

DISS. ETH NO. 26943

THE BEHAVIOUR OF LITHIUM IN SILICIC MAGMATIC SYSTEMS

A thesis submitted to attain the degree of
DOCTOR OF SCIENCES of ETH ZURICH
(Dr. sc. ETH Zurich)

presented by
Julia Neukampf
Master of Science (MSc) in Geological Science
Freie Universität Berlin, Germany

born on 18.02.1989
citizen of Germany

accepted on the recommendation of
Prof. Dr. Olivier Bachmann
Dr. Ben Ellis
Dr. Oscar Laurent
Prof. Dr. Colin Macpherson

2020

“Many of the truths that we cling to depend on our point of view.”

Obi-Wan Kenobi (1983)

Star Wars: Episode VI - Return of the Jedi

Summary

The interest in lithium (Li) and its two stable isotopes (^6Li and ^7Li) has increased over the last two decades due to the economic importance of lithium-ion batteries in different electronic devices, e.g., hybride vehicles. Because of major analytical advances over the past 30 years, it has now become easier to analyse lithium isotopes not only by multi-collector-inductively-coupled-plasma mass spectrometry (MC-ICP-MS) but also *in situ* by secondary ion mass spectrometry (SIMS) or femtosecond laser coupled to a multi-collector ICP-MS (fs-LA-MC-ICP-MS). Previous studies have focused on geological processes related to the subduction cycle or basaltic systems, but studies focusing on more evolved systems are scarce even though the economical demand of lithium has increased and lithium is mined from lithium-rich deposits, e.g., pegmatites, brines, and to a lesser degree from weathered rhyolitic rocks.

In this thesis, I provide the first systematic insight into lithium distribution and concentration and lithium isotopic composition of minerals in dry, rhyolitic systems and how they are affected by processes such as degassing. Additionally, I consider and discuss the potential of lithium isotopes fractionation at high temperatures.

I here present the lithium concentrations and isotopic compositions ($\delta^7\text{Li}$) of all major minerals (quartz, sanidine, plagioclase, clinopyroxene, fayalite, and orthopyroxene) and groundmass glass from non-welded samples of Mesa Falls Tuff (the smallest eruption of the Yellowstone caldera system; 1.3 Ma). These samples were selected to avoid alteration by post-eruptive processes. The groundmass glass of the sample has no microlite growth, verifying that the glass was rapidly quenched and was not modified post-eruption. The $\delta^7\text{Li}$ of all minerals was determined using a MC-ICP-MS and trace element compositions were analysed by LA-ICP-MS. The lithium concentrations in the analysed minerals was low compared to the groundmass glass, where lithium concentrations range from 36 to 52 ppm. Quartz has the highest lithium concentration of all mineral phases (13 to 25 ppm), followed in descending order by plagioclase (5 to 29 ppm), fayalite (14 to 19 ppm), clinopyroxene (10 to 14 ppm), orthopyroxene (8 to 9 ppm), and sanidine (1 to 12 ppm). Lithium concentrations found in quartz-hosted crystallised melt inclusions ranged between 70 and 397 ppm. The $\delta^7\text{Li}$ composition of the different phases varies by $\sim 10\text{‰}$ with the groundmass glass being the heaviest (+6.5 to +7.5‰), and decreasing from quartz (+6.7 to +7.2‰), fayalite (+3.1‰), clinopyroxene (-0.1 to -0.1‰), sanidine (-0.1 to -0.6‰), plagioclase (-1.4 to -2.4‰) to orthopyroxene (-2 to -2.1‰). Furthermore, I calculated apparent partition coefficients between the groundmass glass and the co-existing mineral phases for Mesa Falls Tuff and for 15 other ignimbrites from the Yellowstone-Snake River Plain province. The apparent partition coefficients showed that lithium is more compatible in quartz and the least compatible in sanidine. Additionally, I identified lithium concentration profiles in plagioclase and sanidine, where I observed lithium decreasing towards their rims, suggesting the potential of kinetic isotopic fractionation being preserved.

To verify this potentially preserved kinetic isotopic fractionation I analysed plagioclase crystals *in situ* by fs-LA-MC-ICP-MS to determine their $\delta^7\text{Li}$ composition from rim to core, and by LA-ICP-MS to determine trace element compositions associated with the $\delta^7\text{Li}$ profiles. This revealed large systematic isotopic differences across grain profiles, with rims ranging from -3.8 to +5.9‰ and cores

ranging from -11 to $+2\%$. With these findings I show that there is a negative correlation between the concentration and isotopic composition of these crystals and that this correlation is independent of any other major or trace element. I interpreted the formation of these isotopically heavy rims as kinetic isotopic fractionation due to the disequilibrium between the plagioclase crystals and their surrounding melt. The concentration and $\delta^7\text{Li}$ gradients formed as ^6Li fractionated into the vapour phase during vesiculation, depleting the melt in ^6Li . This led to a flux of ^6Li from the rims of feldspars into the melt enriching the rims in ^7Li . Diffusion modelling was applied to the lithium concentration and $\delta^7\text{Li}$ profiles to quantify the time scales in which they formed. The results show that the gradients formed within tens of minutes before eruption, making lithium and its isotopes a powerful tool to quantify late-stage processes in a magmatic system.

This finding indicates that there should be significant $\delta^7\text{Li}$ fractionation between the melt and the erupted, degassed groundmass glass. This is supported by the difference in lithium concentration in the crystallised melt inclusions compared to the groundmass glass. Therefore, the $\delta^7\text{Li}$ composition of different quartz-hosted melt inclusions and groundmass glass was analysed *in situ* by SIMS and trace elements were determined by LA-ICP-MS. Their H_2O and CO_2 concentrations were determined by Fourier transform infrared (FTIR) spectrometer measurements and only glassy inclusions with ~ 3 to 4 wt.% H_2O were used for further analyses. Lithium concentrations between the two populations of host-quartz vary by more than a factor of 2. The quartz population with crystallised inclusions has increasing lithium concentration towards their rims, indicating a diffusional exchange between melt and quartz. Diffusion modelling shows that these gradients formed in less than three hours. The $\delta^7\text{Li}$ composition of the groundmass glass and glassy melt inclusions verified a large isotopic fractionation of up to 25% . Glassy melt inclusions have a lower lithium concentration compared to the groundmass glass, which hints at a diffusional exchange between melt inclusions and host-quartz.

In this thesis, I show that lithium in mineral phases in evolved magmatic systems can vary significantly and that their isotopic composition is strongly influenced by high-temperature fractionation. This can have implications for studies focusing on the subduction cycle or basaltic systems as the measured lithium isotopes compositions might reflect late-stage processes and not represent mantle values. It highlights that Li and its isotopes combined with *in situ* measurements are a robust proxy to understand late-stage magmatic processes, such as time scales of degassing.

Zusammenfassung

Das Interesse an Lithium (Li) und seinen zwei stabilen Isotopen (^6Li und ^7Li) hat in den letzten zwei Jahrzehnten aufgrund der wirtschaftlichen Bedeutung von Lithium-Ionen-Batterien in verschiedenen elektronischen Geräten, z. B. Hybridfahrzeugen, zugenommen. Aufgrund der großen analytischen Fortschritte in den letzten 30 Jahren ist es jetzt einfacher geworden, Lithiumisotope nicht nur mit Hilfe von Multikollektor-induktiv gekoppelter Plasma-Massenspektrometrie (MC-ICP-MS) zu analysieren, sondern auch *in situ* mit Hilfe von Sekundärionen-Massenspektrometrie (SIMS) oder eines Femtosekundenlasers, welcher an eine Multikollektor-ICP-MS (fs-LA-MC-ICP-MS) gekoppelt ist. Frühere Studien haben sich auf geologische Prozesse im Zusammenhang mit dem Subduktionszyklus oder basaltischen Zusammensetzungen konzentriert. Studien, die sich mit felsische Zusammensetzungen befassen, sind selten, obwohl der wirtschaftliche Bedarf an Lithium gestiegen ist und Lithium aus lithiumreichen Lagerstätten abgebaut wird, z. B. Pegmatiten, Solen, und in geringerem Maße aus verwitterten rhyolitischen Gesteinen.

In dieser Arbeit gebe ich den ersten systematischen Einblick in die Lithiumverteilung und -konzentration sowie die Lithiumisotopenzusammensetzung von Mineralen in trockenen, rhyolitischen Gesteinen und wie sie durch Prozesse wie Magmenausgasung beeinflusst werden. Zusätzlich betrachte und diskutiere ich das Potenzial der Lithiumisotopenfraktionierung bei hohen Temperaturen.

Ich präsentiere die Lithiumkonzentrationen und Isotopenzusammensetzungen ($\delta^7\text{Li}$) aller wichtigen Minerale (Quarz, Sanidin, Plagioklas, Klinopyroxen, Fayalit und Orthopyroxen) und der glasigen Grundmasse aus nicht gefrittetten Proben vom Mesa Falls Tuff (der kleinsten Eruption des Yellowstone-Caldera-Systems; 1,3 Ma). Diese Proben wurden ausgewählt, um eine Veränderung durch posteruptive Prozesse ausschließen zu können. Die glasige Grundmasse der Probe weist kein Mikrolitwachstum auf, was bestätigt, dass das Glas schnell abgeschreckt und nach dem Ausbruch nicht modifiziert wurde. Das $\delta^7\text{Li}$ aller Minerale wurde mit einem MC-ICP-MS bestimmt und die Spurenelementzusammensetzungen mit dem LA-ICP-MS analysiert. Die Lithiumkonzentrationen in den gemessenen Mineralen waren im Vergleich zur glasigen Grundmasse, wo die Lithiumkonzentrationen zwischen 36 und 52 ppm liegen, niedrig. Quarz hat die höchste Lithiumkonzentration aller Mineralphasen (13 bis 25 ppm), gefolgt von Plagioklas (5 bis 29 ppm), Fayalit (14 bis 19 ppm), Klinopyroxen (10 bis 14 ppm) und Orthopyroxen (8 bis 25 ppm) 9 ppm) bis Sanidin (1 bis 12 ppm).

Die Lithiumkonzentrationen von kristallisierten Schmelzeinschlüssen, die sich in Quarz befinden, lagen zwischen 70 und 397 ppm. Die $\delta^7\text{Li}$ -Zusammensetzung der verschiedenen Phasen variiert um $\sim 10\text{‰}$, wobei die glasige Grundmasse am schwersten ist (+6,5 bis +7,5‰) und von Quarz (+6,7 bis +7,2‰) über Fayalit (+3,1‰), Klinopyroxen (−0,1 bis +1‰), Sanidin (−0,1 bis −0,6‰), Plagioklas (−1,4 bis −2,4‰) bis Orthopyroxen (−2 bis −2,1‰) abnimmt. Außerdem habe ich scheinbare Verteilungskoeffizienten zwischen der glasigen Grundmasse und den Mineralphasen des Mesa Falls Tuff und für 15 weitere Ignimbrite aus der Provinz Yellowstone-Snake River Plain, berechnet. Die scheinbaren Verteilungskoeffizienten zeigten, dass Lithium in Quarz am kompatibelsten ist und in Sanidin am wenigsten kompatibel ist. Zusätzlich habe ich Lithiumkonzentrationsprofile in Plagioklas und Sanidin identifiziert. Dort habe ich beobachtet, dass Lithium zu ihren Rändern hin abnahm, was darauf hindeutet, dass einer kinetischen Isotopenfraktionierung möglicherweise erhalten geblieben ist.

Um diese potenziell erhaltene kinetische Isotopenfraktionierung zu verifizieren, habe ich Plagioklaskristalle *in situ* mit Hilfe eines fs-LA-MC-ICP-MS analysiert, um ihre $\delta^7\text{Li}$ -Zusammensetzung vom Rand bis zum Kern zu bestimmen. Zusätzlich habe ich die Spurenelementzusammensetzungen mit Hilfe des LA-ICP-MS entlang der $\delta^7\text{Li}$ Profile gemessen. Dies ergab große systematische Isotopenunterschiede innerhalb der Profile mit Rändern von $-3,8$ bis $+5,9\%$ und Kernen von -11 bis $+2\%$. Mit diesen Ergebnissen zeige ich, dass es eine negative Korrelation zwischen der Konzentration und der Isotopenzusammensetzung dieser Kristalle gibt und dass diese Korrelation unabhängig ist von anderen Haupt- oder Spurenelementen. Die Bildung dieser isotopisch schweren Ränder wird als kinetische Isotopenfraktionierung interpretiert, welche sich aufgrund eines Ungleichgewichts zwischen den Plagioklaskristallen und ihrer umgebenden Schmelze bildete. Die Konzentrations- und $\delta^7\text{Li}$ -Gradienten, bildeten sich dadurch, dass ^6Li während der Vesikulation in die Gasphase fraktionierte, wodurch die Schmelze in ^6Li abgereichert wurde. Dies führte zu einer Diffusion von ^6Li aus den Feldspaträndern in die Schmelze, wodurch die Ränder in ^7Li angereichert wurden. Diffusionsmodellierung wurde auf die Lithiumkonzentrations- und $\delta^7\text{Li}$ -Profile angewendet, um die Zeitskalen zu quantifizieren, in denen sie sich bildeten. Die Ergebnisse zeigen, dass sich die Gradienten innerhalb von zehner Minuten vor dem Ausbruch gebildet haben. Dies macht Lithium und seine Isotope zu einem guten Hilfsmittel um Prozesse, die im späten Stadium des magmatischen Systems stattfinden, zu quantifizieren.

Dieses Ergebnis weist darauf hin, dass zwischen der Schmelze und der abgelagerten, entgasen glasigen Grundmasse eine signifikante $\delta^7\text{Li}$ -Fraktionierung bestehen sollte. Dies wird durch den Unterschied in der Lithiumkonzentration in den kristallisierten Schmelzeinschlüssen im Vergleich zur glasigen Grundmasse unterstützt. Daher wurde die $\delta^7\text{Li}$ -Zusammensetzung verschiedener Schmelzeinschlüsse, welche sich in Quarz befinden, und der glasigen Grundmasse *in situ* mit Hilfe der SIMS gemessen und die Spurenelemente wurden per LA-ICP-MS bestimmt. Ihre H_2O - und CO_2 -Konzentrationen wurden durch Fourier-Transformations-Infrarot (FTIR)-Spektrometer-Messungen ermittelt und nur glasige Einschlüsse mit rund 3 bis 4 Gew.% H_2O wurden für weitere Analysen verwendet. Die Lithiumkonzentrationen zwischen den beiden Quarzpopulationen variieren um mehr als den Faktor 2. Die Quarzpopulation mit kristallisierten Einschlüssen weist eine zunehmende Lithiumkonzentration in Richtung ihrer Ränder auf, was auf einen Diffusionsaustausch zwischen Schmelze und Quarz hinweist. Die Diffusionsmodellierung zeigte, dass sich diese Gradienten in weniger als drei Stunden bildeten. Die $\delta^7\text{Li}$ -Zusammensetzung der glasigen Grundmasse und der glasigen Schmelzeinschlüsse bestätigte eine große Isotopenfraktionierung von bis zu 25%. Glasige Schmelzeinschlüsse weisen im Vergleich zur glasigen Grundmasse eine geringere Lithiumkonzentration auf, was auf einen Diffusionsaustausch zwischen Schmelzeinschlüssen und Quarz hindeutet.

In dieser Arbeit zeige ich, dass Lithium in Mineralen aus felsischen Schmelzen stark variieren kann und dass deren Isotopenzusammensetzung stark durch Fraktionierung bei hohen Temperaturen beeinflusst wird. Dies kann Auswirkungen auf Studien haben, die sich auf den Subduktionszyklus oder basaltische Zusammensetzungen konzentrieren, da die gemessenen Lithiumisotopenzusammensetzungen möglicherweise Prozesse im Spätstadium widerspiegeln und keine Mantelwerte darstellen. Ich hebe hervor, dass Li und seine Isotope in Kombination mit *in situ* Messungen eine robuste Methode sind, um magmatischer Prozesse zu verstehen, die im späten Stadium des magmatischen Systems stattfinden, z. B. Zeitskalen der Ausgasung von Magma.

Acknowledgements

First and foremost, I would like to thank Ben Ellis and Olivier Bachmann for giving me the opportunity to come to ETH to carry out this thesis. Over these four years we had numerous fruitful scientific discussions that allowed me to develop the scope of my PhD. I am grateful that Olivier always supported me and my research and gave me the freedom to follow my ideas and that he provides a harmonious atmosphere within our group by hosting events outside of work. Thank you for the seminars, support, ideas and motivation during the last years.

I would like to express my gratitude to Prof. Dr. Colin Macpherson (University of Durham) for agreeing to be part of my dissertation committee and Prof. Dr. Maria Schönbacher. I want to thank Peter Ulmer and Jörn Wotzlaw for inspirational discussion and always having an open door. A special thank you goes to Oscar Laurent with whom I not only had very long discussions about our data, and who was open to trying new things on the LA-ICP-MS and letting me analyse as much as I needed even if it was quartz, but was a very strong moral support over the past four years. I want to thank my co-authors and all the people that made this thesis possible: Marcel Guillong, Tomas Magna, Lena Steinmann, Stefan Weyer, Ralf Dohmen, Chris Harris, Theresa Ubide, Peter Tollan, Anne-Sophie Bouvier.

I am grateful for all the people that provided technical support during my PhD: Lydia Zehnder, Eric Reuser, Claudia Büchel, Julian Allaz, Andreas Jalles and all the other great people of IGP and ETH: Alina, Angus, Christian, Enico, Fabian, Franziska, Friedrich, Gino, Giuliano, Giulio, Henner, Jakub, Kenneth, Manuel, Mapu, Matthias, Micheal M., Nolwenn, Lena, Paul, Paolo and many more.

I was lucky to share my office with such awesome people with whom I had great scientific discussions as well as a lot of laughter and beers, so a special thank you to Julian S., Matthias L., Razvan P. and Michael F. I want to thank Julien C. for not only being a great office mate the past years and providing an extra spirit in the office by for example singing different songs and making me laugh a lot, but being a great friend, being there for me no matter what and keeping me sane. A special thank you and a lot of appreciations goes to Felix M. Not only did he never give up on me learning to understand Swiss German but provided me over the years with high quality carbon coating for SEM and EPMA measurements and spent a lot of time with me at the probe trying to figure out the various problems the old machine was throwing at us.

I want to thank my friends here that made me feel at home in Switzerland and with whom I spend a lot of time outside of ETH and away from the microprobe and not thinking about work. A big thank you to Emily who welcomed me when I started at ETH and for being the other half of chaotic power. I want to thank Theo, Fabi, Edi, Julien C, Daria for always being up for a kicker match. Special thanks to the “Dog Royal” group, I enjoyed our BBQs and board game evenings a lot. Thank you to Dani, Hannes, Anmi, Peter, Nele, Padde and Linus for a great time!

I want to specially thank my family and friends back from home that weren't in Switzerland but always with me in spirit, provided moral support and gave me the chance to relax over a beer or wine and to gather new strength for the tasks ahead of me. Huge thank you to Sascha and Tina, Nadine, Anja and Basti, Daniel, Lukas, Robbin, Moritz, Esther, Caro, Robert, Sami. I want to thank people that left ETH for new endeavours. Kathi, Basti, Stephané, Dawid and Francesca. Thank you to Dr. Hammer-schmidt and Prof. Timm John for always believing in me.

Contents

Summary	V
Zusammenfassung	VII
Acknowledgements	IX
Chapter 1: Introduction	15
1.1 Motivation and outline of thesis	16
1.2 A general introduction to non-traditional stable isotopes	17
1.3 Current state of research in the field – Introduction to lithium isotopes	19
1.3.1 Lithium coordination, diffusion and partition coefficients	22
1.3.2 Geospeedometry	24
1.3.3 Lithium as a resource	25
1.4 Geological background	27
1.5 References	28
Chapter 2: Partitioning and isotopic fractionation of lithium in mineral phases of hot, dry rhyolites: The case of the Mesa Falls Tuff, Yellowstone	37
2.1 Introduction	38
2.2 Geological background	39
2.3 Analytical methods	40
2.3.1 Trace element measurements	41
2.3.2 Lithium isotopic measurements	42
2.4 Results	42
2.4.1 Quartz	42
2.4.2 Sanidine	43
2.4.3 Plagioclase	44
2.4.4 Pyroxenes	45
2.4.5 Fayalite	46
2.4.6 Groundmass glass and melt inclusions	46
2.4.7 Other phases	48
2.4.7 Lithium isotopes	48
2.5 Discussion	49
2.5.1 Partitioning coefficients for Li in MFT	49
2.5.1.1 Apparent partition coefficient for feldspar	52
2.5.1.2 Lithium distribution in fayalite	53
2.5.2 Lithium elemental variation within feldspars	53
2.5.3 Magmatic fractionation of lithium isotopes	54

2.6 Conclusions and future perspectives	56
2.7 References	58

Chapter 3: Time scales of syn-eruptive volatile loss in silicic magmas quantified by Li-isotopes63

3.1 INTRODUCTION	64
3.2 LITHIUM CONCENTRATION MAPS AND PROFILES	65
3.3 IN SITU $\delta^7\text{Li}$ MEASUREMENTS	67
3.4 DIFFUSION MODELLING OF LI CONCENTRATIONS AND $\delta^7\text{Li}$	68
3.5 REFERENCES	72
3.6 Supplementary Materials	74
3.6.1 Methods	74
3.6.1.1 Major element measurements	74
3.6.1.2 Laser ablation inductively coupled plasma mass spectrometry (LA-ICPMS) mapping.	74
3.6.1.3 In situ Lithium isotope analysis of plagioclase crystals by femtosecond laser ablation-MC-ICPMS	73
3.6.1.4 Trace element measurements	78
3.6.2 Diffusion modelling.	78
3.6.2 References	79

Chapter 4: Li elemental and isotopic composition of rhyolitic melt inclusions and their host quartz: a record blurred by multiple diffusive re-equilibration81

4.1 Introduction	82
4.2 Geological setting and samples	84
4.3 Analytical methods	85
4.3.1 Sample preparation	85
4.3.2 Fourier transform infrared (FTIR) spectroscopy	85
4.3.3 Secondary Ionization Mass Spectrometry measurements	86
4.3.4 Major element measurements	86
4.3.5 Laser ablation inductively coupled plasma mass spectrometry (LA-ICP-MS).	87
4.4 Results	87
4.4.1 Melt inclusions	87
4.4.2 Groundmass glass	88
4.4.3 Quartz	89
4.4.4 Lithium isotopes	90
4.5 Discussion	91
4.5.1 Lithium concentrations and isotopic composition in melt inclusions and groundmass glass	91
4.5.2 Lithium abundance in host-quartz.	93

4.5.3 Diffusion modelling.....	95
4.6 Conclusions.....	96
4.7 References.....	97
Chapter 5: Conclusions and outlook.....	101
5.1 Conclusion.....	102
5.2 Outlook.....	103
5.3 References.....	105
Appendix.....	107
Appendix A: Supplementary material for Chapter 2.....	107
Appendix B: Supplementary material for Chapter 3.....	229
Appendix C: Supplementary material for Chapter 4.....	281
Curriculum vitae.....	

Chapter 1

Introduction

1.1 Motivation and outline of thesis

Non-traditional isotopes have gained increasing attention over the past three decades as they are a useful tool to study geological processes such as the subduction cycle. Lithium and its isotopes have become a more frequently used isotope system to look at mantle, subduction or surface processes. Hundreds of papers focus on the behaviour of lithium in different geological reservoirs by studying natural samples and performing experiments to identify processes leading to changes in lithium concentration and isotopic composition in the melt and mineral phases present, e.g. olivine. These studies (summarised in Tomascak et al., 2016 and Penniston-Dorland et al., 2017) determined that lithium diffusivity can result in large lithium isotopic differences between melt and mineral phases and fluids present. Pioneering work by Richter et al. (2003), who experimentally studied the lithium diffusion between basalt and rhyolite, determined that the fast diffusion of lithium can result in an isotopic fractionation of ~40%. This study also showed that diffusional fractionation increases with increasing temperatures, whereas previous studies assumed lithium fractionation would be greater at temperatures below 350 °C (e.g., Chan et al., 1994).

However, all these previous studies only focus on the behaviour of lithium in more primitive melts, with the exception of a single study by Ellis et al. (2018) that addresses the lithium systematics in more evolved systems. This study showed that the lithium concentration and isotopic composition of mineral phases in rhyolitic ignimbrites can be changed due to post-eruptive mobility of lithium. Due to the increasing demand of lithium as an economic resource (e.g. Kesler et al., 2012; Benson et al., 2017) and the association of lithium deposits with evolved rocks, further studies of the lithium behaviour in evolved magmatic systems are needed. To address this need and current knowledge gap, the primary aim of my thesis is to quantify the lithium budget in rhyolites. The work herein is also guided by the aim to identify and evaluate the processes that lead to changes in lithium concentration and isotopic composition of rhyolites and their associated mineral phases in magmatic systems and to determine potential high-temperature isotopic fractionation.

Furthermore, a lot of studies focus on caldera forming eruptions which are associated with voluminous rhyolitic magma bodies (e.g., Bachmann et al., 2002; Hildreth & Wilson, 2007; Stelten et al., 2015). Most of these studies investigate the time scales of magma storage and assembly and the processes leading to it, but only few studies look at the tipping point of the system that leads to these explosive eruptions. Using lithium concentration and lithium isotopes gives the opportunity to study the last moments of the system prior or during eruption. The Yellowstone caldera system (USA), which is one of the largest volcanic systems on Earth, had three caldera forming eruptions with Huckleberry Ridge Tuff (2.08 Ma; Rivera et al., 2014; Singer et al., 2014), Mesa Falls Tuff (1.30 Ma; Rivera et al., 2016) and Lava Creek Tuff (0.63 Ma; Matthews et al., 2015). Mesa Falls Tuff's eruption history is the simplest out of the three eruptions with being smallest and having erupted in one single pulse (Christiansen, 2001). It has been well characterised in terms of geochemistry, petrography, volcanology (Christiansen, 2001) and as a result, deemed fairly representative of a typical hot, dry rhyolite. As Mesa Falls Tuff has little to no post-eruptive modification these characteristics make it an appropriate choice to solve the different scientific questions using lithium concentrations and isotopes that will be addressed in this thesis.

The thesis is structured into a total of five chapters. Following the introduction, chapters two to four present three independent papers that used Mesa Falls Tuff (Yellowstone, USA) as a case study, while Chapter five provides a general conclusion and an outlook for future research in this field. Chapter two only uses bulk separate measurements to have a general understanding of the lithium isotopic distribution between different mineral phases within a rhyolite. Chapter three and four address scientific questions that were left unanswered and/or were identified in chapter two. In chapters three and four only *in situ* measurements are used as they provide a better spatial resolution which helps to identify disequilibrium processes and quantify the timescales in which they have formed. The specific content of each chapter is briefly summarised below.

Chapter two is a paper published in *Chemical Geology* (2019) and focuses on the partitioning and isotopic fractionation of lithium in minerals in rhyolite. The paper investigates the distribution of lithium concentration (measured *in situ* by LA-ICP-MS) and isotopic composition (measured as bulk separates by MC-ICP-MS) of the different mineral phases present in Mesa Falls Tuff. Additionally, it provides apparent partition coefficients for lithium between the groundmass glass and the co-existing minerals. In this paper lithium variations between rims and cores in sanidine and plagioclase were identified, suggesting a possible kinetic isotopic fractionation between melt and feldspar crystals.

Chapter three is a paper published in *Geology* (2020) and represents the first detailed study of $\delta^7\text{Li}$ in plagioclase crystals measured *in situ* using a femtosecond laser that is coupled to a MC-ICP-MS. With the isotope data it was possible to show that due to the large mass difference between the two isotopes the analysed plagioclase grains record kinetic effects that were a result of volatile degassing prior to eruption. Diffusion modelling of lithium concentration and isotope profiles in plagioclase was applied to determine the time scales of volatile degassing of Mesa Falls Tuff.

Chapter four is a paper draft and examines the lithium isotopic fractionation between melt and deposited groundmass glass. Lithium concentration (measured *in situ* by LA-ICP-MS), isotopic composition (measured *in situ* by SIMS), major elements (measured by EPMA), H_2O as well as CO_2 concentrations (measured *in situ* by FTIR) in melt inclusions hosted in quartz crystals from Mesa Falls Tuff were examined. The melt inclusion data is discussed in context with the groundmass glass from Mesa Falls Tuff to identify processes taking place between entrapment of the melt inclusions and the deposition of the groundmass glass. Furthermore, this chapter deals with potential processes leading to the enrichment of lithium in crystallised melt inclusions compared to their glassy counterparts.

Chapter five is the final chapter, providing a general summary of the dissertation, how the goals were accomplished and gives a future perspective of which questions are still to be answered and how they can guide future studies in this field.

1.2 A general introduction to non-traditional stable isotopes

Numerous stable isotope systems (e.g., H, C, N, O, S; Valley et al., 1986; Valley and Cole, 2001) have been used as tracers to identify geochemical reservoirs, reconstruct temperatures, classify meteorites, among a multitude of applications. The recent improvements in mass spectrometry make it possible to measure even small isotopic effects. Over the past decade non-traditional stable isotope systems (e.g., magnesium, iron, chlorine, lithium) have been developed or expanded to explain geological processes. Non-traditional stable isotope systems have some advantages compared to the traditional stable isotope

systems. For example, the elements span a wide range from highly volatile (e.g., Zn and K) to refractory (e.g., Ca and Ti). Further, most of them are redox-sensitive, and have high atomic numbers with more than two stable isotopes (Teng et al., 2017), which makes analysing them easier. When the isotopes are in disequilibrium with each other their isotopic composition can be used to understand processes leading to disequilibrium and to determine time scales of geological processes (Watkins et al., 2017). The mass difference between the different isotopes of an element, the possible changes of oxidation state of the different isotopes, and volatility of the isotopes influence the amount of isotope fractionation (Teng et al., 2017).

To better understand geological processes and for a correct interpretation of stable isotope data it is important to know the equilibrium isotope fractionation factors between phases as they help to identify isotopic equilibrium or unmask disequilibrium between phases. These factors are usually determined first by theoretical predictions that are then linked to experimental results (Young et al., 2015). Pioneering work on stable isotopic fractionation was done by Lindemann and Aston (1919), Lindemann (1919), Urey and Greiff (1935), and Urey (1947) who calculated theoretical equilibrium isotope fractionations. Urey (1947) developed an equation that calculates the isotopic partition function ratios for molecules that was further modified from Kieffer (1982) for crystals and amorphous solids.

Some general rules for equilibrium stable isotope fractionation, based on the theoretical findings of Bigeleisen and Mayer (1947), have been developed and are summarised in O'Neil (1986) and Schauble (2004). The first general rule is that *equilibrium isotopic fractionation decreases with increasing temperature*, meaning that the largest isotopic fractionation occurs at the lowest temperatures (Schauble, 2004). Exceptions can arise when fractionation is minor and/or when the element is bonded to hydrogen. The second rule is that *isotopic fractionation is greater for light elements and isotopic systems where the isotopes have large mass differences (e.g., lithium)*. The third rule is when looking at an equilibrium state, *heavy isotopes prefer substances where the element forms the strongest bonds*, where the coordination number is low and valence is high. The last rule is that *substances (e.g. crystals) where an element is in a bond with hydrogen or associated with a low-mass molecule will be less enriched in the heavier isotope* (Schauble, 2004).

For kinetic fractionation, however, it is difficult to determine general rules. Kinetic fractionation is defined as a one-directional process under disequilibrium conditions where the exchange of the isotopes was not complete, and the lighter isotopes are enriched in the reaction products (Schauble, 2004). In contrast to equilibrium fractionation, diffusive kinetic fractionation does not decrease with increasing temperature (Schauble, 2004). The isotope fractionation factor is described by the term α (equation 1) with the isotopes $^{\text{light}}\text{X}$ (light isotope) and $^{\text{heavy}}\text{X}$ (heavy isotope) fractionating between two phases or two compounds within a phase (XA and XB):

$$\alpha_{\text{XA-XB}} = \frac{(^{\text{heavy}}\text{X}/^{\text{light}}\text{X})_{\text{XA}}}{(^{\text{heavy}}\text{X}/^{\text{light}}\text{X})_{\text{XB}}} \quad (1)$$

The fraction is usually small and, therefore, $1000 \cdot \ln(\alpha)$ or $1000 \cdot (\alpha - 1)$ are used to highlight the difference between α and 1 with $\alpha = 1.001(1000 \cdot [\alpha - 1] = 1)$ representing the fractionation of one per mil (‰) (Schauble, 2004).

When an isotopic gradient is created within a phase, a net flux forms, which can lead to large isotopic fractionation. According to Fick's first law the flux of a chemical species (i) is proportional to

the concentration gradient and the proportionality constant is the diffusion coefficient (D ; m^2s^{-1}). This can be expressed as:

$$J_i = -D_i \nabla C_i \quad (2)$$

with J_i being the flux ($\text{moles m}^{-2}\text{s}^{-1}$) and C_i the concentration (moles m^{-3}). Equation (2) can, for example, be applied to diffusion of a trace species in silicate melt. The diffusion coefficient depends on various parameters such as temperature, pressure, oxygen fugacity, and water concentration (e.g., Chakraborty 2008). The difference between the diffusion coefficients of the isotopes of one element is mass dependent. This ratio is defined as:

$$D_2/D_1 = (m_1/m_2)^\beta \quad (3)$$

with (D_2/D_1) being the ratio of the diffusion coefficients of the isotopes of the element and (m_2/m_1) being the ratio of masses of the isotopes (Richter et al., 1999). β is a dimensionless empirical parameter that is derived experimentally and is used to compare different elements. β values higher than one mean that the diffusivity is more sensitive to isotope mass. Richter et al. (1999) were the first to study the mass dependence of diffusion in silicate melts. Using calcium isotopes, they experimentally showed that isotopes can experience high-temperature fractionation as the light isotope diffuses faster than the heavier isotopes. Richter et al. (2009) systematically compiled the β factor for different cations in metals (e.g. magnesium) and metalloids (e.g., silicon) with all being less than 0.5, and showed that when plotted against temperature it reflects the sensitivity of mass discrimination. Additionally, Richter et al. (2003, 2008) and Watkins et al. (2009) showed that trace elements (e.g., lithium) have a stronger mass discrimination compared to major elements (e.g., magnesium, iron).

1.3 Current state of research in the field – Introduction to lithium isotopes

Lithium (Li) is the lightest alkali metal and one of the fastest diffusing elements in minerals and silicate melt (e.g., Jambon and Semet, 1978; Giletti and Shanahan, 1997; Richter et al., 2003). Lithium is considered moderately incompatible in clinopyroxene (e.g., Caciagli et al., 2011), olivine (e.g., Brenan et al., 1998a), plagioclase (e.g., Blundy et al., 1998) and mobile when aqueous fluids are involved (e.g., Edmond et al., 1979; Brenan et al., 1998b; Chan and Kastner, 2000). It has two stable isotopes, ^6Li (7.4% atomic abundance) and ^7Li (92.6% atomic abundance), exhibiting one of the largest mass differences (~17%) compared to other stable isotope systems (e.g., ^{10}B - ^{11}B with ~10%, ^{16}O - ^{18}O with ~12.5%). Lithium isotope ratios are reported in the δ -notation (equation 4) relative to the Li Carbonate L-SVEC reference solution (Flesch et al., 1973):

$$\delta^7\text{Li} (\text{‰}) = \left[\frac{(^7\text{Li}/^6\text{Li})_{\text{sample}}}{(^7\text{Li}/^6\text{Li})_{\text{L-SVEC}}} - 1 \right] \times 1000 \quad (4)$$

Therefore, positive values reflect an enrichment in ^7Li and are referred to as isotopically heavy, whereas negative values represent a higher amount of ^6Li and are considered to be isotopically light.

The large mass difference between the two isotopes can lead to considerable differences in the isotopic composition in different reservoirs due to equilibrium/disequilibrium and kinetic fractionation in the Earth system. Recent studies demonstrated the existence of large lithium isotopic differences in geological reservoirs, with up to 50‰ variation (Fig. 1.1; summarised in Tomascak et al., 2016 and

Penniston-Dorland et al., 2017). Studies using lithium are driven by different scientific problems, e.g., crust–mantle recycling (e.g., Moriguti and Nakamura, 1998), silicate weathering and alteration (e.g., Seyfried et al., 1984; Liu and Rudnick, 2011; Misra and Froelich, 2012), and fluid–rock interaction and processes involved in the subduction cycle (e.g., Brenan et al., 1998b; Marschall et al., 2006; Qiu et al., 2009, 2011b). Lithium is typically used as a tracer of metamorphic, hydrothermal, and magmatic

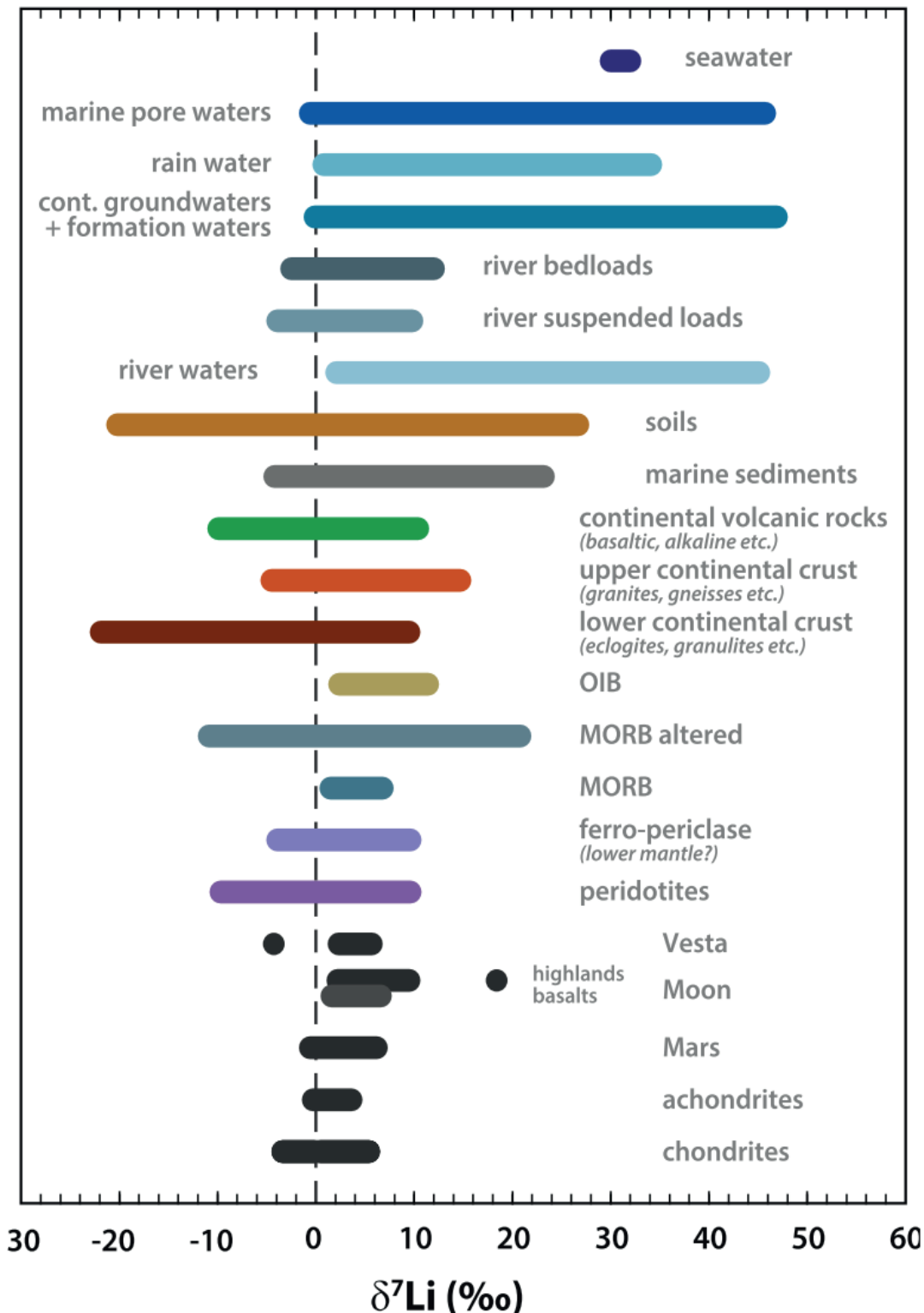


Fig. 1.1: Range in lithium isotopic composition in terrestrial and extra-terrestrial reservoirs (from Tomascak et al., 2016).

processes (e.g., Matsui et al., 1977; Tomascak et al., 1999; Schuessler et al., 2009), especially as lithium is not incorporated by biological systems. Lithium is considered moderately incompatible during crystal fractionation and its concentration increases during magmatic differentiation from basalt to rhyolite (e.g., Schuessler et al., 2009). Most studies published to date focus on very primitive compositions (e.g., Chan et al., 1992; Tomascak et al., 1999; Elliott et al., 2006), whereas, more evolved compositions are less well studied (e.g., Schiavi et al., 2012). Additionally, lithium concentrations and isotopic composition are used to study meteorites as well as lunar and Martian materials, to provide information about the isotopic composition of the solar system (e.g., Tomascak et al., 2016).

Previous studies suggest that lithium isotopic fractionation up to 50‰ only exists during low-temperature reactions that are related to water at the Earth's surface. At temperatures above 350°C the isotopic fractionation is very small and fractional crystallisation and partial melting can only fractionate lithium isotopes by ~1‰ (e.g., Chan et al., 1994; Tomascak et al., 1999). In contrast, experimental studies have demonstrated the existence of isotopic fractionation at temperatures above 350°C (e.g., Richter et al., 1999, 2009, 2014). It has been shown that different reservoirs on Earth have different bulk lithium concentrations and isotopic compositions (e.g., Tomascak et al. 2016; Penniston-Dorland et al., 2017). Different studies determined that secondary clay minerals are enriched in ^6Li during continental weathering, whereas, ^7Li is enriched in the fluid, e.g., rivers (~0.2 ppb to 20 ppb, $\delta^7\text{Li} = +1$ to $+44\%$), groundwater (+6 to $+29\%$), meteoric water (<3 ppb and $\delta^7\text{Li} = +0.8$ to $+33.3\%$), lakes (0.11 ppb to 22 ppm, $\delta^7\text{Li} = +17$ to $+35\%$), seawater (~ 0.18 ppm and $\delta^7\text{Li} = +31\%$), submarine hydrothermal fluids (0.1 to 10 ppm and $\delta^7\text{Li} = +5$ to $+11\%$), or geothermal waters (0.2–150 ppm and $\delta^7\text{Li} = -3$ to $+26\%$) (e.g., Chan and Edmond, 1988; Chan et al., 1993, 1994; Moriguti and Nakamura, 1998; Huh et al., 1998; Pistiner and Henderson, 2003; Tomascak et al., 2003; Millot et al., 2004, 2010, 2012; Pogge von Strandmann et al., 2006, 2014; Millot and Negrel 2007; Witherow et al., 2010; Godfrey et al., 2013; Liu et al., 2015; Verney-Carron et al., 2015).

Samples from fresh mid-ocean ridge basalts (MORB) as well as ocean island basalts (OIB) range in lithium isotopic composition from $+1.5$ to $+5.6\%$ (e.g., Chan et al., 1992; Tomascak et al., 1999; Elliott et al., 2006) and from 2.9 to 34 ppm in lithium concentration, though on average the latter is below 8 ppm (e.g., Ryan and Langmuir, 1987; Niu et al., 1999; Tomascak et al., 2008). These studies showed that there is no significant variation between different ridges. The minor differences found are attributed to different MORB sources. E-MORB (high K_2O to TiO_2 ratio) has a $\delta^7\text{Li}$ average of $+4.0\%$ whereas N-MORB (low K_2O to TiO_2 ratio) has an average of $+3.4\%$, but both sources overlap within their uncertainties (Tomascak et al., 2008). In contrast, OIB samples show heterogeneity even for samples from a single location, yet still fall in the range of MORB values. This heterogeneity in samples is attributed to mixing of altered oceanic crust in the OIB source (e.g., Chan and Frey, 2003; Kobayashi et al., 2004; Chan et al., 2009).

Arc lavas (ranging from basaltic to rhyolitic composition) have a spread in $\delta^7\text{Li}$ from -0.3 to $+11\%$ and in lithium concentration from 5.6 to 11.1 ppm (e.g., Chan et al., 2002; Magna et al., 2006a; Tang et al., 2014), but most data fall within the range exhibited by MORB (e.g., Moriguti and Nakamura, 1998; Tomascak et al., 2000; Moriguti et al., 2004). Arc lavas falling in the range of MORB values are interpreted as being unaffected by subduction processes or arc magma genesis (e.g., Leeman et al., 2004; Moriguti et al., 2004). Moriguti and Nakamura (1998), Moriguti et al. (2004) and Magna

et al. (2006a) found that $\delta^7\text{Li}$ values decrease from forearc to backarc and interpreted this as lithium being released from the hydrating slab. Variation between different arcs were associated with different sources, e.g., different amounts of sedimentary rock input, different amount of alteration of the oceanic crust (e.g., Tang et al., 2004), different slab fluid signatures or a slab melting signature (e.g., Tomascak et al., 2000).

Upper and lower mantle are comparable to MORB, with a $\delta^7\text{Li}$ of $\sim+4\text{‰}$ (e.g., Seitz et al., 2004; Magna et al., 2006b; Jeffcoate et al., 2007). In contrast, the $\delta^7\text{Li}$ for the upper (35 ± 11 ppm and $\delta^7\text{Li} = 0 \pm 4\text{‰}$), lower and middle continental crust (~ 8 ppm and $\delta^7\text{Li} = -17.9$ to $+15.7\text{‰}$) show a wider range (e.g., Teng et al., 2004, 2008, 2009; Qiu et al., 2011a, b; Sauzeat et al., 2015). Most studies only focus on bulk mineral separate or bulk rock measurements, but it has been determined that crystals are often in disequilibrium with their host magma, with the crystals being isotopically lighter compared to their matrix, leading to a large zonation of $\delta^7\text{Li}$ within crystals (e.g., Jeffcoate et al., 2007; Parkinson et al., 2007; Weyer and Seitz, 2012). This indicates that using bulk mineral, or bulk rock, measurements may conceal additional information about the mantle and the crust that could be identified using *in situ* measurement techniques.

The lithium signature of samples from the upper crust, namely volcanic rocks, can be changed by post-eruptive processes. Ellis et al. (2018) studied eight rhyolitic ignimbrites from the Yellowstone–Snake River Plain system (USA) and determined that the lithium composition of crystals differed depending on the portion of the ignimbrite with high lithium concentrations found in the microcrystalline interior (e.g., plagioclase ranging from 35.3 to 36.8 ppm for the Tuff of Knob) and low lithium abundance in the vitrophyre (e.g., plagioclase ranging from 6.5 to 6.7 ppm for the Tuff of Knob). The authors interpreted this as lithium still being mobile in the slowly cooled part of the eruptive products and leading to the diffusion of lithium into the crystals while progressive crystallisation of the groundmass enriches the last melt pockets in lithium. They pointed out that degassing at the surface can alter the lithium abundance found in crystals and groundmass glass. Therefore, lithium concentration and isotopic composition of volcanic groundmass glass might not represent the lithium composition found in the magma chamber, which can be studied by analysing lithium composition of melt inclusions.

Only few studies published to date investigated the lithium concentration and isotopic composition of melt inclusions hosted in different minerals, and often neglected to measure the corresponding groundmass glass (e.g., Hostra et al., 2013; Lui et al., 2006; Benson et al., 2017). Data from dacitic to rhyolitic arc lavas from the island of Dominica, with glassy melt inclusions hosted in orthopyroxene and plagioclase, returned high $\delta^7\text{Li}$ values ($+4.2$ to $+11.6\text{‰}$ and $+7.4$ to $+14.7\text{‰}$, respectively) with lithium concentration between 20 to 60 ppm and groundmass glass with 19 ppm (Gurenko et al., 2005). In contrast, olivine-hosted melt inclusions from St. Vincent Island had lower lithium concentrations (2.6 to 9.2 ppm) with $\delta^7\text{Li}$ as low as -10‰ (Bouvier et al. 2008) and olivine-hosted melt inclusions from Grenada (Lesser Antilles) range from 1.1–12 ppm and $\delta^7\text{Li}$ values of -24 to $+8.2\text{‰}$ (Bouvier et al., 2010). Schiavi et al. (2012) had similar findings in olivine-hosted melt inclusions from Stromboli volcano. Rowe et al. (2008) investigated glassy melt inclusions ($+0.9$ to $+2.2\text{‰}$; corresponding amphibole-host has values ranging from -13.8 to -20.5‰) in amphibole (all measured amphiboles range from -20.4 to $+9\text{‰}$) from dacitic lava samples from Mount St. Helenes and found that the melt inclusions were isotopically heavier compared to the surrounding host-amphibole, which had heavier

rims compared to their interior. The authors explained the zonation within the amphiboles by lithium diffusion from the melt into the amphibole.

Similarly, to the lack of studies focusing on melt inclusions, studies addressing the fractionation of lithium from the fluid/melt into the vapour phase are also rare (e.g., Dubois et al., 1994; Blundy et al., 2010; Schiavi et al., 2010; Schiavi et al., 2012). Audetat et al. (1998) suggests that phase separation-induced fractionation can lead lithium to partition into vapour or brine. Experiments of Liebscher et al. (2007) focus on lithium isotopic composition of vapour and liquid at 400°C and found minor vapour–liquid fractionation. Kent et al. (2007) suggested that lithium concentration gradients in plagioclase recorded lithium transfer of exsolved brines to the upper part of the magma chamber. The study of Vlastelic et al. (2011) is the only one that measured $\delta^{7}\text{Li}$ of gas condensates (−2.8 to −1.3‰). Watson (2017) determined theoretically that ^6Li should partition into the vapour phase preferentially to ^7Li , making the vapour phase isotopically lighter compared to the melt.

1.3.1 Lithium coordination, diffusion and partition coefficients

To better understand the behaviour of lithium concentration and lithium isotopes in different minerals and melt, it is necessary to understand the site occupancy and its behaviour in the different mineral phases, fluids and melt. Lithium has a valence state of +1 and its ionic radius is 0.92 Å in eight-fold coordination, 0.76 Å in six-fold coordination and 0.59 Å in four-fold coordination (Shannon, 1976). ^7Li preferentially partitions into the site with the highest bond energy (Schauble 2004). In most minerals lithium partitions into or out of the minerals by a coupled substitution, e.g., $\text{Si}^{4+} \leftrightarrow \text{Al}^{3+} + \text{Li}^+$ (Denen, 1966; Perny et al., 1992). The bond energy for lithium depends on the coordination number (low coordination number equals high bond energy). In most minerals lithium has a six-fold coordination (e.g., in olivine, pyroxenes and biotite), with ^7Li substituting for magnesium that has a valence state of +2 (0.89 Å in octahedral coordination, 0.57 Å in tetrahedral coordination) or iron (+2; ~0.7 Å) in the octahedral coordinated sites (e.g., Li and Peacor, 1968; Robert et al., 1983; Wenger and Armbruster, 1991; Bertoldi et al., 2004). In pyroxenes and olivine, lithium can substitute for sodium (1.18 Å in octahedral coordination; Shannon 1976) and for trivalent cations, e.g. Cr^{3+} , Sc^{3+} , REE^{3+} (Grant and Wood, 2010). In plagioclase, lithium is more compatible with the albite crystal structure than with the anorthite structure, even though sodium (+1) is larger than calcium (+2). However, due to the difference in radii lithium substitution for sodium is limited (e.g., Shannon, 1976; Tomascak et al., 2016). There is only one published experimental study (Giletti and Shanahan, 1997) that focused on ^6Li diffusion in feldspar. Therefore, it is unknown if ^6Li and ^7Li diffuse differently in plagioclase and if ^6Li moves 3 to 3.5% faster than ^7Li as shown for “dry” and “wet” melt (Richter et al., 2003; Richter et al., 2006; Holycross et al., 2017). It is possible that lithium in plagioclase behaves in the same way as proven for olivine. Dohmen et al. (2010) demonstrated that the lithium diffusivity depends on the olivine-melt boundary conditions, the crystallographic axis, and the partition behaviour between the octahedral and an interstitial site. For example, olivine has a fast (interstitial site) and a slow (octahedral site) diffusion mechanism, with both operating at the same time and ^6Li moving 5% faster than ^7Li on the interstitial site. Experiments for clinopyroxene (e.g., Richter et al., 2014) found similar lithium behaviour as described for olivine (e.g., Dohmen et al., 2010).

In quartz, lithium is in either two- or four-fold coordination and preferably incorporates ^7Li (Larsen et al., 2004; Sartbaeva et al., 2004). There are two mechanisms by which lithium can diffuse and be incorporated into the crystal lattice: 1) fast diffusion of lithium in interstitials along crystallographic channels perpendicular to the c -axis, and 2) a slower diffusion process along a - and b -axis (Sartbaeva et al., 2005). Charlier et al., (2012) stated lithium diffuses up to four times faster in quartz compared to feldspar.

The coordination of lithium in minerals has an influence on the equilibrium partition coefficients (K_d) between mineral and melt (e.g., Hart and Dunn, 1993; Evensen and London, 2003; Ottolini et al., 2009), between mineral and aqueous fluid (e.g., Brenan et al., 1998b; Caciagli et al., 2011), as well as mineral and mineral (e.g., Coogan et al., 2005; Ottolini et al., 2009; Yakob et al., 2012). In general, lithium is moderately incompatible in basaltic systems (e.g., Marks et al., 2007) and partitions into aqueous fluids rather than minerals, but values for more evolved systems are scarce (e.g., Icenhower and London, 1995; Iveson et al., 2018). Available partition coefficients were determined by experiments (summarised in Tomascak et al., 2016 and Penniston-Dorland et al., 2017). In the following, only mineral-melt partition coefficients are covered as they are most relevant for this thesis.

Partition coefficients for plagioclase-melt vary from 0.09 to 0.6 as the partition coefficient of lithium in plagioclase is a function of the anorthite composition (e.g., Blundy, 1997; Bindeman et al., 1998; Coogan, 2011; Dohmen and Blundy, 2014). Olivine-melt and clinopyroxene-melt partition coefficients range from 0.01 to 1.0 and 0.02 to 1.05, respectively (e.g., Taura et al., 1998; Klemme et al., 2002; Bennett et al., 2004; Zanetti et al., 2004; Kuzyura et al., 2010; Spandler and O'Neill, 2010). In a magnesium-rich olivine the lithium concentration correlates with the Sc^{3+} and Ga^{3+} concentrations in the melt. In iron-rich olivine the lithium concentration can depend on the Fe^{3+} concentration in the olivine (Grand and Wood, 2010). In clinopyroxene the lithium concentration depends on the major element composition, e.g. the concentration of Al (e.g., Lundstrom et al., 1998; Blundy and Dalton, 2000; Hill et al., 2000). Orthopyroxenes vary from 0.13 to 0.48 (e.g., Adam and Green, 2006; Brenan et al., 1998a, b; Frei et al., 2009) and the different experiments identified that even with changing composition, temperature and pressure the variability in lithium concentration was minor compared to clinopyroxene or olivine.

1.3.2 . Geospeedometry

Lithium geospeedometry has been established as a useful tool to study processes that occur over short-time scales (e.g., Coogan et al., 2005; Beck et al., 2006; Jeffcoate et al., 2007; Parkinson et al., 2007; Charlier et al., 2012; Richter et al., 2016). The increase of this application is due to the improvement of *in situ* measurement techniques and the increasing amount of available reference standards.

Geospeedometry uses equilibrium partitioning of lithium and its isotopes between minerals, within minerals or mineral and their associated melt to estimate time scales of geological processes, e.g. cooling rates of the oceanic crust (e.g., Coogan et al., 2005). The lithium concentration and isotope profiles used for geospeedometry can form under different conditions, e.g., lithium isotopes can be fractionated through kinetic fractionation (e.g., Lundstrom et al., 2005). Studies have shown that minerals reflect isotopic disequilibrium between coexisting phases, indicating kinetic fractionation (e.g., Teng et al., 2006; Liu et al., 2010; Ireland and Penniston-Dorland, 2015). This disequilibrium can form due to

lithium diffusing into or out of the minerals at their grain boundary (e.g., Jeffcoate et al., 2007; Rudnick and Ionov, 2007) or by diffusion exchange between minerals due to a change in partition coefficients during cooling (e.g., Ionov and Seitz, 2008; Kaliwoda et al., 2008; Gao et al., 2011).

Coogan et al. (2005) experimentally calibrated a Li-geospeedometer by determining the partition behaviour of Li between plagioclase and clinopyroxene. The geospeedometer depends on temperature and it establishes that Li favours clinopyroxene with decreasing temperature. Coogan et al. (2005) then concluded that this can be used as a geospeedometer as the diffusivity depends on the cooling rate of the solid. Solid phases that cool rapidly are favoured over solids that cool over long periods of time, as their original diffusion profile can be overprinted. Geospeedometry is applied to lithium concentration zoning in different minerals to determine, for example, the time scales of degassing (e.g., Charlier et al., 2012). Parkinson et al. (2007) studied lithium concentration and lithium isotopic composition of zoned olivine and pyroxene from arc lavas (New Georgia Group in the Solomon Islands) and showed that the $\delta^7\text{Li}$ composition overprinted the major element zonation with low $\delta^7\text{Li}$ in the rims and high $\delta^7\text{Li}$ in the cores. The time scales estimated by Mg-Fe diffusion and lithium geospeedometry showed that lithium diffuses at the same rate as Mg-Fe in olivine and lithium diffuses faster in clinopyroxene compared to olivine. The authors point out that crystals of porphyritic lavas are not suitable to study mantle processes and any primary $\delta^7\text{Li}$ signal within clinopyroxenes and olivine will be overprinted during melt migration and might not capture the primary signal. Gallagher and Elliott (2009) tested with a quantitative model if the $\delta^7\text{Li}$ diffusion profiles of a clinopyroxene phenocryst presented by Jeffcoate et al. (2007) could be reproduced by just assuming a natural cooling history of the lavas. Their calculations proved that the $\delta^7\text{Li}$ diffusion profiles are a consequence of the cooling history of the lavas and this kind of profile can be used for geospeedometry. Additionally, they concluded that $\delta^7\text{Li}$ diffusion profiles deviating from the one shown in Jeffcoate et al. (2007) and can have different and more complex cooling histories.

1.3.3 Lithium as a resource

Lithium is considered a rare element as its concentration in the upper crust is low (e.g., Teng et al., 2004; Teng et al., 2009; Sauzeat et al., 2015). Until the early 1990s, lithium was mined mostly from



Fig. 1.2: Map showing economically important lithium deposits with pegmatites in squares, brines as crosses and rectangles highlighting the distribution of salars (from Kesler et al., 2012).

minerals like spodumene, but, since the late 1990s, processing of brines has increased (e.g., USGS, 2009; Hostra et al., 2013). Different countries consider lithium as an energy-critical and technologically important element (e.g., Chakhmouradian et al., 2015). The classification is based on the increase of the use of lithium as a resource, e.g., for Li-ion rechargeable batteries (e.g., Jaskula, 2012) in portable electronic devices, electrical power grid, hybrid and electric cars, wind and solar energy plants (e.g., Grosjean et al., 2012) and in ceramics, glass, lubricants, light-weight alloys, and pharmaceutical products (e.g., Kesler et al., 2012; Jaskula, 2012; Vikström et al., 2013). The current demand for lithium is small, with 32.5 kilotons (kt) per year but is predicted to go up to 3 to 35 megatons (Mt) in 2050 (Jaskula, 2016). Most of the lithium is currently produced by Australia, China and Chile (e.g., Jaskula, 2016).

Extractable lithium can be found in 1) pegmatites 2) continental brines and 3) “unusual deposits” (Kesler et al., 2012; Fig. 1.2). To meet the new lithium demands of the market, understanding the formation and origin of these deposits is economically important. Forty percent of the global lithium extraction comes from pegmatite deposits and about 60 percent come from brine deposits (e.g., Jaskula, 2016). Lithium is used by industry in mineral form (e.g., spodumene $[\text{LiAlSi}_2\text{O}_6]$, petalite $[\text{LiAlSi}_4\text{O}_{10}]$ and lepidolite), but extracted as its chemical compounds (Li_2CO_3 , LiCl , LiBr and LiOH) from the minerals found in pegmatites or precipitated from brines (e.g., Ebensperger et al., 2005; Kesler et al., 2012).

Pegmatites are relatively common, but rare metal pegmatites (0.1% of the total) and lithium-rich pegmatites are limited (Laznicka, 2006). Lithium-rich pegmatites are often enriched in other rare elements, e.g. tin, beryllium and tantalum–niobium (Kesler et al., 2012). Pegmatites that are zoned often have large minerals enriched in lithium, e.g., in Namibia, U.S.A. and Canada (Kesler et al., 2012). The melt, forming pegmatites, could originate from lithium-rich sediments or strong differentiation of low-calcium granites (e.g., London, 2008a, b; Norton, 1977, Stewart, 1978). London (2017) states that Li-rich pegmatites can originate from sediments that accumulated in ocean basins, which later, due to metamorphism, are melting and release Li into the melt (Kesler, 2012).

One of the economically important pegmatite deposits is Kings Mountain pegmatite belt in North Carolina and South Carolina (USA). The pegmatites found in the Kings Mountain pegmatite belt are homogeneous and produce 0.32 Mt lithium per year at the Kings Mountain deposit and 0.42 Mt lithium per year at the Bessemer City deposit (Kesler, 1978). Another important pegmatite is the Tanco deposit (Bernic Lake, Manitoba), which produces 0.14 Mt lithium per year (Kesler, 2012).

Brine deposits are enclosed basins with lacustrine evaporates. Economically important deposits of this type, which are more enriched in lithium compared to marine evaporites, are found in Chile, Argentina and China (Kesler, 2012). The current theory for the formation of lithium-rich brines is that lithium is leached from rhyolitic tuffs and lavas by hydrothermal fluids and meteoric water and bound to secondary clay minerals that are deposited in basins close to the source rocks (e.g., Ide and Kunasz, 1989; Zheng and Liu, 2009; Lowenstein and Risacher, 2009). Garrett (2004) stated that lithium can only be leached from rocks and minerals at temperatures over 300–350 °C.

The Andean salars, located in Bolivia, Argentina and Chile, have waters and brines that are enriched in lithium with concentrations of several grams per litre (e.g., Moraga et al., 1974; Ericksen et al., 1978; Risacher and Fritz, 1991). Salar de Atacama in Chile (3000 km²) is the brine that economically produces the highest amount of lithium, with lithium concentration of over 4000 ppm

(Garrett, 2004; Lowenstein and Risacher, 2009; Kesler et al., 2012). The Salar de Hombre Muerto (Argentina) has lithium concentrations ranging from 220 to 1000 ppm, which supports the idea that there is a shallow lithium-brine aquifer present (Garrett, 2004). Risacher and Frith (2009) determined that lithium concentration in spring waters and ground waters of Andean salars is not a function of their temperature, leading them to conclude that hydrothermal alteration is not solely responsible for the enrichment of lithium in brines and waters of the Andean salars.

Other “unusual” lithium-rich deposits form due to the interaction between clastic sedimentary or volcanic material and hydrothermal solutions or evaporative brines (Kesler et al., 2012). One example is King Valley/McDermitt (Nevada, USA) with lithium-rich smectite clay hectorite layers (Castor and Henry, 2020), which are clay minerals that form due to the hydrothermal alteration of volcanic ash by fluids (Kesler et., 2012). This deposit produces around 2 megatons per year (Benson et al., 2017).

1.4 Geological background

The Yellowstone Volcanic Field (USA; Idaho - Montana - Wyoming) is located at the northern end of the Snake River Plain hotspot track (USA) and represents the current location of a continental hotspot. Three of the largest caldera forming eruptions in the Quaternary have taken place in this volcanic field (e.g., Christiansen, 2001; Selten et al., 2018). The first and largest one was Huckleberry Ridge Tuff (HRT, 2.08 Ma; Rivera et al., 2014; Singer et al., 2014) forming the Island Park Caldera. The second one was Mesa Falls Tuff (MFT, 1.30 Ma; Rivera et al., 2016) producing the Henry’s Fork Caldera. The youngest of the three caldera forming eruptions is Lava Creek Tuff (LCT; 0.63 Ma; Matthews et al., 2015), which formed the Yellowstone Caldera. These calderas formed in three cycles and ~6500 km² of material has been erupted in the Yellowstone Volcanic Field over this period of these three cycles. Rhyolite flows and basalts predating and postdating the caldera forming eruptions (Christiansen et al., 2007; Rivera et al., 2016) represent the larger part of the volcanism (~2.1 Myr; e.g., Christiansen, 2001) at the Yellowstone Volcanic Field (Christiansen, 2001).

The Huckleberry Ridge Tuff was the most voluminous eruption (~2500 km³; Christiansen, 2001) of the three eruptions within the Yellowstone Volcanic Field. It is considered as a single eruptive event but is split into three members (A, B, C; Christiansen & Blank, 1972; Christiansen, 2001). All three members consist of quartz, sanidine, plagioclase, titanium oxides, clinopyroxene, and accessory phases with different abundance and grain size between the different members (Christiansen, 2001).

The Mesa Falls Tuff was part of the second cycle and forms the Henry’s Fork caldera in the Island Park (Idaho, USA). MFT is a single eruption unit. It has a thick ash and pumice deposit at its base with large pumice blocks (up to 30 cm in diameter) (Christiansen, 2001; Rivera et al., 2016). Below this base are several rhyolite flows (Christiansen, 2001). The upper part of MFT are welded ash flows (Rivera et al., 2016). MFT consists of quartz, plagioclase, sanidine, orthopyroxene, clinopyroxene, olivine, and accessory phases.

Lava Creek Tuff was part of the third cycle and represents the youngest caldera forming eruption (> 1000 km³; Christiansen, 2001). LCT has two ignimbrite members (A and B) but they are believed to belong to one cooling unit as significant stratigraphic gaps are missing. The two members vary in welding and crystal content (Christiansen, 2001). Both members consist of sanidine, quartz, magnetite, ilmenite, fayalite and zircon. Only member A has amphibole present.

1.5 References

- Adam, J., Green, T. (2006) Trace element partitioning between mica- and amphibole-bearing garnet lherzolite and hydrous basanitic melt: 1. Experimental results and the investigation of controls on partitioning behaviour. *Contributions to Mineralogy and Petrology*, 152, 1–17.
- Audétat, A., Günther, D., Heinrich, C.A. (1998) Formation of a magmatic-hydrothermal ore deposit: insights with LA-ICP-MS analysis of fluid inclusions. *Science*, 279, 2091–2094.
- Bachmann, O., Dungan, M. A., Lipman, P. W. (2002). The Fish Canyon magma body, San Juan Volcanic Field, Colorado: rejuvenation and eruption of an upper-crustal batholith. *Journal of Petrology*, 43, 1469–1503.
- Bennett, S., Blundy, J., Elliott, J. (2004) The effect of sodium and titanium on crystal-melt partitioning of trace elements. *Geochimica et Cosmochimica Acta*, 68, 2335–2347.
- Benson, T. R., Coble, M. A., Rytuba, J. J., Mahood, G. A. (2017) Lithium enrichment in intracontinental rhyolite magmas leads to Li deposits in caldera basins. *Nature Communications*, 8, 270.
- Bertoldi, C., Proyer, A., Garbe-Schonberg, D., Behrens, H., Dachs, E. (2004) Comprehensive chemical analyses of natural cordierites: implications for exchange mechanisms. *Lithos*, 78, 389–409.
- Bigeleisen, J. (1949) The relative velocities of isotopic molecules. *The Journal of Chemical Physics*, 17, 675–678.
- Bindeman, I. N., Davis, A. M., Drake, M. J. (1998) Ion microprobe study of plagioclase-basalt partition experiments at natural concentration level of trace elements. *Geochimica et Cosmochimica Acta*, 62, 1175–1193.
- Blundy, J. (1997) Experimental study of a Kiglapait marginal rock and implications for trace element partitioning in layered intrusions. *Chemical Geology*, 141, 73–92.
- Blundy, J. D., Robinson, J. A. C., Wood, B. J. (1998) Heavy REE are compatible in clinopyroxene on the spinel lherzolite solidus. *Earth and Planetary Science Letters*. 160, 493–504.
- Blundy, J., Dalton, J. (2000) Experimental comparison of trace element partitioning between clinopyroxene and melt in carbonate and silicate systems, and implications for mantle metasomatism. *Contributions to Mineralogy and Petrology*, 139, 356–371.
- Blundy, J., Cashman, K. V., Rust, A., Witham, F. (2010) A case for CO₂-rich arc magmas. *Earth and Planetary Sciences Letters*, 290, 289–301.
- Bouman, C., Elliott T., Vroon, P. Z. (2004) Lithium inputs to subduction zones. *Chemical Geology*, 212, 59–79.
- Bouvier, A.-S., Métrich, N., Deloule, E. (2008) Slab-derived fluids in magma sources of St. Vincent (Lesser Antilles Arc): volatile and light element imprints. *Journal of Petrology*, 49, 1427–1448.
- Bouvier, A.-S., Métrich, N., Deloule, E. (2010) Light elements, volatiles, and stable isotopes in basaltic melt inclusions from Grenada, Lesser Antilles: Inferences for magma genesis. *Geochemistry, Geophysics, Geosystems*, 11 (9).
- Brenan, J. M., Neroda, E., Lundstrom, C. C., Shaw, H. F., Ryerson, F. J., Phinney, D. L. (1998a) Behaviour of boron, beryllium, and lithium during melting and crystallization: Constraints from mineral–melt partitioning experiments. *Geochimica et Cosmochimica Acta*, 62, 2129–2141.
- Brenan J. M., Ryerson F. J., Shaw H. F. (1998b) The role of aqueous fluids in the slab-to-mantle transfer of boron, beryllium, and lithium during subduction: Experiments and models. *Geochimica et Cosmochimica Acta*, 62 (19-20), 3337–3347.
- Bryant, C. J., Chappell B. W., V. C. Bennett, M. T. McCulloch (2004), Lithium isotopic compositions of the New England Batholith: Correlations with inferred source rock compositions. *Transactions of the Royal Society of Edinburgh: Earth Sciences*, 95, 199–214.
- Caciagli-Warman N. (2010) Experimental constraints on lithium exchange between clinopyroxene, olivine and aqueous fluid at high pressures and temperatures (Ph.D. thesis). Univ. Toronto, Toronto, Canada.
- Caciagli, N., Brenan, J. M., McDonough, W. F., Phinney, D. (2011) Mineral- fluid partitioning of lithium and implications for slab-mantle interaction. *Chemical Geology*, 280, 384–398.
- Castor, S. B.; Henry, C. D. (2020) Lithium-Rich Claystone in the McDermitt Caldera, Nevada, USA: Geologic, Mineralogical, and Geochemical Characteristics and Possible Origin. *Minerals*, 10, 68.
- Chakmouradian, A. R., Smith, M. P., Kynicky, J. (2015) From ‘strategic’ tungsten to ‘green’ neodymium: a century of critical metals at a glance. *Ore Geology Reviews*, 64, 455–458.
- Chakraborty, S. (2008) Diffusion in solid silicates: a tool to track timescales of processes comes of age. *Earth and Planetary Science Letters*, 36,153–190.
- Chan, L. H., Edmond, J.M. (1988) Variation of lithium isotope composition in the marine environment: a preliminary report. *Geochimica et Cosmochimica Acta*, 52, 1711–1717.

- Chan, L. H., Edmond, J. M., Thompson, G., Gillis, K. (1992) Lithium isotope composition of submarine basalts—Implications for the lithium cycle in the oceans. *Earth and Planetary Science Letters*, 108, 151–160.
- Chan, L. H., Edmond, J. M., Thompson, G. (1993) A lithium isotope study of hot springs and metabasalts from Mid-Ocean Ridge Hydrothermal Systems. *Journal of Geophysical Research: Solid Earth*, 98 (B6), 9653–9659.
- Chan, L. H., Frey, F. A. (2003) Lithium isotope geochemistry of the Hawaiian plume: Results from the Hawaii Scientific Drilling Project and Koolau Volcano. *Geochemistry, Geophysics, Geosystems*, 4 (3), 8707.
- Chan, L. H., Gieskes, J. M., You, C. F., Edmond, J. M. (1994) Lithium isotope geochemistry of sediments and hydrothermal fluids of the Guaymas Basin, Gulf of California. *Geochimica et Cosmochimica Acta*, 58, 4443–4454.
- Chan L.-H., Kastner M. (2000) Lithium isotopic compositions of pore fluids and sediments in the Costa Rica subduction zone: implications for fluid processes and sediment contribution to the arc volcanoes. *Earth and Planetary Science Letters*, 183 (1-2), 275–290.
- Chan, L. H., Leeman, W.P., You, C. F. (2002) Lithium isotopic composition of Central American volcanic arc lavas: implications for modification of subarc mantle by slab-derived fluids: correction. *Chemical Geology*, 182, 293–300.
- Charlier, B. L. A., Morgan, D. J., Wilson, C. J. N., Wooden, J. L., Allan, A. S. R., Baker, J. A. (2012) Lithium concentration gradients in feldspar and quartz record the final minutes of magma ascent in an explosive supereruption. *Earth and Planetary Science Letters*, 319 – 320, 218–227.
- Chopra, R., Richter, F. M., Watson, E. B., Scullard, C. R. (2012) Magnesium isotope fractionation by chemical diffusion in natural settings and in laboratory analogues. *Geochimica et Cosmochimica Acta*, 88, 1–18.
- Christiansen, R.L., 2001. The Quaternary and Pliocene Yellowstone Plateau Volcanic Field of Wyoming, Idaho, and Montana. US Geological Survey (Professional Paper 729-G).
- Christiansen, R. L., Blank, R.Jr (1972). Volcanic stratigraphy of the Quaternary rhyolite plateau in Yellowstone National Park. US Geological Survey, Professional Papers 729-B.
- Christiansen, R. L., Lowenstern, J. B., Smith, R. B., Heasler, H., Morgan, L. A., Nathenson, M., Mastin, L. G., Muffler, L. J. P., Robinson, J. E. (2007). Preliminary assessment of volcanic and hydrothermal hazards in Yellowstone National Park and vicinity. US Geological Survey, Open-file Report, 2007-1071.
- Coogan, L. A., Kasemann, S. A., Chakraborty, S. (2005) Rates of hydrothermal cooling of new oceanic upper crust derived from lithium-geospeedometry. *Earth and Planetary Science Letters*, 240, 415–424.
- Coogan, L. A. (2011) Preliminary experimental determination of the partitioning of lithium between plagioclase crystals of different anorthite contents. *Lithos*, 125, 711–715.
- Denen, W. H. (1966) Stoichiometric substitution in natural quartz. *Geochimica et Cosmochimica Acta*, 30, 1235–1241.
- Dohmen, R., Kasemann, S. A., Coogan, L. A., Chakraborty, S. (2010) Diffusion of Li in olivine. Part 1: Experimental observations and a multiple species diffusion model. *Geochimica et Cosmochimica Acta*, 74, 274–292.
- Dohmen, R., Blundy, J. (2014) A predictive thermodynamic model for element partitioning between plagioclase and melt as a function of pressure, temperature and composition. *American Journal of Science*, 314, 1319–1372.
- Dubois, M., Weisbrod, A., Shtuka, A. (1994) Experimental determination of the two-phase (liquid and vapour) region in water-alkali chloride binary systems at 500° and 600°C using synthetic fluid inclusions. *Chemical Geology*, 115, 227–38.
- Ebensperger, A., Maxwell, P., Moscoso, C. (2005) The lithium industry: its recent evolution and future prospects. *Resources Policy*, 30, 218–231.
- Edmond J. M., Measures C., McDuff R. E., Chan L. H., Collier R., Grant B., Gordon L. I., Corliss J. B. (1979) Ridge Crest Hydrothermal Activity and the Balances of the Major and Minor Elements in the Ocean - Galapagos Data. *Earth and Planetary Science Letters*, 46 (1), 1–18.
- Elliott, T., Thomas, A., Jeffcoate, A., Niu, Y.L. (2006) Lithium isotope evidence for subduction-enriched mantle in the source of mid-ocean-ridge basalts. *Nature*, 443, 565–568.
- Ellis, B.S., Szymanowski, D., Magna, T., J. Neukampf, Dohmen, R., Bachmann, O., Ulmer, P., Guillong, M. (2018) Post-eruptive mobility of lithium in volcanic rocks. *Nature Communications*, 9, 3228.
- Ericksen, G. E., Salas, R. (1987) Geology and resources of salars in the central Andes. Houston, Texas, Circum-Pacific Council for Energy and Mineral Resources Earth Science Series, 88–210, 51.
- Evensen, J. M., London, D. (2003) Experimental partitioning of Be, Cs, and other trace elements between cordierite and felsic melt, and the chemical signature of S-type granite. *Contributions to Mineralogy and Petrology*, 144, 739–757.

- Flesch, G. D., Anderson, Jr., A. R., Svec, H. J. (1973) A secondary isotopic standard for $^6\text{Li}/^7\text{Li}$ determination, *International Journal of Mass Spectrometry and Ion Physics*, 12, 265–272.
- Frei, D., Liebscher, A., Franz, G., Wunder, B., Klemme, S., Blundy, J. (2009) Trace element partitioning between orthopyroxene and anhydrous silicate melt on the Iherzolite solidus from 1.1 to 3.2 GPa and 1,230 to 1,535 degrees C in the model system $\text{Na}_2\text{O}-\text{CaO}-\text{MgO}-\text{Al}_2\text{O}_3-\text{SiO}_2$. *Contributions to Mineralogy and Petrology*, 157, 473 – 490.
- Garrett, D. E. (2004) *Handbook of Lithium and Natural Calcium Chloride*. Elsevier, Amsterdam.
- Giletti, B. J., Shanahan, T. M. (1997) Alkali diffusion in plagioclase feldspar. *Chemical Geology*, 139, 3–20.
- Gao, Y., Snow, J. E., Casey, J. F., Yu, J. (2011) Cooling-induced fractionation of mantle Li isotopes from the ultraslow-spreading Gakkel Ridge. *Earth and Planetary Science Letters*, 301, 231–240.
- Godfrey, L. V., Chan, L. H., Alonso, R. N., Lowenstein, T. K., McDonough, W. F., Houston, J., Li, J., Bobst, A., Jordan, T. E. (2013) The role of climate in the accumulation of lithium-rich brine in the Central Andes. *Applied Geochemistry*, 38, 92–102.
- Grosjean, C., Miranda, P. H., Perrin, M., Poggi, P. (2012) Assessment of world lithium resources and consequences of their geographic distribution on the expected development of the electric vehicle industry. *Renewable and Sustainable Energy Reviews*, 16, 1735–1744.
- Grant, K.J., Wood, B.J. (2010) Experimental study of the incorporation of Li, Sc, Al and other trace elements into olivine. *Geochimica et Cosmochimica Acta*, 74, 2412–2428.
- Gurenko, A. A., Trumbull, R. B., Thomas, R., Lindsay, J. M. (2005) A melt inclusion record of volatiles, trace elements and Li – B isotope variations in a single magma system from the Plat Pays Volcanic Complex, Dominica, Lesser Antilles. *Journal of Petrology*, 46, 2495–2526.
- Hacini, M., Kherici, N., Oelkers, E. H. (2008) Mineral precipitation rates during the complete evaporation of Merouane Chott ephemeral lake. *Geochimica et Cosmochimica Acta*, 72, 1583–1597.
- Hart, S. R., Dunn, T. (1993) Experimental cpx/melt partitioning of 24 trace elements. *Contributions to Mineralogy and Petrology*, 113, 1–8.
- Hildreth, W., Wilson, C. J. N. (2007). Compositional zoning of the Bishop Tuff. *Journal of Petrology*, 48, 951–999.
- Hill, E., Wood, B., Blundy, J. (2000) The effect of Ca-Tschermaks component on trace element partitioning between clinopyroxene and silicate melt. *Lithos*, 53, 203–215.
- Hofstra, A. H., Todorov, T. I., Mercer, C. N., Adams, D. T., Marsh, E. E. (2013) Silicate Melt Inclusion Evidence for Extreme Pre-eruptive Enrichment and Post-eruptive Depletion of Lithium in Silicic Volcanic Rocks of the Western United States: Implications for the Origin of Lithium-Rich Brines. *Economic Geology*, 108, 1691-1701.
- Holycross, M. E., Watson, E. B., Richter, F. M., Villeneuve, J. (2018) Diffusive fractionation of Li isotopes in wet, silicic melts. *Geochemical Perspectives Letters*, 6, 39–42.
- Huh, Y., Chan, L. H., Zhang, L., Edmond, J. M. (1998) Lithium and its isotopes in major world rivers: Implications for weathering and the oceanic budget. *Geochimica et Cosmochimica Acta*, 62, 2039–2051.
- Icenhower, J., London, D. (1995) An experimental study of element partitioning among biotite, muscovite, and coexisting peraluminous silicic melt at 200 MPa (H_2O). *American Mineralogist*, 80, 1229–1251.
- Ide, F., Kunasz, I. A. (1989) Origin of lithium in Salar de Atacama, northern Chile G.E. in Ericksen, M.T. Cañas Pinochet, J.A. Reinemund (Eds.), *Geology of the Andes and Its Relation to Hydrocarbon and Mineral Resources, Circum-Pacific Council for Energy and Mineral Resources Earth Science Series*, 11, 165–172.
- Ireland, R. H. P., Penniston-Dorland, S. C. (2015) Chemical interactions between a sedimentary diapir and surrounding magma: Evidence from the Phepane Dome and Bushveld Complex, South Africa. *American Mineralogist*, 100, 1985–2000.
- Ionov, D. A., Seitz, H.-M. (2008) Lithium abundances and isotopic compositions in mantle xenoliths from subduction and intra-plate settings: mantle sources vs. eruption histories. *Earth and Planetary Science Letters*, 266, 316–331.
- Iveson, A. A., Rowe, M. C., Webster, J. D., Neill, O. K. (2018). Amphibole-, Clinopyroxene- and Plagioclase-Melt Partitioning of Trace and Economic Metals in Halogen-Bearing Rhyodacitic Melts. *Journal of Petrology*, 59 (8), 1579–1604.
- Jambon, A., Semet, M.P. (1978) Lithium diffusion in silicate glasses of albite, orthoclase and obsidian composition: an ion-microprobe determination. *Earth and Planetary Science Letters*, 37, 445–450.
- Jaskula B.W. (2012) Lithium. *Mineral Commodities Summaries*, U.S. Geological Survey, Reston, Virginia.
- Jaskula, B. W. (2016) Lithium. *U.S. Geological Survey Mineral Commodity Summaries 100–101 (USGS)*.
- Jeffcoate, A. B., Elliott, T., Kasemann, S. A., Ionov, D., Cooper, K., Brooker, R. (2007) Li isotope fractionation in peridotites and mafic melts. *Geochimica et Cosmochimica Acta*, 71, 202–218.

- Kaliwoda, M., Ludwig, T., Altherr, R. (2008) A new SIMS study of Li, Be, B and $\delta^7\text{Li}$ in mantle xenoliths from Harrat Uwayrid (Saudi Arabia). *Lithos* 106, 261–279.
- Kent, A. J. R., Blundy, J., Cashman, K., Cooper, K. M., Donnelly, C., Pallister, J. S., Reagan, M., Rowe, M. C., Thornber, C. R. (2007) Vapor transport prior to the October 2004 eruption of Mount St. Helens, Washington. *Geology*, 35, 231–235.
- Kesler, T.L. (1978) Raw lithium supplies. *Mining Engineering*, 283–285.
- Kesler, S. E., Gruber, P. W., Medina, P. A., Keoleian, G. A., Everson, M. P., Wallington, T. J. (2012). Global lithium resources: Relative importance of pegmatite, brine and other deposits. *Ore Geology Reviews*, 48, 55–69.
- Kieffer, S. W. (1982) Thermodynamics and lattice vibrations of minerals: 5. Applications to phase equilibria, isotopic fractionation, and high-pressure thermodynamic properties. *Reviews of Geophysics*, 20, 827–849.
- Klemme, S., Blundy, J. D., Wood, B. J. (2002) Experimental constraints on major and trace element partitioning during partial melting of eclogite. *Geochimica et Cosmochimica Acta*, 66, 3109–3123.
- Kuzyura, A. V., Wall, F., Jeffries, T., Litvin, YuA. (2010) Partitioning of trace elements between garnet, clinopyroxene and diamond-forming carbonate-silicate melt at 7 GPa. *Mineralogical Magazine*, 74, 227–239.
- Larsen, R. B., Henderson, I., Ihlen, P. M., Jacamon, F. (2004) Distribution and petrogenetic behaviour of trace elements in granitic pegmatite quartz from South Norway. *Contributions to Mineralogy and Petrology*, 147, 615–628.
- Leeman, W. P., Tonarini, S., Chan, L. H., Borg, L. E. (2004) Boron and lithium isotopic variations in a hot subduction zone—The southern Washington Cascades. *Chemical Geology*, 212, 101–124.
- Li, C. T., Peacor, D. R. (1968) Crystal structure of $\text{LiAlSi}_2\text{O}_6$ -II (beta spodumene). *Zeitschrift für Kristallographie - Crystalline Materials*, 126, 46–65.
- Liebscher, A., Meixner, A., Romer, R. L., Heinrich, W. (2007) Experimental calibration of the vapour–liquid phase relations and lithium isotope fractionation in the system H_2O – LiCl at 400 °C / 20–28 MPa. *Geofluids* 7, 369–375.
- Lindemann, F. A. (1919) Note of the vapor pressure and affinity of isotopes. *The London, Edinburgh, and Dublin Philosophical Magazine and Journal of Science*, 38, 173–181.
- Lindemann, F. A., Aston, F. W. (1919) The possibility of separating isotopes. *The London, Edinburgh, and Dublin Philosophical Magazine and Journal of Science*, 37, 523–535.
- Liu, X. M., Rudnick, R. L., Hier-Majumder, S., Sirbescu, M. L. C. (2010) Processes controlling lithium isotopic distribution in contact aureoles: A case study of the Florence County pegmatites, Wisconsin. *Geochemistry, Geophysics, Geosystems*, 11 (8), Q08014.
- Liu, X. M., Rudnick, R. L. (2011) Constraints on continental crustal mass loss via chemical weathering using lithium and its isotopes. *Proceedings of the National Academy of Sciences of the United States of America*, 108, 20873–20880.
- Liu, X. M., Wanner, C., Rudnick, R. L., McDonough, W. F. (2015) Processes controlling $\delta^7\text{Li}$ in rivers illuminated by study of streams and groundwaters draining basalts. *Earth and Planetary Science Letters*, 409, 212–224.
- Liu, Y., Anderson, A. T., Wilson, C. J. N., Davis, A. M., Steele, I. M. (2006) Mixing and differentiation in the Oruanui rhyolitic magma, Taupo, New Zealand: evidence from volatiles and trace elements in melt inclusions. *Contributions to Mineralogy and Petrology*, 151, 71–87.
- London, D. (2008a) Pegmatites. *Mineralogical Association of Canada, Special Publication*, Quebec, 10, 347.
- London, D. (2008b) The transition from granite to pegmatite. *Joint Meeting of the Geological Society America. Abstr. Programs*, 40 (6), 336.
- London, D. (2017) Reading Pegmatites: Part 3—What Lithium Minerals Say. *Rocks & Minerals*, 92 (2), 144–157.
- Lowenstein, T., Risacher, F. (2009) Closed basin brine evolution and the influence of Ca–Cl inflow waters. Death Valley and Bristol Dry Lake, California, Qaidam Basin, China, and Salar de Atacama, Chile. *Aquatic Geochemistry*, 15, 71–94.
- Lundstrom, C. C., Shaw, H. F., Ryerson, F. J., Williams, Q., Gill, J. (1998) Crystal chemical control of clinopyroxene-melt partitioning in the Di-Ab-An system: implications for elemental fractionations in the depleted mantle. *Geochimica et Cosmochimica Acta*, 62, 2849–2862.
- Magna, T., Wiechert, U., Grove, T. L., Halliday, A. N. (2006a) Lithium isotope fractionation in the southern Cascadia subduction zone. *Earth and Planetary Science Letters*, 250, 428–443.
- Magna, T., Wiechert, U., Halliday, A. N. (2006b) New constraints on the lithium isotope compositions of the Moon and terrestrial planets. *Earth and Planetary Science Letters*, 243, 336–353.

- Marks, M. A. W., Rudnick, R. L., McCammon, C., Vennemann, T., Markl, G. (2007) Arrested kinetic Li isotope fractionation at the margin of the Llimaussaq complex, South Greenland: Evidence for open-system processes during final cooling of peralkaline igneous rocks. *Chemical Geology*, 246, 207–230.
- Marschall, H. R., Altherr, R., Ludwig, T., Kalt, A., Gmeling, K., Kasztovszky, Z. (2006) Partitioning and budget of Li, Be and B in high-pressure metamorphic rocks. *Geochimica et Cosmochimica Acta*, 70, 4750–4769.
- Matsui, Y., Onuma, N., Nagasawa, H., Higuchi, H., Banno, S. (1977) Crystal structure control in trace element partition between crystal and magma. *Bulletin de Minéralogie*, 100, 315–324.
- Matthews, N. E., Vazquez, J. A., Calvert, A. (2015). Age of the Lava Creek supereruption and magma chamber assembly at Yellowstone based on $^{40}\text{Ar}/^{39}\text{Ar}$ and U–Pb dating of sanidine and zircon crystals. *Geochemistry, Geophysics, Geosystems*, 16, doi:10.1002/2015GC005881.
- Millot, R., Guerrot, C., Vigier, N. (2004) Accurate and high-precision measurement of lithium isotopes in two reference materials by MC-ICP-MS. *Geostandards and Geoanalytical Research*, 28, 153–159.
- Millot, R., Negrel, P. (2007) Multi-isotopic tracing ($\delta^7\text{Li}$, $\delta^{11}\text{B}$, $^{87}\text{Sr}/^{86}\text{Sr}$) and chemical geothermometry: evidence from hydro-geothermal systems in France. *Chemical Geology*, 244, 664–678.
- Millot, R., Scaillet, B., Sanjuan, B. (2010) Lithium isotopes in island arc geothermal systems: Guadeloupe, Martinique (French West Indies) and experimental approach. *Geochimica et Cosmochimica Acta*, 74, 1852–1871.
- Millot, R., Hegan, A., Negrel, P. (2012) Geothermal waters from the Taupo Volcanic Zone, New Zealand: Li, B and Sr isotopes characterization. *Applied Geochemistry*, 27, 677–688.
- Misra, S., Froelich, P.N. (2012) Lithium isotope history of Cenozoic seawater: changes in silicate weathering and reverse weathering. *Science*, 335, 818–823.
- Moraga, A., Chong, G., Fortt, M. A., Henriquez, H. (1974) Estudio geológico del salar de Atacama, Provincia de Antofagasta Boletín del Instituto de Investigaciones Geológicas, Santiago, Chile, 29, 56.
- Moriguti, T., Nakamura, E. (1998) Across-arc variation of Li isotopes in lavas and implications for crust/mantle recycling at subduction zones. *Earth and Planetary Science Letters*, 163, 167–174.
- Moriguti, T., Shibata, T., Nakamura, E. (2004) Lithium, boron and lead isotope and trace element systematics of Quaternary basaltic volcanic rocks in northeastern Japan: Mineralogical controls on slab-derived fluid composition. *Chemical Geology*, 212, 81–100.
- Negrel, P., Millot, R., Brenot, A., Bertin, C. (2010) Lithium isotopes as tracers of groundwater circulation in a peat land. *Chemical Geology*, 276, 119–127.
- Negrel, P., Millot, R., Guerrot, C., Petelet-Giraud, E., Brenot, A., Malcuit, E. (2012) Heterogeneities and interconnections in groundwaters: Coupled B, Li and stable-isotope variations in a large aquifer system (Eocene Sand aquifer, Southwestern France). *Chemical Geology*, 296, 83–95.
- Niu, Y. L., Collerson, K. D., Batiza, R., Wendt, J. I., Regelous, M. (1999) Origin of enriched-type mid-ocean ridge basalt at ridges far from mantle plumes: The East Pacific Rise at $11^\circ 20'$ N. *Journal of Geophysical Research Solid Earth*, 104 (B4), 7067–7087.
- Norton, J. J. (1977) Lithium, cesium and rubidium — the rare alkali metals. *Geological Survey Professional Paper*, 820, 365–378.
- Ottolini, L., Laporte, D., Raffone, N., Devidal, J. L., Le Fevre, B. (2009) New experimental determination of Li and B partition coefficients during upper mantle partial melting. *Contributions to Mineralogy and Petrology*, 157, 313–325.
- Parkinson, I. J., Hammond, S. J., James, R. H., Rogers, N. W. (2007) High-temperature lithium isotope fractionation: Insights from lithium isotope diffusion in magmatic systems. *Earth and Planetary Science Letters*, 257, 609–621.
- Patterson, J. (2009) Fracture mechanics and geochemical factors influencing the emplacement mechanisms of the Stewart Lithia gem bearing granitic pegmatite, Pala District, San Diego County, California. Ph.D. dissertation. University of Calgary, 531.
- Penniston-Dorland, S., Liu, X.M., Rudnick, R.L. (2017) Lithium isotope geochemistry. *Reviews in Mineralogy and Geochemistry*, 82 (1), 165–217.
- Perny, B., Eberhardt, P., Ramseyer, K., Mullis, J., Pankrath, R. (1992) Microdistribution of Al, Li, and Na in α quartz: Possible causes and correlation with short-lived cathodoluminescence. *American Mineralogist*, 77 (5-6), 534–544.
- Pistiner, J. S., Henderson, G. M. (2003) Lithium-isotope fractionation during continental weathering processes. *Earth and Planetary Science Letters*, 214, 327–339.
- Pogge von Strandmann, P.A.E., Burton, K. W., James, R. H., van Calsteren, P., Gislason, S. R., Mokadem, F. (2006) Riverine behaviour of uranium and lithium isotopes in an actively glaciated basaltic terrain. *Earth and Planetary Science Letters*, 251, 134–147.

- Pogge von Strandmann, P. A. E., Porcelli, D., James, R. H., van Calsteren, P., Schaefer, B., Cartwright, I., Reynolds, B. C., Burton, K. W. (2014) Chemical weathering processes in the Great Artesian Basin: Evidence from lithium and silicon isotopes. *Earth and Planetary Science Letters*, 406, 24–36.
- Qiu, L., Rudnick, R. L., McDonough, W. F., Merriman, R. J. (2009) Li and $\delta^7\text{Li}$ in mudrocks from the British Caledonides: Metamorphism and source influences. *Geochimica et Cosmochimica Acta*, 73, 7325–7340.
- Qiu, L., Rudnick, R. L., Ague, J. J., McDonough, W. F. (2011a) A lithium isotopic study of sub-greenschist to greenschist facies metamorphism in an accretionary prism, New Zealand. *Earth and Planetary Science Letters*, 301, 213–221.
- Qiu, L., Rudnick, R. L., McDonough, W. F., Bea, F. (2011b) The behavior of lithium in amphibolite- to granulite-facies rocks of the Ivrea-Verbano Zone, NW Italy. *Chemical Geology*, 289, 76–85.
- O’Neil, J. R. (1986) Theoretical and experimental aspects of isotopic fractionation. Valley, J. W., Taylor Jr., H. P., O’Neil, J. R. (Eds.), *Stable Isotopes in High Temperature Geological Processes*, Reviews in Mineralogy, Mineralogical Society of America, Washington, D.C, 16, 1–40.
- Richter, F. M., Liang, Y., Davis, A. M. (1999) Isotope fractionation by diffusion in molten oxides. *Geochimica et Cosmochimica Acta*, 63, 2853–2861.
- Richter, F. M., Davis, A. M., DePaolo, D. J., Watson, E. B. (2003) Isotope fractionation by chemical diffusion between molten basalt and rhyolite. *Geochimica et Cosmochimica Acta*, 67, 3905–3923.
- Richter, F. M., Mendybaev, R. A., Christensen, J. N., Hutcheon, I. D., Williams, R. W., Sturchio, N. C., Beloso, A. D. Jr. (2006) Kinetic isotope fractionation during diffusion of ionic species in water. *Geochimica et Cosmochimica Acta*, 70, 277–289.
- Richter, F. M., Watson, E. B., Mendybaev, R. A., Teng, F-Z., Janney, P. E. (2008) Magnesium isotope fractionation in silicate melts by chemical and thermal diffusion. *Geochimica et Cosmochimica Acta*, 72, 206–220.
- Richter, F. M., Watson, E. B., Mendybaev, R., Dauphas, N., Georg, B., Watkins, J., Valley, J. (2009) Isotopic fractionation of the major elements of molten basalt by chemical and thermal diffusion. *Geochimica et Cosmochimica Acta*, 73, 4250–4263.
- Richter, F., Watson, B., Chaussidon, M., Mendybaev, R., Ruscitto, D. (2014) Lithium isotope fractionation by diffusion in minerals. Part 1: Pyroxenes. *Geochimica et Cosmochimica Acta*, 126, 352–370.
- Richter, F., Chaussidon, M., Mendybaev, R., Kite, E. (2016) Reassessing the cooling rate and geologic setting of Martian meteorites MIL 03346 and NWA 817. *Geochimica et Cosmochimica Acta*, 182, 1–23.
- Risacher, F., Fritz, B. (1991) Quaternary geochemical evolution of the salars of Uyuni and Coipasa. central Altiplano, Bolivia. *Chemical Geology*, 90, 211–231.
- Risacher, F., Fritz, B. (2009) Origin of Salts and Brine Evolution of Bolivian and Chilean Salars. *Aquatic Geochemistry*, 15, 123–157.
- Rivera, T. A., Schmitz, M. D., Crowley, J. L., Storey, M. (2014). Rapid magma evolution constrained by zircon petrochronology and $^{40}\text{Ar}/^{39}\text{Ar}$ sanidine ages for the Huckleberry Ridge Tuff, Yellowstone, USA. *Geology*, 42, 643–646.
- Rivera, T.A., Schmitz, M.D., Jicha, B.R., Crowley, J.L., (2016). Zircon petrochronology and $^{40}\text{Ar}/^{39}\text{Ar}$ sanidine dates for the Mesa Falls Tuff: crystal-scale records of magmatic evolution and the short lifespan of a large Yellowstone magma chamber. *Journal of Petrology*, 57 (9), 1677–1704.
- Robert, J. L., Volfinger, M., Barrandon, J. N., Basutcu, M. (1983) Lithium in the interlayer space of synthetic trioctahedral micas. *Chemical Geology*, 40, 337–351.
- Rowe, M. C., Kent, A. J. R., Thornber, C. R. (2008) Using amphibole phenocrysts to track vapor transfer during magma crystallization and transport: an example from Mount St. Helens, Washington. *Journal of Volcanology and Geothermal Research*, 178, 593–607.
- Rudnick, R. L., Ionov, D. A. (2007) Lithium elemental and isotopic disequilibrium in minerals from peridotite xenoliths from far-east Russia: Product of recent melt/fluid – rock reaction. *Earth and Planetary Science Letters*, 56, 278–293.
- Ryan, J. G., Langmuir, C. H. (1987) The systematics of lithium abundances in young volcanic rocks. *Geochimica et Cosmochimica Acta*, 51, 1727–1741.
- Ryan, J. G., Kyle, P. R. (2004) Lithium abundance and lithium isotope variations in mantle sources: insights from intraplate volcanic rocks from Ross Island and Marie Byrd Land (Antarctica) and other oceanic islands. *Chemical Geology*, 212, 125–142.
- Sartbaeva, A., Wells, S. A., Redfern, S. A. T. (2004) Li^+ ion motion in quartz and beta-eucryptite studied by dielectric spectroscopy and atomistic simulations. *Journal of Physics: Condensed Matter*, 16, 8173–8189.
- Sartbaeva, A., Wells, S. A., Redfern, S. A. T., Hinton, R. W., Reed, S. J. B. (2005) Ionic diffusion in quartz studied by transport measurements, SIMS and atomistic simulations. *Journal of Physics: Condensed Matter*, 17, 1099–1112.

- Sauzeat, L., Rudnick, R. L., Chauvel, C., Garcon, M., Tang, M. (2015) New perspectives on the Li isotopic composition of the upper continental crust and its weathering signature. *Earth and Planetary Science Letters*, 428, 181–192.
- Schauble, E. A. (2004) Applying stable isotope fractionation theory to new systems. *Reviews in Mineralogy and Geochemistry*, 55, 65–111.
- Schiavi, F., Katsura Kobayashi, K., Moriguti, T., Nakamura, E., Pompilio, M., Tiepolo, M., Vannucci, R. (2010) Degassing, crystallization and eruption dynamics at Stromboli: trace element and lithium isotopic evidence from 2003 ashes. *Contributions to Mineralogy and Petrology*, 159, 541–561.
- Schiavi, F., Kobayashi, K., Nakamura, E., Tiepolo, M., Vannucci, R. (2012) Trace element and Pb-B-Li isotope systematics of olivine-hosted melt inclusions: insights into source metasomatism beneath Stromboli (southern Italy). *Contributions to Mineralogy and Petrology*, 163, 1011–1031.
- Schuessler, J. A., Schoenberg, R., Srsoson, O. (2009) Iron and lithium isotope systematics of the Hekla volcano, Iceland—Evidence for Fe isotope fractionation during magma differentiation. *Chemical Geology*, 258, 78–91.
- Seitz, H. M., Brey, G. P., Lahaye, Y., Durali, S., Weyer, S. (2004) Lithium isotopic signatures of peridotite xenoliths and isotopic fractionation at high temperature between olivine and pyroxenes. *Chemical Geology*, 212, 163–177.
- Seyfried, W. E., Janecky, D. R., Mottl, M. J. (1984) Alteration of the oceanic crust: Implications for geochemical cycles of lithium and boron. *Geochimica et Cosmochimica Acta*, 48, 557–569.
- Singer, B. S., Jicha, B. R., Condon, D. J., Macho, A. S., Hoffman, K. A., Dierkhising, J., Brown, M. C., Feinberg, J. M., Kidane, T. (2014). Precise ages of the Reunion event and Huckleberry Ridge excursion: episodic clustering of geomagnetic instabilities and the dynamics of flow within the outer core. *Earth and Planetary Science Letters* 405, 25–38.
- Shannon, R. D. (1976) Revised effective ionic radii in oxides and fluorides. *Acta Crystallographica Section A*, 32, 751–767.
- Spandler, C., O'Neill, H. S. (2010) Diffusion and partition coefficients of minor and trace elements in San Carlos olivine at 1,300°C with some geochemical implications. *Contributions to Mineralogy and Petrology*, 159, 791–818.
- Stelten, M. E., Cooper, K. M., Vazquez, J. A., Calvert, A. T., Glessner, J. J. G. (2015). Mechanisms and timescales of generating eruptible rhyolitic magmas at Yellowstone caldera from zircon and sanidine geochronology and geochemistry. *Journal of Petrology*, 56, 1607–1642.
- Stewart, D. B. (1978) Petrogenesis of lithium-rich pegmatites. *American Mineralogist*, 63, 970–980.
- Tang, Y. J., Zhang, H. F., Deloule, E., Su, B. X., Ying, J. F., Santosh, M., Xiao, Y. (2014) Abnormal lithium isotope composition from the ancient lithospheric mantle beneath the North China Craton. *Scientific Reports*, 4, 4274.
- Taura, H., Yurimoto, H., Kurita, K., Sueno, S. (1998) Pressure dependence on partition coefficients for trace elements between olivine and the coexisting melts. *Physics and Chemistry of Minerals*, 25, 469–484.
- Teng, F.-Z., McDonough, W. F., Rudnick, R. L., Dalpé, C., Tomascak, P. B., Chappell, B. W., Gao, S. (2004) Lithium isotopic composition and concentration of the upper continental crust. *Geochimica et Cosmochimica Acta*, 68, 4167–4178.
- Teng, F. Z., McDonough, W. F., Rudnick, R. L., Walker, R. J. (2006) Diffusion-driven extreme lithium isotopic fractionation in country rocks of the Tin Mountain pegmatite. *Earth and Planetary Science Letters*, 243, 701–710.
- Teng, F. Z., McDonough, W. F., Rudnick, R. L., Wing, B. A. (2007) Limited lithium isotopic fractionation during progressive metamorphic dehydration in metapelites: A case study from the Onawa contact aureole, Maine. *Chemical Geology*, 239, 1–12.
- Teng, F. Z., Rudnick, R. L., McDonough, W. F., Gao, S., Tomascak, P. B., Liu, Y. S. (2008) Lithium isotopic composition and concentration of the deep continental crust. *Chemical Geology*, 255, 47–59.
- Teng, F. Z., Rudnick, R. L., McDonough, W. F., Wu, F. Y. (2009) Lithium isotopic systematics of A-type granites and their mafic enclaves: Further constraints on the Li isotopic composition of the continental crust. *Chemical Geology*, 262, 370–379.
- Teng, F. Z., Dauphas, N., Watkins, J. M. (2017) Non-Traditional Stable Isotopes: Retrospective and Prospective. *Reviews in Mineralogy and Geochemistry*, 82 (1), 1–26.
- Tepley, F. J. III, Lundstrom, C. C., McDonough, W. F., Thompson, A. (2010) Trace element partitioning between high-An plagioclase and basaltic to basaltic andesite melt at 1 atmosphere pressure. *Lithos*, 118, 82–94.

- Tomascak, P. B., Helz, R. T., Walker, R. J. (1999) The absence of lithium isotope fractionation during basalt differentiation: New measurements by multi-collector ICP-MS. *Geochimica et Cosmochimica Acta*, 63, 907–910.
- Tomascak, P. B., Ryan, J. G., Defant, M. J. (2000) Lithium isotope evidence for light element decoupling in the Panama subarc mantle. *Geology*, 28, 507–510.
- Tomascak, P. B., Hemming, N. G., Hemming, S. R. (2003) The lithium isotopic composition of waters of the Mono Basin, California. *Geochimica et Cosmochimica Acta*, 67, 601–611.
- Tomascak, P.B., Langmuir, C. H., le Roux, P. J., Shirey, S.B. (2008) Lithium isotopes in global mid-ocean ridge basalts. *Geochimica et Cosmochimica Acta*, 72, 1626–1637.
- Tomascak, P. B., Magna, T.S., Dohmen, R. (2016) *Advances in Lithium Isotope Geochemistry*. Springer International Publishing.
- Urey, H. C. (1947) The thermodynamic properties of isotopic substances. *Journal of the Chemical Society (London)*, 562–581.
- Urey, H. C., Greiff, L. J. (1935) Isotopic exchange equilibria. *Journal of the Chemical Society*, 57, 321–327.
- USGS (2009) Mineral commodity summaries, United States Geological Survey, Reston.
- Valley, J. W. Taylor, H. P., O'Neil, J. R. (1986) *Stable Isotopes in High-Temperature Geological Processes*. Reviews in Mineralogy, 16. The Mineralogical Society of America, Washington DC.
- Valley, J. W., Cole, D. R. E. (2001) Stable isotope thermometry at high temperatures. *Reviews in mineralogy and geochemistry*, 43 (1), 365–413.
- Verney-Carron, A., Vigier, N., Millot, R. (2011) Experimental determination of the role of diffusion on Li isotope fractionation during basaltic glass weathering. *Geochimica et Cosmochimica Acta*, 75, 3452–3468.
- Verney-Carron, A., Vigier, N., Millot, R., Hardarson, B. S. (2015) Lithium isotopes in hydrothermally altered basalts from Hengill (SW Iceland). *Earth and Planetary Science Letters*, 411, 62–71.
- Vikström, H., Davidsson, S., Höök, M. (2013) Lithium availability and future production outlooks. *Applied Energy*, 110, 252–266.
- Vlastelic, I., Staudacher, T., Bachelery, P., Telouk, P., Neuville, D., Benbakkar, M. (2011). Lithium isotope fractionation during magma degassing: Constraints from silicic differentiates and natural gas condensates from Piton de la Fournaise volcano (Réunion Island). *Chemical Geology*, 284, 26–34.
- Watkins, J. M., DePaolo, D. J., Huber, C., Ryerson, F. J. (2009) Liquid composition-dependence of calcium isotope fractionation during diffusion in molten silicates. *Geochimica et Cosmochimica Acta*, 73, 7341–7359.
- Watkins, J. M., DePaolo, D. J., Bruce, W. E. (2017) Kinetic Fractionation of Non-Traditional Stable Isotopes by Diffusion and Crystal Growth Reactions. *Reviews in Mineralogy and Geochemistry*, 82 (1), 85–125.
- Watson, E. B. (2017). Diffusive fractionation of volatiles and their isotopes during bubble growth in magmas. *Contributions to Mineralogy and Petrology*, 177, 61.
- Wenger, M., Armbruster, T. (1991) Crystal-chemistry of lithium—oxygen coordination and bonding. *European Journal of Mineralogy*, 3, 387–399.
- Witherow, R. A., Lyons, W. B., Henderson, G. M (2010) Lithium isotopic composition of the McMurdo Dry Valleys aquatic systems. *Chemical Geology*, 275, 139–147.
- Yakob, J. L., Feineman, M. D., Deane, J. A., Eggler, D. H., Penniston-Dorland, S. C. (2012) Lithium partitioning between olivine and diopside at upper mantle conditions: An experimental study. *Earth and Planetary Science Letters*, 329, 11–21.
- Yamaji, K., Makita, Y., Watanabe, H., Sonoda, A., Kanoh, H., Hirotsu, T., Ooi, K. (2001) Theoretical estimation of lithium isotopic reduced partition function ratio for lithium ions in aqueous solution. *The Journal of Physical Chemistry A*, 105, 602–613.
- Young, E. D., Manning, C. E., Schauble, E. A., Shahar, A., Macris, C. A., Lazar, C., Jordan, M. (2015) High-temperature equilibrium isotope fractionation of non-traditional stable isotopes: experiments, theory, and applications *Chemical Geology*, 395, 176–195.
- Zanetti, A., Tiepolo, M., Obertina, R., Vannuccia, R. (2004) Trace-element partitioning in olivine: modelling of a complete data set from a synthetic hydrous basanite melt. *Lithos*, 75, 39–54.
- Zheng, M., Liu, X. (2009) Hydrochemistry of salt lakes of the Qinghai–Tibet plateau, China. *Aquatic Geochemistry*, 15, 293–320.

Chapter 2

Partitioning and isotopic fractionation of lithium in mineral phases of hot, dry rhyolites: The case of the Mesa Falls Tuff, Yellowstone

Neukampf, J.¹; Ellis, B.S.¹; Magna, T.²; Laurent, O.¹; Bachmann, O.¹

¹Institute of Geochemistry and Petrology, ETH Zürich, NW, Clausiusstrasse 25, CH-8092 Zürich, Switzerland

²Czech Geological Survey, Klárov 3, CZ-11821 Prague 1, Czech Republic

Published in *Chemical Geology*, 2019, vol. 506, pp. 175-186

Abstract

Studying the inventory and distribution of lithium (Li) in rhyolitic magmas, and the potential Li isotope fractionation during progressive crystallisation is crucial to understand the formation of economic Li deposits. Lithium concentrations and isotopic compositions of co-existing groundmass glass, quartz, sanidine, plagioclase, clinopyroxene, fayalite, and orthopyroxene from the Mesa Falls Tuff (Yellowstone) were determined using LA-ICP-MS and MC-ICP-MS. The highest Li contents were obtained from quartz-hosted melt inclusions (avg. 244 ppm) and groundmass glass (avg. 43 ppm). Lithium concentrations are lower in mineral phases, decreasing from quartz (avg. 18 ppm), plagioclase (avg. 17 ppm), fayalite (avg. 16 ppm), clinopyroxene (avg. 11 ppm), orthopyroxene (avg. 8 ppm) to sanidine (avg. 6 ppm). Lithium isotopic compositions of bulk tuff samples and major mineral phases reveal a range in $\delta^7\text{Li}$ values (per mil deviation of $^7\text{Li}/^6\text{Li}$ ratio relative to L-SVEC reference material), spanning $\sim 10\%$ between the co-existing phases and decreasing from groundmass glass (+6.5 – +7.5‰) to feldspars (plagioclase from -2.3 to -1.4% ; sanidine from -0.6 to -0.1%). Lithium concentration profiles across sanidine and plagioclase crystals show a decrease towards the crystal rims, which is not observed in the other mineral phases of the Mesa Falls Tuff. The variations identified in feldspar are decoupled from both the major and all other trace element compositions, precluding an origin related to mafic recharge and magma mixing. We propose that they result from Li loss from the melt to a vapour or fluid phase taking place immediately prior to, or synchronously with, eruption. This is supported by the observation that Li contents in quartz-hosted melt inclusions are a factor of six greater than those found in groundmass glass while the concentrations of immobile trace elements are identical. The low-Li rims on sanidine and plagioclase crystals observed in the high-silica Mesa Falls Tuff rhyolite are potential candidates to preserve Li isotopic disequilibrium as has been observed in less evolved systems. The variation in Li abundances within feldspar crystals hints at the potential for kinetic isotopic fractionation to play a role in the reported isotopic compositions of bulk separates. The large elemental database of Li concentrations from the MFT allows us to calculate apparent partition coefficients between groundmass glass and co-existing minerals. These data are compared to fifteen other ignimbrites from the Yellowstone-Snake River Plain province to provide a coherent picture of Li partitioning in hot and dry rhyolites with Li most compatible in quartz and olivine, and least compatible in sanidine.

2.1 Introduction

The last twenty-five years have seen an increased interest in the geochemistry and global cycling of lithium (Li). Studies have used Li contents and isotope systematics to investigate the composition of the Earth's mantle (e.g., Elliott et al., 2006; Tomascak et al., 2008; Marschall et al., 2017), the transfer of mass at subduction zones (e.g., Leeman et al., 2004; Magna et al., 2006; Plank, 2014), degassing and cooling (Coogan et al., 2005; Beck et al., 2006; Kent et al., 2007; Charlier et al., 2012; Benson et al., 2017; Rubin et al., 2017; Ellis et al., 2018; Holycross et al., 2018), and continental weathering (e.g., Pistiner and Henderson, 2003; Rudnick et al., 2004; Teng et al., 2004; Pogge von Strandmann et al., 2010; Pogge von Strandmann et al., 2017), among other applications. With an increasing drive towards

renewable energy sources, Li has also become an economically important element in the manufacture of fuel cells.

Despite the recognised association between economic deposits of Li (mainly brines and pegmatites) and evolved magmas (e.g., Kesler et al., 2012), relatively little is known about the behaviour of Li in such evolved magmas compared with more mafic systems. The latest compilations of partitioning data of Li between minerals and co-existing melt (Tomascak et al., 2016; Penniston-Dorland et al., 2017) lack data for mineral phases common in felsic systems (e.g., quartz, sanidine) even though they could be an important source for Li through weathering and erosion. Studies about Li isotopic fractionation among coexisting mineral phases in evolved systems are equally rare. A study of Fe and Li isotopes from the Hekla system in Iceland using bulk rock samples suggested that little Li isotopic fractionation occurred during a fractional crystallisation-dominated evolution from basaltic to rhyolitic compositions (Schuessler et al., 2009), consistent with earlier results for the Kilauea Iki lava lake (Tomascak et al., 1999). However, detailed studies indicate that Li isotopic fractionation between co-existing minerals commonly exists on order of 10–20‰ in mafic and/or highly evolved systems (e.g., Teng et al., 2006; Weyer and Seitz, 2012; Magna et al., 2016), and up to ca. 40‰ within single phenocrysts (e.g., Jeffcoate et al., 2007; Cabato et al., 2013). Lithium isotopic variability between mineral phases is even preserved within granitoid rocks (Teng et al., 2006), which cool over long timescales. It is therefore possible that sequential crystallisation of mineral phases could induce Li isotopic fractionation and drive evolution of $\delta^7\text{Li}$ in the system. Such evolution could be of interest to fingerprint the source and mechanisms of formation of the economic Li deposits related to magmatic processes, such as pegmatites.

We aimed to further constrain and understand the elemental and isotopic behaviour of Li throughout the crystallisation and emplacement of evolved, silicic magmas. For this purpose, we selected the ca. 1.30 Ma Mesa Falls Tuff (Yellowstone, USA) as a case study as it is a well-documented high-silica rhyolite system with relatively simple crystallisation history (e.g., Christiansen and Blank, 1972; Rivera et al., 2016), and mostly lacking post-eruptive alteration. We combined in situ major and trace element analyses of co-existing mineral phases and groundmass glasses (including quartz-hosted melt inclusions), coupled with Li isotopic measurements of bulk mineral separates, to constrain the major hosts of Li and first-order approximation of Li isotopic fractionation among major mineral phases in rhyolitic magmatic systems.

2.2 Geological background

The Yellowstone Volcanic Field (Idaho/Wyoming, USA) represents the current manifestation of the Columbia River–Yellowstone volcanic province which has been active for the last ~16.5 Myr (Lowenstern et al., 2006; Hooper et al., 2007). Following the early flood basalt eruptions, volcanism has been dominantly bimodal (basalt–rhyolite) and for the last 14 Myr the silicic volcanism has been broadly time transgressive along the track of the Snake River Plain to the presently active Yellowstone Volcanic Field (e.g., Nash et al., 2006). Yellowstone has been erupting rhyolitic and basaltic magmas for the past ~ 2 Myr with three voluminous ignimbrites (Huckleberry Ridge, Mesa Falls, and Lava Creek tuffs) separated by periods of relative quiescence dominated by the effusion of rhyolitic lavas (Christiansen, 2001).

The Mesa Falls Tuff (MFT) erupted at 1.30 Ma (Rivera et al., 2016; Ellis et al., 2017a) as part of the second volcanic cycle of Yellowstone forming the Henry's Fork caldera, located south-west of the Yellowstone National Park (Christiansen, 2001; Fig. 2.1). The MFT ignimbrite has an estimated deposit volume of 280 km³ and covers an area of ~2,700 km² in south-eastern Idaho and western Wyoming (Christiansen, 2001) with ashfall dispersed regionally. The MFT is typical for the rhyolites of the Yellowstone Volcanic Field with a mineral assemblage of sanidine, quartz, plagioclase, fayalite, clino- and orthopyroxene, ilmenite, magnetite, zircon and apatite. Samples for this study come from one location (described in Ellis et al., 2017a) of the non-welded portion of the MFT with juvenile clasts preserving glassy groundmass indicative of rapid quenching upon eruption. Using only glassy samples minimises the potential for post-eruptive mobility of Li as has been observed in the slowly-cooled welded ignimbrites of the Snake River Plain (Ellis et al., 2015, Ellis et al., 2018).

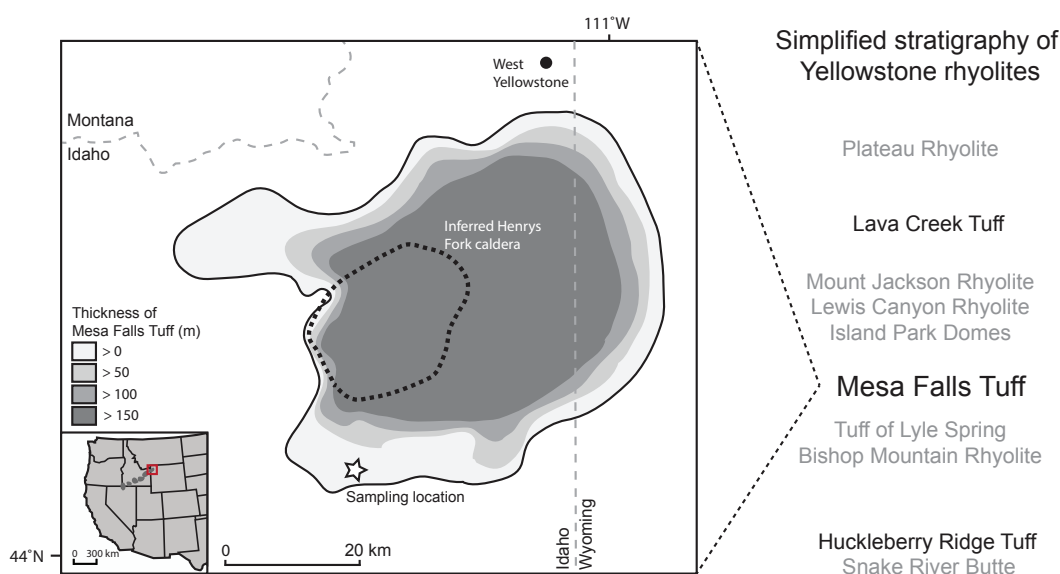


Fig. 2.1: Map showing the sampling location of the Mesa Falls Tuff, the thickness of the deposit (in grey) and the inferred source of the deposit (Henry's Folk caldera; after Christiansen, 2001) as well as the simplified stratigraphy of Yellowstone rhyolites (after Christiansen, 2001 and Rivera et al., 2018). Inset map shows the location of Yellowstone hotspot track in North America.

2.3 Analytical methods

Samples were crushed with aliquots reserved for bulk rock powder and the rest of the sample was cleaned, sieved and used to separate crystals for *in situ* geochemical work and Li isotopic determinations. Prior to *in situ* geochemical analyses, groundmass glass, sanidine, plagioclase, clinopyroxene, orthopyroxene, fayalite (embedded in epoxy mounts) were backscatter electron (BSE) imaged using a JEOL JSM-6390 scanning electron microscope (SEM) at ETH Zürich. The SEM was also used to image the quartz and sanidine by cathodoluminescence (CL). The major element compositions of minerals were determined using a JEOL JXA 8200 Superprobe at ETH Zürich. For pyroxenes and fayalite, operating conditions were 15 kV and 20 nA beam current with a focused beam while sanidine and plagioclase were analysed with a 10 µm beam diameter with counting times of 20 s on peak and 10 s on background.

All analyses were organised so that the potentially mobile elements (Na, K) were measured first. Natural and synthetic minerals were used as standards (see Appendix A1: Supplementary data 1).

2.3.1 Trace element measurements

Trace element concentrations in groundmass glass, sanidine, plagioclase, clinopyroxene, orthopyroxene, fayalite, zircon, apatite, ilmenite, and magnetite were measured using an Excimer 193 nm (ArF) Resolution laser ablation system coupled to a Thermo Element XR ICP-MS at the Institute of Geochemistry and Petrology, ETH Zürich. The spot size was 43 μm for all minerals except for groundmass glass, smaller crystals and detailed profiles of feldspar crystals for which a 29 μm spot was employed. We used a repetition rate of 5 Hz and on-sample energy density of the laser beam of $\sim 3.5 \text{ J}\cdot\text{cm}^{-2}$. The ablation was performed under a flow of high-purity He (ca. $0.7 \text{ L}\cdot\text{min}^{-1}$) and Ar make-up gas (ca. $1.0 \text{ L}\cdot\text{min}^{-1}$) from the ICP-MS. The list of elements and details of the analytical conditions are reported in the Appendix A1: Supplementary data 1. For all minerals and groundmass glass (except quartz), concentrations were quantified against the NIST SRM 612 silicate glass wafer as the primary standard (Jochum et al., 2011), using standard–sample bracketing with a block of 25 samples between the standards. The USGS basaltic glass GSD-1G was used as the secondary standard to check for the accuracy and reproducibility of the analyses (see results in the Appendix A1: Supplementary data 1). The average 2 standard deviation (2 SD) reproducibility of concentrations in the GSD-1G standard for all analytical sessions was used to determine uncertainties on the concentrations of unknowns (5% relative for Li).

Trace element concentrations in quartz and melt inclusions in quartz were determined using an Excimer 193 nm (ArF) GeoLas (Coherent) laser system coupled to a Perkin Elmer Elan 6100 DRC quadrupole ICP-MS. The on-sample energy density of the laser beam was $15\text{--}20 \text{ J}\cdot\text{cm}^{-2}$. All quartz was measured with a spot size of 40 μm whereas for the melt inclusions the spot size was adjusted to fully ablate the entire inclusion. The ablation was performed under a flow of He (ca. $1.0 \text{ L}\cdot\text{min}^{-1}$) and Ar make-up gas from the ICP-MS (ca. $1 \text{ L}\cdot\text{min}^{-1}$) was admixed downstream of the ablation chamber. The list of elements and details of the analytical conditions are reported in the Appendix A1: Supplementary data 1. Concentrations were quantified against the NIST SRM 610 silicate glass wafer as the primary standard (Jochum et al., 2011) and a natural quartz crystal characterised by Audétat et al. (2015) was employed as a secondary standard (see results in the Appendix A:1 Supplementary data 1). The average 2 SD reproducibility of concentrations in the secondary quartz standard for all analytical sessions was used to determine uncertainties on the concentrations of unknowns (9% relative for Li).

Raw data were reduced using the Matlab-based SILLS program (Guillong et al., 2008) by using one of the major elements (Si, Ca, Al) that were determined from microprobe analysis as an internal standard. As no microprobe data were obtained for quartz-hosted melt inclusions we used two internal standards: (i) the assumption that the sum of major oxides was 95 wt.% (to account for the possible presence of volatiles in the melt that are not quantifiable by LA-ICP-MS); and (ii) a SiO_2 content of 70 wt.%. The latter estimate would encompass most of the compositional range of silicic magmas within $\pm 10\%$ (which is a lower estimate for the bulk reproducibility of the melt inclusion data in any case). The uncertainties on melt inclusion concentrations were set to 15% relative (2 SE).

2.3.2 Lithium isotopic measurements

For Li isotopic analyses, grains containing mineral inclusions or cracks were avoided and only the highest-purity crystals were selected. The bulk mineral separates were washed in an ultra-sonic bath with dilute HNO₃ and again with double-distilled ultra-pure water in order to remove potential adherent contamination on grain boundaries. Clinopyroxene, orthopyroxene, sanidine and plagioclase separates were analysed using a Dilor LabRaman with an ILD – Laser (532.1 nm) to ensure their purity. Lithium analytical procedures, including sample digestion, ion-exchange chemistry, and concentration and isotopic measurements for bulk whole rock and handpicked bulk mineral separates were performed at the Czech Geological Survey, following procedures given in Magna et al. (2004). For mass spectrometry measurements, a Neptune MC-ICP-MS (Thermo Fisher Scientific, Bremen, Germany) was used. The lithium concentrations were analysed in clean Li fractions against the L-SVEC reference solution (Flesch et al., 1973). A standard–sample–standard bracketing method using L-SVEC solution was employed to determine natural Li isotopic variations in unknown samples. The results of Li isotopic measurements are reported in the δ -notation relative to the L-SVEC reference solution and calculated as $\delta^7\text{Li} (\text{‰}) = [({}^7\text{Li}/{}^6\text{Li})_{\text{sample}} / ({}^7\text{Li}/{}^6\text{Li})_{\text{L-SVEC}} - 1] \times 1000$. The reference rock materials JR-2 (rhyolite; GSJ), BHVO-2 (basalt; USGS), JG-2 (granite; GSJ), BCR-2 (basalt; USGS) and UB-N (serpentinite; CRPG-CNRS) were analysed to monitor the reliability of the entire procedure. The resulting $\delta^7\text{Li}$ values are provided in Appendix A1: Supplementary data 1 and are all in agreement with published values for these standards (e.g., Pistiner and Henderson, 2003; Parkinson et al., 2007). The reproducibility of Li isotopic measurements was generally better than $\pm 0.4\text{‰}$ (2 SD). All analytical results are provided in the Appendix A1: Supplementary data 1. Trace element concentrations in dissolved aliquots of each sample were acquired using an Agilent 7900 \times ICP-MS, housed at the Czech Geological Survey.

2.4 Results

2.4.1 Quartz

Quartz is the most abundant mineral phase in the MFT with subhedral grains reaching 2–4 mm and often containing large (100–200 μm), glassy, melt inclusions. The quartz crystals show multiple internal growth zones revealed as variations in brightness in CL images (see Appendix A1: Supplementary data 1). CL-bright rims are relatively common in MFT quartz; however, no coherent pattern of internal zoning occurs across the quartz population. Titanium contents in quartz correlate with the CL intensity in the different growth zones, the CL-bright domains being Ti and Al-rich and mostly Li-poor (Fig. 2.2b and Appendix A1: Supplementary data 1). The Ti concentrations are variable (60–182 ppm), with one anomalous grain returning values as low as 37–47 ppm, while having Li, P, and Al concentrations comparable with other grains. The abundances of these trace elements (Al = 76–125 ppm; P = 39–80 ppm; Li = 13.2–24.5 ppm; $n = 718$) appear more homogenous (see full dataset in Appendix A1: Supplementary data 1). Magnesium and Fe contents are close to the detection limits and concentrations of other trace elements (Ca, Mn, K, Rb, Sr, Cs, Pb, and Ba) are below the respective detection limits. Lithium contents of MFT quartz show a small increase from core (mean 17.4 ppm; $n = 571$) to rim (mean 19.0; $n = 147$) and are comparable to previously published Li contents of Yellowstone quartz

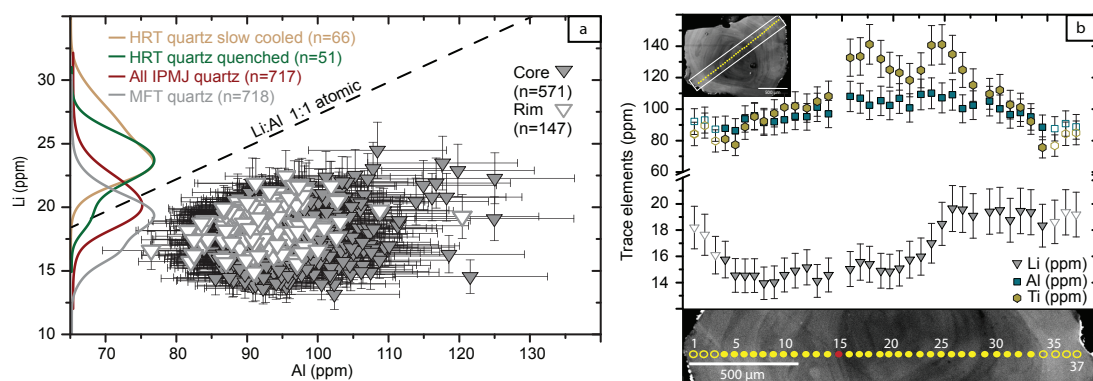


Fig. 2.2: Trace element compositions of MFT quartz. **(a)** Plot of Li vs. Al concentration ($\pm 9\%$ error bars) of all analysed quartz grains from MFT (cores as grey filled triangles, rims as open triangles, measured with $40\ \mu\text{m}$ spot size), compared to the probability density distribution of Li concentrations in literature data from Yellowstone (IPMJ quartz in red, data from Troch et al., 2017; HRT quartz from slowly cooled part in brown and HRT quartz from quenched part in green, data from Ellis et al., 2018). The isoatomic Li:Al 1:1 line, illustrating the ideal $\text{Si}^{4+} \leftrightarrow \text{Al}^{3+} + \text{Li}^{+}$ substitution, is shown for reference. **(b)** Li (grey filled triangle), Al (green filled square) and Ti (yellow hexagon) concentration profile ($\pm 9\%$ error bars) in one representative quartz crystal. Lithium shows an increase towards the rims represented by open symbols, Al exhibits a limited variability, and Ti follows the growth zones that were identified by the CL image. CL image with position of trace element analyses indicated in yellow, open symbols represent rim measurements, filled represent measurements in the core and red indicate excluded data point.

(Fig. 2.2a) from the Island Park–Mount Jackson lava series (Troch et al., 2017) and slightly lower than those from Huckleberry Ridge Tuff (Ellis et al., 2018).

2.4.2 Sanidine

Sanidine is ubiquitous in the MFT, occurring as large (up to a few mm), euhedral, clear, crystals which may contain glassy melt inclusions. CL images reveal multiple growth zones with alternating bright and dark CL domains (Fig. 2.3). Sanidine compositions from the MFT have been well-characterised in previous studies of major and trace element concentrations, and $^{40}\text{Ar}/^{39}\text{Ar}$ ages (Ganseccki et al., 1998; Lanphere et al., 2002; Rivera et al., 2016; Ellis et al., 2017a). Our results are in good agreement with those studies, showing little compositional variability in major elements (Or_{55-65}) either within or between crystals. Trace elements, however, exhibit large ranges of concentration; our results ($\text{Ti} = 34\text{--}155\ \text{ppm}$, $\text{Sr} = 27\text{--}331\ \text{ppm}$, $\text{Rb} = 85\text{--}145\ \text{ppm}$) are in excellent agreement with existing data (Ellis et al., 2017a). Our results for Ba ($208\text{--}15,180\ \text{ppm}$) exceed the previously described range (up to $8,721\ \text{ppm}$) with the highest Ba contents found in the rims of the sanidine, as previously reported for Yellowstone rhyolites (Troch et al., 2017). Barium and Ti zoning in the sanidine correlates with the zoning patterns identified by CL images. Lithium contents in MFT sanidine crystals measured in this study span from 1.1 to $11.9\ \text{ppm}$ (average $5.8\ \text{ppm}$; $n = 688$), overlapping the data of Ellis et al. (2017a) who reported 2.7 to $5.1\ \text{ppm}$ (average $4.4\ \text{ppm}$; $n = 163$). Traverses across crystals revealed systematic variation in Li (Fig. 2.3) with higher Li content in the cores ($1.7\text{--}11.9\ \text{ppm}$, average $6.0\ \text{ppm}$) and on average lower concentrations in the rims ($1.1\text{--}7.8\ \text{ppm}$, average $4.3\ \text{ppm}$). In addition to the common occurrence of low Li contents at sanidine rims, analyses located near cracks (not shown in Fig. 2.3, for more CL images see Appendix A1: Supplementary data 1) in crystals often returned lower Li values.

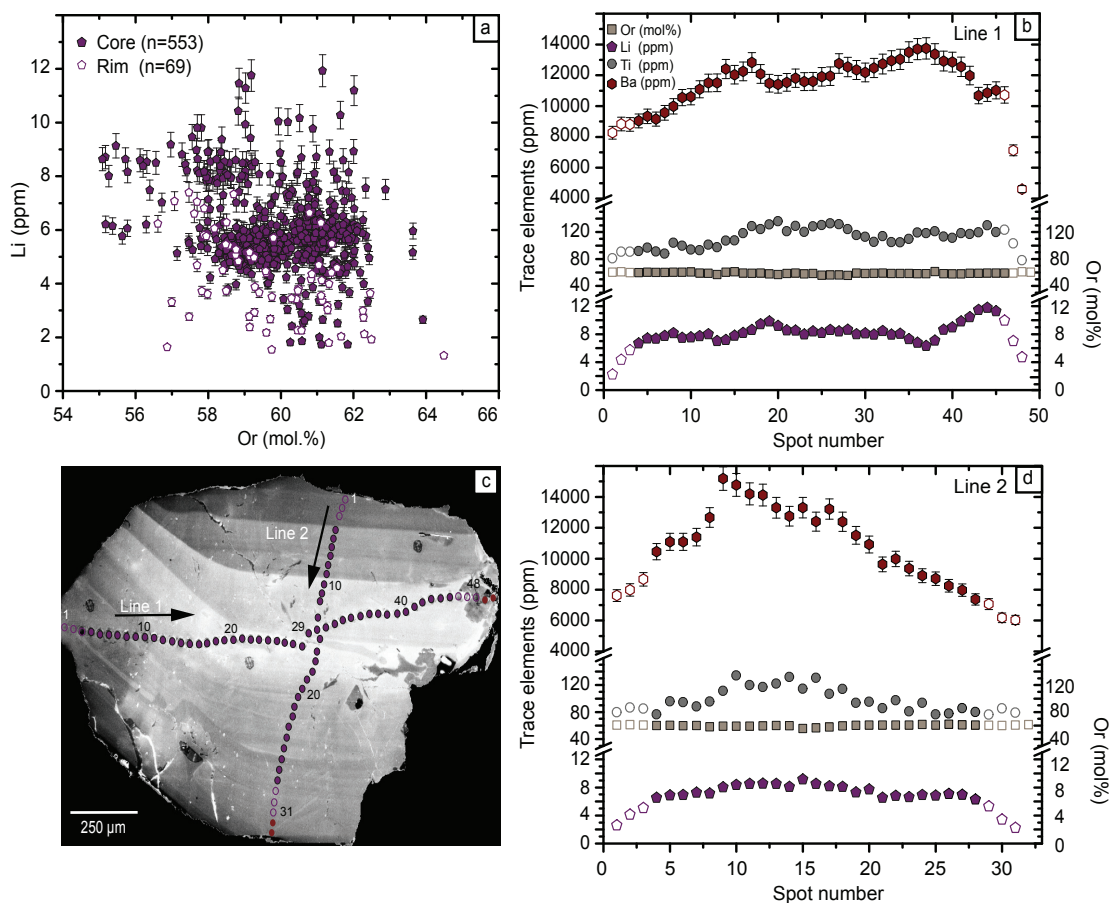


Fig. 2.3: Major and trace element compositions of MFT sanidine. (a) Li concentrations (measured with 29 μm spot size) in all analysed crystal rims (open purple pentagon) and cores (filled purple pentagon) relative to the orthoclase (Or mol.%) component. Two traverses were measured, represented as line 1 (b) and line 2 (d). (c) CL image of one representative sanidine grain with analysis locations indicated in purple, excluded data points indicated in red. (b & d) results of traverses showing variations of orthoclase, Li (filled purple pentagon), Ti (grey filled circle) (uncertainties on the analyses are smaller than the symbols) and Ba contents (red hexagon; $\pm 5\%$ error bars) across the crystal in (b).

2.4.3 Plagioclase

Plagioclase is relatively rare in the MFT compared to sanidine. The crystals are euhedral (up to 2 mm) and transparent to milky in appearance. There is a limited compositional range in plagioclase from the MFT with variability predominantly between grains ($\text{Ab}_{66-74}\text{An}_{16-29}\text{Or}_{5-11}$). As with sanidine, despite a limited range in major elemental composition, trace elements show significant variations up to one to two orders of magnitude (Ba = 13–1,140 ppm, Ti = 27–106 ppm, Sr = 21–289 ppm). Lithium concentrations are less variable but still exhibit a range between 4.7 and 28.5 ppm (average = 17.3 ppm; $n = 653$) that appears unrelated to the major element composition, size or shape of the crystals (Fig. 2.4). Profiles across crystals indicate a large Li concentration heterogeneity within the crystals and three different zones can be identified (Fig. 2.4). The first zone corresponds to crystal cores showing homogeneous, intermediate concentrations (average of 17.6 ppm). Between core and rim, there appears a zone on average slightly enriched in Li compared with the core (average of 21.2 ppm and up to 26.9 ppm), while the rims, which were directly in contact with the melt, are slightly depleted in Li (average 15.7 ppm and down to 4.7 ppm). Similarly, to sanidine, analyses in plagioclase crystals that were close to cracks return lower Li contents.

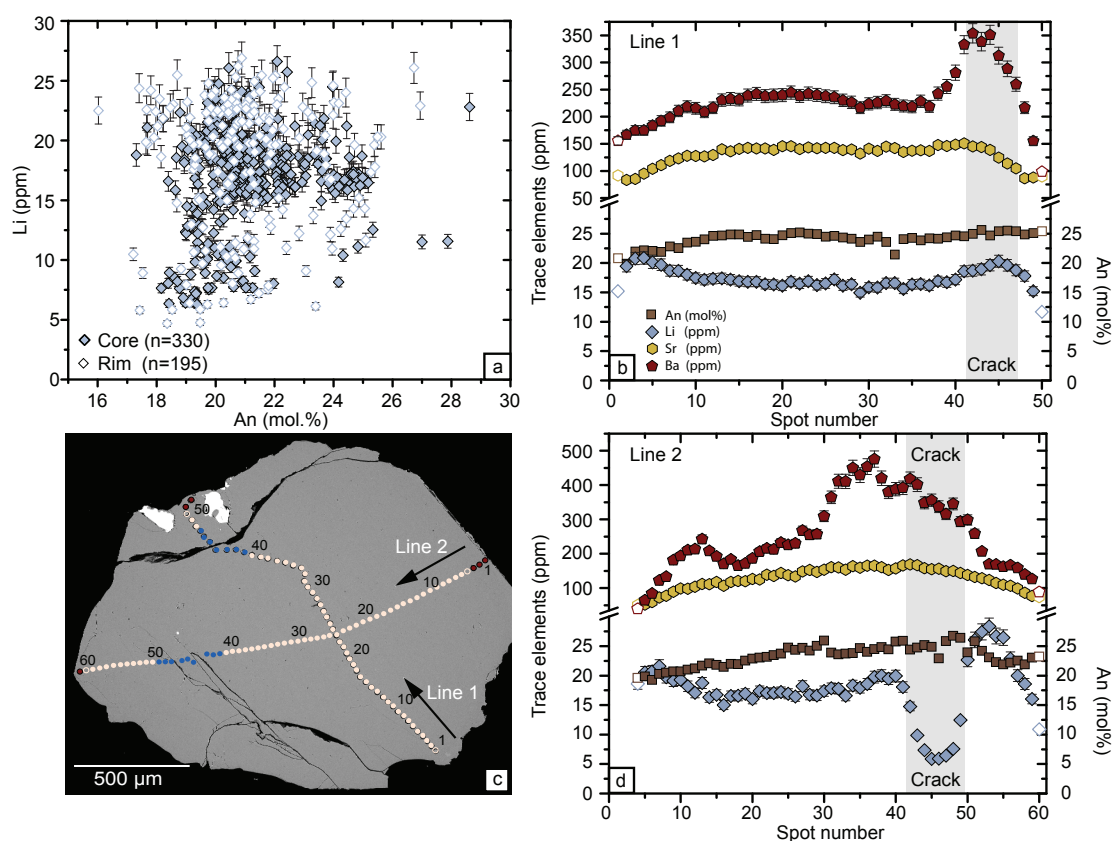


Fig. 2.4: Major and trace element compositions of MFT plagioclase. (a) Li concentrations (measured with 29 μm spot size; ±5% error bars) in all analysed crystal rims (open blue diamond) and cores (filled blue diamond) relative to the anorthite (An mol.%) component. (b) and (d) represent two of the measured traverses shown as line 1 (b) and line 2 (d). (c) BSE image of plagioclase grain with analysis locations for the traverses indicated in pink, excluded data points indicated in red and measurements influenced by cracks shown in blue. (c & d) results of traverses showing variations of anorthite (brown square), Li (blue diamond), Sr (yellow hexagon) (uncertainties on the analyses are smaller than the symbols) and Ba contents (red pentagon; ±5% error bars) across the crystal in (b).

2.4.4 Pyroxenes

The MFT contains both clinopyroxene and orthopyroxene. Orthopyroxene rarely forms single crystals and commonly occurs as cores surrounded by rims of clinopyroxene (Fig. 2.5). In addition to these rims around orthopyroxene, clinopyroxene frequently occurs as single euhedral to subhedral grains. Notably, the smaller clinopyroxenes do not contain any core of orthopyroxene. Both clinopyroxene and orthopyroxene commonly exhibit inclusions of Fe-Ti oxides, apatite, and zircon (Fig. 2.5).

Clinopyroxenes are augitic ($\text{Wo}_{32-42}\text{En}_{13-33}\text{Fs}_{25-48}$) in composition. Their compositions do not vary significantly as a function of grain size or texture (i.e., single crystals or rims enveloping orthopyroxene). The clinopyroxenes exhibit a variation in some trace elements for the entire population such as Ti (749–1,679 ppm) and Mn (4,381–7,974 ppm). Lithium concentrations are rather homogeneous (9.9–13.6 ppm, average 11.2 ppm; $n = 259$) and show no correlation with any major element. Traverses across single crystals indicate that the clinopyroxenes are homogeneous (Appendix A1: Supplementary data 1), notably lacking the low-Li rims observed in the plagioclase and sanidine crystals.

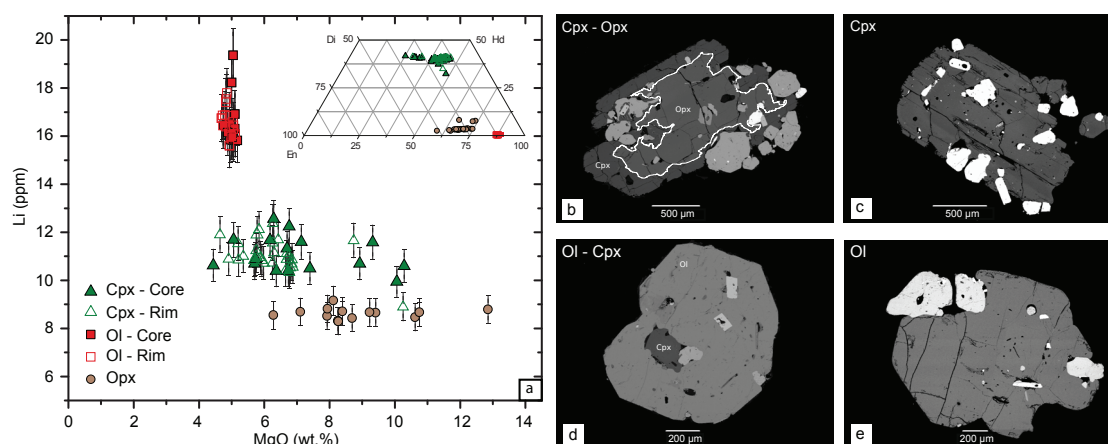


Fig. 2.5: Major and trace element compositions of MFT mafic minerals showing (a) variations between augite (green triangle), orthopyroxene (brown circle) and olivine (red square) in Li relative to MgO and inset with pyroxene classification diagram; the composition of olivine is included for comparison. (b) to (e) BSE images of the mafic minerals (cpx with opx core, cpx, olivine with cpx core, and olivine, respectively) that occur in the MFT. Clinopyroxene, orthopyroxene and olivine have inclusions of Fe-Ti oxides, apatite, and zircon.

The orthopyroxenes ($Wo_{2-8}En_{18-39}Fs_{59-75}$) are moderately uniform in their major and trace elements. There are modest variations in the major elements CaO (1.1–3.6 wt.%), FeO (37.6–42.2 wt.%) and MgO (5.7–10.8 wt.%). The minor elements are relatively homogeneous with TiO_2 ranging 0.14–1.0 wt.% and Mn from 1.2 to 1.6 wt.%. The Li concentrations are strikingly homogeneous, from 7.8 to 9.3 ppm (Fig. 2.5 and Appendix A1: Supplementary data 1).

2.4.5 Fayalite

Fayalite is the least abundant of the major phases in the MFT. Homogeneous fayalite (Fa_{87-89}) crystals are subhedral and rarely enclose clinopyroxene while commonly containing magnetite and ilmenite inclusions (Fig. 2.5). Titanium (43–205 ppm) and P (25–97 ppm) are variable within fayalite crystals with lower values occurring at crystal rims. The other trace elements are relatively homogeneous with Li ranging between 13.9 and 19.4 ppm (average 16.2 ppm; $n = 127$). Profiles across the grains show no significant variations (see Appendix A1: Supplementary data 1), and specifically, no Li decrease towards the rims.

2.4.6 Groundmass glass and melt inclusions

MFT groundmass glasses are all high-silica rhyolite (>75 wt.% SiO_2 , recalculated on volatile-free basis) with K_2O and Na_2O contents ranging from 5.2–6.5 wt.% and 2.9–3.4 wt.%, respectively. In terms of trace elements, the MFT groundmass glasses are similar to others from the Yellowstone–Snake River Plain province ($Zr = 155$ – 198 ppm, $Ba = 91$ – 221 ppm, $Rb = 230$ – 281 ppm, $Ti = 647$ – 851 ppm). Strontium contents are very low (<32 ppm), interpreted as a result of extensive plagioclase fractionation. These compositions are in good agreement with previously published MFT groundmass glass data (Pearce et al., 1996; Perkins and Nash, 2002). Lithium contents of the groundmass glass vary between 36.1 and 51.9 ppm (average 43.1 ppm; $n = 73$). The groundmass glass exhibits a strong negative Eu anomaly with an enrichment in light rare earth elements (LREE) and a decrease towards the heavy rare

earth elements (HREE), but is enriched relative to the Bulk Silicate Earth-normalised rare earth element (REE) pattern (Fig. 2.6) which is typical for rhyolites from the Yellowstone–Snake River Plain province (Ellis et al., 2013).

Quartz-hosted melt inclusions contain significantly more Li (69.5–397 ppm, average 243.7 ppm; $n = 29$) than the groundmass glasses. These Li contents are similar to, or slightly lower than, those reported by Benson et al. (2017) for other quartz-hosted melt inclusions in rhyolites from the McDermitt volcanic field in Oregon and Nevada, and the Huckleberry Ridge Tuff from Yellowstone. Further, while we did not observe bubbles within our melt inclusions, Benson et al. (2017) demonstrated that re-homogenisation of melt inclusions tends to result in higher Li contents by approximately 10% compared

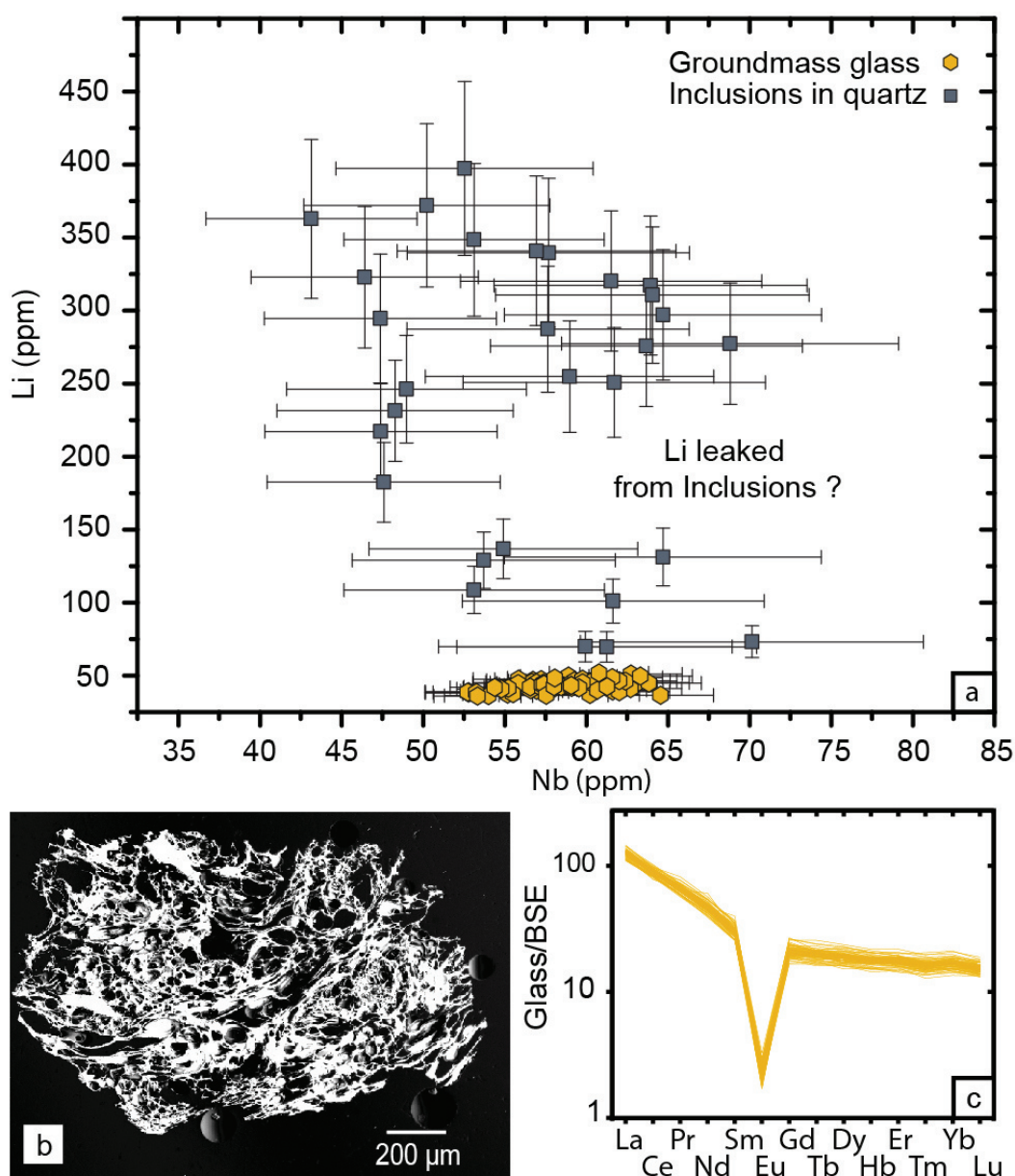


Fig. 2.6: Trace element compositions of the quartz-hosted melt inclusions (blue square) and groundmass glass (yellow hexagon) of MFT. (a) Plot of Li relative to Nb (immobile during degassing) concentrations in groundmass glass ($\pm 5\%$ error bars) and melt-inclusions in quartz ($\pm 15\%$ error bars). (b) BSE image of the vesicular groundmass glass. (c) Rare earth element patterns (concentrations normalised to the Bulk Silicate Earth; McDonough and Sun, 1995) for the groundmass glass, showing strong negative Eu anomaly typical of rhyolites from the Yellowstone–Snake River Plain province.

to un-homogenised inclusions. Thus, our values may be considered as minima. Besides these higher Li contents, the quartz-hosted melt inclusions notably show similar trace element compositions as the groundmass glass, illustrated in Fig. 2.6 by comparable ranges in Nb contents (49–70 ppm, average 58 ppm in the groundmass glass; 43–70 ppm, average 57 ppm in the inclusions).

2.4.7 Other phases

The MFT also contains magnetite, ilmenite, apatite and zircon but all those minerals have Li concentrations below the typical limits of detection for our analytical system (between 0.3 and 0.7 ppm depending on the analytical session). Therefore, these phases are not considered further here.

2.4.8 Lithium isotopes

Lithium isotopic compositions of bulk samples and mineral separates show a significant variability, with a range of $\delta^7\text{Li}$ values between different phases of nearly 10‰ from -2.3‰ in plagioclase to $+7.5\text{‰}$ in groundmass glass (Table 1.1; Fig. 2.7). Notably, the isotopically heaviest materials are groundmass glass ($6.5\text{--}7.5\text{‰}$) and quartz ($6.7\text{--}7.2\text{‰}$). The bulk rock MFT ($3.9\text{--}4.3\text{‰}$) and fayalite (3.1‰) show intermediate $\delta^7\text{Li}$ values whereas clinopyroxene, orthopyroxene and sanidine all show slightly positive to negative $\delta^7\text{Li}$ values (-0.1 to $+1.0\text{‰}$, $\sim -2.0\text{‰}$ and -0.6 to -0.1‰ , respectively).

Table 1.1: Lithium contents and isotopic compositions (with 2 SD error) in bulk whole rock aliquots and bulk mineral separates from this study.

Sample	Li (ppm)	$\delta^7\text{Li}$ (‰)	2SD
Bulk 1	39.0	4.28	0.15
Bulk 2	37.3	3.94	0.29
Groundmass glass 1	32.8	6.92	0.57
Groundmass glass 2	27.2	6.48	0.42
Groundmass glass 3	26.5	7.31	0.27
Groundmass glass 4	27.3	7.46	0.47
Quartz 1	17.1	7.24	0.19
Quartz 2	18.8	6.69	0.34
Olivine 1	30.6	3.05	0.41
Olivine 2	24.1	3.10	0.19
Clinopyroxene 1	13.7	-0.11	0.16
Clinopyroxene 2	11.1	1.02	0.22
Orthopyroxene 1	11.9	-2.10	0.41
Orthopyroxene 2	13.7	-1.95	0.33
Plagioclase 1	12.9	-1.39	0.36
Plagioclase 2	13.4	-2.31	0.54
Sanidine 1	4.16	-0.11	0.18
Sanidine 2	4.74	-0.58	0.37

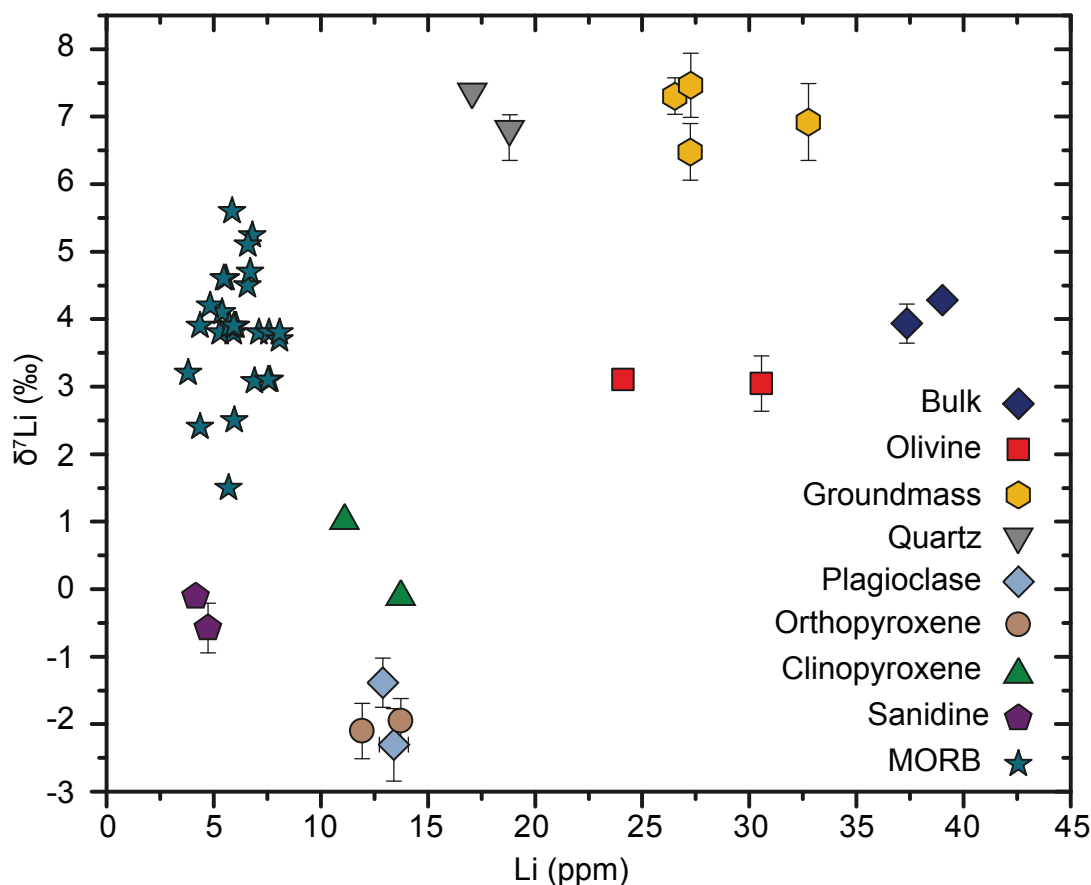


Fig. 2.7: Plot of $\delta^7\text{Li}$ versus Li concentrations for different mineral separates and bulk rock samples from MFT. Error bars correspond to 2 SD uncertainty on the $\delta^7\text{Li}$ values (Table 1.1) and are shown where they exceed symbol size. Literature data (Moriguti and Nakamura, 1998; Elliott et al., 2006; Tomascak et al., 2008) for unaltered MORB samples are shown for comparison.

2.5 Discussion

2.5.1 Partitioning coefficients for Li in MFT

In contrast to more mafic systems, there has been relatively little work addressing the crystal/melt partitioning of Li in silicic magmatic systems. Based on >2,500 new analyses from this study combined with literature data for major and trace elements on MFT crystals and glasses, we can constrain in detail the inventory of Li in the MFT. Lithium is found in the following order of decreasing abundance: melt inclusions (243.7 ± 198.5 ppm; $n = 29$) > groundmass glass (43.1 ± 7.2 ppm; $n = 73$) > quartz (17.9 ± 3.9 ppm; $n = 718$) \approx plagioclase (17.3 ± 9.6 ppm; $n = 653$) \approx fayalite (16.2 ± 2.2 ppm; $n = 127$) > clinopyroxene (11.2 ± 1 ppm; $n = 259$) > orthopyroxene (8.3 ± 0.7 ppm; $n = 58$) \approx sanidine (5.8 ± 3.2 ppm; $n = 688$).

The significant difference between Li contents of quartz-hosted melt inclusions and the groundmass glass, both in our data from the MFT (Fig. 2.6) and from other rhyolites (Stix and Layne, 1996; Kent et al., 2007; Charlier et al., 2012; Hofstra et al., 2013) requires that Li readily passes into a fluid or vapour phase during the latest stages of magmatic evolution. This is supported by the concentrations of all other trace elements, especially those expected to be “immobile” during such degassing process (e.g., Nb, Ta, Zr, Hf, Y, REE), because they are similar between the melt inclusions and the groundmass glass. The range in Li contents of the melt inclusions from higher values down towards those approaching the

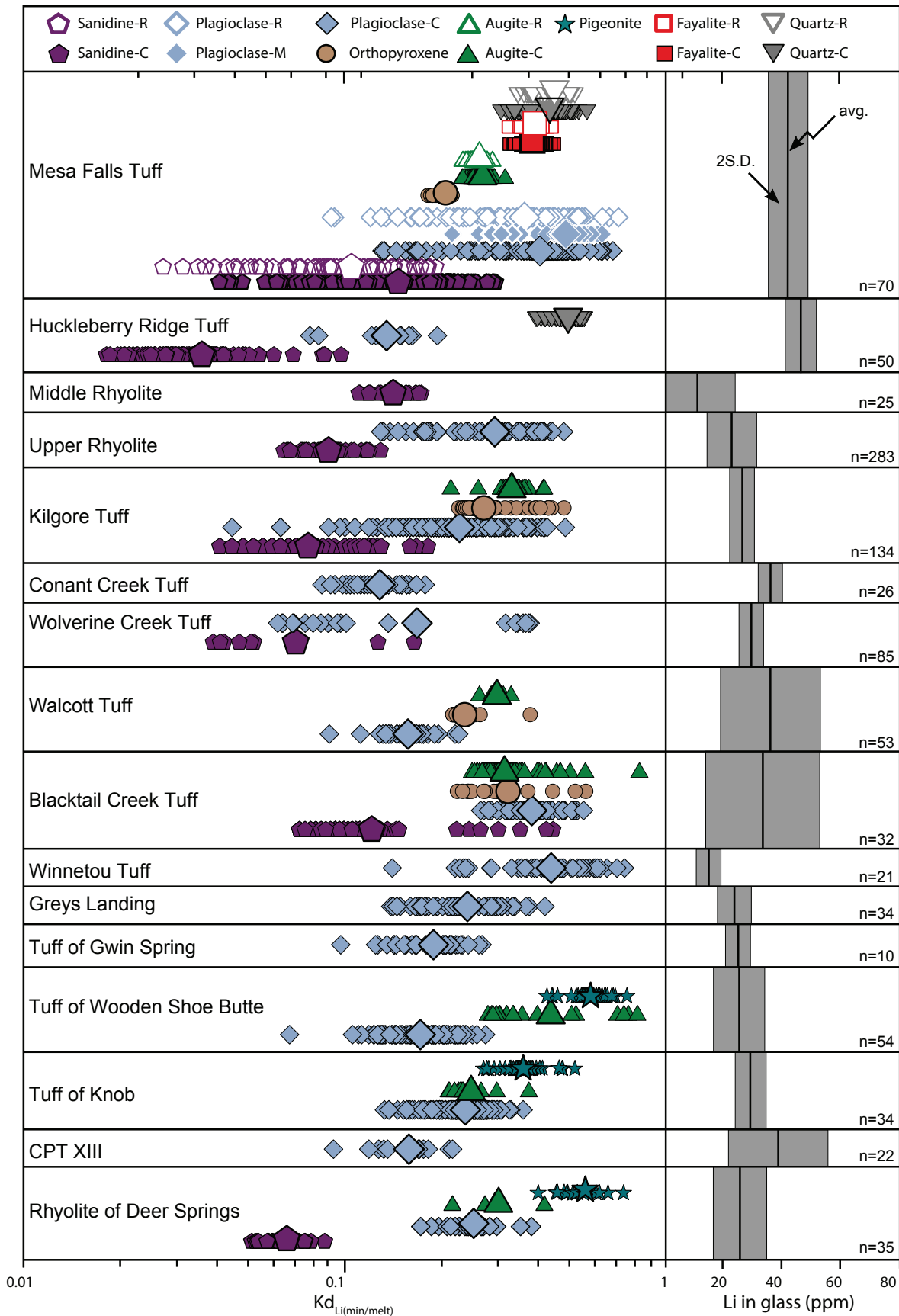


Fig. 2.8: Partitioning of Li between co-existing minerals and groundmass glass in rhyolitic systems, obtained using the filtering and calculation procedure described in text. On the left hand side of the diagram, apparent partition coefficients ($Kd_{Li(min/melt)}$) are shown for minerals from the MFT, compared to other rhyolites from the Yellowstone-Snake River Plain province from the literature (Szymanowski et al., 2015; Ellis et al., 2015; Ellis et al., 2017b, Ellis et al., 2018). Larger symbols indicate the average value of each mineral phase (with plagioclase

data obtained close to cracks excluded). MFT partition coefficients for plagioclase are subdivided into core (C), middle zone (M) and rim (R). On the right hand side of the diagram, Li concentration in the co-existing glass for each eruptive unit is presented as mean values (black bar) with their spread represented by 2 SD (grey bar).

groundmass values suggests either heterogeneous entrapment of inclusions throughout degassing, or ‘leakage’ of Li that may have occurred from some of the inclusions.

The effect of this loss of Li from the matrix melt on estimating partitioning behaviour requires further consideration since pairing groundmass glass values or melt inclusion values with minerals returns different apparent partition coefficients. In the case of the MFT plagioclase, the average outermost rim which is directly in contact with the melt (considered later) returns an apparent partition coefficient of 0.37 when paired with the groundmass glass but would give a partition coefficient of 0.06 using the average Li content of the ‘non-leaked’ quartz-hosted melt inclusion. Estimated partition coefficients from Ellis et al. (2018), using the model of Dohmen and Blundy (2014) for a Snake River Plain (SRP) rhyolite of similar composition (Tuff of Knob; Fig. 2.8) gave values of 0.3 for plagioclase/glass, while the experimental results of Iveson et al. (2018) returned partition coefficients of 0.23 ± 0.02 for hydrous rhyodacite. Given that the apparent partition coefficient of plagioclase paired with the groundmass glass is in good agreement with the experimentally determined partition coefficients, we prefer to use the groundmass glass values rather than the values for melt inclusions in our calculations. However, these apparent partition coefficients should be considered as maximum values.

With the new extensive dataset of trace element measurements from all major Li-bearing phases in the MFT, we can calculate the apparent partition coefficients for Li between groundmass glass and co-existing minerals (Fig. 2.8), taking into consideration that Li can be highly variable within each phase, the apparent partition coefficients based on MFT data are shown in Table 1.2.

Table 1.2: Apparent partition coefficients for Li in co-existing mineral phases of MFT.

MFT	Mean	Min	Max	n
Sanidine (R)	0.10	0.03	0.18	88
Sanidine (C)	0.14	0.04	0.28	600
Plagioclase (R)	0.37	0.11	0.67	112
Plagioclase (M)	0.50	0.24	0.63	123
Plagioclase (C)	0.41	0.15	0.67	368
Orthopyroxene	0.20	0.18	0.22	58
Clinopyroxene (R)	0.26	0.23	0.29	74
Clinopyroxene (C)	0.27	0.23	0.32	185
Fayalite (R)	0.39	0.31	0.58	53
Fayalite (C)	0.38	0.33	0.46	74
Quartz (R)	0.45	0.35	0.53	148
Quartz (C)	0.41	0.31	0.58	570

All values are calculated relative to groundmass glass. R, M and C stand for rim, middle and core, respectively.

To further understand the apparent distribution coefficients calculated for the minerals of MFT (Table 1.2) and, in more general, assess where Li is partitioned in hot (>850 °C) and dry ($<3.5\%$ H_2O) rhyolitic settings, we compared the new results with natural mineral and groundmass glass data from 15 other rhyolite bodies from the Yellowstone–Snake River Plain (YSRP) province (Szymanowski et

al., 2015; Ellis et al., 2015, Ellis et al., 2017b, Ellis et al., 2018). The majority of these ignimbrites are high-grade, lava-like, rheomorphic deposits, which underwent prolonged post-emplacement cooling on the Earth's surface. This post-eruptive history has the potential to significantly affect the inventory and behaviour of Li in mineral phases, with phenocrysts from slowly cooled microcrystalline lithologies having Li contents higher by up to a factor of 5 than their counterparts from the rapidly chilled vitrophyres (e.g., Ellis et al., 2015, Ellis et al., 2018). To minimise these effects for this comparison, we only use literature data from vitrophyric samples. To mitigate against the well-known potential of Li to be mobilised from volcanic glass (e.g., Hofstra et al., 2013), we took all glass Li compositions and imposed an iterative filter which excluded values outside 2 SD of the mean until no measurements were excluded, and used this 'filtered' Li concentration value as the glass composition. By using this iterative filter 3 out of 73 data points for MFT were excluded and on average 94% of the glass data for the other ignimbrites was included. All mineral data (without filtering) were then plotted with this new glass value (Fig. 2.8; also see Appendix A2: Supplementary data 2). The Li groundmass glass composition of the other ignimbrites shown in Fig. 2.8 varies from 4 to 54 ppm (average of 29 ppm).

2.5.1.1 Apparent partition coefficient for feldspar

Overall, these results reveal a coherent picture of where Li is partitioned in hot and dry rhyolitic settings. Considering only the units (seven out of fifteen) where data from co-existing plagioclase and sanidine are available, the overall average of all ignimbrites (Fig. 2.8) of their Kd_{plag} (0.28) is 2–3 times higher than that determined for Kd_{san} (0.10). Huckleberry Ridge Tuff has the lowest average Kd_{san} (0.04) whereas the sanidine cores of MFT have the highest average Kd_{san} of 0.14.

For quartz the overall average apparent Kd value is higher (0.43) than the overall average Kd_{plag} . The overall average Kd values are 0.48, 0.38, 0.29 and 0.26 for pigeonite, fayalite, augite and orthopyroxene, respectively. In the Tuff of Wood Shoe Butte, Tuff of Knob and Rhyolite of Deer Spring most Li is found in pigeonite whereas in Kilgore Tuff and Walcott Tuff, with pigeonite absent, clinopyroxene and orthopyroxene incorporate the highest amount of Li.

These results confirm that Li is a moderately incompatible element in all phases of rhyolitic systems, as has been shown for basaltic systems (e.g., Blundy et al., 1998; Brenan et al., 1998; Ottolini et al., 2009). For basaltic systems and phenocrysts in peridotite xenoliths, several partition coefficients have been established experimentally (summarised in Tomascak et al., 2016 and Penniston-Dorland et al., 2017). These studies show that in mantle minerals Li preferentially partitions into olivine ($Kd = 0.20\text{--}0.56$; Ryan, 1989; Brenan et al., 1998; Taura et al., 1998; McDade et al., 2003; Ottolini et al., 2009), to a lesser extent into plagioclase ($Kd = 0.15\text{--}0.7$; Ryan, 1989; Blundy et al., 1998; Aigner-Torres et al., 2007), followed by clinopyroxene ($Kd = 0.11\text{--}0.59$; Ryan, 1989; Hart and Dunn, 1993; Blundy et al., 1998; Brenan et al., 1998; McDade et al., 2003; Ottolini et al., 2009) and orthopyroxene ($Kd = 0.17\text{--}0.26$; Brenan et al., 1998; McDade et al., 2003; Ottolini et al., 2009). In rhyodacitic glass the partition coefficients that have been established experimentally show that Li preferentially partitions into clinopyroxene ($Kd = 0.26 \pm 0.04$; Iveson et al., 2018) followed by plagioclase ($Kd = 0.23 \pm 0.02$; Iveson et al., 2018). Thus, in terms of preference for Li, rhyolitic systems appear to mirror basaltic systems (e.g., Seitz and Woodland, 2000; Jeffcoate et al., 2007; Weyer and Seitz, 2012) with most Li found in olivine, followed by plagioclase, clinopyroxene and orthopyroxene.

2.5.1.2 Lithium distribution in fayalite

The major element compositions of fayalite in the MFT (Fa₈₇₋₈₉) are significantly more Fe-rich than most compositions studied both from natural samples, such as mantle xenoliths (see above) or in experimental studies (i.e., almost pure forsterite; Grant and Wood, 2010). The study of Grant and Wood (2010) employed constant olivine compositions, temperature, and pressure (at 1 atm) to study the effect of variable trivalent trace element composition of olivine on Kd(Li) values. Their results span two orders of magnitude between 0.01 and 1.04 with those from their DiFoScFe suite of experiments that are the most compositionally appropriate for natural basalts (~20 ppm Li and ~7–20 ppm Sc in the melt) returning Kd(Li) values of 0.1 to 0.23, somewhat lower than our average fayalite Kd(Li) value of 0.38. Interestingly, in these experiments, the highest-Fe olivine (at 9,380 ppm Fe) returned the highest Kd value suggesting that higher FeO contents in olivine are associated with an increased Li content in olivine (Caciagli et al., 2011). Several studies (e.g., Purton et al., 1997; Taura et al., 1998) have established that incorporation of Li into olivine requires a charge balance, preferentially from a coupled substitution with a trivalent cation (Fe, Al, Sc, Ga). Dohmen et al. (2010) verified experimentally that Li can partition into two sites in olivine, one being the octahedral site and the other interstitial sites.

This ‘two-site’ model for the incorporation of Li in olivine has previously been proposed to be responsible for unusual diffusional profiles and isotopic gradients observed in olivine as Li diffuses faster in interstitial sites than in the metal site (Dohmen et al., 2010; Tomascak et al., 2016). However, several authors (e.g., Jeffcoate et al., 2007; Parkinson et al., 2007) concluded that diffusion in the metal site is more common in nature. In the fayalite from MFT we do not observe any diffusion profiles; therefore, we speculate that only a minor proportion of Li is in the interstitial sites and the majority is in the metal site coupled to a slower moving trivalent cation that prevents the formation of diffusion profiles that can be found in plagioclase from MFT.

2.5.2 Lithium elemental variation within feldspars

An interesting feature of the feldspar data (Fig. 2.3, Fig. 2.4) is a resolvable decrease in the Li content in both plagioclase and, to a lesser extent, sanidine towards the crystal rims. Previous studies on Li partitioning into plagioclase show little agreement, with some suggesting a Li partition coefficient almost independent of plagioclase composition (Bindeman et al., 1998) while others indicate that the major element composition of plagioclase exerts a major control on Li partitioning (Coogan, 2011). In the case of the MFT, this discussion is rendered moot by the limited variability in An content of the plagioclase crystals (An₁₆₋₂₉ with only six out of 555 measurements above An₂₅). The decrease in Li at the feldspar rims could reflect either (1) a mixing event with Li-poor magma, or (2) some Li loss shortly prior to or during eruption. As there are no coherent relationships between decreasing Li to the rims of the feldspar crystals and either major or other trace elements (e.g., Rb, Sr, Ba) that would indicate a new magma input, the prior hypothesis can be excluded. In favour of the latter interpretation, low-Li rims in feldspar crystals were already suggested to reflect degassing (Giuffrida et al., 2018; Charlier et al., 2012). This interpretation is supported by the melt inclusion data discussed above, clearly showing that the melt underwent dramatic Li loss between its entrapment as inclusions in quartz and the quenching of the groundmass glass.

Although it is clear that Li leaves the melt phase at some point prior to quenching, the mechanism by which this translates into the patterns observed in MFT feldspars is uncertain. One explanation is that Li partitions in a fluid/vapour phase together with H₂O, and CO₂ while feldspar growth continues and the feldspar rims are growing in a liquid progressively depleted in Li. This is one possibility since feldspar stability is more sensitive to loss of water than that of the other mineral phases where low-Li rims are not observed. We would infer that the other mineral phases are growing up to the point of eruption, or the rims are much thinner than the laser spot size (<40 µm). An alternative explanation is suggested in which degassing outpaces crystallisation and the low-Li rims in feldspar reflect the attempts of the crystal to re-equilibrate with the changing conditions. In this case, the lack of gradients observed in quartz is a potential consequence of the relatively inert behaviour of Li within quartz. During slow post-eruption cooling in the interiors of thick deposits, Ellis et al. (2018) have shown that the Li content in plagioclase significantly increases (by a factor of five or more), yet the Li content of quartz crystals remains unaffected by post-eruptive processes. Lithium in quartz typically correlates with Al (Müller et al., 2003; Larsen et al., 2009; Rusk et al., 2011; Breiter et al., 2013) with Al³⁺ and Li¹⁺ acting as a part of coupled substitution for Si⁴⁺ in the quartz lattice (Rusk et al., 2011). Therefore, the lack of mobility of Li within quartz may result from coupling to a slowly diffusing element, as indicated by the absence of diffusion profiles in our data set. However, while our samples show no clear relationship between Li and excess Al (Fig. 2.2), the departure from a 1:1 line in terms of atomic Li:Al likely reflects a role of H⁺ in this substitution. Charlier et al. (2012) suggested yet another mechanism whereby Li⁺ diffuses into the quartz lattice along the *c*-axis channels and moves independently from more slowly moving cations. Interestingly, they also describe an increase of Li concentration towards quartz rims, which can also be observed in MFT quartz.

In contrast, none of the mafic phases in the MFT show the low-Li rim signal. Rhyolite-MELTS models for MFT bulk and glass compositions (see Appendix A2: Supplement data 2) suggest that feldspars, fayalite and clinopyroxene should be crystallising up to the point of eruption. Despite the suggestion by Ellis et al. (2018) that the most commonly used rates of Li diffusion in plagioclase determined experimentally are faster than those occurring in nature, Li diffusion in feldspar is thought to be faster than in clinopyroxene or olivine (Giletti and Shanahan, 1997; Spandler and O'Neill, 2010; Richer et al., 2014; Tomascak et al., 2016). Thus, if the formation of the volatile phase (into which Li partitions together with H₂O, and CO₂ depleting the residual melt) occurs shortly before, or perhaps synchronously with, eruption as recently suggested by Stock et al. (2016), then the differing rates of diffusive re-equilibration between feldspars and the mafic phases may explain their different Li profiles. Distinguishing between potential processes could be aided by in situ Li isotopic measurements. Unfortunately, these techniques are hampered by the lack of matrix-matched standards in the case of SIMS and remain in a development stage for femtosecond laser ablation instruments (e.g., Oeser et al., 2014).

2.5.3 Magmatic fractionation of lithium isotopes

Stable isotopic variability between co-existing minerals may reflect either equilibrium isotopic partitioning resulting from isotopes of differing mass being preferentially incorporated into different bonding environments, or kinetic fractionation arising from the trapping (in the volcanic case, by quenching) of transient isotopic signals that result from differential movement of different isotopes. The

rapid diffusion of lithium in most geologically relevant materials (Tomascak et al., 2016; Holycross et al., 2018) and the large mass difference between ${}^7\text{Li}$ and ${}^6\text{Li}$ render Li particularly susceptible to kinetic fractionation in magmatic systems. Thus, the question of the ultimate cause of the remarkable $\sim 10\%$ isotopic variability recorded for the MFT requires addressing. Unfortunately, in the Li isotopic system, there are so far no experimentally derived isotopic fractionation factors compared to other stable isotope systems, such as oxygen (e.g., O'Neil and Taylor Jr., 1969; Kulla and Anderson, 1978; Chiba et al., 1989). In the better-characterised mafic systems, Seitz et al. (2004) found a systematic relationship between mafic minerals representing the upper mantle, whereby the olivine shows similar $\delta^7\text{Li}$ values to MORB, and ortho- and clinopyroxene are isotopically lighter, with clinopyroxene being the isotopically lightest phase. By compiling the data from natural systems, Penniston-Dorland et al. (2017) proposed that mafic minerals with $\delta^7\text{Li}$ within $\pm 2\%$ of one another are in isotopic equilibrium. In terms of bulk compositions, Schuessler et al. (2009) have shown that differentiation from the mafic series at Hekla, Iceland, (average $\delta^7\text{Li} = +4.89 \pm 0.69\%$, 2 SD) to the silicic series ($\delta^7\text{Li} = +4.27 \pm 0.57\%$, 2 SD) causes limited Li isotopic fractionation.

MFT bulk whole rock $\delta^7\text{Li}$ values ($+3.9 - +4.3\%$) are similar to the published MORB data ($4 \pm 2\%$; Moriguti and Nakamura, 1998; Elliott et al., 2006; Tomascak et al., 2008). In the case of the MFT mafic minerals, clinopyroxene paired with orthopyroxene and clinopyroxene paired with fayalite return $\delta^7\text{Li}$ values within $\pm 2\%$ (Penniston-Dorland et al., 2017). Therefore, we infer that these pairs are in equilibrium. Only orthopyroxene and fayalite pairs are in apparent disequilibrium. This could be due to fayalite having heavier Li isotopic compositions through the incorporation of Fe^{3+} on the tetrahedral position. In forsteritic olivine, Li usually enters the octahedrally co-ordinated Mg site due to their almost identical ionic radii, or it fills the interstitial sites (Dohmen et al., 2010). However, in fayalitic olivine, it is also possible to substitute Fe^{3+} or Al^{3+} for Si^{4+} with Li^+ in the interstitial sites (as shown for quartz; Soltay and Henderson, 2005) and, therefore, occurring in tetrahedral co-ordination. This would lead to the preferential incorporation of ${}^7\text{Li}$ over ${}^6\text{Li}$ and explain the isotopically heavy values for the fayalite compared to pyroxenes. To estimate the amount of Fe^{3+} occupying the tetrahedral position is beyond the scope of this paper as it would require carefully characterised experiments because Fe^{3+} in olivine strongly depends on the fayalite content, $f\text{O}_2$ and temperature (Dohmen and Chakraborty, 2007).

Quartz and groundmass glass separates from the MFT return the isotopically heaviest values, where Li is expected to occur in tetrahedral co-ordination (e.g., Soltay and Henderson, 2005). We note here that the solution measurements for groundmass glass are systematically lower in Li content than the LA-ICP-MS measurements. When a broad range of trace elements for groundmass glass are compared between the dissolutions and in situ data (see Appendix A1: Supplementary data 1) it is apparent that the groundmass separates contained some trace of sanidine and Fe-Ti-oxides that were too small to be separated. This slight contamination means that the quoted Li abundances and $\delta^7\text{Li}$ values are likely slightly too low for the groundmass glass. The recognition of this effect also helps removing the issue of the bulk MFT having a higher Li abundance than any of its individual components. If Li concentration of the groundmass glass is taken from the LA-ICP-MS measurements, then mass balance constraints are satisfied. Mineral phases in which Li is octahedrally co-ordinated (e.g. mafics and feldspars) are isotopically lighter, which confirms that the $\delta^7\text{Li}$ variability could be a consequence of the co-ordination of Li

in the different mineral phases, consistent with more general findings (e.g., Teng et al., 2006; Wunder et al., 2006; Magna et al., 2016).

The potential for the groundmass glass $\delta^7\text{Li}$ to have undergone large and rapid shifts as a result of degassing makes it difficult to assess what the equilibrium melt–mineral Li isotopic fractionation should be. Recent studies investigating stable isotopic behaviour during volcanic degassing have suggested that where bubble growth is diffusion-limited, an isotopic fractionation arising from the variable diffusivities of the different isotopes in the melt may occur (Fortin et al., 2017; Watson, 2017). The models of Watson (2017) and Holycross et al. (2018) suggest that Li isotopic fractionations arising from degassing may be as large as 20‰. If the Li depletion in feldspar rims is a result of degassing, then intra-mineral isotopic variability likely exists and the bulk mineral $\delta^7\text{Li}$ values contain some component of kinetic fractionation. The other phases that show no zonation in Li abundances (i.e., mafic phases, quartz) may better preserve the equilibrium pre-eruptive $\delta^7\text{Li}$ signature.

2.6 Conclusions and future perspectives

The extensive MFT dataset allows, for the first time, the Li budget of a rhyolitic magma to be defined. Lithium is variably incompatible in all phases occurring in the MFT with average Li contents in the liquid from ~250 ppm (melt inclusions) to ~40 ppm (groundmass glass), and major mineral phases ranging from quartz (mean ~18 ppm) to sanidine (mean ~6 ppm). The apparent partitioning behaviour observed in the MFT is reproduced from glassy samples from a number of other rhyolites of the Yellowstone-Snake River Plain province, suggesting these values may approach mineral–melt equilibrium. Intra-crystal variations in Li abundances in plagioclase and sanidine are interpreted as reflecting pre/syn eruptive degassing and likely impart a kinetic fractionation on the Li isotopic signature. Lithium isotopic measurements on bulk mineral separates display a remarkable $\delta^7\text{Li}$ variation of almost 10‰ from $\delta^7\text{Li}$ of $+7.46 \pm 0.47\text{‰}$ in groundmass glass to $\delta^7\text{Li}$ of $-2.31 \pm 0.54\text{‰}$ in plagioclase. Such variations will require further investigation with *in situ* methods.

The highly elevated Li abundances in MFT melt inclusions (as also reported in studies of other rhyolites; Hofstra et al., 2013; Benson et al., 2017) and the low-Li rims on feldspar crystals together make a compelling case that between melt inclusion entrapment and quenching of the glass at eruption the majority of Li is lost from the system. The fate of this ‘lost-Li’ remains a key question – does it pass into a vapour phase together with H_2O , and CO_2 (and so is ultimately lost from the system), or does it pass into a magmatic brine (allowing it to be ‘pre-concentrated’) and potentially be a source for economic deposits? Understanding the extent to which these processes occur and the conditions favouring Li passing to a gas phase as opposed to a brine will require a carefully planned campaign of experimental petrology.

Despite the general agreement that evolved magmas either directly or indirectly appear to be crucial to the generation of economic lithium deposits (Kesler et al., 2012), this study represents the first attempt to define the various reservoirs for Li. For hot, dry rhyolites (and we note that similar studies involving rhyolites from subduction zones which follow different fractionation trajectories with different mineral assemblages would be illuminating) it appears that 20–60 ppm Li is a characteristic abundance for the quenched groundmass glass. Particularly this has a bearing on whether leaching of

volcanic rocks alone could be sufficient or magmatic fluids are required to form economically important Li deposits.

Acknowledgements

This work was supported by the Swiss National Science Foundation (grant 200021_166281 to BE). We thank Sebastian Cionoiu for help with the Raman measurements and Marcel Guillong for assistance in generating the LA-ICP-MS data. We thank Ralf Dohmen and Peter Ulmer for inspiring discussions. The manuscript benefited from detailed reviews by Gail Mahood and two anonymous reviewers. Don Dingwell is acknowledged for editorial handling

2.7 References

- Aigner-Torres, M., Blundy, J., Ulmer, P., Pettke, T., 2007. Laser Ablation ICPMS study of trace element partitioning between plagioclase and basaltic melts: an experimental approach. *Contrib. Mineral. Petrol.* 153 (6), 647–667.
- Audétat, A., Garbe-Schönberg, D., Kronz, A., Pettke, T., Rusk, B., Donovan, J.J., Lowers, H.A., 2015. Characterisation of a natural quartz crystal as a reference material for microanalytical determination of Ti, Al, Li, Fe, Mn, Ga and Ge. *Geostand. Geoanal. Res.* 39 (2), 171–184.
- Beck, P., Chaussidon, M., Barrat, J.A., Gillet, P., Bohn, M., 2006. Diffusion induced Li isotopic fractionation during the cooling of magmatic rocks: the case of pyroxene phenocrysts from Nakhilite meteorites. *Geochim. Cosmochim. Acta* 70 (18), 4813–4825.
- Benson, T.R., Coble, M.A., Rytuba, J.J., Mahood, G.A., 2017. Lithium enrichment in intracontinental rhyolite magmas leads to Li deposits in Caldera Basins. *Nat. Commun.* 8 (1), 270. <https://doi.org/10.1038/s41467-017-00234-y>.
- Bindeman, I.N., Davis, A.M., Drake, M.J., 1998. Ion microprobe study of plagioclase-basalt partition experiments at natural concentration levels of trace elements. *Geochim. Cosmochim. Acta* 62 (7), 1175–1193.
- Blundy, J.D., Robinson, J.A.C., Wood, B.J., 1998. Heavy REE are compatible in clinopyroxene on the spinel lherzolite solidus. *Earth Planet. Sci. Lett.* 160, 493–504.
- Breiter, K., Ackerman, L., Svojtka, M., Müller, A., 2013. Behavior of trace elements in quartz from plutons of different geochemical signature: a case study from the Bohemian Massif, Czech Republic. *Lithos* 175–176, 54–67.
- Brenan, J.M., Neroda, E., Lundstrom, C.C., Shaw, H.F., Ryerson, F.J., Phinney, D.L., 1998. Behaviour of boron, beryllium, and lithium during melting and crystallization: constraints from mineral–melt partitioning experiments. *Geochim. Cosmochim. Acta* 62 (12), 2129–2141.
- Cabato, J., Altherr, R., Ludwig, T., Meyer, H.P., 2013. Li, Be, B concentrations and $\delta^7\text{Li}$ values in plagioclase phenocrysts of dacites from Nea Kameni (Santorini, Greece). *Contrib. Mineral. Petrol.* 165 (6), 1135–1154.
- Caciagli, N., Brenan, J.M., McDonough, W.F., Phinney, D., 2011. Mineral–fluid partitioning of lithium and implications for slab–mantle interaction. *Chem. Geol.* 280 (2–3), 384–398.
- Charlier, B.L.A., Morgan, D.J., Wilson, C.J.N., Wooden, J.L., Allan, A.S.R., Baker, J.A., 2012. Lithium concentration gradients in feldspar and quartz record the final minutes of magma ascent in an explosive super-eruption. *Earth Planet. Sci. Lett.* 319–320, 218–227.
- Chiba, H., Chacko, T., Clayton, R.N., Goldsmith, J.R., 1989. Oxygen isotope fractionation involving diopside, magnetite, and calcite: application to geothermometry. *Geochim. Cosmochim. Acta* 53 (11), 2985–2995.
- Christiansen, R.L., 2001. The Quaternary and Pliocene Yellowstone Plateau Volcanic Field of Wyoming, Idaho, and Montana. US Geological Survey (Professional Paper 729-G).
- Christiansen, R.L., Blank, R.Jr, 1972. Volcanic stratigraphy of the Quaternary rhyolite plateau in Yellowstone National Park. US Geological Survey (Professional Papers 729-B).
- Coogan, L.A., 2011. Preliminary experimental determination of the partitioning of lithium between plagioclase crystals of different anorthite contents. *Lithos* 125 (1–2), 711–715.
- Coogan, L.A., Kasemann, S.A., Chakraborty, S., 2005. Rates of hydrothermal cooling of new oceanic upper crust derived from lithium-geospeedometry. *Earth Planet. Sci. Lett.* 240 (2), 415–424.
- Dohmen, R., Blundy, J., 2014. A predictive thermodynamic model for element partitioning between plagioclase and melt as a function of pressure, temperature and composition. *Am. J. Sci.* 314 (9), 1319–1372.
- Dohmen, R., Chakraborty, S., 2007. Fe-Mg diffusion in olivine II: point defect chemistry, change of diffusion mechanisms and a model for calculation of diffusion coefficients in natural olivine. *Phys. Chem. Miner.* 34 (6), 409–430.
- Dohmen, R., Kasemann, S.A., Coogan, L.A., Chakraborty, S., 2010. Diffusion of Li in olivine. Part 1: experimental observations and a multiple species diffusion model. *Geochim. Cosmochim. Acta* 74 (1), 274–292.
- Elliott, T., Thomas, A., Jeffcoate, A., Niu, Y., 2006. Lithium isotope evidence for subduction-enriched mantle in the source of Mid-Ocean-Ridge Basalts. *Nature* 443 (7111), 565–568.
- Ellis, B.S., Wolff, J.A., Boroughs, S., Mark, D.F., Starkel, W.A., Bonnicksen, B., 2013. Rhyolitic volcanism of the Central Snake River Plain: a review. *Bull. Volcanol.* 75 (8), 745. <https://doi.org/10.1007/s00445-013-0745-y>.

- Ellis, B.S., Cordonnier, B., Rowe, M.C., Szymanowski, D., Bachmann, O., Andrews, G.D.M., 2015. Groundmass crystallisation and cooling rates of lava-like ignimbrites: the Grey's landing ignimbrite, southern Idaho, USA. *Bull. Volcanol.* 77 (10), 87. <https://doi.org/10.1007/s00445-015-0972-5>.
- Ellis, B.S., Mark, D.F., Troch, J., Bachmann, O., Guillong, M., von Kent, A.J.R., Quadt, A., 2017a. Split-Grain $^{40}\text{Ar}/^{39}\text{Ar}$ dating: integrating temporal and geochemical data from crystal cargoes. *Chem. Geol.* 457, 15–23.
- Ellis, B.S., Szymanowski, D., Wotzlav, J.F., Schmitt, A.K., Bindeman, I.N., Troch, J., Harris, C., Guillong, M., 2017b. Post-caldera volcanism at the Heise volcanic field: implications for petrogenetic models. *J. Petrol.* 58, 115–136.
- Ellis, B.S., Szymanowski, D., Magna, T., Neukampf, J., Dohmen, R., Bachmann, O., Ulmer, P., Guillong, M., 2018. Post-eruptive mobility of lithium in volcanic rocks. *Nat. Commun.* 9, 3228. <https://doi.org/10.1038/s41467-018-05688-2>.
- Flesch, G.D., Anderson Jr., A.R., Svec, H.J., 1973. A secondary isotopic standard for $^6\text{Li}/^7\text{Li}$ determinations. *Int. J. Mass Spectrom. Ion Phys.* 12 (3), 265–272.
- Fortin, M.A., Watson, B., Stern, R., 2017. The isotope mass effect on chlorine diffusion in dacite melt, with implications for fractionation during bubble growth. *Earth Planet. Sci. Lett.* 480, 15–24.
- Gansecki, C.A., Mahood, G.A., McWilliams, M., 1998. New ages for the climactic eruptions at Yellowstone: single-crystal $^{40}\text{Ar}/^{39}\text{Ar}$ dating identifies contamination. *Geology* 26 (4), 343–346.
- Giletti, B.J., Shanahan, T.M., 1997. Alkali diffusion in plagioclase feldspar. *Chem. Geol.* 139 (1–4), 3–20.
- Giuffrida, M., Viccaro, M., Ottolini, L., 2018. Ultrafast syn-eruptive degassing and ascent trigger high-energy basic eruptions. *Sci. Rep.* 8 (1), 147. <https://doi.org/10.1038/s41598-017-18580-8>.
- Grant, K.J., Wood, B.J., 2010. Experimental study of the incorporation of Li, Sc, Al and other trace elements into olivine. *Geochim. Cosmochim. Acta* 74, 2412–2428.
- Guillong, M., Meier, D.K., Allan, M.M., Heinrich, C.A., Yardley, B.W.D., 2008. SILLS: A Matlab-Based Program for the Reduction of Laser Ablation ICP–MS Data of Homogeneous Materials and Inclusions. Vol. 40. Mineralogical Association of Canada Short Course, Vancouver, B.C, pp. 328–333.
- Hart, S.R., Dunn, T., 1993. Experimental cpx/melt partitioning of 24 trace elements. *Contrib. Mineral. Petrol.* 113, 1–8.
- Hofstra, A.H., Todorov, T.I., Mercer, C.N., Adams, D.T., Marsh, E.E., 2013. Silicate melt inclusion evidence for extreme pre-eruptive enrichment and post-eruptive depletion of lithium in silicic volcanic rocks of the western United States: implications for the origin of lithium-rich brines. *Econ. Geol.* 108 (7), 1691–1701.
- Holycross, M.E., Watson, E.B., Richter, F.M., Villeneuve, J., 2018. Diffusive fractionation of Li isotopes in wet, silicic melts. *Geochem. Perspect. Lett.* 6, 39–42.
- Hooper, P.R., Camp, V.E., Reidel, S.P., Ross, M.E., 2007. The origin of the Columbia River flood basalt province: plume versus nonplume models. In: *Special Paper 430: Plates, Plumes and Planetary Processes*. 430. Geological Society of America, pp. 635–668.
- Iveson, A.A., Rowe, M.C., Webster, J.D., Neill, O.K., 2018. Amphibole-, clinopyroxene-, and plagioclase-melt partitioning of trace and economic metals in halogen-bearing rhyodacitic melts. *J. Petrol.* 59 (8), 1579–1604.
- Jeffcoate, A.B., Elliott, T., Kasemann, S.A., Ionov, D., Cooper, K., Brooker, R., 2007. Li isotope fractionation in peridotites and mafic melts. *Geochim. Cosmochim. Acta* 71, 202–218.
- Jochum, K.P., Weis, U., Stoll, B., Kuzmin, D., Yang, Q., Raczek, I., Jacob, D.E., Stracke, A., Birbaum, K., Frick, D.A., Günther, D., Enzweiler, J., 2011. Determination of reference values for NIST SRM 610–617 glasses following ISO guidelines. *Geostand. Geoanal. Res.* 35, 397–429.
- Kent, A.J.R., Blundy, J., Cashman, K.V., Cooper, K.M., Donnelly, C., Pallister, J.S., Reagan, M., Rowe, M.C., Thornber, C.R., 2007. Vapor transfer prior to the October 2004 eruption of Mount St. Helens, Washington. *Geology* 35 (3), 231–234.
- Kesler, S.E., Gruber, P.W., Medina, P.A., Keoleian, G.A., Everson, M.P., Wallington, T.J., 2012. Global lithium resources: relative importance of pegmatite, brine and other deposits. *Ore Geol. Rev.* 48, 55–69.
- Kulla, J.B., Anderson, T.F., Zartman, R.E., 1978. Experimental oxygen isotope fractionation between kaolinite and water. In: *Short Papers of the 4th Int. Conf. on Geochronology, Cosmochronology, and Isotope Geology*. 78–70. US Geol. Surv. Open File Rep, pp. 234–235.
- Lanphere, M.A., Champion, D.E., Christiansen, R.L., Izett, G.A., Obradovich, J.D., 2002. Revised ages for tuffs of the Yellowstone Plateau Volcanic field: assignment of the Huckleberry Ridge Tuff to a new geomagnetic polarity event. *Geol. Soc. Am. Bull.* 114 (5), 559–568.
- Larsen, R.B., Jacamon, F., Krantz, A., 2009. Trace element chemistry and textures of quartz during the magmatic-hydrothermal transition of Oslo Rift granites. *Mineral. Mag.* 73, 691–707.

- Leeman, W.P., Tonarini, S., Chan, L.H., Borg, L.E., 2004. Boron and lithium isotopic variations in a hot subduction zone—the southern Washington Cascades. *Chem. Geol.* 212 (1), 101–124.
- Lowenstern, J.B., Smith, R.B., Hill, D.P., 2006. Monitoring super-volcanoes: geophysical and geochemical signals at Yellowstone and other large caldera systems. *Philos. Trans. R. Soc. London, Ser. A* 364 (1845), 2055–2072.
- Magna, T., Wiechert, U.H., Halliday, A.N., 2004. Low-blank isotope ratio measurement of small samples of lithium using multiple-collector ICPMS. *Int. J. Mass Spectrom.* 239 (1), 67–76.
- Magna, T., Wiechert, U., Grove, T.L., Halliday, A.N., 2006. Lithium isotope fractionation in the southern Cascadia subduction zone. *Earth Planet. Sci. Lett.* 250 (3), 428–443.
- Magna, T., Novák, M., Cempírek, J., Janoušek, V., Ullmann, C.V., Wiechert, U., 2016. Crystallographic control on lithium isotope fractionation in Archean to Cenozoic lithium-cesium-tantalum pegmatites. *Geology* 44 (8), 655–658.
- Marschall, H.R., Wanless, D.V., Shimizu, N., Pogge von Strandmann, P.A.E., Elliott, T., Monteleone, B.D., 2017. The boron and lithium isotopic composition of Mid-Ocean Ridge Basalts and the mantle. *Geochim. Cosmochim. Acta* 207, 102–138.
- McDade, P., Blundy, J., Wood, B.J., 2003. Trace element partitioning on the Tinaquillo Lherzolite solidus at 1.5 GPa. *Phys. Earth Planet. Inter.* 139, 129–147.
- McDonough, W.F., Sun, S.S., 1995. The composition of the Earth. *Chem. Geol.* 120, 223–253.
- Moriguti, T., Nakamura, E., 1998. Across-arc variation of Li isotopes in lavas and implications for crust/mantle recycling at subduction zones. *Earth Planet. Sci. Lett.* 163 (1–4), 167–174.
- Müller, A., Wiedenbeck, M., Van den Kerkhof, A.M., Kronz, A., Simon, K., 2003. Trace elements in quartz: a combined electron microprobe, secondary ion mass spectrometry, laser-ablation ICPMS, and cathodoluminescence study. *Eur. J. Mineral.* 15, 747–763.
- Nash, B.P., Perkins, M.E., Christensen, J.N., Lee, D.C., Halliday, A.N., 2006. The Yellowstone hotspot in space and time: Nd and Hf isotopes in silicic magmas. *Earth Planet. Sci. Lett.* 247 (1–2), 143–156.
- Oeser, M., Weyer, S., Horn, I., Schuth, S., 2014. High-precision Fe and Mg isotope ratios of silicate reference glasses determined in situ by femtosecond LA-MC-ICP-MS and by solution nebulisation MC-ICP-MS. *Geostand. Geoanal. Res.* 38 (3), 311–328.
- O’Neil, J.R., Taylor Jr., H.P., 1969. Oxygen isotope equilibrium between muscovite and water. *J. Geophys. Res.* B74, 6012–6022.
- Ottolini, L., Laporte, D., Raffone, N., Devidal, J.L., Le Fevre, B., 2009. New experimental determination of Li and B partition coefficients during upper mantle partial melting. *Contrib. Mineral. Petrol.* 157, 313–325.
- Parkinson, I.J., Hammond, S.J., James, R.H., Rogers, N.W., 2007. High-temperature lithium isotope fractionation: insights from lithium isotope diffusion in magmatic systems. *Earth Planet. Sci. Lett.* 257 (3–4), 609–621.
- Pearce, N.J.G., Westgate, J.A., Perkins, W.T., 1996. Developments in the analysis of volcanic glass shards by laser ablation ICP-MS: quantitative and single internal standard-multielement methods. *Quat. Int.* 34–36, 213–227.
- Penniston-Dorland, S., Liu, X.M., Rudnick, R.L., 2017. Lithium isotope geochemistry. *Rev. Mineral. Geochem.* 82 (1), 165–217.
- Perkins, M.E., Nash, B.P., 2002. Explosive silicic volcanism of the Yellowstone hotspot: the ash fall tuff record. *Geol. Soc. Am. Bull.* 114 (3), 367–381.
- Pistiner, J.S., Henderson, G.M., 2003. Lithium-isotope fractionation during continental weathering processes. *Earth Planet. Sci. Lett.* 214 (1–2), 327–339.
- Plank, T., 2014. The chemical composition of subducting sediments. In: Rudnick, R.L. (Ed.), *Treatise on Geochemistry*, 2nd edn., 4, 607–629.
- Pogge von Strandmann, P.A.E., Burton, K.W., James, R.H., van Calsteren, P., Gislason, S.R., 2010. Assessing the role of climate on uranium and lithium isotope behaviour in rivers draining a basaltic terrain. *Chem. Geol.* 270, 227–239.
- Pogge von Strandmann, P.A.E., Frings, P.J., Murphy, M.J., 2017. Lithium isotope behaviour during weathering in the Ganges Alluvial Plain. *Geochim. Cosmochim. Acta* 198, 17–31.
- Purton, J.A., Allan, N.L., Blundy, J.D., 1997. Calculated solution energies of heterovalent cations in forsterite and diopside: implications for trace element partitioning. *Geochim. Cosmochim. Acta* 61 (18), 3927–3936.

- Richer, F., Watson, E.B., Chaussidon, M., Mendybaev, R., Ruscitto, D., 2014. Lithium isotope fractionation by diffusion in minerals. Part 1: pyroxenes. *Geochim. Cosmochim. Acta* 126, 352–370.
- Rivera, T.A., Schmitz, M.D., Jicha, B.R., Crowley, J.L., 2016. Zircon petrochronology and $^{40}\text{Ar}/^{39}\text{Ar}$ sanidine dates for the Mesa Falls Tuff: crystal-scale records of magmatic evolution and the short lifespan of a large Yellowstone magma chamber. *J. Petrol.* 57 (9), 1677–1704.
- Rivera, T.A., Furlong, R., Vincent, J., Gardiner, S., Jicha, B.J., Schmitz, M.D., Lippert, P.C., 2018. Volcanism at 1.45 Ma within the Yellowstone volcanic field, United States. *J. Volcanol. Geotherm. Res.* 357, 224–238.
- Rubin, A.E., Cooper, K.M., Till, C.B., Kent, A.J.R., Costa, F., Bose, M., Cole, J., 2017. Rapid cooling and cold storage in a silicic magma reservoir recorded in individual crystals. *Science* 356 (6343), 1154–1156.
- Rudnick, R.L., Tomascak, P.B., Njo, H.B., Gardner, L.R., 2004. Extreme lithium isotopic fractionation during continental weathering revealed in Saprolites from South Carolina. *Chem. Geol.* 212 (1–2), 45–57.
- Rusk, B., Koenig, A., Lowers, H., 2011. Visualizing trace element distribution in quartz using cathodoluminescence, electron microprobe, and laser ablation-inductively coupled plasma-mass spectrometry. *Am. Mineral.* 96 (5–6), 703–708.
- Ryan, J.G., 1989. The Systematics of Lithium, Beryllium and Boron in Young Volcanic Rocks (PhD Dissertation). Columbia University, New York, NY 313 pp.
- Schuessler, J.A., Schoenberg, R., Sigmarsson, O., 2009. Iron and lithium isotope systematics of the Hekla volcano, Iceland—evidence for Fe isotope fractionation during magma differentiation. *Chem. Geol.* 258 (1), 78–91.
- Seitz, H.M., Woodland, A.B., 2000. The distribution of lithium in peridotitic and pyroxenitic mantle lithologies – an Indicator of magmatic and metasomatic processes. *Chem. Geol.* 166 (1–2), 47–64.
- Seitz, H.M., Brey, G.P., Lahaye, Y., Durali, S., Weyer, S., 2004. Lithium isotopic signatures of peridotite xenoliths and isotopic fractionation at high temperature between olivine and pyroxenes. *Chem. Geol.* 212, 163–177.
- Soltay, L.G., Henderson, G.S., 2005. Structural differences between lithium silicate and lithium germanate glasses by Raman spectroscopy. *Phys. Chem. Glasses* 46, 381–384.
- Spandler, C., O'Neill, H.S., 2010. Diffusion and partition coefficients of minor and trace elements in San Carlos olivine at 1,300 °C with some geochemical implications. *Contrib. Mineral. Petrol.* 159, 791–818.
- Stix, J., Layne, G.D., 1996. Gas saturation and evolution of volatile and light lithophile elements in the bandelier magma chamber between two caldera-forming eruptions. *J. Geophys. Res. Solid Earth* 101 (B11), 25181–25196.
- Stock, M.J., Humphreys, M.C.S., Smith, V.C., Isaia, R., Pyle, D.M., 2016. Late-stage volatile saturation as a potential trigger for explosive volcanic eruptions. *Nat. Geosci.* 9, 249–254.
- Szymanowski, D., Ellis, B.S., Bachmann, O., Guillong, M., Phillips, W.M., 2015. Bridging basalts and rhyolites in the Yellowstone–Snake River Plain volcanic province: the elusive intermediate step. *Earth Planet. Sci. Lett.* 415, 80–89.
- Taura, H., Yurimoto, H., Kurita, K., Sueno, S., 1998. Pressure dependence on partition coefficients for trace elements between olivine and the coexisting melts. *Phys. Chem. Miner.* 25, 469–484.
- Teng, F.Z., McDonough, W.F., Rudnick, R.L., Dalpé, C., Tomascak, P.B., Chappell, B.W., Gao, S., 2004. Lithium isotopic composition and concentration of the upper continental crust. *Geochim. Cosmochim. Acta* 68 (20), 4167–4178.
- Teng, F.Z., McDonough, W.F., Rudnick, R.L., Walker, R.J., 2006. Diffusion-driven extreme lithium isotopic fractionation in country rocks of the Tin Mountain pegmatite. *Earth Planet. Sci. Lett.* 243 (3), 701–710.
- Tomascak, P.B., Tera, F., Helz, R.T., Walker, R.J., 1999. The absence of lithium isotope fractionation during basalt differentiation: new measurements by multicollector sector ICP-MS. *Geochim. Cosmochim. Acta* 63, 907–910.
- Tomascak, P.B., Langmuir, C.H., le Roux, P.J., Shirey, S.B., 2008. Lithium isotopes in global mid-ocean ridge basalts. *Geochim. Cosmochim. Acta* 72 (6), 1626–1637.
- Tomascak, P.B., Magna, T., Dohmen, R., 2016. *Advances in Lithium Isotope Geochemistry*. Springer International Publishing, Cham, Switzerland 195 pp.
- Troch, J., Ellis, B.S., Mark, D.F., Bindeman, I.N., Kent, A.J.R., Guillong, M., Bachmann, O., 2017. Rhyolite generation prior to a Yellowstone Supereruption: insights from the Island Park–Mount Jackson rhyolite series. *J. Petrol.* 58 (1), 29–52.
- Watson, E.B., 2017. Diffusive fractionation of volatiles and their isotopes during bubble growth in magmas. *Contrib. Mineral. Petrol.* 172 (8). <https://doi.org/10.1007/s00410-017-1384-7>. (paper 61).

- Weyer, S., Seitz, H.M., 2012. Coupled lithium- and iron isotope fractionation during magmatic differentiation. *Chem. Geol.* 294–295, 42–50.
- Wunder, B., Meixner, A., Romer, R.L., Heinrich, W., 2006. Temperature dependent isotopic fractionation of lithium between clinopyroxene and high pressure hydrous fluids. *Contrib. Mineral. Petrol.* 151, 112–120.

Chapter 3

Time scales of syn-eruptive volatile loss in silicic magmas quantified by Li-isotopes

J. Neukampf^{1*}, B.S. Ellis¹, O. Laurent², L.K. Steinmann³, T. Ubide⁴, M. Oeser³, T. Magna⁵, S. Weyer³, and O. Bachmann¹

¹Institute of Geochemistry and Petrology, ETH Zurich, CH-8092, Zurich, Switzerland

²CNRS, Géosciences Environnement Toulouse, Observatoire Midi-Pyrénées, F-31400 Toulouse, France

³Institut für Mineralogie, Leibniz Universität Hannover, D-30167, Hannover, Germany

⁴School of Earth and Environmental Sciences, University of Queensland, QLD 4072, Brisbane, Australia

⁵Czech Geological Survey, CZ-11821, Prague, Czech Republic

Published in *Geology*, 2020, vol. 49

ABSTRACT

Most explosive, silicic volcanoes spend thousands of years in repose between eruptive events. The timing of the switch from repose to eruption is key to interpreting monitoring signals and improving the safety of people living close to active volcanoes. We addressed this question using a novel technique based on lithium isotopic ($\delta^7\text{Li}$) and elemental concentration profiles within plagioclase crystals from the Mesa Falls Tuff of the Yellowstone volcanic system (Idaho and Wyoming, USA), constraining volatile degassing to occur on minimum time scales of tens of minutes prior to eruption. During this ephemeral time, Li abundances drop by a factor of four to 10 from crystal cores to rims, accompanied by an increase in $\delta^7\text{Li}$ of as much as 10‰, reflecting diffusion-driven equilibration between plagioclase cores and outgassed, Li-poor melt. New times scales obtained in this study show the potential for rapid syneruptive changes in the volatile inventory of magmas.

3.1 INTRODUCTION

A key aim of volcanology is to improve the forecasting of volcanic eruptions in order to safeguard millions of people who live in volcanically prolific regions. Understanding magma dynamics, particularly the time scales of bubble nucleation and magma degassing, which control eruptive explosivity (e.g., Sparks et al., 1994; Mangan and Sisson, 2000), can help minimise this hazard. The study of volcanic deposits remains fundamental to understanding and quantifying the processes occurring immediately prior to eruption (Humphreys et al., 2006; Cashman et al., 2017). This requires the ability to define and characterise the factors that lead to changes in chemical (major and trace elements, volatile contents) (Shea et al., 2015) and isotopic compositions in melt and associated crystals (Oeser et al., 2015). In particular, crystals in rapidly quenched, nonwelded deposits can record magmatic histories from storage in the magma chamber to eruption and provide information about changes in volatile concentration, magma composition, temperature, and pressure before and during eruptions (e.g., Sparks, 1978; Ellis et al., 2018).

The Yellowstone volcanic system (Idaho and Wyoming, USA) represents the archetypal supervolcano. Silicic volcanism at Yellowstone has predominantly produced rhyolitic lavas punctuated by three voluminous caldera-forming eruptions (Huckleberry Ridge Tuff, Mesa Falls Tuff, and Lava Creek Tuff) (Christiansen, 2001). The 1.3 Ma Mesa Falls Tuff (MFT; Fig. 3.1) represents a large-volume explosive event that produced a variably welded ignimbrite sheet overlying fallout deposits (Rivera et al., 2016). While the MFT is well characterised in many respects, the final processes that tipped the system from stability to eruption remain unknown.

The groundmass glass from the MFT is depleted in lithium (Li) (36–52 ppm) relative to quartz-hosted melt inclusions (70–397 ppm) (Neukampf et al., 2019). We propose that Li was lost with a H_2O -rich fluid upon syneruptive degassing. Although the fluid-melt partitioning behaviour of Li is debated, natural fluid-melt inclusion pairs consistently show that Li tends to partition in favour of a H_2O - and Cl-rich fluid phase, thereby depleting the melt in Li (Zajacz et al., 2008; Fiedrich et al., 2020), as supported by some experimental results (Webster et al., 1989). Kinetic isotopic fractionation has been proposed to occur between the faster-diffusing ^6Li and the slower-diffusing ^7Li during bubble formation, enriching the vapour in ^6Li and, conversely, the melt in ^7Li (Vlastélic et al., 2011). These processes, as

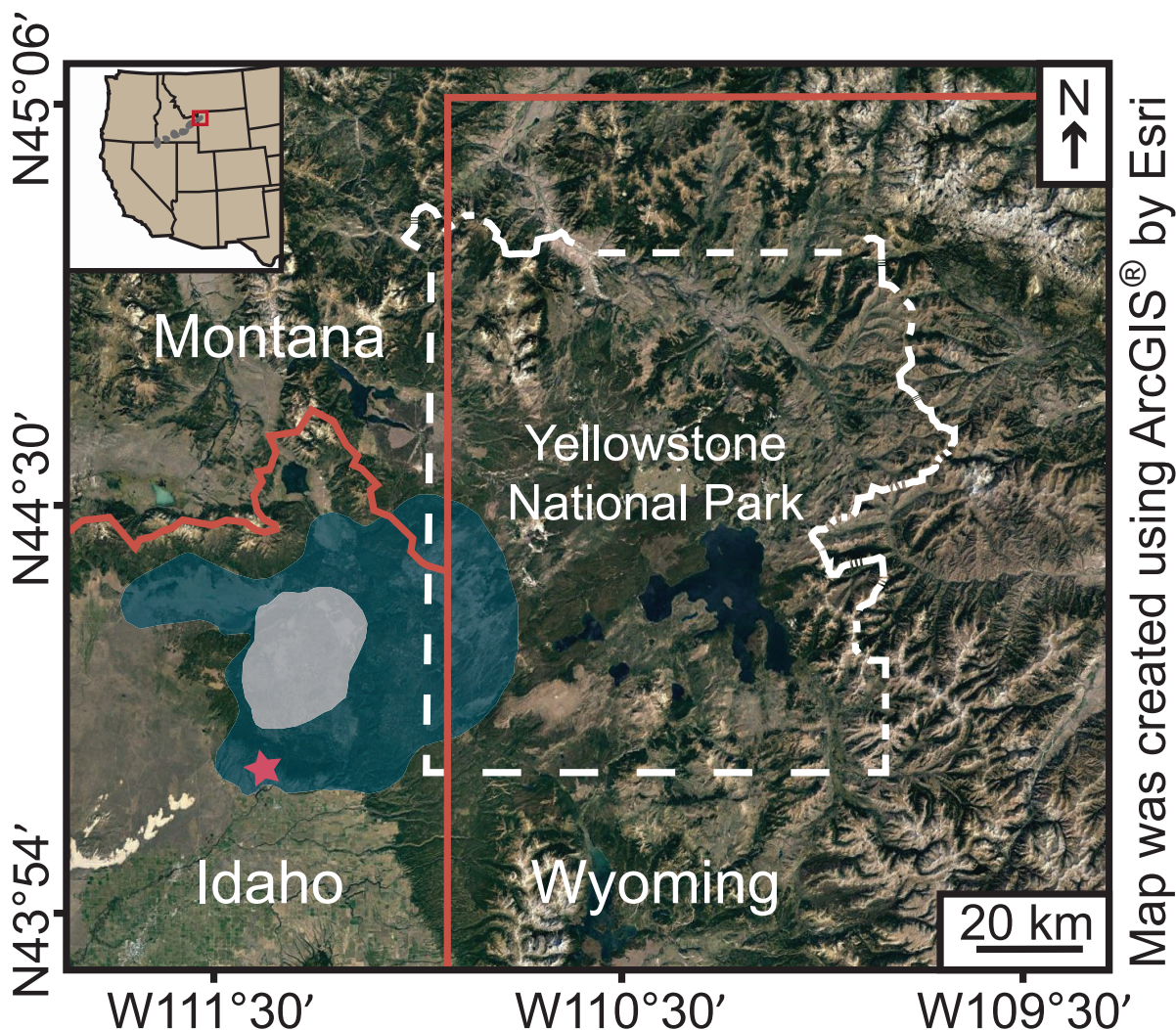


Fig. 3.1: Map showing sample location ($44^{\circ}7'8.49''\text{N}$, $111^{\circ}26'39.49''\text{W}$; Ellis et al., 2017) of Mesa Falls Tuff (in blue), indicated with a red star. Inferred Henry's Folk caldera (Christiansen, 2001) is in light gray, and state borders are in red.

shown experimentally (Holycross et al., 2018) and theoretically (Watson, 2017), can produce significant Li elemental and isotopic variations between groundmass glass and mineral phases as the system strives to re-establish equilibrium. The extent to which diffusion can homogenise these records reflects the time between onset and termination of diffusion upon quenching. Here, we use a novel technique combining Li concentration and Li stable-isotope ratios (Steinmann et al., 2020) in plagioclase phenocrysts from the MFT and applying diffusion modelling to constrain time scales of Li loss from the melt.

3.2 LITHIUM CONCENTRATION MAPS AND PROFILES

Seven plagioclase crystals from the non-welded portion of the MFT were geochemically characterised by electron microprobe and laser ablation inductively coupled plasma mass spectrometry (LA-ICPMS). Only plagioclase crystals rimmed by groundmass glass were used, to ensure that crystal rim measurements truly reflect plagioclase in contact with the surrounding melt. Lithium concentration maps obtained by LA-ICPMS (Figs. 3.2A and 3.2B) reveal homogeneous crystal interiors with high Li concentrations mantled by a narrow zone ($\leq 200 \mu\text{m}$) where Li contents continuously decrease toward crystal edges (Figs. 3.2C and 3.2D).

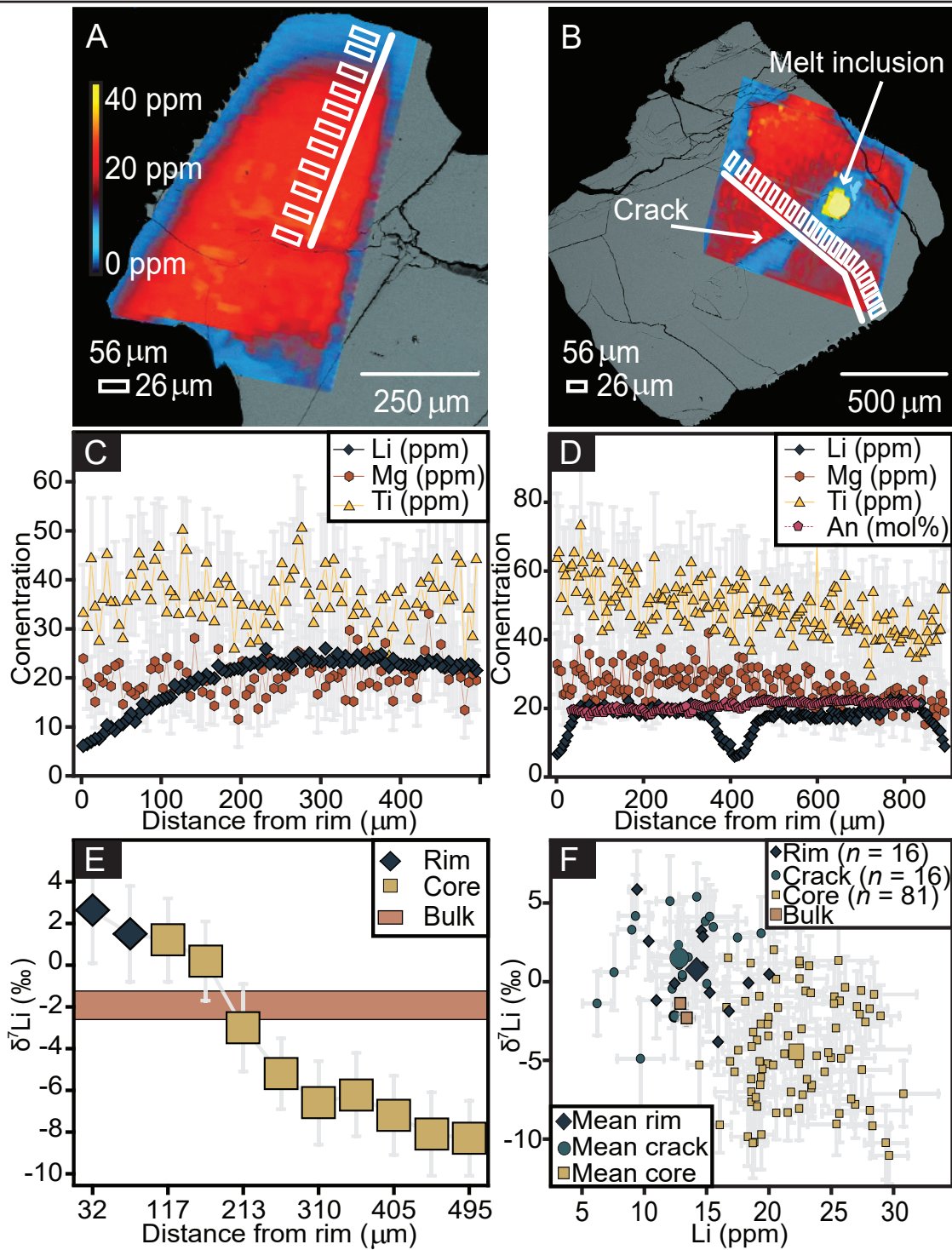


Fig. 3.2: Lithium elemental and isotopic zoning in Mesa Falls Tuff plagioclase (Yellowstone volcanic system, Idaho and Wyoming, USA). (A,B) Backscatter electron images combined with Li concentration maps (by laser ablation–inductively coupled plasma–mass spectrometry [LA-ICPMS]). White lines indicate measurement area of concentration profiles, and white boxes represent areas used for $\delta^7\text{Li}$ measurements. Representative plagioclase crystal with magmatic cracks is shown in B. (C,D) Concentration profiles measured from core to rim of crystals shown in A (grain 27 in the Supplemental Material) and B (grain 21 in the Supplemental Material), respectively, with Li (error within symbol size; two standard deviations, 2 SD) depletion toward the rim and magmatic crack (D) while other trace and major elements, e.g., magnesium (Mg) and titanium (Ti), and anorthite concentration (An), remain homogenous. Errors on the measurements are represented as grey error bars (2 SD). (E) $\delta^7\text{Li}$ profile within the crystal shown in A. $\delta^7\text{Li}$ value of bulk plagioclase separate (Neukampf et al., 2019) is illustrated with a brown bar. Symbol width represents size of laser spot (~ 55 μm). Errors on the measurements are represented as grey error bars (2 SD). (F) All $\delta^7\text{Li}$ measurements (2 SE) with corresponding Li concentrations. Large symbols represent average (mean) values of rims, cracks, and cores.

Concentration profiles through crystals confirm high-Li cores, from 12 to 33 ppm depending on the crystal (mean 22 ppm; $n = 1440$), decreasing to 19 to ~ 5 ppm at the very edge of the crystals (mean 12 ppm; $n = 208$). The anorthite content (An) varies between crystals (An 17–31) but is homogenous within grains, and all other major and trace elements lack any strong, systematic core-to-rim variation (Fig. 3.2C and 3.2D).

Some crystals exhibit Li depletion along cracks within the crystal interior similar to that in rims. These cracks likely formed due to depressurisation during eruptive ascent allowing melt inclusions to expand and fracture their host plagioclase (Fig. 3.2B). Interestingly, concentration profiles perpendicular to magmatic cracks return steeper depletion profiles (Fig. 3.2D) compared to measurements at crystal rims. This supports the interpretation that the cracks developed at a later stage during ascent, leading to shorter Li diffusion times.

3.3 *IN SITU* $\delta^7\text{Li}$ MEASUREMENTS

Lithium isotopic composition ($\delta^7\text{Li}$) was measured in situ using a femtosecond laser ablation system coupled to a multicollector ICPMS (fs-LA-MC-ICPMS) along transects following crystal zoning patterns. The $\delta^7\text{Li}$ profiles exhibit large but systematic differences (of as much as 10‰; Fig. 3.2E), with Li-poor plagioclase rims isotopically heavier (-3.8‰ to $+5.9\text{‰}$; mean $+1.0\text{‰} \pm 2.5\text{‰}$; two standard errors [2 SE], $n = 19$) than the Li-rich cores (-11‰ to $+2\text{‰}$; mean $-4.2\text{‰} \pm 2\text{‰}$; 2 SE, $n = 85$). Measurements associated with magmatic cracks mimic those from crystal rims (-4.9‰ to $+5.4\text{‰}$; mean $+1.2\text{‰} \pm 2.6\text{‰}$; 2 SE, $n = 13$), resulting in a broad negative correlation between Li concentrations and $\delta^7\text{Li}$ across all crystals (Fig. 3.2F).

The observed Li loss toward crystal edges and magmatic cracks requires charge balancing by other elements. Hydrogen is unsuitable, as it would behave similarly to Li. The charge balance can occur by an exchange reaction of $\text{Li}^+ + \text{Al}^{3+} \rightarrow \text{Si}^{4+}$ and/or oxidation of Fe^{2+} to Fe^{3+} during eruption. Although none of these elements correlates with the observed edge ward decrease in Li, their higher abundance relative to the small concentration change (~ 20 ppm) observed in Li challenges the identification of the charge-balance mechanism. We favour the oxidation of Fe^{2+} to Fe^{3+} because it is independent from elemental diffusion.

The variation in Li abundance cannot result from simple crystal-liquid equilibrium partitioning during crystal growth because Li is moderately incompatible in plagioclase [apparent partition coefficient $Kd_{\text{Li(plag/melt)}} = 0.1\text{--}0.7$; Neukampf et al., 2019) and other mineral phases present in the MFT (Tomascak et al., 2016; Neukampf et al., 2019). Hence, continued crystal growth would enrich Li in the melt, thereby increasing the Li concentration toward the plagioclase rim assuming that Li is not lost into the volatile phase. This process would result in isotopically lighter rims because the resulting concentration gradient would foster ^6Li diffusion into the crystal as observed for magmatic olivine and clinopyroxene (Jeffcoate et al., 2007). Magma recharge with a Li-poor, ^7Li -enriched melt can be excluded because no other element correlates with the decrease in Li toward plagioclase rims.

The decreased Li concentration and elevated $\delta^7\text{Li}$ toward crystal edges can be explained by scavenging of Li from the melt into the vapour phase during magma ascent and degassing (e.g., Genareau et al., 2009; Giuffrida et al., 2018; Steinmann et al., 2020). ^6Li preferentially moves into the vapour phase during vesiculation (Watson, 2017), resulting in the depletion of ^6Li along with Li concentrations in the

melt, inducing a disequilibrium between plagioclase and melt (Fig. 3.3). This disequilibrium causes diffusion of Li—preferentially ${}^6\text{Li}$ because it diffuses faster than ${}^7\text{Li}$ —from the rim of the plagioclase into the melt. This in turn leads to a disequilibrium within the plagioclase between the Li-depleted rim and its interior, driving Li diffusion toward the rims. Such a scenario results in the observed depletion of Li and enrichment of ${}^7\text{Li}$ in the plagioclase rims.

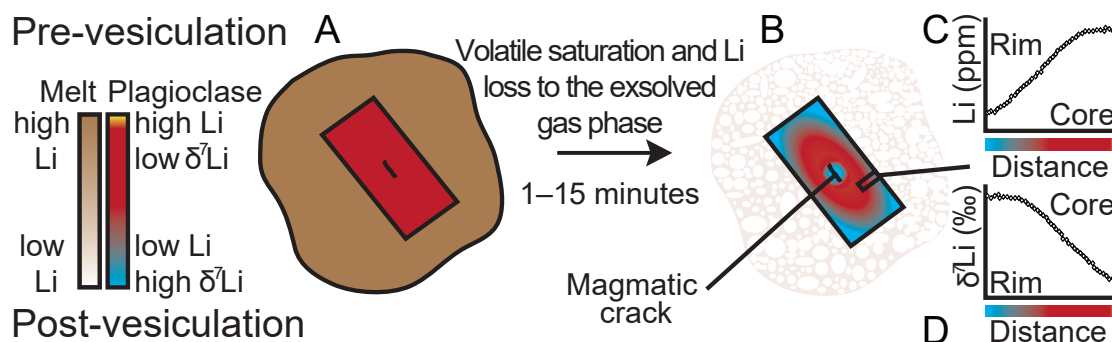


Fig. 3.3: Schematic sketch of processes recorded in Mesa Falls Tuff plagioclase (Yellowstone volcanic system, Idaho and Wyoming, USA). Plagioclase colour bar indicates low Li concentration and high $\delta^7\text{Li}$ isotopic composition in blue, and red colour represents higher Li concentrations with low $\delta^7\text{Li}$ values. Melt Li contents are shown by light brown (low Li) and dark brown (high Li). (A) Plagioclase in H_2O -undegassed melt with homogenous Li concentration and isotopic composition. (B) Diffusion profile formed in plagioclase due to the loss of Li during vesiculation of melt. (C) Theoretical concentration profile across a crystal. (D) Theoretical $\delta^7\text{Li}$ profile.

3.4 DIFFUSION MODELLING OF LI CONCENTRATIONS AND $\delta^7\text{Li}$

Lithium diffusion profiles in plagioclase can be used to determine time spans of this disequilibrium process (Fig. 3.4). Estimating such time scales depends on the applied diffusion coefficient (D), requiring an accurate temperature determination. Here, we investigated a temperature range based on different mineral thermometers for the MFT (Tollan et al., 2019). Diffusion coefficients are calculated using the Arrhenius parameters for Li that were experimentally determined for an anorthitic plagioclase (Giletti and Shanahan, 1997). The published ${}^6\text{Li}$ diffusion coefficient can be applied because Li diffusivity in feldspar is compositionally independent (Giletti and Shanahan, 1997). The minimum applied temperature is 789 °C based on a sanidine-melt thermometer (Putirka, 2008) with a corresponding $D^{6\text{Li}}=1.05\times 10^{-11}$ m²/s. Lower temperatures are implausible because the melt was rapidly quenched upon eruption as supported by the absence of microlites. Moreover, the pre-eruptive water content of the MFT melt was ~3 wt% (Tollan et al., 2019). At the pre-eruptive storage pressure of the MFT (<1.5 kbar; Befus and Gardner, 2016), this implies minimum temperatures of 770–780 °C (Holtz et al., 2001). The maximum temperature is 856 °C, which is determined by a magnetite-ilmenite thermometer (Sauerzapf et al., 2008), with a corresponding $D^{6\text{Li}}=2.79\times 10^{-11}$ m²/s. Both calculated diffusion coefficients are applied to the concentration profiles.

To calculate time scales for the isotope profiles, ${}^6\text{Li}$ and ${}^7\text{Li}$ are considered as two independent species with different diffusion coefficients. Because no published diffusion coefficient is available for ${}^7\text{Li}$ in plagioclase (Giletti and Shanahan, 1997), we recalculated the diffusion coefficients based on those used for ${}^6\text{Li}$ and considering that ${}^6\text{Li}$ moves 3.5% faster than ${}^7\text{Li}$ in melt (Holycross et al., 2018). This

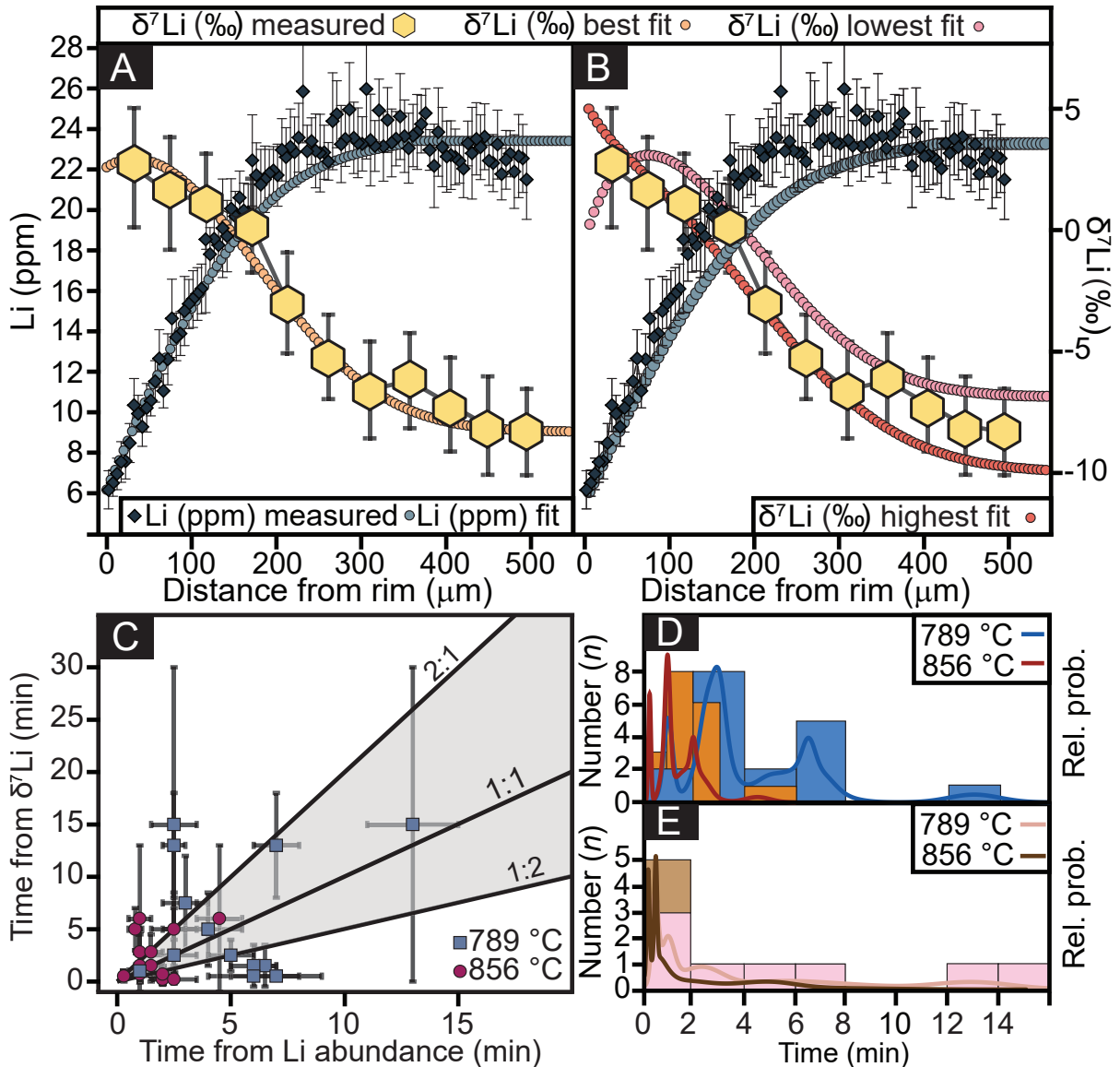


Fig. 3.4: Example of one-dimensional Li diffusion model for Mesa Falls Tuff plagioclase (Yellowstone volcanic system, Idaho and Wyoming, USA). **(A)** Representative diffusion profile with measured (blue diamonds) concentration profile and its modelled best fit (blue circles), in situ measured $\delta^7\text{Li}$ data (yellow hexagons), and best fit for $\delta^7\text{Li}$ profile (orange circles). **(B)** Profiles shown in A with boundary conditions set to highest (red) and lowest (pink) isotopic value within analytical error. **(C)** Comparison of time scales obtained by diffusion modelling of Li concentration (Li abundance) and isotope ($\delta^7\text{Li}$) profiles. Blue squares represent time scales at 789 °C, and red circles refer to time scales at 856 °C. Errors are provided as dark grey error bars. Lines labelled 1:1, 2:1, and 1:2 and the grey shaded area indicate the field of best agreement between time scales obtained for Li concentration and isotope profiles. **(D)** Time scales obtained from Li concentration profiles ($n = 18$) shown as lines at 789 °C (blue) and 856 °C (red) for their relative probability (Rel. prob.). Histogram (789 °C in blue, 856 °C in orange) shows distribution of time scales. **(E)** Time scales obtained from all eight (two profiles in the same crystal) analysed $\delta^7\text{Li}$ profiles at 789 °C (pink) and at 856 °C (brown). Histogram (789 °C in pink, 856 °C in brown) shows distribution of the time scales.

calculation yields $D^{7\text{Li}}=1.01\times 10^{-11}$ m²/s for 789 °C and $D^{7\text{Li}}=2.69\times 10^{-11}$ m²/s for 856 °C. We recognise that the relative diffusivity of the two isotopes in plagioclase could differ from that in melt and may furthermore be composition dependent, as observed for olivine (in which ⁶Li moves 3% faster; Dohmen et al., 2010) and clinopyroxene (in which ⁶Li moves 4% faster; Richter et al., 2014). However, these differences in relative isotope diffusivities between phases are much smaller than that resulting from our

inferred temperature range. The $\delta^7\text{Li}$ fit is calculated as the ratio of individual Li isotope paths (Equation S1 in the Supplemental Material 2.1). Estimated time scales are 1–13 min at 789 °C and 0.3–4.5 min at 856 °C for concentration profiles, and 0.5–15 min at 789 °C and 0.2–6 min at 856 °C for $\delta^7\text{Li}$ profiles. The results for the diffusion modelling of concentration and isotopic profiles are thus mutually consistent.

Figure 3.4C shows that for some profiles, a slight mismatch exists between time scales derived from concentration profiles and isotope profiles. This can be a result of different errors that are introduced into the model, e.g., different spatial resolution and analytical errors on the measurements and/or inaccurate diffusion coefficients. To better estimate errors on the time scales, the model boundary conditions (Tables S2.1–S2.3 in the Supplemental Material) were set to match the highest and the lowest $^7\text{Li}/^6\text{Li}$ ratio within analytical uncertainty (Fig. 3.4B) and modelled for the best fit. The time difference between the best fit and the model using the highest and the lowest $^7\text{Li}/^6\text{Li}$ ratio is used as a more realistic uncertainty (Fig. 3.4C) on the time scales derived from the diffusion models.

Crystal size has no influence on the estimated time scales, but crystal geometry and magmatic cracks can have a non-negligible impact. There might be a diffusional anisotropy of Li isotopes along different crystallographic directions, as reported for olivine (Dohmen et al., 2010). Audétat et al. (2018) recognised that Li has two, slow- versus fast-diffusing pathways in plagioclase. If the used diffusion coefficients represent the latter, the resulting time scales are minima. However, even considering that Li diffusion could be two orders of magnitude slower, the maximum time scales would increase to only a few hours.

Our results agree well with decompression time scales from a study of the Huckleberry Ridge Tuff (Myers et al., 2016), which yields durations of <12 h to 5 days. A recent study of Li concentration profiles in plagioclase from Mount Etna (Italy; Giuffrida et al., 2018) predicts time scales of ascent and degassing within minutes. Other studies have also recognised Li gradients in plagioclase (e.g., Kent et al., 2007; Charlier et al., 2012), but these investigations have suggested magmatic processes other than degassing to be responsible for formation of Li gradients.

With particular attention to the suitability of individual crystals, e.g., identifying the rims that were in contact with melt, crystal geometry, and three-dimensional effects, the new combination of Li concentrations and *in situ* $\delta^7\text{Li}$ measurements in phenocrysts represents a powerful tool and affords new opportunities for understanding time scales of late magmatic processes. Our results show that at minimum a few tens of minutes elapse between the onset of the eruptive volatile degassing of the magma and quenching. The possibility of such rapid shifts from quiescence to explosivity underscores the need for the improved understanding of the dynamics of magmatic systems and the causes for the formation of a magmatic volatile phase. This study strengthens the role of petrology in assisting in the key observations in monitoring potentially explosive volcanoes in real time.

ACKNOWLEDGMENTS

We thank R. Dohmen for help with, and discussions on, the diffusion modelling. This work was supported by the Swiss National Science Foundation (grant 200021_166281 to Ellis). The manuscript benefited from detailed reviews by Megan Holycross, Bruce Watson, and one anonymous reviewer. Chris Clark is acknowledged for editorial handling.

3.5 REFERENCES

- Audétat, A., Zhang, L., and Ni, H., 2018, Copper and Li diffusion in plagioclase, pyroxenes, olivine and apatite, and consequences for the composition of melt inclusions: *Geochimica et Cosmochimica Acta*, v. 243, p. 99–115, <https://doi.org/10.1016/j.gca.2018.09.016>.
- Befus, K.S. and Gardner, J.E., 2016, Magma storage and evolution of the most recent effusive and explosive eruptions from Yellowstone Caldera: *Contributions to Mineralogy and Petrology*, v. 171, p. 30, <https://doi.org/10.1007/s00410-016-1244-x>.
- Cashman, K. V., Sparks, R. S. J. and Blundy, J. D., 2017, Vertically extensive and unstable magmatic systems: A unified view of igneous processes: *Science*, v. 355 (6331), eaag3055, <https://doi.org/10.1126/science.aag3055>.
- Charlier, B., Morgan, D., Wilson, C., Wooden, J., Allan, A. and Baker, J., 2012, Lithium concentration gradients in feldspar and quartz record the final minutes of magma ascent in an explosive supereruption: *Earth and Planetary Science Letters*, v. 319–320, p. 218–227, <https://doi.org/10.1016/j.epsl.2011.12.016>.
- Christiansen, R.L., 2001, The Quaternary and Pliocene Yellowstone Plateau Volcanic Field of Wyoming, Idaho, and Montana: US Geological Survey Professional Paper 729-G, <https://doi.org/10.3133/pp729G>.
- Dohmen, R., Kasemann, S.A., Coogan, L. and Chakraborty, S., 2010, Diffusion of Li in olivine. Part I: Experimental observations and a multi species diffusion model: *Geochimica et Cosmochimica Acta*, v. 74, p. 274–292, <https://doi.org/10.1016/j.gca.2009.10.016>.
- Ellis, B.S., Mark, D.F., Troch, J., Bachmann, O., Guillong, M., von Kent, A.J.R. and Quadt, A., 2017, Split-Grain $^{40}\text{Ar}/^{39}\text{Ar}$ dating: integrating temporal and geochemical data from crystal cargoes: *Chemical Geology*, v. 457, p. 15–23, <https://doi.org/10.1016/j.chemgeo.2017.03.005>.
- Ellis, B.S., Szymanowski, D., Magna, T., J. Neukampf, Dohmen, R., Bachmann, O., Ulmer, P. and Guillong, M., 2018, Post-eruptive mobility of lithium in volcanic rocks: *Nature Communications*, v. 9, 3228, <https://doi.org/10.1038/s41467-018-05688-2>.
- Fiedrich, A.M., Laurent, O., Heinrich, C.A., and Bachmann, O., 2020, Melt and fluid evolution in an upper-crustal magma reservoir, preserved by inclusions in juvenile clasts from the Kos Plateau Tuff, Aegean Arc, Greece: *Geochimica et Cosmochimica Acta*, v. 280, p. 237–262, <https://doi.org/10.1016/j.gca.2020.03.038>.
- Genareau, K., Clarke, A.B., and Hervig, R.L., 2009, New insight into explosive volcanic eruptions: Connecting crystal-scale chemical changes with conduit-scale dynamics: *Geology*, v. 37, p. 367–370, <https://doi.org/10.1130/G25561A.1>.
- Giletti, B.J. and Shanahan, T.M., 1997, Alkali diffusion in plagioclase feldspar: *Chemical Geology*, v. 139, p. 3–20, [https://doi.org/10.1016/S0009-2541\(97\)00026-0](https://doi.org/10.1016/S0009-2541(97)00026-0).
- Giuffrida, M. Viccaro, L and Ottolini, M., 2018, Ultrafast syn-eruptive degassing and ascent trigger high-energy basic eruptions: *Scientific Reports*, v. 8 (147), <https://doi.org/10.1038/s41598-017-18580-8>.
- Holtz, F., Johannes, W., Tamic, N. and Behrens, H., 2001, Maximum and minimum water contents of granitic melts generated in the crust: a reevaluation and implications: *Lithos*, v. 56, p. 1–14, [https://doi.org/10.1016/S0024-4937\(00\)00056-6](https://doi.org/10.1016/S0024-4937(00)00056-6).
- Holycross, M.E., Watson, E.B., Richter, F.M., and Villeneuve, J., 2018, Diffusive fractionation of Li isotopes in wet, silicic melts: *Geochemical Perspectives Letters*, v. 6, p. 39–42, <https://doi.org/10.7185/geochemlet.1807>.
- Humphreys, M. C. S., Blundy, J. D. and Sparks, R. S. J., 2006, Magma evolution and open-system processes at Shiveluch Volcano: Insights from phenocryst zoning: *Journal of Petrology*, v. 47, p. 2303–2334, <https://doi.org/10.1093/petrology/egl045>.
- Jeffcoate, A.B., Elliott, T., Kasemann, S.A., Ionov, D., Cooper, K. and Brooker, R., 2007, Li isotope fractionation in peridotites and mafic melts: *Geochimica et Cosmochimica Acta*, v. 71, p. 202–218, <https://doi.org/10.1016/j.gca.2006.06.1611>.
- Kent, A.J.R., Blundy, J., Cashman, K.V., Cooper, K.M., Donnelly, C., Pallister, J.S., Reagan, M., Rowe, M.C. and Thornber, C.R., 2007, Vapor transfer prior to the October 2004 eruption of Mount StHelens, Washington: *Geology*, v. 35 (3), p. 231–234, <https://doi.org/10.1130/G22809A.1>.
- Mangan, M. and Sisson, T., 2000, Delayed, disequilibrium degassing in rhyolite magma: decompression experiments and implications for explosive volcanism: *Earth and Planetary Science Letters*, v. 183, p. 441–455, [https://doi.org/10.1016/S0012-821X\(00\)00299-5](https://doi.org/10.1016/S0012-821X(00)00299-5).
- Myers, M.L., Wallace, P.J., Wilson, C.J., Morter, B.K. and Swallow, E.J., 2016, Prolonged ascent and episodic venting of discrete magma batches at the onset of the Huckleberry Ridge supereruption, Yellowstone: *Earth and Planetary Science Letters*, v.451, p. 285–297, <https://doi.org/10.1016/j.epsl.2016.07.023>.

- Neukampf, J., Ellis, B.S., Magna, T., Laurent O. and Bachmann, O., 2019, Partitioning and isotopic fractionation of lithium in mineral phases of hot, dry rhyolites: The case of the Mesa Falls Tuff, Yellowstone: *Chemical Geology*, v. 506, p. 175–186, <https://doi.org/10.1016/j.chemgeo.2018.12.031>.
- Oeser, M., Dohmen, R., Horn, I., Schuth, S. and Weyer, S., 2015, Processes and time scales of magmatic evolution as revealed by Fe-Mg chemical and isotopic zoning in natural olivines: *Geochimica et Cosmochimica Acta*, v. 154, p. 130–150, <https://doi.org/10.1016/j.gca.2015.01.025>.
- Putirka, K.D., 2008, Thermometers and barometers for volcanic systems: *Reviews in Mineralogy and Geochemistry*, v. 69, p. 61–120, <https://doi.org/10.2138/rmg.2008.69.3>.
- Richter, F., Watson, B., Chaussidon, M., Mendybaev, R. and Ruscitto, D., 2014, Lithium isotope fractionation by diffusion in minerals. Part 1: Pyroxenes: *Geochimica et Cosmochimica Acta*, v. 126, p. 352–370, <https://doi.org/10.1016/j.gca.2013.11.008>.
- Rivera, T.A., Schmitz, M.D., Jicha, B.R. and Crowley, J.L., 2016, Zircon petrochronology and $^{40}\text{Ar}/^{39}\text{Ar}$ sanidine dates for the Mesa Falls Tuff: crystal-scale records of magmatic evolution and the short lifespan of a large Yellowstone magma chamber: *Journal of Petrology*, v. 57, p. 1677–1704, <https://doi.org/10.1093/petrology/egw053>.
- Sauerzapf, U., Lattard, D., Burchard, M. and Engelmann, R., 2008, The titanomagnetite–ilmenite equilibrium: new experimental data and thermo-oxybarometric application to the crystallization of basic to intermediate rocks: *Journal of Petrology*, v. 49, p. 1161–1185, <https://doi.org/10.1093/petrology/egn021>.
- Shea, T., Lynn, K.J. and Garcia, M.O., 2015, Cracking the olivine zoning code: distinguishing between crystal growth and diffusion: *Geology*, v. 43, p. 935–938, <https://doi.org/10.1130/G37082.1>.
- Sparks, R.S.J., 1978, The dynamics of bubble formation and growth in magmas: *Journal of Volcanology and Geothermal Research*, v. 3, p. 1–37, [https://doi.org/10.1016/0377-0273\(78\)90002-1](https://doi.org/10.1016/0377-0273(78)90002-1).
- Sparks, R.S.J., Barclay, J., Jaupart, C., Mader, H.M. and Phillips, J.C., 1994, Physical aspects of magmatic degassing I. Experimental and theoretical constraints on vesiculation: In: Carrol, M.R., Holloway, J.R. (Eds.), *Volatiles in Magmas*. *Reviews in Mineralogy*, v. 30, p. 413–445.
- Steinmann, L.K., Oeser, M., Horn, I., and Weyer, S., 2020, Multi-stage magma evolution in intra-plate volcanoes: Insights from combined in situ Li and Mg-Fe chemical and isotopic diffusion profiles in olivine: *Frontiers in Earth Science*, v. 8, 201, <https://doi.org/10.3389/feart.2020.00201>.
- Tollan, P., Ellis, B., Troch, J. and Neukampf, J., 2019, Assessing magmatic volatile equilibria through FTIR spectroscopy of unexposed melt inclusions and their host quartz: a new technique and application to the Mesa Falls Tuff, Yellowstone: *Contributions to Mineralogy and Petrology*, v. 174 (24), <https://doi.org/10.1007/s00410-019-1561-y>.
- Tomascak, P.B., Magna, T. and Dohmen, R., 2016, *Advances in Lithium Isotope Geochemistry*. Springer International Publishing, Cham, Switzerland.
- Vlastélic, I., Staudacher, T., Bachèlery, P., Télouk, P., Neuville, D., and Benbakkar, M., 2011, Lithium isotope fractionation during magma degassing: Constraints from silicic differentiates and natural gas condensates from Piton de la Fournaise volcano (Réunion Island): *Chemical Geology*, v. 284, p. 26–34, <https://doi.org/10.1016/j.chemgeo.2011.02.002>.
- Watson, E.B., 2017, Diffusive fractionation of volatiles and their isotopes during bubble growth in magmas: *Contributions to Mineralogy and Petrology*, v. 172, <https://doi.org/10.1007/s00410-017-1384-7>.
- Webster, J.D., Holloway, J.R., and Hervig, R.L., 1989, Partitioning of lithophile trace elements between H_2O and $\text{H}_2\text{O}+\text{CO}_2$ fluids and topaz rhyolite melts: *Economic Geology and the Bulletin of the Society of Economic Geologists*, v. 84, p. 116–134, <https://doi.org/10.2113/gsecongeo.84.1.116>.
- Zajacz, Z., Halter, W.E., Pettke, T., and Guillong, M., 2008, Determination of fluid/melt partition coefficients by LA-ICPMS analysis of co-existing fluid and silicate melt inclusions: Controls on element partitioning: *Geochimica et Cosmochimica Acta*, v. 72, p. 2169–2197, <https://doi.org/10.1016/j.gca.2008.01.034>.

3.6 Supplementary Materials

3.6.1 Methods

3.6.1.1 Major element measurements

Backscattered electron imaging by scanning electron microscope (SEM) and electron probe (EPMA) analyses (Si, Na, Mg, Al, Ca, K, Sr, Ti, Fe, Ba) of plagioclase grains were obtained at the Institute of Geochemistry and Petrology, ETH Zürich. Profiles were measured from core to rim with 5 to 10 μm steps with standards every 30 to 40 measurements. All analyses were measured with 15 kV acceleration voltage, a beam diameter of 10 μm and a beam current of 20 nA with counting times of 20 s on peak and 10 s on background. All analyses were performed so that the mobile elements (Na, K) were measured first. To ensure measurement accuracy, in-house reference minerals (albite, anorthite and microcline) from the ETH collection were used as secondary standards and reproducibility was better than 5 %.

3.6.1.2 Laser ablation inductively coupled plasma mass spectrometry (LA-ICPMS) mapping

Laser ablation inductively coupled plasma mass spectrometry (LA-ICPMS) mapping was undertaken at The University of Queensland Centre for Geoanalytical Mass Spectrometry, Radiogenic Isotope Facility (UQ RIF-lab). Plagioclase crystals embedded in 1-inch polished resin mounts were analysed following a published mapping method (Ubide et al., 2015; Ubide et al., 2019). The analytical set up comprised an ASI RESolution 193 nm excimer UV ArF laser ablation system with a dual-volume Laurin Technic ablation cell, coupled to a Thermo iCap RQ quadrupole mass spectrometer. Ablation was performed in ultra-pure He to which Ar make-up gas with a trace amount of N_2 was added for efficient transport and to aid ionization. The mapping area was built by overlapping ablation lines to form a rectangular grid, using a 20x20 μm square-shaped laser aperture, 20 $\mu\text{m}/\text{s}$ translation speed, 10 Hz repetition rate, 3 J/cm^2 fluence, and 1 μm overlap between lines. A baseline measurement of 20-30 s was programmed between lines. Pre-ablation of the crystals using large, quick rasters (100 μm spot, 200 $\mu\text{m}/\text{s}$ speed and 20 Hz repetition rate) was found to improve the subsequent mapping. The total dwell cycle was 115 ms, including maximised dwell time for ^7Li (50 ms). The instrument was tuned with scans on NIST SRM 612 silicate wafer reference material. NIST SRM 612 silicate wafer was employed as calibration standard and silicon concentrations (homogenous throughout single crystals) obtained by EPMA for each of the plagioclase crystals as internal standard. Spatially registered, quantitative multi-elemental maps were built with Iolite (Paton et al., 2011) v2.5, using CellSpace (Paul et al., 2012). Accuracy and precision were monitored via analysis of BHVO-2G, BCR-2G and GSD-1G glasses as secondary standards, using the same parameters as for the unknowns. Accuracy was better than 5 % for Li and better than 10 % for all other analysed elements. Limits of detection (Longerich et al., 1996) were at the sub-ppm level for Li as well as all other trace elements.

3.6.1.3 *In situ* Lithium isotope analysis of plagioclase crystals by femtosecond laser ablation-MC-ICPMS

For the *in situ* determination of Li isotope composition in plagioclase phenocrysts a femtosecond laser based ablation system (Spectra-Physics Solstice) coupled to a multi-collector-ICP-MS (Thermo-Finnigan Neptune Plus) at the Leibniz Universität Hannover, Germany, was used. The ablation beam had a pulse duration of ~100 fs and wavelength of 194 nm which was generated via frequency conversion from an infrared beam with 775 nm wavelength in an in-house built mirror and lens system and focused on the sample surface via a modified New Wave (ESI) stage combined with an optical microscope (Horn et al., 2006). The laser spot size of ~26 μm on the komatiite reference glass wafer GOR132-G (MPI DING) allowed for sufficient spatial resolution. Isotope measurements were performed according to the published method of Steinmann et al., (2019), by employing standard-sample-bracketing with the GOR132-G glass as a bracketing standard according to Equation 5 and recalculation to IRMM-16.

$$\delta^7\text{Li} = \left[\left(\frac{{}^7\text{Li}}{{}^6\text{Li}} \right)_{\text{sample}} / \left(\frac{{}^7\text{Li}}{{}^6\text{Li}} \right)_{\text{GOR132-G}} - 1 \right] \times 1000 \quad (5)$$

Due to low Li concentrations (5-30 ppm) in the plagioclase a device was implemented for gas flow homogenisation into the tubing system behind the ablation cell to homogenise the ablated aerosol with the transport Helium gas. Afterwards the make-up Ar gas was added and the gas-aerosol mixture was transported to the mass spectrometer. The homogenisation of the gas flow was necessary to enhance signal stability and decrease the analytical error. In order to decrease matrix effects by avoiding the ionisation of matrix elements in the plasma, relatively cool plasma conditions (RF power 900 W) were applied. *In situ* Li isotope ratio measurements were performed in static mode at low mass resolution which is sufficient to resolve atomic interferences. In order to keep background Li signals low, the measurements were performed under dry plasma conditions. For the detection of ${}^7\text{Li}$, a Faraday cup equipped with a slow-response $10^{13} \Omega$ amplifier was deployed whereas a secondary ion multiplier was used for the detection of ${}^6\text{Li}$. Due to the slower signal response of the $10^{13} \Omega$ amplifier a tau correction (Kimura et al., 2016) was applied for data evaluation.

Measurements of the bracketing standard were performed in raster ablation mode with a scan speed of 20 $\mu\text{m}/\text{s}$. The plagioclase profiles were measured in line ablation mode at the rims and raster ablation mode (26 μm by 56 μm) further into the grains, with lines and rasters arranged perpendicular to the crystal rim, each line/raster accounting for one measurement value. Individual measurements consisted of 180 cycles with an integration time of 1.049 s per cycle. The first ~35 cycles were used for background correction using only the gas blank reading, followed by ~130 cycles of laser ablation. All analyses that represent one isotopic profile were measured during a single analytical session. As an internal control, the MPI DING reference glass T1-G was measured yielding a long-term reproducibility of 2.1 ‰ ($\delta^7\text{Li} = 0.4 \text{ ‰}$, 2 SD, n=64 in 16 sessions during 22 months) in agreement with Steinmann et al., (2019). The results of Li isotopic measurements were recalculated to the δ -notation relative to the L-SVEC reference material.

Table S1. Time scales of Li diffusion from Li concentration in plagioclase crystals from MFT and boundary conditions for each profile. Timescales are calculated for 789°C and 856°C using D of $1.05 \times 10^{-11} \text{ m}^2/\text{s}$ and $2.79 \times 10^{-11} \text{ m}^2/\text{s}$, respectively.

Grain	Line	C_0 - Core (ppm)*	Rim (ppm)*	789 °C		856 °C	
				Time (min)	S.D.	Time (min)	S.D.
7	L1	20.2	5.3	3	0.5	1.5	0.5
	L2	19.6	6.7	3	1	1	0.2
11	L1.1	27.7	6.2	5	1	2	0.6
	L1.2	28.3	5.9	2.5	1	1	0.3
13	L1.1	27.2	5.0	6.5	0.5	2	0.5
	L1.2	30.0	6.8	6	1	2	0.2
15	L2.1	27.8	5.1	7	2	2.5	1
	L2.2	28.6	6.4	6	2	2	0.5
	L3.1	25.6	4.9	3	1	1	0.2
	L3.2	21.1	6.5	3	1	1	0.2
21	L1.1	20.1	6.7	1	0	0.3	0.1
	L1.2	22.3	8.5	1	1	0.3	0.1
	L3.1	28.6	7.7	3	1	1	0.2
	L3.2	28.7	7.4	4	2	1.5	0.5
25	L1	23.6	8.8	2.5	0.5	0.8	0.3
	L2	23.6	7.0	7	1	2.5	0.5
27	L1	23.4	6.2	13	2	4.5	1
	L2	28.4	8.4	3	1	1	0.5

Note: Samples are stored in the collection of ETH Zurich, Department of Earth Sciences, Zurich, Switzerland.

*Measured using a LA-ICPMS.

Table S2. Time scales of Li diffusion from $\delta^7\text{Li}$ profiles in plagioclase crystals from MFT and boundary conditions for each profile. Timescales are calculated for 789°C and 856°C using D of $1.05 \times 10^{-11} \text{ m}^2/\text{s}$ and $2.79 \times 10^{-11} \text{ m}^2/\text{s}$, respectively.

Grain	Line	C_0 - Core ($\delta^7\text{Li}$)*	Rim ($\delta^7\text{Li}$)*	789 °C		856 °C	
				Time (min)	S.D.	Time (min)	S.D.
7	L1	-9.1	-0.8	7.5	1	2.8	0.2
11	L1.1	-2.6	3.2	2.5	1	0.7	0.2
13	L1.1	-9.2	-1.2	1.5	1	0.5	0.5
15	L2.1	-1.4	0.7	0.5	0.1	0.2	0.1
21	L1.1	-7.0	-3.8	1	0.5	0.5	0.1
21	L3.1	-9.0	-1.9	5	1	1.5	0.5
25	L1	-7.0	2.9	13	5	5	2
27	L1	-8.3	2.6	15	3	6	2

Note: Samples are stored in the collection of ETH Zurich, Department of Earth Sciences, Zurich, Switzerland.

*Measured using a LA-ICPMS.

Table S3. Time scales of Li diffusion from $\delta^7\text{Li}$ profiles in plagioclase crystals from MFT and boundary conditions for each profile. Timescales are calculated for 789°C and 856°C using D of $1.05 \times 10^{-11} \text{ m}^2/\text{s}$ and $2.79 \times 10^{-11} \text{ m}^2/\text{s}$, respectively. The highest and lowest Li isotopic value within the error are taken as boundary conditions for the diffusion modelling.

Grain	Line	C_0 - Core ($\delta^7\text{Li}$)*	Rim ($\delta^7\text{Li}$)*	789 °C		856 °C	
				Time (min)	Time (min)	Time (min)	Time (min)
upper values							
7	L1	-10.9	1.5	12		6	
11	L1.1	-4.4	5.7	4		1.5	
13	L1.1	-11.2	1.2	3.5		1.1	
15	L2.1	-3.6	3.0	0.75		0.3	
21	L1.1	-7.4	-1.7	0.75		0.3	
21	L3.1	-11.0	1.0	8.5		3.25	
25	L1	-9.0	5.1	16		6	
27	L1	-10.1	5.0	30		12	
lower value							
7	L1	-7.3	-3.0	4.5		1.6	
11	L1.1	-0.7	0.8	1		0.35	
13	L1.1	-7.1	-3.6	0.9		0.4	
15	L2.1	-1.6	0.8	0.3		0.1	
21	L1.1	-2.7	-5.9	0.15		0.05	
21	L3.1	-7.0	-4.7	2.75		1	
25	L1	-5.1	0.6	5.5		2.2	
27	L1	-6.5	0.1	10		4	

Note: Samples are stored in the collection of ETH Zurich, Department of Earth Sciences, Zurich, Switzerland.

*Measured using a LA-ICPMS.

3.6.1.4 Trace element measurements

Plagioclase trace element concentration profiles were obtained by LA-ICPMS using an Excimer 193 nm (ArF) Resolution (Australian Scientific Instruments) nanosecond laser ablation system coupled to a Nexion2000 (Perkin Elmer, Canada/USA) fast-scanning quadrupole ICPMS, at the Institute of Geochemistry and Petrology, ETH Zürich. The trace element concentration profiles in the plagioclase crystals were measured parallel to the previously analysed chemical and Li isotopic profiles. The ablation was performed in a S-155 dual-volume ablation cell (Laurin Technic, Australia) under a carrier gas flow consisting of high-purity He (ca. 0.5 l.min⁻¹), N₂ (cica 2 ml.min⁻¹) and Ar make-up gas (ca. 1.0 l.min⁻¹) from the ICPMS. Line scans were ablated with a spot diameter of 29 µm, a repetition rate of 10 Hz, a laser energy density of ca. 3.5 J.cm⁻² and a scan velocity of 1 µm.s⁻¹. All concentrations were quantified against the NIST SRM 612 silicate glass wafer as the primary standard (Jochum et al., 2011), using conventional standard-sample bracketing with one line between two standards. The USGS basaltic glass GSD-1G was used as the secondary standard to monitor for the accuracy and reproducibility of the analyses. Both reference materials were ablated with line scans under the same conditions as the unknown samples. The resulting raw intensities were processed using the Igor Pro-based Iolite v2.5 software (Hellstrom et al., 2008), using the implemented data reduction scheme for trace element quantification. The baseline-corrected intensities for each line scan were averaged over integration periods of 5 s (corresponding to 20 mass cycles with a sweep time of 0.25 s each), resulting in a spatial resolution of 5 µm for the final concentrations along the profiles. We used Si as an internal standard to correct for differences in relative sensitivities, based on the average SiO₂ content of the analysed plagioclase crystals (63±0.5 wt.%) measured by EPMA. The uncertainties on concentrations at each step of the profiles correspond to the scatter of the 20 measurement cycles integrated within the corresponding time step, quoted at 95% confidence level (2 S.D.).

3.6.2 Diffusion modelling

Diffusion modelling as shown in Fig. 4 was conducted using the diffusion coefficient of Li in an anorthitic plagioclase (Giletti and Shanahan, 1997). Each profile was modelled using a one-dimensional model, and a diffusion exchange at a constant temperature with an infinite medium (core is unaffected by diffusion) is assumed. The shape of the Li concentration profiles as well as the δ⁷Li profiles can be described by an error function. Therefore, the following equation (6) can be applied:

$$C_x = (C_{0-1})(1 - \text{erf}(x/(2\sqrt{Dt}))) + 1 \quad (6)$$

where C_x represents the composition at a distance x (in µm) from the crystal surface, D is the Li diffusion coefficient in plagioclase, and t is the time since the diffusion started. C_0 represents the composition in the core (used values are given in Table S1, S2 and S3). To calculate the timescales for the isotope profiles, the ⁶Li and ⁷Li are considered as two independent species with different diffusion coefficients. The temperature range used in this study is between 789 °C (sanidine–melt thermometer; Putirka, 2008) to 856 °C (ilmenite–magnetite thermometer; Sauerzapf et al., 2008). Only ilmenite–magnetite pairs passing the equilibrium criteria (Bacon and Hirschmann, 1988) were used for temperature estimations.

3.6.3 References

- Bacon, C.R. and Hirschmann, M.M., 1988, Mg/Mn partitioning as a test for equilibrium between coexisting Fe–Ti oxides: *American Mineralogist*, v. 73, p.57-61.
- Hellstrom, J., Paton, C., Woodhead, J. and Hergt, J., 2008, Iolite: software for spatially resolved LA-(Quad and MC)-ICP-MS analysis Laser Ablation-ICP-MS in the Earth Sciences: Current Practices and Outstanding Issues. P. Sylvester, Editor. Mineralogical Association of Canada:Vancouver. p. 343-348.
- Horn, I., von Blanckenburg, F., Schoenberg, R., Steinhöfel, G. and Markl, G., 2006, In situ iron isotope ratio determination using UV-femtosecond laser ablation with application to hydrothermal ore formation processes: *Geochimica et Cosmochimica Acta*, v. 70, p. 3677–3688, <https://doi.org/10.1016/j.gca.2006.05.002>.
- Jochum, K.P., Weis, U., Stoll, B., Kuzmin, D., Yang, Q., Raczek, I., Jacob, D.E., Stracke, A., Birbaum, K., Frick, D.A., Günther, D. and Enzweiler, J., 2011, Determination of reference values for NIST SRM 610–617 glasses following ISO guidelines: *Geostandards and Geoanalytical Research*, v. 35, p. 397–429, <https://doi.org/10.1111/j.1751-908X.2011.00120.x>.
- Kimura, J.I., Chang, Q., Kanazawa, N., Sasaki, S. and Vaglarov, B.S., 2016, High-precision in situ analysis of Pb isotopes in glasses using 1013 Ω resistor high gain amplifiers with ultraviolet femtosecond laser ablation multiple Faraday collector inductively coupled plasma mass spectrometry: *Journal of Analytical Atomic Spectrometry*, v. 31, p. 790–800, <https://doi.org/10.1039/C5JA00374A>.
- Longerich, H.P., Jackson, S.E. and Günther, D., 1996, Inter-laboratory note. Laser ablation inductively coupled plasma mass spectrometric signal data acquisition and analyte concentration calculation: *Journal of Analytical Atomic Spectrometry*. v. 11, p. 899–904, <https://doi.org/10.1039/JA9961100899>.
- Paton, C., Hellstrom, J., Paul, B., Woodhead, J. and Hergt, J., 2011, Iolite: freeware for the visualisation and processing of mass spectrometric data: *Journal of Analytical Atomic Spectrometry*, v. 26, p. 2508–2518, <https://doi.org/10.1039/C1JA10172B>.
- Paul, B., Paton, C., Norris, A., Woodhead, J., Hellstrom, J., Hergt, J. and Greig, A., 2012, Cell Space: a module for creating spatially registered laser ablation images within the Iolite freeware environment: *Journal of Analytical Atomic Spectrometry*, v. 27, p. 700–706, <https://doi.org/10.1039/C2JA10383D>.
- Steinmann, L.K., Oeser, M., Horn, I., Seitz, H-M. and Weyer, S., 2019, In situ high-precision lithium isotope analyses at low concentration levels with femtosecond-LA-MC-ICP-MS: *Journal of Analytical Atomic Spectrometry*, v. 7, p. 1447-1458, <https://doi.org/10.1039/C9JA00088G>.
- Ubide, T., McKenna, C.A., Chew, D. M. and Kamber, B.S., 2015, High-resolution LA-ICP-MS trace element mapping of igneous minerals: in search of magma histories: *Chemical Geology*, v. 409, p. 157–168, <https://doi.org/10.1016/j.chemgeo.2015.05.020>.
- Ubide, T., Mollo, S., Zhao, J.X., Nazzari, M. and Scarlato, P., 2019, Sector-zoned clinopyroxene as a recorder of magma history, eruption triggers, and ascent rates: *Geochimica et Cosmochimica Acta*, v. 251, p. 265–283, <https://doi.org/10.1016/j.gca.2019.02.021>.

Chapter 4

Li elemental and isotopic composition of rhyolitic melt inclusions and their host quartz: a record blurred by multiple diffusive re-equilibration

Julia Neukampf¹, Ben S. Ellis¹, Anne-Sophie Bouvier², Peter Tollan¹, Peter Ulmer¹, Oscar Laurent^{1,3}, Marcel Guillong¹, Tomas Magna⁴, and Olivier Bachmann¹

¹Institute of Geochemistry and Petrology, ETH Zurich, NW Clausiusstrasse 25, CH-8092, Zurich, Switzerland

²Institut des Sciences de la Terre, University of Lausanne, CH-1015, Lausanne, Switzerland

³CNRS, Géosciences Environnement Toulouse, Observatoire Midi-Pyrénées, 14 avenue Édouard Belin F-31400 Toulouse, France

⁴Czech Geological Survey, Klárov 3, CZ-11821 Prague 1, Czech Republic

Paper in preparation

Abstract

Ion-microprobe measurements of Li isotopic composition and Li concentration of quartz-hosted melt inclusions and groundmass glass from the rhyolitic Mesa Falls Tuff were obtained in order to reconstruct the Li concentration and isotopic composition within the magma chamber. The $\delta^7\text{Li}$ values between melt inclusions and groundmass glass vary by up to 25%. Lithium concentrations in the glassy melt inclusions (10 to 37 ppm) are lower compared to the groundmass glass (28 to 46 ppm) and overlap with their host quartz (8 to 15 ppm). This indicates a diffusional exchange between entrapped melt inclusions and their host-quartz resulting in a potential re-equilibration of the melt inclusions. The re-equilibration between inclusion and host-quartz modified the $\delta^7\text{Li}$ values of the melt inclusions, therefore, they are not recording the isotopic composition of the melt. Crystallised melt inclusions from the same eruption have higher Li concentrations (6 to 160 ppm) compared to the groundmass glass and their host-quartz (15 to 24 ppm) reflecting the loss of H_2O from the melt inclusions and leading to an enrichment of Li during the crystallisation of the melt inclusions.

Two quartz populations were identified as they differ in Li concentration by up to a factor of two, but are similar in other trace elements. One quartz population has homogenous Li concentrations and the other is heterogeneous in its Li concentration with an increase of Li concentration towards their rims. The heterogeneous quartz population indicates a diffusive exchange between quartz and surrounding melt which formed during ascent due to a change in pressure and resulting H^+ diffusion. By diffusion modelling it was determined that the Li diffusion profiles in the quartz crystals formed within a few hours. The quartz crystals with homogenous Li concentration erupted earlier, therefore experienced only small amounts of diffusive exchange and no Li diffusion profiles formed.

4.1 Introduction

The economic importance of lithium (Li) has increased over the past decades because Li is a major component in energy storage devices that are key in many technologies (Kesler et al., 2012). The majority of economic Li deposits are found in salars, predominantly located close to the silicic volcanic deposits like Andes in Bolivia, Chile and China (Kesler et al. 2012), but pegmatites, associated with mineralized granitic rocks, represent another important repository of Li (e.g., Australia, Canada, USA, Congo). A number of studies (e.g., Kesler et al., 2012; Hofstra et al., 2013; Benson et al., 2017) have focused on the origin of Li-rich brines and pegmatite deposits and linked them to silicic magmatism where either Li-rich rhyolites are leached due to weathering, with Li further enriched due to its affinity to transport during weathering, combined with the incompatibility of Li in most rock-forming minerals (e.g., Tomascak et al., 2016) or enriched by hydrothermal fluids. Hofstra et al. (2013) and Benson et al. (2017) showed that quartz-hosted rhyolitic melt inclusions can contain up to 9,400 ppm Li with significant enrichments compared to the host groundmass glass, this trend was also recognised elsewhere (e.g., Stix and Layne, 1996; Lindsay et al., 2001). Therefore, the cycling of Li in magmatic systems needs to be further addressed to understand the formation of economically important Li-rich deposits.

Processes related to the enrichment of Li in silicic magmas at mid to upper crustal conditions are still not fully disentangled and studies focusing on Li concentration and isotopic composition of

pre-eruptive magmas in chemically more evolved systems are infrequent. Available studies have shown that the Li concentration of groundmass glass and minerals in evolved systems can be modified by syn- (e.g., Neukampf et al., 2019; Neukampf et al. 2020) and post-eruptive processes (e.g., Ellis et al., 2018) and may not represent the original Li inventory elemental/isotope data of the melt. A recent study (Neukampf et al., 2020) on the Mesa Falls Tuff (MFT; Fig.4.1), Yellowstone, USA, showed that diffusive (kinetic) fractionation can lead to sizeable Li isotopic differences of >10‰ within plagioclase crystals. The large Li isotopic diffusion profiles in plagioclase can be formed within tens of minutes prior to eruption as a response to expeditious degassing whereby ^6Li moves preferentially into the volatile phase and ^7Li remains in the melt. Indeed, this change of the original Li concentration and isotopic composition of melt was theoretically predicted by Watson (2017). Holycross et al. (2018) and Richter et al. (2009) experimentally demonstrated that Li isotopes diffuse at a different speed, depending on the water content of the melt (^6Li moves ~3 to 3.5 % faster compared to ^7Li). The large mass difference (17%) between the two Li isotopes (^6Li and ^7Li) has been recognised as the mechanism that leads to natural Li isotopic differences of >50‰ between different geological reservoirs (e.g., Tomascak et al. 2016). The fast diffusivity of Li and its isotopes (Richter et al., 2003) and the resulting diffusive fractionation driven by concentration gradients can cause large isotopic variations within minerals on the micron scale (e.g., Jeffcoate et al., 2007; Parkinson et al., 2007) to variations on the meter scale (e.g., Lundstrom et al., 2005; Marschall et al., 2007, John et al. 2012, Beinlich et al., 2020). Even though high-temperature fractionation has been recognised as an important process to influence the Li isotopic composition of igneous systems (e.g., Jeffcoate et al., 2007, Magna et al., 2008), the elemental and isotopic composition of chemically evolved melts in the magma chamber before eruption has not been studied in detail and previous studies only focused on arc setting (e.g., Gurenko et al., 2005; Bouvier et al., 2008, 2010; Schiavi et al., 2010, 2012).

Melt inclusions in phenocrysts are used to study magmatic processes because they are considered to preserve the original melt composition after their entrapment (e.g., Roedder, 1979). It has been shown that melt inclusions can be modified prior to eruption leading to compositional changes as a result of crystallisation on the inclusion walls or leakage of the inclusions through cracks (e.g., Nielsen et al., 1998; Frezzotti, 2001), diffusive exchange between inclusions and host minerals and/or between host minerals and a surrounding melt (e.g., Qin et al. 1992; Danyushevsky et al., 2000). The modification of melt inclusions due to crystallisation can, to a certain extent, be experimentally reversed, but re-equilibration with the host mineral/melt cannot be reversed (Danyushevsky et al., 2000). Therefore, care must be exercised in unravelling the intrinsic to potential process that can modify the chemistry of melt inclusions.

In this study, we report Li concentrations and isotopic compositions of quartz-hosted melt inclusions (MI) and groundmass glass, complemented with the Li concentrations of the host quartz from the rhyolitic Mesa Falls Tuff (Yellowstone, USA) in order to test whether diffusional exchange between melt inclusions and host quartz can lead to the modification of the original Li elemental and isotopic inventory of melt inclusions.

4.2 Geological setting and samples

The Yellowstone caldera system is located at the northern end of the Snake River Plain hotspot track. It had three caldera-forming eruptions with Huckleberry Ridge Tuff representing the most voluminous (~2500 km³; Christiansen, 2001) and the earliest eruption (2.08 Ma; Rivera et al., 2014; Singer et al., 2014), which forms the Island Park Caldera. The youngest eruption (0.63 Ma; Matthews et al., 2015) produced the Lava Creek Tuff (~1000 km³; Christiansen, 2001) which formed the Yellowstone Caldera. The Huckleberry Ridge Tuff and Lava Creek Tuff erupted in multiple pulses whereas the Mesa Falls Tuff (MFT, 1.30 Ma; Rivera et al., 2016), the smallest of the caldera forming eruptions, erupted in a single pulse (Christiansen, 2001) and formed the Henry's Fork Caldera. Mesa Falls Tuff was a voluminous explosive event with fallout and pumice deposits at its base were covered with a welded ignimbrite sheet (Rivera et al., 2016). This eruption is a high-silica rhyolite containing quartz, plagioclase, sanidine, fayalite, clinopyroxene, orthopyroxene and accessory phases and shows no large chemical differences throughout the unit (Christiansen, 2001).

Samples used in this study come from one sampling location and were collected from a thick ash and pumice deposited at the base of Mesa Falls Tuff that can be found at a road cut along Highway 20 in the north of Ashton, Idaho. One sample are loose grains from highly vesicular MFT fallout (11022) and the other a large piece of highly vesicular pumice (13005). Both samples were collected close to each other and represent the same eruption as MFT is single-eruptive unit. The non-welded part of the MFT deposit was used to minimise the potential of post-eruptive changes in the Li concentration.

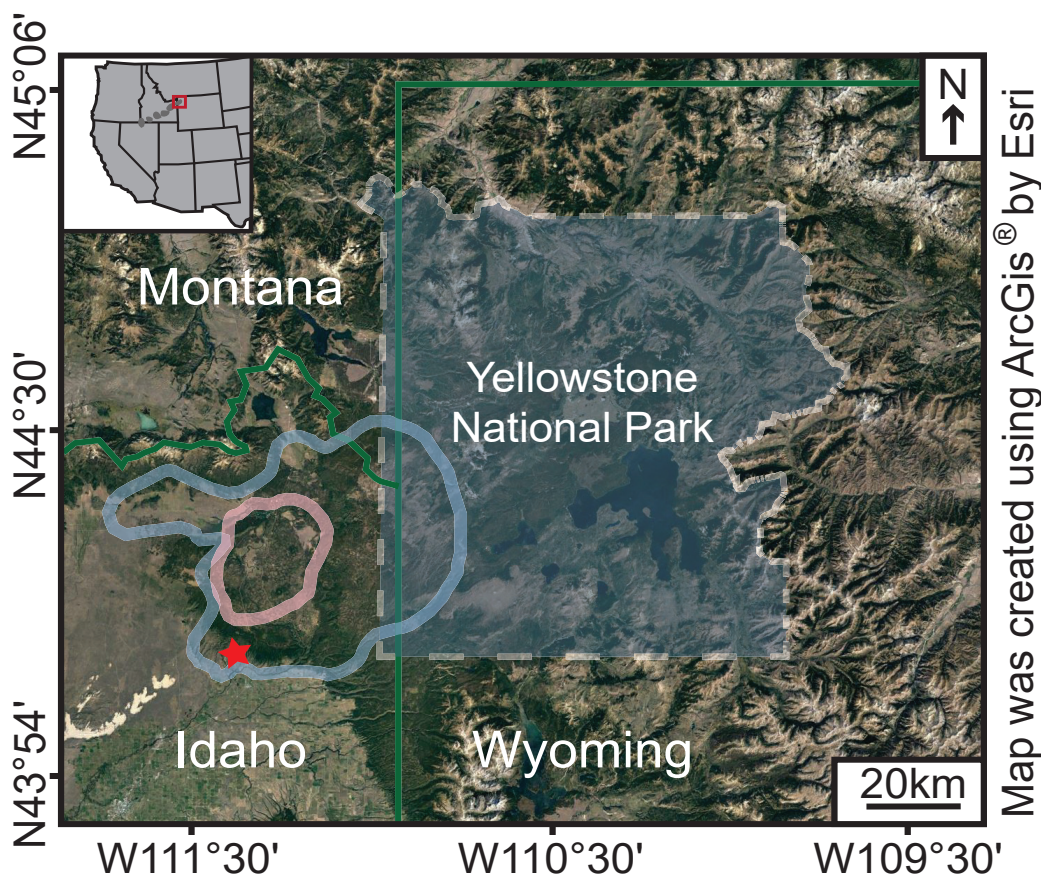


Fig. 4.1: Location map of the two samples (44°7'8.49"N, 111°26'39.49"W; Ellis et al., 2017) of MFT (light blue line) indicated with a red star (changed after Neukampf et al., 2020). Inferred Henry's Folk caldera (Christiansen, 2001) in light pink line and state lines in green.

4.3 Analytical methods

4.3.1 Sample preparation

Quartz crystals with melt inclusions and groundmass glass were hand-picked under a binocular microscope from crushed samples and mounted in 1-inch epoxy mounts. The quartz mounts were then double polished down to a variable thickness of ~ 350 to ~ 450 μm . H_2O and CO_2 contents of the melt inclusions were determined using the Fourier transform infrared spectroscopy (FTIR). Following the FTIR measurements single melt inclusions were selected for $\delta^7\text{Li}$ measurements using SIMS. The selected melt inclusions were exposed, polished and the quartz crystals hosting the melt inclusions were excavated from the epoxy mount and mounted into a 1-inch indium mount for SIMS measurements. Major and trace element contents were measured after the SIMS analyses to minimise potential modifications of the melt inclusions.

4.3.2 Fourier transform infrared (FTIR) spectroscopy

The H_2O and CO_2 contents of quartz-hosted melt inclusions were determined by employing a transmitted light FTIR spectroscopy following the technique described in Tollan et al. (2019). In short, this method involves measuring the melt inclusions that remain fully enclosed in the crystal and then correcting for the absorbance contribution from the crystal host itself. First, the transmitted light images of quartz crystals and their melt inclusions were taken at the University of Bern using an optical microscope recording their position, appearance, and geometry (Fig. 4. 2). The thickness of each quartz crystal was then measured using a Mitutoyo ID-S IP42 digital depth gauge (3 μm precision). FTIR spectra were obtained at the University of Bern with a Bruker Hyperion 3000 microscope attached to a Bruker Tensor II spectrometer. The measurements were conducted in a dry air-purged measurement chamber, using non-polarised light, a 15x Cassegrain objective and a mercury-cadmium-telluride detector. The light source and beamsplitter were composed of SiC and KBr, respectively. Background and sample measurements were made with 64 scans and a resolution of 8 cm^{-1} . Three measurements with a varying spot size were made on each melt inclusion, followed by the measurement immediately adjacent through the host quartz (without any inclusions in the beam pathway). The host quartz has relatively little to no interfering absorption at the wavelengths of total H_2O and CO_2 in rhyolitic glass. Therefore, this latter step is solely used to obtain the Si–O overtone bands of the quartz for the calculation of the size of the melt inclusion, critical in the calculation of volatile concentration. The concentrations of H_2O and CO_2 were calculated using the (non-integrated) absorbance of the bands centred at 5200 cm^{-1} , 4500 cm^{-1} and 2345 cm^{-1} , with a direct baseline correction in each case. Conversion from the absorption to concentration was achieved using Zhang et al. (1997) for H_2O and Behren et al. (2004) for CO_2 . Three individual measurements on each melt inclusion were monitored for the consistency and any significant deviation in concentration resulted in discarding of the data. As noted by Tollan et al. (2019), any melt inclusion whose size was less than 15% of the thickness of the host quartz typically did not yield reliable values of concentration.

4.3.3 Secondary Ionization Mass Spectrometry measurements

Lithium isotope compositions were determined using a CAMECA ims1280-HR secondary ionization mass spectrometer at the Swiss SIMS laboratory (University of Lausanne). Samples were mounted in indium together with a reference material (either NIST SRM 612 or BHVO-2G; Jochum et al., 2011). Prior to the analysis samples were coated with 35 nm thick gold layer. Sample surfaces were bombarded using O^- beam generated by a Hyperion RF source. The analyses were performed in three separate SIMS sessions; the intensity of the primary O^- ion beam was ~ 2 nA in the first session whereas it was ~ 5 nA in the second and third session, respectively. The $^6Li^+$ and $^7Li^+$ ion beams were collected in multi-collection mode on two opposing electron multipliers. The mass resolution was set to 2400, using an entrance slit width of 121 μm and multi-collector slits 1. The field aperture was closed to 1360, in order to avoid possible surface contamination. Prior to each analysis, the surface was pre-sputtered for 200 s using a 15- μm raster in order to remove the gold layer and any potential Li surface contamination. Automatic centring of the field aperture and contrast aperture deflectors were conducted at the end of the pre-sputtering. Measurements were performed using a 5- μm rastered primary beam. Each Li measurement consisted of 70 cycles, with each cycle 12 s long.

Calibration was made using StH, Atho and TI MPI-DING reference glass materials (Jochum et al., 2006). NIST SRM 612 and BHVO-2G were used to monitor the instrumental stability during the analytical sessions. Analyses of melt inclusions were bracketed every four to five analyses by either NIST SRM 612 or BHVO-2G.

The measured data were corrected for an instrumental drift for each analytical session (typically 2–3‰ over an eight-hour period) using the δ^7Li isotopic composition of NIST SRM 612 or BHVO-2G measured throughout each session. The long-term reproducibility of the reference materials (2SD) after a drift correction is $\pm 1.6\text{‰}$ for NIST SRM 612 and $\pm 2.3\text{‰}$ for BHVO. The internal error for each measurement is dependent on the Li content and it varied between ± 0.3 and $\pm 1.5\text{‰}$ (2SE) during the course of this study.

4.3.4 Major element measurements

Backscattered electron (BSE) and cathodoluminescence (CL) images of the melt inclusions, the quartz host and groundmass glass were acquired using a scanning electron microscope (SEM). Major element compositions of the exposed melt inclusions and the groundmass glass were determined with a Jeol JXA-8230 electron microprobe (EMPA) probe analysis (Si, Na, Mg, Al, Ca, K, Ti, Fe, P, Cl, Cr, Mn), housed at the Institute of Geochemistry and Petrology, ETH Zürich. All analyses were measured with 15 kV acceleration voltage. The beam diameter for the melt inclusions was either 2 μm with a beam current of 2 nA, 5 μm with a beam current of 4 nA or 20 μm with a beam current of 10 nA, depending on the size of the melt inclusions. The beam diameter for the groundmass glass was 5 μm with a beam current of 4 nA. For Si, Na, Al, Mg, Ca and P a counting time of 30 s on peak was used whereas a counting time of 20 s on peak was employed for K, Ti, Cl, Fe, Mn and Cr. To ensure the reliability of the technique, the rhyolitic reference material from Smithsonian (VG-568) was used as a secondary standard with the reproducibility better than 5% (SD). Two to five individual measurements per melt inclusion were obtained.

4.3.5 Laser ablation inductively coupled plasma mass spectrometry (LA-ICP-MS)

Trace element concentrations in host quartz and quartz-hosted melt inclusions were analysed using an Excimer 193 nm (ArF) GeoLas (Coherent) laser system coupled to a Nexion2000 (Perkin Elmer, Canada/USA) fast-scanning quadrupole ICP-MS, at the Institute of Geochemistry and Petrology, ETH Zürich. The on-sample energy density of the laser beam was $20 \text{ J}\cdot\text{cm}^{-2}$. All quartz was measured with a spot size of $40 \mu\text{m}$; for the melt inclusions the spot size was $40 \mu\text{m}$ with one to nine measurements per inclusion depending on the inclusion size. The ablation was performed with ca. $1.0 \text{ L}\cdot\text{min}^{-1}$ He carrier gas flow and ca. $1 \text{ L}\cdot\text{min}^{-1}$ Ar make-up gas was admixed downstream of the ablation chamber. Concentrations were quantified against the NIST SRM 610 glass wafer as the primary reference material (Jochum et al., 2011) and a natural quartz crystal characterised by Audétat et al. (2015) was employed as a secondary standard (see results in Data S1). The average 2 SD reproducibility of concentrations in the secondary quartz standard for all analytical sessions was used to determine the uncertainties on the concentrations of unknown samples (5% relative for Li).

The raw data were reduced using the Matlab-based SILLS program (Guillong et al., 2008) by using the Si concentration of the melt inclusions as an internal standard that were determined by EMPA. The uncertainties on melt inclusion concentrations were 5% relative (2 SD).

4.4 Results

4.4.1 Melt inclusions

Eight glassy and sixteen crystallised quartz-hosted melt inclusions were selected for further geochemical investigation. The studied quartz crystals host a variety of glassy melt inclusion types (Fig. 4.2 A, B and C) from brown to colourless or bubble-bearing in either spherical shapes (sample 11022) (Tollan et al. 2019), or cubic-shaped fully crystallised melt inclusions (sample 13005), all ranging in

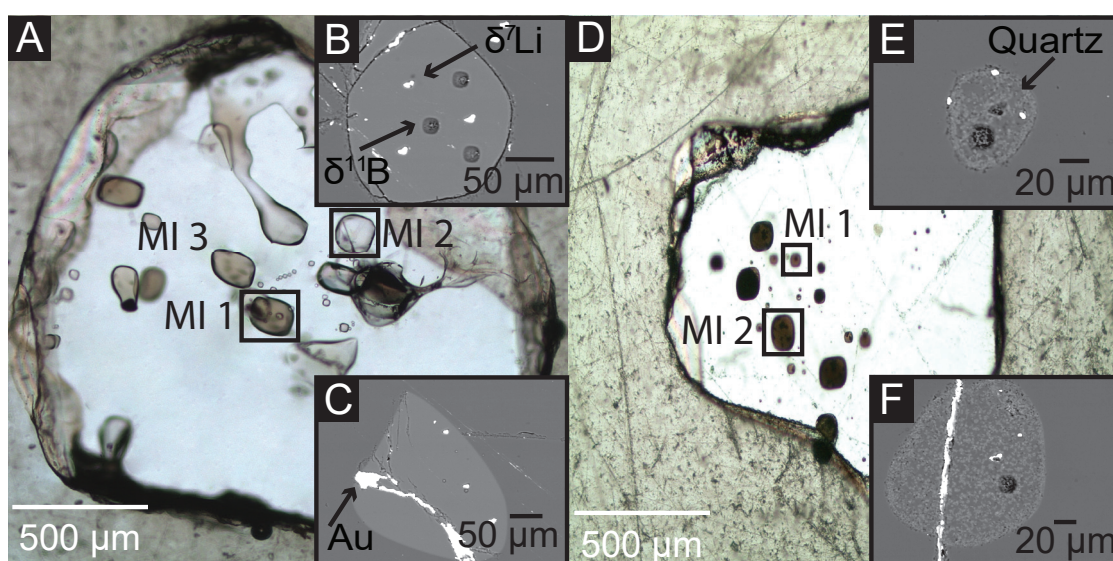


Fig. 4.2: (A) Transmitted light image of a quartz with glassy melt inclusion (MI1 = brown MI; MI2 = colourless MI, sample 11022). (B) BSE image of MI2 with SIMS spots indicated for $\delta^7\text{Li}$ and $\delta^{11}\text{B}$. (C) BSE image of MI1 with gold (Au) coating in a crack. (D) Transmitted light image of a quartz with crystallised MIs (sample 13005). (E) and (F) BSE images of the crystallised MI1 and MI2 showing small quartz crystallising at the rim of the melt inclusions as in the MIs.

size between 10 and 400 μm . The crystallinity of the melt inclusions in sample 13005 varies among individual inclusions, but all crystallised melt inclusions have a thin film of a few microns of new small quartz needles (approx. 5 to 15 μm) on the rims of the inclusions, and feldspar and quartz crystallised within the inclusion (Fig. 4.2D, E and F). Quartz grains from sample 11022 contain mostly glassy melt inclusions with a subordinate proportion of crystallised melt inclusions, whilst; quartz grains from sample 13005 only contain minor amounts of glassy melt inclusions and the majority of melt inclusions are crystallised.

Major element composition the MFT glass melt inclusions are all high-silica rhyolite (> 75 wt.% SiO_2 , recalculated to a volatile-free basis) with K_2O and Na_2O ranging from 5.2 to 5.7 wt.% and 1.6 to 2.7 wt.%, respectively. The concentration of dissolved H_2O and CO_2 in the glassy melt inclusions ranges from 2.8–3.7 wt.% and 68–416 ppm CO_2 , respectively (Tollan et al., 2019) (Appendix C: Supplementary data - Table 1).

Glassy melt inclusions contain less Li (10–37 ppm; average 21 ppm; $n = 26$) compared to the crystallised melt inclusions (6–160 ppm; average 72 ppm; $n = 46$). The Li concentration of the glassy melt inclusions is lower compared to the concentration measured in the groundmass glass (36–52 ppm; Neukampf et al., 2019) and the crystallised melt inclusions have less Li than the previously studied crystallised melt inclusions from MFT (70–397 ppm, average 244 ppm; $n = 29$; Neukampf et al., 2019). The glass melt inclusions are similar in their trace element composition, which is in contrast to other data published on groundmass glass from MFT (Pearce et al., 1996; Perkins and Nash, 2002; Neukampf et al., 2019) with Zr ranging 144–177 ppm, Rb 192–273 ppm, Sm 8–14 ppm and Ti 522–747 ppm. The crystallised melt inclusions show a wider range in their trace element inventories with Zr ranging 73–204 ppm, Rb 115–370 ppm, Sm 4–13 ppm and Ti 330–1051 ppm.

4.4.2 Groundmass glass

The major element composition of the groundmass glass from sample 13005 are in good agreement with the published data (Neukampf et al., 2019) attesting to a high-silica rhyolite (> 75 wt.% SiO_2 ,

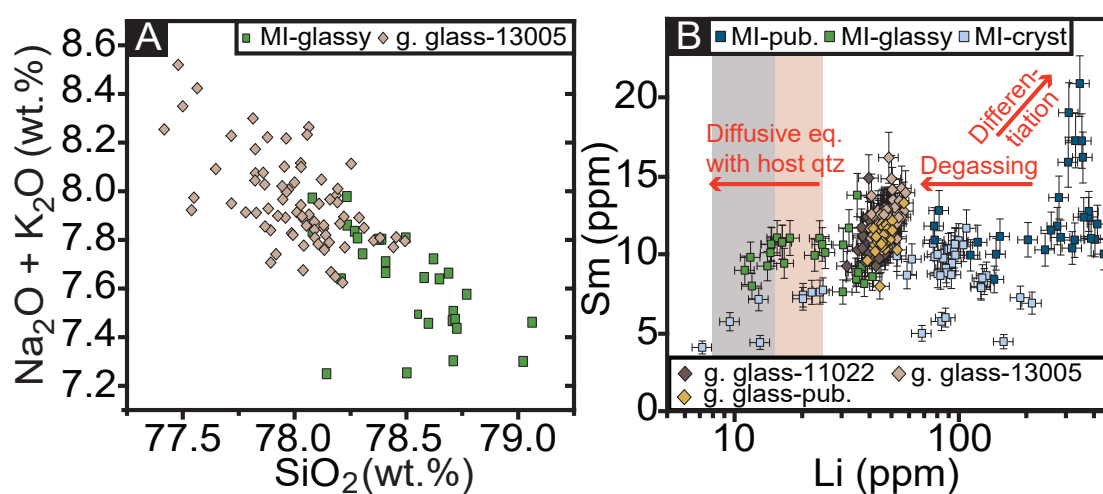


Fig. 4.3:(A) Alkalis vs. SiO_2 of the glassy melt inclusions and the groundmass glass. (B) Lithium versus Samarium concentration (Sm; also immobile during degassing) plot of analysed MIs, corresponding groundmass glass (g. glass) and published data from Neukampf et al. (2019) for comparison. Only crystallised MIs are enriched in Li and glassy melt inclusions have a lower Li concentration than corresponding groundmass glass.

recalculated to a volatile-free basis) with Na₂O ranging 2.1–2.5 wt.% and K₂O 5.3–6.3 wt.%. (Fig. 4.3A). The trace element abundances of both investigated samples are mutually similar (Zr = 128–174 ppm and 133–175 ppm, Ba = 85–165 ppm and 43–303 ppm, Rb = 216–243 ppm and 225–281 ppm, Ti = 555–743 and 510–858 ppm, for sample 13005 and 11022 respectively). Lithium concentration in the groundmass glass from sample 13005 ranges 35–51 ppm (average 42 ppm; n = 35) whereas it is 28–46 ppm in sample 11022 (average 40; n = 59 (Fig. 4.3B).

4.4.3 Quartz

Quartz crystals from both samples are subhedral and range in size from 1 to 5 mm. The CL images of the two quartz samples show different growth zones (Fig. 4.3A and 4.3B; Appendix C: Supplementary data - Fig. C1). The observed elemental patterns are in a good agreement with the previously revealed internal zoning (Neukampf et al., 2019). In the quartz crystals from sample 13005 (Fig. 4.3A and 4.3.C) Ti concentration varies 60–151 ppm in the core (n= 106) and 79–97 ppm in the rim. Titanium and all other measured elements (e.g., Al=93–147 ppm) are in good agreement with the previously

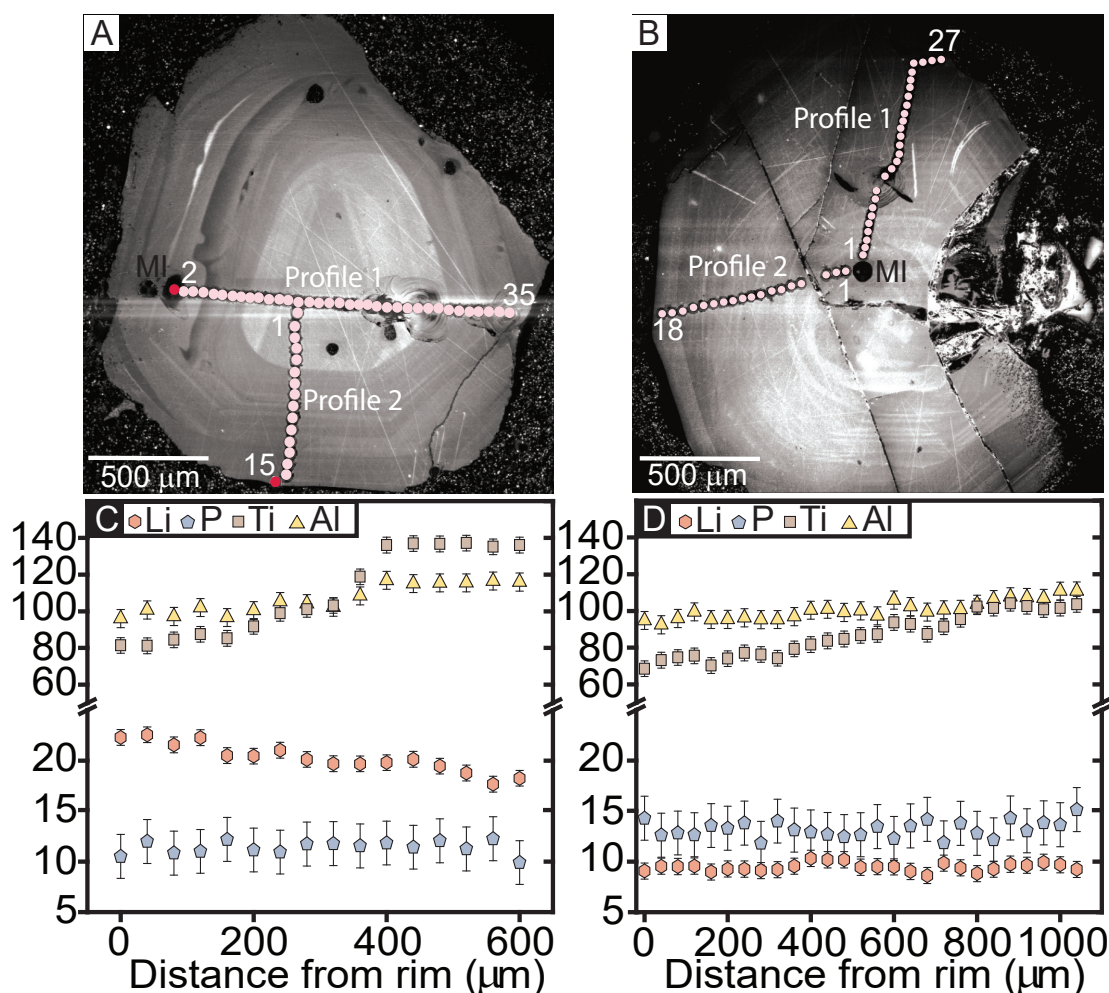


Fig. 4.4: Trace element composition in two different quartz samples. (A) CL image of a quartz with crystallised melt inclusion (MI) and measured (by LA-ICP-MS) trace element profiles in pink (red indicates failed measurement). (B) CL image of quartz with glassy melt inclusion (MI). (C) Trace element composition (in ppm, with 2SD error) of the quartz profile 2 shown in (A) with lithium (Li), phosphorus (P), titanium (Ti) and aluminium (Al). Showing an increase of Li concentration towards the rim. (D) Represents the trace element composition of the profile 1 shown in (B).

published values (Neukampf et al., 2019). Lithium concentrations in sample 13005 increase from the core (15–24 ppm; $n=106$) to the crystal edge (22–24 ppm; $n=7$). Quartz crystals with crystallised melt inclusions have up to a factor of two higher Li concentrations (Fig. 4.6) compared to quartz crystals from sample 11022 (Fig. 4.3B and 4.3D). Those latter quartz crystals show more homogenous Li concentration (8–15 ppm, average: 10 ppm; $n=184$) but, at the same time, they are similar in other trace elements (e.g., Al = 88–117 ppm, Ti = 63–126 ppm).

4.4.4 Lithium isotopes

The brown glassy inclusions have $\delta^7\text{Li}$ values from -7.8‰ to $+2.8\text{‰}$, colorless glassy MIs display almost identical Li systematics ($\delta^7\text{Li}$ from -8.0 to $+3.3\text{‰}$) and a single analysed bubble-bearing glassy MI falls in the same range (-7.1‰). Some melt inclusions vary in their isotopic composition from rim to core, with the rims being isotopically light and the cores isotopically heavy. No $\delta^7\text{Li}$ data for crystallised melt inclusions is presented because there is no SIMS reference material that can be reliably applied to a multi-component matrix. Compared to the inclusions, the groundmass glass from sample 13005 ($+7.6$ to $+20.5\text{‰}$) is up to 25‰ higher (Fig. 4.5).

The $\delta^7\text{Li}$ values of the groundmass glass that were measured by SIMS are not in agreement with the published $\delta^7\text{Li}$ values measured by MC-ICP-MS, that might be due to matrix effects during SIMS measurement, the use of different reference material for the measurements, which could lead to a discrepancy between MC-ICP-MS and SIMS or the bulk glass contained minor amounts of other

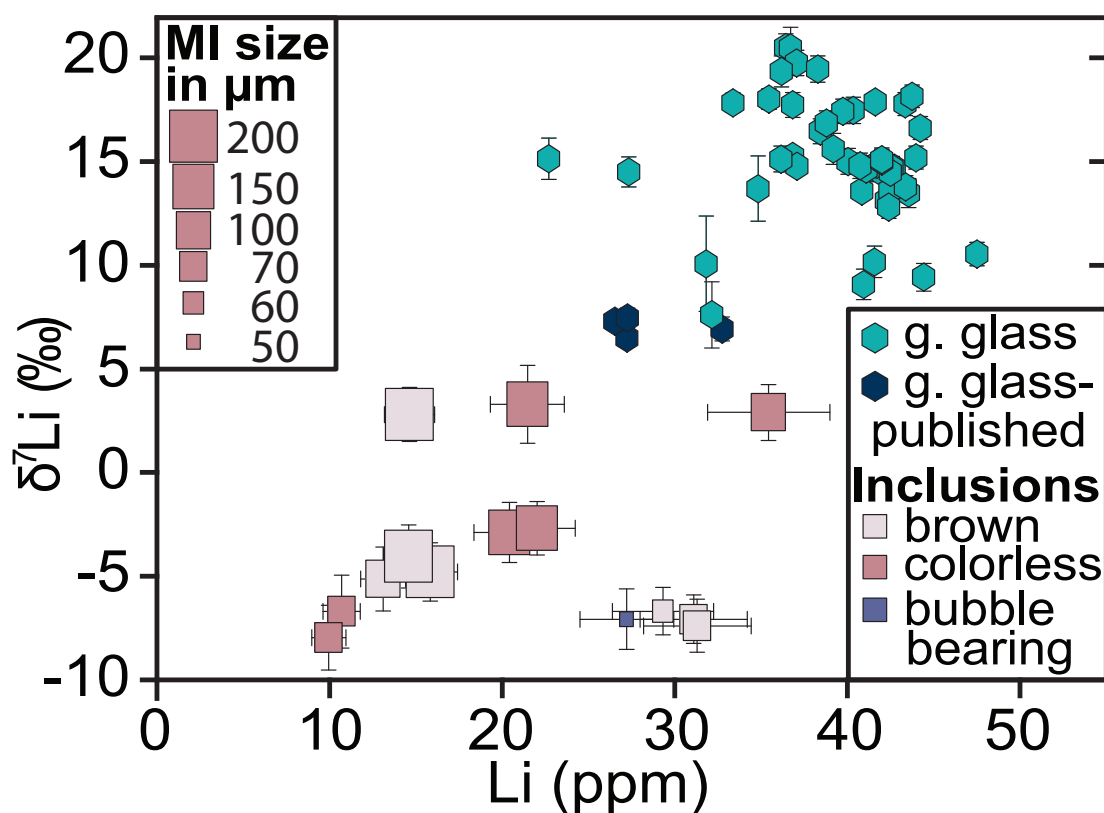


Fig. 4.5: Li concentration (by LA-ICP-MS; 2SD error) vs. isotopic composition ($\delta^7\text{Li}$) of different kinds of glassy melt inclusions (by SIMS; 2SE error) and groundmass glass (by SIMS; 2SE error) compared to isotopic composition of groundmass glass measured by MC-ICPMS (Neukampf et al., 2019). Symbol sizes represent melt inclusion size (see table 4.1).

mineral-phases which would lower the $\delta^7\text{Li}$ value as they are all isotopically lighter than the groundmass glass. The third explanation is more probable as it also explains the differences in the lithium concentrations between MC-ICP-MS and LA-ICP-MS described by Neukampf et al. (2019). Since these are preliminary results the isotope value still may change.

4.5 Discussion

It has been experimentally shown that the trace element composition (e.g., Ag, Cu, Na, Li) of quartz-hosted melt inclusions can be altered within a few days as a result of a concentration gradient, a gradient in pressure or change in water fugacity (e.g., Audétat and Günther, 1999; Zajacz et al., 2009; Rottier et al., 2017) and it was inferred that H_2O can diffuse out of melt inclusions within hours to days when high temperatures are maintained (e.g., Qin et al., 1992; Massare et al., 1998; Massare et al., 2002; Severs et al., 2007). The re-homogenisation of devitrified melt inclusions is used to study processes that lead to volcanic eruptions and to reconstruct their P-T conditions during entrapment. However, Zajacz et al. (2009) have shown that the elemental composition of melt inclusions may change as a result of reheating. Indeed, laboratory-controlled reheating of the melt inclusions can lead to changes in their composition. Errors in the heating temperature, errors on the time span used to reheat the melt inclusions, diffusive re-equilibration with the host crystal, cracking of the melt inclusions can lead to the modification of melt inclusions (Nielsen et al., 1998), therefore in this study the crystallised melt inclusions were not re-homogenised.

4.5.1 Lithium concentrations and isotopic composition in melt inclusions and groundmass glass

The Li isotopic composition varies up to 25‰ between the groundmass glass and glassy melt inclusions; at the same time the Li concentrations of the melt inclusions are up to 50% lower compared to the presumably degassed groundmass glass. Assuming that Li moves into the vapour phase leaving the melt Li-depleted (e.g., Neukampf et al., 2020), the final Li concentration in the groundmass glass represents the minimum Li content of the source melt. The isotopic variation within the groundmass glass (7.6 to 20.5 ‰) could be explained by different bubble sizes during degassing. Whereby a big sized bubble would lead to more ^6Li diffusing from the melt into the vapour leading to heavier values whereas smaller bubbles would lead to less depletion of ^6Li in the melt and lighter values. This has only been theoretically addressed by Watson (2017) and still needs to be experimentally confirmed.

One explanation for the compositional and isotopic difference between the glassy melt inclusions and groundmass glass could be that those are representative of two distinct stages of melt evolution through early and late differentiation, respectively. Even considering a purely incompatible behaviour of Li, over 50% of crystallisation would be required to explain the compositional difference between the melt inclusions (~20 ppm) and the groundmass glass (>40 ppm). This is, however, not supported by any other major- or trace element indicator, since the groundmass glass and melt inclusions are strikingly similar in their chemistry (Fig. 4.3A and B) and petrographic relationships. Therefore, the fractional crystallisation can be excluded to play a major role in the variations of Li concentrations and $\delta^7\text{Li}$ values

of the melt inclusions. By inference, the Li concentration measured in the melt inclusions cannot represent the original Li concentration of the melt at the time of MI entrapment.

The experimental results of Zajacz et al. (2009) showed that the trace element composition of melt inclusions after entrapment can be modified due to the migration of molecular H₂ and H₂O into and out of a melt inclusion and/or host quartz as a consequence of a concentration gradient at temperature and pressure conditions that are typical for upper crustal felsic volcanism. This gradient can result in a rapid diffusion in quartz of H⁺, Li⁺ and Na⁺ parallel to the c-axis as H⁺ loss needs to be charge balanced with a slower diffusion along a- and b-axis (e.g., Audétat and Günther, 1999, Rottier et al., 2017). Qin et al. (1992) determined experimentally that molecular H₂O can diffuse through the host quartz on geologically reasonable time scales and that the diffusion is a result of the pressure gradient that the melt inclusions experienced. The melt inclusions are entrapped at a high pressure and this is followed by a period of residence at a lower pressure in the magma chamber/conduit during degassing of a melt which introduces the pressure gradient. Experiments of Severs et al. (2007) on melt inclusions hosted in quartz from the Bishop Tuff showed that diffusive loss of H-bearing species (OH⁻, H₂O) can occur through the quartz crystal during ascent. Considering these experimental results, we propose equilibration of melt inclusions with their host quartz as an alternative explanation during ascent. As shown for the different H-bearing species Li diffuses from the melt inclusion into the quartz. This is supported by the different lithium concentrations and isotopic composition of some of the melt inclusions, where the melt inclusions are higher in Li concentration and isotopically heavier in the core and lower in concentration and isotopically lighter towards the rims of the melt inclusions. As quartz preferentially incorporates ⁷Li over ⁶Li (e.g., Soltay and Henderson, 2005; Teng et al., 2006), any re-equilibration with quartz would deplete the melt inclusion in ⁷Li and consequently result in low $\delta^7\text{Li}$ values. This may explain why the melt inclusions are 10–30‰ lighter than the groundmass glass (Fig. 4.5) and published MORB data ($\delta^7\text{Li} = 3.5 \pm 1.5\text{‰}$; e.g., Moriguti and Nakamura, 1998; Elliott et al., 2006; Tomascak et al., 2008). A possible explanation for the observed scatter of $\delta^7\text{Li}$ values in the melt inclusions could be related to the size and perhaps shape of the melt inclusions. Smaller melt inclusions (50–100 μm) appear to have lower $\delta^7\text{Li}$ values (–8.9 to –5.1‰) compared to larger melt inclusions (100–200 μm) that are isotopically heavier (–4.8 to +2.8‰) and would have, suffered less diffusive re-equilibration. There is no clear correlation between Li concentration and $\delta^7\text{Li}$ in the melt inclusions, presumably because quartz shows some variability in Li concentrations (8–15 ppm).

Gurenko et al. (2005) investigated the Li systematics of melt inclusions (20–60 ppm, +4 to +15‰) in plagioclase and orthopyroxene from a dacitic pumice (Plat Pays Volcanic Complex, Dominica, Lesser Antilles) and Bouvier et al. (2010) presented an even larger range in Li elemental and isotopic composition (1.1–12 ppm, –24 to +8.2‰) for mafic olivine-hosted melt inclusions from basaltic lavas (Grenada Island, Lesser Antilles). The authors explained the range of $\delta^7\text{Li}$ to be caused by the contribution of dehydration/aqueous fluids from to the underlying slab, possible influence of sediments and/or melting of a metasomatised mantle, which was also shown for Stromboli, Italy (Schiavi et al., 2012). This cannot explain the variation of the melt inclusions from MFT quartz as MFT is in a continental setting whereas Lesser Antilles are in an arc setting and no differences in major or trace elements are observed that would support different origins of the samples.

Kobayashi et al. (2004) measured lithium isotopes in olivine-hosted melt inclusions from Hawaiian lavas that showed variations from -10.2% to $+8.4\%$. The authors stated that these variations represent different mantle sources. However, their melt inclusions were homogenised prior to their measurements which may have changed the Li elemental and isotopic composition of the melt inclusions.

Table 4.1: Lithium isotopic composition (by SIMS) and Li concentration (by LA-ICP-MS) of different glassy quartz-hosted melt inclusions from MFT.

Sample	melt inclusion type	size (in μm)	Li (ppm)	$\delta^7\text{Li}$ (‰)	2 SE
11022-g11-MI3-1	Brown MI	100	13	-5.1	1.5
11022-g11-MI2-1	Colourless MI	150	20	-2.9	1.5
11022-g11-MI2-2	Colourless MI	150	22	3.3	1.9
11022-g11-MI2-3	Colourless MI	150	22	-2.7	1.3
11022-g11-MI1-1	Brown MI	200	16	-4.8	1.4
11022-g11-MI1-2	Brown MI	200	15	2.8	1.3
11022-g11-MI1-3	Brown MI	200	15	-4.1	1.5
11022-g8-MI2-1	Colourless MI	100	34	2.9	1.3
11022-g14-MI1-1	Colourless MI	70	11	-6.7	1.8
11022-g14-MI1-2	Colourless MI	70	10	-8.0	1.6
11022-g10-MI2-1	Brown MI	70	31	-7.1	1.2
11022-g10-MI2-2	Brown MI	70	31	-7.4	1.3
11022-g10-MI3-1	Brown MI	60	29	-6.7	1.2
11022-g1-MI1-1	Bubble-bearing MI	50	27	-7.1	1.5

4.5.2 Lithium abundance in host-quartz

The most common charge balance in quartz is the substitution of $\text{Si}^{4+} \leftrightarrow \text{Al}^{3+} + \text{Li}^+$ (Denen, 1966; Perny et al., 1992). However, in Fig. 4.6A it is shown that there is an excess of Al relative to Li, indicating that Al is additionally charge balanced by H^+ and/or Na^+ . Fig. 4.6A also highlights that the Li concentration between the two quartz populations varies by more than a factor of 2, but with both populations overlapping. Additionally, it also shows that quartz from sample 11022 is further away from the isoatomic Li:Al 1:1 line compared to quartz in sample 13005, perhaps due to a more pronounced Li deficit in 11022. Since the determined Na contents are the same in quartz from both samples, quartz from sample 11022 must have a higher concentration of H^+ than sample 13005 to charge balance this Li deficit. Tollan et al. (2019) described a core-to-rim decrease of H^+ for sample 11022 and their published Li and Al data are in good agreement with the data in this study. The data of Tollan et al. (2019) indicates a diffusive exchange of H^+ between quartz crystals and the surrounding melt as H^+ decreases towards the rims of the crystals. Additional FTIR measurements of sample 13005 are required in order to determine if there is a close relationship between H^+ and Li^+ diffusion in the quartz crystals of MFT.

Reheating of the deposits by the overlying ignimbrite may offer an explanation for the wide range of Li concentrations in quartz, but no microlite growth in the groundmass glass was observed which would be indicative of a long cooling period of the sample and post-eruptive mobility was previously excluded for the pumice sample 13005 as no microlites were observed (Neukampf et al., 2020). Both

samples were collected only few meters apart and they should thus undergo a similar extent of reheating, and would, in all likelihood, preserve the same Li profiles.

An alternative explanation for the Li diffusion profiles in quartz from the sample 13005 could be that due to a general Li enrichment in the melt due to the continuous crystallisation of mineral phases and the general incompatibility of lithium into minerals the quartz crystals would grow Li-rich rims compared to the cores. This would then involve a diffusion of Li between Li-enriched rims and Li-depleted cores. However, the enrichment in Li of the melt would also affect the other mineral phases such as plagioclase and sanidine (Neukampf et al., 2019), whilst their Li systematics hint at a decrease of Li in the melt rather than an increase. Moreover, as discussed earlier, this cannot explain the >50% difference in Li concentration between the two quartz samples as it would require an unreasonable amount of melt differentiation. This is, however, unsupported by other geochemical proxies.

Charlier et al. (2012) reported the Li gradients in plagioclase and quartz for the rhyolitic Oruanui super eruption (Taupo, New Zealand) with an increase of Li towards the rims of feldspar and quartz and explained this by Li re-partitioning from fluid phase into the melt phase due to the extraction of chloride into the gas phase. However, this does not explain the reversed Li diffusion profiles observed for MFT quartz on one hand (Fig. 4.6B), and plagioclase and sanidine (Neukampf et al., 2019; Neukampf et al., 2020) on the other.

Magma mixing with a less evolved melt can be excluded as an explanation for the Li concentration differences in the quartz samples because their associated groundmass glass would differ in major- and trace element compositions. Moreover, due to a moderately incompatible character of Li, mixing of rhyolitic materials with a more mafic melt would lower the Li concentration towards the rim, while an opposite is observed. Additionally, none of the other minerals present in MFT (plagioclase, sanidine, clinopyroxene, orthopyroxene, olivine) indicate magma mixing or cumulate melting, which would equally decrease the Li concentration. Fluxing of a new volatile phase that is enriched in Li (e.g., plagioclase), described for Mount St. Helens by Berlo et al. (2004), Kent et al., (2007) and Rowe et al. (2008), can be excluded because it would again lead to Li-enriched and isotopically light rims in the feldspar crystals. It has been shown that ^6Li favours the vapour phase (Neukampf et al., 2020).

We propose a scenario where the core-to-rim diffusion profiles of Li concentrations in sample 13005 are caused by H^+ diffusing out of the quartz lattice into the melt and Li^+ diffusing inwards to replace these vacancies. The H^+ diffusing out of the quartz occurs due to H^+ moving into the vapour phase during degassing and thereby depleting the melt in H^+ leading to a disequilibrium between quartz and melt. This disequilibrium imparts diffusion of H^+ outwards which is then replaced by Li^+ diffusing into the quartz crystal lattice. This is supported by experiments from Audétat and Günther (1999) and other others who determined the rapid diffusion of H^+ , Li^+ and Na^+ parallel to the c-axis and slower diffusion along a- and b-axis occurs when a gradient between quartz and melt is introduced. A way to test this hypothesis would entail measurements of the $\delta^7\text{Li}$ profiles in the quartz following the observation of Sartbaeva et al. (2005) who determined that ^6Li moves faster through quartz compared to ^7Li . However, this hypothesis cannot currently be tested using Li isotopes because no suitable $\delta^7\text{Li}$ quartz reference material is available for in situ analysis.

However, it is unclear which mechanism drives Li to move into the quartz lattice during degassing of the melt as it should move into the vapour phase. A reason why quartz crystals from sample 11022

have not formed Li diffusion profiles could be that they were not kept at lower pressures as long as the quartz crystals from sample 13005, which would also explain why they preserved their glassy melt inclusions.

4.5.3 Diffusion modelling

The Li diffusion profiles from quartz in sample 13005 can be used to estimate the time scales of the disequilibrium between melt and quartz. Quartz from the fallout sample 11022 is not considered due to the homogenous concentrations. The time scales calculated here should only be considered as an oversimplified approximation as only a single diffusion coefficient (D) value for Li along the c-axis in quartz at 720 °C was determined by Verhoogen (1952) ($D^{\text{Li}}=1.9\times 10^{-11}$ m²/s) and verified more recently by Zajacz et al. (2009) ($D^{\text{Li}}=10^{-11}$ m²/s at 710 °C). Because no Arrhenius parameters for Li were experimentally determined it is impossible to recalculate the diffusion coefficient for the accurate temperatures of MFT (789 to 856 °C; Neukampf et al. 2020). The diffusivity of Li is strongly temperature-dependent as shown for plagioclase (Giletti and Shanahan, 1997), using the diffusion coefficient obtained for 720°C will result in the overestimation of the diffusion time scales for the Li diffusion profiles in quartz. In addition, the diffusion coefficient was only determined along the c-axis. Applying this coefficient to profiles along the a- and b-axis will result in an underestimation of the time scales. Orientation of the crystals during sample preparation in the mounts was not considered and most profiles were measured along the a- and b-axis. The time scales estimated for Li diffusion profiles (sample 13005 – this study, and Neukampf et al., 2019) (Fig. 4.6B) range from 2 to 150±20 minutes with a majority of the estimates longer than 40 minutes ($n=21$, average: 48 min). The measured concentration profiles and variations from short to long estimated time scales support the diffusional anisotropy of Li along different crystallographic axes which has been shown for olivine (Dohmen et al., 2010). The estimated time scales

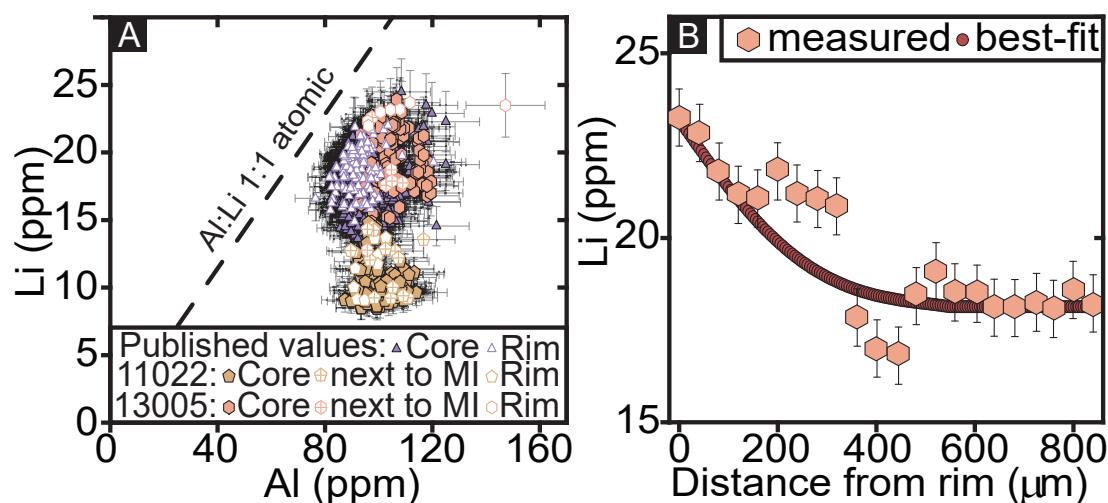


Fig. 4.6: (A) Plot of Li vs. Al with isoatomic Li:Al 1:1 line (substitution of $\text{Si}^{4+} \leftrightarrow \text{Al}^{3+} + \text{Li}^{+}$). Purple triangle (core: $n=570$; rim: $n=148$) represents data from Neukampf et al., (2019), the brown pentagram refers to the quartz sample with glassy melt inclusions (core: $n=160$; next to MI: $n=13$; rim: $n=11$) and the pink hexagon indicates the quartz with crystallised melt inclusions (sample 13005). (B) Example of a one-dimensional Li diffusion model for quartz (profile 1 shown in Fig 4.4A) with crystallised MIs. The pink hexagon represents (symbol size representing size of the analysed spot) the measured Li concentration and red circle the best-fit.

between 2 to 20 minutes are in a good agreement with the time scales estimated for Li diffusion in plagioclase from MFT which ranges from 1 to 15 minutes. Our findings are also in a good agreement with the estimates from Li diffusion in plagioclase from MFT and decompression time scales (<12 hours to 5 days) published for the Huckleberry Ridge Tuff (Myers et al., 2016).

4.6 Conclusions

This study shows that particular attention needs to be paid to the selection of melt inclusions for geochemical analyses and homogenisation of MIs can change their composition. The combination of lithium concentration, *in situ* $\delta^7\text{Li}$ measurements in quartz-hosted melt inclusions and groundmass glass and diffusion modelling of lithium concentration gradients in quartz could present a powerful tool to understand late stage magmatic processes. The results of this study suggest that the lithium concentration in quartz can double within hours and quartz-hosted melt inclusions do not necessarily preserve the original melt composition and trace element and isotopic composition can be overprinted prior to eruption during ascent due to changes in pressure and as a result of the diffusion of the different H species that need to be charge balanced. Earlier erupted material experienced less diffusion and re-equilibration, therefore preserved the glassy melt inclusion. Later erupted samples experience a longer diffusional exchange leading to the re-crystallisation of the melt inclusions and to a modification of the Li concentration of the host quartz. Further measurements are needed to confirm or exclude theories presented here and may change part of the interpretation.

Acknowledgements

We thank Julien Allaz for his help during probe analyses. This work was supported by Swiss National Science Foundation grant 200021_166281 to BE.

4.7 References

- Audétat, A. and Günther, D., 1999, Mobility and H₂O loss from fluid inclusions in natural quartz crystals: Contributions to Mineralogy and Petrology, v. 137, p. 1-14, <https://doi.org/10.1007/s004100050578>.
- Audétat, A., Garbe-Schönberg, D., Kronz, A., Pettke, T., Rusk, B., Donovan, J. J., Lowers, H. A., 2015, Characterisation of a natural quartz crystal as a reference material for microanalytical determination of Ti, Al, Li, Fe, Mn, Ga and Ge. *Geostandards and Geoanalytical Research*, v. 39 (2), p. 171–184.
- Beinlich, A., John, T., Vrijmoed, J.C., Tominaga, M., Magna T. Podladchikov, Y. Y., 2020, Instantaneous rock transformations in the deep crust driven by reactive fluid flow. *Nature Geoscience*, v. 13, p. 307–311. <https://doi.org/10.1038/s41561-020-0554-9>.
- Behrens, H., Tamic, N., Holtz, F., 2004, Determination of the molar absorption coefficient for the infrared absorption band of CO₂ in rhyolitic glasses. *American Mineralogist*, v.89, p. 301–306.
- Benson, T. R., Coble, M. A., Rytuba, J. J., Mahood, G. A., 2017, Lithium enrichment in intracontinental rhyolite magmas leads to Li deposits in caldera basins. *Nature Communications*, v. 8, 270, <https://doi.org/10.1038/s41467-017-00234-y>.
- Berlo, K., Blundy, J., Turner, S., Cashman, K., Hawkesworth, C., Black, S., 2004, Geochemical precursors to volcanic activity at Mount St. Helens, USA. *Science*, v. 306, p. <https://doi.org/1167-1169>, 10.1126/science.1103869.
- Bouvier, A.-S., Métrich, N., Delouie, E., 2008, Slab-derived fluids in magma sources of St. Vincent (Lesser Antilles Arc): volatile and light element imprints. *Journal of Petrology*, v. 49 (8), p. 1427–1448, <https://doi.org/10.1093/petrology/egn031>.
- Bouvier, A.-S., Métrich, N., Delouie, E., 2010, Light elements, volatiles, and stable isotopes in basaltic melt inclusions from Grenada, Lesser Antilles: Inferences for magma genesis. *Geochemistry, Geophysics, Geosystems*, v. 11 (9), <https://doi.org/10.1029/2010GC003051>.
- Chan, L. H., Edmond, J. M., Thompson, G., Gillis, K., 1992, Lithium isotopic composition of submarine basalts: implications for the lithium cycle in the oceans. *Earth and Planetary Science Letters*, v. 108, p. 151-160.
- Charlier, B., Morgan, D., Wilson, C., Wooden, J., Allan, A., Baker, J., 2012, Lithium concentration gradients in feldspar and quartz record the final minutes of magma ascent in an explosive supereruption. *Earth and Planetary Science Letters*, v. 319–320, p. 218-227, <https://doi.org/10.1016/j.epsl.2011.12.016>.
- Christiansen, R.L., 2001, The Quaternary and Pliocene Yellowstone Plateau Volcanic Field of Wyoming, Idaho, and Montana. US Geological Survey Professional Paper 729-G, <https://doi.org/10.3133/pp729G>.
- Danyushevsky, L. V., Della-Pasqua, F. N., Sokolov, S., 2000, Re-equilibration of melt inclusions trapped by magnesian olivine phenocrysts from subduction-related magmas. petrological implications. *Contributions to Mineralogy and Petrology*, v. 138, p. 68–83.
- Denen, W. H., 1966, Stoichiometric substitution in natural quartz. *Geochimica et Cosmochimica Acta*, v. 30, p. 1235–1241.
- Elliott, T., Thomas, A., Jeffcoate, A., Niu, Y., 2006, Lithium isotope evidence for subduction-enriched mantle in the source of Mid-Ocean-Ridge Basalts. *Nature*, v. 443 (7111), p. 565–568.
- Ellis, B.S., Mark, D.F., Troch, J., Bachmann, O., Guillong, M., von Kent, A.J.R., Quadt, A., 2017, Split-Grain ⁴⁰Ar/³⁹Ar dating: integrating temporal and geochemical data from crystal cargoes. *Chemical Geology*, v. 457, p. 15-23, <https://doi.org/10.1016/j.chemgeo.2017.03.005>.
- Ellis, B.S., Szymanowski, D., Magna, T., J. Neukampf, Dohmen, R., Bachmann, O., Ulmer, P., Guillong, M., 2018, Post-eruptive mobility of lithium in volcanic rocks. *Nature Communications*, v. 9, p. 3228, <https://doi.org/10.1038/s41467-018-05688-2>.
- Frezzotti, M.L., 2001, Silicate-melt inclusions in magmatic rocks: applications to petrology. *Lithos*, v. 55, p. 273–299.
- Giletti, B.J., and Shanahan, T.M., 1997, Alkali diffusion in plagioclase feldspar: *Chemical Geology*, v. 139, p. 3–20, [https://doi.org/10.1016/S0009-2541\(97\)00026-0](https://doi.org/10.1016/S0009-2541(97)00026-0).
- Guillong, M., Meier, D.K., Allan, M.M., Heinrich, C.A., Yardley, B.W.D., 2008, SILLS: A Matlab-Based Program for the Reduction of Laser Ablation ICP–MS Data of Homogeneous Materials and Inclusions. *Mineralogical Association of Canada Short Course, Vancouver, B.C.*, v. 40, p. 328–333.
- Gurenko, A. A., Trumbull, R. B., Thomas, R., Lindsay, J. M., 2005, A melt inclusion record of volatiles, trace elements and Li – B isotope variations in a single magma system from the Plat Pays Volcanic Complex,

- Dominica, Lesser Antilles. *Journal of Petrology*, v. 46, p. 2495–2526, <https://doi.org/10.1093/petrology/egi063>.
- Hofstra, A. H., Todorov, T. I., Mercer, C. N., Adams, D. T., Marsh, E. E., 2013, Silicate Melt Inclusion Evidence for Extreme Pre-eruptive Enrichment and Post-eruptive Depletion of Lithium in Silicic Volcanic Rocks of the Western United States: Implications for the Origin of Lithium-Rich Brines. *Economic Geology*, v. 108, p. 1691-1701, <https://doi.org/10.2113/econgeo.108.7.1691>.
- Holycross, M. E., Watson, E. B., Richter, F. M., Villeneuve, J., 2018, Diffusive fractionation of Li isotopes in wet, silicic melts. *Geochemical Perspectives Letters*, v. 6, p. 39-42, <https://doi.org/10.7185/geochemlet.1807>.
- Jeffcoate, A. B., Elliott, T., Kasemann, S. A., Ionov, D., Cooper, K., Brooker R., 2007, Li isotope fractionation in peridotites and mafic melts. *Geochimica et Cosmochimica Acta*, v. 71, p. 202-218.
- Jochum, K. P., Weis, U., Stoll, B., Kuzmin, D., Yang, Q., Raczek, I., Jacob, D. E., Stracke, A., Birbaum, K., Frick, D. A., Günther, D., Enzweiler, J., 2011, Determination of reference values for NIST SRM 610–617 glasses following ISO guidelines. *Geostandards and Geoanalytical Research*, v. 35, p. 397–429.
- John, T., Gussone, N., Podladchikov, Y. Y., Bebout, G. E., Dohmen, R., Halama, R., Klemd, R., Magna, T., Seitz, H-M, 2012, Volcanic arcs fed by rapid pulsed fluid flow through subducting slabs. *Nature Geoscience*, v. 5, 489–492.
- Johnson, E. A., Rossman, G. R., 2013, The diffusion behavior of hydrogen in plagioclase feldspar at 800–1000 °C: implications for re-equilibration of hydroxyl in volcanic phenocrysts. *American Mineralogist*, v. 98, p. 1779-1787.
- Kent, A. J. R., Blundy, J., Cashman, K. V., Cooper, K. M., Donnelly, C., Pallister, J. S., Reagan, M., Rowe, M. C., Thornber, C. R., 2007, Vapor transfer prior to the October 2004 eruption of Mount St. Helens, Washington. *Geology*, v. 35 (3), p. 231–234, <https://doi.org/10.1130/G22809A.1>.
- Kesler, S. E., Gruber, P. W., Medina, P. A., Keoleian, G. A., Everson, M. P., Wallington, T. J., 2012, Global lithium resources: Relative importance of pegmatite, brine and other deposits. *Ore Geology Reviews*, v. 48, p. 55-69, <https://doi.org/10.1016/j.oregeorev.2012.05.006>.
- Kobayashi, K., Tanaka, R., Moriguti, T., Shimizu, K., Nakamura, E., 2004, Lithium, boron, and lead isotope systematics of glass inclusions in olivines from Hawaiian lavas: evidence for recycled components in the Hawaiian plume. *Chemical Geology*, v. 212 (1), p. 143-161.
- Lindsay, J. M., Schmitt, A. K., Trumbull, R. B., de Silva, S. L., Siebel, W., Emmermann, R., 2001, Magmatic evolution of the La Pacana Caldera system, central Andes, Chile: compositional variation of two cogenetic, large-volume felsic ignimbrites and implications for contrasting eruption mechanisms. *Journal of Petrology*, v. 42, p. 459–486, <https://doi.org/10.1093/petrology/42.3.459>.
- Lundstrom, C. C., Chaussidon, M., Hsui, A.T., Kelemen, P., Zimmerman, M., 2005, Observations of Li isotopic variations in the Trinity ophiolite: evidence for isotopic fractionation by diffusion during mantle melting. *Geochimica et Cosmochimica Acta*, v. 69, p. 735-751.
- Magna, T., Ionov, D. A., Oberli, F., Wiechert, U., 2008, Links between mantle metasomatism and lithium isotopes: Evidence from glass-bearing and cryptically metasomatized xenoliths from Mongolia. *Earth and Planetary Science Letters*, 276:214–222.
- Marschall, H. R., Pogge von Strandmann, P. A. E., Seitz, H. M., Elliott, T., Niu, Y. L., 2007, The lithium isotopic composition of orogenic eclogites and deep subducted slabs. *Earth and Planetary Science Letters*, v. 262, p. 563-580.
- Massare, D., Metrich, N., Thellier, B., Clocchiatti, R., 1998, Evidence of H₂O loss in melt inclusions after a series of heating stage experiments. *Terra Abstracts*, v. 10, p. 39.
- Massare, D., Metrich, N., Clocchiatti, R., 2002, High-temperature experiments on silicate melt inclusions in olivine at 1 atm: inferences on temperature of homogenization and H₂O concentrations. *Chemical Geology*, v. 183, p. 87-98.
- Matthews, N. E., Vazquez, J. A., Calvert, A., 2015, Age of the Lava Creek supereruption and magma chamber assembly at Yellowstone based on ⁴⁰Ar/³⁹Ar and U–Pb dating of sanidine and zircon crystals. *Geochemistry, Geophysics, Geosystems*, v. 16, doi:10.1002/2015GC005881.
- Moriguti, T., Nakamura, E., 1998, Across-arc variation of Li isotopes in lavas and implications for crust/mantle recycling at subduction zones. *Earth and Planetary Science Letters*, v.163(1–4), p. 167–174.
- Myers, M.L., Wallace, P.J., Wilson, C.J., Morter, B.K., Swallow, E.J., 2016, Prolonged ascent and episodic venting of discrete magma batches at the onset of the Huckleberry Ridge supereruption, Yellowstone. *Earth and Planetary Science Letters*, v. 451, p. 285-297, <https://doi.org/10.1016/j.epsl.2016.07.023>.
- Neukampf, J., Ellis, B.S., Magna, T., Laurent, O., and Bachmann, O., 2019, Partitioning and isotopic fractionation of lithium in mineral phases of hot, dry rhyolites: The case of the Mesa Falls Tuff, Yellowstone. *Chemical Geology*, v. 506, p. 175–186, <https://doi.org/10.1016/j.chemgeo.2018.12.031>.

- Neukampf, J., Ellis, B.S., Laurent, O., Steinmann, L. K., Ubide, T., Oeser, M., Magna, T., Weyer, S., Bachmann, O. (2020) Time scales of syn-eruptive volatile loss in silicic magmas quantified by Li-isotopes. *Geology*, v. 49, p. xxx-xxx, <https://doi.org/10.1130/G47764.1>.
- Nielsen, R. L., Michael, P. J., Sours-Page, R., 1998, Chemical and physical indicators of compromised melt inclusions. *Geochimica et Cosmochimica Acta*, v. 62, p. 831–839.
- Parkinson, I. J., Hammond, S. J., James, R. H., Rogers, N. W., 2007, High-temperature lithium isotope fractionation: insights from lithium isotope diffusion in magmatic systems. *Earth and Planetary Science Letters*, v. 257, p. 609–621.
- Pearce, N. J. G., Westgate, J. A., Perkins, W. T., 1996, Developments in the analysis of volcanic glass shards by laser ablation ICP-MS: quantitative and single internal standard-multielement methods. *Quaternary International*, v. 34–36, p. 213–227.
- Perkins, M. E., Nash, B. P., 2002, Explosive silicic volcanism of the Yellowstone hotspot: the ash fall tuff record. *Geological Society of America Bulletin*, v. 114 (3), p. 367–381.
- Perny, B., Eberhardt, P., Ramseyer, K., Mullis, J., Pankrath, R., 1992, Microdistribution of Al, Li, and Na in α quartz: Possible causes and correlation with short-lived cathodoluminescence. *American Mineralogist*, v. 77 (5-6), p. 534–544.
- Qin, Z., Lu, F., Anderson Jr., A., T., 1992, Diffusive reequilibration of melt and fluid inclusions. *American Mineralogist*, v. 77, p. 565–576.
- Richter, F. M., Watson, E. B., Mendybaev, R., Dauphas, N., Georg, B., Watkins, J., Valley, J., 2009, Isotopic fractionation of the major elements of molten basalt by chemical and thermal diffusion. *Geochimica et Cosmochimica Acta*, v. 73, p. 4250–4263.
- Richter, F. M., Davis, A. M., DePaolo, D. J., Watson, E. B., 2003, Isotope fractionation by chemical diffusion between molten basalt and rhyolite. *Geochimica et Cosmochimica Acta*, v. 67, p. 3905–3923.
- Rivera, T. A., Schmitz, M. D., Crowley, J. L., Storey, M., 2014, Rapid magma evolution constrained by zircon petrochronology and $^{40}\text{Ar}/^{39}\text{Ar}$ sanidine ages for the Huckleberry Ridge Tuff, Yellowstone, USA. *Geology*, v. 42, p. 643–646.
- Rivera, T.A., Schmitz, M.D., Jicha, B.R., Crowley, J.L., 2016, Zircon petrochronology and $^{40}\text{Ar}/^{39}\text{Ar}$ sanidine dates for the Mesa Falls Tuff: crystal-scale records of magmatic evolution and the short lifespan of a large Yellowstone magma chamber. *Journal of Petrology*, v. 57, p. 1677–1704, <https://doi.org/10.1093/petrology/egw053>.
- Roedder, E., 1979, Origin and significance of magmatic inclusions. *Bulletin de Mineralogie*, v. 102, p. 487–510.
- Rottier, B., Rezeau, H., Casanova, V., Kouzmanov, K., Moritz, R., Schlöglöva, K., Wälle, M., and Fontboté, L., 2017, Trace element diffusion and incorporation in quartz during heating experiments. *Contributions to Mineralogy and Petrology*, v. 172, p. 23, <https://doi.org/10.1007/s00410-017-1350-4>.
- Rowe, M. C., Kent, A. J. R., Thornber, C.R., 2008, Using amphibole phenocrysts to track vapor transfer during magma crystallization and transport: an example from Mount St. Helens, Washington. *Journal of Volcanology and Geothermal Research*, v. 178, p. 593–607, 10.1016/j.jvolgeores.2008.01.012.
- Sartbaeva, A., Wells, S. A., Redfern, S. A. T., Hinton, R. W., Reed, S. J. B., 2005, ionic diffusion in quartz studied by transport measurements, SIMS and atomistic simulations. *Journal of Physics: Condensed Matter*, v. 17, p. 1099–1112, <http://dx.doi.org/10.1080/01411599008206882>.
- Schiavi, F., Katsura Kobayashi, K., Moriguti, T., Nakamura, E., Pompilio, M., Tiepolo, M., Vannucci, R., 2010, Degassing, crystallization and eruption dynamics at Stromboli: trace element and lithium isotopic evidence from 2003 ashes. *Contributions to Mineralogy and Petrology*, v. 159, p. 541–561, <https://doi.org/10.1029/96JB00815>.
- Schiavi, F., Kobayashi, K., Nakamura, E., Tiepolo, M., Vannucci, R., 2012, Trace element and Pb-B-Li isotope systematics of olivine-hosted melt inclusions: insights into source metasomatism beneath Stromboli (southern Italy). *Contributions to Mineralogy and Petrology*, v. 163, p. 1011–1031, <https://doi.org/10.1007/s00410-011-0713-5>.
- Severs, M. J., Azbej, T., Thomas, J. B., Mandeville, C. W., Bodnar, R. J., 2007, Experimental determination of H_2O loss from melt inclusions during laboratory heating: evidence from Raman spectroscopy. *Chemical Geology*, v. 237, p. 358–371.
- Singer, B. S., Jicha, B. R., Condon, D. J., Macho, A. S., Hoffman, K. A., Dierkhising, J., Brown, M. C., Feinberg, J. M., Kidane, T., 2014, Precise ages of the Reunion event and Huckleberry Ridge excursion: episodic clustering of geomagnetic instabilities and the dynamics of flow within the outer core. *Earth and Planetary Science Letters*, v. 405, p. 25–38.
- Soltay, L. G., Henderson, G. S., 2005, Structural differences between lithium silicate and lithium germanate glasses by Raman spectroscopy. *Physics and Chemistry of Glasses*, 46, 381–384.

- Stix, J., Layne, G. D., 1996, Gas saturation and evolution of volatile and light lithophile elements in the Bandelier magma chamber between two caldera-forming eruptions. *Journal of Geophysical Research*, v. 101, p. 25181–25196.
- Teng, F. Z., McDonough, W. F., Rudnick, R. L., Walker, R. J. (2006) Diffusion-driven extreme lithium isotopic fractionation in country rocks of the Tin Mountain pegmatite. *Earth and Planetary Science Letters*, 243, 701–710.
- Tollan, P., Ellis, B., Troch, J., Neukampf, J., 2019, Assessing magmatic volatile equilibria through FTIR spectroscopy of unexposed melt inclusions and their host quartz: a new technique and application to the Mesa Falls Tuff, Yellowstone. *Contributions to Mineralogy and Petrology*, v. 174 (24), <https://doi.org/10.1007/s00410-019-1561-y>.
- Tomascak, P. B., Johnson, C. M., Beard, B. Albarède, L., F. (Eds.), 2004, Developments in the understanding and application of lithium isotopes in the Earth and planetary sciences. *Geochemistry of Non-traditional Stable Isotopes*, Mineralogical Society of America, Washington, D.C., p. 153-195.
- Tomascak, P. B., Langmuir, C. H., le Roux, P. J., Shirey, S. B., 2008, Lithium isotopes in global mid-ocean ridge basalts. *Geochimica et Cosmochimica Acta*, v. 72 (6), p. 1626–1637.
- Tomascak, P. B., Magna, T. and Dohmen, R., 2016, *Advances in Lithium Isotope Geochemistry*. Springer International Publishing, Cham, Switzerland.
- Verhoogen, J., 1952, Ionic diffusion and electrical conductivity in quartz. *American Mineralogist*, v. 37 (7-8), p. 637–655.
- Watson, E.B., 2017, Diffusive fractionation of volatiles and their isotopes during bubble growth in magmas. *Contributions to Mineralogy and Petrology*, v. 172, <https://doi.org/10.1007/s00410-017-1384-7>.
- Zajacz, Z., Hanley, J.J., Heinrich, C.A., Halter, W.E., Guillong, M., 2009, Diffusive reequilibration of quartz-hosted silicate melt and fluid inclusions: are all metal concentrations unmodified? *Geochimica et Cosmochimica Acta*, v. 73, p. 3013-3027, <https://doi.org/10.1016/j.gca.2009.02.023>.
- Zhang, Y., Belcher, R., Ihinger, P. D., Wang, L., Xu, Z., Newman, S., 1997, New calibration of infrared measurement of dissolved water in rhyolitic glasses. *Geochimica et Cosmochimica Acta*, v. 61, p. 3089–3100.

Chapter 5

Conclusions and outlook

5.1 Conclusion

In this thesis, I investigated the lithium distribution and isotopic composition between different mineral phases, groundmass glass and melt inclusions of a dry high-silica rhyolite from Yellowstone (USA) as a first detailed study of lithium in an evolved magmatic system. The smallest of the three caldera-forming eruptions, Mesa Falls Tuff, was used for all studies presented in my thesis as the samples were taken from the non-welded part of the eruption and, due to the fast quenching, post-eruptive modification can be excluded. Additionally, none of the minerals is strongly zoned in terms of major elements, making it a simpler system to study. This thesis covers different disciplines within Earth Sciences, e.g., geochemistry, volcanology, igneous petrology, by looking at high-temperature fractionation of lithium isotopes by applying different measurement techniques (MC-ICP-MS, fs-LA-MC-ICP-MS; SIMS). This thesis is one of the first studies to show that high-temperature kinetic isotopic fractionation in evolved magmatic systems exist and gives a systematic overview on the lithium distribution in an evolved magmatic system. Further, the applied measurement techniques can be used to identify economically important Li deposits, however, Mesa Fall Tuff does not represent an economically important Li deposit.

The lithium data of the different minerals and groundmass glass present in the Mesa Falls Tuff showed that lithium is variably incompatible, with quartz-hosted crystallised melt inclusions exhibiting the highest lithium concentration, followed by the groundmass glass and minimising with sanidine. Calculated apparent partition coefficients for lithium between the groundmass glass and the different mineral phases showed that lithium is most compatible in quartz and most incompatible in sanidine. Lithium isotopic composition measurements by MC-ICP-MS show that high-temperature fractionation can span over ~10‰ between different mineral phases and groundmass glass in one single eruption.

By studying plagioclase crystals from Mesa Falls Tuff, it is shown that a single phase can preserve high-temperature kinetic isotopic fractionation that spans over ~15‰ and is, therefore, greater than the fractionation between different mineral phases. The groundmass glass of Mesa Falls Tuff is the isotopically heaviest phase present, resulting from ^6Li fractionating into the vapour phase during vesiculation, thereby, depleting the melt in ^6Li and enriching it in ^7Li . The loss of lithium from the melt then led to the diffusion of ^6Li from the plagioclase rims into the melt, depleting the rims in ^6Li and resulting in a large isotopic fractionation within plagioclase crystals. This leads to the conclusion that disequilibrium between melt and mineral phases prior to eruption can result in large inter-mineral fractionation. Applying diffusion modelling to lithium concentration profiles and to the $\delta^7\text{Li}$ diffusion profiles can allow to determine the time scales in which this isotopic fractionation appeared and can help track late-stage magmatic processes. This can be applied to different magmatic systems, but magma mixing or cumulate melting needs to be excluded as it would change the isotopic signature that is preserved. Additionally, this shows that ^6Li can be lost from the systems due to degassing, and, therefore, the groundmass glass does not represent the original value of the melt, neither in concentration nor in the isotopic composition. However, to be able to apply this to other systems there is the need for more experimental studies on lithium diffusion coefficients that cover a wider range in feldspar composition as well as temperature and pressure. It also shows that collecting $\delta^7\text{Li}$ diffusion profile measurements by fs-LA-MC-ICP-MS combined with diffusion modelling is a powerful tool and should be used more routinely especially

when combined with concentration maps acquired by LA-ICP-MS. This technique could be applied to other caldera forming eruption, e.g., Kos Plateau Tuff to study which influence the geological setting (e.g., arc setting) has on the degassing time scales.

It was further shown that the lithium composition can not only be altered in feldspar but in quartz and quartz-hosted melt inclusions as well. Attention needs to be paid to the selection of melt inclusions and their interpretation. The lithium concentration in quartz appears to be linked to H₂O present in the quartz, but further measurements are needed to confirm this. Diffusion modelling showed that due to diffusional exchange between quartz crystals and melt, the lithium concentration in quartz can change within a few hours. Additionally, quartz-hosted melt inclusions do not necessarily preserve the isotopic composition of the melt and their composition can be changed due to lithium diffusion between host-quartz and melt inclusions. This leads to the conclusion that at magmatic temperature lithium diffusion within melt and crystals is fast and degassing of the melt induces disequilibrium resulting in lithium gradients within feldspars and quartz. However, the mechanism responsible for the enrichment in the quartz is not fully understood, as degassing should lead to a depletion of lithium from the quartz, as shown for the feldspar, rather than to an enrichment. Further measurements are needed to address this contradiction.

In conclusion, by using different *in situ* measurement techniques, preserved lithium compositional and isotopic zonation in different mineral phases that have formed at magmatic temperatures can be identified, while using column chemistry might mask inter-mineral fractionation. High-temperature kinetic isotopic fractionation of lithium can span over ~15‰ and the lithium concentration and isotopic composition of different mineral phases and melt can change within hours prior to eruption. The measurement techniques used in this thesis can also be applied to other volcanic eruptions (e.g., Bishop Tuff) and this would further contribute to the understanding of the lithium cycle.

When studying lithium isotopes, close attention needs to be paid to which processes they preserve and if they represent the actual magmatic values or if they were overprinted. Lithium and its isotopes is a powerful tool to study process that take place on short time scales. However, as it is a fast diffuser these primary signals of a process can be overprinted within a short time span. This is also crucial for studies that use lithium as geochemical tracer of crustal recycling as the lithium isotope ratios they obtain may not represent the processes they want to study. The applicability of lithium isotopes and Li concentration to study melt inclusions is limited as their primary signal can be overprinted by different processes which makes it very challenging to identify the original lithium isotopic composition. Selecting different eruption that have not undergone reheating and measuring melt inclusions that are bigger in size might minimise the effect of diffusion between melt inclusion and host mineral.

I hope that these results might inspire the development of more lithium reference materials, increasing the applicability of *in situ* measurements for minerals of different composition.

5.2 Outlook

The results I present in this thesis have significant implications for the lithium cycle in evolved magmatic systems, while also paving the way for new avenues of research as several questions remain unanswered and new ones have emerged. On one hand, there is still work needed to fully understand large scale processes that lead to the enrichment of lithium in evolved systems and the variations that

arise from different settings (e.g. arc setting vs. continental setting). On the other hand, processes happening on the crystal scale, e.g., $\delta^{7}\text{Li}$ diffusion in quartz, require further investigation. Some of this work is hindered by the lack of standards available for *in situ* measurements by SIMS.

My results from chapter 4 show that we still do not fully understand the diffusion of lithium and its isotopes in quartz. Therefore, a more detailed study of different eruptions is needed. A study of $\delta^{7}\text{Li}$ of glassy melt inclusions in different minerals and their associated groundmass glass from different eruptions and compositions would aid the formation of a more coherent picture and foster the understanding of the high and low $\delta^{7}\text{Li}$ that have been found by multiple authors. Additionally, experiments are needed to fully understand the enrichment of lithium in melt inclusions due to the loss of H^{+} . The factor by which lithium will be enriched in a quartz-hosted melt inclusion due to homogenizing them is unknown and needs to be determined. The development of a quartz standard for SIMS would further help to better understand the movement of lithium in quartz, as chapter 4 shows that lithium is diffusing out of the melt inclusions and SIMS measurements of $\delta^{7}\text{Li}$ profiles along the different axis in quartz could aid our understanding of lithium diffusion in quartz.

I show in chapter 2 and 4 that dry high-silica rhyolite has around 40 ppm of lithium in the groundmass glass and the same trend of lithium enrichment in the groundmass glass has the wet high silica rhyolite of Kos Plateau Tuff. Fiedrich et al. (2020), who also used the LA-ICP-MS to determine the trace element concentrations, found that for Kos Plateau Tuff the quartz crystals vary in lithium concentration from ~4 ppm in the pumice quartz to between 6 and 16 ppm in the granite sample, this differs from the results of the quartz crystals of Mesa Falls Tuff that have up to 25 ppm of lithium. The mechanism by which lithium is incorporated into the quartz lattice is, thus, still not fully understood. Richter et al., 2003, Richter et al., 2006 and Holycross et al., 2018 have shown that ${}^6\text{Li}$ diffuses 3% faster than ${}^7\text{Li}$ in dry rhyolite and 3.5% faster in wet rhyolite. My results suggest that a similar behaviour could be found for lithium isotope diffusivity in quartz. Experiments are needed to understand if the different diffusivity can lead to different enrichment of Li in the mineral phases that are present or if higher H_2O content in quartz leads to less lithium as more aluminium is charge balanced by H^{+} .

Furthermore, the Kos Plateau Tuff also presents mica minerals, which incorporated large amounts of lithium. Lynton et al., (2005) studied the partition behaviour of lithium between quartz, mica and fluid and showed that there is a significant isotopic fractionation in this system and that lithium exchange is more rapid in quartz compared to muscovite. However, this study only looks at a temperature range of 400 to 500°C and pressures of 50–100 MPa. Extending this study to a wider temperature and pressure range and applying this to the system of quartz-mica-melt could help to understand the enrichment of lithium in pegmatites and the differences of lithium composition between wet and dry rhyolites.

In chapters 2, 3 and 4 I predict that ${}^6\text{Li}$ fractionates into the vapour phase. This had been theoretically predicted by Watson (2017), but so far only one study has measured the lithium isotopic composition of gas (Vlastelic et al., 2011). Experiments and measurements of natural gasses are needed to fully understand the extent to which lithium diffuses into the vapour phase and how much lithium is lost from the magmatic system due to degassing.

Thus, more experimental work in addition to studying different systems at different scales and settings will help to improve our understanding of the lithium cycle between the Earth's interior and exterior reservoirs.

5.3 References

- Fiedrich, F. M., Laurent, O., Heinrich, C. A., Bachmann, O. (2020) Melt and fluid evolution in an upper-crustal magma reservoir, preserved by inclusions in juvenile clasts from the Kos Plateau Tuff, Aegean Arc, Greece. *Geochimica et Cosmochimica Acta*, 280, 237-262.
- Holycross, M. E., Watson, E. B., Richter, F. M., Villeneuve, J. (2018) Diffusive fractionation of Li isotopes in wet, silicic melts. *Geochemical Perspectives Letters*, 6, 39-42.
- Lynton, S. J., Walker, R. J., Candela, P. A. (2005) Lithium isotopes in the system Qz–Ms–fluid: An experimental study. *Geochimica et Cosmochimica Acta*, 69, 3337–3347.
- Richter, F. M., Davis, A. M., DePaolo, D. J., Watson, E. B. (2003) Isotope fractionation by chemical diffusion between molten basalt and rhyolite. *Geochimica et Cosmochimica Acta*, 67, 3905–3923.
- Richter, F. M., Mendybaev, R. A., Christensen, J. N., Hutcheon, I. D., Williams, R. W., Sturchio, N. C., Beloso, A. D. Jr. (2006) Kinetic isotope fractionation during diffusion of ionic species in water. *Geochimica et Cosmochimica Acta*, 70, 277–289.
- Watson, E. B. (2017) Diffusive fractionation of volatiles and their isotopes during bubble growth in magmas. *Contributions to Mineralogy and Petrology*, 177, 61.



Appendix

Appendix A: Supplementary material for Chapter 2

A1: Major and trace element data of phases from MFT

Table A1.1: Major elements - groundmass glass

	SiO ₂	Na ₂ O	CaO	K ₂ O	FeO	Al ₂ O ₃	Cr ₂ O ₃	TiO ₂	MnO	MgO	P ₂ O ₅	Total
MFT Mount 1 grain 2 - 1	73.83	2.92	0.47	5.11	1.20	11.72	0.05	0.12	0.05	0.08	0.10	95.66
MFT Mount 1 grain 2 - 2	74.51	3.04	0.37	5.20	1.14	11.89	0.00	0.12	0.12	0.04	0.00	96.43
MFT Mount 1 grain 2 - 4	75.04	2.62	0.55	5.29	1.16	11.39	0.03	0.16	0.03	0.02	0.00	96.27
MFT Mount 1 grain 2 - 5	74.11	2.73	0.45	5.55	1.03	11.36	0.05	0.14	0.03	0.01	0.05	95.51
MFT Mount 1 grain 6 - 2	74.02	3.01	0.54	5.05	1.13	11.43	0.01	0.11	0.12	0.04	0.13	95.58
MFT Mount 1 grain 6 - 3	73.17	2.94	0.52	5.16	1.28	12.02	0.05	0.14	0.00	0.00	0.01	95.29
MFT Mount 1 grain 6 - 4	74.46	2.87	0.38	5.55	1.19	11.61	0.00	0.08	0.05	0.00	0.00	96.20
MFT Mount 1 grain 7 - 4	74.05	2.94	0.40	5.21	1.22	11.64	0.01	0.12	0.06	0.05	0.08	95.77
MFT Mount 1 grain 7 - 5	73.97	3.20	0.56	5.21	1.21	11.57	0.04	0.17	0.02	0.00	0.07	96.02
MFT Mount 1 grain 12 - 5	74.48	2.79	0.51	5.14	1.19	11.70	0.00	0.14	0.00	0.00	0.04	95.99
MFT Mount 2 grain 1 - 4	74.82	2.52	0.27	6.26	0.88	11.68	0.07	0.18	0.07	0.05	0.10	96.90
MFT Mount 2 grain 2 - 2	75.01	3.00	0.34	5.61	1.25	11.94	0.00	0.15	0.00	0.06	0.00	97.36
MFT Mount 2 grain 2 - 3	74.19	2.94	0.53	5.06	1.17	11.61	0.00	0.15	0.10	0.02	0.06	95.83
MFT Mount 2 grain 2 - 4	76.00	2.98	0.42	5.56	1.28	11.57	0.08	0.14	0.08	0.08	0.00	98.19
MFT Mount 2 grain 3 - 1	74.58	2.86	0.39	5.27	1.27	11.79	0.02	0.13	0.00	0.03	0.00	96.35
MFT Mount 2 grain 3 - 2	73.98	2.96	0.49	5.01	1.09	11.43	0.00	0.15	0.05	0.03	0.10	95.28
MFT Mount 2 grain 3 - 4	74.85	2.83	0.41	5.44	1.13	11.67	0.00	0.15	0.00	0.00	0.03	96.50
MFT Mount 2 grain 4 - 1	74.03	2.76	0.38	5.43	1.20	11.43	0.03	0.08	0.08	0.04	0.00	95.46
MFT Mount 2 grain 4 - 3	74.27	2.87	0.41	5.71	1.27	11.52	0.00	0.14	0.01	0.01	0.02	96.24
MFT Mount 2 grain 4 - 4	74.22	3.20	0.48	5.01	1.25	11.65	0.00	0.07	0.06	0.08	0.00	96.02
MFT Mount 2 grain 5 - 4	73.92	2.73	0.44	5.05	1.23	11.45	0.01	0.07	0.00	0.07	0.05	95.02
MFT Mount 2 grain 6 - 1	74.45	3.10	0.51	5.04	1.31	11.37	0.00	0.10	0.04	0.04	0.01	95.97
MFT Mount 2 grain 6 - 2	74.46	2.67	0.39	5.65	1.05	11.42	0.00	0.13	0.01	0.01	0.00	95.79
MFT Mount 2 grain 6 - 3	74.51	2.75	0.44	5.44	1.23	11.55	0.00	0.10	0.06	0.00	0.00	96.07
MFT Mount 2 grain 6 - 4	74.79	2.95	0.39	5.55	1.23	11.88	0.00	0.15	0.00	0.01	0.03	96.99
MFT Mount 2 grain 6 - 5	74.46	2.93	0.45	5.39	1.19	11.66	0.05	0.14	0.00	0.01	0.11	96.39
MFT Mount 2 grain 7 - 1	74.40	3.11	0.43	5.18	1.29	11.46	0.00	0.12	0.04	0.00	0.10	96.14
MFT Mount 2 grain 7 - 2	74.30	2.81	0.57	4.95	1.37	11.38	0.00	0.11	0.08	0.02	0.02	95.61
MFT Mount 2 grain 7 - 5	73.66	3.23	0.54	5.03	1.24	11.45	0.02	0.18	0.00	0.08	0.04	95.48
MFT Mount 2 grain 9 - 8	74.54	2.60	0.35	5.75	1.20	11.71	0.00	0.14	0.06	0.02	0.00	96.38
MFT Mount 2 grain 10 - 1	73.98	2.94	0.41	5.23	1.04	11.75	0.03	0.16	0.08	0.00	0.08	95.71
MFT Mount 2 grain 10 - 3	73.75	2.65	0.39	5.73	1.01	11.35	0.02	0.12	0.07	0.02	0.00	95.10
MFT Mount 2 grain 10 - 4	74.39	2.87	0.46	5.36	1.16	11.50	0.00	0.11	0.06	0.07	0.08	96.07
MFT Mount 2 grain 10 - 5	74.32	2.96	0.48	5.20	1.23	11.67	0.00	0.15	0.00	0.00	0.00	96.01
MFT Mount 2 grain 11 - 1	74.79	2.80	0.42	5.65	1.09	11.90	0.08	0.10	0.07	0.02	0.00	96.92
MFT Mount 2 grain 11 - 2	74.36	3.21	0.45	5.16	1.36	11.47	0.01	0.10	0.05	0.00	0.00	96.17
MFT Mount 2 grain 12 - 1	74.52	2.74	0.39	5.21	1.25	11.90	0.00	0.11	0.10	0.08	0.00	96.30
MFT Mount 2 grain 12 - 2	74.15	3.10	0.54	4.97	1.24	11.57	0.00	0.15	0.04	0.02	0.02	95.79
MFT Mount 2 grain 12 - 5	73.88	2.72	0.45	5.09	1.16	11.78	0.01	0.13	0.02	0.01	0.02	95.26
MFT Mount 2 grain 15 - 2	74.78	3.31	0.48	5.05	1.21	11.82	0.02	0.10	0.00	0.05	0.00	96.81
MFT Mount 2 grain 15 - 3	74.71	2.52	0.33	5.74	0.94	12.10	0.00	0.18	0.04	0.04	0.00	96.59
MFT Mount 2 grain 15 - 5	74.03	3.22	0.53	4.99	1.12	11.56	0.02	0.09	0.00	0.03	0.01	95.62
MFT Mount 2 grain 15 - 6	74.87	2.61	0.53	5.68	0.97	11.54	0.09	0.12	0.05	0.06	0.00	96.53

Table A1.2: Trace elements - groundmass glass

Sample#-grain#	Li ⁺	Li ⁺	Na	Mg	Al	Si	P	K	Ca	Sc	Ti	V	Mn	Fe	Rb	Sr	Y	Zr	Nb	Cs	Ba	La	Ce	Pr	Nd	Sm	Eu	Gd	Tb	Dy	Ho	Er	Tm	Yb	Hf	Ta	Pb	Th	U		
MFT_Mount 1 grain 2 - 1	50.3	46.9	23793	370	695	14	359948	46.3	59500	3919	3.1	719	0.4	243	13338	245.6	9.7	75.2	176.3	56.7	5.9	91.0	80.0	152.5	16.6	38.4	12.2	0.4	11.3	2.0	13.0	2.6	8.0	1.1	7.2	1.1	6.9	4.1	38.5	32.0	7.6
MFT_Mount 1 grain 2 - 5	46.4	45.1	20009	560	79026	359948	44.7	69620	3543	2.8	80.1	0.0	232	12119	258.6	20.9	87.9	189.5	63.1	8.5	43.5	83.8	56.0	17.0	62.9	13.0	0.4	12.9	2.1	14.8	3.1	8.5	1.2	8.5	1.1	7.1	4.3	44.2	34.0	7.2	
MFT_Mount 1 grain 5 - 1	45.8	41.2	23610	509	72990	359948	34.9	63731	3965	3.1	677.2	1.5	241	12358	257.6	13.9	77.1	195.7	62.7	7.2	13.7	81.5	157.3	17.0	60.0	12.9	0.4	11.1	2.0	13.4	2.7	8.0	1.1	7.3	1.0	7.9	4.3	37.5	32.7	7.7	
MFT_Mount 1 grain 6 - 4	52.8	46.6	22736	387	74308	359948	45.3	63188	4107	2.8	754	0.4	238	12017	253.0	13.1	75.1	175.5	58.1	6.8	22.7	81.1	151.4	16.9	59.9	12.2	0.4	11.6	1.9	13.1	2.7	7.7	1.1	7.6	1.0	7.2	4.0	38.9	32.2	7.8	
MFT_Mount 1 grain 6 - 5	47.4	40.0	22782	288	70731	359948	39.6	67433	3492	2.1	655	0.3	222	10303	256.0	12.2	68.5	157.7	52.8	7.4	11.9	73.6	137.8	16.3	57.6	11.5	0.3	11.1	1.9	11.9	2.5	7.4	1.1	7.2	1.0	6.9	3.9	34.1	31.6	7.4	
MFT_Mount 1 grain 8 - 1	36.9	38.2	21669	365	65440	359948	33.8	63413	3492	2.1	647	0.3	224	10428	236.3	9.8	64.1	155.1	52.8	5.3	11.9	72.3	140.4	15.0	54.7	11.3	0.4	9.6	1.8	10.9	2.2	6.3	0.9	6.3	0.9	6.5	3.7	41.5	28.6	7.2	
MFT_Mount 1 grain 9 - 3	45.1	38.8	22439	290	64156	359948	42.2	64461	2757	2.4	665	0.2	232	10075	250.2	9.8	64.6	155.7	52.7	5.9	12.1	72.6	139.0	15.0	52.5	11.6	0.3	9.1	1.7	10.8	2.3	6.9	1.0	6.7	0.9	6.7	3.9	42.7	30.0	7.4	
MFT_Mount 1 grain 10 - 1	39.6	39.5	22245	578	6694	359948	30.5	66538	3693	3.4	787	1.0	235	10941	253.7	15.4	77.7	188.9	61.6	7.6	120.1	82.2	136.0	17.7	36.7	12.3	0.3	11.0	2.0	13.3	2.8	7.6	1.1	8.0	1.1	7.1	4.1	39.2	32.7	7.4	
MFT_Mount 1 grain 13 - 1	49.3	51.0	21596	686	8285	359948	44.7	58130	3475	3.4	852	0.8	217	12215	251.5	30.3	84.8	189.8	62.7	8.1	217.6	83.9	156.1	17.3	65.0	12.8	0.4	12.6	2.1	14.1	2.8	8.2	1.3	7.8	1.1	7.3	4.3	43.8	32.4	7.5	
MFT_Mount 1 grain 14 - 1	39.3	45.1	23630	455	69221	359948	51.1	55513	3840	2.8	756	1.3	249	12828	255.8	11.1	74.0	178.5	60.3	6.6	108.8	82.0	136.8	16.7	58.2	12.9	0.3	10.7	2.0	12.3	2.7	7.4	1.1	7.6	1.0	7.3	3.9	40.4	32.4	7.8	
MFT_Mount 1 grain 15 - 2	44.2	44.4	23636	448	70306	359948	42.4	53125	3741	2.8	761	0.4	239	12255	244.8	11.9	74.9	181.0	57.4	5.2	114.1	82.9	157.2	17.0	57.9	11.9	0.4	10.6	2.0	13.1	2.7	7.5	1.2	7.6	1.0	7.1	4.1	36.2	33.2	7.6	
MFT_Mount 1 grain 15 - 3	48.8	49.7	23893	419	74543	359948	54.0	55232	3683	2.8	751	0.3	241	12425	257.1	13.8	73.7	174.3	57.2	6.3	118.2	80.6	149.5	16.5	55.6	11.0	0.3	10.8	1.9	11.9	2.5	7.4	1.1	7.5	1.0	6.5	3.9	39.9	31.5	7.5	
MFT_Mount 1 grain 15 - 4	44.9	45.2	20397	242	68414	359948	43.3	50727	3616	3.1	764	0.4	243	12324	257.2	14.7	77.3	181.0	58.9	5.7	121.1	85.1	155.6	17.4	60.4	12.4	0.4	11.9	2.0	12.9	2.6	7.8	1.1	7.5	1.0	7.1	4.0	37.8	33.9	7.9	
MFT_Mount 1 grain 17 - 3	41.9	44.8	25152	777	77144	359948	55.2	54000	3727	3.1	850	2.3	235	14307	240.8	21.9	99.3	193.2	63.8	7.5	167.1	93.0	161.6	19.5	67.6	14.9	0.4	14.3	2.4	15.1	3.2	8.8	1.4	9.3	1.2	7.1	4.1	42.9	35.3	7.1	
MFT_Mount 1 grain 17 - 5	47.1	45.5	28358	354	55566	359948	47.1	53785	3963	3.1	744	0.6	244	12635	242.4	13.9	77.9	181.0	56.7	5.5	131.0	85.5	159.6	17.2	61.2	13.0	0.4	11.5	2.1	13.4	2.8	7.7	1.2	7.6	1.1	7.0	4.0	43.0	32.7	7.3	
MFT_Mount 1 grain 19 - 3	45.0	46.4	22821	444	73113	359948	51.1	60657	3471	2.9	767	0.4	241	11408	266.6	14.5	81.7	183.5	62.0	6.9	128.2	85.9	159.9	17.6	61.2	12.8	0.3	12.8	2.1	14.3	2.8	8.0	1.2	8.1	1.2	7.1	4.1	39.9	34.0	7.8	
MFT_Mount 1 grain 19 - 4	45.0	46.4	22821	444	73113	359948	51.1	60657	3471	2.9	767	0.4	241	11408	266.6	14.5	81.7	183.5	62.0	6.9	128.2	85.9	159.9	17.6	61.2	12.8	0.3	12.8	2.1	14.3	2.8	8.0	1.2	8.1	1.2	7.1	4.1	39.9	34.0	7.8	
MFT_Mount 1 grain 19 - 6	42.7	45.1	23962	317	68989	359948	36.3	53018	3526	2.7	707	0.2	243	11954	245.7	10.0	73.1	175.1	56.9	6.2	106.7	80.2	153.2	16.5	57.4	12.1	0.3	11.1	1.9	13.2	2.6	7.8	1.1	7.4	1.0	7.1	4.1	37.6	32.2	7.8	
MFT_Mount 1 grain 20 - 3	38.5	42.2	22123	374	67749	359948	48.8	58754	2639	2.7	714	0.5	242	1240	265.9	13.8	64.6	158.9	55.3	7.4	112.3	75.7	142.2	14.8	52.9	10.5	0.3	10.2	1.6	10.8	2.3	6.6	1.0	6.7	0.9	5.8	3.7	46.2	28.7	7.1	
MFT_Mount 1 grain 21 - 3	35.1	44.9	25486	287	71340	359948	29.4	54447	4295	2.7	766	0.3	251	11454	248.2	9.7	75.6	180.0	57.4	5.1	99.8	85.4	159.0	17.5	59.4	12.7	0.4	11.6	2.0	12.8	2.7	7.1	1.1	7.3	1.1	6.8	3.9	35.7	32.4	7.6	
MFT_Mount 1 grain 22 - 3	50.7	44.8	22247	510	74778	359948	50.5	58016	3929	2.6	802	0.5	248	1578	250.6	16.3	77.0	180.8	60.6	6.4	49.2	83.4	155.6	16.9	61.4	12.2	0.4	11.8	2.0	13.1	2.7	7.6	1.1	7.6	1.0	7.4	4.4	41.7	32.6	7.6	
MFT_Mount 1 grain 22 - 5	46.8	46.4	22845	254	62913	359948	20.9	52027	3782	2.5	689	0.3	226	10774	230.4	10.5	64.0	155.3	54.0	5.0	122.4	73.3	142.5	15.3	52.1	11.1	0.4	10.2	1.8	11.2	2.3	7.0	1.0	6.4	0.9	6.3	3.7	37.1	29.6	7.4	
MFT_Mount 1 grain 23 - 2	39.9	43.1	23449	497	75126	359948	44.9	56035	3530	2.6	811	1.9	236	11022	248.1	15.4	75.4	179.1	58.6	6.1	138.2	83.5	153.8	16.9	59.0	12.3	0.5	11.0	2.0	12.5	2.6	7.5	1.1	7.6	1.0	7.1	3.9	35.2	31.4	7.3	
MFT_Mount 1 grain 24 - 4	35.7	41.7	20692	535	73386	359948	59.9	60333	2767	3.1	747	0.7	212	9736	253.2	15.7	74.8	175.0	57.3	7.2	125.2	80.5	144.6	16.7	57.4	13.0	0.3	11.0	2.0	12.3	2.5	7.5	1.1	7.4	1.1	6.6	4.1	44.9	32.0	7.3	
MFT_Mount 1 grain 24 - 5	38.4	44.0	22012	483	74184	359948	57.2	58488	3630	2.8	733	0.6	240	11173	251.3	4.4	80.6	170.3	60.9	7.9	115.1	77.4	146.9	16.2	76.0	12.6	0.3	10.9	1.9	11.9	2.9	7.0	1.0	7.3	1.0	6.4	4.1	39.1	30.6	8.2	
MFT_Mount 1 grain 25 - 1	43.5	46.3	22952	526	74567	359948	76.4	54830	3501	2.9	820	1.1	219	11857	239.0	15.3	83.1	186.9	62.4	6.8	122.3	86.3	153.2	18.6	65.2	13.2	0.3	13.0	2.2	14.6	2.9	8.3	1.2	8.0	1.2	7.3	4.3	41.3	34.3	7.4	
MFT_Mount 1 grain 25 - 2	45.3	43.6	22321	428	71775	359948	55.7	58977	3448	2.9	774	0.5	222	11153	247.2	4.1	75.1	168.3	57.9	7.7	149.6	83.2	144.7	16.7	58.6	11.8	0.3	11.0	2.0	12.7	2.7	7.7	1.1	7.4	1.0	6.7	4.0	39.4	31.4	7.2	
MFT_Mount 1 grain 26 - 1	50.0	47.5	24697	386	71525	359948	37.7	52864	3924	2.8	747	0.3	247	11127	235.7	12.5	76.6	176.9	58.3	5.4	137.7	82.4	151.0	16.9	58.7	12.6	0.4	11.0	1.9	12.0	2.6	7.4	1.1	6.9	1.0	6.9	3.8	35.5	31.9	7.4	
MFT_Mount 1 grain 26 - 2	40.0	40.4	22128	357	67960	359948	63.9	53520	3524	2.3	700	0.5	230	11732	233.6	14.8	74.7	166.3	56.6	5.5	148.3	80.2	146.7	16.4	57.7	12.6	0.4	10.1	2.0	12.7	2.6	8.1	1.1	7.7	1.0	6.7	3.8	39.5	31.4	7.1	
MFT_Mount 1 grain 26 - 5	42.3	44.5	20295	598	74366	359948	76.2	60714	3230	2.8	738	1.2	219	11011	249.7	25.8	83.9	161.6	55.8	8.1	182.2	81.1	130.7	16.8	59.0	11.7	0.4	12.1	2.2	12.7	2.6	7.2	1.0	6.6	1.0	6.3	3.7	45.6	29.2	6.1	
MFT_Mount 1 grain 29 - 1	48.3	42.2	21445	377	70696	359948	46.0	62381	3384	2.7	703	0.5	224	10172	263.2	5.0	72.3	170.7	56.6	6.9	126.3	79.8	149.3	16.0	58.2	11.7	0.3	10.9	1.9	11.5	2.7	7.3	1.0	6.8	1.0	6.9	4.1	40.4	30.5	7.2	
MFT_Mount 1 grain 30 - 1	47.1	43.8	22932	298	70594	359948	30.9	61425	3678	2.9	750	0.2	236	10185	252.0	11.1	73.1	176.5	58.2	6.0	116.2	79.6	153.5	16.0	57.2	11.8	0.3	10.9	1.8	11.9	2.5	7.5									

Table A1.2: continued

	Li ⁺	Li ⁺	Na	Mg	Al	Si	P	K	Ca	Sc	Ti	V	Mn	Fe	Rb	Sr	Y	Zr	Nb	Cs	Ba	La	Ce	Pr	Nd	Sm	Eu	Gd	Tb	Dy	Ho	Er	Tm	Yb	Lu	Hf	Ta	Pb	Th	U
MFT_Mount 2 grain 5 - 1	44.3	41.4	22726	294	71118	359948	35.6	58068	3728	3.0	748	0.3	234	10268	250.2	10.7	75.3	180.5	57.3	5.7	114.0	83.3	157.4	168	59.4	12.8	0.4	11.7	2.0	12.6	2.6	8.2	1.2	7.4	1.1	7.3	4.1	34.0	33.5	7.8
MFT_Mount 2 grain 5 - 2	45.4	42.4	21971	321	69543	359948	34.7	58652	3796	2.8	701	0.2	248	11168	254.0	11.6	74.3	171.0	58.6	5.4	118.3	81.5	151.8	16.1	57.5	12.2	0.4	10.6	1.8	12.5	2.7	7.6	1.0	7.0	1.0	6.7	4.1	42.0	32.0	7.5
MFT_Mount 2 grain 5 - 3	40.2	43.8	23910	266	70054	359948	43.3	56328	3291	2.4	746	0.2	238	10010	250.2	9.6	74.8	179.8	57.3	5.1	109.9	84.2	159.3	17.1	61.5	12.6	0.4	11.3	2.0	13.3	2.7	8.0	1.1	7.4	1.1	7.1	4.1	35.0	33.7	8.0
MFT_Mount 2 grain 7 - 1	37.9	37.1	19113	757	77728	359948	37.1	61288	3334	2.8	784	0.5	201	9934	267.9	23.6	79.5	182.2	60.2	9.3	162.3	81.1	148.4	16.5	58.7	12.5	0.3	11.7	1.9	13.1	2.9	8.2	1.1	8.0	1.1	7.1	4.0	46.6	32.1	7.2
MFT_Mount 2 grain 8 - 3	35.1	42.3	21651	378	72164	359948	38.1	57201	3434	3.1	764	0.4	216	12164	249.7	14.3	76.9	180.0	58.8	6.4	147.6	81.8	151.3	17.0	60.1	12.8	0.4	11.7	2.0	12.6	2.8	7.9	1.2	7.7	1.0	7.3	4.1	39.1	33.3	7.7
MFT_Mount 2 grain 8 - 3	38.8	37.5	20628	298	67978	359948	38.4	56522	2849	2.8	751	0.5	214	11291	252.2	13.6	72.0	176.5	58.4	7.1	130.2	78.1	150.9	15.9	56.1	11.4	0.3	10.7	1.7	11.9	2.4	7.1	1.0	7.1	0.9	6.5	3.6	37.7	30.2	7.1
MFT_Mount 2 grain 9 - 7	36.9	41.3	22585	269	70812	359948	30.9	55660	3887	2.6	711	0.3	233	10814	241.8	10.5	71.1	173.4	55.2	5.4	101.4	80.8	152.8	16.6	59.1	12.0	0.3	11.4	2.1	12.5	2.6	7.5	1.2	7.3	1.0	6.9	4.0	35.7	32.0	7.6
MFT_Mount 2 grain 9 - 9	42.7	41.9	21316	602	70913	359948	25.4	59224	3021	2.6	738	0.6	218	11685	251.8	19.1	72.1	170.5	59.1	7.6	144.1	78.9	142.7	16.3	58.1	11.6	0.3	11.2	1.9	11.8	2.5	7.3	1.1	7.1	1.0	6.6	3.8	37.6	30.3	7.0
MFT_Mount 2 grain 10 - 2	42.9	44.2	22869	275	69953	359948	30.4	59773	3214	2.6	729	0.2	241	10389	254.8	11.1	70.4	175.7	57.4	5.7	106.6	80.7	155.3	16.7	58.9	12.4	0.3	11.0	1.8	12.5	2.6	7.4	1.1	7.5	1.1	6.9	4.2	37.3	32.3	7.8
MFT_Mount 2 grain 11 - 2	47.6	47.6	24128	280	71056	359948	45.7	55041	3939	2.8	739	0.2	241	11952	249.9	9.5	75.4	179.7	59.8	5.9	104.4	80.0	158.5	17.5	61.9	12.7	0.4	11.8	2.0	13.1	2.6	8.0	1.2	7.9	1.1	7.5	3.9	40.9	33.7	8.0
MFT_Mount 2 grain 11 - 3	46.1	45.5	23501	331	72735	359948	35.5	58667	3539	3.2	756	0.3	242	11874	256.4	11.3	79.1	192.8	60.3	5.9	124.3	88.5	168.4	18.4	62.4	13.5	0.4	12.0	2.1	13.8	3.0	8.1	1.2	7.8	1.2	7.5	4.2	40.3	35.7	8.2
MFT_Mount 2 grain 12 - 3	33.3	36.6	19825	583	72066	359948	41.9	63381	3208	3.2	741	0.6	230	12594	261.0	17.6	76.5	171.4	57.5	8.4	154.1	183.5	142.8	16.9	61.1	12.6	0.4	11.6	2.0	12.5	2.5	7.5	1.1	7.2	1.0	6.8	4.1	41.7	31.8	7.3
mft-16 - 3	50.6	46.5	19052	786	78138	359948	59.9	55261	3580	2.8	769	0.8	230	13531	260.8	23.9	75.9	169.2	62.0	15.3	179.7	73.9	132.0	15.8	54.0	13.0	0.4	11.5	2.1	12.3	2.5	7.3	1.1	6.4	1.0	6.7	4.7	52.7	28.0	6.3
mft-16 - 4	50.3	48.7	20563	645	83955	359948	55.5	60288	3555	3.1	792	0.6	259	14614	258.9	18.8	78.6	181.8	61.6	9.1	160.0	82.7	141.3	17.1	59.9	13.5	0.4	13.1	2.0	12.8	2.7	7.4	1.1	7.4	1.0	6.8	4.3	44.3	30.9	6.7
mft-13 - 2	44.8	40.1	22623	463	80875	359948	53.5	61039	3900	3.0	761	0.8	286	10452	259.8	24.0	83.1	181.8	60.7	7.3	220.7	83.6	164.6	17.2	62.0	12.6	0.4	12.5	2.0	12.6	2.7	7.8	1.1	8.0	0.9	6.5	3.9	45.1	31.7	6.6
mft-11 - 1	42.0	42.4	22694	325	76196	359948	35.1	61591	3906	3.0	772	0.5	226	9413	267.7	14.1	81.6	186.4	58.0	6.9	125.6	87.1	153.1	17.4	63.8	12.0	0.3	12.1	1.9	13.5	2.9	7.5	1.0	7.2	1.2	6.7	3.9	37.0	31.4	7.1
mft-11 - 3	51.8	49.9	21475	461	81641	359948	51.6	59431	3781	3.3	820	0.6	241	11353	263.3	17.7	92.5	195.9	63.3	10.8	156.0	94.6	163.3	20.8	71.0	14.3	0.5	14.4	2.4	15.5	3.1	9.0	1.3	8.5	1.2	7.0	4.3	42.6	35.1	7.1
mft-10 - 1	46.4	43.2	21283	456	76016	359948	35.8	62417	3225	3.1	751	0.7	216	11572	269.9	20.6	81.2	185.1	59.1	8.4	211.2	81.5	151.4	16.5	58.4	12.9	0.4	11.9	2.0	12.9	2.7	8.1	1.1	7.8	1.1	6.9	4.2	44.3	31.9	7.4
mft-10 - 5	44.5	42.6	22059	438	73549	359948	43.8	60876	3196	3.4	776	0.7	233	10673	272.1	19.4	85.9	186.4	61.3	8.2	169.3	85.8	158.5	17.7	62.4	12.9	0.4	11.7	2.1	13.9	3.1	8.4	1.2	8.2	1.1	7.3	4.5	46.5	34.1	7.6
mft-9 - 1	51.0	48.3	22703	375	73773	359948	39.8	56452	3976	2.9	757	0.4	255	11921	261.3	12.3	74.9	180.8	58.1	9.2	119.7	81.5	154.6	16.7	58.6	12.4	0.4	11.2	2.0	12.3	2.7	8.0	1.0	7.6	1.0	7.3	4.1	39.8	32.9	7.8
mft-9 - 1	54.5	51.9	21696	644	80735	359948	50.1	59663	3908	3.0	796	0.6	244	13639	254.1	18.9	80.7	185.6	60.8	8.2	177.0	85.2	153.9	18.0	61.6	14.0	0.4	12.2	2.0	13.3	2.7	8.3	1.1	7.5	1.0	6.8	4.1	42.1	32.6	7.3
mft-8 - 1	48.7	45.2	23755	339	74426	359948	34.0	59370	3424	2.8	806	0.4	252	9916	263.8	13.0	85.7	198.2	59.8	5.8	46.0	92.5	171.5	18.4	67.6	14.2	0.4	12.6	2.3	14.3	3.0	8.8	1.4	8.7	1.2	8.6	4.3	41.4	35.9	8.2
mft-8 - 2	41.6	40.8	20719	339	64393	359948	34.7	56642	2660	2.5	703	0.3	225	9011	260.3	12.6	64.6	160.4	54.8	8.6	111.1	71.8	136.3	15.0	49.1	10.3	0.3	10.0	1.7	10.8	2.1	16.4	0.9	6.5	0.9	6.1	13.6	48.7	27.6	7.1
mft-8 - 6	45.6	41.6	21728	334	74960	359948	44.6	61658	2940	3.0	789	0.4	242	9111	269.2	13.3	81.3	186.3	59.6	7.1	138.8	86.4	165.6	18.1	61.5	12.6	0.4	11.8	2.1	13.2	2.8	8.2	1.2	8.2	1.2	7.4	4.1	40.6	34.6	8.0

Table A1.3.3: Trace elements - quartz

Info	Position	Lj ^o	Lj ⁱ	Na	Mg	Al	Si	P	K	Ca	Sc	Ti	Mn	Fe	Ge	Rb	Sr	Sn	Cs	Pb	Ba
16de20b12.xl	Core	18.2	16.1	b.d.l.	0.7	93.2	466998	57.6	b.d.l.	b.d.l.		80.9	b.d.l.	6.3	0.6	b.d.l.	b.d.l.	1.9	b.d.l.	b.d.l.	b.d.l.
16de20b13.xl	Core	16.5	15.9	b.d.l.	0.7	90.1	466998	54.9	b.d.l.	b.d.l.		76.4	b.d.l.	b.d.l.	0.6	b.d.l.	b.d.l.	1.6	b.d.l.	b.d.l.	b.d.l.
16de20b14.xl	Core	18.4	16.8	b.d.l.	0.8	97.0	466998	55.2	b.d.l.	b.d.l.		79.8	0.2	10.0	b.d.l.	b.d.l.	b.d.l.	1.5	b.d.l.	b.d.l.	b.d.l.
16de20b15.xl	Core	17.7	16.9	b.d.l.	0.6	96.5	466998	53.8	b.d.l.	b.d.l.		79.5	b.d.l.	7.5	b.d.l.	b.d.l.	b.d.l.	1.4	b.d.l.	b.d.l.	b.d.l.
16de20b16.xl	Core	14.1	16.5	b.d.l.	0.8	94.4	466998	54.1	b.d.l.	b.d.l.		76.3	b.d.l.	b.d.l.	0.9	b.d.l.	b.d.l.	1.6	b.d.l.	b.d.l.	b.d.l.
16de20b18.xl	Rim	21.9	20.6	b.d.l.	0.7	102.5	466998	54.1	b.d.l.	b.d.l.		87.2	0.2	9.1	0.6	b.d.l.	b.d.l.	1.1	b.d.l.	b.d.l.	b.d.l.
17ia16a68.xl	Core	14.6	13.7	b.d.l.	0.7	95.5	466998	45.2	b.d.l.	b.d.l.		89.8	b.d.l.	6.9	b.d.l.	b.d.l.	0.0	0.5	b.d.l.	0.1	b.d.l.
17ia16a69.xl	Core	13.6	14.4	b.d.l.	0.8	93.9	466998	44.4	b.d.l.	b.d.l.		83.9	b.d.l.	6.9	0.7	b.d.l.	b.d.l.	0.4	b.d.l.	b.d.l.	b.d.l.
17ia16a70.xl	Core	16.7	15.5	0.3	0.7	93.3	466998	46.1	b.d.l.	b.d.l.		88.5	b.d.l.	6.9	b.d.l.	b.d.l.	b.d.l.	0.4	b.d.l.	b.d.l.	b.d.l.
17ia16a71.xl	Core	18.7	16.5	0.4	0.7	90.9	466998	45.1	b.d.l.	b.d.l.		92.0	0.4	b.d.l.	b.d.l.	b.d.l.	b.d.l.	0.5	b.d.l.	b.d.l.	0.0
17ia16a72.xl	Core	17.9	18.1	b.d.l.	0.7	98.7	466998	42.5	b.d.l.	b.d.l.		99.1	b.d.l.	b.d.l.	b.d.l.	b.d.l.	0.0	0.8	b.d.l.	0.0	b.d.l.
17ia16a73.xl	Core	18.1	17.0	b.d.l.	0.7	98.3	466998	43.7	b.d.l.	b.d.l.		97.5	b.d.l.	7.2	b.d.l.	b.d.l.	0.0	0.4	b.d.l.	b.d.l.	b.d.l.
17ia16a74.xl	Rim	20.3	18.7	b.d.l.	0.7	100.6	466998	44.5	b.d.l.	b.d.l.		104.8	b.d.l.	11.3	b.d.l.	b.d.l.	b.d.l.	0.5	b.d.l.	b.d.l.	b.d.l.
16de20b46.xl	Rim	20.7	20.4	0.2	0.6	88.7	466998	57.1	b.d.l.	b.d.l.		83.0	0.2	b.d.l.	0.5	b.d.l.	0.0	1.3	b.d.l.	0.0	b.d.l.
16de20b47.xl	Core	19.2	19.6	0.2	0.8	89.8	466998	55.7	b.d.l.	b.d.l.		84.7	0.2	6.7	0.8	b.d.l.	b.d.l.	1.3	b.d.l.	0.0	b.d.l.
16de20b48.xl	Core	19.0	17.9	0.2	0.6	86.5	466998	57.7	b.d.l.	b.d.l.		78.7	0.2	7.2	0.6	b.d.l.	0.0	1.3	b.d.l.	b.d.l.	b.d.l.
16de20b49.xl	Core	19.0	19.0	b.d.l.	0.4	86.3	466998	57.0	b.d.l.	b.d.l.		75.6	b.d.l.	4.9	b.d.l.	b.d.l.	b.d.l.	1.3	b.d.l.	0.0	b.d.l.
16de20b50.xl	Core	22.8	21.2	0.1	0.7	90.4	466998	55.8	b.d.l.	b.d.l.		74.0	0.2	6.9	0.4	b.d.l.	b.d.l.	1.3	b.d.l.	b.d.l.	b.d.l.
16de20b51.xl	Core	21.4	20.8	0.2	0.5	88.7	466998	55.2	b.d.l.	b.d.l.		71.9	0.2	6.7	0.4	b.d.l.	b.d.l.	1.2	b.d.l.	b.d.l.	b.d.l.
16de20b52.xl	Core	22.6	21.9	0.3	0.7	90.8	466998	55.1	b.d.l.	b.d.l.		68.0	0.2	6.7	0.6	b.d.l.	b.d.l.	1.2	b.d.l.	b.d.l.	b.d.l.
16de20b54.xl	Core	18.4	17.6	b.d.l.	0.7	95.9	466998	53.1	b.d.l.	b.d.l.		90.2	b.d.l.	8.4	b.d.l.	b.d.l.	b.d.l.	1.2	b.d.l.	0.0	b.d.l.
16de20b55.xl	Core	19.3	18.8	0.2	0.5	94.5	466998	52.8	b.d.l.	b.d.l.		91.0	0.2	8.2	0.4	b.d.l.	b.d.l.	1.1	b.d.l.	0.0	b.d.l.
16de20b56.xl	Core	19.1	19.4	0.3	0.7	91.4	466998	51.6	b.d.l.	b.d.l.		90.6	0.2	6.8	0.7	b.d.l.	0.0	1.1	0.0	0.0	b.d.l.
16de20b57.xl	Core	19.4	19.8	0.4	0.5	90.6	466998	49.7	b.d.l.	b.d.l.		92.1	0.1	9.1	0.7	b.d.l.	0.0	1.2	b.d.l.	b.d.l.	b.d.l.
16de20b58.xl	Core	22.2	21.2	0.4	0.6	95.3	466998	51.3	b.d.l.	b.d.l.		101.0	0.2	7.2	0.4	b.d.l.	0.0	1.1	b.d.l.	0.0	b.d.l.
17ia10a25.xl	Rim	19.8	20.7	b.d.l.	0.6	94.5	466998	66.4	b.d.l.	b.d.l.		71.6	b.d.l.	7.0	0.7	b.d.l.	b.d.l.	0.8	b.d.l.	b.d.l.	b.d.l.
17ia10a26.xl	Rim	19.9	20.0	0.2	0.5	95.8	466998	64.2	b.d.l.	b.d.l.		77.6	b.d.l.	5.7	0.9	b.d.l.	b.d.l.	1.0	b.d.l.	b.d.l.	b.d.l.
17ia10a27.xl	Core	18.2	19.1	b.d.l.	0.8	92.3	466998	64.9	b.d.l.	b.d.l.		79.0	b.d.l.	5.7	1.1	b.d.l.	b.d.l.	1.0	b.d.l.	b.d.l.	b.d.l.
17ia10a28.xl	Core	20.3	19.7	0.1	0.4	90.4	466998	63.6	b.d.l.	b.d.l.		67.5	0.2	4.4	0.8	b.d.l.	b.d.l.	1.0	b.d.l.	b.d.l.	b.d.l.
17ia10a29.xl	Core	18.2	18.1	0.2	0.6	91.6	466998	65.3	b.d.l.	b.d.l.		77.5	b.d.l.	5.7	b.d.l.	b.d.l.	b.d.l.	0.9	b.d.l.	b.d.l.	b.d.l.
17ia10a30.xl	Core	19.3	18.8	b.d.l.	0.6	95.9	466998	65.5	b.d.l.	b.d.l.		89.0	b.d.l.	8.2	b.d.l.	b.d.l.	b.d.l.	0.8	b.d.l.	b.d.l.	b.d.l.
17ia10a33.xl	Core	19.4	18.7	0.2	0.9	101.3	466998	67.4	b.d.l.	b.d.l.		97.5	b.d.l.	7.4	b.d.l.	b.d.l.	b.d.l.	0.7	b.d.l.	b.d.l.	b.d.l.
17ia10a34.xl	Core	18.5	17.9	0.2	0.6	95.5	466998	67.6	b.d.l.	b.d.l.		90.9	b.d.l.	8.7	0.7	b.d.l.	b.d.l.	0.8	b.d.l.	b.d.l.	b.d.l.
17ia10a35.xl	Core	19.2	17.6	0.2	0.5	91.1	466998	69.3	b.d.l.	b.d.l.		78.9	b.d.l.	5.4	0.6	b.d.l.	b.d.l.	0.8	b.d.l.	b.d.l.	b.d.l.
17ia10a36.xl	Core	17.5	17.8	0.2	0.7	91.6	466998	69.8	b.d.l.	b.d.l.		77.7	b.d.l.	7.6	0.6	b.d.l.	b.d.l.	0.9	b.d.l.	b.d.l.	b.d.l.
17ia10a37.xl	Core	18.8	18.5	b.d.l.	0.5	92.4	466998	72.0	b.d.l.	b.d.l.		77.3	0.2	6.1	b.d.l.	b.d.l.	b.d.l.	0.7	b.d.l.	b.d.l.	b.d.l.
17ia10a38.xl	Core	19.2	18.6	0.2	0.7	90.8	466998	72.5	b.d.l.	b.d.l.		72.1	b.d.l.	5.4	b.d.l.	b.d.l.	b.d.l.	0.7	b.d.l.	b.d.l.	b.d.l.
17ia10a39.xl	Rim	19.9	19.5	0.2	0.5	91.7	466998	72.5	b.d.l.	b.d.l.		76.0	b.d.l.	6.0	b.d.l.	b.d.l.	b.d.l.	0.8	b.d.l.	b.d.l.	b.d.l.
17ia10a12.xl	Rim	19.8	19.5	b.d.l.	0.4	90.0	466998	71.9	b.d.l.	b.d.l.		64.6	b.d.l.	5.3	b.d.l.	b.d.l.	b.d.l.	0.9	b.d.l.	b.d.l.	b.d.l.
17ia10a13.xl	Rim	15.5	15.8	b.d.l.	0.7	97.0	466998	72.2	b.d.l.	b.d.l.		69.1	0.2	8.4	0.6	b.d.l.	b.d.l.	0.9	b.d.l.	b.d.l.	b.d.l.
17ia10a14.xl	Core	16.2	15.6	b.d.l.	0.8	97.1	466998	73.8	b.d.l.	b.d.l.		67.8	0.2	6.5	0.7	b.d.l.	b.d.l.	1.0	b.d.l.	b.d.l.	b.d.l.
17ia10a16.xl	Core	20.7	18.9	1.0	0.8	99.1	466998	75.8	b.d.l.	b.d.l.		73.0	b.d.l.	5.8	0.7	b.d.l.	b.d.l.	0.9	b.d.l.	b.d.l.	b.d.l.
17ia10a17.xl	Core	19.1	19.2	0.7	0.8	95.5	466998	72.8	b.d.l.	b.d.l.		67.8	0.2	5.8	0.7	b.d.l.	b.d.l.	0.9	b.d.l.	b.d.l.	b.d.l.
17ia10a18.xl	Core	20.7	18.8	0.5	0.6	90.0	466998	72.0	b.d.l.	b.d.l.		66.4	b.d.l.	6.1	b.d.l.	b.d.l.	b.d.l.	0.9	b.d.l.	b.d.l.	b.d.l.
16de20e26.xl	Core	14.7	14.9	b.d.l.	0.7	90.2	466998	62.3	b.d.l.	b.d.l.		79.3	0.2	4.8	0.6	b.d.l.	b.d.l.	0.7	b.d.l.	b.d.l.	b.d.l.
16de20e29.xl	Core	18.9	17.2	0.4	0.6	94.4	466998	62.3	b.d.l.	b.d.l.		80.3	0.2	9.3	0.4	b.d.l.	b.d.l.	0.9	b.d.l.	b.d.l.	b.d.l.
16de20e30.xl	Core	19.6	18.0	0.3	0.6	99.4	466998	62.0	b.d.l.	b.d.l.		94.4	0.2	7.6	0.5	b.d.l.	b.d.l.	0.8	b.d.l.	b.d.l.	b.d.l.
16de20e31.xl	Core	18.3	17.8	0.1	0.6	102.4	466998	64.9	b.d.l.	b.d.l.		89.8	0.2	7.2	0.4	b.d.l.	b.d.l.	0.9	b.d.l.	b.d.l.	b.d.l.
16de20e32.xl	Rim	19.5	19.3	0.3	0.9	120.4	466998	67.2	b.d.l.	b.d.l.		91.2	0.2	7.2	0.5	b.d.l.	b.d.l.	0.9	b.d.l.	b.d.l.	b.d.l.

Table A1.3: continued

Info	Position	Li ⁶	Li ⁷	Na	Mg	Al	Si	P	K	Ca	Sc	Ti	Mn	Fe	Ge	Rb	Sr	Sn	Cs	Pb	Ba
16de20e16.xl	Core	20.5	20.0	0.1	0.6	95.8	466998	61.1	b.d.l.	b.d.l.	b.d.l.	63.7	0.1	5.5	0.6	b.d.l.	b.d.l.	0.6	b.d.l.	b.d.l.	b.d.l.
16de20e17.xl	Core	16.8	18.8	b.d.l.	0.6	92.4	466998	60.4	b.d.l.	b.d.l.	b.d.l.	59.6	0.2	5.4	0.6	b.d.l.	b.d.l.	0.6	b.d.l.	b.d.l.	b.d.l.
16de20e18.xl	Core	17.0	16.1	b.d.l.	0.6	91.3	466998	60.6	b.d.l.	b.d.l.	b.d.l.	62.3	0.2	4.7	0.5	b.d.l.	b.d.l.	0.5	b.d.l.	b.d.l.	b.d.l.
16de20e19.xl	Core	14.0	14.2	0.1	0.5	88.0	466998	60.4	b.d.l.	b.d.l.	b.d.l.	61.7	b.d.l.	5.9	0.5	b.d.l.	b.d.l.	0.8	b.d.l.	b.d.l.	b.d.l.
16de20e20.xl	Rim	14.2	16.1	b.d.l.	0.8	93.8	466998	59.2	b.d.l.	b.d.l.	b.d.l.	88.3	b.d.l.	6.2	0.7	b.d.l.	b.d.l.	0.6	b.d.l.	b.d.l.	b.d.l.
16de20e21.xl	Rim	13.9	14.9	0.1	0.7	91.0	466998	60.6	b.d.l.	b.d.l.	b.d.l.	82.6	b.d.l.	7.7	0.6	b.d.l.	b.d.l.	0.7	b.d.l.	b.d.l.	b.d.l.
16de20e22.xl	Rim	17.3	16.8	0.2	0.8	93.1	466998	58.4	b.d.l.	b.d.l.	b.d.l.	82.5	b.d.l.	5.1	0.5	b.d.l.	b.d.l.	0.5	b.d.l.	b.d.l.	b.d.l.
17fal6a77.xl	Rim	18.7	16.3	b.d.l.	0.5	94.9	466998	57.1	b.d.l.	b.d.l.	b.d.l.	80.4	b.d.l.	6.9	b.d.l.	b.d.l.	b.d.l.	0.5	b.d.l.	b.d.l.	b.d.l.
17fal6a79.xl	Core	16.1	16.5	b.d.l.	0.8	94.9	466998	58.0	b.d.l.	b.d.l.	b.d.l.	80.7	b.d.l.	6.8	b.d.l.	b.d.l.	b.d.l.	b.d.l.	b.d.l.	b.d.l.	b.d.l.
17fal6a80.xl	Core	16.9	16.9	1.3	0.7	94.5	466998	56.4	b.d.l.	b.d.l.	b.d.l.	81.0	b.d.l.	7.5	b.d.l.	b.d.l.	b.d.l.	0.4	b.d.l.	b.d.l.	b.d.l.
17fal6a81.xl	Core	17.8	16.5	1.0	0.5	96.4	466998	58.2	b.d.l.	b.d.l.	b.d.l.	82.2	b.d.l.	8.9	0.9	b.d.l.	b.d.l.	0.7	b.d.l.	b.d.l.	b.d.l.
17fal6a82.xl	Core	20.9	18.9	b.d.l.	0.7	103.2	466998	55.3	b.d.l.	b.d.l.	b.d.l.	79.0	b.d.l.	6.4	b.d.l.	b.d.l.	b.d.l.	0.4	b.d.l.	b.d.l.	b.d.l.
17fal6a83.xl	Rim	19.1	18.6	b.d.l.	0.9	99.1	466998	55.9	b.d.l.	b.d.l.	b.d.l.	78.5	b.d.l.	6.5	b.d.l.	b.d.l.	b.d.l.	0.5	b.d.l.	b.d.l.	b.d.l.
17fal6a84.xl	Rim	19.5	18.7	b.d.l.	0.5	96.6	466998	54.9	b.d.l.	b.d.l.	b.d.l.	86.8	b.d.l.	7.6	b.d.l.	b.d.l.	b.d.l.	0.4	b.d.l.	b.d.l.	b.d.l.
16de20e06.xl	Core	24.4	23.0	0.9	1.0	107.8	466998	62.2	b.d.l.	b.d.l.	b.d.l.	101.8	0.2	9.4	0.7	b.d.l.	b.d.l.	0.6	b.d.l.	b.d.l.	b.d.l.
16de20e07.xl	Core	23.2	22.5	0.5	0.8	105.3	466998	60.9	b.d.l.	b.d.l.	b.d.l.	104.3	0.2	7.0	0.6	b.d.l.	b.d.l.	0.6	b.d.l.	b.d.l.	b.d.l.
16de20e08.xl	Core	23.9	22.2	0.2	0.8	107.1	466998	61.4	b.d.l.	b.d.l.	b.d.l.	107.4	0.2	7.1	0.4	b.d.l.	b.d.l.	0.6	b.d.l.	b.d.l.	b.d.l.
16de20e10.xl	Core	20.4	19.8	0.3	0.6	106.0	466998	61.6	b.d.l.	b.d.l.	b.d.l.	107.9	0.2	7.0	0.5	b.d.l.	b.d.l.	0.6	b.d.l.	b.d.l.	b.d.l.
16de20e11.xl	Core	19.3	18.5	0.4	0.8	100.3	466998	60.6	b.d.l.	b.d.l.	b.d.l.	102.5	0.2	6.1	0.4	b.d.l.	b.d.l.	0.6	b.d.l.	b.d.l.	b.d.l.
16de20e12.xl	Rim	18.7	19.6	0.3	0.6	92.9	466998	61.5	b.d.l.	b.d.l.	b.d.l.	79.2	0.2	6.8	0.4	b.d.l.	b.d.l.	0.6	b.d.l.	b.d.l.	b.d.l.
16de20e13.xl	Rim	20.0	19.4	0.7	0.6	94.1	466998	62.4	b.d.l.	b.d.l.	b.d.l.	76.3	b.d.l.	6.3	0.8	b.d.l.	b.d.l.	0.7	b.d.l.	b.d.l.	b.d.l.
16de20e14.xl	Rim	20.4	20.3	1.1	0.8	97.8	466998	62.6	b.d.l.	b.d.l.	b.d.l.	63.9	0.1	5.3	0.5	b.d.l.	b.d.l.	0.7	b.d.l.	b.d.l.	b.d.l.
16de20e15.xl	Rim	20.8	20.2	0.6	0.6	91.9	466998	60.2	b.d.l.	b.d.l.	b.d.l.	67.1	0.1	5.0	0.5	b.d.l.	b.d.l.	0.5	b.d.l.	b.d.l.	b.d.l.
16de20b30.xl	Rim	19.2	19.1	0.3	0.6	93.5	466998	60.4	b.d.l.	b.d.l.	b.d.l.	87.8	0.2	6.3	0.5	b.d.l.	b.d.l.	1.4	b.d.l.	b.d.l.	b.d.l.
16de20b31.xl	Rim	19.4	18.0	0.9	0.6	99.0	466998	61.5	b.d.l.	b.d.l.	b.d.l.	88.0	0.2	5.3	0.7	b.d.l.	b.d.l.	1.1	b.d.l.	b.d.l.	b.d.l.
16de20b32.xl	Rim	16.7	16.8	0.3	0.6	89.0	466998	56.7	b.d.l.	b.d.l.	b.d.l.	78.8	0.2	6.5	0.4	b.d.l.	b.d.l.	1.2	b.d.l.	b.d.l.	b.d.l.
16de20b33.xl	Core	17.3	16.3	0.4	0.6	91.4	466998	55.7	b.d.l.	b.d.l.	b.d.l.	88.2	0.1	8.1	0.6	b.d.l.	b.d.l.	1.2	b.d.l.	b.d.l.	b.d.l.
16de20b34.xl	Core	17.1	16.3	0.3	0.7	98.8	466998	57.0	b.d.l.	b.d.l.	b.d.l.	105.0	0.3	7.8	0.5	b.d.l.	b.d.l.	1.1	b.d.l.	b.d.l.	b.d.l.
16de20b35.xl	Core	16.3	16.1	0.2	0.7	100.9	466998	58.4	b.d.l.	b.d.l.	b.d.l.	107.9	0.2	8.1	0.5	b.d.l.	b.d.l.	1.4	b.d.l.	b.d.l.	b.d.l.
16de20b36.xl	Core	17.0	15.8	0.2	0.7	98.9	466998	57.9	b.d.l.	b.d.l.	b.d.l.	110.1	0.2	8.3	0.4	b.d.l.	b.d.l.	1.4	b.d.l.	b.d.l.	b.d.l.
16de20b37.xl	Core	18.5	16.8	0.2	0.8	99.9	466998	56.4	b.d.l.	b.d.l.	b.d.l.	110.0	0.2	9.7	0.5	b.d.l.	b.d.l.	1.2	b.d.l.	b.d.l.	b.d.l.
16de20b39.xl	Rim	17.6	16.9	0.3	0.6	98.2	466998	57.2	b.d.l.	b.d.l.	b.d.l.	104.3	0.2	7.9	0.4	b.d.l.	b.d.l.	1.3	b.d.l.	b.d.l.	b.d.l.
16de20b40.xl	Rim	18.3	17.5	0.2	0.7	96.0	466998	57.7	b.d.l.	b.d.l.	b.d.l.	99.2	0.2	7.4	0.5	b.d.l.	b.d.l.	1.3	b.d.l.	b.d.l.	b.d.l.
16de20b41.xl	Rim	23.3	21.9	0.2	0.8	91.3	466998	57.1	b.d.l.	b.d.l.	b.d.l.	71.3	0.2	7.4	0.6	b.d.l.	b.d.l.	1.3	b.d.l.	b.d.l.	b.d.l.
16de20e58.xl	Rim	19.8	20.5	b.d.l.	0.5	94.1	466998	74.2	b.d.l.	b.d.l.	b.d.l.	70.1	0.2	5.6	0.6	b.d.l.	b.d.l.	1.1	b.d.l.	b.d.l.	b.d.l.
16de20e59.xl	Rim	22.0	21.3	0.1	0.7	98.1	466998	71.9	b.d.l.	b.d.l.	b.d.l.	80.3	0.2	7.2	0.5	b.d.l.	b.d.l.	1.0	b.d.l.	b.d.l.	b.d.l.
16de20e60.xl	Core	23.1	21.5	0.2	0.7	98.3	466998	72.6	b.d.l.	b.d.l.	b.d.l.	86.3	0.1	6.4	0.5	b.d.l.	b.d.l.	1.0	b.d.l.	b.d.l.	b.d.l.
16de20e61.xl	Core	22.0	21.7	0.3	0.6	98.8	466998	71.5	b.d.l.	b.d.l.	b.d.l.	87.3	0.2	8.5	0.7	b.d.l.	b.d.l.	1.0	b.d.l.	b.d.l.	b.d.l.
16de20e62.xl	Core	20.1	19.6	0.2	0.8	92.6	466998	71.4	b.d.l.	b.d.l.	b.d.l.	75.6	0.2	6.1	0.4	b.d.l.	b.d.l.	1.1	b.d.l.	b.d.l.	b.d.l.
16de20e63.xl	Core	18.8	19.0	0.2	0.6	92.4	466998	71.4	b.d.l.	b.d.l.	b.d.l.	81.4	0.2	6.0	0.4	b.d.l.	b.d.l.	1.0	b.d.l.	b.d.l.	b.d.l.
16de20e64.xl	Core	19.6	18.0	0.3	0.5	92.0	466998	71.8	b.d.l.	b.d.l.	b.d.l.	85.9	0.2	5.6	0.8	b.d.l.	b.d.l.	1.0	b.d.l.	b.d.l.	b.d.l.
16de20e65.xl	Core	19.2	17.8	0.1	0.8	93.4	466998	74.1	b.d.l.	b.d.l.	b.d.l.	87.2	b.d.l.	6.1	0.5	b.d.l.	b.d.l.	1.0	b.d.l.	b.d.l.	b.d.l.
16de20e70.xl	Rim	18.0	18.3	0.2	0.8	92.7	466998	71.4	b.d.l.	b.d.l.	b.d.l.	85.4	0.2	6.1	0.4	b.d.l.	b.d.l.	0.9	b.d.l.	b.d.l.	b.d.l.
16de20e71.xl	Rim	19.4	18.0	0.2	0.7	92.4	466998	72.1	b.d.l.	b.d.l.	b.d.l.	86.8	0.1	6.6	0.5	b.d.l.	b.d.l.	0.8	b.d.l.	b.d.l.	b.d.l.
16de20e72.xl	Rim	17.8	18.1	0.2	0.7	94.3	466998	71.9	b.d.l.	b.d.l.	b.d.l.	88.9	0.2	6.3	0.6	b.d.l.	b.d.l.	0.9	b.d.l.	b.d.l.	b.d.l.
16de20e73.xl	Core	20.5	19.1	b.d.l.	0.6	92.3	466998	73.9	b.d.l.	b.d.l.	b.d.l.	66.7	0.2	5.6	0.6	b.d.l.	b.d.l.	0.9	b.d.l.	b.d.l.	b.d.l.
16de20e74.xl	Core	19.0	19.4	0.1	0.7	94.9	466998	73.3	b.d.l.	b.d.l.	b.d.l.	70.5	0.2	6.9	0.4	b.d.l.	b.d.l.	0.9	b.d.l.	b.d.l.	b.d.l.
16de20e75.xl	Rim	18.3	17.3	0.2	0.6	92.3	466998	71.9	b.d.l.	b.d.l.	b.d.l.	84.0	0.2	6.5	0.7	b.d.l.	b.d.l.	0.8	b.d.l.	b.d.l.	b.d.l.

Table A1.3: continued

Info	Position	Li*	Li†	Na	Mg	Al	Si	P	K	Ca	Sc	Ti	Mn	Fe	Ge	Rb	Sr	Sn	Cs	Pb	Ba
17ja10a04.xl	Rim	22.0	19.9	b.d.l.	0.6	94.5	466998	67.0	b.d.l.	b.d.l.		65.1	b.d.l.	6.5	b.d.l.	b.d.l.	b.d.l.	0.6	b.d.l.	b.d.l.	b.d.l.
17ja10a05.xl	Rim	19.7	20.6	0.1	0.8	92.1	466998	67.3	b.d.l.	b.d.l.		66.1	0.3	b.d.l.	0.7	b.d.l.	b.d.l.	0.7	b.d.l.	b.d.l.	b.d.l.
17ja10a06.xl	Core	21.0	20.7	0.2	0.8	103.8	466998	67.5	b.d.l.	b.d.l.		105.0	0.2	5.0	0.6	b.d.l.	b.d.l.	0.8	b.d.l.	b.d.l.	b.d.l.
17ja10a07.xl	Core	21.4	20.5	0.2	0.7	103.3	466998	63.2	b.d.l.	b.d.l.		107.5	b.d.l.	7.9	0.5	b.d.l.	b.d.l.	0.8	b.d.l.	b.d.l.	b.d.l.
17ja10a08.xl	Core	22.3	21.2	0.3	0.7	103.0	466998	63.5	b.d.l.	b.d.l.		106.4	0.2	8.8	0.7	b.d.l.	b.d.l.	0.9	b.d.l.	b.d.l.	b.d.l.
17ja10a09.xl	Core	24.5	22.0	0.2	0.8	104.2	466998	64.3	b.d.l.	b.d.l.		106.3	0.4	7.3	b.d.l.	b.d.l.	b.d.l.	0.9	b.d.l.	b.d.l.	b.d.l.
17ja10a10.xl	Core	28.1	24.5	0.4	1.0	108.4	466998	64.3	b.d.l.	b.d.l.		102.2	0.3	8.3	0.5	b.d.l.	b.d.l.	0.8	b.d.l.	b.d.l.	b.d.l.
17ja10a11.xl	Rim	23.3	22.5	0.2	0.5	95.5	466998	65.8	b.d.l.	b.d.l.		77.3	0.2	6.1	0.7	b.d.l.	b.d.l.	0.8	b.d.l.	b.d.l.	b.d.l.
17ja10a11.xl	Core	13.8	13.2	b.d.l.	0.8	102.3	466998	76.4	b.d.l.	b.d.l.		104.8	b.d.l.	8.2	b.d.l.	b.d.l.	b.d.l.	0.9	b.d.l.	b.d.l.	b.d.l.
17ja10a11.xl	Core	14.4	14.0	b.d.l.	0.7	102.3	466998	66.6	b.d.l.	b.d.l.		106.0	0.2	8.1	0.5	b.d.l.	b.d.l.	0.7	b.d.l.	b.d.l.	b.d.l.
17ja10a12.xl	Core	15.6	14.5	0.3	0.8	101.8	466998	65.0	b.d.l.	b.d.l.		110.8	0.2	7.5	0.6	b.d.l.	b.d.l.	0.7	b.d.l.	b.d.l.	b.d.l.
17ja10a13.xl	Core	15.7	15.7	b.d.l.	1.0	105.1	466998	63.7	b.d.l.	b.d.l.		111.1	0.3	7.4	0.8	b.d.l.	b.d.l.	0.5	b.d.l.	b.d.l.	b.d.l.
17ja10a15.xl	Core	19.8	17.7	b.d.l.	0.6	100.0	466998	64.6	b.d.l.	b.d.l.		96.0	0.3	6.4	0.5	b.d.l.	b.d.l.	0.7	b.d.l.	b.d.l.	b.d.l.
17ja10a16.xl	Core	15.7	15.1	b.d.l.	0.6	104.0	466998	66.6	b.d.l.	b.d.l.		104.3	0.2	8.6	0.7	b.d.l.	b.d.l.	0.6	b.d.l.	b.d.l.	b.d.l.
17ja10a17.xl	Core	15.8	15.6	0.1	0.7	98.5	466998	64.5	b.d.l.	b.d.l.		99.2	0.2	5.2	0.5	b.d.l.	b.d.l.	0.5	b.d.l.	b.d.l.	b.d.l.
17ja10a95.xl	Rim	20.7	20.5	0.1	0.6	97.2	466998	67.0	b.d.l.	b.d.l.		83.5	b.d.l.	7.6	0.8	b.d.l.	b.d.l.	0.7	b.d.l.	b.d.l.	b.d.l.
17ja10a96.xl	Rim	19.2	19.7	b.d.l.	0.7	92.6	466998	66.3	b.d.l.	b.d.l.		72.5	b.d.l.	5.4	0.8	b.d.l.	b.d.l.	0.6	b.d.l.	b.d.l.	b.d.l.
17ja10a97.xl	Core	20.1	19.9	0.2	0.6	93.1	466998	64.1	b.d.l.	b.d.l.		82.0	b.d.l.	5.8	1.0	b.d.l.	b.d.l.	0.6	b.d.l.	b.d.l.	b.d.l.
17ja10a98.xl	Core	20.2	20.3	0.2	0.9	97.0	466998	64.3	b.d.l.	b.d.l.		87.8	0.2	7.5	1.0	b.d.l.	b.d.l.	0.5	b.d.l.	b.d.l.	b.d.l.
17ja10a99.xl	Core	19.7	19.7	0.2	0.5	95.4	466998	63.0	b.d.l.	b.d.l.		88.9	b.d.l.	8.3	0.8	b.d.l.	b.d.l.	0.5	b.d.l.	b.d.l.	b.d.l.
17ja10a100.xl	Core	20.0	19.5	0.2	0.6	95.8	466998	61.7	b.d.l.	b.d.l.		88.7	b.d.l.	7.2	0.6	b.d.l.	b.d.l.	0.6	b.d.l.	b.d.l.	b.d.l.
17ja10a101.xl	Core	20.8	19.0	0.2	0.6	94.0	466998	64.6	b.d.l.	b.d.l.		87.8	b.d.l.	6.8	0.9	b.d.l.	b.d.l.	0.7	b.d.l.	b.d.l.	b.d.l.
17ja10a102.xl	Core	18.1	18.5	0.2	0.5	92.5	466998	63.9	b.d.l.	b.d.l.		86.1	b.d.l.	6.0	0.7	b.d.l.	b.d.l.	0.6	b.d.l.	b.d.l.	b.d.l.
17ja10a103.xl	Core	20.0	18.8	0.2	0.6	93.7	466998	65.7	b.d.l.	b.d.l.		84.1	0.2	7.6	b.d.l.	b.d.l.	b.d.l.	0.8	b.d.l.	b.d.l.	b.d.l.
17ja10a104.xl	Core	20.6	18.5	0.2	0.6	91.2	466998	64.1	b.d.l.	b.d.l.		78.2	b.d.l.	6.4	0.6	b.d.l.	b.d.l.	0.5	b.d.l.	b.d.l.	b.d.l.
16de20c34.xl	Rim	19.7	19.8	b.d.l.	0.8	108.8	466998	75.5	b.d.l.	b.d.l.		89.2	0.2	8.9	0.5	b.d.l.	b.d.l.	0.9	b.d.l.	b.d.l.	b.d.l.
16de20c35.xl	Rim	19.2	18.4	b.d.l.	0.8	100.9	466998	74.4	b.d.l.	b.d.l.		84.1	0.2	6.8	0.7	b.d.l.	b.d.l.	1.0	b.d.l.	b.d.l.	b.d.l.
16de20c36.xl	Core	17.4	17.5	b.d.l.	0.6	93.1	466998	74.2	b.d.l.	b.d.l.		79.6	b.d.l.	6.5	0.5	b.d.l.	b.d.l.	1.0	b.d.l.	b.d.l.	b.d.l.
16de20c37.xl	Core	18.7	17.9	b.d.l.	0.7	94.7	466998	74.4	b.d.l.	b.d.l.		80.4	0.2	6.8	0.6	b.d.l.	b.d.l.	0.9	b.d.l.	b.d.l.	b.d.l.
16de20c38.xl	Core	19.4	19.1	0.1	0.6	98.0	466998	74.5	b.d.l.	b.d.l.		84.0	0.2	8.1	0.6	b.d.l.	b.d.l.	1.0	b.d.l.	b.d.l.	b.d.l.
16de20c39.xl	Core	21.0	20.0	b.d.l.	0.8	102.5	466998	74.6	b.d.l.	b.d.l.		84.1	0.2	7.9	0.4	b.d.l.	b.d.l.	1.0	b.d.l.	b.d.l.	b.d.l.
16de20c40.xl	Core	21.2	21.0	0.1	0.6	106.6	466998	73.5	b.d.l.	b.d.l.		83.1	0.2	7.5	0.6	b.d.l.	b.d.l.	1.0	b.d.l.	b.d.l.	b.d.l.
16de20c41.xl	Core	19.4	19.8	0.1	0.6	98.5	466998	75.8	b.d.l.	b.d.l.		77.8	0.2	5.6	0.6	b.d.l.	b.d.l.	0.9	b.d.l.	b.d.l.	b.d.l.
16de20c42.xl	Core	20.0	19.5	0.1	0.6	94.1	466998	73.1	b.d.l.	b.d.l.		70.4	b.d.l.	5.4	0.4	b.d.l.	b.d.l.	1.0	b.d.l.	b.d.l.	b.d.l.
16de20c43.xl	Core	18.8	18.7	0.1	0.7	90.1	466998	73.9	b.d.l.	b.d.l.		68.5	b.d.l.	4.9	0.5	b.d.l.	b.d.l.	0.9	b.d.l.	b.d.l.	b.d.l.
16de20c44.xl	Core	18.4	19.0	0.2	0.7	92.8	466998	73.0	b.d.l.	b.d.l.		68.8	0.2	6.7	0.4	b.d.l.	b.d.l.	1.0	b.d.l.	b.d.l.	b.d.l.
16de20c48.xl	Core	17.7	17.7	0.2	0.6	90.5	466998	73.9	b.d.l.	b.d.l.		70.0	0.1	5.8	0.5	b.d.l.	b.d.l.	1.0	b.d.l.	b.d.l.	b.d.l.
16de20c49.xl	Core	17.7	17.8	0.1	0.5	91.4	466998	75.3	b.d.l.	b.d.l.		74.6	b.d.l.	6.2	0.5	b.d.l.	b.d.l.	1.1	b.d.l.	b.d.l.	b.d.l.
16de20c50.xl	Core	17.2	16.6	0.2	0.5	90.9	466998	73.6	b.d.l.	b.d.l.		79.1	b.d.l.	6.5	0.5	b.d.l.	b.d.l.	0.9	b.d.l.	b.d.l.	b.d.l.
16de20c51.xl	Core	17.9	16.7	0.3	0.8	94.0	466998	72.8	b.d.l.	b.d.l.		84.8	0.2	5.2	0.5	b.d.l.	b.d.l.	0.9	b.d.l.	b.d.l.	b.d.l.
16de20c52.xl	Core	16.4	15.7	0.2	0.5	92.0	466998	73.7	b.d.l.	b.d.l.		86.8	b.d.l.	5.3	0.5	b.d.l.	b.d.l.	0.9	b.d.l.	b.d.l.	b.d.l.
16de20c53.xl	Core	16.6	16.3	0.2	0.7	91.5	466998	73.3	b.d.l.	b.d.l.		83.3	0.2	5.6	0.4	b.d.l.	b.d.l.	0.9	b.d.l.	b.d.l.	b.d.l.
16de20c54.xl	Core	16.6	16.1	0.3	0.6	89.9	466998	73.6	b.d.l.	b.d.l.		78.8	0.2	7.8	0.4	b.d.l.	b.d.l.	1.0	b.d.l.	b.d.l.	b.d.l.
16de20c55.xl	Core	17.3	15.7	0.2	0.5	87.9	466998	73.5	b.d.l.	b.d.l.		69.2	b.d.l.	5.4	0.4	b.d.l.	b.d.l.	0.9	b.d.l.	b.d.l.	b.d.l.
16de20c56.xl	Core	20.3	17.8	0.1	0.7	91.5	466998	72.7	b.d.l.	b.d.l.		74.4	0.2	7.1	0.4	b.d.l.	b.d.l.	0.9	b.d.l.	b.d.l.	b.d.l.
16de20c57.xl	Rim	19.9	18.2	b.d.l.	0.6	88.0	466998	73.1	b.d.l.	b.d.l.		71.1	b.d.l.	6.7	0.5	b.d.l.	b.d.l.	1.0	b.d.l.	b.d.l.	b.d.l.
17ja10a73.xl	Rim	18.1	18.0	b.d.l.	0.7	96.3	466998	74.1	b.d.l.	b.d.l.		74.2	b.d.l.	b.d.l.	b.d.l.	b.d.l.	b.d.l.	1.2	b.d.l.	b.d.l.	b.d.l.
17ja10a74.xl	Core	16.1	17.3	b.d.l.	0.5	95.5	466998	74.5	b.d.l.	b.d.l.		b.d.l.	b.d.l.	6.6	b.d.l.	b.d.l.	b.d.l.	0.9	b.d.l.	b.d.l.	b.d.l.
17ja10a76.xl	Core	16.0	15.8	b.d.l.	0.8	95.9	466998	75.6	b.d.l.	b.d.l.		73.4	0.3	6.9	0.8	b.d.l.	b.d.l.	0.9	b.d.l.	b.d.l.	b.d.l.
17ja10a77.xl	Core	17.5	15.7	b.d.l.	0.6	93.6	466998	75.2	b.d.l.	b.d.l.		72.4	b.d.l.	8.1	b.d.l.	b.d.l.	b.d.l.	0.9	b.d.l.	b.d.l.	b.d.l.
17ja10a78.xl	Core	17.4	16.1	b.d.l.	0.5	90.9	466998	75.4	b.d.l.	b.d.l.		71.9	b.d.l.	5.1	0.8	b.d.l.	b.d.l.	0.8	b.d.l.	b.d.l.	b.d.l.
17ja10a79.xl	Core	18.4	17.6	b.d.l.	0.5	89.0	466998	74.4	b.d.l.	b.d.l.		67.8	b.d.l.	5.0	b.d.l.	b.d.l.	b.d.l.	0.9	b.d.l.	b.d.l.	b.d.l.

Table A1.3: continued

Info	Position	I ^o	I ^z	Na	Mg	Al	Si	P	K	Ca	Sc	Ti	Mn	Fe	Ge	Rb	Sr	Sn	Cs	Pb	Ba
17ia0a83.xl	Rim	21.3	19.7	b.d.l.	0.7	91.0	466998	72.1	b.d.l.	b.d.l.		71.6	b.d.l.	5.6	b.d.l.	b.d.l.	b.d.l.	0.8	b.d.l.	b.d.l.	b.d.l.
17ia0a84.xl	Core	18.4	18.9	b.d.l.	0.6	88.4	466998	72.9	b.d.l.	b.d.l.		61.4	b.d.l.	6.6	0.9	b.d.l.	b.d.l.	0.8	b.d.l.	b.d.l.	b.d.l.
17ia0a85.xl	Core	18.5	19.3	b.d.l.	0.7	97.3	466998	75.1	b.d.l.	b.d.l.		80.5	b.d.l.	6.8	0.8	b.d.l.	b.d.l.	0.6	b.d.l.	b.d.l.	b.d.l.
17ia0a86.xl	Core	18.8	18.5	b.d.l.	0.7	94.1	466998	74.9	b.d.l.	b.d.l.		77.3	b.d.l.	6.8	b.d.l.	b.d.l.	b.d.l.	0.7	b.d.l.	b.d.l.	b.d.l.
17ia0a89.xl	Core	17.0	17.6	b.d.l.	0.7	97.5	466998	75.9	b.d.l.	b.d.l.		89.8	b.d.l.	b.d.l.	0.8	b.d.l.	b.d.l.	0.8	b.d.l.	b.d.l.	b.d.l.
17ia0a91.xl	Rim	20.1	19.6	b.d.l.	0.7	94.0	466998	73.0	b.d.l.	b.d.l.		75.9	b.d.l.	5.7	0.9	b.d.l.	b.d.l.	0.8	b.d.l.	b.d.l.	b.d.l.
17ia0a92.xl	Core	18.3	18.5	0.2	0.6	100.0	466998	71.3	b.d.l.	b.d.l.		98.4	b.d.l.	7.7	0.6	b.d.l.	b.d.l.	0.9	b.d.l.	b.d.l.	b.d.l.
17ia0a93.xl	Core	15.9	16.0	b.d.l.	0.6	92.6	466998	75.8	b.d.l.	b.d.l.		86.5	0.3	5.9	b.d.l.	b.d.l.	b.d.l.	1.0	b.d.l.	b.d.l.	b.d.l.
17ia0a94.xl	Core	15.7	16.3	b.d.l.	0.5	93.1	466998	78.1	b.d.l.	b.d.l.		83.9	b.d.l.	5.5	b.d.l.	b.d.l.	b.d.l.	1.0	b.d.l.	b.d.l.	b.d.l.
17ia10a140.xl	Rim	18.6	18.5	b.d.l.	0.4	97.4	466998	75.5	b.d.l.	b.d.l.		95.0	b.d.l.	5.7	0.9	b.d.l.	b.d.l.	0.7	b.d.l.	b.d.l.	b.d.l.
17ia10a141.xl	Rim	18.4	17.6	0.2	0.7	102.7	466998	75.8	b.d.l.	b.d.l.		101.1	b.d.l.	8.5	0.7	b.d.l.	b.d.l.	0.9	b.d.l.	b.d.l.	b.d.l.
17ia10a144.xl	Core	15.5	15.8	0.6	0.6	101.2	466998	74.4	b.d.l.	b.d.l.		99.0	0.3	8.1	b.d.l.	b.d.l.	b.d.l.	0.7	b.d.l.	b.d.l.	b.d.l.
17ia10a146.xl	Core	16.6	15.3	b.d.l.	0.6	103.0	466998	75.5	b.d.l.	b.d.l.		96.5	b.d.l.	8.0	b.d.l.	b.d.l.	b.d.l.	0.8	b.d.l.	b.d.l.	b.d.l.
17ia10a147.xl	Core	17.0	15.4	b.d.l.	0.8	99.0	466998	74.3	b.d.l.	b.d.l.		89.1	0.3	7.0	b.d.l.	b.d.l.	b.d.l.	0.8	b.d.l.	b.d.l.	b.d.l.
17ia10a148.xl	Core	19.8	19.0	b.d.l.	0.5	91.8	466998	72.3	b.d.l.	b.d.l.		79.1	b.d.l.	4.6	b.d.l.	b.d.l.	b.d.l.	0.8	b.d.l.	b.d.l.	b.d.l.
17ia10a149.xl	Core	18.6	17.8	b.d.l.	0.4	89.6	466998	73.3	b.d.l.	b.d.l.		75.3	b.d.l.	5.3	0.6	b.d.l.	b.d.l.	0.8	b.d.l.	b.d.l.	b.d.l.
17ia10a150.xl	Rim	21.5	19.3	0.2	0.6	90.9	466998	70.3	b.d.l.	b.d.l.		80.9	0.3	6.2	b.d.l.	b.d.l.	b.d.l.	1.0	b.d.l.	b.d.l.	b.d.l.
17ia10a151.xl	Rim	21.9	20.3	b.d.l.	0.7	95.6	466998	72.7	b.d.l.	b.d.l.		109.6	b.d.l.	6.5	0.8	b.d.l.	b.d.l.	0.9	b.d.l.	b.d.l.	b.d.l.
17ia10a152.xl	Rim	19.5	19.8	0.2	0.7	89.3	466998	70.7	b.d.l.	b.d.l.		78.7	b.d.l.	4.8	b.d.l.	b.d.l.	b.d.l.	0.8	b.d.l.	b.d.l.	b.d.l.
17ia16a07.xl	Rim	22.8	21.8	0.5	0.6	97.4	466998	39.2	b.d.l.	b.d.l.		81.6	b.d.l.	9.0	1.0	b.d.l.	b.d.l.	b.d.l.	b.d.l.	b.d.l.	b.d.l.
17ia16a08.xl	Core	20.4	19.8	b.d.l.	0.6	87.3	466998	42.6	b.d.l.	b.d.l.		70.1	b.d.l.	b.d.l.	0.8	b.d.l.	b.d.l.	0.3	b.d.l.	b.d.l.	b.d.l.
17ia16a09.xl	Core	20.3	20.2	b.d.l.	0.7	91.1	466998	41.7	b.d.l.	b.d.l.		81.2	b.d.l.	7.3	b.d.l.	b.d.l.	b.d.l.	0.3	b.d.l.	b.d.l.	b.d.l.
17ia16a10.xl	Core	23.0	21.1	0.3	0.6	100.1	466998	42.3	b.d.l.	b.d.l.		99.0	b.d.l.	8.2	0.8	b.d.l.	b.d.l.	0.3	b.d.l.	b.d.l.	b.d.l.
17ia16a11.xl	Core	22.7	20.4	0.5	0.9	105.6	466998	42.9	b.d.l.	b.d.l.		122.6	b.d.l.	b.d.l.	b.d.l.	b.d.l.	b.d.l.	b.d.l.	b.d.l.	b.d.l.	b.d.l.
17ia16a12.xl	Core	22.2	20.9	0.3	0.6	103.0	466998	42.5	b.d.l.	b.d.l.		107.6	0.3	9.3	b.d.l.	b.d.l.	b.d.l.	b.d.l.	b.d.l.	b.d.l.	b.d.l.
17ia16a14.xl	Core	20.9	20.6	0.8	0.6	101.4	466998	43.9	b.d.l.	b.d.l.		106.7	b.d.l.	b.d.l.	0.8	b.d.l.	b.d.l.	0.4	b.d.l.	b.d.l.	b.d.l.
17ia16a16.xl	Core	19.7	19.5	0.2	0.5	90.6	466998	41.0	b.d.l.	b.d.l.		82.8	b.d.l.	7.4	b.d.l.	b.d.l.	b.d.l.	0.4	b.d.l.	b.d.l.	b.d.l.
17ia16a17.xl	Core	20.7	19.7	0.2	0.7	91.2	466998	43.1	b.d.l.	b.d.l.		74.2	b.d.l.	6.2	0.6	b.d.l.	b.d.l.	0.3	b.d.l.	b.d.l.	b.d.l.
17ia16a18.xl	Core	19.5	18.7	0.3	0.4	86.4	466998	43.7	b.d.l.	b.d.l.		73.0	b.d.l.	6.1	0.9	b.d.l.	b.d.l.	0.3	b.d.l.	b.d.l.	b.d.l.
17ia16a19.xl	Rim	21.9	20.0	b.d.l.	0.8	95.0	466998	42.6	b.d.l.	b.d.l.		76.7	b.d.l.	6.3	b.d.l.	b.d.l.	b.d.l.	b.d.l.	b.d.l.	b.d.l.	b.d.l.
17ia16a24.xl	Rim	19.9	20.3	b.d.l.	0.4	93.3	466998	48.8	b.d.l.	b.d.l.		66.1	0.4	b.d.l.	b.d.l.	b.d.l.	b.d.l.	0.4	b.d.l.	b.d.l.	b.d.l.
17ia16a25.xl	Core	21.0	20.3	b.d.l.	0.7	96.5	466998	46.3	b.d.l.	b.d.l.		76.3	b.d.l.	7.9	b.d.l.	b.d.l.	b.d.l.	0.4	b.d.l.	b.d.l.	b.d.l.
17ia16a26.xl	Core	22.3	20.1	b.d.l.	0.5	94.4	466998	46.5	b.d.l.	b.d.l.		68.7	b.d.l.	7.2	0.9	b.d.l.	b.d.l.	0.4	b.d.l.	b.d.l.	b.d.l.
17ia16a27.xl	Core	20.0	19.9	b.d.l.	0.4	96.0	466998	47.7	b.d.l.	b.d.l.		77.0	b.d.l.	7.0	b.d.l.	b.d.l.	b.d.l.	0.3	b.d.l.	b.d.l.	b.d.l.
17ia16a28.xl	Core	22.6	19.8	0.2	0.8	95.2	466998	45.5	b.d.l.	b.d.l.		78.8	b.d.l.	5.8	0.7	b.d.l.	b.d.l.	0.5	b.d.l.	b.d.l.	b.d.l.
17ia16a29.xl	Core	19.6	19.5	b.d.l.	0.7	95.2	466998	48.4	b.d.l.	b.d.l.		79.5	b.d.l.	b.d.l.	0.9	b.d.l.	b.d.l.	0.4	b.d.l.	b.d.l.	b.d.l.
17ia16a31.xl	Core	19.9	19.2	0.2	0.7	94.8	466998	46.8	b.d.l.	b.d.l.		78.1	b.d.l.	6.4	0.8	b.d.l.	b.d.l.	0.5	b.d.l.	b.d.l.	b.d.l.
17ia16a32.xl	Core	18.7	18.4	0.3	0.4	92.9	466998	48.1	b.d.l.	b.d.l.		77.8	b.d.l.	b.d.l.	b.d.l.	b.d.l.	b.d.l.	0.4	b.d.l.	b.d.l.	b.d.l.
17ia16a33.xl	Core	18.2	17.7	b.d.l.	0.7	92.7	466998	48.7	b.d.l.	b.d.l.		77.7	b.d.l.	b.d.l.	b.d.l.	b.d.l.	b.d.l.	0.4	b.d.l.	b.d.l.	b.d.l.
17ia16a34.xl	Core	18.0	18.2	b.d.l.	0.6	91.7	466998	45.5	b.d.l.	b.d.l.		81.4	0.4	b.d.l.	0.9	b.d.l.	b.d.l.	0.5	b.d.l.	b.d.l.	b.d.l.
17ia16a35.xl	Core	19.0	19.2	0.3	0.4	92.0	466998	46.3	b.d.l.	b.d.l.		82.3	b.d.l.	5.7	b.d.l.	b.d.l.	b.d.l.	b.d.l.	b.d.l.	b.d.l.	b.d.l.
17ia16a36.xl	Rim	21.5	20.1	b.d.l.	0.7	93.6	466998	45.7	b.d.l.	b.d.l.		82.1	b.d.l.	b.d.l.	b.d.l.	b.d.l.	b.d.l.	0.5	b.d.l.	b.d.l.	b.d.l.
17ia10a61.xl	Core	16.5	16.2	b.d.l.	0.8	108.9	466998	79.8	b.d.l.	b.d.l.		115.7	b.d.l.	b.d.l.	b.d.l.	b.d.l.	b.d.l.	0.8	b.d.l.	b.d.l.	b.d.l.
17ia10a64.xl	Core	16.2	16.0	b.d.l.	0.6	100.6	466998	69.2	b.d.l.	b.d.l.		101.1	0.2	7.2	0.9	b.d.l.	b.d.l.	0.7	b.d.l.	b.d.l.	b.d.l.
17ia10a65.xl	Core	16.2	16.1	0.2	0.5	99.9	466998	69.5	b.d.l.	b.d.l.		105.2	b.d.l.	6.6	0.6	b.d.l.	b.d.l.	0.8	b.d.l.	b.d.l.	b.d.l.
17ia10a66.xl	Core	17.1	16.4	0.3	0.7	103.8	466998	67.9	b.d.l.	b.d.l.		107.7	0.2	8.1	0.7	b.d.l.	b.d.l.	0.8	b.d.l.	b.d.l.	b.d.l.
17ia10a67.xl	Core	13.9	14.6	0.2	0.6	90.6	466998	68.3	b.d.l.	b.d.l.		80.6	b.d.l.	6.4	0.8	b.d.l.	b.d.l.	0.6	b.d.l.	b.d.l.	b.d.l.
17ia10a68.xl	Core	17.1	16.0	0.1	0.5	93.9	466998	69.5	b.d.l.	b.d.l.		88.6	b.d.l.	5.9	0.7	b.d.l.	b.d.l.	0.7	b.d.l.	b.d.l.	b.d.l.
17ia10a69.xl	Rim	16.9	16.4	b.d.l.	0.5	97.8	466998	69.3	b.d.l.	b.d.l.		95.4	0.2	8.0	b.d.l.	b.d.l.	b.d.l.	0.8	b.d.l.	b.d.l.	b.d.l.
17ia10a70.xl	Rim	18.8	17.0	b.d.l.	0.5	94.3	466998	66.6	b.d.l.	b.d.l.		83.2	b.d.l.	7.8	0.6	b.d.l.	b.d.l.	0.8	b.d.l.	b.d.l.	b.d.l.

Table A1.3: continued

Info	Position	Lj*	Lj†	Na	Mg	Al	Si	P	K	Ca	Sc	Ti	Mn	Fe	Ce	Rb	Sr	Sn	Cs	Pb	Ba
17ja 0a118.xl	Rim	19.5	19.7	b.d.l.	0.5	93.5	466998	64.8	b.d.l.	b.d.l.		76.9	b.d.l.	6.9	b.d.l.	b.d.l.	b.d.l.	0.7	b.d.l.	b.d.l.	b.d.l.
17ja 0a119.xl	Rim	18.1	18.8	b.d.l.	0.6	93.6	466998	63.9	b.d.l.	b.d.l.		78.9	b.d.l.	6.7	b.d.l.	b.d.l.	b.d.l.	0.7	b.d.l.	b.d.l.	b.d.l.
17ja 0a121.xl	Core	18.1	18.3	0.2	0.7	93.2	466998	67.4	b.d.l.	b.d.l.		88.6	b.d.l.	7.3	0.7	b.d.l.	b.d.l.	0.9	b.d.l.	b.d.l.	b.d.l.
17ja 0a122.xl	Core	20.7	20.5	0.2	0.6	91.2	466998	69.2	b.d.l.	b.d.l.		89.2	b.d.l.	6.4	0.5	b.d.l.	b.d.l.	0.7	b.d.l.	b.d.l.	b.d.l.
17ja 0a123.xl	Core	20.3	18.7	0.2	0.7	90.8	466998	67.8	b.d.l.	b.d.l.		89.0	b.d.l.	4.5	0.6	b.d.l.	b.d.l.	0.7	b.d.l.	b.d.l.	b.d.l.
17ja 0a124.xl	Core	21.8	19.7	b.d.l.	0.6	90.3	466998	70.2	b.d.l.	b.d.l.		87.7	b.d.l.	6.0	0.5	b.d.l.	b.d.l.	0.7	b.d.l.	b.d.l.	b.d.l.
17ja 0a125.xl	Core	21.8	21.1	0.1	0.7	95.9	466998	71.9	b.d.l.	b.d.l.		92.8	0.2	7.9	0.7	b.d.l.	b.d.l.	0.7	b.d.l.	b.d.l.	b.d.l.
17ja 0a126.xl	Core	22.9	21.9	0.2	0.7	97.7	466998	72.1	b.d.l.	b.d.l.		74.8	0.2	6.4	0.7	b.d.l.	b.d.l.	0.8	b.d.l.	b.d.l.	b.d.l.
17ja 0a130.xl	Rim	20.4	18.8	b.d.l.	0.6	86.9	466998	72.8	b.d.l.	b.d.l.		61.2	b.d.l.	5.8	b.d.l.	b.d.l.	b.d.l.	0.6	b.d.l.	b.d.l.	b.d.l.
17ja 0a131.xl	Rim	21.0	19.6	0.3	0.6	88.8	466998	71.7	b.d.l.	b.d.l.		66.1	b.d.l.	6.4	0.8	b.d.l.	b.d.l.	0.9	b.d.l.	b.d.l.	b.d.l.
17ja 0a132.xl	Core	20.4	19.0	0.2	0.7	89.0	466998	69.8	b.d.l.	b.d.l.		65.2	b.d.l.	6.1	0.6	b.d.l.	b.d.l.	0.7	b.d.l.	b.d.l.	b.d.l.
17ja 0a133.xl	Core	17.4	17.7	b.d.l.	0.5	90.0	466998	71.4	b.d.l.	b.d.l.		65.8	0.2	5.9	0.5	b.d.l.	b.d.l.	1.0	b.d.l.	b.d.l.	b.d.l.
17ja 0a134.xl	Core	19.4	18.5	0.1	0.6	91.5	466998	70.4	b.d.l.	b.d.l.		69.0	0.2	6.2	0.6	b.d.l.	b.d.l.	0.6	b.d.l.	b.d.l.	b.d.l.
17ja 0a135.xl	Core	17.3	16.9	0.2	0.7	94.2	466998	71.6	b.d.l.	b.d.l.		76.4	b.d.l.	7.0	b.d.l.	b.d.l.	b.d.l.	0.9	b.d.l.	b.d.l.	b.d.l.
17ja 0a136.xl	Core	17.6	18.5	0.2	0.8	94.3	466998	74.2	b.d.l.	b.d.l.		86.3	b.d.l.	6.7	0.6	b.d.l.	b.d.l.	0.7	b.d.l.	b.d.l.	b.d.l.
17ja 0a137.xl	Core	17.5	17.6	0.1	0.6	88.9	466998	70.7	b.d.l.	b.d.l.		74.2	0.2	5.7	0.8	b.d.l.	b.d.l.	0.6	b.d.l.	b.d.l.	b.d.l.
17ja 0a138.xl	Core	18.3	17.1	b.d.l.	0.6	87.1	466998	72.2	b.d.l.	b.d.l.		69.8	b.d.l.	5.2	0.7	b.d.l.	b.d.l.	0.8	b.d.l.	b.d.l.	b.d.l.
17ja 0a139.xl	Rim	20.6	19.1	b.d.l.	0.6	91.0	466998	73.0	b.d.l.	b.d.l.		66.9	b.d.l.	4.7	b.d.l.	b.d.l.	b.d.l.	0.9	b.d.l.	b.d.l.	b.d.l.
17ja 0a43.xl	Core	22.6	21.7	b.d.l.	0.8	114.9	466998	66.3	b.d.l.	b.d.l.		151.8	0.3	9.4	b.d.l.	b.d.l.	b.d.l.	0.7	b.d.l.	b.d.l.	b.d.l.
17ja 0a44.xl	Core	19.9	20.8	0.2	0.6	118.2	466998	63.3	b.d.l.	b.d.l.		156.2	0.3	9.2	b.d.l.	b.d.l.	b.d.l.	0.9	b.d.l.	b.d.l.	b.d.l.
17ja 0a46.xl	Core	19.3	19.1	b.d.l.	0.9	125.0	466998	66.4	b.d.l.	b.d.l.		160.0	0.3	9.6	b.d.l.	b.d.l.	b.d.l.	0.6	b.d.l.	b.d.l.	b.d.l.
17ja 0a48.xl	Rim	21.2	20.2	b.d.l.	0.6	97.0	466998	63.1	b.d.l.	b.d.l.		82.9	b.d.l.	6.4	0.6	b.d.l.	b.d.l.	0.9	b.d.l.	b.d.l.	b.d.l.
17ja 0a50.xl	Core	16.8	16.3	b.d.l.	0.7	118.5	466998	61.6	b.d.l.	b.d.l.		164.6	0.3	9.8	0.6	b.d.l.	b.d.l.	0.6	b.d.l.	b.d.l.	b.d.l.
17ja 0a51.xl	Core	16.2	14.5	0.2	0.8	121.5	466998	61.2	b.d.l.	b.d.l.		178.8	0.4	11.1	b.d.l.	b.d.l.	b.d.l.	0.8	b.d.l.	b.d.l.	b.d.l.
17ja 0a52.xl	Rim	17.4	16.6	b.d.l.	0.7	100.0	466998	62.5	b.d.l.	b.d.l.		91.0	0.3	6.4	b.d.l.	b.d.l.	b.d.l.	0.7	b.d.l.	b.d.l.	b.d.l.
17ja 0a53.xl	Rim	17.7	18.1	b.d.l.	0.6	97.2	466998	62.4	b.d.l.	b.d.l.		85.5	0.2	6.6	b.d.l.	b.d.l.	b.d.l.	0.6	b.d.l.	b.d.l.	b.d.l.
17ja 0a54.xl	Rim	21.9	20.5	b.d.l.	0.9	102.8	466998	63.4	b.d.l.	b.d.l.		103.5	b.d.l.	6.3	b.d.l.	b.d.l.	b.d.l.	0.9	b.d.l.	b.d.l.	b.d.l.
17ja 0a55.xl	Rim	22.3	21.7	0.2	0.6	101.9	466998	62.0	b.d.l.	b.d.l.		86.7	0.2	7.1	0.7	b.d.l.	b.d.l.	0.9	b.d.l.	b.d.l.	b.d.l.
17ja 6a44.xl	Core	21.9	20.6	b.d.l.	0.8	91.8	466998	50.6	b.d.l.	b.d.l.		37.4	b.d.l.	6.4	1.0	b.d.l.	b.d.l.	0.5	b.d.l.	b.d.l.	b.d.l.
17ja 6a45.xl	Core	20.2	20.2	0.2	0.3	91.9	466998	52.2	b.d.l.	b.d.l.		38.0	b.d.l.	7.0	b.d.l.	b.d.l.	b.d.l.	0.6	b.d.l.	b.d.l.	b.d.l.
17ja 6a46.xl	Core	18.9	18.5	b.d.l.	0.6	91.7	466998	51.1	b.d.l.	b.d.l.		39.7	b.d.l.	5.4	0.7	b.d.l.	b.d.l.	0.4	b.d.l.	b.d.l.	b.d.l.
17ja 6a48.xl	Core	20.6	19.6	b.d.l.	0.5	93.4	466998	51.9	b.d.l.	b.d.l.		40.6	b.d.l.	5.7	b.d.l.	b.d.l.	b.d.l.	0.4	b.d.l.	b.d.l.	b.d.l.
17ja 6a49.xl	Core	20.3	19.5	b.d.l.	0.5	93.9	466998	50.3	b.d.l.	b.d.l.		43.2	b.d.l.	7.8	0.7	b.d.l.	b.d.l.	0.5	b.d.l.	b.d.l.	b.d.l.
17ja 6a50.xl	Core	20.0	18.5	b.d.l.	0.6	92.3	466998	53.6	b.d.l.	b.d.l.		43.2	b.d.l.	5.4	b.d.l.	b.d.l.	b.d.l.	0.3	b.d.l.	b.d.l.	b.d.l.
17ja 6a51.xl	Rim	20.6	18.8	0.2	0.6	98.8	466998	52.2	b.d.l.	b.d.l.		46.8	b.d.l.	7.8	b.d.l.	b.d.l.	b.d.l.	b.d.l.	b.d.l.	b.d.l.	b.d.l.
17ja 6a52.xl	Rim	21.0	19.5	b.d.l.	0.7	94.5	466998	53.5	b.d.l.	b.d.l.		45.3	b.d.l.	5.6	b.d.l.	b.d.l.	b.d.l.	0.6	b.d.l.	b.d.l.	b.d.l.
17ja 6a53.xl	Rim	18.4	18.9	b.d.l.	0.6	89.0	466998	55.1	b.d.l.	b.d.l.		37.5	b.d.l.	6.4	b.d.l.	b.d.l.	b.d.l.	0.5	b.d.l.	b.d.l.	b.d.l.

Appendix A

Table A1.3: continued

Info	Position	Li ⁶	Li ⁷	Na	Mg	Al	Si	P	Sc	Ti	Ge
Qz-1-1	Rim	20.0	19.2	b.d.l.	0.6	88.5	466998	22.7	1.2	87.0	b.d.l.
Qz-1-2	Rim	19.5	18.9	b.d.l.	0.5	89.2	466998	21.9	1.2	97.2	b.d.l.
Qz-1-3	Rim	20.3	19.8	b.d.l.	0.9	94.4	466998	28.7	1.2	107.5	b.d.l.
Qz-1-4	Core	19.7	19.6	b.d.l.	0.8	96.9	466998	26.2	1.2	110.1	0.7
Qz-1-5	Core	18.8	18.2	b.d.l.	0.7	91.9	466998	19.5	1.2	103.4	b.d.l.
Qz-1-6	Core	18.4	18.0	b.d.l.	0.9	94.4	466998	22.7	1.2	111.9	b.d.l.
Qz-1-7	Core	18.2	17.9	b.d.l.	0.8	97.5	466998	25.3	1.2	122.8	b.d.l.
Qz-1-8	Core	17.4	17.4	b.d.l.	0.8	96.8	466998	20.8	1.2	117.8	b.d.l.
Qz-1-9	Core	17.7	17.5	b.d.l.	0.9	98.5	466998	26.3	1.1	122.6	b.d.l.
Qz-1-10	Core	18.2	17.7	b.d.l.	0.7	99.8	466998	22.6	1.1	127.7	b.d.l.
Qz-1-11	Core	18.1	17.6	b.d.l.	0.9	98.6	466998	27.9	1.2	128.8	b.d.l.
Qz-1-12	Core	19.2	18.4	b.d.l.	0.9	101.0	466998	25.4	1.2	139.8	b.d.l.
Qz-1-13	Core	20.0	19.7	b.d.l.	0.9	109.3	466998	21.6	1.1	145.9	b.d.l.
Qz-1-14	Core	23.4	22.3	b.d.l.	1.0	125.0	466998	17.1	1.1	163.5	b.d.l.
Qz-1-15	Core	20.5	20.4	b.d.l.	1.1	113.9	466998	29.5	1.2	157.0	b.d.l.
Qz-1-16	Core	18.4	18.3	b.d.l.	1.1	107.9	466998	25.5	1.1	150.5	b.d.l.
Qz-1-17	Core	16.6	16.5	b.d.l.	0.9	107.6	466998	26.6	1.1	152.7	b.d.l.
Qz-1-18	Core	17.8	17.3	b.d.l.	0.9	106.3	466998	22.8	1.2	154.7	b.d.l.
Qz-1-19	Core	19.2	18.5	b.d.l.	0.9	111.3	466998	21.5	1.2	171.4	b.d.l.
Qz-1-20	Core	21.1	20.8	b.d.l.	1.2	116.2	466998	24.0	1.1	176.3	0.7
Qz-1-21	Core	22.3	21.9	b.d.l.	1.2	116.7	466998	22.2	1.1	180.0	0.9
Qz-1-22	Core	23.3	22.9	0.6	1.0	119.8	466998	24.7	1.1	179.5	b.d.l.
Qz-1-23	Core	24.2	23.5	b.d.l.	1.0	117.6	466998	23.3	1.1	181.8	0.9
Qz-2-1	Rim	19.7	19.6	b.d.l.	0.6	90.2	466998	23.4	1.1	94.7	b.d.l.
Qz-2-2	Core	21.1	20.9	b.d.l.	0.7	95.8	466998	23.7	1.1	103.3	b.d.l.
Qz-2-3	Core	20.7	20.7	b.d.l.	0.6	95.1	466998	25.9	1.2	104.4	b.d.l.
Qz-2-4	Core	20.9	20.9	b.d.l.	0.7	97.9	466998	24.6	1.1	109.5	b.d.l.
Qz-2-5	Core	20.2	20.4	b.d.l.	0.8	96.6	466998	25.9	1.1	107.0	b.d.l.
Qz-2-6	Core	20.2	19.9	b.d.l.	0.6	95.8	466998	23.4	1.1	106.8	b.d.l.
Qz-2-7	Core	18.9	18.4	b.d.l.	0.7	90.2	466998	26.3	1.1	92.9	b.d.l.
Qz-2-8	Core	17.8	17.8	b.d.l.	0.6	89.3	466998	25.6	1.1	85.8	0.9
Qz-2-9	Core	17.6	17.6	b.d.l.	0.8	91.6	466998	21.9	1.1	84.8	b.d.l.
Qz-2-10	Core	18.0	17.5	b.d.l.	0.7	91.2	466998	25.8	1.1	90.9	0.9
Qz-2-11	Core	17.5	17.2	b.d.l.	0.7	89.7	466998	20.9	1.1	88.1	b.d.l.
Qz-2-12	Core	17.4	17.5	b.d.l.	0.6	91.9	466998	25.7	1.1	102.4	b.d.l.
Qz-2-13	Core	17.9	17.4	b.d.l.	0.6	93.5	466998	20.0	1.1	97.8	b.d.l.
Qz-2-14	Core	17.4	17.3	b.d.l.	0.8	91.6	466998	26.3	1.1	100.3	b.d.l.
Qz-2-15	Core	17.2	17.2	b.d.l.	0.7	90.6	466998	23.8	1.0	99.9	0.9
Qz-2-16	Core	17.6	17.4	b.d.l.	0.7	89.7	466998	17.3	1.0	98.7	0.7
Qz-2-17	Core	18.0	17.4	b.d.l.	0.8	90.7	466998	22.6	1.0	97.6	0.9
Qz-2-18	Core	17.5	17.3	b.d.l.	0.7	91.2	466998	28.9	1.1	96.6	b.d.l.
Qz-2-19	Core	17.8	17.4	0.3	0.9	89.4	466998	26.2	1.1	95.2	0.9
Qz-2-20	Core	17.8	17.6	b.d.l.	0.6	90.5	466998	28.0	1.1	94.7	b.d.l.
Qz-2-21	Core	17.7	17.8	b.d.l.	0.7	91.2	466998	24.4	1.1	94.4	b.d.l.
Qz-2-22	Core	17.5	17.6	b.d.l.	0.9	89.8	466998	21.2	1.1	91.6	0.8
Qz-2-23	Core	18.0	18.0	b.d.l.	0.6	90.4	466998	20.8	1.0	90.4	b.d.l.
Qz-2-24	Core	18.5	18.2	b.d.l.	0.6	90.3	466998	21.3	1.0	91.7	b.d.l.
Qz-2-25	Core	18.5	18.4	b.d.l.	0.5	92.0	466998	26.4	1.1	91.1	b.d.l.
Qz-2-26	Core	19.2	18.6	b.d.l.	0.7	92.5	466998	20.2	1.1	90.1	0.9
Qz-2-27	Core	19.1	18.6	b.d.l.	0.8	90.6	466998	25.3	1.0	86.0	b.d.l.
Qz-2-28	Core	19.3	18.9	b.d.l.	0.6	91.5	466998	25.3	1.0	87.2	0.8
Qz-2-29	Core	19.2	18.8	b.d.l.	0.8	92.3	466998	16.7	1.1	88.7	b.d.l.
Qz-2-30	Core	19.1	18.8	b.d.l.	0.7	91.5	466998	22.4	1.0	83.3	b.d.l.
Qz-2-31	Core	19.5	19.0	b.d.l.	0.6	91.2	466998	21.4	1.1	79.4	b.d.l.
Qz-2-32	Core	20.0	19.4	b.d.l.	0.9	93.3	466998	21.1	1.0	80.1	0.8
Qz-2-33	Core	20.0	19.9	b.d.l.	0.8	94.5	466998	23.2	1.1	99.4	0.9
Qz-2-34	Core	19.9	20.0	b.d.l.	0.7	95.9	466998	21.4	1.1	104.7	b.d.l.
Qz-2-35	Core	20.7	20.2	b.d.l.	0.8	95.7	466998	21.9	1.0	101.4	b.d.l.
Qz-2-36	Rim	20.1	20.3	b.d.l.	0.6	95.1	466998	24.2	1.1	98.4	b.d.l.
Qz-2-37	Rim	20.6	20.3	b.d.l.	0.8	94.4	466998	20.0	1.0	95.3	0.9
Qz-2-38	Rim	20.7	20.0	b.d.l.	0.6	91.5	466998	18.0	1.0	86.2	b.d.l.
Qz-2-39	Rim	20.3	20.0	b.d.l.	0.7	89.5	466998	16.9	1.0	85.2	b.d.l.
Qz-2-40	Rim	21.4	21.1	b.d.l.	0.7	94.0	466998	19.3	1.0	86.1	b.d.l.
Qz-2-41	Rim	21.7	21.2	b.d.l.	0.8	94.4	466998	22.3	1.0	95.1	b.d.l.
Qz-3-1	Rim	20.4	20.0	b.d.l.	0.5	91.7	466998	24.2	0.9	87.1	b.d.l.
Qz-3-2	Rim	20.5	20.2	b.d.l.	0.8	93.0	466998	21.7	1.0	75.0	1.0
Qz-3-3	Core	19.0	18.9	b.d.l.	0.6	87.1	466998	15.8	1.0	73.6	b.d.l.
Qz-3-4	Core	19.5	19.5	b.d.l.	0.8	91.5	466998	21.2	0.9	90.8	b.d.l.
Qz-3-5	Core	20.0	19.8	b.d.l.	0.7	95.1	466998	21.1	1.0	98.1	b.d.l.
Qz-3-6	Core	20.4	20.1	b.d.l.	0.8	99.2	466998	21.7	1.0	105.6	b.d.l.
Qz-3-7	Core	21.1	20.3	b.d.l.	0.9	106.1	466998	22.8	1.1	121.7	b.d.l.
Qz-3-8	Core	20.2	20.4	b.d.l.	0.9	100.1	466998	24.8	1.1	125.0	b.d.l.
Qz-3-9	Core	19.7	19.0	b.d.l.	0.9	101.9	466998	20.9	1.1	125.9	b.d.l.
Qz-3-10	Core	19.3	19.0	b.d.l.	1.1	111.5	466998	19.9	1.0	129.8	0.9
Qz-3-11	Core	18.6	18.2	b.d.l.	1.0	103.1	466998	20.0	1.0	127.8	b.d.l.
Qz-3-12	Core	18.2	18.0	b.d.l.	0.9	104.1	466998	19.8	1.0	129.2	b.d.l.
Qz-3-13	Core	17.8	17.5	b.d.l.	0.9	102.7	466998	19.5	1.0	128.6	b.d.l.
Qz-3-14	Core	17.6	17.3	b.d.l.	1.1	101.7	466998	16.4	1.0	127.5	b.d.l.
Qz-3-15	Core	17.6	17.1	b.d.l.	1.2	107.4	466998	19.9	1.0	135.3	b.d.l.
Qz-3-16	Core	17.4	17.4	b.d.l.	0.9	96.0	466998	17.7	1.0	131.0	b.d.l.
Qz-3-17	Core	17.4	17.0	b.d.l.	1.0	103.4	466998	20.5	1.1	132.1	b.d.l.
Qz-3-18	Core	18.3	18.0	b.d.l.	0.9	100.5	466998	18.6	1.0	130.7	b.d.l.
Qz-3-20	Core	18.4	18.1	b.d.l.	1.1	101.5	466998	20.5	0.9	122.3	b.d.l.
Qz-3-21	Core	19.0	18.4	b.d.l.	1.0	105.8	466998	19.1	1.0	124.1	b.d.l.
Qz-3-22	Core	19.3	19.1	b.d.l.	0.7	102.0	466998	22.1	1.0	123.5	b.d.l.
Qz-3-23	Core	19.8	19.5	b.d.l.	1.0	102.6	466998	16.7	0.9	123.6	b.d.l.
Qz-3-24	Core	20.6	20.1	b.d.l.	1.1	104.8	466998	17.3	0.9	123.2	b.d.l.

Table A1.3: continued

Info	Position	Li ^c	Li ^r	Na	Mg	Al	Si	P	Sc	Ti	Ge
Qz-4 - 1	Rim	19.4	19.1	b.d.l.	0.6	89.6	466998	18.2	1.0	80.3	b.d.l.
Qz-4 - 3	Rim	18.6	18.2	b.d.l.	0.7	87.6	466998	18.1	1.0	79.8	b.d.l.
Qz-4 - 4	Core	19.2	18.5	b.d.l.	0.8	90.7	466998	15.7	0.9	79.6	b.d.l.
Qz-4 - 5	Core	18.3	18.0	b.d.l.	0.8	89.5	466998	23.5	0.9	86.2	b.d.l.
Qz-4 - 6	Core	18.0	17.2	b.d.l.	0.6	86.9	466998	16.3	0.9	88.4	b.d.l.
Qz-4 - 7	Core	17.9	17.1	b.d.l.	0.8	87.7	466998	17.1	0.9	94.5	b.d.l.
Qz-4 - 8	Core	17.6	17.4	b.d.l.	0.8	90.3	466998	18.1	0.9	101.6	b.d.l.
Qz-4 - 9	Core	17.5	17.4	b.d.l.	0.7	93.1	466998	18.0	0.9	106.8	b.d.l.
Qz-4 - 10	Core	17.5	17.2	b.d.l.	0.8	93.5	466998	19.2	1.0	106.9	0.8
Qz-4 - 11	Core	17.3	17.1	b.d.l.	0.7	94.9	466998	21.1	0.9	108.5	0.9
Qz-4 - 12	Core	17.1	16.8	b.d.l.	0.6	95.3	466998	21.6	1.0	110.3	b.d.l.
Qz-4 - 13	Core	17.1	16.7	b.d.l.	1.0	96.1	466998	15.7	0.9	111.2	b.d.l.
Qz-4 - 14	Core	17.3	16.9	b.d.l.	0.8	96.7	466998	13.5	0.9	114.5	b.d.l.
Qz-4 - 15	Core	17.4	17.1	b.d.l.	0.8	99.9	466998	17.7	0.9	116.6	0.8
Qz-4 - 16	Core	17.7	17.1	0.2	1.0	101.5	466998	17.9	0.9	115.6	b.d.l.
Qz-4 - 17	Core	17.7	17.0	b.d.l.	0.9	102.9	466998	18.7	0.9	112.1	b.d.l.
Qz-4 - 18	Core	16.9	16.7	b.d.l.	0.9	102.4	466998	19.0	1.0	111.6	b.d.l.
Qz-4 - 19	Core	16.8	16.5	b.d.l.	0.9	101.2	466998	15.7	0.9	112.1	b.d.l.
Qz-4 - 20	Core	16.4	16.2	b.d.l.	0.8	99.2	466998	18.9	1.0	117.0	0.8
Qz-4 - 21	Core	16.2	15.5	b.d.l.	0.8	96.2	466998	21.2	0.9	108.3	0.8
Qz-4 - 22	Core	16.3	15.4	b.d.l.	0.9	93.3	466998	18.5	0.9	110.7	b.d.l.
Qz-4 - 23	Core	16.3	15.9	b.d.l.	0.7	95.6	466998	22.3	1.0	107.6	b.d.l.
Qz-4 - 24	Core	16.7	16.4	b.d.l.	0.9	94.1	466998	20.3	0.9	111.4	b.d.l.
Qz-4 - 25	Core	17.7	17.8	b.d.l.	0.7	94.5	466998	17.2	0.9	112.7	0.8
Qz-4 - 26	Core	19.6	19.0	b.d.l.	0.8	92.7	466998	15.7	0.9	105.6	0.9
Qz-6 - 1	Rim	19.8	19.4	b.d.l.	0.7	87.6	466998	18.4	0.9	72.1	b.d.l.
Qz-6 - 2	Core	20.1	19.5	b.d.l.	0.6	90.0	466998	18.4	0.9	76.0	b.d.l.
Qz-6 - 3	Core	20.6	19.7	b.d.l.	0.6	89.2	466998	23.2	0.9	81.0	0.8
Qz-6 - 4	Core	19.8	19.6	b.d.l.	0.7	90.1	466998	19.0	0.9	79.5	b.d.l.
Qz-6 - 5	Core	21.2	20.5	b.d.l.	0.8	97.3	466998	20.5	0.9	81.4	0.8
Qz-6 - 6	Core	18.8	18.6	b.d.l.	0.7	89.4	466998	16.5	0.9	80.7	b.d.l.
Qz-6 - 7	Core	18.7	18.5	b.d.l.	0.5	90.0	466998	15.8	0.9	84.8	b.d.l.
Qz-6 - 8	Core	18.3	18.2	b.d.l.	0.7	91.1	466998	18.6	0.9	84.4	b.d.l.
Qz-6 - 9	Core	17.5	17.0	b.d.l.	0.5	87.1	466998	18.5	0.9	83.2	b.d.l.
Qz-6 - 10	Core	17.1	17.1	b.d.l.	0.6	88.4	466998	15.6	0.9	84.3	b.d.l.
Qz-6 - 11	Core	16.0	16.0	b.d.l.	0.7	87.1	466998	15.1	0.9	82.6	b.d.l.
Qz-6 - 12	Core	16.4	16.0	b.d.l.	0.5	87.2	466998	25.7	0.9	86.6	0.7
Qz-6 - 13	Core	16.4	16.0	b.d.l.	0.6	90.2	466998	17.0	1.0	88.7	b.d.l.
Qz-6 - 14	Core	16.4	15.3	b.d.l.	0.7	88.2	466998	16.8	0.8	87.3	b.d.l.
Qz-6 - 15	Core	15.5	15.2	b.d.l.	0.7	87.7	466998	19.1	0.9	89.7	b.d.l.
Qz-6 - 16	Core	16.3	15.4	b.d.l.	0.7	86.9	466998	16.0	0.9	90.6	b.d.l.
Qz-6 - 17	Core	15.2	14.8	b.d.l.	0.9	89.3	466998	23.1	0.9	95.3	b.d.l.
Qz-6 - 18	Core	15.0	14.8	b.d.l.	0.7	91.2	466998	18.4	0.9	95.9	b.d.l.
Qz-6 - 19	Core	15.3	14.8	b.d.l.	0.8	90.6	466998	19.2	0.8	98.2	b.d.l.
Qz-6 - 20	Core	15.3	15.0	b.d.l.	0.7	91.6	466998	17.1	0.9	98.3	b.d.l.
Qz-6 - 21	Core	16.0	15.2	b.d.l.	0.7	91.2	466998	17.9	0.9	96.1	b.d.l.
Qz-6 - 22	Core	16.7	16.3	b.d.l.	0.6	90.0	466998	18.5	0.9	98.0	b.d.l.
Qz-6 - 23	Core	18.4	18.5	b.d.l.	0.5	90.3	466998	18.8	0.9	98.7	b.d.l.
Qz-6 - 24	Core	20.6	19.7	b.d.l.	0.7	90.7	466998	24.6	0.9	101.0	b.d.l.
Qz-6 - 25	Core	21.1	20.4	b.d.l.	0.9	92.5	466998	15.6	0.9	102.3	b.d.l.
Qz-7 - 1	Rim	18.4	18.1	b.d.l.	0.6	91.5	466998	21.1	0.9	83.5	b.d.l.
Qz-7 - 2	Rim	17.9	17.5	b.d.l.	0.8	92.4	466998	19.5	0.9	88.8	b.d.l.
Qz-7 - 3	Rim	16.4	16.0	b.d.l.	0.7	86.5	466998	19.8	0.9	79.1	b.d.l.
Qz-7 - 4	Core	16.2	15.6	b.d.l.	0.7	87.0	466998	18.7	0.9	80.1	b.d.l.
Qz-7 - 5	Core	14.8	14.4	b.d.l.	0.7	85.5	466998	21.9	0.9	76.6	b.d.l.
Qz-7 - 6	Core	14.9	14.4	b.d.l.	0.9	93.1	466998	16.2	0.9	88.0	b.d.l.
Qz-7 - 7	Core	14.6	14.4	b.d.l.	0.9	95.0	466998	15.8	0.8	94.6	b.d.l.
Qz-7 - 8	Core	14.0	13.8	b.d.l.	0.6	90.8	466998	14.9	0.9	91.6	b.d.l.
Qz-7 - 9	Core	13.9	13.9	b.d.l.	0.9	91.2	466998	17.9	0.9	96.7	0.9
Qz-7 - 10	Core	14.9	14.4	b.d.l.	0.7	92.5	466998	18.6	0.8	100.5	b.d.l.
Qz-7 - 11	Core	15.1	14.8	b.d.l.	0.9	94.8	466998	17.3	0.9	101.3	0.8
Qz-7 - 12	Core	15.6	15.0	b.d.l.	0.8	94.4	466998	14.3	1.0	100.0	0.9
Qz-7 - 13	Core	14.4	14.0	b.d.l.	1.1	100.5	466998	18.6	1.0	104.2	b.d.l.
Qz-7 - 14	Core	14.7	14.4	b.d.l.	0.9	96.3	466998	16.8	0.9	107.6	b.d.l.
Qz-7 - 16	Core	14.7	14.9	b.d.l.	1.2	107.5	466998	13.9	0.9	132.2	b.d.l.
Qz-7 - 17	Core	15.8	15.4	b.d.l.	0.9	106.4	466998	13.5	0.9	133.1	b.d.l.
Qz-7 - 18	Core	16.0	15.3	b.d.l.	1.1	101.9	466998	18.1	0.9	140.8	b.d.l.
Qz-7 - 19	Core	15.5	14.8	b.d.l.	0.8	104.7	466998	18.8	1.0	131.5	1.0
Qz-7 - 20	Core	15.2	14.7	b.d.l.	0.9	101.7	466998	17.9	0.9	124.5	b.d.l.
Qz-7 - 21	Core	14.9	14.9	0.3	0.9	106.2	466998	20.1	0.9	122.5	b.d.l.
Qz-7 - 22	Core	15.8	15.6	b.d.l.	0.7	100.1	466998	18.6	0.9	117.9	b.d.l.
Qz-7 - 23	Core	16.0	15.8	b.d.l.	1.0	108.7	466998	17.6	0.9	124.2	b.d.l.
Qz-7 - 24	Core	16.7	16.9	b.d.l.	1.2	109.5	466998	17.4	1.0	140.2	b.d.l.
Qz-7 - 25	Core	18.6	18.3	b.d.l.	1.2	106.6	466998	15.3	0.8	140.7	b.d.l.
Qz-7 - 26	Core	19.9	19.5	0.3	0.9	108.5	466998	15.7	0.9	134.5	b.d.l.
Qz-7 - 27	Core	20.3	19.5	b.d.l.	1.2	99.6	466998	17.5	0.9	124.4	b.d.l.
Qz-7 - 28	Core	19.2	19.0	b.d.l.	0.9	101.9	466998	21.6	0.9	114.7	b.d.l.
Qz-7 - 29	Core	19.9	19.3	b.d.l.	0.8	104.5	466998	15.8	0.8	109.1	1.0
Qz-7 - 30	Core	19.7	19.4	b.d.l.	0.8	99.5	466998	17.2	0.8	111.5	b.d.l.
Qz-7 - 31	Core	19.3	18.6	b.d.l.	0.8	95.8	466998	20.7	0.8	102.2	b.d.l.
Qz-7 - 32	Core	19.5	19.4	b.d.l.	0.8	97.1	466998	17.0	0.9	100.5	b.d.l.
Qz-7 - 33	Rim	19.9	19.2	b.d.l.	0.9	94.4	466998	17.7	0.9	91.5	b.d.l.
Qz-7 - 34	Rim	18.5	18.2	b.d.l.	0.7	87.7	466998	17.2	0.8	74.9	b.d.l.
Qz-7 - 35	Rim	18.6	18.5	b.d.l.	0.6	86.8	466998	15.0	0.9	76.0	b.d.l.
Qz-7 - 36	Rim	19.8	19.2	b.d.l.	0.7	90.1	466998	20.2	0.9	83.6	b.d.l.
Qz-7 - 37	Rim	19.3	19.1	b.d.l.	0.7	88.0	466998	15.4	0.9	84.2	b.d.l.

Appendix A

Table A1.3: continued

Info	Position	Li ⁶	Li ⁷	Na	Mg	Al	Si	P	Sc	Ti	Ge
Qz-8 - 1	Core	21.1	20.4	b.d.l.	0.6	96.7	466998	19.7	0.8	106.9	1.1
Qz-8 - 2	Core	20.5	20.2	b.d.l.	0.7	95.6	466998	18.0	0.8	105.4	b.d.l.
Qz-8 - 3	Core	18.9	19.0	b.d.l.	0.7	95.5	466998	20.6	0.8	106.0	1.1
Qz-8 - 4	Core	18.0	17.7	b.d.l.	0.8	96.2	466998	17.4	0.9	106.7	b.d.l.
Qz-8 - 5	Core	17.3	17.3	b.d.l.	0.8	98.1	466998	15.2	0.8	109.1	b.d.l.
Qz-8 - 6	Core	17.2	16.9	b.d.l.	0.8	98.2	466998	14.4	0.8	107.1	b.d.l.
Qz-8 - 7	Core	17.7	17.9	b.d.l.	0.8	99.5	466998	15.7	0.8	112.2	1.0
Qz-8 - 8	Core	17.9	17.4	b.d.l.	0.8	99.1	466998	20.1	0.8	109.1	b.d.l.
Qz-8 - 9	Core	16.8	16.5	b.d.l.	0.9	95.9	466998	18.0	0.8	113.8	1.0
Qz-8 - 11	Core	14.9	14.8	0.5	0.8	99.4	466998	15.1	0.8	114.8	1.3
Qz-8 - 24	Core	16.5	16.4	0.3	0.9	97.4	466998	16.3	0.8	102.7	b.d.l.
Qz-8 - 25	Core	16.4	16.2	b.d.l.	0.7	93.9	466998	15.5	0.8	95.2	0.8
Qz-8 - 26	Core	16.6	16.4	b.d.l.	0.8	91.2	466998	17.3	0.8	91.5	b.d.l.
Qz-8 - 27	Core	17.3	16.9	b.d.l.	0.7	90.6	466998	16.9	0.8	92.1	b.d.l.
Qz-8 - 28	Core	18.5	18.5	b.d.l.	0.7	93.6	466998	12.2	0.8	90.7	0.7
Qz-8 - 29	Core	19.0	18.6	b.d.l.	0.6	88.7	466998	15.2	0.8	84.3	b.d.l.
Qz-8 - 30	Rim	19.7	18.9	b.d.l.	0.7	88.1	466998	12.7	0.8	85.5	b.d.l.
Qz-8 - 31	Rim	19.9	19.6	b.d.l.	0.7	89.7	466998	16.5	0.9	91.1	b.d.l.
Qz-8 - 32	Rim	19.5	19.4	b.d.l.	0.7	88.0	466998	17.4	0.8	90.0	b.d.l.
Qz-8 - 33	Rim	20.6	20.1	b.d.l.	0.6	90.9	466998	15.1	0.8	88.6	1.0
Qz-9 - 1	Rim	20.4	20.4	b.d.l.	0.8	92.5	466998	12.4	0.8	70.5	b.d.l.
Qz-9 - 2	Rim	19.7	18.9	b.d.l.	0.7	84.1	466998	11.2	0.8	66.2	b.d.l.
Qz-9 - 3	Rim	19.4	18.9	b.d.l.	0.5	84.3	466998	17.6	0.8	67.1	b.d.l.
Qz-9 - 4	Rim	20.8	20.8	b.d.l.	0.6	94.4	466998	10.8	0.8	69.1	b.d.l.
Qz-9 - 5	Rim	20.4	19.5	b.d.l.	0.6	88.6	466998	13.3	0.8	68.9	0.8
Qz-9 - 6	Rim	19.5	19.4	b.d.l.	0.7	87.1	466998	16.3	0.9	71.8	b.d.l.
Qz-9 - 7	Rim	20.0	19.8	b.d.l.	0.6	89.8	466998	13.9	0.8	77.5	b.d.l.
Qz-9 - 8	Rim	20.8	20.5	b.d.l.	0.8	94.4	466998	14.7	0.8	106.6	0.9
Qz-9 - 9	Core	21.0	20.8	b.d.l.	0.9	96.2	466998	17.6	0.8	114.9	b.d.l.
Qz-9 - 10	Core	21.1	20.5	b.d.l.	0.9	96.2	466998	14.6	0.8	115.7	b.d.l.
Qz-9 - 11	Core	21.3	20.5	b.d.l.	0.8	97.9	466998	13.6	0.8	118.2	b.d.l.
Qz-9 - 12	Core	20.2	20.1	b.d.l.	0.7	98.0	466998	17.1	0.8	124.2	b.d.l.
Qz-9 - 13	Core	20.3	19.8	b.d.l.	0.7	98.1	466998	12.5	0.8	119.6	b.d.l.
Qz-9 - 14	Core	19.2	18.5	b.d.l.	1.1	96.6	466998	13.8	0.8	115.7	b.d.l.
Qz-9 - 15	Core	18.1	17.6	b.d.l.	1.0	95.6	466998	14.0	0.7	113.9	b.d.l.
Qz-9 - 16	Core	18.3	17.7	b.d.l.	1.1	95.9	466998	11.9	0.8	114.4	0.8
Qz-9 - 17	Core	18.1	17.8	b.d.l.	1.1	94.9	466998	14.5	0.8	117.9	b.d.l.
Qz-9 - 18	Core	18.4	17.7	b.d.l.	1.1	102.3	466998	17.1	0.8	131.4	b.d.l.
Qz-9 - 19	Core	17.9	17.0	b.d.l.	0.8	94.7	466998	13.8	0.9	129.7	b.d.l.
Qz-9 - 20	Core	17.3	16.6	b.d.l.	0.7	103.3	466998	17.1	0.8	132.4	0.9
Qz-9 - 21	Core	17.0	16.6	b.d.l.	0.8	97.7	466998	15.6	0.8	132.7	b.d.l.
Qz-9 - 22	Core	17.1	17.0	b.d.l.	1.0	100.3	466998	16.8	0.8	119.9	1.0
Qz-9 - 23	Core	17.0	17.0	b.d.l.	1.3	110.1	466998	11.2	0.9	135.1	b.d.l.
Qz-9 - 24	Core	16.6	16.2	b.d.l.	1.0	101.7	466998	20.8	0.8	128.5	b.d.l.
Qz-9 - 25	Core	17.9	16.7	0.6	1.6	107.8	466998	16.0	0.9	130.5	b.d.l.
Qz-9 - 26	Core	19.0	18.4	b.d.l.	1.6	107.1	466998	14.7	0.9	125.7	b.d.l.
Qz-9 - 27	Core	17.1	16.9	b.d.l.	1.1	104.0	466998	17.7	0.9	120.1	b.d.l.
Qz-9 - 28	Core	16.5	16.3	b.d.l.	0.9	96.7	466998	13.3	0.9	123.4	b.d.l.
Qz-9 - 29	Core	16.0	15.8	b.d.l.	0.8	97.6	466998	19.5	0.9	122.1	b.d.l.
Qz-9 - 30	Core	15.8	15.5	b.d.l.	1.0	99.0	466998	b.d.l.	0.8	118.9	b.d.l.
Qz-9 - 31	Rim	16.9	17.3	b.d.l.	1.1	96.8	466998	b.d.l.	0.8	117.0	b.d.l.
Qz-9 - 32	Rim	17.3	17.0	b.d.l.	1.1	94.3	466998	11.1	0.8	87.4	b.d.l.
Qz-9 - 33	Rim	17.3	16.9	b.d.l.	0.9	92.8	466998	10.7	0.8	84.6	b.d.l.
Qz-9 - 34	Rim	16.3	16.1	b.d.l.	0.7	87.1	466998	12.0	0.8	79.6	b.d.l.
Qz-9 - 35	Rim	15.7	15.7	b.d.l.	0.6	82.0	466998	10.9	0.8	74.7	b.d.l.
Qz-10 - 1	Rim	20.7	20.4	b.d.l.	0.8	93.3	466998	11.1	0.8	87.3	b.d.l.
Qz-10 - 2	Rim	21.0	20.6	b.d.l.	0.8	93.5	466998	14.7	0.7	90.1	b.d.l.
Qz-10 - 3	Rim	20.3	19.8	b.d.l.	0.7	91.5	466998	15.0	0.7	89.7	b.d.l.
Qz-10 - 4	Rim	20.9	20.3	b.d.l.	0.7	95.4	466998	14.6	0.8	95.5	b.d.l.
Qz-10 - 5	Rim	20.2	20.1	b.d.l.	0.8	93.7	466998	14.2	0.7	91.9	1.1
Qz-10 - 6	Core	19.8	19.5	b.d.l.	0.7	92.3	466998	16.5	0.8	83.7	b.d.l.
Qz-10 - 7	Core	18.9	18.5	b.d.l.	0.7	88.9	466998	14.9	0.8	84.7	b.d.l.
Qz-10 - 8	Core	18.7	18.4	b.d.l.	1.0	90.4	466998	12.6	0.8	84.2	b.d.l.
Qz-10 - 9	Core	18.5	18.5	b.d.l.	0.6	91.4	466998	10.1	0.8	79.4	b.d.l.
Qz-10 - 10	Core	19.2	18.2	b.d.l.	0.7	91.7	466998	13.8	0.8	77.1	b.d.l.
Qz-10 - 11	Core	18.2	17.9	b.d.l.	0.7	91.7	466998	14.8	0.8	81.0	b.d.l.
Qz-10 - 12	Core	17.9	17.8	b.d.l.	1.1	92.3	466998	12.9	0.8	82.2	b.d.l.
Qz-10 - 13	Core	18.2	17.8	b.d.l.	0.8	94.6	466998	14.9	0.8	85.9	b.d.l.
Qz-10 - 14	Core	17.7	17.5	b.d.l.	0.7	92.7	466998	16.0	0.8	86.5	b.d.l.
Qz-10 - 15	Core	17.9	17.0	b.d.l.	0.7	93.2	466998	19.5	0.8	86.0	b.d.l.
Qz-10 - 16	Core	17.1	16.7	b.d.l.	0.7	91.8	466998	17.3	0.8	84.2	0.8
Qz-10 - 17	Core	16.6	16.3	b.d.l.	0.8	90.0	466998	12.1	0.8	85.3	b.d.l.
Qz-10 - 18	Core	16.7	16.2	b.d.l.	0.7	91.4	466998	16.6	0.8	86.6	b.d.l.
Qz-10 - 19	Core	16.9	16.2	b.d.l.	0.6	91.5	466998	16.4	0.8	84.1	b.d.l.
Qz-10 - 20	Core	17.0	16.0	b.d.l.	0.9	91.3	466998	16.5	0.7	85.5	b.d.l.
Qz-10 - 21	Core	16.8	16.1	b.d.l.	0.8	90.7	466998	11.3	0.8	85.0	b.d.l.
Qz-10 - 22	Core	16.3	16.2	b.d.l.	0.8	89.7	466998	15.9	0.8	86.7	b.d.l.
Qz-10 - 23	Core	16.5	16.1	b.d.l.	0.7	89.1	466998	15.2	0.7	83.7	1.1
Qz-10 - 24	Core	16.9	16.3	b.d.l.	0.4	89.8	466998	16.4	0.7	83.1	b.d.l.
Qz-10 - 25	Core	16.8	17.1	b.d.l.	0.9	90.0	466998	12.0	0.7	84.6	b.d.l.
Qz-10 - 26	Core	18.0	17.7	b.d.l.	0.8	91.2	466998	13.7	0.7	83.6	b.d.l.

Table A1.3: continued

Info	Position	Li ^e	Li ⁱ	Na	Mg	Al	Si	P	Sc	Ti	Ge
Qz-13 - 1	Rim	21.1	20.7	b.d.l.	0.7	95.9	466998	9.4	0.8	92.3	1.1
Qz-13 - 2	Rim	20.2	19.8	b.d.l.	0.7	90.2	466998	15.2	0.8	81.0	b.d.l.
Qz-13 - 3	Core	20.1	19.4	b.d.l.	0.7	88.4	466998	14.9	0.8	79.3	b.d.l.
Qz-13 - 4	Core	20.3	19.6	b.d.l.	0.7	90.2	466998	14.1	0.7	88.9	b.d.l.
Qz-13 - 5	Core	19.8	19.5	b.d.l.	0.5	90.3	466998	11.4	0.8	89.0	0.9
Qz-13 - 6	Core	20.1	19.5	b.d.l.	1.1	92.0	466998	12.8	0.8	87.2	b.d.l.
Qz-13 - 7	Core	19.8	19.4	b.d.l.	0.9	94.1	466998	12.5	0.8	92.4	b.d.l.
Qz-13 - 8	Core	18.8	18.6	b.d.l.	0.7	90.1	466998	10.1	0.8	90.1	b.d.l.
Qz-13 - 9	Core	19.0	18.5	b.d.l.	0.6	89.8	466998	10.3	0.7	90.8	1.0
Qz-13 - 10	Core	18.2	17.9	b.d.l.	0.7	89.4	466998	14.4	0.8	89.6	0.8
Qz-13 - 11	Core	17.1	17.1	b.d.l.	0.6	89.9	466998	11.6	0.7	95.3	b.d.l.
Qz-13 - 12	Core	17.3	16.9	b.d.l.	0.7	90.9	466998	14.5	0.7	96.1	b.d.l.
Qz-13 - 13	Core	18.0	17.8	b.d.l.	0.6	90.3	466998	13.8	0.8	89.5	b.d.l.
Qz-13 - 14	Core	18.7	18.3	b.d.l.	0.8	89.4	466998	13.7	0.8	92.6	b.d.l.
Qz-13 - 15	Core	18.9	18.5	b.d.l.	0.6	89.4	466998	10.7	0.8	89.6	b.d.l.
Qz-13 - 16	Core	19.7	18.7	b.d.l.	0.8	88.4	466998	14.4	0.8	89.3	1.0
Qz-13 - 17	Core	20.0	19.5	b.d.l.	0.6	91.9	466998	15.7	0.8	91.4	b.d.l.
Qz-13 - 18	Core	19.8	19.2	b.d.l.	0.5	90.1	466998	10.7	0.8	92.9	b.d.l.
Qz-13 - 19	Core	19.3	19.2	b.d.l.	0.8	88.8	466998	b.d.l.	0.7	86.2	b.d.l.
Qz-13 - 20	Core	20.7	19.9	b.d.l.	0.7	91.3	466998	13.2	0.8	91.8	0.9
Qz-14 - 1	Rim	18.9	18.1	b.d.l.	0.5	83.5	466998	14.8	0.7	73.5	0.9
Qz-14 - 2	Rim	18.3	18.2	b.d.l.	0.7	87.0	466998	13.9	0.8	74.4	1.2
Qz-14 - 3	Rim	17.8	17.0	b.d.l.	0.6	83.9	466998	9.8	0.7	70.9	1.0
Qz-14 - 4	Rim	17.9	17.4	b.d.l.	0.4	87.2	466998	9.9	0.8	79.8	b.d.l.
Qz-14 - 5	Core	18.2	17.7	b.d.l.	0.7	90.1	466998	10.8	0.8	88.7	b.d.l.
Qz-14 - 6	Core	17.7	17.5	b.d.l.	0.8	89.3	466998	11.7	0.7	90.5	0.8
Qz-14 - 7	Core	18.1	17.6	b.d.l.	0.6	90.4	466998	8.7	0.8	94.1	b.d.l.
Qz-14 - 8	Core	17.0	16.6	b.d.l.	0.7	88.6	466998	10.3	0.8	84.4	b.d.l.
Qz-14 - 9	Core	16.5	16.2	b.d.l.	0.8	88.7	466998	11.7	0.7	82.5	b.d.l.
Qz-14 - 10	Core	16.6	16.3	b.d.l.	0.6	88.2	466998	11.1	0.7	85.1	b.d.l.
Qz-14 - 11	Core	16.7	16.4	b.d.l.	0.7	92.7	466998	b.d.l.	0.8	102.7	b.d.l.
Qz-14 - 12	Core	17.2	16.3	b.d.l.	1.0	96.6	466998	b.d.l.	0.8	104.1	b.d.l.
Qz-14 - 13	Core	17.0	16.5	b.d.l.	0.5	94.8	466998	9.6	0.8	102.2	b.d.l.
Qz-14 - 14	Core	17.2	16.5	b.d.l.	0.8	96.0	466998	14.2	0.7	105.6	b.d.l.
Qz-14 - 15	Core	16.6	16.5	b.d.l.	0.7	97.8	466998	12.3	0.7	109.3	b.d.l.
Qz-14 - 16	Core	16.9	16.4	b.d.l.	0.7	97.7	466998	11.2	0.8	106.8	1.1
Qz-14 - 17	Core	15.6	15.9	b.d.l.	0.7	95.5	466998	10.6	0.8	104.7	1.0
Qz-14 - 19	Core	15.8	15.5	0.4	0.9	92.1	466998	12.3	0.8	103.1	b.d.l.
Qz-14 - 20	Core	15.0	15.0	b.d.l.	0.7	93.6	466998	10.1	0.8	97.7	b.d.l.
Qz-14 - 22	Core	15.6	14.9	0.4	0.8	91.4	466998	17.3	0.8	96.7	b.d.l.
Qz-14 - 23	Core	15.4	15.2	b.d.l.	0.7	96.5	466998	b.d.l.	0.8	107.0	b.d.l.
Qz-14 - 24	Core	14.5	14.2	b.d.l.	0.8	93.7	466998	14.9	0.8	95.0	b.d.l.
Qz-14 - 25	Core	14.1	14.1	b.d.l.	0.9	96.0	466998	14.4	0.8	97.3	b.d.l.
Qz-14 - 26	Core	15.4	15.0	b.d.l.	0.8	95.8	466998	11.8	0.8	101.3	b.d.l.
Qz-14 - 27	Core	15.7	14.9	b.d.l.	1.1	93.8	466998	15.3	0.8	96.3	b.d.l.
Qz-14 - 28	Core	16.0	16.0	b.d.l.	1.0	92.4	466998	12.7	0.8	96.1	b.d.l.
Qz-14 - 29	Core	16.4	15.8	b.d.l.	0.7	90.6	466998	b.d.l.	0.8	92.2	0.9
Qz-14 - 30	Core	16.4	16.5	b.d.l.	0.8	92.3	466998	12.7	0.8	93.7	b.d.l.
Qz-14 - 31	Core	16.7	16.4	0.4	0.6	92.3	466998	14.1	0.7	94.8	b.d.l.
Qz-14 - 32	Core	16.8	16.4	b.d.l.	0.7	88.4	466998	10.5	0.7	88.6	b.d.l.
Qz-14 - 33	Core	18.1	17.2	b.d.l.	0.7	90.8	466998	9.7	0.8	84.8	b.d.l.
Qz-14 - 34	Rim	18.1	17.4	b.d.l.	0.7	89.9	466998	9.0	0.8	81.2	b.d.l.
Qz-14 - 35	Rim	17.8	17.4	b.d.l.	0.8	86.6	466998	15.0	0.8	78.5	b.d.l.
Qz-14 - 36	Rim	18.1	17.5	b.d.l.	0.5	84.2	466998	15.5	0.8	71.4	b.d.l.
Qz-15 - 1	Rim	19.7	19.7	b.d.l.	0.4	87.5	466998	b.d.l.	0.8	87.3	b.d.l.
Qz-15 - 2	Rim	19.0	18.2	b.d.l.	0.6	82.0	466998	11.8	0.7	73.6	0.9
Qz-15 - 3	Rim	18.1	18.1	b.d.l.	0.8	81.7	466998	b.d.l.	0.7	74.9	b.d.l.
Qz-15 - 4	Core	19.8	19.5	b.d.l.	0.5	89.3	466998	10.6	0.8	83.6	b.d.l.
Qz-15 - 5	Core	18.2	18.6	b.d.l.	0.8	87.5	466998	13.5	0.8	78.1	1.1
Qz-15 - 6	Core	18.2	17.7	b.d.l.	0.6	84.7	466998	b.d.l.	0.7	77.0	0.8
Qz-15 - 7	Core	17.4	17.0	b.d.l.	0.6	84.2	466998	15.8	0.8	75.0	b.d.l.
Qz-15 - 8	Core	16.9	16.7	b.d.l.	0.5	83.9	466998	10.3	0.8	76.1	b.d.l.
Qz-15 - 9	Core	16.7	16.6	b.d.l.	0.6	85.1	466998	8.9	0.8	78.8	b.d.l.
Qz-15 - 10	Core	17.2	16.5	b.d.l.	0.6	88.0	466998	12.8	0.8	80.0	b.d.l.
Qz-15 - 11	Core	16.2	16.1	b.d.l.	0.5	87.6	466998	12.5	0.8	83.9	b.d.l.
Qz-15 - 12	Core	16.1	15.7	b.d.l.	0.7	88.1	466998	11.6	0.8	92.2	1.0
Qz-15 - 13	Core	15.9	15.7	b.d.l.	0.6	90.5	466998	13.8	0.7	107.6	b.d.l.
Qz-15 - 14	Core	15.9	15.7	b.d.l.	0.6	91.7	466998	12.7	0.8	107.9	0.8
Qz-15 - 15	Core	16.0	15.5	b.d.l.	0.6	90.9	466998	10.3	0.9	109.8	b.d.l.
Qz-15 - 16	Core	15.6	15.1	b.d.l.	0.8	90.6	466998	9.0	0.8	110.6	b.d.l.
Qz-15 - 17	Core	14.7	14.5	b.d.l.	0.7	91.4	466998	11.0	0.8	109.7	b.d.l.
Qz-15 - 18	Core	15.4	14.7	b.d.l.	0.7	89.8	466998	13.0	0.8	107.9	0.9
Qz-15 - 19	Core	15.3	14.8	b.d.l.	0.7	89.6	466998	14.9	0.8	109.3	b.d.l.
Qz-15 - 20	Core	15.7	15.4	b.d.l.	0.7	91.8	466998	10.9	0.8	112.6	b.d.l.
Qz-15 - 21	Core	15.2	15.3	b.d.l.	0.7	91.2	466998	12.8	0.7	108.9	b.d.l.
Qz-15 - 22	Core	16.5	16.5	b.d.l.	0.7	92.5	466998	13.4	0.7	110.6	b.d.l.
Qz-15 - 23	Core	17.5	17.0	b.d.l.	0.6	92.6	466998	b.d.l.	0.8	109.2	b.d.l.
Qz-15 - 24	Core	18.0	17.8	b.d.l.	0.6	92.6	466998	9.2	0.8	107.0	b.d.l.
Qz-15 - 25	Core	19.1	18.9	b.d.l.	0.7	92.2	466998	13.9	0.7	98.7	b.d.l.
Qz-15 - 26	Core	19.3	19.1	b.d.l.	0.6	90.3	466998	10.9	0.7	89.8	b.d.l.
Qz-15 - 27	Core	19.9	19.4	b.d.l.	0.6	89.1	466998	14.7	0.8	90.7	b.d.l.

Appendix A

Table A1.3: continued

Info	Position	Li ⁶	Li ⁷	Na	Mg	Al	Si	P	Sc	Ti	Ge
Qz-16-1	Rim	17.7	17.2	b.d.l.	0.7	91.0	466998	11.1	0.8	98.8	b.d.l.
Qz-16-2	Rim	16.7	16.1	b.d.l.	0.7	90.9	466998	13.9	0.8	100.6	b.d.l.
Qz-16-3	Rim	16.2	15.8	b.d.l.	0.7	89.9	466998	12.0	0.8	104.3	b.d.l.
Qz-16-4	Rim	16.3	16.2	b.d.l.	0.8	91.6	466998	10.5	0.8	103.8	b.d.l.
Qz-16-5	Rim	16.0	16.1	b.d.l.	0.8	95.6	466998	12.4	0.8	108.7	b.d.l.
Qz-16-6	Core	15.7	15.4	b.d.l.	0.7	94.4	466998	8.9	0.7	110.5	0.9
Qz-16-13	Core	14.0	14.2	b.d.l.	0.8	95.6	466998	11.3	0.8	109.9	b.d.l.
Qz-16-14	Core	14.4	14.1	b.d.l.	0.7	94.7	466998	11.2	0.8	120.2	b.d.l.
Qz-16-15	Core	14.1	13.7	b.d.l.	0.5	92.6	466998	8.9	0.8	115.6	b.d.l.
Qz-16-16	Core	14.0	13.6	b.d.l.	0.6	92.3	466998	9.5	0.8	106.6	b.d.l.
Qz-16-17	Core	14.4	14.0	b.d.l.	0.8	94.1	466998	12.3	0.8	112.7	b.d.l.
Qz-16-18	Core	16.1	15.5	b.d.l.	0.8	98.9	466998	9.5	0.8	125.7	b.d.l.
Qz-16-19	Core	16.2	15.4	b.d.l.	1.0	104.5	466998	12.3	0.8	155.1	b.d.l.
Qz-16-20	Core	16.8	16.6	b.d.l.	0.8	106.5	466998	b.d.l.	0.7	142.4	b.d.l.
Qz-16-21	Core	16.6	16.4	b.d.l.	0.8	105.0	466998	10.2	0.8	147.0	b.d.l.
Qz-16-22	Core	17.2	16.6	b.d.l.	0.8	105.5	466998	9.1	0.8	144.1	1.1
Qz-16-23	Core	16.8	16.3	b.d.l.	0.9	100.7	466998	11.7	0.8	116.6	b.d.l.
Qz-16-24	Core	17.4	16.9	b.d.l.	0.6	99.0	466998	10.6	0.8	124.1	1.0
Qz-16-25	Core	17.8	17.0	b.d.l.	0.9	96.8	466998	12.2	0.7	108.4	b.d.l.
Qz-16-26	Core	18.0	17.8	b.d.l.	0.7	98.4	466998	11.8	0.7	102.3	b.d.l.
Qz-17-1	Rim	19.6	19.1	b.d.l.	0.7	91.8	466998	13.9	0.7	91.4	b.d.l.
Qz-17-2	Rim	19.4	18.7	b.d.l.	0.7	91.8	466998	14.6	0.8	92.5	b.d.l.
Qz-17-3	Rim	17.0	16.6	b.d.l.	0.7	82.8	466998	b.d.l.	0.8	71.8	0.9
Qz-17-4	Core	16.1	16.2	b.d.l.	0.6	82.6	466998	14.6	0.7	74.6	b.d.l.
Qz-17-5	Core	17.7	17.2	b.d.l.	0.7	88.1	466998	12.9	0.8	84.9	1.0
Qz-17-6	Core	16.7	16.3	b.d.l.	0.6	86.2	466998	13.0	0.8	80.8	b.d.l.
Qz-17-7	Core	16.8	16.6	b.d.l.	0.9	90.2	466998	10.1	0.8	91.3	b.d.l.
Qz-17-8	Core	17.2	16.4	b.d.l.	0.7	90.7	466998	12.8	0.8	87.0	b.d.l.
Qz-17-9	Core	17.1	16.3	b.d.l.	0.8	89.4	466998	10.2	0.8	83.0	1.1
Qz-17-10	Core	16.6	15.5	b.d.l.	0.6	88.1	466998	11.9	0.8	83.2	b.d.l.
Qz-17-11	Core	15.1	15.2	b.d.l.	0.7	86.5	466998	12.1	0.7	80.4	b.d.l.
Qz-17-12	Core	16.0	15.5	b.d.l.	0.8	89.1	466998	b.d.l.	0.8	91.8	0.9
Qz-17-13	Core	16.2	15.7	0.3	0.9	93.4	466998	11.6	0.8	102.7	b.d.l.
Qz-17-14	Core	16.1	15.5	b.d.l.	0.9	92.1	466998	13.0	0.8	98.2	0.9
Qz-17-15	Core	15.9	15.5	b.d.l.	0.8	91.5	466998	10.7	0.7	102.0	b.d.l.
Qz-17-16	Core	16.2	15.5	b.d.l.	1.2	93.1	466998	18.5	0.7	108.5	b.d.l.
Qz-17-18	Core	16.3	15.7	b.d.l.	1.0	99.4	466998	11.9	0.7	116.6	b.d.l.
Qz-17-19	Core	16.8	16.7	b.d.l.	1.0	97.4	466998	b.d.l.	0.8	120.3	b.d.l.
Qz-17-20	Core	16.9	16.8	b.d.l.	1.2	104.7	466998	b.d.l.	0.8	120.2	b.d.l.
Qz-17-22	Core	16.1	16.2	0.8	0.9	98.3	466998	14.1	0.7	120.0	b.d.l.
Qz-17-23	Core	16.9	16.4	b.d.l.	0.8	99.0	466998	9.6	0.8	116.1	b.d.l.
Qz-17-24	Core	17.1	16.5	b.d.l.	0.8	95.9	466998	12.9	0.8	109.8	b.d.l.
Qz-17-25	Core	16.1	15.4	b.d.l.	0.8	92.7	466998	14.4	0.8	102.8	b.d.l.
Qz-17-26	Core	16.7	16.3	b.d.l.	0.7	92.0	466998	13.9	0.8	108.5	b.d.l.
Qz-17-27	Core	16.4	16.1	b.d.l.	0.9	92.7	466998	b.d.l.	0.8	101.7	b.d.l.
Qz-17-28	Core	16.2	15.8	b.d.l.	0.6	87.6	466998	13.1	0.7	95.2	b.d.l.
Qz-17-29	Core	16.2	15.6	b.d.l.	0.6	87.1	466998	b.d.l.	0.7	87.5	b.d.l.
Qz-17-30	Core	16.9	16.3	b.d.l.	0.7	85.2	466998	12.1	0.8	87.0	0.8
Qz-17-31	Core	16.6	16.2	0.6	0.9	85.3	466998	9.5	0.7	83.4	b.d.l.
Qz-17-32	Core	18.5	18.1	b.d.l.	0.8	90.5	466998	10.9	0.8	83.0	b.d.l.
Qz-17-33	Core	18.2	17.9	b.d.l.	0.7	91.7	466998	b.d.l.	0.7	80.0	b.d.l.
Qz-17-34	Core	17.6	17.4	b.d.l.	0.6	86.9	466998	12.7	0.7	74.8	b.d.l.
Qz-17-35	Rim	17.8	17.5	b.d.l.	0.7	84.4	466998	11.3	0.7	68.2	0.9
Qz-17-36	Rim	18.2	17.4	b.d.l.	0.8	82.5	466998	13.3	0.7	74.3	0.8
Qz-19-1	Rim	18.9	18.2	b.d.l.	0.7	87.0	466998	11.2	0.7	78.0	b.d.l.
Qz-19-2	Rim	19.1	18.7	b.d.l.	0.8	89.6	466998	11.7	0.7	75.5	0.8
Qz-19-3	Rim	17.0	16.3	b.d.l.	0.7	82.5	466998	14.1	0.8	72.7	1.1
Qz-19-4	Rim	17.6	17.2	b.d.l.	0.6	87.8	466998	b.d.l.	0.7	73.5	b.d.l.
Qz-19-5	Rim	17.9	17.4	b.d.l.	0.6	89.5	466998	11.7	0.7	77.7	b.d.l.
Qz-19-6	Core	18.1	17.2	b.d.l.	0.8	91.5	466998	9.0	0.8	87.5	1.1
Qz-19-7	Core	19.9	19.2	b.d.l.	1.0	103.2	466998	9.5	0.8	117.6	b.d.l.
Qz-19-8	Core	19.5	18.4	b.d.l.	0.7	98.7	466998	9.8	0.7	114.9	b.d.l.
Qz-19-9	Core	18.2	17.9	b.d.l.	0.7	98.0	466998	10.1	0.7	114.4	b.d.l.
Qz-19-10	Core	18.0	17.5	b.d.l.	0.8	98.4	466998	8.5	0.7	115.2	b.d.l.
Qz-19-11	Core	18.6	17.8	b.d.l.	0.9	98.8	466998	10.8	0.7	120.3	b.d.l.
Qz-19-12	Core	18.8	18.5	b.d.l.	0.9	99.7	466998	12.1	0.8	122.6	b.d.l.
Qz-19-13	Core	18.1	17.9	b.d.l.	0.8	96.7	466998	12.0	0.8	127.1	b.d.l.
Qz-19-14	Core	18.2	17.9	b.d.l.	1.1	100.2	466998	8.3	0.8	126.9	b.d.l.
Qz-19-15	Core	18.5	17.9	b.d.l.	1.0	107.3	466998	10.2	0.8	139.9	b.d.l.
Qz-19-16	Core	19.2	17.7	b.d.l.	1.0	104.9	466998	13.1	0.7	147.1	b.d.l.
Qz-19-17	Core	18.5	17.8	0.4	1.0	103.3	466998	11.7	0.7	139.4	b.d.l.
Qz-19-18	Core	18.0	17.4	b.d.l.	0.9	100.3	466998	12.3	0.8	126.1	b.d.l.
Qz-19-19	Core	18.1	18.3	b.d.l.	0.8	101.1	466998	10.3	0.8	121.5	b.d.l.
Qz-19-20	Core	19.1	18.6	b.d.l.	0.7	100.7	466998	14.6	0.7	120.6	b.d.l.
Qz-19-21	Core	19.7	19.1	b.d.l.	0.9	101.4	466998	10.2	0.7	120.9	b.d.l.
Qz-19-22	Core	20.2	19.6	b.d.l.	0.8	101.3	466998	12.3	0.8	117.6	b.d.l.
Qz-19-23	Core	21.7	20.5	b.d.l.	0.8	101.2	466998	12.7	0.8	117.8	b.d.l.
Qz-19-24	Core	20.7	20.4	b.d.l.	0.9	99.0	466998	11.2	0.7	115.3	b.d.l.
Qz-19-25	Core	21.6	21.1	b.d.l.	0.8	100.7	466998	9.1	0.8	117.3	b.d.l.
Qz-19-26	Core	21.9	21.7	b.d.l.	1.0	101.7	466998	10.9	0.8	120.0	b.d.l.
Qz-19-27	Core	22.7	22.4	0.3	1.0	101.1	466998	12.7	0.7	120.9	b.d.l.
Qz-19-28	Rim	22.4	22.0	b.d.l.	0.8	103.4	466998	10.6	0.8	118.3	b.d.l.
Qz-19-29	Rim	22.3	21.7	b.d.l.	0.9	96.7	466998	14.6	0.8	104.4	b.d.l.
Qz-19-30	Rim	20.4	20.1	b.d.l.	0.7	90.6	466998	13.9	0.7	75.7	b.d.l.
Qz-19-31	Rim	20.8	20.3	b.d.l.	0.7	90.0	466998	b.d.l.	0.7	74.4	0.9
Qz-19-32	Rim	20.5	19.8	b.d.l.	0.6	86.9	466998	10.2	0.8	70.7	b.d.l.

Table A1.3: continued

Info	Position	Li ⁶	Li ⁷	Na	Mg	Al	Si	P	Sc	Ti	Ge
Qz-20 - 1	Rim	22.0	21.6	b.d.l.	0.9	97.3	466998	9.5	0.8	86.3	b.d.l.
Qz-20 - 2	Rim	21.8	21.2	b.d.l.	0.5	93.2	466998	11.0	0.7	80.2	b.d.l.
Qz-20 - 3	Core	20.1	19.9	b.d.l.	0.6	86.7	466998	9.9	0.8	74.0	1.0
Qz-20 - 4	Core	19.1	18.7	b.d.l.	0.7	83.5	466998	b.d.l.	0.7	73.1	1.0
Qz-20 - 5	Core	20.7	20.0	b.d.l.	0.8	89.0	466998	b.d.l.	0.8	81.9	b.d.l.
Qz-20 - 6	Core	20.8	20.7	b.d.l.	0.7	92.1	466998	12.2	0.8	88.5	b.d.l.
Qz-20 - 7	Core	21.0	20.6	b.d.l.	0.8	92.6	466998	11.2	0.8	93.2	0.8
Qz-20 - 8	Core	20.0	19.6	b.d.l.	0.6	88.7	466998	9.9	0.7	95.5	b.d.l.
Qz-20 - 9	Core	20.0	19.6	b.d.l.	0.7	92.3	466998	11.6	0.7	100.4	b.d.l.
Qz-20 - 10	Core	20.0	19.4	b.d.l.	0.8	93.1	466998	b.d.l.	0.8	101.4	b.d.l.
Qz-20 - 11	Core	19.7	18.9	b.d.l.	0.6	93.9	466998	9.8	0.8	105.1	b.d.l.
Qz-20 - 12	Core	18.9	18.5	b.d.l.	0.8	91.9	466998	8.4	0.8	90.4	b.d.l.
Qz-20 - 13	Core	18.8	18.2	b.d.l.	0.8	93.5	466998	11.7	0.7	95.3	b.d.l.
Qz-20 - 14	Core	19.0	17.8	b.d.l.	0.7	93.6	466998	13.2	0.8	102.5	b.d.l.
Qz-20 - 15	Core	17.5	17.0	b.d.l.	0.7	90.3	466998	11.0	0.8	97.0	b.d.l.
Qz-20 - 16	Core	17.2	16.4	b.d.l.	0.7	88.5	466998	8.8	0.7	93.6	1.0
Qz-20 - 17	Core	16.4	16.1	b.d.l.	0.7	88.1	466998	b.d.l.	0.7	95.0	b.d.l.
Qz-20 - 18	Core	15.8	15.7	b.d.l.	0.8	87.6	466998	13.6	0.8	97.3	0.9
Qz-20 - 19	Core	16.1	16.1	b.d.l.	0.8	89.9	466998	8.7	0.8	103.1	b.d.l.
Qz-20 - 20	Core	17.0	16.6	b.d.l.	0.8	91.6	466998	8.7	0.7	105.8	b.d.l.
Qz-20 - 21	Core	18.0	16.9	b.d.l.	0.9	95.3	466998	13.2	0.9	106.3	b.d.l.
Qz-20 - 22	Core	16.1	15.8	b.d.l.	0.8	93.4	466998	13.7	0.8	104.1	b.d.l.
Qz-20 - 27	Core	16.4	16.1	b.d.l.	0.9	90.4	466998	14.7	0.9	107.6	b.d.l.
Qz-20 - 28	Core	16.5	15.7	b.d.l.	0.8	92.3	466998	10.3	0.8	107.3	b.d.l.
Qz-20 - 29	Core	15.6	15.8	b.d.l.	0.7	95.5	466998	b.d.l.	0.7	111.7	1.2
Qz-20 - 30	Core	16.2	15.6	b.d.l.	0.8	92.2	466998	11.7	0.7	104.3	b.d.l.
Qz-20 - 31	Core	17.3	16.7	b.d.l.	0.9	94.4	466998	11.3	0.8	107.2	b.d.l.
Qz-21 - 1	Rim	16.4	16.6	b.d.l.	0.5	76.5	466998	11.7	0.7	65.7	b.d.l.
Qz-21 - 2	Core	19.2	18.5	0.2	0.6	88.9	466998	9.6	0.8	74.3	0.9
Qz-21 - 3	Core	18.5	18.1	b.d.l.	0.6	88.9	466998	10.8	0.8	81.1	b.d.l.
Qz-21 - 4	Core	17.9	17.3	b.d.l.	0.6	87.0	466998	11.2	0.7	77.8	b.d.l.
Qz-21 - 5	Core	17.2	17.2	b.d.l.	0.6	87.2	466998	9.2	0.9	85.1	b.d.l.
Qz-21 - 6	Core	17.6	17.4	b.d.l.	0.7	88.7	466998	b.d.l.	0.8	85.2	b.d.l.
Qz-21 - 7	Core	18.0	17.3	b.d.l.	0.6	90.5	466998	12.1	0.9	91.2	b.d.l.
Qz-21 - 8	Core	15.9	15.8	b.d.l.	0.8	90.6	466998	10.3	0.7	92.4	b.d.l.
Qz-21 - 9	Core	16.8	15.9	b.d.l.	0.7	86.1	466998	10.8	0.8	96.8	b.d.l.
Qz-21 - 10	Core	15.9	15.4	b.d.l.	0.6	87.0	466998	11.0	0.8	98.1	b.d.l.
Qz-21 - 11	Core	15.7	15.4	b.d.l.	0.8	92.8	466998	10.4	0.8	104.1	b.d.l.
Qz-21 - 12	Core	15.2	15.0	b.d.l.	0.8	98.3	466998	10.5	0.8	107.3	0.9
Qz-21 - 13	Core	15.7	15.4	0.3	0.9	96.3	466998	9.6	0.8	106.9	0.9
Qz-21 - 14	Core	16.4	15.7	0.6	1.4	103.6	466998	12.3	0.8	115.6	1.1
Qz-21 - 15	Core	15.7	14.7	b.d.l.	0.8	97.7	466998	b.d.l.	0.8	102.4	b.d.l.
Qz-21 - 16	Core	15.3	14.6	b.d.l.	0.9	94.9	466998	11.8	0.8	102.0	0.9
Qz-21 - 17	Core	15.3	14.9	b.d.l.	0.7	96.9	466998	9.1	0.8	102.7	b.d.l.
Qz-21 - 18	Core	15.4	14.6	b.d.l.	0.8	95.8	466998	10.2	0.7	104.0	b.d.l.
Qz-21 - 19	Core	15.7	15.1	b.d.l.	0.8	98.5	466998	b.d.l.	0.8	109.7	b.d.l.
Qz-21 - 20	Core	15.7	15.2	b.d.l.	0.8	97.1	466998	11.0	0.8	112.1	0.9
Qz-21 - 21	Core	15.1	15.1	b.d.l.	0.8	94.5	466998	10.4	0.8	107.6	b.d.l.
Qz-21 - 22	Core	14.7	14.5	b.d.l.	0.6	92.3	466998	b.d.l.	0.8	104.8	1.1
Qz-21 - 23	Core	14.8	14.4	b.d.l.	0.8	88.6	466998	8.9	0.8	96.8	b.d.l.
Qz-21 - 24	Core	15.0	14.3	b.d.l.	0.7	88.1	466998	10.9	0.8	91.6	b.d.l.
Qz-21 - 25	Core	15.0	14.5	b.d.l.	0.7	87.5	466998	13.1	0.7	95.9	b.d.l.
Qz-21 - 26	Core	14.6	14.1	b.d.l.	0.7	89.7	466998	10.4	0.8	88.9	b.d.l.
Qz-21 - 27	Core	15.5	14.7	b.d.l.	0.6	89.7	466998	9.5	0.8	92.7	b.d.l.
Qz-21 - 28	Core	15.8	15.2	b.d.l.	0.7	88.9	466998	14.4	0.7	88.8	b.d.l.
Qz-21 - 29	Core	16.2	15.7	b.d.l.	0.7	87.5	466998	12.2	0.7	86.5	b.d.l.
Qz-21 - 30	Core	16.6	15.9	b.d.l.	0.6	86.1	466998	13.5	0.8	81.8	1.0
Qz-21 - 31	Core	17.0	16.3	b.d.l.	0.5	86.6	466998	17.0	0.7	82.3	b.d.l.
Qz-21 - 32	Core	17.9	17.5	b.d.l.	0.6	90.7	466998	11.8	0.7	82.0	0.9
Qz-21 - 33	Rim	19.0	18.3	b.d.l.	0.8	90.5	466998	12.8	0.8	79.4	b.d.l.
Qz-21 - 34	Rim	20.0	19.1	b.d.l.	0.7	91.6	466998	10.6	0.7	81.7	b.d.l.

Appendix A

Table A1.4: Major elements - sanidine

Info	Position	SiO ₂	TiO ₂	Al ₂ O ₃	FeO	MgO	CaO	Na ₂ O	K ₂ O	SrO	BaO	Total	An	Ab	Or
MFT-grain1-1	Rim	65.5	0.0	19.4	0.1	0.0	0.3	4.2	10.2	0.0	0.4	100.1	2	38	60
MFT-grain1-2	Rim	65.4	0.1	19.4	0.1	0.0	0.5	4.4	9.6	0.0	0.6	100.2	3	40	57
MFT-grain1-3	Rim	65.3	0.1	19.5	0.1	0.0	0.5	4.4	9.7	0.0	0.6	100.2	2	40	58
MFT-grain1-4	Rim	65.8	0.0	19.6	0.1	0.0	0.6	4.5	9.5	0.0	0.6	100.9	3	41	56
MFT-grain1-5	Rim	65.5	0.1	19.5	0.1	0.0	0.5	4.5	9.6	0.0	0.5	100.4	3	40	57
MFT-grain1-6	Rim	65.4	0.1	19.4	0.1	0.0	0.4	4.2	10.0	0.0	0.5	100.1	2	38	60
MFT-grain1-7	Rim	65.3	0.1	19.1	0.1	0.0	0.3	4.2	10.2	0.0	0.5	99.7	2	38	60
MFT-grain1-8	Rim	65.7	0.1	19.3	0.1	0.0	0.4	4.2	10.3	0.1	0.5	100.5	2	38	60
MFT-grain1-9	Rim	65.7	0.1	19.3	0.1	0.0	0.3	4.2	10.3	0.0	0.5	100.4	2	38	60
MFT-grain1-10	Rim	65.7	0.1	19.3	0.1	0.0	0.3	4.1	10.4	0.0	0.5	100.4	2	37	61
MFT-grain1-11	Rim	65.7	0.1	19.3	0.1	0.0	0.3	4.2	10.3	0.0	0.6	100.5	2	37	61
MFT-grain1-12	Rim	65.7	0.1	19.4	0.1	0.0	0.3	4.1	10.3	0.0	0.5	100.5	2	37	61
MFT-grain1-13	Rim	65.6	0.1	19.0	0.1	0.0	0.3	4.1	10.3	0.0	0.6	100.1	2	37	61
MFT-grain1-14	Rim	65.6	0.0	19.2	0.1	0.0	0.3	4.2	10.4	0.0	0.6	100.5	2	37	61
MFT-grain1-15	Rim	64.7	0.1	19.2	0.1	0.0	0.3	4.3	10.3	0.0	0.5	99.5	2	38	60
MFT-grain1-16	Core	65.1	0.1	19.3	0.1	0.0	0.4	4.2	10.4	0.0	0.5	100.0	2	38	61
MFT-grain1-17	Core	64.7	0.1	19.3	0.1	0.0	0.4	4.2	10.4	0.0	0.5	99.6	2	37	61
MFT-grain1-18	Core	64.9	0.1	19.4	0.1	0.0	0.3	4.2	10.3	0.0	0.5	99.8	2	37	61
MFT-grain1-19	Core	65.2	0.1	19.1	0.1	0.0	0.3	4.2	10.4	0.0	0.7	100.0	1	37	61
MFT-grain1-20	Core	65.1	0.1	19.3	0.1	0.0	0.3	4.1	10.6	0.0	0.7	100.2	1	37	62
MFT-grain1-21	Core	65.4	0.1	19.0	0.1	0.0	0.2	4.0	10.5	0.0	0.9	100.2	1	36	62
MFT-grain1-22	Core	65.1	0.1	19.4	0.1	0.0	0.3	4.1	10.1	0.0	1.0	100.2	2	37	61
MFT-grain1-23	Core	64.9	0.1	19.3	0.1	0.0	0.3	4.2	10.2	0.0	1.0	100.2	2	38	61
MFT-grain1-24	Core	65.2	0.1	19.4	0.1	0.0	0.3	4.2	10.2	0.0	0.9	100.4	2	38	60
MFT-grain1-25	Core	65.5	0.1	19.4	0.1	0.0	0.3	4.1	10.2	0.0	1.1	100.8	2	37	61
MFT-grain1-26	Core	65.2	0.1	19.5	0.1	0.0	0.4	4.1	10.3	0.0	1.0	100.7	2	37	61
MFT-grain1-27	Core	65.2	0.1	19.5	0.1	0.0	0.3	4.1	10.3	0.0	1.0	100.6	2	37	61
MFT-grain1-28	Core	65.4	0.1	19.4	0.1	0.0	0.3	4.1	10.3	0.0	1.0	100.8	2	37	61
MFT-grain1-29	Core	65.3	0.1	19.4	0.1	0.0	0.3	4.2	10.3	0.0	1.0	100.8	2	38	61
MFT-grain1-30	Core	65.0	0.1	19.4	0.1	0.0	0.3	4.2	10.1	0.0	1.0	100.2	2	38	61
MFT-grain1-31	Core	65.1	0.1	19.4	0.1	0.0	0.3	4.2	10.3	0.0	1.0	100.4	2	37	61
MFT-grain1-32	Core	65.1	0.1	19.6	0.1	0.0	0.4	4.2	10.1	0.0	1.2	100.7	2	38	60
MFT-grain1-33	Core	65.3	0.1	19.7	0.1	0.0	0.4	4.3	9.9	0.0	1.3	101.1	2	39	59
MFT-grain1-34	Core	65.8	0.1	19.4	0.2	0.0	0.3	4.1	10.4	0.0	0.7	100.9	1	37	62
MFT-grain1-35	Core	65.2	0.1	19.7	0.1	0.0	0.4	4.1	10.3	0.0	0.9	100.8	2	37	61
MFT-grain1-36	Core	65.3	0.0	19.6	0.1	0.0	0.3	4.2	10.2	0.0	0.9	100.6	2	38	60
MFT-grain1-37	Core	65.1	0.1	19.6	0.1	0.0	0.4	4.1	10.1	0.0	0.8	100.3	2	37	61
MFT-grain1-38	Core	64.9	0.1	19.4	0.1	0.0	0.4	4.1	10.2	0.0	0.9	100.0	2	37	61
MFT-grain1-39	Core	65.0	0.1	19.5	0.1	0.0	0.4	4.3	10.1	0.0	0.9	100.3	2	38	60
MFT-grain1-40	Core	65.1	0.1	19.5	0.1	0.0	0.4	4.3	10.0	0.0	0.8	100.5	2	39	59
MFT-grain1-41	Core	65.2	0.1	19.6	0.1	0.0	0.4	4.2	10.2	0.0	0.9	100.6	2	38	60
MFT-grain1-42	Core	64.9	0.1	19.5	0.1	0.0	0.4	4.3	10.0	0.0	0.9	100.2	2	38	59
MFT-grain1-43	Core	65.0	0.1	19.6	0.1	0.0	0.4	4.4	10.1	0.1	0.9	100.6	2	39	59
MFT-grain1-44	Core	65.2	0.1	19.6	0.1	0.0	0.4	4.2	10.0	0.1	1.3	100.9	2	38	60
MFT-grain1-45	Core	64.8	0.1	19.4	0.1	0.0	0.4	4.3	10.0	0.0	0.9	100.0	2	38	59
MFT-grain1-46	Core	64.9	0.1	19.5	0.1	0.0	0.4	4.2	10.2	0.0	1.0	100.2	2	38	61
MFT-grain1-47	Core	65.1	0.1	19.5	0.1	0.0	0.4	4.1	10.2	0.0	1.1	100.7	2	37	61
MFT-grain1-48	Core	64.9	0.1	19.4	0.1	0.0	0.3	4.1	10.2	0.0	0.9	100.0	2	37	61
MFT-grain1-49	Core	65.4	0.1	19.5	0.1	0.0	0.3	4.2	10.2	0.0	1.1	100.8	2	38	61
MFT-grain1-50	Core	65.2	0.1	19.4	0.1	0.0	0.3	4.1	10.2	0.0	1.0	100.4	2	37	61
MFT-grain1-51	Core	65.1	0.1	19.6	0.1	0.0	0.3	4.1	10.1	0.0	1.1	100.5	2	38	61
MFT-grain1-52	Core	64.7	0.1	19.8	0.1	0.0	0.4	4.2	9.9	0.0	1.4	100.5	2	38	60
MFT-grain1-53	Core	65.1	0.1	19.9	0.1	0.0	0.4	4.2	9.9	0.0	1.4	101.1	2	38	60
MFT-grain1-54	Core	64.5	0.1	19.6	0.1	0.0	0.4	4.2	9.9	0.0	1.3	100.1	2	38	60
MFT-grain1-55	Core	64.1	0.1	19.8	0.1	0.0	0.6	4.2	9.5	0.0	1.5	100.0	3	39	58
MFT-grain1-56	Core	64.5	0.1	19.9	0.1	0.0	0.6	4.2	9.5	0.0	1.6	100.4	3	39	58
MFT-grain1-57	Core	64.1	0.1	20.0	0.1	0.0	0.8	4.4	9.1	0.0	1.8	100.3	4	40	56
MFT-grain1-58	Core	64.2	0.1	20.1	0.1	0.0	0.7	4.4	9.1	0.0	1.8	100.7	4	41	55
MFT-grain1-59	Core	63.8	0.1	19.8	0.1	0.0	0.8	4.3	9.1	0.0	1.7	99.9	4	40	56
MFT-grain1-60	Core	64.7	0.1	20.1	0.1	0.0	0.6	4.3	9.2	0.0	1.7	100.8	3	40	57
MFT-San1 - 1	Rim	64.8	0.1	19.6	0.1	0.0	0.4	4.2	10.7	0.4	0.0	100.2	2	37	62
MFT-San1 - 2	Rim	64.8	0.1	19.6	0.1	0.0	0.4	4.2	10.6	0.4	0.0	100.2	2	37	61
MFT-San1 - 3	Rim	65.3	0.0	19.5	0.1	0.0	0.3	4.2	10.6	0.5	0.0	100.6	2	37	62
MFT-San1 - 4	Rim	65.1	0.1	19.5	0.1	0.0	0.3	4.2	10.5	0.5	0.0	100.3	2	37	61
MFT-San1 - 5	Rim	65.2	0.1	19.5	0.1	0.0	0.3	4.2	10.5	0.6	0.0	100.6	2	37	61
MFT-San1 - 6	Core	65.1	0.0	19.4	0.1	0.0	0.4	4.1	10.5	0.5	0.0	100.3	2	36	62
MFT-San1 - 7	Core	65.0	0.1	19.4	0.1	0.0	0.4	4.1	10.5	0.6	0.0	100.1	2	37	62
MFT-San1 - 8	Core	65.3	0.1	19.7	0.1	0.0	0.4	4.2	10.3	0.7	0.0	100.8	2	37	61
MFT-San1 - 9	Core	64.7	0.1	19.8	0.1	0.0	0.4	4.4	10.3	1.0	0.0	100.8	2	39	59
MFT-San1 - 10	Core	64.5	0.0	19.6	0.1	0.0	0.4	4.2	10.2	1.0	0.0	100.1	2	38	60
MFT-San1 - 11	Core	64.4	0.1	19.8	0.1	0.0	0.5	4.3	10.0	1.1	0.0	100.2	3	38	59
MFT-San1 - 12	Core	64.5	0.1	19.5	0.1	0.0	0.4	4.2	10.3	1.0	0.0	100.1	2	38	60
MFT-San1 - 13	Core	64.5	0.1	19.7	0.1	0.0	0.5	4.2	10.1	1.1	0.0	100.3	2	38	60
MFT-San1 - 14	Core	64.9	0.1	19.7	0.1	0.0	0.4	4.0	10.3	1.0	0.0	100.4	2	36	62
MFT-San1 - 15	Core	64.3	0.1	19.8	0.1	0.0	0.4	4.1	10.2	1.3	0.0	100.2	2	37	61
MFT-San1 - 16	Core	64.3	0.1	19.8	0.1	0.0	0.5	4.1	10.0	1.4	0.0	100.3	2	37	60
MFT-San1 - 17	Core	64.2	0.1	19.6	0.1	0.0	0.4	4.0	10.3	1.4	0.0	100.1	2	36	61
MFT-San1 - 18	Core	64.2	0.1	19.9	0.1	0.0	0.4	4.1	10.0	1.2	0.0	100.0	2	37	61
MFT-San1 - 19	Core	64.1	0.1	20.1	0.1	0.0	0.5	4.3	9.9	1.5	0.0	100.5	3	38	59
MFT-San1 - 20	Core	64.1	0.1	20.0	0.1	0.0	0.5	4.2	9.9	1.6	0.0	100.5	3	38	59
MFT-San1 - 21	Core	63.8	0.1	20.0	0.1	0.0	0.6	4.3	9.5	1.7	0.0	100.1	3	39	57
MFT-San1 - 22	Core	63.8	0.1	20.2	0.1	0.0	0.8	4.5	9.3	1.6	0.0	100.3	4	41	55
MFT-San1 - 23	Core	63.9	0.1	20.1	0.1	0.0	0.8	4.4	9.5	1.7	0.0	100.5	4	40	56
MFT-San1 - 24	Core	64.2	0.1	20.0	0.1	0.0	0.6	4.2	9.7	1.8	0.0	100.8	3	39	58
MFT-San1 - 25	Core	64.6	0.1	20.1	0.1	0.0	0.5	4.2	9.9	1.6	0.0	101.1	3	38	59
MFT-San1 - 26	Core	64.4	0.1	20.2	0.1	0.0	0.5	4.3	9.7	1.7	0.0	101.0	3	39	58

Table A1.4: continued

Info	Position	SiO ₂	TiO ₂	Al ₂ O ₃	FeO	MgO	CaO	Na ₂ O	K ₂ O	SrO	BaO	Total	An	Ab	Or
MFT-San1 - 27	Core	64.6	0.1	20.2	0.1	0.0	0.6	4.3	9.6	1.6	0.0	101.2	3	39	58
MFT-San1 - 28	Core	65.0	0.1	19.8	0.1	0.0	0.5	4.2	9.9	1.5	0.0	101.2	3	38	59
MFT-San1 - 29	Core	64.8	0.1	19.4	0.1	0.0	0.3	4.1	10.5	1.1	0.0	100.4	2	36	62
MFT-San1 - 30	Core	64.8	0.1	19.4	0.1	0.0	0.3	4.1	10.5	0.9	0.0	100.3	2	37	62
MFT-San1 - 31	Core	65.1	0.1	19.7	0.1	0.0	0.4	4.2	10.3	0.9	0.0	100.7	2	37	61
MFT-San1 - 32	Core	64.7	0.1	19.4	0.1	0.0	0.5	4.1	10.3	0.9	0.0	100.2	2	37	61
MFT-San1 - 33	Core	65.6	0.1	19.4	0.1	0.0	0.3	4.1	10.6	0.6	0.0	100.8	1	37	62
MFT-San1 - 34	Core	65.6	0.1	19.5	0.1	0.0	0.3	4.1	10.6	0.6	0.0	100.9	1	37	62
MFT-San1 - 35	Core	65.3	0.1	19.3	0.1	0.0	0.3	4.2	10.5	0.4	0.0	100.3	2	37	61
MFT-San1 - 36	Core	65.3	0.1	19.6	0.1	0.0	0.3	4.2	10.4	0.5	0.0	100.4	2	37	61
MFT-San1 - 37	Core	65.6	0.0	19.3	0.1	0.0	0.4	4.2	10.5	0.4	0.0	100.5	2	37	61
MFT-San1 - 38	Core	65.2	0.1	19.4	0.1	0.0	0.3	4.2	10.5	0.4	0.0	100.2	2	37	61
MFT-San1 - 39	Core	65.1	0.1	19.5	0.1	0.0	0.4	4.3	10.5	0.5	0.0	100.5	2	38	61
MFT-San1 - 40	Core	65.2	0.0	19.6	0.1	0.0	0.3	4.3	10.4	0.5	0.0	100.6	2	38	60
MFT-San1 - 41	Core	65.3	0.0	19.4	0.1	0.0	0.4	4.2	10.4	0.5	0.0	100.2	2	38	61
MFT-San1 - 42	Core	65.4	0.1	19.5	0.1	0.0	0.4	4.2	10.4	0.4	0.0	100.4	2	37	61
MFT-San1 - 43	Core	65.1	0.0	19.4	0.1	0.0	0.4	4.2	10.4	0.4	0.0	100.2	2	37	61
MFT-San1 - 44	Core	65.4	0.1	19.5	0.1	0.0	0.4	4.3	10.3	0.4	0.0	100.4	2	38	60
MFT-San1 - 45	Core	65.8	0.0	19.7	0.1	0.0	0.4	4.2	10.4	0.6	0.0	101.3	2	38	61
MFT-San1 - 46	Core	65.0	0.1	19.5	0.1	0.0	0.4	4.2	10.4	0.3	0.0	100.0	2	37	61
MFT-San1 - 47	Core	65.5	0.1	19.4	0.1	0.0	0.3	4.1	10.5	0.4	0.0	100.4	2	37	62
MFT-San1 - 48	Core	65.5	0.1	19.2	0.1	0.0	0.4	4.1	10.5	0.4	0.0	100.2	2	37	61
grain5-1	Core	65.8	0.0	19.3	0.1	0.0	0.4	4.2	10.2	0.0	0.2	100.2	2	38	61
grain5-2	Core	65.9	0.0	19.3	0.1	0.0	0.4	4.2	10.1	0.0	0.3	100.4	2	38	60
grain5-3	Core	66.0	0.0	19.2	0.1	0.0	0.4	4.2	10.1	0.0	0.2	100.2	2	38	60
grain5-4	Core	65.9	0.1	19.4	0.1	0.0	0.3	4.2	10.1	0.0	0.2	100.2	2	38	60
grain5-5	Core	65.8	0.0	19.4	0.1	0.0	0.4	4.2	10.2	0.0	0.2	100.3	2	38	60
grain5-6	Core	65.9	0.0	19.6	0.1	0.0	0.3	4.2	10.3	0.0	0.3	100.6	2	37	61
grain5-7	Core	65.9	0.1	19.4	0.1	0.0	0.4	4.2	10.3	0.0	0.2	100.6	2	37	61
grain5-8	Core	65.8	0.1	19.4	0.1	0.0	0.3	4.2	10.2	0.0	0.3	100.4	2	38	61
grain5-9	Core	66.0	0.1	19.6	0.1	0.0	0.4	4.2	10.2	0.0	0.3	100.9	2	38	60
grain5-10	Core	65.6	0.0	19.4	0.1	0.0	0.4	4.2	10.1	0.0	0.2	100.1	2	38	60
grain5-11	Core	65.8	0.0	19.4	0.1	0.0	0.4	4.2	10.1	0.0	0.2	100.2	2	38	60
grain5-12	Core	65.9	0.0	19.4	0.1	0.0	0.4	4.2	10.1	0.0	0.2	100.3	2	38	60
grain5-13	Core	65.9	0.1	19.3	0.1	0.0	0.4	4.2	10.1	0.0	0.3	100.4	2	38	60
grain5-14	Core	66.1	0.0	19.4	0.1	0.0	0.4	4.3	10.2	0.0	0.2	100.8	2	38	60
grain5-15	Core	66.1	0.0	19.3	0.1	0.0	0.4	4.2	10.2	0.0	0.2	100.5	2	38	60
grain5-16	Core	66.2	0.1	19.4	0.1	0.0	0.4	4.3	10.0	0.0	0.2	100.5	2	39	59
grain5-17	Core	66.2	0.0	19.5	0.1	0.0	0.4	4.3	10.0	0.0	0.3	100.7	2	38	60
grain5-18	Core	66.0	0.0	19.5	0.1	0.0	0.4	4.3	10.2	0.0	0.3	100.8	2	38	60
grain5-19	Core	65.9	0.1	19.2	0.1	0.0	0.4	4.2	10.2	0.0	0.2	100.2	2	38	60
grain5-20	Core	66.1	0.1	19.3	0.1	0.0	0.4	4.3	10.2	0.0	0.3	100.6	2	38	60
grain5-21	Core	66.0	0.0	19.3	0.1	0.0	0.4	4.2	10.2	0.0	0.3	100.5	2	38	60
grain5-22	Core	66.3	0.0	19.4	0.1	0.0	0.4	4.3	10.2	0.0	0.3	101.0	2	38	60
grain5-23	Rim	66.0	0.0	19.5	0.1	0.0	0.4	4.3	9.9	0.0	0.3	100.4	2	39	59
grain5-24	Rim	65.8	0.1	19.3	0.1	0.0	0.3	4.3	10.0	0.0	0.3	100.1	2	39	60
grain5-25	Rim	65.7	0.1	19.4	0.1	0.0	0.4	4.4	10.1	0.0	0.3	100.5	2	39	59
grain5-26	Rim	66.0	0.0	19.5	0.1	0.0	0.4	4.3	10.1	0.0	0.2	100.6	2	39	60
grain5-27	Rim	65.9	0.1	19.6	0.1	0.0	0.4	4.3	10.0	0.0	0.2	100.6	2	39	59
grain5-28	Rim	66.1	0.1	19.3	0.1	0.0	0.4	4.3	10.1	0.0	0.2	100.6	2	39	59
MFT-San5 - 1	Rim	65.0	0.1	18.8	0.1	0.0	0.3	4.1	10.8	0.1	0.0	99.3	2	36	62
MFT-San5 - 2	Core	64.3	0.0	19.2	0.1	0.0	0.3	4.2	10.7	0.1	0.0	99.0	1	37	62
MFT-San5 - 3	Core	64.6	0.1	19.3	0.1	0.0	0.3	4.2	10.8	0.2	0.0	99.6	2	37	62
MFT-San5 - 4	Core	65.2	0.0	19.0	0.1	0.0	0.3	4.1	10.6	0.2	0.0	99.6	2	36	62
MFT-San5 - 5	Core	64.9	0.0	19.1	0.1	0.0	0.3	4.2	10.6	0.3	0.0	99.6	2	37	62
MFT-San5 - 6	Core	65.1	0.1	19.2	0.1	0.0	0.3	4.2	10.6	0.4	0.0	99.9	2	37	62
MFT-San5 - 7	Core	64.5	0.1	19.1	0.1	0.0	0.4	4.2	10.4	0.4	0.0	99.1	2	37	61
MFT-San5 - 8	Core	65.4	0.0	19.1	0.1	0.0	0.3	4.1	10.7	0.4	0.0	100.2	2	36	62
MFT-San5 - 9	Core	65.3	0.0	19.4	0.1	0.0	0.4	4.2	10.4	0.3	0.0	100.2	2	37	61
MFT-San5 - 10	Core	65.4	0.1	19.4	0.1	0.0	0.4	4.2	10.6	0.2	0.0	100.3	2	37	61
MFT-San5 - 11	Core	65.4	0.0	19.3	0.1	0.0	0.4	4.2	10.7	0.3	0.0	100.4	2	37	61
MFT-San5 - 12	Core	65.1	0.1	19.1	0.1	0.0	0.4	4.2	10.5	0.2	0.0	99.6	2	37	61
MFT-San5 - 13	Core	65.4	0.0	19.1	0.1	0.0	0.3	4.2	10.7	0.2	0.0	100.1	2	37	62
MFT-San5 - 14	Core	65.2	0.1	19.1	0.1	0.0	0.4	4.1	10.6	0.2	0.0	99.6	2	36	62
MFT-San5 - 15	Core	65.4	0.1	19.2	0.1	0.0	0.4	4.2	10.6	0.2	0.0	100.1	2	37	61
MFT-San5 - 16	Core	65.4	0.1	19.1	0.1	0.0	0.4	4.3	10.6	0.3	0.0	100.1	2	37	61
MFT-San5 - 17	Core	65.4	0.0	19.1	0.1	0.0	0.3	4.1	10.6	0.2	0.0	100.0	2	37	62
MFT-San5 - 18	Core	65.4	0.0	19.2	0.1	0.0	0.4	4.1	10.6	0.2	0.0	100.0	2	36	62
MFT-San5 - 19	Core	65.4	0.1	19.1	0.1	0.0	0.4	4.2	10.5	0.2	0.0	100.0	2	37	61
MFT-San5 - 20	Core	65.4	0.0	19.4	0.1	0.0	0.4	4.3	10.6	0.2	0.0	100.3	2	37	61
MFT-San5 - 21	Core	65.2	0.1	19.0	0.1	0.0	0.4	4.2	10.6	0.4	0.0	99.9	2	37	61
MFT-San5 - 22	Core	65.1	0.0	19.2	0.1	0.0	0.4	4.2	10.6	0.3	0.0	99.8	2	37	61
MFT-San5 - 23	Core	65.2	0.1	19.1	0.1	0.0	0.4	4.1	10.6	0.3	0.0	99.8	2	37	62
MFT-San5 - 24	Core	65.0	0.0	19.4	0.1	0.0	0.3	4.2	10.5	0.4	0.0	100.1	2	37	61
MFT-San5 - 25	Core	65.2	0.1	19.3	0.1	0.0	0.4	4.3	10.4	0.4	0.0	100.1	2	38	61
MFT-San5 - 26	Core	64.9	0.1	19.3	0.1	0.0	0.4	4.2	10.4	0.3	0.0	99.6	2	37	61
MFT-San5 - 27	Core	65.2	0.1	19.3	0.1	0.0	0.4	4.2	10.5	0.3	0.0	100.0	2	37	61
MFT-San5 - 28	Core	65.2	0.0	19.3	0.1	0.0	0.4	4.2	10.4	0.4	0.0	100.1	2	37	61
MFT-San5 - 29	Core	65.2	0.0	19.2	0.1	0.0	0.4	4.2	10.5	0.5	0.0	100.2	2	37	61
MFT-San5 - 30	Core	65.1	0.1	19.2	0.1	0.0	0.4	4.2	10.4	0.5	0.0	100.0	2	37	61
MFT-San5 - 31	Core	65.0	0.1	19.3	0.1	0.0	0.4	4.2	10.5	0.5	0.0	100.0	2	37	61
MFT-San5 - 32	Core	65.2	0.0	19.2	0.1	0.0	0.4	4.2	10.4	0.5	0.0	100.0	2	37	61
MFT-San5 - 33	Core	65.4	0.1	19.3	0.1	0.0	0.4	4.2	10.4	0.4	0.0	100.3	2	37	61
MFT-San5 - 34	Core	65.5	0.0	19.5	0.1	0.0	0.4	4.3	10.2	0.4	0.0	100.5	2	38	60

Appendix A

Table A1.4: continued

Info	Position	SiO ₂	TiO ₂	Al ₂ O ₃	FeO	MgO	CaO	Na ₂ O	K ₂ O	SrO	BaO	Total	An	Ab	Or
MFT-San5 - 35	Core	65.4	0.1	19.4	0.1	0.0	0.5	4.4	10.2	0.4	0.0	100.5	2	39	59
MFT-San5 - 36	Core	65.6	0.0	18.9	0.1	0.0	0.3	4.1	10.6	0.3	0.0	99.9	1	36	62
MFT-San5 - 37		65.6	0.0	18.9	0.1	0.0	0.3	4.1	10.8	0.3	0.0	100.2	1	36	63
grain6-1	Rim	65.1	0.1	19.7	0.1	0.0	0.5	4.4	9.7	0.0	0.9	100.5	3	40	57
grain6-2	Rim	65.4	0.1	19.8	0.1	0.0	0.5	4.3	9.7	0.0	1.0	100.9	3	39	58
grain6-3	Rim	65.3	0.1	19.8	0.1	0.0	0.5	4.4	9.7	0.0	0.8	100.6	3	40	58
grain6-4	Rim	65.2	0.1	19.9	0.1	0.0	0.5	4.4	9.6	0.0	0.8	100.8	3	40	57
grain6-5	Core	65.2	0.1	19.7	0.1	0.0	0.5	4.3	9.6	0.0	0.9	100.5	3	40	58
grain6-6	Core	65.0	0.1	19.7	0.1	0.0	0.5	4.4	9.7	0.0	0.9	100.3	3	40	58
grain6-7	Core	65.2	0.1	19.8	0.1	0.0	0.5	4.4	9.7	0.0	0.8	100.6	3	39	58
grain6-8	Core	65.1	0.1	19.8	0.1	0.0	0.5	4.3	9.6	0.0	0.9	100.4	3	39	58
grain6-9	Core	65.0	0.1	19.8	0.1	0.0	0.5	4.4	9.7	0.0	1.0	100.5	3	40	58
grain6-10	Core	64.6	0.0	19.7	0.1	0.0	0.5	4.2	9.6	0.0	0.9	99.8	3	39	58
grain6-11	Core	65.1	0.1	19.7	0.1	0.0	0.5	4.3	9.6	0.0	0.8	100.2	2	40	58
grain6-12	Core	64.6	0.1	19.7	0.1	0.0	0.5	4.4	9.7	0.0	0.9	100.1	3	40	58
grain6-13	Core	64.8	0.1	19.8	0.1	0.0	0.5	4.4	9.7	0.0	0.9	100.2	3	39	58
grain6-14	Core	65.1	0.1	19.6	0.1	0.0	0.5	4.4	9.7	0.0	1.0	100.3	2	40	58
grain6-15	Core	64.8	0.0	19.7	0.1	0.0	0.5	4.4	9.8	0.1	0.9	100.4	2	39	58
grain6-16	Core	65.0	0.1	19.8	0.1	0.0	0.5	4.4	9.6	0.0	0.9	100.5	3	40	57
grain6-17	Core	64.9	0.1	19.5	0.1	0.0	0.5	4.4	9.6	0.0	1.0	100.0	2	40	57
grain6-18	Core	65.0	0.1	19.6	0.1	0.0	0.5	4.3	9.6	0.0	0.9	100.1	3	39	58
grain6-19	Core	64.9	0.0	19.5	0.1	0.0	0.4	4.2	9.6	0.0	1.0	99.9	2	39	59
grain6-20	Core	64.6	0.1	19.8	0.1	0.0	0.5	4.3	9.6	0.1	0.9	99.9	2	39	58
grain6-21	Core	65.0	0.1	19.5	0.1	0.0	0.5	4.2	9.6	0.0	0.9	99.9	3	39	58
grain6-22	Core	64.8	0.1	19.8	0.1	0.0	0.5	4.4	9.6	0.0	0.9	100.1	3	40	58
grain6-23	Core	64.8	0.1	19.7	0.1	0.0	0.4	4.3	9.8	0.0	1.0	100.1	2	39	59
grain6-24	Core	64.5	0.1	19.7	0.1	0.0	0.5	4.5	9.7	0.0	0.9	99.9	2	40	57
grain6-25	Core	64.9	0.1	19.8	0.1	0.0	0.5	4.3	9.6	0.0	0.9	100.2	3	39	58
grain6-26	Core	64.6	0.1	20.1	0.1	0.0	0.6	4.4	9.3	0.1	0.9	100.2	3	41	56
grain6-27	Core	64.4	0.1	20.1	0.1	0.0	0.7	4.5	9.2	0.0	0.9	100.0	4	41	55
grain6-28	Core	64.4	0.1	20.2	0.1	0.0	0.7	4.5	9.1	0.0	0.8	100.0	4	41	55
grain6-29	Core	64.3	0.1	19.9	0.1	0.0	0.7	4.5	9.2	0.0	0.9	99.8	3	41	55
grain6-30	Core	64.7	0.1	19.7	0.1	0.0	0.6	4.5	9.5	0.0	0.8	100.0	3	41	56
grain6-31	Core	64.8	0.1	19.7	0.1	0.0	0.6	4.5	9.7	0.0	0.8	100.2	3	40	57
grain6-32	Core	64.5	0.1	19.9	0.1	0.0	0.5	4.4	9.6	0.0	1.0	100.1	3	40	57
MFT-San6 - 1	Rim	65.7	0.1	19.1	0.1	0.0	0.3	3.7	10.8	0.4	0.0	100.2	1	34	65
MFT-San6 - 2	Core	65.5	0.0	19.1	0.1	0.0	0.3	3.8	10.6	0.4	0.0	99.9	2	34	64
MFT-San6 - 3	Core	64.9	0.1	19.6	0.1	0.0	0.8	4.1	9.7	0.4	0.0	99.5	4	37	59
MFT-San6 - 4	Core	65.2	0.0	19.1	0.1	0.0	0.4	3.7	10.5	0.5	0.0	99.6	2	34	64
MFT-San6 - 5	Core	65.5	0.1	19.3	0.1	0.0	0.4	3.8	10.6	0.5	0.0	100.2	2	35	64
MFT-San6 - 6	Core	65.3	0.1	19.6	0.1	0.0	0.6	4.0	10.0	0.7	0.0	100.4	3	36	61
MFT-San6 - 7	Core	64.5	0.1	19.6	0.1	0.0	0.6	4.0	9.8	0.8	0.0	99.6	3	37	60
MFT-San6 - 8	Core	64.9	0.1	19.6	0.1	0.0	0.6	3.9	10.0	0.8	0.0	100.0	3	36	61
MFT-San6 - 9	Core	64.7	0.1	19.8	0.1	0.0	0.7	4.1	9.6	0.8	0.0	99.9	4	38	59
MFT-San6 - 10	Core	65.2	0.0	19.4	0.1	0.0	0.5	3.9	10.1	0.7	0.0	100.0	3	36	62
MFT-San6 - 11	Core	65.1	0.1	19.7	0.1	0.0	0.5	4.0	10.1	0.8	0.0	100.4	3	36	61
MFT-San6 - 12	Core	64.9	0.1	19.5	0.1	0.0	0.5	3.9	10.1	0.9	0.0	100.0	2	36	62
MFT-San6 - 13	Core	65.3	0.1	19.6	0.1	0.0	0.5	3.9	10.0	0.8	0.0	100.3	3	36	61
MFT-San6 - 14	Core	65.3	0.1	19.7	0.1	0.0	0.5	3.9	10.2	1.0	0.0	100.7	2	36	62
MFT-San6 - 15	Core	64.9	0.1	19.6	0.1	0.0	0.4	4.0	10.2	0.9	0.0	100.1	2	36	61
MFT-San6 - 16	Core	64.8	0.1	19.6	0.1	0.0	0.5	3.8	10.2	1.0	0.0	100.1	2	36	62
MFT-San6 - 17	Core	64.9	0.1	19.3	0.1	0.0	0.4	3.9	10.2	0.8	0.0	99.8	2	36	62
MFT-San6 - 18	Core	64.9	0.1	19.5	0.1	0.0	0.5	3.9	10.0	0.9	0.0	99.9	3	36	61
MFT-San6 - 19	Core	65.2	0.1	19.7	0.1	0.0	0.6	4.0	9.9	1.1	0.0	100.5	3	37	60
MFT-San6 - 20	Core	65.1	0.1	19.7	0.1	0.0	0.5	3.9	10.1	0.9	0.0	100.4	3	36	61
MFT-San6 - 22	Core	65.4	0.1	19.4	0.1	0.0	0.4	3.9	10.3	0.9	0.0	100.5	2	36	62
MFT-San6 - 23	Core	65.1	0.1	19.8	0.1	0.0	0.4	3.9	10.2	1.0	0.0	100.5	2	36	62
MFT-San6 - 24	Core	65.4	0.1	19.5	0.1	0.0	0.5	3.9	10.2	0.8	0.0	100.5	2	36	62
MFT-San6 - 25	Rim	65.7	0.1	19.5	0.1	0.0	0.5	3.9	10.2	1.0	0.0	100.9	2	36	62
grain15-1	Rim	65.4	0.1	18.9	0.1	0.0	0.4	4.3	10.1	0.0	0.2	99.5	2	39	59
grain15-2	Rim	65.5	0.1	18.9	0.1	0.0	0.4	4.3	10.1	0.0	0.1	99.6	2	38	60
grain15-3	Core	65.4	0.0	18.9	0.1	0.0	0.3	4.4	10.1	0.0	0.1	99.4	2	39	59
grain15-4	Core	65.9	0.1	19.0	0.1	0.0	0.3	4.4	10.3	0.0	0.1	100.2	2	39	60
grain15-5	Core	65.8	0.1	19.1	0.1	0.0	0.4	4.3	10.1	0.0	0.2	100.2	2	39	60
grain15-6	Core	65.6	0.0	19.1	0.1	0.0	0.4	4.4	10.2	0.0	0.2	100.0	2	39	60
grain15-7	Core	65.9	0.0	19.2	0.1	0.0	0.4	4.4	10.3	0.0	0.2	100.5	2	38	60
grain15-8	Core	65.8	0.1	19.3	0.1	0.0	0.4	4.3	10.3	0.0	0.1	100.4	2	38	60
grain15-9	Core	65.2	0.1	19.1	0.1	0.0	0.4	4.3	9.9	0.0	0.2	99.3	2	39	59
grain15-10	Core	65.2	0.0	18.9	0.1	0.0	0.4	4.3	9.9	0.0	0.2	99.1	2	39	59
grain15-11	Core	65.5	0.0	18.9	0.1	0.0	0.4	4.3	10.0	0.0	0.2	99.3	2	39	59
grain15-12	Core	65.4	0.1	19.1	0.1	0.0	0.4	4.4	10.2	0.0	0.2	99.7	2	39	59
grain15-13	Core	65.4	0.1	18.9	0.1	0.0	0.3	4.3	10.1	0.0	0.2	99.4	2	39	60
grain15-14	Core	65.7	0.1	19.0	0.1	0.0	0.3	4.3	10.2	0.0	0.2	99.9	2	38	60
grain15-15	Core	65.6	0.0	19.2	0.1	0.0	0.4	4.3	10.2	0.0	0.2	100.0	2	38	60
grain15-16	Core	65.6	0.1	19.2	0.1	0.0	0.3	4.3	10.1	0.0	0.2	99.9	2	38	60
grain15-17	Core	65.6	0.1	19.0	0.1	0.0	0.4	4.3	10.1	0.0	0.2	99.8	2	38	60
grain15-18	Core	66.1	0.1	19.2	0.1	0.0	0.3	4.3	10.1	0.0	0.2	100.4	2	38	60
grain15-19	Core	65.9	0.1	19.1	0.1	0.0	0.3	4.3	10.0	0.0	0.2	100.0	2	39	60
grain15-20	Core	65.6	0.0	19.1	0.1	0.0	0.4	4.3	10.1	0.0	0.2	99.8	2	38	60
grain15-21	Core	65.5	0.0	19.0	0.1	0.0	0.4	4.3	10.0	0.0	0.2	99.5	2	39	59
grain15-22	Core	65.4	0.0	18.9	0.1	0.0	0.4	4.2	10.0	0.0	0.2	99.3	2	39	60
grain15-23	Core	65.7	0.1	19.0	0.1	0.0	0.3	4.3	10.2	0.0	0.1	99.8	2	38	60
grain15-24	Core	65.7	0.0	19.1	0.1	0.0	0.3	4.3	10.0	0.0	0.2	99.8	2	39	60

Table A1.4: continued

Info	Position	SiO ₂	TiO ₂	Al ₂ O ₃	FeO	MgO	CaO	Na ₂ O	K ₂ O	SrO	BaO	Total	An	Ab	Or
grain15-25	Core	65.4	0.0	19.1	0.1	0.0	0.3	4.3	10.0	0.0	0.2	99.6	2	39	59
grain15-26	Core	65.3	0.1	19.1	0.1	0.0	0.3	4.4	10.0	0.0	0.3	99.6	2	39	59
grain15-27	Core	65.7	0.1	19.1	0.1	0.0	0.3	4.3	10.0	0.0	0.3	99.9	2	39	60
grain15-28	Core	65.6	0.1	19.0	0.1	0.0	0.3	4.2	10.0	0.0	0.3	99.7	2	38	60
grain15-29	Core	65.8	0.1	19.3	0.1	0.0	0.4	4.2	10.2	0.0	0.3	100.3	2	38	60
grain15-30	Core	65.5	0.1	19.0	0.1	0.0	0.4	4.4	10.0	0.0	0.2	99.7	2	39	59
grain15-31	Core	65.5	0.1	19.1	0.1	0.0	0.3	4.3	10.0	0.0	0.2	99.6	2	39	59
grain15-32	Core	65.7	0.0	19.0	0.1	0.0	0.3	4.3	10.0	0.0	0.3	99.7	2	39	60
grain15-33	Core	65.6	0.1	19.1	0.1	0.0	0.4	4.3	10.1	0.0	0.3	99.9	2	38	60
grain15-34	Core	65.4	0.0	19.0	0.2	0.0	0.4	4.3	9.9	0.0	0.4	99.6	2	39	59
grain15-35	Core	65.8	0.1	19.0	0.1	0.0	0.4	4.3	10.1	0.0	0.4	100.2	2	38	60
grain15-36	Core	65.0	0.1	18.9	0.1	0.0	0.4	4.3	9.9	0.0	0.3	99.0	2	39	59
grain15-37	Core	65.2	0.0	19.0	0.1	0.0	0.4	4.3	9.9	0.0	0.3	99.3	2	39	59
grain15-38	Rim	65.3	0.1	19.0	0.1	0.0	0.3	4.3	10.0	0.0	0.3	99.4	2	39	60
grain15-39	Rim	65.6	0.1	19.0	0.1	0.0	0.4	4.3	9.9	0.0	0.3	99.7	2	39	59
grain15-40	Rim	65.8	0.1	19.0	0.1	0.0	0.4	4.2	9.9	0.0	0.3	99.8	2	38	60
grain16-1	Rim	65.1	0.0	19.0	0.1	0.0	0.4	4.4	9.9	0.0	0.1	98.9	2	39	59
grain16-3	Rim	65.1	0.0	19.0	0.1	0.0	0.4	4.4	9.9	0.0	0.1	99.0	2	39	59
grain16-4	Rim	65.4	0.0	19.0	0.1	0.0	0.4	4.3	10.0	0.0	0.1	99.2	2	39	59
grain16-5	Rim	65.3	0.0	18.8	0.1	0.0	0.4	4.3	9.9	0.0	0.1	99.0	2	39	59
grain16-6	Core	65.3	0.0	19.0	0.1	0.0	0.4	4.4	9.9	0.0	0.0	99.2	2	39	59
grain16-7	Core	65.0	0.0	18.9	0.1	0.0	0.3	4.3	9.8	0.0	0.1	98.6	2	39	59
grain16-8	Core	65.2	0.1	18.9	0.1	0.0	0.4	4.3	10.0	0.0	0.1	99.0	2	39	59
grain16-9	Core	65.4	0.0	19.0	0.1	0.0	0.3	4.3	10.0	0.0	0.1	99.2	2	39	60
grain16-10	Core	65.7	0.0	18.7	0.1	0.0	0.4	4.3	9.9	0.0	0.1	99.2	2	39	59
grain16-11	Core	65.3	0.1	18.9	0.1	0.0	0.4	4.3	9.9	0.0	0.0	99.0	2	39	59
grain16-12	Core	65.4	0.0	18.9	0.1	0.0	0.3	4.2	10.0	0.0	0.1	99.1	2	39	60
grain16-13	Core	65.6	0.0	18.9	0.1	0.0	0.3	4.4	10.0	0.0	0.2	99.5	2	39	59
grain16-14	Core	65.4	0.0	19.0	0.1	0.0	0.4	4.4	10.0	0.0	0.1	99.5	2	39	59
grain16-15	Core	65.6	0.1	19.0	0.1	0.0	0.4	4.3	10.1	0.0	0.1	99.6	2	39	59
grain16-16	Core	65.5	0.1	18.9	0.1	0.0	0.4	4.4	10.0	0.0	0.0	99.3	2	39	59
grain16-17	Core	65.6	0.0	18.9	0.1	0.0	0.3	4.4	10.0	0.0	0.1	99.4	2	39	59
grain16-18	Core	65.7	0.1	19.0	0.1	0.0	0.4	4.4	9.9	0.0	0.1	99.6	2	40	58
grain16-19	Core	65.9	0.1	19.1	0.1	0.0	0.4	4.4	10.0	0.0	0.1	100.0	2	39	59
grain16-20	Core	65.7	0.0	19.1	0.1	0.0	0.3	4.3	10.1	0.0	0.1	99.9	2	39	59
grain16-21	Core	65.6	0.1	18.9	0.1	0.0	0.3	4.3	10.2	0.0	0.0	99.3	2	38	60
grain16-22	Core	65.8	0.1	19.1	0.1	0.0	0.4	4.3	10.2	0.0	0.0	99.9	2	39	60
grain16-23	Core	66.1	0.1	19.0	0.1	0.0	0.4	4.4	10.0	0.0	0.1	100.1	2	39	59
grain16-24	Core	65.8	0.1	19.0	0.1	0.0	0.3	4.3	9.9	0.0	0.0	99.5	2	39	59
grain16-25	Core	65.9	0.1	19.1	0.1	0.0	0.3	4.3	10.1	0.0	0.0	100.0	1	39	60
grain16-26	Core	65.8	0.0	19.1	0.1	0.0	0.4	4.2	10.0	0.0	0.0	99.7	2	38	60
grain16-27	Core	65.7	0.1	19.0	0.1	0.0	0.3	4.4	10.0	0.0	0.0	99.6	2	40	59
grain16-28	Core	66.0	0.1	19.2	0.1	0.0	0.3	4.3	10.1	0.0	0.0	100.1	2	39	60
grain16-29	Core	65.9	0.1	19.0	0.1	0.0	0.3	4.3	10.1	0.0	0.0	99.9	2	38	60
grain16-30	Core	65.8	0.1	19.0	0.1	0.0	0.3	4.4	10.1	0.0	0.0	99.9	2	39	59
grain16-31	Core	65.8	0.0	19.0	0.1	0.0	0.3	4.3	10.0	0.0	0.0	99.6	2	39	59
grain16-32	Core	65.9	0.0	18.8	0.1	0.0	0.4	4.3	10.0	0.0	0.0	99.5	2	39	59
grain16-33	Core	65.4	0.0	19.0	0.1	0.0	0.3	4.3	9.9	0.0	0.1	99.2	2	39	59
grain16-34	Core	65.2	0.0	19.0	0.1	0.0	0.3	4.4	10.0	0.0	0.0	99.1	2	39	59
grain16-35	Core	65.4	0.0	18.9	0.1	0.0	0.3	4.4	10.0	0.0	0.0	99.2	2	40	59
grain16-36	Core	65.4	0.0	18.9	0.1	0.0	0.4	4.4	9.9	0.0	0.0	99.1	2	39	59
grain16-37	Core	65.6	0.1	18.9	0.1	0.0	0.4	4.3	9.9	0.0	0.0	99.3	2	39	59
grain16-38	Core	65.4	0.1	18.8	0.1	0.0	0.4	4.4	9.9	0.0	0.0	99.0	2	39	59
grain16-39	Core	65.7	0.0	18.8	0.1	0.0	0.3	4.4	10.0	0.0	0.0	99.4	2	39	59
grain16-40	Core	65.7	0.0	18.9	0.1	0.0	0.3	4.4	9.8	0.0	0.0	99.3	2	40	59
grain16-41	Core	65.3	0.1	18.9	0.1	0.0	0.4	4.3	9.8	0.0	0.1	98.8	2	39	59
grain16-42	Core	65.5	0.0	18.6	0.1	0.0	0.4	4.4	9.8	0.0	0.1	98.9	2	40	59
grain16-43	Core	65.5	0.0	18.8	0.1	0.0	0.3	4.3	10.0	0.0	0.0	99.1	2	39	60
grain16-44	Core	65.4	0.1	18.7	0.1	0.0	0.4	4.3	9.9	0.0	0.0	98.9	2	39	59
grain16-45	Core	65.3	0.0	18.7	0.1	0.0	0.4	4.4	10.0	0.0	0.1	99.0	2	39	59
grain16-46	Core	65.6	0.1	18.9	0.1	0.0	0.4	4.4	10.0	0.0	0.0	99.4	2	39	59
grain16-47	Core	65.8	0.0	18.9	0.1	0.0	0.3	4.4	9.9	0.0	0.0	99.5	2	40	59
grain16-48	Core	65.4	0.0	19.0	0.1	0.0	0.4	4.4	9.9	0.0	0.0	99.1	2	39	59
grain16-49	Core	65.4	0.1	19.0	0.1	0.0	0.4	4.5	10.0	0.0	0.1	99.4	2	40	58
grain16-50	Core	65.4	0.1	18.9	0.1	0.0	0.4	4.4	9.9	0.0	0.1	99.3	2	40	58
grain16-51	Core	65.2	0.1	18.8	0.1	0.0	0.4	4.4	9.9	0.0	0.1	98.9	2	39	59
grain16-52	Core	65.3	0.1	18.9	0.1	0.0	0.4	4.3	9.9	0.0	0.0	98.9	2	39	59
grain16-53	Core	65.1	0.1	18.7	0.1	0.0	0.4	4.3	9.9	0.0	0.1	98.6	2	39	59
grain16-54	Core	64.8	0.1	18.8	0.1	0.0	0.3	4.3	9.9	0.0	0.1	98.3	2	39	59
grain16-55	Core	65.3	0.1	18.9	0.1	0.0	0.4	4.4	9.7	0.0	0.0	98.8	2	40	58
grain16-56	Core	65.1	0.1	18.8	0.1	0.0	0.3	4.3	9.8	0.0	0.1	98.7	2	39	59
grain16-57	Core	64.9	0.0	18.8	0.1	0.0	0.4	4.4	9.8	0.0	0.0	98.3	2	40	59
grain16-58	Core	64.9	0.0	18.8	0.1	0.0	0.4	4.3	9.9	0.0	0.1	98.4	2	39	59
grain16-59	Core	65.7	0.1	18.9	0.1	0.0	0.4	4.3	10.0	0.0	0.1	99.5	2	39	59
grain16-60	Core	65.4	0.1	19.1	0.1	0.0	0.4	4.3	10.0	0.0	0.1	99.5	2	39	59
grain16-61	Core	65.5	0.1	18.8	0.1	0.0	0.3	4.3	9.9	0.0	0.0	99.0	2	39	59
grain16-62	Core	65.4	0.1	19.0	0.1	0.0	0.3	4.3	9.9	0.0	0.1	99.2	2	39	59
grain16-63	Core	65.4	0.0	18.8	0.2	0.0	0.3	4.3	10.0	0.0	0.0	99.0	2	39	60
grain16-64	Core	65.4	0.0	18.8	0.1	0.0	0.3	4.3	10.0	0.0	0.1	99.1	2	39	59
grain16-65	Core	65.5	0.0	19.1	0.1	0.0	0.4	4.3	10.0	0.0	0.0	99.3	2	39	60
grain16-66	Core	65.5	0.1	19.1	0.1	0.0	0.3	4.4	10.0	0.0	0.1	99.6	2	39	59
grain16-67	Core	65.4	0.0	19.0	0.1	0.0	0.4	4.2	10.0	0.0	0.0	99.2	2	38	60
grain16-68	Core	65.3	0.1	19.0	0.1	0.0	0.3	4.3	9.9	0.0	0.0	99.1	2	39	59
grain16-69	Core	65.3	0.0	18.8	0.1	0.0	0.4	4.3	9.9	0.0	0.1	98.9	2	39	59
grain16-70	Core	65.3	0.0	18.8	0.1	0.0	0.4	4.3	9.8	0.0	0.0	98.8	2	39	59

Appendix A

Table A1.4: continued

Info	Position	SiO ₂	TiO ₂	Al ₂ O ₃	FeO	MgO	CaO	Na ₂ O	K ₂ O	SrO	BaO	Total	An	Ab	Or
grain17-1	Core	64.6	0.1	19.3	0.1	0.0	0.4	4.3	9.7	0.0	0.9	99.4	2	39	58
grain17-2	Core	64.8	0.1	19.0	0.1	0.0	0.4	4.2	9.5	0.0	0.8	99.0	2	39	58
grain17-3	Core	64.7	0.1	19.2	0.1	0.0	0.4	4.3	9.7	0.0	1.0	99.5	2	39	58
grain17-4	Core	64.8	0.1	19.2	0.1	0.0	0.4	4.3	9.7	0.0	0.9	99.6	2	39	58
grain17-5	Core	64.6	0.1	19.3	0.1	0.0	0.5	4.2	9.7	0.0	1.2	99.7	2	39	59
grain17-6	Core	64.5	0.1	19.3	0.1	0.0	0.4	4.3	9.9	0.0	0.9	99.6	2	39	59
grain17-7	Core	65.1	0.1	19.4	0.1	0.0	0.4	4.3	10.0	0.1	1.0	100.4	2	39	59
grain17-8	Core	65.2	0.1	19.5	0.1	0.0	0.4	4.2	9.6	0.0	0.9	100.1	2	39	59
grain17-9	Core	65.1	0.1	19.3	0.1	0.0	0.4	4.2	9.8	0.0	0.8	99.7	2	39	59
grain17-10	Core	64.8	0.1	18.9	0.1	0.0	0.4	4.2	9.6	0.0	0.9	99.0	2	39	59
grain17-11	Core	65.1	0.1	19.5	0.1	0.0	0.4	4.3	9.8	0.0	1.0	100.3	2	39	59
grain17-12	Core	64.7	0.1	19.4	0.1	0.0	0.4	4.3	9.8	0.0	1.0	99.7	2	39	59
grain17-13	Core	64.8	0.1	19.4	0.1	0.0	0.5	4.3	9.7	0.0	1.0	99.9	2	39	58
grain17-14	Core	64.8	0.1	19.4	0.1	0.0	0.4	4.2	9.7	0.0	1.1	100.0	2	39	59
grain17-15	Core	64.8	0.1	19.4	0.2	0.0	0.4	4.2	9.6	0.0	1.3	100.0	2	39	59
grain17-16	Core	65.1	0.1	19.4	0.1	0.0	0.4	4.3	9.7	0.0	1.0	100.2	2	39	59
grain17-17	Core	64.9	0.1	19.7	0.1	0.0	0.4	4.3	9.6	0.0	1.4	100.4	2	40	58
grain17-18	Core	64.3	0.1	19.1	0.1	0.0	0.4	4.3	9.5	0.0	1.1	98.9	2	40	58
grain17-19	Core	64.7	0.0	19.2	0.1	0.0	0.4	4.3	9.6	0.0	0.8	99.3	2	40	58
grain17-20	Core	65.0	0.1	19.1	0.1	0.0	0.4	4.3	9.8	0.0	0.6	99.4	2	39	59
grain17-21	Core	65.2	0.0	19.1	0.1	0.0	0.4	4.3	9.8	0.0	0.7	99.8	2	39	59
grain17-22	Core	64.8	0.1	19.3	0.1	0.0	0.4	4.4	9.8	0.0	0.8	99.7	2	40	59
grain17-23	Core	63.5	0.1	18.8	0.1	0.0	0.4	4.2	9.5	0.0	0.5	97.1	2	39	59
grain17-24	Core	65.3	0.1	19.3	0.1	0.0	0.4	4.3	9.7	0.0	0.6	99.9	2	39	58
grain17-25	Core	65.1	0.1	19.4	0.1	0.0	0.4	4.3	9.7	0.0	0.9	100.1	2	40	58
grain17-26	Rim	64.5	0.1	19.2	0.1	0.0	0.4	4.3	9.5	0.0	1.1	99.3	2	40	58
grain17-27	Rim	64.9	0.1	19.2	0.1	0.0	0.4	4.4	9.6	0.0	1.1	99.8	2	40	58
grain17-28	Rim	64.9	0.1	19.5	0.2	0.0	0.4	4.3	9.6	0.0	1.1	100.0	2	40	58
grain17-29	Rim	64.8	0.1	19.5	0.2	0.0	0.5	4.4	9.6	0.0	1.3	100.2	2	40	58
grain17-30	Rim	64.6	0.1	19.2	0.1	0.0	0.5	4.3	9.2	0.0	1.5	99.6	2	41	57
MFT-San17 - 1	Rim	63.80	0.07	18.95	0.12	0.00	0.45	4.01	10.25	0.54	0.00	98.18	2	36	61
MFT-San17 - 2	Core	63.45	0.04	18.94	0.16	0.01	0.33	4.12	10.34	0.57	0.00	97.95	2	37	61
MFT-San17 - 3	Core	62.54	0.06	19.12	0.14	0.00	0.38	3.98	10.32	0.91	0.00	97.44	2	36	62
MFT-San17 - 4	Core	62.64	0.06	19.16	0.10	0.00	0.38	4.00	10.33	0.95	0.00	97.63	2	36	62
MFT-San17 - 5	Core	61.85	0.07	19.13	0.09	0.00	0.53	4.06	9.99	1.33	0.04	97.09	3	37	60
MFT-San17 - 6	Core	62.09	0.09	19.02	0.10	0.00	0.40	3.93	10.07	1.26	0.00	96.96	2	36	61
MFT-San17 - 7	Core	61.89	0.06	19.11	0.11	0.00	0.38	4.03	10.11	1.03	0.00	96.72	2	37	61
MFT-San17 - 8	Core	61.73	0.08	18.81	0.11	0.01	0.39	4.02	10.31	0.84	0.02	96.31	2	36	62
MFT-San17 - 9	Core	63.16	0.06	19.14	0.12	0.00	0.39	4.09	10.26	0.93	0.00	98.14	2	37	61
MFT-San17 - 10	Core	62.96	0.07	19.11	0.12	0.02	0.42	4.01	10.25	0.82	0.03	97.80	2	37	61
MFT-San17 - 11	Core	62.58	0.09	19.11	0.13	0.00	0.42	4.01	10.15	0.96	0.00	97.45	2	37	61
MFT-San17 - 12	Core	62.25	0.08	19.31	0.08	0.01	0.44	4.05	10.18	0.98	0.00	97.39	2	37	61
MFT-San17 - 13	Core	62.45	0.05	19.31	0.12	0.00	0.40	4.08	10.14	1.21	0.04	97.81	2	37	61
MFT-San17 - 14	Core	62.21	0.09	19.21	0.10	0.00	0.39	4.07	10.12	1.15	0.00	97.36	2	37	61
MFT-San17 - 15	Core	62.31	0.09	19.29	0.13	0.00	0.40	3.94	10.16	1.01	0.02	97.34	2	36	62
MFT-San17 - 17	Core	62.84	0.10	19.42	0.10	0.01	0.40	4.04	10.20	1.18	0.01	98.31	2	37	61
MFT-San17 - 18	Core	62.78	0.10	19.22	0.12	0.00	0.43	4.07	10.23	1.16	0.00	98.10	2	37	61
MFT-San17 - 19	Core	62.98	0.08	19.16	0.08	0.00	0.40	4.04	10.34	0.86	0.00	97.94	2	37	61
MFT-San17 - 20	Core	63.09	0.07	19.24	0.10	0.00	0.39	4.04	10.34	0.58	0.00	97.84	2	37	62
MFT-San17 - 21	Core	63.35	0.06	19.20	0.11	0.00	0.39	4.02	10.44	0.62	0.01	98.20	2	36	62
MFT-San17 - 22	Core	63.29	0.09	19.13	0.11	0.00	0.39	4.04	10.25	0.79	0.02	98.10	2	37	61
MFT-San17 - 23	Core	63.31	0.09	19.05	0.11	0.00	0.41	4.15	10.26	0.62	0.00	97.99	2	37	61
MFT-San17 - 24	Core	62.24	0.09	19.52	0.11	0.00	0.51	4.17	9.90	1.20	0.00	97.73	3	38	59
MFT-San17 - 25	Core	62.64	0.09	19.11	0.13	0.00	0.42	4.07	10.02	1.12	0.04	97.64	2	37	61
MFT-San17 - 26	Core	62.66	0.04	19.20	0.13	0.01	0.45	4.17	10.04	0.93	0.04	97.67	2	38	60
MFT-San17 - 27	Core	62.26	0.07	19.26	0.13	0.00	0.41	4.16	9.93	1.14	0.00	97.36	2	38	60
MFT-San17 - 28	Core	61.82	0.09	19.17	0.12	0.01	0.44	4.08	9.90	1.30	0.01	96.93	2	38	60
MFT-San17 - 29	Core	61.93	0.08	19.21	0.11	0.00	0.46	4.03	9.90	1.23	0.00	96.94	2	37	60
MFT-San17 - 30	Core	62.96	0.07	19.49	0.13	0.00	0.46	4.18	10.03	1.18	0.00	98.50	2	38	60
MFT-San17 - 31	Core	62.71	0.08	19.66	0.11	0.00	0.54	4.08	9.80	1.75	0.01	98.73	3	38	60
MFT-San17 - 32	Core	62.54	0.10	19.83	0.08	0.00	0.48	4.03	9.83	1.43	0.02	98.35	2	37	60
MFT-San17 - 33	Core	62.55	0.08	19.37	0.09	0.00	0.50	4.03	9.96	1.37	0.00	97.94	3	37	60
MFT-San17 - 34	Core	62.42	0.08	19.46	0.13	0.00	0.45	4.03	9.94	1.26	0.01	97.77	2	37	60
MFT-San17 - 35	Core	63.28	0.07	19.25	0.12	0.00	0.38	4.25	10.09	0.64	0.00	98.07	2	38	60
MFT-San17 - 36	Core	63.09	0.07	19.25	0.11	0.01	0.42	4.13	10.16	0.63	0.00	97.87	2	37	61
MFT-San17 - 37	Core	62.89	0.06	19.52	0.10	0.00	0.43	4.12	10.05	0.65	0.06	97.89	2	38	60
grain18-1	Rim	65.3	0.1	19.2	0.1	0.0	0.4	4.1	10.4	0.0	0.4	100.0	2	37	61
grain18-2	Rim	65.8	0.1	19.3	0.1	0.0	0.3	4.0	10.6	0.0	0.4	100.6	2	36	62
grain18-3	Core	65.5	0.1	19.2	0.1	0.0	0.3	4.1	10.5	0.0	0.3	100.1	2	37	61
grain18-4	Core	65.3	0.1	19.1	0.1	0.0	0.4	4.1	10.2	0.0	0.6	99.8	2	37	61
grain18-5	Core	65.5	0.0	19.3	0.1	0.0	0.4	4.3	10.3	0.0	0.6	100.5	2	38	60
grain18-6	Core	65.4	0.1	19.2	0.1	0.0	0.4	4.1	10.3	0.0	0.6	100.1	2	37	61
grain18-7	Core	65.6	0.1	19.3	0.1	0.0	0.4	4.2	10.3	0.0	0.6	100.5	2	37	61
grain18-8	Core	65.7	0.1	19.0	0.2	0.0	0.4	4.1	10.0	0.0	0.6	100.2	2	38	60
grain18-9	Core	65.7	0.0	19.3	0.1	0.0	0.3	4.1	10.6	0.0	0.4	100.5	2	36	62
grain18-10	Core	65.6	0.1	19.4	0.1	0.0	0.5	4.2	10.1	0.0	0.6	100.7	2	38	60
grain18-11	Core	65.4	0.1	19.4	0.1	0.0	0.5	4.4	9.9	0.0	0.4	100.2	3	39	58
grain18-12	Core	65.6	0.0	19.0	0.1	0.0	0.3	4.1	10.6	0.0	0.3	100.1	1	37	62
grain18-13	Core	65.8	0.1	19.1	0.1	0.0	0.3	4.1	10.5	0.0	0.0	100.0	1	37	62
grain18-14	Core	66.2	0.0	19.2	0.1	0.0	0.3	4.2	10.6	0.0	0.0	100.6	2	37	61
grain18-15	Core	65.9	0.1	19.3	0.1	0.0	0.4	4.2	10.5	0.0	0.0	100.4	2	37	61
grain18-16	Core	65.6	0.0	19.1	0.1	0.0	0.4	4.2	10.6	0.0	0.1	100.0	2	37	61
grain18-17	Core	66.1	0.1	19.2	0.1	0.0	0.4	4.3	10.5	0.0	0.1	100.7	2	37	61
grain18-18	Core	66.3	0.1	19.3	0.1	0.0	0.3	4.2	10.4	0.0	0.1	100.9	2	38	61

Table A1.4: continued

Info	Position	SiO ₂	TiO ₂	Al ₂ O ₃	FeO	MgO	CaO	Na ₂ O	K ₂ O	SrO	BaO	Total	An	Ab	Or
grain18-19	Core	66.2	0.0	19.4	0.1	0.0	0.4	4.2	10.4	0.0	0.1	100.7	2	37	61
grain18-20	Core	66.3	0.1	19.6	0.1	0.0	0.4	4.2	10.5	0.0	0.1	101.1	2	37	61
grain18-21	Core	66.2	0.1	19.3	0.1	0.0	0.4	4.2	10.5	0.0	0.1	100.8	2	37	61
grain18-22	Core	66.4	0.0	19.2	0.1	0.0	0.4	4.2	10.5	0.0	0.0	100.9	2	37	61
grain18-23	Core	66.2	0.0	19.4	0.1	0.0	0.4	4.2	10.4	0.0	0.0	100.7	2	37	61
grain18-24	Core	66.0	0.1	19.1	0.1	0.0	0.3	4.3	10.6	0.0	0.1	100.5	2	37	61
grain18-25	Core	65.9	0.0	19.2	0.1	0.0	0.3	4.2	10.5	0.0	0.1	100.4	2	37	61
grain18-26	Core	66.1	0.1	19.3	0.1	0.0	0.4	4.2	10.5	0.0	0.1	100.8	2	37	61
grain18-27	Core	66.2	0.0	19.3	0.1	0.0	0.4	4.2	10.6	0.0	0.1	100.8	2	37	61
grain18-28	Core	66.0	0.1	19.3	0.1	0.0	0.4	4.3	10.5	0.0	0.1	100.6	2	38	61
grain18-29	Core	66.0	0.0	19.2	0.1	0.0	0.4	4.3	10.4	0.0	0.1	100.4	2	38	60
grain18-30	Core	66.1	0.1	19.0	0.1	0.0	0.4	4.2	10.4	0.0	0.1	100.4	2	37	61
grain18-31	Core	66.1	0.1	19.3	0.1	0.0	0.4	4.3	10.5	0.0	0.1	100.8	2	38	60
grain18-32	Core	66.0	0.0	19.2	0.1	0.0	0.4	4.2	10.4	0.0	0.1	100.5	2	37	61
grain18-33	Core	66.0	0.0	19.2	0.1	0.0	0.4	4.2	10.4	0.0	0.1	100.4	2	37	61
grain18-34	Core	66.3	0.0	19.4	0.1	0.0	0.4	4.2	10.4	0.0	0.1	100.9	2	38	61
grain18-35	Core	66.2	0.0	19.4	0.1	0.0	0.4	4.2	10.4	0.0	0.0	100.8	2	38	61
grain18-36	Core	66.1	0.1	19.1	0.1	0.0	0.3	4.2	10.4	0.0	0.1	100.4	2	37	61
grain18-37	Core	66.0	0.1	19.4	0.1	0.0	0.3	4.2	10.4	0.0	0.1	100.6	2	37	61
grain18-38	Core	66.3	0.1	19.2	0.1	0.0	0.3	4.1	10.5	0.0	0.1	100.7	2	37	61
grain18-39	Core	66.2	0.0	19.3	0.1	0.0	0.3	4.2	10.5	0.0	0.1	100.8	2	37	61
grain18-40	Core	66.2	0.0	19.2	0.1	0.0	0.3	4.2	10.4	0.0	0.1	100.7	2	37	61
grain18-41	Core	66.1	0.1	19.3	0.1	0.0	0.3	4.2	10.5	0.0	0.2	100.9	2	37	61
grain18-42	Core	66.2	0.1	19.2	0.1	0.0	0.4	4.2	10.5	0.0	0.1	100.7	2	37	61
grain18-43	Core	65.8	0.0	19.2	0.1	0.0	0.4	4.2	10.4	0.1	0.1	100.2	2	37	61
grain18-44	Core	66.1	0.0	19.4	0.1	0.0	0.4	4.2	10.3	0.0	0.1	100.6	2	38	60
grain18-45	Core	66.1	0.0	19.5	0.1	0.0	0.4	4.1	10.5	0.0	0.1	100.8	2	37	61
grain18-46	Core	66.0	0.0	19.2	0.1	0.0	0.3	4.2	10.4	0.0	0.2	100.5	2	37	61
grain18-47	Core	65.9	0.0	19.4	0.1	0.0	0.4	4.3	10.4	0.0	0.1	100.6	2	38	61
grain18-48	Core	66.0	0.0	19.1	0.1	0.0	0.4	4.2	10.5	0.0	0.1	100.4	2	37	61
grain18-49	Core	65.9	0.0	19.1	0.1	0.0	0.3	4.2	10.6	0.0	0.1	100.3	2	37	61
grain18-50	Core	66.1	0.0	19.1	0.1	0.0	0.3	4.1	10.6	0.0	0.2	100.5	2	36	62
grain18-51	Core	66.1	0.1	19.1	0.1	0.0	0.3	4.1	10.5	0.0	0.1	100.4	2	37	61
grain18-52	Core	66.0	0.0	19.0	0.2	0.0	0.3	4.1	10.6	0.0	0.2	100.4	2	37	62
grain18-53	Core	66.0	0.1	19.3	0.1	0.0	0.3	4.1	10.6	0.0	0.3	100.7	2	37	62
grain18-54	Core	66.1	0.0	19.1	0.1	0.0	0.3	4.1	10.5	0.0	0.4	100.6	2	37	62
grain18-55	Core	66.3	0.1	19.1	0.1	0.0	0.3	4.0	10.5	0.0	0.3	100.7	1	36	62
grain18-56	Core	65.7	0.0	19.6	0.1	0.0	0.4	4.2	10.1	0.0	0.6	100.9	2	38	60
grain18-57	Core	65.7	0.1	19.4	0.1	0.0	0.4	4.1	10.2	0.0	0.6	100.5	2	37	61
MFT-San18 - 1	Core	65.3	0.0	19.0	0.1	0.0	0.3	4.3	10.6	0.0	0.1	99.7	2	38	61
MFT-San18 - 2	Core	65.5	0.0	19.0	0.1	0.0	0.3	4.3	10.7	0.0	0.0	99.9	2	37	61
MFT-San18 - 3	Core	65.3	0.0	19.0	0.1	0.0	0.3	4.2	10.6	0.0	0.0	99.6	2	37	61
MFT-San18 - 4	Core	65.6	0.1	19.0	0.1	0.0	0.4	4.2	10.6	0.0	0.0	99.9	2	37	62
MFT-San18 - 5	Core	65.5	0.0	19.0	0.1	0.0	0.4	4.2	10.6	0.0	0.0	99.8	2	37	61
MFT-San18 - 6	Core	65.4	0.1	18.9	0.1	0.0	0.4	4.3	10.6	0.0	0.0	99.8	2	37	61
MFT-San18 - 7	Core	65.7	0.1	19.0	0.1	0.0	0.3	4.2	10.6	0.0	0.0	100.1	2	37	61
MFT-San18 - 8	Core	65.5	0.0	19.0	0.1	0.0	0.3	4.2	10.7	0.1	0.0	99.9	2	37	62
MFT-San18 - 9	Core	65.5	0.1	19.1	0.1	0.0	0.4	4.2	10.6	0.0	0.0	99.9	2	37	61
MFT-San18 - 10	Core	65.7	0.1	19.1	0.1	0.0	0.3	4.1	10.7	0.0	0.0	100.1	2	36	62
MFT-San18 - 11	Core	65.7	0.0	19.1	0.1	0.0	0.3	4.2	10.6	0.0	0.0	100.2	2	37	61
MFT-San18 - 12	Core	65.5	0.0	19.2	0.1	0.0	0.3	4.2	10.6	0.0	0.0	100.0	2	37	61
MFT-San18 - 13	Core	65.7	0.1	19.2	0.1	0.0	0.3	4.2	10.7	0.1	0.0	100.4	2	37	62
MFT-San18 - 14	Core	65.5	0.0	19.0	0.1	0.0	0.3	4.2	10.7	0.0	0.0	99.8	2	37	62
MFT-San18 - 15	Core	65.5	0.0	19.0	0.1	0.0	0.4	4.2	10.6	0.0	0.0	99.8	2	37	61
MFT-San18 - 16	Core	65.3	0.1	19.1	0.1	0.0	0.3	4.2	10.7	0.1	0.0	99.8	2	37	62
MFT-San18 - 17	Core	65.9	0.1	18.9	0.1	0.0	0.3	4.1	10.7	0.1	0.0	100.2	2	36	62
MFT-San18 - 18	Core	65.6	0.0	19.2	0.1	0.0	0.4	4.2	10.6	0.1	0.0	100.2	2	37	61
MFT-San18 - 19	Core	65.7	0.1	19.2	0.1	0.0	0.4	4.3	10.5	0.1	0.0	100.2	2	38	61
MFT-San18 - 20	Core	65.8	0.0	19.1	0.1	0.0	0.3	4.2	10.7	0.1	0.0	100.5	1	37	61
MFT-San18 - 21	Core	65.6	0.0	19.1	0.1	0.0	0.4	4.2	10.5	0.1	0.0	100.1	2	37	61
MFT-San18 - 22	Core	65.6	0.0	19.3	0.1	0.0	0.4	4.3	10.6	0.1	0.0	100.3	2	37	61
MFT-San18 - 23	Core	65.7	0.0	19.3	0.1	0.0	0.3	4.2	10.6	0.1	0.0	100.4	2	37	61
MFT-San18 - 24	Core	66.0	0.1	19.4	0.1	0.0	0.4	4.3	10.6	0.1	0.0	100.8	2	37	61
MFT-San18 - 25	Core	65.8	0.1	19.2	0.1	0.0	0.3	4.2	10.6	0.0	0.0	100.3	2	37	62
MFT-San18 - 26	Core	65.7	0.0	19.1	0.1	0.0	0.4	4.1	10.5	0.0	0.0	99.9	2	37	62
MFT-San18 - 27	Core	65.5	0.1	19.2	0.1	0.0	0.3	4.2	10.7	0.1	0.0	100.1	2	37	62
MFT-San18 - 28	Core	65.6	0.0	19.3	0.1	0.0	0.3	4.1	10.7	0.2	0.0	100.4	1	37	62
MFT-San18 - 29	Core	65.5	0.0	19.0	0.1	0.0	0.3	4.0	10.8	0.3	0.0	100.1	1	36	63
MFT-San18 - 30	Core	65.4	0.1	19.1	0.1	0.0	0.3	4.1	10.7	0.4	0.0	100.1	1	36	62
MFT-San18 - 31	Core	65.0	0.1	19.3	0.1	0.0	0.5	4.4	10.1	0.5	0.0	100.0	3	39	59
MFT-San18 - 32	Core	65.2	0.1	19.3	0.1	0.0	0.4	4.2	10.3	0.7	0.0	100.2	2	37	61
MFT-San18 - 33	Core	64.9	0.1	19.5	0.1	0.0	0.4	4.3	10.4	0.6	0.0	100.3	2	38	60
MFT-San18 - 34	Core	65.1	0.1	19.4	0.1	0.0	0.4	4.2	10.4	0.6	0.0	100.2	2	38	60
MFT-San18 - 35	Core	65.2	0.1	19.7	0.1	0.0	0.4	4.3	10.4	0.7	0.0	100.8	2	38	60
MFT-San18 - 36	Core	65.0	0.1	19.5	0.1	0.0	0.4	4.2	10.4	0.6	0.0	100.3	2	37	61
MFT-San18 - 37	Core	65.0	0.1	19.4	0.1	0.0	0.4	4.1	10.4	0.5	0.0	100.0	2	37	61
MFT-San18 - 38	Rim	65.7	0.0	19.4	0.1	0.0	0.3	4.1	10.7	0.4	0.0	100.6	1	36	62
MFT-San18 - 39	Rim	65.5	0.0	19.2	0.1	0.0	0.3	4.1	10.7	0.4	0.0	100.2	2	36	63
grain19-1	Rim	65.3	0.1	19.4	0.1	0.0	0.4	4.2	10.2	0.0	1.0	100.6	2	38	60
grain19-2	Rim	65.4	0.1	19.6	0.1	0.0	0.4	4.1	10.2	0.0	1.1	101.0	2	37	61
grain19-3	Rim	65.6	0.1	19.6	0.1	0.0	0.4	4.2	10.1	0.0	0.9	101.1	2	38	60
grain19-4	Core	65.4	0.1	19.8	0.1	0.0	0.5	4.2	10.0	0.0	1.2	101.2	2	38	60
grain19-5	Core	65.3	0.1	19.7	0.1	0.0	0.4	4.2	10.2	0.0	1.1	101.0	2	38	60

Appendix A

Table A1.4: continued

Info	Position	SiO ₂	TiO ₂	Al ₂ O ₃	FeO	MgO	CaO	Na ₂ O	K ₂ O	SrO	BaO	Total	An	Ab	Or
grain19-6	Core	65.0	0.1	19.9	0.1	0.0	0.4	4.2	10.2	0.0	1.0	101.0	2	38	60
grain19-7	Core	65.1	0.1	19.7	0.1	0.0	0.4	4.2	10.2	0.0	0.9	100.6	2	38	60
grain19-8	Core	65.3	0.1	19.7	0.1	0.0	0.4	4.1	10.1	0.0	1.2	101.0	2	37	60
grain19-9	Core	64.9	0.1	19.6	0.1	0.0	0.4	4.1	9.9	0.0	1.4	100.5	2	37	60
grain19-10	Core	65.1	0.1	19.7	0.1	0.0	0.4	4.1	10.1	0.1	1.2	100.8	2	37	61
grain19-11	Core	64.8	0.1	19.5	0.1	0.0	0.5	4.2	9.8	0.0	1.4	100.3	3	38	59
grain19-12	Core	64.7	0.1	19.8	0.1	0.0	0.6	4.2	9.7	0.0	1.6	100.9	3	39	59
grain19-13	Core	64.5	0.1	20.0	0.1	0.0	0.7	4.4	9.5	0.0	1.6	100.8	3	40	57
grain19-14	Core	65.3	0.1	19.5	0.1	0.0	0.4	4.2	10.1	0.0	1.3	101.0	2	38	60
grain19-15	Core	65.4	0.1	19.8	0.1	0.0	0.4	4.1	10.2	0.0	1.2	101.1	2	37	61
grain19-16	Core	64.8	0.0	20.0	0.1	0.0	0.6	4.2	9.8	0.0	1.6	101.1	3	38	59
grain19-17	Core	64.6	0.1	19.7	0.1	0.0	0.5	4.3	9.8	0.0	1.6	100.7	3	39	59
grain19-18	Core	64.8	0.1	19.9	0.1	0.0	0.5	4.2	9.8	0.0	1.5	100.9	3	38	59
grain19-19	Core	64.7	0.1	20.3	0.1	0.0	0.7	4.3	9.7	0.0	1.6	101.3	3	39	58
grain19-20	Core	64.6	0.1	20.1	0.1	0.0	0.7	4.4	9.6	0.0	1.5	101.0	4	39	57
grain19-21	Core	65.0	0.1	19.9	0.1	0.0	0.5	4.3	9.8	0.0	1.5	101.2	3	39	58
grain19-22	Core	64.7	0.1	19.9	0.1	0.0	0.6	4.1	9.8	0.1	1.5	100.9	3	38	59
grain19-23	Core	65.0	0.1	19.9	0.1	0.0	0.6	4.3	9.7	0.0	1.6	101.2	3	39	58
grain19-24	Core	64.7	0.1	20.1	0.1	0.0	0.6	4.3	9.8	0.0	1.5	101.1	3	39	58
grain19-25	Core	64.4	0.1	20.1	0.1	0.0	0.8	4.4	9.3	0.1	1.4	100.7	4	40	56
grain19-26	Core	64.5	0.1	20.2	0.1	0.0	0.7	4.4	9.3	0.0	1.6	100.9	4	40	56
grain19-27	Core	64.5	0.1	20.2	0.1	0.0	0.8	4.3	9.3	0.0	1.5	100.8	4	40	56
grain19-28	Core	64.4	0.1	20.2	0.1	0.0	0.8	4.5	9.3	0.0	1.5	100.8	4	40	56
grain19-29	Core	64.7	0.1	19.9	0.1	0.0	0.5	4.2	9.7	0.0	1.7	100.9	3	38	59
grain19-30	Core	64.6	0.1	19.8	0.1	0.0	0.6	4.2	9.7	0.0	1.7	100.8	3	39	58
grain19-31	Core	64.7	0.1	19.9	0.1	0.0	0.6	4.2	9.7	0.0	1.7	100.9	3	39	59
grain19-32	Core	64.8	0.1	19.8	0.1	0.0	0.6	4.1	9.7	0.0	1.6	100.8	3	38	59
grain19-33	Core	64.7	0.1	19.7	0.1	0.0	0.6	4.2	9.7	0.0	1.6	100.7	3	39	58
grain19-34	Core	64.9	0.1	19.9	0.1	0.0	0.6	4.2	9.8	0.0	1.6	101.1	3	39	59
grain19-35	Core	64.9	0.1	19.8	0.1	0.0	0.6	4.2	9.6	0.0	1.7	101.0	3	39	58
grain19-36	Core	64.9	0.1	19.9	0.1	0.0	0.6	4.2	9.6	0.0	1.6	101.1	3	39	58
grain19-37	Core	64.6	0.1	19.6	0.1	0.0	0.6	4.2	9.6	0.0	1.5	100.3	3	39	58
grain19-38	Core	64.8	0.1	19.4	0.1	0.0	0.4	4.0	10.2	0.0	1.4	100.3	2	37	61
grain19-39	Core	64.7	0.1	19.9	0.1	0.0	0.6	4.2	9.6	0.0	1.6	100.9	3	39	58
grain19-40	Core	64.9	0.1	20.0	0.1	0.0	0.7	4.3	9.6	0.0	1.4	101.1	3	39	58
grain19-41	Core	65.0	0.1	19.9	0.1	0.0	0.7	4.3	9.7	0.0	1.3	101.1	3	39	58
grain19-42	Core	65.2	0.1	19.8	0.1	0.0	0.5	4.3	9.9	0.0	1.1	100.9	2	39	59
grain19-43	Core	65.0	0.1	19.9	0.2	0.0	0.5	4.3	9.9	0.0	1.1	100.9	2	39	59
grain19-44	Core	65.1	0.1	19.5	0.1	0.0	0.5	4.2	9.9	0.0	1.1	100.5	3	38	59
grain19-45	Core	65.2	0.1	19.7	0.1	0.0	0.5	4.3	10.0	0.0	1.2	101.1	3	38	59
grain19-46	Core	65.3	0.1	19.8	0.1	0.0	0.5	4.2	9.9	0.0	1.1	101.1	3	38	59
grain19-47	Core	65.1	0.1	19.6	0.1	0.0	0.5	4.2	9.9	0.0	1.0	100.5	3	38	59
grain19-48	Rim	66.0	0.1	19.5	0.1	0.0	0.3	4.2	10.4	0.0	0.4	101.0	2	37	61
grain19-49	Rim	65.6	0.0	19.3	0.1	0.0	0.4	4.3	10.3	0.0	0.5	100.3	2	38	60
grain19-50	Rim	65.4	0.1	19.8	0.1	0.0	0.6	4.4	10.0	0.0	0.8	101.2	3	39	58
MFT-San19 - 1	Core	63.6	0.1	19.1	0.1	0.0	0.4	4.2	10.3	0.8	0.0	98.7	2	37	61
MFT-San19 - 2	Core	62.6	0.1	19.1	0.1	0.0	0.4	4.1	10.2	0.9	0.0	97.5	2	37	61
MFT-San19 - 3	Core	62.7	0.1	19.1	0.1	0.0	0.4	4.1	10.1	1.2	0.0	97.7	2	37	61
MFT-San19 - 4	Core	62.9	0.1	19.4	0.1	0.0	0.5	4.1	10.0	1.2	0.0	98.3	2	38	60
MFT-San19 - 5	Core	62.8	0.1	19.1	0.1	0.0	0.4	4.1	10.1	1.3	0.0	97.9	2	37	60
MFT-San19 - 6	Core	62.7	0.1	19.3	0.1	0.0	0.5	4.2	10.0	1.3	0.0	98.2	2	38	60
MFT-San19 - 7	Core	62.8	0.1	19.4	0.1	0.0	0.4	4.2	10.0	1.5	0.0	98.4	2	38	60
MFT-San19 - 8	Core	62.3	0.1	19.7	0.1	0.0	0.6	4.3	9.7	1.8	0.0	98.6	3	39	58
MFT-San19 - 9	Core	62.7	0.1	19.4	0.1	0.0	0.6	4.2	9.8	1.5	0.0	98.4	3	38	59
MFT-San19 - 10	Core	62.5	0.1	19.5	0.1	0.0	0.6	4.1	9.8	1.5	0.0	98.3	3	38	59
MFT-San19 - 11	Core	63.0	0.1	19.6	0.1	0.0	0.5	4.2	9.7	1.5	0.0	98.7	3	38	59
MFT-San19 - 12	Core	62.8	0.1	19.6	0.1	0.0	0.5	4.2	9.9	1.5	0.1	98.7	3	38	59
MFT-San19 - 13	Core	62.9	0.1	19.8	0.1	0.0	0.5	4.1	10.0	1.7	0.0	99.2	3	37	60
MFT-San19 - 14	Core	63.3	0.1	19.5	0.1	0.0	0.5	4.1	10.0	1.5	0.0	99.0	3	38	60
MFT-San19 - 15	Core	62.8	0.1	19.8	0.1	0.0	0.8	4.5	9.3	1.5	0.0	98.8	4	41	55
MFT-San19 - 16	Core	63.1	0.1	19.7	0.1	0.0	0.7	4.4	9.5	1.5	0.0	99.1	3	40	57
MFT-San19 - 17	Core	63.3	0.1	19.6	0.1	0.0	0.6	4.3	9.6	1.5	0.0	99.1	3	39	58
MFT-San19 - 18	Core	63.1	0.1	19.4	0.1	0.0	0.5	4.1	9.9	1.5	0.0	98.7	3	38	59
MFT-San19 - 19	Core	63.6	0.1	19.4	0.1	0.0	0.5	4.1	10.0	1.4	0.0	99.1	2	37	60
MFT-San19 - 20	Core	63.7	0.1	19.3	0.1	0.0	0.4	4.1	10.2	1.2	0.0	99.2	2	37	61
MFT-San19 - 21	Core	63.6	0.1	19.4	0.1	0.0	0.4	4.1	10.2	1.2	0.0	99.1	2	37	61
MFT-San19 - 22	Core	63.8	0.1	19.3	0.1	0.0	0.4	4.2	10.2	1.1	0.0	99.2	2	37	61
MFT-San19 - 23	Core	64.0	0.1	19.4	0.1	0.0	0.5	4.1	10.3	1.1	0.0	99.5	2	37	61
MFT-San19 - 24	Core	64.0	0.1	19.2	0.1	0.0	0.4	4.1	10.4	1.1	0.0	99.1	2	37	61
MFT-San19 - 25	Core	64.0	0.1	19.4	0.1	0.0	0.4	4.1	10.2	1.1	0.0	99.3	2	37	61
MFT-San19 - 26	Core	64.2	0.1	19.3	0.1	0.0	0.3	4.0	10.4	0.9	0.0	99.3	2	37	62
MFT-San19 - 27	Core	64.0	0.1	19.2	0.1	0.0	0.4	4.1	10.3	0.9	0.0	99.0	2	37	61
MFT-San19 - 28	Core	64.3	0.1	19.1	0.1	0.0	0.4	4.2	10.3	1.0	0.0	99.4	2	37	61
MFT-San19 - 29	Core	64.0	0.0	19.3	0.1	0.0	0.4	4.2	10.2	0.8	0.0	99.1	2	38	60
MFT-San19 - 30	Core	64.2	0.0	19.3	0.1	0.0	0.4	4.3	10.3	0.8	0.0	99.5	2	38	60
MFT-San19 - 31	Rim	64.4	0.1	19.2	0.1	0.0	0.4	4.2	10.3	0.7	0.0	99.4	2	37	61
MFT-San19 - 32	Rim	64.4	0.1	19.1	0.1	0.0	0.4	4.1	10.3	0.8	0.0	99.3	2	37	61
MFT-San19 - 33	Rim	64.5	0.1	19.1	0.1	0.0	0.4	4.2	10.3	0.6	0.0	99.3	2	37	61
MFT-San27 - 1	Rim	64.26	0.03	18.79	0.10	0.00	0.34	4.00	10.38	0.38	0.00	98.27	2	36	62
MFT-San27 - 2	Rim	63.95	0.07	18.90	0.09	0.00	0.39	4.08	10.36	0.49	0.00	98.34	2	37	61
MFT-San27 - 3	Core	63.58	0.06	18.80	0.12	0.00	0.35	4.05	10.34	0.38	0.05	97.73	2	37	62
MFT-San27 - 4	Core	63.40	0.05	18.88	0.09	0.00	0.38	4.15	10.44	0.40	0.00	97.79	2	37	61
MFT-San27 - 5	Core	63.24	0.06	18.86	0.09	0.01	0.40	4.16	10.38	0.43	0.00	97.63	2	37	61
MFT-San27 - 6	Core	63.07	0.07	19.00	0.10	0.00	0.41	4.13	10.34	0.46	0.00	97.58	2	37	61
MFT-San27 - 7	Core	63.05	0.05	18.98	0.09	0.00	0.44	4.25	10.20	0.46	0.02	97.53	2	38	60

Table A1.4: continued

Info	Position	SiO ₂	TiO ₂	Al ₂ O ₃	FeO	MgO	CaO	Na ₂ O	K ₂ O	SrO	BaO	Total	An	Ab	Or
MFT-San27 - 8	Core	62.95	0.06	18.84	0.14	0.00	0.34	4.08	10.49	0.38	0.00	97.27	2	37	62
MFT-San27 - 9	Core	64.00	0.04	18.87	0.09	0.00	0.31	4.10	10.57	0.33	0.01	98.32	2	37	62
MFT-San27 - 10	Core	64.02	0.03	18.93	0.08	0.00	0.33	4.09	10.61	0.39	0.00	98.47	2	36	62
MFT-San27 - 11	Core	63.78	0.07	18.91	0.10	0.00	0.33	4.08	10.63	0.30	0.00	98.20	2	36	62
MFT-San27 - 12	Core	63.59	0.04	18.82	0.11	0.00	0.34	4.16	10.51	0.36	0.02	97.95	2	37	61
MFT-San27 - 13	Core	63.46	0.06	18.92	0.10	0.00	0.37	4.03	10.48	0.21	0.01	97.63	2	36	62
MFT-San27 - 14	Core	63.58	0.05	18.93	0.09	0.00	0.30	4.14	10.60	0.21	0.00	97.91	1	37	62
MFT-San27 - 15	Core	63.47	0.05	18.93	0.08	0.01	0.32	4.05	10.60	0.33	0.01	97.85	2	36	62
MFT-San27 - 16	Core	63.26	0.04	19.10	0.10	0.01	0.36	4.17	10.50	0.21	0.00	97.74	2	37	61
MFT-San27 - 17	Core	63.11	0.08	18.82	0.12	0.00	0.31	4.08	10.59	0.21	0.00	97.32	2	36	62
MFT-San27 - 18	Core	64.08	0.04	19.16	0.10	0.00	0.36	4.09	10.52	0.24	0.00	98.59	2	36	62
MFT-San27 - 19	Core	63.86	0.04	19.03	0.10	0.00	0.36	4.19	10.48	0.19	0.00	98.25	2	37	61
MFT-San27 - 20	Core	63.89	0.07	19.22	0.11	0.02	0.40	4.15	10.46	0.22	0.03	98.57	2	37	61
MFT-San27 - 21	Core	64.06	0.06	19.09	0.10	0.00	0.36	4.15	10.53	0.18	0.03	98.57	2	37	61
MFT-San27 - 22	Core	63.79	0.05	18.93	0.13	0.03	0.32	4.11	10.57	0.17	0.01	98.10	2	37	62
MFT-San27 - 23	Core	63.73	0.04	18.81	0.11	0.00	0.31	4.14	10.58	0.18	0.00	97.90	2	37	62
MFT-San27 - 24	Core	63.60	0.07	18.97	0.08	0.00	0.33	4.18	10.65	0.12	0.00	98.00	2	37	62
MFT-San27 - 25	Core	63.87	0.08	19.08	0.13	0.01	0.32	4.05	10.66	0.15	0.03	98.36	2	36	62
MFT-San27 - 26	Rim	63.49	0.06	19.05	0.10	0.00	0.30	4.07	10.65	0.11	0.00	97.83	1	36	62
MFT-San27 - 27	Rim	63.54	0.05	18.87	0.08	0.00	0.33	4.18	10.69	0.07	0.00	97.81	2	37	62
mount1-1-1	Rim	65.2	0.0	19.4	bdl	0.1	0.4	4.2	9.2			98.5	2	40	58
mount1-1-3	Core	64.9	0.1	19.6	bdl	0.1	0.4	4.1	9.1			98.2	2	40	58
mount1-5-1	Rim	65.4	0.1	19.3	bdl	0.1	0.3	4.2	9.4			98.9	2	40	58
mount1-5-2	Core	65.5	0.1	19.4	0.1	0.0	0.4	4.2	9.2			98.8	2	40	58
mount1-6-1	Rim	64.9	0.1	19.8	bdl	0.1	0.5	4.2	9.0			98.6	3	40	57
mount2-10-1	Rim	65.0	0.0	19.3	0.1	0.0	0.5	4.3	9.0			98.2	3	41	57
mount2-10-2	Core	65.0	0.1	19.5	bdl	0.1	0.5	4.1	9.0			98.1	2	40	58
mount2-14-1	Rim	65.5	0.0	19.1	bdl	0.1	0.4	4.0	9.2			98.3	2	39	59
mount2-14-2	Rim	65.5	0.0	19.1	bdl	0.1	0.4	4.0	9.3			98.3	2	39	59
mount2-14-3	Core	66.4	0.0	19.1	bdl	0.1	0.3	4.0	9.2			99.3	2	39	59
mount2-14-4	Core	66.3	0.0	19.2	bdl	0.1	0.4	4.1	9.2			99.2	2	40	58
mount2-14-5	Core	66.0	0.0	19.2	bdl	0.1	0.3	4.1	9.2			99.0	2	39	59
mount2-14-6	Rim	66.2	0.0	19.1	0.1	0.0	0.4	4.1	9.2			99.1	2	40	58
mount2-14-7	Rim	66.4	0.0	19.2	bdl	0.1	0.4	4.1	9.3			99.6	2	39	59
mount1-15-1	Rim	65.2	0.0	19.2	bdl	0.1	0.4	4.2	9.5			98.6	2	39	59
mount1-16-1	Rim	65.1	0.0	19.2	bdl	0.1	0.4	4.2	9.4			98.5	2	40	58
mount1-16-2	Core	65.3	0.0	19.3	bdl	0.1	0.4	4.2	9.4			98.7	2	40	58
mount1-17-1	Rim	65.1	0.0	19.4	bdl	0.1	0.4	4.2	9.3			98.4	2	40	58
mount1-17-3	Rim	64.7	0.1	19.8	bdl	0.1	0.5	4.2	8.9			98.2	3	41	57
mount1-18-2	Core	65.7	0.0	19.2	bdl	0.1	0.4	4.3	9.3			98.9	2	40	58
mount1-19-1	Rim	64.8	0.1	19.5	bdl	0.1	0.4	4.2	9.0			98.2	2	41	57
mount1-22-1	Rim	65.2	0.1	19.2	bdl	0.1	0.4	4.2	9.2			98.4	2	40	58
mount1-22-2	Core	64.6	0.1	19.5	0.1	0.0	0.4	4.2	9.1			98.0	2	40	57
mount2-8-1	Rim	65.7	0.0	19.1	bdl	0.1	0.4	4.1	9.2			98.6	2	40	58
mount2-8-2	Core	65.3	0.0	18.9	bdl	0.1	0.4	4.0	9.2			98.0	2	39	59
mount2-8-3	Core	65.5	0.0	19.3	bdl	0.1	0.4	4.1	9.1			98.5	2	40	58
mount2-8-4	Rim	65.5	0.1	19.0	bdl	0.1	0.4	4.1	9.1			98.4	2	40	58
mount2-16-2	Rim	65.6	0.0	19.4	bdl	0.1	0.4	4.0	9.2			98.8	2	39	59
mount2-16-3	Core	65.0	0.1	19.3	0.1	0.0	0.4	4.1	8.9			98.0	2	40	57
mount2-16-4	Core	65.5	0.0	19.1	0.1	0.0	0.4	4.0	9.0			98.1	2	40	58
mount2-16-5	Core	65.5	0.1	19.3	bdl	0.1	0.4	4.1	9.0			98.5	2	40	58
mount2-20-1	Rim	66.2	0.0	19.2	0.1	0.0	0.3	4.1	9.2			99.2	2	40	58
mount2-20-2	Core	66.4	0.1	19.3	bdl	0.1	0.4	4.0	9.1			99.4	2	39	59
mount2-20-3	Core	66.7	0.0	19.2	bdl	0.1	0.4	4.1	9.3			99.7	2	39	59
mount2-20-4	Rim	66.2	0.1	19.1	0.1	0.0	0.4	4.1	9.2			99.1	2	39	59
mount2-20-5	Core	66.1	0.0	19.2	0.1	0.0	0.4	4.0	9.3			99.1	2	39	59
mount2-21-1	Rim	66.0	0.0	19.1	0.1	0.0	0.4	4.0	9.3			98.9	2	39	59
mount2-21-2	Core	66.0	0.0	19.2	bdl	0.1	0.4	4.0	9.4			99.0	2	38	60
mount2-22-1	Rim	65.8	0.1	19.2	bdl	0.1	0.4	4.0	9.2			98.8	2	39	59
mount2-22-2	Core	65.5	0.1	19.2	bdl	0.1	0.4	4.0	9.1			98.3	2	39	59
mount2-28-2	Rim	66.0	0.0	19.0	bdl	0.1	0.4	4.1	9.0			98.7	2	40	58
mount2-28-3	Rim	65.7	0.0	19.2	0.1	0.0	0.4	4.1	9.0			98.5	2	40	57
mount2-28-4	Core	65.6	0.0	19.1	0.1	0.0	0.4	4.0	8.9			98.1	2	40	58
mount2-28-5	Core	65.5	0.0	19.2	bdl	0.1	0.4	4.1	9.2			98.4	2	40	58
mount2-28-6	Core	65.8	0.0	19.2	0.1	0.0	0.4	4.0	9.1			98.7	2	39	59

Table A1.5: Trace elements - saninde

Info	Position	Li6	Li7	Na	Mg	Al	Si	P	K	Ca	Sc	Ti	V	Mn	Fe	Rb	Sr	Y	Zr	Nb	Cs	Ba	La	Ce	Pr	Nd	Sm	Eu	Gd	Th	Dy	Ho
MFT-grain1-5	Rim	b.d.l.	1.6	32218.0	25.5	97575	303853	b.d.l.	74793	42670	0.6	34.2	b.d.l.	b.d.l.	7250	89.0	287.0	0.1	0.3	0.1	0.0	4440	4.7	2.9	0.1	0.2	0.0	7.6	b.d.l.	b.d.l.	b.d.l.	b.d.l.
MFT-grain1-6	Rim	b.d.l.	2.7	31806.4	b.d.l.	96432	303853	b.d.l.	78614	4055.8	1.1	46.3	b.d.l.	0.8	746.1	74.5	266.6	b.d.l.	b.d.l.	b.d.l.	b.d.l.	4196	5.3	2.4	0.1	0.2	b.d.l.	7.1	b.d.l.	b.d.l.	b.d.l.	b.d.l.
MFT-grain1-7	Rim	b.d.l.	3.4	30254.2	b.d.l.	96002	303853	b.d.l.	78443	3290.2	0.8	69.7	b.d.l.	0.9	714.7	99.5	237.4	b.d.l.	b.d.l.	b.d.l.	b.d.l.	3092	7.1	4.8	0.2	0.5	b.d.l.	6.1	b.d.l.	b.d.l.	b.d.l.	b.d.l.
MFT-grain1-8	Rim	b.d.l.	3.8	29595.6	b.d.l.	97400	303853	b.d.l.	79698	3585.1	0.9	67.1	b.d.l.	0.9	764.8	98.4	234.7	b.d.l.	b.d.l.	b.d.l.	b.d.l.	3076	7.4	5.4	0.3	0.5	0.0	6.1	b.d.l.	b.d.l.	b.d.l.	b.d.l.
MFT-grain1-9	Rim	b.d.l.	3.7	29366.1	b.d.l.	94180	303853	29.1	77327	2954.0	b.d.l.	70.8	b.d.l.	b.d.l.	714.3	98.5	229.6	b.d.l.	b.d.l.	b.d.l.	b.d.l.	3211	7.5	5.2	0.2	0.6	b.d.l.	6.1	b.d.l.	b.d.l.	b.d.l.	b.d.l.
MFT-grain1-10	Rim	b.d.l.	4.0	30038.7	b.d.l.	95851	303853	b.d.l.	79696	3492.7	0.9	73.3	b.d.l.	b.d.l.	751.9	100.8	229.8	b.d.l.	b.d.l.	b.d.l.	b.d.l.	3500	8.0	5.5	0.3	0.4	b.d.l.	6.2	b.d.l.	b.d.l.	b.d.l.	b.d.l.
MFT-grain1-11	Rim	b.d.l.	4.2	29959.5	b.d.l.	95387	303853	b.d.l.	79267	3130.3	0.8	73.5	b.d.l.	b.d.l.	772.3	99.1	221.8	b.d.l.	b.d.l.	b.d.l.	b.d.l.	3548	7.5	5.2	0.2	0.4	0.0	6.4	b.d.l.	b.d.l.	b.d.l.	b.d.l.
MFT-grain1-12	Rim	b.d.l.	4.1	29610.2	7.0	96048	303853	b.d.l.	79294	3011.4	1.0	74.5	b.d.l.	1.1	701.1	99.5	219.2	0.0	b.d.l.	b.d.l.	b.d.l.	3493	7.4	5.2	0.3	0.5	b.d.l.	6.0	b.d.l.	b.d.l.	b.d.l.	b.d.l.
MFT-grain1-13	Rim	b.d.l.	3.3	30893.4	b.d.l.	96681	303853	14.0	79307	2974.0	b.d.l.	77.5	b.d.l.	0.9	759.3	100.5	221.4	b.d.l.	b.d.l.	b.d.l.	b.d.l.	3491	7.5	5.1	0.2	0.5	b.d.l.	5.8	b.d.l.	b.d.l.	b.d.l.	b.d.l.
MFT-grain1-14	Rim	b.d.l.	3.5	30032.6	b.d.l.	95589	303853	29.3	79525	2964.8	0.8	74.0	b.d.l.	b.d.l.	756.9	100.1	218.9	0.0	b.d.l.	b.d.l.	b.d.l.	3758	7.2	5.2	0.3	0.4	0.0	5.7	b.d.l.	b.d.l.	b.d.l.	b.d.l.
MFT-grain1-15	Rim	b.d.l.	3.4	30244.9	6.4	93919	303853	19.6	78270	2749.0	0.8	68.8	b.d.l.	b.d.l.	747.0	99.4	208.9	b.d.l.	b.d.l.	b.d.l.	b.d.l.	3914	7.3	5.1	0.2	0.4	b.d.l.	5.8	b.d.l.	b.d.l.	b.d.l.	b.d.l.
MFT-grain1-16	Core	b.d.l.	4.1	30156.3	b.d.l.	96673	303853	b.d.l.	81093	2805.5	0.6	75.9	b.d.l.	0.7	765.3	100.8	212.6	b.d.l.	b.d.l.	b.d.l.	b.d.l.	4355	7.6	4.9	0.3	0.5	b.d.l.	5.8	b.d.l.	b.d.l.	b.d.l.	b.d.l.
MFT-grain1-17	Core	b.d.l.	4.6	29429.5	4.6	94420	303853	19.2	78723	3010.0	0.9	70.3	b.d.l.	0.8	766.8	101.0	209.0	0.1	b.d.l.	b.d.l.	b.d.l.	4399	7.2	4.9	0.2	0.5	b.d.l.	5.5	b.d.l.	b.d.l.	b.d.l.	b.d.l.
MFT-grain1-18	Core	b.d.l.	4.9	29038.7	b.d.l.	95236	303853	b.d.l.	79186	2867.6	b.d.l.	70.3	b.d.l.	b.d.l.	749.5	98.9	204.8	b.d.l.	b.d.l.	b.d.l.	b.d.l.	4180	7.5	5.2	0.2	0.4	b.d.l.	5.8	b.d.l.	b.d.l.	b.d.l.	b.d.l.
MFT-grain1-19	Core	b.d.l.	5.3	30080.2	b.d.l.	97389	303853	42.8	81748	3053.8	1.1	66.6	b.d.l.	b.d.l.	818.8	103.6	209.9	0.0	b.d.l.	b.d.l.	b.d.l.	4703	7.6	5.2	0.3	0.4	b.d.l.	5.7	b.d.l.	b.d.l.	b.d.l.	b.d.l.
MFT-grain1-20	Core	b.d.l.	5.1	30681.7	4.8	97511	303853	42.8	81581	3289.5	1.0	76.5	b.d.l.	b.d.l.	765.3	102.0	211.8	0.0	b.d.l.	b.d.l.	b.d.l.	4797	8.1	5.3	0.3	0.3	b.d.l.	5.5	b.d.l.	b.d.l.	b.d.l.	b.d.l.
MFT-grain1-21	Core	b.d.l.	5.3	29849.4	b.d.l.	93321	303853	25.9	81090	2443.7	0.7	71.9	b.d.l.	b.d.l.	785.7	103.2	193.1	b.d.l.	b.d.l.	b.d.l.	b.d.l.	5271	7.1	4.9	0.2	0.5	b.d.l.	5.1	b.d.l.	b.d.l.	b.d.l.	b.d.l.
MFT-grain1-22	Core	b.d.l.	5.5	30229.7	b.d.l.	96024	303853	b.d.l.	82500	2537.0	0.8	71.8	b.d.l.	0.9	813.8	107.2	196.7	b.d.l.	b.d.l.	b.d.l.	b.d.l.	5677	7.6	5.0	0.2	0.4	b.d.l.	5.5	b.d.l.	b.d.l.	b.d.l.	b.d.l.
MFT-grain1-23	Core	b.d.l.	4.8	30160.4	b.d.l.	97884	303853	b.d.l.	80576	3043.2	0.7	75.2	b.d.l.	b.d.l.	770.3	101.0	210.1	b.d.l.	b.d.l.	b.d.l.	b.d.l.	5977	7.5	4.9	0.3	0.4	b.d.l.	6.1	b.d.l.	b.d.l.	b.d.l.	b.d.l.
MFT-grain1-30	Core	b.d.l.	5.1	30830.9	b.d.l.	95434	303853	b.d.l.	79284	3502.1	b.d.l.	83.3	b.d.l.	0.7	758.4	99.9	230.3	b.d.l.	b.d.l.	b.d.l.	b.d.l.	7573	8.7	5.8	0.3	0.5	b.d.l.	6.5	b.d.l.	b.d.l.	b.d.l.	b.d.l.
MFT-grain1-31	Core	b.d.l.	4.9	30708.0	b.d.l.	98612	303853	b.d.l.	79504	3540.6	0.8	85.5	b.d.l.	0.6	791.1	104.1	244.4	0.0	b.d.l.	b.d.l.	b.d.l.	7510	9.0	6.2	0.3	0.6	0.0	6.6	b.d.l.	b.d.l.	b.d.l.	b.d.l.
MFT-grain1-32	Core	b.d.l.	4.5	29255.1	b.d.l.	94602	303853	22.7	76840	3215.2	0.8	80.1	b.d.l.	b.d.l.	764.9	102.6	240.1	0.1	b.d.l.	b.d.l.	b.d.l.	7436	8.7	6.3	0.3	0.6	0.1	6.8	b.d.l.	b.d.l.	b.d.l.	b.d.l.
MFT-grain1-33	Core	b.d.l.	4.6	30112.6	b.d.l.	98239	303853	b.d.l.	80715	3364.0	0.8	82.4	b.d.l.	b.d.l.	778.8	102.9	239.0	0.0	0.1	b.d.l.	b.d.l.	7661	8.5	6.1	0.3	0.6	b.d.l.	6.7	b.d.l.	b.d.l.	b.d.l.	b.d.l.
MFT-grain1-34	Core	b.d.l.	4.3	29971.0	b.d.l.	96568	303853	b.d.l.	80880	3285.7	0.9	84.4	b.d.l.	0.8	744.3	102.1	237.3	b.d.l.	b.d.l.	b.d.l.	b.d.l.	7360	7.9	5.8	0.3	0.5	b.d.l.	6.4	b.d.l.	b.d.l.	b.d.l.	b.d.l.
MFT-grain1-35	Core	b.d.l.	5.4	29417.5	b.d.l.	98639	303853	27.1	79374	3265.6	0.7	80.7	b.d.l.	0.9	827.8	103.6	225.0	0.0	b.d.l.	b.d.l.	b.d.l.	8013	6.8	4.5	0.2	0.5	0.0	6.2	b.d.l.	b.d.l.	b.d.l.	b.d.l.
MFT-grain1-36	Core	b.d.l.	5.1	30302.7	b.d.l.	98537	303853	b.d.l.	78730	3684.2	0.8	85.1	b.d.l.	b.d.l.	777.7	98.3	263.0	b.d.l.	b.d.l.	b.d.l.	b.d.l.	9320	8.6	6.2	0.3	0.6	0.0	7.6	b.d.l.	b.d.l.	b.d.l.	b.d.l.
MFT-grain1-37	Core	b.d.l.	5.0	30768.8	5.3	100981	303853	b.d.l.	80531	3902.8	0.6	89.3	b.d.l.	b.d.l.	797.5	101.6	264.8	b.d.l.	b.d.l.	b.d.l.	b.d.l.	9444	9.0	6.2	0.3	0.4	b.d.l.	7.4	b.d.l.	b.d.l.	b.d.l.	b.d.l.
MFT-grain1-38	Core	b.d.l.	5.0	30924.6	b.d.l.	98339	303853	48.6	81090	3965.3	0.9	92.4	b.d.l.	0.7	793.2	98.7	265.2	0.0	b.d.l.	b.d.l.	b.d.l.	9384	9.1	6.0	0.3	0.6	0.0	7.6	b.d.l.	b.d.l.	b.d.l.	b.d.l.
MFT-grain1-39	Core	b.d.l.	4.7	30505.2	b.d.l.	101036	303853	b.d.l.	78938	4142.4	b.d.l.	94.7	b.d.l.	b.d.l.	823.3	100.9	265.4	0.0	b.d.l.	b.d.l.	b.d.l.	9461	9.0	6.2	0.3	0.7	0.0	7.3	b.d.l.	b.d.l.	b.d.l.	b.d.l.
MFT-grain1-40	Core	b.d.l.	5.2	29897.7	b.d.l.	95706	303853	19.2	81174	2699.2	0.9	81.1	b.d.l.	b.d.l.	796.8	111.0	218.5	0.0	0.1	0.0	b.d.l.	7694	6.7	4.8	0.2	0.7	b.d.l.	5.9	b.d.l.	b.d.l.	b.d.l.	b.d.l.
MFT-grain1-41	Core	b.d.l.	5.0	29139.2	b.d.l.	95874	303853	29.7	80552	3270.5	0.7	79.8	b.d.l.	0.6	781.9	102.4	217.9	b.d.l.	b.d.l.	b.d.l.	b.d.l.	7661	6.9	4.8	0.2	0.6	b.d.l.	6.3	b.d.l.	b.d.l.	b.d.l.	b.d.l.
MFT-grain1-42	Core	b.d.l.	5.6	30695.8	b.d.l.	99057	303853	b.d.l.	82424	2913.3	b.d.l.	77.4	b.d.l.	0.7	768.0	105.3	219.5	0.0	b.d.l.	b.d.l.	b.d.l.	7829	7.3	4.7	0.2	0.3	b.d.l.	6.2	b.d.l.	b.d.l.	b.d.l.	b.d.l.
MFT-grain1-43	Core	b.d.l.	5.2	29497.3	b.d.l.	96295	303853	23.2	81727	2523.3	b.d.l.	88.6	b.d.l.	b.d.l.	814.0	103.4	211.5	b.d.l.	b.d.l.	b.d.l.	b.d.l.	7893	6.6	4.5	0.2	0.4	b.d.l.	5.8	b.d.l.	b.d.l.	b.d.l.	b.d.l.
MFT-grain1-44	Core	b.d.l.	5.6	29444.8	b.d.l.	98248	303853	b.d.l.	80843	2852.3	1.1	88.6	b.d.l.	b.d.l.	793.3	106.9	212.4	0.0	b.d.l.	b.d.l.	b.d.l.	7943	7.0	4.6	0.2	0.4	0.1	5.7	b.d.l.	b.d.l.	b.d.l.	b.d.l.
MFT-grain1-45	Core	b.d.l.	5.8	30179.5	6.7	96936	303853	b.d.l.	79707	2954.4	b.d.l.	86.8	b.d.l.	b.d.l.	848.2	107.2	212.1	0.0	b.d.l.	b.d.l.	b.d.l.	8606	6.8	4.6	0.2	0.6	b.d.l.	6.0	b.d.l.	b.d.l.	b.d.l.	b.d.l.
MFT-grain1-46	Core	b.d.l.	5.5	29399.9	b.d.l.	96674	303853	18.1	76972	2742.7	0.8	84.6	b.d.l.	b.d.l.	768.9	100.2	223.9	b.d.l.	b.d.l.	b.d.l.	b.d.l.	9043	7.5	5.0	0.3	0.5	b.d.l.	6.6	b.d.l.	b.d.l.	b.d.l.	b.d.l.
MFT-grain1-47	Core	b.d.l.	5.2	30494.2	6.6	98666	303853	b.d.l.	79254	3728.7	0.7	91.0	b.d.l.	0.7	799.3	100.0	226.2	0.1	0.1	0.0	b.d.l.	10468	9.4	6.3	0.3	0.6	b.d.l.	7.2	b.d.l.	b.d.l.	b.d.l.	b.d.l.
MFT-grain1-48	Core	b.d.l.	5.6	30972.1	b.d.l.	98277	303853	23.0	79532	3692.9	b.d.l.	92.3	b.d.l.	b.d.l.	763.4	97.7	233.3	0.1	0.1	b.d.l.	b.d.l.	10288	9.1	6.2	0.3	0.6	b.d.l.	7.2	b.d.l.	b.d.l.	b.d.l.	b.d.l.
MFT-grain1-49</																																

Table A1.5: continued

Info	Position	Lj ^a	Lj ^b	Na	Mg	Al	Si	P	K	Ca	Sc	Ti	V	Mn	Fe	Rb	Sr	Y	Zr	Nb	Cs	Ba	La	Ce	Pr	Nd	Sm	Eu	Gd	Tb	Dy	Ho
MFT-grain1-55	Core	b.d.l.	5.9	30034.8	b.d.l.	987.82	299178	b.d.l.	77837	3298.9	b.d.l.	92.1	111.8	b.d.l.	0.8	853.7	100.6	246.4	0.0	b.d.l.	b.d.l.	0.0	1456	7.1	5.2	0.3	0.6	b.d.l.	6.9	b.d.l.	b.d.l.	b.d.l.
MFT-grain1-56	Core	b.d.l.	5.8	30058.4	8.6	991.73	299178	b.d.l.	72470	4989.8	1.1	111.8	b.d.l.	0.9	833.3	90.2	331.3	0.0	b.d.l.	b.d.l.	0.0	13856	10.6	8.3	0.5	0.8	b.d.l.	9.2	b.d.l.	b.d.l.	b.d.l.	
MFT-grain1-57	Core	b.d.l.	5.8	29962.7	b.d.l.	981.07	299178	b.d.l.	75270	4081.8	b.d.l.	105.8	b.d.l.	b.d.l.	866.5	96.7	280.4	0.1	b.d.l.	0.0	0.0	13357	7.7	5.3	0.3	0.6	b.d.l.	8.1	b.d.l.	b.d.l.	b.d.l.	
MFT-grain1-58	Core	b.d.l.	6.1	30394.3	b.d.l.	973.81	299178	29.0	75372	4325.0	0.6	116.6	b.d.l.	0.7	868.8	97.9	283.6	0.1	b.d.l.	b.d.l.	b.d.l.	13458	7.9	5.6	0.3	0.7	b.d.l.	8.0	b.d.l.	b.d.l.	b.d.l.	
MFT-grain1-59	Core	b.d.l.	6.1	30470.2	b.d.l.	992.12	299178	20.7	73726	3753.9	b.d.l.	104.3	b.d.l.	1.2	854.7	95.3	293.0	0.1	b.d.l.	0.0	0.0	13576	6.1	6.0	0.3	0.7	b.d.l.	8.3	b.d.l.	b.d.l.	b.d.l.	
Sandine grain 2 - Line 2																																
MFT-San1 - 1	Rim	2.4	2.0	30372.1	2.7	106930	308527	79.6	78080	2917.5	1.0	66.1	b.d.l.	b.d.l.	737.8	120.9	126.3	0.2	b.d.l.	b.d.l.	0.1	3220	6.4	4.5	0.2	0.5	b.d.l.	3.7	b.d.l.	b.d.l.	b.d.l.	
MFT-San1 - 2	Rim	2.7	3.2	29822.5	4.1	104592	308527	b.d.l.	75283	2748.9	b.d.l.	70.0	b.d.l.	b.d.l.	625.2	116.4	130.7	0.2	b.d.l.	b.d.l.	b.d.l.	3473	6.5	4.3	0.2	0.5	b.d.l.	3.7	b.d.l.	b.d.l.	b.d.l.	
MFT-San1 - 3	Rim	4.4	4.6	32120.8	1.6	112736	308527	b.d.l.	79851	3399.0	b.d.l.	68.5	b.d.l.	b.d.l.	734.1	123.1	145.3	0.2	0.1	b.d.l.	0.1	4046	7.2	5.0	0.2	0.4	b.d.l.	4.3	b.d.l.	b.d.l.	b.d.l.	
MFT-San1 - 4	Rim	3.3	5.5	30350.0	1.2	107538	308527	87.1	76018	3725.4	b.d.l.	74.5	b.d.l.	b.d.l.	746.9	119.3	146.0	0.3	0.1	0.0	0.1	4186	6.7	4.7	0.2	0.4	b.d.l.	4.4	b.d.l.	b.d.l.	b.d.l.	
MFT-San1 - 5	Rim	5.6	6.3	31126.9	1.7	110362	308527	82.1	78375	3220.5	b.d.l.	78.3	b.d.l.	b.d.l.	847.1	123.0	163.4	0.2	0.0	b.d.l.	b.d.l.	4809	7.1	5.0	0.3	0.5	b.d.l.	4.5	b.d.l.	b.d.l.	b.d.l.	
MFT-San1 - 6	Core	7.8	6.5	31584.6	2.4	110489	308527	b.d.l.	77852	3413.7	0.8	79.8	b.d.l.	b.d.l.	816.0	121.4	162.4	0.3	0.0	b.d.l.	0.2	5219	7.4	5.3	0.3	0.4	b.d.l.	4.5	b.d.l.	b.d.l.	b.d.l.	
MFT-San1 - 7	Core	7.3	6.5	30293.0	1.2	108596	308527	b.d.l.	75193	3171.9	b.d.l.	75.2	b.d.l.	b.d.l.	868.3	112.9	169.2	0.4	0.0	0.0	0.0	5800	7.7	5.4	0.3	0.5	b.d.l.	4.9	b.d.l.	b.d.l.	b.d.l.	
MFT-San1 - 8	Core	6.3	6.8	31661.2	3.0	112221	308527	b.d.l.	75607	3932.5	b.d.l.	77.4	b.d.l.	b.d.l.	842.1	118.3	179.7	0.4	0.0	0.0	0.1	6550	8.1	5.6	0.2	0.6	b.d.l.	5.5	b.d.l.	b.d.l.	b.d.l.	
MFT-San1 - 9	Core	7.6	6.9	33479.5	1.8	119038	308527	91.7	81400	3811.7	b.d.l.	80.9	b.d.l.	b.d.l.	891.1	122.2	198.4	0.4	b.d.l.	b.d.l.	0.2	8016	8.4	6.1	0.3	0.8	b.d.l.	5.9	b.d.l.	b.d.l.	b.d.l.	
MFT-San1 - 10	Core	7.0	6.3	30042.1	2.7	107705	308527	b.d.l.	73001	3412.1	b.d.l.	72.7	b.d.l.	b.d.l.	815.5	107.4	191.4	0.3	0.1	b.d.l.	b.d.l.	7736	8.2	5.4	0.2	0.5	b.d.l.	5.6	b.d.l.	b.d.l.	b.d.l.	
MFT-San1 - 11	Core	5.8	6.4	30398.8	1.2	108656	308527	49.3	75378	2745.9	b.d.l.	85.0	b.d.l.	b.d.l.	888.6	110.8	184.8	0.4	b.d.l.	b.d.l.	b.d.l.	8087	6.8	4.6	0.3	0.5	b.d.l.	5.5	b.d.l.	b.d.l.	b.d.l.	
MFT-San1 - 12	Core	6.6	5.8	30830.8	2.0	109790	308527	b.d.l.	73773	4501.6	b.d.l.	86.6	b.d.l.	b.d.l.	752.8	107.3	217.4	0.4	0.1	b.d.l.	b.d.l.	9129	8.2	6.1	0.3	0.6	b.d.l.	6.5	b.d.l.	b.d.l.	b.d.l.	
MFT-San1 - 13	Core	4.7	5.7	30252.7	3.4	107239	308527	b.d.l.	73609	3717.0	b.d.l.	86.6	b.d.l.	b.d.l.	841.5	105.7	213.4	0.5	0.1	0.0	b.d.l.	9311	7.9	5.8	0.4	0.6	b.d.l.	6.0	b.d.l.	b.d.l.	b.d.l.	
MFT-San1 - 14	Core	4.7	6.1	31224.5	b.d.l.	112374	308527	b.d.l.	75355	3523.7	0.7	94.4	b.d.l.	b.d.l.	807.5	110.2	206.5	0.7	b.d.l.	0.0	0.0	9720	8.1	5.6	0.3	0.6	b.d.l.	6.5	b.d.l.	b.d.l.	b.d.l.	
MFT-San1 - 15	Core	7.2	5.6	30928.0	2.5	111548	308527	b.d.l.	75129	3151.1	1.1	85.3	b.d.l.	b.d.l.	790.1	114.2	205.7	0.5	0.0	b.d.l.	b.d.l.	9925	7.9	5.3	0.3	0.6	0.1	6.1	b.d.l.	b.d.l.	b.d.l.	
MFT-San1 - 16	Core	6.0	5.7	29451.0	4.6	102003	308527	b.d.l.	70904	3705.3	0.6	81.2	b.d.l.	b.d.l.	763.9	103.4	201.0	0.9	b.d.l.	b.d.l.	0.0	9908	7.5	5.4	0.3	0.7	b.d.l.	6.3	b.d.l.	b.d.l.	b.d.l.	
MFT-San1 - 17	Core	5.6	5.9	29830.0	1.6	108435	308527	47.0	72027	3628.9	b.d.l.	90.1	b.d.l.	b.d.l.	881.8	106.9	232.9	0.6	b.d.l.	b.d.l.	b.d.l.	10848	8.5	6.0	0.3	0.7	b.d.l.	7.1	b.d.l.	b.d.l.	b.d.l.	
MFT-San1 - 18	Core	5.9	6.0	31901.2	2.0	113467	308527	50.2	74522	4022.6	b.d.l.	118.0	b.d.l.	b.d.l.	860.0	106.6	256.4	0.6	0.0	b.d.l.	0.0	11908	8.2	6.1	0.4	0.7	b.d.l.	7.7	b.d.l.	b.d.l.	b.d.l.	
MFT-San1 - 19	Core	6.6	6.0	31000.6	2.7	112119	308527	b.d.l.	71795	4424.6	b.d.l.	102.9	b.d.l.	b.d.l.	793.6	110.6	271.0	0.7	0.1	0.1	b.d.l.	12869	8.5	6.4	0.3	0.9	b.d.l.	7.8	b.d.l.	b.d.l.	b.d.l.	
MFT-San1 - 20	Core	7.0	5.9	31077.3	1.9	113293	308527	64.2	73260	4759.3	b.d.l.	105.9	b.d.l.	b.d.l.	834.8	101.3	281.1	0.7	b.d.l.	b.d.l.	b.d.l.	13378	7.8	5.7	0.3	0.9	b.d.l.	8.3	b.d.l.	b.d.l.	b.d.l.	
MFT-San1 - 21	Core	5.6	5.6	31422.5	b.d.l.	109286	308527	b.d.l.	69779	5342.0	b.d.l.	132.6	b.d.l.	b.d.l.	797.7	95.1	291.2	0.6	b.d.l.	0.0	b.d.l.	13792	7.2	5.6	0.3	0.5	b.d.l.	8.7	b.d.l.	b.d.l.	b.d.l.	
MFT-San1 - 22	Core	6.7	6.2	32835.0	3.0	113193	308527	b.d.l.	67910	6469.4	b.d.l.	105.8	b.d.l.	b.d.l.	817.0	91.2	317.8	0.7	b.d.l.	b.d.l.	b.d.l.	14358	7.0	6.0	0.4	0.9	b.d.l.	9.4	b.d.l.	b.d.l.	b.d.l.	
MFT-San1 - 23	Core	6.0	6.2	32110.4	5.8	113081	308527	b.d.l.	67547	6486.5	b.d.l.	120.6	b.d.l.	b.d.l.	709.8	90.3	330.6	0.8	0.0	0.0	b.d.l.	14737	7.6	5.9	0.3	1.0	b.d.l.	9.4	b.d.l.	b.d.l.	b.d.l.	
MFT-San1 - 24	Core	3.8	6.2	32315.5	2.3	112429	308527	b.d.l.	68800	6574.7	b.d.l.	119.9	b.d.l.	b.d.l.	822.1	93.0	327.1	0.6	0.1	b.d.l.	b.d.l.	14481	8.2	6.9	0.4	0.6	b.d.l.	9.1	b.d.l.	b.d.l.	b.d.l.	
MFT-San1 - 25	Core	7.3	6.0	31758.5	3.5	112284	308527	80.0	69272	5420.7	b.d.l.	117.4	b.d.l.	b.d.l.	848.7	94.4	301.0	0.6	b.d.l.	b.d.l.	0.1	14120	8.1	6.1	0.3	0.5	0.1	8.8	b.d.l.	b.d.l.	b.d.l.	
MFT-San1 - 26	Core	7.4	5.7	31363.5	b.d.l.	111602	308527	b.d.l.	71169	5253.7	0.8	103.3	b.d.l.	b.d.l.	855.0	96.0	299.0	0.7	b.d.l.	b.d.l.	0.1	13465	7.6	6.1	0.3	0.7	b.d.l.	8.4	b.d.l.	b.d.l.	b.d.l.	
MFT-San1 - 27	Core	4.1	5.2	30483.5	1.5	106803	308527	b.d.l.	66468	5207.6	0.7	102.0	b.d.l.	b.d.l.	742.8	91.6	298.7	0.4	b.d.l.	b.d.l.	b.d.l.	12921	9.2	7.4	0.4	1.0	b.d.l.	8.8	b.d.l.	b.d.l.	b.d.l.	
MFT-San1 - 28	Core	7.0	5.9	30131.9	1.5	109102	308527	54.0	71105	3572.2	b.d.l.	95.8	b.d.l.	b.d.l.	740.1	94.5	245.2	0.4	b.d.l.	0.0	0.0	10825	7.0	5.1	0.3	0.6	b.d.l.	7.2	b.d.l.	b.d.l.	b.d.l.	
MFT-San1 - 29	Core	6.4	6.1	31163.2	3.8	114324	308527	53.1	78534	3382.6	b.d.l.	83.6	b.d.l.	b.d.l.	920.3	112.5	215.9	0.5	0.0	b.d.l.	b.d.l.	8980	7.1	5.0	0.3	0.5	b.d.l.	6.3	b.d.l.	b.d.l.	b.d.l.	
MFT-San1 - 30	Core	4.9	6.1	30391.1	b.d.l.	109557	308527	b.d.l.	75440	3613.1	b.d.l.	72.2	b.d.l.	b.d.l.	769.3	103.7	215.4	0.5	b.d.l.	b.d.l.	0.1	8266	6.9	4.7	0.2	0.4	b.d.l.	6.1	b.d.l.	b.d.l.	b.d.l.	
MFT-San1 - 31	Core	7.1	6.1	31614.5	3.4	112133	308527	b.d.l.	75895	3426.1	b.d.l.	95.4	b.d.l.	b.d.l.	841.2	105.0	249.0	0.5	b.d.l.	0.0	0.0	7982	8.5	5.5	0.3	0.5	b.d.l.	7.0	b.d.l.	b.d.l.	0.0	
MFT-San1 - 32	Core	7.6	5.8	31519.4	b.d.l.	110503	308527	53.8	77484	3971.6	0.8	81.3	b.d.l.	b.d.l.	776.0	106.1	250.4	0.3	b.d.l.	b.d.l.	0.0	7343	8.4	5.8	0.3	0.6	b.d.l.	7.3	b.d.l.	b.d.l.	b.d.l.	
MFT-San1 - 33	Core	6.0	5.2	29798.3	2.6	106946	308527	57.3	74763	3015.0	0.8	70.1	b.d.l.	b.d.l.	807.0	103.9	197.5	0.2	b.d.l.	b.d.l.	b.d.l.	5197	6.2	4.1	0.2	0.4	b.d.l.	5.1	b.d.l.	b.d.l.	b.d.l.	
MFT-San1 - 34	Core	4.5	4.4	29326.6	0.7	104386	308527	58.4	7299																							

Table A1.5: continued

Er	Tm	Yb	Lu	Hf	Ta	Pb	Th	U
b.d.l.	b.d.l.	b.d.l.	b.d.l.	b.d.l.	b.d.l.	20.3	b.d.l.	b.d.l.
b.d.l.	b.d.l.	b.d.l.	b.d.l.	b.d.l.	b.d.l.	26.2	b.d.l.	b.d.l.
b.d.l.	b.d.l.	b.d.l.	b.d.l.	b.d.l.	b.d.l.	24.3	b.d.l.	b.d.l.
b.d.l.	b.d.l.	b.d.l.	b.d.l.	b.d.l.	b.d.l.	23.8	b.d.l.	b.d.l.
b.d.l.	b.d.l.	b.d.l.	b.d.l.	b.d.l.	b.d.l.	23.8	b.d.l.	b.d.l.
b.d.l.	b.d.l.	b.d.l.	b.d.l.	b.d.l.	0.0	24.2	b.d.l.	b.d.l.
b.d.l.	b.d.l.	b.d.l.	b.d.l.	b.d.l.	b.d.l.	25.6	b.d.l.	b.d.l.
b.d.l.	b.d.l.	b.d.l.	b.d.l.	b.d.l.	b.d.l.	28.4	b.d.l.	b.d.l.
b.d.l.	b.d.l.	b.d.l.	b.d.l.	b.d.l.	b.d.l.	26.9	b.d.l.	b.d.l.
b.d.l.	b.d.l.	b.d.l.	b.d.l.	0.0	0.0	26.8	b.d.l.	b.d.l.
b.d.l.	b.d.l.	b.d.l.	b.d.l.	0.0	b.d.l.	26.1	b.d.l.	b.d.l.
b.d.l.	b.d.l.	b.d.l.	b.d.l.	b.d.l.	b.d.l.	27.2	b.d.l.	b.d.l.
b.d.l.	b.d.l.	b.d.l.	b.d.l.	b.d.l.	0.0	27.2	b.d.l.	b.d.l.
b.d.l.	b.d.l.	b.d.l.	b.d.l.	b.d.l.	0.0	29.8	b.d.l.	b.d.l.
b.d.l.	b.d.l.	b.d.l.	b.d.l.	b.d.l.	0.0	25.1	b.d.l.	b.d.l.
b.d.l.	b.d.l.	b.d.l.	b.d.l.	0.0	b.d.l.	23.5	b.d.l.	b.d.l.
b.d.l.	b.d.l.	b.d.l.	b.d.l.	b.d.l.	b.d.l.	26.2	b.d.l.	b.d.l.
b.d.l.	b.d.l.	b.d.l.	b.d.l.	0.1	0.0	24.7	b.d.l.	b.d.l.
b.d.l.	b.d.l.	b.d.l.	b.d.l.	b.d.l.	b.d.l.	24.2	b.d.l.	b.d.l.
b.d.l.	b.d.l.	b.d.l.	b.d.l.	0.0	0.0	23.3	b.d.l.	b.d.l.
b.d.l.	b.d.l.	b.d.l.	b.d.l.	b.d.l.	b.d.l.	22.6	b.d.l.	b.d.l.
b.d.l.	b.d.l.	b.d.l.	b.d.l.	0.1	b.d.l.	23.7	b.d.l.	b.d.l.
b.d.l.	b.d.l.	b.d.l.	b.d.l.	0.1	b.d.l.	26.2	b.d.l.	b.d.l.
b.d.l.	b.d.l.	b.d.l.	b.d.l.	b.d.l.	b.d.l.	25.9	b.d.l.	b.d.l.
b.d.l.	b.d.l.	b.d.l.	b.d.l.	b.d.l.	0.0	27.5	b.d.l.	b.d.l.
b.d.l.	b.d.l.	b.d.l.	b.d.l.	b.d.l.	b.d.l.	27.4	b.d.l.	b.d.l.
b.d.l.	b.d.l.	b.d.l.	b.d.l.	0.0	0.0	28.9	b.d.l.	b.d.l.
b.d.l.	b.d.l.	b.d.l.	b.d.l.	0.1	b.d.l.	28.3	b.d.l.	b.d.l.
b.d.l.	b.d.l.	b.d.l.	b.d.l.	0.2	0.1	26.4	b.d.l.	b.d.l.
b.d.l.	b.d.l.	b.d.l.	b.d.l.	0.0	b.d.l.	27.8	b.d.l.	b.d.l.
b.d.l.	b.d.l.	b.d.l.	b.d.l.	b.d.l.	0.0	28.0	b.d.l.	b.d.l.
b.d.l.	b.d.l.	b.d.l.	b.d.l.	b.d.l.	b.d.l.	25.8	b.d.l.	b.d.l.
b.d.l.	b.d.l.	b.d.l.	b.d.l.	0.0	0.0	23.6	b.d.l.	b.d.l.
b.d.l.	b.d.l.	b.d.l.	b.d.l.	b.d.l.	b.d.l.	19.6	b.d.l.	b.d.l.
b.d.l.	b.d.l.	b.d.l.	b.d.l.	b.d.l.	b.d.l.	20.2	b.d.l.	b.d.l.
b.d.l.	b.d.l.	b.d.l.	b.d.l.	b.d.l.	b.d.l.	23.6	0.0	0.0
b.d.l.	b.d.l.	b.d.l.	b.d.l.	b.d.l.	0.0	24.7	0.0	b.d.l.
b.d.l.	b.d.l.	b.d.l.	0.0	b.d.l.	0.1	18.5	b.d.l.	b.d.l.
b.d.l.	b.d.l.	b.d.l.	b.d.l.	b.d.l.	0.0	17.2	b.d.l.	b.d.l.
b.d.l.	b.d.l.	b.d.l.	b.d.l.	0.1	b.d.l.	19.5	b.d.l.	0.0
b.d.l.	b.d.l.	b.d.l.	b.d.l.	0.1	b.d.l.	18.8	b.d.l.	b.d.l.
0.1	b.d.l.	b.d.l.	b.d.l.	b.d.l.	0.0	19.1	0.0	b.d.l.
b.d.l.	0.0	b.d.l.	b.d.l.	b.d.l.	0.1	20.8	b.d.l.	b.d.l.
b.d.l.	b.d.l.	b.d.l.	b.d.l.	b.d.l.	0.0	22.4	b.d.l.	b.d.l.
b.d.l.	b.d.l.	b.d.l.	0.0	0.1	b.d.l.	20.4	0.0	b.d.l.
b.d.l.	b.d.l.	b.d.l.	b.d.l.	b.d.l.	0.0	23.1	b.d.l.	b.d.l.
0.0	b.d.l.	b.d.l.	b.d.l.	0.0	0.0	20.3	b.d.l.	b.d.l.
b.d.l.	b.d.l.	b.d.l.	b.d.l.	0.1	b.d.l.	20.3	b.d.l.	b.d.l.
b.d.l.	b.d.l.	b.d.l.	b.d.l.	b.d.l.	b.d.l.	21.9	b.d.l.	0.0
b.d.l.	b.d.l.	b.d.l.	b.d.l.	0.1	0.1	21.4	b.d.l.	b.d.l.
b.d.l.	b.d.l.	b.d.l.	b.d.l.	b.d.l.	b.d.l.	20.7	0.0	0.0

Table A1.5: continued

Info	Position	L [†]	Na	Mg	Al	Si	P	K	Ca	Sc	Ti	V	Mn	Fe	Rb	Sr	Y	Zr	Nb	Cs	Ba	La	Ce	Pr	Nd	Sm	Eu	Gd	Tb	Dy	Ho
MFT-San1-47	Core	4.9	4.6	29915.6	0.4	103344	308527	74894	3196.6	b.d.l.	78.6	b.d.l.	11.4	794.1	97.9	214.6	b.d.l.	b.d.l.	0.1	b.d.l.	2243	7.3	5.2	0.2	0.4	b.d.l.	5.5	b.d.l.	b.d.l.	b.d.l.	
MFT-San1-48	Core	4.0	4.6	30056.5	2.2	105145	308527	74172	3413.3	b.d.l.	83.8	b.d.l.	b.d.l.	765.2	99.6	216.3	0.1	b.d.l.	0.0	b.d.l.	2580	7.5	4.6	0.2	0.4	b.d.l.	5.3	b.d.l.	b.d.l.	b.d.l.	
Sandstone grain 5 - Line 1																															
grain5-1	Core	b.d.l.	5.7	30786.5	b.d.l.	99504	308527	84116	3166.4	b.d.l.	65.9	b.d.l.	b.d.l.	722.7	121.0	128.3	b.d.l.	b.d.l.	b.d.l.	0.1	1985	6.6	4.5	0.2	0.5	b.d.l.	3.7	b.d.l.	b.d.l.	b.d.l.	
grain5-2	Core	b.d.l.	5.7	31046.4	b.d.l.	99092	308527	82542	2904.3	0.7	69.2	b.d.l.	1.1	730.6	118.0	130.3	b.d.l.	b.d.l.	b.d.l.	0.1	1959	6.7	4.5	0.2	0.4	0.0	3.4	b.d.l.	b.d.l.	b.d.l.	
grain5-3	Core	b.d.l.	5.7	31269.8	b.d.l.	100515	308527	88117	2881.6	b.d.l.	68.7	b.d.l.	b.d.l.	720.8	123.8	127.3	b.d.l.	b.d.l.	b.d.l.	0.1	1983	6.7	4.6	0.2	0.5	b.d.l.	3.8	b.d.l.	b.d.l.	b.d.l.	
grain5-4	Core	b.d.l.	5.8	30834.5	b.d.l.	98060	308527	83327	2953.8	b.d.l.	71.4	b.d.l.	b.d.l.	757.0	119.6	123.0	b.d.l.	b.d.l.	b.d.l.	0.1	1987	6.7	4.6	0.2	0.4	0.1	3.3	b.d.l.	b.d.l.	b.d.l.	
grain5-5	Core	b.d.l.	5.3	30292.7	b.d.l.	96415	308527	81293	3038.4	b.d.l.	68.5	b.d.l.	b.d.l.	710.8	119.7	123.0	b.d.l.	b.d.l.	b.d.l.	0.1	1979	6.5	4.6	0.2	0.4	0.0	3.5	b.d.l.	b.d.l.	b.d.l.	
grain5-6	Core	b.d.l.	5.1	29676.1	b.d.l.	95965	308527	80523	2691.7	b.d.l.	73.2	b.d.l.	b.d.l.	676.5	116.3	115.6	b.d.l.	b.d.l.	b.d.l.	0.1	1972	6.5	4.3	0.2	0.4	0.0	3.2	b.d.l.	b.d.l.	b.d.l.	
grain5-7	Core	b.d.l.	5.5	31443.7	9.7	99827	308527	83332	2644.8	b.d.l.	69.9	b.d.l.	1.0	695.1	121.7	118.0	0.0	b.d.l.	b.d.l.	0.1	2054	6.8	4.5	0.2	0.5	b.d.l.	3.6	b.d.l.	b.d.l.	b.d.l.	
grain5-8	Core	b.d.l.	5.2	30664.6	6.4	93986	303853	80942	2425.8	0.8	66.7	b.d.l.	0.7	698.9	116.2	109.5	b.d.l.	b.d.l.	b.d.l.	0.1	1914	5.9	4.3	0.2	0.4	b.d.l.	3.1	b.d.l.	b.d.l.	b.d.l.	
grain5-9	Core	b.d.l.	5.2	30454.0	b.d.l.	97873	308527	88413	2730.1	b.d.l.	71.7	b.d.l.	0.7	716.3	121.5	114.3	b.d.l.	b.d.l.	b.d.l.	0.1	2044	6.4	4.4	0.2	0.4	0.0	3.1	b.d.l.	b.d.l.	b.d.l.	
grain5-10	Core	b.d.l.	5.6	30595.2	b.d.l.	99333	308527	81767	3135.8	b.d.l.	71.8	b.d.l.	b.d.l.	661.1	127.8	111.7	b.d.l.	b.d.l.	b.d.l.	0.1	2041	6.4	4.5	0.2	0.4	0.1	3.2	b.d.l.	b.d.l.	b.d.l.	
grain5-11	Core	b.d.l.	5.4	31750.9	b.d.l.	95994	308527	83039	2949.9	b.d.l.	70.0	b.d.l.	0.9	784.3	128.6	111.7	b.d.l.	b.d.l.	b.d.l.	0.1	2034	6.4	4.5	0.2	0.4	0.1	3.2	b.d.l.	b.d.l.	b.d.l.	
grain5-12	Core	b.d.l.	5.4	30685.1	b.d.l.	100679	308527	84776	2960.1	0.6	78.5	b.d.l.	b.d.l.	689.6	120.8	113.8	b.d.l.	b.d.l.	b.d.l.	0.1	2092	6.6	4.4	0.2	0.4	0.0	3.3	b.d.l.	b.d.l.	b.d.l.	
grain5-13	Core	b.d.l.	5.0	31360.7	b.d.l.	100168	308527	84247	2951.5	0.7	73.5	0.1	b.d.l.	751.1	121.9	112.0	0.0	b.d.l.	b.d.l.	0.1	2080	6.7	4.4	0.2	0.4	0.1	3.3	b.d.l.	b.d.l.	b.d.l.	
grain5-14	Core	b.d.l.	5.3	30504.6	b.d.l.	98498	308527	84241	2783.9	b.d.l.	68.9	b.d.l.	b.d.l.	684.6	119.0	107.2	b.d.l.	b.d.l.	0.0	0.1	2019	6.5	4.3	0.2	0.4	b.d.l.	3.0	b.d.l.	b.d.l.	0.0	
grain5-15	Core	b.d.l.	5.2	30258.9	b.d.l.	99053	308527	82817	2603.0	b.d.l.	70.2	b.d.l.	1.0	692.0	118.0	105.3	0.0	b.d.l.	b.d.l.	0.1	2016	6.3	4.4	0.2	0.4	b.d.l.	3.3	b.d.l.	b.d.l.	b.d.l.	
grain5-16	Core	b.d.l.	5.4	31965.5	8.0	101174	308527	84912	3105.5	b.d.l.	66.7	b.d.l.	b.d.l.	725.0	121.5	111.5	b.d.l.	b.d.l.	b.d.l.	0.1	2087	6.7	4.6	0.2	0.5	b.d.l.	3.4	b.d.l.	b.d.l.	b.d.l.	
grain5-17	Core	b.d.l.	5.6	31564.0	8.8	100244	308527	84879	2810.0	1.0	76.3	b.d.l.	b.d.l.	716.5	126.7	112.6	b.d.l.	b.d.l.	b.d.l.	0.1	2071	6.6	4.4	0.2	0.4	b.d.l.	3.2	b.d.l.	b.d.l.	b.d.l.	
grain5-18	Core	b.d.l.	5.0	30549.6	b.d.l.	97235	303853	84433	2440.6	b.d.l.	79.9	b.d.l.	b.d.l.	696.1	120.4	109.0	b.d.l.	b.d.l.	0.0	0.1	2024	6.4	4.3	0.2	0.5	0.0	3.2	b.d.l.	b.d.l.	b.d.l.	
grain5-19	Core	b.d.l.	5.1	31406.8	b.d.l.	100006	308527	85001	3080.4	b.d.l.	69.0	b.d.l.	b.d.l.	710.7	122.7	111.4	b.d.l.	b.d.l.	b.d.l.	0.1	2052	6.5	4.5	0.2	0.5	0.1	3.4	b.d.l.	b.d.l.	b.d.l.	
grain5-20	Core	b.d.l.	5.3	32153.5	7.9	99979	308527	83933	3038.2	0.6	70.1	b.d.l.	b.d.l.	705.9	120.6	112.3	b.d.l.	b.d.l.	b.d.l.	0.1	2031	6.6	4.5	0.2	0.5	0.1	3.3	b.d.l.	b.d.l.	b.d.l.	
grain5-21	Core	b.d.l.	4.7	30946.5	b.d.l.	99005	308527	83785	2982.5	0.6	67.3	b.d.l.	1.1	724.8	120.0	112.3	b.d.l.	b.d.l.	b.d.l.	0.1	2045	6.5	4.5	0.2	0.5	b.d.l.	3.2	b.d.l.	b.d.l.	b.d.l.	
grain5-22	Core	b.d.l.	4.9	32444.4	b.d.l.	99567	308527	84827	3287.2	b.d.l.	75.5	b.d.l.	b.d.l.	763.6	120.4	112.6	b.d.l.	b.d.l.	b.d.l.	0.1	2081	6.3	4.6	0.2	0.4	b.d.l.	3.3	b.d.l.	b.d.l.	b.d.l.	
grain5-23	Rim	b.d.l.	3.9	30940.3	b.d.l.	100766	308527	82886	2854.2	b.d.l.	72.4	b.d.l.	b.d.l.	728.2	119.3	111.3	b.d.l.	b.d.l.	b.d.l.	0.1	2094	6.8	4.5	0.2	0.5	b.d.l.	3.4	b.d.l.	b.d.l.	b.d.l.	
grain5-24	Rim	b.d.l.	3.5	30263.9	b.d.l.	92941	308527	79036	2997.0	b.d.l.	72.4	b.d.l.	0.9	722.0	117.8	110.4	b.d.l.	b.d.l.	b.d.l.	0.1	1940	6.5	4.4	0.2	0.6	b.d.l.	3.1	b.d.l.	b.d.l.	b.d.l.	
grain5-25	Rim	b.d.l.	2.9	31522.5	b.d.l.	101714	303853	80765	3031.6	b.d.l.	72.8	b.d.l.	b.d.l.	721.7	113.8	120.9	0.0	b.d.l.	b.d.l.	0.1	2052	7.3	4.9	0.2	0.5	0.0	3.5	b.d.l.	b.d.l.	b.d.l.	
grain5-26	Rim	b.d.l.	2.2	30249.3	b.d.l.	97600	303853	79284	2855.5	b.d.l.	69.4	b.d.l.	b.d.l.	703.2	115.6	118.2	b.d.l.	b.d.l.	b.d.l.	0.1	1953	6.8	4.7	0.2	0.4	b.d.l.	3.6	b.d.l.	b.d.l.	b.d.l.	
grain5-27	Rim	b.d.l.	2.4	29753.1	b.d.l.	96238	303853	78034	3034.3	b.d.l.	68.2	b.d.l.	b.d.l.	703.2	110.9	119.6	b.d.l.	b.d.l.	b.d.l.	0.1	1873	7.0	4.8	0.2	0.4	b.d.l.	3.5	b.d.l.	b.d.l.	b.d.l.	
Sandstone grain 5 - Line 2																															
MFT-San5-1	Rim	3.7	3.6	28590.7	1.2	107250	308527	73987	2667.2	b.d.l.	61.8	b.d.l.	b.d.l.	675.7	121.1	61.3	b.d.l.	b.d.l.	b.d.l.	0.1	821	6.2	4.4	0.2	0.4	b.d.l.	2.3	b.d.l.	b.d.l.	b.d.l.	
MFT-San5-2	Core	2.7	3.7	29289.1	2.4	105892	308527	75017	2238.8	0.7	71.8	b.d.l.	b.d.l.	708.5	127.4	71.2	b.d.l.	b.d.l.	b.d.l.	0.1	1090	6.1	4.4	0.3	0.4	b.d.l.	2.6	0.1	b.d.l.	b.d.l.	
MFT-San5-3	Core	3.4	3.8	31024.3	2.0	110440	308527	78523	2464.8	0.7	64.8	b.d.l.	b.d.l.	745.3	129.1	87.7	0.1	b.d.l.	b.d.l.	0.0	1500	6.7	4.4	0.3	0.5	b.d.l.	3.0	b.d.l.	b.d.l.	b.d.l.	
MFT-San5-4	Core	5.5	4.4	30804.7	1.3	112288	308527	79389	3027.9	b.d.l.	76.5	b.d.l.	1.2	774.2	130.4	96.9	0.1	0.1	b.d.l.	0.1	2106	6.6	4.6	0.2	0.4	0.1	3.1	b.d.l.	b.d.l.	b.d.l.	
MFT-San5-5	Core	5.1	4.8	30733.9	1.5	109072	308527	79189	3124.6	b.d.l.	68.2	b.d.l.	b.d.l.	793.3	125.8	112.5	0.3	0.0	b.d.l.	0.1	2862	6.5	4.6	0.2	0.5	b.d.l.	3.3	b.d.l.	b.d.l.	b.d.l.	
MFT-San5-6	Core	5.0	4.8	31243.6	1.2	112368	308527	80311	3344.0	b.d.l.	70.9	b.d.l.	b.d.l.	857.8	125.1	126.8	0.2	b.d.l.	b.d.l.	0.1	3407	7.2	4.7	0.3	0.4	b.d.l.	3.6	b.d.l.	b.d.l.	b.d.l.	
MFT-San5-7	Core	7.0	4.9	34611.1	3.4	116930	308527	79777	3430.2	0.7	71.3	b.d.l.	b.d.l.	836.3	127.1	142.1	0.2	b.d.l.	b.d.l.	0.1	3335	7.1	5.2	0.2	0.5	b.d.l.	3.7	b.d.l.	b.d.l.	b.d.l.	
MFT-San5-8	Core	4.2	4.8	30158.0	4.1	100839	308527	77135	2422.3	b.d.l.	68.7	b.d.l.	b.d.l.	765.3	117.2	117.2	0.1	b.d.l.	0.0	0.0	2519	6.1	4.6	0.2	0.5	b.d.l.	3.5	b.d.l.	b.d.l.	b.d.l.	
MFT-San5-9	Core	6.9	4.9	32628.0	2.1	116608	308527	82191	3550.9	1.1	61.0	b.d.l.	b.d.l.	800.8	128.0	131.6	0.1	b.d.l.	0.0	b.d.l.	2333	6.9	4.6	0.2	0.4	b.d.l.	3.6	b.d.l.	b.d.l.	b.d.l.	
MFT-San5-10	Core	6.4	4.8	30857.5	b.d.l.	110471	308527	78600	3320.0	1.1	67.1	b.d.l.	b.d.l.	795.9	120.8	123.4	0.2	b.d.l.	b.d.l.	0.2	1962	6.4	4.6	0.3	0.4	b.d.l.	3.7	b.d.l.	b.d.l.	b.d.l.	
MFT-San5-11	Core	6.5	5.3	33756.4	2.3	119719	308527	83220	3399.4	b.d.l.	75.8	b.d.l.	b.d.l.	771.6	125.7	130.5	b.d.l.	b.d.l.	b.d.l.	0.1	1969	7.2	4.9	0.3	0.4	b.d.l.	3.8	b.d.l.	b.d.l.		

Table A1.5: continued

Er	Tm	Yb	Lu	Hf	Ta	Pb	Th	U
b.d.l.	b.d.l.	b.d.l.	0.0	b.d.l.	0.0	21.3	b.d.l.	b.d.l.
b.d.l.	b.d.l.	b.d.l.	b.d.l.	b.d.l.	b.d.l.	19.7	b.d.l.	b.d.l.
b.d.l.	b.d.l.	b.d.l.	0.0	b.d.l.	b.d.l.	26.6	b.d.l.	b.d.l.
b.d.l.	b.d.l.	b.d.l.	b.d.l.	b.d.l.	b.d.l.	27.2	b.d.l.	b.d.l.
b.d.l.	b.d.l.	b.d.l.	0.0	b.d.l.	0.0	27.8	b.d.l.	b.d.l.
b.d.l.	b.d.l.	b.d.l.	b.d.l.	b.d.l.	b.d.l.	27.5	b.d.l.	b.d.l.
b.d.l.	b.d.l.	b.d.l.	b.d.l.	b.d.l.	b.d.l.	26.9	b.d.l.	b.d.l.
0.0	b.d.l.	b.d.l.	b.d.l.	b.d.l.	b.d.l.	26.2	b.d.l.	b.d.l.
b.d.l.	b.d.l.	b.d.l.	b.d.l.	b.d.l.	b.d.l.	26.9	b.d.l.	b.d.l.
b.d.l.	b.d.l.	b.d.l.	0.0	b.d.l.	b.d.l.	24.7	b.d.l.	b.d.l.
b.d.l.	b.d.l.	b.d.l.	b.d.l.	b.d.l.	b.d.l.	25.6	b.d.l.	b.d.l.
b.d.l.	b.d.l.	b.d.l.	b.d.l.	b.d.l.	b.d.l.	26.5	b.d.l.	b.d.l.
b.d.l.	b.d.l.	b.d.l.	b.d.l.	b.d.l.	b.d.l.	26.4	b.d.l.	b.d.l.
b.d.l.	b.d.l.	b.d.l.	b.d.l.	b.d.l.	0.0	26.5	b.d.l.	b.d.l.
b.d.l.	b.d.l.	b.d.l.	0.0	b.d.l.	b.d.l.	27.3	b.d.l.	b.d.l.
b.d.l.	b.d.l.	b.d.l.	b.d.l.	b.d.l.	b.d.l.	26.5	b.d.l.	b.d.l.
b.d.l.	b.d.l.	b.d.l.	b.d.l.	b.d.l.	b.d.l.	25.8	b.d.l.	b.d.l.
b.d.l.	b.d.l.	b.d.l.	b.d.l.	0.0	b.d.l.	27.4	b.d.l.	b.d.l.
b.d.l.	b.d.l.	b.d.l.	b.d.l.	b.d.l.	b.d.l.	27.1	b.d.l.	b.d.l.
b.d.l.	b.d.l.	b.d.l.	b.d.l.	b.d.l.	b.d.l.	26.1	b.d.l.	b.d.l.
b.d.l.	b.d.l.	b.d.l.	b.d.l.	b.d.l.	b.d.l.	26.9	b.d.l.	b.d.l.
b.d.l.	b.d.l.	b.d.l.	b.d.l.	b.d.l.	b.d.l.	27.9	b.d.l.	b.d.l.
b.d.l.	b.d.l.	b.d.l.	b.d.l.	b.d.l.	b.d.l.	26.5	b.d.l.	b.d.l.
b.d.l.	b.d.l.	b.d.l.	b.d.l.	b.d.l.	b.d.l.	27.3	b.d.l.	b.d.l.
b.d.l.	b.d.l.	b.d.l.	0.0	b.d.l.	b.d.l.	26.6	b.d.l.	b.d.l.
b.d.l.	b.d.l.	b.d.l.	b.d.l.	b.d.l.	b.d.l.	26.7	b.d.l.	b.d.l.
b.d.l.	b.d.l.	b.d.l.	b.d.l.	b.d.l.	b.d.l.	28.6	b.d.l.	b.d.l.
b.d.l.	b.d.l.	b.d.l.	b.d.l.	b.d.l.	b.d.l.	27.6	b.d.l.	b.d.l.
b.d.l.	b.d.l.	b.d.l.	b.d.l.	b.d.l.	b.d.l.	26.5	b.d.l.	b.d.l.
0.0	b.d.l.	b.d.l.	b.d.l.	0.0	0.0	26.7	b.d.l.	b.d.l.
b.d.l.	b.d.l.	b.d.l.	b.d.l.	0.0	b.d.l.	27.7	b.d.l.	b.d.l.
b.d.l.	b.d.l.	b.d.l.	b.d.l.	b.d.l.	0.0	29.6	b.d.l.	b.d.l.
b.d.l.	b.d.l.	b.d.l.	b.d.l.	0.1	b.d.l.	30.2	0.0	0.0
b.d.l.	b.d.l.	0.1	b.d.l.	0.0	b.d.l.	30.8	b.d.l.	b.d.l.
b.d.l.	b.d.l.	b.d.l.	b.d.l.	b.d.l.	0.0	29.7	b.d.l.	b.d.l.
b.d.l.	b.d.l.	b.d.l.	b.d.l.	b.d.l.	0.0	30.7	b.d.l.	b.d.l.
b.d.l.	b.d.l.	b.d.l.	b.d.l.	0.0	0.1	27.7	b.d.l.	b.d.l.
b.d.l.	b.d.l.	b.d.l.	b.d.l.	b.d.l.	b.d.l.	28.7	b.d.l.	b.d.l.
b.d.l.	b.d.l.	b.d.l.	b.d.l.	b.d.l.	b.d.l.	25.4	b.d.l.	b.d.l.
b.d.l.	b.d.l.	b.d.l.	b.d.l.	b.d.l.	b.d.l.	29.8	b.d.l.	b.d.l.
b.d.l.	b.d.l.	b.d.l.	b.d.l.	b.d.l.	b.d.l.	28.3	0.0	b.d.l.
b.d.l.	b.d.l.	b.d.l.	b.d.l.	b.d.l.	b.d.l.	27.6	b.d.l.	b.d.l.
b.d.l.	b.d.l.	b.d.l.	b.d.l.	b.d.l.	b.d.l.	27.3	b.d.l.	0.0
b.d.l.	b.d.l.	b.d.l.	b.d.l.	b.d.l.	b.d.l.	30.3	b.d.l.	0.1
0.0	b.d.l.	b.d.l.	b.d.l.	0.0	b.d.l.	28.0	b.d.l.	b.d.l.
b.d.l.	b.d.l.	b.d.l.	0.1	b.d.l.	0.1	29.1	b.d.l.	b.d.l.
b.d.l.	b.d.l.	b.d.l.	0.0	b.d.l.	b.d.l.	30.3	b.d.l.	b.d.l.
b.d.l.	b.d.l.	b.d.l.	b.d.l.	b.d.l.	b.d.l.	31.3	b.d.l.	b.d.l.
b.d.l.	b.d.l.	b.d.l.	0.0	0.1	b.d.l.	29.7	0.0	b.d.l.
b.d.l.	b.d.l.	b.d.l.	b.d.l.	b.d.l.	0.0	28.6	b.d.l.	0.0
b.d.l.	b.d.l.	b.d.l.	b.d.l.	b.d.l.	b.d.l.	29.3	b.d.l.	b.d.l.

Table A1.5: continued

Info	Position	Li ⁺	Na	Mg	Al	Si	P	K	Ca	Sc	Ti	V	Mn	Fe	Rb	Sr	Y	Zr	Nb	Cs	Ba	La	Ce	Pr	Nd	Sm	Eu	Gd	Tb	Dy	HfO	
MFT-San5-23	Core	4.4	5.8	3.10233.5	1.2	110451	308527	b.d.l.	75653	32471.0	0.8	79.7	b.d.l.	b.d.l.	712.9	117.2	22.1	0.2	b.d.l.	0.1	3306	8.0	4.9	0.2	0.2	b.d.l.	3.5	0.1	b.d.l.	b.d.l.	b.d.l.	
MFT-San5-24	Core	5.4	5.8	30742.1	2.0	110470	308527	b.d.l.	75965	33433.4	0.6	67.9	b.d.l.	10.5	760.9	116.6	116.6	0.2	b.d.l.	0.1	3647	7.2	5.3	0.2	0.4	b.d.l.	3.3	b.d.l.	b.d.l.	b.d.l.		
MFT-San5-25	Core	6.5	5.7	29484.9	1.5	105891	308527	b.d.l.	73309	34429.9	b.d.l.	72.1	b.d.l.	b.d.l.	739.7	115.2	112.6	0.2	b.d.l.	0.1	3610	7.4	4.6	0.3	0.5	b.d.l.	3.2	0.1	b.d.l.	b.d.l.		
MFT-San5-26	Core	5.5	5.6	31007.2	b.d.l.	111853	308527	b.d.l.	76239	34889	b.d.l.	70.4	b.d.l.	b.d.l.	774.1	115.8	116.8	0.3	b.d.l.	0.1	4045	7.7	5.0	0.3	0.4	b.d.l.	3.1	b.d.l.	b.d.l.	b.d.l.		
MFT-San5-27	Core	4.9	5.7	31930.9	1.7	113269	308527	b.d.l.	79838	31344.0	0.6	77.4	b.d.l.	b.d.l.	868.2	118.6	120.7	0.2	0.1	b.d.l.	0.1	4215	7.7	5.3	0.3	0.6	b.d.l.	3.3	b.d.l.	b.d.l.	b.d.l.	
MFT-San5-28	Core	5.0	5.6	31314.9	b.d.l.	112998	308527	b.d.l.	80226	30029.9	b.d.l.	73.7	b.d.l.	b.d.l.	799.1	118.0	116.6	0.3	b.d.l.	0.1	4183	7.5	5.1	0.2	0.6	0.1	3.1	b.d.l.	b.d.l.	b.d.l.		
MFT-San5-29	Core	7.7	6.1	33574.8	3.0	120398	308527	b.d.l.	82633	30633.0	0.8	81.8	b.d.l.	b.d.l.	915.9	123.3	126.5	0.3	b.d.l.	0.1	4470	8.3	5.6	0.3	0.5	b.d.l.	3.5	b.d.l.	b.d.l.	b.d.l.		
MFT-San5-30	Core	4.3	5.7	31688.4	1.6	113358	308527	b.d.l.	77749	35466.9	b.d.l.	84.5	b.d.l.	b.d.l.	769.2	119.6	123.2	0.1	b.d.l.	0.0	4234	8.1	5.7	0.3	0.4	b.d.l.	3.6	b.d.l.	b.d.l.	b.d.l.		
MFT-San5-31	Core	6.9	5.6	32384.1	1.2	114671	308527	b.d.l.	77730	36855.9	b.d.l.	79.2	b.d.l.	b.d.l.	876.9	116.7	128.3	0.3	b.d.l.	0.1	4032	7.9	5.3	0.3	0.7	b.d.l.	3.7	b.d.l.	b.d.l.	b.d.l.		
MFT-San5-32	Core	5.2	5.2	33301.7	3.0	117291	308527	79.2	77481	42155.5	b.d.l.	83.5	b.d.l.	b.d.l.	813.2	113.1	139.8	0.2	b.d.l.	0.1	3881	9.6	7.2	0.3	0.6	b.d.l.	4.0	b.d.l.	b.d.l.	b.d.l.		
MFT-San5-33	Core	5.5	5.5	29872.7	3.6	107616	308527	72.4	76984	24426.0	0.7	69.4	b.d.l.	b.d.l.	819.6	118.5	91.7	0.1	b.d.l.	0.1	2556	5.6	3.2	0.1	0.3	b.d.l.	2.8	b.d.l.	b.d.l.	b.d.l.		
MFT-San5-34	Core	7.0	5.5	29867.9	2.0	108233	308527	b.d.l.	77856	27947.0	0.7	69.1	b.d.l.	b.d.l.	707.3	118.3	91.8	0.2	b.d.l.	0.1	2197	5.9	3.8	0.2	0.4	b.d.l.	2.6	b.d.l.	b.d.l.	b.d.l.		
MFT-San5-35	Core	6.0	5.2	30364.5	4.9	106615	308527	b.d.l.	79277	25161.0	b.d.l.	64.9	b.d.l.	b.d.l.	715.9	120.1	91.3	0.1	0.0	b.d.l.	0.1	1594	5.8	4.2	0.2	0.4	b.d.l.	2.5	b.d.l.	b.d.l.	b.d.l.	
MFT-San5-36	Core	5.8	4.9	28596.5	6.7	103356	308527	b.d.l.	83271	25735.5	b.d.l.	60.4	b.d.l.	b.d.l.	739.3	116.9	89.7	0.3	b.d.l.	0.1	0.2	1292	5.7	4.0	0.3	0.7	b.d.l.	2.7	b.d.l.	0.0	0.1	
MFT-San5-37	Core																															
Sandstone grain 6 - Line 1																																
grain6-1	Rim																															
grain6-2	Rim	b.d.l.	3.6	31040.5	11.6	100530	303853	34.3	79768	3618.6	0.8	87.8	b.d.l.	1.6	832.8	116.6	116.4	b.d.l.	b.d.l.	0.1	6902	7.6	5.2	0.3	0.6	0.0	3.7	b.d.l.	b.d.l.	b.d.l.	b.d.l.	
grain6-3	Rim	b.d.l.	5.8	31041.1	13.6	100062	303853	23.6	78343	3978.7	b.d.l.	93.8	b.d.l.	b.d.l.	768.7	117.8	110.9	0.0	b.d.l.	0.1	7004	7.9	5.2	0.3	0.6	0.1	3.7	b.d.l.	b.d.l.	b.d.l.	0.0	
grain6-4	Rim	b.d.l.	7.2	31737.2	10.5	102833	303853	b.d.l.	80258	3693.1	b.d.l.	90.8	b.d.l.	0.9	840.2	117.1	114.7	0.0	b.d.l.	0.1	7024	8.0	5.4	0.3	0.5	0.1	3.9	b.d.l.	b.d.l.	b.d.l.	b.d.l.	
grain6-5	Core	b.d.l.	8.2	31492.6	b.d.l.	102362	303853	b.d.l.	82546	4070.0	0.6	96.3	b.d.l.	1.0	891.5	118.6	113.4	0.0	b.d.l.	0.1	7165	8.2	5.4	0.3	0.7	b.d.l.	3.7	b.d.l.	b.d.l.	b.d.l.		
grain6-6	Core	b.d.l.	8.6	31319.3	b.d.l.	101345	303853	b.d.l.	80356	3758.7	b.d.l.	90.7	b.d.l.	1.2	853.3	120.3	109.9	0.0	b.d.l.	0.1	7196	7.6	5.2	0.3	0.6	b.d.l.	3.5	0.1	b.d.l.	b.d.l.		
grain6-7	Core	b.d.l.	8.9	32409.1	b.d.l.	105189	303853	b.d.l.	82856	3681.0	b.d.l.	93.2	b.d.l.	b.d.l.	899.6	120.7	107.6	0.0	b.d.l.	0.1	7210	7.8	5.6	0.3	0.7	b.d.l.	3.5	b.d.l.	b.d.l.	b.d.l.		
grain6-8	Core	b.d.l.	8.5	31305.6	b.d.l.	102380	303853	b.d.l.	81728	4003.8	b.d.l.	89.5	b.d.l.	0.9	890.0	119.6	107.4	0.0	b.d.l.	0.1	7161	8.0	5.3	0.3	0.4	0.1	3.3	b.d.l.	0.0	b.d.l.		
grain6-9	Core	b.d.l.	9.5	31625.1	b.d.l.	101953	303853	b.d.l.	81219	4227.6	b.d.l.	97.3	b.d.l.	0.9	838.5	119.1	104.9	b.d.l.	b.d.l.	0.0	7136	7.9	5.1	0.3	0.6	b.d.l.	3.4	b.d.l.	b.d.l.	b.d.l.		
grain6-10	Core	b.d.l.	8.9	31119.7	b.d.l.	102956	303853	b.d.l.	81529	3820.4	0.9	93.7	b.d.l.	0.9	884.0	121.1	103.6	0.1	b.d.l.	0.1	7172	7.7	5.3	0.3	0.6	0.0	3.4	0.1	0.0	b.d.l.	b.d.l.	
grain6-11	Core	b.d.l.	8.9	30959.0	b.d.l.	100666	303853	b.d.l.	80389	3466.5	b.d.l.	94.4	b.d.l.	0.9	857.1	118.1	105.0	0.0	b.d.l.	0.1	7315	8.1	5.3	0.2	0.5	b.d.l.	3.7	b.d.l.	b.d.l.	b.d.l.		
grain6-12	Core	b.d.l.	8.2	30603.8	b.d.l.	99324	303853	b.d.l.	79451	3473.5	b.d.l.	94.0	b.d.l.	0.9	848.4	117.1	110.3	0.0	b.d.l.	0.1	7534	8.1	5.6	0.3	0.5	0.1	3.8	b.d.l.	b.d.l.	b.d.l.		
grain6-13	Core	b.d.l.	8.0	31429.3	b.d.l.	101778	303853	b.d.l.	79419	4013.2	0.7	92.3	b.d.l.	b.d.l.	868.7	117.9	116.1	b.d.l.	b.d.l.	0.1	7653	8.9	5.9	0.3	0.6	b.d.l.	3.6	b.d.l.	b.d.l.	b.d.l.		
grain6-14	Core	b.d.l.	7.8	31376.2	7.3	103371	303853	b.d.l.	79816	3732.5	b.d.l.	89.8	b.d.l.	b.d.l.	829.3	119.7	118.1	b.d.l.	b.d.l.	0.1	7839	8.7	5.9	0.3	0.7	b.d.l.	4.0	0.1	b.d.l.	b.d.l.		
grain6-15	Core	b.d.l.	8.2	32040.9	b.d.l.	102560	303853	b.d.l.	83326	3668.3	0.6	94.4	b.d.l.	0.8	809.0	125.5	119.3	b.d.l.	b.d.l.	0.1	7668	8.5	5.7	0.3	0.6	0.1	4.3	b.d.l.	b.d.l.	b.d.l.		
grain6-16	Core	b.d.l.	8.4	31122.6	b.d.l.	103943	303853	b.d.l.	80192	3778.9	1.0	84.7	b.d.l.	0.9	877.4	119.9	122.0	0.1	b.d.l.	0.1	7576	8.5	5.6	0.3	0.7	b.d.l.	4.1	b.d.l.	b.d.l.	b.d.l.		
grain6-17	Core	b.d.l.	8.2	30912.9	b.d.l.	103478	303853	25.9	80647	4089.8	0.8	84.2	b.d.l.	0.8	868.1	122.0	120.3	b.d.l.	b.d.l.	0.1	7647	8.1	5.8	0.3	0.6	b.d.l.	4.0	0.0	b.d.l.	b.d.l.		
grain6-18	Core	b.d.l.	7.8	30980.6	b.d.l.	100403	303853	b.d.l.	81010	3679.5	0.6	89.4	b.d.l.	b.d.l.	826.8	122.6	117.7	0.0	b.d.l.	0.0	7365	7.7	5.3	0.3	0.5	0.1	3.7	b.d.l.	b.d.l.	b.d.l.		
grain6-19	Core	b.d.l.	8.5	30997.6	b.d.l.	101647	303853	b.d.l.	80693	4199.5	0.7	85.5	b.d.l.	0.8	801.4	124.7	119.5	0.0	b.d.l.	0.1	7481	7.7	5.5	0.3	0.7	b.d.l.	4.2	b.d.l.	b.d.l.	b.d.l.		
grain6-20	Core	b.d.l.	7.9	30822.2	b.d.l.	101317	303853	b.d.l.	81598	3594.2	b.d.l.	92.7	b.d.l.	b.d.l.	773.0	125.6	128.9	0.0	0.1	b.d.l.	0.1	7499	7.8	5.4	0.3	0.5	0.1	4.6	b.d.l.	b.d.l.	b.d.l.	
grain6-21	Core	b.d.l.	7.7	31385.1	7.1	103643	303853	b.d.l.	80270	3598.3	0.8	93.2	b.d.l.	0.8	832.1	126.7	131.5	b.d.l.	b.d.l.	0.0	7404	7.5	5.4	0.3	0.5	b.d.l.	4.7	b.d.l.	b.d.l.	0.0		
grain6-22	Core	b.d.l.	8.1	31715.1	b.d.l.	102662	303853	b.d.l.	80280	3731.4	0.9	91.3	b.d.l.	b.d.l.	854.7	126.2	130.6	b.d.l.	b.d.l.	0.1	7349	7.5	5.2	0.3	0.6	b.d.l.	4.8	b.d.l.	b.d.l.	b.d.l.		
grain6-23	Core	b.d.l.	7.9	31257.8	10.6	103058	303853	b.d.l.	80844	3890.3	0.8	93.1	b.d.l.	b.d.l.	779.1	123.7	135.1	b.d.l.	b.d.l.	0.1	7668	8.6	5.8	0.3	0.5	b.d.l.	4.4	0.1	b.d.l.	0.0		
grain6-24	Core	b.d.l.	8.8	32537.7	b.d.l.	103390	303853	b.d.l.	86474	4320.2	0.7	91.4	b.d.l.	1.0	847.3	127.7	137.5	b.d.l.	b.d.l.	0.1	7651	8.4	5.9	0.3	0.6	0.0	4.7	b.d.l.	b.d.l.	b.d.l.		
grain6-25	Core	b.d.l.	7.9	31018.6	b.d.l.	103394	303853	b.d.l.	80754	3528.5	b.d.l.	88.0	b.d.l.	b.d.l.	908.4	123.7	137.5	b.d.l.	b.d.l.	0.1	7592	8.3	5.8	0.3	0.4	b.d.l.	4.6	b.d.l.	b.d.l.	b.d.l.		
grain6-26	Core	b.d.l.	8.5	30785.6	6.4	99230	299178	b.d.l.																								

Table A1.5: continued

Er	Tm	Yb	Lu	Hf	Ta	Pb	Th	U
b.d.l.	b.d.l.	b.d.l.	b.d.l.	b.d.l.	b.d.l.	29.8	b.d.l.	b.d.l.
0.1	b.d.l.	b.d.l.	b.d.l.	0.0	0.0	30.9	0.0	b.d.l.
b.d.l.	b.d.l.	b.d.l.	b.d.l.	0.1	b.d.l.	28.1	b.d.l.	b.d.l.
0.1	b.d.l.	b.d.l.	b.d.l.	b.d.l.	b.d.l.	28.2	b.d.l.	b.d.l.
b.d.l.	b.d.l.	b.d.l.	b.d.l.	b.d.l.	b.d.l.	29.7	b.d.l.	0.0
b.d.l.	b.d.l.	b.d.l.	b.d.l.	0.0	0.0	29.5	b.d.l.	b.d.l.
b.d.l.	b.d.l.	0.1	b.d.l.	b.d.l.	0.0	33.0	0.0	0.0
b.d.l.	b.d.l.	b.d.l.	b.d.l.	b.d.l.	b.d.l.	31.7	b.d.l.	b.d.l.
b.d.l.	b.d.l.	b.d.l.	b.d.l.	b.d.l.	b.d.l.	33.6	b.d.l.	b.d.l.
b.d.l.	b.d.l.	b.d.l.	b.d.l.	b.d.l.	0.0	37.5	b.d.l.	b.d.l.
b.d.l.	b.d.l.	b.d.l.	b.d.l.	0.1	b.d.l.	24.8	b.d.l.	b.d.l.
b.d.l.	b.d.l.	b.d.l.	b.d.l.	0.0	b.d.l.	26.8	b.d.l.	b.d.l.
b.d.l.	b.d.l.	b.d.l.	b.d.l.	b.d.l.	b.d.l.	24.0	b.d.l.	b.d.l.
b.d.l.	b.d.l.	b.d.l.	b.d.l.	0.1	b.d.l.	27.1	0.0	b.d.l.
b.d.l.	b.d.l.	b.d.l.	b.d.l.	b.d.l.	b.d.l.	33.2	b.d.l.	b.d.l.
b.d.l.	b.d.l.	b.d.l.	b.d.l.	0.0	b.d.l.	33.0	b.d.l.	b.d.l.
b.d.l.	b.d.l.	b.d.l.	b.d.l.	b.d.l.	b.d.l.	34.2	b.d.l.	b.d.l.
b.d.l.	0.0	b.d.l.	b.d.l.	b.d.l.	b.d.l.	34.2	b.d.l.	b.d.l.
b.d.l.	b.d.l.	b.d.l.	0.0	b.d.l.	b.d.l.	33.7	b.d.l.	b.d.l.
b.d.l.	b.d.l.	b.d.l.	b.d.l.	b.d.l.	b.d.l.	34.8	b.d.l.	b.d.l.
b.d.l.	b.d.l.	b.d.l.	b.d.l.	b.d.l.	b.d.l.	34.0	b.d.l.	b.d.l.
b.d.l.	b.d.l.	b.d.l.	b.d.l.	b.d.l.	b.d.l.	34.1	b.d.l.	b.d.l.
b.d.l.	b.d.l.	b.d.l.	b.d.l.	0.0	b.d.l.	34.3	b.d.l.	b.d.l.
b.d.l.	b.d.l.	b.d.l.	b.d.l.	b.d.l.	b.d.l.	34.3	b.d.l.	b.d.l.
b.d.l.	b.d.l.	b.d.l.	b.d.l.	b.d.l.	b.d.l.	33.9	b.d.l.	b.d.l.
b.d.l.	b.d.l.	b.d.l.	0.0	b.d.l.	b.d.l.	34.0	b.d.l.	0.0
b.d.l.	b.d.l.	b.d.l.	b.d.l.	b.d.l.	b.d.l.	34.9	b.d.l.	0.0
b.d.l.	b.d.l.	b.d.l.	b.d.l.	b.d.l.	b.d.l.	35.0	0.0	b.d.l.
b.d.l.	b.d.l.	b.d.l.	b.d.l.	0.0	0.0	33.7	b.d.l.	b.d.l.
b.d.l.	b.d.l.	b.d.l.	b.d.l.	b.d.l.	b.d.l.	35.5	b.d.l.	b.d.l.
b.d.l.	b.d.l.	b.d.l.	b.d.l.	b.d.l.	b.d.l.	34.3	0.0	b.d.l.
b.d.l.	b.d.l.	b.d.l.	b.d.l.	0.0	0.0	34.2	b.d.l.	b.d.l.
b.d.l.	b.d.l.	b.d.l.	b.d.l.	b.d.l.	b.d.l.	32.8	b.d.l.	b.d.l.
b.d.l.	b.d.l.	b.d.l.	b.d.l.	b.d.l.	b.d.l.	32.3	b.d.l.	b.d.l.
b.d.l.	b.d.l.	b.d.l.	b.d.l.	b.d.l.	b.d.l.	32.0	b.d.l.	b.d.l.
b.d.l.	b.d.l.	b.d.l.	b.d.l.	b.d.l.	b.d.l.	33.8	b.d.l.	b.d.l.
b.d.l.	b.d.l.	b.d.l.	b.d.l.	0.0	b.d.l.	34.6	b.d.l.	b.d.l.
b.d.l.	b.d.l.	b.d.l.	b.d.l.	b.d.l.	b.d.l.	34.7	b.d.l.	b.d.l.
b.d.l.	b.d.l.	b.d.l.	b.d.l.	b.d.l.	b.d.l.	34.8	b.d.l.	0.0
0.0	b.d.l.	b.d.l.	b.d.l.	b.d.l.	b.d.l.	33.0	b.d.l.	b.d.l.
0.0	b.d.l.	b.d.l.	b.d.l.	b.d.l.	b.d.l.	33.9	b.d.l.	b.d.l.
b.d.l.	b.d.l.	b.d.l.	b.d.l.	0.0	b.d.l.	32.1	b.d.l.	b.d.l.
b.d.l.	b.d.l.	b.d.l.	b.d.l.	b.d.l.	b.d.l.	33.6	b.d.l.	b.d.l.
b.d.l.	b.d.l.	b.d.l.	b.d.l.	b.d.l.	b.d.l.	34.9	b.d.l.	b.d.l.
b.d.l.	b.d.l.	b.d.l.	b.d.l.	b.d.l.	0.0	36.3	b.d.l.	b.d.l.
b.d.l.	b.d.l.	b.d.l.	b.d.l.	b.d.l.	0.0	34.5	0.0	b.d.l.
b.d.l.	b.d.l.	b.d.l.	b.d.l.	b.d.l.	b.d.l.	33.6	b.d.l.	b.d.l.
b.d.l.	b.d.l.	b.d.l.	b.d.l.	0.0	0.0	33.4	b.d.l.	b.d.l.
b.d.l.	b.d.l.	0.1	b.d.l.	0.1	0.0	32.2	b.d.l.	b.d.l.

Table A1.5: continued

Info	Position	L ⁱ	L ^j	Na	Mg	Al	Si	P	K	Ca	Sc	Ti	V	Mn	Fe	Rb	Sr	Y	Zr	Nb	Cs	Ba	La	Ce	Pr	Nd	Sm	Eu	Gd	Tb	Dy	Ho	
MFT-San6-6	Core	7.2	6.0	32144.7	4.3	115495	308527	b.d.l.	76805	3985.6	b.d.l.	88.8	b.d.l.	b.d.l.	7942	121.0	116.0	0.5	b.d.l.	0.0	0.1	8235	9.5	6.5	0.3	0.6	b.d.l.	4.2	b.d.l.	b.d.l.	b.d.l.		
MFT-San6-7	Core	7.9	6.0	30984.4	2.4	100588	308527	b.d.l.	73913	4145.5	b.d.l.	94.6	b.d.l.	b.d.l.	7303	143.4	119.7	0.4	b.d.l.	0.0	0.1	7997	9.4	7.0	0.3	0.6	b.d.l.	4.1	b.d.l.	b.d.l.	b.d.l.		
MFT-San6-8	Core	11.0	7.4	31870.9	1.2	12396	308527	b.d.l.	76460	3531.9	b.d.l.	87.0	b.d.l.	b.d.l.	7935	117.7	113.9	0.5	b.d.l.	0.1	0.1	8004	9.0	6.2	0.3	0.6	b.d.l.	4.0	0.1	b.d.l.	b.d.l.		
MFT-San6-9	Core	7.5	7.0	29629.3	1.9	106986	308527	b.d.l.	73128	3193.3	b.d.l.	86.4	b.d.l.	b.d.l.	8001.6	118.5	105.6	0.5	0.1	b.d.l.	0.1	7234	7.4	5.6	0.2	0.5	b.d.l.	3.6	b.d.l.	b.d.l.	b.d.l.		
MFT-San6-10	Core	8.9	7.9	32265.6	2.7	116039	308527	b.d.l.	76661	3800.9	0.9	92.3	b.d.l.	b.d.l.	852.3	123.7	120.4	0.5	b.d.l.	0.0	0.0	8232	8.4	6.0	0.3	0.5	0.1	4.2	b.d.l.	b.d.l.	b.d.l.		
MFT-San6-11	Core	10.3	8.7	33002.8	2.8	119796	308527	b.d.l.	81075	4040.3	0.8	98.8	b.d.l.	b.d.l.	885.5	122.3	124.8	0.5	b.d.l.	b.d.l.	b.d.l.	8264	8.7	6.4	0.4	0.7	b.d.l.	4.2	b.d.l.	b.d.l.	b.d.l.		
MFT-San6-12	Core	5.1	7.5	30177.7	3.9	107588	308527	b.d.l.	74145	3841.1	b.d.l.	91.5	b.d.l.	b.d.l.	846.3	112.1	111.1	0.6	0.0	b.d.l.	0.0	7603	8.6	5.6	0.4	0.6	b.d.l.	3.8	b.d.l.	b.d.l.	b.d.l.		
MFT-San6-13	Core	8.8	8.2	31158.4	2.5	113798	308527	b.d.l.	74946	3837.9	b.d.l.	80.1	b.d.l.	b.d.l.	841.3	125.1	118.8	0.4	0.0	b.d.l.	0.0	7182	7.4	5.4	0.3	0.4	b.d.l.	3.9	b.d.l.	b.d.l.	b.d.l.		
MFT-San6-14	Core	8.1	8.6	31381.1	3.5	109935	308527	b.d.l.	76470	3899.1	b.d.l.	78.2	b.d.l.	b.d.l.	874.9	114.9	127.1	0.5	b.d.l.	b.d.l.	b.d.l.	7262	8.4	5.8	0.3	0.7	b.d.l.	4.0	b.d.l.	b.d.l.	b.d.l.		
MFT-San6-15	Core	9.2	8.9	32551.9	4.9	114770	308527	b.d.l.	76260	4240.6	b.d.l.	79.7	b.d.l.	b.d.l.	874.0	111.0	133.3	0.4	0.1	b.d.l.	0.1	7240	8.1	5.5	0.3	0.7	b.d.l.	4.1	b.d.l.	b.d.l.	b.d.l.		
MFT-San6-16	Core																																
MFT-San6-17	Core	8.2	8.1	30028.6	2.0	105778	308527	b.d.l.	76960	4154.7	b.d.l.	85.0	b.d.l.	b.d.l.	749.9	102.4	129.7	0.4	0.1	0.0	0.1	6327	7.9	6.2	0.3	0.8	b.d.l.	3.9	b.d.l.	b.d.l.	b.d.l.		
MFT-San6-18	Core	9.5	8.1	32656.9	2.5	115653	308527	b.d.l.	74818	4470.1	0.7	84.0	b.d.l.	b.d.l.	832.0	108.2	144.7	0.4	b.d.l.	b.d.l.	b.d.l.	6551	9.3	7.3	0.4	1.1	b.d.l.	4.7	b.d.l.	b.d.l.	b.d.l.		
MFT-San6-19	Core	8.2	8.0	33163.3	3.9	111498	308527	b.d.l.	74084	4976.0	b.d.l.	88.9	b.d.l.	b.d.l.	792.7	115.7	129.4	0.3	0.1	b.d.l.	0.0	4898	9.3	7.2	0.5	0.8	0.1	3.9	b.d.l.	0.0	b.d.l.		
MFT-San6-20	Core	7.5	6.4	31710.8	1.9	115835	308527	b.d.l.	79862	3552.8	b.d.l.	92.9	b.d.l.	b.d.l.	782.6	124.3	119.2	0.2	b.d.l.	b.d.l.	0.2	b.d.l.	0.2	4630	7.5	5.1	0.3	0.5	b.d.l.	3.8	b.d.l.	b.d.l.	b.d.l.
MFT-San6-22	Core	5.6	4.0	31738.0	b.d.l.	114813	308527	b.d.l.	79014	2830.2	b.d.l.	74.4	b.d.l.	b.d.l.	809.3	127.9	112.0	0.1	0.1	b.d.l.	b.d.l.	4001	7.5	5.2	0.3	0.4	b.d.l.	3.4	b.d.l.	b.d.l.	b.d.l.		
MFT-San6-23	Core	2.1	2.5	31795.3	3.8	117019	308527	b.d.l.	81842	3857.2	1.0	73.8	b.d.l.	b.d.l.	860.2	126.4	113.5	0.2	b.d.l.	0.0	b.d.l.	0.0	3806	7.9	5.2	0.3	0.5	0.1	3.6	b.d.l.	b.d.l.	b.d.l.	
MFT-San6-24	Core	b.d.l.	1.7	31138.6	3.4	113334	308527	b.d.l.	80275	2519.3	0.6	77.7	b.d.l.	b.d.l.	797.8	128.9	105.3	0.1	b.d.l.	b.d.l.	0.1	3261	7.3	4.8	0.2	0.4	b.d.l.	3.2	b.d.l.	b.d.l.	b.d.l.		
MFT-San6-25	Rim																																
Sandstone grain 15 - Line 1																																	
grain15-1	Rim	b.d.l.	3.7	31355.4	b.d.l.	98392	308527	28.3	83729	3392.5	0.5	93.8	b.d.l.	b.d.l.	841.1	125.4	99.0	b.d.l.	b.d.l.	b.d.l.	1459	7.4	5.1	0.3	0.5	b.d.l.	2.8	b.d.l.	b.d.l.	b.d.l.			
grain15-2	Rim	b.d.l.	4.4	30831.9	b.d.l.	96435	308527	b.d.l.	83590	2693.8	0.7	91.5	b.d.l.	b.d.l.	838.7	122.7	96.4	b.d.l.	b.d.l.	b.d.l.	0.1	1372	7.1	5.2	0.2	0.4	b.d.l.	2.5	b.d.l.	b.d.l.	b.d.l.		
grain15-3	Core	b.d.l.	5.2	31496.2	b.d.l.	97978	308527	32.2	84923	2720.1	0.7	91.9	b.d.l.	0.9	828.5	127.1	94.3	0.0	b.d.l.	0.0	b.d.l.	1336	7.6	5.1	0.2	0.4	0.0	2.7	b.d.l.	b.d.l.	b.d.l.		
grain15-4	Core	b.d.l.	5.3	31325.4	b.d.l.	95745	308527	16.7	82984	2667.0	0.8	91.7	b.d.l.	0.7	834.2	125.9	91.1	b.d.l.	b.d.l.	b.d.l.	0.1	1200	7.6	5.3	0.2	0.4	b.d.l.	2.5	b.d.l.	b.d.l.	b.d.l.		
grain15-5	Core	6.5	5.5	30797.0	5.9	94795	308527	16.1	83335	2814.8	0.8	97.4	b.d.l.	b.d.l.	804.2	124.8	84.9	b.d.l.	b.d.l.	b.d.l.	0.1	1377	7.3	4.9	0.2	0.5	b.d.l.	2.4	b.d.l.	b.d.l.	b.d.l.		
grain15-6	Core	b.d.l.	5.5	31669.2	b.d.l.	98218	308527	17.9	86400	2803.8	0.6	100.9	b.d.l.	0.8	859.3	129.2	87.5	b.d.l.	b.d.l.	0.0	0.1	1382	7.8	5.3	0.3	0.5	b.d.l.	2.3	b.d.l.	b.d.l.	b.d.l.		
grain15-7	Core	b.d.l.	5.9	31539.2	b.d.l.	96477	308527	26.9	85775	2666.9	0.6	93.8	b.d.l.	b.d.l.	864.5	126.6	84.5	b.d.l.	b.d.l.	b.d.l.	0.1	1409	7.6	5.3	0.2	0.5	0.0	2.3	b.d.l.	0.0	0.0	b.d.l.	
grain15-8	Core	b.d.l.	5.6	32369.3	b.d.l.	99144	308527	b.d.l.	86037	2982.4	0.9	96.8	b.d.l.	0.9	877.0	128.5	82.5	b.d.l.	b.d.l.	b.d.l.	0.1	1423	7.6	5.2	0.3	0.4	b.d.l.	2.2	b.d.l.	b.d.l.	b.d.l.		
grain15-9	Core	b.d.l.	5.5	32729.3	b.d.l.	96440	308527	16.1	88461	2848.4	0.6	94.2	b.d.l.	b.d.l.	865.4	132.4	79.7	b.d.l.	b.d.l.	b.d.l.	0.1	1480	7.6	5.7	0.3	0.6	b.d.l.	2.2	b.d.l.	0.0	b.d.l.		
grain15-10	Core	b.d.l.	5.6	30360.7	b.d.l.	92521	308527	25.7	83900	3135.6	0.8	89.7	b.d.l.	b.d.l.	823.7	123.9	76.0	b.d.l.	b.d.l.	b.d.l.	0.1	1491	7.7	5.4	0.3	0.5	0.0	2.2	0.0	0.0	b.d.l.		
grain15-11	Core	b.d.l.	5.5	31739.2	b.d.l.	94474	308527	15.2	85198	3045.8	1.0	96.7	b.d.l.	0.6	853.7	128.7	76.0	0.0	b.d.l.	b.d.l.	0.1	1526	7.7	5.6	0.2	0.5	b.d.l.	2.1	b.d.l.	b.d.l.	0.0		
grain15-12	Core	6.4	5.1	31308.8	6.0	93065	308527	19.2	85806	2512.0	0.6	88.7	b.d.l.	0.6	830.2	125.7	70.8	b.d.l.	b.d.l.	b.d.l.	0.1	1499	7.6	5.4	0.3	0.5	b.d.l.	1.9	b.d.l.	b.d.l.	b.d.l.		
grain15-13	Core	b.d.l.	5.4	30770.7	8.6	93100	308527	18.0	87495	2639.2	0.9	97.2	b.d.l.	0.6	817.7	129.8	66.6	b.d.l.	b.d.l.	b.d.l.	0.1	1469	7.2	5.1	0.2	0.3	b.d.l.	1.8	b.d.l.	b.d.l.	b.d.l.		
grain15-14	Core	6.2	5.6	32340.0	b.d.l.	96984	308527	b.d.l.	86191	2466.7	0.6	100.4	b.d.l.	b.d.l.	854.7	131.3	63.7	b.d.l.	b.d.l.	b.d.l.	0.1	1489	7.2	5.0	0.2	0.4	b.d.l.	1.8	b.d.l.	b.d.l.	b.d.l.		
grain15-15	Core	b.d.l.	5.3	31359.6	6.8	94608	308527	13.3	86317	3134.1	0.7	86.7	b.d.l.	b.d.l.	824.4	128.7	64.1	b.d.l.	b.d.l.	b.d.l.	0.1	1548	7.6	5.6	0.3	0.4	b.d.l.	1.7	b.d.l.	b.d.l.	b.d.l.		
grain15-16	Core	b.d.l.	5.4	32207.8	b.d.l.	88602	308527	13.8	80109	2821.1	0.5	88.5	b.d.l.	b.d.l.	823.6	129.9	58.4	b.d.l.	b.d.l.	0.0	0.1	1507	6.7	4.8	0.2	0.4	0.0	1.5	b.d.l.	b.d.l.	b.d.l.		
grain15-17	Core	b.d.l.	5.1	31984.0	b.d.l.	98250	308527	14.9	86891	2568.2	0.6	99.7	b.d.l.	0.8	846.6	132.7	62.1	b.d.l.	b.d.l.	b.d.l.	0.1	1601	7.6	5.1	0.3	0.6	0.0	1.7	0.1	b.d.l.	b.d.l.	b.d.l.	
grain15-18	Core	b.d.l.	4.7	30619.3	b.d.l.	92864	308527	15.1	85512	2666.1	0.6	91.5	b.d.l.	0.6	784.2	125.4	59.2	b.d.l.	b.d.l.	b.d.l.	0.1	1513	6.8	4.8	0.2	0.4	b.d.l.	1.5	0.0	b.d.l.	b.d.l.		
grain15-19	Core	5.5	5.0	30866.5	b.d.l.	88720	308527	11.9	82591	2403.0	0.6	87.2	b.d.l.	0.7	771.2	120.5	54.8	b.d.l.	b.d.l.	b.d.l.	0.1	1490	6.8	4.8	0.3	0.4	0.0	1.5	b.d.l.	b.d.l.	b.d.l.		
grain15-20	Core	6.0	5.1	31460.4	b.d.l.	94170	308527	b.d.l.	83646	2477.2	0.7	88.4	b.d.l.	b.d.l.	768.3	130.2	54.5	b.d.l.	b.d.l.	b.d.l.	0.1	1546	7.0	4.8	0.2	0.4	b.d.l.	1.5	b.d.l.	b.d.l.	b.d.l.		
grain15-21	Core	6.1	5.1	31648.2	5.9	96909	308527	b.d.l.	86124	2739.6	0.8																						

Table A1.5: continued

Er	Tm	Yb	Lu	Hf	Ta	Pb	Th	U
b.d.l.	b.d.l.	b.d.l.	0.1	0.0	36.2	0.0	0.0	
b.d.l.	b.d.l.	b.d.l.	b.d.l.	b.d.l.	0.1	36.2	b.d.l.	0.0
b.d.l.	b.d.l.	b.d.l.	b.d.l.	b.d.l.	0.0	35.4	b.d.l.	0.0
b.d.l.	b.d.l.	b.d.l.	b.d.l.	0.0	34.6	b.d.l.	b.d.l.	
b.d.l.	b.d.l.	b.d.l.	b.d.l.	0.0	b.d.l.	34.6	b.d.l.	b.d.l.
b.d.l.	b.d.l.	b.d.l.	b.d.l.	0.2	b.d.l.	37.7	b.d.l.	0.0
b.d.l.	b.d.l.	b.d.l.	0.0	0.0	b.d.l.	35.9	b.d.l.	b.d.l.
b.d.l.	0.0	b.d.l.	b.d.l.	0.1	b.d.l.	35.1	b.d.l.	0.0
b.d.l.	b.d.l.	b.d.l.	b.d.l.	0.1	b.d.l.	35.0	b.d.l.	b.d.l.
b.d.l.	b.d.l.	b.d.l.	b.d.l.	0.1	0.0	36.9	b.d.l.	b.d.l.
b.d.l.	b.d.l.	b.d.l.	b.d.l.	0.1	0.0	34.6	b.d.l.	b.d.l.
b.d.l.	b.d.l.	b.d.l.	b.d.l.	0.0	0.0	37.5	b.d.l.	b.d.l.
b.d.l.	b.d.l.	b.d.l.	b.d.l.	0.1	b.d.l.	34.3	b.d.l.	0.0
b.d.l.	b.d.l.	b.d.l.	b.d.l.	0.0	b.d.l.	29.5	b.d.l.	0.0
b.d.l.	b.d.l.	b.d.l.	b.d.l.	0.1	0.0	30.0	b.d.l.	b.d.l.
b.d.l.	b.d.l.	b.d.l.	b.d.l.	b.d.l.	b.d.l.	31.8	b.d.l.	b.d.l.
b.d.l.	b.d.l.	b.d.l.	b.d.l.	b.d.l.	0.0	29.4	0.0	0.0
b.d.l.	b.d.l.	b.d.l.	b.d.l.	b.d.l.	b.d.l.	28.5	b.d.l.	b.d.l.
b.d.l.	b.d.l.	b.d.l.	b.d.l.	b.d.l.	b.d.l.	27.6	b.d.l.	b.d.l.
b.d.l.	b.d.l.	b.d.l.	0.0	b.d.l.	b.d.l.	28.0	b.d.l.	b.d.l.
b.d.l.	b.d.l.	b.d.l.	b.d.l.	b.d.l.	b.d.l.	27.5	b.d.l.	b.d.l.
b.d.l.	b.d.l.	b.d.l.	b.d.l.	b.d.l.	b.d.l.	27.3	b.d.l.	b.d.l.
b.d.l.	b.d.l.	b.d.l.	b.d.l.	b.d.l.	b.d.l.	29.3	b.d.l.	0.0
b.d.l.	b.d.l.	b.d.l.	b.d.l.	0.0	b.d.l.	28.7	b.d.l.	b.d.l.
b.d.l.	b.d.l.	b.d.l.	b.d.l.	b.d.l.	b.d.l.	29.2	b.d.l.	b.d.l.
b.d.l.	b.d.l.	b.d.l.	b.d.l.	b.d.l.	b.d.l.	29.8	b.d.l.	b.d.l.
0.0	b.d.l.	b.d.l.	b.d.l.	b.d.l.	0.0	29.8	b.d.l.	b.d.l.
b.d.l.	b.d.l.	b.d.l.	b.d.l.	b.d.l.	b.d.l.	30.0	b.d.l.	b.d.l.
b.d.l.	b.d.l.	b.d.l.	b.d.l.	b.d.l.	b.d.l.	29.5	b.d.l.	b.d.l.
b.d.l.	b.d.l.	b.d.l.	b.d.l.	0.0	b.d.l.	28.8	b.d.l.	b.d.l.
b.d.l.	b.d.l.	b.d.l.	b.d.l.	b.d.l.	0.0	28.4	b.d.l.	b.d.l.
b.d.l.	b.d.l.	b.d.l.	b.d.l.	b.d.l.	0.0	30.5	0.0	b.d.l.
b.d.l.	0.0	b.d.l.	b.d.l.	b.d.l.	b.d.l.	27.4	b.d.l.	0.0
b.d.l.	b.d.l.	b.d.l.	0.0	b.d.l.	b.d.l.	30.1	b.d.l.	b.d.l.
b.d.l.	b.d.l.	b.d.l.	b.d.l.	b.d.l.	b.d.l.	28.5	b.d.l.	b.d.l.
b.d.l.	0.0	b.d.l.	b.d.l.	b.d.l.	b.d.l.	27.9	b.d.l.	b.d.l.
b.d.l.	b.d.l.	b.d.l.	b.d.l.	b.d.l.	0.0	28.4	b.d.l.	b.d.l.
b.d.l.	b.d.l.	b.d.l.	b.d.l.	b.d.l.	b.d.l.	29.8	b.d.l.	b.d.l.
b.d.l.	b.d.l.	b.d.l.	b.d.l.	b.d.l.	0.0	28.0	b.d.l.	b.d.l.
b.d.l.	b.d.l.	b.d.l.	b.d.l.	b.d.l.	b.d.l.	30.4	b.d.l.	b.d.l.
b.d.l.	b.d.l.	b.d.l.	0.0	b.d.l.	b.d.l.	27.5	b.d.l.	b.d.l.
b.d.l.	b.d.l.	b.d.l.	b.d.l.	b.d.l.	0.0	30.3	b.d.l.	b.d.l.
b.d.l.	b.d.l.	b.d.l.	b.d.l.	b.d.l.	b.d.l.	30.5	b.d.l.	b.d.l.
b.d.l.	b.d.l.	b.d.l.	b.d.l.	b.d.l.	0.0	29.4	b.d.l.	b.d.l.
b.d.l.	b.d.l.	b.d.l.	b.d.l.	b.d.l.	b.d.l.	29.2	b.d.l.	b.d.l.
b.d.l.	b.d.l.	b.d.l.	b.d.l.	b.d.l.	b.d.l.	29.3	b.d.l.	b.d.l.
0.0	b.d.l.	b.d.l.	b.d.l.	b.d.l.	0.0	33.0	b.d.l.	b.d.l.
b.d.l.	b.d.l.	b.d.l.	b.d.l.	b.d.l.	0.0	32.6	b.d.l.	b.d.l.
b.d.l.	b.d.l.	b.d.l.	b.d.l.	b.d.l.	b.d.l.	33.0	b.d.l.	b.d.l.
b.d.l.	b.d.l.	b.d.l.	b.d.l.	b.d.l.	b.d.l.	31.7	b.d.l.	0.0

Table A1.5: continued

Info	Position	Li ^β	Li ^γ	Na	Mg	Al	Si	P	K	Ca	Sc	Ti	V	Mn	Fe	Rb	Sr	Y	Zr	Nb	Cs	Ba	La	Ce	Pr	Nd	Sm	Eu	Gd	Tb	Dy	Ho			
grain15-34	Core	b.d.l.	6.0	31849.4	b.d.l.	96326	308527	17.9	84731	2866.0	0.6	87.9	b.d.l.	b.d.l.	794.8	134.0	55.7	b.d.l.	b.d.l.	0.0	0.1	2632	7.7	5.7	0.3	0.5	b.d.l.	1.5	b.d.l.	b.d.l.	b.d.l.	b.d.l.			
grain15-35	Core	7.8	6.0	30800.8	5.4	91481	308527	12.8	81239	2630.3	0.6	93.7	b.d.l.	0.7	855.1	130.2	53.3	0.0	b.d.l.	b.d.l.	b.d.l.	0.1	2417	7.3	5.3	0.3	0.4	0.0	1.5	b.d.l.	b.d.l.	b.d.l.	b.d.l.		
grain15-36	Core	b.d.l.	6.0	30492.9	9.2	92038	308527	17.3	82123	2855.0	0.6	94.9	b.d.l.	0.7	826.7	125.2	53.6	0.0	b.d.l.	b.d.l.	0.1	2374	7.4	5.0	0.2	0.5	0.1	1.6	b.d.l.	b.d.l.	b.d.l.	b.d.l.			
grain15-37	Core	b.d.l.	5.7	30830.3	b.d.l.	92927	308527	15.0	83866	2938.9	0.7	84.6	b.d.l.	0.8	813.5	126.5	55.4	b.d.l.	b.d.l.	0.0	0.1	2330	7.7	5.5	0.3	0.4	0.0	1.6	b.d.l.	b.d.l.	b.d.l.	b.d.l.			
grain15-38	Rim	b.d.l.	4.5	31207.5	5.6	92960	308527	25.6	86782	2997.3	0.5	91.5	b.d.l.	b.d.l.	799.2	129.8	58.5	b.d.l.	0.2	b.d.l.	0.1	2260	7.9	5.6	0.3	0.6	0.0	1.6	b.d.l.	b.d.l.	b.d.l.	b.d.l.			
grain15-39	Rim	b.d.l.	2.8	32974.2	b.d.l.	90882	308527	37.7	86768	2958.8	0.4	91.4	b.d.l.	1.0	793.2	128.5	56.9	0.0	b.d.l.	0.0	0.1	2134	7.6	5.5	0.3	0.4	0.0	1.6	b.d.l.	0.0	b.d.l.	b.d.l.			
grain15-40	Rim	b.d.l.	1.5	31077.7	b.d.l.	94305	308527	16.7	84774	2929.4	0.6	86.5	b.d.l.	1.0	810.4	128.9	58.2	b.d.l.	b.d.l.	b.d.l.	0.1	2071	7.7	5.3	0.3	0.4	0.0	1.6	b.d.l.	b.d.l.	b.d.l.	b.d.l.			
Sandline grain 16 - Line 1																																			
grain16-1	Rim	b.d.l.	4.8	31208.6	b.d.l.	97028	308527	18.8	85812	2556.4	0.4	67.0	b.d.l.	b.d.l.	672.3	122.9	88.8	b.d.l.	b.d.l.	b.d.l.	0.1	499	6.4	4.4	0.2	0.4	0.0	2.2	b.d.l.	b.d.l.	b.d.l.	b.d.l.			
grain16-2	Rim	b.d.l.	4.7	30582.2	b.d.l.	96772	308527	b.d.l.	85550	2848.6	0.4	68.5	b.d.l.	b.d.l.	660.5	121.3	88.0	b.d.l.	b.d.l.	b.d.l.	b.d.l.	0.1	522	6.6	4.3	0.2	0.4	b.d.l.	2.4	b.d.l.	b.d.l.	b.d.l.	b.d.l.		
grain16-3	Rim	b.d.l.	5.1	30820.8	b.d.l.	97863	308527	18.0	84653	2587.3	0.8	63.9	b.d.l.	0.7	700.4	122.8	87.8	b.d.l.	b.d.l.	b.d.l.	0.1	584	6.7	4.6	0.2	0.5	b.d.l.	2.5	b.d.l.	b.d.l.	b.d.l.	b.d.l.			
grain16-4	Rim	b.d.l.	5.0	31300.8	b.d.l.	97210	308527	15.0	87247	2489.5	0.7	67.8	b.d.l.	b.d.l.	655.4	124.1	83.9	b.d.l.	b.d.l.	b.d.l.	0.1	584	6.6	4.4	0.2	0.5	b.d.l.	2.2	0.0	b.d.l.	b.d.l.	b.d.l.			
grain16-5	Rim	b.d.l.	5.0	32591.3	b.d.l.	100568	308527	b.d.l.	86550	2940.2	0.7	65.7	b.d.l.	0.6	722.3	126.5	83.6	b.d.l.	b.d.l.	b.d.l.	b.d.l.	0.1	622	6.7	4.3	0.2	0.4	b.d.l.	2.1	b.d.l.	b.d.l.	b.d.l.	b.d.l.		
grain16-6	Core	b.d.l.	5.2	30727.7	b.d.l.	98197	308527	15.3	84654	2897.3	0.7	62.7	b.d.l.	b.d.l.	734.6	123.7	82.3	b.d.l.	b.d.l.	0.0	0.1	663	6.5	4.5	0.2	0.4	0.0	2.1	0.0	b.d.l.	b.d.l.	b.d.l.	b.d.l.		
grain16-7	Core	b.d.l.	5.2	31438.5	b.d.l.	93273	308527	b.d.l.	85753	2803.0	0.6	76.8	b.d.l.	0.7	718.1	122.2	79.0	b.d.l.	b.d.l.	b.d.l.	0.1	693	6.6	4.6	0.2	0.5	0.0	2.2	b.d.l.	b.d.l.	b.d.l.	b.d.l.	b.d.l.		
grain16-8	Core	6.5	5.2	31809.2	b.d.l.	95455	308527	24.2	87114	2916.1	0.7	73.3	b.d.l.	b.d.l.	754.9	124.7	77.3	b.d.l.	b.d.l.	b.d.l.	0.1	725	6.4	4.4	0.2	0.4	0.0	2.0	b.d.l.	0.0	b.d.l.	b.d.l.	b.d.l.		
grain16-9	Core	b.d.l.	5.1	30380.9	b.d.l.	92045	308527	b.d.l.	83307	2836.3	0.6	62.9	b.d.l.	0.7	705.7	117.5	72.7	b.d.l.	b.d.l.	0.0	0.1	713	5.9	4.1	0.2	0.4	0.0	1.7	b.d.l.	b.d.l.	b.d.l.	b.d.l.	b.d.l.		
grain16-10	Core	b.d.l.	5.7	32812.1	b.d.l.	95724	308527	33.0	89106	2452.1	0.7	69.5	b.d.l.	0.8	730.9	125.7	78.4	b.d.l.	b.d.l.	b.d.l.	0.1	783	6.6	4.4	0.2	0.4	b.d.l.	2.2	b.d.l.	b.d.l.	b.d.l.	b.d.l.	b.d.l.		
grain16-11	Core	b.d.l.	4.9	32182.6	b.d.l.	94353	308527	b.d.l.	88166	2701.8	0.5	73.1	b.d.l.	b.d.l.	726.4	123.3	75.5	b.d.l.	b.d.l.	0.0	0.1	796	6.3	4.5	0.2	0.4	b.d.l.	2.1	0.0	b.d.l.	0.0	b.d.l.	0.0	b.d.l.	
grain16-12	Core	b.d.l.	4.5	31700.3	9.4	96648	308527	20.9	83948	2747.4	0.4	67.2	b.d.l.	b.d.l.	727.6	124.4	74.2	0.0	b.d.l.	0.0	0.1	797	6.5	4.7	0.2	0.4	b.d.l.	1.9	b.d.l.	b.d.l.	b.d.l.	0.0	b.d.l.		
grain16-13	Core	b.d.l.	4.5	30938.9	b.d.l.	94158	308527	31.8	85475	2583.8	0.4	68.9	b.d.l.	b.d.l.	719.6	122.1	71.0	b.d.l.	b.d.l.	b.d.l.	0.1	792	6.4	4.3	0.2	0.4	0.0	2.0	b.d.l.	b.d.l.	b.d.l.	b.d.l.	b.d.l.		
grain16-14	Core	b.d.l.	4.7	30172.5	b.d.l.	93937	308527	29.4	84991	2670.9	0.7	71.8	b.d.l.	1.0	730.0	120.5	71.8	b.d.l.	b.d.l.	b.d.l.	0.1	766	6.4	4.5	0.2	0.3	b.d.l.	1.8	0.0	b.d.l.	b.d.l.	b.d.l.	b.d.l.		
grain16-15	Core	b.d.l.	4.9	31152.5	b.d.l.	94863	308527	b.d.l.	84703	2888.5	0.6	70.7	b.d.l.	b.d.l.	713.3	125.7	73.4	b.d.l.	b.d.l.	0.0	0.1	766	7.0	5.1	0.2	0.4	b.d.l.	1.8	b.d.l.	b.d.l.	b.d.l.	b.d.l.	b.d.l.		
grain16-17	Core	6.1	5.1	30440.9	7.3	90318	308527	15.0	88631	2491.9	0.7	71.8	b.d.l.	0.8	732.8	125.3	62.5	b.d.l.	b.d.l.	b.d.l.	0.1	651	5.5	4.0	0.2	0.4	0.0	1.8	b.d.l.	0.0	b.d.l.	0.0	b.d.l.	b.d.l.	
grain16-18	Core	6.0	5.3	32599.8	b.d.l.	96994	308527	13.6	85353	3026.1	0.6	76.7	b.d.l.	0.7	742.8	122.8	70.0	b.d.l.	b.d.l.	b.d.l.	0.1	662	7.1	4.9	0.2	0.5	b.d.l.	1.9	b.d.l.	b.d.l.	b.d.l.	b.d.l.	b.d.l.		
grain16-19	Core	b.d.l.	5.1	31051.3	b.d.l.	92231	308527	b.d.l.	84677	2536.8	0.6	76.7	b.d.l.	0.7	732.4	125.0	63.0	b.d.l.	b.d.l.	b.d.l.	0.1	548	6.0	4.3	0.2	0.3	b.d.l.	1.7	b.d.l.	0.0	b.d.l.	0.0	b.d.l.	b.d.l.	
grain16-20	Core	b.d.l.	4.8	31554.0	b.d.l.	95709	308527	b.d.l.	86406	2766.1	0.8	69.5	b.d.l.	0.8	711.0	128.7	59.5	0.0	b.d.l.	b.d.l.	0.1	498	5.6	3.9	0.2	0.5	b.d.l.	1.6	0.1	b.d.l.	b.d.l.	0.0	b.d.l.	0.0	
grain16-21	Core	b.d.l.	4.2	30678.3	b.d.l.	94393	308527	20.2	88450	2759.9	0.8	68.6	b.d.l.	b.d.l.	693.7	121.0	58.2	b.d.l.	b.d.l.	b.d.l.	0.1	430	5.7	3.9	0.2	0.3	0.0	1.6	b.d.l.	b.d.l.	b.d.l.	b.d.l.	b.d.l.	b.d.l.	
grain16-22	Core	b.d.l.	4.2	31461.0	b.d.l.	97396	308527	b.d.l.	84474	2734.4	0.9	72.0	b.d.l.	0.7	739.6	125.4	59.3	b.d.l.	b.d.l.	b.d.l.	0.1	392	5.3	4.1	0.2	0.2	0.0	1.5	0.0	b.d.l.	b.d.l.	b.d.l.	b.d.l.	b.d.l.	
grain16-23	Core	6.7	4.5	31657.2	b.d.l.	95481	308527	19.2	90877	2711.6	0.5	71.4	b.d.l.	0.7	767.6	124.4	57.1	b.d.l.	b.d.l.	b.d.l.	0.1	336	5.5	3.8	0.2	0.3	b.d.l.	1.5	b.d.l.	0.0	b.d.l.	0.0	b.d.l.	b.d.l.	
grain16-24	Core	b.d.l.	4.3	31743.1	b.d.l.	95237	308527	b.d.l.	86872	2331.9	0.8	69.8	b.d.l.	0.7	747.2	125.0	57.2	b.d.l.	b.d.l.	b.d.l.	0.1	301	5.7	3.9	0.2	0.3	0.0	1.4	b.d.l.	b.d.l.	b.d.l.	b.d.l.	b.d.l.	b.d.l.	
grain16-25	Core	6.3	4.0	29334.3	b.d.l.	92426	308527	b.d.l.	85319	2664.2	0.5	73.0	b.d.l.	0.6	729.1	132.4	53.5	b.d.l.	b.d.l.	b.d.l.	0.1	258	5.3	3.6	0.2	0.3	0.0	1.3	b.d.l.	b.d.l.	b.d.l.	b.d.l.	b.d.l.	b.d.l.	
grain16-26	Core	b.d.l.	4.0	31650.3	b.d.l.	93273	308527	b.d.l.	84420	2702.7	1.1	73.1	b.d.l.	0.8	758.6	125.1	53.2	b.d.l.	b.d.l.	b.d.l.	0.1	236	5.4	3.8	0.2	0.4	b.d.l.	1.2	b.d.l.	b.d.l.	b.d.l.	b.d.l.	b.d.l.	b.d.l.	
grain16-27	Core	b.d.l.	4.0	31321.8	b.d.l.	93437	308527	b.d.l.	85202	2691.7	0.6	77.5	b.d.l.	b.d.l.	739.9	127.4	52.8	b.d.l.	b.d.l.	b.d.l.	0.1	224	5.6	3.8	0.2	0.3	0.0	1.3	b.d.l.	b.d.l.	b.d.l.	b.d.l.	0.0	b.d.l.	0.0
grain16-28	Core	b.d.l.	4.3	31754.0	6.1	92782	308527	b.d.l.	85254	3068.0	0.7	78.7	b.d.l.	b.d.l.	736.7	122.8	51.8	b.d.l.	b.d.l.	0.0	0.1	215	5.7	3.9	0.2	0.3	0.0	1.3	b.d.l.	b.d.l.	b.d.l.	b.d.l.	b.d.l.	b.d.l.	
grain16-29	Core	b.d.l.	4.7	31113.0	b.d.l.	93711	308527	25.5	84890	2723.3	b.d.l.	73.8	b.d.l.	0.6	760.3	127.9	51.6	b.d.l.	b.d.l.	0.0	0.1	212	5.6	4.1	0.2	0.3	b.d.l.	1.4	b.d.l.	b.d.l.	b.d.l.	b.d.l.	b.d.l.	b.d.l.	
grain16-30	Core	b.d.l.	5.1	30664.3	b.d.l.	93883	308527	b.d.l.	84998	2662.1	0.7	73.0	b.d.l.	b.d.l.	729.7	123.8	48.8	b.d.l.	b.d.l.	0.0	0.1	208	5.6	3.8	0.2	0.3	0.0	1.3	b.d.l.	b.d.l.	b.d.l.	b.d.l.	b.d.l.	b.d.l.	
grain16-31	Core	7.1	6.8	31866.1	b.d.l.	95606	308527	27.2	87278	2649.7	1.0	72.5	b.d.l.	b.d.l.	753.2	128.0	50.8	b.d.l.	b.d.l.	0.0	0.1	211	6.0	4.0	0.2	0.3	0.0	1.3	0.0	b.d.l.	b.d.l.	b.d.l.	b.d.l.	b.d.l.	
grain16-32	Core	b.d.l.	6.5	31187.8	b.d.l.	94333	308527	b.d.l.	93028	2781.0	0.6	76.6	b.d.l.	b.d.l.	753.9	128.7	50.9	b.d.l.	b.d.l.	b.d.l.	0.1	227	6.1	4.4	0.2	0.3	0.0	1.4	b.d.l.	b.d.l.	b.d.l.	b.d.l.	b.d.l.	b.d.l.	
grain16-33	Core	b.d.l.	5.9	32070.2	b.d.l.	97712	308527	20.8	87712	2425.8	0.9	76.0	b.d.l.	0.6	780.5	129.7	49.6	b.d.l.	b.d.l.	b.d.l.	0.1	227	6.2	4.1	0.2	0.3	0.0	1.4	b.d.l.	b.d.l.	b.d.l.	b.d.l.	b.d.l.	b.d.l.	
grain16-34	Core	6.9	5.7	31746.8	b.d.l.	96994	308527	b.d.l.	89615	2500.2	0.6	78.9	b.d.l.	0.8	803.2	128.4	47.3	b.d.l.	b.d.l.	0.0	0.1	228	6.0	4.2	0.2	0.4	b.d.l.	1.2	b.d.l.	b.d.l.	b.d.l.	b.d.l.	b.d.l.	b.d.l.	
grain16-35	Core	6.2	5.4	30668.9	5.7	94193	308527	b.d.l.	84875	2506.6	0.7	77.8	b.d.l.	0.7	783.9	128.1	48.5	b.d.l.	b.d.l.	b.d.l.	0.1	235	6.0	4.2	0.2	0.4	b.d.l.	1.2	b.d.l.	0.0	b.d.l.	0.0	b.d.l.	b.d.l.	
grain16-36	Core	b.d.l.	5.2	31851.8	b.d.l.	96955	30																												

Table A1.5: continued

Er	Tm	Yb	Lu	Hf	Ta	Pb	Th	U
b.d.l.	b.d.l.	b.d.l.	b.d.l.	b.d.l.	b.d.l.	32.7	b.d.l.	b.d.l.
b.d.l.	b.d.l.	b.d.l.	b.d.l.	b.d.l.	b.d.l.	30.8	b.d.l.	b.d.l.
b.d.l.	b.d.l.	b.d.l.	0.0	0.0	b.d.l.	31.4	b.d.l.	b.d.l.
b.d.l.	b.d.l.	b.d.l.	b.d.l.	b.d.l.	0.0	31.3	b.d.l.	b.d.l.
b.d.l.	b.d.l.	b.d.l.	b.d.l.	b.d.l.	b.d.l.	31.6	b.d.l.	b.d.l.
b.d.l.	b.d.l.	b.d.l.	b.d.l.	b.d.l.	b.d.l.	32.5	0.0	0.0
b.d.l.	b.d.l.	b.d.l.	b.d.l.	b.d.l.	b.d.l.	31.3	b.d.l.	b.d.l.
b.d.l.	b.d.l.	b.d.l.	b.d.l.	b.d.l.	b.d.l.	28.9	b.d.l.	b.d.l.
b.d.l.	b.d.l.	b.d.l.	b.d.l.	b.d.l.	b.d.l.	28.7	b.d.l.	b.d.l.
b.d.l.	b.d.l.	b.d.l.	b.d.l.	b.d.l.	b.d.l.	28.6	b.d.l.	b.d.l.
b.d.l.	b.d.l.	b.d.l.	b.d.l.	b.d.l.	b.d.l.	28.0	b.d.l.	b.d.l.
b.d.l.	0.0	b.d.l.	b.d.l.	b.d.l.	b.d.l.	28.5	b.d.l.	b.d.l.
b.d.l.	b.d.l.	b.d.l.	b.d.l.	b.d.l.	0.0	28.9	b.d.l.	b.d.l.
b.d.l.	b.d.l.	b.d.l.	b.d.l.	b.d.l.	b.d.l.	28.5	b.d.l.	b.d.l.
b.d.l.	b.d.l.	b.d.l.	b.d.l.	b.d.l.	b.d.l.	28.0	b.d.l.	b.d.l.
b.d.l.	b.d.l.	b.d.l.	b.d.l.	b.d.l.	0.0	26.9	b.d.l.	b.d.l.
b.d.l.	b.d.l.	b.d.l.	b.d.l.	b.d.l.	b.d.l.	29.7	b.d.l.	b.d.l.
b.d.l.	b.d.l.	b.d.l.	b.d.l.	b.d.l.	b.d.l.	28.5	b.d.l.	b.d.l.
b.d.l.	b.d.l.	b.d.l.	b.d.l.	b.d.l.	b.d.l.	28.4	b.d.l.	b.d.l.
b.d.l.	0.0	b.d.l.	b.d.l.	b.d.l.	b.d.l.	29.2	b.d.l.	b.d.l.
b.d.l.	b.d.l.	b.d.l.	b.d.l.	b.d.l.	b.d.l.	28.6	b.d.l.	b.d.l.
0.0	b.d.l.	b.d.l.	b.d.l.	0.0	b.d.l.	29.2	b.d.l.	b.d.l.
b.d.l.	b.d.l.	0.0	b.d.l.	b.d.l.	0.0	30.9	b.d.l.	b.d.l.
b.d.l.	b.d.l.	b.d.l.	b.d.l.	b.d.l.	b.d.l.	27.0	b.d.l.	b.d.l.
b.d.l.	0.0	b.d.l.	0.0	b.d.l.	b.d.l.	31.5	b.d.l.	b.d.l.
b.d.l.	b.d.l.	b.d.l.	b.d.l.	b.d.l.	0.0	28.1	b.d.l.	b.d.l.
b.d.l.	b.d.l.	b.d.l.	b.d.l.	b.d.l.	b.d.l.	29.6	b.d.l.	b.d.l.
b.d.l.	0.0	b.d.l.	b.d.l.	b.d.l.	b.d.l.	28.2	b.d.l.	b.d.l.
b.d.l.	b.d.l.	b.d.l.	b.d.l.	b.d.l.	b.d.l.	28.5	b.d.l.	b.d.l.
b.d.l.	b.d.l.	b.d.l.	b.d.l.	b.d.l.	b.d.l.	29.4	b.d.l.	b.d.l.
b.d.l.	b.d.l.	b.d.l.	b.d.l.	0.0	b.d.l.	29.8	b.d.l.	b.d.l.
b.d.l.	b.d.l.	b.d.l.	b.d.l.	b.d.l.	b.d.l.	28.4	b.d.l.	b.d.l.
b.d.l.	b.d.l.	b.d.l.	b.d.l.	b.d.l.	b.d.l.	30.0	b.d.l.	b.d.l.
b.d.l.	b.d.l.	b.d.l.	b.d.l.	b.d.l.	b.d.l.	29.2	b.d.l.	b.d.l.
b.d.l.	b.d.l.	b.d.l.	b.d.l.	b.d.l.	b.d.l.	30.9	b.d.l.	b.d.l.
b.d.l.	b.d.l.	b.d.l.	b.d.l.	b.d.l.	b.d.l.	30.5	b.d.l.	b.d.l.
b.d.l.	0.0	b.d.l.	b.d.l.	b.d.l.	b.d.l.	30.1	b.d.l.	b.d.l.
b.d.l.	b.d.l.	b.d.l.	b.d.l.	b.d.l.	b.d.l.	30.6	b.d.l.	0.0
b.d.l.	b.d.l.	b.d.l.	b.d.l.	b.d.l.	b.d.l.	30.9	b.d.l.	b.d.l.
b.d.l.	b.d.l.	b.d.l.	b.d.l.	b.d.l.	b.d.l.	29.9	b.d.l.	b.d.l.
b.d.l.	b.d.l.	b.d.l.	b.d.l.	b.d.l.	b.d.l.	31.4	b.d.l.	b.d.l.
b.d.l.	b.d.l.	b.d.l.	0.0	b.d.l.	b.d.l.	32.6	b.d.l.	b.d.l.
0.0	b.d.l.	b.d.l.	b.d.l.	b.d.l.	b.d.l.	32.4	b.d.l.	b.d.l.
b.d.l.	b.d.l.	b.d.l.	b.d.l.	b.d.l.	b.d.l.	31.2	b.d.l.	b.d.l.
b.d.l.	b.d.l.	b.d.l.	b.d.l.	b.d.l.	b.d.l.	30.8	b.d.l.	b.d.l.
b.d.l.	b.d.l.	b.d.l.	b.d.l.	b.d.l.	b.d.l.	31.2	b.d.l.	b.d.l.
b.d.l.	b.d.l.	b.d.l.	b.d.l.	b.d.l.	b.d.l.	32.6	b.d.l.	b.d.l.
b.d.l.	b.d.l.	b.d.l.	b.d.l.	b.d.l.	b.d.l.	31.6	b.d.l.	b.d.l.
b.d.l.	b.d.l.	b.d.l.	0.0	b.d.l.	b.d.l.	31.6	b.d.l.	b.d.l.
b.d.l.	b.d.l.	b.d.l.	b.d.l.	b.d.l.	b.d.l.	30.4	b.d.l.	b.d.l.
b.d.l.	b.d.l.	b.d.l.	b.d.l.	b.d.l.	b.d.l.	30.6	0.0	b.d.l.
b.d.l.	b.d.l.	b.d.l.	b.d.l.	b.d.l.	b.d.l.	31.5	b.d.l.	b.d.l.

Table A1.5: continued

Info	Position	L ^β	Li ^γ	Na	Mg	Al	Si	P	K	Ca	Sc	Ti	V	Mn	Fe	Rb	Sr	Y	Zr	Nb	Cs	Ba	La	Ce	Pr	Nd	Sm	Eu	Gd	Tb	Dy	Ho	
gram16-46	Core	6.3	5.4	31525.8	b.d.l.	97409	308527	20.0	89567	2418.2	0.9	85.3	b.d.l.	800.1	130.6	44.5	b.d.l.	b.d.l.	0.0	0.1	362	6.3	4.4	0.2	0.3	0.0	1.1	b.d.l.	b.d.l.	b.d.l.	b.d.l.		
gram16-47	Core	b.d.l.	5.3	31164.9	b.d.l.	94603	308527	b.d.l.	87151	2348.4	1.0	90.6	b.d.l.	821.5	126.6	44.7	b.d.l.	b.d.l.	0.0	0.1	367	6.3	4.4	0.2	0.4	0.0	1.1	b.d.l.	b.d.l.	b.d.l.	b.d.l.		
gram16-48	Core	b.d.l.	5.7	31011.3	b.d.l.	96959	308527	b.d.l.	87272	3080.7	0.6	86.2	b.d.l.	821.0	124.8	45.2	b.d.l.	b.d.l.	b.d.l.	b.d.l.	b.d.l.	390	6.5	4.7	0.2	0.5	0.0	1.3	b.d.l.	b.d.l.	b.d.l.	b.d.l.	
gram16-49	Core	6.5	5.4	31810.2	5.5	96205	308527	b.d.l.	88114	2835.5	0.5	88.7	b.d.l.	832.0	129.4	45.8	b.d.l.	b.d.l.	b.d.l.	0.1	420	6.4	4.7	0.2	0.4	0.1	1.2	b.d.l.	b.d.l.	b.d.l.	b.d.l.		
gram16-50	Core	b.d.l.	5.2	31109.3	b.d.l.	91866	308527	b.d.l.	85355	2589.5	0.6	81.5	b.d.l.	839.5	125.3	44.4	b.d.l.	b.d.l.	0.0	0.1	430	6.4	4.6	0.2	0.4	0.0	1.3	b.d.l.	b.d.l.	b.d.l.	b.d.l.		
gram16-51	Core	6.3	5.2	31989.5	b.d.l.	93887	308527	b.d.l.	85701	2559.3	0.7	84.9	b.d.l.	804.7	123.2	44.3	b.d.l.	b.d.l.	b.d.l.	0.1	438	6.5	4.9	0.3	0.5	b.d.l.	1.2	b.d.l.	0.0	b.d.l.	b.d.l.		
gram16-52	Core	b.d.l.	5.5	31657.8	b.d.l.	95537	308527	b.d.l.	86687	2484.8	0.6	86.3	b.d.l.	811.5	125.0	45.3	b.d.l.	b.d.l.	b.d.l.	0.1	438	6.9	5.0	0.2	0.5	0.1	1.2	b.d.l.	b.d.l.	b.d.l.	b.d.l.		
gram16-53	Core	b.d.l.	5.6	31706.6	b.d.l.	96064	308527	20.8	86687	2762.2	0.7	86.3	b.d.l.	822.2	123.4	45.0	b.d.l.	b.d.l.	b.d.l.	0.1	449	6.8	4.8	0.2	0.3	0.0	1.3	b.d.l.	b.d.l.	b.d.l.	b.d.l.		
gram16-54	Core	b.d.l.	5.0	31456.9	6.6	92897	308527	b.d.l.	84963	2745.8	0.9	88.4	b.d.l.	850.3	121.6	43.8	b.d.l.	b.d.l.	0.0	b.d.l.	451	6.5	4.5	0.2	0.4	b.d.l.	1.3	b.d.l.	b.d.l.	b.d.l.	b.d.l.		
gram16-55	Core	b.d.l.	5.2	31539.5	b.d.l.	93427	308527	21.9	83375	3046.8	0.7	90.1	b.d.l.	820.0	124.5	43.6	b.d.l.	b.d.l.	0.0	0.1	445	6.5	4.7	0.2	0.4	b.d.l.	1.3	b.d.l.	b.d.l.	b.d.l.	b.d.l.		
gram16-56	Core	b.d.l.	5.8	32111.8	b.d.l.	98177	308527	21.9	87894	3046.4	0.7	84.7	b.d.l.	820.0	128.5	45.1	b.d.l.	b.d.l.	b.d.l.	0.1	488	6.9	4.7	0.2	0.5	0.0	1.2	b.d.l.	0.0	b.d.l.	b.d.l.		
gram16-57	Core	b.d.l.	4.9	31603.1	b.d.l.	96659	308527	17.0	93907	3077.8	0.8	80.1	b.d.l.	869.5	127.9	44.7	0.0	b.d.l.	b.d.l.	0.1	495	6.8	4.8	0.2	0.4	b.d.l.	1.2	b.d.l.	0.0	b.d.l.	b.d.l.		
gram16-58	Core	b.d.l.	5.4	31273.0	b.d.l.	99363	308527	22.1	90474	2765.4	0.4	86.2	b.d.l.	850.4	127.6	45.3	b.d.l.	b.d.l.	b.d.l.	0.1	499	6.5	4.5	0.2	0.4	b.d.l.	1.3	0.0	0.0	b.d.l.	b.d.l.		
gram16-59	Core	b.d.l.	5.1	30495.9	8.2	95064	308527	20.3	86369	3117.5	b.d.l.	87.8	b.d.l.	871.1	126.4	46.3	b.d.l.	b.d.l.	0.0	0.1	492	6.4	4.5	0.2	0.4	0.0	1.3	b.d.l.	b.d.l.	b.d.l.	b.d.l.		
gram16-60	Core	b.d.l.	5.3	31030.6	b.d.l.	94062	308527	18.0	84100	2311.9	0.5	83.2	b.d.l.	822.3	122.3	46.5	b.d.l.	b.d.l.	b.d.l.	0.1	504	6.4	4.5	0.2	0.4	b.d.l.	1.1	b.d.l.	b.d.l.	b.d.l.	b.d.l.		
gram16-61	Core	b.d.l.	5.3	32112.6	b.d.l.	94425	308527	b.d.l.	88791	2724.8	0.6	80.4	b.d.l.	869.0	125.3	47.8	b.d.l.	b.d.l.	b.d.l.	0.1	515	6.3	4.4	0.2	0.5	0.0	1.3	b.d.l.	b.d.l.	b.d.l.	b.d.l.		
gram16-62	Core	b.d.l.	5.2	31075.9	b.d.l.	94149	308527	b.d.l.	87521	2875.8	0.7	80.8	b.d.l.	842.9	127.1	48.9	0.0	b.d.l.	b.d.l.	0.1	513	6.5	4.5	0.2	0.4	b.d.l.	1.3	b.d.l.	b.d.l.	0.0	b.d.l.		
gram16-63	Core	b.d.l.	5.4	31561.8	b.d.l.	95213	308527	b.d.l.	86735	2510.9	0.7	77.4	b.d.l.	810.5	126.5	48.0	b.d.l.	b.d.l.	b.d.l.	0.1	515	6.0	4.1	0.2	0.5	b.d.l.	1.2	b.d.l.	b.d.l.	b.d.l.	b.d.l.		
gram16-64	Core	7.5	5.6	32661.0	7.1	99146	308527	21.7	91406	2724.9	0.6	86.6	b.d.l.	871.6	133.0	50.6	b.d.l.	b.d.l.	b.d.l.	0.1	522	6.6	4.4	0.2	0.4	b.d.l.	1.2	b.d.l.	b.d.l.	0.0	b.d.l.		
gram16-65	Core	b.d.l.	5.9	31376.2	b.d.l.	96590	308527	13.7	86587	2126.0	0.7	83.1	b.d.l.	860.2	124.9	48.7	b.d.l.	b.d.l.	b.d.l.	0.1	517	6.1	4.1	0.2	0.3	b.d.l.	1.1	b.d.l.	b.d.l.	b.d.l.	b.d.l.		
gram16-66	Core	b.d.l.	6.0	30574.3	b.d.l.	94031	308527	b.d.l.	86813	2521.7	0.7	84.1	b.d.l.	879.1	125.9	48.5	b.d.l.	b.d.l.	b.d.l.	0.1	488	6.1	4.2	0.2	0.3	0.0	1.2	b.d.l.	b.d.l.	b.d.l.	b.d.l.		
gram16-67	Core	b.d.l.	6.2	31858.9	b.d.l.	95471	308527	16.2	91349	2591.9	0.8	85.6	b.d.l.	879.5	126.0	51.0	b.d.l.	b.d.l.	b.d.l.	0.1	496	6.1	4.1	0.2	0.3	0.0	1.3	0.1	b.d.l.	b.d.l.	b.d.l.	b.d.l.	
gram16-68	Core	b.d.l.	5.7	30560.8	b.d.l.	96629	308527	b.d.l.	86090	2381.0	0.7	87.2	b.d.l.	879.7	124.6	50.9	b.d.l.	b.d.l.	b.d.l.	0.1	467	6.2	4.1	0.2	0.3	0.0	1.3	b.d.l.	b.d.l.	b.d.l.	b.d.l.		
gram16-69	Core	b.d.l.	5.8	39101.0	b.d.l.	101009	308527	b.d.l.	69730	8758.7	0.6	71.2	b.d.l.	2.4	903.3	89.7	54.9	b.d.l.	b.d.l.	b.d.l.	0.0	347	8.0	6.9	0.4	0.9	b.d.l.	1.4	b.d.l.	b.d.l.	b.d.l.	b.d.l.	
gram16-70	Core	b.d.l.	5.7	32960.0	6.6	97313	308527	b.d.l.	88758	2684.4	0.8	85.3	b.d.l.	0.8	892.4	125.4	52.8	b.d.l.	b.d.l.	b.d.l.	0.1	475	6.5	4.5	0.2	0.4	b.d.l.	1.2	b.d.l.	b.d.l.	b.d.l.	b.d.l.	
Sanidine grain 17 - Line 1																																	
gram17-1	Core	b.d.l.	4.6	30415.1	b.d.l.	99669	303853	b.d.l.	83160	2655.4	0.6	97.0	b.d.l.	0.9	823.3	111.1	207.9	b.d.l.	b.d.l.	b.d.l.	0.1	7457	9.8	7.1	0.4	0.7	b.d.l.	5.3	b.d.l.	b.d.l.	b.d.l.	0.0	
gram17-2	Core	7.3	4.7	30294.9	b.d.l.	99619	303853	28.3	83463	3226.5	0.6	96.3	b.d.l.	828.8	111.7	227.2	0.1	0.1	b.d.l.	0.1	8125	10.1	6.9	0.4	0.8	b.d.l.	6.1	b.d.l.	b.d.l.	b.d.l.	b.d.l.	0.0	
gram17-3	Core	b.d.l.	5.2	30423.6	b.d.l.	101225	303853	20.2	83710	3243.6	0.6	94.9	b.d.l.	888.4	110.7	247.7	b.d.l.	b.d.l.	b.d.l.	0.1	8285	10.5	7.4	0.4	0.8	0.1	6.3	0.1	b.d.l.	b.d.l.	b.d.l.	b.d.l.	
gram17-4	Core	b.d.l.	5.3	31218.1	8.4	102635	303853	19.2	83666	4010.0	0.6	109.3	b.d.l.	912.0	104.7	285.5	b.d.l.	b.d.l.	b.d.l.	0.0	10577	13.2	9.6	0.6	1.1	b.d.l.	7.2	b.d.l.	b.d.l.	b.d.l.	b.d.l.	b.d.l.	
gram17-5	Core	b.d.l.	4.8	30933.7	7.1	98308	303853	b.d.l.	83622	3570.1	0.5	112.4	b.d.l.	1.0	837.6	100.6	290.8	b.d.l.	b.d.l.	0.0	10981	10.5	7.8	0.4	0.6	0.0	7.0	b.d.l.	b.d.l.	b.d.l.	b.d.l.	b.d.l.	
gram17-6	Core	b.d.l.	4.9	30530.5	b.d.l.	96939	303853	20.6	84497	3509.6	0.8	89.8	b.d.l.	0.7	831.2	101.1	250.7	0.0	b.d.l.	b.d.l.	b.d.l.	7982	7.9	5.6	0.3	0.6	b.d.l.	6.7	b.d.l.	b.d.l.	b.d.l.	b.d.l.	
gram17-7	Core	b.d.l.	4.8	30934.9	b.d.l.	100220	303853	b.d.l.	87874	3525.6	0.5	89.1	b.d.l.	0.7	879.0	102.4	257.2	b.d.l.	b.d.l.	b.d.l.	b.d.l.	8183	8.1	5.8	0.3	0.6	0.0	7.2	b.d.l.	b.d.l.	b.d.l.	b.d.l.	
gram17-8	Core	b.d.l.	4.7	30741.5	b.d.l.	97542	303853	b.d.l.	84216	3395.6	0.8	84.2	b.d.l.	852.2	98.3	239.8	0.0	b.d.l.	b.d.l.	0.1	7392	7.4	5.4	0.3	0.6	0.0	6.9	b.d.l.	b.d.l.	b.d.l.	b.d.l.	b.d.l.	
gram17-9	Core	b.d.l.	5.1	31039.2	b.d.l.	98936	303853	15.9	83571	3492.1	0.4	85.3	b.d.l.	0.7	850.2	100.9	236.5	0.0	b.d.l.	b.d.l.	0.1	6424	7.7	5.3	0.3	0.5	b.d.l.	6.8	b.d.l.	b.d.l.	b.d.l.	b.d.l.	
gram17-10	Core	b.d.l.	5.1	29379.0	b.d.l.	98210	303853	b.d.l.	84245	3256.7	0.7	86.6	b.d.l.	847.5	99.5	238.8	b.d.l.	b.d.l.	b.d.l.	0.1	7277	7.4	5.6	0.3	0.3	b.d.l.	6.8	b.d.l.	b.d.l.	b.d.l.	b.d.l.	b.d.l.	
gram17-11	Core	b.d.l.	4.9	31683.8	b.d.l.	99143	303853	b.d.l.	84137	3406.8	0.7	88.1	b.d.l.	0.7	826.0	98.4	245.0	0.0	b.d.l.	b.d.l.	b.d.l.	7879	8.0	5.6	0.3	0.6	0.0	6.9	b.d.l.	b.d.l.	b.d.l.	b.d.l.	b.d.l.
gram17-12	Core	b.d.l.	4.8	30455.4	7.8	96232	303853	14.7	83885	3087.0	0.4	86.5	b.d.l.	0.6	867.2	99.2	242.3	b.d.l.	b.d.l.	b.d.l.	7922	7.6	5.5	0.3	0.4	0.0	7.0	b.d.l.	b.d.l.	b.d.l.	b.d.l.	b.d.l.	
gram17-13	Core	b.d.l.	5.4	30586.8	b.d.l.	99982	303853	b.d.l.	83268	3239.1	0.6	90.2	b.d.l.	0.6	858.8	101.6	252.5	0.0	b.d.l.	0.0	0.0	8674	8.0	5.6	0.3	0.5	0.0	7.1	b.d.l.	b.d.l.	b.d.l.	b.d.l.	b.d.l.
gram17-14	Core	b.d.l.	5.7	30500.9	b.d.l.	95875	303853	b.d.l.	87329	3252.1	0.7	88.0	b.d.l.	0.7	855.0	96.2	258.5	0.0	b.d.l.	0.0	0.0	9686	8.0	5.8	0.3	0.8	0.0	7.2	b.d.l.	0.0	b.d.l.	b.d.l.	b.d.l.
gram17-15	Core	b.d.l.	5.2	30971.1	8.6	99415	303853	b.d.l.	82976	3065.0	0.7	91.9	b.d.l.	870.8	100.3	258.8	0.1	b.d.l.	b.d.l.	0.1	9663	8.3	6.1	0.3	0.5	0.0	7.2	b.d.l.	0.0	b.d.l.	b.d.l.	b.d.l.	
gram17-16	Core	6.4	5.4	31137.3	10.6	99190	303853	b.d.l.	85009	3610.8	0.6	89.5	b.d.l.	0.9	875.7	95.5	246.5	b.d.l.	b.d.l.	b.d.l.	9247	8.4	5.8	0.3	0.7	b.d.l.	7.1	b.d.l.	b.d.l.	b.d.l.	b.d.l.	b.d.l.	
gram17-17	Core	b.d.l.	5.1	31860.6	b.d.l.	99753	303853	b.d.l.	85358	3694.8	0.9	92.6	b.d.l.	882.0	98.9	254.2	0.0	b.d.l.	b.d.l.	0.1	10645	8.3	6.2	0.3	0.6	b.d.l.	7.2	b.d.l.	0.0	b.d.l.	b.d.l.	b.d.l.	
gram17-18	Core	b.d.l.	5.3	32308.4	b.d.l.	99769	303853	19.5	83618	3652.8	0.9	97.2	b.d.l.	0.7	844.5	99.5	258.9	0.1	b.d.l.	b.d.l.	0.1	9848	8.6	6.0	0.3	0.5	0.0	7.3	b.d.l.	b.d.l.	b.d.l.	b.d.l.	b.d.l.
gram17-19	Core	b.d.l.	5.6	31488.7																													

Table A1.5: continued

Er	Tm	Yb	Lu	Hf	Ta	Pb	Th	U
b.d.l.	b.d.l.	b.d.l.	b.d.l.	b.d.l.	0.0	31.7	b.d.l.	b.d.l.
b.d.l.	b.d.l.	b.d.l.	b.d.l.	b.d.l.	b.d.l.	30.9	b.d.l.	b.d.l.
b.d.l.	b.d.l.	b.d.l.	0.0	b.d.l.	b.d.l.	32.2	b.d.l.	b.d.l.
b.d.l.	b.d.l.	b.d.l.	b.d.l.	b.d.l.	b.d.l.	33.1	b.d.l.	b.d.l.
b.d.l.	b.d.l.	b.d.l.	b.d.l.	b.d.l.	b.d.l.	32.0	b.d.l.	b.d.l.
b.d.l.	b.d.l.	b.d.l.	b.d.l.	b.d.l.	0.0	32.8	b.d.l.	b.d.l.
b.d.l.	b.d.l.	b.d.l.	b.d.l.	b.d.l.	b.d.l.	32.5	b.d.l.	b.d.l.
b.d.l.	b.d.l.	b.d.l.	b.d.l.	b.d.l.	b.d.l.	32.1	b.d.l.	b.d.l.
b.d.l.	b.d.l.	b.d.l.	b.d.l.	b.d.l.	b.d.l.	31.3	b.d.l.	b.d.l.
b.d.l.	b.d.l.	b.d.l.	b.d.l.	b.d.l.	b.d.l.	31.5	b.d.l.	b.d.l.
b.d.l.	b.d.l.	b.d.l.	b.d.l.	b.d.l.	b.d.l.	33.3	b.d.l.	b.d.l.
b.d.l.	b.d.l.	b.d.l.	b.d.l.	b.d.l.	b.d.l.	31.9	b.d.l.	b.d.l.
b.d.l.	b.d.l.	b.d.l.	b.d.l.	b.d.l.	b.d.l.	32.1	b.d.l.	b.d.l.
b.d.l.	b.d.l.	b.d.l.	b.d.l.	b.d.l.	b.d.l.	30.3	b.d.l.	b.d.l.
b.d.l.	b.d.l.	0.0	0.0	b.d.l.	b.d.l.	31.8	b.d.l.	b.d.l.
b.d.l.	b.d.l.	b.d.l.	b.d.l.	b.d.l.	b.d.l.	30.5	b.d.l.	b.d.l.
b.d.l.	b.d.l.	b.d.l.	b.d.l.	0.0	b.d.l.	30.9	b.d.l.	b.d.l.
b.d.l.	b.d.l.	b.d.l.	b.d.l.	b.d.l.	b.d.l.	30.0	b.d.l.	b.d.l.
b.d.l.	b.d.l.	b.d.l.	b.d.l.	b.d.l.	b.d.l.	30.3	b.d.l.	b.d.l.
b.d.l.	b.d.l.	b.d.l.	b.d.l.	b.d.l.	b.d.l.	29.3	b.d.l.	b.d.l.
b.d.l.	b.d.l.	b.d.l.	b.d.l.	b.d.l.	b.d.l.	30.2	b.d.l.	b.d.l.
b.d.l.	b.d.l.	b.d.l.	b.d.l.	b.d.l.	b.d.l.	26.8	b.d.l.	b.d.l.
b.d.l.	b.d.l.	b.d.l.	b.d.l.	b.d.l.	b.d.l.	30.7	b.d.l.	b.d.l.
b.d.l.	b.d.l.	b.d.l.	b.d.l.	b.d.l.	b.d.l.	25.0	b.d.l.	b.d.l.
b.d.l.	b.d.l.	b.d.l.	b.d.l.	b.d.l.	b.d.l.	24.6	b.d.l.	b.d.l.
b.d.l.	b.d.l.	b.d.l.	b.d.l.	b.d.l.	b.d.l.	26.0	b.d.l.	b.d.l.
b.d.l.	b.d.l.	b.d.l.	b.d.l.	0.0	b.d.l.	23.8	b.d.l.	b.d.l.
b.d.l.	b.d.l.	b.d.l.	b.d.l.	b.d.l.	b.d.l.	21.6	b.d.l.	b.d.l.
b.d.l.	b.d.l.	b.d.l.	b.d.l.	b.d.l.	b.d.l.	22.5	b.d.l.	b.d.l.
0.0	b.d.l.	b.d.l.	b.d.l.	b.d.l.	b.d.l.	21.6	b.d.l.	b.d.l.
b.d.l.	b.d.l.	b.d.l.	b.d.l.	b.d.l.	b.d.l.	21.8	b.d.l.	b.d.l.
b.d.l.	b.d.l.	b.d.l.	b.d.l.	0.0	b.d.l.	21.7	b.d.l.	b.d.l.
b.d.l.	b.d.l.	b.d.l.	b.d.l.	b.d.l.	0.0	b.d.l.	21.0	b.d.l.
b.d.l.	b.d.l.	b.d.l.	0.0	b.d.l.	b.d.l.	22.4	b.d.l.	b.d.l.
b.d.l.	b.d.l.	b.d.l.	b.d.l.	b.d.l.	b.d.l.	21.8	b.d.l.	b.d.l.
b.d.l.	b.d.l.	b.d.l.	b.d.l.	0.0	b.d.l.	22.0	b.d.l.	b.d.l.
b.d.l.	b.d.l.	b.d.l.	b.d.l.	b.d.l.	b.d.l.	21.1	b.d.l.	b.d.l.
b.d.l.	b.d.l.	b.d.l.	b.d.l.	b.d.l.	0.0	22.7	b.d.l.	b.d.l.
b.d.l.	b.d.l.	b.d.l.	0.0	b.d.l.	b.d.l.	23.1	b.d.l.	b.d.l.
b.d.l.	b.d.l.	b.d.l.	b.d.l.	b.d.l.	b.d.l.	22.0	b.d.l.	b.d.l.
b.d.l.	b.d.l.	b.d.l.	b.d.l.	b.d.l.	b.d.l.	22.0	b.d.l.	b.d.l.
b.d.l.	b.d.l.	b.d.l.	b.d.l.	b.d.l.	b.d.l.	21.3	b.d.l.	b.d.l.
b.d.l.	b.d.l.	b.d.l.	b.d.l.	b.d.l.	0.0	22.1	b.d.l.	b.d.l.
b.d.l.	b.d.l.	b.d.l.	b.d.l.	b.d.l.	0.0	22.4	0.0	b.d.l.
b.d.l.	b.d.l.	b.d.l.	b.d.l.	b.d.l.	b.d.l.	22.3	b.d.l.	b.d.l.
b.d.l.	b.d.l.	0.0	b.d.l.	0.0	0.0	24.3	b.d.l.	b.d.l.
b.d.l.	b.d.l.	b.d.l.	b.d.l.	b.d.l.	b.d.l.	22.8	b.d.l.	b.d.l.

Table A1.5: continued

Info	Position	Li ⁺	Na	Mg	Al	Si	P	K	Ca	Sc	Ti	V	Mn	Fe	Rb	Sr	Y	Zr	Nb	Cs	Ba	La	Ce	Pr	Nd	Sm	Eu	Gd	Tb	Dy	Ho
grain17-28	Rim	b.d.l.	6.0	31581.4	b.d.l.	97137	303853	19.2	85626	3207.1	0.7	87.2	b.d.l.	904.6	101.6	247.3	0.0	b.d.l.	b.d.l.	0.1	8220	8.4	6.3	0.3	0.5	0.0	7.1	b.d.l.	b.d.l.	b.d.l.	b.d.l.
grain17-29	Rim	b.d.l.	4.7	31771.7	b.d.l.	100272	303853	b.d.l.	88168	3204.2	0.8	92.4	b.d.l.	894.0	99.5	248.3	b.d.l.	b.d.l.	b.d.l.	0.1	9167	8.9	6.4	0.3	0.9	0.1	7.0	b.d.l.	0.0	b.d.l.	b.d.l.
grain17-30	Rim	b.d.l.	3.3	33312.8	b.d.l.	100113	303853	16.4	80321	3705.6	0.9	100.6	b.d.l.	0.9	878.8	94.0	255.0	0.1	0.0	0.0	11068	8.7	6.5	0.4	0.7	0.0	7.0	0.1	b.d.l.	b.d.l.	b.d.l.
grain17-31	Rim	b.d.l.	1.4	33257.0	b.d.l.	98834	303853	15.7	84532	4028.8	0.6	94.5	b.d.l.	914.1	96.7	247.7	0.0	b.d.l.	0.0	0.1	10386	8.8	6.5	0.3	0.6	b.d.l.	7.1	b.d.l.	b.d.l.	b.d.l.	
Sanidine grain 17 - Line 2																															
MFT-San17 - 1	Rim	2.9	30626.1	4.0	109218	308527	b.d.l.	74245	3579.5	b.d.l.	73.8	b.d.l.	b.d.l.	759.2	113.6	168.7	0.3	b.d.l.	0.0	0.1	5052	8.9	6.0	0.3	0.3	0.3	b.d.l.	4.7	b.d.l.	b.d.l.	b.d.l.
MFT-San17 - 2	Core	4.2	31770.2	4.4	116247	308527	b.d.l.	78235	4759.4	b.d.l.	111.7	b.d.l.	b.d.l.	896.3	114.5	203.5	0.7	b.d.l.	b.d.l.	0.1	9077	9.7	8.2	0.5	0.8	b.d.l.	5.8	b.d.l.	b.d.l.	0.1	0.0
MFT-San17 - 3	Core	5.5	4.6	29082.7	2.3	105554	308527	b.d.l.	73511	3603.6	b.d.l.	89.4	b.d.l.	764.2	109.4	174.3	0.5	b.d.l.	b.d.l.	0.1	6564	9.3	6.5	0.3	0.6	0.1	4.4	b.d.l.	b.d.l.	b.d.l.	
MFT-San17 - 4	Core	5.8	5.0	31098.0	b.d.l.	111874	308527	59.6	78467	3678.5	b.d.l.	89.3	b.d.l.	841.4	114.9	204.4	0.4	b.d.l.	b.d.l.	0.1	7928	10.3	7.4	0.4	0.6	b.d.l.	5.5	0.1	b.d.l.	b.d.l.	
MFT-San17 - 5	Core	4.9	5.3	31067.5	3.1	111727	308527	b.d.l.	80355	3951.8	b.d.l.	85.8	b.d.l.	825.4	117.8	246.8	0.4	0.0	0.0	0.1	8344	10.3	7.6	0.3	0.5	b.d.l.	7.0	b.d.l.	b.d.l.		
MFT-San17 - 6	Core	4.1	4.7	31030.9	3.9	112361	308527	73.5	74597	5231.8	b.d.l.	110.8	b.d.l.	805.0	104.6	197.7	0.4	0.1	b.d.l.	b.d.l.	10564	15.2	11.3	0.7	1.1	b.d.l.	7.8	0.1	b.d.l.	b.d.l.	
MFT-San17 - 7	Core	5.0	4.9	30810.6	3.8	112885	308527	b.d.l.	77427	4428.1	b.d.l.	104.8	b.d.l.	877.3	100.3	287.1	0.5	b.d.l.	0.0	0.1	10191	10.4	7.7	0.5	0.7	0.1	7.7	b.d.l.	b.d.l.	0.0	
MFT-San17 - 8	Core	5.6	4.6	28366.8	1.3	102258	308527	b.d.l.	71143	3412.4	b.d.l.	77.3	b.d.l.	868.5	92.7	254.8	0.4	0.0	b.d.l.	0.1	7277	7.7	5.6	0.3	0.6	0.1	5.9	b.d.l.	b.d.l.	b.d.l.	
MFT-San17 - 9	Core	7.0	5.3	31106.4	3.2	108233	308527	65.9	80913	3951.6	b.d.l.	78.0	b.d.l.	889.5	99.6	257.7	0.4	b.d.l.	b.d.l.	0.1	7866	7.9	5.4	0.2	0.6	b.d.l.	7.0	b.d.l.	b.d.l.		
MFT-San17 - 10	Core	5.9	5.5	30422.0	4.3	110743	308527	b.d.l.	77486	3901.5	b.d.l.	84.0	b.d.l.	857.3	95.0	257.6	0.4	b.d.l.	0.0	0.1	8004	7.7	5.4	0.2	0.6	b.d.l.	7.1	b.d.l.	b.d.l.		
MFT-San17 - 11	Core	6.0	5.3	30287.1	1.9	110750	308527	40.5	75530	3905.4	0.8	76.6	b.d.l.	852.7	98.1	253.1	0.4	b.d.l.	b.d.l.	0.1	7504	7.8	5.7	0.3	0.6	b.d.l.	7.0	b.d.l.	b.d.l.		
MFT-San17 - 12	Core	5.9	5.7	30316.4	4.0	107949	308527	b.d.l.	74628	3838.6	0.5	83.0	b.d.l.	879.2	94.6	245.3	0.3	0.1	b.d.l.	b.d.l.	7361	8.0	5.8	0.3	0.5	0.1	7.0	b.d.l.	b.d.l.		
MFT-San17 - 13	Core	5.9	5.6	30262.9	3.5	109972	308527	b.d.l.	74523	3652.8	0.5	79.5	b.d.l.	870.8	93.2	244.2	0.3	b.d.l.	b.d.l.	0.1	7539	8.3	5.5	0.3	0.6	b.d.l.	7.3	b.d.l.	b.d.l.		
MFT-San17 - 14	Core	8.0	6.6	29991.7	4.2	106403	308527	b.d.l.	74187	4185.6	0.8	82.0	b.d.l.	902.9	93.7	249.4	0.4	0.1	0.0	b.d.l.	8101	8.0	5.8	0.3	0.5	b.d.l.	6.9	b.d.l.	b.d.l.		
MFT-San17 - 15	Core	10.3	10.3	31373.1	1.6	105168	308527	b.d.l.	75688	4060.9	0.5	89.0	0.9	b.d.l.	887.8	92.8	257.5	0.4	0.1	b.d.l.	8553	8.2	5.8	0.3	0.6	b.d.l.	7.5	b.d.l.	b.d.l.		
MFT-San17 - 16	Core	13.4	11.9	31296.6	3.0	110401	308527	65.5	77839	3791.8	b.d.l.	81.1	b.d.l.	961.2	104.5	265.1	0.8	b.d.l.	0.1	9300	8.3	5.9	0.4	0.5	b.d.l.	7.5	b.d.l.	b.d.l.			
MFT-San17 - 17	Core	7.2	7.5	30578.9	3.2	107214	308527	b.d.l.	80478	3887.5	b.d.l.	92.3	b.d.l.	901.7	102.8	256.2	0.7	0.3	0.3	b.d.l.	9708	8.0	5.8	0.3	0.4	b.d.l.	7.1	b.d.l.	b.d.l.		
MFT-San17 - 18	Core	6.4	5.9	29768.8	4.8	106948	308527	b.d.l.	80478	3887.5	b.d.l.	92.3	b.d.l.	943.9	95.9	249.8	0.7	0.4	0.1	0.3	0.0	10354	8.4	7.5	0.4	1.3	b.d.l.	7.0	b.d.l.	b.d.l.	
MFT-San17 - 19	Core	6.0	5.8	30141.6	4.9	104198	308527	49.2	79370	3659.0	b.d.l.	74.8	b.d.l.	851.6	96.0	219.8	0.4	0.1	0.1	0.2	8346	7.4	5.6	0.2	0.5	0.1	6.3	0.1	0.0	b.d.l.	
MFT-San17 - 20	Core	6.5	5.9	30931.5	4.9	104198	308527	b.d.l.	76364	3595.0	b.d.l.	81.8	b.d.l.	127	928.6	101.1	213.7	0.2	0.1	0.2	6009	7.0	5.2	0.2	0.5	b.d.l.	6.0	b.d.l.	b.d.l.		
MFT-San17 - 21	Core	6.6	5.8	30809.0	4.5	113197	308527	b.d.l.	79918	4104.1	b.d.l.	82.1	b.d.l.	853.7	98.9	233.5	0.3	b.d.l.	b.d.l.	0.1	5628	7.7	6.0	0.4	0.4	b.d.l.	6.5	0.1	b.d.l.		
MFT-San17 - 22	Core	5.2	5.3	30294.5	1.9	106778	308527	b.d.l.	76672	3883.8	1.1	91.0	b.d.l.	880.0	97.0	229.9	0.5	0.0	0.1	0.1	8400	7.7	5.9	0.2	0.5	b.d.l.	6.3	b.d.l.	b.d.l.		
MFT-San17 - 23	Core	5.2	5.7	32605.2	2.4	108672	308527	47.6	78504	4899.9	b.d.l.	91.5	b.d.l.	889.9	93.4	246.6	0.4	b.d.l.	b.d.l.	0.1	9362	8.7	6.2	0.3	0.5	b.d.l.	6.5	b.d.l.	b.d.l.		
MFT-San17 - 24	Core	5.5	6.1	31291.1	1.9	111694	308527	66.3	73981	4142.4	b.d.l.	81.7	b.d.l.	895.0	91.0	246.9	0.5	0.1	0.1	0.1	8595	8.3	6.2	0.3	0.5	0.1	7.3	b.d.l.	b.d.l.		
MFT-San17 - 25	Core	4.8	5.7	30113.2	1.8	105665	308527	b.d.l.	76432	3663.0	b.d.l.	82.5	b.d.l.	120	792.5	93.5	217.5	0.4	0.0	0.0	10581	8.6	6.6	0.3	0.6	b.d.l.	7.0	b.d.l.	b.d.l.		
MFT-San17 - 26	Core	6.6	5.8	30809.0	4.5	113197	308527	b.d.l.	79918	4104.1	b.d.l.	82.1	b.d.l.	853.7	98.9	233.5	0.3	b.d.l.	b.d.l.	0.1	5628	7.7	6.0	0.4	0.4	b.d.l.	6.5	0.1	b.d.l.		
MFT-San17 - 27	Core	5.2	5.3	30294.5	1.9	106778	308527	b.d.l.	76672	3883.8	1.1	91.0	b.d.l.	880.0	97.0	229.9	0.5	0.0	0.1	0.1	8400	7.7	5.9	0.2	0.5	b.d.l.	6.3	b.d.l.	b.d.l.		
MFT-San17 - 28	Core	5.2	5.7	32605.2	2.4	108672	308527	47.6	78504	4899.9	b.d.l.	91.5	b.d.l.	889.9	93.4	246.6	0.4	b.d.l.	b.d.l.	0.1	9362	8.7	6.2	0.3	0.5	b.d.l.	6.5	b.d.l.	b.d.l.		
MFT-San17 - 29	Core	5.5	6.1	31291.1	1.9	111694	308527	66.3	73981	4142.4	b.d.l.	81.7	b.d.l.	895.0	91.0	246.9	0.5	0.1	0.1	0.1	8595	8.3	6.2	0.3	0.5	0.1	7.3	b.d.l.	b.d.l.		
MFT-San17 - 30	Core	5.8	5.5	30088.3	3.1	106466	308527	66.3	73981	4142.4	b.d.l.	93.9	b.d.l.	855.3	86.5	243.0	0.7	b.d.l.	b.d.l.	0.0	8595	8.3	6.2	0.4	0.6	b.d.l.	7.1	0.1	b.d.l.		
MFT-San17 - 31	Core	7.4	6.4	31742.6	1.5	108470	308527	b.d.l.	76744	4152.9	b.d.l.	92.8	b.d.l.	828.8	96.4	254.8	0.4	0.0	0.0	0.1	10581	8.6	6.6	0.3	0.6	b.d.l.	7.0	b.d.l.	b.d.l.		
MFT-San17 - 32	Core	7.5	6.4	29753.0	2.2	105927	308527	b.d.l.	70077	3838.7	b.d.l.	78.4	b.d.l.	828.2	84.7	251.8	0.6	b.d.l.	b.d.l.	0.1	10723	8.4	6.4	0.3	0.5	b.d.l.	7.4	0.1	b.d.l.		
MFT-San17 - 33	Core	6.6	6.2	31593.3	4.3	108840	308527	b.d.l.	74812	4697.9	b.d.l.	99.2	b.d.l.	927.3	90.7	273.2	0.6	b.d.l.	0.1	0.1	12922	8.3	7.0	0.3	0.9	b.d.l.	7.5	b.d.l.			
MFT-San17 - 34	Core	6.2	5.6	31507.8	3.3	111114	308527	b.d.l.	73572	4618.5	b.d.l.	110.6	b.d.l.	837.7	91.4	264.7	0.8	b.d.l.	b.d.l.	0.1	12368	9.6	7.1	0.4	0.6	b.d.l.	7.1	b.d.l.			
MFT-San17 - 35	Core	5.3	4.7	30522.5	2.0	108656	308527	b.d.l.	73981	4142.4	b.d.l.	85.9	b.d.l.	830.8	93.1	224.1	0.3	0.0	0.0	0.1	5285	9.2	6.2	0.3	0.3	b.d.l.	6.6	0.1	b.d.l.		
MFT-San17 - 36	Core	3.4	3.2	30779.1	4.8	107455	308527	b.d.l.	72851	3991.9	b.d.l.	83.9	b.d.l.	841.3	88.9	225.2	0.2	b.d.l.	b.d.l.	0.0	5321	9.0	6.4	0.3	0.6	b.d.l.					

Table A1.5: continued

Er	Tm	Yb	Lu	Hf	Ta	Pb	Th	U
b.d.l.	b.d.l.	b.d.l.	b.d.l.	0.0	0.0	22.8	b.d.l.	b.d.l.
b.d.l.	b.d.l.	b.d.l.	b.d.l.	b.d.l.	b.d.l.	23.7	b.d.l.	b.d.l.
b.d.l.	b.d.l.	b.d.l.	0.0	0.0	b.d.l.	23.9	b.d.l.	b.d.l.
b.d.l.	b.d.l.	b.d.l.	b.d.l.	b.d.l.	b.d.l.	23.3	b.d.l.	b.d.l.
b.d.l.	b.d.l.	b.d.l.	b.d.l.	b.d.l.	b.d.l.	27.9	b.d.l.	b.d.l.
b.d.l.	b.d.l.	b.d.l.	b.d.l.	b.d.l.	b.d.l.	34.5	b.d.l.	0.0
b.d.l.	b.d.l.	b.d.l.	0.0	0.1	0.0	27.9	b.d.l.	b.d.l.
b.d.l.	b.d.l.	b.d.l.	b.d.l.	b.d.l.	b.d.l.	25.6	b.d.l.	0.0
b.d.l.	b.d.l.	b.d.l.	b.d.l.	b.d.l.	b.d.l.	26.6	b.d.l.	b.d.l.
b.d.l.	b.d.l.	b.d.l.	b.d.l.	0.0	0.0	24.9	b.d.l.	b.d.l.
0.0	b.d.l.	b.d.l.	0.0	b.d.l.	b.d.l.	22.9	b.d.l.	b.d.l.
b.d.l.	b.d.l.	b.d.l.	b.d.l.	0.1	0.0	23.1	0.0	b.d.l.
b.d.l.	b.d.l.	b.d.l.	b.d.l.	b.d.l.	b.d.l.	25.4	b.d.l.	0.0
b.d.l.	b.d.l.	b.d.l.	b.d.l.	b.d.l.	b.d.l.	22.4	b.d.l.	b.d.l.
b.d.l.	b.d.l.	b.d.l.	b.d.l.	0.2	0.0	22.9	b.d.l.	b.d.l.
b.d.l.	b.d.l.	b.d.l.	b.d.l.	0.1	b.d.l.	22.2	b.d.l.	b.d.l.
b.d.l.	b.d.l.	b.d.l.	b.d.l.	b.d.l.	b.d.l.	22.4	0.0	b.d.l.
b.d.l.	b.d.l.	b.d.l.	b.d.l.	0.1	b.d.l.	21.5	0.0	0.0
0.0	b.d.l.	b.d.l.	b.d.l.	b.d.l.	b.d.l.	22.3	0.0	0.0
b.d.l.	b.d.l.	b.d.l.	b.d.l.	b.d.l.	0.0	23.0	0.0	b.d.l.
b.d.l.	0.0	b.d.l.	b.d.l.	b.d.l.	0.0	24.4	0.1	0.0
b.d.l.	b.d.l.	b.d.l.	b.d.l.	0.1	0.0	22.6	0.0	0.0
b.d.l.	b.d.l.	b.d.l.	0.0	0.0	0.0	21.9	0.0	0.0
b.d.l.	b.d.l.	b.d.l.	b.d.l.	b.d.l.	b.d.l.	23.1	b.d.l.	b.d.l.
b.d.l.	b.d.l.	b.d.l.	b.d.l.	0.1	0.0	24.9	b.d.l.	b.d.l.
b.d.l.	b.d.l.	b.d.l.	b.d.l.	0.1	b.d.l.	25.4	b.d.l.	b.d.l.
b.d.l.	b.d.l.	b.d.l.	b.d.l.	0.0	0.0	24.8	b.d.l.	b.d.l.
b.d.l.	b.d.l.	b.d.l.	b.d.l.	b.d.l.	b.d.l.	24.1	0.0	0.0
b.d.l.	b.d.l.	b.d.l.	b.d.l.	0.2	b.d.l.	22.3	b.d.l.	b.d.l.
b.d.l.	b.d.l.	b.d.l.	b.d.l.	b.d.l.	b.d.l.	25.7	b.d.l.	b.d.l.
b.d.l.	b.d.l.	b.d.l.	0.0	0.1	0.0	25.2	b.d.l.	b.d.l.
b.d.l.	b.d.l.	b.d.l.	0.0	b.d.l.	0.0	21.9	b.d.l.	b.d.l.
b.d.l.	b.d.l.	b.d.l.	b.d.l.	0.1	0.0	23.5	0.0	0.0
b.d.l.	b.d.l.	b.d.l.	b.d.l.	0.1	b.d.l.	21.3	b.d.l.	0.0
b.d.l.	b.d.l.	b.d.l.	b.d.l.	0.2	b.d.l.	26.5	0.0	0.0
0.0	b.d.l.	b.d.l.	b.d.l.	b.d.l.	0.0	24.8	b.d.l.	b.d.l.
b.d.l.	b.d.l.	b.d.l.	b.d.l.	0.1	b.d.l.	20.0	b.d.l.	b.d.l.
b.d.l.	b.d.l.	b.d.l.	b.d.l.	0.1	b.d.l.	22.0	b.d.l.	b.d.l.
b.d.l.	b.d.l.	b.d.l.	b.d.l.	0.0	0.1	23.4	b.d.l.	b.d.l.
b.d.l.	b.d.l.	b.d.l.	b.d.l.	b.d.l.	b.d.l.	24.7	b.d.l.	b.d.l.
b.d.l.	b.d.l.	b.d.l.	b.d.l.	b.d.l.	b.d.l.	28.8	b.d.l.	b.d.l.
b.d.l.	0.0	b.d.l.	b.d.l.	0.0	b.d.l.	29.8	b.d.l.	b.d.l.
b.d.l.	b.d.l.	b.d.l.	b.d.l.	b.d.l.	b.d.l.	28.3	b.d.l.	b.d.l.
b.d.l.	b.d.l.	b.d.l.	b.d.l.	b.d.l.	0.0	28.3	b.d.l.	b.d.l.
b.d.l.	b.d.l.	b.d.l.	0.0	b.d.l.	b.d.l.	25.5	0.0	b.d.l.
b.d.l.	b.d.l.	b.d.l.	b.d.l.	0.0	b.d.l.	28.1	0.0	b.d.l.
0.0	0.0	0.1	b.d.l.	0.0	0.1	27.7	0.2	0.1
0.0	b.d.l.	b.d.l.	b.d.l.	b.d.l.	0.0	23.9	b.d.l.	0.0
b.d.l.	b.d.l.	b.d.l.	b.d.l.	b.d.l.	0.0	22.6	0.0	b.d.l.
b.d.l.	b.d.l.	b.d.l.	b.d.l.	b.d.l.	b.d.l.	22.8	b.d.l.	b.d.l.

Table A1.5: continued

Info	Position	Li ⁺	Li	Na	Mg	Al	Si	P	K	Ca	Sc	Ti	V	Mn	Fe	Rb	Sr	Y	Zr	Nb	Cs	Ba	La	Ce	Pr	Nd	Sm	Eu	Gd	Tb	Dy	Ho
grain18-13	Core	7.0	7.4	30171.9	b.d.i.	96727	308527	b.d.i.	85601	2760.2	0.6	64.7	b.d.i.	b.d.i.	718.7	122.8	142.8	b.d.i.	b.d.i.	b.d.i.	b.d.i.	818	6.1	4.2	0.2	0.4	b.d.i.	3.7	b.d.i.	b.d.i.	b.d.i.	
grain18-14	Core	b.d.i.	6.7	31379.6	7.2	95977	308527	b.d.i.	87767	2686.3	0.5	67.7	b.d.i.	b.d.i.	751.6	127.4	145.5	b.d.i.	b.d.i.	b.d.i.	0.1	657	6.1	4.4	0.2	0.4	b.d.i.	3.7	0.0	b.d.i.	b.d.i.	
grain18-15	Core	b.d.i.	6.7	30732.7	b.d.i.	95199	308527	20.0	86156	3170.9	0.6	69.4	b.d.i.	b.d.i.	738.8	123.0	144.1	b.d.i.	b.d.i.	b.d.i.	0.1	650	6.2	4.3	0.2	0.4	0.0	3.6	b.d.i.	0.0	b.d.i.	
grain18-16	Core	b.d.i.	6.3	31666.7	b.d.i.	97597	308527	19.8	85657	3145.2	0.7	75.4	b.d.i.	b.d.i.	781.0	121.5	149.7	b.d.i.	b.d.i.	b.d.i.	0.0	b.d.i.	646	6.7	4.7	0.2	0.4	0.0	3.6	b.d.i.	b.d.i.	
grain18-17	Core	7.5	6.6	31387.1	b.d.i.	96111	308527	20.3	86527	3137.8	0.9	75.4	b.d.i.	b.d.i.	733.4	123.5	145.3	b.d.i.	b.d.i.	b.d.i.	0.1	687	6.6	4.7	0.2	0.4	b.d.i.	3.4	b.d.i.	b.d.i.	b.d.i.	
grain18-18	Core	7.5	7.2	33544.5	b.d.i.	95424	308527	19.9	89309	2836.7	0.5	77.3	b.d.i.	b.d.i.	764.6	125.0	142.7	b.d.i.	b.d.i.	b.d.i.	0.1	706	6.4	4.5	0.2	0.4	b.d.i.	3.3	b.d.i.	b.d.i.	b.d.i.	
grain18-19	Core	8.4	7.1	32176.1	b.d.i.	95036	308527	b.d.i.	86966	3011.5	0.5	72.9	b.d.i.	b.d.i.	725.1	122.6	145.3	b.d.i.	b.d.i.	b.d.i.	0.1	715	6.9	4.8	0.2	0.3	b.d.i.	3.3	b.d.i.	b.d.i.	b.d.i.	
grain18-20	Core	8.4	7.1	32194.1	b.d.i.	95932	308527	22.9	85132	3009.3	0.5	73.6	b.d.i.	0.9	703.1	120.3	141.9	b.d.i.	b.d.i.	b.d.i.	0.0	0.1	727	6.8	4.7	0.2	0.4	b.d.i.	3.5	b.d.i.	b.d.i.	b.d.i.
grain18-21	Core	b.d.i.	6.7	32365.1	7.4	96524	308527	20.5	85480	2588.0	0.6	78.5	b.d.i.	b.d.i.	732.5	116.6	139.6	b.d.i.	b.d.i.	b.d.i.	0.1	722	6.7	4.7	0.2	0.4	b.d.i.	3.4	b.d.i.	0.0	b.d.i.	
grain18-22	Core	6.8	6.5	29988.0	b.d.i.	94122	308527	b.d.i.	86510	2847.9	0.7	83.6	b.d.i.	b.d.i.	742.2	114.0	134.4	b.d.i.	b.d.i.	b.d.i.	0.0	0.1	696	6.6	4.5	0.2	0.4	0.0	3.3	b.d.i.	b.d.i.	b.d.i.
grain18-23	Core	b.d.i.	6.3	32894.0	b.d.i.	99347	308527	b.d.i.	88829	3006.2	0.7	80.6	b.d.i.	b.d.i.	765.1	122.2	143.4	b.d.i.	b.d.i.	b.d.i.	0.1	712	7.1	5.0	0.2	0.4	b.d.i.	3.5	b.d.i.	b.d.i.	b.d.i.	
grain18-24	Core	b.d.i.	6.3	30376.3	b.d.i.	97095	308527	19.6	86957	2399.3	0.6	77.7	b.d.i.	b.d.i.	751.5	116.2	134.9	b.d.i.	b.d.i.	b.d.i.	0.1	679	6.6	4.5	0.2	0.4	b.d.i.	3.2	0.0	b.d.i.	b.d.i.	
grain18-25	Core	b.d.i.	5.7	31760.9	5.7	99022	308527	20.8	85007	2621.1	0.7	75.3	b.d.i.	b.d.i.	751.5	116.8	132.7	0.0	b.d.i.	b.d.i.	0.1	663	6.8	4.8	0.3	0.3	0.0	3.0	b.d.i.	b.d.i.	b.d.i.	
grain18-26	Core	b.d.i.	6.5	30970.2	8.5	96862	308527	18.2	90684	2817.8	0.6	74.4	b.d.i.	0.9	772.2	122.0	134.8	b.d.i.	b.d.i.	b.d.i.	0.1	662	6.5	4.6	0.2	0.4	b.d.i.	3.1	b.d.i.	b.d.i.	b.d.i.	
grain18-27	Core	b.d.i.	6.1	32160.1	b.d.i.	94695	308527	b.d.i.	85793	2659.3	0.7	75.2	b.d.i.	b.d.i.	735.1	120.1	128.3	b.d.i.	b.d.i.	b.d.i.	0.1	633	6.2	4.3	0.2	0.5	b.d.i.	2.8	b.d.i.	b.d.i.	b.d.i.	
grain18-28	Core	b.d.i.	6.3	32143.2	8.7	94770	308527	b.d.i.	87131	2751.3	0.6	76.8	b.d.i.	b.d.i.	730.5	119.8	128.3	0.0	b.d.i.	b.d.i.	0.1	620	6.2	4.4	0.2	0.3	b.d.i.	3.0	b.d.i.	b.d.i.	b.d.i.	
grain18-29	Core	b.d.i.	5.9	30694.8	b.d.i.	92195	308527	17.1	83490	2562.5	0.5	68.9	b.d.i.	b.d.i.	707.1	114.4	125.6	0.0	b.d.i.	b.d.i.	0.1	613	6.2	4.2	0.2	0.5	b.d.i.	3.0	b.d.i.	b.d.i.	b.d.i.	
grain18-30	Core	b.d.i.	6.3	33865.9	b.d.i.	95122	308527	b.d.i.	89514	2978.3	0.5	77.7	b.d.i.	b.d.i.	718.9	122.9	135.6	0.0	b.d.i.	b.d.i.	0.1	678	6.9	4.8	0.2	0.4	b.d.i.	3.3	0.0	b.d.i.	b.d.i.	
grain18-31	Core	b.d.i.	5.8	33111.9	6.4	98280	308527	b.d.i.	89266	2511.9	0.5	78.8	b.d.i.	b.d.i.	777.3	116.7	144.1	b.d.i.	b.d.i.	b.d.i.	0.0	696	7.0	4.7	0.2	0.4	0.1	3.5	b.d.i.	0.0	b.d.i.	
grain18-32	Core	7.3	6.6	33445.9	b.d.i.	94961	308527	18.8	85399	2744.3	0.7	78.9	b.d.i.	0.8	767.8	117.2	143.5	b.d.i.	b.d.i.	b.d.i.	0.1	706	7.0	4.6	0.2	0.5	0.0	3.6	b.d.i.	b.d.i.	b.d.i.	
grain18-33	Core	8.1	6.5	34189.1	7.0	99608	308527	22.9	87413	2927.0	0.7	85.8	b.d.i.	0.8	745.0	131.7	143.7	b.d.i.	b.d.i.	b.d.i.	0.1	700	6.8	4.8	0.2	0.5	b.d.i.	3.4	b.d.i.	b.d.i.	b.d.i.	
grain18-34	Core	6.7	6.1	32387.7	6.0	98650	308527	22.9	87413	2927.0	0.7	85.8	b.d.i.	0.8	745.0	131.7	143.7	b.d.i.	b.d.i.	b.d.i.	0.1	700	6.8	4.8	0.2	0.5	b.d.i.	3.4	b.d.i.	b.d.i.	b.d.i.	
grain18-35	Core	6.7	6.1	32387.7	6.0	98650	308527	22.9	87413	2927.0	0.7	85.8	b.d.i.	0.8	745.0	131.7	143.7	b.d.i.	b.d.i.	b.d.i.	0.1	700	6.8	4.8	0.2	0.5	b.d.i.	3.4	b.d.i.	b.d.i.	b.d.i.	
grain18-36	Core	6.3	5.8	30567.7	8.2	93187	308527	b.d.i.	87867	3269.6	0.6	78.2	b.d.i.	b.d.i.	729.0	114.3	135.4	b.d.i.	b.d.i.	b.d.i.	0.1	686	6.6	4.6	0.2	0.4	0.0	3.1	b.d.i.	b.d.i.	b.d.i.	
grain18-37	Core	b.d.i.	5.8	32962.6	8.4	98522	308527	b.d.i.	87867	3269.6	0.6	78.2	b.d.i.	b.d.i.	729.0	114.3	135.4	b.d.i.	b.d.i.	b.d.i.	0.1	686	6.6	4.6	0.2	0.4	0.0	3.1	b.d.i.	b.d.i.	b.d.i.	
grain18-38	Core	b.d.i.	5.9	32920.3	6.2	96417	308527	b.d.i.	86800	3034.3	b.d.i.	81.1	b.d.i.	0.7	749.4	119.6	145.6	b.d.i.	b.d.i.	b.d.i.	0.1	737	6.9	5.3	0.3	0.3	0.0	3.4	b.d.i.	b.d.i.	b.d.i.	
grain18-39	Core	b.d.i.	6.0	31006.8	b.d.i.	95343	308527	15.6	88931	2662.6	0.8	77.2	b.d.i.	b.d.i.	727.1	120.3	140.2	b.d.i.	b.d.i.	b.d.i.	0.0	711	6.6	4.5	0.2	0.4	b.d.i.	3.2	b.d.i.	b.d.i.	b.d.i.	
grain18-40	Core	b.d.i.	6.0	31373.4	b.d.i.	92335	308527	23.2	86291	2619.9	0.9	76.7	b.d.i.	0.7	755.8	122.4	136.5	b.d.i.	b.d.i.	b.d.i.	0.1	685	6.1	4.3	0.2	0.4	b.d.i.	3.3	0.1	b.d.i.	b.d.i.	b.d.i.
grain18-41	Core	b.d.i.	6.1	32127.1	b.d.i.	96594	308527	18.2	86901	2733.4	b.d.i.	74.8	b.d.i.	0.9	746.5	122.7	142.7	b.d.i.	b.d.i.	b.d.i.	0.1	719	6.4	4.4	0.2	0.3	0.0	3.4	b.d.i.	b.d.i.	b.d.i.	
grain18-42	Core	b.d.i.	6.4	32889.4	b.d.i.	97451	308527	b.d.i.	86371	2640.5	0.7	77.1	b.d.i.	b.d.i.	766.8	121.0	141.9	b.d.i.	b.d.i.	b.d.i.	0.1	724	6.4	4.6	0.2	0.5	b.d.i.	3.5	b.d.i.	b.d.i.	b.d.i.	
grain18-43	Core	b.d.i.	6.1	32733.6	b.d.i.	99618	308527	15.6	89593	3012.4	0.8	79.1	b.d.i.	b.d.i.	758.2	122.3	150.9	b.d.i.	b.d.i.	b.d.i.	0.0	0.1	748	6.9	4.6	0.3	0.4	b.d.i.	3.7	b.d.i.	b.d.i.	b.d.i.
grain18-44	Core	b.d.i.	5.9	32074.3	6.6	96657	308527	26.4	87994	2992.1	0.6	77.5	b.d.i.	b.d.i.	740.8	123.8	151.8	b.d.i.	b.d.i.	b.d.i.	0.1	777	6.9	4.9	0.2	0.4	0.0	3.7	b.d.i.	0.0	b.d.i.	b.d.i.
grain18-45	Core	b.d.i.	5.8	31988.8	5.6	97785	308527	b.d.i.	90496	2976.8	0.6	73.5	b.d.i.	0.8	799.2	125.9	153.6	0.0	b.d.i.	b.d.i.	0.0	0.1	764	6.8	4.7	0.2	0.4	b.d.i.	3.9	b.d.i.	b.d.i.	0.0
grain18-46	Core	b.d.i.	6.0	31695.2	b.d.i.	95632	308527	b.d.i.	87113	2857.6	b.d.i.	78.3	b.d.i.	b.d.i.	742.9	119.5	149.3	b.d.i.	b.d.i.	b.d.i.	0.0	0.1	739	6.2	4.6	0.2	0.3	0.0	3.7	b.d.i.	b.d.i.	b.d.i.
grain18-47	Core	b.d.i.	5.5	31795.9	b.d.i.	87140	308527	b.d.i.	83834	2490.0	0.5	72.9	b.d.i.	b.d.i.	738.9	121.1	141.2	b.d.i.	b.d.i.	b.d.i.	0.1	715	5.9	4.3	0.2	0.3	b.d.i.	3.4	b.d.i.	b.d.i.	b.d.i.	
grain18-48	Core	b.d.i.	6.2	32568.5	5.5	100350	308527	14.8	86168	2766.1	0.8	78.4	b.d.i.	b.d.i.	733.5	126.9	152.4	b.d.i.	b.d.i.	b.d.i.	0.1	779	6.6	4.3	0.2	0.4	b.d.i.	3.9	b.d.i.	b.d.i.	b.d.i.	
grain18-49	Core	7.3	6.2	32627.0	b.d.i.	95006	308527	b.d.i.	88720	3183.3	0.9	76.3	b.d.i.	0.7	775.8	127.9	151.2	b.d.i.	b.d.i.	b.d.i.	0.1	793	6.5	4.5	0.2	0.4	b.d.i.	3.9	b.d.i.	b.d.i.	b.d.i.	
grain18-50	Core	b.d.i.	6.0	31815.9	b.d.i.	93388	308527	b.d.i.	84596	2480.6	0.4	75.6	b.d.i.	0.8	718.7	124.0	145.5	b.d.i.	b.d.i.	b.d.i.	0.1	815	6.7	4.7	0.2	0.4	b.d.i.	3.8	b.d.i.	b.d.i.	b.d.i.	
grain18-51	Core	b.d.i.	5.7	31919.4	b.d.i.	94985	308527	b.d.i.	84406	2528.5	0.6	72.0	b.d.i.	0.6	759.2	121.6	143.0	b.d.i.	b.d.i.	b.d.i.	0.1	950	6.1	4.5	0.2	0.4	0.1	3.7	b.d.i.	b.d.i.	b.d.i.	
grain18-52	Core	b.d.i.	5.6	31063.9	b.d.i.	96450	308527	b.d.i.	83680	3025.9	0.7	73.1	b.d.i.	b.d.i.	745.4	121.1	137.8	b.d.i.	b.d.i.	b.d.i.	0.1	1075	6.3	4.5	0.2	0.4	0.0	3.4	b.d.i.	b.d.i.	b.d.i.	
grain18-53	Core	b.d.i.	5.8	32022.9	b.d.i.	97099	308527	14.9	86268	2657.8	0.8	67.4	b.d.i.	0.7	753.9	127.2	135.5	0.0	b.d.i.	b.d.i.	0.0	0.1	1225	6.3	4.3	0.2	0.4	b.d.i.	3.7	b.d.i.	b.d.i.	b.d.i.
grain18-54	Core	b.d.i.	5.8	31938.4	b.d.i.	98444	308527	b.d.i.	87293	2892.7	0.5	72.0	b.d.i.	0.7	773.0	128.1	143.7	b.d.i.	b.d.i.	b.d.i.	0.0	0.1	1492	6.2	4.2	0.2	0.4	0.0	3.8	b.d.i.	b.d.i.	b.d.i.
grain18-55	Core	b.d.i.	5.9	34039.3	b.d.i.	96572	308527	b.d.i.	86603	2568.3	0.7	72.0	b.d.i.	b.d.i.	754.9	127.5	144.2	b.d.i.	b.d.i.	b.d.i.	0.1	1973	6.7	4.5	0.2	0.4	b.d.i.	3.9	b.d.i.	b.d.i.	b.d.i.	
grain18-56	Core	b.d.i.	6.7	30468.0	11.2	94785	308527	15.0	89247	2431.4	0.6	64.3	b.d.i.	1.																		

Table A1.5: continued

Er	Tm	Yb	Lu	Hf	Ta	Pb	Th	U
b.d.l.	b.d.l.	b.d.l.	0.0	b.d.l.	b.d.l.	23.2	b.d.l.	b.d.l.
b.d.l.	b.d.l.	b.d.l.	b.d.l.	b.d.l.	b.d.l.	23.8	b.d.l.	b.d.l.
b.d.l.	b.d.l.	b.d.l.	b.d.l.	b.d.l.	b.d.l.	24.2	0.0	b.d.l.
b.d.l.	b.d.l.	b.d.l.	b.d.l.	0.0	b.d.l.	25.9	b.d.l.	b.d.l.
b.d.l.	b.d.l.	b.d.l.	b.d.l.	0.0	b.d.l.	26.1	b.d.l.	b.d.l.
b.d.l.	b.d.l.	b.d.l.	0.0	b.d.l.	b.d.l.	26.8	b.d.l.	b.d.l.
b.d.l.	0.0	b.d.l.	b.d.l.	b.d.l.	b.d.l.	26.9	b.d.l.	b.d.l.
b.d.l.	b.d.l.	b.d.l.	b.d.l.	b.d.l.	0.0	25.9	b.d.l.	b.d.l.
b.d.l.	b.d.l.	b.d.l.	b.d.l.	b.d.l.	b.d.l.	27.0	b.d.l.	b.d.l.
b.d.l.	b.d.l.	b.d.l.	b.d.l.	0.0	b.d.l.	25.4	b.d.l.	b.d.l.
b.d.l.	b.d.l.	b.d.l.	b.d.l.	b.d.l.	b.d.l.	27.6	b.d.l.	b.d.l.
b.d.l.	b.d.l.	b.d.l.	b.d.l.	b.d.l.	b.d.l.	26.1	b.d.l.	b.d.l.
b.d.l.	b.d.l.	b.d.l.	b.d.l.	b.d.l.	b.d.l.	26.2	b.d.l.	b.d.l.
b.d.l.	b.d.l.	b.d.l.	b.d.l.	0.0	b.d.l.	26.5	b.d.l.	b.d.l.
b.d.l.	0.0	b.d.l.	b.d.l.	b.d.l.	b.d.l.	26.2	b.d.l.	0.0
b.d.l.	b.d.l.	b.d.l.	b.d.l.	b.d.l.	b.d.l.	25.5	b.d.l.	b.d.l.
b.d.l.	b.d.l.	b.d.l.	b.d.l.	b.d.l.	b.d.l.	24.5	b.d.l.	b.d.l.
b.d.l.	b.d.l.	b.d.l.	b.d.l.	b.d.l.	b.d.l.	27.1	b.d.l.	b.d.l.
b.d.l.	0.0	b.d.l.	b.d.l.	b.d.l.	b.d.l.	26.1	b.d.l.	b.d.l.
b.d.l.	b.d.l.	b.d.l.	b.d.l.	b.d.l.	b.d.l.	27.0	b.d.l.	b.d.l.
b.d.l.	b.d.l.	0.0	b.d.l.	b.d.l.	b.d.l.	27.2	b.d.l.	b.d.l.
b.d.l.	b.d.l.	b.d.l.	b.d.l.	b.d.l.	b.d.l.	30.7	b.d.l.	b.d.l.
b.d.l.	b.d.l.	b.d.l.	b.d.l.	b.d.l.	b.d.l.	26.3	b.d.l.	b.d.l.
b.d.l.	b.d.l.	b.d.l.	b.d.l.	b.d.l.	b.d.l.	28.2	b.d.l.	b.d.l.
b.d.l.	b.d.l.	b.d.l.	b.d.l.	b.d.l.	b.d.l.	27.4	b.d.l.	b.d.l.
b.d.l.	b.d.l.	b.d.l.	b.d.l.	b.d.l.	b.d.l.	25.8	b.d.l.	b.d.l.
b.d.l.	b.d.l.	b.d.l.	b.d.l.	b.d.l.	b.d.l.	25.8	b.d.l.	b.d.l.
b.d.l.	b.d.l.	b.d.l.	b.d.l.	b.d.l.	b.d.l.	25.4	b.d.l.	b.d.l.
b.d.l.	b.d.l.	b.d.l.	b.d.l.	0.0	b.d.l.	25.2	b.d.l.	b.d.l.
b.d.l.	b.d.l.	b.d.l.	b.d.l.	b.d.l.	b.d.l.	26.7	b.d.l.	b.d.l.
b.d.l.	b.d.l.	b.d.l.	b.d.l.	b.d.l.	b.d.l.	26.2	b.d.l.	b.d.l.
b.d.l.	b.d.l.	b.d.l.	b.d.l.	b.d.l.	b.d.l.	25.2	b.d.l.	b.d.l.
b.d.l.	b.d.l.	b.d.l.	b.d.l.	b.d.l.	b.d.l.	25.3	b.d.l.	b.d.l.
b.d.l.	b.d.l.	b.d.l.	b.d.l.	b.d.l.	b.d.l.	25.0	b.d.l.	b.d.l.
b.d.l.	b.d.l.	b.d.l.	b.d.l.	b.d.l.	b.d.l.	24.5	b.d.l.	b.d.l.
b.d.l.	b.d.l.	b.d.l.	b.d.l.	b.d.l.	b.d.l.	25.7	b.d.l.	b.d.l.
b.d.l.	b.d.l.	b.d.l.	b.d.l.	b.d.l.	b.d.l.	25.6	b.d.l.	b.d.l.
b.d.l.	0.0	b.d.l.	b.d.l.	b.d.l.	b.d.l.	24.3	b.d.l.	b.d.l.
b.d.l.	b.d.l.	b.d.l.	b.d.l.	b.d.l.	b.d.l.	23.9	b.d.l.	b.d.l.
b.d.l.	b.d.l.	b.d.l.	b.d.l.	b.d.l.	b.d.l.	23.9	b.d.l.	b.d.l.
b.d.l.	b.d.l.	0.0	b.d.l.	b.d.l.	b.d.l.	23.2	b.d.l.	b.d.l.
b.d.l.	b.d.l.	b.d.l.	b.d.l.	b.d.l.	b.d.l.	23.1	b.d.l.	b.d.l.
b.d.l.	b.d.l.	b.d.l.	b.d.l.	b.d.l.	b.d.l.	22.0	b.d.l.	b.d.l.
b.d.l.	b.d.l.	b.d.l.	b.d.l.	b.d.l.	b.d.l.	20.6	b.d.l.	b.d.l.
b.d.l.	b.d.l.	b.d.l.	0.0	b.d.l.	b.d.l.	24.3	b.d.l.	b.d.l.
b.d.l.	b.d.l.	b.d.l.	b.d.l.	b.d.l.	b.d.l.	28.3	b.d.l.	b.d.l.
b.d.l.	b.d.l.	b.d.l.	0.0	b.d.l.	b.d.l.	27.1	0.1	0.0
b.d.l.	b.d.l.	b.d.l.	b.d.l.	0.1	0.0	27.9	b.d.l.	b.d.l.
0.0	b.d.l.	b.d.l.	b.d.l.	b.d.l.	b.d.l.	26.9	b.d.l.	b.d.l.
b.d.l.	b.d.l.	b.d.l.	b.d.l.	0.1	b.d.l.	27.9	b.d.l.	b.d.l.
b.d.l.	b.d.l.	0.1	b.d.l.	b.d.l.	b.d.l.	25.6	b.d.l.	b.d.l.

Table A1.5: continued

Info	Position	Li ^β	Li ^γ	Na	Mg	Al	Si	P	K	Ca	Sc	Ti	V	Mn	Fe	Rb	Sr	Y	Zr	Nb	Cs	Ba	La	Ce	Pr	Nd	Sm	Eu	Gd	Tb	Dy	Ho
MFT-San18-6	Core	5.4	5.6	31228.6	4.0	109558	308527	b.d.l.	78352	3389.0	b.d.l.	70.3	b.d.l.	b.d.l.	743.8	118.3	126.5	0.1	b.d.l.	0.1	b.d.l.	248	63.4	4.0	0.3	0.5	b.d.l.	2.8	b.d.l.	b.d.l.	b.d.l.	
MFT-San18-7	Core	5.1	5.6	31906.0	1.3	114165	308527	b.d.l.	79319	2772.9	0.9	71.4	1.0	b.d.l.	766.7	116.9	126.2	0.0	b.d.l.	0.1	b.d.l.	250	61.4	4.0	0.3	0.3	b.d.l.	2.9	b.d.l.	b.d.l.	b.d.l.	
MFT-San18-8	Core	6.0	5.8	30892.7	2.3	108550	308527	b.d.l.	77767	2424.9	b.d.l.	64.7	b.d.l.	b.d.l.	732.2	118.7	119.2	b.d.l.	b.d.l.	b.d.l.	0.1	234	5.6	3.7	0.2	0.4	b.d.l.	2.9	b.d.l.	b.d.l.	b.d.l.	
MFT-San18-9	Core	6.6	5.5	29780.6	1.3	106366	308527	b.d.l.	76490	2703.6	0.9	69.6	b.d.l.	b.d.l.	633.8	113.6	122.8	b.d.l.	b.d.l.	b.d.l.	0.1	238	5.3	3.6	0.2	0.4	b.d.l.	2.6	b.d.l.	b.d.l.	b.d.l.	
MFT-San18-10	Core	6.3	5.6	30281.0	b.d.l.	106725	308527	b.d.l.	76385	3033.0	b.d.l.	64.5	b.d.l.	b.d.l.	633.1	112.8	125.9	0.0	0.2	b.d.l.	0.1	262	5.5	3.9	0.1	0.3	b.d.l.	2.8	b.d.l.	b.d.l.	b.d.l.	
MFT-San18-11	Core	7.4	5.9	31774.0	3.0	113063	308527	b.d.l.	81916	3155.1	b.d.l.	77.3	b.d.l.	b.d.l.	786.0	120.6	132.5	b.d.l.	b.d.l.	b.d.l.	0.1	293	6.1	4.4	0.3	0.4	b.d.l.	3.0	b.d.l.	b.d.l.	b.d.l.	
MFT-San18-12	Core	5.4	6.0	30520.9	0.5	109600	308527	b.d.l.	78471	2801.5	b.d.l.	79.1	b.d.l.	b.d.l.	703.0	116.8	128.6	b.d.l.	0.1	b.d.l.	0.2	317	5.7	3.7	0.2	0.2	b.d.l.	2.9	0.1	b.d.l.	0.0	
MFT-San18-13	Core	5.7	5.5	30552.9	2.3	108010	308527	b.d.l.	76675	3166.0	b.d.l.	80.9	b.d.l.	b.d.l.	742.8	117.1	125.0	b.d.l.	0.1	b.d.l.	0.1	355	5.8	3.8	0.2	0.2	b.d.l.	3.1	b.d.l.	b.d.l.	b.d.l.	
MFT-San18-14	Core	6.9	6.0	30515.3	2.4	109566	308527	90.4	78613	2541.7	b.d.l.	68.9	b.d.l.	b.d.l.	752.8	119.4	122.1	0.0	b.d.l.	0.0	0.1	395	5.5	3.5	0.2	0.3	b.d.l.	2.9	b.d.l.	b.d.l.	b.d.l.	
MFT-San18-15	Core	6.4	5.6	30123.0	1.9	107169	308527	b.d.l.	76154	2962.4	1.2	65.5	b.d.l.	b.d.l.	677.5	114.4	126.7	0.1	b.d.l.	b.d.l.	0.1	494	6.1	4.1	0.2	0.4	b.d.l.	2.9	b.d.l.	b.d.l.	b.d.l.	
MFT-San18-16	Core	6.8	5.8	30687.1	1.3	109348	308527	62.0	77818	3307.6	b.d.l.	78.4	b.d.l.	b.d.l.	690.0	118.6	128.4	b.d.l.	b.d.l.	0.0	b.d.l.	545	6.1	4.4	0.2	0.4	b.d.l.	3.3	b.d.l.	b.d.l.	b.d.l.	
MFT-San18-17	Core	5.1	5.9	30879.8	b.d.l.	108878	308527	b.d.l.	77469	3059.7	b.d.l.	69.1	b.d.l.	b.d.l.	719.9	118.2	129.9	b.d.l.	b.d.l.	0.0	b.d.l.	561	6.0	4.0	0.2	0.3	b.d.l.	3.3	b.d.l.	b.d.l.	b.d.l.	
MFT-San18-18	Core	6.8	5.7	30466.1	2.1	109730	308527	b.d.l.	75492	3146.7	0.6	72.5	b.d.l.	b.d.l.	756.1	117.6	138.2	b.d.l.	0.0	b.d.l.	0.1	675	6.2	4.5	0.2	0.4	b.d.l.	3.0	b.d.l.	b.d.l.	0.0	
MFT-San18-19	Core	6.9	5.8	30531.3	2.4	106480	308527	b.d.l.	75315	3002.9	b.d.l.	82.4	b.d.l.	b.d.l.	701.6	113.1	136.2	0.1	b.d.l.	0.0	0.1	683	6.5	4.7	0.2	0.4	0.1	3.2	b.d.l.	b.d.l.	b.d.l.	
MFT-San18-20	Core	4.5	6.0	31505.7	b.d.l.	112109	308527	b.d.l.	78030	3306.0	b.d.l.	64.8	b.d.l.	b.d.l.	11.8	694.2	119.6	147.7	0.1	0.0	b.d.l.	752	7.0	4.9	0.2	0.4	b.d.l.	3.4	b.d.l.	b.d.l.	0.0	
MFT-San18-21	Core	8.9	5.5	30042.8	1.7	106730	308527	b.d.l.	77528	3169.4	b.d.l.	68.6	b.d.l.	b.d.l.	663.6	114.6	137.8	0.1	b.d.l.	0.0	b.d.l.	718	6.1	4.2	0.2	0.3	0.1	3.4	b.d.l.	b.d.l.	b.d.l.	
MFT-San18-22	Core	7.2	5.9	30040.8	3.1	107348	308527	b.d.l.	74694	2999.5	b.d.l.	74.5	b.d.l.	b.d.l.	728.3	111.8	144.5	0.0	b.d.l.	b.d.l.	0.2	682	6.5	4.7	0.2	0.6	b.d.l.	3.6	b.d.l.	b.d.l.	b.d.l.	
MFT-San18-23	Core	4.8	5.5	30612.2	2.0	106826	308527	56.2	75267	3336.9	b.d.l.	65.6	0.6	b.d.l.	697.9	116.8	145.6	0.0	b.d.l.	0.0	b.d.l.	623	6.9	4.5	0.2	0.5	b.d.l.	3.5	b.d.l.	b.d.l.	b.d.l.	
MFT-San18-24	Core	6.8	6.3	31203.5	b.d.l.	109189	308527	b.d.l.	77680	2920.5	0.7	70.1	0.6	b.d.l.	805.9	118.8	148.0	b.d.l.	b.d.l.	0.0	0.1	601	6.3	4.2	0.2	0.4	b.d.l.	3.7	b.d.l.	b.d.l.	b.d.l.	
MFT-San18-25	Core	6.0	6.1	30679.8	2.1	108513	308527	b.d.l.	77558	3154.0	b.d.l.	70.4	b.d.l.	b.d.l.	661.4	122.0	142.0	0.0	b.d.l.	b.d.l.	0.1	575	6.6	4.3	0.2	0.3	b.d.l.	3.7	b.d.l.	b.d.l.	b.d.l.	
MFT-San18-26	Core	8.6	6.0	30553.0	b.d.l.	108296	308527	b.d.l.	76167	3238.2	b.d.l.	62.8	b.d.l.	b.d.l.	726.7	115.1	148.7	0.0	0.0	b.d.l.	0.1	669	6.2	4.1	0.2	0.3	b.d.l.	3.5	b.d.l.	b.d.l.	b.d.l.	
MFT-San18-27	Core	7.4	6.0	30225.6	2.5	107240	308527	b.d.l.	76164	2928.7	b.d.l.	65.7	b.d.l.	b.d.l.	741.8	118.3	147.4	b.d.l.	b.d.l.	0.1	866	6.6	4.4	0.2	0.4	b.d.l.	3.5	b.d.l.	b.d.l.	b.d.l.		
MFT-San18-28	Core	4.9	6.8	30344.0	3.4	108338	308527	b.d.l.	77735	2832.5	b.d.l.	67.2	b.d.l.	b.d.l.	671.8	117.6	140.1	0.1	b.d.l.	b.d.l.	0.1	1228	6.3	4.1	0.2	0.3	b.d.l.	3.8	b.d.l.	b.d.l.	b.d.l.	
MFT-San18-29	Core	8.3	7.5	29865.9	1.3	111878	308527	b.d.l.	77795	2991.1	b.d.l.	57.9	b.d.l.	b.d.l.	709.2	124.6	141.0	0.1	0.0	b.d.l.	0.1	1885	6.9	4.9	0.2	0.6	b.d.l.	3.5	b.d.l.	b.d.l.	b.d.l.	
MFT-San18-30	Core	6.7	7.6	29092.6	3.8	106592	308527	b.d.l.	78273	2594.0	b.d.l.	68.3	b.d.l.	b.d.l.	699.6	121.0	139.1	0.1	0.1	b.d.l.	0.1	2583	6.2	4.5	0.2	0.5	b.d.l.	3.3	b.d.l.	b.d.l.	b.d.l.	
MFT-San18-31	Core	6.6	7.4	30791.9	3.4	105504	308527	b.d.l.	79130	4571.0	0.8	72.2	b.d.l.	b.d.l.	692.4	105.4	179.4	0.2	b.d.l.	b.d.l.	0.1	3924	9.0	6.5	0.4	0.6	b.d.l.	4.9	b.d.l.	b.d.l.	b.d.l.	
MFT-San18-32	Core	8.4	8.7	31472.0	2.1	110635	308527	b.d.l.	75032	3684.3	b.d.l.	87.2	b.d.l.	b.d.l.	767.8	111.8	179.1	0.3	b.d.l.	0.1	b.d.l.	5125	9.4	6.6	0.4	0.6	b.d.l.	4.6	b.d.l.	b.d.l.	b.d.l.	
MFT-San18-33	Core																															
MFT-San18-34	Core	9.1	8.1	31395.1	1.8	112856	308527	b.d.l.	78413	3691.4	0.6	84.0	b.d.l.	b.d.l.	786.3	119.8	163.5	0.4	b.d.l.	0.0	0.1	5667	9.5	6.6	0.3	0.8	b.d.l.	4.5	b.d.l.	b.d.l.	b.d.l.	
MFT-San18-35	Core	8.9	6.8	31121.5	2.1	112783	308527	b.d.l.	76846	3933.5	0.9	82.3	b.d.l.	b.d.l.	847.4	114.9	164.1	0.3	0.1	b.d.l.	0.0	5612	9.4	6.6	0.3	0.6	b.d.l.	4.7	b.d.l.	b.d.l.	b.d.l.	
MFT-San18-36	Core	4.1	5.7	29754.3	2.5	106930	308527	60.1	73446	3976.6	0.6	84.6	b.d.l.	b.d.l.	824.3	114.8	156.5	0.3	b.d.l.	0.0	0.1	5028	9.1	6.5	0.3	0.6	b.d.l.	4.2	0.1	b.d.l.	b.d.l.	
MFT-San18-37	Core	4.5	4.5	30840.9	1.2	111072	308527	b.d.l.	76716	3466.2	b.d.l.	89.7	b.d.l.	b.d.l.	763.7	118.9	159.8	0.4	b.d.l.	b.d.l.	0.1	4780	9.4	6.5	0.4	0.6	b.d.l.	4.5	b.d.l.	b.d.l.	b.d.l.	
MFT-San18-38	Rim	3.4	3.0	31035.5	3.8	115032	308527	b.d.l.	80904	3210.5	0.9	74.0	b.d.l.	b.d.l.	830.3	130.9	134.4	0.2	b.d.l.	0.0	0.0	3695	6.4	4.3	0.2	0.3	0.1	3.7	b.d.l.	b.d.l.	b.d.l.	
MFT-San18-39	Rim	2.2	1.9	30513.2	2.1	111698	308527	62.2	79555	2361.5	b.d.l.	58.0	b.d.l.	b.d.l.	721.8	127.4	118.9	0.2	b.d.l.	b.d.l.	0.1	3104	6.0	3.7	0.2	0.3	b.d.l.	3.6	b.d.l.	b.d.l.	b.d.l.	
Sandine grain 19 - Line 1																																
grain19-1	Rim	b.d.l.	2.2	31572.6	b.d.l.	100202	303853	b.d.l.	82960	3554.2	0.5	80.9	b.d.l.	b.d.l.	821.9	118.6	176.4	0.1	b.d.l.	b.d.l.	b.d.l.	8270	7.4	5.6	0.3	0.5	b.d.l.	5.3	b.d.l.	b.d.l.	b.d.l.	
grain19-2	Rim	b.d.l.	4.3	32137.8	8.0	100495	303853	20.0	81609	3646.6	b.d.l.	90.6	b.d.l.	b.d.l.	810.7	113.5	188.5	b.d.l.	b.d.l.	b.d.l.	b.d.l.	8844	8.7	6.2	0.3	0.8	b.d.l.	5.7	b.d.l.	0.0	b.d.l.	
grain19-3	Rim	7.4	5.7	31152.8	b.d.l.	98660	303853	b.d.l.	81645	3568.4	b.d.l.	90.7	b.d.l.	0.8	789.1	115.6	177.5	0.0	b.d.l.	0.0	0.1	8809	8.1	5.8	0.3	0.4	b.d.l.	5.5	b.d.l.	b.d.l.	b.d.l.	
grain19-4	Core	b.d.l.	6.7	30556.4	b.d.l.	99085	303853	21.9	80938	3166.5	0.6	91.6	b.d.l.	b.d.l.	792.5	116.7	174.8	0.0	0.1	b.d.l.	0.1	9044	8.3	5.5	0.3	0.8	b.d.l.	5.3	b.d.l.	b.d.l.	b.d.l.	
grain19-5	Core	b.d.l.	7.4	30997.9	b.d.l.	98762	303853	30.8	82854	2655.3	0.8	96.8	b.d.l.	0.8	848.9	118.4	174.1	0.0	b.d.l.	b.d.l.	0.1	9360	8.2	6.0	0.3	0.6	0.0	5.4	b.d.l.	b.d.l.	b.d	

Table A1.5: continued

Er	Tm	Yb	Lu	Hf	Ta	Pb	Th	U
b.d.l.	b.d.l.	b.d.l.	b.d.l.	b.d.l.	b.d.l.	267	b.d.l.	b.d.l.
b.d.l.	b.d.l.	b.d.l.	b.d.l.	0.1	b.d.l.	270	b.d.l.	b.d.l.
b.d.l.	b.d.l.	b.d.l.	b.d.l.	0.0	0.0	273	b.d.l.	b.d.l.
b.d.l.	b.d.l.	b.d.l.	b.d.l.	b.d.l.	b.d.l.	252	b.d.l.	0.0
b.d.l.	b.d.l.	0.1	b.d.l.	b.d.l.	b.d.l.	281	b.d.l.	b.d.l.
b.d.l.	b.d.l.	b.d.l.	b.d.l.	0.0	b.d.l.	280	b.d.l.	b.d.l.
b.d.l.	b.d.l.	b.d.l.	b.d.l.	b.d.l.	b.d.l.	260	b.d.l.	b.d.l.
b.d.l.	b.d.l.	b.d.l.	b.d.l.	0.0	b.d.l.	270	b.d.l.	b.d.l.
b.d.l.	b.d.l.	b.d.l.	0.0	b.d.l.	0.0	256	b.d.l.	b.d.l.
b.d.l.	b.d.l.	b.d.l.	b.d.l.	0.1	b.d.l.	269	b.d.l.	b.d.l.
b.d.l.	b.d.l.	b.d.l.	b.d.l.	b.d.l.	0.0	266	b.d.l.	b.d.l.
b.d.l.	b.d.l.	b.d.l.	b.d.l.	b.d.l.	b.d.l.	269	b.d.l.	0.0
b.d.l.	b.d.l.	b.d.l.	b.d.l.	b.d.l.	0.0	257	b.d.l.	b.d.l.
b.d.l.	b.d.l.	b.d.l.	b.d.l.	b.d.l.	b.d.l.	265	b.d.l.	b.d.l.
b.d.l.	b.d.l.	b.d.l.	b.d.l.	b.d.l.	0.0	296	b.d.l.	b.d.l.
b.d.l.	b.d.l.	0.1	b.d.l.	b.d.l.	b.d.l.	247	b.d.l.	b.d.l.
b.d.l.	b.d.l.	b.d.l.	b.d.l.	0.0	0.0	271	0.0	0.0
b.d.l.	b.d.l.	b.d.l.	b.d.l.	b.d.l.	b.d.l.	253	0.0	b.d.l.
b.d.l.	b.d.l.	b.d.l.	b.d.l.	0.0	b.d.l.	246	b.d.l.	0.0
b.d.l.	b.d.l.	b.d.l.	b.d.l.	b.d.l.	b.d.l.	251	b.d.l.	b.d.l.
b.d.l.	b.d.l.	b.d.l.	b.d.l.	b.d.l.	b.d.l.	240	b.d.l.	0.0
b.d.l.	b.d.l.	b.d.l.	b.d.l.	b.d.l.	0.0	238	0.0	0.0
b.d.l.	b.d.l.	b.d.l.	b.d.l.	b.d.l.	b.d.l.	223	b.d.l.	b.d.l.
b.d.l.	b.d.l.	b.d.l.	b.d.l.	b.d.l.	0.0	211	b.d.l.	0.0
b.d.l.	b.d.l.	b.d.l.	b.d.l.	b.d.l.	b.d.l.	223	b.d.l.	b.d.l.
b.d.l.	b.d.l.	b.d.l.	b.d.l.	b.d.l.	b.d.l.	280	b.d.l.	b.d.l.
b.d.l.	b.d.l.	b.d.l.	b.d.l.	0.1	0.0	282	b.d.l.	b.d.l.
b.d.l.	b.d.l.	b.d.l.	b.d.l.	b.d.l.	0.0	270	b.d.l.	b.d.l.
b.d.l.	b.d.l.	b.d.l.	b.d.l.	b.d.l.	b.d.l.	260	b.d.l.	b.d.l.
b.d.l.	b.d.l.	b.d.l.	b.d.l.	0.1	b.d.l.	287	b.d.l.	b.d.l.
b.d.l.	b.d.l.	b.d.l.	b.d.l.	0.1	b.d.l.	291	b.d.l.	b.d.l.
b.d.l.	b.d.l.	b.d.l.	b.d.l.	b.d.l.	0.0	274	b.d.l.	0.0
0.1	b.d.l.	b.d.l.	b.d.l.	b.d.l.	b.d.l.	257	b.d.l.	b.d.l.
b.d.l.	b.d.l.	b.d.l.	b.d.l.	b.d.l.	b.d.l.	274	0.0	b.d.l.
b.d.l.	b.d.l.	b.d.l.	b.d.l.	b.d.l.	b.d.l.	288	b.d.l.	b.d.l.
0.0	b.d.l.	b.d.l.	b.d.l.	0.0	0.0	271	b.d.l.	b.d.l.
b.d.l.	b.d.l.	b.d.l.	b.d.l.	b.d.l.	b.d.l.	261	b.d.l.	b.d.l.
b.d.l.	b.d.l.	b.d.l.	b.d.l.	b.d.l.	b.d.l.	259	b.d.l.	b.d.l.
b.d.l.	b.d.l.	b.d.l.	b.d.l.	0.0	b.d.l.	244	b.d.l.	b.d.l.
b.d.l.	b.d.l.	b.d.l.	b.d.l.	b.d.l.	0.0	262	b.d.l.	b.d.l.
0.0	b.d.l.	b.d.l.	b.d.l.	b.d.l.	b.d.l.	253	b.d.l.	b.d.l.
0.0	b.d.l.	b.d.l.	b.d.l.	b.d.l.	b.d.l.	267	b.d.l.	b.d.l.
b.d.l.	b.d.l.	b.d.l.	b.d.l.	b.d.l.	0.0	271	b.d.l.	b.d.l.
b.d.l.	b.d.l.	b.d.l.	b.d.l.	b.d.l.	b.d.l.	278	b.d.l.	b.d.l.
b.d.l.	b.d.l.	b.d.l.	b.d.l.	b.d.l.	0.0	277	b.d.l.	b.d.l.
b.d.l.	b.d.l.	b.d.l.	b.d.l.	b.d.l.	b.d.l.	289	b.d.l.	b.d.l.
b.d.l.	b.d.l.	b.d.l.	b.d.l.	0.0	b.d.l.	307	b.d.l.	b.d.l.
b.d.l.	b.d.l.	b.d.l.	b.d.l.	b.d.l.	b.d.l.	311	b.d.l.	b.d.l.
b.d.l.	b.d.l.	b.d.l.	0.0	0.0	b.d.l.	332	0.0	0.0
b.d.l.	b.d.l.	b.d.l.	b.d.l.	b.d.l.	b.d.l.	345	b.d.l.	b.d.l.
0.0	b.d.l.	b.d.l.	b.d.l.	b.d.l.	b.d.l.	324	b.d.l.	b.d.l.

Table A1.5: continued

Info	Position	Li ⁸	Li ⁷	Na	Mg	Al	Si	P	K	Ca	Sc	Ti	V	Mn	Fe	Rb	Sr	Y	Zr	Nb	Cs	Ba	La	Ce	Pr	Nd	Sm	Eu	Gd	Tb	Dy	Ho	
grain19-19	Core	7.9	9.8	34530.9	b.d.l.	101015	299178	b.d.l.	72531	5838.5	0.5	131.1	b.d.l.	1.3	849.8	102.6	224.1	0.1	b.d.l.	0.0	0.1	11482	9.3	8.3	0.5	1.3	0.1	6.4	b.d.l.	b.d.l.	b.d.l.	b.d.l.	
grain19-20	Core	9.1	9.2	31384.9	b.d.l.	100535	299178	b.d.l.	82589	4116.8	0.6	136.0	b.d.l.	1.0	813.3	117.2	184.8	0.1	b.d.l.	0.0	0.1	11416	9.9	5.5	0.3	0.7	0.1	5.5	0.0	b.d.l.	b.d.l.	b.d.l.	
grain19-21	Core	8.1	8.5	33592.9	b.d.l.	98997	299178	27.2	74677	8259.8	0.5	121.1	b.d.l.	1.0	807.3	108.4	216.6	0.1	b.d.l.	0.0	0.1	11541	9.0	7.5	0.5	0.8	0.2	6.3	b.d.l.	b.d.l.	b.d.l.	0.0	
grain19-22	Core	11.0	8.5	32861.2	b.d.l.	99817	299178	b.d.l.	76728	6464.4	b.d.l.	128.8	b.d.l.	1.1	833.7	109.1	227.4	0.1	0.1	0.0	b.d.l.	11813	8.9	8.2	0.5	1.2	0.0	7.2	b.d.l.	b.d.l.	0.0	b.d.l.	
grain19-23	Core	8.5	8.0	32665.6	b.d.l.	97207	299178	17.0	78172	5725.1	b.d.l.	120.0	b.d.l.	0.9	836.0	103.3	220.0	0.1	b.d.l.	0.0	b.d.l.	11596	8.9	8.1	0.5	1.1	b.d.l.	6.8	b.d.l.	b.d.l.	b.d.l.	b.d.l.	
grain19-24	Core	8.7	8.4	33028.7	6.5	100069	299178	b.d.l.	74590	6328.5	0.8	128.5	b.d.l.	1.1	843.5	103.6	221.5	b.d.l.	0.1	b.d.l.	0.1	11602	8.6	8.1	0.5	1.1	0.1	7.0	b.d.l.	b.d.l.	b.d.l.	b.d.l.	
grain19-25	Core	10.5	8.2	33462.6	b.d.l.	101906	299178	b.d.l.	79665	5711.3	0.6	130.4	b.d.l.	1.3	843.5	110.6	225.3	0.1	b.d.l.	0.0	0.0	11902	9.4	8.1	0.5	1.0	0.2	6.8	b.d.l.	b.d.l.	b.d.l.	0.0	
grain19-26	Core	9.6	8.6	33671.9	b.d.l.	101635	299178	b.d.l.	74370	6342.2	0.6	132.8	b.d.l.	1.3	824.8	104.5	235.8	0.1	b.d.l.	0.0	0.1	11945	9.4	8.5	0.6	1.1	0.1	7.2	b.d.l.	b.d.l.	0.0	b.d.l.	
grain19-27	Core	11.1	8.4	36014.5	6.3	102858	299178	b.d.l.	76789	6067.5	0.7	131.4	b.d.l.	1.0	769.4	103.3	236.3	0.1	0.1	0.0	b.d.l.	12766	8.9	8.0	0.5	0.8	b.d.l.	7.1	b.d.l.	b.d.l.	b.d.l.	b.d.l.	
grain19-28	Core	10.5	8.6	33392.5	6.0	100959	299178	b.d.l.	76566	6282.3	0.5	124.3	b.d.l.	1.4	869.9	104.7	237.4	0.0	b.d.l.	0.1	b.d.l.	12345	8.9	7.9	0.4	0.9	0.1	7.1	b.d.l.	b.d.l.	b.d.l.	b.d.l.	
grain19-29	Core	7.4	8.0	33198.6	8.3	96880	299178	18.6	79050	4349.2	0.7	115.3	b.d.l.	0.1	789.7	110.4	217.1	0.0	b.d.l.	0.1	12345	9.1	12345	9.1	6.0	0.3	0.7	0.0	6.8	b.d.l.	b.d.l.	b.d.l.	b.d.l.
grain19-30	Core	7.7	8.1	32610.3	8.4	96960	299178	16.4	78690	4098.6	0.4	112.7	b.d.l.	0.1	807.4	111.7	213.8	0.1	b.d.l.	0.1	12190	8.4	5.9	0.3	0.7	b.d.l.	6.7	b.d.l.	b.d.l.	b.d.l.	0.0		
grain19-31	Core	8.2	7.9	33456.8	5.4	100145	299178	b.d.l.	79011	3952.2	0.5	105.3	b.d.l.	0.7	810.9	112.8	219.4	0.1	0.1	b.d.l.	0.1	12479	8.1	6.1	0.3	0.7	b.d.l.	6.8	b.d.l.	b.d.l.	b.d.l.	b.d.l.	
grain19-32	Core	8.3	8.4	32343.3	5.5	99022	299178	24.8	81363	4440.8	0.6	113.7	b.d.l.	0.1	798.9	113.3	218.7	0.1	0.1	b.d.l.	0.0	12732	8.6	6.4	0.3	0.6	0.1	6.8	b.d.l.	b.d.l.	b.d.l.	b.d.l.	
grain19-33	Core	8.7	7.9	32530.1	8.4	100042	299178	b.d.l.	77752	3786.4	0.7	105.1	b.d.l.	0.7	798.5	110.5	218.4	0.1	b.d.l.	0.1	12942	8.9	6.5	0.3	0.9	b.d.l.	6.5	b.d.l.	b.d.l.	b.d.l.	b.d.l.		
grain19-34	Core	8.6	8.1	32595.0	7.5	99716	299178	b.d.l.	79419	4082.3	0.9	104.5	b.d.l.	0.1	816.5	111.7	219.9	0.0	0.1	b.d.l.	0.1	13036	9.2	7.0	0.4	0.7	0.0	6.8	b.d.l.	0.0	b.d.l.	0.0	
grain19-35	Core	8.1	7.3	31916.0	b.d.l.	99909	299178	b.d.l.	82393	4020.3	0.8	109.6	b.d.l.	0.1	820.2	113.9	216.4	0.1	b.d.l.	0.0	0.1	13504	9.8	7.8	0.4	0.8	0.1	6.5	b.d.l.	b.d.l.	b.d.l.	b.d.l.	
grain19-36	Core	b.d.l.	6.8	31118.9	7.7	102052	299178	24.5	82281	4312.4	0.4	119.1	b.d.l.	0.8	816.1	115.2	218.9	0.1	b.d.l.	0.0	0.1	13702	10.3	7.9	0.4	0.9	b.d.l.	6.8	b.d.l.	b.d.l.	b.d.l.	b.d.l.	
grain19-37	Core	8.2	6.3	33460.0	b.d.l.	100901	299178	b.d.l.	83343	4518.1	0.5	118.1	b.d.l.	0.1	761.2	114.8	232.1	0.1	b.d.l.	0.0	0.1	13745	9.7	7.1	0.4	0.6	b.d.l.	6.7	b.d.l.	0.0	b.d.l.	b.d.l.	
grain19-38	Core	10.0	7.1	33440.6	b.d.l.	102159	303853	17.3	84463	4549.7	b.d.l.	121.0	0.1	0.9	788.8	113.0	220.0	0.0	b.d.l.	0.0	0.0	12924	8.7	6.5	0.3	0.7	0.0	6.7	b.d.l.	b.d.l.	b.d.l.	b.d.l.	
grain19-39	Core	8.1	8.6	32459.4	b.d.l.	98715	299178	b.d.l.	80362	3974.1	0.7	113.0	b.d.l.	0.9	788.8	113.0	220.0	0.0	b.d.l.	0.0	0.0	12924	8.7	6.5	0.3	0.7	0.0	6.7	b.d.l.	b.d.l.	b.d.l.	b.d.l.	
grain19-40	Core	9.9	9.0	31149.0	b.d.l.	96071	299178	24.2	78684	4031.8	0.5	111.1	b.d.l.	0.1	830.4	107.4	213.4	0.0	b.d.l.	0.0	0.0	12861	8.9	6.5	0.3	0.7	0.1	6.4	b.d.l.	b.d.l.	b.d.l.	b.d.l.	
grain19-41	Core	10.3	9.8	32986.8	b.d.l.	103831	299178	b.d.l.	82942	4728.3	0.7	118.3	b.d.l.	0.7	914.6	110.7	232.3	0.0	0.1	0.0	0.1	12554	9.5	7.1	0.4	0.8	0.1	6.4	b.d.l.	b.d.l.	b.d.l.	b.d.l.	
grain19-42	Core	10.1	10.4	32729.3	b.d.l.	101700	303853	15.6	79258	4979.3	0.5	116.9	b.d.l.	0.1	913.0	110.5	240.4	0.1	b.d.l.	0.1	11983	9.1	7.0	0.4	0.7	0.1	7.4	b.d.l.	b.d.l.	b.d.l.	b.d.l.		
grain19-43	Core	10.5	11.5	32142.8	b.d.l.	99357	299178	b.d.l.	77776	5162.1	0.6	119.6	b.d.l.	0.9	886.1	105.5	241.6	0.0	b.d.l.	0.0	0.0	10681	9.0	7.4	0.4	0.7	b.d.l.	7.1	b.d.l.	b.d.l.	b.d.l.	b.d.l.	
grain19-44	Core	12.1	11.8	33383.3	b.d.l.	104638	303853	18.9	79787	5628.9	0.7	129.8	b.d.l.	0.9	931.3	106.3	249.3	0.1	b.d.l.	0.0	0.1	10851	9.1	7.4	0.4	0.8	0.1	7.3	b.d.l.	b.d.l.	b.d.l.	b.d.l.	
grain19-45	Core	11.9	11.3	31346.3	b.d.l.	98958	299178	15.3	75024	4907.1	0.6	119.6	b.d.l.	0.7	860.3	99.7	232.1	0.1	b.d.l.	0.0	0.1	11025	8.6	6.8	0.4	0.9	0.0	7.2	b.d.l.	b.d.l.	b.d.l.	b.d.l.	
grain19-46	Core	9.5	9.9	32051.3	b.d.l.	103132	303853	b.d.l.	78001	5508.0	0.7	123.4	b.d.l.	4.4	941.3	105.1	233.5	0.2	0.6	0.2	0.0	10724	9.2	7.9	0.4	0.9	0.1	6.9	b.d.l.	b.d.l.	b.d.l.	0.0	
grain19-47	Core	8.3	7.0	31318.6	5.5	99922	303853	b.d.l.	79467	4677.0	0.7	102.9	b.d.l.	1.1	790.7	113.5	193.3	0.0	0.1	b.d.l.	0.1	1733	9.8	7.9	0.4	0.9	0.1	5.7	b.d.l.	b.d.l.	0.0	b.d.l.	
grain19-48	Rim	b.d.l.	4.7	30615.5	6.7	100125	303853	18.5	84474	2640.5	0.6	77.9	b.d.l.	0.7	772.0	125.3	128.6	0.0	b.d.l.	0.0	0.1	4614	6.6	4.4	0.2	0.5	b.d.l.	3.8	b.d.l.	b.d.l.	b.d.l.		
Sandline grain 19 - Line 2																																	
MFT-San19-1	Core	2.7	2.6	31249.1	1.4	113989	308527	63.4	76185	3910.1	0.8	79.5	b.d.l.	11.6	850.2	118.1	191.9	0.4	b.d.l.	0.1	7617	7.9	5.6	0.3	0.6	b.d.l.	5.9	b.d.l.	b.d.l.	b.d.l.	0.0		
MFT-San19-2	Core	3.2	4.1	30716.4	3.4	111291	308527	79.9	76556	3479.5	b.d.l.	86.7	b.d.l.	11.6	912.5	110.9	173.8	0.4	b.d.l.	0.1	7984	7.9	5.4	0.3	0.7	b.d.l.	5.6	b.d.l.	b.d.l.	b.d.l.	b.d.l.		
MFT-San19-3	Core	5.8	5.1	29947.7	2.9	108986	308527	b.d.l.	72797	3595.7	b.d.l.	85.1	b.d.l.	11.6	894.3	110.6	187.0	0.7	0.0	b.d.l.	0.0	8672	8.1	5.7	0.3	0.7	0.1	5.5	b.d.l.	b.d.l.	b.d.l.	b.d.l.	
MFT-San19-4	Core	6.8	6.5	31721.0	7.1	114234	308527	b.d.l.	76234	4407.2	0.9	76.5	b.d.l.	11.6	839.0	111.5	218.2	0.4	b.d.l.	0.1	10459	9.7	7.1	0.3	0.7	b.d.l.	7.3	b.d.l.	0.0	b.d.l.	b.d.l.		
MFT-San19-5	Core	8.2	6.9	31981.7	2.7	117071	308527	90.1	77324	3939.3	b.d.l.	95.8	b.d.l.	11.6	910.5	117.0	211.7	0.6	b.d.l.	0.0	11089	9.5	6.8	0.3	0.8	b.d.l.	6.4	b.d.l.	b.d.l.	b.d.l.	b.d.l.		
MFT-San19-6	Core	7.8	6.9	30954.6	2.1	111860	308527	b.d.l.	75550	3614.2	b.d.l.	94.6	b.d.l.	11.6	864.3	114.8	192.8	0.6	b.d.l.	0.1	11089	8.8	6.3	0.3	0.7	b.d.l.	5.9	b.d.l.	b.d.l.	b.d.l.	b.d.l.		
MFT-San19-7	Core	6.5	7.3	30260.7	2.9	111359	308527	b.d.l.	72912	3978.5	b.d.l.	88.2	b.d.l.	11.6	886.9	110.4	198.6	0.5	0.1	0.0	b.d.l.	11397	9.1	6.4	0.3	0.6	b.d.l.	6.2	b.d.l.	b.d.l.	b.d.l.	b.d.l.	
MFT-San19-8	Core	8.3	7.1	30648.0	b.d.l.																												

Table A1.5: continued

Er	Tm	Yb	Lu	Hf	Ta	Pb	Th
b.d.l.	b.d.l.	b.d.l.	b.d.l.	b.d.l.	b.d.l.	32.4	b.d.l.
b.d.l.	b.d.l.	b.d.l.	b.d.l.	0.0	b.d.l.	28.5	b.d.l.
b.d.l.	b.d.l.	b.d.l.	0.0	0.0	b.d.l.	32.1	b.d.l.
b.d.l.	b.d.l.	b.d.l.	b.d.l.	0.0	b.d.l.	31.8	b.d.l.
b.d.l.	b.d.l.	b.d.l.	b.d.l.	b.d.l.	b.d.l.	30.9	b.d.l.
b.d.l.	b.d.l.	b.d.l.	b.d.l.	0.0	b.d.l.	30.8	b.d.l.
b.d.l.	b.d.l.	b.d.l.	b.d.l.	0.0	b.d.l.	31.9	b.d.l.
b.d.l.	b.d.l.	b.d.l.	b.d.l.	0.0	b.d.l.	31.3	0.0
b.d.l.	0.0	b.d.l.	b.d.l.	b.d.l.	b.d.l.	32.5	b.d.l.
b.d.l.	b.d.l.	b.d.l.	b.d.l.	0.0	b.d.l.	31.3	b.d.l.
b.d.l.	b.d.l.	b.d.l.	b.d.l.	b.d.l.	0.0	29.4	b.d.l.
b.d.l.	b.d.l.	b.d.l.	b.d.l.	0.0	b.d.l.	29.3	b.d.l.
b.d.l.	b.d.l.	b.d.l.	b.d.l.	b.d.l.	b.d.l.	29.1	b.d.l.
b.d.l.	b.d.l.	b.d.l.	b.d.l.	b.d.l.	b.d.l.	31.0	b.d.l.
b.d.l.	b.d.l.	b.d.l.	b.d.l.	b.d.l.	b.d.l.	30.8	b.d.l.
b.d.l.	b.d.l.	b.d.l.	b.d.l.	b.d.l.	0.0	30.5	b.d.l.
b.d.l.	b.d.l.	b.d.l.	b.d.l.	b.d.l.	0.0	31.6	b.d.l.
b.d.l.	b.d.l.	b.d.l.	b.d.l.	b.d.l.	0.0	31.7	0.0
b.d.l.	b.d.l.	b.d.l.	b.d.l.	0.0	b.d.l.	32.7	b.d.l.
b.d.l.	b.d.l.	b.d.l.	b.d.l.	0.0	b.d.l.	33.3	b.d.l.
b.d.l.	b.d.l.	b.d.l.	b.d.l.	b.d.l.	b.d.l.	31.4	b.d.l.
0.0	b.d.l.	b.d.l.	b.d.l.	b.d.l.	b.d.l.	31.9	b.d.l.
0.0	b.d.l.	b.d.l.	b.d.l.	0.0	0.0	35.5	b.d.l.
b.d.l.	b.d.l.	b.d.l.	b.d.l.	0.0	b.d.l.	36.1	0.0
b.d.l.	b.d.l.	b.d.l.	b.d.l.	0.0	b.d.l.	37.1	b.d.l.
b.d.l.	0.0	b.d.l.	b.d.l.	0.0	0.0	39.6	b.d.l.
b.d.l.	b.d.l.	0.0	b.d.l.	0.0	0.0	36.6	0.0
0.0	b.d.l.	0.0	0.0	0.0	b.d.l.	38.7	0.1
b.d.l.	b.d.l.	b.d.l.	b.d.l.	b.d.l.	b.d.l.	33.6	b.d.l.
b.d.l.	b.d.l.	b.d.l.	b.d.l.	0.0	b.d.l.	24.8	b.d.l.
b.d.l.	b.d.l.	b.d.l.	b.d.l.	0.0	b.d.l.	24.4	b.d.l.
b.d.l.	b.d.l.	b.d.l.	b.d.l.	b.d.l.	b.d.l.	23.3	b.d.l.
b.d.l.	b.d.l.	b.d.l.	b.d.l.	0.0	b.d.l.	24.3	b.d.l.
b.d.l.	b.d.l.	b.d.l.	b.d.l.	b.d.l.	0.0	29.4	b.d.l.
b.d.l.	b.d.l.	b.d.l.	b.d.l.	0.2	b.d.l.	28.0	b.d.l.
b.d.l.	b.d.l.	b.d.l.	b.d.l.	0.1	b.d.l.	27.4	b.d.l.
b.d.l.	b.d.l.	b.d.l.	b.d.l.	b.d.l.	0.0	27.0	0.0
b.d.l.	b.d.l.	b.d.l.	b.d.l.	b.d.l.	b.d.l.	27.3	0.0
b.d.l.	b.d.l.	b.d.l.	b.d.l.	0.1	b.d.l.	34.1	b.d.l.
b.d.l.	b.d.l.	b.d.l.	b.d.l.	0.0	0.0	31.7	b.d.l.
b.d.l.	b.d.l.	b.d.l.	b.d.l.	0.2	b.d.l.	31.7	0.0
b.d.l.	b.d.l.	b.d.l.	b.d.l.	0.0	0.0	32.5	b.d.l.
b.d.l.	b.d.l.	b.d.l.	b.d.l.	0.2	b.d.l.	26.6	b.d.l.
b.d.l.	b.d.l.	b.d.l.	b.d.l.	b.d.l.	0.0	34.4	0.0
b.d.l.	b.d.l.	b.d.l.	b.d.l.	b.d.l.	b.d.l.	32.5	b.d.l.
b.d.l.	b.d.l.	b.d.l.	b.d.l.	b.d.l.	b.d.l.	35.6	b.d.l.
b.d.l.	b.d.l.	b.d.l.	b.d.l.	0.2	0.1	32.5	b.d.l.
b.d.l.	b.d.l.	b.d.l.	b.d.l.	0.0	b.d.l.	31.4	0.0
b.d.l.	b.d.l.	0.1	b.d.l.	b.d.l.	0.0	28.7	b.d.l.

Table A1.5: continued

Info	Position	Li ⁺	Li ⁺	Na	Mg	Al	Si	P	K	Ca	Sc	Ti	V	Mn	Fe	Rb	Sr	Y	Zr	Nb	Cs	Ba	La	Ce	Pr	Nd	Sm	Eu	Gd	Tb	Dy	Ho
MFT-San19 - 21	Core	9.5	6.5	29538.2	3.0	104716	308527	b.d.l.	75038	3789.2	0.7	85.7	b.d.l.	b.d.l.	821.3	121.5	172.5	0.4	b.d.l.	b.d.l.	b.d.l.	9635	7.4	5.3	0.3	0.5	b.d.l.	5.7	b.d.l.	b.d.l.	b.d.l.	0.0
MFT-San19 - 22	Core	6.6	6.8	31841.7	3.6	114094	308527	b.d.l.	79388	3714.9	b.d.l.	97.2	b.d.l.	b.d.l.	858.7	121.5	194.6	0.6	b.d.l.	0.0	0.1	9987	8.5	5.3	0.3	0.4	b.d.l.	6.1	b.d.l.	b.d.l.	b.d.l.	0.0
MFT-San19 - 23	Core	7.0	6.6	31107.2	3.4	113271	308527	b.d.l.	77753	3476.6	0.9	80.8	b.d.l.	b.d.l.	850.9	116.5	184.9	0.6	0.0	0.0	0.2	9369	8.4	5.5	0.3	0.4	b.d.l.	5.7	b.d.l.	b.d.l.	b.d.l.	0.0
MFT-San19 - 24	Core	6.5	6.9	31182.3	2.9	116382	308527	130.8	81093	3184.2	b.d.l.	93.5	b.d.l.	b.d.l.	802.9	117.4	174.4	0.5	b.d.l.	0.1	8902	7.8	5.1	0.3	0.4	b.d.l.	5.4	b.d.l.	b.d.l.	b.d.l.	b.d.l.	
MFT-San19 - 25	Core	7.5	6.8	30916.2	0.4	111241	308527	b.d.l.	75438	3619.5	b.d.l.	76.5	b.d.l.	b.d.l.	803.9	118.3	176.8	0.5	b.d.l.	0.1	8712	8.4	6.3	0.3	0.7	b.d.l.	5.5	b.d.l.	b.d.l.	b.d.l.	b.d.l.	
MFT-San19 - 26	Core	7.4	7.1	30717.9	2.0	110524	308527	b.d.l.	77218	4258.4	0.9	77.7	b.d.l.	b.d.l.	838.4	117.5	168.6	0.3	b.d.l.	b.d.l.	b.d.l.	8252	7.4	5.2	0.2	0.5	b.d.l.	5.1	b.d.l.	b.d.l.	b.d.l.	0.0
MFT-San19 - 27	Core	6.6	6.9	30315.8	3.1	112076	308527	b.d.l.	76409	4003.3	b.d.l.	85.8	b.d.l.	b.d.l.	830.8	113.1	171.9	0.6	b.d.l.	b.d.l.	b.d.l.	7966	7.7	5.6	0.3	0.6	b.d.l.	5.3	b.d.l.	b.d.l.	b.d.l.	0.0
MFT-San19 - 28	Core	5.5	6.3	30047.4	1.2	110109	308527	67.1	75498	3580.5	b.d.l.	79.9	b.d.l.	b.d.l.	829.9	117.7	166.2	0.3	0.1	b.d.l.	0.0	7372	8.3	6.1	0.3	0.8	b.d.l.	4.8	b.d.l.	b.d.l.	b.d.l.	0.0
MFT-San19 - 29	Core	5.3	5.3	31346.2	2.9	113488	308527	b.d.l.	77099	3694.3	b.d.l.	76.1	b.d.l.	b.d.l.	850.1	117.7	168.1	0.4	0.1	b.d.l.	b.d.l.	7067	8.6	5.7	0.3	1.1	b.d.l.	5.1	b.d.l.	b.d.l.	b.d.l.	b.d.l.
MFT-San19 - 30	Core	4.0	3.4	30646.1	2.9	110079	308527	b.d.l.	75820	3679.6	b.d.l.	85.2	b.d.l.	b.d.l.	796.0	116.0	158.7	0.4	b.d.l.	0.0	0.0	6180	8.1	5.8	0.3	0.8	b.d.l.	4.6	b.d.l.	b.d.l.	b.d.l.	b.d.l.
MFT-San19 - 31	Rim	b.d.l.	2.2	31206.8	3.7	111697	308527	b.d.l.	78766	3961.3	b.d.l.	79.1	b.d.l.	b.d.l.	784.8	117.4	167.5	0.3	b.d.l.	b.d.l.	0.1	6040	7.7	5.9	0.2	0.5	b.d.l.	4.7	b.d.l.	b.d.l.	b.d.l.	b.d.l.
Sandine grain 22 - Line 1																																
MFT-San22 - 1	Core	2.6	1.7	29782.8	3.2	108495	308527	b.d.l.	78093	2444.4	b.d.l.	62.7	b.d.l.	b.d.l.	813.4	121.8	103.9	0.2	b.d.l.	b.d.l.	b.d.l.	2877	5.0	2.6	0.1	0.2	b.d.l.	3.0	b.d.l.	b.d.l.	b.d.l.	b.d.l.
MFT-San22 - 2	Core	2.3	2.3	30461.9	2.6	109121	308527	54.5	81812	2458.9	b.d.l.	73.0	b.d.l.	b.d.l.	782.5	133.2	107.4	0.2	b.d.l.	0.0	0.0	3059	4.9	3.2	0.1	0.4	b.d.l.	3.0	0.1	b.d.l.	b.d.l.	b.d.l.
MFT-San22 - 3	Core	2.3	2.5	28834.6	1.9	105962	308527	b.d.l.	74449	2059.7	b.d.l.	66.1	b.d.l.	b.d.l.	762.4	118.5	113.3	0.3	b.d.l.	0.0	b.d.l.	3265	5.3	3.4	0.1	b.d.l.	3.6	b.d.l.	b.d.l.	b.d.l.	b.d.l.	b.d.l.
MFT-San22 - 4	Core	3.8	3.3	30629.1	b.d.l.	108017	308527	b.d.l.	80092	2364.8	b.d.l.	57.4	b.d.l.	b.d.l.	792.2	125.8	117.9	0.2	b.d.l.	b.d.l.	0.1	3451	5.7	3.6	0.2	0.3	b.d.l.	3.6	b.d.l.	b.d.l.	b.d.l.	b.d.l.
MFT-San22 - 5	Core	4.6	3.8	29905.9	0.8	104826	308527	b.d.l.	81173	2615.4	0.6	64.0	b.d.l.	b.d.l.	749.0	121.9	147.5	0.1	b.d.l.	b.d.l.	0.1	3849	7.7	5.4	0.3	0.3	b.d.l.	4.1	b.d.l.	b.d.l.	b.d.l.	b.d.l.
MFT-San22 - 6	Core	4.8	4.1	29694.1	1.3	104431	308527	b.d.l.	76634	2500.0	1.0	76.4	b.d.l.	b.d.l.	734.5	115.1	137.3	0.2	b.d.l.	b.d.l.	0.1	3720	6.4	4.4	0.2	0.5	b.d.l.	4.2	b.d.l.	b.d.l.	b.d.l.	b.d.l.
MFT-San22 - 7	Core	6.7	4.3	29479.0	1.2	106592	308527	b.d.l.	73345	3286.0	b.d.l.	76.3	b.d.l.	b.d.l.	778.2	109.3	160.8	0.2	b.d.l.	b.d.l.	0.1	3851	5.9	4.0	0.2	0.3	b.d.l.	4.7	b.d.l.	b.d.l.	b.d.l.	b.d.l.
MFT-San22 - 8	Core	5.6	5.4	32048.5	5.6	110319	308527	52.4	73808	4521.8	0.8	95.3	0.7	b.d.l.	806.5	107.6	240.8	0.4	b.d.l.	0.0	0.1	5836	9.8	7.4	0.4	0.9	b.d.l.	6.6	b.d.l.	b.d.l.	b.d.l.	0.0
MFT-San22 - 10	Core	5.0	5.7	30294.8	3.5	107432	308527	b.d.l.	71725	4407.6	b.d.l.	84.6	b.d.l.	b.d.l.	776.5	102.1	218.0	0.4	b.d.l.	b.d.l.	0.1	5407	7.7	5.7	0.3	0.6	b.d.l.	6.0	b.d.l.	b.d.l.	b.d.l.	b.d.l.
MFT-San22 - 11	Core	6.4	6.5	31962.7	3.6	108863	308527	56.7	74416	4597.2	b.d.l.	84.1	b.d.l.	b.d.l.	844.2	105.4	223.4	0.3	b.d.l.	b.d.l.	0.1	5852	8.0	5.9	0.3	0.6	b.d.l.	6.1	b.d.l.	b.d.l.	b.d.l.	b.d.l.
MFT-San22 - 12	Core	6.3	6.5	32216.5	2.1	110195	308527	b.d.l.	75265	4887.3	b.d.l.	80.6	b.d.l.	b.d.l.	861.9	103.0	226.0	0.2	0.1	0.0	0.1	6642	8.1	6.0	0.3	0.6	b.d.l.	6.1	b.d.l.	b.d.l.	b.d.l.	0.0
MFT-San22 - 13	Core	8.3	6.7	31336.5	2.0	110597	308527	b.d.l.	75061	3828.8	b.d.l.	83.3	b.d.l.	b.d.l.	811.3	100.9	216.7	0.3	0.0	b.d.l.	0.1	6642	8.1	6.0	0.3	0.6	b.d.l.	6.6	b.d.l.	b.d.l.	b.d.l.	b.d.l.
MFT-San22 - 14	Core	8.8	6.6	30568.0	2.1	108961	308527	b.d.l.	73519	3713.0	b.d.l.	78.9	b.d.l.	b.d.l.	849.9	99.4	206.5	0.3	0.0	b.d.l.	b.d.l.	7040	8.6	6.5	0.3	0.6	b.d.l.	5.5	b.d.l.	0.0	b.d.l.	b.d.l.
MFT-San22 - 15	Core	8.2	7.1	29983.9	2.6	103625	308527	b.d.l.	70714	3217.9	0.5	67.8	b.d.l.	b.d.l.	784.4	116.4	179.8	0.3	b.d.l.	b.d.l.	0.1	6559	7.8	5.7	0.2	0.5	b.d.l.	5.0	b.d.l.	b.d.l.	b.d.l.	b.d.l.
MFT-San22 - 16	Core	7.0	6.0	29833.0	2.9	101347	308527	b.d.l.	70800	3201.7	b.d.l.	82.7	b.d.l.	b.d.l.	794.9	95.8	177.1	0.3	b.d.l.	b.d.l.	0.1	6521	7.2	5.0	0.3	0.5	b.d.l.	5.1	b.d.l.	b.d.l.	b.d.l.	b.d.l.
MFT-San22 - 17	Core	6.3	6.8	30722.5	b.d.l.	108596	308527	83.0	75006	3992.3	b.d.l.	80.4	b.d.l.	b.d.l.	837.5	102.6	183.8	0.4	b.d.l.	b.d.l.	0.1	7446	7.4	5.2	0.2	0.3	b.d.l.	5.3	b.d.l.	b.d.l.	b.d.l.	b.d.l.
MFT-San22 - 18	Core	6.2	6.0	31143.7	2.1	109367	308527	b.d.l.	74695	4259.5	b.d.l.	92.8	b.d.l.	b.d.l.	926.9	106.9	195.8	0.4	b.d.l.	0.0	b.d.l.	8245	8.6	6.1	0.3	0.6	b.d.l.	5.9	b.d.l.	b.d.l.	b.d.l.	b.d.l.
MFT-San22 - 19	Core	6.8	6.8	30631.7	b.d.l.	106734	308527	56.7	74970	3570.3	b.d.l.	98.1	b.d.l.	b.d.l.	868.6	117.8	193.0	0.4	b.d.l.	b.d.l.	0.0	7904	7.9	5.4	0.3	0.4	b.d.l.	5.3	b.d.l.	b.d.l.	b.d.l.	b.d.l.
MFT-San22 - 20	Core	7.6	6.2	30766.5	1.7	110816	308527	b.d.l.	74263	3932.6	b.d.l.	71.3	b.d.l.	b.d.l.	873.2	109.7	205.6	0.5	b.d.l.	0.0	b.d.l.	8548	8.1	6.0	0.3	0.7	b.d.l.	5.5	b.d.l.	b.d.l.	b.d.l.	b.d.l.
MFT-San22 - 21	Core	6.8	6.0	31402.3	1.6	114030	308527	b.d.l.	76026	4377.6	b.d.l.	91.4	b.d.l.	b.d.l.	856.3	111.4	224.2	0.5	0.0	b.d.l.	0.1	9692	8.0	6.3	0.3	0.6	b.d.l.	6.4	b.d.l.	b.d.l.	b.d.l.	b.d.l.
MFT-San22 - 22	Core	6.0	6.1	30859.8	2.0	10901	308527	63.3	76193	3661.1	b.d.l.	94.6	b.d.l.	b.d.l.	928.0	112.1	192.4	0.5	b.d.l.	b.d.l.	0.1	8569	6.8	5.2	0.3	0.4	b.d.l.	5.8	b.d.l.	b.d.l.	b.d.l.	b.d.l.
MFT-San22 - 23	Core	7.3	5.9	30442.0	3.1	110361	308527	91.0	74308	3643.3	b.d.l.	93.7	b.d.l.	b.d.l.	796.8	110.4	215.1	0.5	0.1	0.0	0.1	9587	8.5	5.9	0.3	0.9	b.d.l.	6.5	b.d.l.	b.d.l.	b.d.l.	b.d.l.
MFT-San22 - 24	Core	7.0	6.0	31172.4	3.7	107700	308527	47.1	73824	4342.1	0.6	88.9	b.d.l.	b.d.l.	877.4	113.5	216.2	0.4	b.d.l.	0.0	0.1	9922	8.7	7.2	0.4	0.8	b.d.l.	6.4	b.d.l.	b.d.l.	b.d.l.	b.d.l.
MFT-San22 - 25	Core	7.1	6.5	33023.5	b.d.l.	112291	308527	105.0	75824	3694.5	0.6	100.0	b.d.l.	b.d.l.	834.9	112.0	183.6	0.4	0.2	b.d.l.	0.1	8362	7.0	5.0	0.2	0.4	b.d.l.	5.3	b.d.l.	b.d.l.	b.d.l.	b.d.l.
MFT-San22 - 26	Core	6.1	6.1	29743.8	3.6	106895	308527	b.d.l.	78182	3734.6	0.9	90.9	b.d.l.	b.d.l.	864.1	113.5	204.2	0.6	0.0	b.d.l.	0.1	9295	8.8	6.2	0.3	0.8	b.d.l.	5.8	b.d.l.	0.0	b.d.l.	b.d.l.
MFT-San22 - 27	Core	6.8	6.0	30484.0	1.7	110252	308527	b.d.l.	75454	3819.1	b.d.l.	86.7	b.d.l.	b.d.l.	864.1	113.5	204.2	0.6	0.0	b.d.l.	0.1	9295	8.8	6.2	0.3	0.8	b.d.l.	5.8	b.d.l.	b.d.l.	b.d.l.	b.d.l.
MFT-San22 - 28	Core	6.8	5.7	30595.3	4.2	111500	308527	b.d.l.	78575	36																						

Table A1.5: continued

Er	Tm	Yb	Lu	Hf	Ta	Pb	Th	U
b.d.l.	b.d.l.	b.d.l.	b.d.l.	0.2	0.1	28.3	0.0	b.d.l.
b.d.l.	b.d.l.	b.d.l.	b.d.l.	0.1	0.0	28.0	b.d.l.	b.d.l.
b.d.l.	b.d.l.	b.d.l.	0.0	b.d.l.	b.d.l.	26.7	b.d.l.	b.d.l.
b.d.l.	b.d.l.	b.d.l.	b.d.l.	0.1	b.d.l.	28.1	b.d.l.	b.d.l.
b.d.l.	b.d.l.	0.1	b.d.l.	b.d.l.	0.0	30.2	b.d.l.	b.d.l.
b.d.l.	b.d.l.	b.d.l.	b.d.l.	b.d.l.	b.d.l.	27.4	b.d.l.	b.d.l.
b.d.l.	b.d.l.	b.d.l.	b.d.l.	0.1	0.0	27.0	b.d.l.	b.d.l.
b.d.l.	b.d.l.	b.d.l.	b.d.l.	b.d.l.	0.0	30.0	b.d.l.	b.d.l.
b.d.l.	b.d.l.	b.d.l.	b.d.l.	b.d.l.	b.d.l.	29.8	0.0	b.d.l.
b.d.l.	b.d.l.	b.d.l.	b.d.l.	b.d.l.	0.0	30.1	b.d.l.	0.0
b.d.l.	b.d.l.	b.d.l.	b.d.l.	b.d.l.	0.0	28.4	b.d.l.	b.d.l.
b.d.l.	b.d.l.	b.d.l.	b.d.l.	b.d.l.	b.d.l.	21.0	b.d.l.	b.d.l.
b.d.l.	b.d.l.	b.d.l.	b.d.l.	b.d.l.	b.d.l.	20.9	b.d.l.	b.d.l.
b.d.l.	b.d.l.	b.d.l.	b.d.l.	b.d.l.	b.d.l.	19.5	b.d.l.	0.0
b.d.l.	b.d.l.	b.d.l.	b.d.l.	b.d.l.	0.0	24.5	b.d.l.	b.d.l.
b.d.l.	b.d.l.	b.d.l.	b.d.l.	b.d.l.	0.0	25.6	b.d.l.	b.d.l.
b.d.l.	b.d.l.	b.d.l.	0.0	b.d.l.	0.0	21.3	b.d.l.	b.d.l.
b.d.l.	b.d.l.	b.d.l.	b.d.l.	0.0	b.d.l.	22.1	b.d.l.	b.d.l.
b.d.l.	b.d.l.	b.d.l.	b.d.l.	0.1	0.0	22.3	0.0	b.d.l.
0.0	b.d.l.	b.d.l.	b.d.l.	0.0	0.0	31.8	b.d.l.	b.d.l.
b.d.l.	b.d.l.	b.d.l.	b.d.l.	0.0	0.0	28.8	b.d.l.	b.d.l.
b.d.l.	b.d.l.	b.d.l.	0.0	0.1	0.0	29.4	b.d.l.	b.d.l.
b.d.l.	b.d.l.	b.d.l.	b.d.l.	0.0	b.d.l.	31.0	b.d.l.	b.d.l.
b.d.l.	b.d.l.	b.d.l.	b.d.l.	b.d.l.	b.d.l.	29.6	b.d.l.	b.d.l.
b.d.l.	b.d.l.	b.d.l.	b.d.l.	0.2	b.d.l.	27.0	0.0	b.d.l.
b.d.l.	b.d.l.	b.d.l.	b.d.l.	b.d.l.	0.0	27.2	b.d.l.	b.d.l.
b.d.l.	b.d.l.	b.d.l.	b.d.l.	b.d.l.	0.0	22.5	b.d.l.	b.d.l.
b.d.l.	b.d.l.	b.d.l.	b.d.l.	b.d.l.	0.0	24.5	b.d.l.	b.d.l.
b.d.l.	b.d.l.	b.d.l.	b.d.l.	b.d.l.	0.1	29.7	0.0	b.d.l.
b.d.l.	b.d.l.	b.d.l.	0.0	0.0	b.d.l.	27.8	b.d.l.	b.d.l.
b.d.l.	b.d.l.	b.d.l.	b.d.l.	0.0	0.0	25.5	b.d.l.	b.d.l.
b.d.l.	b.d.l.	b.d.l.	b.d.l.	0.1	b.d.l.	26.0	b.d.l.	b.d.l.
b.d.l.	b.d.l.	b.d.l.	b.d.l.	0.2	b.d.l.	27.9	b.d.l.	b.d.l.
b.d.l.	b.d.l.	b.d.l.	b.d.l.	0.0	0.0	26.1	b.d.l.	0.0
b.d.l.	b.d.l.	b.d.l.	b.d.l.	b.d.l.	0.0	30.0	b.d.l.	b.d.l.
b.d.l.	b.d.l.	b.d.l.	b.d.l.	0.0	0.0	26.0	b.d.l.	b.d.l.
b.d.l.	b.d.l.	b.d.l.	b.d.l.	0.0	0.1	28.3	b.d.l.	0.0
0.0	b.d.l.	b.d.l.	b.d.l.	0.1	0.0	25.7	b.d.l.	b.d.l.
b.d.l.	b.d.l.	b.d.l.	b.d.l.	0.1	b.d.l.	25.6	b.d.l.	b.d.l.
b.d.l.	b.d.l.	b.d.l.	b.d.l.	b.d.l.	0.0	28.6	b.d.l.	0.0
b.d.l.	b.d.l.	b.d.l.	b.d.l.	0.1	0.0	25.9	0.0	b.d.l.
b.d.l.	b.d.l.	0.1	b.d.l.	b.d.l.	0.0	28.1	0.0	b.d.l.
b.d.l.	b.d.l.	b.d.l.	b.d.l.	b.d.l.	b.d.l.	27.3	b.d.l.	b.d.l.
b.d.l.	b.d.l.	b.d.l.	0.0	0.1	b.d.l.	27.6	b.d.l.	b.d.l.
b.d.l.	b.d.l.	b.d.l.	b.d.l.	0.1	b.d.l.	27.9	b.d.l.	b.d.l.
b.d.l.	0.0	b.d.l.	b.d.l.	b.d.l.	b.d.l.	29.5	b.d.l.	0.0
b.d.l.	b.d.l.	0.1	b.d.l.	0.1	b.d.l.	28.0	b.d.l.	b.d.l.
b.d.l.	b.d.l.	0.1	b.d.l.	b.d.l.	b.d.l.	29.2	b.d.l.	0.0
b.d.l.	b.d.l.	b.d.l.	b.d.l.	0.1	0.0	29.7	b.d.l.	b.d.l.
b.d.l.	b.d.l.	b.d.l.	b.d.l.	0.0	0.0	28.9	b.d.l.	0.0

Table A1.5: continued

Info	Position	Li ^o	Li ⁱ	Na	Mg	Al	Si	P	K	Ca	Sc	Ti	V	Mn	Fe	Rb	Sr	Y	Zr	Nb	Cs	Ba	La	Ce	Pr	Nd	Sm	Eu	Gd	Tb	Dy	Ho	
MFT-San22 - 40	Rim	5.2	5.1	32275.1	1.7	116963	308527	b.d.l.	81667	3727.7	b.d.l.	788	b.d.l.	b.d.l.	739.8	119.9	178.9	0.2	0.1	b.d.l.	0.1	3421	16.6	4.3	0.2	0.5	b.d.l.	3.8	b.d.l.	b.d.l.	b.d.l.	b.d.l.	
MFT-San22 - 41	Rim	4.4	4.5	30606.4	1.6	111635	308527	b.d.l.	78370	3309.0	b.d.l.	80.6	b.d.l.	b.d.l.	829.1	119.5	160.4	0.2	0.1	b.d.l.	0.0	0.1	5447	7.3	5.3	0.3	0.6	b.d.l.	4.7	b.d.l.	b.d.l.	0.0	b.d.l.
MFT-San22 - 42	Rim	2.2	3.5	30693.9	b.d.l.	109075	308527	b.d.l.	77824	3153.0	b.d.l.	81.0	b.d.l.	b.d.l.	781.9	116.4	158.3	0.1	b.d.l.	b.d.l.	b.d.l.	5106	7.6	5.2	0.2	0.7	b.d.l.	4.7	b.d.l.	b.d.l.	b.d.l.	b.d.l.	
MFT-San22 - 43	Rim	3.9	2.5	30744.0	1.3	110826	308527	b.d.l.	77562	3073.1	b.d.l.	78.2	b.d.l.	b.d.l.	770.2	118.6	155.5	0.3	0.1	b.d.l.	0.1	4786	7.3	5.4	0.3	0.5	b.d.l.	4.4	b.d.l.	b.d.l.	b.d.l.	b.d.l.	
MFT-San22 - 44	Rim	2.3	1.9	30279.7	1.9	109617	308527	65.1	77750	3176.9	0.6	61.3	b.d.l.	b.d.l.	732.6	117.4	146.9	0.3	0.0	b.d.l.	b.d.l.	4329	7.2	4.7	0.3	0.4	b.d.l.	4.1	b.d.l.	b.d.l.	b.d.l.	b.d.l.	
MFT-San22 - 45	Rim	b.d.l.	1.1	30203.1	2.4	105895	308527	b.d.l.	76764	2891.0	0.7	72.3	b.d.l.	b.d.l.	798.9	123.3	139.0	0.2	0.2	b.d.l.	b.d.l.	4008	6.8	5.0	0.2	0.5	b.d.l.	4.2	b.d.l.	b.d.l.	b.d.l.	b.d.l.	
Sanidine grain 27 - Line 1																																	
MFT-San27 - 2	Rim	3.2	1.8	30215.0	2.9	107862	308527	b.d.l.	76124	3540.2	1.1	71.2	b.d.l.	b.d.l.	739.8	119.9	125.2	0.1	b.d.l.	b.d.l.	0.1	3421	16.6	4.3	0.2	0.5	b.d.l.	3.8	b.d.l.	b.d.l.	b.d.l.	b.d.l.	
MFT-San27 - 3	Core	4.0	3.2	29171.8	3.6	107644	308527	b.d.l.	74405	2985.6	b.d.l.	64.2	b.d.l.	b.d.l.	729.3	114.5	124.1	0.1	b.d.l.	b.d.l.	b.d.l.	3456	6.1	4.2	0.2	0.4	0.1	3.6	b.d.l.	b.d.l.	b.d.l.	b.d.l.	
MFT-San27 - 4	Core	5.2	4.5	32402.1	2.7	117634	308527	b.d.l.	81004	3248.3	b.d.l.	78.9	b.d.l.	b.d.l.	777.2	126.5	147.4	0.3	b.d.l.	b.d.l.	0.1	3783	6.9	4.8	0.3	0.5	b.d.l.	4.0	b.d.l.	b.d.l.	b.d.l.	b.d.l.	
MFT-San27 - 5	Core	6.3	5.7	32159.5	1.8	117263	308527	b.d.l.	82066	3152.5	b.d.l.	78.9	b.d.l.	b.d.l.	788.6	122.9	148.2	0.2	b.d.l.	0.1	0.1	3601	6.6	4.6	0.2	0.3	b.d.l.	4.2	b.d.l.	b.d.l.	b.d.l.	b.d.l.	
MFT-San27 - 6	Core	6.3	5.9	31226.5	1.3	113207	308527	b.d.l.	78023	3484.8	0.6	70.8	b.d.l.	b.d.l.	774.7	122.7	155.1	0.4	b.d.l.	0.0	0.1	3612	6.8	4.6	0.2	0.5	b.d.l.	4.4	b.d.l.	b.d.l.	b.d.l.	b.d.l.	
MFT-San27 - 7	Core	7.1	6.2	31521.5	2.2	113465	308527	b.d.l.	76384	3879.6	b.d.l.	63.9	b.d.l.	b.d.l.	753.5	114.7	163.6	0.3	b.d.l.	b.d.l.	0.1	3657	7.4	5.1	0.2	0.5	b.d.l.	4.6	b.d.l.	b.d.l.	b.d.l.	b.d.l.	
MFT-San27 - 8	Core	6.1	6.3	32680.9	2.6	117970	308527	79.4	80605	3454.0	b.d.l.	72.4	b.d.l.	b.d.l.	821.7	123.3	154.9	0.1	b.d.l.	b.d.l.	b.d.l.	3404	7.0	5.2	0.2	0.5	b.d.l.	4.3	b.d.l.	b.d.l.	b.d.l.	b.d.l.	
MFT-San27 - 9	Core	5.0	7.2	31980.0	1.9	118079	308527	b.d.l.	82458	2655.8	b.d.l.	80.8	b.d.l.	b.d.l.	767.0	131.8	132.0	0.2	b.d.l.	b.d.l.	0.0	3005	6.6	3.9	0.2	0.4	b.d.l.	3.6	b.d.l.	b.d.l.	0.0	b.d.l.	
MFT-San27 - 10	Core	5.7	6.1	30678.6	2.1	110666	308527	b.d.l.	77936	2808.3	b.d.l.	69.8	b.d.l.	b.d.l.	707.1	120.7	126.8	0.1	b.d.l.	b.d.l.	0.0	2699	6.4	4.4	0.2	0.3	b.d.l.	3.7	b.d.l.	0.0	b.d.l.	b.d.l.	
MFT-San27 - 11	Core	5.8	6.1	29816.1	2.4	110392	308527	b.d.l.	76391	3179.6	b.d.l.	71.6	b.d.l.	b.d.l.	700.3	115.5	126.3	b.d.l.	b.d.l.	b.d.l.	0.1	2548	6.1	4.1	0.2	0.4	b.d.l.	3.5	b.d.l.	b.d.l.	b.d.l.	b.d.l.	
MFT-San27 - 12	Core	6.6	5.8	30094.5	4.6	109175	308527	70.8	75594	2699.9	b.d.l.	73.9	b.d.l.	b.d.l.	712.7	114.3	132.0	0.1	b.d.l.	b.d.l.	0.1	2376	6.2	4.3	0.2	0.4	b.d.l.	4.1	b.d.l.	b.d.l.	b.d.l.	b.d.l.	
MFT-San27 - 13	Core	7.4	5.7	30302.5	2.6	110229	308527	b.d.l.	76727	3001.8	b.d.l.	61.6	b.d.l.	b.d.l.	618.3	120.4	134.1	0.1	0.1	b.d.l.	b.d.l.	0.1	2236	6.0	4.4	0.2	0.4	b.d.l.	3.6	b.d.l.	b.d.l.	0.0	b.d.l.
MFT-San27 - 14	Core	6.5	5.8	30930.0	2.1	111925	308527	b.d.l.	78059	2517.9	b.d.l.	59.6	b.d.l.	b.d.l.	726.3	122.0	126.5	0.1	b.d.l.	0.0	0.1	2068	5.8	3.8	0.2	0.4	b.d.l.	3.5	b.d.l.	b.d.l.	b.d.l.	b.d.l.	
MFT-San27 - 15	Core	6.4	6.4	30097.1	2.6	110948	308527	88.7	76814	2778.2	b.d.l.	63.8	b.d.l.	b.d.l.	722.8	120.3	128.7	0.1	b.d.l.	b.d.l.	0.1	1949	5.8	3.8	0.2	0.3	b.d.l.	3.9	b.d.l.	0.0	b.d.l.	0.0	
MFT-San27 - 16	Core	7.4	6.1	30132.5	1.3	111540	308527	b.d.l.	76026	2566.4	b.d.l.	70.2	b.d.l.	b.d.l.	714.6	115.3	125.8	b.d.l.	b.d.l.	b.d.l.	0.1	1936	6.3	4.4	0.2	0.4	b.d.l.	3.5	b.d.l.	b.d.l.	b.d.l.	b.d.l.	
MFT-San27 - 17	Core	6.5	6.0	29280.9	0.4	107207	308527	b.d.l.	74475	2568.4	b.d.l.	62.8	b.d.l.	b.d.l.	639.0	115.7	144.4	0.2	0.1	0.0	0.1	1841	6.3	4.4	0.2	0.5	b.d.l.	3.7	b.d.l.	b.d.l.	b.d.l.	b.d.l.	
MFT-San27 - 18	Core	6.8	6.2	30408.7	2.1	109631	308527	b.d.l.	76054	2864.1	b.d.l.	62.8	b.d.l.	b.d.l.	639.0	115.7	144.4	0.2	0.1	0.0	0.1	1777	6.5	4.4	0.2	0.5	b.d.l.	3.7	b.d.l.	b.d.l.	b.d.l.	b.d.l.	
MFT-San27 - 19	Core	6.1	6.3	30546.1	3.6	109410	308527	b.d.l.	75940	3527.5	0.8	67.0	b.d.l.	b.d.l.	671.1	115.4	144.3	0.2	0.1	0.0	0.1	1693	6.4	4.4	0.2	0.7	0.1	3.8	b.d.l.	b.d.l.	b.d.l.	b.d.l.	
MFT-San27 - 20	Core	7.6	5.9	29123.4	1.2	110367	308527	b.d.l.	71097	2986.2	b.d.l.	70.4	b.d.l.	b.d.l.	647.0	108.2	139.9	0.1	b.d.l.	0.0	0.1	1693	6.5	4.3	0.2	0.5	b.d.l.	3.6	b.d.l.	b.d.l.	b.d.l.	b.d.l.	
MFT-San27 - 21	Core	6.2	6.3	31890.0	1.8	113671	308527	b.d.l.	80022	3242.0	b.d.l.	61.0	1.0	b.d.l.	718.4	121.1	140.5	0.1	b.d.l.	b.d.l.	0.0	1649	6.2	4.5	0.2	0.4	b.d.l.	3.5	b.d.l.	b.d.l.	0.0	b.d.l.	
MFT-San27 - 22	Core	5.6	5.6	30681.5	2.6	111732	308527	b.d.l.	76097	2972.5	1.2	64.4	b.d.l.	b.d.l.	627.3	118.6	127.7	0.1	b.d.l.	b.d.l.	0.2	1491	5.9	3.9	0.2	0.3	b.d.l.	3.5	b.d.l.	b.d.l.	b.d.l.	b.d.l.	
MFT-San27 - 23	Core	7.1	5.1	30135.9	1.3	109545	308527	b.d.l.	76039	3145.3	b.d.l.	65.5	b.d.l.	b.d.l.	627.3	118.6	127.7	0.1	0.0	b.d.l.	0.1	1378	6.2	3.9	0.2	b.d.l.	0.1	3.5	b.d.l.	b.d.l.	b.d.l.	b.d.l.	
MFT-San27 - 24	Core	4.6	4.4	31255.1	1.3	113692	308527	b.d.l.	80764	2379.9	0.9	76.6	b.d.l.	b.d.l.	732.7	125.0	132.8	b.d.l.	b.d.l.	b.d.l.	0.1	1326	5.9	4.0	0.2	0.3	b.d.l.	3.7	b.d.l.	b.d.l.	b.d.l.	b.d.l.	
MFT-San27 - 25	Core	3.3	3.3	30769.2	1.8	110403	308527	b.d.l.	77140	3043.7	0.8	68.2	b.d.l.	b.d.l.	698.3	121.3	126.4	b.d.l.	b.d.l.	b.d.l.	0.0	1132	6.4	4.1	0.2	0.5	b.d.l.	3.5	b.d.l.	b.d.l.	b.d.l.	b.d.l.	
MFT-San27 - 26	Rim	2.5	2.1	31417.7	1.5	112008	308527	95.1	78328	2329.9	b.d.l.	66.7	b.d.l.	b.d.l.	774.0	122.6	129.6	0.1	b.d.l.	0.0	0.1	1006	6.5	4.3	0.2	0.5	b.d.l.	3.5	b.d.l.	b.d.l.	b.d.l.	b.d.l.	
mount1-1-1	Rim	4.1	3.7	30174.3	b.d.l.	99512	303853	24.2	91426	3025.7	0.6	80.7	b.d.l.	0.6	800.8	98.2	240.5	0.0	b.d.l.	0.0	0.0	3156	7.7	5.4	0.3	0.5	b.d.l.	6.2	b.d.l.	b.d.l.	b.d.l.	b.d.l.	
mount1-1-2	Rim	6.4	4.9	30960.9	b.d.l.	102877	303853	25.1	87024	4135.6	0.6	114.0	b.d.l.	0.7	927.7	99.1	272.1	0.1	0.1	0.0	0.0	11669	9.0	6.3	0.3	0.8	0.0	8.0	b.d.l.	b.d.l.	b.d.l.	b.d.l.	
mount1-4	Core	5.7	4.8	30626.6	3.0	102141	303853	23.6	88475	3603.1	0.6	98.7	b.d.l.	0.6	894.3	97.8	265.5	0.0	b.d.l.	0.0	0.0	9222	8.8	6.2	0.3	0.6	0.0	7.7	b.d.l.	b.d.l.	b.d.l.	b.d.l.	
mount1-5-3	Rim	5.4	3.0	30500.7	b.d.l.	98827	303853	21.8	88864	2741.5	0.7	71.3	b.d.l.	0.4	752.2	116.1	118.9	0.0	b.d.l.	0.0	0.1	2335	6.2	4.3	0.2	0.3	b.d.l.	3.4	b.d.l.	b.d.l.	b.d.l.	b.d.l.	
mount1-6-1	Rim	7.1	7.1	31796.0	4.7	101815	303853	21.9	86291	4061.9	0.6	97.9	b.d.l.	0.7	908.2	112.5	115.9	0.1	b.d.l.	b.d.l.	0.1	7139	8.8	6.6	0.3	0.7	0.0	3.9	b.d.l.	b.d.l.	b.d.l.	b.d.l.	
mount1-6-2	Core	8.0	7.8	31086.0	b.d.l.	99879	303853	20.5	87061	3694.5	0.6	94.4	b.d.l.	0.5	837.1	122.7	127.6	0.0	b.d.l.	0.0	0.1	6854	7.2	5.4	0.3	0.5	0.0	4.4	b.d.l.	b.d.l.	b.d.l.	b.d.l.	
mount1-6-3	Rim	9.6	7.5	30805.3	b.d.l.	100325	303853	2																									

Table A1.5: continued

Er	Tm	Yb	Lu	Hf	Ta	Pb	Th	U
b.d.l.	0.0	b.d.l.	b.d.l.	b.d.l.	0.0	28.1	b.d.l.	0.0
b.d.l.	b.d.l.	0.1	b.d.l.	0.1	b.d.l.	28.7	b.d.l.	b.d.l.
b.d.l.	b.d.l.	b.d.l.	b.d.l.	b.d.l.	0.0	27.3	b.d.l.	b.d.l.
b.d.l.	b.d.l.	b.d.l.	b.d.l.	b.d.l.	0.0	28.4	0.0	0.0
b.d.l.	0.0	b.d.l.	b.d.l.	b.d.l.	0.0	26.4	b.d.l.	b.d.l.
b.d.l.	b.d.l.	b.d.l.	b.d.l.	b.d.l.	0.0	25.1	0.0	b.d.l.
b.d.l.	b.d.l.	b.d.l.	b.d.l.	0.1	b.d.l.	26.8	0.0	b.d.l.
b.d.l.	0.0	b.d.l.	b.d.l.	0.1	b.d.l.	25.8	b.d.l.	b.d.l.
b.d.l.	b.d.l.	0.1	b.d.l.	0.0	b.d.l.	28.6	b.d.l.	b.d.l.
b.d.l.	b.d.l.	b.d.l.	b.d.l.	b.d.l.	b.d.l.	27.9	b.d.l.	0.0
b.d.l.	b.d.l.	b.d.l.	b.d.l.	b.d.l.	b.d.l.	30.6	b.d.l.	b.d.l.
b.d.l.	b.d.l.	b.d.l.	b.d.l.	b.d.l.	0.0	32.0	b.d.l.	b.d.l.
b.d.l.	b.d.l.	b.d.l.	b.d.l.	0.0	b.d.l.	27.8	b.d.l.	b.d.l.
b.d.l.	b.d.l.	b.d.l.	b.d.l.	b.d.l.	b.d.l.	24.6	b.d.l.	b.d.l.
b.d.l.	b.d.l.	b.d.l.	b.d.l.	b.d.l.	b.d.l.	24.7	b.d.l.	0.0
b.d.l.	b.d.l.	b.d.l.	b.d.l.	b.d.l.	b.d.l.	24.8	b.d.l.	b.d.l.
b.d.l.	b.d.l.	b.d.l.	0.0	b.d.l.	0.0	24.1	b.d.l.	b.d.l.
b.d.l.	b.d.l.	b.d.l.	b.d.l.	b.d.l.	0.0	23.4	b.d.l.	b.d.l.
b.d.l.	b.d.l.	b.d.l.	b.d.l.	0.0	0.0	23.0	0.0	b.d.l.
b.d.l.	b.d.l.	b.d.l.	b.d.l.	0.1	b.d.l.	24.3	b.d.l.	b.d.l.
b.d.l.	b.d.l.	b.d.l.	b.d.l.	b.d.l.	0.0	25.1	b.d.l.	b.d.l.
b.d.l.	b.d.l.	0.1	0.0	b.d.l.	b.d.l.	23.2	b.d.l.	b.d.l.
b.d.l.	b.d.l.	0.1	b.d.l.	b.d.l.	0.0	24.7	b.d.l.	b.d.l.
b.d.l.	b.d.l.	b.d.l.	b.d.l.	b.d.l.	0.0	24.4	b.d.l.	0.0
0.1	b.d.l.	b.d.l.	b.d.l.	b.d.l.	0.0	25.5	b.d.l.	b.d.l.
b.d.l.	b.d.l.	b.d.l.	b.d.l.	b.d.l.	b.d.l.	25.8	0.0	b.d.l.
b.d.l.	b.d.l.	b.d.l.	b.d.l.	b.d.l.	b.d.l.	22.8	b.d.l.	0.0
b.d.l.	b.d.l.	b.d.l.	b.d.l.	b.d.l.	b.d.l.	24.0	b.d.l.	b.d.l.
b.d.l.	b.d.l.	b.d.l.	b.d.l.	b.d.l.	b.d.l.	24.8	b.d.l.	b.d.l.
b.d.l.	b.d.l.	b.d.l.	0.0	0.0	b.d.l.	23.5	b.d.l.	b.d.l.
b.d.l.	b.d.l.	b.d.l.	b.d.l.	b.d.l.	0.0	25.1	b.d.l.	0.0
b.d.l.	b.d.l.	b.d.l.	b.d.l.	b.d.l.	b.d.l.	b.d.l.	b.d.l.	b.d.l.
b.d.l.	b.d.l.	b.d.l.	b.d.l.	0.0	0.0	26.3	b.d.l.	b.d.l.
b.d.l.	b.d.l.	b.d.l.	b.d.l.	b.d.l.	b.d.l.	22.8	b.d.l.	b.d.l.
b.d.l.	b.d.l.	b.d.l.	b.d.l.	0.0	0.0	26.4	b.d.l.	b.d.l.
b.d.l.	b.d.l.	b.d.l.	b.d.l.	0.0	0.0	37.9	b.d.l.	b.d.l.
b.d.l.	b.d.l.	b.d.l.	b.d.l.	0.0	0.0	33.7	b.d.l.	b.d.l.
b.d.l.	b.d.l.	b.d.l.	b.d.l.	0.0	0.0	32.9	b.d.l.	b.d.l.
b.d.l.	b.d.l.	b.d.l.	b.d.l.	0.0	0.0	27.6	b.d.l.	b.d.l.
b.d.l.	b.d.l.	b.d.l.	b.d.l.	0.0	0.0	26.3	b.d.l.	b.d.l.
b.d.l.	b.d.l.	b.d.l.	b.d.l.	0.0	0.0	21.3	b.d.l.	b.d.l.
b.d.l.	b.d.l.	b.d.l.	b.d.l.	b.d.l.	0.0	23.6	b.d.l.	b.d.l.
b.d.l.	b.d.l.	b.d.l.	b.d.l.	b.d.l.	b.d.l.	31.7	b.d.l.	b.d.l.
b.d.l.	b.d.l.	b.d.l.	b.d.l.	b.d.l.	b.d.l.	33.9	b.d.l.	b.d.l.
b.d.l.	b.d.l.	b.d.l.	b.d.l.	b.d.l.	0.0	34.2	b.d.l.	b.d.l.
b.d.l.	b.d.l.	b.d.l.	b.d.l.	0.0	b.d.l.	34.3	b.d.l.	b.d.l.

Table A1.5: continued

Info	Position	Li ⁶	Li ⁷	Na	Mg	Al	Si	P	K	Ca	Sc	Ti	V	Mn	Fe	Rb	Sr	Y	Zr	Nb	Cs	Ba	La	Ce	Pr	Nd	Sm	Eu	Gd	Tb	Dy	Ho
mount2-14-5	Core	4.7	4.9	31044.9	3.2	101272	303853	20.8	93143	2934.8	0.4	83.6	b.d.l.	0.3	763.5	141.2	41.7	b.d.l.	0.0	0.1	778	6.7	4.6	0.2	0.4	b.d.l.	1.4	b.d.l.	b.d.l.	b.d.l.	b.d.l.	
mount2-14-6	Rim	5.4	4.5	30770.9	b.d.l.	101327	303853	22.5	92807	2846.1	0.4	79.0	b.d.l.	0.5	741.1	145.1	27.5	0.0	b.d.l.	0.1	261	6.7	4.7	0.2	0.4	b.d.l.	1.0	b.d.l.	b.d.l.	b.d.l.	b.d.l.	
mount1-15-1	Rim	5.6	5.4	30484.1	4.6	99650	303853	28.5	91627	2872.5	0.5	102.4	b.d.l.	0.6	859.8	120.8	78.9	b.d.l.	0.0	0.1	1389	7.5	5.3	0.3	0.5	b.d.l.	2.2	b.d.l.	b.d.l.	b.d.l.	b.d.l.	
mount1-16-1	Rim	4.1	5.5	30755.5	3.1	98941	303853	24.4	91174	2853.1	0.6	93.4	b.d.l.	0.7	828.0	120.6	44.0	b.d.l.	0.0	0.1	571	6.7	4.9	0.2	0.4	b.d.l.	1.2	b.d.l.	b.d.l.	b.d.l.	b.d.l.	
mount1-16-2	Core	6.0	4.2	30504.8	2.8	97036	303853	19.8	92249	2730.9	0.5	85.7	b.d.l.	0.5	808.6	120.9	67.8	0.0	b.d.l.	0.1	649	5.8	4.2	0.2	0.4	b.d.l.	1.8	b.d.l.	b.d.l.	b.d.l.	b.d.l.	
mount1-16-3	Rim	6.9	7.8	30679.1	4.1	97789	303853	21.3	91703	2803.3	0.6	78.7	b.d.l.	0.5	758.3	118.7	83.0	b.d.l.	0.0	0.1	683	5.9	3.9	0.2	0.3	0.0	2.1	b.d.l.	b.d.l.	b.d.l.	0.0	
mount1-17-2	Core	5.6	4.9	29461.9	b.d.l.	99718	303853	23.6	89032	3309.0	0.5	94.1	b.d.l.	0.5	845.0	95.0	250.4	0.0	b.d.l.	0.0	b.d.l.	8605	7.5	5.6	0.3	0.6	0.0	7.2	b.d.l.	b.d.l.	b.d.l.	0.0
mount1-18-2	Core	5.2	7.7	30853.7	b.d.l.	98501	303853	21.0	91276	3216.5	0.6	84.0	b.d.l.	0.6	737.3	114.7	138.9	0.0	b.d.l.	0.0	725	6.4	4.6	0.2	0.5	0.0	3.3	b.d.l.	b.d.l.	b.d.l.	b.d.l.	
mount1-19-2	Core	7.7	5.3	31155.0	b.d.l.	102766	303853	26.3	87706	4348.4	0.6	155.5	b.d.l.	0.7	839.5	108.0	210.7	0.0	b.d.l.	0.0	11077	8.0	6.9	0.4	0.8	0.0	6.3	b.d.l.	b.d.l.	b.d.l.	b.d.l.	
mount1-22-2	Core	5.4	5.5	30875.6	5.4	105960	303853	25.0	91688	3835.3	0.5	103.5	b.d.l.	0.7	901.3	110.5	225.7	0.0	b.d.l.	0.0	9243	9.1	6.5	0.3	0.8	b.d.l.	6.7	b.d.l.	b.d.l.	b.d.l.	b.d.l.	
mount1-27-2	Core	6.6	5.8	30177.4	4.0	99505	303853	26.5	92439	2710.2	0.5	71.4	b.d.l.	0.6	753.2	117.4	132.7	b.d.l.	0.0	0.1	2358	6.3	4.3	0.2	0.4	b.d.l.	3.8	b.d.l.	b.d.l.	b.d.l.	b.d.l.	
mount2-8-4	Rim	6.4	5.8	31222.5	3.7	98718	303853	21.7	91153	2785.3	0.4	90.8	b.d.l.	0.6	835.5	104.1	128.1	0.0	b.d.l.	0.0	494	6.0	4.3	0.2	0.3	0.0	3.0	0.0	0.1	b.d.l.	b.d.l.	b.d.l.
mount2-16-1	Rim	5.5	7.4	31136.8	b.d.l.	101276	303853	18.5	89687	3797.5	0.4	98.9	b.d.l.	0.7	859.4	108.3	230.3	0.0	b.d.l.	0.0	8448	8.4	6.2	0.3	0.7	b.d.l.	6.9	b.d.l.	b.d.l.	b.d.l.	b.d.l.	
mount2-16-2	Rim	6.3	7.3	30791.4	b.d.l.	100401	303853	24.1	92636	3170.2	0.3	83.7	b.d.l.	0.4	830.4	115.6	163.4	0.0	b.d.l.	0.0	4709	7.1	5.2	0.3	0.5	b.d.l.	4.8	b.d.l.	b.d.l.	0.0	b.d.l.	
mount2-16-4	Core	8.0	5.1	30886.7	b.d.l.	98624	303853	23.8	91876	3030.3	0.3	99.6	b.d.l.	0.5	874.1	108.7	181.2	b.d.l.	0.0	0.1	1965	6.9	4.8	0.2	0.4	b.d.l.	5.1	b.d.l.	b.d.l.	b.d.l.	b.d.l.	
mount2-16-5	Core	7.0	5.4	31044.6	b.d.l.	99977	303853	24.8	91792	2786.1	0.4	101.6	b.d.l.	0.6	886.6	110.3	180.0	0.0	b.d.l.	0.0	2036	7.1	5.1	0.3	0.5	b.d.l.	5.0	b.d.l.	b.d.l.	b.d.l.	b.d.l.	
mount2-16-6	Core	4.3	5.8	31124.1	2.8	101207	303853	22.5	90139	3660.2	0.4	94.3	b.d.l.	0.6	880.8	105.4	233.8	0.0	b.d.l.	0.0	8553	8.2	6.3	0.3	0.7	b.d.l.	7.0	b.d.l.	b.d.l.	0.0	b.d.l.	
mount2-20-1	Rim	4.0	3.7	30686.2	3.6	101789	303853	22.2	93680	2936.3	0.4	78.2	b.d.l.	0.6	757.0	121.8	120.5	0.0	b.d.l.	0.0	2677	6.1	4.4	0.2	0.4	0.0	3.4	b.d.l.	b.d.l.	b.d.l.	b.d.l.	
mount2-20-2	Core	5.3	5.7	30937.2	4.1	100967	303853	19.1	95856	2778.0	0.4	70.1	b.d.l.	0.6	747.6	124.6	59.5	b.d.l.	0.0	0.1	489	5.8	4.1	0.2	0.4	0.0	1.7	b.d.l.	b.d.l.	b.d.l.	b.d.l.	
mount2-20-3	Core	5.9	5.1	31563.0	4.5	99582	303853	22.0	93435	2794.2	0.4	76.3	b.d.l.	0.7	736.4	125.9	60.3	b.d.l.	0.0	0.1	561	6.1	4.7	0.2	0.3	0.0	1.7	b.d.l.	b.d.l.	b.d.l.	0.0	
mount2-20-4	Rim	8.2	6.3	30496.9	b.d.l.	99505	303853	20.3	93469	2749.5	0.4	71.4	b.d.l.	0.6	681.2	121.4	82.0	b.d.l.	0.0	0.1	1188	6.1	4.3	0.2	0.3	b.d.l.	2.3	b.d.l.	b.d.l.	b.d.l.	b.d.l.	
mount2-21-3	Core	4.9	5.2	29937.9	2.2	97660	303853	22.7	92977	2670.7	0.4	74.7	b.d.l.	0.3	689.4	124.1	62.6	b.d.l.	0.0	0.1	426	5.7	4.1	0.2	0.3	b.d.l.	1.7	b.d.l.	b.d.l.	b.d.l.	b.d.l.	
mount2-21-1	Rim	5.0	5.0	30500.4	5.7	100153	303853	22.7	93687	2556.8	0.5	68.1	b.d.l.	0.3	689.4	124.4	77.5	b.d.l.	0.0	0.1	819	5.4	3.9	0.2	0.3	b.d.l.	2.1	b.d.l.	b.d.l.	b.d.l.	b.d.l.	
mount2-21-2	Core	5.6	4.9	30440.6	6.4	99613	303853	17.8	94423	2685.0	0.3	71.9	b.d.l.	0.3	698.1	126.8	70.6	b.d.l.	0.0	0.1	887	5.8	4.2	0.2	0.4	0.0	2.0	b.d.l.	b.d.l.	b.d.l.	b.d.l.	
mount2-22-1	Rim	7.1	5.2	30465.5	4.3	101573	303853	18.5	96303	2558.9	0.4	83.9	b.d.l.	0.6	751.8	129.2	78.1	b.d.l.	0.0	0.1	852	5.9	4.0	0.2	0.3	0.0	1.9	b.d.l.	b.d.l.	b.d.l.	b.d.l.	
mount2-22-2	Core	5.4	4.8	30978.8	2.9	100495	303853	20.6	96066	2557.1	0.4	65.5	b.d.l.	0.6	702.3	121.5	106.0	b.d.l.	0.0	0.1	773	5.5	3.8	0.2	0.3	0.0	3.0	b.d.l.	b.d.l.	b.d.l.	b.d.l.	
mount2-22-3	Rim	7.1	5.2	30465.5	4.3	101573	303853	18.5	96303	2558.9	0.4	83.9	b.d.l.	0.6	751.8	129.2	78.1	b.d.l.	0.0	0.1	3213	6.0	4.2	0.2	0.4	0.0	2.2	0.1	b.d.l.	b.d.l.	b.d.l.	
mount2-28-1	Rim	6.6	6.7	31271.4	3.6	102874	303853	27.1	93072	3580.3	0.4	92.6	b.d.l.	0.4	808.1	113.6	185.9	0.0	b.d.l.	0.0	6101	8.3	5.8	0.3	0.5	b.d.l.	5.4	b.d.l.	b.d.l.	b.d.l.	b.d.l.	
mount2-28-2	Rim	4.7	7.0	30519.8	b.d.l.	100274	303853	21.3	93529	2644.4	0.3	68.0	b.d.l.	0.4	694.3	116.1	145.0	b.d.l.	0.0	0.1	1685	5.7	3.8	0.2	0.4	0.0	4.2	b.d.l.	b.d.l.	b.d.l.	b.d.l.	
mount2-28-3	Rim	5.0	2.8	31522.1	2.4	101681	303853	20.9	94344	2925.4	0.4	80.7	b.d.l.	0.4	740.5	114.5	156.4	b.d.l.	0.0	0.1	1324	6.8	4.7	0.2	0.4	b.d.l.	4.4	b.d.l.	b.d.l.	b.d.l.	b.d.l.	
mount2-28-6	Core	5.5	5.8	31044.2	4.4	101312	303853	23.8	94125	2810.0	0.5	75.3	b.d.l.	0.6	753.6	114.1	147.4	b.d.l.	0.0	0.1	1108	6.5	4.3	0.2	0.3	0.0	4.1	b.d.l.	b.d.l.	b.d.l.	b.d.l.	

Table A1.5: continued

Er	Tm	Yb	Lu	Hf	Ta	Pb	Th	U
b.d.l.	b.d.l.	b.d.l.	b.d.l.	b.d.l.	0.0	33.5	b.d.l.	b.d.l.
0.0	b.d.l.	b.d.l.	b.d.l.	b.d.l.	b.d.l.	35.4	b.d.l.	b.d.l.
b.d.l.	b.d.l.	b.d.l.	b.d.l.	0.0	b.d.l.	29.5	b.d.l.	b.d.l.
b.d.l.	b.d.l.	b.d.l.	b.d.l.	0.0	b.d.l.	33.1	b.d.l.	b.d.l.
0.0	b.d.l.	b.d.l.	b.d.l.	b.d.l.	b.d.l.	29.9	b.d.l.	b.d.l.
b.d.l.	b.d.l.	b.d.l.	b.d.l.	b.d.l.	b.d.l.	29.8	b.d.l.	b.d.l.
b.d.l.	b.d.l.	b.d.l.	b.d.l.	0.0	0.0	22.1	b.d.l.	b.d.l.
b.d.l.	b.d.l.	b.d.l.	0.0	b.d.l.	b.d.l.	27.5	0.0	b.d.l.
b.d.l.	b.d.l.	b.d.l.	b.d.l.	0.0	0.0	33.8	b.d.l.	b.d.l.
b.d.l.	b.d.l.	0.0	b.d.l.	b.d.l.	b.d.l.	28.5	b.d.l.	b.d.l.
b.d.l.	b.d.l.	b.d.l.	b.d.l.	b.d.l.	b.d.l.	25.2	b.d.l.	b.d.l.
b.d.l.	b.d.l.	b.d.l.	b.d.l.	b.d.l.	b.d.l.	27.2	b.d.l.	b.d.l.
b.d.l.	b.d.l.	b.d.l.	b.d.l.	b.d.l.	0.0	24.5	b.d.l.	b.d.l.
b.d.l.	b.d.l.	b.d.l.	b.d.l.	0.0	0.0	26.2	b.d.l.	b.d.l.
b.d.l.	b.d.l.	b.d.l.	b.d.l.	b.d.l.	0.0	21.1	b.d.l.	b.d.l.
b.d.l.	b.d.l.	b.d.l.	b.d.l.	b.d.l.	b.d.l.	22.4	b.d.l.	b.d.l.
b.d.l.	b.d.l.	b.d.l.	b.d.l.	b.d.l.	0.0	24.5	b.d.l.	b.d.l.
b.d.l.	b.d.l.	b.d.l.	b.d.l.	b.d.l.	0.0	28.7	b.d.l.	b.d.l.
b.d.l.	b.d.l.	b.d.l.	b.d.l.	b.d.l.	0.0	29.9	b.d.l.	b.d.l.
b.d.l.	b.d.l.	b.d.l.	b.d.l.	b.d.l.	b.d.l.	31.7	b.d.l.	b.d.l.
b.d.l.	b.d.l.	b.d.l.	b.d.l.	b.d.l.	0.0	29.7	b.d.l.	b.d.l.
b.d.l.	b.d.l.	b.d.l.	b.d.l.	b.d.l.	b.d.l.	31.1	b.d.l.	b.d.l.
b.d.l.	b.d.l.	0.0	b.d.l.	b.d.l.	b.d.l.	28.4	b.d.l.	b.d.l.
0.0	b.d.l.	b.d.l.	b.d.l.	b.d.l.	0.0	30.0	b.d.l.	b.d.l.
b.d.l.	b.d.l.	b.d.l.	b.d.l.	b.d.l.	b.d.l.	29.9	b.d.l.	b.d.l.
b.d.l.	b.d.l.	b.d.l.	b.d.l.	b.d.l.	b.d.l.	29.7	b.d.l.	b.d.l.
0.0	b.d.l.	0.0	b.d.l.	b.d.l.	b.d.l.	27.1	b.d.l.	b.d.l.
b.d.l.	b.d.l.	b.d.l.	b.d.l.	b.d.l.	b.d.l.	29.7	b.d.l.	b.d.l.
b.d.l.	b.d.l.	b.d.l.	b.d.l.	b.d.l.	b.d.l.	26.8	b.d.l.	b.d.l.
0.0	b.d.l.	b.d.l.	b.d.l.	0.0	b.d.l.	22.3	b.d.l.	b.d.l.
b.d.l.	b.d.l.	b.d.l.	b.d.l.	b.d.l.	b.d.l.	25.6	b.d.l.	b.d.l.
b.d.l.	b.d.l.	b.d.l.	b.d.l.	b.d.l.	b.d.l.	25.4	b.d.l.	b.d.l.

Table A1.6: Major elements - plagioclase

Info	Position	SiO ₂	TiO ₂	Al ₂ O ₃	FeO	MgO	CaO	Na ₂ O	K ₂ O	SrO	BaO	Total	An	Ab	Or
MFT-Mount1-plag2-1	Rim	63.6	0.1	22.4	0.2	0.0	4.0	8.1	1.7	0.0	0.0	100.0	19	71	10
MFT-Mount1-plag2-2	Rim	64.1	0.0	22.4	0.2	0.0	3.6	8.2	1.8	0.0	0.0	100.4	18	72	11
MFT-Mount1-plag2-3	Middle	64.1	0.1	22.4	0.2	0.0	3.6	8.1	1.8	0.0	0.0	100.2	18	72	11
MFT-Mount1-plag2-4	Middle	63.9	0.1	22.5	0.2	0.0	3.8	8.2	1.7	0.0	0.0	100.4	19	72	10
MFT-Mount1-plag2-5	Middle	64.0	0.0	22.6	0.2	0.0	3.8	8.1	1.7	0.0	0.0	100.4	18	72	10
MFT-Mount1-plag2-6	Middle	64.0	0.0	22.7	0.2	0.0	3.9	8.1	1.6	0.0	0.0	100.6	19	72	9
MFT-Mount1-plag2-7	Middle	64.0	0.0	22.8	0.2	0.0	3.7	8.2	1.7	0.0	0.0	100.6	18	72	10
MFT-Mount1-plag2-8	Middle	64.1	0.0	22.4	0.2	0.0	3.6	8.1	1.8	0.0	0.0	100.2	18	72	10
MFT-Mount1-plag2-9	Core	64.0	0.0	22.6	0.2	0.0	3.7	8.2	1.7	0.0	0.0	100.5	18	72	10
MFT-Mount1-plag2-10	Core	63.5	0.1	22.8	0.2	0.0	3.8	8.2	1.7	0.0	0.0	100.2	19	72	10
MFT-Mount1-plag2-11	Core	63.7	0.0	22.6	0.1	0.0	3.8	8.0	1.7	0.0	0.0	100.0	19	71	10
MFT-Mount1-plag2-12	Core - close to crack	63.5	0.0	22.9	0.1	0.0	3.8	7.9	1.7	0.0	0.0	100.1	19	71	10
MFT-Mount1-plag2-13	Core - close to crack	63.6	0.0	22.8	0.2	0.0	3.8	8.1	1.7	0.0	0.0	100.3	19	72	10
MFT-Mount1-plag2-14	Core - close to crack	63.5	0.0	23.1	0.2	0.0	4.1	8.2	1.5	0.0	0.0	100.7	20	71	9
MFT-Mount1-plag2-15	Core - close to crack	63.4	0.0	22.5	0.2	0.0	3.9	8.3	1.6	0.0	0.0	100.1	19	72	9
MFT-Mount1-plag2-16	Core - close to crack	63.6	0.0	23.0	0.2	0.0	4.0	8.1	1.6	0.0	0.0	100.5	20	71	9
MFT-Mount1-plag2-17	Core	63.5	0.0	23.0	0.2	0.0	4.2	8.1	1.5	0.0	0.0	100.6	20	71	9
MFT-Mount1-plag2-18	Core	63.3	0.0	23.0	0.2	0.0	4.2	8.1	1.5	0.0	0.0	100.2	20	71	9
MFT-Mount1-plag2-19	Core	63.1	0.0	23.2	0.2	0.0	4.3	8.1	1.5	0.0	0.0	100.4	21	71	9
MFT-Mount1-plag2-20	Core	62.9	0.0	23.1	0.2	0.0	4.3	8.0	1.5	0.0	0.0	100.0	21	71	8
MFT-Mount1-plag2-21	Core	62.7	0.0	23.4	0.2	0.0	4.6	8.0	1.4	0.0	0.0	100.2	22	70	8
MFT-Mount1-plag2-22	Core	62.8	0.0	23.4	0.2	0.0	4.6	8.0	1.3	0.0	0.0	100.2	22	70	8
MFT-Mount1-plag2-23	Core	62.9	0.0	23.4	0.2	0.0	4.5	8.1	1.4	0.0	0.0	100.4	22	70	8
MFT-Mount1-plag2-24	Core	62.6	0.0	23.4	0.2	0.0	4.5	7.9	1.4	0.0	0.0	99.9	22	70	8
MFT-Mount1-plag2-25	Core	63.1	0.0	23.3	0.2	0.0	4.4	8.0	1.4	0.0	0.0	100.3	21	71	8
MFT-Mount1-plag2-26	Core	62.8	0.0	23.2	0.2	0.0	4.4	8.1	1.4	0.0	0.0	100.2	21	71	8
MFT-Mount1-plag2-27	Middle	62.9	0.0	23.0	0.2	0.0	4.3	8.1	1.5	0.0	0.0	100.0	21	71	8
MFT-Mount1-plag2-28	Middle	63.8	0.0	22.7	0.2	0.0	4.0	8.1	1.6	0.0	0.0	100.4	19	71	9
MFT-Mount1-plag2-29	Middle	63.5	0.0	23.0	0.2	0.0	4.2	8.0	1.5	0.0	0.0	100.4	20	71	9
MFT-Mount1-plag2-30	Middle	63.4	0.1	23.2	0.2	0.0	4.3	8.1	1.5	0.0	0.0	100.8	21	71	9
MFT-Mount1-plag2-31	Middle - close to crack	63.6	0.1	23.1	0.2	0.0	4.2	8.1	1.5	0.1	0.0	100.9	20	71	9
MFT-Mount1-plag2-32	Middle - close to crack	63.3	0.1	22.8	0.2	0.0	4.0	8.1	1.6	0.0	0.0	100.1	19	71	9
MFT-Mount1-plag2-33	Middle - close to crack	63.6	0.0	22.8	0.2	0.0	4.0	8.2	1.6	0.0	0.0	100.4	19	71	9
MFT-Mount1-plag2-34	Rim - close to crack	63.7	0.0	22.7	0.2	0.0	3.8	8.4	1.7	0.0	0.0	100.5	18	72	10
MFT-Mount1-plag2-35	Rim - close to crack	63.5	0.0	22.9	0.2	0.0	4.0	8.2	1.7	0.0	0.0	100.5	19	71	9
MFT-Mount1-plag2-36	Rim - close to crack	63.7	0.1	22.8	0.2	0.0	3.7	8.2	1.6	0.1	0.0	100.5	18	72	9
grain3-1	Rim	62.4	0.0	23.9	0.2	0.0	4.9	7.9	1.2	0.0	0.0	100.4	24	69	7
grain3-2	Rim	62.5	0.1	23.7	0.2	0.0	4.9	7.9	1.2	0.0	0.0	100.5	24	69	7
grain3-3	Rim	62.4	0.1	23.6	0.2	0.0	5.0	8.0	1.2	0.0	0.0	100.4	24	69	7
grain3-4	Middle	62.3	0.0	23.9	0.2	0.0	5.0	8.0	1.1	0.0	0.0	100.6	24	69	7
grain3-5	Middle	62.4	0.1	23.7	0.2	0.0	4.8	8.0	1.2	0.0	0.0	100.3	23	70	7
grain3-6	Middle	62.2	0.1	23.7	0.2	0.0	5.0	8.0	1.1	0.0	0.0	100.4	24	70	6
grain3-7	Middle	62.3	0.0	23.9	0.2	0.0	5.1	7.9	1.1	0.0	0.0	100.7	24	69	7
grain3-8	Middle	62.2	0.1	23.8	0.2	0.0	5.1	8.0	1.1	0.0	0.0	100.5	24	69	6
grain3-9	Middle	62.9	0.0	23.5	0.2	0.0	4.8	8.1	1.2	0.0	0.0	100.8	23	70	7
grain3-10	Middle	62.6	0.0	23.7	0.2	0.0	4.8	8.1	1.2	0.0	0.0	100.6	23	70	7
grain3-11	Middle	62.5	0.0	23.7	0.2	0.0	5.0	8.0	1.2	0.1	0.0	100.6	24	69	7
grain3-12	Middle	62.3	0.1	23.7	0.2	0.0	4.9	7.9	1.2	0.0	0.1	100.4	24	69	7
grain3-13	Core	62.2	0.0	23.7	0.2	0.0	4.9	8.0	1.2	0.0	0.0	100.2	24	70	7
grain3-14	Core	62.2	0.1	23.8	0.2	0.0	5.1	7.9	1.1	0.0	0.0	100.4	24	69	7
grain3-15	Core	62.5	0.1	23.7	0.2	0.0	4.8	7.9	1.1	0.0	0.0	100.3	23	70	7
grain3-16	Core	62.5	0.0	23.7	0.2	0.0	4.9	8.0	1.2	0.0	0.0	100.5	24	70	7
grain3-17	Core	62.4	0.0	23.7	0.2	0.0	4.8	8.1	1.2	0.0	0.0	100.4	23	70	7
grain3-18	Core	62.2	0.1	23.8	0.2	0.0	5.0	8.0	1.2	0.0	0.0	100.4	24	69	7
grain3-19	Core	62.4	0.1	23.7	0.2	0.0	4.9	8.0	1.2	0.0	0.0	100.6	24	70	7
grain3-20	Core	62.3	0.1	23.8	0.2	0.0	4.9	8.1	1.2	0.0	0.0	100.6	23	70	7
grain3-21	Core	63.0	0.0	23.3	0.2	0.0	4.5	8.0	1.3	0.0	0.0	100.3	22	71	7
grain3-22	Core	62.8	0.1	23.6	0.2	0.0	4.8	8.1	1.2	0.0	0.0	101.0	23	70	7
grain3-23	Core	62.9	0.0	23.3	0.2	0.0	4.4	8.3	1.4	0.0	0.0	100.4	21	71	8
grain3-24	Core	62.6	0.0	23.7	0.2	0.0	4.7	8.2	1.2	0.0	0.0	100.5	22	71	7
grain3-25	Core	62.8	0.0	23.4	0.2	0.0	4.7	8.1	1.3	0.0	0.0	100.5	22	70	7
grain3-26	Core	62.8	0.1	23.5	0.2	0.0	4.7	8.3	1.2	0.0	0.0	100.6	22	71	7
grain3-27	Core	62.8	0.0	23.5	0.2	0.0	4.5	8.2	1.3	0.0	0.0	100.6	22	71	7
grain3-28	Core	62.9	0.1	23.0	0.2	0.0	4.5	8.0	1.3	0.0	0.0	100.0	22	71	8
grain3-29	Core	62.8	0.0	23.2	0.2	0.0	4.4	8.2	1.3	0.1	0.0	100.1	21	71	8
grain3-30	Core	62.8	0.1	23.3	0.2	0.0	4.4	8.2	1.3	0.0	0.0	100.3	21	71	8
grain3-31	Core	62.9	0.0	23.5	0.2	0.0	4.6	8.0	1.3	0.0	0.0	100.6	22	70	7
grain3-32	Core	63.1	0.0	23.3	0.2	0.0	4.5	8.1	1.3	0.1	0.0	100.6	22	71	8
grain3-33	Core	63.3	0.0	23.1	0.2	0.0	4.3	8.2	1.4	0.0	0.0	100.4	21	72	8
grain3-34	Core	63.1	0.0	23.1	0.2	0.0	4.2	8.2	1.4	0.0	0.0	100.3	20	72	8
grain3-35	Core	63.3	0.0	23.0	0.2	0.0	4.2	8.4	1.4	0.0	0.0	100.5	20	72	8
grain3-36	Core	63.4	0.0	22.9	0.2	0.0	4.0	8.3	1.5	0.0	0.0	100.1	19	72	8
grain3-37	Core	63.8	0.0	22.4	0.2	0.0	3.6	8.4	1.6	0.0	0.0	100.0	17	73	9
grain3-38	Core	63.3	0.0	23.1	0.2	0.0	4.1	8.3	1.5	0.0	0.0	100.5	20	72	8
grain3-39	Core	63.6	0.0	22.8	0.2	0.0	3.9	8.3	1.5	0.0	0.0	100.3	19	72	9
grain3-40	Core	63.3	0.0	23.0	0.2	0.0	4.1	8.3	1.5	0.0	0.0	100.4	20	72	9
grain3-41	Core - close to crack	63.3	0.0	23.0	0.2	0.0	4.0	8.2	1.5	0.0	0.0	100.3	19	72	9
grain3-42	Core - close to crack	62.9	0.1	23.1	0.2	0.0	4.3	8.0	1.5	0.0	0.0	100.1	21	70	9
grain3-43	Core - close to crack	63.4	0.1	22.6	0.2	0.0	4.0	8.1	1.6	0.0	0.0	100.0	19	71	9
grain3-44	Core	63.0	0.0	23.2	0.2	0.0	4.2	8.1	1.5	0.0	0.0	100.2	20	71	8
grain3-45	Core	63.3	0.1	22.8	0.2	0.0	4.0	8.2	1.5	0.0	0.0	100.0	19	72	9
grain3-46	Middle	63.2	0.0	23.1	0.2	0.0	4.1	8.1	1.5	0.1	0.0	100.4	20	71	9
grain3-47	Middle	62.8	0.0	23.2	0.2	0.0	4.2	8.3	1.5	0.0	0.0	100.3	20	72	9
grain3-48	Middle	63.7	0.1	22.9	0.2	0.0	3.9	8.1	1.6	0.0	0.0	100.4	19	72	9
grain3-49	Middle	64.5	0.0	22.4	0.2	0.0	3.3	8.4	1.9	0.0	0.0	100.6	16	73	11
grain3-50	Middle	63.9	0.0	22.8	0.2	0.0	3.8	8.2	1.7	0.0	0.0	100.6	18	72	10

Table A1.6: continued

Info	Position	SiO ₂	TiO ₂	Al ₂ O ₃	FeO	MgO	CaO	Na ₂ O	K ₂ O	SrO	BaO	Total	An	Ab	Or
grain3-51	Middle	63.8	0.0	22.8	0.2	0.0	3.9	8.1	1.6	0.0	0.0	100.5	19	72	9
grain3-52	Middle	63.7	0.0	22.9	0.2	0.0	4.0	8.2	1.6	0.0	0.0	100.5	19	72	9
grain3-53	Rim	63.8	0.0	22.9	0.2	0.0	4.0	8.1	1.6	0.0	0.0	100.7	19	71	9
Mount1-plag4-1	Rim	62.0	0.1	23.8	0.2	0.0	5.1	7.9	1.1	0.0	0.0	100.3	25	69	7
Mount1-plag4-2	Middle	61.9	0.1	23.6	0.2	0.0	4.8	7.9	1.2	0.1	0.0	99.8	23	70	7
Mount1-plag4-3	Middle	61.8	0.1	23.7	0.2	0.0	5.0	8.0	1.2	0.0	0.0	100.0	24	70	7
Mount1-plag4-4	Core	62.0	0.0	23.8	0.2	0.0	4.9	7.9	1.2	0.0	0.0	100.0	24	69	7
Mount1-plag4-5	Core	61.9	0.0	23.6	0.2	0.0	4.9	8.0	1.2	0.0	0.0	99.9	24	70	7
Mount1-plag4-6	Core	62.2	0.0	23.6	0.2	0.0	4.9	8.0	1.2	0.0	0.0	100.1	24	69	7
Mount1-plag4-7	Core	62.0	0.0	23.6	0.2	0.0	4.9	8.0	1.2	0.0	0.0	100.0	23	70	7
Mount1-plag4-8	Core	61.9	0.0	23.6	0.2	0.0	4.8	8.1	1.2	0.1	0.0	100.0	23	70	7
Mount1-plag4-9	Core	62.1	0.1	23.6	0.2	0.0	4.8	8.1	1.2	0.0	0.0	100.1	23	70	7
Mount1-plag4-10	Core	62.3	0.0	23.6	0.2	0.0	4.8	8.0	1.3	0.0	0.0	100.2	23	70	7
Mount1-plag4-11	Core	62.3	0.0	23.5	0.2	0.0	4.8	8.0	1.3	0.0	0.0	100.1	23	70	7
Mount1-plag4-12	Core	62.0	0.0	23.4	0.2	0.0	4.6	8.0	1.3	0.0	0.0	99.7	22	70	8
Mount1-plag4-13	Core	62.6	0.1	23.3	0.3	0.0	4.6	8.0	1.3	0.0	0.0	100.1	22	70	8
Mount1-plag4-14	Core	62.5	0.0	23.4	0.2	0.0	4.6	8.0	1.3	0.0	0.0	100.1	22	70	8
Mount1-plag4-15	Core	62.3	0.1	23.1	0.2	0.0	4.7	8.1	1.3	0.0	0.0	99.7	22	70	7
Mount1-plag4-16	Core	62.6	0.1	23.5	0.2	0.0	4.8	8.0	1.3	0.0	0.0	100.5	23	70	7
Mount1-plag4-17	Core	62.5	0.0	23.5	0.2	0.0	4.6	8.0	1.3	0.0	0.0	100.3	22	70	8
Mount1-plag4-18	Core	62.6	0.0	23.2	0.2	0.0	4.7	8.0	1.3	0.0	0.0	100.0	23	70	7
Mount1-plag4-19	Core	62.3	0.0	23.5	0.2	0.0	4.7	8.0	1.3	0.0	0.0	100.1	23	70	7
Mount1-plag4-20	Core	62.4	0.0	23.2	0.2	0.0	4.7	8.1	1.3	0.1	0.0	100.0	23	70	7
Mount1-plag4-21	Core	62.5	0.0	23.5	0.2	0.0	4.7	8.0	1.3	0.0	0.0	100.2	23	70	7
Mount1-plag4-22	Core	62.7	0.0	23.4	0.2	0.0	4.6	8.0	1.3	0.0	0.0	100.1	22	70	8
Mount1-plag4-23	Core	62.7	0.0	23.3	0.2	0.0	4.6	8.1	1.3	0.0	0.0	100.2	22	70	8
Mount1-plag4-24	Core	62.7	0.0	23.5	0.2	0.0	4.6	8.1	1.3	0.0	0.0	100.5	22	70	8
Mount1-plag4-25	Core	62.7	0.0	23.4	0.2	0.0	4.6	8.0	1.3	0.1	0.0	100.3	22	70	8
Mount1-plag4-26	Core	62.8	0.1	23.5	0.2	0.0	4.6	8.1	1.3	0.1	0.0	100.5	22	70	8
Mount1-plag4-27	Core	62.7	0.0	23.2	0.2	0.0	4.7	7.9	1.3	0.0	0.0	100.0	23	70	8
Mount1-plag4-28	Core	62.4	0.0	23.4	0.2	0.0	4.6	8.0	1.3	0.0	0.0	99.9	22	70	7
Mount1-plag4-29	Core	62.7	0.1	23.4	0.2	0.0	4.4	8.1	1.4	0.0	0.0	100.2	21	71	8
Mount1-plag4-30	Core	62.6	0.0	23.1	0.2	0.0	4.5	8.0	1.4	0.0	0.0	99.7	22	70	8
Mount1-plag4-31	Core	62.6	0.0	23.1	0.2	0.0	4.4	8.0	1.4	0.0	0.0	99.7	22	70	8
Mount1-plag4-32	Core	62.9	0.0	23.4	0.2	0.0	4.5	8.0	1.4	0.0	0.0	100.3	22	70	8
Mount1-plag4-33	Core	62.8	0.1	23.1	0.2	0.0	4.3	8.0	1.4	0.0	0.0	99.9	21	71	8
Mount1-plag4-34	Core	63.1	0.0	23.3	0.2	0.0	4.5	8.0	1.4	0.0	0.0	100.5	22	71	8
Mount1-plag4-35	Core	62.8	0.0	23.1	0.2	0.0	4.4	8.2	1.4	0.0	0.0	100.0	21	71	8
Mount1-plag4-36	Core	62.9	0.0	23.3	0.2	0.0	4.5	8.2	1.3	0.0	0.0	100.4	21	71	8
Mount1-plag4-37	Core	62.9	0.0	23.2	0.2	0.0	4.5	8.0	1.3	0.0	0.0	100.1	22	71	8
Mount1-plag4-38	Core	62.8	0.1	23.4	0.2	0.0	4.4	8.0	1.4	0.0	0.0	100.3	21	70	8
Mount1-plag4-39	Core	62.4	0.0	23.4	0.2	0.0	4.4	8.2	1.4	0.0	0.0	99.9	21	71	8
Mount1-plag4-40	Core	62.6	0.0	23.4	0.2	0.0	4.6	8.0	1.3	0.0	0.0	100.2	22	70	8
Mount1-plag4-41	Core	62.8	0.0	23.4	0.2	0.0	4.6	8.0	1.3	0.0	0.0	100.4	22	70	8
Mount1-plag4-42	Core	62.9	0.0	23.1	0.2	0.0	4.4	8.1	1.4	0.0	0.0	100.2	21	71	8
Mount1-plag4-43	Core	62.9	0.0	23.2	0.2	0.0	4.2	8.0	1.4	0.0	0.0	100.1	21	71	8
Mount1-plag4-44	Core	62.7	0.1	23.0	0.2	0.0	4.3	8.1	1.5	0.0	0.0	99.8	21	71	8
Mount1-plag4-45	Core	62.8	0.0	23.1	0.2	0.0	4.3	8.1	1.4	0.0	0.0	99.9	21	71	8
Mount1-plag4-46	Core	62.7	0.0	23.1	0.2	0.0	4.3	8.1	1.4	0.0	0.0	99.9	21	71	8
Mount1-plag4-47	Core	62.8	0.1	23.2	0.2	0.0	4.4	8.2	1.4	0.0	0.0	100.3	21	71	8
Mount1-plag4-48	Core	62.5	0.0	23.2	0.2	0.0	4.4	8.1	1.4	0.0	0.0	99.8	21	71	8
Mount1-plag4-49	Core	62.7	0.0	23.3	0.2	0.0	4.5	8.1	1.4	0.0	0.0	100.2	22	70	8
Mount1-plag4-50	Core	62.5	0.0	23.4	0.3	0.0	4.4	8.1	1.4	0.0	0.0	100.1	21	71	8
Mount1-plag4-51	Core	62.9	0.0	23.1	0.2	0.0	4.3	8.1	1.4	0.0	0.0	100.0	21	71	8
Mount1-plag4-52	Core	63.0	0.0	23.2	0.2	0.0	4.3	8.2	1.4	0.0	0.0	100.3	21	71	8
Mount1-plag4-53	Core	63.0	0.0	23.1	0.2	0.0	4.3	8.1	1.4	0.0	0.0	100.1	21	71	8
Mount1-plag4-54	Core	63.1	0.1	23.2	0.2	0.0	4.3	8.1	1.5	0.0	0.0	100.4	21	71	8
Mount1-plag4-55	Core	63.0	0.0	23.4	0.2	0.0	4.3	8.3	1.4	0.0	0.0	100.7	21	71	8
Mount1-plag4-56	Core	62.8	0.0	23.4	0.2	0.0	4.3	8.2	1.4	0.0	0.0	100.4	21	71	8
Mount1-plag4-57	Core	63.0	0.1	23.0	0.2	0.0	4.3	8.2	1.5	0.0	0.0	100.3	20	71	9
Mount1-plag4-58	Middle	62.9	0.0	23.1	0.2	0.0	4.4	8.0	1.5	0.0	0.0	100.1	21	71	8
Mount1-plag4-59	Middle	63.3	0.0	23.3	0.2	0.0	4.2	8.1	1.5	0.0	0.0	100.5	20	71	8
Mount1-plag4-60	Middle	63.1	0.1	23.1	0.2	0.0	4.3	8.2	1.4	0.0	0.0	100.3	21	71	8
Mount1-plag4-61	Middle	63.3	0.1	23.2	0.2	0.0	4.3	8.2	1.5	0.0	0.0	100.7	21	71	9
Mount1-plag4-62	Middle	63.3	0.0	23.2	0.2	0.0	4.3	8.1	1.5	0.0	0.0	100.6	21	71	8
grain8-1	Rim	62.9	0.1	23.2	0.2	0.0	4.4	8.4	1.3	0.0	0.0	100.5	21	72	8
grain8-2	Rim	62.7	0.0	23.0	0.2	0.0	4.1	8.3	1.4	0.0	0.0	99.9	20	72	8
grain8-3	Middle	62.5	0.1	23.2	0.2	0.0	4.6	8.1	1.3	0.0	0.0	100.0	22	71	8
grain8-4	Middle	62.5	0.0	23.4	0.2	0.0	4.6	8.2	1.3	0.0	0.0	100.2	22	71	7
grain8-5	Middle	62.4	0.1	23.4	0.2	0.0	4.6	8.2	1.3	0.0	0.0	100.2	22	71	7
grain8-6	Middle	62.3	0.0	23.2	0.2	0.0	4.6	8.2	1.3	0.0	0.0	99.9	22	71	7
grain8-7	Core	62.1	0.0	23.5	0.2	0.0	4.7	8.1	1.2	0.0	0.0	99.8	23	71	7
grain8-8	Core	62.2	0.0	23.3	0.2	0.0	4.7	8.1	1.2	0.0	0.0	99.8	23	71	7
grain8-9	Core	61.8	0.0	23.5	0.2	0.0	4.8	8.0	1.1	0.0	0.0	99.5	23	70	7
grain8-10	Core	61.7	0.1	23.6	0.2	0.0	4.9	8.0	1.1	0.0	0.0	99.6	24	70	6
grain8-11	Core	61.7	0.1	23.8	0.2	0.0	5.0	8.1	1.1	0.0	0.0	100.0	24	70	6
grain8-12	Core	62.0	0.1	23.8	0.2	0.0	5.1	8.0	1.1	0.1	0.0	100.3	25	69	6
grain8-13	Core	61.7	0.1	23.7	0.2	0.0	5.1	7.9	1.1	0.0	0.0	99.8	25	69	6
grain8-14	Core	61.6	0.0	23.8	0.2	0.0	5.1	7.9	1.0	0.0	0.0	99.8	25	69	6
grain8-15	Core	61.8	0.0	23.7	0.2	0.0	5.2	8.0	1.1	0.1	0.0	100.1	25	69	6
grain8-16	Core	61.9	0.0	23.7	0.2	0.0	5.0	7.9	1.1	0.0	0.0	99.9	24	69	6
grain8-17	Core	62.0	0.0	23.5	0.2	0.0	5.1	7.9	1.0	0.0	0.0	99.8	25	69	6
grain8-18	Core	61.9	0.1	23.6	0.2	0.0	5.0	8.0	1.1	0.0	0.0	99.9	24	70	6
grain8-19	Core	62.1	0.0	23.6	0.2	0.0	5.1	8.1	1.0	0.0	0.0	100.2	24	70	6
grain8-20	Core	62.0	0.0	23.8	0.2	0.0	5.1	7.9	1.0	0.0	0.0	100.2	25	69	6

Table A1.6: continued

Info	Position	SiO ₂	TiO ₂	Al ₂ O ₃	FeO	MgO	CaO	Na ₂ O	K ₂ O	SrO	BaO	Total	An	Ab	Or
grain8-21	Core	62.2	0.1	23.7	0.2	0.0	5.2	7.9	1.0	0.0	0.0	100.2	25	69	6
grain8-22	Core	61.9	0.0	23.9	0.2	0.0	5.2	7.9	1.0	0.0	0.0	100.3	25	69	6
grain8-23	Core	62.2	0.1	23.9	0.2	0.0	5.2	7.9	1.0	0.1	0.0	100.6	25	69	6
grain8-24	Core	62.3	0.0	23.9	0.2	0.0	5.2	8.0	1.0	0.0	0.0	100.6	25	69	6
grain8-25	Core	61.9	0.1	23.8	0.2	0.0	5.1	8.0	1.0	0.0	0.1	100.0	24	70	6
grain8-26	Core	62.2	0.0	23.8	0.2	0.0	5.1	7.9	1.0	0.0	0.0	100.3	25	70	6
grain8-27	Core	61.8	0.1	23.7	0.2	0.0	5.1	8.0	1.0	0.1	0.0	100.0	24	70	6
grain8-28	Core	61.9	0.1	23.6	0.2	0.0	5.0	8.0	1.1	0.0	0.0	99.8	24	70	6
grain8-29	Core	62.3	0.0	23.7	0.2	0.0	4.9	8.1	1.1	0.0	0.0	100.4	24	70	6
grain8-30	Core	61.9	0.0	23.6	0.2	0.0	5.0	8.0	1.0	0.1	0.0	99.7	24	70	6
grain8-31	Core	62.0	0.1	23.6	0.2	0.0	5.1	8.0	1.0	0.0	0.0	100.0	24	70	6
grain8-32	Core	62.3	0.0	23.6	0.2	0.0	4.8	7.9	1.1	0.0	0.0	100.0	24	70	6
grain8-33	Core	62.6	0.0	23.3	0.2	0.0	4.5	8.3	1.2	0.0	0.0	100.1	21	72	7
grain8-34	Core	62.2	0.0	23.9	0.2	0.0	5.0	8.0	1.1	0.0	0.0	100.5	24	69	6
grain8-35	Core	62.1	0.1	23.8	0.2	0.0	5.0	8.0	1.1	0.1	0.0	100.4	24	69	6
grain8-36	Core	62.0	0.1	23.6	0.2	0.0	5.0	8.0	1.1	0.0	0.1	100.0	24	70	6
grain8-37	Core	61.9	0.0	23.6	0.2	0.0	5.0	8.0	1.1	0.0	0.0	99.9	24	69	6
grain8-38	Core	61.7	0.1	23.9	0.2	0.0	5.0	8.0	1.1	0.0	0.0	100.0	24	70	6
grain8-39	Core	61.7	0.1	23.9	0.2	0.0	5.1	8.0	1.0	0.0	0.0	100.0	24	70	6
grain8-40	Core	61.8	0.0	23.9	0.2	0.0	5.2	8.0	1.1	0.0	0.0	100.2	25	69	6
grain8-41	Core	61.8	0.1	23.8	0.2	0.0	5.1	7.9	1.1	0.0	0.0	100.1	25	69	6
grain8-42	Core	61.7	0.0	23.9	0.3	0.0	5.2	8.0	1.0	0.0	0.0	100.1	25	69	6
grain8-43	Middle	61.5	0.1	23.8	0.2	0.0	5.3	7.8	1.0	0.1	0.0	99.8	26	68	6
grain8-44	Middle	61.5	0.0	24.0	0.2	0.0	5.2	8.0	1.1	0.0	0.0	100.0	25	69	6
grain8-45	Middle	61.6	0.0	23.6	0.2	0.0	5.2	7.8	1.0	0.0	0.0	99.5	25	69	6
grain8-46	Middle	62.0	0.1	23.7	0.2	0.0	5.2	7.8	1.1	0.0	0.0	100.1	25	68	6
grain8-47	Rim	61.9	0.0	23.8	0.2	0.0	5.3	7.9	1.1	0.1	0.0	100.3	25	69	6
grain8-48	Rim	61.9	0.1	23.8	0.2	0.0	5.1	7.9	1.1	0.0	0.0	100.1	25	69	6
grain8-49	Rim	61.3	0.1	24.1	0.3	0.0	5.2	7.9	1.0	0.0	0.0	99.9	25	69	6
grain8-50	Rim	61.4	0.1	24.1	0.5	0.0	5.3	8.0	1.1	0.0	0.0	100.5	25	69	6
MFT-plag8 - 1	Rim	63.2	0.0	22.5	0.2	0.0	3.7	8.2	1.7	0.0	0.0	99.6	18	72	10
MFT-plag8 - 2	Rim	62.8	0.1	22.9	0.2	0.0	4.0	8.1	1.7	0.0	0.0	99.7	19	71	10
MFT-plag8 - 3	Middle	63.0	0.0	22.6	0.1	0.0	3.7	8.1	1.7	0.0	0.0	99.3	18	72	10
MFT-plag8 - 4	Middle	62.9	0.0	23.1	0.2	0.0	4.0	8.0	1.6	0.0	0.0	99.8	20	71	9
MFT-plag8 - 5	Core	62.4	0.0	22.9	0.2	0.0	4.1	8.0	1.6	0.0	0.0	99.2	20	71	9
MFT-plag8 - 6	Core	62.8	0.0	22.9	0.1	0.0	3.9	8.0	1.6	0.1	0.0	99.5	19	71	10
MFT-plag8 - 7	Core	62.6	0.0	23.1	0.2	0.0	4.1	7.9	1.6	0.0	0.0	99.4	20	71	9
MFT-plag8 - 8	Core	62.4	0.0	23.3	0.2	0.0	4.2	8.0	1.5	0.0	0.0	99.6	20	71	9
MFT-plag8 - 9	Core	62.6	0.0	22.9	0.2	0.0	4.1	7.8	1.5	0.0	0.0	99.2	21	70	9
MFT-plag8 - 10	Core	62.3	0.0	23.1	0.2	0.0	4.2	7.8	1.5	0.1	0.0	99.2	21	70	9
MFT-plag8 - 11	Core	62.5	0.0	22.9	0.2	0.0	4.3	7.9	1.5	0.0	0.0	99.3	21	70	9
MFT-plag8 - 12	Core	62.2	0.0	22.9	0.2	0.0	4.3	7.8	1.5	0.0	0.0	98.9	21	70	9
MFT-plag8 - 13	Core	62.3	0.0	23.3	0.2	0.0	4.3	7.8	1.4	0.1	0.0	99.4	22	70	8
MFT-plag8 - 14	Core	62.0	0.1	23.3	0.2	0.0	4.4	7.7	1.4	0.0	0.0	99.0	22	70	8
MFT-plag8 - 15	Core	62.0	0.1	23.1	0.2	0.0	4.4	7.8	1.4	0.0	0.0	99.0	22	70	8
MFT-plag8 - 16	Core	62.3	0.0	23.2	0.2	0.0	4.3	7.9	1.4	0.0	0.0	99.3	21	71	8
MFT-plag8 - 17	Core	62.0	0.1	23.2	0.2	0.0	4.4	7.8	1.3	0.0	0.0	99.1	22	70	8
MFT-plag8 - 18	Core	62.0	0.1	23.4	0.2	0.0	4.4	7.9	1.3	0.0	0.0	99.2	22	70	8
MFT-plag8 - 19	Core	61.8	0.1	23.5	0.2	0.0	4.6	7.9	1.3	0.0	0.0	99.3	23	70	8
MFT-plag8 - 20	Core	61.6	0.1	23.4	0.2	0.0	4.7	7.8	1.3	0.0	0.0	99.0	23	70	7
MFT-plag8 - 21	Core	61.4	0.0	23.2	0.2	0.0	4.7	7.8	1.2	0.0	0.1	98.7	23	70	7
MFT-plag8 - 22	Core	61.4	0.0	23.5	0.2	0.0	4.7	7.8	1.2	0.0	0.0	99.0	23	70	7
MFT-plag8 - 23	Core	61.4	0.0	23.6	0.2	0.0	4.7	7.7	1.2	0.0	0.0	98.8	23	69	7
MFT-plag8 - 24	Core	61.3	0.0	23.5	0.2	0.0	4.9	7.9	1.2	0.0	0.0	99.0	24	70	7
MFT-plag8 - 25	Core	61.6	0.0	23.7	0.2	0.0	5.1	7.8	1.1	0.0	0.0	99.6	25	69	7
MFT-plag8 - 26	Core	61.5	0.0	23.9	0.2	0.0	4.9	7.7	1.1	0.1	0.0	99.6	24	69	7
MFT-plag8 - 27	Core	61.5	0.1	23.8	0.2	0.0	5.0	7.7	1.1	0.0	0.0	99.4	25	69	6
MFT-plag8 - 28	Core	61.4	0.0	23.8	0.2	0.0	4.9	7.8	1.1	0.0	0.0	99.3	24	69	6
MFT-plag8 - 29	Core	61.5	0.0	23.8	0.2	0.0	5.0	7.6	1.1	0.0	0.0	99.4	25	69	6
MFT-plag8 - 30	Core	61.0	0.0	23.9	0.2	0.0	5.3	7.7	1.0	0.1	0.0	99.2	26	68	6
MFT-plag8 - 31	Core	61.7	0.1	23.6	0.2	0.0	4.9	7.8	1.2	0.0	0.0	99.4	24	69	7
MFT-plag8 - 32	Core	61.5	0.1	23.3	0.2	0.0	4.8	7.8	1.1	0.1	0.0	98.8	24	70	7
MFT-plag8 - 33	Core	61.4	0.1	23.9	0.2	0.0	4.8	7.7	1.2	0.0	0.0	99.3	24	69	7
MFT-plag8 - 34	Core	61.5	0.1	23.7	0.2	0.0	4.7	7.6	1.2	0.1	0.0	99.0	24	69	7
MFT-plag8 - 35	Core	61.4	0.0	23.4	0.2	0.0	4.9	7.6	1.1	0.0	0.0	98.6	25	69	7
MFT-plag8 - 36	Core	61.4	0.1	23.4	0.2	0.0	4.8	7.7	1.1	0.0	0.1	98.7	24	69	7
MFT-plag8 - 37	Core	61.5	0.0	23.4	0.2	0.0	4.9	7.5	1.1	0.0	0.0	98.7	24	69	7
MFT-plag8 - 38	Core	61.5	0.0	23.6	0.3	0.0	4.9	7.5	1.1	0.1	0.0	99.0	25	69	7
MFT-plag8 - 39	Core	61.2	0.1	23.4	0.2	0.0	4.8	7.5	1.1	0.1	0.1	98.5	24	69	7
MFT-plag8 - 40	Core	60.8	0.1	23.7	0.2	0.0	5.2	7.5	1.0	0.0	0.0	98.6	26	68	6
MFT-plag8 - 41	Core	60.9	0.1	23.6	0.2	0.0	5.1	7.4	1.1	0.1	0.0	98.5	26	68	6
MFT-plag8 - 42	Core	61.3	0.0	23.3	0.2	0.0	4.9	7.6	1.1	0.1	0.0	98.5	24	69	7
MFT-plag8 - 43	Core - close to crack	61.0	0.1	23.5	0.2	0.0	4.9	7.5	1.1	0.0	0.0	98.3	25	69	7
MFT-plag8 - 44	Core - close to crack	61.0	0.1	23.6	0.2	0.0	5.0	7.6	1.1	0.1	0.0	98.7	25	68	7
MFT-plag8 - 45	Core - close to crack	60.8	0.0	23.5	0.2	0.0	5.0	7.6	1.1	0.1	0.0	98.4	25	69	7
MFT-plag8 - 46	Core - close to crack	61.7	0.0	23.3	0.2	0.0	4.6	7.7	1.2	0.1	0.0	98.7	23	70	7
MFT-plag8 - 47	Core - close to crack	60.9	0.0	24.0	0.2	0.0	5.2	7.5	1.1	0.0	0.0	98.9	26	68	6
MFT-plag8 - 48	Core - close to crack	60.8	0.1	24.2	0.2	0.0	5.4	7.5	1.0	0.0	0.0	99.2	27	67	6
MFT-plag8 - 49	Core - close to crack	60.7	0.1	23.9	0.2	0.0	5.3	7.5	1.0	0.1	0.0	98.7	26	68	6
MFT-plag8 - 50	Core	61.3	0.0	23.4	0.2	0.0	4.8	7.7	1.1	0.1	0.0	98.7	24	69	7
MFT-plag8 - 51	Core	61.3	0.0	23.8	0.2	0.0	5.2	7.6	1.1	0.0	0.0	99.2	26	68	6
MFT-plag8 - 52	Core	61.4	0.0	23.3	0.2	0.0	4.9	7.7	1.2	0.0	0.0	98.7	24	69	7
MFT-plag8 - 53	Core	62.0	0.1	23.5	0.2	0.0	4.7	7.9	1.2	0.0	0.0	99.4	23	70	7
MFT-plag8 - 54	Core	61.7	0.1	23.0	0.2	0.0	4.5	7.9	1.3	0.0	0.0	98.7	22	70	8
MFT-plag8 - 55	Core	62.4	0.0	23.0	0.2	0.0	4.5	7.9	1.4	0.0	0.0	99.3	22	70	8

Table A1.6: continued

Info	Position	SiO ₂	TiO ₂	Al ₂ O ₃	FeO	MgO	CaO	Na ₂ O	K ₂ O	SrO	BaO	Total	An	Ab	Or
MFT-plag8 - 56	Core	62.3	0.0	22.8	0.2	0.0	4.5	7.8	1.3	0.0	0.0	98.9	22	70	8
MFT-plag8 - 57	Core	62.1	0.0	22.9	0.2	0.0	4.5	7.7	1.3	0.0	0.0	98.7	23	70	8
MFT-plag8 - 58	Core	61.9	0.0	22.8	0.2	0.0	4.4	7.8	1.4	0.0	0.0	98.6	22	70	8
MFT-plag8 - 59	Core	61.9	0.1	23.1	0.2	0.0	4.6	7.7	1.3	0.1	0.0	98.9	23	69	8
MFT-plag8 - 60	Core	62.0	0.0	23.1	0.2	0.0	4.7	7.7	1.3	0.1	0.0	99.2	23	69	8
MFT-plag8 - 61	Rim	62.1	0.0	23.2	0.2	0.0	4.5	7.7	1.3	0.0	0.0	99.0	22	70	8
grain9-1	Rim	62.7	0.0	23.0	0.2	0.0	4.5	8.1	1.3	0.0	0.0	99.9	22	71	7
grain9-2	Rim	63.3	0.0	22.8	0.2	0.0	3.9	8.3	1.6	0.0	0.0	100.1	19	72	9
grain9-3	Middle	63.4	0.0	22.9	0.2	0.0	4.2	8.2	1.6	0.0	0.0	100.4	20	71	9
grain9-4	Middle	62.8	0.0	23.2	0.2	0.0	4.5	8.2	1.4	0.0	0.0	100.3	21	71	8
grain9-5	Middle	62.8	0.1	23.1	0.2	0.0	4.4	8.3	1.4	0.0	0.0	100.2	21	71	8
grain9-6	Middle	62.7	0.0	22.8	0.2	0.0	4.3	8.2	1.5	0.1	0.0	99.8	21	71	8
grain9-7	Middle	62.7	0.0	23.2	0.2	0.0	4.5	8.2	1.4	0.0	0.0	100.2	21	71	8
grain9-8	Core	62.6	0.1	23.1	0.2	0.0	4.3	8.2	1.4	0.1	0.0	99.9	21	71	8
grain9-9	Core	62.7	0.1	22.8	0.2	0.0	4.2	8.3	1.5	0.0	0.0	99.7	20	72	8
grain9-10	Core	62.6	0.1	22.8	0.2	0.0	4.3	8.1	1.4	0.0	0.0	99.5	21	71	8
grain9-11	Core	62.6	0.1	22.9	0.2	0.0	4.2	8.2	1.4	0.0	0.0	99.7	20	72	8
grain9-12	Core	62.4	0.0	23.1	0.2	0.0	4.4	8.1	1.4	0.0	0.0	99.6	21	71	8
grain9-13	Core	62.5	0.1	23.0	0.2	0.0	4.4	8.3	1.4	0.0	0.0	99.9	21	71	8
grain9-14	Core	63.7	0.0	22.9	0.2	0.0	3.9	8.3	1.6	0.0	0.0	100.6	19	72	9
grain9-15	Core	63.7	0.0	22.9	0.2	0.0	4.0	8.4	1.6	0.1	0.0	100.9	19	72	9
grain9-16	Core	63.6	0.0	22.7	0.2	0.0	4.1	8.2	1.6	0.0	0.0	100.3	20	71	9
grain9-17	Core	63.8	0.0	22.6	0.2	0.0	3.7	8.4	1.8	0.0	0.0	100.6	18	72	10
grain9-18	Core	63.5	0.0	22.6	0.2	0.0	4.0	8.3	1.6	0.0	0.0	100.3	19	72	9
grain9-19	Core	63.5	0.0	22.5	0.2	0.0	4.1	8.4	1.6	0.0	0.0	100.3	19	72	9
grain9-20	Core - close to crack	63.1	0.1	22.7	0.2	0.0	4.1	8.4	1.6	0.0	0.0	100.1	19	72	9
grain9-24	Core - close to crack	61.8	1.2	22.2	1.4	0.0	4.1	8.3	1.5	0.1	0.0	100.6	20	72	8
grain9-25	Core - close to crack	63.0	0.1	22.3	0.3	0.0	4.0	8.3	1.6	0.1	0.0	99.6	19	72	9
grain9-26	Core - close to crack	63.7	0.1	22.5	0.2	0.0	4.0	8.4	1.6	0.0	0.0	100.4	19	72	9
grain9-27	Core	62.4	0.1	22.6	0.3	0.0	4.6	8.2	1.3	0.0	0.0	99.6	22	71	8
grain9-28	Middle	62.0	0.1	22.7	0.2	0.0	4.6	8.2	1.3	0.0	0.0	99.1	22	71	8
grain9-29	Middle	62.2	0.1	22.8	0.2	0.0	4.6	8.2	1.3	0.0	0.0	99.4	22	71	8
grain9-30	Rim	62.7	0.0	23.2	0.2	0.0	4.5	8.2	1.4	0.0	0.0	100.1	21	71	8
grain9-31	Rim	63.0	0.0	22.8	0.2	0.0	4.4	8.3	1.4	0.0	0.0	100.2	21	71	8
grain9-32	Rim	63.0	0.0	23.0	0.2	0.0	4.4	8.2	1.4	0.0	0.0	100.3	21	71	8
grain9-33	Rim	62.6	0.1	23.2	0.2	0.0	4.4	8.5	1.4	0.0	0.0	100.3	21	72	8
grain10-1	Rim	62.4	0.0	22.8	0.2	0.0	4.4	8.4	1.2	0.0	0.0	99.6	21	72	7
grain10-2	Middle	62.7	0.1	22.5	0.2	0.0	4.0	8.6	1.4	0.0	0.0	99.4	19	74	8
grain10-3	Middle	62.5	0.0	22.4	0.2	0.0	4.5	8.3	1.2	0.0	0.0	99.2	21	72	7
grain10-4	Middle	62.2	0.1	22.7	0.2	0.0	4.4	8.2	1.2	0.0	0.0	99.0	21	72	7
grain10-5	Middle	63.4	0.0	22.8	0.2	0.0	4.3	8.4	1.3	0.0	0.0	100.5	21	72	7
grain10-6	Middle	63.1	0.1	22.7	0.2	0.0	4.3	8.2	1.3	0.0	0.0	99.8	21	72	8
grain10-7	Middle	63.0	0.0	22.8	0.2	0.0	4.6	8.4	1.3	0.0	0.0	100.3	22	71	7
grain10-8	Middle	63.2	0.0	22.7	0.2	0.0	4.3	8.3	1.4	0.0	0.0	100.0	21	72	8
grain10-9	Core	63.0	0.0	22.6	0.2	0.0	4.3	8.3	1.3	0.0	0.0	99.8	20	72	8
grain10-10	Core	62.7	0.0	22.8	0.2	0.0	4.3	8.5	1.3	0.0	0.0	99.9	20	72	7
grain10-11	Core	62.7	0.1	22.7	0.2	0.0	4.3	8.3	1.3	0.0	0.0	99.6	21	72	7
grain10-12	Core	62.7	0.0	22.8	0.2	0.0	4.4	8.3	1.4	0.0	0.0	99.8	21	72	8
grain10-13	Core	62.7	0.0	23.1	0.2	0.0	4.5	8.3	1.3	0.1	0.0	100.1	21	71	7
grain10-14	Core	62.8	0.0	22.5	0.2	0.0	4.3	8.3	1.3	0.0	0.0	99.5	21	72	8
grain10-15	Middle	62.6	0.0	22.7	0.2	0.0	4.2	8.4	1.4	0.0	0.0	99.4	20	72	8
grain10-16	Middle	63.0	0.0	22.6	0.2	0.0	4.2	8.5	1.4	0.0	0.0	100.0	20	72	8
grain10-17	Middle	63.4	0.0	22.1	0.2	0.0	3.7	8.7	1.5	0.0	0.0	99.6	17	74	9
grain10-18	Middle	63.6	0.0	22.0	0.2	0.0	3.8	8.6	1.5	0.0	0.0	99.7	18	74	8
grain10-19	Middle	63.7	0.0	22.0	0.2	0.0	3.8	8.5	1.5	0.0	0.0	99.7	18	73	9
grain10-20	Middle	63.5	0.0	22.1	0.2	0.0	3.8	8.4	1.5	0.0	0.0	99.6	18	73	9
grain10-21	Middle	64.0	0.0	21.7	0.2	0.0	3.5	8.5	1.7	0.0	0.0	99.7	17	74	9
grain10-22	Middle - close to crack	63.5	0.1	21.9	0.2	0.0	3.8	8.5	1.5	0.0	0.0	99.6	18	73	9
grain10-23	Rim - close to crack	63.9	0.0	21.9	0.2	0.0	3.7	8.6	1.6	0.0	0.0	100.1	18	74	9
grain10-24	Rim - close to crack	63.5	0.0	22.3	0.2	0.0	3.9	8.5	1.5	0.0	0.0	99.8	19	73	8
grain10-25	Rim - close to crack	63.2	0.0	22.4	0.2	0.0	4.0	8.3	1.5	0.0	0.0	99.7	19	72	9
grain10-26	Rim - close to crack	63.4	0.0	22.3	0.2	0.0	3.9	8.4	1.5	0.0	0.0	99.7	19	73	9
grain10-27	Rim - close to crack	63.5	0.0	22.1	0.2	0.0	3.6	8.6	1.7	0.1	0.0	99.8	17	73	9
grain10-28	Rim	63.2	0.0	22.2	0.2	0.0	4.0	8.5	1.5	0.0	0.0	99.5	19	73	8
grain10-29	Rim	63.3	0.0	22.3	0.2	0.0	4.1	8.4	1.5	0.0	0.0	99.8	20	72	8
grain12-1	Rim	63.0	0.1	22.6	0.2	0.0	4.1	8.3	1.5	0.0	0.0	99.6	20	72	8
grain12-2	Rim	62.7	0.0	22.8	0.2	0.0	4.3	8.3	1.5	0.0	0.0	99.8	20	71	8
grain12-3	Rim	62.8	0.0	22.9	0.2	0.0	4.4	8.1	1.4	0.0	0.0	99.9	21	71	8
grain12-4	Middle	62.8	0.0	22.8	0.2	0.0	4.4	8.2	1.4	0.0	0.0	99.9	21	71	8
grain12-5	Middle	62.9	0.0	23.1	0.2	0.0	4.4	8.2	1.4	0.0	0.0	100.2	21	71	8
grain12-6	Middle	62.7	0.0	23.1	0.3	0.0	4.7	8.2	1.3	0.0	0.0	100.2	22	70	8
grain12-7	Middle	62.5	0.0	23.0	0.2	0.0	4.6	8.2	1.3	0.0	0.0	99.9	22	70	7
grain12-8	Middle	62.9	0.0	23.0	0.2	0.0	4.4	8.1	1.4	0.0	0.0	100.0	21	71	8
grain12-9	Middle	62.9	0.0	23.1	0.2	0.0	4.5	8.1	1.3	0.0	0.0	100.3	22	71	8
grain12-10	Core	62.9	0.1	23.1	0.2	0.0	4.6	8.2	1.4	0.0	0.0	100.4	22	71	8
grain12-11	Core	62.8	0.0	22.9	0.2	0.0	4.5	8.3	1.4	0.1	0.0	100.2	21	71	8
grain12-12	Core	63.2	0.0	23.0	0.2	0.0	4.3	8.3	1.5	0.0	0.0	100.4	20	71	8
grain12-13	Core	63.2	0.1	22.9	0.2	0.0	4.3	8.2	1.5	0.0	0.0	100.3	20	71	8
grain12-14	Core	63.3	0.1	22.8	0.2	0.0	4.2	8.3	1.5	0.0	0.0	100.4	20	71	9
grain12-15	Core - close to crack	63.6	0.0	22.8	0.2	0.0	4.0	8.3	1.6	0.0	0.0	100.5	19	72	9
grain12-16	Core - close to crack	63.4	0.0	22.7	0.2	0.0	4.0	8.3	1.6	0.0	0.0	100.2	19	71	9
grain12-17	Core - close to crack	63.2	0.0	22.7	0.2	0.0	4.1	8.2	1.6	0.0	0.0	100.0	20	71	9
grain12-18	Core - close to crack	63.7	0.0	22.6	0.2	0.0	3.9	8.3	1.7	0.0	0.0	100.4	19	72	9

Table A1.6: continued

Info	Position	SiO ₂	TiO ₂	Al ₂ O ₃	FeO	MgO	CaO	Na ₂ O	K ₂ O	SrO	BaO	Total	An	Ab	Or
grain12-19	Core - close to crack	62.5	0.0	23.3	0.2	0.0	4.4	8.5	1.4	0.0	0.0	100.4	21	71	8
grain12-20	Core - close to crack	63.2	0.0	22.6	0.2	0.0	4.0	8.4	1.6	0.0	0.0	100.0	19	72	9
grain12-21	Core - close to crack	63.1	0.1	22.6	0.2	0.0	3.9	8.4	1.7	0.0	0.0	99.8	18	72	9
grain12-22	Core - close to crack	62.7	0.0	23.1	0.2	0.0	4.5	8.3	1.3	0.0	0.0	100.1	21	71	8
grain12-23	Core - close to crack	63.2	0.0	22.7	0.2	0.0	4.1	8.3	1.6	0.0	0.0	100.2	20	71	9
grain12-24	Core - close to crack	63.4	0.0	22.8	0.2	0.0	4.0	8.4	1.7	0.0	0.0	100.5	19	72	9
grain12-25	Core - close to crack	60.7	0.0	23.0	0.2	0.0	4.2	8.3	1.6	0.0	0.0	98.0	20	71	9
grain12-26	Core - close to crack	62.7	0.0	22.8	0.2	0.0	4.2	8.4	1.5	0.0	0.0	99.8	20	72	8
grain12-27	Core - close to crack	63.2	0.1	23.0	0.2	0.0	4.4	8.2	1.4	0.0	0.0	100.4	21	71	8
grain12-28	Core - close to crack	62.7	0.1	22.7	0.2	0.0	4.3	8.3	1.4	0.0	0.0	99.8	21	71	8
grain12-29	Core - close to crack	62.4	0.0	23.1	0.2	0.0	4.4	8.3	1.4	0.0	0.0	99.9	21	71	8
grain12-30	Core - close to crack	63.3	0.0	22.7	0.2	0.0	4.2	8.3	1.5	0.0	0.0	100.2	20	71	9
grain12-31	Core	63.2	0.0	22.7	0.2	0.0	4.2	8.2	1.5	0.0	0.0	100.1	20	71	9
grain12-32	Middle	63.0	0.0	22.8	0.2	0.0	4.5	8.2	1.4	0.0	0.0	100.1	21	71	8
grain12-33	Middle	63.4	0.0	22.7	0.2	0.0	4.0	8.3	1.6	0.0	0.0	100.2	19	72	9
grain12-34	Middle	63.3	0.0	22.3	0.2	0.0	3.7	8.5	1.8	0.0	0.0	99.9	17	73	10
grain12-35	Rim	62.5	0.1	22.9	0.2	0.0	4.2	8.5	1.6	0.1	0.0	100.0	19	72	9
grain12-37	Rim	63.1	0.0	22.5	0.2	0.0	3.9	8.4	1.7	0.1	0.0	99.9	18	72	10
grain12-38	Rim	63.2	0.0	22.7	0.2	0.0	4.0	8.2	1.7	0.0	0.0	100.0	19	71	9
grain13-1	Rim	62.8	0.1	22.9	0.2	0.0	4.1	8.4	1.5	0.0	0.0	99.9	19	72	9
grain13-2	Rim	63.0	0.1	22.9	0.2	0.0	4.2	8.3	1.5	0.0	0.0	100.3	20	72	9
grain13-3	Rim	63.1	0.0	22.9	0.2	0.0	4.3	8.2	1.5	0.0	0.0	100.2	20	71	9
grain13-4	Middle	63.1	0.0	22.9	0.2	0.0	4.3	8.3	1.4	0.0	0.0	100.3	20	71	8
grain13-5	Middle	63.2	0.0	22.7	0.2	0.0	4.2	8.1	1.5	0.0	0.0	100.0	20	71	9
grain13-6	Middle	63.1	0.1	23.2	0.2	0.0	4.5	8.1	1.5	0.0	0.0	100.5	21	70	8
grain13-7	Middle	63.0	0.0	23.0	0.2	0.0	4.4	8.3	1.5	0.0	0.0	100.5	21	71	8
grain13-8	Middle	62.8	0.1	23.1	0.3	0.0	4.5	8.2	1.5	0.0	0.0	100.4	21	70	8
grain13-9	Core	63.1	0.0	22.6	0.2	0.0	4.2	8.3	1.5	0.0	0.0	100.0	20	71	9
grain13-10	Core	63.0	0.1	22.9	0.2	0.0	4.4	8.2	1.5	0.1	0.0	100.3	21	70	8
grain13-11	Core	63.1	0.0	22.6	0.2	0.0	4.3	8.2	1.5	0.0	0.0	100.0	20	71	9
grain13-12	Core	63.2	0.1	22.7	0.2	0.0	4.2	8.3	1.6	0.1	0.0	100.3	20	71	9
grain13-13	Core	63.2	0.1	22.8	0.2	0.0	4.0	8.2	1.6	0.0	0.0	100.1	19	72	9
grain13-14	Core	62.9	0.0	22.8	0.2	0.0	4.3	8.2	1.5	0.0	0.0	99.9	21	71	8
grain13-15	Core	63.0	0.0	22.7	0.2	0.0	4.3	8.3	1.5	0.0	0.0	100.1	20	71	9
grain13-16	Core	63.1	0.0	22.8	0.2	0.0	4.5	8.0	1.5	0.1	0.0	100.2	21	70	9
grain13-17	Core	63.0	0.0	22.9	0.2	0.0	4.4	8.3	1.5	0.0	0.0	100.4	21	71	8
grain13-18	Core	62.7	0.1	23.1	0.2	0.0	4.4	8.3	1.4	0.0	0.0	100.1	21	71	8
grain13-19	Core	63.1	0.0	23.1	0.2	0.0	4.3	8.1	1.5	0.1	0.0	100.5	21	71	9
grain13-20	Core	62.7	0.0	23.0	0.2	0.0	4.3	8.2	1.5	0.1	0.0	100.0	21	71	9
grain13-21	Core	63.1	0.1	23.2	0.2	0.0	4.4	8.3	1.5	0.1	0.0	100.8	21	71	8
grain13-22	Core	62.7	0.0	23.0	0.2	0.0	4.5	8.2	1.5	0.1	0.0	100.3	21	70	8
grain13-23	Core	62.8	0.0	22.9	0.3	0.0	4.5	8.2	1.5	0.1	0.0	100.1	21	70	8
grain13-24	Core	63.3	0.0	22.6	0.2	0.0	4.3	8.1	1.6	0.1	0.0	100.2	21	71	9
grain13-25	Core	63.5	0.0	22.4	0.2	0.0	4.0	8.2	1.6	0.1	0.0	100.0	19	71	9
grain13-26	Core	63.0	0.1	22.9	0.3	0.0	4.3	8.0	1.5	0.1	0.0	100.1	21	70	9
grain13-27	Core	62.8	0.0	22.8	0.2	0.0	4.3	8.2	1.5	0.1	0.0	100.0	21	71	9
grain13-28	Core	62.9	0.0	22.9	0.2	0.0	4.4	8.2	1.5	0.1	0.0	100.2	21	71	8
grain13-29	Core	62.9	0.0	22.9	0.2	0.0	4.4	8.2	1.5	0.1	0.0	100.3	21	70	9
grain13-30	Core	62.5	0.0	22.7	0.2	0.0	4.3	8.1	1.5	0.1	0.0	99.6	21	71	9
grain13-31	Core	62.8	0.1	22.4	0.2	0.0	4.2	8.2	1.6	0.1	0.0	99.6	20	71	9
grain13-32	Core	63.1	0.0	22.5	0.2	0.0	4.1	8.1	1.6	0.1	0.0	99.8	20	71	9
grain13-33	Core	63.5	0.1	22.1	0.2	0.0	3.8	8.2	1.7	0.1	0.0	99.8	18	72	10
grain13-34	Core	63.4	0.1	22.1	0.2	0.0	4.0	8.3	1.7	0.1	0.0	99.8	19	72	9
grain13-35	Core	63.2	0.0	22.4	0.2	0.0	4.0	8.2	1.6	0.1	0.0	99.8	19	71	9
grain13-36	Core	63.4	0.0	22.3	0.2	0.0	4.0	8.3	1.7	0.1	0.0	100.0	19	72	9
grain13-37	Core	63.3	0.1	22.5	0.2	0.0	4.1	8.3	1.6	0.1	0.0	100.2	19	72	9
grain13-38	Core	62.7	0.0	22.3	0.2	0.0	4.1	8.4	1.6	0.1	0.0	99.5	19	71	9
grain13-39	Core	62.8	0.1	22.5	0.2	0.0	4.1	8.2	1.6	0.2	0.0	99.7	20	71	9
grain13-40	Core	62.9	0.0	22.4	0.2	0.0	4.1	8.3	1.6	0.1	0.1	99.7	20	71	9
grain13-41	Core	63.1	0.1	22.3	0.2	0.0	4.0	8.2	1.6	0.1	0.0	99.7	19	71	9
grain13-42	Core	62.9	0.0	22.5	0.2	0.0	4.2	8.2	1.6	0.2	0.0	99.9	20	71	9
grain13-43	Core	62.9	0.1	22.5	0.2	0.0	4.1	8.2	1.6	0.2	0.0	99.8	20	71	9
grain13-44	Core	63.0	0.0	22.6	0.2	0.0	4.0	8.2	1.6	0.1	0.0	99.7	19	71	9
grain13-45	Core	62.9	0.0	22.5	0.2	0.0	4.3	8.2	1.6	0.1	0.0	99.8	20	71	9
grain13-46	Core	63.1	0.0	22.7	0.3	0.0	4.1	8.1	1.6	0.1	0.0	100.0	20	71	9
grain13-47	Core	63.2	0.0	22.7	0.2	0.0	4.1	8.2	1.6	0.1	0.0	100.1	20	71	9
grain13-48	Core	62.0	0.1	22.6	0.2	0.0	4.4	8.1	1.4	0.1	0.0	98.9	21	71	8
grain13-49	Core	62.0	0.0	22.7	0.2	0.0	4.5	8.2	1.4	0.0	0.0	99.1	21	70	8
grain13-50	Core	62.2	0.1	23.0	0.2	0.0	4.6	8.0	1.4	0.1	0.0	99.6	22	70	8
grain13-51	Core	63.0	0.1	22.6	0.2	0.0	4.1	8.1	1.6	0.1	0.0	99.7	20	71	9
grain13-52	Core	62.9	0.0	22.6	0.2	0.0	4.1	8.2	1.6	0.1	0.0	99.8	20	71	9
grain13-53	Core	62.6	0.0	23.1	0.2	0.0	4.4	8.2	1.5	0.1	0.0	100.2	21	71	8
grain13-54	Core	62.9	0.1	22.8	0.3	0.0	4.3	8.2	1.6	0.1	0.0	100.2	20	71	9
grain13-55	Core	62.6	0.0	22.7	0.2	0.0	4.3	8.2	1.6	0.1	0.0	99.7	20	71	9
grain13-56	Core	63.0	0.0	22.9	0.2	0.0	4.3	8.2	1.6	0.1	0.1	100.3	21	71	9
grain13-57	Core	62.3	0.0	23.2	0.2	0.0	4.7	8.0	1.4	0.0	0.0	99.8	22	69	8
grain13-58	Core	62.9	0.0	23.0	0.2	0.0	4.2	8.1	1.6	0.1	0.0	100.2	20	71	9
grain13-59	Middle	62.9	0.0	23.2	0.2	0.0	4.5	8.2	1.4	0.1	0.0	100.5	21	71	8
grain13-60	Middle	62.8	0.0	23.2	0.2	0.0	4.6	8.1	1.4	0.1	0.0	100.4	22	70	8
grain13-61	Middle	63.0	0.1	23.3	0.2	0.0	4.5	8.1	1.3	0.1	0.0	100.6	22	71	8
grain13-62	Middle	62.8	0.0	23.5	0.2	0.0	4.6	8.1	1.3	0.1	0.0	100.6	22	70	7
grain13-63	Middle	62.6	0.0	23.6	0.2	0.0	4.8	8.1	1.3	0.1	0.0	100.7	23	70	7
grain13-64	Middle	62.7	0.0	23.3	0.2	0.0	4.7	8.0	1.3	0.1	0.0	100.5	23	70	7
grain13-65	Rim	62.0	0.0	23.5	0.2	0.0	5.0	8.0	1.3	0.0	0.0	100.1	24	69	7

Table A1.6: continued

Info	Position	SiO ₂	TiO ₂	Al ₂ O ₃	FeO	MgO	CaO	Na ₂ O	K ₂ O	SrO	BaO	Total	An	Ab	Or
grain13-66	Rim	62.9	0.0	23.1	0.2	0.0	4.7	8.1	1.3	0.0	0.0	100.4	22	70	8
grain13-67	Rim	62.9	0.0	23.2	0.2	0.0	4.6	8.1	1.3	0.1	0.0	100.3	22	71	7
grain14-1	Rim	62.8	0.0	22.8	0.2	0.0	4.2	8.3	1.5	0.0	0.0	99.8	20	71	9
grain14-2	Rim	62.6	0.1	22.7	0.2	0.0	4.3	8.3	1.4	0.1	0.0	99.6	20	72	8
grain14-3	Rim	62.5	0.1	22.4	0.2	0.0	4.2	8.2	1.5	0.0	0.0	99.1	20	72	8
grain14-4	Middle	62.8	0.0	22.8	0.2	0.0	4.1	8.4	1.6	0.1	0.0	99.9	19	72	9
grain14-5	Middle	62.6	0.0	23.1	0.2	0.0	4.2	8.2	1.5	0.1	0.0	99.9	20	71	8
grain14-6	Middle	62.4	0.0	22.7	0.2	0.0	4.3	8.2	1.5	0.1	0.0	99.4	21	71	8
grain14-7	Middle	62.2	0.1	22.8	0.2	0.0	4.2	8.2	1.5	0.0	0.0	99.2	20	71	9
grain14-8	Middle	62.4	0.0	22.6	0.2	0.0	4.2	8.3	1.6	0.1	0.0	99.5	20	71	9
grain14-9	Middle	62.4	0.0	22.4	0.2	0.0	4.1	8.2	1.5	0.1	0.0	99.0	20	71	9
grain14-10	Middle	62.4	0.0	22.7	0.2	0.0	4.2	8.1	1.5	0.1	0.0	99.2	20	71	9
grain14-11	Middle	62.5	0.1	22.5	0.2	0.0	4.0	8.2	1.6	0.1	0.0	99.1	20	71	9
grain14-12	Core	62.4	0.0	22.5	0.2	0.0	4.1	8.2	1.5	0.1	0.0	99.1	20	72	9
grain14-13	Core - close to crack	62.4	0.0	22.5	0.2	0.0	4.1	8.5	1.6	0.1	0.0	99.4	19	72	9
grain14-14	Core - close to crack	62.0	0.0	22.4	0.2	0.0	4.2	8.3	1.5	0.2	0.0	98.9	20	72	9
grain14-15	Core	62.2	0.0	22.5	0.2	0.0	4.3	8.3	1.5	0.1	0.0	99.1	20	71	8
grain14-16	Core	63.2	0.0	22.9	0.2	0.0	4.1	8.3	1.6	0.2	0.0	100.7	20	71	9
grain14-17	Core - close to crack	63.1	0.0	22.7	0.2	0.0	4.2	8.2	1.5	0.1	0.0	99.9	20	71	9
grain14-18	Core - close to crack	62.9	0.1	23.1	0.2	0.0	4.4	8.1	1.5	0.1	0.0	100.3	21	71	8
grain14-19	Core - close to crack	62.7	0.0	23.0	0.2	0.0	4.4	8.1	1.4	0.1	0.0	100.1	21	71	8
grain14-20	Core - close to crack	62.8	0.0	23.0	0.2	0.0	4.3	8.2	1.4	0.1	0.0	100.1	21	71	8
grain14-21	Core - close to crack	63.3	0.0	22.7	0.2	0.0	4.0	8.2	1.6	0.1	0.0	100.3	19	72	9
grain14-22	Core - close to crack	63.2	0.1	22.5	0.2	0.0	4.0	8.3	1.7	0.1	0.0	100.1	19	72	9
grain14-23	Core	63.4	0.0	22.6	0.2	0.0	4.0	8.2	1.6	0.1	0.0	100.2	19	71	9
grain14-24	Core	63.1	0.1	22.6	0.2	0.0	4.1	8.3	1.6	0.1	0.0	100.1	19	72	9
grain14-25	Core	63.0	0.0	22.6	0.2	0.0	4.0	8.3	1.5	0.0	0.0	99.8	19	72	9
grain14-26	Core	63.3	0.1	22.7	0.2	0.0	4.0	8.3	1.6	0.1	0.0	100.2	19	72	9
grain14-27	Core	63.5	0.1	22.4	0.2	0.0	3.9	8.4	1.7	0.1	0.0	100.3	18	72	10
grain14-28	Core	63.4	0.0	22.5	0.2	0.0	4.0	8.3	1.7	0.1	0.0	100.3	19	72	10
grain14-29	Core	63.3	0.0	22.1	0.2	0.0	3.8	8.4	1.7	0.1	0.1	99.8	18	72	10
grain14-30	Core	62.7	0.0	22.5	0.2	0.0	3.9	8.4	1.7	0.1	0.0	99.5	18	72	9
grain14-31	Core	62.8	0.0	22.7	0.2	0.0	4.3	8.3	1.4	0.1	0.0	99.8	20	71	8
grain14-32	Core	62.6	0.1	22.8	0.2	0.0	4.2	8.0	1.4	0.1	0.0	99.5	20	71	8
grain14-33	Core	62.4	0.0	22.6	0.2	0.0	4.2	8.2	1.5	0.1	0.0	99.3	20	72	9
grain14-34	Core	62.6	0.0	22.6	0.2	0.0	4.1	8.1	1.5	0.1	0.0	99.3	20	71	9
grain14-35	Core	62.6	0.0	22.5	0.2	0.0	4.2	8.3	1.5	0.0	0.0	99.4	20	71	9
grain14-36	Core - close to crack	62.1	0.0	22.8	0.2	0.0	4.3	8.3	1.5	0.0	0.0	99.2	20	71	8
grain14-37	Core - close to crack	62.5	0.0	22.5	0.2	0.0	4.2	8.2	1.5	0.1	0.0	99.1	20	72	8
grain14-38	Core - close to crack	61.9	0.0	22.9	0.2	0.0	4.6	8.2	1.3	0.1	0.0	99.2	22	71	7
grain14-39	Core - close to crack	63.3	0.0	22.7	0.2	0.0	4.2	8.2	1.5	0.1	0.0	100.3	20	71	9
grain14-40	Core	63.0	0.0	22.8	0.2	0.0	4.2	8.2	1.5	0.1	0.0	100.1	20	71	9
grain14-41	Core	62.9	0.1	23.0	0.2	0.0	4.4	8.2	1.4	0.1	0.0	100.3	21	71	8
grain14-42	Core	62.1	0.1	23.6	0.2	0.0	5.1	8.1	1.1	0.0	0.0	100.2	24	69	6
grain14-43	Core	62.8	0.0	22.9	0.2	0.0	4.3	8.2	1.4	0.1	0.0	100.0	21	71	8
grain14-44	Core	62.4	0.0	22.8	0.2	0.0	4.3	8.3	1.4	0.1	0.0	99.5	21	72	8
grain14-45	Core	61.4	0.0	23.6	0.2	0.0	5.1	8.1	1.1	0.1	0.0	99.6	24	69	6
grain14-46	Core	61.0	0.1	23.8	0.2	0.0	5.6	7.8	0.9	0.1	0.0	99.6	27	68	5
grain14-47	Core	60.5	0.1	24.0	0.2	0.0	5.9	7.8	0.9	0.0	0.0	99.3	28	67	5
grain14-48	Core	61.2	0.1	23.6	0.2	0.0	5.3	8.0	1.0	0.0	0.0	99.4	25	69	6
grain14-49	Core	61.0	0.0	23.5	0.2	0.0	5.2	8.1	1.1	0.1	0.0	99.2	25	69	6
grain14-50	Middle	60.7	0.1	23.7	0.2	0.0	5.3	8.1	1.0	0.1	0.0	99.3	25	69	6
grain14-51	Middle	61.7	0.0	23.7	0.2	0.0	5.1	8.0	1.2	0.1	0.0	100.1	24	69	7
grain14-52	Middle	61.9	0.0	23.7	0.2	0.0	5.1	8.0	1.1	0.0	0.0	100.0	24	69	6
grain14-53	Middle	62.2	0.0	23.5	0.2	0.0	4.9	8.2	1.1	0.1	0.1	100.1	23	70	6
grain14-54	Rim	62.2	0.0	23.2	0.2	0.0	4.8	8.0	1.2	0.0	0.0	99.6	23	70	7
grain14-55	Rim	62.4	0.0	22.9	0.2	0.0	4.5	8.1	1.3	0.1	0.0	99.3	22	71	7
grain14-56	Rim	62.0	0.1	22.9	0.2	0.0	4.5	8.3	1.4	0.1	0.0	99.3	21	71	8
grain20-5	Middle	62.9	0.0	23.0	0.2	0.0	4.3	8.0	1.5	0.0	0.0	99.9	21	71	8
grain20-6	Middle	62.7	0.0	23.2	0.2	0.0	4.5	7.9	1.4	0.0	0.0	100.0	22	70	8
grain20-7	Middle	62.9	0.0	23.2	0.2	0.0	4.4	7.9	1.5	0.0	0.0	100.1	22	70	9
grain20-8	Middle	63.5	0.0	22.8	0.2	0.0	4.3	8.0	1.5	0.0	0.0	100.3	21	70	9
grain20-9	Middle	63.1	0.0	22.9	0.2	0.0	4.2	7.9	1.5	0.1	0.0	100.0	21	70	9
grain20-10	Middle	63.4	0.1	22.7	0.2	0.0	4.1	8.0	1.7	0.0	0.0	100.1	20	71	10
grain20-11	Middle	63.2	0.0	22.8	0.2	0.0	4.1	8.0	1.6	0.1	0.0	100.1	20	71	9
grain20-12	Middle	63.4	0.1	22.7	0.2	0.0	4.1	8.0	1.6	0.0	0.0	100.1	20	70	9
grain20-13	Middle	63.9	0.0	22.7	0.2	0.0	4.0	7.9	1.8	0.1	0.1	100.6	20	70	10
grain20-14	Core	63.6	0.0	22.7	0.2	0.0	4.0	8.0	1.7	0.2	0.0	100.5	19	71	10
grain20-15	Core	63.6	0.1	22.8	0.2	0.0	3.9	7.9	1.7	0.1	0.0	100.3	19	71	10
grain20-16	Core	63.8	0.1	22.6	0.2	0.0	4.0	8.0	1.8	0.1	0.0	100.6	19	71	10
grain20-17	Core	63.5	0.0	22.7	0.2	0.0	4.1	8.1	1.6	0.1	0.0	100.3	20	71	9
grain20-18	Core	63.0	0.0	22.9	0.2	0.0	4.2	8.0	1.6	0.1	0.0	100.0	20	70	9
grain20-19	Core	63.1	0.0	23.0	0.2	0.0	3.9	8.0	1.7	0.1	0.0	100.2	19	71	10
grain20-20	Core	63.7	0.0	22.6	0.2	0.0	3.9	8.0	1.7	0.1	0.0	100.4	19	71	10
grain20-21	Core	63.1	0.1	22.9	0.2	0.0	4.1	8.0	1.6	0.1	0.0	100.1	20	71	9
grain20-22	Core	63.5	0.0	22.8	0.2	0.0	4.2	7.9	1.6	0.1	0.0	100.3	20	70	9
grain20-23	Core	63.5	0.0	22.9	0.2	0.0	4.0	7.9	1.7	0.1	0.0	100.3	20	71	10
grain20-24	Core	63.3	0.1	23.2	0.2	0.0	4.2	8.0	1.6	0.1	0.0	100.7	20	70	9
grain20-25	Core	63.1	0.1	23.2	0.2	0.0	4.4	8.0	1.5	0.1	0.0	100.7	21	70	8
grain20-26	Core	63.0	0.0	23.2	0.2	0.0	4.3	8.0	1.5	0.1	0.0	100.3	21	71	9
grain20-27	Core	63.4	0.0	23.1	0.2	0.0	4.2	8.0	1.5	0.1	0.0	100.6	21	71	9
grain20-28	Core	63.4	0.0	23.1	0.2	0.0	4.1	8.0	1.6	0.1	0.0	100.5	20	71	9
grain20-29	Core	63.3	0.0	23.1	0.2	0.0	4.3	7.9	1.5	0.1	0.0	100.5	21	70	9
grain20-30	Core	63.6	0.0	22.8	0.2	0.0	4.2	7.9	1.6	0.0	0.0	100.2	21	70	9

Table A1.6: continued

Info	Position	SiO ₂	TiO ₂	Al ₂ O ₃	FeO	MgO	CaO	Na ₂ O	K ₂ O	SrO	BaO	Total	An	Ab	Or
grain20-31	Core	63.4	0.1	22.4	0.2	0.0	4.3	7.9	1.6	0.2	0.0	100.1	21	70	9
grain20-32	Core	63.3	0.0	22.6	0.2	0.0	4.2	7.9	1.5	0.1	0.0	99.9	21	70	9
grain20-33	Core	63.1	0.0	22.8	0.2	0.0	4.5	7.8	1.5	0.1	0.0	100.1	22	69	9
grain20-34	Core	63.2	0.0	22.6	0.2	0.0	4.2	7.9	1.6	0.1	0.0	99.8	21	70	9
grain20-35	Middle	63.2	0.1	22.6	0.2	0.0	4.1	7.8	1.6	0.1	0.0	99.7	20	70	9
grain20-36	Middle	63.2	0.0	22.6	0.2	0.0	4.2	7.9	1.6	0.1	0.0	99.8	21	70	9
grain20-37	Middle	63.1	0.0	22.6	0.2	0.0	4.2	7.9	1.6	0.1	0.1	99.7	21	70	9
grain20-38	Middle	63.9	0.0	22.6	0.2	0.0	4.1	7.9	1.6	0.1	0.0	100.4	20	70	9
grain20-39	Middle	63.0	0.0	22.8	0.2	0.0	4.2	8.0	1.6	0.0	0.0	99.8	20	70	9
grain20-40	Middle	63.0	0.1	22.9	0.2	0.0	4.5	8.0	1.4	0.2	0.0	100.2	22	70	8
grain20-41	Rim	63.5	0.0	22.7	0.2	0.0	4.4	7.9	1.5	0.1	0.0	100.3	21	70	9
grain20-42	Rim	63.6	0.1	22.8	0.2	0.0	4.4	7.8	1.5	0.0	0.0	100.4	21	70	9
grain20-43	Rim	63.4	0.0	22.6	0.2	0.0	4.2	7.9	1.6	0.1	0.1	100.0	21	70	9
grain20-44	Rim	63.1	0.0	22.6	0.2	0.0	4.3	7.9	1.5	0.1	0.0	99.7	21	70	9
grain20-45	Rim	63.1	0.1	22.6	0.2	0.0	4.4	7.9	1.5	0.1	0.0	99.7	21	70	9
grain20-46	Rim	62.9	0.0	22.6	0.2	0.0	4.4	7.8	1.5	0.1	0.0	99.5	22	70	9
grain20-47	Rim	62.8	0.0	22.5	0.2	0.0	4.4	7.9	1.5	0.1	0.0	99.4	22	70	9
grain20-48	Rim	63.0	0.0	22.7	0.2	0.0	4.3	7.8	1.5	0.1	0.0	99.5	21	70	9
grain20-49	Rim	63.0	0.0	22.6	0.2	0.0	4.5	7.8	1.4	0.1	0.0	99.7	22	70	8
mount1-1-10-1	Rim	63.2	0.0	22.7	0.2	0.0	3.9	8.1	1.5			99.7	19	72	9
mount1-1-10-2	Core	62.9	0.0	22.8	0.2	0.0	4.0	8.2	1.3			99.4	20	72	8
mount1-11-1	Rim	62.4	0.0	23.3	bdl	0.2	4.5	7.8	1.3			99.5	22	70	8
mount1-12-1	Rim	63.1	0.1	22.7	bdl	0.2	3.9	8.1	1.5			99.5	19	72	9
mount1-12-2	Core	62.7	0.0	22.9	bdl	0.2	4.1	8.0	1.4			99.3	20	72	8
mount1-13-1	Rim	62.5	0.0	23.0	0.2	0.0	4.1	7.9	1.4			99.0	21	71	8
mount1-13-2	Core	62.4	0.0	22.9	0.2	0.0	4.1	8.0	1.5			99.1	20	71	8
mount1-14-1	Rim	62.6	0.1	22.7	bdl	0.2	4.2	7.9	1.4			99.1	21	71	8
mount1-14-2	Rim	61.7	0.0	23.5	bdl	0.2	4.7	7.8	1.2			99.1	23	70	7
mount1-20-1	Core	62.9	0.0	22.9	bdl	0.2	4.0	8.1	1.5			99.6	20	72	9
mount1-20-2	Rim	63.3	0.0	22.8	0.2	0.0	4.1	8.2	1.4			100.0	20	72	8
mount1-21-1	Rim	63.1	0.1	22.7	bdl	0.2	4.1	7.9	1.5			99.6	20	71	9
mount1-21-2	Rim	62.8	0.1	23.0	0.2	0.0	4.3	8.0	1.3			99.7	21	71	8
mount1-2-1-1	Rim	63.2	0.0	22.6	bdl	0.2	3.8	8.1	1.5			99.4	19	72	9
mount1-2-1-2	Core	63.4	0.0	22.4	bdl	0.2	3.8	8.3	1.6			99.6	18	73	9
mount1-2-1-3	Rim	62.8	0.0	22.9	0.2	0.0	4.2	8.0	1.4			99.5	21	71	8
mount1-23-1	Rim	62.7	0.0	22.9	bdl	0.2	4.3	7.9	1.3			99.4	21	71	8
mount1-23-2	Core	63.3	0.0	22.8	bdl	0.2	4.1	8.1	1.4			99.9	20	72	8
mount1-24-1	Rim	62.9	0.0	22.8	0.2	0.0	4.0	8.1	1.4			99.5	20	72	8
mount1-24-2	Core	62.9	0.0	22.9	0.2	0.0	4.1	8.1	1.4			99.5	20	72	8
mount1-25-1	Rim	62.5	0.0	23.5	0.2	0.0	4.5	8.0	1.1			99.8	22	71	7
mount1-25-2	Core	63.0	0.0	22.8	bdl	0.2	4.0	8.1	1.3			99.5	20	72	8
mount1-26-1	Rim	62.8	0.0	23.2	0.2	0.0	4.3	8.0	1.4			100.0	21	71	8
mount1-26-2	Core	63.2	0.0	22.9	0.2	0.0	4.1	8.1	1.5			99.9	20	71	9
mount1-3-1-1	Rim	61.9	0.1	23.8	bdl	0.2	4.9	8.0	1.0			99.8	24	70	6
mount1-3-1-2	Core	62.4	0.1	23.5	bdl	0.2	4.5	8.2	1.2			99.9	22	71	7
mount1-4-1	Rim	62.2	0.0	23.4	0.2	0.0	4.6	8.1	1.2			99.7	22	71	7
mount1-4-2	Core	62.3	0.0	22.9	bdl	0.2	4.5	8.0	1.2			99.2	22	71	7
mount1-7-1	Rim	63.2	0.0	22.9	0.2	0.0	4.0	8.0	1.5			99.8	20	72	9
mount1-7-2	Core	63.0	0.1	23.1	0.2	0.0	4.1	8.0	1.5			99.9	20	71	9
mount1-8-1	Rim	61.4	0.0	23.7	bdl	0.2	5.1	7.7	1.0			99.1	25	69	6
mount1-8-2	Core	62.8	0.0	23.2	0.2	0.0	4.5	8.0	1.1			99.7	22	71	6
mount1-9-1	Rim	62.9	0.1	22.8	bdl	0.2	4.1	8.1	1.4			99.6	20	72	8
mount1-9-2	Core	62.7	0.0	23.0	0.2	0.0	4.3	8.1	1.3			99.7	21	71	8
mount2-1-1	Rim	62.5	0.1	23.0	bdl	0.2	4.3	8.0	1.3			99.3	21	71	8
mount2-1-2	Core	61.1	0.0	23.7	bdl	0.2	4.9	7.7	1.1			98.7	24	69	6
mount2-11-1	Rim	61.4	0.0	23.2	0.2	0.0	4.6	7.6	1.2			98.2	23	70	7
mount2-11-2	Core	62.8	0.0	22.7	0.2	0.0	4.2	7.7	1.4			99.0	21	70	8
mount2-11-3	Core	62.5	0.0	22.9	0.2	0.0	4.3	7.6	1.4			98.9	22	70	8
mount2-11-4	Core	62.4	0.0	22.9	0.2	0.0	4.2	7.7	1.4			98.8	21	70	8
mount2-11-5	Core	62.7	0.1	23.0	bdl	0.2	4.2	7.7	1.3			99.2	21	71	8
mount2-12-1	Rim	62.9	0.0	22.8	bdl	0.2	3.9	7.8	1.4			99.1	20	72	9
mount2-12-2	Core	62.5	0.0	22.9	bdl	0.2	4.2	8.0	1.4			99.2	21	71	8
mount2-12-3	Rim	62.8	0.0	22.9	bdl	0.2	4.1	7.9	1.4			99.4	20	71	8
mount2-13-1	Rim	63.1	0.1	22.7	bdl	0.2	4.1	7.6	1.5			99.1	21	70	9
mount2-13-2	Rim	63.0	0.0	22.7	0.2	0.0	4.0	7.8	1.4			99.1	20	71	8
mount2-13-3	Rim	62.5	0.0	23.0	0.2	0.0	4.4	7.7	1.3			99.1	22	70	8
mount2-13-4	Core	62.2	0.0	23.6	bdl	0.2	4.7	7.6	1.1			99.5	24	69	7
mount2-13-5	Core	62.6	0.0	23.1	bdl	0.2	4.5	7.7	1.2			99.3	22	70	7
mount2-15-1	Rim	62.7	0.0	22.9	bdl	0.2	4.0	7.8	1.3			99.0	20	72	8
mount2-15-2	Core	63.7	0.0	22.5	bdl	0.2	3.8	8.0	1.5			99.7	19	72	9
mount2-15-3	Core	63.4	0.0	22.7	bdl	0.2	4.0	7.9	1.4			99.7	20	71	8
mount2-15-4	Rim	62.9	0.0	23.0	0.2	0.0	4.2	7.7	1.4			99.4	21	71	8
mount2-15-5	Core	63.4	0.0	22.9	bdl	0.2	4.1	7.8	1.4			99.8	21	71	8
mount2-17-1	Core	63.6	0.0	22.7	bdl	0.2	4.1	7.6	1.4			99.7	21	70	9
mount2-17-2	Rim	63.5	0.0	22.8	0.2	0.0	4.0	7.8	1.3			99.7	20	72	8
mount2-17-3	Core	63.3	0.0	22.9	0.2	0.0	4.2	7.8	1.3			99.8	21	71	8
mount2-17-4	Core	62.9	0.0	23.0	0.2	0.0	4.2	7.7	1.3			99.4	21	71	8
mount2-17-5	Core	63.7	0.0	22.6	bdl	0.2	3.8	7.8	1.5			99.6	19	72	9
mount2-17-6	Core	63.5	0.0	22.8	bdl	0.2	4.0	7.8	1.5			99.8	20	71	9
mount2-17-7	Core	63.0	0.1	23.0	0.2	0.0	4.2	7.7	1.3			99.4	21	71	8
mount2-2-1	Rim	63.1	0.0	22.6	0.2	0.0	3.9	8.0	1.5			99.2	19	72	9
mount2-2-2	Core	62.1	0.0	23.4	bdl	0.2	4.5	7.8	1.2			99.3	23	70	7
mount2-2-3	Core	62.2	0.0	23.3	0.2	0.0	4.6	7.9	1.2			99.5	23	70	7
mount2-2-4	Core	62.7	0.0	23.0	0.2	0.0	4.1	8.0	1.4			99.3	20	71	8
mount2-24-1	Rim	62.9	0.0	23.1	bdl	0.2	4.3	7.7	1.3			99.5	22	70	8

Table A1.6: continued

Info	Position	SiO ₂	TiO ₂	Al ₂ O ₃	FeO	MgO	CaO	Na ₂ O	K ₂ O	SrO	BaO	Total	An	Ab	Or
mount2-24-2	Core	62.7	0.0	23.0	bdl	0.2	4.4	7.7	1.3			99.2	22	70	8
mount2-24-3	Core	62.6	0.0	23.1	bdl	0.2	4.3	7.8	1.3			99.2	21	71	8
mount2-24-4	Rim	62.8	0.0	22.7	0.2	0.0	4.1	7.8	1.4			99.0	21	71	8
mount2-3-1	Rim	62.3	0.0	23.1	0.2	0.0	4.3	8.0	1.4			99.3	21	71	8
mount2-3-2	Core	62.2	0.0	23.3	bdl	0.2	4.5	7.9	1.3			99.4	22	70	8
mount2-3-3	Core	62.7	0.0	22.9	0.2	0.0	4.1	8.0	1.4			99.5	20	72	8
mount2-3-4	Core	62.7	0.0	22.6	0.2	0.0	4.0	8.0	1.5			99.0	20	71	9
mount2-4-1	Rim	62.7	0.0	23.0	0.2	0.0	4.1	8.0	1.5			99.6	20	71	9
mount2-4-2	Rim	62.8	0.0	23.1	bdl	0.2	4.0	8.0	1.4			99.6	20	72	8
mount2-4-3	Core	62.7	0.1	22.7	bdl	0.2	4.1	7.9	1.4			99.1	21	71	8
mount2-4-4	Core	63.1	0.0	22.9	bdl	0.2	3.9	8.0	1.5			99.7	19	72	9
mount2-5-1	Rim	62.7	0.0	23.0	bdl	0.2	4.4	7.9	1.3			99.4	22	71	8
mount2-5-2	Rim	62.8	0.0	23.0	bdl	0.2	4.3	8.0	1.3			99.5	21	71	7
mount2-5-3	Core	62.8	0.0	22.8	bdl	0.2	4.2	8.0	1.4			99.2	21	71	8
mount2-6-1	Rim	62.8	0.1	23.0	0.2	0.0	4.3	8.0	1.4			99.7	21	71	8
mount2-6-2	Core	62.8	0.0	22.9	bdl	0.2	4.3	7.9	1.3			99.4	21	71	8
mount2-6-3	Core	62.5	0.0	22.8	bdl	0.2	4.2	7.8	1.4			99.0	21	71	8
mount2-6-4	Core	62.5	0.1	23.2	0.2	0.0	4.4	7.9	1.3			99.5	22	71	8
mount2-6-5	Core	62.9	0.0	22.9	bdl	0.2	4.1	7.7	1.4			99.3	21	70	9
mount2-7-4	Core	60.9	0.0	24.3	bdl	0.2	5.9	7.5	0.9			99.7	29	66	5
mount2-9-1	Rim	61.8	0.0	23.0	bdl	0.2	4.5	7.5	1.2			98.2	23	70	7
mount2-9-2	Rim	61.3	0.1	24.0	0.2	0.0	5.4	7.4	0.9			99.3	27	67	6
mount2-9-3	Rim	61.1	0.0	23.9	bdl	0.2	5.3	7.4	0.9			98.8	27	68	6
mount2-9-4	Rim	62.3	0.1	23.2	0.2	0.0	4.5	7.8	1.3			99.2	22	70	7

Table A1.7: trace elements - plagioclase

Info	Position	Li ⁺	L ⁺	Na	Mg	Al	Si	P	K	Ca	Sc	Ti	V	Mn	Fe	Rb	Sr	Zr	Nb	Cs	Ba	La	Ce	Pr	Nd	Sm	Eu	Gd	Tb	Dy	
MFT-Mount1-plag2-1	Rim	15.6	14.2	58199	21.5	113908	299178	21.2	13295	26524	0.8	41.6	b.d.l.	6.6	1309.5	4.3	59.3	0.2	b.d.l.	b.d.l.	b.d.l.	58.4	19.6	20.6	1.5	39.0	0.3	1.5	0.2	0.0	0.1
MFT-Mount1-plag2-2	Rim	16.8	17.6	58359	24.8	113403	299178	28.0	12722	28755	0.8	40.0	b.d.l.	8.1	1354.9	4.4	56.5	0.2	b.d.l.	b.d.l.	b.d.l.	56.5	20.3	21.6	1.6	39.0	0.3	1.6	0.2	0.0	0.1
MFT-Mount1-plag2-3	Middle	20.6	19.7	59227	21.1	115060	299178	22.6	12947	27669	1.0	38.8	b.d.l.	7.8	1339.2	4.3	50.5	0.3	b.d.l.	b.d.l.	b.d.l.	57.3	19.6	21.6	1.5	38.0	0.4	1.6	0.2	0.0	0.1
MFT-Mount1-plag2-4	Middle	23.2	22.6	59569	19.4	112489	299178	19.0	13044	26772	b.d.l.	41.6	b.d.l.	7.7	1350.1	4.6	47.1	0.3	0.1	0.1	b.d.l.	50.3	18.9	19.8	1.4	38.0	0.4	1.4	0.1	0.0	0.1
MFT-Mount1-plag2-5	Middle	22.4	23.0	58812	19.0	113591	299178	b.d.l.	12793	26854	b.d.l.	42.0	b.d.l.	7.4	1250.0	4.2	45.8	0.2	b.d.l.	b.d.l.	b.d.l.	44.6	19.0	20.0	1.6	35.0	0.3	1.3	0.2	0.0	0.0
MFT-Mount1-plag2-6	Middle	24.2	22.7	59575	18.7	114298	299178	b.d.l.	13747	26836	0.8	36.5	b.d.l.	6.3	1294.5	4.6	45.8	0.2	b.d.l.	b.d.l.	b.d.l.	41.7	19.1	20.8	1.4	39.0	0.4	1.2	0.3	0.0	0.1
MFT-Mount1-plag2-7	Middle	25.1	23.2	58548	22.2	111512	299178	30.0	13282	26080	b.d.l.	39.5	b.d.l.	6.4	1249.3	4.5	44.2	0.3	b.d.l.	b.d.l.	b.d.l.	39.2	19.9	20.6	1.5	40.0	0.2	1.1	0.2	0.0	0.1
MFT-Mount1-plag2-8	Middle	22.1	22.4	58155	21.2	108886	299178	b.d.l.	13184	25353	b.d.l.	38.0	b.d.l.	6.7	1183.8	4.2	42.0	0.2	b.d.l.	b.d.l.	b.d.l.	37.6	18.9	19.9	1.3	35.0	0.2	1.2	0.2	b.d.l.	0.1
MFT-Mount1-plag2-9	Core	20.5	21.8	59561	18.8	111093	299178	b.d.l.	14195	24782	0.7	39.5	b.d.l.	6.3	1207.9	4.6	42.9	0.2	b.d.l.	b.d.l.	b.d.l.	35.7	19.2	20.0	1.3	33.0	0.2	1.2	0.2	b.d.l.	0.1
MFT-Mount1-plag2-10	Core	21.2	18.6	57182	24.2	111849	294503	19.4	13670	25527	0.6	37.7	b.d.l.	6.5	1201.5	4.4	42.8	0.2	b.d.l.	b.d.l.	b.d.l.	36.6	20.8	20.6	1.5	35.0	0.2	1.1	0.2	b.d.l.	b.d.l.
MFT-Mount1-plag2-11	Core	18.4	15.8	60315	16.9	109259	299178	b.d.l.	12845	26629	b.d.l.	40.2	b.d.l.	7.7	1278.1	4.2	45.1	0.3	b.d.l.	b.d.l.	b.d.l.	37.2	18.7	19.8	1.3	35.0	0.3	1.1	0.2	0.0	b.d.l.
MFT-Mount1-plag2-12	Core - close to crack	11.7	12.3	58791	16.2	108425	294503	b.d.l.	13704	24017	0.7	41.7	b.d.l.	6.5	1161.3	4.8	41.8	0.2	b.d.l.	b.d.l.	b.d.l.	37.3	19.6	20.3	1.4	34.0	0.2	1.2	0.1	0.0	0.0
MFT-Mount1-plag2-13	Core - close to crack	9.5	8.5	58802	24.3	109796	294503	23.3	13970	24334	0.9	39.1	b.d.l.	6.3	1164.9	4.7	42.3	0.2	b.d.l.	b.d.l.	b.d.l.	32.8	20.9	21.2	1.5	33.0	0.2	1.3	0.2	b.d.l.	0.1
MFT-Mount1-plag2-14	Core - close to crack	11.5	11.2	56671	19.2	110196	294503	b.d.l.	12742	27230	b.d.l.	44.7	b.d.l.	6.9	1289.4	4.2	43.2	0.2	b.d.l.	0.0	b.d.l.	34.3	19.4	21.2	1.4	40.0	0.3	1.1	0.1	b.d.l.	0.1
MFT-Mount1-plag2-15	Core - close to crack	b.d.l.	7.6	57014	21.5	114868	294503	b.d.l.	12938	27853	b.d.l.	43.6	b.d.l.	7.6	1335.2	4.3	44.1	0.2	0.2	0.1	b.d.l.	34.9	20.1	21.6	1.5	39.0	0.4	1.2	0.1	0.0	0.0
MFT-Mount1-plag2-16	Core - close to crack	8.9	8.9	60425	23.2	113072	294503	b.d.l.	12845	26629	b.d.l.	40.2	b.d.l.	7.7	1278.1	4.2	45.1	0.3	b.d.l.	b.d.l.	b.d.l.	37.1	19.8	21.2	1.5	41.0	0.4	1.2	0.1	b.d.l.	0.1
MFT-Mount1-plag2-17	Core	12.7	13.2	57695	20.2	105218	294503	b.d.l.	13013	26383	0.6	43.5	b.d.l.	7.3	1220.5	4.4	42.9	0.2	b.d.l.	b.d.l.	b.d.l.	39.1	18.6	20.1	1.4	36.0	0.3	1.1	0.1	0.0	0.1
MFT-Mount1-plag2-18	Core	15.5	15.1	59037	19.0	111579	294503	b.d.l.	13549	26209	b.d.l.	43.2	b.d.l.	6.9	1272.2	4.5	44.7	0.2	b.d.l.	b.d.l.	b.d.l.	37.8	19.1	20.1	1.4	39.0	0.2	1.3	0.2	0.0	0.1
MFT-Mount1-plag2-19	Core	15.6	16.7	60618	21.1	110994	294503	b.d.l.	13078	26656	b.d.l.	44.5	b.d.l.	7.4	1286.6	4.4	45.2	0.2	b.d.l.	b.d.l.	b.d.l.	38.2	19.4	20.4	1.4	36.0	0.3	1.2	0.2	b.d.l.	0.1
MFT-Mount1-plag2-20	Core	18.5	17.3	58637	22.9	111981	294503	b.d.l.	12989	26218	0.7	47.9	b.d.l.	7.9	1294.6	4.1	45.7	0.2	b.d.l.	b.d.l.	b.d.l.	37.7	19.4	21.1	1.5	37.0	0.3	1.3	0.3	b.d.l.	0.1
MFT-Mount1-plag2-21	Core	18.3	18.4	57672	22.2	109706	294503	b.d.l.	12243	27614	0.6	41.2	b.d.l.	7.8	1268.5	4.1	45.1	0.2	b.d.l.	b.d.l.	b.d.l.	37.6	20.1	21.9	1.5	40.0	0.3	1.2	0.2	0.0	0.1
MFT-Mount1-plag2-22	Core	21.0	19.4	57897	24.3	111891	294503	34.4	11878	28731	b.d.l.	47.1	b.d.l.	8.1	1286.5	4.0	46.5	0.3	b.d.l.	b.d.l.	b.d.l.	34.8	20.3	23.2	1.6	40.0	0.4	1.3	0.2	0.0	0.1
MFT-Mount1-plag2-23	Core	22.9	19.6	57392	25.0	113386	294503	26.0	11614	29070	0.7	50.2	b.d.l.	8.4	1311.1	3.8	43.9	0.3	b.d.l.	b.d.l.	b.d.l.	33.3	21.2	23.2	1.6	42.0	0.3	1.2	0.2	b.d.l.	b.d.l.
MFT-Mount1-plag2-24	Core	18.0	18.3	59585	25.5	111275	294503	b.d.l.	11661	29058	0.6	41.7	b.d.l.	8.7	1315.6	3.6	40.7	0.3	b.d.l.	b.d.l.	b.d.l.	29.0	19.8	22.2	1.5	39.0	0.2	1.2	0.3	0.0	0.1
MFT-Mount1-plag2-25	Core	22.3	18.9	57376	20.9	108375	294503	18.7	11381	27663	0.6	43.2	b.d.l.	7.9	1330.3	3.6	37.6	0.3	b.d.l.	b.d.l.	b.d.l.	27.6	19.4	21.9	1.6	42.0	0.3	1.1	0.1	0.0	0.1
MFT-Mount1-plag2-26	Core	21.3	19.8	59505	25.3	114514	294503	24.0	11829	28712	b.d.l.	47.9	b.d.l.	8.1	1333.4	3.9	37.9	0.3	b.d.l.	b.d.l.	b.d.l.	28.2	20.5	22.6	1.6	40.0	0.3	1.1	0.2	b.d.l.	b.d.l.
MFT-Mount1-plag2-27	Middle	20.8	19.9	59834	16.7	113759	294503	19.7	13240	27843	b.d.l.	45.0	b.d.l.	7.6	1262.4	3.9	38.5	0.2	b.d.l.	b.d.l.	b.d.l.	31.2	20.7	22.3	1.7	39.0	0.5	1.1	0.1	0.0	b.d.l.
MFT-Mount1-plag2-28	Middle	23.0	21.3	59051	21.4	113628	299178	b.d.l.	12739	28083	b.d.l.	44.4	b.d.l.	8.2	1336.0	3.8	39.6	0.3	b.d.l.	b.d.l.	b.d.l.	35.7	21.3	23.4	1.6	43.0	0.4	1.2	0.2	0.0	0.0
MFT-Mount1-plag2-29	Middle	21.0	19.6	57279	27.2	108434	294503	b.d.l.	11646	26736	0.9	41.4	b.d.l.	8.0	1275.2	3.5	39.5	0.3	b.d.l.	b.d.l.	b.d.l.	34.7	20.0	22.1	1.6	40.0	0.2	1.0	0.2	0.0	0.1
MFT-Mount1-plag2-30	Middle	16.1	16.5	59916	21.1	113990	294503	b.d.l.	12766	28061	b.d.l.	40.9	b.d.l.	7.7	1305.1	4.0	39.9	0.2	b.d.l.	b.d.l.	b.d.l.	40.4	21.3	23.0	1.6	43.0	0.4	1.2	0.3	0.0	0.0
MFT-Mount1-plag2-31	Middle - close to crack	b.d.l.	8.0	57093	17.0	105850	294503	b.d.l.	13353	23538	0.8	36.2	b.d.l.	6.2	1199.1	4.8	34.7	0.2	b.d.l.	b.d.l.	b.d.l.	40.9	19.8	19.5	1.4	34.0	0.2	1.0	0.1	b.d.l.	0.1
MFT-Mount1-plag2-32	Middle - close to crack	b.d.l.	6.4	57510	20.6	108550	294503	b.d.l.	14661	33020	b.d.l.	38.3	b.d.l.	6.9	1235.8	6.4	35.7	0.3	0.4	0.1	b.d.l.	43.9	18.8	18.8	1.2	28.0	0.2	1.0	0.1	b.d.l.	0.1
MFT-Mount1-plag2-33	Middle - close to crack	b.d.l.	5.9	59916	19.2	108975	294503	b.d.l.	13185	26503	0.8	40.8	b.d.l.	8.0	1270.2	5.6	38.7	0.4	0.3	0.2	b.d.l.	35.8	19.4	20.1	1.3	39.0	0.3	1.2	b.d.l.	0.0	0.1
grain3-1	Rim	b.d.l.	7.2	57290	18.2	114577	289829	26.7	10005	31303	0.9	71.7	b.d.l.	8.6	1313.0	3.5	62.1	0.3	b.d.l.	b.d.l.	b.d.l.	97.9	27.3	30.3	2.2	56.0	0.5	1.6	0.3	0.0	0.1
grain3-2	Rim	14.7	12.1	57563	18.4	113364	289829	b.d.l.	10265	29712	0.8	63.9	b.d.l.	8.7	1252.5	3.2	60.8	0.2	b.d.l.	b.d.l.	b.d.l.	109.9	25.6	28.2	2.1	52.0	0.5	1.6	0.2	0.0	0.1
grain3-3	Rim	19.5	17.9	57531	24.5	114450	289829	b.d.l.	10050	31362	b.d.l.	65.2	b.d.l.	8.9	1285.8	3.1	63.7	0.3	b.d.l.	b.d.l.	b.d.l.	127.6	26.4	29.4	2.1	52.0	0.6	1.6	0.2	0.0	0.1
grain3-4	Middle	21.3	21.6	56143	22.5	111753	289829	34.0	10266	29764	1.2	57.3	b.d.l.	8.7	1255.6	3.2	64.0	0.3	b.d.l.	0.0	b.d.l.	135.4	25.2	28.7	2.0	55.0	0.4	1.6	0.2	0.0	0.1
grain3-5	Middle	24.6	23.2	55851	20.5	111106	289829	27.8	9944	30585	b.d.l.	64.3	b.d.l.	8.6	1300.5	3.0	66.6	0.3	b.d.l.	b.d.l.	b.d.l.	147.7									

Table A1.7: continued

Ho	Er	Tm	Yb	Lu	Hf	Ta	Pb	Th	U
0.0	0.0	b.d.l.	b.d.l.	b.d.l.	b.d.l.	b.d.l.	17.2	b.d.l.	b.d.l.
0.0	0.0	0.0	b.d.l.	b.d.l.	b.d.l.	b.d.l.	16.9	b.d.l.	b.d.l.
0.0	b.d.l.	b.d.l.	b.d.l.	b.d.l.	b.d.l.	b.d.l.	16.8	b.d.l.	b.d.l.
b.d.l.	0.0	0.0	0.0	b.d.l.	b.d.l.	b.d.l.	16.4	0.0	b.d.l.
0.0	0.0	0.0	b.d.l.	0.0	b.d.l.	b.d.l.	16.3	b.d.l.	0.0
b.d.l.	0.0	b.d.l.	b.d.l.	b.d.l.	b.d.l.	b.d.l.	16.7	b.d.l.	b.d.l.
0.0	b.d.l.	b.d.l.	b.d.l.	b.d.l.	b.d.l.	b.d.l.	16.4	b.d.l.	b.d.l.
0.0	0.0	0.0	b.d.l.	b.d.l.	b.d.l.	b.d.l.	15.8	b.d.l.	b.d.l.
0.0	b.d.l.	b.d.l.	b.d.l.	b.d.l.	b.d.l.	b.d.l.	15.8	b.d.l.	b.d.l.
b.d.l.	b.d.l.	b.d.l.	b.d.l.	b.d.l.	0.0	b.d.l.	16.8	b.d.l.	b.d.l.
0.0	b.d.l.	0.0	b.d.l.	b.d.l.	b.d.l.	b.d.l.	16.4	b.d.l.	b.d.l.
0.0	0.0	0.0	b.d.l.	b.d.l.	b.d.l.	b.d.l.	16.1	b.d.l.	b.d.l.
0.0	b.d.l.	b.d.l.	b.d.l.	b.d.l.	b.d.l.	b.d.l.	15.8	b.d.l.	b.d.l.
0.0	0.0	b.d.l.	b.d.l.	b.d.l.	b.d.l.	b.d.l.	16.5	b.d.l.	b.d.l.
0.0	0.1	b.d.l.	b.d.l.	0.0	b.d.l.	0.0	17.4	0.0	b.d.l.
0.0	0.0	b.d.l.	b.d.l.	b.d.l.	b.d.l.	b.d.l.	16.3	b.d.l.	b.d.l.
0.0	0.0	b.d.l.	0.0	b.d.l.	b.d.l.	b.d.l.	15.3	b.d.l.	b.d.l.
b.d.l.	b.d.l.	b.d.l.	b.d.l.	b.d.l.	b.d.l.	b.d.l.	16.7	b.d.l.	b.d.l.
0.0	0.0	b.d.l.	b.d.l.	b.d.l.	b.d.l.	b.d.l.	15.9	b.d.l.	b.d.l.
0.0	b.d.l.	b.d.l.	b.d.l.	b.d.l.	b.d.l.	b.d.l.	16.4	b.d.l.	b.d.l.
b.d.l.	0.0	b.d.l.	0.0	b.d.l.	b.d.l.	b.d.l.	16.0	b.d.l.	b.d.l.
0.0	0.0	b.d.l.	b.d.l.	b.d.l.	b.d.l.	b.d.l.	17.0	0.0	b.d.l.
b.d.l.	0.0	b.d.l.	b.d.l.	b.d.l.	b.d.l.	b.d.l.	17.1	b.d.l.	b.d.l.
0.0	b.d.l.	b.d.l.	b.d.l.	b.d.l.	b.d.l.	b.d.l.	15.9	b.d.l.	b.d.l.
b.d.l.	0.0	b.d.l.	b.d.l.	0.0	b.d.l.	b.d.l.	16.7	b.d.l.	b.d.l.
0.0	b.d.l.	b.d.l.	b.d.l.	0.0	b.d.l.	b.d.l.	17.3	b.d.l.	b.d.l.
0.0	0.0	b.d.l.	b.d.l.	b.d.l.	b.d.l.	b.d.l.	17.2	b.d.l.	b.d.l.
0.0	0.0	0.0	b.d.l.	b.d.l.	b.d.l.	b.d.l.	16.9	0.0	b.d.l.
b.d.l.	0.0	b.d.l.	0.0	b.d.l.	b.d.l.	b.d.l.	16.2	b.d.l.	b.d.l.
0.0	b.d.l.	b.d.l.	b.d.l.	b.d.l.	b.d.l.	b.d.l.	17.6	b.d.l.	b.d.l.
0.0	0.0	b.d.l.	b.d.l.	0.0	b.d.l.	b.d.l.	16.0	b.d.l.	b.d.l.
b.d.l.	0.0	b.d.l.	0.0	b.d.l.	0.0	b.d.l.	16.2	0.0	0.0
0.0	0.0	b.d.l.	b.d.l.	b.d.l.	0.0	b.d.l.	17.2	0.1	0.0
b.d.l.	0.0	b.d.l.	b.d.l.	b.d.l.	b.d.l.	b.d.l.	16.1	b.d.l.	b.d.l.
0.0	b.d.l.	b.d.l.	b.d.l.	b.d.l.	b.d.l.	b.d.l.	15.9	0.0	b.d.l.
b.d.l.	b.d.l.	b.d.l.	b.d.l.	b.d.l.	b.d.l.	b.d.l.	15.3	0.0	b.d.l.
0.0	0.0	b.d.l.	0.0	b.d.l.	b.d.l.	b.d.l.	15.2	b.d.l.	b.d.l.
0.0	0.0	0.0	b.d.l.	0.0	b.d.l.	b.d.l.	15.2	b.d.l.	b.d.l.
0.0	b.d.l.	b.d.l.	b.d.l.	b.d.l.	0.0	b.d.l.	15.7	0.0	b.d.l.
0.0	b.d.l.	b.d.l.	b.d.l.	b.d.l.	b.d.l.	b.d.l.	15.8	b.d.l.	b.d.l.
0.0	0.0	b.d.l.	b.d.l.	b.d.l.	b.d.l.	b.d.l.	16.6	b.d.l.	0.0
b.d.l.	0.0	b.d.l.	b.d.l.	b.d.l.	b.d.l.	b.d.l.	16.0	b.d.l.	b.d.l.
b.d.l.	0.0	b.d.l.	0.0	b.d.l.	b.d.l.	b.d.l.	16.1	b.d.l.	b.d.l.
b.d.l.	0.0	b.d.l.	0.0	b.d.l.	b.d.l.	b.d.l.	15.7	0.0	b.d.l.
0.0	b.d.l.	b.d.l.	b.d.l.	b.d.l.	b.d.l.	b.d.l.	16.1	b.d.l.	b.d.l.
0.0	b.d.l.	b.d.l.	b.d.l.	b.d.l.	b.d.l.	b.d.l.	15.5	b.d.l.	0.0
b.d.l.	0.0	b.d.l.	b.d.l.	b.d.l.	b.d.l.	b.d.l.	16.3	b.d.l.	b.d.l.
0.0	0.0	0.0	b.d.l.	b.d.l.	b.d.l.	b.d.l.	15.5	b.d.l.	b.d.l.
0.0	b.d.l.	b.d.l.	b.d.l.	b.d.l.	b.d.l.	b.d.l.	15.7	b.d.l.	b.d.l.
0.0	0.0	b.d.l.	b.d.l.	b.d.l.	b.d.l.	b.d.l.	16.1	b.d.l.	b.d.l.
0.0	0.0	b.d.l.	b.d.l.	b.d.l.	b.d.l.	b.d.l.	16.8	b.d.l.	b.d.l.
0.0	0.0	b.d.l.	0.0	b.d.l.	b.d.l.	b.d.l.	15.6	b.d.l.	b.d.l.
0.0	b.d.l.	b.d.l.	0.0	b.d.l.	b.d.l.	b.d.l.	15.9	b.d.l.	b.d.l.

Table A1.7: continued

Info	Position	Li ⁶	Li ⁷	Na	Mg	Al	Si	P	K	Ca	Sc	Ti	V	Mn	Fe	Rb	Sr	Y	Zr	Nb	Cs	Ba	La	Ce	Pr	Nd	Sm	Eu	Gd	Tb	Dy	
grain3-22	Core	17.9	17.8	58500	24.6	116683	289829	b.d.l.	9692	29028	b.d.l.	653	b.d.l.	9.3	1425.5	30	67.9	0.3	b.d.l.	b.d.l.	b.d.l.	b.d.l.	126.5	27.4	29.1	22.5	4.4	1.6	b.d.l.	0.0	0.1	
grain3-23	Core	18.6	18.2	58060	26.7	116260	294503	31.5	10449	29021	b.d.l.	60.7	b.d.l.	8.3	1468.9	33	68.7	0.3	b.d.l.	b.d.l.	b.d.l.	b.d.l.	118.4	25.9	29.2	21.1	4.9	0.5	1.6	0.2	0.0	
grain3-24	Core	19.1	18.4	58118	26.0	116545	289829	b.d.l.	9962	31932	0.7	57.4	b.d.l.	9.9	1505.5	30	68.1	0.3	b.d.l.	0.0	b.d.l.	0.0	104.5	28.0	30.9	22.2	5.7	0.7	1.6	b.d.l.	0.0	
grain3-25	Core	17.3	17.6	58225	24.1	114582	289829	b.d.l.	10269	29357	b.d.l.	56.3	b.d.l.	10.2	1458.9	33	63.3	0.3	b.d.l.	b.d.l.	b.d.l.	b.d.l.	88.2	25.3	28.3	20.2	5.2	0.4	1.6	0.3	0.0	
grain3-26	Core	17.4	17.4	56572	25.3	113790	289829	30.8	10418	30735	b.d.l.	57.3	b.d.l.	8.6	1379.0	33	61.0	0.4	b.d.l.	b.d.l.	b.d.l.	b.d.l.	80.3	25.7	27.8	21.1	5.8	0.6	1.5	b.d.l.	0.1	
grain3-27	Core	20.6	17.7	57863	25.4	115300	289829	22.0	10938	29669	b.d.l.	58.0	b.d.l.	8.7	1502.9	33	57.6	0.3	b.d.l.	b.d.l.	b.d.l.	b.d.l.	72.6	26.4	28.9	20.5	5.7	0.7	1.5	0.3	0.0	
grain3-28	Core	16.6	18.1	57711	30.6	112598	294503	19.9	10713	29672	0.7	55.7	b.d.l.	8.9	1431.2	33	54.0	0.4	b.d.l.	b.d.l.	b.d.l.	b.d.l.	47.1	25.1	27.2	18.1	4.6	0.4	1.3	0.2	0.0	
grain3-29	Core	20.1	18.1	57870	27.9	114253	294503	b.d.l.	10684	29027	b.d.l.	58.3	b.d.l.	8.9	1459.5	33	49.9	0.3	b.d.l.	b.d.l.	b.d.l.	b.d.l.	58.5	24.7	27.1	21.1	4.6	0.5	1.4	0.2	0.0	
grain3-30	Core	23.0	18.8	57687	27.8	115771	294503	23.3	10787	29647	b.d.l.	54.5	b.d.l.	8.9	1478.3	33	49.3	0.3	b.d.l.	b.d.l.	b.d.l.	b.d.l.	52.4	25.6	27.2	20.5	4.4	1.3	0.2	0.0	0.1	
grain3-31	Core	20.0	19.3	59116	28.0	111094	294503	22.2	10384	30158	b.d.l.	55.3	b.d.l.	8.7	1475.3	33	45.5	0.3	b.d.l.	b.d.l.	b.d.l.	b.d.l.	45.0	24.6	27.1	19.1	4.9	0.1	1.1	0.3	b.d.l.	0.1
grain3-32	Core	19.4	15.7	57010	24.4	110812	294503	b.d.l.	10614	29150	b.d.l.	44.5	0.1	8.0	1353.1	33	43.1	0.3	b.d.l.	b.d.l.	b.d.l.	b.d.l.	34.7	23.3	25.9	18.1	5.2	0.5	1.1	0.3	b.d.l.	0.1
grain3-33	Core	12.6	10.6	57660	25.2	113329	294503	20.1	11079	28545	0.8	48.8	b.d.l.	7.6	1338.3	33	42.7	0.3	b.d.l.	b.d.l.	b.d.l.	b.d.l.	25.5	21.8	24.3	17.4	4.2	0.4	1.1	0.2	0.0	0.1
grain3-34	Core	21.2	20.1	57510	25.1	111785	294503	b.d.l.	10946	26732	b.d.l.	40.8	b.d.l.	7.5	1372.5	38	43.0	0.3	b.d.l.	b.d.l.	b.d.l.	b.d.l.	20.2	20.7	22.2	15.3	3.7	0.4	1.2	0.2	0.0	
grain3-35	Core	22.1	21.1	58557	22.5	114450	294503	27.4	12488	26818	b.d.l.	46.1	b.d.l.	7.4	1288.2	44	65.1	0.2	0.2	0.0	b.d.l.	b.d.l.	21.9	20.3	22.1	15.1	4.1	0.4	1.2	0.2	0.0	
grain3-36	Core	20.8	19.7	58428	24.0	113040	294503	b.d.l.	11613	27877	b.d.l.	41.3	b.d.l.	7.3	1285.8	42	46.1	0.3	b.d.l.	b.d.l.	b.d.l.	b.d.l.	20.7	20.2	21.9	17.4	4.2	0.4	1.2	b.d.l.	0.0	
grain3-37	Core	21.7	18.8	59277	15.3	111550	294503	22.6	13130	24144	0.8	46.1	b.d.l.	6.4	1243.1	47	50.1	0.2	b.d.l.	b.d.l.	b.d.l.	b.d.l.	28.1	20.0	20.0	14.1	3.4	0.1	0.0	0.0	0.0	
grain3-38	Core	20.9	18.9	58075	24.1	112884	294503	22.1	11393	27331	b.d.l.	43.9	b.d.l.	7.8	1296.5	44	53.2	0.2	b.d.l.	b.d.l.	b.d.l.	b.d.l.	24.1	20.9	22.9	15.1	4.2	0.3	1.3	0.1	0.0	
grain3-39	Core	16.4	18.4	58768	20.9	114131	294503	21.1	11692	27430	b.d.l.	45.7	b.d.l.	7.2	1274.2	41	56.4	0.2	b.d.l.	b.d.l.	b.d.l.	b.d.l.	35.6	20.8	22.6	16.4	4.0	0.5	1.4	0.2	0.0	
grain3-40	Core	16.6	15.3	58920	22.2	115219	294503	33.5	12793	26563	b.d.l.	50.9	b.d.l.	6.4	1282.2	44	61.4	0.2	b.d.l.	b.d.l.	b.d.l.	b.d.l.	49.9	19.1	20.2	15.3	3.4	0.3	1.6	b.d.l.	0.0	
grain3-41	Core - close to crack	b.d.l.	11.5	57801	17.6	112435	294503	b.d.l.	12488	26818	b.d.l.	46.1	b.d.l.	7.4	1288.2	44	65.1	0.2	0.2	0.0	b.d.l.	b.d.l.	71.5	19.5	21.7	15.1	3.9	0.5	1.7	b.d.l.	0.0	
grain3-42	Core - close to crack	b.d.l.	8.2	59246	22.1	110979	294503	20.0	12973	26679	0.8	44.7	b.d.l.	7.0	1277.0	48	68.6	0.2	b.d.l.	b.d.l.	b.d.l.	b.d.l.	98.3	19.8	21.2	16.3	3.7	0.4	1.7	0.1	b.d.l.	0.0
grain3-43	Core - close to crack	b.d.l.	9.8	56673	23.7	111341	294503	20.6	12395	25986	0.6	45.5	b.d.l.	6.5	1274.5	41	67.9	0.2	b.d.l.	b.d.l.	b.d.l.	b.d.l.	123.2	20.3	21.5	16.1	3.9	0.3	1.8	0.2	0.0	
grain3-44	Core	14.6	13.4	58802	19.6	114592	294503	b.d.l.	12637	27224	1.1	49.9	b.d.l.	7.1	1356.4	41	71.8	0.2	b.d.l.	b.d.l.	b.d.l.	b.d.l.	136.6	20.8	23.6	17.1	3.9	0.5	2.1	0.2	0.0	
grain3-45	Core	18.9	18.3	60342	16.3	117061	294503	b.d.l.	13007	26969	b.d.l.	48.3	b.d.l.	7.5	1309.1	44	67.1	0.2	b.d.l.	b.d.l.	b.d.l.	b.d.l.	134.3	20.5	21.7	16.4	4.4	0.2	2.0	0.3	b.d.l.	0.1
grain3-46	Middle	23.8	20.4	60269	21.0	110039	294503	b.d.l.	12584	27129	b.d.l.	43.0	b.d.l.	7.3	1307.8	42	61.5	0.2	b.d.l.	b.d.l.	b.d.l.	b.d.l.	0.0	0.0	0.0	0.0	0.0	0.0	0.0	0.0	0.0	0.0
grain3-47	Middle	22.1	20.4	58324	25.5	112027	294503	b.d.l.	13027	25852	b.d.l.	48.4	b.d.l.	7.2	1280.0	46	59.8	0.2	b.d.l.	b.d.l.	b.d.l.	b.d.l.	98.6	20.1	21.3	16.1	4.1	0.4	1.9	0.3	0.0	
grain3-48	Middle	20.1	21.6	59363	18.2	112823	294503	b.d.l.	13125	25748	b.d.l.	42.2	b.d.l.	7.2	1254.9	47	58.6	0.2	b.d.l.	b.d.l.	b.d.l.	b.d.l.	63.7	18.7	20.0	14.3	3.6	0.3	1.6	0.2	0.0	
grain3-49	Middle	20.9	21.9	60743	11.1	116838	299178	b.d.l.	13050	26683	b.d.l.	44.3	b.d.l.	7.7	1323.0	49	61.0	0.2	0.1	0.1	b.d.l.	b.d.l.	0.1	0.1	0.1	0.1	0.1	0.1	0.1	0.1	0.1	
grain3-50	Middle	24.7	22.5	59117	18.6	113847	299178	b.d.l.	13847	27324	b.d.l.	43.1	b.d.l.	6.7	1382.3	53	68.0	0.3	0.1	0.1	b.d.l.	b.d.l.	83.3	18.5	20.2	14.1	3.4	0.4	1.9	b.d.l.	0.0	
grain3-51	Middle	23.4	21.8	56950	15.6	112134	294503	29.5	12651	26651	b.d.l.	39.0	b.d.l.	7.2	1254.0	44	66.7	0.3	b.d.l.	b.d.l.	b.d.l.	b.d.l.	115.3	18.8	20.7	14.3	3.8	0.4	1.9	0.2	0.0	
grain3-52	Middle	18.3	20.5	57426	19.9	111510	294503	b.d.l.	13385	25963	b.d.l.	43.0	b.d.l.	7.0	1179.6	48	68.0	0.2	b.d.l.	b.d.l.	b.d.l.	b.d.l.	88.7	17.9	19.6	14.1	3.4	0.3	1.8	0.2	0.0	
Mount1-plag4-1	Rim	15.4	16.7	57340	22.0	107312	294503	24.4	12953	25570	b.d.l.	36.0	b.d.l.	6.7	1209.5	47	85.2	0.2	b.d.l.	b.d.l.	b.d.l.	b.d.l.	89.9	17.6	18.7	14.1	3.4	0.4	2.1	0.2	0.0	
Mount1-plag4-2	Middle	18.8	19.6	56789	25.1	115129	289829	22.6	9599	32231	b.d.l.	56.4	b.d.l.	9.6	1432.0	29	94.2	0.4	b.d.l.	b.d.l.	b.d.l.	b.d.l.	130.4	26.6	30.2	22.2	5.6	0.5	1.9	0.4	0.0	
Mount1-plag4-3	Middle	20.8	19.1	55934	22.0	115438	289829	b.d.l.	9956	32313	b.d.l.	54.6	b.d.l.	9.0	1381.4	29	90.7	0.3	b.d.l.	b.d.l.	b.d.l.	b.d.l.	112.3	25.3	28.0	21.1	5.7	0.4	1.9	b.d.l.	0.1	
Mount1-plag4-4	Core	18.9	18.5	56705	26.8	114819	289829	b.d.l.	9963	30125	b.d.l.	60.9	b.d.l.	9.0	1418.0	32	98.0	0.3	b.d.l.	b.d.l.	b.d.l.	b.d.l.	140.9	26.1	29.3	21.1	5.5	0.3	2.1	0.2	0.0	
Mount1-plag4-5	Core	17.9	18.5	56165	27.5	114957	289829	b.d.l.	9824	30567	b.d.l.	50.6	b.d.l.	9.1	1425.6	29	98.5	0.3	b.d.l.	b.d.l.	b.d.l.	b.d.l.	141.4	26.3	29.1	22.2	5.5	0.4	2.1	0.3	0.0	
Mount1-plag4-6	Core	17.8	18.4	56900	23.0	113268	289829	32.5	10099	29425	b.d.l.	54.7	b.d.l.	9.7	1441.5	31	95.8	0.3	b.d.l.	b.d.l.	b.d.l.	b.d.l.	135.8	25.6	28.9	21.1	5.4	0.4	2.1	0.3	0.0	
Mount1-plag4-7	Core	20.7	18.9	55643	22.3	112441	289829	b.d.l.	9940	30785	0.9	50.9	b.d.l.	8.9	1426.8	30	94.7	0.3	b.d.l.	b.d.l.	b.d.l.	b.d.l.	124.0	26.0	28.9	20.5	4.4	0.5	2.1	0.3	0.0	
Mount1-plag4-8	Core	19.2	18.5	58030																												

Table A1.7: continued

Ho	Er	Tm	Yb	Lu	Hf	Ta	Pb	Th	U
0.0	0.0	b.d.l.	b.d.l.	b.d.l.	b.d.l.	b.d.l.	15.4	b.d.l.	0.0
0.0	0.0	0.0	b.d.l.	b.d.l.	0.0	b.d.l.	16.5	b.d.l.	b.d.l.
0.0	b.d.l.	b.d.l.	0.0	b.d.l.	b.d.l.	b.d.l.	16.6	b.d.l.	b.d.l.
b.d.l.	0.0	0.0	b.d.l.	b.d.l.	b.d.l.	b.d.l.	16.2	b.d.l.	b.d.l.
b.d.l.	b.d.l.	b.d.l.	b.d.l.	b.d.l.	b.d.l.	0.0	15.7	b.d.l.	b.d.l.
0.0	0.0	0.0	b.d.l.	b.d.l.	b.d.l.	b.d.l.	15.9	b.d.l.	b.d.l.
b.d.l.	b.d.l.	b.d.l.	b.d.l.	b.d.l.	b.d.l.	b.d.l.	16.4	b.d.l.	b.d.l.
0.0	0.0	b.d.l.	b.d.l.	b.d.l.	b.d.l.	b.d.l.	16.1	b.d.l.	b.d.l.
0.0	b.d.l.	b.d.l.	b.d.l.	b.d.l.	b.d.l.	b.d.l.	16.8	b.d.l.	b.d.l.
0.0	0.0	b.d.l.	b.d.l.	b.d.l.	b.d.l.	b.d.l.	16.8	b.d.l.	b.d.l.
0.0	0.0	b.d.l.	b.d.l.	b.d.l.	b.d.l.	b.d.l.	16.3	b.d.l.	b.d.l.
b.d.l.	0.0	b.d.l.	b.d.l.	b.d.l.	b.d.l.	b.d.l.	16.2	b.d.l.	0.0
0.0	b.d.l.	b.d.l.	b.d.l.	b.d.l.	b.d.l.	b.d.l.	15.8	b.d.l.	b.d.l.
0.0	b.d.l.	0.0	b.d.l.	b.d.l.	b.d.l.	b.d.l.	16.7	b.d.l.	0.0
0.0	b.d.l.	0.0	b.d.l.	0.0	b.d.l.	b.d.l.	16.7	b.d.l.	b.d.l.
0.0	0.0	b.d.l.	b.d.l.	b.d.l.	b.d.l.	b.d.l.	15.2	b.d.l.	0.0
b.d.l.	b.d.l.	b.d.l.	b.d.l.	b.d.l.	b.d.l.	b.d.l.	16.0	b.d.l.	b.d.l.
b.d.l.	0.0	b.d.l.	b.d.l.	b.d.l.	b.d.l.	b.d.l.	16.3	0.0	b.d.l.
0.0	0.0	b.d.l.	b.d.l.	b.d.l.	b.d.l.	b.d.l.	15.6	0.0	b.d.l.
0.0	0.0	0.0	0.0	b.d.l.	0.0	b.d.l.	16.3	0.0	b.d.l.
b.d.l.	0.0	b.d.l.	0.0	b.d.l.	0.0	b.d.l.	17.4	b.d.l.	b.d.l.
b.d.l.	0.0	b.d.l.	b.d.l.	b.d.l.	b.d.l.	b.d.l.	15.9	b.d.l.	b.d.l.
b.d.l.	b.d.l.	b.d.l.	0.0	b.d.l.	b.d.l.	b.d.l.	16.4	b.d.l.	b.d.l.
0.0	b.d.l.	b.d.l.	0.0	b.d.l.	b.d.l.	b.d.l.	16.3	b.d.l.	b.d.l.
b.d.l.	0.0	b.d.l.	b.d.l.	b.d.l.	b.d.l.	b.d.l.	16.2	0.0	b.d.l.
0.0	0.0	b.d.l.	b.d.l.	b.d.l.	b.d.l.	b.d.l.	17.0	0.0	b.d.l.
0.0	0.0	b.d.l.	b.d.l.	b.d.l.	b.d.l.	b.d.l.	15.8	b.d.l.	b.d.l.
0.0	0.0	b.d.l.	0.0	0.0	b.d.l.	b.d.l.	16.3	0.0	0.0
b.d.l.	b.d.l.	b.d.l.	b.d.l.	b.d.l.	b.d.l.	b.d.l.	16.8	0.0	b.d.l.
b.d.l.	b.d.l.	b.d.l.	b.d.l.	b.d.l.	b.d.l.	b.d.l.	15.8	b.d.l.	b.d.l.
0.0	b.d.l.	b.d.l.	0.0	b.d.l.	b.d.l.	b.d.l.	16.3	b.d.l.	b.d.l.
b.d.l.	b.d.l.	0.0	b.d.l.	0.0	b.d.l.	b.d.l.	15.1	0.0	b.d.l.
0.0	b.d.l.	b.d.l.	0.0	b.d.l.	b.d.l.	b.d.l.	16.3	b.d.l.	b.d.l.
0.0	0.0	b.d.l.	b.d.l.	b.d.l.	b.d.l.	b.d.l.	15.0	b.d.l.	0.0
b.d.l.	0.0	b.d.l.	b.d.l.	b.d.l.	b.d.l.	b.d.l.	15.0	b.d.l.	b.d.l.
0.0	0.0	b.d.l.	b.d.l.	b.d.l.	b.d.l.	b.d.l.	15.1	b.d.l.	b.d.l.
0.0	b.d.l.	0.0	b.d.l.	b.d.l.	b.d.l.	b.d.l.	15.3	b.d.l.	b.d.l.
0.0	0.0	b.d.l.	0.0	b.d.l.	b.d.l.	b.d.l.	14.9	b.d.l.	0.0
b.d.l.	b.d.l.	0.0	0.0	b.d.l.	b.d.l.	b.d.l.	14.8	b.d.l.	b.d.l.
b.d.l.	0.0	0.0	b.d.l.	b.d.l.	b.d.l.	b.d.l.	15.4	b.d.l.	b.d.l.
0.0	0.0	b.d.l.	b.d.l.	b.d.l.	b.d.l.	b.d.l.	15.1	b.d.l.	b.d.l.
0.0	0.0	b.d.l.	b.d.l.	b.d.l.	b.d.l.	b.d.l.	16.2	b.d.l.	0.0
0.0	b.d.l.	b.d.l.	b.d.l.	b.d.l.	b.d.l.	b.d.l.	15.1	b.d.l.	b.d.l.
0.0	0.0	b.d.l.	b.d.l.	b.d.l.	b.d.l.	b.d.l.	15.7	b.d.l.	b.d.l.
0.0	b.d.l.	b.d.l.	b.d.l.	b.d.l.	b.d.l.	b.d.l.	14.7	b.d.l.	b.d.l.
0.0	0.0	b.d.l.	b.d.l.	b.d.l.	b.d.l.	b.d.l.	15.2	0.0	0.0
0.0	0.0	b.d.l.	0.0	b.d.l.	0.0	b.d.l.	15.2	b.d.l.	b.d.l.
b.d.l.	0.0	b.d.l.	b.d.l.	b.d.l.	b.d.l.	b.d.l.	15.1	b.d.l.	b.d.l.
0.0	0.0	b.d.l.	b.d.l.	b.d.l.	b.d.l.	b.d.l.	15.2	b.d.l.	b.d.l.
b.d.l.	0.0	0.0	b.d.l.	b.d.l.	b.d.l.	b.d.l.	15.0	b.d.l.	b.d.l.
0.0	0.0	b.d.l.	b.d.l.	b.d.l.	b.d.l.	b.d.l.	14.9	b.d.l.	b.d.l.
b.d.l.	0.0	b.d.l.	b.d.l.	b.d.l.	0.0	b.d.l.	14.6	b.d.l.	b.d.l.

Table A1.7: continued

Info	Position	Li ⁶	Li ⁷	Na	Mg	Al	Si	P	K	Ca	Sc	Ti	V	Mn	Fe	Rb	Sr	Y	Zr	Nb	Cs	Ba	La	Ce	Pr	Nd	Sm	Eu	Gd	Tb	Dy
Mount1-plaq4-22	Core	16.7	16.4	59954	20.4	115474	294503	b.d.l.	11198	30539	b.d.l.	49.0	b.d.l.	9.4	14917	3.2	88.6	0.3	b.d.l.	b.d.l.	b.d.l.	72.6	26.1	2.0	4.7	10.5	2.0	0.2	b.d.l.	0.1	
Mount1-plaq4-23	Core	17.0	16.6	56476	18.8	112687	294503	22.3	10643	28034	0.8	44.8	b.d.l.	8.9	13583	3.1	87.7	0.3	b.d.l.	b.d.l.	b.d.l.	68.7	22.2	25.5	1.8	4.8	10.5	2.0	0.2	b.d.l.	0.0
Mount1-plaq4-24	Core	19.4	16.2	57184	26.7	114909	299829	b.d.l.	10710	29810	0.6	48.4	b.d.l.	8.9	13967	3.2	86.5	0.3	b.d.l.	b.d.l.	b.d.l.	73.3	23.4	26.5	1.8	4.7	10.4	2.0	0.2	0.0	0.1
Mount1-plaq4-25	Core	15.7	16.4	56638	27.2	117197	29924	0.6	10797	29924	0.7	46.7	b.d.l.	8.4	14470	3.3	88.2	0.3	b.d.l.	b.d.l.	b.d.l.	71.4	23.4	25.7	2.0	5.1	10.4	1.9	0.2	b.d.l.	0.1
Mount1-plaq4-26	Core	14.9	16.3	56853	20.9	110688	299829	28.4	10538	29913	0.6	48.9	b.d.l.	8.2	14190	3.0	85.3	0.2	b.d.l.	b.d.l.	b.d.l.	69.2	22.4	25.1	1.9	5.0	10.4	1.8	0.2	0.0	0.1
Mount1-plaq4-27	Core	15.5	16.1	57542	23.6	112901	294503	b.d.l.	10874	29994	b.d.l.	47.8	b.d.l.	8.9	14286	3.4	86.1	0.3	b.d.l.	b.d.l.	b.d.l.	69.1	22.6	26.1	1.8	5.1	10.5	1.7	0.2	0.0	b.d.l.
Mount1-plaq4-28	Core	18.7	16.1	56617	25.8	116822	299829	21.0	10679	30906	1.2	44.7	b.d.l.	9.0	14369	3.1	84.4	0.3	b.d.l.	b.d.l.	b.d.l.	67.4	23.1	26.3	1.9	4.8	10.5	1.9	0.3	b.d.l.	0.1
Mount1-plaq4-29	Core	15.5	16.6	57463	26.9	116832	294503	38.9	10678	29989	b.d.l.	54.7	b.d.l.	9.2	14652	3.2	82.2	0.3	b.d.l.	b.d.l.	b.d.l.	67.6	23.0	26.4	1.9	4.6	10.5	1.8	0.1	0.0	0.1
Mount1-plaq4-30	Core	16.8	15.6	56613	22.2	110740	294503	b.d.l.	10277	29017	b.d.l.	49.3	b.d.l.	9.1	14853	3.1	80.3	0.3	b.d.l.	b.d.l.	b.d.l.	65.6	22.9	24.7	1.9	4.6	10.5	1.6	0.2	0.0	0.1
Mount1-plaq4-31	Core	17.3	16.3	57638	19.9	118254	294503	b.d.l.	10837	32279	b.d.l.	52.5	b.d.l.	9.3	14269	3.6	81.2	0.3	b.d.l.	b.d.l.	b.d.l.	69.8	22.6	25.9	1.9	5.3	10.4	2.0	0.2	b.d.l.	0.0
Mount1-plaq4-32	Core	15.2	15.5	55416	16.3	111046	294503	27.3	10397	29406	0.6	50.4	b.d.l.	9.0	14392	3.2	77.9	0.3	b.d.l.	b.d.l.	b.d.l.	66.2	22.2	24.8	1.8	4.8	10.4	1.7	0.3	0.0	0.1
Mount1-plaq4-33	Core	17.0	16.2	59815	27.9	118772	294503	b.d.l.	10670	32464	b.d.l.	50.0	b.d.l.	9.0	14617	3.3	81.8	0.3	b.d.l.	b.d.l.	b.d.l.	71.1	23.7	27.1	2.0	5.0	10.4	1.8	0.3	b.d.l.	0.1
Mount1-plaq4-34	Core	16.6	14.9	56830	23.4	114579	294503	b.d.l.	10637	31444	b.d.l.	50.4	b.d.l.	8.7	14665	3.1	82.0	0.3	b.d.l.	b.d.l.	b.d.l.	70.8	23.8	26.4	1.9	5.2	10.4	1.7	0.2	0.0	0.1
Mount1-plaq4-35	Core	16.8	15.9	56980	25.1	115884	294503	b.d.l.	10701	31003	0.7	46.6	b.d.l.	9.1	14591	3.2	81.4	0.3	b.d.l.	b.d.l.	b.d.l.	68.7	23.6	25.7	1.9	4.6	10.4	1.7	0.4	0.0	b.d.l.
Mount1-plaq4-36	Core	15.5	15.1	57586	30.1	115844	294503	b.d.l.	10896	31687	b.d.l.	51.7	b.d.l.	9.3	14666	3.3	80.7	0.3	b.d.l.	b.d.l.	b.d.l.	70.1	23.2	25.8	1.9	5.3	10.5	1.9	0.2	0.0	0.1
Mount1-plaq4-37	Core	16.6	15.2	58038	22.0	111791	294503	b.d.l.	10589	29936	0.7	44.4	b.d.l.	8.3	13851	3.1	76.2	0.3	b.d.l.	b.d.l.	b.d.l.	62.3	22.6	24.3	1.9	5.0	10.3	1.5	0.2	0.0	0.1
Mount1-plaq4-38	Core	17.4	15.9	56908	25.2	113612	294503	b.d.l.	10722	29587	b.d.l.	50.7	b.d.l.	8.6	14533	3.5	76.6	0.3	b.d.l.	b.d.l.	b.d.l.	61.0	22.4	25.0	1.8	4.3	10.4	1.6	0.3	b.d.l.	0.1
Mount1-plaq4-39	Core	15.9	15.8	57698	20.7	114348	299829	b.d.l.	11606	29205	b.d.l.	49.4	b.d.l.	8.6	14586	3.3	75.3	0.3	b.d.l.	b.d.l.	b.d.l.	59.4	22.3	24.5	1.8	4.8	10.4	1.6	0.2	0.0	0.1
Mount1-plaq4-40	Core	17.4	15.8	57402	19.8	115257	294503	b.d.l.	11343	28036	0.9	45.2	b.d.l.	8.2	13935	3.6	78.1	0.2	b.d.l.	b.d.l.	b.d.l.	76.3	20.8	23.0	1.7	4.3	10.4	1.6	b.d.l.	b.d.l.	
Mount1-plaq4-41	Core	16.9	15.2	59513	19.3	115884	294503	b.d.l.	10883	29989	b.d.l.	46.7	b.d.l.	8.1	14092	3.4	72.3	0.3	b.d.l.	b.d.l.	b.d.l.	78.4	20.0	22.8	1.6	3.9	10.6	1.9	0.2	b.d.l.	0.1
Mount1-plaq4-42	Core	15.6	15.3	58608	23.4	11254	294503	b.d.l.	10986	29619	0.8	47.6	b.d.l.	8.9	14500	3.7	70.3	0.3	b.d.l.	b.d.l.	b.d.l.	57.0	21.3	23.5	1.7	4.4	10.4	2.1	0.2	0.0	0.1
Mount1-plaq4-43	Core	15.4	15.5	58359	16.2	114602	294503	b.d.l.	11008	28650	1.0	48.1	b.d.l.	8.2	1477	8.1	72.7	0.2	b.d.l.	b.d.l.	b.d.l.	58.1	21.1	24.0	1.7	4.6	10.3	1.7	b.d.l.	0.0	0.1
Mount1-plaq4-44	Core	15.3	15.6	58592	20.1	113105	294503	b.d.l.	11066	28484	b.d.l.	43.2	b.d.l.	8.0	14443	3.7	72.6	0.3	b.d.l.	b.d.l.	b.d.l.	56.9	21.1	24.0	1.6	4.1	10.4	1.7	0.3	0.0	0.1
Mount1-plaq4-45	Core	15.2	15.7	59772	17.9	116362	294503	32.9	11616	29363	0.6	47.3	b.d.l.	9.2	14405	3.7	75.1	0.2	b.d.l.	b.d.l.	b.d.l.	66.3	21.3	23.8	1.7	4.5	10.4	1.9	0.2	b.d.l.	0.1
Mount1-plaq4-46	Core	16.4	16.7	58980	20.5	113735	294503	b.d.l.	11343	28036	0.9	45.2	b.d.l.	8.2	13935	3.6	78.1	0.2	b.d.l.	b.d.l.	b.d.l.	76.3	20.8	23.0	1.7	4.3	10.4	1.6	b.d.l.	b.d.l.	
Mount1-plaq4-47	Core	17.2	15.4	57123	17.8	111708	294503	b.d.l.	11301	27531	0.8	43.4	b.d.l.	8.7	13860	3.6	78.4	0.2	b.d.l.	b.d.l.	b.d.l.	78.4	20.0	22.8	1.6	3.9	10.6	1.9	0.2	b.d.l.	0.1
Mount1-plaq4-48	Core	17.6	16.0	59123	27.3	114037	294503	b.d.l.	11451	29018	0.8	44.5	b.d.l.	8.4	14769	3.7	87.5	0.3	b.d.l.	b.d.l.	b.d.l.	91.1	21.1	23.2	1.7	4.4	10.4	2.1	0.2	0.0	0.1
Mount1-plaq4-49	Core	16.2	16.6	60115	20.1	113713	294503	22.3	11367	28947	0.7	48.1	b.d.l.	7.9	14659	3.8	101.8	0.3	b.d.l.	b.d.l.	b.d.l.	137.3	20.6	23.4	1.7	4.9	10.4	2.5	0.2	0.0	b.d.l.
Mount1-plaq4-50	Core	14.6	15.6	57099	23.2	110947	299829	b.d.l.	11413	26908	0.7	39.8	b.d.l.	7.9	13893	3.7	94.1	0.2	b.d.l.	b.d.l.	b.d.l.	116.2	19.9	23.0	1.6	4.2	10.4	2.2	0.2	b.d.l.	0.1
Mount1-plaq4-51	Core	16.6	16.5	61708	16.6	116066	294503	b.d.l.	12077	29213	b.d.l.	47.6	b.d.l.	7.5	14437	3.6	107.4	0.2	b.d.l.	b.d.l.	b.d.l.	155.7	21.3	23.6	1.7	4.6	10.3	2.8	b.d.l.	b.d.l.	
Mount1-plaq4-52	Core	17.6	16.7	58980	24.1	113766	294503	b.d.l.	11595	30533	0.8	47.0	b.d.l.	8.3	14532	3.7	125.7	0.3	b.d.l.	b.d.l.	b.d.l.	225.1	21.9	24.3	1.7	4.7	10.4	3.2	0.2	0.0	0.2
Mount1-plaq4-53	Core	14.4	16.5	60145	24.5	115815	294503	b.d.l.	11917	29471	b.d.l.	50.3	b.d.l.	8.4	14068	4.0	144.5	0.3	b.d.l.	0.0	b.d.l.	321.0	22.3	24.0	1.7	4.5	10.6	3.7	0.2	b.d.l.	0.1
Mount1-plaq4-54	Core	17.1	16.6	57182	22.4	112971	294503	b.d.l.	11776	27324	b.d.l.	47.1	b.d.l.	8.0	13927	3.9	154.3	0.3	b.d.l.	b.d.l.	b.d.l.	382.7	21.7	24.2	1.7	4.8	10.6	4.2	b.d.l.	b.d.l.	
Mount1-plaq4-55	Core	16.2	17.8	58960	20.0	115444	294503	b.d.l.	11370	29780	0.8	53.4	b.d.l.	8.7	1387	4.3	154.4	0.3	b.d.l.	b.d.l.	b.d.l.	348.3	22.0	23.9	1.7	4.5	10.4	4.2	0.2	0.0	0.1
Mount1-plaq4-56	Core	14.0	18.1	57123	13.8	112453	294503	b.d.l.	11476	28256	b.d.l.	46.2	b.d.l.	8.3	13994	3.3	147.9	0.3	b.d.l.	b.d.l.	b.d.l.	295.7	21.1	24.1	1.8	4.5	10.4	4.0	b.d.l.	0.0	
Mount1-plaq4-57	Core	19.1	18.4	58127	19.9	112523	294503	b.d.l.	12052	29516	0.9	52.4	b.d.l.	8.3	13746	3.6	135.3	0.3	b.d.l.	b.d.l.	b.d.l.	259.0	22.0	24.5	1.8	4.4	10.4	3.7	0.3	0.0	0.1
Mount1-plaq4-58	Middle	20.2	18.9	58354	19.4	112353	294503	b.d.l.	11503	29073	0.6	53.1	b.d.l.	7.7	13521	3.9	120.5	0.2	b.d.l.	b.d.l.	b.d.l.	218.4	21.1	23.7	1.6	4.4	10.5	3.3	0.2	b.d.l.	0.1
Mount1-plaq4-59	Middle	21.1	19.8	59012	20.9	116842	294503	b.d.l.	11599	30382	b.d.l.	45.6	b.d.l.	8.2	14023	3.9	116.1	0.3	0.1	b.d.l.	b.d.l.	183.2	21.1	23.6	1.7	4.8	10.4	3.2	0.3	b.d.l.	0.1
Mount1-plaq4-60	Middle	18.7	20.4	58510	24.6	115065																									

Table A1.7: continued

Ho	Er	Tm	Yb	Lu	Hf	Ta	Pb	Th	U
b.d.l.	0.0	b.d.l.	b.d.l.	b.d.l.	b.d.l.	b.d.l.	15.1	0.0	b.d.l.
0.0	0.0	b.d.l.	b.d.l.	b.d.l.	b.d.l.	b.d.l.	15.1	0.0	b.d.l.
0.0	0.0	0.0	b.d.l.	b.d.l.	b.d.l.	b.d.l.	15.3	0.0	b.d.l.
0.0	0.0	b.d.l.	b.d.l.	b.d.l.	b.d.l.	b.d.l.	15.8	b.d.l.	b.d.l.
0.0	b.d.l.	b.d.l.	b.d.l.	b.d.l.	b.d.l.	b.d.l.	14.9	b.d.l.	b.d.l.
0.0	0.0	b.d.l.	b.d.l.	b.d.l.	b.d.l.	b.d.l.	15.0	b.d.l.	b.d.l.
0.0	0.1	b.d.l.	b.d.l.	b.d.l.	b.d.l.	b.d.l.	15.6	b.d.l.	b.d.l.
0.0	0.0	b.d.l.	0.0	b.d.l.	b.d.l.	b.d.l.	15.4	b.d.l.	b.d.l.
0.0	b.d.l.	0.0	b.d.l.	0.0	b.d.l.	b.d.l.	14.9	b.d.l.	b.d.l.
0.0	0.0	b.d.l.	b.d.l.	0.0	b.d.l.	b.d.l.	15.7	b.d.l.	b.d.l.
0.0	b.d.l.	b.d.l.	b.d.l.	b.d.l.	b.d.l.	b.d.l.	14.7	0.0	b.d.l.
0.0	0.0	0.0	b.d.l.	b.d.l.	b.d.l.	b.d.l.	15.8	b.d.l.	b.d.l.
0.0	0.0	b.d.l.	b.d.l.	b.d.l.	b.d.l.	b.d.l.	16.1	b.d.l.	b.d.l.
b.d.l.	0.0	b.d.l.	b.d.l.	b.d.l.	b.d.l.	b.d.l.	15.5	b.d.l.	b.d.l.
0.0	0.0	b.d.l.	b.d.l.	b.d.l.	0.0	0.0	15.4	b.d.l.	b.d.l.
0.0	0.0	b.d.l.	b.d.l.	b.d.l.	b.d.l.	b.d.l.	14.9	b.d.l.	b.d.l.
0.0	b.d.l.	b.d.l.	0.0	0.0	b.d.l.	b.d.l.	15.3	0.0	b.d.l.
0.0	0.1	b.d.l.	b.d.l.	b.d.l.	b.d.l.	b.d.l.	15.2	b.d.l.	b.d.l.
0.0	b.d.l.	b.d.l.	b.d.l.	b.d.l.	b.d.l.	b.d.l.	15.5	0.0	b.d.l.
0.0	0.0	b.d.l.	b.d.l.	b.d.l.	b.d.l.	b.d.l.	15.7	b.d.l.	b.d.l.
0.0	b.d.l.	b.d.l.	b.d.l.	b.d.l.	b.d.l.	b.d.l.	15.3	b.d.l.	b.d.l.
b.d.l.	0.0	b.d.l.	b.d.l.	b.d.l.	b.d.l.	b.d.l.	14.7	b.d.l.	b.d.l.
b.d.l.	b.d.l.	b.d.l.	b.d.l.	b.d.l.	b.d.l.	b.d.l.	15.0	b.d.l.	b.d.l.
b.d.l.	0.0	b.d.l.	b.d.l.	b.d.l.	b.d.l.	b.d.l.	14.7	b.d.l.	b.d.l.
0.0	b.d.l.	b.d.l.	b.d.l.	b.d.l.	b.d.l.	b.d.l.	14.4	b.d.l.	b.d.l.
0.0	0.0	b.d.l.	b.d.l.	b.d.l.	b.d.l.	b.d.l.	14.2	b.d.l.	b.d.l.
0.0	0.0	b.d.l.	b.d.l.	b.d.l.	b.d.l.	b.d.l.	14.8	b.d.l.	b.d.l.
0.0	0.0	b.d.l.	0.0	b.d.l.	b.d.l.	b.d.l.	14.3	b.d.l.	b.d.l.
0.0	0.0	b.d.l.	b.d.l.	b.d.l.	b.d.l.	b.d.l.	15.0	b.d.l.	b.d.l.
b.d.l.	0.0	b.d.l.	b.d.l.	0.0	b.d.l.	b.d.l.	14.4	b.d.l.	b.d.l.
b.d.l.	0.0	b.d.l.	b.d.l.	b.d.l.	b.d.l.	b.d.l.	13.8	b.d.l.	b.d.l.
b.d.l.	0.0	b.d.l.	b.d.l.	0.0	0.0	b.d.l.	14.6	b.d.l.	b.d.l.
0.0	b.d.l.	b.d.l.	b.d.l.	b.d.l.	b.d.l.	b.d.l.	14.6	b.d.l.	b.d.l.
b.d.l.	0.0	b.d.l.	b.d.l.	b.d.l.	b.d.l.	b.d.l.	15.4	b.d.l.	b.d.l.
b.d.l.	0.0	b.d.l.	b.d.l.	b.d.l.	b.d.l.	b.d.l.	15.4	b.d.l.	b.d.l.
0.0	0.0	b.d.l.	b.d.l.	b.d.l.	b.d.l.	b.d.l.	14.7	b.d.l.	b.d.l.
0.0	0.0	b.d.l.	b.d.l.	b.d.l.	b.d.l.	b.d.l.	14.8	b.d.l.	b.d.l.
b.d.l.	b.d.l.	b.d.l.	b.d.l.	b.d.l.	b.d.l.	b.d.l.	15.1	b.d.l.	b.d.l.
0.0	b.d.l.	0.0	b.d.l.	b.d.l.	b.d.l.	b.d.l.	14.9	b.d.l.	b.d.l.
b.d.l.	b.d.l.	b.d.l.	b.d.l.	0.0	b.d.l.	b.d.l.	15.1	b.d.l.	b.d.l.
0.0	0.0	b.d.l.	0.1	b.d.l.	0.0	b.d.l.	15.5	b.d.l.	b.d.l.
b.d.l.	b.d.l.	b.d.l.	b.d.l.	b.d.l.	0.0	b.d.l.	15.4	b.d.l.	b.d.l.
0.0	0.0	b.d.l.	b.d.l.	b.d.l.	b.d.l.	b.d.l.	15.8	b.d.l.	b.d.l.
0.0	0.0	b.d.l.	b.d.l.	b.d.l.	b.d.l.	b.d.l.	15.8	b.d.l.	b.d.l.
0.0	0.0	0.0	0.0	b.d.l.	b.d.l.	b.d.l.	15.7	b.d.l.	b.d.l.
0.0	0.0	0.0	b.d.l.	0.0	b.d.l.	b.d.l.	15.2	b.d.l.	b.d.l.
0.0	b.d.l.	b.d.l.	0.1	b.d.l.	b.d.l.	b.d.l.	15.7	b.d.l.	b.d.l.
0.0	0.0	b.d.l.	b.d.l.	b.d.l.	0.0	0.0	15.2	b.d.l.	b.d.l.
0.0	0.1	b.d.l.	b.d.l.	b.d.l.	b.d.l.	b.d.l.	15.0	b.d.l.	b.d.l.
b.d.l.	b.d.l.	b.d.l.	0.0	b.d.l.	b.d.l.	b.d.l.	15.3	0.0	b.d.l.

Table A1.7: continued

Info	Position	Li ⁶	Li ⁷	Na	Mg	Al	Si	P	K	Ca	Sc	Ti	V	Mn	Fe	Rb	Sr	Y	Zr	Nb	Cs	Ba	La	Ce	Pr	Nd	Sm	Eu	Gd	Tb	Dy
grain8-13	Core	15.4	17.4	59020	22.5	119920	289829	31.3	8781	343633	b.d.l.	70.7	b.d.l.	11.4	1579.8	2.6	1399.9	0.4	b.d.l.	b.d.l.	b.d.l.	230.7	31.7	356	2.7	6.9	0.6	2.7	0.4	0.0	0.1
grain8-14	Core	15.5	17.2	55281	33.9	115514	298829	b.d.l.	8935	34698	b.d.l.	71.0	0.1	10.8	1520.2	2.4	1363.3	0.4	b.d.l.	b.d.l.	b.d.l.	232.9	31.6	357	2.5	6.5	0.5	2.6	0.3	0.0	0.1
grain8-15	Core	17.6	16.9	58404	27.1	116582	298829	b.d.l.	8959	33737	1.0	68.9	b.d.l.	11.1	1561.0	2.6	1407.7	0.4	b.d.l.	b.d.l.	b.d.l.	231.7	31.7	358	2.7	7.2	0.7	2.8	0.2	0.0	0.1
grain8-16	Core	15.1	16.8	57792	28.2	117773	298829	44.2	8667	34428	b.d.l.	63.0	b.d.l.	10.3	1552.4	2.9	1425.0	0.4	b.d.l.	b.d.l.	b.d.l.	239.1	31.3	355	2.6	6.3	0.6	2.6	0.3	0.0	0.1
grain8-17	Core	16.8	16.8	56940	30.9	116055	298829	b.d.l.	8799	33410	b.d.l.	70.7	b.d.l.	11.4	1529.1	2.4	1414.4	0.3	b.d.l.	b.d.l.	b.d.l.	242.1	31.6	358	2.6	6.7	0.6	2.6	0.2	b.d.l.	0.1
grain8-18	Core	16.9	16.4	57077	29.8	116272	298829	b.d.l.	8584	33688	b.d.l.	69.0	b.d.l.	10.6	1539.8	2.5	1415.5	0.3	b.d.l.	b.d.l.	b.d.l.	238.0	31.6	358	2.6	6.8	0.7	2.6	0.2	0.0	0.1
grain8-19	Core	17.7	16.3	55948	27.6	119208	298829	b.d.l.	8361	33124	0.9	72.4	b.d.l.	11.0	1547.5	2.5	1389.4	0.4	b.d.l.	b.d.l.	b.d.l.	239.0	31.0	352	2.6	6.7	0.6	2.7	0.3	0.0	0.1
grain8-20	Core	18.8	16.1	54996	26.6	118255	298829	b.d.l.	8285	34366	b.d.l.	69.8	b.d.l.	11.0	1612.9	2.6	1456.4	0.4	b.d.l.	b.d.l.	b.d.l.	244.6	31.0	356	2.6	6.2	0.6	2.5	0.1	0.0	0.1
grain8-21	Core	17.4	16.8	59069	24.0	118174	298829	b.d.l.	8874	34377	b.d.l.	70.7	b.d.l.	11.2	1612.9	2.6	1456.4	0.4	b.d.l.	b.d.l.	b.d.l.	244.6	31.0	356	2.6	6.2	0.6	2.5	0.1	0.0	0.1
grain8-22	Core	16.4	16.5	58466	29.4	115872	298829	42.4	8267	31641	0.8	69.6	b.d.l.	10.8	1534.2	2.7	1402.4	0.4	b.d.l.	b.d.l.	b.d.l.	238.5	29.7	34.5	2.4	6.3	0.5	2.5	0.3	0.0	0.1
grain8-23	Core	19.3	16.9	59311	34.5	118294	298829	b.d.l.	9290	32391	0.8	71.4	b.d.l.	11.4	1638.5	2.9	1433.3	0.3	b.d.l.	0.0	b.d.l.	242.5	30.4	34.5	2.6	6.6	0.5	2.6	b.d.l.	b.d.l.	0.1
grain8-24	Core	14.8	16.2	57572	32.4	115532	298829	b.d.l.	8916	32873	b.d.l.	68.3	b.d.l.	10.3	1530.6	2.7	1418.4	0.4	b.d.l.	b.d.l.	b.d.l.	240.3	28.8	34.2	2.4	5.7	0.6	2.4	0.1	0.0	0.1
grain8-25	Core	17.8	16.5	58813	28.3	119393	298829	26.9	8966	32841	b.d.l.	69.5	b.d.l.	11.2	1553.7	2.9	1425.0	0.3	b.d.l.	b.d.l.	b.d.l.	237.9	29.9	34.7	2.5	6.9	0.5	2.5	0.2	0.0	0.1
grain8-26	Core	15.4	17.2	59174	28.7	116370	298829	30.6	8936	33376	b.d.l.	62.3	0.1	10.9	1618.8	2.8	1426.4	0.4	b.d.l.	b.d.l.	b.d.l.	236.0	29.1	33.5	2.4	6.4	0.4	2.6	0.3	0.0	0.1
grain8-27	Core	14.9	16.1	57896	26.0	114684	298829	b.d.l.	8584	30787	b.d.l.	67.0	b.d.l.	10.5	1524.9	2.9	1382.0	0.4	b.d.l.	b.d.l.	b.d.l.	230.2	28.7	32.4	2.5	5.6	0.5	2.8	0.3	0.0	0.1
grain8-28	Core	15.6	16.4	56293	27.5	114945	298829	b.d.l.	8821	32488	0.8	67.3	b.d.l.	10.3	1522.9	2.9	1396.6	0.4	b.d.l.	b.d.l.	b.d.l.	226.5	28.5	32.8	2.3	6.3	0.4	2.6	0.2	b.d.l.	0.1
grain8-29	Core	17.0	14.9	54271	24.9	108307	298829	b.d.l.	8367	30113	b.d.l.	58.2	b.d.l.	9.5	1430.5	2.8	1321.1	0.3	b.d.l.	b.d.l.	b.d.l.	216.6	26.7	30.6	2.1	5.8	0.7	2.3	0.2	0.0	0.1
grain8-30	Core	18.1	15.9	57087	26.9	114169	298829	24.0	9115	32774	0.8	66.5	b.d.l.	10.5	1504.9	3.0	1410.0	0.3	b.d.l.	b.d.l.	b.d.l.	223.9	28.3	32.2	2.3	6.5	0.4	2.5	0.2	0.0	b.d.l.
grain8-31	Core	16.6	15.8	54167	32.7	111946	298829	b.d.l.	8759	30366	b.d.l.	63.1	b.d.l.	10.0	1480.1	2.8	1368.3	0.3	b.d.l.	b.d.l.	b.d.l.	226.1	29.2	32.4	2.3	6.2	0.6	2.3	0.2	0.0	0.1
grain8-32	Core	18.8	16.6	58275	28.5	117588	298829	50.3	9247	32444	b.d.l.	66.7	b.d.l.	9.9	1547.4	2.9	1448.8	0.3	b.d.l.	b.d.l.	b.d.l.	229.2	30.1	34.6	2.7	5.8	0.6	2.8	0.2	0.0	0.1
grain8-33	Core	15.1	16.6	58475	32.7	118747	294503	b.d.l.	9254	35058	b.d.l.	67.2	b.d.l.	10.6	1562.5	2.9	1420.0	0.3	b.d.l.	b.d.l.	b.d.l.	222.8	30.5	35.1	2.5	6.5	0.5	2.8	0.4	b.d.l.	0.1
grain8-34	Core	16.6	15.6	56783	27.6	114381	298829	b.d.l.	9019	30951	b.d.l.	65.6	b.d.l.	10.2	1537.4	2.8	1352.3	0.3	b.d.l.	b.d.l.	b.d.l.	219.8	28.4	33.0	2.3	6.2	0.6	2.6	0.2	0.0	0.1
grain8-35	Core	17.8	16.4	55900	29.2	116323	298829	b.d.l.	8925	34191	b.d.l.	64.6	b.d.l.	10.5	1500.2	2.8	1372.0	0.4	b.d.l.	b.d.l.	b.d.l.	218.4	28.7	32.6	2.4	6.2	0.5	2.6	0.3	b.d.l.	0.1
grain8-36	Core	18.1	16.4	56584	33.3	114835	298829	b.d.l.	8940	31770	b.d.l.	65.9	b.d.l.	10.2	1579.7	2.8	1380.0	0.3	b.d.l.	b.d.l.	b.d.l.	228.4	28.4	32.6	2.4	6.1	0.5	2.4	0.3	0.0	0.1
grain8-37	Core	16.4	16.2	55111	31.0	113862	298829	b.d.l.	8649	31922	1.2	62.8	b.d.l.	10.2	1554.7	2.8	1369.4	0.4	b.d.l.	b.d.l.	b.d.l.	219.0	28.4	32.2	2.4	6.7	0.6	2.7	0.3	0.0	0.1
grain8-38	Core	17.5	16.9	57146	26.6	115820	298829	27.8	8805	33826	0.7	69.3	0.1	10.9	1519.1	2.7	1479.9	0.3	b.d.l.	b.d.l.	b.d.l.	242.6	30.8	34.6	2.6	7.1	0.8	2.8	0.4	b.d.l.	0.1
grain8-39	Core	15.9	16.7	56056	24.2	118925	298829	b.d.l.	8865	34169	b.d.l.	67.7	b.d.l.	10.5	1505.5	2.6	1459.0	0.3	b.d.l.	b.d.l.	b.d.l.	255.7	31.0	35.7	2.6	6.8	0.3	2.6	0.3	0.0	0.1
grain8-40	Core	17.7	17.2	56466	34.6	118738	298829	b.d.l.	8604	32989	b.d.l.	73.0	b.d.l.	11.0	1484.5	2.4	1484.4	0.4	b.d.l.	b.d.l.	b.d.l.	281.2	32.9	37.8	2.9	7.0	0.7	2.7	0.2	0.0	0.1
grain8-41	Core	18.8	18.6	56290	30.0	119279	298829	b.d.l.	9401	33678	b.d.l.	82.8	0.1	11.2	1505.9	2.6	1509.9	0.4	b.d.l.	b.d.l.	b.d.l.	333.0	34.9	39.3	2.9	7.0	0.6	2.9	0.3	0.0	0.1
grain8-42	Core	18.4	18.7	56210	26.4	114985	298829	25.0	9216	31862	1.1	81.3	b.d.l.	9.7	1466.1	2.7	1450.0	0.4	b.d.l.	b.d.l.	b.d.l.	353.8	33.7	36.0	2.7	7.1	0.4	2.9	0.3	0.0	0.1
grain8-43	Middle	20.0	18.9	56922	28.0	119214	298829	b.d.l.	8706	33959	b.d.l.	76.7	b.d.l.	11.2	1487.1	2.7	1439.4	0.4	b.d.l.	b.d.l.	b.d.l.	338.4	35.0	38.5	2.8	7.4	0.7	2.7	0.3	b.d.l.	0.1
grain8-44	Middle	20.2	19.6	54999	26.2	117005	298829	37.9	8544	33752	b.d.l.	74.6	0.1	10.6	1417.9	2.5	1386.6	0.3	b.d.l.	0.0	b.d.l.	351.1	34.0	38.5	2.8	8.0	0.6	2.7	0.4	0.0	0.1
grain8-45	Middle	24.0	20.3	55860	20.8	117277	298829	b.d.l.	8737	33615	0.8	73.2	b.d.l.	9.8	1378.9	2.3	1244.4	0.4	b.d.l.	b.d.l.	b.d.l.	312.6	34.1	38.7	2.9	7.3	0.6	2.6	0.4	b.d.l.	0.1
grain8-46	Middle	22.6	19.6	56402	23.9	117151	298829	b.d.l.	8974	34356	b.d.l.	84.5	b.d.l.	11.3	1399.9	2.2	1136.6	0.4	b.d.l.	b.d.l.	b.d.l.	288.5	34.2	39.6	2.7	7.0	0.6	2.7	0.2	0.0	0.1
grain8-47	Rim	20.7	18.8	57303	24.7	117903	298829	b.d.l.	9411	34343	0.7	77.8	b.d.l.	11.3	1322.8	2.5	1049.9	0.3	b.d.l.	b.d.l.	b.d.l.	259.8	34.0	38.4	2.7	6.9	0.5	2.4	0.2	b.d.l.	0.1
grain8-48	Rim	18.6	17.8	54097	21.5	116504	298829	37.2	8875	33431	b.d.l.	72.4	b.d.l.	10.2	1290.6	2.5	86.5	0.3	b.d.l.	b.d.l.	b.d.l.	216.7	33.7	37.8	2.7	7.3	0.5	2.0	0.2	0.0	0.1
grain8-49	Rim	17.4	15.2	56176	28.8	124990	298829	b.d.l.	9008	35820	b.d.l.	81.6	b.d.l.	10.9	1290.5	2.8	87.8	0.4	b.d.l.	b.d.l.	b.d.l.	155.2	35.9	38.9	2.8	8.0	0.5	2.3	0.3	b.d.l.	0.1
grain8-50	Rim	11.3	11.7	56041	17.9	116255	298829	25.3	8794	34426	b.d.l.	74.7	b.d.l.	10.9	1284.3	2.3	89.9	0.4	b.d.l.	b.d.l.	b.d.l.	98.8	32.9	36.6	2.7	6.8	0.8	2.4	0.3	0.0	0.1

Table A1.7: continued

Ho	Er	Tm	Yb	Lu	Hf	Ta	Pb	Th	U
0.0	0.0	b.d.l.	0.0	b.d.l.	b.d.l.	b.d.l.	15.9	b.d.l.	b.d.l.
0.0	0.0	b.d.l.	0.0	b.d.l.	0.0	b.d.l.	15.6	b.d.l.	b.d.l.
b.d.l.	b.d.l.	0.0	b.d.l.	b.d.l.	b.d.l.	b.d.l.	15.8	b.d.l.	b.d.l.
0.0	0.0	b.d.l.	0.0	b.d.l.	b.d.l.	b.d.l.	15.8	b.d.l.	b.d.l.
0.0	0.0	b.d.l.	0.0	b.d.l.	b.d.l.	b.d.l.	15.9	b.d.l.	b.d.l.
0.0	0.0	b.d.l.	0.0	b.d.l.	b.d.l.	b.d.l.	15.1	b.d.l.	0.0
0.0	b.d.l.	b.d.l.	0.0	b.d.l.	b.d.l.	b.d.l.	15.6	b.d.l.	b.d.l.
b.d.l.	b.d.l.	b.d.l.	0.0	b.d.l.	b.d.l.	b.d.l.	15.8	b.d.l.	b.d.l.
0.0	0.0	b.d.l.	0.0	b.d.l.	b.d.l.	b.d.l.	15.9	b.d.l.	0.0
0.0	0.0	b.d.l.	0.0	b.d.l.	b.d.l.	b.d.l.	14.7	b.d.l.	b.d.l.
b.d.l.	0.0	b.d.l.	0.0	b.d.l.	b.d.l.	b.d.l.	15.0	b.d.l.	0.0
b.d.l.	0.0	b.d.l.	0.0	b.d.l.	b.d.l.	0.0	15.7	b.d.l.	b.d.l.
b.d.l.	0.0	b.d.l.	0.0	b.d.l.	b.d.l.	b.d.l.	15.1	b.d.l.	b.d.l.
0.0	0.0	b.d.l.	0.0	b.d.l.	b.d.l.	b.d.l.	15.6	0.0	b.d.l.
0.0	b.d.l.	0.0	b.d.l.	b.d.l.	b.d.l.	b.d.l.	14.6	b.d.l.	b.d.l.
0.0	b.d.l.	0.0	b.d.l.	b.d.l.	b.d.l.	b.d.l.	15.4	b.d.l.	b.d.l.
b.d.l.	b.d.l.	0.0	b.d.l.	b.d.l.	b.d.l.	b.d.l.	15.4	b.d.l.	b.d.l.
b.d.l.	b.d.l.	0.0	b.d.l.	b.d.l.	b.d.l.	b.d.l.	16.3	b.d.l.	b.d.l.
0.0	0.0	b.d.l.	0.0	b.d.l.	b.d.l.	b.d.l.	16.0	b.d.l.	b.d.l.
0.0	0.0	b.d.l.	0.0	b.d.l.	b.d.l.	b.d.l.	15.5	b.d.l.	b.d.l.
0.0	0.1	0.0	0.0	b.d.l.	0.0	b.d.l.	15.4	0.0	b.d.l.
0.0	0.0	b.d.l.	0.0	b.d.l.	0.0	b.d.l.	15.5	b.d.l.	b.d.l.
b.d.l.	0.0	b.d.l.	0.0	b.d.l.	0.0	b.d.l.	14.6	b.d.l.	b.d.l.
0.0	b.d.l.	0.0	b.d.l.	0.0	b.d.l.	b.d.l.	15.6	b.d.l.	b.d.l.
0.0	0.1	b.d.l.	0.0	0.0	b.d.l.	b.d.l.	15.4	b.d.l.	0.0
0.0	0.0	b.d.l.	0.0	b.d.l.	b.d.l.	b.d.l.	15.6	b.d.l.	b.d.l.
0.0	b.d.l.	0.0	0.0	b.d.l.	0.0	15.7	0.0	b.d.l.	b.d.l.
0.0	0.0	b.d.l.	0.0	b.d.l.	b.d.l.	b.d.l.	15.6	b.d.l.	b.d.l.
0.0	0.0	b.d.l.	0.0	b.d.l.	b.d.l.	b.d.l.	16.5	b.d.l.	b.d.l.
b.d.l.	0.0	b.d.l.	0.0	b.d.l.	b.d.l.	b.d.l.	15.3	b.d.l.	b.d.l.
0.0	0.0	0.0	0.0	b.d.l.	0.0	b.d.l.	15.6	b.d.l.	b.d.l.
b.d.l.	0.0	0.0	0.0	b.d.l.	b.d.l.	b.d.l.	16.3	b.d.l.	b.d.l.
b.d.l.	0.0	b.d.l.	0.0	b.d.l.	b.d.l.	b.d.l.	15.3	b.d.l.	b.d.l.
0.0	b.d.l.	0.0	0.0	b.d.l.	b.d.l.	b.d.l.	15.7	0.0	b.d.l.
0.0	0.0	b.d.l.	0.0	b.d.l.	b.d.l.	b.d.l.	15.1	b.d.l.	0.0
b.d.l.	b.d.l.	b.d.l.	b.d.l.	b.d.l.	b.d.l.	b.d.l.	15.9	b.d.l.	b.d.l.
b.d.l.	b.d.l.	b.d.l.	b.d.l.	b.d.l.	b.d.l.	b.d.l.	16.8	0.0	b.d.l.
b.d.l.	b.d.l.	b.d.l.	b.d.l.	b.d.l.	0.0	17.6	b.d.l.	b.d.l.	b.d.l.
b.d.l.	b.d.l.	b.d.l.	b.d.l.	b.d.l.	b.d.l.	b.d.l.	17.8	b.d.l.	0.0
b.d.l.	b.d.l.	0.0	b.d.l.	0.0	b.d.l.	b.d.l.	16.3	b.d.l.	b.d.l.
b.d.l.	b.d.l.	b.d.l.	b.d.l.	b.d.l.	b.d.l.	b.d.l.	16.2	b.d.l.	b.d.l.
b.d.l.	b.d.l.	b.d.l.	b.d.l.	b.d.l.	0.1	0.0	18.0	b.d.l.	b.d.l.
0.0	b.d.l.	b.d.l.	b.d.l.	b.d.l.	b.d.l.	b.d.l.	15.9	b.d.l.	b.d.l.
b.d.l.	b.d.l.	b.d.l.	b.d.l.	b.d.l.	b.d.l.	b.d.l.	15.9	b.d.l.	b.d.l.
b.d.l.	b.d.l.	b.d.l.	b.d.l.	b.d.l.	b.d.l.	b.d.l.	17.4	0.0	b.d.l.
b.d.l.	b.d.l.	b.d.l.	b.d.l.	b.d.l.	b.d.l.	b.d.l.	15.6	0.0	0.0
0.0	b.d.l.	b.d.l.	b.d.l.	b.d.l.	0.0	b.d.l.	16.4	b.d.l.	0.0
b.d.l.	b.d.l.	b.d.l.	b.d.l.	b.d.l.	b.d.l.	b.d.l.	16.5	b.d.l.	0.0
b.d.l.	b.d.l.	b.d.l.	b.d.l.	b.d.l.	b.d.l.	b.d.l.	17.2	b.d.l.	b.d.l.
b.d.l.	b.d.l.	b.d.l.	b.d.l.	b.d.l.	b.d.l.	b.d.l.	18.1	0.0	b.d.l.

Table A1.7: continued

Info	Position	Li ⁶	Li ⁷	Na	Mg	Al	Si	P	K	Ca	Sc	Ti	V	Mn	Fe	Rb	Sr	Y	Zr	Nb	Cs	Ba	La	Ce	Pr	Nd	Sm	Eu	Gd	Tb	Dy	
MFT-plag8 - 19	Core	15.7	16.9	59844	38.5	130038	299178	54.4	9988	29986	b.d.l.	56.9	b.d.l.	1594.1	3.2	120.4	0.3	0.1	0.0	0.1	171.8	27.6	30.5	2.5	5.8	0.3	2.6	0.4	b.d.l.	0.1		
MFT-plag8 - 20	Core	17.7	16.0	58517	25.1	126639	299178	b.d.l.	9660	29986	b.d.l.	63.9	b.d.l.	22.1	1627.2	2.8	126.4	0.3	b.d.l.	0.0	b.d.l.	186.5	28.1	31.4	2.2	5.6	0.5	2.4	0.2	b.d.l.	b.d.l.	
MFT-plag8 - 21	Core	16.0	17.4	59152	25.8	128916	299178	45.9	9631	31262	b.d.l.	62.9	b.d.l.	14.9	1649.4	2.9	124.9	0.2	b.d.l.	0.0	b.d.l.	206.1	29.1	32.5	2.3	6.3	0.5	2.5	0.1	0.0	b.d.l.	
MFT-plag8 - 22	Core	16.6	17.0	61657	30.8	137973	299178	b.d.l.	10057	33875	1.1	69.2	b.d.l.	13.9	1670.3	3.3	139.3	0.2	0.1	b.d.l.	b.d.l.	215.5	29.1	35.1	2.6	6.2	0.4	2.8	0.3	0.0	0.1	
MFT-plag8 - 23	Core	18.3	17.1	63665	31.1	135572	299178	b.d.l.	10166	30288	b.d.l.	79.3	b.d.l.	14.8	1606.1	3.1	135.1	0.3	b.d.l.	b.d.l.	b.d.l.	212.9	28.1	31.5	2.3	6.3	0.5	2.6	b.d.l.	0.0	b.d.l.	
MFT-plag8 - 24	Core	20.8	17.2	61498	27.1	136517	299178	b.d.l.	9450	34053	0.6	69.0	b.d.l.	12.7	1646.7	2.9	144.3	0.3	b.d.l.	0.0	b.d.l.	232.3	31.7	35.8	2.6	7.0	0.6	2.8	b.d.l.	b.d.l.	b.d.l.	
MFT-plag8 - 25	Core	18.2	16.9	60660	29.1	132505	299178	b.d.l.	9250	32787	b.d.l.	64.3	b.d.l.	14.7	1553.6	3.5	137.8	0.4	b.d.l.	b.d.l.	b.d.l.	226.2	30.5	34.3	2.7	6.5	0.7	2.6	0.2	b.d.l.	b.d.l.	
MFT-plag8 - 26	Core	16.1	16.5	57496	31.9	127312	299178	61.1	8858	31826	b.d.l.	57.2	b.d.l.	11.7	1463.9	2.7	134.1	0.3	b.d.l.	b.d.l.	b.d.l.	230.1	28.6	32.0	2.3	6.4	0.7	2.3	0.3	0.0	0.1	
MFT-plag8 - 27	Core	20.3	18.2	62325	31.6	139603	299178	b.d.l.	9217	36188	0.6	74.1	0.7	21.6	1800.6	3.2	148.3	0.3	b.d.l.	b.d.l.	b.d.l.	267.5	35.2	39.5	2.6	7.7	0.5	2.8	0.4	b.d.l.	b.d.l.	
MFT-plag8 - 28	Core	19.0	16.8	60454	29.4	135150	299178	58.1	8946	34450	0.9	72.1	b.d.l.	15.1	1591.6	2.6	152.7	0.3	b.d.l.	b.d.l.	b.d.l.	254.7	32.9	37.9	2.7	7.1	0.5	2.7	0.3	0.0	0.2	
MFT-plag8 - 29	Core	16.4	16.6	58031	27.0	128878	299178	b.d.l.	8458	33134	b.d.l.	71.3	b.d.l.	b.d.l.	1527.4	2.3	147.0	0.3	0.0	b.d.l.	b.d.l.	257.3	32.7	37.2	2.7	6.7	0.5	2.7	0.4	b.d.l.	b.d.l.	
MFT-plag8 - 30	Core	16.7	17.4	60645	23.6	134228	299178	b.d.l.	8811	33878	b.d.l.	85.1	b.d.l.	85.1	1563.8	2.6	153.8	0.4	0.1	0.1	b.d.l.	b.d.l.	309.4	34.9	37.4	2.8	7.5	0.5	2.8	0.3	0.0	b.d.l.
MFT-plag8 - 31	Core	18.3	17.9	60906	23.3	136779	299178	b.d.l.	8831	36205	b.d.l.	91.8	0.8	11.8	1566.9	2.2	161.1	0.4	b.d.l.	0.0	b.d.l.	b.d.l.	364.9	38.0	44.0	3.2	8.2	0.7	2.6	0.2	b.d.l.	b.d.l.
MFT-plag8 - 32	Core	16.4	17.8	60772	27.5	134497	299178	78.5	9830	33098	b.d.l.	86.6	b.d.l.	11.6	1645.7	3.4	160.1	0.2	0.0	b.d.l.	b.d.l.	411.3	36.8	38.7	2.8	7.5	0.6	2.9	0.4	0.0	0.1	
MFT-plag8 - 33	Core	18.1	16.6	58100	24.7	125164	299178	45.8	9126	30606	b.d.l.	73.2	b.d.l.	b.d.l.	1480.5	3.7	153.4	0.3	b.d.l.	b.d.l.	b.d.l.	410.9	33.5	37.9	2.6	6.7	0.3	2.6	0.5	b.d.l.	b.d.l.	
MFT-plag8 - 34	Core	22.1	18.3	59887	31.6	133270	299178	b.d.l.	9227	33482	0.9	80.4	b.d.l.	21.0	1479.7	3.0	163.9	0.2	b.d.l.	b.d.l.	b.d.l.	450.3	36.5	40.0	2.8	7.0	0.7	3.1	0.4	b.d.l.	0.2	
MFT-plag8 - 35	Core	20.4	17.9	59224	28.9	128921	299178	b.d.l.	9373	32362	b.d.l.	65.0	b.d.l.	b.d.l.	1566.6	2.6	159.4	0.3	b.d.l.	b.d.l.	b.d.l.	429.3	33.9	36.8	2.5	6.3	0.5	2.7	0.3	b.d.l.	b.d.l.	
MFT-plag8 - 36	Core	19.8	18.6	59504	30.5	131732	299178	b.d.l.	9152	33186	b.d.l.	87.5	b.d.l.	11.9	1580.9	2.6	165.2	0.2	0.0	b.d.l.	b.d.l.	b.d.l.	454.0	35.6	39.3	2.8	7.2	0.6	3.0	0.3	0.0	b.d.l.
MFT-plag8 - 37	Core	23.0	19.8	61046	28.6	132623	299178	b.d.l.	9202	32715	b.d.l.	87.2	b.d.l.	11.5	1628.9	2.9	165.3	0.3	b.d.l.	0.0	b.d.l.	b.d.l.	475.7	35.7	38.8	2.9	7.7	0.5	2.8	b.d.l.	b.d.l.	
MFT-plag8 - 38	Core	22.5	20.0	60399	34.3	135603	299178	b.d.l.	9612	33079	b.d.l.	72.2	0.8	14.5	1715.3	2.7	161.2	0.4	b.d.l.	0.0	b.d.l.	b.d.l.	420.2	34.9	38.3	2.7	7.2	0.6	3.0	0.4	0.0	b.d.l.
MFT-plag8 - 39	Core	21.2	19.5	57465	33.5	124637	299178	b.d.l.	8804	31741	b.d.l.	77.9	b.d.l.	b.d.l.	1577.4	2.9	152.5	0.5	b.d.l.	b.d.l.	b.d.l.	380.0	32.0	35.1	2.6	6.5	0.6	2.7	0.3	0.0	b.d.l.	
MFT-plag8 - 40	Core	19.2	18.1	60327	33.6	132280	299178	b.d.l.	9381	33805	0.7	84.7	b.d.l.	15.0	1697.1	3.1	166.0	0.5	0.0	b.d.l.	b.d.l.	b.d.l.	392.6	33.6	37.4	2.7	7.5	0.7	2.9	b.d.l.	b.d.l.	
MFT-plag8 - 41	Core	13.0	14.8	63116	33.8	139756	299178	87.9	9610	35307	b.d.l.	74.8	b.d.l.	23.8	1677.9	2.8	168.7	0.3	b.d.l.	b.d.l.	b.d.l.	417.8	34.5	40.6	2.8	7.8	0.4	3.0	0.2	0.0	b.d.l.	
MFT-plag8 - 42	Core - close to crack	9.8	9.9	60262	35.0	134738	299178	b.d.l.	9551	33512	1.1	76.6	b.d.l.	14.0	1569.3	3.0	167.0	0.4	0.1	0.0	b.d.l.	b.d.l.	401.6	33.2	39.5	2.9	6.5	0.5	3.2	0.4	b.d.l.	0.1
MFT-plag8 - 43	Core - close to crack	9.4	7.4	58854	22.0	132868	299178	b.d.l.	9002	32899	b.d.l.	76.9	b.d.l.	b.d.l.	1599.1	2.3	157.7	0.4	b.d.l.	0.0	b.d.l.	b.d.l.	348.7	33.7	38.2	2.7	6.7	0.6	2.8	0.3	b.d.l.	0.1
MFT-plag8 - 44	Core - close to crack	7.5	5.9	60353	20.8	129934	299178	b.d.l.	9769	32915	0.6	62.8	b.d.l.	b.d.l.	1551.4	2.9	155.2	0.3	0.0	b.d.l.	b.d.l.	b.d.l.	356.1	31.4	34.1	2.5	6.6	0.5	2.8	0.3	0.0	b.d.l.
MFT-plag8 - 45	Core - close to crack	6.8	5.9	60877	24.5	132626	299178	b.d.l.	10238	32445	b.d.l.	74.7	b.d.l.	11.9	1579.5	2.9	156.5	0.8	0.6	0.1	b.d.l.	b.d.l.	337.1	32.3	35.1	2.3	6.7	0.5	3.0	b.d.l.	b.d.l.	
MFT-plag8 - 46	Core - close to crack	6.8	5.9	60877	24.5	132626	299178	b.d.l.	10238	32445	b.d.l.	74.7	b.d.l.	11.9	1579.5	2.9	156.5	0.8	0.6	0.1	b.d.l.	b.d.l.	337.1	32.3	35.1	2.3	6.7	0.5	3.0	b.d.l.	b.d.l.	
MFT-plag8 - 47	Core - close to crack	5.1	6.4	59679	29.3	129475	299178	b.d.l.	9729	31959	b.d.l.	75.8	b.d.l.	10.6	1478.9	3.1	149.4	0.3	b.d.l.	b.d.l.	b.d.l.	315.6	30.6	33.9	2.4	6.6	0.6	2.7	0.2	b.d.l.	b.d.l.	
MFT-plag8 - 48	Core - close to crack	6.2	7.6	60529	22.3	132741	299178	b.d.l.	10151	31749	b.d.l.	68.6	b.d.l.	13.0	15158.8	2.7	144.0	0.4	b.d.l.	b.d.l.	b.d.l.	293.5	32.1	35.1	2.7	7.1	0.7	2.9	0.3	b.d.l.	b.d.l.	
MFT-plag8 - 49	Core - close to crack	14.2	12.4	58456	21.7	130173	299178	76.5	9013	33409	b.d.l.	71.9	0.7	13.9	1520.8	2.7	144.0	0.4	b.d.l.	b.d.l.	b.d.l.	298.6	31.1	36.2	2.5	6.9	0.4	2.6	b.d.l.	b.d.l.		
MFT-plag8 - 50	Core	21.2	22.7	57591	21.9	130780	299178	b.d.l.	9038	33651	b.d.l.	70.1	b.d.l.	18.2	1327.3	2.5	138.3	0.4	b.d.l.	b.d.l.	b.d.l.	298.6	31.1	36.2	2.5	6.9	0.4	2.6	b.d.l.	b.d.l.		
MFT-plag8 - 51	Core	24.6	26.1	57139	23.3	127879	299178	78.6	9229	32144	b.d.l.	71.1	b.d.l.	23.4	1404.3	1.8	132.7	0.3	b.d.l.	b.d.l.	b.d.l.	258.7	29.7	34.6	2.4	6.8	0.6	2.4	0.3	b.d.l.	0.0	
MFT-plag8 - 52	Core	27.8	27.4	58868	20.8	132638	299178	b.d.l.	9017	34082	b.d.l.	64.8	b.d.l.	1373.2	2.4	128.5	0.5	b.d.l.	0.0	0.0	0.0	206.9	31.3	36.8	2.5	7.2	0.5	2.7	b.d.l.	0.0	b.d.l.	
MFT-plag8 - 53	Core	33.5	28.4	63816	24.2	136027	299178	b.d.l.	9029	36630	b.d.l.	72.0	b.d.l.	12.5	1416.6	2.7	123.4	0.5	b.d.l.	0.0	0.1	169.5	31.9	35.8	2.5	7.4	0.5	2.5	b.d.l.	b.d.l.		
MFT-plag8 - 54	Core	23.6	26.7	59708	22.7	132182	299178	71.3	9923	32176	b.d.l.	45.9	b.d.l.	18.0	1388.3	3.1	114.7	0.5	b.d.l.	b.d.l.	0.0	169.0	25.6	29.5	2.1	5.5	0.4	2.7	b.d.l.	0.0		
MFT-plag8 - 55	Core	25.9	26.5	58715	21.1	129747	299178	54.2	10754	30141	b.d.l.	48.3	b.d.l.	11.9	1342.5	2.9	86.2	0.3	b.d.l.	b.d.l.	b.d.l.	139.6	22.3	25.6	1.8	5.4	0.4	2.3	0.3	b.d.l.	0.1	
MFT-plag8 - 56	Core	22.0	22.9	61352	20.2	131771	299178	b.d.l.	11696	30254	b.d.l.	37.3	b.d.l.	20.0	1388.7	3.3	106.7	0.3	b.d.l.	b.d.l.	0.0	166.8	23.2	26.7	2.0							

Table A1.7: continued

Ho	Er	Tm	Yb	Lu	Hf
b.d.l.	b.d.l.	b.d.l.	b.d.l.	b.d.l.	b.d.l.
b.d.l.	b.d.l.	b.d.l.	b.d.l.	b.d.l.	b.d.l.
0.0	b.d.l.	b.d.l.	b.d.l.	0.0	b.d.l.
b.d.l.	0.1	0.0	b.d.l.	b.d.l.	b.d.l.
b.d.l.	b.d.l.	b.d.l.	b.d.l.	b.d.l.	b.d.l.
0.0	b.d.l.	b.d.l.	b.d.l.	b.d.l.	b.d.l.
0.0	b.d.l.	b.d.l.	b.d.l.	b.d.l.	b.d.l.
b.d.l.	b.d.l.	b.d.l.	b.d.l.	b.d.l.	b.d.l.
b.d.l.	b.d.l.	b.d.l.	b.d.l.	b.d.l.	b.d.l.
b.d.l.	b.d.l.	b.d.l.	0.1	b.d.l.	0.1
b.d.l.	b.d.l.	b.d.l.	b.d.l.	b.d.l.	b.d.l.
0.0	b.d.l.	b.d.l.	b.d.l.	b.d.l.	b.d.l.
b.d.l.	b.d.l.	b.d.l.	b.d.l.	b.d.l.	b.d.l.
b.d.l.	b.d.l.	b.d.l.	b.d.l.	b.d.l.	b.d.l.
0.0	0.1	0.0	b.d.l.	b.d.l.	b.d.l.
b.d.l.	0.1	b.d.l.	b.d.l.	b.d.l.	b.d.l.
b.d.l.	b.d.l.	b.d.l.	b.d.l.	b.d.l.	b.d.l.
b.d.l.	0.0	b.d.l.	b.d.l.	b.d.l.	b.d.l.
b.d.l.	b.d.l.	b.d.l.	b.d.l.	b.d.l.	0.0
b.d.l.	b.d.l.	b.d.l.	b.d.l.	b.d.l.	b.d.l.
0.0	b.d.l.	b.d.l.	0.1	b.d.l.	b.d.l.
b.d.l.	b.d.l.	b.d.l.	b.d.l.	0.0	b.d.l.
b.d.l.	b.d.l.	b.d.l.	0.1	b.d.l.	b.d.l.
0.0	b.d.l.	b.d.l.	b.d.l.	b.d.l.	b.d.l.
b.d.l.	b.d.l.	b.d.l.	b.d.l.	b.d.l.	0.0
b.d.l.	b.d.l.	b.d.l.	b.d.l.	b.d.l.	0.0
b.d.l.	b.d.l.	b.d.l.	b.d.l.	b.d.l.	b.d.l.
0.0	0.1	b.d.l.	b.d.l.	b.d.l.	b.d.l.
b.d.l.	b.d.l.	b.d.l.	b.d.l.	b.d.l.	0.1
b.d.l.	b.d.l.	b.d.l.	0.1	b.d.l.	0.0
0.0	0.0	b.d.l.	b.d.l.	b.d.l.	b.d.l.
0.0	0.0	b.d.l.	b.d.l.	b.d.l.	b.d.l.
b.d.l.	0.1	b.d.l.	b.d.l.	b.d.l.	b.d.l.
0.0	b.d.l.	b.d.l.	b.d.l.	b.d.l.	b.d.l.
b.d.l.	0.0	b.d.l.	0.0	b.d.l.	b.d.l.
0.0	0.0	b.d.l.	b.d.l.	0.0	0.0
0.0	0.0	b.d.l.	b.d.l.	b.d.l.	b.d.l.
0.0	b.d.l.	b.d.l.	0.0	b.d.l.	b.d.l.
b.d.l.	b.d.l.	b.d.l.	b.d.l.	b.d.l.	0.0

Table A1.7: continued

Info	Position	Li ⁶	Li ⁷	Na	Mg	Al	Si	P	K	Ca	Sc	Ti	V	Mn	Fe	Rb	Sr	Y	Zr	Nb	Cs	Ba	La	Ce	Pr	Nd	Sm	Eu	Gd	Tb	Dy
grain9-11	Core	26.2	22.6	57231	27.6	113555	294503	b.d.l.	11668	28318	b.d.l.	55.5	b.d.l.	8.5	1473.8	3.5	53.8	0.3	b.d.l.	0.0	b.d.l.	42.1	21.4	23.7	1.8	4.4	0.4	1.5	0.2	b.d.l.	0.1
grain9-12	Core	22.7	22.5	58361	26.1	113690	294503	24.6	11534	29966	b.d.l.	51.0	b.d.l.	8.8	1435.9	3.5	53.3	0.2	b.d.l.	0.0	b.d.l.	40.5	20.9	23.6	1.7	4.2	0.5	1.3	0.2	b.d.l.	0.1
grain9-13	Core	21.7	23.4	57349	22.9	113967	294503	28.5	11976	28241	0.7	51.7	b.d.l.	7.5	1465.7	3.9	58.5	0.3	b.d.l.	0.0	b.d.l.	38.4	20.5	23.7	1.7	4.6	0.3	1.5	0.2	0.0	0.2
grain9-14	Core	25.8	22.3	57667	25.0	113754	294503	21.9	13172	26543	b.d.l.	53.5	b.d.l.	7.9	1389.7	4.3	61.1	0.2	b.d.l.	0.0	b.d.l.	39.1	20.3	22.1	1.6	4.2	0.4	1.6	0.1	0.0	b.d.l.
grain9-15	Core	19.7	20.8	56676	20.6	107121	294503	b.d.l.	13797	24049	b.d.l.	48.9	b.d.l.	6.7	1288.1	4.7	59.4	0.2	b.d.l.	0.0	b.d.l.	40.8	17.6	18.9	1.3	3.1	0.3	1.4	0.1	0.0	b.d.l.
grain9-16	Core	20.8	23.1	58312	23.0	113319	294503	b.d.l.	13199	26242	0.6	52.0	b.d.l.	7.5	1396.3	4.3	63.6	0.3	b.d.l.	0.0	b.d.l.	38.7	18.8	20.8	1.5	3.6	0.4	1.4	0.2	0.0	0.0
grain9-17	Core	22.5	21.1	57470	27.6	111383	294503	b.d.l.	13599	26562	b.d.l.	49.4	b.d.l.	8.1	1430.3	4.2	69.1	0.2	b.d.l.	0.0	b.d.l.	39.8	18.8	20.2	1.6	3.3	0.4	1.7	0.3	b.d.l.	0.1
grain9-18	Core	16.2	18.1	58739	20.5	112955	294503	b.d.l.	12966	26494	b.d.l.	52.0	b.d.l.	8.1	1430.3	4.2	69.1	0.2	b.d.l.	0.0	b.d.l.	39.4	18.4	20.2	1.5	3.3	0.3	1.5	0.2	b.d.l.	0.1
grain9-19	Core	12.3	14.4	59253	23.9	113033	294503	b.d.l.	13153	26678	0.9	50.6	b.d.l.	8.0	1380.1	4.3	77.8	0.3	b.d.l.	0.0	b.d.l.	45.0	18.3	20.3	1.5	3.8	0.5	1.9	0.2	0.0	0.0
grain9-20	Core - close to crack	12.6	10.8	61118	24.3	114521	294503	b.d.l.	13618	27076	0.6	46.7	b.d.l.	8.6	1441.7	4.4	89.0	0.2	0.1	0.0	b.d.l.	64.5	17.8	20.1	1.6	3.8	0.2	2.1	0.2	b.d.l.	0.1
grain9-24	Core - close to crack	b.d.l.	7.5	58685	21.6	111808	294503	24.1	13961	26147	b.d.l.	49.9	b.d.l.	11.8	1436.9	4.4	100.4	0.8	0.3	0.2	b.d.l.	114.9	19.2	22.7	1.6	4.3	0.5	2.8	b.d.l.	0.0	0.1
grain9-25	Core - close to crack	b.d.l.	7.3	58693	25.0	113639	294503	b.d.l.	11761	30299	b.d.l.	64.5	b.d.l.	33.4	1481.8	3.7	113.0	0.4	0.2	0.9	b.d.l.	165.8	22.7	38.3	1.9	4.7	0.4	3.1	0.3	0.0	0.1
grain9-26	Core - close to crack	12.4	12.2	57459	26.0	116073	294503	b.d.l.	11261	29472	0.7	51.1	b.d.l.	15.7	1448.8	3.6	103.7	0.4	b.d.l.	0.0	b.d.l.	115.8	24.6	27.1	1.9	5.5	0.5	3.0	0.3	0.0	0.1
grain9-27	Core	17.8	17.6	58387	22.8	117240	294503	b.d.l.	10943	30377	b.d.l.	52.7	b.d.l.	9.4	1422.9	3.2	88.5	0.3	b.d.l.	0.0	b.d.l.	74.8	24.1	29.3	2.0	5.5	0.3	2.3	0.1	0.0	0.1
grain9-28	Middle	20.1	19.8	58224	24.8	117800	294503	b.d.l.	11078	30466	0.7	52.1	b.d.l.	9.9	1397.4	3.3	74.4	0.3	b.d.l.	0.1	b.d.l.	67.3	22.5	26.0	1.8	4.8	0.4	2.0	0.2	0.0	0.1
grain9-29	Middle	19.4	18.1	57559	23.9	116847	294503	b.d.l.	11244	29286	b.d.l.	44.0	b.d.l.	9.2	1359.3	3.2	69.6	0.3	b.d.l.	0.0	b.d.l.	74.0	21.6	24.8	1.7	4.8	0.4	1.8	0.3	0.0	0.1
grain9-30	Rim	14.7	14.8	58149	17.2	121558	294503	25.2	11390	30951	b.d.l.	44.4	b.d.l.	8.7	1411.3	3.5	74.7	0.3	b.d.l.	0.0	b.d.l.	97.6	21.4	24.4	1.7	4.6	0.4	2.0	0.3	b.d.l.	0.1
grain9-31	Rim	b.d.l.	7.2	57111	21.4	115210	289829	b.d.l.	10872	28585	b.d.l.	38.5	b.d.l.	9.0	1398.7	3.2	82.3	0.3	b.d.l.	0.0	b.d.l.	107.7	20.9	23.5	1.7	4.5	0.6	2.1	0.3	0.0	0.1
grain10-1	Rim	19.6	20.2	63698	35.8	123943	294503	b.d.l.	11208	33414	b.d.l.	56.2	b.d.l.	9.0	1431.6	3.4	30.1	0.3	b.d.l.	0.0	b.d.l.	21.6	22.5	25.4	1.9	4.7	0.5	0.9	0.2	0.0	0.1
grain10-2	Middle	23.2	21.9	58109	27.0	115360	294503	29.2	10579	28128	b.d.l.	50.7	b.d.l.	8.0	1399.1	3.6	28.7	0.3	b.d.l.	0.0	b.d.l.	23.2	21.5	23.3	1.8	4.2	0.5	0.9	0.2	0.0	0.1
grain10-3	Middle	21.2	25.5	58659	31.8	115389	294503	b.d.l.	10647	28653	0.7	51.5	0.1	8.6	1400.8	3.6	28.9	0.3	b.d.l.	0.0	b.d.l.	23.2	21.3	23.3	1.8	4.3	0.5	1.0	0.2	b.d.l.	0.1
grain10-5	Middle	22.3	22.9	58236	30.0	117775	294503	b.d.l.	10504	29263	0.7	42.3	b.d.l.	8.2	1423.5	3.5	29.3	0.4	b.d.l.	0.0	b.d.l.	23.6	22.4	25.4	1.8	4.7	0.7	1.1	0.2	0.0	0.1
grain10-6	Middle	22.5	22.9	58597	24.9	115679	294503	b.d.l.	10321	30995	b.d.l.	50.9	b.d.l.	9.0	1479.8	3.7	29.1	0.3	b.d.l.	0.0	b.d.l.	22.8	22.9	25.8	1.9	4.6	0.5	1.0	0.2	0.0	0.1
grain10-7	Middle	24.5	23.2	57573	23.5	115194	294503	29.0	10413	30048	0.7	48.8	b.d.l.	8.3	1437.5	3.6	28.4	0.4	b.d.l.	0.0	b.d.l.	21.4	20.8	24.3	1.8	4.5	0.4	1.0	0.2	0.0	0.1
grain10-8	Middle	19.4	19.0	59655	30.4	114405	294503	b.d.l.	10786	30475	b.d.l.	45.9	b.d.l.	8.2	1410.5	3.9	26.2	0.2	b.d.l.	0.0	b.d.l.	18.8	20.6	22.3	1.5	4.6	0.4	1.0	0.1	b.d.l.	0.1
grain10-9	Core	22.6	21.0	58978	21.9	118310	294503	24.3	10515	30231	b.d.l.	49.9	b.d.l.	7.9	1361.6	3.5	26.5	0.3	b.d.l.	0.0	b.d.l.	19.8	20.8	23.9	1.6	4.4	0.3	1.0	0.4	0.0	0.1
grain10-11	Core	16.9	17.4	59849	28.8	119435	294503	b.d.l.	11056	30381	b.d.l.	48.7	b.d.l.	8.3	1456.7	3.5	27.2	0.3	b.d.l.	0.0	b.d.l.	17.6	20.8	23.1	1.8	4.6	0.4	0.9	b.d.l.	0.0	0.1
grain10-12	Core	15.6	18.4	59964	32.8	116417	294503	b.d.l.	11081	30569	1.2	48.7	b.d.l.	7.9	1453.1	3.7	26.2	0.3	b.d.l.	0.0	b.d.l.	15.8	21.4	23.7	1.8	4.3	0.5	0.9	0.3	b.d.l.	0.1
grain10-13	Core	19.6	18.2	58495	25.1	112754	294503	b.d.l.	10458	29372	b.d.l.	46.7	b.d.l.	7.6	1440.2	3.5	25.3	0.3	b.d.l.	0.0	b.d.l.	14.4	19.1	21.8	1.5	3.9	0.4	0.8	b.d.l.	0.0	0.1
grain10-14	Core	19.8	21.2	58943	25.5	113943	294503	25.6	10997	28494	b.d.l.	44.2	b.d.l.	7.6	1438.9	3.8	25.3	0.3	b.d.l.	0.0	b.d.l.	13.3	19.2	21.4	1.5	4.1	0.5	0.8	0.3	0.0	0.0
grain10-15	Middle	24.3	23.4	58737	26.8	113751	294503	b.d.l.	11162	27061	b.d.l.	44.1	b.d.l.	7.7	1396.7	4.2	26.4	0.3	b.d.l.	0.0	b.d.l.	15.9	19.1	20.5	1.5	4.0	0.5	0.9	0.2	0.0	0.1
grain10-16	Middle	24.0	23.8	59188	17.6	110317	294503	b.d.l.	11314	27139	b.d.l.	40.9	b.d.l.	7.1	1407.6	4.0	29.2	0.2	b.d.l.	0.0	b.d.l.	24.8	19.6	21.7	1.6	3.9	0.3	0.9	0.2	0.0	0.1
grain10-17	Middle	29.2	24.8	60154	27.1	114962	294503	b.d.l.	11817	27080	b.d.l.	41.1	b.d.l.	7.3	1361.1	4.2	29.8	0.3	b.d.l.	0.0	b.d.l.	25.0	20.2	21.1	1.5	3.5	0.5	1.0	0.1	0.0	0.1
grain10-18	Middle	25.3	24.4	59471	28.5	113565	294503	b.d.l.	12441	24606	b.d.l.	42.6	b.d.l.	6.6	1379.5	4.4	27.8	0.2	b.d.l.	0.0	b.d.l.	21.9	19.2	20.5	1.4	3.7	0.4	0.9	0.2	0.0	0.1
grain10-19	Middle	24.3	24.2	60036	29.1	113649	294503	b.d.l.	11912	26427	b.d.l.	40.2	b.d.l.	7.5	1378.8	4.2	26.2	0.3	b.d.l.	0.0	b.d.l.	26.1	19.0	20.9	1.5	3.7	0.4	0.9	b.d.l.	0.1	
grain10-20	Middle	25.5	23.5	59823	24.8	112111	299178	b.d.l.	12112	25528	b.d.l.	37.2	b.d.l.	6.3	1358.0	4.6	22.3	0.3	b.d.l.	0.0	b.d.l.	18.1	18.3	20.0	1.3	3.4	0.3	0.7	b.d.l.	0.0	0.1
grain10-21	Middle	21.9	21.2	61433	20.9	111946	299178	b.d.l.	13133	24931	b.d.l.	35.4	b.d.l.	6.9	1358.8	4.6	21.4	0.2	0.1	0.0	b.d.l.	22.4	18.3	19.1	1.3	3.6	0.3	0.6	b.d.l.	0.0	0.0
grain10-23	Rim - close to crack	13.9	11.4	61320	22.3	114716	294503	29.5	12386	26829	b.d.l.	40.4	b.d.l.	7.2	1359.6	4.2	21.0	0.2	b.d.l.	0.0	b.d.l.	14.3	19.4	20.9	1.4	3.7	0.2	0.5	0.2	0.0	0.1
grain10-24	Rim - close to crack	b.d.l.	8.9</																												

Table A1.7: continued

Ho	Er	Tm	Yb	Lu	Hf	Ta	Pb	Th	U
b.d.l.	0.0	0.0	b.d.l.	b.d.l.	b.d.l.	b.d.l.	168	b.d.l.	b.d.l.
0.0	b.d.l.	b.d.l.	b.d.l.	b.d.l.	b.d.l.	b.d.l.	165	b.d.l.	b.d.l.
b.d.l.	0.0	b.d.l.	b.d.l.	b.d.l.	b.d.l.	b.d.l.	170	b.d.l.	b.d.l.
0.0	0.0	b.d.l.	0.1	b.d.l.	b.d.l.	b.d.l.	166	0.0	b.d.l.
b.d.l.	b.d.l.	b.d.l.	b.d.l.	b.d.l.	b.d.l.	b.d.l.	169	b.d.l.	b.d.l.
0.0	0.0	0.0	b.d.l.	b.d.l.	b.d.l.	b.d.l.	168	b.d.l.	b.d.l.
b.d.l.	0.0	b.d.l.	b.d.l.	b.d.l.	b.d.l.	b.d.l.	163	b.d.l.	b.d.l.
0.0	b.d.l.	b.d.l.	0.0	b.d.l.	b.d.l.	b.d.l.	167	b.d.l.	b.d.l.
b.d.l.	0.0	b.d.l.	b.d.l.	b.d.l.	b.d.l.	b.d.l.	160	0.0	b.d.l.
b.d.l.	0.0	b.d.l.	b.d.l.	0.0	b.d.l.	b.d.l.	154	b.d.l.	b.d.l.
0.0	0.1	b.d.l.	0.0	0.0	b.d.l.	b.d.l.	168	0.1	b.d.l.
0.0	0.0	b.d.l.	b.d.l.	b.d.l.	b.d.l.	b.d.l.	219	0.1	0.0
0.0	0.0	b.d.l.	b.d.l.	b.d.l.	0.0	b.d.l.	162	0.0	b.d.l.
0.0	0.0	b.d.l.	b.d.l.	0.0	b.d.l.	b.d.l.	149	0.0	b.d.l.
0.0	0.0	b.d.l.	b.d.l.	b.d.l.	b.d.l.	b.d.l.	145	b.d.l.	b.d.l.
0.0	0.0	b.d.l.	b.d.l.	b.d.l.	b.d.l.	b.d.l.	150	b.d.l.	b.d.l.
0.0	b.d.l.	b.d.l.	b.d.l.	b.d.l.	b.d.l.	b.d.l.	152	b.d.l.	b.d.l.
0.0	b.d.l.	b.d.l.	b.d.l.	b.d.l.	b.d.l.	b.d.l.	145	b.d.l.	b.d.l.
0.0	0.1	b.d.l.	b.d.l.	b.d.l.	b.d.l.	b.d.l.	177	0.2	b.d.l.
0.0	0.0	0.0	b.d.l.	0.0	b.d.l.	b.d.l.	172	0.0	b.d.l.
0.0	b.d.l.	0.0	b.d.l.	b.d.l.	b.d.l.	b.d.l.	174	0.0	b.d.l.
0.0	0.0	b.d.l.	0.0	b.d.l.	0.0	b.d.l.	180	b.d.l.	b.d.l.
0.0	0.1	0.0	b.d.l.	b.d.l.	b.d.l.	b.d.l.	176	0.0	b.d.l.
0.0	b.d.l.	b.d.l.	b.d.l.	b.d.l.	b.d.l.	b.d.l.	176	b.d.l.	b.d.l.
b.d.l.	0.0	b.d.l.	0.0	b.d.l.	b.d.l.	b.d.l.	178	b.d.l.	b.d.l.
0.0	b.d.l.	b.d.l.	b.d.l.	b.d.l.	b.d.l.	b.d.l.	168	b.d.l.	b.d.l.
0.0	b.d.l.	b.d.l.	b.d.l.	b.d.l.	b.d.l.	b.d.l.	170	b.d.l.	b.d.l.
b.d.l.	0.0	b.d.l.	b.d.l.	b.d.l.	b.d.l.	b.d.l.	176	b.d.l.	b.d.l.
b.d.l.	0.0	0.0	b.d.l.	b.d.l.	b.d.l.	b.d.l.	179	b.d.l.	b.d.l.
0.0	0.0	b.d.l.	b.d.l.	b.d.l.	b.d.l.	b.d.l.	166	b.d.l.	b.d.l.
0.0	0.0	b.d.l.	b.d.l.	b.d.l.	b.d.l.	b.d.l.	174	b.d.l.	b.d.l.
0.0	0.0	b.d.l.	b.d.l.	b.d.l.	b.d.l.	b.d.l.	175	b.d.l.	b.d.l.
b.d.l.	0.0	b.d.l.	b.d.l.	b.d.l.	b.d.l.	b.d.l.	167	b.d.l.	b.d.l.
0.0	0.0	b.d.l.	b.d.l.	b.d.l.	b.d.l.	b.d.l.	177	b.d.l.	b.d.l.
0.0	0.0	b.d.l.	b.d.l.	b.d.l.	b.d.l.	b.d.l.	172	0.0	b.d.l.
b.d.l.	0.0	b.d.l.	b.d.l.	b.d.l.	b.d.l.	b.d.l.	177	b.d.l.	b.d.l.
0.0	0.0	b.d.l.	b.d.l.	b.d.l.	b.d.l.	b.d.l.	177	0.0	b.d.l.
0.0	0.0	b.d.l.	b.d.l.	b.d.l.	0.0	b.d.l.	174	b.d.l.	0.0
0.0	b.d.l.	b.d.l.	b.d.l.	b.d.l.	b.d.l.	b.d.l.	183	b.d.l.	0.0
b.d.l.	0.0	b.d.l.	b.d.l.	b.d.l.	b.d.l.	b.d.l.	173	b.d.l.	b.d.l.
0.0	0.0	b.d.l.	b.d.l.	0.0	b.d.l.	b.d.l.	166	0.0	b.d.l.
0.0	b.d.l.	b.d.l.	b.d.l.	b.d.l.	b.d.l.	b.d.l.	175	b.d.l.	b.d.l.
0.0	b.d.l.	b.d.l.	b.d.l.	b.d.l.	b.d.l.	0.0	16.1	b.d.l.	b.d.l.
b.d.l.	0.0	b.d.l.	b.d.l.	b.d.l.	b.d.l.	b.d.l.	164	b.d.l.	b.d.l.
b.d.l.	0.0	b.d.l.	b.d.l.	b.d.l.	b.d.l.	b.d.l.	170	b.d.l.	b.d.l.
0.0	b.d.l.	0.0	0.0	b.d.l.	0.0	b.d.l.	177	0.0	b.d.l.
0.0	0.0	b.d.l.	b.d.l.	b.d.l.	b.d.l.	b.d.l.	167	0.0	b.d.l.

Table A1.7: continued

Info	Position	Li ⁺	Li ⁺	Na	Mg	Al	Si	P	K	Ca	Sc	Ti	V	Mn	Fe	Rb	Sr	Y	Zr	Nb	Cs	Ba	La	Ce	Pr	Nd	Sm	Eu	Gd	Tb	Dy
grain12-6	Middle	25.4	22.7	58482	21.3	115233	294503	b.d.l.	11740	29955	b.d.l.	52.2	b.d.l.	8.5	1442.6	3.8	45.8	0.2	b.d.l.	b.d.l.	b.d.l.	39.4	22.9	25.0	1.7	4.7	0.4	1.2	b.d.l.	0.0	0.0
grain12-7	Middle	27.0	24.5	59179	24.5	116677	294503	b.d.l.	11659	30135	b.d.l.	53.0	b.d.l.	9.6	1531.1	3.5	49.1	0.4	b.d.l.	b.d.l.	b.d.l.	41.8	23.2	26.2	1.9	5.2	0.4	1.3	0.2	0.0	0.1
grain12-8	Middle	25.7	25.4	58410	21.4	115464	294503	b.d.l.	11022	30197	b.d.l.	53.3	b.d.l.	8.8	1492.9	3.6	50.7	0.3	b.d.l.	0.0	b.d.l.	37.2	23.0	26.4	1.7	4.4	0.3	1.1	0.3	0.0	0.1
grain12-9	Middle	25.8	24.9	59939	20.5	117224	294503	b.d.l.	11165	30850	b.d.l.	55.5	b.d.l.	9.2	1503.7	3.3	51.9	0.3	b.d.l.	b.d.l.	b.d.l.	34.7	23.1	25.0	1.9	4.4	0.3	1.4	0.2	0.0	0.1
grain12-10	Core	23.8	21.0	56446	16.8	108741	294503	43.1	10691	29084	0.7	53.4	b.d.l.	8.7	1396.2	3.2	49.9	0.3	b.d.l.	b.d.l.	b.d.l.	32.7	21.5	23.9	1.7	4.7	0.4	1.3	0.2	0.0	0.1
grain12-11	Core	22.8	19.6	59083	26.7	115007	294503	b.d.l.	11921	29593	b.d.l.	54.9	b.d.l.	8.1	1447.1	3.6	56.8	0.2	0.1	b.d.l.	b.d.l.	40.5	21.1	22.9	1.7	4.1	0.4	1.3	0.3	0.0	0.1
grain12-12	Core	27.3	20.6	60705	20.2	114091	294503	27.7	13683	25835	0.8	58.8	b.d.l.	7.9	1487.5	5.3	59.4	0.6	0.2	0.1	b.d.l.	45.0	21.7	23.2	1.7	4.3	0.6	1.4	0.2	0.0	0.1
grain12-13	Core	29.4	26.1	57948	24.2	116022	294503	27.7	13683	27744	b.d.l.	53.7	b.d.l.	7.7	1452.8	4.1	59.2	0.2	b.d.l.	b.d.l.	b.d.l.	41.3	22.1	24.1	1.7	3.9	0.5	1.5	0.2	0.0	0.1
grain12-14	Core	27.4	24.7	57442	24.9	112899	294503	29.7	11980	28071	b.d.l.	55.9	b.d.l.	8.0	1492.4	3.9	57.6	0.3	b.d.l.	b.d.l.	b.d.l.	36.2	21.7	23.5	1.8	4.1	0.6	1.3	0.2	b.d.l.	0.1
grain12-15	Core - close to crack	b.d.l.	8.8	59311	33.2	116257	294503	b.d.l.	12593	27919	b.d.l.	53.2	b.d.l.	7.7	1497.8	4.0	51.6	0.5	0.4	0.1	b.d.l.	31.6	20.8	23.1	1.6	4.3	0.4	1.4	b.d.l.	0.0	0.1
grain12-16	Core - close to crack	b.d.l.	12.9	58582	31.6	115176	294503	32.4	12481	28181	b.d.l.	49.1	b.d.l.	7.7	1446.2	4.5	50.9	0.2	b.d.l.	b.d.l.	b.d.l.	29.1	21.0	22.3	1.6	4.1	0.4	1.2	0.2	0.0	0.2
grain12-17	Core - close to crack	12.9	10.2	58619	28.9	114181	294503	b.d.l.	13205	27825	b.d.l.	44.7	b.d.l.	7.3	1473.0	4.4	47.9	0.2	b.d.l.	b.d.l.	b.d.l.	24.6	18.7	20.3	1.5	3.4	0.3	1.3	0.2	0.0	0.1
grain12-18	Core - close to crack	b.d.l.	8.1	59182	35.4	113298	294503	b.d.l.	11350	29734	b.d.l.	50.3	b.d.l.	11.6	1691.1	6.1	47.9	0.6	1.0	0.5	0.1	25.1	20.0	22.6	1.6	4.4	0.5	1.2	0.3	0.0	0.1
grain12-22	Core - close to crack	b.d.l.	9.1	57031	25.1	111252	294503	b.d.l.	12469	26253	b.d.l.	37.9	b.d.l.	7.1	1304.7	4.7	53.0	0.2	0.1	b.d.l.	b.d.l.	17.8	16.1	17.1	1.3	2.9	0.2	1.3	0.2	0.0	0.1
grain12-23	Core - close to crack	b.d.l.	10.8	58802	22.6	114593	294503	b.d.l.	12338	29293	0.8	34.1	b.d.l.	7.0	1392.3	4.0	60.0	0.2	b.d.l.	0.1	b.d.l.	16.5	16.5	17.9	1.3	3.3	0.3	1.3	0.2	0.0	0.1
grain12-24	Core - close to crack	b.d.l.	8.2	61323	23.1	114738	294503	b.d.l.	13608	27695	0.7	48.5	b.d.l.	7.2	1392.5	4.8	65.7	0.2	b.d.l.	b.d.l.	b.d.l.	18.8	17.5	18.8	1.3	3.6	0.3	1.6	b.d.l.	0.0	0.1
grain12-25	Core - close to crack	b.d.l.	7.7	57824	31.4	112369	294503	b.d.l.	12217	27665	0.6	47.9	b.d.l.	8.6	1382.9	3.9	65.0	0.5	0.4	0.2	b.d.l.	15.2	17.9	19.9	1.4	3.4	0.3	1.3	0.2	0.0	0.1
grain12-26	Core - close to crack	13.0	10.1	59371	23.0	114380	294503	b.d.l.	12982	27245	b.d.l.	40.1	b.d.l.	6.9	1396.0	4.3	74.3	0.2	b.d.l.	b.d.l.	b.d.l.	17.9	17.8	19.3	1.3	3.1	0.3	1.7	b.d.l.	0.0	0.2
grain12-27	Core - close to crack	14.9	13.9	58762	18.6	112798	294503	b.d.l.	12653	27794	b.d.l.	45.7	b.d.l.	7.9	1415.4	4.6	82.6	0.2	b.d.l.	0.0	b.d.l.	27.8	17.7	19.8	1.3	3.7	0.4	1.9	0.2	0.0	0.1
grain12-28	Core - close to crack	b.d.l.	9.9	58702	27.2	114299	294503	b.d.l.	11665	29200	0.6	43.3	b.d.l.	9.3	1401.4	3.9	86.7	0.3	0.3	0.0	b.d.l.	34.2	19.3	21.8	1.6	3.3	0.3	2.0	0.2	0.0	0.1
grain12-29	Core - close to crack	14.5	14.2	60094	22.9	112665	294503	b.d.l.	11642	28170	b.d.l.	41.7	b.d.l.	7.9	1383.6	3.7	92.4	0.2	b.d.l.	b.d.l.	b.d.l.	47.8	18.9	21.6	1.6	4.3	0.4	2.2	b.d.l.	0.0	0.1
grain12-31	Core	18.0	17.1	60058	30.8	117228	294503	b.d.l.	12516	28298	b.d.l.	47.5	b.d.l.	8.6	1445.4	4.0	103.9	0.2	b.d.l.	b.d.l.	b.d.l.	90.5	20.4	22.4	1.7	4.1	0.5	2.6	0.2	b.d.l.	0.1
grain12-32	Middle	12.7	11.8	59513	25.7	113333	294503	b.d.l.	12092	29330	b.d.l.	46.7	b.d.l.	8.1	1420.3	4.2	113.2	0.2	b.d.l.	b.d.l.	b.d.l.	118.4	20.6	22.3	1.7	4.1	0.5	2.6	0.2	b.d.l.	0.1
grain12-33	Middle	16.7	13.4	58930	18.3	112866	294503	b.d.l.	13652	26295	b.d.l.	41.2	b.d.l.	7.2	1319.3	4.6	119.2	0.2	b.d.l.	b.d.l.	b.d.l.	152.6	18.3	20.2	1.4	4.0	0.4	2.9	0.2	0.0	0.0
grain12-34	Middle	13.2	12.6	59103	24.0	114565	294503	b.d.l.	13845	27796	b.d.l.	47.3	b.d.l.	7.3	1441.6	4.5	133.7	0.2	b.d.l.	b.d.l.	b.d.l.	207.0	19.1	20.7	1.6	4.2	0.4	3.1	0.2	b.d.l.	0.1
grain12-35	Rim	b.d.l.	5.8	57408	27.8	109929	294503	23.2	14423	23538	b.d.l.	43.4	b.d.l.	10.5	1332.6	5.3	134.8	0.2	b.d.l.	b.d.l.	b.d.l.	258.4	18.3	19.1	1.4	3.3	0.4	3.8	0.1	0.0	b.d.l.
grain12-36	Rim	b.d.l.	4.8	58433	27.2	113600	294503	b.d.l.	13127	27180	0.8	49.7	b.d.l.	7.7	1437.3	4.5	139.8	0.3	0.3	0.1	b.d.l.	259.2	20.3	21.9	1.5	3.7	0.5	3.7	0.2	0.0	0.0
grain12-37	Rim	b.d.l.	8.3	57379	19.0	112116	294503	b.d.l.	13570	26733	0.8	52.6	b.d.l.	7.1	1420.5	4.6	140.5	0.2	0.1	0.0	b.d.l.	262.3	20.0	21.2	1.5	4.2	0.4	3.8	0.2	0.0	b.d.l.
grain12-38	Rim	b.d.l.	4.7	58634	22.2	110701	294503	21.8	13860	26021	0.7	42.8	b.d.l.	6.7	1345.3	4.9	134.1	0.2	b.d.l.	b.d.l.	b.d.l.	211.5	19.2	20.9	1.4	3.9	0.4	3.6	0.2	b.d.l.	0.1
grain13-1	Rim	11.2	11.6	59253	20.4	112282	294503	b.d.l.	12403	27328	1.0	42.0	b.d.l.	7.4	1332.1	4.1	94.3	0.3	b.d.l.	b.d.l.	b.d.l.	106.4	20.1	22.1	1.6	4.2	0.3	2.7	0.3	0.0	0.0
grain13-2	Rim	18.8	18.0	58299	20.0	113056	294503	21.2	12227	28337	0.6	43.0	b.d.l.	7.8	1354.6	4.0	112.5	0.2	b.d.l.	b.d.l.	b.d.l.	154.1	20.6	22.7	1.7	4.4	0.4	3.2	0.2	0.0	0.0
grain13-3	Rim	22.4	21.1	57011	19.4	110663	294503	b.d.l.	12288	27350	0.5	47.1	b.d.l.	8.3	1367.1	3.7	129.1	0.3	b.d.l.	b.d.l.	b.d.l.	207.5	20.6	23.0	1.6	4.5	0.4	3.6	0.2	b.d.l.	0.1
grain13-4	Middle	25.2	22.6	59182	20.7	111454	294503	15.7	11798	29135	b.d.l.	43.1	b.d.l.	7.9	1420.8	3.7	146.0	0.3	b.d.l.	b.d.l.	b.d.l.	259.9	21.0	24.5	1.7	4.9	0.5	3.8	0.3	0.0	0.1
grain13-5	Middle	22.8	23.0	57892	38.9	109944	294503	17.1	12432	27203	0.6	40.8	b.d.l.	7.8	1393.4	3.8	149.5	0.3	0.2	0.1	b.d.l.	260.8	20.7	23.7	1.7	4.6	0.4	4.2	0.2	0.0	0.0
grain13-6	Middle	22.9	22.2	58449	24.6	110281	294503	20.0	11755	27507	0.7	45.3	b.d.l.	8.5	1390.4	3.8	158.4	0.2	b.d.l.	0.0	b.d.l.	260.8	20.7	23.7	1.7	4.6	0.4	4.2	0.2	0.0	0.0
grain13-7	Middle	22.8	22.4	61076	23.9	109425	294503	13.9	12639	27386	0.7	44.8	b.d.l.	8.1	1432.7	3.8	162.8	0.3	0.0	b.d.l.	b.d.l.	260.5	19.5	22.4	1.6	4.2	0.3	4.1	0.2	0.0	0.1
grain13-8	Middle	22.2	21.6	59066	22.5	113062	294503	b.d.l.	12410	28322	0.9	49.1	b.d.l.	8.3	1507.8	3.9	169.1	0.2	b.d.l.	b.d.l.	b.d.l.	274.4	20.2	23.5	1.8	4.4	0.5	4.4	0.1	0.0	0.1
grain13-9	Core	21.0	20.6	57828	18.9	108105	294503	13.4	11915	28734	0.7	46.2	b.d.l.	8.3	1461.0	3.8	166.8	0.2	b.d.l.	b.d.l.	b.d.l.	293.7	20.6	24.2	1.7	4.5	0.4	4.2	0.2	0.0	0.1

Table A1.7: continued

Ho	Er	Tm	Yb	Lu	Hf	Ta	Pb	Th	U
0.0	0.0	b.d.l.	b.d.l.	b.d.l.	b.d.l.	b.d.l.	17.5	b.d.l.	b.d.l.
0.0	b.d.l.	b.d.l.	b.d.l.	b.d.l.	b.d.l.	b.d.l.	17.5	b.d.l.	b.d.l.
b.d.l.	0.0	b.d.l.	0.0	b.d.l.	b.d.l.	b.d.l.	17.0	b.d.l.	b.d.l.
0.0	b.d.l.	0.0	b.d.l.	0.0	b.d.l.	b.d.l.	17.2	b.d.l.	0.0
0.0	0.0	b.d.l.	0.0	b.d.l.	b.d.l.	b.d.l.	16.3	b.d.l.	b.d.l.
0.0	0.0	b.d.l.	b.d.l.	b.d.l.	b.d.l.	b.d.l.	16.8	b.d.l.	b.d.l.
b.d.l.	0.1	0.0	b.d.l.	0.0	0.0	b.d.l.	15.9	0.1	0.0
0.0	0.0	b.d.l.	0.0	b.d.l.	b.d.l.	b.d.l.	16.7	b.d.l.	0.0
0.0	0.0	b.d.l.	0.0	b.d.l.	b.d.l.	b.d.l.	17.0	b.d.l.	b.d.l.
0.0	b.d.l.	0.0	b.d.l.	b.d.l.	0.0	b.d.l.	16.7	0.1	b.d.l.
0.0	b.d.l.	b.d.l.	b.d.l.	b.d.l.	b.d.l.	b.d.l.	17.4	0.0	0.0
0.0	0.0	b.d.l.	b.d.l.	b.d.l.	b.d.l.	b.d.l.	17.3	b.d.l.	b.d.l.
0.0	0.1	b.d.l.	b.d.l.	b.d.l.	0.1	0.0	16.4	0.2	0.1
0.0	0.0	b.d.l.	b.d.l.	b.d.l.	b.d.l.	b.d.l.	15.9	0.0	0.0
b.d.l.	0.0	b.d.l.	b.d.l.	b.d.l.	b.d.l.	b.d.l.	16.6	0.0	b.d.l.
0.0	0.0	b.d.l.	b.d.l.	b.d.l.	b.d.l.	b.d.l.	16.9	b.d.l.	b.d.l.
0.0	0.1	b.d.l.	b.d.l.	b.d.l.	b.d.l.	b.d.l.	15.6	0.0	b.d.l.
0.0	b.d.l.	b.d.l.	b.d.l.	0.0	b.d.l.	b.d.l.	15.6	b.d.l.	b.d.l.
0.0	b.d.l.	b.d.l.	b.d.l.	0.0	b.d.l.	b.d.l.	15.8	0.0	b.d.l.
b.d.l.	0.0	b.d.l.	b.d.l.	b.d.l.	b.d.l.	0.0	16.2	0.0	b.d.l.
b.d.l.	0.0	b.d.l.	b.d.l.	b.d.l.	b.d.l.	b.d.l.	15.8	0.0	b.d.l.
0.0	0.0	b.d.l.	0.1	b.d.l.	b.d.l.	b.d.l.	15.9	b.d.l.	b.d.l.
b.d.l.	0.0	b.d.l.	b.d.l.	b.d.l.	b.d.l.	b.d.l.	15.8	b.d.l.	b.d.l.
b.d.l.	b.d.l.	b.d.l.	0.1	b.d.l.	b.d.l.	b.d.l.	15.2	b.d.l.	b.d.l.
0.0	b.d.l.	0.0	b.d.l.	b.d.l.	b.d.l.	b.d.l.	15.8	b.d.l.	b.d.l.
b.d.l.	b.d.l.	b.d.l.	b.d.l.	b.d.l.	b.d.l.	b.d.l.	15.8	b.d.l.	b.d.l.
0.0	b.d.l.	0.0	b.d.l.	b.d.l.	0.0	b.d.l.	15.8	b.d.l.	0.0
b.d.l.	b.d.l.	b.d.l.	b.d.l.	b.d.l.	b.d.l.	b.d.l.	15.7	0.0	b.d.l.
b.d.l.	b.d.l.	b.d.l.	0.0	b.d.l.	b.d.l.	b.d.l.	15.8	0.0	b.d.l.
0.0	b.d.l.	b.d.l.	b.d.l.	0.0	b.d.l.	b.d.l.	15.3	b.d.l.	b.d.l.
0.0	0.0	b.d.l.	b.d.l.	b.d.l.	b.d.l.	b.d.l.	14.2	b.d.l.	b.d.l.
0.0	0.0	b.d.l.	b.d.l.	b.d.l.	b.d.l.	b.d.l.	14.2	b.d.l.	b.d.l.
0.0	0.0	0.0	0.0	b.d.l.	b.d.l.	b.d.l.	13.9	b.d.l.	b.d.l.
0.0	b.d.l.	b.d.l.	b.d.l.	b.d.l.	b.d.l.	b.d.l.	14.5	0.0	b.d.l.
0.0	0.0	0.0	0.0	0.0	b.d.l.	b.d.l.	13.6	0.0	b.d.l.
0.0	0.0	b.d.l.	0.0	b.d.l.	b.d.l.	b.d.l.	13.7	b.d.l.	b.d.l.
0.0	b.d.l.	b.d.l.	b.d.l.	b.d.l.	b.d.l.	b.d.l.	13.5	b.d.l.	b.d.l.
0.0	b.d.l.	b.d.l.	b.d.l.	b.d.l.	b.d.l.	b.d.l.	13.7	b.d.l.	b.d.l.
0.0	0.0	0.0	b.d.l.	b.d.l.	b.d.l.	b.d.l.	13.7	b.d.l.	b.d.l.
0.0	0.0	b.d.l.	b.d.l.	0.0	b.d.l.	b.d.l.	13.7	b.d.l.	b.d.l.
0.0	0.0	b.d.l.	b.d.l.	b.d.l.	b.d.l.	b.d.l.	13.3	b.d.l.	b.d.l.
b.d.l.	0.0	0.0	b.d.l.	b.d.l.	b.d.l.	b.d.l.	12.9	b.d.l.	b.d.l.
0.0	0.0	b.d.l.	b.d.l.	b.d.l.	b.d.l.	b.d.l.	12.8	0.0	0.0
b.d.l.	b.d.l.	b.d.l.	b.d.l.	b.d.l.	b.d.l.	b.d.l.	13.0	b.d.l.	b.d.l.
b.d.l.	b.d.l.	b.d.l.	0.0	b.d.l.	b.d.l.	b.d.l.	13.3	b.d.l.	b.d.l.
b.d.l.	b.d.l.	b.d.l.	b.d.l.	b.d.l.	b.d.l.	b.d.l.	13.0	b.d.l.	b.d.l.
0.0	0.0	b.d.l.	b.d.l.	b.d.l.	b.d.l.	b.d.l.	13.0	0.0	b.d.l.
0.0	0.0	b.d.l.	b.d.l.	b.d.l.	b.d.l.	b.d.l.	12.7	b.d.l.	b.d.l.
0.0	0.0	b.d.l.	b.d.l.	b.d.l.	b.d.l.	b.d.l.	13.0	b.d.l.	b.d.l.
b.d.l.	0.0	b.d.l.	b.d.l.	0.0	b.d.l.	b.d.l.	13.0	b.d.l.	b.d.l.
b.d.l.	b.d.l.	0.0	b.d.l.	b.d.l.	0.0	b.d.l.	12.5	b.d.l.	b.d.l.

Table A1.7: continued

Info	Position	Li ⁶	Li ⁷	Na	Mg	Al	Si	P	K	Ca	Sc	Ti	V	Mn	Fe	Rb	Sr	Y	Zr	Nb	Cs	Ba	La	Ce	Pr	Nd	Sm	Eu	Gd	Tb	Dy
grain13-22	Core	18.4	16.7	57120	26.0	107509	294503	b.d.l.	12510	27646	0.6	52.3	b.d.l.	7.8	1471.6	3.9	244.1	0.2	b.d.l.	b.d.l.	b.d.l.	706.3	21.6	24.7	1.6	4.5	0.4	6.5	0.1	0.0	0.1
grain13-23	Core	17.6	16.7	56136	18.0	108575	294503	13.3	12510	27281	0.6	53.7	b.d.l.	8.2	1493.1	3.9	253.6	0.2	b.d.l.	b.d.l.	b.d.l.	747.1	22.7	25.7	1.8	4.7	0.4	6.7	0.1	0.0	b.d.l.
grain13-24	Core	18.3	16.1	56526	16.1	103112	294503	19.6	12573	25095	0.8	55.4	b.d.l.	7.7	1467.7	4.3	250.7	0.2	b.d.l.	b.d.l.	b.d.l.	766.6	20.4	23.3	1.7	4.3	0.4	6.3	0.2	0.0	b.d.l.
grain13-25	Core	17.4	16.8	56081	15.2	102458	294503	16.8	13815	23460	0.7	48.7	b.d.l.	7.1	1392.2	4.3	238.7	0.2	b.d.l.	0.0	b.d.l.	787.4	18.8	21.3	1.5	3.8	0.2	6.1	0.2	0.0	0.0
grain13-26	Core	20.0	18.5	60852	24.0	108123	294503	b.d.l.	13091	27830	0.9	54.8	b.d.l.	8.1	1487.4	4.3	257.5	0.4	0.1	0.0	b.d.l.	787.4	20.9	23.5	1.7	5.0	0.4	6.6	0.1	0.0	0.1
grain13-27	Core	19.2	18.3	58097	18.9	108444	294503	25.9	13347	26572	0.7	53.1	b.d.l.	7.9	1522.7	4.1	254.8	0.2	b.d.l.	b.d.l.	b.d.l.	808.9	20.8	24.5	1.7	4.6	0.3	6.6	0.2	0.0	0.0
grain13-28	Core	21.7	19.3	60725	25.4	110746	294503	b.d.l.	13274	27322	0.6	56.9	b.d.l.	8.2	1525.6	4.0	263.8	0.2	b.d.l.	b.d.l.	b.d.l.	890.7	21.0	24.5	1.7	4.4	0.3	6.7	0.2	0.0	0.0
grain13-29	Core	17.5	19.4	58791	24.5	111481	294503	12.3	13471	27392	0.6	59.7	b.d.l.	7.8	1562.1	4.0	263.8	0.2	b.d.l.	b.d.l.	b.d.l.	890.7	21.8	24.6	1.8	4.7	0.4	6.9	0.2	0.0	0.0
grain13-30	Core	20.8	19.5	57688	16.0	111302	294503	b.d.l.	13659	28483	0.6	61.5	b.d.l.	8.1	1524.9	3.9	266.8	0.2	b.d.l.	b.d.l.	b.d.l.	915.2	22.3	25.4	1.9	5.1	0.3	6.9	0.1	0.0	0.1
grain13-31	Core	20.2	19.0	60570	16.7	114645	294503	17.0	13870	27932	0.8	59.9	b.d.l.	7.7	1564.8	4.7	264.5	0.1	b.d.l.	b.d.l.	b.d.l.	944.3	22.8	26.0	1.9	5.1	0.3	7.0	0.2	0.0	0.1
grain13-32	Core	17.5	16.4	61154	16.7	105179	294503	21.7	13088	26784	0.8	60.1	b.d.l.	7.3	1484.0	4.3	246.3	0.1	b.d.l.	b.d.l.	b.d.l.	872.9	21.8	24.6	1.7	4.6	0.4	6.4	0.2	0.0	0.0
grain13-33	Core	16.4	16.6	62247	17.6	111524	294503	b.d.l.	13697	26817	1.0	61.3	b.d.l.	8.1	1534.9	4.3	254.1	0.2	b.d.l.	b.d.l.	b.d.l.	895.8	23.0	26.2	1.8	4.8	0.4	6.7	0.2	0.0	0.0
grain13-34	Core	13.8	12.8	58423	18.7	106020	294503	b.d.l.	12030	25267	0.4	57.2	b.d.l.	6.6	1456.6	4.2	235.3	0.2	b.d.l.	b.d.l.	b.d.l.	831.6	21.0	23.9	1.6	4.5	0.3	6.1	0.1	0.0	0.0
grain13-35	Core	15.0	13.1	56083	16.1	102425	294503	26.5	12545	24865	0.6	53.4	b.d.l.	7.5	1421.3	4.3	235.5	0.2	b.d.l.	b.d.l.	b.d.l.	834.8	20.7	22.9	1.6	4.4	0.3	6.0	0.1	0.0	0.1
grain13-36	Core	14.1	12.8	59247	17.6	111021	294503	b.d.l.	14140	26719	0.9	64.6	b.d.l.	8.0	1536.2	4.4	253.2	0.2	b.d.l.	b.d.l.	b.d.l.	873.5	22.9	25.1	1.8	4.8	0.4	6.6	0.1	0.0	0.0
grain13-37	Core	12.1	13.0	58545	17.9	109951	294503	16.2	13853	26097	1.0	56.1	b.d.l.	7.2	1529.8	4.2	246.2	0.2	b.d.l.	0.0	b.d.l.	852.1	23.1	25.6	1.8	4.5	0.4	6.3	0.2	0.0	0.1
grain13-38	Core	12.5	12.2	60418	14.7	111146	294503	b.d.l.	13642	25722	0.9	60.1	b.d.l.	7.5	1521.1	4.5	250.0	0.2	b.d.l.	b.d.l.	b.d.l.	849.1	22.9	25.6	1.7	4.4	0.5	6.3	0.2	0.0	0.1
grain13-39	Core	12.6	11.4	58137	16.6	107187	294503	16.2	13596	27612	0.6	53.4	b.d.l.	7.4	1518.1	4.1	237.1	0.2	b.d.l.	0.0	b.d.l.	856.5	21.8	25.3	1.7	4.4	0.5	6.3	0.2	0.0	0.1
grain13-40	Core	13.3	13.9	59822	17.1	108544	294503	b.d.l.	13902	26233	0.7	58.1	b.d.l.	7.5	1562.4	4.2	248.7	0.2	b.d.l.	b.d.l.	b.d.l.	901.3	22.7	25.6	1.8	4.6	0.4	6.4	0.1	0.0	0.0
grain13-41	Core	15.3	13.9	59822	17.1	108544	294503	b.d.l.	13902	26233	0.7	58.1	b.d.l.	7.5	1562.4	4.2	248.7	0.2	b.d.l.	b.d.l.	b.d.l.	901.3	22.7	25.6	1.8	4.6	0.4	6.4	0.1	0.0	0.0
grain13-42	Core	15.5	14.2	57288	16.3	108581	294503	21.5	12996	26213	0.6	60.8	b.d.l.	7.5	1543.7	4.0	253.3	0.1	b.d.l.	b.d.l.	b.d.l.	863.9	22.4	24.7	1.7	4.6	0.3	6.6	0.2	0.0	0.1
grain13-43	Core	15.9	14.7	61094	20.8	110544	294503	15.1	13699	27084	0.5	61.9	b.d.l.	8.2	1611.9	4.2	269.4	0.2	b.d.l.	b.d.l.	b.d.l.	859.2	22.2	25.1	1.9	4.7	0.4	6.7	0.2	0.0	0.1
grain13-44	Core	17.7	16.4	60780	14.3	107190	294503	b.d.l.	13574	26151	0.6	61.7	b.d.l.	7.3	1547.4	4.5	261.6	0.2	b.d.l.	b.d.l.	b.d.l.	1029.1	23.1	25.0	1.7	4.2	0.3	6.9	0.2	0.0	0.1
grain13-45	Core	19.4	17.9	60674	20.3	113174	294503	12.4	13991	27060	0.4	63.5	b.d.l.	7.8	1609.5	4.5	289.5	0.2	b.d.l.	0.0	b.d.l.	1103.7	23.7	26.7	1.8	4.7	0.4	6.8	0.1	0.0	0.0
grain13-46	Core	17.4	18.3	59536	17.3	109954	294503	b.d.l.	12831	27386	0.7	67.3	b.d.l.	7.6	1617.8	4.2	265.9	0.2	0.0	b.d.l.	b.d.l.	1056.1	23.1	25.1	1.8	4.5	0.2	7.0	0.2	0.0	b.d.l.
grain13-47	Core	20.4	19.3	63350	16.5	114241	294503	b.d.l.	13509	28350	0.6	79.9	b.d.l.	8.2	1696.4	4.1	270.7	0.2	b.d.l.	b.d.l.	b.d.l.	1063.2	22.6	25.8	1.8	5.3	0.4	7.0	0.2	0.0	0.1
grain13-48	Core	19.9	19.1	57774	20.8	111516	294503	20.2	12295	29171	0.6	84.3	b.d.l.	8.2	1667.7	3.7	265.7	0.2	b.d.l.	b.d.l.	b.d.l.	1024.4	22.3	25.4	1.8	4.7	0.4	6.7	0.2	0.0	0.1
grain13-49	Core	21.1	19.3	59809	23.3	110011	294503	18.5	11711	28599	0.8	84.5	b.d.l.	8.2	1680.0	3.8	256.2	0.2	b.d.l.	b.d.l.	b.d.l.	962.8	20.8	24.3	1.7	4.5	0.4	6.6	0.1	0.0	0.0
grain13-50	Core	19.1	19.6	56389	16.2	108537	294503	16.5	12108	28079	0.4	83.7	b.d.l.	7.9	1644.8	3.7	257.3	0.2	b.d.l.	b.d.l.	b.d.l.	943.3	20.7	23.6	1.6	4.3	0.4	6.6	0.2	0.0	0.0
grain13-51	Core	20.2	19.8	61973	16.0	110734	294503	18.1	15057	27306	0.7	58.1	b.d.l.	7.3	1679.9	4.4	255.8	0.2	b.d.l.	b.d.l.	b.d.l.	952.2	21.0	23.4	1.7	4.2	0.3	6.5	0.1	0.0	0.0
grain13-52	Core	20.9	18.7	59106	18.0	109992	294503	b.d.l.	13424	26571	0.7	56.7	b.d.l.	8.0	1653.6	4.0	249.2	0.2	b.d.l.	b.d.l.	b.d.l.	899.2	20.5	22.9	1.6	4.4	0.3	6.1	0.1	0.0	0.1
grain13-53	Core	20.0	18.5	58709	18.6	104371	294503	17.9	12823	26238	0.6	52.5	b.d.l.	7.5	1585.3	4.0	239.1	0.2	b.d.l.	b.d.l.	b.d.l.	807.0	21.0	23.8	1.6	4.4	0.4	6.2	0.2	0.0	0.0
grain13-54	Core	20.9	19.2	59452	23.0	113398	294503	17.7	12944	28893	0.7	57.9	b.d.l.	8.1	1625.7	4.0	250.8	0.2	b.d.l.	0.0	b.d.l.	812.4	22.2	24.7	1.8	4.8	0.4	6.5	0.2	0.0	0.1
grain13-55	Core	21.9	19.3	58330	23.9	109469	294503	b.d.l.	12588	27874	0.7	50.6	b.d.l.	8.3	1712.3	4.4	249.6	0.2	b.d.l.	b.d.l.	b.d.l.	787.4	22.3	24.9	1.7	4.8	0.3	6.1	0.2	0.0	0.0
grain13-56	Core	20.0	18.6	59254	20.9	110353	294503	b.d.l.	12981	27370	0.7	53.9	b.d.l.	8.0	1612.9	4.4	245.0	0.2	b.d.l.	b.d.l.	b.d.l.	807.0	21.0	23.8	1.6	4.4	0.3	6.4	0.2	0.0	0.0
grain13-57	Core	19.8	18.8	59345	19.9	112769	294503	20.6	13712	28039	0.9	56.1	b.d.l.	7.5	1616.6	4.6	248.5	0.2	b.d.l.	b.d.l.	b.d.l.	833.8	22.2	25.6	1.8	4.6	0.3	6.5	0.2	0.0	0.0
grain13-58	Core	19.8	18.2	56585	18.0	107066	294503	b.d.l.	12565	27390	0.6	59.6	b.d.l.	8.2	1601.5	3.8	231.6	0.2	b.d.l.	0.0	b.d.l.	787.4	22.3	24.9	1.7	4.8	0.3	6.1	0.2	0.0	0.0
grain13-59	Middle	20.9	19.0	57932	21.1	109126	294503	21.6	12532	27395	0.8	60.6	b.d.l.	7.6	1588.8	3.9	227.3	0.2	0.1	b.d.l.	b.d.l.	751.7	2								

Table A1.7: continued

Ho	Er	Tm	Yb	Lu	Hf	Ta	Pb	Th	U
0.0	0.0	b.d.l.	b.d.l.	b.d.l.	b.d.l.	0.0	12.4	b.d.l.	b.d.l.
b.d.l.	0.0	b.d.l.	0.0	0.0	b.d.l.	0.0	12.6	b.d.l.	b.d.l.
0.0	b.d.l.	b.d.l.	b.d.l.	b.d.l.	b.d.l.	b.d.l.	12.0	b.d.l.	b.d.l.
0.0	0.0	0.0	b.d.l.	b.d.l.	b.d.l.	b.d.l.	11.9	b.d.l.	0.0
0.0	b.d.l.	b.d.l.	0.0	0.0	0.0	b.d.l.	12.6	0.0	b.d.l.
0.0	0.0	0.0	b.d.l.	b.d.l.	b.d.l.	b.d.l.	12.7	b.d.l.	b.d.l.
0.0	0.0	b.d.l.	b.d.l.	0.0	b.d.l.	b.d.l.	12.6	b.d.l.	b.d.l.
b.d.l.	0.0	b.d.l.	b.d.l.	b.d.l.	b.d.l.	b.d.l.	12.8	b.d.l.	b.d.l.
0.0	b.d.l.	b.d.l.	b.d.l.	b.d.l.	b.d.l.	0.0	13.0	b.d.l.	b.d.l.
0.0	b.d.l.	b.d.l.	0.0	b.d.l.	b.d.l.	0.0	13.3	b.d.l.	b.d.l.
0.0	b.d.l.	b.d.l.	b.d.l.	b.d.l.	b.d.l.	b.d.l.	12.3	b.d.l.	b.d.l.
b.d.l.	0.0	0.0	b.d.l.	0.0	b.d.l.	b.d.l.	13.0	b.d.l.	b.d.l.
0.0	0.0	b.d.l.	b.d.l.	b.d.l.	b.d.l.	0.0	12.8	b.d.l.	b.d.l.
0.0	b.d.l.	b.d.l.	0.0	b.d.l.	b.d.l.	b.d.l.	12.1	b.d.l.	b.d.l.
b.d.l.	b.d.l.	0.0	b.d.l.	0.0	b.d.l.	b.d.l.	12.8	b.d.l.	b.d.l.
0.0	0.0	b.d.l.	b.d.l.	b.d.l.	b.d.l.	b.d.l.	13.3	b.d.l.	0.0
0.0	0.0	b.d.l.	b.d.l.	b.d.l.	b.d.l.	0.0	13.2	b.d.l.	b.d.l.
0.0	0.0	b.d.l.	b.d.l.	b.d.l.	b.d.l.	b.d.l.	12.6	b.d.l.	b.d.l.
b.d.l.	b.d.l.	b.d.l.	b.d.l.	0.0	b.d.l.	b.d.l.	12.6	b.d.l.	b.d.l.
0.0	0.0	0.0	b.d.l.	b.d.l.	b.d.l.	b.d.l.	12.4	0.0	b.d.l.
b.d.l.	0.0	b.d.l.	b.d.l.	b.d.l.	b.d.l.	b.d.l.	12.7	b.d.l.	b.d.l.
0.0	0.0	0.0	b.d.l.	b.d.l.	b.d.l.	b.d.l.	12.9	b.d.l.	b.d.l.
0.0	0.0	b.d.l.	b.d.l.	b.d.l.	b.d.l.	b.d.l.	12.5	b.d.l.	b.d.l.
0.0	0.0	b.d.l.	b.d.l.	b.d.l.	b.d.l.	b.d.l.	13.1	0.0	b.d.l.
0.0	0.0	b.d.l.	b.d.l.	b.d.l.	b.d.l.	b.d.l.	12.8	b.d.l.	b.d.l.
0.0	0.0	b.d.l.	b.d.l.	b.d.l.	b.d.l.	b.d.l.	13.2	b.d.l.	b.d.l.
0.0	0.0	b.d.l.	b.d.l.	b.d.l.	b.d.l.	b.d.l.	13.0	b.d.l.	b.d.l.
0.0	b.d.l.	b.d.l.	b.d.l.	b.d.l.	b.d.l.	b.d.l.	13.4	b.d.l.	b.d.l.
0.0	0.0	b.d.l.	0.0	b.d.l.	b.d.l.	b.d.l.	12.3	b.d.l.	b.d.l.
b.d.l.	0.0	b.d.l.	b.d.l.	b.d.l.	b.d.l.	b.d.l.	13.1	b.d.l.	b.d.l.
b.d.l.	b.d.l.	b.d.l.	b.d.l.	0.0	b.d.l.	b.d.l.	12.3	b.d.l.	b.d.l.
0.0	b.d.l.	b.d.l.	b.d.l.	b.d.l.	b.d.l.	b.d.l.	12.7	b.d.l.	b.d.l.
0.0	0.0	b.d.l.	b.d.l.	b.d.l.	b.d.l.	b.d.l.	12.9	b.d.l.	b.d.l.
0.0	b.d.l.	b.d.l.	b.d.l.	b.d.l.	0.0	b.d.l.	13.6	b.d.l.	0.0
b.d.l.	0.0	b.d.l.	b.d.l.	b.d.l.	b.d.l.	b.d.l.	13.0	b.d.l.	b.d.l.
b.d.l.	0.0	b.d.l.	0.0	b.d.l.	0.0	b.d.l.	13.7	b.d.l.	b.d.l.
0.0	b.d.l.	b.d.l.	0.0	0.0	b.d.l.	b.d.l.	12.8	b.d.l.	b.d.l.
b.d.l.	b.d.l.	b.d.l.	b.d.l.	b.d.l.	b.d.l.	b.d.l.	12.9	b.d.l.	b.d.l.
0.0	0.0	b.d.l.	b.d.l.	b.d.l.	b.d.l.	b.d.l.	13.2	b.d.l.	b.d.l.
b.d.l.	0.0	b.d.l.	b.d.l.	b.d.l.	b.d.l.	b.d.l.	13.6	0.0	b.d.l.
0.0	0.0	0.0	b.d.l.	b.d.l.	b.d.l.	b.d.l.	13.7	b.d.l.	b.d.l.
0.0	0.0	b.d.l.	0.0	b.d.l.	0.0	0.0	13.1	b.d.l.	b.d.l.
b.d.l.	0.0	b.d.l.	b.d.l.	b.d.l.	b.d.l.	b.d.l.	13.6	0.0	b.d.l.
0.0	0.0	0.0	b.d.l.	b.d.l.	b.d.l.	b.d.l.	14.0	b.d.l.	b.d.l.
0.0	0.0	b.d.l.	b.d.l.	b.d.l.	b.d.l.	b.d.l.	13.8	b.d.l.	b.d.l.
0.0	0.0	b.d.l.	b.d.l.	b.d.l.	b.d.l.	b.d.l.	14.1	b.d.l.	b.d.l.
0.0	b.d.l.	b.d.l.	b.d.l.	b.d.l.	b.d.l.	b.d.l.	13.9	0.0	b.d.l.
0.0	0.0	b.d.l.	b.d.l.	0.0	b.d.l.	b.d.l.	13.5	b.d.l.	b.d.l.
0.0	b.d.l.	b.d.l.	0.0	b.d.l.	b.d.l.	b.d.l.	14.1	b.d.l.	b.d.l.
0.0	0.0	b.d.l.	0.0	0.0	b.d.l.	b.d.l.	14.3	0.0	b.d.l.
0.0	0.0	b.d.l.	0.0	0.0	0.0	b.d.l.	14.2	b.d.l.	b.d.l.
0.0	0.0	b.d.l.	0.0	b.d.l.	b.d.l.	b.d.l.	13.7	b.d.l.	b.d.l.

Table A1.7: continued

Info	Position	Li ⁶	Li ⁷	Na	Mg	Al	Si	P	K	Ca	Sc	Ti	V	Mn	Fe	Rb	Sr	Y	Zr	Nb	Cs	Ba	La	Ce	Pr	Nd	Sm	Eu	Gd	Tb	Dy
grain14-10	Middle	21.6	20.3	57357	24.2	122178	294503	27.2	8519	38633	b.d.l.	92.6	b.d.l.	12.1	1539.4	1.21	2103.0	0.5	b.d.l.	b.d.l.	b.d.l.	408.8	36.7	41.8	3.1	7.8	0.9	5.5	0.4	0.0	0.1
grain14-11	Middle	21.1	19.4	56289	25.8	121016	294503	16.5	7951	39331	0.7	91.6	0.2	12.8	1481.8	1.9	2199.0	0.5	b.d.l.	b.d.l.	b.d.l.	388.6	36.6	42.8	3.2	8.0	0.7	5.7	0.3	0.0	0.1
grain14-12	Core	14.4	14.5	58759	21.2	18297	294503	17.4	8608	37274	0.6	79.4	b.d.l.	12.0	1498.0	2.3	2184.0	0.4	b.d.l.	b.d.l.	b.d.l.	414.5	32.6	38.8	2.7	7.5	0.4	6.0	0.4	0.0	0.1
grain14-13	Core - close to crack	6.7	6.7	161809	28.2	115359	294503	15.2	11001	32895	0.9	75.8	b.d.l.	13.0	1604.9	4.5	2221.1	1.3	1.8	0.7	0.1	493.9	28.0	33.4	2.4	6.7	0.5	5.9	0.5	0.1	0.2
grain14-14	Core - close to crack	8.2	7.7	58516	23.4	116343	294503	27.1	8857	34285	0.7	73.3	b.d.l.	11.3	1511.6	2.6	2238.0	0.4	b.d.l.	0.0	b.d.l.	463.1	30.5	36.0	2.6	6.6	0.6	5.7	0.3	0.0	0.1
grain14-15	Core	11.7	10.3	58474	24.5	119445	294503	15.2	9885	35397	0.7	67.8	b.d.l.	11.5	1536.1	1.29	2210.0	0.6	0.2	0.1	b.d.l.	482.8	29.7	35.5	2.6	6.9	0.6	5.9	0.3	0.0	0.1
grain14-16	Core	9.9	9.7	62352	20.1	116200	294503	19.2	10226	32233	0.8	69.6	b.d.l.	11.1	1631.8	3.1	2264.0	0.6	0.3	0.2	b.d.l.	512.6	29.6	33.5	2.4	6.1	0.5	5.7	0.3	0.0	0.1
grain14-17	Core - close to crack	8.6	8.5	58393	18.5	109141	294503	16.5	12882	28683	0.8	67.5	b.d.l.	9.4	1607.5	4.1	2262.0	0.2	b.d.l.	b.d.l.	b.d.l.	627.9	24.8	28.8	2.0	5.0	0.4	6.0	0.3	0.0	0.1
grain14-18	Core - close to crack	7.1	8.2	59377	23.5	111314	294503	13.3	12830	29246	0.6	60.1	b.d.l.	8.3	1576.6	4.0	2358.0	0.2	b.d.l.	b.d.l.	b.d.l.	663.7	23.7	27.4	2.1	5.3	0.3	6.3	0.2	0.0	0.1
grain14-19	Core - close to crack	8.3	7.7	58528	18.4	108414	294503	14.8	12630	27343	0.6	54.1	0.1	9.7	1555.5	4.4	2194.4	0.4	2.6	0.0	0.1	660.7	22.2	25.3	1.8	4.7	0.3	5.9	0.2	0.0	0.1
grain14-21	Core - close to crack	5.9	6.4	54528	37.8	104183	280479	38.1	12326	24880	1.0	59.0	0.1	9.7	1555.5	4.4	2194.4	0.4	2.6	0.0	0.1	660.7	22.2	25.3	1.8	4.7	0.3	5.9	0.2	0.0	0.1
grain14-22	Core - close to crack	7.0	6.4	55675	28.1	100747	280479	42.5	12949	24970	0.7	61.3	b.d.l.	8.6	1498.1	4.4	2142.2	1.4	0.9	0.3	0.1	618.6	21.6	27.5	2.0	5.7	0.8	5.5	0.5	0.1	0.3
grain14-23	Core	6.5	7.4	54722	22.4	102384	280479	42.8	13237	27138	0.4	55.3	b.d.l.	7.8	1513.7	3.9	2159.0	0.6	0.3	0.1	b.d.l.	590.5	20.4	25.2	1.9	5.2	0.5	5.7	0.2	0.0	0.1
grain14-24	Core	7.2	7.2	54944	22.1	102514	280479	19.0	12953	26856	0.5	54.6	b.d.l.	7.8	1433.8	3.9	2191.0	0.5	0.1	0.1	b.d.l.	605.7	20.9	24.2	1.7	4.5	0.5	5.6	0.2	0.0	0.1
grain14-25	Core	7.0	6.4	55933	23.4	102887	294503	22.4	12341	26303	0.7	56.1	b.d.l.	7.3	1448.5	4.3	2175.0	0.3	0.4	0.1	b.d.l.	628.2	20.4	23.1	1.9	4.5	0.4	5.6	0.1	0.0	0.1
grain14-26	Core	b.d.l.	6.3	58459	21.5	105596	294503	b.d.l.	12352	27545	0.8	55.5	b.d.l.	8.5	1452.6	4.3	2151.0	0.4	0.3	0.2	b.d.l.	615.6	21.2	24.4	1.9	4.8	0.3	5.4	0.2	0.0	0.1
grain14-27	Core	7.0	6.3	60251	24.2	113760	294503	36.2	13451	28493	0.7	57.9	b.d.l.	8.2	1636.5	4.4	2437.0	0.9	0.3	0.1	b.d.l.	708.7	22.8	25.9	1.9	5.2	0.4	6.1	0.3	0.0	0.2
grain14-28	Core	6.8	6.8	58009	18.8	107687	294503	23.1	11955	26642	0.8	56.8	b.d.l.	7.8	1576.5	3.8	2316.0	0.2	b.d.l.	0.0	b.d.l.	675.9	21.4	24.9	1.6	4.2	0.5	5.6	b.d.l.	0.0	0.1
grain14-29	Core	8.3	7.6	59121	20.7	109643	294503	b.d.l.	12690	28140	1.0	57.4	b.d.l.	9.1	1608.5	4.5	2402.0	0.2	b.d.l.	0.1	b.d.l.	678.3	22.1	24.9	1.7	4.3	0.4	6.4	0.1	0.0	b.d.l.
grain14-30	Core	9.1	8.9	56989	18.4	107046	294503	b.d.l.	11809	27475	0.7	52.8	b.d.l.	7.7	1546.7	3.9	2404.0	0.3	b.d.l.	b.d.l.	611.8	22.1	24.8	1.7	4.3	0.4	6.0	0.2	0.0	0.1	
grain14-31	Core	10.6	10.0	56960	20.7	108609	294503	14.3	12829	27606	0.6	53.0	b.d.l.	7.6	1574.5	4.3	2413.0	0.2	b.d.l.	0.0	b.d.l.	626.8	22.0	24.8	1.7	4.5	0.3	6.3	0.2	0.0	0.1
grain14-32	Core	12.0	12.3	57985	18.1	104793	294503	b.d.l.	12366	25666	0.7	52.4	b.d.l.	7.3	1422.5	4.1	2273.0	0.2	0.1	b.d.l.	b.d.l.	605.2	20.8	23.2	1.6	4.2	0.4	5.6	0.2	0.0	0.1
grain14-33	Core	10.0	11.0	61199	16.8	108247	294503	b.d.l.	12771	27042	0.7	56.4	b.d.l.	8.0	1498.7	4.4	2433.0	0.2	b.d.l.	b.d.l.	612.0	21.8	25.1	1.7	4.6	0.3	6.4	0.1	b.d.l.	0.0	0.1
grain14-34	Core	10.3	10.5	58724	13.1	109154	294503	b.d.l.	14758	26230	0.9	59.0	b.d.l.	7.5	1505.9	3.7	250.8	0.4	0.9	0.2	b.d.l.	618.6	22.9	26.2	1.8	4.8	0.3	6.3	b.d.l.	0.0	0.1
grain14-35	Core	10.2	10.5	59837	22.2	107703	294503	b.d.l.	11563	27839	0.8	51.4	b.d.l.	9.3	1593.8	3.3	241.4	0.3	b.d.l.	0.0	b.d.l.	590.8	22.8	27.2	1.9	5.3	0.5	6.2	0.2	0.0	0.1
grain14-36	Core - close to crack	9.1	8.0	53510	19.2	100569	294503	21.5	11837	25495	0.6	57.4	b.d.l.	8.1	1425.3	4.4	2325.0	0.5	0.6	0.2	b.d.l.	581.9	22.7	26.3	1.9	5.3	0.4	6.0	0.3	0.0	0.1
grain14-37	Core - close to crack	7.8	8.7	57463	18.3	109106	294503	17.7	12904	26163	0.4	67.2	b.d.l.	7.7	1538.7	4.5	2599.0	0.2	b.d.l.	0.0	b.d.l.	755.0	22.7	25.7	1.8	4.7	0.5	6.8	0.2	0.0	0.1
grain14-40	Core	8.4	7.7	57548	20.9	105489	294503	13.3	12890	25743	0.6	54.1	0.1	7.5	1493.3	4.5	2514.4	0.3	b.d.l.	0.0	b.d.l.	786.2	21.7	25.3	1.7	4.5	0.5	6.4	0.2	0.0	0.1
grain14-41	Core	9.8	8.1	58439	32.2	104306	289829	b.d.l.	13224	24987	0.7	64.5	b.d.l.	9.1	1671.7	5.6	2584.2	2.2	2.6	0.8	0.2	771.6	22.7	24.7	2.1	5.7	0.9	6.8	0.5	0.1	0.4
grain14-42	Core	7.9	7.8	58218	18.3	106989	294503	14.3	13615	26511	0.8	58.4	b.d.l.	8.0	1504.3	4.4	2614.0	0.2	0.1	0.0	b.d.l.	780.3	21.5	23.8	1.7	4.2	0.2	6.7	0.1	0.0	0.0
grain14-43	Core	8.7	9.4	59920	23.0	111873	294503	21.4	14065	27287	0.6	61.4	b.d.l.	8.0	1596.6	4.5	2765.0	0.3	b.d.l.	0.0	b.d.l.	827.5	23.5	25.4	1.9	4.5	0.4	7.2	b.d.l.	0.0	0.1
grain14-44	Core	11.6	10.4	58581	18.3	11447	289829	15.1	13198	26425	0.8	61.1	b.d.l.	7.6	1586.1	4.2	2761.0	0.2	b.d.l.	b.d.l.	798.5	22.7	25.3	1.9	4.6	0.3	7.0	b.d.l.	0.0	0.1	
grain14-45	Core	12.6	11.5	58505	19.0	109087	285154	b.d.l.	13277	25998	b.d.l.	59.2	b.d.l.	7.7	1597.5	4.4	2681.0	0.2	b.d.l.	b.d.l.	790.3	22.4	24.5	1.8	4.6	0.4	6.9	0.2	0.0	0.0	
grain14-46	Core	11.0	11.6	57074	13.9	102493	285154	21.2	12898	25338	0.7	58.1	b.d.l.	6.8	1446.2	4.5	2493.0	0.2	b.d.l.	b.d.l.	743.8	20.4	22.5	1.6	4.1	0.3	6.5	0.2	0.0	0.0	
grain14-47	Core	14.1	12.5	59709	20.8	106344	289829	13.4	13777	26581	0.7	53.9	b.d.l.	7.6	1543.9	4.2	2614.0	0.2	0.1	0.0	b.d.l.	783.9	20.9	23.9	1.7	4.5	0.4	6.8	0.2	0.0	0.1
grain14-48	Core	11.6	11.1	55742	16.3	101024	285154	20.6	12307	25210	0.6	53.1	b.d.l.	7.0	1495.1	4.0	2441.0	0.2	b.d.l.	b.d.l.	724.8	19.9	22.0	1.6	3.7	0.3	6.3	0.1	0.0	0.1	
grain14-49	Core	13.9	12.7	56081	16.6	105584	285154	b.d.l.	12810	25720	0.6	52.9	b.d.l.	7.8	1492.9	4.2	2518.0	0.2	b.d.l.	b.d.l.	762.3	21.2	24.2	1.7	4.8	0.3	6.7	0.2	b.d.l.	0.1	
grain14-50	Middle	15.3	14.3	59917	18.0	109248	289829	b.d.l.	12495	26643	0.7	56.5	b.d.l.	8.6	1554.1	3.9	2495.0	0.2	b.d.l.	b.d.l.											

Table A1.7: continued

Ho	Er	Tm	Yb	Lu	Hf	Ta	Pb	Th	U
b.d.l.	0.0	b.d.l.	b.d.l.	b.d.l.	b.d.l.	b.d.l.	132	b.d.l.	b.d.l.
0.0	0.0	b.d.l.	0.0	b.d.l.	b.d.l.	b.d.l.	129	b.d.l.	b.d.l.
0.0	0.0	0.0	b.d.l.	b.d.l.	b.d.l.	b.d.l.	127	b.d.l.	b.d.l.
0.1	0.1	0.0	0.1	0.0	0.1	0.1	146	0.2	0.0
0.0	0.0	b.d.l.	b.d.l.	b.d.l.	b.d.l.	b.d.l.	131	0.0	b.d.l.
0.0	0.1	b.d.l.	0.0	b.d.l.	b.d.l.	b.d.l.	132	0.0	b.d.l.
0.0	0.0	0.0	b.d.l.	b.d.l.	0.0	0.0	137	0.1	b.d.l.
0.0	0.0	b.d.l.	b.d.l.	b.d.l.	b.d.l.	b.d.l.	138	b.d.l.	b.d.l.
0.0	0.0	b.d.l.	b.d.l.	b.d.l.	0.0	0.0	136	b.d.l.	b.d.l.
0.0	0.0	b.d.l.	b.d.l.	b.d.l.	b.d.l.	b.d.l.	131	b.d.l.	b.d.l.
0.1	0.2	0.0	0.2	0.0	0.1	0.1	131	0.5	0.0
0.1	0.1	0.0	0.1	b.d.l.	0.1	0.0	137	0.3	0.0
0.0	0.0	0.0	0.1	b.d.l.	0.0	0.0	137	0.1	b.d.l.
0.0	0.0	0.0	0.0	b.d.l.	b.d.l.	b.d.l.	129	0.0	b.d.l.
0.0	0.0	b.d.l.	0.0	b.d.l.	0.0	b.d.l.	126	0.0	b.d.l.
0.0	0.0	0.0	b.d.l.	b.d.l.	b.d.l.	b.d.l.	126	0.0	b.d.l.
0.0	0.1	0.0	0.0	b.d.l.	0.0	b.d.l.	134	0.1	0.0
b.d.l.	b.d.l.	b.d.l.	0.0	b.d.l.	b.d.l.	b.d.l.	127	b.d.l.	b.d.l.
b.d.l.	0.0	b.d.l.	b.d.l.	b.d.l.	0.0	0.0	137	0.0	b.d.l.
0.0	0.0	b.d.l.	b.d.l.	0.0	b.d.l.	b.d.l.	129	0.0	b.d.l.
0.0	0.1	b.d.l.	b.d.l.	b.d.l.	b.d.l.	b.d.l.	134	0.0	0.0
0.0	0.0	b.d.l.	0.0	b.d.l.	0.0	b.d.l.	129	0.0	0.0
0.0	0.0	b.d.l.	0.0	b.d.l.	0.0	0.0	122	b.d.l.	b.d.l.
0.0	0.0	b.d.l.	b.d.l.	b.d.l.	b.d.l.	b.d.l.	127	b.d.l.	b.d.l.
0.0	0.1	b.d.l.	0.0	b.d.l.	0.0	0.0	131	0.1	0.0
0.0	0.0	b.d.l.	0.0	b.d.l.	b.d.l.	b.d.l.	123	0.0	b.d.l.
0.0	0.0	b.d.l.	0.0	b.d.l.	0.0	b.d.l.	117	0.1	b.d.l.
b.d.l.	0.0	0.0	b.d.l.	b.d.l.	b.d.l.	b.d.l.	129	b.d.l.	b.d.l.
0.0	0.0	0.0	0.0	b.d.l.	b.d.l.	0.0	122	0.0	b.d.l.
0.1	0.2	0.0	0.2	0.0	0.1	0.0	156	0.5	0.0
0.0	b.d.l.	0.0	0.0	b.d.l.	b.d.l.	b.d.l.	129	0.0	0.0
b.d.l.	b.d.l.	b.d.l.	0.0	b.d.l.	b.d.l.	b.d.l.	128	b.d.l.	b.d.l.
0.0	0.0	b.d.l.	b.d.l.	0.0	b.d.l.	b.d.l.	130	b.d.l.	b.d.l.
0.0	0.0	b.d.l.	b.d.l.	b.d.l.	0.0	b.d.l.	135	b.d.l.	b.d.l.
0.0	b.d.l.	0.0	b.d.l.	b.d.l.	b.d.l.	b.d.l.	121	b.d.l.	b.d.l.
0.0	b.d.l.	b.d.l.	b.d.l.	0.0	b.d.l.	b.d.l.	127	b.d.l.	b.d.l.
b.d.l.	0.0	b.d.l.	b.d.l.	b.d.l.	b.d.l.	b.d.l.	121	b.d.l.	b.d.l.
0.0	b.d.l.	0.0	b.d.l.	b.d.l.	b.d.l.	b.d.l.	125	b.d.l.	b.d.l.
0.0	b.d.l.	b.d.l.	b.d.l.	b.d.l.	0.0	b.d.l.	133	b.d.l.	b.d.l.
0.0	0.0	b.d.l.	b.d.l.	b.d.l.	b.d.l.	b.d.l.	125	b.d.l.	b.d.l.
0.0	0.0	b.d.l.	b.d.l.	b.d.l.	0.0	b.d.l.	121	0.0	0.0
0.0	b.d.l.	b.d.l.	0.0	b.d.l.	b.d.l.	b.d.l.	125	0.0	0.0
0.0	b.d.l.	b.d.l.	b.d.l.	b.d.l.	b.d.l.	b.d.l.	132	b.d.l.	b.d.l.
0.0	0.1	0.0	0.0	b.d.l.	b.d.l.	b.d.l.	138	0.0	b.d.l.
0.0	0.0	b.d.l.	b.d.l.	b.d.l.	b.d.l.	b.d.l.	151	b.d.l.	b.d.l.
0.0	0.0	0.0	b.d.l.	b.d.l.	b.d.l.	b.d.l.	148	b.d.l.	b.d.l.
0.0	b.d.l.	b.d.l.	b.d.l.	b.d.l.	b.d.l.	b.d.l.	135	0.0	b.d.l.
0.0	0.0	0.0	b.d.l.	b.d.l.	b.d.l.	0.0	144	b.d.l.	b.d.l.
0.0	b.d.l.	b.d.l.	0.0	b.d.l.	b.d.l.	b.d.l.	139	b.d.l.	b.d.l.
b.d.l.	b.d.l.	0.0	b.d.l.	b.d.l.	b.d.l.	b.d.l.	141	b.d.l.	b.d.l.

Table A1.7: continued

Info	Position	Li ⁺	Li ⁺	Na	Mg	Al	Si	P	K	Ca	Sc	Ti	V	Mn	Fe	Rb	Sr	Y	Zr	Nb	Cs	Ba	La	Ce	Pr	Nd	Sm	Eu	Gd	Tb	Dy
grain20-7	Middle	28.0	25.2	58234	17.2	109190	294503	b.d.l.	12076	28664	0.6	51.9	0.1	9.2	14459	4.0	217.0	0.2	b.d.l.	b.d.l.	b.d.l.	595.3	22.2	25.4	1.8	4.7	0.4	5.8	b.d.l.	b.d.l.	0.0
grain20-8	Middle	25.4	25.4	55758	21.4	110368	294503	26.2	10999	27168	0.5	58.4	b.d.l.	9.2	15136	3.7	221.2	0.3	b.d.l.	b.d.l.	b.d.l.	652.8	21.9	24.4	1.8	5.1	0.4	6.0	0.3	0.0	0.0
grain20-9	Middle	28.4	26.9	61739	16.1	111700	294503	25.3	13549	28179	b.d.l.	52.7	b.d.l.	7.9	15533	4.1	226.1	0.2	b.d.l.	b.d.l.	b.d.l.	674.4	21.4	23.9	1.8	4.1	0.3	6.2	b.d.l.	b.d.l.	0.0
grain20-10	Middle	28.4	25.3	57691	25.7	109626	294503	19.1	13162	26371	0.8	53.2	b.d.l.	7.7	15258	4.4	225.4	0.2	b.d.l.	0.0	b.d.l.	731.5	20.7	23.2	1.6	4.2	0.5	6.0	b.d.l.	0.0	0.1
grain20-11	Middle	24.6	22.7	60943	24.4	112146	294503	b.d.l.	12501	27198	0.5	56.4	b.d.l.	8.2	15579	4.3	230.0	0.2	0.1	0.0	b.d.l.	747.8	21.8	24.6	1.7	4.4	0.5	6.2	0.3	0.0	0.1
grain20-12	Middle	21.6	22.3	58514	23.2	111164	294503	b.d.l.	13181	28324	0.7	56.5	b.d.l.	7.7	15519	4.3	224.7	0.2	b.d.l.	b.d.l.	b.d.l.	758.7	22.7	24.7	1.8	4.4	0.3	6.2	0.2	0.0	0.1
grain20-13	Middle	23.0	20.5	62450	27.5	112269	299178	15.5	14077	27984	0.7	60.0	b.d.l.	7.6	15928	4.5	241.6	0.2	0.2	0.0	b.d.l.	804.5	23.8	25.7	1.7	4.8	0.4	6.7	0.1	b.d.l.	0.1
grain20-14	Core	21.1	20.4	60104	22.9	110715	294503	b.d.l.	13467	26268	0.6	57.0	b.d.l.	7.3	15343	4.7	238.9	0.2	0.1	0.0	b.d.l.	810.4	22.9	25.0	1.8	4.7	0.5	6.6	0.1	0.0	0.0
grain20-15	Core	22.8	20.2	56809	25.3	109451	294503	b.d.l.	13010	28211	0.5	53.0	b.d.l.	7.2	15184	4.0	239.2	0.2	0.2	b.d.l.	0.0	782.2	23.2	25.6	1.9	4.6	0.3	6.3	0.2	b.d.l.	0.1
grain20-16	Core	19.2	19.1	55650	26.7	108620	294503	b.d.l.	12718	28818	0.5	57.2	b.d.l.	8.1	14634	3.8	233.8	0.2	0.1	0.0	b.d.l.	729.3	22.5	25.2	1.8	5.0	0.4	6.2	0.3	0.0	0.1
grain20-17	Core	20.9	20.4	58171	18.4	111169	294503	b.d.l.	12300	28581	0.7	56.4	b.d.l.	8.3	14719	4.1	235.0	0.2	b.d.l.	0.0	b.d.l.	708.1	22.6	25.1	1.8	4.8	0.4	6.0	0.2	b.d.l.	0.1
grain20-18	Core	22.7	20.6	61055	20.1	112910	294503	b.d.l.	13031	28906	0.6	58.9	b.d.l.	8.0	15765	4.2	248.5	0.2	b.d.l.	b.d.l.	807.6	24.7	26.2	1.9	4.7	0.4	6.5	b.d.l.	b.d.l.	b.d.l.	
grain20-19	Core	18.2	19.2	58089	17.6	109106	294503	b.d.l.	13031	26906	0.6	53.5	b.d.l.	7.3	14847	4.2	234.3	0.3	0.2	0.0	b.d.l.	769.9	23.0	25.9	1.9	4.8	0.3	6.6	b.d.l.	b.d.l.	
grain20-20	Core	19.2	19.5	64006	22.0	110566	294503	22.0	12194	29313	0.6	59.7	b.d.l.	8.1	15808	4.3	246.1	0.2	b.d.l.	b.d.l.	b.d.l.	754.4	23.9	27.3	1.8	4.9	0.3	6.7	0.2	0.0	0.0
grain20-21	Core	23.2	20.0	60234	23.4	109015	294503	19.1	12517	27911	0.4	59.5	b.d.l.	7.8	15762	3.9	239.9	0.2	b.d.l.	b.d.l.	720.7	23.2	25.3	1.9	4.9	0.4	6.9	b.d.l.	0.0	0.1	
grain20-22	Core	19.3	19.3	59017	19.1	108727	294503	20.8	13698	26759	0.6	56.5	b.d.l.	7.1	15057	4.5	238.4	0.2	b.d.l.	b.d.l.	745.7	22.6	25.3	1.7	4.5	0.3	6.6	b.d.l.	0.0	0.1	
grain20-23	Core	20.2	19.2	59456	27.3	112951	294503	b.d.l.	13874	27462	0.6	58.5	b.d.l.	8.1	15664	5.2	265.0	0.3	0.2	0.1	b.d.l.	891.8	24.0	25.9	1.9	4.6	0.4	7.1	0.2	b.d.l.	0.1
grain20-24	Core	19.4	19.7	59976	23.7	114142	294503	17.8	14156	27195	0.7	61.6	b.d.l.	7.0	15344	4.6	245.3	0.2	b.d.l.	b.d.l.	847.6	23.3	25.4	1.8	4.8	0.3	6.8	b.d.l.	0.0	0.1	
grain20-25	Core	22.6	20.2	58004	22.5	109256	294503	b.d.l.	13832	26043	b.d.l.	61.4	b.d.l.	7.4	15138	4.5	252.0	0.2	b.d.l.	b.d.l.	866.6	22.7	24.7	1.7	4.6	0.5	6.8	0.2	b.d.l.	b.d.l.	
grain20-26	Core	22.5	21.2	61580	28.3	111119	294503	19.3	14832	27359	0.6	66.8	b.d.l.	7.4	15681	4.4	267.1	0.2	b.d.l.	b.d.l.	898.5	22.8	24.6	1.8	4.8	0.4	7.2	0.2	0.0	0.0	
grain20-27	Core	22.1	20.5	57499	24.5	110364	294503	21.6	14807	26115	0.4	68.8	b.d.l.	7.0	15786	4.7	263.6	0.2	b.d.l.	b.d.l.	802.3	21.4	23.6	1.7	3.9	0.4	6.2	0.1	0.0	0.1	
grain20-28	Core	19.2	18.4	57501	16.7	112541	294503	b.d.l.	15147	28025	0.7	63.6	0.1	7.4	15470	4.8	265.9	0.2	0.1	b.d.l.	886.0	21.8	23.8	1.7	4.3	0.4	7.0	0.2	0.0	0.0	
grain20-29	Core	17.0	16.0	57123	20.4	107301	294503	17.9	13787	25566	0.6	59.2	b.d.l.	7.0	15344	4.6	245.3	0.2	b.d.l.	b.d.l.	854.9	22.3	23.7	1.6	4.4	0.3	6.8	b.d.l.	0.0	0.1	
grain20-30	Core	20.8	18.8	62324	18.6	113064	294503	b.d.l.	13984	26896	0.6	60.1	b.d.l.	7.8	15929	4.7	251.0	0.2	b.d.l.	b.d.l.	847.6	23.3	25.4	1.8	4.8	0.3	6.6	b.d.l.	0.0	0.1	
grain20-31	Core	24.4	20.5	59816	25.2	109560	294503	b.d.l.	14279	26725	0.9	57.6	b.d.l.	7.7	15327	4.0	243.9	0.1	b.d.l.	b.d.l.	826.6	21.3	25.1	1.6	4.1	0.3	6.6	b.d.l.	0.0	0.0	
grain20-32	Core	22.1	20.7	60553	25.3	104056	294503	b.d.l.	12976	25234	0.6	60.0	b.d.l.	7.4	15621	4.4	229.6	0.2	b.d.l.	b.d.l.	800.3	21.4	23.6	1.7	3.9	0.4	6.2	0.1	0.0	0.1	
grain20-33	Middle	24.3	22.3	61499	21.8	111720	294503	b.d.l.	14353	26914	0.7	65.5	0.1	7.6	16456	5.0	243.3	0.2	b.d.l.	b.d.l.	882.4	23.7	26.3	1.9	4.5	0.4	6.8	0.2	0.0	0.1	
grain20-34	Middle	23.1	22.4	57333	20.8	108242	294503	b.d.l.	14730	26340	0.9	61.3	0.1	6.5	15075	4.9	228.7	0.2	b.d.l.	b.d.l.	850.0	22.2	24.5	1.7	3.8	0.4	6.3	0.2	0.0	0.0	
grain20-35	Middle	24.3	24.2	63114	25.6	115885	294503	b.d.l.	14571	27044	0.6	62.9	b.d.l.	7.2	16218	4.9	227.5	0.2	b.d.l.	b.d.l.	842.9	23.0	25.2	1.8	4.4	0.3	6.5	0.2	0.0	0.1	
grain20-36	Middle	21.6	22.6	54256	18.8	101100	294503	b.d.l.	12794	25351	0.4	59.1	0.1	6.5	14622	4.1	199.9	0.2	b.d.l.	b.d.l.	684.5	20.8	23.4	1.6	4.2	0.4	5.4	b.d.l.	0.0	0.0	
grain20-37	Middle	24.7	23.6	56157	24.5	110383	294503	b.d.l.	13559	27329	0.5	51.2	b.d.l.	7.9	15386	4.1	204.7	0.2	b.d.l.	b.d.l.	647.1	21.5	25.1	1.8	4.8	0.4	5.4	0.2	0.0	0.1	
grain20-38	Middle	21.2	19.9	54678	22.0	104111	294503	b.d.l.	13725	24608	b.d.l.	60.6	b.d.l.	7.0	16103	3.9	180.5	1.1	4.2	0.7	0.1	574.4	20.7	23.7	1.7	4.8	0.5	4.9	0.4	0.0	0.3
grain20-39	Middle	18.1	16.7	58301	16.8	109612	294503	b.d.l.	14074	27442	0.5	54.3	b.d.l.	8.8	15208	4.6	178.8	0.3	0.3	0.1	0.0	513.2	20.8	23.6	1.7	4.6	0.3	4.7	0.2	0.0	0.1
grain20-40	Rim	17.4	16.3	58922	24.9	114724	294503	b.d.l.	12058	29208	0.4	58.7	b.d.l.	8.8	14941	3.7	175.9	0.3	0.1	0.0	b.d.l.	439.7	22.0	25.4	1.8	5.0	0.4	4.5	0.2	b.d.l.	0.1
grain20-41	Rim	15.9	14.8	58347	25.6	112302	294503	b.d.l.	11852	27969	0.4	51.8	b.d.l.	8.4	15241	4.1	160.8	0.3	b.d.l.	b.d.l.	351.7	22.1	25.6	1.8	5.4	0.4	4.2	0.3	0.0	0.0	
grain20-42	Rim	12.2	10.5	59342	24.0	115193	294503	15.0	11900	26970	0.5	50.2	b.d.l.	8.1	14922	3.9	155.0	0.3	b.d.l.	b.d.l.	321.8	20.9	24.2	1.8	4.4	0.4	3.9	0.1	0.0	0.1	
MFT-plag25-1	Rim	11.9	9.2	61472	28.7	127670	299178	b.d.l.	12034	26223	b.d.l.	49.8	b.d.l.	b.d.l.	1377.1	3.9	55.4	0.2	b.d.l.	b.d.l.	51.3	21.1	23.6	1.6	4.1	0.5	1.8	b.d.l.	b.d.l.		
MFT-plag25-2	Rim	13.5	15.6	59926	26.8	126765	299178	46.6	11534	26331	b.d.l.	45.1	b.d.l.	b.d.l.	1440.6	3.7	54.9	0.3	b.d.l.	0.0	b.d.l.	52.9	22.0	23.5	1.7	4.3	0.5	1.3	0.2	0.0	0.1
MFT-plag25-3	Middle	21.3	19.8	61373	29.3	128879	299178	b.d.l.	11807	26969	b.d.l.	46.0	b.d.l.	19.0	14318	3.8															

Table A1.7: continued

Ho	Er	Tm	Yb	Lu	Hf	Ta	Pb	Th	U
0.0	0.0	b.d.l.	b.d.l.	b.d.l.	b.d.l.	b.d.l.	13.4	b.d.l.	b.d.l.
0.0	b.d.l.	b.d.l.	0.0	b.d.l.	b.d.l.	b.d.l.	12.9	0.0	b.d.l.
b.d.l.	b.d.l.	b.d.l.	0.0	b.d.l.	b.d.l.	b.d.l.	14.1	0.0	b.d.l.
0.0	b.d.l.	b.d.l.	b.d.l.	b.d.l.	b.d.l.	b.d.l.	13.3	0.0	b.d.l.
0.0	0.0	b.d.l.	b.d.l.	0.0	b.d.l.	b.d.l.	13.8	b.d.l.	b.d.l.
b.d.l.	0.0	b.d.l.	b.d.l.	0.0	b.d.l.	b.d.l.	14.3	b.d.l.	b.d.l.
b.d.l.	b.d.l.	b.d.l.	b.d.l.	b.d.l.	0.0	b.d.l.	15.0	b.d.l.	b.d.l.
0.0	0.1	b.d.l.	0.1	0.0	b.d.l.	b.d.l.	14.5	0.1	b.d.l.
0.0	b.d.l.	b.d.l.	b.d.l.	b.d.l.	0.0	b.d.l.	14.7	b.d.l.	b.d.l.
b.d.l.	0.0	b.d.l.	b.d.l.	0.0	b.d.l.	b.d.l.	13.7	0.0	b.d.l.
b.d.l.	0.0	b.d.l.	0.0	b.d.l.	b.d.l.	b.d.l.	13.4	0.0	b.d.l.
b.d.l.	0.0	b.d.l.	b.d.l.	b.d.l.	b.d.l.	b.d.l.	12.8	b.d.l.	b.d.l.
b.d.l.	0.0	b.d.l.	b.d.l.	b.d.l.	0.0	b.d.l.	13.9	b.d.l.	b.d.l.
0.0	0.0	b.d.l.	b.d.l.	b.d.l.	b.d.l.	b.d.l.	13.6	0.0	b.d.l.
b.d.l.	b.d.l.	b.d.l.	b.d.l.	b.d.l.	b.d.l.	b.d.l.	14.3	b.d.l.	b.d.l.
0.0	b.d.l.	b.d.l.	b.d.l.	b.d.l.	b.d.l.	0.0	14.2	0.0	b.d.l.
b.d.l.	b.d.l.	b.d.l.	0.0	b.d.l.	b.d.l.	b.d.l.	14.9	b.d.l.	b.d.l.
b.d.l.	0.0	b.d.l.	0.0	b.d.l.	b.d.l.	b.d.l.	14.0	b.d.l.	b.d.l.
0.0	0.0	b.d.l.	0.0	b.d.l.	b.d.l.	b.d.l.	13.9	b.d.l.	b.d.l.
0.0	0.0	b.d.l.	b.d.l.	b.d.l.	b.d.l.	b.d.l.	14.8	0.0	0.0
b.d.l.	b.d.l.	b.d.l.	b.d.l.	b.d.l.	b.d.l.	b.d.l.	14.9	0.0	b.d.l.
0.0	b.d.l.	b.d.l.	0.0	b.d.l.	b.d.l.	b.d.l.	13.6	b.d.l.	b.d.l.
0.0	b.d.l.	0.0	b.d.l.	b.d.l.	b.d.l.	b.d.l.	13.6	0.0	b.d.l.
0.0	0.0	b.d.l.	0.0	b.d.l.	b.d.l.	b.d.l.	14.0	b.d.l.	b.d.l.
b.d.l.	0.0	b.d.l.	0.0	b.d.l.	b.d.l.	b.d.l.	14.3	0.0	b.d.l.
0.0	b.d.l.	b.d.l.	b.d.l.	b.d.l.	0.0	b.d.l.	14.1	b.d.l.	b.d.l.
b.d.l.	b.d.l.	b.d.l.	b.d.l.	0.0	b.d.l.	b.d.l.	14.4	b.d.l.	b.d.l.
0.0	0.0	b.d.l.	0.0	0.0	b.d.l.	b.d.l.	13.9	b.d.l.	b.d.l.
b.d.l.	b.d.l.	b.d.l.	0.0	b.d.l.	b.d.l.	b.d.l.	13.6	b.d.l.	b.d.l.
b.d.l.	b.d.l.	b.d.l.	b.d.l.	b.d.l.	b.d.l.	b.d.l.	14.4	b.d.l.	b.d.l.
b.d.l.	b.d.l.	b.d.l.	b.d.l.	b.d.l.	b.d.l.	b.d.l.	14.6	b.d.l.	b.d.l.
0.0	0.0	b.d.l.	b.d.l.	b.d.l.	b.d.l.	b.d.l.	15.4	b.d.l.	b.d.l.
0.0	0.0	b.d.l.	b.d.l.	b.d.l.	0.0	b.d.l.	13.4	b.d.l.	b.d.l.
b.d.l.	b.d.l.	b.d.l.	b.d.l.	b.d.l.	b.d.l.	b.d.l.	14.2	b.d.l.	b.d.l.
0.0	0.1	0.0	0.2	0.0	0.1	0.1	14.8	0.4	0.2
0.0	0.0	b.d.l.	0.0	b.d.l.	b.d.l.	0.0	15.3	0.0	0.0
0.0	b.d.l.	b.d.l.	b.d.l.	b.d.l.	b.d.l.	b.d.l.	15.2	b.d.l.	b.d.l.
b.d.l.	b.d.l.	b.d.l.	b.d.l.	0.0	b.d.l.	b.d.l.	14.5	b.d.l.	b.d.l.
0.0	0.0	0.0	b.d.l.	b.d.l.	b.d.l.	b.d.l.	14.8	0.0	b.d.l.
0.0	b.d.l.	b.d.l.	b.d.l.	0.0	0.0	b.d.l.	17.5	b.d.l.	b.d.l.
b.d.l.	b.d.l.	b.d.l.	b.d.l.	b.d.l.	b.d.l.	b.d.l.	16.7	b.d.l.	b.d.l.
b.d.l.	b.d.l.	b.d.l.	b.d.l.	b.d.l.	0.0	17.5	b.d.l.	b.d.l.	b.d.l.
b.d.l.	b.d.l.	b.d.l.	b.d.l.	b.d.l.	b.d.l.	b.d.l.	18.3	b.d.l.	b.d.l.
b.d.l.	b.d.l.	b.d.l.	b.d.l.	b.d.l.	b.d.l.	b.d.l.	18.1	b.d.l.	b.d.l.
b.d.l.	b.d.l.	b.d.l.	b.d.l.	b.d.l.	b.d.l.	b.d.l.	17.2	0.0	b.d.l.
b.d.l.	b.d.l.	b.d.l.	b.d.l.	b.d.l.	b.d.l.	b.d.l.	16.3	b.d.l.	b.d.l.
b.d.l.	b.d.l.	b.d.l.	b.d.l.	b.d.l.	0.0	0.0	18.3	b.d.l.	b.d.l.
b.d.l.	b.d.l.	b.d.l.	b.d.l.	b.d.l.	b.d.l.	b.d.l.	17.6	b.d.l.	b.d.l.
b.d.l.	b.d.l.	0.0	b.d.l.	b.d.l.	b.d.l.	0.0	16.6	0.0	b.d.l.
b.d.l.	b.d.l.	b.d.l.	b.d.l.	b.d.l.	0.0	b.d.l.	15.8	b.d.l.	b.d.l.
b.d.l.	b.d.l.	b.d.l.	b.d.l.	b.d.l.	0.0	b.d.l.	17.3	b.d.l.	0.0
b.d.l.	b.d.l.	b.d.l.	b.d.l.	b.d.l.	b.d.l.	b.d.l.	16.3	b.d.l.	b.d.l.
b.d.l.	0.1	b.d.l.	b.d.l.	b.d.l.	0.0	0.0	17.1	b.d.l.	b.d.l.

Table A1.7: continued

Info	Position	Li ⁶	Li ⁷	Na	Mg	Al	Si	P	K	Ca	Sc	Ti	V	Mn	Fe	Rb	Sr	Y	Zr	Nb	Cs	Ba	La	Ce	Pr	Nd	Sm	Eu	Gd	Tb	Dy
MFT-plag25 - 16	Core	18.8	16.5	59389	20.1	125616	299178	b.d.l.	11063	27586	1317.7	3.2	54.4	0.5	46.0	23.6	26.5	2.0	4.8	0.5	1.4	0.2	b.d.l.	b.d.l.	b.d.l.	b.d.l.	b.d.l.	b.d.l.	b.d.l.	b.d.l.	b.d.l.
MFT-plag25 - 17	Core	15.0	17.5	60851	26.1	131754	299178	b.d.l.	11694	29136	163.7	b.d.l.	1460.2	3.4	58.7	0.5	25.7	28.7	2.2	5.0	0.6	1.7	0.3	b.d.l.	b.d.l.	b.d.l.	b.d.l.	b.d.l.	b.d.l.	b.d.l.	b.d.l.
MFT-plag25 - 18	Core	17.7	17.5	61145	25.7	135076	299178	65.4	1382	29657	b.d.l.	15.5	b.d.l.	17.5	157.6	3.7	60.0	0.2	b.d.l.	b.d.l.	b.d.l.	55.3	25.9	29.5	2.1	5.2	0.4	1.6	0.2	0.0	b.d.l.
MFT-plag25 - 19	Core	18.9	17.3	59061	28.0	131182	299178	b.d.l.	11123	29332	b.d.l.	63.3	0.7	11.4	1434.5	3.5	55.7	0.4	0.1	b.d.l.	b.d.l.	0.0	52.3	24.7	28.0	2.0	5.4	0.5	1.3	0.0	b.d.l.
MFT-plag25 - 20	Core	17.5	16.6	57235	25.5	123887	299178	b.d.l.	10422	27827	b.d.l.	54.2	b.d.l.	b.d.l.	1392.8	3.3	55.2	0.3	b.d.l.	b.d.l.	b.d.l.	53.4	23.8	26.5	2.0	5.1	0.5	1.4	0.3	0.0	b.d.l.
MFT-plag25 - 21	Core	20.2	17.8	59826	23.6	131348	299178	57.2	10790	29872	b.d.l.	58.4	b.d.l.	12.4	1461.7	3.9	58.9	0.3	b.d.l.	b.d.l.	b.d.l.	56.7	26.1	29.0	2.1	5.1	0.6	1.7	0.2	0.0	b.d.l.
MFT-plag25 - 22	Core	18.7	17.9	59647	23.7	130782	299178	49.3	10843	29963	b.d.l.	58.4	b.d.l.	18.6	1416.8	4.1	58.8	0.4	0.0	b.d.l.	b.d.l.	62.3	25.1	29.0	1.9	5.4	0.6	1.5	0.4	b.d.l.	
MFT-plag25 - 23	Core	17.9	18.5	59651	22.7	131939	299178	b.d.l.	10279	30052	b.d.l.	53.0	b.d.l.	b.d.l.	1299.9	2.8	61.1	0.4	b.d.l.	b.d.l.	b.d.l.	71.4	26.6	28.9	2.2	5.7	0.6	1.6	0.2	0.0	b.d.l.
MFT-plag25 - 24	Core	22.3	18.6	59476	25.6	132201	299178	47.8	10398	31064	0.7	62.0	b.d.l.	23.7	1487.3	3.6	64.0	0.3	b.d.l.	b.d.l.	0.0	70.9	27.8	29.8	2.3	6.1	0.5	1.5	0.3	b.d.l.	
MFT-plag25 - 25	Core	20.6	19.0	59634	26.0	133201	299178	b.d.l.	10356	31204	0.8	60.5	b.d.l.	16.1	1443.9	3.2	61.4	0.4	0.1	0.0	b.d.l.	74.6	26.6	31.0	2.1	5.6	0.5	1.6	0.3	b.d.l.	
MFT-plag25 - 26	Core	18.5	19.0	59305	28.5	127795	299178	b.d.l.	10035	29590	0.8	61.4	b.d.l.	21.3	1487.3	2.9	61.3	0.3	b.d.l.	b.d.l.	b.d.l.	65.7	26.0	30.2	2.2	5.7	0.6	1.6	0.3	b.d.l.	
MFT-plag25 - 27	Core	21.8	20.5	60807	20.2	131466	299178	b.d.l.	11042	30292	b.d.l.	55.9	b.d.l.	b.d.l.	1518.1	3.5	62.1	0.3	b.d.l.	b.d.l.	0.0	74.3	24.5	28.5	2.0	5.4	0.4	1.5	0.3	b.d.l.	
MFT-plag25 - 28	Middle	22.8	21.5	58711	23.1	125505	299178	b.d.l.	9731	28183	b.d.l.	63.7	b.d.l.	b.d.l.	1460.2	3.0	59.7	0.3	b.d.l.	b.d.l.	0.0	71.4	24.7	28.3	1.9	5.0	0.5	1.5	0.3	b.d.l.	
MFT-plag25 - 29	Middle	27.2	21.8	62379	24.8	134402	299178	b.d.l.	11311	31329	0.6	70.4	b.d.l.	b.d.l.	1596.8	3.3	63.8	0.2	b.d.l.	b.d.l.	0.0	66.7	24.8	28.6	2.1	5.1	0.5	1.7	0.3	0.0	b.d.l.
MFT-plag25 - 30	Middle	12.9	11.7	56418	18.5	105527	280479	20.1	14154	24041	1.0	39.7	b.d.l.	6.5	1214.9	4.1	61.4	0.2	b.d.l.	b.d.l.	b.d.l.	57.6	22.8	25.4	1.8	4.7	0.4	1.5	0.3	b.d.l.	
MFT-plag25 - 31	Middle	21.2	21.6	58260	26.5	123034	299178	b.d.l.	10766	28258	b.d.l.	51.6	b.d.l.	b.d.l.	1426.0	2.9	57.0	0.4	b.d.l.	b.d.l.	b.d.l.	54.3	22.2	24.6	1.6	4.9	0.6	1.4	0.3	b.d.l.	
MFT-plag25 - 32	Middle	21.4	20.4	60738	22.3	128332	299178	b.d.l.	11346	28128	0.8	51.9	0.8	b.d.l.	1327.6	3.4	58.3	0.2	0.1	0.0	b.d.l.	51.8	21.5	24.0	1.9	5.0	0.4	1.5	0.3	b.d.l.	
MFT-plag25 - 33	Middle	12.9	11.7	56418	18.5	105527	280479	20.1	14154	24041	1.0	39.7	b.d.l.	6.5	1214.9	4.1	61.4	0.2	b.d.l.	b.d.l.	b.d.l.	57.6	22.8	25.4	1.8	4.7	0.4	1.5	0.3	b.d.l.	
MFT-plag25 - 34	Rim	22.2	21.9	55940	27.8	112106	280479	21.3	11544	29934	0.6	62.2	b.d.l.	7.1	1376.6	3.9	79.7	0.2	b.d.l.	b.d.l.	b.d.l.	82.6	17.1	19.3	1.4	3.5	0.3	2.0	0.1	0.0	0.1
MFT-plag25 - 35	Rim	7.6	7.5	60568	23.5	130501	299178	b.d.l.	10822	29080	0.6	43.2	b.d.l.	b.d.l.	1426.2	3.3	55.5	0.3	b.d.l.	b.d.l.	0.0	51.9	21.5	23.7	1.7	4.4	0.4	1.4	0.3	0.0	0.1
MFT-Mount1-2 - 1	Rim	12.3	10.8	55888	18.1	105278	280479	16.5	14584	23826	0.6	45.1	b.d.l.	6.5	1207.8	4.3	40.3	0.2	b.d.l.	b.d.l.	b.d.l.	35.4	17.9	19.0	1.3	3.3	0.3	1.1	0.1	0.0	0.1
MFT-Mount1-2 - 2	Core	22.6	19.7	55351	20.8	110527	280479	20.1	14154	24041	1.0	39.7	b.d.l.	6.5	1214.9	4.1	61.4	0.2	b.d.l.	b.d.l.	b.d.l.	43.3	17.4	18.7	1.3	3.3	0.3	1.3	0.2	0.0	0.1
MFT-Mount1-2 - 3	Core	22.2	21.9	55940	27.8	112106	280479	21.3	11544	29934	0.6	62.2	b.d.l.	7.1	1376.6	3.9	79.7	0.2	b.d.l.	b.d.l.	b.d.l.	82.6	17.1	19.3	1.4	3.5	0.3	2.0	0.1	0.0	0.1
MFT-Mount1-2 - 4	Rim	20.4	21.6	57510	27.3	108919	280479	22.6	11581	26674	0.5	50.1	b.d.l.	7.5	1392.2	3.7	29.0	0.2	b.d.l.	b.d.l.	0.0	22.2	18.4	21.0	1.5	3.8	0.3	1.0	0.2	0.0	0.0
mount1-1-10-1	Rim	22.2	21.9	55940	27.8	112106	280479	21.3	11544	29934	0.6	62.2	b.d.l.	7.1	1376.6	3.9	79.7	0.2	b.d.l.	b.d.l.	b.d.l.	82.6	17.1	19.3	1.4	3.5	0.3	2.0	0.1	0.0	0.1
mount1-1-10-2	Core	21.9	20.3	56624	24.2	106917	280479	24.5	14424	23706	0.5	45.9	b.d.l.	6.8	1365.5	4.0	27.0	0.2	b.d.l.	b.d.l.	0.0	65.8	16.8	18.5	1.3	3.2	0.3	1.3	0.2	0.0	0.0
mount1-1-10-3	Rim	13.4	13.0	56254	21.8	106640	280479	21.9	14424	23706	0.5	45.9	b.d.l.	6.8	1365.5	4.0	27.0	0.2	b.d.l.	b.d.l.	0.0	65.8	16.8	18.5	1.3	3.2	0.3	1.3	0.2	0.0	0.0
mount1-11-1	Rim	27.4	27.1	55538	28.3	114010	280479	24.1	10115	30762	0.5	66.8	b.d.l.	9.2	1576.8	2.9	184.3	0.3	b.d.l.	b.d.l.	b.d.l.	651.4	28.9	32.2	2.3	6.2	0.4	5.1	0.2	0.0	0.1
mount1-11-2	Core	23.5	22.7	55429	23.6	110888	280479	23.9	12443	28272	0.5	63.3	b.d.l.	8.0	1569.9	3.4	195.5	0.2	b.d.l.	b.d.l.	0.0	739.2	23.2	25.4	1.8	4.8	0.4	5.4	0.2	0.0	0.1
mount1-11-3	Rim	26.2	23.5	55894	25.1	108878	280479	20.3	13347	26057	0.5	47.2	b.d.l.	7.1	1376.6	3.9	79.7	0.2	b.d.l.	b.d.l.	b.d.l.	82.6	17.1	19.3	1.4	3.5	0.3	2.0	0.1	0.0	0.1
mount1-12-2	Core	24.8	23.4	55874	23.8	109866	280479	17.0	12368	27488	0.5	42.9	b.d.l.	7.7	1362.2	3.5	82.6	0.2	b.d.l.	b.d.l.	b.d.l.	75.1	17.3	20.1	1.4	3.8	0.4	2.1	0.1	0.0	0.1
mount1-12-3	Rim	10.8	10.7	55893	23.5	109545	280479	22.0	13001	26780	0.5	52.8	b.d.l.	7.4	1371.9	3.7	62.0	0.2	b.d.l.	b.d.l.	b.d.l.	35.9	18.0	20.3	1.4	3.5	0.3	1.6	0.1	0.0	0.1
mount1-13-2	Core	16.3	15.4	54922	20.7	109709	280479	19.3	13547	27859	0.5	65.6	b.d.l.	7.7	1568.0	3.8	251.8	0.2	b.d.l.	b.d.l.	b.d.l.	745.7	20.1	22.6	1.6	4.2	0.3	5.7	0.1	0.0	0.1
mount1-13-3	Rim	18.7	16.9	56202	19.6	108717	280479	22.5	13967	25913	0.5	54.0	0.0	7.1	1401.8	4.0	179.3	0.2	b.d.l.	b.d.l.	b.d.l.	873.6	22.1	24.9	1.8	4.5	0.4	6.6	0.2	0.0	0.1
mount1-14-1	Rim	24.4	23.0	54980	24.4	107869	280479	17.1	13153	26598	0.5	47.5	b.d.l.	7.4	1405.9	3.9	168.4	0.2	b.d.l.	b.d.l.	b.d.l.	275.8	19.0	21.0	1.5	4.0	0.3	4.4	0.2	0.0	0.1
mount1-14-2	Rim	23.4	22.8	55651	26.0	111645	280479	21.9	1925	29567	0.4	68.1	0.1	8.3	1571.1	3.3	224.6	0.2	b.d.l.	b.d.l.	b.d.l.	622.0	22.1	25.8	1.9	5.2	0.4	5.6	0.2	0.0	0.1
mount1-14-3	Rim	14.5	13.7	55804	24.8	110723	280479	19.6	13383	27917	0.5	65.9	b.d.l.	7.3	1602.9	3.5	259.6	0.2	b.d.l.	b.d.l.	b.d.l.	744.6	22.0	24.3	1.7	4.8	0.3	6.7	0.2	0.0	0.1
mount1-20-1	Core	24.2	20.1	55558	23.3	109504	280479	25.4	13511	27535	0.5	63.7	b.d.l.	7.6	1520.0	3.9	233.1	0.2	b.d.l.	b.d.l.	0.0	745.1	22.3	24.6	1.8	4.4	0.3	6.4	0.2	0.0	0.0
mount1-20-2	Rim	27.0	23.8																												

Table A1.7: continued

Ho	Er	Tm	Yb	Lu	Hf	Ta	Pb	Th	U
b.d.l.	b.d.l.	b.d.l.	b.d.l.	b.d.l.	b.d.l.	b.d.l.	16.8	b.d.l.	0.0
b.d.l.	b.d.l.	b.d.l.	b.d.l.	b.d.l.	b.d.l.	b.d.l.	16.2	b.d.l.	b.d.l.
b.d.l.	b.d.l.	b.d.l.	b.d.l.	b.d.l.	0.0	b.d.l.	17.6	0.0	b.d.l.
b.d.l.	b.d.l.	b.d.l.	b.d.l.	b.d.l.	b.d.l.	b.d.l.	17.3	b.d.l.	b.d.l.
0.0	b.d.l.	b.d.l.	b.d.l.	b.d.l.	b.d.l.	0.0	16.7	b.d.l.	b.d.l.
b.d.l.	b.d.l.	b.d.l.	b.d.l.	b.d.l.	b.d.l.	b.d.l.	17.9	0.0	0.0
b.d.l.	0.1	b.d.l.	b.d.l.	b.d.l.	0.1	0.0	16.2	b.d.l.	b.d.l.
b.d.l.	b.d.l.	b.d.l.	b.d.l.	b.d.l.	b.d.l.	b.d.l.	17.2	b.d.l.	b.d.l.
b.d.l.	b.d.l.	b.d.l.	b.d.l.	b.d.l.	b.d.l.	b.d.l.	16.5	0.0	0.0
b.d.l.	b.d.l.	b.d.l.	b.d.l.	b.d.l.	0.0	b.d.l.	17.4	b.d.l.	b.d.l.
b.d.l.	b.d.l.	b.d.l.	b.d.l.	b.d.l.	b.d.l.	b.d.l.	17.1	b.d.l.	b.d.l.
0.0	b.d.l.	b.d.l.	b.d.l.	b.d.l.	b.d.l.	b.d.l.	17.1	b.d.l.	b.d.l.
0.0	b.d.l.	b.d.l.	b.d.l.	b.d.l.	b.d.l.	0.0	15.9	b.d.l.	b.d.l.
b.d.l.	b.d.l.	b.d.l.	b.d.l.	b.d.l.	b.d.l.	0.0	17.1	0.0	b.d.l.
0.0	0.0	b.d.l.	b.d.l.	b.d.l.	b.d.l.	b.d.l.	20.0	b.d.l.	b.d.l.
0.0	b.d.l.	b.d.l.	b.d.l.	b.d.l.	b.d.l.	b.d.l.	17.9	b.d.l.	0.0
b.d.l.	b.d.l.	b.d.l.	b.d.l.	b.d.l.	b.d.l.	0.0	16.9	b.d.l.	b.d.l.
b.d.l.	b.d.l.	b.d.l.	b.d.l.	b.d.l.	0.1	b.d.l.	18.5	b.d.l.	b.d.l.
b.d.l.	b.d.l.	b.d.l.	b.d.l.	0.0	b.d.l.	0.0	16.4	b.d.l.	b.d.l.
b.d.l.	b.d.l.	b.d.l.	b.d.l.	b.d.l.	b.d.l.	b.d.l.	16.4	b.d.l.	b.d.l.
0.0	0.0	b.d.l.	b.d.l.	b.d.l.	b.d.l.	b.d.l.	15.7	b.d.l.	b.d.l.
0.0	b.d.l.	b.d.l.	b.d.l.	b.d.l.	b.d.l.	b.d.l.	15.8	b.d.l.	b.d.l.
0.0	0.0	b.d.l.	b.d.l.	b.d.l.	b.d.l.	b.d.l.	16.5	b.d.l.	b.d.l.
0.0	0.0	0.0	0.0	b.d.l.	b.d.l.	b.d.l.	17.2	0.0	b.d.l.
0.0	0.0	b.d.l.	b.d.l.	b.d.l.	b.d.l.	b.d.l.	16.7	b.d.l.	b.d.l.
0.0	b.d.l.	b.d.l.	b.d.l.	b.d.l.	b.d.l.	b.d.l.	17.0	b.d.l.	b.d.l.
0.0	0.0	b.d.l.	0.0	b.d.l.	0.0	b.d.l.	14.1	b.d.l.	b.d.l.
0.0	0.0	b.d.l.	0.0	b.d.l.	b.d.l.	b.d.l.	13.9	b.d.l.	b.d.l.
0.0	0.0	b.d.l.	b.d.l.	b.d.l.	b.d.l.	b.d.l.	15.9	b.d.l.	b.d.l.
0.0	b.d.l.	b.d.l.	b.d.l.	b.d.l.	b.d.l.	b.d.l.	15.7	b.d.l.	b.d.l.
0.0	0.0	b.d.l.	b.d.l.	b.d.l.	b.d.l.	b.d.l.	16.3	b.d.l.	b.d.l.
0.0	b.d.l.	b.d.l.	0.0	b.d.l.	b.d.l.	b.d.l.	13.5	b.d.l.	b.d.l.
0.0	b.d.l.	b.d.l.	b.d.l.	b.d.l.	b.d.l.	b.d.l.	13.2	b.d.l.	b.d.l.
0.0	b.d.l.	b.d.l.	b.d.l.	b.d.l.	b.d.l.	b.d.l.	13.7	b.d.l.	b.d.l.
0.0	0.0	b.d.l.	0.0	b.d.l.	0.0	b.d.l.	14.0	b.d.l.	b.d.l.
0.0	b.d.l.	b.d.l.	0.0	b.d.l.	b.d.l.	b.d.l.	13.2	b.d.l.	b.d.l.
0.0	0.0	b.d.l.	b.d.l.	b.d.l.	b.d.l.	b.d.l.	12.9	b.d.l.	b.d.l.
0.0	0.0	0.0	0.0	b.d.l.	b.d.l.	b.d.l.	13.7	b.d.l.	b.d.l.
b.d.l.	0.0	0.0	0.0	b.d.l.	0.0	b.d.l.	13.9	0.0	b.d.l.
0.0	0.0	0.0	b.d.l.	b.d.l.	0.0	b.d.l.	13.7	b.d.l.	b.d.l.
b.d.l.	0.0	b.d.l.	b.d.l.	b.d.l.	b.d.l.	b.d.l.	13.2	b.d.l.	b.d.l.
0.0	0.0	b.d.l.	b.d.l.	b.d.l.	b.d.l.	b.d.l.	12.9	0.0	0.0
0.0	0.0	b.d.l.	b.d.l.	b.d.l.	b.d.l.	b.d.l.	14.4	b.d.l.	b.d.l.
0.0	b.d.l.	b.d.l.	b.d.l.	b.d.l.	b.d.l.	b.d.l.	16.3	b.d.l.	b.d.l.
0.0	0.0	0.0	0.0	b.d.l.	b.d.l.	b.d.l.	16.3	b.d.l.	b.d.l.
b.d.l.	b.d.l.	b.d.l.	b.d.l.	b.d.l.	b.d.l.	b.d.l.	16.6	0.0	b.d.l.
0.0	b.d.l.	0.0	b.d.l.	b.d.l.	b.d.l.	b.d.l.	13.1	b.d.l.	b.d.l.
0.0	0.0	0.0	0.0	b.d.l.	b.d.l.	b.d.l.	13.6	b.d.l.	b.d.l.
0.0	0.0	0.0	b.d.l.	b.d.l.	b.d.l.	b.d.l.	13.1	b.d.l.	b.d.l.
0.0	b.d.l.	b.d.l.	b.d.l.	b.d.l.	b.d.l.	b.d.l.	16.5	b.d.l.	b.d.l.

Table A1.7: continued

Info	Position	Li ⁱ	Li ⁱⁱ	Na	Mg	Al	Si	P	K	Ca	Sc	Ti	V	Mn	Fe	Rb	Sr	Y	Zr	Nb	Cs	Ba	La	Ce	Pr	Nd	Sm	Eu	Gd	Tb	Dy	
mount1-25-2	Core	18.1	15.9	56475	28.0	109772	280479	21.3	11864	27452	0.4	57.3	b.d.l.	7.4	14129.9	3.6	53.7	0.2	b.d.l.	b.d.l.	b.d.l.	47.9	23.4	25.1	1.8	4.5	0.3	1.3	0.2	0.0	0.1	
mount1-25-3	Rim	16.1	15.6	56735	30.4	111431	280479	22.8	11298	28689	0.5	64.9	b.d.l.	7.9	14624.9	3.2	54.4	0.2	b.d.l.	b.d.l.	b.d.l.	51.8	22.7	26.5	1.9	5.0	0.4	1.4	0.1	0.0	0.1	
mount1-26-1	Rim	19.5	18.8	56324	22.5	109529	280479	24.7	14060	26196	0.6	54.9	b.d.l.	7.3	14299.9	4.1	154.7	0.2	b.d.l.	0.0	b.d.l.	357.1	19.2	21.6	1.6	4.2	0.3	1.4	0.2	0.0	0.1	
mount1-26-2	Core	16.4	15.0	56181	19.9	109521	280479	20.4	13694	27079	0.5	44.4	b.d.l.	7.6	13342.2	3.8	59.3	0.2	b.d.l.	b.d.l.	b.d.l.	23.9	18.4	20.8	1.5	3.8	0.3	1.2	0.1	0.0	0.1	
mount1-3-1-1	Rim	24.4	23.4	55966	29.1	112387	280479	21.0	10115	31607	0.5	71.3	b.d.l.	9.5	14827.1	2.6	55.4	0.3	b.d.l.	b.d.l.	b.d.l.	94.0	27.1	31.1	2.2	5.7	0.6	1.4	0.2	0.0	0.1	
mount1-3-1-2	Core	18.0	16.6	55913	26.7	111042	280479	22.3	10783	29225	0.6	61.0	b.d.l.	8.4	13831.0	3.1	59.2	0.3	b.d.l.	b.d.l.	b.d.l.	83.4	23.8	27.3	1.9	4.9	0.5	1.5	0.2	0.0	0.1	
mount1-3-1-3	Rim	16.3	16.8	56220	22.5	105255	280479	21.8	13559	24804	0.6	45.6	b.d.l.	6.5	13055.4	4.2	56.0	0.2	b.d.l.	b.d.l.	b.d.l.	102.6	18.5	20.5	1.4	3.5	0.3	1.6	0.2	b.d.l.	0.0	
mount1-4-1	Rim	19.4	17.9	55732	24.9	110115	280479	22.0	11113	30068	0.4	54.8	b.d.l.	8.7	14283.3	3.1	84.1	0.3	b.d.l.	b.d.l.	b.d.l.	86.7	22.1	25.8	1.8	4.9	0.4	1.8	0.1	0.0	0.1	
mount1-4-2	Core	15.0	15.5	55504	24.8	110159	280479	18.3	11448	28430	0.5	48.6	b.d.l.	8.3	14522.2	3.1	74.0	0.2	b.d.l.	b.d.l.	b.d.l.	57.7	20.6	23.5	1.8	4.2	0.4	1.7	0.2	0.0	0.1	
mount1-4-3	Rim	16.1	15.2	55974	23.9	108672	280479	22.1	12211	27576	0.5	55.4	0.1	7.8	14332.2	3.5	147.5	0.2	b.d.l.	b.d.l.	b.d.l.	363.2	20.8	23.3	1.7	4.3	0.4	1.7	0.2	0.0	0.1	
mount1-7-3	Rim	10.4	9.7	55554	23.3	111472	280479	23.1	13281	27571	0.5	65.6	b.d.l.	7.7	15073.3	3.8	217.4	0.2	0.1	b.d.l.	b.d.l.	751.0	22.8	24.7	1.8	4.6	0.4	1.6	0.2	0.0	0.1	
mount1-8-1	Rim	21.7	20.6	56080	25.4	111370	280479	22.8	12515	27914	0.6	48.9	b.d.l.	8.0	13977.6	3.5	72.7	0.3	b.d.l.	b.d.l.	b.d.l.	150.1	21.1	23.3	1.7	4.3	0.4	2.1	0.3	0.0	0.1	
mount1-8-2	Core	17.1	15.5	56120	33.2	116053	280479	28.2	9554	32641	0.6	69.6	b.d.l.	10.1	16034.2	2.8	135.3	0.3	b.d.l.	0.0	b.d.l.	600.7	23.2	33.2	2.5	6.2	0.6	2.6	0.3	0.0	0.1	
mount1-8-3	Rim	19.6	17.3	55492	33.0	115518	280479	26.1	9230	33320	0.6	81.5	b.d.l.	10.3	16357.7	2.5	157.9	0.3	b.d.l.	0.0	b.d.l.	336.0	29.2	36.2	2.6	7.0	0.6	2.8	0.3	0.0	0.1	
mount1-9-1	Rim	16.5	16.3	56241	23.8	108986	280479	19.1	13178	26085	0.4	52.6	b.d.l.	7.2	1357.0	3.8	51.4	0.2	b.d.l.	0.0	b.d.l.	35.2	18.4	20.1	1.5	3.5	0.3	1.3	0.2	0.0	0.1	
mount1-9-2	Core	21.4	19.8	55975	25.5	108176	280479	22.2	13312	25411	0.6	55.8	b.d.l.	6.9	1408.7	4.0	52.5	0.2	b.d.l.	b.d.l.	b.d.l.	35.1	18.6	20.5	1.4	3.7	0.3	1.2	0.1	0.0	0.1	
mount1-9-3	Rim	13.9	15.6	56145	25.6	110529	280479	25.9	11928	28598	0.6	51.2	b.d.l.	8.1	14127.2	3.2	124.1	0.2	b.d.l.	b.d.l.	b.d.l.	96.0	20.9	24.1	1.7	4.2	0.3	1.3	0.2	0.0	0.1	
mount2-1-1	Rim	9.9	8.7	56104	26.1	113420	280479	20.4	13227	28574	0.5	64.8	b.d.l.	7.6	1589.2	3.8	258.4	0.2	b.d.l.	b.d.l.	b.d.l.	666.8	21.6	24.6	1.7	4.4	0.4	1.5	0.1	0.0	0.0	
mount2-1-1-1	Rim	18.4	17.4	56609	23.3	111511	280479	17.1	13243	27591	0.4	67.7	b.d.l.	7.6	1552.9	3.7	255.5	0.3	b.d.l.	0.0	b.d.l.	870.2	22.2	24.5	1.7	4.7	0.3	1.6	0.2	0.0	0.1	
mount2-1-1-2	Core	20.2	17.2	55866	21.5	110482	280479	18.4	12964	27553	0.4	67.0	b.d.l.	7.6	1538.1	3.7	255.0	0.2	b.d.l.	b.d.l.	b.d.l.	919.7	21.2	24.1	1.7	4.5	0.5	1.6	0.2	0.0	0.1	
mount2-1-1-3	Core	17.9	18.7	56171	19.3	111466	280479	21.7	13916	27053	0.5	64.0	b.d.l.	7.5	1546.4	4.1	248.7	0.2	b.d.l.	b.d.l.	b.d.l.	986.5	20.8	22.8	1.6	4.2	0.3	1.6	0.2	0.0	0.1	
mount2-1-1-4	Core	13.3	10.3	56704	25.7	111345	280479	17.9	13328	27717	0.3	64.0	b.d.l.	7.5	1532.2	3.9	248.7	0.2	b.d.l.	b.d.l.	b.d.l.	926.1	21.5	24.1	1.7	4.6	0.3	1.6	0.2	0.0	0.1	
mount2-1-1-5	Core	24.4	24.0	56755	23.5	113056	280479	21.5	13190	28563	0.4	61.9	b.d.l.	7.9	1533.9	3.8	258.4	0.2	b.d.l.	b.d.l.	b.d.l.	1140.0	21.9	24.0	1.7	4.5	0.3	1.6	0.2	0.0	0.0	
mount2-1-1-6	Rim	5.1	6.1	57219	35.4	111594	280479	20.2	12242	29029	0.3	73.2	b.d.l.	8.6	1497.3	3.6	218.8	0.3	0.2	0.1	b.d.l.	0.0	575.2	23.8	25.5	1.8	4.7	0.4	1.5	0.2	0.0	0.1
mount2-1-2-1	Rim	16.1	16.5	56486	23.7	112839	280479	23.8	13086	28053	0.4	60.8	b.d.l.	8.0	1516.1	3.9	193.4	0.2	b.d.l.	b.d.l.	0.0	716.1	22.5	24.5	1.7	4.4	0.4	1.5	0.1	0.0	0.1	
mount2-1-2-2	Core	18.6	19.3	56135	25.7	113706	280479	24.2	13118	28907	0.4	62.1	b.d.l.	7.9	1514.1	3.8	218.3	0.2	b.d.l.	b.d.l.	b.d.l.	716.1	22.5	24.5	1.7	4.4	0.4	1.5	0.1	0.0	0.1	
mount2-1-2-3	Rim	20.8	19.4	56663	22.8	111969	280479	22.3	13889	26531	0.3	57.8	b.d.l.	7.3	1585.7	4.1	255.6	0.2	b.d.l.	b.d.l.	b.d.l.	910.8	21.0	23.0	1.7	4.2	0.4	1.6	0.2	0.0	0.1	
mount2-1-2-4	Rim	22.8	22.7	56699	22.9	114536	280479	21.9	13862	28944	0.4	67.0	b.d.l.	7.5	1643.3	4.1	250.1	0.2	b.d.l.	0.0	b.d.l.	798.7	24.6	26.5	1.9	5.0	0.4	1.6	0.2	0.0	0.1	
mount2-1-2-5	Core	7.0	7.2	56841	24.7	112796	280479	26.8	14296	26936	0.4	66.2	b.d.l.	7.3	1553.7	4.4	240.7	0.2	b.d.l.	0.0	b.d.l.	869.3	23.3	24.6	1.8	4.6	0.3	1.6	0.2	0.0	0.0	
mount2-1-3-1	Rim	25.3	23.0	56450	21.6	112677	280479	22.3	13889	26531	0.3	57.8	b.d.l.	7.3	1585.7	4.1	255.6	0.2	b.d.l.	b.d.l.	b.d.l.	910.8	21.0	23.0	1.7	4.2	0.4	1.6	0.2	0.0	0.1	
mount2-1-3-2	Rim	9.4	8.9	57000	22.2	111471	280479	25.2	13413	26893	0.3	50.8	b.d.l.	7.6	1412.6	4.0	156.4	0.2	b.d.l.	0.0	b.d.l.	317.3	20.3	21.9	1.6	4.2	0.3	1.4	0.2	0.0	0.1	
mount2-1-3-3	Rim	19.4	16.2	56725	28.1	116592	280479	23.5	11632	31406	0.3	63.1	b.d.l.	9.2	1594.6	3.3	237.7	0.3	b.d.l.	0.0	b.d.l.	581.3	25.7	28.8	2.1	5.3	0.6	1.5	0.2	0.0	0.1	
mount2-1-3-4	Core	28.1	24.5	56852	24.0	113905	280479	26.3	12829	28758	0.4	52.4	b.d.l.	8.4	1546.0	3.8	259.0	0.2	0.1	0.0	b.d.l.	817.3	20.3	21.9	1.6	4.2	0.3	1.4	0.2	0.0	0.1	
mount2-1-3-5	Core	25.9	25.7	56863	23.0	113735	280479	24.2	12399	29076	0.4	66.1	b.d.l.	8.7	1613.9	3.4	241.9	0.3	b.d.l.	b.d.l.	b.d.l.	281.7	25.1	27.9	2.0	5.1	0.4	1.5	0.2	0.0	0.1	
mount2-1-3-6	Rim	23.5	23.0	55852	29.8	120456	280479	18.4	9171	37561	0.3	64.7	b.d.l.	11.9	1607.4	2.2	226.1	0.4	b.d.l.	b.d.l.	499.9	30.6	35.7	2.6	7.0	0.6	1.5	0.2	0.0	0.1		
mount2-1-5-1	Rim	15.0	14.1	56392	26.5	113209	280479	17.2	13291	29254	0.4	62.5	b.d.l.	8.3	1557.7	3.7	253.9	0.2	0.1	0.0	b.d.l.	752.9	24.8	27.6	2.0	5.2	0.4	1.5	0.2	0.0	0.1	
mount2-1-5-2	Core	19.7	19.5	56304	24.6	112924	280479	21.3	13751	27513	0.5	62.8	b.d.l.	7.4	1532.9	4.2	264.7	0.2	b.d.l.	b.d.l.	b.d.l.	774.3	21.4	23.9	1.7	4.4	0.3	1.7	0.2	0.0	0.1	
mount2-1-5-3	Rim	18.0	21.2	56528	24.0	111874	280479	20.3	13098	27844	0.4	62.9	b.d.l.	7.6	1546.0	3.9	214.8	0.2														

Table A1.7: continued

Ho	Er	Tm	Yb	Lu	Hf	Ta	Pb	Th	U
0.0	0.0	b.d.l.	b.d.l.	b.d.l.	b.d.l.	b.d.l.	17.0	b.d.l.	b.d.l.
0.0	0.0	b.d.l.	b.d.l.	b.d.l.	b.d.l.	b.d.l.	17.3	b.d.l.	b.d.l.
0.0	b.d.l.	b.d.l.	b.d.l.	b.d.l.	b.d.l.	b.d.l.	14.5	b.d.l.	b.d.l.
0.0	0.0	b.d.l.	b.d.l.	b.d.l.	b.d.l.	b.d.l.	16.4	b.d.l.	b.d.l.
0.0	0.0	0.0	0.0	b.d.l.	b.d.l.	b.d.l.	15.8	b.d.l.	b.d.l.
0.0	0.0	b.d.l.	b.d.l.	b.d.l.	b.d.l.	b.d.l.	16.0	b.d.l.	b.d.l.
b.d.l.	b.d.l.	b.d.l.	b.d.l.	b.d.l.	b.d.l.	b.d.l.	16.1	b.d.l.	b.d.l.
0.0	0.0	b.d.l.	b.d.l.	b.d.l.	0.0	b.d.l.	15.3	b.d.l.	b.d.l.
0.0	0.0	b.d.l.	b.d.l.	b.d.l.	b.d.l.	b.d.l.	15.2	b.d.l.	b.d.l.
0.0	b.d.l.	b.d.l.	b.d.l.	b.d.l.	b.d.l.	b.d.l.	14.2	b.d.l.	b.d.l.
0.0	0.0	b.d.l.	b.d.l.	b.d.l.	0.0	b.d.l.	14.2	0.0	b.d.l.
0.0	0.0	b.d.l.	0.0	0.0	0.0	b.d.l.	16.3	b.d.l.	b.d.l.
0.0	0.0	b.d.l.	0.0	b.d.l.	b.d.l.	b.d.l.	16.1	b.d.l.	b.d.l.
0.0	0.0	b.d.l.	b.d.l.	b.d.l.	b.d.l.	b.d.l.	16.0	b.d.l.	b.d.l.
0.0	b.d.l.	b.d.l.	b.d.l.	b.d.l.	b.d.l.	b.d.l.	16.4	b.d.l.	b.d.l.
0.0	0.0	0.0	0.0	b.d.l.	b.d.l.	b.d.l.	16.2	b.d.l.	b.d.l.
0.0	0.0	0.0	0.0	b.d.l.	0.0	b.d.l.	14.3	b.d.l.	b.d.l.
0.0	0.0	b.d.l.	b.d.l.	b.d.l.	b.d.l.	b.d.l.	14.8	b.d.l.	b.d.l.
0.0	b.d.l.	b.d.l.	b.d.l.	b.d.l.	0.0	b.d.l.	14.5	0.0	0.0
0.0	0.0	0.0	0.0	b.d.l.	b.d.l.	b.d.l.	12.9	0.0	b.d.l.
0.0	0.0	0.0	0.0	b.d.l.	b.d.l.	b.d.l.	12.7	b.d.l.	b.d.l.
0.0	b.d.l.	b.d.l.	b.d.l.	b.d.l.	b.d.l.	b.d.l.	13.6	0.0	b.d.l.
b.d.l.	b.d.l.	b.d.l.	b.d.l.	b.d.l.	b.d.l.	b.d.l.	13.1	b.d.l.	b.d.l.
b.d.l.	0.0	b.d.l.	b.d.l.	b.d.l.	b.d.l.	b.d.l.	13.3	b.d.l.	b.d.l.
0.0	0.0	b.d.l.	0.0	b.d.l.	0.0	0.0	14.1	0.0	b.d.l.
0.0	b.d.l.	b.d.l.	b.d.l.	b.d.l.	b.d.l.	b.d.l.	14.5	b.d.l.	b.d.l.
0.0	0.0	b.d.l.	0.0	b.d.l.	b.d.l.	b.d.l.	14.4	b.d.l.	b.d.l.
0.0	b.d.l.	b.d.l.	0.0	b.d.l.	b.d.l.	b.d.l.	14.4	0.0	b.d.l.
b.d.l.	0.0	b.d.l.	b.d.l.	b.d.l.	b.d.l.	b.d.l.	14.0	b.d.l.	b.d.l.
0.0	0.0	b.d.l.	b.d.l.	b.d.l.	b.d.l.	b.d.l.	14.3	b.d.l.	b.d.l.
0.0	b.d.l.	b.d.l.	b.d.l.	b.d.l.	b.d.l.	b.d.l.	13.9	b.d.l.	b.d.l.
0.0	0.0	b.d.l.	b.d.l.	b.d.l.	b.d.l.	b.d.l.	14.7	b.d.l.	b.d.l.
0.0	0.0	b.d.l.	b.d.l.	b.d.l.	b.d.l.	b.d.l.	13.8	b.d.l.	b.d.l.
0.0	b.d.l.	b.d.l.	0.0	b.d.l.	0.0	b.d.l.	13.4	b.d.l.	b.d.l.
0.0	0.0	0.0	0.0	b.d.l.	b.d.l.	b.d.l.	12.9	b.d.l.	0.0
0.0	b.d.l.	b.d.l.	b.d.l.	b.d.l.	b.d.l.	b.d.l.	13.3	b.d.l.	b.d.l.
b.d.l.	b.d.l.	b.d.l.	b.d.l.	b.d.l.	b.d.l.	b.d.l.	13.7	b.d.l.	b.d.l.
b.d.l.	b.d.l.	b.d.l.	b.d.l.	b.d.l.	b.d.l.	b.d.l.	13.5	b.d.l.	b.d.l.
0.0	b.d.l.	0.0	b.d.l.	b.d.l.	b.d.l.	b.d.l.	14.1	b.d.l.	b.d.l.
0.0	0.0	b.d.l.	0.0	b.d.l.	b.d.l.	b.d.l.	14.6	b.d.l.	b.d.l.
0.0	b.d.l.	b.d.l.	b.d.l.	b.d.l.	b.d.l.	b.d.l.	12.9	b.d.l.	b.d.l.
0.0	b.d.l.	b.d.l.	b.d.l.	b.d.l.	b.d.l.	b.d.l.	14.3	0.0	b.d.l.
b.d.l.	0.0	b.d.l.	b.d.l.	b.d.l.	b.d.l.	b.d.l.	13.7	b.d.l.	b.d.l.
0.0	b.d.l.	b.d.l.	b.d.l.	b.d.l.	b.d.l.	b.d.l.	13.6	b.d.l.	b.d.l.
0.0	0.0	b.d.l.	b.d.l.	b.d.l.	b.d.l.	b.d.l.	14.0	b.d.l.	b.d.l.
0.0	0.0	b.d.l.	b.d.l.	b.d.l.	b.d.l.	b.d.l.	13.6	b.d.l.	b.d.l.
b.d.l.	b.d.l.	b.d.l.	b.d.l.	b.d.l.	b.d.l.	b.d.l.	13.8	b.d.l.	b.d.l.
b.d.l.	0.0	b.d.l.	b.d.l.	b.d.l.	b.d.l.	b.d.l.	13.3	b.d.l.	b.d.l.
b.d.l.	0.0	b.d.l.	b.d.l.	b.d.l.	b.d.l.	b.d.l.	15.9	0.0	b.d.l.

Table A1.7: continued

Info	Position	Li ⁺	Li ⁺	Na	Mg	Al	Si	P	K	Ca	Sc	Ti	V	Mn	Fe	Rb	Sr	Y	Zr	Nb	Cs	Ba	La	Ce	Pr	Nd	Sm	Eu	Gd	Tb	Dy
mount2-2-2	Core	16.5	17.2	56160	30.6	119375	280479	20.6	10959	32353	0.4	62.2	b.d.l.	9.8	1495.6	3.0	82.7	0.2	b.d.l.	0.0	b.d.l.	90.9	25.5	29.9	2.2	5.5	0.4	1.7	0.2	0.0	0.1
mount2-2-3	Core	29.3	21.2	57119	30.0	116904	280479	20.2	11846	31033	0.4	58.8	b.d.l.	9.1	1463.8	3.1	63.6	0.3	b.d.l.	0.0	b.d.l.	97.8	25.1	28.4	2.1	5.4	0.5	1.6	0.3	0.0	0.1
mount2-2-4	Core	22.9	20.2	56088	30.0	116227	280479	22.3	11533	31339	0.3	67.3	b.d.l.	9.3	1538.6	3.1	100.5	0.3	b.d.l.	0.0	b.d.l.	99.2	25.2	28.4	2.0	5.2	0.5	2.4	0.2	0.0	0.1
mount2-2-5	Rim	19.3	19.8	56733	26.2	114637	280479	20.9	12807	29008	0.3	60.6	b.d.l.	8.0	1448.7	3.5	61.3	0.2	b.d.l.	b.d.l.	b.d.l.	76.8	25.5	28.1	2.0	5.1	0.4	1.4	0.2	0.0	0.1
mount2-2-1	Rim	16.5	13.9	56809	23.7	111939	280479	16.6	14169	26724	0.4	56.7	b.d.l.	7.5	1388.2	4.1	121.3	0.2	b.d.l.	b.d.l.	b.d.l.	283.2	20.9	22.8	1.6	4.3	0.3	3.4	0.2	0.0	0.1
mount2-2-4-2	Core	21.2	21.8	56342	24.2	109176	280479	20.0	14182	25980	0.2	54.1	b.d.l.	7.0	1289.4	4.0	122.8	0.2	b.d.l.	0.0	b.d.l.	280.4	20.6	22.4	1.6	4.0	0.3	3.5	0.2	0.0	0.1
mount2-2-4-3	Core	24.8	24.5	56864	23.9	113237	280479	25.0	12668	29030	0.4	51.3	b.d.l.	8.5	1345.7	3.5	97.8	0.1	0.3	b.d.l.	b.d.l.	149.2	22.4	25.7	1.9	4.8	0.4	2.5	0.2	0.0	0.1
mount2-2-4-4	Rim	21.3	19.6	56831	25.3	114081	280479	23.4	12792	29384	0.3	56.6	b.d.l.	8.4	1388.5	3.5	97.8	0.2	b.d.l.	b.d.l.	b.d.l.	100.2	23.6	26.1	1.8	4.7	0.5	2.3	0.2	0.0	0.1
mount2-2-4-5	Rim	16.3	18.3	56880	26.3	110536	280479	23.5	13827	27018	0.4	50.8	b.d.l.	7.4	1349.3	3.9	107.7	0.2	b.d.l.	0.0	b.d.l.	197.3	19.9	21.8	1.7	4.4	0.4	3.2	0.2	0.0	0.1
mount2-3-1	Rim	21.1	20.2	55449	24.1	112926	280479	18.1	12397	29200	0.4	62.7	b.d.l.	8.2	1523.4	3.7	201.6	0.2	b.d.l.	b.d.l.	b.d.l.	484.9	22.6	25.9	1.9	5.0	0.4	5.2	0.1	0.0	0.1
mount2-3-2	Core	27.7	26.6	55895	25.3	112996	280479	24.6	12849	29052	0.4	66.8	0.1	8.5	1617.6	3.7	209.6	0.2	b.d.l.	b.d.l.	b.d.l.	705.8	22.8	26.0	1.8	4.9	0.4	5.8	0.2	0.0	0.1
mount2-3-3	Core	22.5	21.2	55782	20.5	112041	280479	21.6	14765	27366	0.5	72.1	0.1	7.4	1629.3	4.1	282.0	0.2	b.d.l.	0.0	b.d.l.	1064.8	22.4	25.2	1.7	4.5	0.4	7.3	0.1	0.0	0.1
mount2-3-4	Core	21.4	20.8	56882	24.3	113956	280479	20.8	13566	28527	0.4	69.3	b.d.l.	7.7	1593.2	4.0	219.5	0.2	b.d.l.	0.0	b.d.l.	791.0	21.4	24.3	1.8	4.7	0.4	5.7	b.d.l.	0.0	0.0
mount2-3-5	Rim	10.2	10.9	55401	21.8	111962	280479	22.5	13835	27938	0.5	88.1	b.d.l.	7.7	1643.0	3.9	272.1	0.2	b.d.l.	b.d.l.	b.d.l.	827.7	18.2	21.0	1.5	4.2	0.3	6.9	0.1	b.d.l.	0.0
mount2-4-1	Rim	16.8	16.0	55135	23.0	109730	280479	19.4	14251	27111	0.4	59.6	b.d.l.	7.1	1591.7	4.3	260.9	0.1	b.d.l.	0.0	b.d.l.	971.2	20.9	23.4	1.6	4.3	0.3	7.0	0.1	0.0	0.0
mount2-4-2	Rim	20.5	19.7	56084	22.9	112710	280479	21.7	13617	28539	0.4	74.8	b.d.l.	7.8	1665.5	3.7	269.9	0.2	b.d.l.	0.0	b.d.l.	874.2	22.8	25.4	1.8	5.1	0.4	6.9	0.1	0.0	0.1
mount2-4-3	Core	15.6	15.3	55503	22.1	110418	280479	21.4	14087	26729	0.5	73.7	0.0	7.4	1590.3	4.0	266.2	0.2	b.d.l.	b.d.l.	b.d.l.	935.7	22.4	24.6	1.7	4.3	0.3	7.0	0.2	0.0	0.1
mount2-4-4	Core	19.3	19.4	55375	22.8	112580	280479	18.5	13141	28508	0.4	67.6	b.d.l.	7.9	1651.4	3.7	270.7	0.2	b.d.l.	0.0	b.d.l.	887.5	22.1	25.1	1.8	4.8	0.3	6.9	0.2	0.0	0.1
mount2-4-5	Rim	22.3	22.3	56360	23.2	112317	280479	21.4	12669	28929	0.4	68.7	b.d.l.	8.4	1597.4	3.6	250.5	0.2	b.d.l.	0.0	b.d.l.	852.5	23.0	26.3	1.9	4.9	0.4	6.3	0.2	0.0	0.1
mount2-5-1	Rim	10.2	9.9	60212	30.4	121454	280479	21.7	13852	29816	0.4	46.7	b.d.l.	8.4	1472.6	4.0	95.5	0.2	b.d.l.	b.d.l.	b.d.l.	66.3	20.2	22.0	1.6	4.5	0.4	2.3	0.2	0.0	0.1
mount2-5-2	Rim	7.2	7.6	59017	27.5	116515	280479	16.8	12768	30104	0.4	50.6	b.d.l.	8.5	1478.4	3.5	121.3	0.3	b.d.l.	0.0	b.d.l.	156.5	22.1	24.9	1.8	4.5	0.5	3.0	0.2	0.0	0.1
mount2-5-3	Core	10.7	9.9	55943	27.4	111684	280479	18.9	12463	28201	0.4	47.5	b.d.l.	7.9	1387.4	3.6	69.3	0.3	0.1	0.0	b.d.l.	82.0	20.2	23.5	1.7	4.2	0.4	1.7	0.2	0.0	0.1
mount2-5-4	Rim	7.2	6.7	56752	24.9	110120	280479	22.5	13140	27153	0.5	48.7	b.d.l.	8.2	1388.5	3.7	74.8	0.3	0.1	0.0	b.d.l.	80.4	19.7	22.5	1.6	4.0	0.3	1.8	0.2	0.0	0.1
mount2-6-1	Rim	22.9	22.7	55570	26.4	112558	280479	20.8	12857	28337	0.4	61.0	b.d.l.	8.1	1536.3	3.6	209.0	0.2	0.1	b.d.l.	b.d.l.	539.2	22.4	25.8	1.8	5.0	0.4	5.6	0.2	0.0	0.1
mount2-6-2	Core	19.2	19.0	56442	25.6	112024	280479	22.4	13400	27537	0.4	61.6	b.d.l.	7.7	1501.0	3.8	206.2	0.2	b.d.l.	b.d.l.	b.d.l.	532.1	21.7	24.5	1.7	4.5	0.4	5.6	0.2	0.0	0.1
mount2-6-3	Core	10.1	11.7	56273	23.8	111454	280479	19.1	13378	28283	0.4	64.0	b.d.l.	7.9	1571.3	3.9	228.2	0.2	b.d.l.	0.0	b.d.l.	690.3	20.8	23.7	1.7	4.3	0.4	5.8	0.2	0.0	0.1
mount2-6-4	Core	15.2	16.1	56153	34.2	112884	280479	17.6	12889	27697	0.4	61.9	b.d.l.	8.3	1576.1	3.6	171.9	0.2	b.d.l.	0.0	b.d.l.	584.3	19.7	22.7	1.6	4.3	0.3	5.9	0.2	0.0	0.1
mount2-6-5	Core	24.0	24.1	55816	22.1	112442	280479	20.1	13582	28014	0.4	64.8	b.d.l.	7.9	1524.8	4.1	225.0	0.2	b.d.l.	b.d.l.	b.d.l.	665.6	20.7	23.3	1.7	4.3	0.4	6.2	0.2	0.0	0.1
mount2-6-6	Rim	23.5	23.0	56166	22.9	110418	280479	22.7	13371	28758	0.4	64.5	0.1	7.6	1520.1	3.8	205.2	0.2	b.d.l.	0.0	b.d.l.	590.2	19.7	22.7	1.6	4.4	0.3	5.6	0.2	0.0	0.1
mount2-7-4	Core	23.3	22.8	55543	30.2	123346	280479	24.9	8649	39039	0.6	105.8	0.1	12.5	1559.2	2.0	245.0	0.4	b.d.l.	b.d.l.	b.d.l.	811.0	38.2	44.6	3.2	8.6	0.7	5.7	0.3	0.0	0.1
mount2-7-5	Rim	28.0	28.5	55023	26.9	119167	280479	21.5	9142	36885	0.4	97.2	0.1	11.2	1549.3	2.2	252.8	0.4	b.d.l.	0.0	b.d.l.	974.1	36.3	42.8	3.1	8.4	0.8	5.6	0.4	0.0	0.1
mount2-9-1	Rim	19.6	19.2	56601	25.5	114921	280479	21.3	11789	30515	0.5	48.9	b.d.l.	8.6	1398.0	3.1	129.7	0.3	b.d.l.	b.d.l.	b.d.l.	184.5	21.2	24.8	1.7	4.8	0.5	3.2	0.2	0.0	0.1
mount2-9-3	Rim	23.4	22.9	56331	27.2	117142	280479	23.4	10605	33033	0.5	101.7	b.d.l.	10.0	1442.2	2.9	127.7	0.3	b.d.l.	b.d.l.	b.d.l.	428.9	28.0	34.9	2.5	6.6	0.5	3.7	0.2	0.0	0.0
mount2-9-4	Rim	28.1	26.1	56960	28.9	117519	280479	27.3	10408	33801	0.4	97.8	0.1	10.4	1421.1	2.7	118.2	0.3	0.2	0.0	b.d.l.	436.1	25.6	30.4	2.2	6.0	0.6	3.1	0.2	0.0	0.1

Table A1.7: continued

Ho	Er	Tm	Yb	Lu	Hf	Ta	Pb	Th	U
0.0	b.d.l.	b.d.l.	b.d.l.	b.d.l.	b.d.l.	b.d.l.	16.8	b.d.l.	b.d.l.
0.0	0.0	b.d.l.	b.d.l.	b.d.l.	b.d.l.	b.d.l.	16.8	b.d.l.	b.d.l.
0.0	0.0	b.d.l.	b.d.l.	0.0	b.d.l.	b.d.l.	15.5	b.d.l.	b.d.l.
0.0	0.0	b.d.l.	b.d.l.	b.d.l.	b.d.l.	b.d.l.	16.7	b.d.l.	b.d.l.
0.0	b.d.l.	b.d.l.	b.d.l.	b.d.l.	b.d.l.	b.d.l.	15.6	b.d.l.	b.d.l.
0.0	0.0	b.d.l.	b.d.l.	b.d.l.	b.d.l.	b.d.l.	15.0	b.d.l.	b.d.l.
0.0	b.d.l.	b.d.l.	0.0	b.d.l.	b.d.l.	b.d.l.	15.7	b.d.l.	b.d.l.
0.0	0.0	b.d.l.	b.d.l.	b.d.l.	b.d.l.	b.d.l.	15.9	b.d.l.	b.d.l.
b.d.l.	b.d.l.	0.0	b.d.l.	b.d.l.	b.d.l.	b.d.l.	15.6	b.d.l.	b.d.l.
0.0	b.d.l.	b.d.l.	b.d.l.	b.d.l.	b.d.l.	b.d.l.	14.0	b.d.l.	b.d.l.
0.0	0.0	b.d.l.	b.d.l.	b.d.l.	b.d.l.	b.d.l.	14.4	b.d.l.	b.d.l.
0.0	b.d.l.	0.0	0.0	b.d.l.	b.d.l.	b.d.l.	13.1	b.d.l.	b.d.l.
0.0	0.0	b.d.l.	b.d.l.	b.d.l.	b.d.l.	b.d.l.	14.4	b.d.l.	b.d.l.
b.d.l.	0.0	b.d.l.	b.d.l.	b.d.l.	b.d.l.	b.d.l.	13.4	b.d.l.	b.d.l.
0.0	b.d.l.	b.d.l.	b.d.l.	b.d.l.	b.d.l.	b.d.l.	13.6	b.d.l.	b.d.l.
0.0	0.0	b.d.l.	b.d.l.	b.d.l.	b.d.l.	b.d.l.	13.7	b.d.l.	b.d.l.
0.0	b.d.l.	b.d.l.	b.d.l.	b.d.l.	b.d.l.	b.d.l.	13.4	0.0	b.d.l.
0.0	0.0	b.d.l.	0.0	b.d.l.	b.d.l.	b.d.l.	13.2	b.d.l.	b.d.l.
0.0	b.d.l.	b.d.l.	b.d.l.	b.d.l.	b.d.l.	b.d.l.	13.5	b.d.l.	b.d.l.
0.0	0.0	b.d.l.	b.d.l.	0.0	b.d.l.	b.d.l.	16.9	b.d.l.	b.d.l.
0.0	0.0	b.d.l.	b.d.l.	b.d.l.	b.d.l.	b.d.l.	16.2	0.0	b.d.l.
b.d.l.	b.d.l.	0.0	0.0	b.d.l.	b.d.l.	0.0	15.6	0.0	b.d.l.
0.0	0.0	b.d.l.	0.0	0.0	0.0	0.0	16.6	0.0	b.d.l.
0.0	b.d.l.	b.d.l.	b.d.l.	b.d.l.	b.d.l.	b.d.l.	14.2	b.d.l.	b.d.l.
0.0	0.0	0.0	b.d.l.	b.d.l.	b.d.l.	b.d.l.	14.1	b.d.l.	b.d.l.
0.0	b.d.l.	b.d.l.	b.d.l.	b.d.l.	0.0	b.d.l.	13.8	b.d.l.	b.d.l.
0.0	b.d.l.	b.d.l.	b.d.l.	b.d.l.	0.0	b.d.l.	13.3	0.0	b.d.l.
0.0	0.0	b.d.l.	0.0	b.d.l.	b.d.l.	b.d.l.	14.3	b.d.l.	b.d.l.
0.0	b.d.l.	b.d.l.	b.d.l.	b.d.l.	b.d.l.	b.d.l.	14.1	b.d.l.	b.d.l.
0.0	0.0	0.0	0.0	0.0	b.d.l.	b.d.l.	14.0	b.d.l.	b.d.l.
0.0	0.0	b.d.l.	0.0	b.d.l.	b.d.l.	b.d.l.	13.6	b.d.l.	b.d.l.
0.0	b.d.l.	b.d.l.	b.d.l.	b.d.l.	b.d.l.	b.d.l.	14.9	b.d.l.	b.d.l.
0.0	0.0	b.d.l.	b.d.l.	b.d.l.	b.d.l.	b.d.l.	16.1	b.d.l.	b.d.l.
0.0	0.0	b.d.l.	b.d.l.	b.d.l.	b.d.l.	b.d.l.	15.6	0.0	b.d.l.

Table A1.8: Major elements - orthopyroxene

Info	Position	SiO ₂	TiO ₂	Al ₂ O ₃	FeO	MgO	CaO	Na ₂ O	K ₂ O	Cr ₂ O ₃	MnO	Total	Wo	En	Fs
MFT-3 - 3	larger grain	48.9	0.2	0.4	38.4	8.4	3.7	0.0	0.0	0.0	1.3	101.3	8	26	66
MFT-4 - 1	larger grain	48.4	0.2	0.2	42.0	7.2	1.6	0.0	0.0	0.0	1.5	101.2	4	23	74
MFT-10 - 6	larger grain	47.7	1.0	0.2	41.0	5.7	3.3	0.0	0.0	0.0	1.6	100.6	8	18	74
MFT-11-1	larger grain	48.2	0.7	0.3	39.8	8.8	1.5	0.0	0.0	0.0	1.4	100.7	3	27	69
MFT-11-2	larger grain	48.5	0.9	0.2	40.2	8.4	1.5	0.0	0.0	0.0	1.5	101.1	3	26	70
MFT-11-3	larger grain	48.0	0.7	0.2	40.9	7.6	1.7	0.0	0.0	0.0	1.5	100.5	4	24	72
MFT-11-5	larger grain	48.1	0.9	0.3	39.6	8.9	1.5	0.0	0.0	0.0	1.4	100.7	3	28	69
MFT-11-6	larger grain	49.8	1.0	0.3	39.3	8.4	1.5	0.0	0.0	0.0	1.3	101.6	3	27	70
MFT-11-7	larger grain	48.8	0.6	0.3	38.8	9.8	1.4	0.0	0.0	0.0	1.2	100.9	3	30	67
MFT-11-8	larger grain	48.7	1.0	0.4	38.5	9.9	1.4	0.0	0.0	0.0	1.2	101.2	3	30	66
MFT-11-9	larger grain	48.8	0.9	0.3	39.2	9.3	1.5	0.0	0.0	0.0	1.3	101.3	3	29	68
MFT-15 - 1	larger grain	48.7	0.2	0.2	41.1	8.0	1.5	0.0	0.0	0.0	1.5	101.2	3	25	72
MFT-17 - 2	larger grain	48.7	0.2	0.3	40.2	8.8	1.5	0.0	0.0	0.0	1.5	101.2	3	27	70
MFT-17 - 4	larger grain														
MFT-25 - 1	larger grain	48.5	0.2	0.2	41.4	8.2	1.5	0.0	0.0	0.0	1.5	101.5	3	25	71
MFT-25 - 4	larger grain														
MFT-27 - 1	larger grain	49.1	0.1	0.2	39.7	9.6	1.3	0.0	0.0	0.0	1.4	101.4	3	29	68
MFT-27 - 3	larger grain														
MFT-34 - 1	larger grain	48.5	0.2	0.2	40.9	8.4	1.5	0.0	0.0	0.0	1.5	101.2	3	26	71
MFT-41 - 1	larger grain	48.8	0.2	0.2	41.3	8.1	1.6	0.0	0.0	0.0	1.5	101.6	4	25	72
MFT-47 - 1	larger grain	49.1	0.1	0.3	38.5	10.8	1.1	0.0	0.0	0.0	1.2	101.2	2	32	65
MFT-49 - 1	larger grain	48.6	0.2	0.2	40.1	9.3	1.3	0.0	0.0	0.0	1.4	101.2	3	28	69
MFT-49 - 2	larger grain	48.5	0.2	0.3	40.9	8.5	1.5	0.0	0.0	0.0	1.5	101.3	3	26	71
MFT-50 - 1	larger grain	47.9	0.2	0.2	42.5	7.0	1.6	0.0	0.0	0.0	1.5	100.9	3	22	75
MFT-54 - 1	larger grain	48.2	0.2	0.3	41.4	8.1	1.4	0.0	0.0	0.0	1.5	101.1	3	25	72
MFT-58 - 1	larger grain	47.8	0.2	0.2	41.4	6.3	3.3	0.1	0.0	0.0	1.6	100.9	7	20	73
MFT-63 - 1	larger grain	48.3	0.2	0.2	40.6	8.5	1.5	0.0	0.0	0.0	1.5	100.9	3	26	70
MFT-64 - 1	larger grain	49.5	0.1	0.3	38.1	10.9	1.3	0.0	0.0	0.0	1.2	101.5	3	33	64
MFT-6 - 1	small grain	48.5	0.8	0.3	39.3	9.2	1.5	0.0	0.0	0.0	1.4	101.0	3	29	68
MFT-6 - 2	small grain	48.6	0.6	0.2	38.8	9.5	1.5	0.0	0.0	0.0	1.3	100.5	3	29	67

Table A1.9: Trace elements - orthopyroxene

Info	Position	Li ⁺	Li ⁻	Na	Mg	Al	Si	P	K	Ca	Sc	Ti	V	Mn	Fe	Rb	Sr	Y	Zr	Nb	Cs	Ba	La	Ce	Pr	Nd	Sm	Eu	Gd	Tb	Dy	Ho		
MFT-4-1	larger grain	8.6	8.3	129.1	57585	1488	233733	94.0	b.d.l.	13301	55.1	1080.7	7.7	10314	347958	b.d.l.	0.1	71.8	3.6	0.1	b.d.l.	b.d.l.	1.0	4.5	0.9	6.3	3.2	0.1	5.6	1.4	11.0	3.0		
MFT-4-2	larger grain	8.8	8.7	121.9	51243	1336	233733	11.6	b.d.l.	12508	46.7	969.9	3.2	10961	364373	b.d.l.	b.d.l.	73.3	3.0	0.1	b.d.l.	b.d.l.	1.0	2.5	0.6	4.5	3.0	0.1	5.2	1.4	11.5	3.0		
MFT-4-3	larger grain	9.3	8.8	122.2	52923	1390	233733	12.3	b.d.l.	12501	45.6	960.7	3.1	10862	363372	b.d.l.	b.d.l.	71.7	3.0	0.1	b.d.l.	b.d.l.	1.0	2.4	0.7	4.6	2.7	0.1	5.2	1.4	11.5	3.0		
MFT-15-3	larger grain	8.4	8.5	109.9	56333	1240	233733	4.4	b.d.l.	11483	42.1	833.8	2.4	10633	328268	b.d.l.	b.d.l.	63.9	2.2	0.1	b.d.l.	b.d.l.	1.0	1.8	0.5	3.3	2.3	0.1	4.4	1.1	9.9	2.5		
MFT-15-4	larger grain	8.8	8.6	112.5	55479	1341	233733	9.0	b.d.l.	11659	46.9	937.9	3.0	10684	321751	b.d.l.	b.d.l.	69.4	2.5	0.1	b.d.l.	b.d.l.	1.0	2.0	0.5	3.7	2.4	0.1	4.9	1.2	10.7	2.8		
MFT-17-2	larger grain	7.9	8.3	120.2	55919	1374	233733	12.4	b.d.l.	12159	53.1	993.6	4.6	10753	326327	0.0	b.d.l.	74.4	3.0	0.1	b.d.l.	b.d.l.	1.0	2.3	0.6	4.1	2.7	0.0	5.0	1.3	11.3	3.0		
MFT-17-4	larger grain	8.8	8.4	113.2	52351	1341	233733	8.4	b.d.l.	12341	51.6	964.3	4.0	11017	330856	b.d.l.	b.d.l.	75.4	2.8	0.1	b.d.l.	b.d.l.	1.0	2.0	0.5	3.8	2.3	0.0	5.0	1.3	11.5	3.1		
MFT-25-1	larger grain	9.3	8.9	118.5	51331	1197	233733	12.6	b.d.l.	11185	43.5	830.0	3.3	10512	332528	b.d.l.	b.d.l.	57.1	2.2	0.1	b.d.l.	b.d.l.	1.0	2.1	0.5	3.7	2.3	0.1	4.2	1.1	9.1	2.4		
MFT-25-4	larger grain	9.6	9.2	122.7	48291	1513	233733	8.6	5.2	11909	55.1	916.5	3.4	10591	332463	0.1	0.3	65.7	3.6	0.6	0.1	2.4	10.6	9.9	0.7	4.5	2.7	0.1	5.0	1.2	10.7	2.8		
MFT-27-1	larger grain	8.8	8.9	112.4	57867	1387	233733	8.2	b.d.l.	10214	43.6	821.3	5.2	9996	314374	b.d.l.	b.d.l.	64.4	2.1	0.0	b.d.l.	b.d.l.	1.0	1.5	0.4	3.2	2.0	0.1	4.2	1.1	9.8	2.6		
MFT-27-3	larger grain	9.1	8.7	109.5	54890	1260	233733	9.6	b.d.l.	11276	46.2	867.2	2.5	10717	326133	b.d.l.	b.d.l.	66.2	2.3	0.1	b.d.l.	b.d.l.	1.0	1.9	0.5	3.7	2.4	0.1	4.2	1.2	10.8	2.7		
MFT-34-1	larger grain	8.5	8.8	125.4	51794	1698	233733	13.4	7.6	11712	39.7	924.2	2.9	10819	314010	0.1	0.3	69.3	3.5	0.3	0.1	1.6	10.4	2.8	0.6	3.9	2.6	0.1	4.9	1.2	10.8	2.9		
MFT-34-3	larger grain	9.1	8.3	120.1	53634	1377	233733	11.9	b.d.l.	12358	51.8	998.8	4.4	10626	309266	b.d.l.	0.0	71.7	3.1	0.1	b.d.l.	b.d.l.	1.0	2.5	0.6	4.4	2.7	0.1	5.0	1.3	11.2	3.0		
MFT-47-1	larger grain	8.6	8.8	95.5	63732	1468	233733	11.5	b.d.l.	8965	40.4	765.5	3.9	9019	302880	b.d.l.	0.0	55.4	1.8	0.0	b.d.l.	b.d.l.	1.0	1.3	0.4	2.6	1.8	0.1	3.4	0.9	8.2	2.1		
MFT-49-1	larger grain	9.1	8.5	104.0	53814	1292	233733	13.6	b.d.l.	10440	45.6	790.4	2.8	10515	325226	b.d.l.	b.d.l.	63.3	2.0	0.1	b.d.l.	b.d.l.	1.0	1.6	0.4	2.9	2.0	0.0	4.2	1.1	9.6	2.5		
MFT-49-2	larger grain	8.7	8.7	112.7	51980	1259	233733	12.0	b.d.l.	11515	46.3	802.7	2.7	10918	335856	b.d.l.	b.d.l.	67.8	2.2	0.1	b.d.l.	b.d.l.	1.0	1.8	0.5	3.5	2.4	0.0	4.4	1.2	10.2	2.8		
MFT-50-1	larger grain	8.8	8.7	119.7	44212	1322	233733	11.6	b.d.l.	12477	48.0	896.6	5.6	11232	347654	b.d.l.	0.0	72.3	3.1	0.1	b.d.l.	b.d.l.	1.0	2.4	0.6	4.3	2.9	0.1	4.9	1.3	11.2	3.0		
MFT-63-1	larger grain	8.6	8.5	117.6	52579	1385	233733	11.0	b.d.l.	12548	50.4	1005.3	4.1	11058	333154	0.0	b.d.l.	73.4	3.0	0.1	b.d.l.	b.d.l.	1.0	2.1	0.5	4.0	2.5	0.1	4.8	1.3	11.2	3.0		
MFT-66-1	larger grain	9.0	8.7	105.8	57747	1496	233733	13.1	b.d.l.	10340	37.7	812.3	6.8	9094	321886	b.d.l.	0.0	57.9	2.4	0.0	b.d.l.	b.d.l.	1.0	2.1	0.5	3.8	2.4	0.1	4.3	1.1	9.3	2.3		
MFT-maf-3-16	larger grain	8.2	8.0	143.5	40273	1471	233733	15.6	10.6	11559	46.7	861.2	6.3	9865	277985	0.3	0.5	57.7	4.0	1.0	0.2	4.5	10.0	11.6	0.7	4.4	2.2	0.1	4.2	1.0	8.4	2.3		
MFT-maf-3-21	larger grain	9.0	8.2	141.5	39866	1438	233733	10.8	21.7	11021	44.6	834.0	6.8	9638	279242	0.2	0.5	57.6	3.5	0.7	0.1	3.3	11.1	8.5	0.8	4.8	2.7	0.1	5.0	1.1	9.7	2.3		
MFT-maf-3-22	larger grain	8.1	8.4	125.1	40328	1372	233733	b.d.l.	4.2	11058	43.5	831.2	6.5	9637	282037	0.1	b.d.l.	57.0	2.9	0.2	b.d.l.	b.d.l.	1.0	3.0	0.6	4.1	2.3	0.1	4.3	1.0	8.8	2.3		
MFT-maf-3-23	larger grain	9.9	9.2	155.8	39030	1630	233733	16.2	15.0	10814	43.8	861.5	6.7	9691	278263	0.2	2.0	57.5	5.9	2.8	0.1	25.8	1.4	30.0	0.8	5.3	2.8	0.1	4.4	1.1	9.4	2.3		
MFT-maf-3-24	larger grain	7.7	7.8	164.4	38043	1306	233733	12.4	68.1	10287	41.5	799.1	6.2	9314	269504	0.4	b.d.l.	53.6	2.7	0.1	b.d.l.	0.4	0.4	2.8	0.5	3.6	2.0	0.1	3.7	1.0	8.6	2.2		
MFT-maf-3-25	larger grain	7.5	8.2	261.9	36847	1461	233733	20.2	147.4	14174	45.7	782.9	6.8	9198	266354	0.8	2.2	62.2	4.4	0.3	0.1	9.4	12.1	8.2	1.6	8.9	3.7	0.1	5.8	1.2	10.9	2.6		
MFT-maf-3-28	larger grain	7.8	8.0	167.9	38475	1620	233733	b.d.l.	47.8	12318	45.3	816.4	6.6	9728	279339	0.5	1.1	60.8	4.4	1.1	0.3	10.7	1.3	16.1	1.0	6.6	3.2	0.1	5.0	1.2	10.1	2.4		
MFT-maf-3-29	larger grain	9.3	9.1	174.6	38341	2857	233733	10.1	57.6	11407	43.9	842.2	6.4	9712	280103	0.6	2.0	60.0	6.0	1.6	0.3	10.5	0.9	9.2	0.7	4.8	2.6	0.1	4.8	1.1	9.5	2.4		
MFT-maf-3-30	larger grain	9.8	8.3	137.9	39353	1411	233733	b.d.l.	10.7	11209	44.6	856.7	6.1	10022	288493	0.3	0.5	59.9	2.9	0.2	0.2	3.6	10.9	7.7	0.8	5.0	2.8	0.1	4.4	1.1	9.5	2.3		
MFT-maf-11-1	larger grain	8.8	8.6	132.8	46339	1751	233733	33.8	5.5	10127	39.0	841.3	18.6	9062	267685	0.2	1.3	53.6	5.3	1.7	0.2	12.5	1.7	21.1	0.8	4.7	2.2	0.1	3.9	0.9	8.1	2.2		
MFT-maf-11-1	larger grain	7.9	8.5	124.8	44122	1667	233733	12.3	6.5	10011	38.1	823.2	17.7	9089	267195	0.1	0.2	54.5	3.7	0.7	0.1	1.8	10.6	5.6	0.5	3.5	2.1	0.1	4.0	0.9	8.1	2.2		
MFT-maf-11-1	larger grain	8.3	7.9	121.2	42369	1594	233733	44.5	8.2	10254	40.2	834.5	17.5	9071	266601	b.d.l.	b.d.l.	57.0	3.1	0.1	b.d.l.	b.d.l.	1.0	1.9	0.9	5.2	0.7	4.2	2.5	0.1	3.8	1.0	8.8	2.3
MFT-maf-11-1	larger grain	7.3	8.3	121.2	43251	1610	233733	b.d.l.	b.d.l.	9853	41.2	798.7	18.2	9523	278815	b.d.l.	0.1	59.9	3.5	0.1	b.d.l.	0.3	0.9	4.1	0.8	4.4	2.5	0.1	4.4	1.1	9.7	2.4		
MFT-maf-11-1	larger grain	7.8	8.5	126.9	43068	1751	233733	b.d.l.	7.2	9980	42.0	779.4	17.8	9538	277376	b.d.l.	0.1	59.2	4.1	1.0	0.2	0.6	10.9	4.1	0.6	5.0	2.2	0.1	4.6	1.0	9.4	2.4		

Table A1.9: T continued

Er	Tm	Yb	Lu	Hf	Ta	Pb	Th	U
10.6	1.8	14.7	2.5	0.2	b.d.l.	0.0	0.1	0.0
10.8	1.9	14.8	2.5	0.2	b.d.l.	0.0	0.1	b.d.l.
10.6	1.8	14.8	2.5	0.1	b.d.l.	0.0	0.0	b.d.l.
9.1	1.6	13.1	2.2	0.1	b.d.l.	0.0	0.0	b.d.l.
10.1	1.8	14.0	2.3	0.2	b.d.l.	0.1	0.0	0.0
10.7	1.9	15.1	2.6	0.2	b.d.l.	0.0	0.0	b.d.l.
11.1	1.9	15.4	2.6	0.2	b.d.l.	0.0	0.0	0.0
8.3	1.5	11.7	1.9	0.1	b.d.l.	b.d.l.	0.0	b.d.l.
9.4	1.7	13.5	2.3	0.2	0.0	1.5	0.1	0.0
9.2	1.7	13.1	2.1	0.1	b.d.l.	0.1	0.0	b.d.l.
9.4	1.7	13.8	2.2	0.1	b.d.l.	0.0	0.0	b.d.l.
10.0	1.8	14.2	2.4	0.2	0.0	0.3	0.0	0.0
10.4	1.8	14.5	2.4	0.2	b.d.l.	0.0	0.0	b.d.l.
7.9	1.3	11.0	1.8	0.1	b.d.l.	b.d.l.	0.0	b.d.l.
9.1	1.6	12.9	2.2	0.1	b.d.l.	0.0	0.0	b.d.l.
10.0	1.7	14.1	2.2	0.1	b.d.l.	b.d.l.	0.0	0.0
10.7	1.9	14.8	2.5	0.2	0.0	0.0	0.0	0.0
8.3	1.4	11.6	2.0	0.1	b.d.l.	b.d.l.	0.0	0.0
8.2	1.5	11.3	1.9	0.2	0.0	2.0	0.1	0.0
8.3	1.4	11.2	1.8	0.1	b.d.l.	3.1	0.1	0.0
8.5	1.5	10.9	1.9	0.2	0.0	3.3	0.1	0.0
8.1	1.5	11.5	1.9	0.1	b.d.l.	0.4	0.0	0.0
8.4	1.5	11.7	1.9	0.2	0.1	8.0	0.3	0.0
7.7	1.4	10.6	1.8	0.1	b.d.l.	0.3	0.0	0.0
8.7	1.5	11.5	1.9	0.2	b.d.l.	0.7	0.3	0.0
9.9	1.7	12.9	2.1	0.3	0.0	0.4	0.2	0.0
8.7	1.5	11.3	1.9	0.2	0.0	5.9	0.2	0.0
8.6	1.4	12.1	2.0	0.3	0.0	2.9	0.2	0.0
8.8	1.5	12.0	1.9	0.2	b.d.l.	4.0	0.1	0.0
7.5	1.3	11.0	1.7	0.2	0.1	9.8	0.2	0.0
7.8	1.4	10.7	1.8	0.2	0.0	2.5	0.1	b.d.l.
7.9	1.5	11.4	2.0	0.2	b.d.l.	0.4	0.0	0.0
8.6	1.5	12.1	2.0	0.1	b.d.l.	0.3	0.0	0.0
8.7	1.5	12.0	1.9	0.2	0.0	0.4	0.0	0.0

Table A1.10: Major elements - clinopyroxene

Info	Position	SiO ₂	TiO ₂	Al ₂ O ₃	FeO	MgO	CaO	Na ₂ O	K ₂ O	Cr ₂ O ₃	MnO	Total	Wo	En	Fs
mft-cpx-6 - 3	smaller grain - Rim	49.5	0.8	0.5	24.1	6.0	18.1	0.3	0.0	0.0	0.8	100.2	40	18	42
mft-cpx-6 - 6	smaller grain - Rim	48.6	0.8	0.7	25.5	5.0	18.4	0.3	0.0	0.0	0.8	100.1	41	15	44
mft-cpx-25 - 1	smaller grain - Rim	48.9	1.1	0.5	23.9	6.0	18.3	0.2	0.0	0.0	0.8	99.9	40	18	41
mft-cpx-25 - 2	smaller grain - Core	48.8	0.7	0.6	25.0	5.0	18.4	0.2	0.0	0.0	0.8	99.6	41	16	43
mft-cpx-25 - 3	smaller grain - Rim	48.6	0.8	0.6	24.0	5.7	18.5	0.2	0.0	0.0	0.8	99.2	41	18	41
mft-cpx-33 - 1	smaller grain - Rim	49.4	0.8	0.5	23.2	6.7	17.9	0.3	0.0	0.0	0.8	99.6	39	21	40
mft-cpx-33 - 2	smaller grain - Core	49.4	0.6	0.5	23.3	6.6	17.9	0.2	0.0	0.0	0.9	99.4	39	20	40
mft-cpx-33 - 3	smaller grain - Rim	49.2	0.6	0.6	23.3	6.8	17.7	0.2	0.0	0.0	0.9	99.2	39	21	40
MFT-2 - 1	larger grain -Core	49.9	0.3	0.6	24.6	6.2	17.9	0.2	0.0	0.0	0.9	100.5	39	19	42
MFT-2 - 2	larger grain - Rim	49.3	0.3	0.6	26.4	4.2	18.3	0.2	0.0	0.0	0.9	100.3	41	13	46
MFT-3 - 1	larger grain -Core	50.1	0.2	0.5	24.3	6.2	18.1	0.2	0.0	0.0	0.9	100.6	40	19	41
MFT-3 - 2	larger grain - Rim	49.7	0.2	0.6	24.9	5.4	18.6	0.2	0.0	0.0	0.8	100.4	41	16	43
MFT-4 - 2	larger grain -Core	50.0	0.2	0.6	24.7	5.9	17.8	0.2	0.0	0.0	0.9	100.4	39	18	42
MFT-4 - 3	larger grain -Core	49.8	0.2	0.5	25.4	5.6	18.1	0.3	0.0	0.0	0.9	100.8	40	17	43
MFT-5 - 1	larger grain - Rim	51.1	0.2	0.6	19.7	8.8	19.4	0.2	0.0	0.0	0.7	100.8	41	26	33
MFT-5 - 2	larger grain -Core	49.6	0.3	0.6	28.0	6.4	14.7	0.2	0.0	0.0	1.0	100.8	32	20	48
MFT-8 - 1	larger grain -Core	49.5	0.3	0.7	24.3	6.1	18.5	0.2	0.0	0.0	0.9	100.4	40	18	41
MFT-8 - 2	larger grain - Rim	49.0	0.2	0.5	23.9	6.2	18.3	0.2	0.0	0.0	0.8	99.3	40	19	41
MFT-9 - 1	larger grain -Core	50.0	0.2	0.5	22.4	7.4	18.5	0.2	0.0	0.0	0.9	100.1	40	22	38
MFT-9 - 2	larger grain - Rim	49.8	0.2	0.5	23.6	6.7	18.2	0.2	0.0	0.0	0.9	100.0	40	20	40
MFT-10 - 1	larger grain - Rim	48.9	1.0	0.6	25.6	4.7	18.3	0.3	0.0	0.0	0.8	100.3	41	14	45
MFT-10 - 2	larger grain -Core	49.3	0.7	0.5	24.4	5.9	18.0	0.2	0.0	0.0	0.9	99.9	40	18	42
MFT-10 - 3	larger grain -Core	49.7	1.1	0.6	22.8	7.2	17.8	0.2	0.0	0.0	0.8	100.2	39	22	39
MFT-10 - 4	larger grain -Core	49.9	1.1	0.5	22.3	7.6	17.6	0.2	0.0	0.0	0.8	100.1	39	23	38
MFT-10 - 5	larger grain -Core	49.1	1.1	0.6	24.1	5.9	18.1	0.2	0.0	0.0	0.8	100.1	40	18	42
MFT-10 - 7	larger grain -Core	48.9	1.2	0.6	25.6	5.0	17.9	0.2	0.0	0.0	0.9	100.4	40	15	45
MFT-10 - 8	larger grain -Core	48.8	0.8	0.6	26.2	4.9	18.0	0.2	0.0	0.0	0.8	100.3	40	15	45
MFT-10 - 9	larger grain -Core	48.9	0.6	0.6	25.7	5.1	17.6	0.3	0.0	0.0	0.8	99.6	39	16	45
MFT-10 - 10	larger grain - Rim	48.9	0.9	0.6	25.4	4.9	18.4	0.3	0.0	0.0	0.9	100.2	41	15	44
MFT-11 - 1	larger grain -Core	51.1	0.3	0.8	18.0	10.0	19.2	0.3	0.0	0.0	0.6	100.3	41	30	30
MFT-11 - 2	larger grain - Rim	49.2	0.3	0.6	25.4	5.2	18.5	0.2	0.0	0.0	0.8	100.2	41	16	44
MFT-11 - 4	larger grain - Rim	49.8	0.2	0.5	25.5	5.0	18.7	0.2	0.0	0.0	0.9	100.9	41	15	44
MFT-12 - 1	larger grain -Core	49.2	0.3	0.6	25.5	5.7	17.7	0.2	0.0	0.0	0.9	100.2	39	17	44
MFT-12 - 2	larger grain - Rim	49.7	0.3	0.7	24.5	6.0	18.4	0.3	0.0	0.0	0.8	100.6	40	18	42
MFT-13 - 1	larger grain -Core	49.6	0.8	0.5	23.0	6.7	18.0	0.2	0.0	0.0	0.9	99.7	40	21	40
MFT-13 - 2	larger grain - Rim	49.5	1.0	0.5	22.7	6.8	18.5	0.3	0.0	0.0	0.8	100.1	40	21	39
MFT-13 - 3	larger grain -Core	49.7	0.8	0.6	23.5	6.4	18.1	0.3	0.0	0.0	0.8	100.2	40	20	40
MFT-15 - 2	larger grain - Rim	49.7	0.2	0.6	23.0	6.8	18.5	0.2	0.0	0.0	0.8	99.8	40	21	39
MFT-16 - 2	larger grain - Rim	49.3	0.3	0.6	24.5	6.5	17.7	0.2	0.0	0.0	0.8	99.9	39	20	42
MFT-17 - 3	larger grain -Core	49.3	0.2	0.5	24.8	6.2	17.7	0.2	0.0	0.0	0.9	99.7	39	19	42
MFT-18 - 1	larger grain -Core	49.7	0.2	0.5	25.0	5.7	18.4	0.2	0.0	0.0	0.8	100.6	40	17	43
MFT-18 - 2	larger grain - Rim	49.5	0.2	0.6	24.2	6.3	18.3	0.3	0.0	0.0	0.9	100.3	40	19	41
MFT-19 - 1	larger grain -Core	49.7	0.2	0.5	24.5	6.0	18.3	0.3	0.0	0.0	0.9	100.3	40	18	42
MFT-19 - 2	larger grain - Rim	49.3	0.2	0.6	24.5	5.9	18.5	0.3	0.0	0.0	0.9	100.2	40	18	42
MFT-21 - 1	larger grain -Core	51.1	0.2	0.5	20.0	9.0	19.2	0.2	0.0	0.0	0.7	100.9	41	26	33
MFT-21 - 2	larger grain - Rim	49.7	0.3	0.6	25.5	5.3	18.4	0.2	0.0	0.0	0.8	100.7	40	16	44
MFT-24 - 1	larger grain - Rim	49.3	1.0	0.5	24.3	5.7	18.2	0.2	0.0	0.0	0.8	100.1	40	18	42
MFT-24 - 2	larger grain -Core	48.9	0.9	0.6	24.1	5.7	18.2	0.3	0.0	0.0	0.8	99.6	41	18	42
MFT-24 - 3	larger grain -Core	49.2	0.7	0.5	24.0	6.4	17.7	0.3	0.0	0.0	0.8	99.6	39	20	41
MFT-24 - 4	larger grain -Core	48.6	1.1	0.6	26.3	4.4	17.7	0.3	0.0	0.0	0.9	100.0	40	14	46
MFT-24 - 5	larger grain - Rim	48.9	1.0	0.5	24.3	5.6	18.3	0.2	0.0	0.0	0.8	99.5	41	17	42
MFT-25 - 2	larger grain - Rim	49.4	0.2	0.6	24.7	6.3	17.5	0.2	0.0	0.0	0.9	99.8	38	19	42
MFT-26 - 1	larger grain -Core	49.3	0.2	0.5	25.2	5.3	18.3	0.3	0.0	0.0	0.9	100.0	40	16	44
MFT-26 - 2	larger grain - Rim	49.4	0.2	0.5	23.9	6.2	18.0	0.2	0.0	0.0	0.8	99.3	40	19	41
MFT-27 - 2	larger grain - Rim	49.2	0.2	0.5	23.2	6.7	18.2	0.2	0.0	0.0	0.9	99.1	40	20	40
MFT-28 - 2	larger grain - Rim	50.3	0.2	0.5	22.9	6.9	18.7	0.2	0.0	0.0	0.8	100.5	40	21	39
MFT-29 - 1	larger grain -Core	51.7	0.2	0.7	15.3	11.4	19.9	0.3	0.0	0.0	0.5	99.9	42	33	25
MFT-34 - 2	larger grain - Rim	48.8	0.2	0.5	25.2	5.3	18.1	0.2	0.0	0.0	0.9	99.1	40	16	44
MFT-36 - 1	larger grain -Core	50.5	0.2	0.6	19.2	9.3	18.9	0.2	0.0	0.0	0.7	99.7	40	28	32
MFT-36 - 2	larger grain - Rim	49.7	0.2	0.6	24.1	5.9	18.2	0.2	0.0	0.0	0.9	99.7	40	18	42
MFT-37 - 2	larger grain - Rim	49.6	0.2	0.5	24.5	6.1	18.5	0.2	0.0	0.0	0.9	100.4	40	18	41
MFT-41 - 2	larger grain - Rim	48.9	0.3	0.6	25.9	4.8	18.1	0.2	0.0	0.0	0.8	99.6	40	15	45
MFT-43 - 1	larger grain -Core	48.8	0.3	0.7	24.5	5.9	17.9	0.3	0.0	0.0	0.8	99.2	40	18	42
MFT-43 - 2	larger grain - Rim	49.4	0.2	0.5	24.5	5.8	18.3	0.2	0.0	0.0	0.8	99.8	40	18	42
MFT-46 - 1	larger grain -Core	50.2	0.2	0.8	18.3	9.8	19.2	0.2	0.0	0.0	0.7	99.4	41	29	30
MFT-46 - 2	larger grain - Rim	49.1	0.2	0.6	24.4	6.1	18.4	0.3	0.0	0.0	0.8	99.9	40	18	41
MFT-47 - 2	larger grain - Rim	49.3	0.3	0.6	26.0	4.9	18.3	0.2	0.0	0.0	0.8	100.4	40	15	45
MFT-49 - 3	larger grain - Rim	50.1	0.2	0.5	23.1	6.8	18.4	0.3	0.0	0.0	0.9	100.1	40	21	39
MFT-50 - 2	larger grain - Rim	49.5	0.2	0.6	24.7	5.8	18.4	0.2	0.0	0.0	0.8	100.1	40	18	42
MFT-52 - 1	larger grain -Core	49.6	0.2	0.5	24.7	6.8	17.0	0.2	0.0	0.0	0.9	100.1	37	21	42
MFT-52 - 2	larger grain - Rim	49.2	0.2	0.6	24.6	6.3	17.8	0.3	0.0	0.0	0.9	99.8	39	19	42
MFT-53 - 1	larger grain -Core	50.5	0.2	0.7	17.8	10.3	19.5	0.2	0.0	0.0	0.6	99.7	41	30	29
MFT-53 - 2	larger grain - Rim	49.5	0.2	0.5	23.3	6.8	18.3	0.2	0.0	0.0	0.8	99.7	40	21	40
MFT-55 - 1	larger grain -Core	49.5	0.2	0.6	23.2	6.7	18.5	0.3	0.0	0.0	0.8	99.7	40	20	39
MFT-55 - 2	larger grain - Rim	49.4	0.2	0.5	26.6	6.5	16.0	0.2	0.0	0.0	1.0	100.3	35	20	45
MFT-57 - 1	larger grain -Core	49.3	0.3	0.7	24.5	6.3	17.9	0.2	0.0	0.0	0.9	100.1	39	19	42
MFT-57 - 2	larger grain - Rim	49.7	0.2	0.5	23.4	6.7	18.7	0.3	0.0	0.0	0.8	100.3	40	20	39
MFT-58 - 2	larger grain - Rim	49.6	0.2	0.6	24.3	5.8	18.8	0.3	0.0	0.0	0.8	100.3	41	18	41
MFT-61 - 1	larger grain -Core	50.2	0.2	0.7	18.0	10.0	19.4	0.2	0.0	0.0	0.6	99.3	41	29	30
MFT-61 - 2	larger grain - Rim	49.3	0.2	0.5	24.2	6.0	18.5	0.2	0.0	0.0	0.9	99.8	40	18	41
MFT-63 - 2	larger grain - Rim	49.6	0.2	0.4	22.9	6.9	18.6	0.2	0.0	0.0	0.9	99.5	40	21	39
MFT-68 - 1	larger grain -Core	49.2	0.2	0.5	24.3	6.0	18.0	0.2	0.0	0.0	0.9	99.3	40	18	42
MFT-68 - 2	larger grain - Rim	49.1	0.2	0.5	25.2	5.5	17.7	0.2	0.0	0.0	0.8	99.3	39	17	44
MFT-69 - 1	larger grain -Core	48.3	0.4	0.8	26.2	4.5	17.9	0.3	0.0	0.0	0.8	99.2	40	14	46
MFT-69 - 2	larger grain - Rim	48.9	0.3	0.7	25.1	5.3	18.1	0.3	0.0	0.0	0.9	99.6	40	16	43

Table A1.11: Trace elements - clinopyroxene

Info	Li ^o	Li ⁱ	Na	Mg	Al	Si	P	K	Ca	Sc	Ti	V	Mn	Fe	Rb	Sr	Y	Zr	Nb	Cs	Ba	La	Pr	Nd	Sm	Eu	Gd	Tb	Dy	Ho	
mft-cpx-1-3	10.6	11.0	1933	35036	2852	233733	20.0	b.d.	132000	186.4	1190.2	15.1	5990	183881	0.1	4.5	256.4	32.3	0.8	0.1	0.2	40.8	160.9	29.8	156.3	49.5	1.3	53.8	9.3	57.8	11.2
mft-cpx-2-1	11.0	11.1	1906	35970	2815	233733	19.0	2.2	135208	184.3	1141.1	18.4	5908	184980	0.1	3.8	263.1	30.2	0.5	0.0	2.6	39.2	157.4	29.0	151.8	50.1	1.3	54.8	9.5	59.2	11.5
mft-cpx-3-1	10.5	10.6	1856	36418	2805	233733	15.2	b.d.	131630	175.4	1076.7	15.9	5770	218480	b.d.	3.4	263.3	28.1	0.3	0.0	b.d.	37.3	147.9	27.8	150.5	48.2	1.1	54.0	9.5	58.6	11.4
mft-cpx-3-2	10.9	10.6	1858	32717	2763	233733	23.1	4.2	130688	190.1	1137.1	19.8	5789	225878	b.d.	3.8	256.4	29.8	0.4	b.d.	b.d.	38.6	154.3	28.7	153.2	49.1	1.3	54.4	9.2	57.1	11.3
mft-cpx-3-3	10.0	10.6	1822	37015	2775	233733	11.9	b.d.	131008	176.4	1076.3	15.8	5776	225878	b.d.	3.5	263.1	27.0	0.2	b.d.	b.d.	36.2	146.7	27.7	147.4	49.2	1.2	54.1	9.5	59.4	11.5
mft-cpx-4-2	11.9	11.1	1845	31345	3178	233733	23.5	b.d.	136185	159.2	1402.4	20.9	5940	241325	b.d.	7.0	234.8	38.3	0.3	b.d.	b.d.	48.7	185.9	33.8	179.6	52.8	2.1	55.2	9.0	53.6	10.5
mft-cpx-4-3	10.3	11.1	1900	28163	3212	233733	20.4	b.d.	131996	177.7	1591.5	20.0	5950	248559	0.1	8.4	229.6	47.2	0.8	b.d.	0.2	51.1	195.4	35.3	186.7	53.0	2.4	53.7	8.8	53.3	9.9
mft-cpx-5-2	11.2	10.7	1872	30661	2986	233733	12.8	6.8	135692	170.1	1306.9	17.1	5836	248559	b.d.	5.4	244.2	36.3	0.2	b.d.	b.d.	44.0	172.4	32.0	169.3	51.5	1.7	54.9	9.2	55.9	10.7
mft-cpx-5-3	11.6	10.9	1869	33520	2850	233733	15.1	b.d.	135639	175.5	1167.0	16.5	5841	241455	b.d.	4.3	255.4	30.5	0.3	b.d.	b.d.	40.6	163.2	30.6	159.3	49.7	1.4	53.6	9.3	57.5	11.2
mft-cpx-6-3	10.1	10.7	1796	41365	2529	233733	15.9	b.d.	130744	157.2	888.0	6.3	5847	236078	b.d.	1.6	282.0	22.1	0.2	b.d.	b.d.	31.3	128.8	24.9	131.7	46.7	0.7	53.5	9.8	62.1	12.3
mft-cpx-6-4	9.9	11.0	1812	41702	2519	233733	19.9	b.d.	131884	154.4	885.5	6.4	5909	230184	b.d.	1.5	278.9	20.9	0.1	b.d.	b.d.	30.9	127.8	24.4	134.5	46.3	0.7	54.0	9.7	62.6	12.3
mft-cpx-8-4	12.2	11.1	1758	39462	2447	233733	18.5	b.d.	129474	124.7	869.3	4.6	6097	237546	b.d.	1.5	283.0	20.6	0.2	b.d.	b.d.	29.7	124.0	23.9	129.9	46.0	0.8	52.0	9.6	61.7	12.2
mft-cpx-9-1	10.3	11.0	1873	32494	3009	233733	15.1	b.d.	134721	172.2	1242.3	16.7	5819	259632	b.d.	5.3	253.7	34.8	0.3	b.d.	b.d.	43.6	168.8	31.0	167.3	51.6	1.6	55.7	9.5	58.1	11.2
mft-cpx-9-2	10.9	11.3	1861	30645	3181	233733	17.4	b.d.	133832	181.2	1415.8	18.1	5978	266108	b.d.	6.5	245.4	40.8	0.3	b.d.	b.d.	50.0	191.6	35.0	185.6	54.5	2.0	56.5	9.3	55.7	11.0
mft-cpx-9-3	11.0	11.7	1847	35387	3110	233733	12.9	9.4	127261	173.1	1274.4	18.0	6119	257241	0.1	4.4	274.3	35.8	0.2	b.d.	b.d.	42.2	166.7	31.8	172.6	55.0	1.7	58.4	9.9	62.2	12.2
mft-cpx-12-1	10.7	10.6	1848	37101	2834	233733	20.6	3.5	133424	186.9	1063.2	17.4	5800	253627	0.1	3.4	272.7	27.3	0.2	b.d.	b.d.	37.3	148.2	27.7	149.6	49.7	1.2	54.9	9.8	60.6	11.9
mft-cpx-12-2	10.8	10.5	1854	34061	2915	233733	20.1	6.1	132973	187.6	1200.1	18.0	5708	258295	0.1	4.8	262.4	33.8	0.9	0.1	1.0	42.7	167.0	30.4	162.3	50.5	1.4	54.4	9.5	58.1	11.6
mft-cpx-12-3	10.7	10.7	1809	35892	2815	233733	14.0	b.d.	135160	149.7	1088.3	12.1	5786	256167	b.d.	3.6	271.2	28.4	0.2	b.d.	b.d.	38.8	155.5	28.8	153.0	51.2	1.3	55.4	9.9	61.4	11.8
mft-cpx-13-1	10.7	10.7	1799	40474	2560	233733	14.3	b.d.	131267	161.1	881.8	6.3	5681	244662	b.d.	1.9	279.8	22.6	0.2	b.d.	b.d.	32.9	134.1	25.3	135.2	46.6	0.8	53.5	9.7	63.2	12.1
mft-cpx-13-2	10.9	10.8	1863	40076	2858	233733	13.3	9.0	129579	164.7	912.3	7.1	5883	247675	0.2	1.9	296.9	32.3	3.6	0.4	1.2	34.2	142.6	25.8	137.7	48.6	0.8	56.4	10.2	65.8	12.9
mft-cpx-13-3	10.7	10.6	1776	39831	2550	233733	15.6	b.d.	132428	158.9	911.4	6.5	5758	245059	b.d.	1.9	279.1	22.7	0.2	b.d.	b.d.	32.8	135.3	25.6	136.2	47.7	0.8	53.5	9.8	62.6	12.2
mft-cpx-14-2	11.1	11.0	1839	35935	3061	233733	19.3	b.d.	127915	172.7	1168.8	8.9	5810	294114	b.d.	1.5	301.5	24.1	0.2	b.d.	b.d.	34.6	142.5	27.3	145.7	52.1	0.6	51.3	10.3	67.4	13.3
mft-cpx-14-3	12.5	11.7	1875	35237	3092	233733	26.0	5.5	127127	194.6	1223.8	18.9	5991	267837	b.d.	4.9	259.9	34.0	0.2	b.d.	b.d.	40.2	162.9	30.6	163.6	52.1	1.6	54.8	9.5	58.0	11.5
mft-cpx-16-1	11.7	11.2	1853	31284	3140	233733	23.3	8.6	131343	165.8	1119.2	16.3	5558	317516	0.1	5.5	248.1	34.0	1.5	b.d.	12.7	42.2	163.9	30.2	157.3	49.8	1.5	53.4	9.0	57.0	11.1
mft-cpx-16-2	12.0	10.7	1863	31588	2948	233733	11.1	b.d.	136399	168.6	1141.5	16.6	5778	297129	b.d.	4.7	249.7	33.7	0.6	b.d.	b.d.	42.7	170.0	30.8	162.7	51.2	1.5	54.8	9.1	58.9	11.1
mft-cpx-17-1	10.6	10.4	1842	39703	2720	233733	13.9	b.d.	133307	175.8	902.6	7.4	5672	273705	0.1	2.0	292.7	24.6	0.2	b.d.	b.d.	34.0	141.0	26.6	142.1	50.0	0.8	57.3	10.3	64.9	12.8
mft-cpx-17-2	11.0	10.4	1890	40485	2757	233733	17.3	4.6	133757	178.2	887.9	4.9	5810	294114	b.d.	1.4	324.3	25.4	0.2	b.d.	b.d.	34.6	142.5	27.3	145.7	52.1	0.6	51.3	11.3	72.0	14.3
mft-cpx-17-3	12.2	10.8	1847	42150	2486	233733	12.7	b.d.	130024	153.3	800.6	5.2	5913	329248	b.d.	1.3	288.1	20.0	0.2	b.d.	b.d.	29.1	123.2	23.3	125.9	45.8	0.6	53.8	9.8	63.8	12.8
mft-cpx-18-4	11.0	10.8	1847	34061	2980	233733	13.8	b.d.	131139	174.8	1268.8	15.2	5601	391806	b.d.	5.8	236.6	34.9	0.2	b.d.	b.d.	42.0	165.4	30.3	160.4	48.7	1.7	51.8	8.8	54.1	10.6
mft-cpx-20-1	12.7	11.3	1846	42557	2606	233733	19.5	b.d.	131208	164.4	868.7	6.5	5912	435033	b.d.	1.7	289.1	22.7	0.1	b.d.	b.d.	31.5	131.1	24.8	134.8	47.9	0.7	53.6	10.1	64.2	12.7
mft-cpx-20-2	11.3	11.8	1816	40710	2685	233733	10.9	b.d.	125653	126.9	960.7	5.2	5745	427975	b.d.	1.8	293.9	25.3	0.7	0.0	1.6	33.6	140.9	26.4	143.0	48.1	0.8	56.3	10.0	64.9	12.7
mft-cpx-20-3	11.2	11.1	1844	41446	2632	233733	22.4	b.d.	126593	148.2	890.0	5.7	6008	481226	0.1	3.8	290.0	23.5	0.6	0.1	4.3	31.4	130.5	24.9	134.2	47.2	0.8	55.0	10.1	64.0	12.7
mft-cpx-21-1	12.0	11.0	1832	37903	2916	233733	17.0	b.d.	127873	161.0	1069.9	13.4	5884	518271	b.d.	3.8	267.7	31.2	0.2	b.d.	b.d.	39.5	159.4	30.0	159.9	50.5	1.4	56.4	9.5	60.1	12.0
mft-cpx-21-2	13.0	11.6	1810	42396	2996	233733	20.8	b.d.	128236	172.6	1140.1	15.8	5921	540722	b.d.	3.5	280.6	31.1	0.2	b.d.	b.d.	41.7	165.5	31.2	168.9	52.7	1.3	58.0	10.0	63.2	12.4
mft-cpx-21-3	12.0	10.9	1811	38423	2826	233733	13.2	b.d.	131826	172.3	1026.5	10.2	5720	538871	0.1	2.9	261.9	28.4	0.6	0.0	b.d.	38.4	153.2	28.4	151.5	49.5	1.2	55.6	9.5	59.9	11.8
mft-cpx-24-1	11.0	11.2	1881	36278	2928	233733	21.5	3.9	129850	167.8	1139.2	13.3	5965	543481	b.d.	4.2	271.4	31.2	0.2	b.d.	b.d.	39.5	158.8	29.9	160.1	50.8	1.4	57.4	9.7	61.8	12.0
mft-cpx-24-2	12.3	10.8	1849	35807	2756	233733	15.5	b.d.	131546	190.7	1061.6	16.2	5770	380203	b																

Table A1.11: continued

Er	Tm	Yb	Lu	Hf	Ta	Pb	Th	U
30.2	4.1	29.3	4.6	1.7	0.1	1.2	0.1	0.0
30.7	4.2	29.4	4.8	1.7	0.0	1.2	0.1	0.0
30.8	4.2	28.6	4.6	1.6	0.0	1.1	0.1	0.0
30.0	4.1	28.8	4.7	1.7	0.0	1.1	0.1	0.0
30.8	4.2	29.5	4.5	1.5	0.0	1.0	0.1	0.0
27.6	3.8	26.2	4.4	2.0	0.0	1.0	0.1	0.0
26.8	3.7	26.4	4.4	2.3	0.0	1.3	0.1	0.0
29.2	4.1	28.2	4.7	1.9	0.0	1.1	0.1	0.0
29.7	4.1	28.5	4.7	1.7	0.0	1.2	0.1	0.0
33.4	4.5	30.5	4.8	1.4	bd.l.	1.0	0.1	0.0
33.1	4.3	30.8	4.7	1.3	0.0	0.9	0.1	0.0
33.7	4.5	30.9	4.8	1.2	0.0	0.9	0.1	0.0
30.6	4.1	29.2	4.8	1.7	0.0	1.1	0.1	0.0
28.8	4.0	28.4	4.7	2.0	0.0	1.0	0.1	0.0
32.8	4.3	30.5	4.7	2.1	0.0	0.9	0.1	0.0
32.3	4.3	29.9	4.8	1.6	0.0	1.0	0.1	0.0
31.1	4.2	28.9	4.7	1.9	0.0	1.6	0.2	0.0
31.7	4.4	29.7	4.7	1.6	0.0	1.1	0.1	0.0
33.0	4.5	30.2	4.8	1.5	bd.l.	1.0	0.1	0.0
35.5	4.6	31.4	4.9	1.8	0.3	2.1	0.7	0.0
33.1	4.3	30.6	4.7	1.4	0.0	1.0	0.1	0.0
29.6	4.0	28.2	4.4	1.7	0.0	1.3	0.1	0.0
30.5	4.2	28.4	4.6	1.9	0.0	0.9	0.1	0.0
29.3	4.0	28.2	4.6	2.0	0.1	8.8	0.4	0.0
30.1	4.1	28.3	4.7	1.8	0.0	1.2	0.2	0.0
34.3	4.5	30.8	5.1	1.6	0.0	1.0	0.1	0.0
35.5	4.7	31.9	5.1	1.7	0.0	1.1	0.1	0.0
37.9	5.1	34.1	5.4	1.9	0.0	1.2	0.1	0.0
33.9	4.4	30.8	4.8	1.2	0.0	1.0	0.1	0.0
27.7	3.8	26.1	4.2	1.7	0.0	1.0	0.1	0.0
34.0	4.5	30.5	4.9	1.4	0.0	1.0	0.1	0.0
34.2	4.8	30.6	4.8	1.6	0.0	1.1	0.1	0.0
33.6	4.6	30.8	5.0	1.6	0.0	1.3	0.1	0.0
30.8	4.2	28.5	4.8	1.7	0.0	1.0	0.1	0.0
32.1	4.4	29.3	4.6	1.7	0.0	0.9	0.1	0.0
30.4	4.1	27.6	4.6	1.5	0.0	1.1	0.1	0.0
32.2	4.4	30.7	4.9	1.8	0.0	1.0	0.1	0.0
31.4	4.2	28.7	4.7	1.5	bd.l.	1.0	0.1	0.0
31.0	4.1	28.4	4.5	2.3	0.2	1.2	0.4	0.0
30.8	4.2	28.2	4.5	2.0	0.0	0.9	0.1	0.0
28.9	3.9	27.5	4.6	1.9	bd.l.	1.0	0.1	0.0
29.5	4.1	28.5	4.8	1.7	0.0	1.0	0.1	0.0
27.8	3.7	26.3	4.4	2.0	bd.l.	1.0	0.1	0.0
30.0	4.1	29.1	4.6	1.8	bd.l.	1.0	0.1	0.0
26.9	3.7	26.4	4.6	2.3	0.0	1.1	0.1	0.0
29.4	4.0	28.3	4.6	1.9	bd.l.	1.1	0.1	0.0
33.1	4.5	30.4	4.7	1.7	bd.l.	1.0	0.1	0.0
30.4	4.2	29.0	4.8	1.8	0.1	1.4	0.2	0.0
31.3	4.2	29.4	4.7	1.5	bd.l.	1.1	0.1	0.0
30.0	4.1	29.1	4.8	2.0	0.0	1.1	0.1	0.0
33.2	4.3	30.7	4.9	2.4	0.1	1.6	0.2	0.0
30.5	4.0	28.8	4.7	1.6	0.0	1.1	0.1	0.0
34.6	4.7	31.5	5.0	2.5	0.0	0.9	0.1	0.0
33.5	4.5	31.8	5.2	2.0	0.0	1.1	0.1	0.0

Table A1: Trace elements - clinopyroxene continued

Info	Position	Li ⁶	Li ⁷	Na	Mg	Al	Si	P	K	Ca	Sc	Ti	V	Mn	Fe	Rb	Sr	Y	Zr	Nb	Cs	Ba	La	Ce	Pr	Nd	Sm	Eu	Gd	Tb	Dy	Ho
MFT-4 - 6	larger grain - Rim	10.9	10.6	1308	43367	2256	233733	12.9	6.5	93947	108.7	1103.2	7.2	7974	204622	0.1	2.9	221.4	22.6	0.4	0.0	0.2	27.2	109.0	20.6	111.1	36.6	1.0	42.2	7.5	48.6	9.8
MFT-5 - 1	larger grain - Rim	11.8	11.7	1821	47240	3217	233733	12.7	14.9	132203	163.1	1314.4	22.0	6229	209159	0.1	6.3	247.8	38.3	0.2	0.0	0.1	43.1	173.4	32.3	171.7	51.9	2.0	55.5	9.3	57.8	11.1
MFT-5 - 3	larger grain - Core	12.7	12.0	1853	45862	3500	233733	14.5	b.d.l.	128822	178.7	1592.8	21.6	6436	215670	0.0	8.4	247.6	48.0	0.3	b.d.l.	b.d.l.	45.1	175.1	32.4	172.4	51.4	2.4	54.8	9.2	55.8	11.0
MFT-8 - 2	larger grain - Rim	11.0	10.7	1918	49038	2423	233733	13.4	b.d.l.	137057	176.7	866.1	5.4	6174	191790	0.0	1.3	304.4	21.9	0.2	b.d.l.	b.d.l.	30.8	127.7	24.5	132.1	48.2	0.6	57.4	10.5	68.4	13.4
MFT-8 - 3	larger grain - Core	11.9	11.6	1965	37926	3193	233733	12.8	b.d.l.	136351	167.1	1416.9	16.7	6106	210745	b.d.l.	5.9	269.6	41.5	0.3	b.d.l.	b.d.l.	49.8	193.1	35.8	189.7	58.0	1.0	61.5	10.2	63.0	12.0
MFT-9 - 1	larger grain - Core	10.7	10.5	1899	52656	2616	233733	13.3	b.d.l.	133151	174.3	963.2	7.5	5895	184117	0.0	1.7	300.8	24.5	0.2	b.d.l.	b.d.l.	34.0	139.7	26.8	143.1	50.3	0.8	58.5	10.6	67.6	13.4
MFT-9 - 2	larger grain - Rim	10.8	10.4	1913	47346	2642	233733	13.0	b.d.l.	133865	166.9	994.8	6.9	6103	191687	0.0	1.9	255.4	26.1	0.2	b.d.l.	b.d.l.	34.3	140.1	26.7	141.9	50.3	0.9	57.6	10.6	66.8	13.0
MFT-10 - 1	larger grain - Rim	12.2	11.9	1874	49341	3064	233733	8.2	b.d.l.	138198	163.1	1022.1	20.9	4566	147727	0.0	2.9	251.1	26.1	0.1	b.d.l.	b.d.l.	35.0	143.3	27.4	145.7	47.3	1.1	53.8	9.1	56.8	11.1
MFT-10 - 3	larger grain - Rim	12.1	11.6	1979	44642	3273	233733	10.0	b.d.l.	130520	193.3	1257.0	28.8	6054	195616	0.0	4.4	270.1	35.8	0.2	b.d.l.	b.d.l.	44.5	174.6	32.5	173.9	53.6	1.6	58.0	9.8	60.9	11.8
MFT-11 - 2	larger grain - Core	11.4	11.5	2006	38787	3232	233733	11.8	6.5	135960	151.9	1386.1	30.9	6156	205975	0.1	7.1	251.1	39.8	0.2	b.d.l.	b.d.l.	44.9	178.1	33.2	174.9	53.7	2.0	55.3	9.2	56.6	11.1
MFT-11 - 4	larger grain - Rim	11.0	10.9	1958	35058	2949	233733	13.2	2.2	137705	186.3	1385.9	20.7	6072	207129	0.0	6.2	252.4	38.5	0.3	b.d.l.	0.2	47.7	183.8	33.8	174.8	54.4	1.8	56.2	9.5	58.6	11.2
MFT-13 - 1	larger grain - Core	10.3	10.4	1912	47430	2550	233733	7.8	b.d.l.	136399	176.0	846.0	6.9	6056	186392	b.d.l.	2.0	299.9	24.6	0.2	b.d.l.	b.d.l.	34.9	143.3	27.3	146.9	52.0	0.8	59.6	10.6	68.4	13.3
MFT-13 - 2	larger grain - Rim	10.6	10.3	1894	47092	2417	233733	9.5	b.d.l.	135191	172.2	874.8	5.2	6056	184546	0.0	1.4	300.6	21.8	0.2	b.d.l.	b.d.l.	31.2	129.1	24.7	131.1	48.8	0.6	57.3	10.4	67.3	13.2
MFT-13 - 3	larger grain - Core	10.2	10.4	1899	46657	2606	233733	7.7	1.5	132958	180.9	952.1	7.2	5997	187379	0.0	2.1	298.1	25.2	0.2	b.d.l.	b.d.l.	34.8	142.8	27.5	144.8	51.2	0.9	59.0	10.6	67.6	13.1
MFT-15 - 2	larger grain - Rim	11.0	10.7	1927	42799	2638	233733	13.1	b.d.l.	134261	170.4	1027.7	8.9	6011	190743	0.0	2.6	286.8	27.7	0.2	b.d.l.	b.d.l.	36.7	148.6	28.2	149.4	51.4	1.0	58.2	10.1	65.0	12.6
MFT-15 - 5	larger grain - Rim	11.1	10.7	1903	41889	2732	233733	12.7	b.d.l.	132127	155.8	1134.0	10.3	5979	192019	0.0	3.2	271.0	29.9	0.2	b.d.l.	0.0	38.7	155.3	29.4	154.7	51.6	1.1	57.1	9.9	61.6	12.1
MFT-18 - 1	larger grain - Core	11.3	10.7	1973	35387	2672	233733	12.8	1.8	135637	193.5	1094.4	18.0	5937	201019	0.0	3.7	265.1	29.6	0.2	b.d.l.	b.d.l.	39.6	155.5	29.2	155.2	51.7	1.3	56.3	9.7	60.6	11.8
MFT-19 - 2	larger grain - Rim	11.0	11.1	1952	34351	2831	233733	12.6	b.d.l.	134353	169.7	1185.7	16.0	6238	203769	0.0	4.1	277.2	33.6	0.2	b.d.l.	b.d.l.	42.2	166.9	31.1	162.7	54.5	1.5	59.0	10.0	64.5	12.2
MFT-19 - 2	larger grain - Rim	11.2	10.8	1969	34846	2824	233733	7.5	b.d.l.	134273	177.4	1146.9	15.7	6038	199361	0.0	4.4	263.2	33.2	0.2	b.d.l.	b.d.l.	41.8	164.7	30.5	160.5	53.0	1.5	58.1	9.7	60.8	11.7
MFT-21 - 1	larger grain - Core	11.4	10.7	1952	56551	3296	233733	11.0	b.d.l.	132703	223.0	140.4	17.1	5153	188344	0.0	1.9	321.7	29.9	0.2	b.d.l.	b.d.l.	38.1	155.2	29.8	162.4	56.2	0.9	66.1	11.3	72.6	14.1
MFT-21 - 2	larger grain - Rim	11.7	10.9	1910	31585	2595	233733	9.1	b.d.l.	127168	120.6	1196.2	10.8	6238	203769	0.0	5.0	258.3	34.1	0.2	b.d.l.	b.d.l.	41.9	164.9	30.8	161.2	52.1	1.7	56.6	9.3	58.8	11.6
MFT-24 - 1	larger grain - Core	10.9	10.8	1933	37572	2704	233733	15.5	b.d.l.	133787	194.5	1070.5	19.6	6080	193148	0.0	3.5	270.5	28.4	0.2	b.d.l.	0.1	37.9	151.9	28.6	150.2	50.4	1.3	56.0	9.8	61.9	12.0
MFT-24 - 2	larger grain - Rim	11.1	10.9	1949	34514	2749	233733	12.8	b.d.l.	132987	209.4	1155.4	23.4	6156	199879	0.0	4.1	262.6	32.2	0.2	b.d.l.	b.d.l.	41.7	164.6	30.5	161.8	52.2	1.4	56.4	9.7	60.6	11.7
MFT-25 - 4	larger grain - Core	11.3	10.6	1929	37706	2957	233733	12.1	b.d.l.	132622	195.7	1056.9	18.8	6078	193091	0.0	3.5	268.1	27.7	0.2	b.d.l.	b.d.l.	37.5	148.0	27.8	150.0	49.8	1.2	55.7	9.7	61.4	11.9
MFT-25 - 3	larger grain - Core	12.2	12.1	1803	38977	2887	233733	10.7	b.d.l.	132825	138.7	1136.4	8.6	6276	200218	0.0	3.8	255.9	32.2	0.3	b.d.l.	b.d.l.	43.2	171.7	31.6	165.7	52.1	1.6	55.4	9.5	58.4	11.3
MFT-28 - 2	larger grain - Rim	11.0	10.6	1951	42452	2537	233733	13.5	b.d.l.	136409	166.8	873.9	5.6	6206	182165	0.0	1.4	299.7	22.8	0.2	b.d.l.	b.d.l.	31.0	128.8	24.5	132.4	47.3	0.7	56.5	10.7	66.5	13.0
MFT-34 - 2	larger grain - Rim	11.3	11.0	1949	38149	2825	233733	16.6	14.8	134465	166.8	1099.2	12.1	6149	187832	0.1	3.5	272.6	32.8	1.0	0.1	1.7	38.4	158.5	28.7	152.9	50.8	1.3	56.7	9.9	62.4	12.1
MFT-36 - 1	larger grain - Core	11.8	11.6	1880	56807	3948	233733	12.9	7.0	136074	136.1	1123.1	60.7	5260	149076	0.1	4.4	266.8	30.0	0.3	0.0	0.5	37.5	157.2	29.8	159.8	51.8	1.7	56.8	9.8	60.4	11.8
MFT-36 - 2	larger grain - Rim	11.4	10.9	1967	36731	2710	233733	13.0	b.d.l.	135277	181.4	1094.3	15.5	6032	184890	0.0	3.8	266.6	29.0	0.2	b.d.l.	b.d.l.	38.7	152.8	28.8	153.1	50.3	1.3	55.9	9.6	60.6	11.7
MFT-43 - 4	larger grain - Rim	11.5	10.8	1957	32068	2819	233733	15.0	b.d.l.	132164	182.3	1238.9	17.5	5957	189165	0.0	5.1	254.4	35.5	0.2	b.d.l.	b.d.l.	43.0	167.2	31.0	164.4	51.8	1.6	55.0	9.4	57.9	11.2
MFT-49 - 3	larger grain - Rim	10.9	10.5	1932	40607	2565	233733	13.2	b.d.l.	134487	166.3	939.8	7.5	5992	188798	0.0	2.0	285.2	25.3	0.2	b.d.l.	b.d.l.	34.3	140.1	26.8	141.5	49.8	0.8	55.7	10.1	62.9	12.4
MFT-50 - 2	larger grain - Rim	11.9	11.2	1959	36773	2713	233733	15.0	b.d.l.	133855	167.3	1074.3	12.5	6190	201204	0.0	3.5	260.9	30.7	0.2	b.d.l.	0.0	40.4	160.2	30.0	160.2	50.9	1.3	55.2	9.4	59.1	11.4
MFT-52 - 1	larger grain - Core	12.2	12.2	1952	41475	2979	233733	15.5	b.d.l.	129966	179.4	1206.6	17.1	6360	197666	0.0	3.4	288.5	34.1	0.3	0.0	0.4	39.3	160.6	30.5	165.1	53.2	1.2	58.6	10.1	63.6	12.6
MFT-52 - 2	larger grain - Core	10.7	10.6	1929	39014	2450	233733	10.3	b.d.l.	136601	173.6	919.4	9.5	6113	191548	0.0	2.7	273.8	25.0	0.2	b.d.l.	b.d.l.	34.8	140.1	26.3	139.2	48.2	1.0	54.4	9.6	61.2	12.1
MFT-53 - 1	larger grain - Rim	12.0	11.6	1944	38756	2820	233733	12.4	b.d.l.	132638	172.7	1121.0	10.8	6212	195928	0.0	3.4	281.0	30.7	0.2	b.d.l.	b.d.l.	39.5	158.2	30.1	159.1	52.3	1.2	57.3	10.1	62.4	12.4

Table A1: Trace elements - clinopyroxene continued

Er	Tm	Yb	Lu	Hf	Ta	Pb	Th	U
26.8	3.9	27.0	4.4	1.3	0.0	0.9	0.2	0.0
29.4	4.0	27.3	4.2	2.0	0.0	0.9	0.1	0.0
29.3	4.0	26.9	4.4	2.3	0.0	0.8	0.1	0.0
35.9	4.9	32.9	5.2	1.4	0.0	1.0	0.1	0.0
32.0	4.4	29.7	5.0	2.5	0.0	1.1	0.1	0.0
36.1	4.8	31.8	5.0	1.6	0.0	0.9	0.1	0.0
34.8	4.7	32.3	5.1	1.7	0.0	1.0	0.1	0.0
29.2	3.9	25.3	3.7	1.6	0.0	0.8	0.1	0.0
31.9	4.3	28.5	4.5	1.9	0.0	0.8	0.1	0.0
29.3	4.0	26.8	4.2	2.0	0.0	0.9	0.1	0.0
29.0	4.0	27.5	4.5	2.4	0.0	1.1	0.2	0.0
29.5	4.1	28.7	4.9	2.0	0.0	1.1	0.1	0.0
35.1	4.7	32.3	5.0	1.6	0.0	1.1	0.1	0.0
35.0	4.8	32.3	5.0	1.4	0.0	1.1	0.1	0.0
34.9	4.7	31.8	5.0	1.7	0.0	1.0	0.1	0.0
33.2	4.5	30.8	4.9	1.7	0.0	1.1	0.1	0.0
31.9	4.3	29.4	4.7	1.7	0.0	1.0	0.1	0.0
30.9	4.3	29.7	4.8	1.7	0.0	1.1	0.1	0.0
32.8	4.5	31.1	5.1	1.8	0.0	1.1	0.1	0.0
31.4	4.4	30.0	4.9	2.0	0.0	1.1	0.1	0.0
37.3	4.9	31.5	4.5	2.1	0.0	0.8	0.1	0.0
30.4	4.3	29.2	4.8	1.8	0.0	1.0	0.1	0.0
32.0	4.4	30.1	4.8	1.7	0.0	1.2	0.1	0.0
31.2	4.3	29.5	4.9	1.9	0.0	1.0	0.1	0.0
31.6	4.4	29.4	4.8	1.6	0.0	1.0	0.1	0.0
30.4	4.1	27.7	4.5	1.9	0.0	1.2	0.1	0.0
29.9	4.1	28.2	4.4	1.8	0.0	0.9	0.1	0.0
34.6	4.8	31.9	5.0	1.4	0.0	1.0	0.1	0.0
35.3	4.7	32.2	5.1	1.6	0.0	1.0	0.1	0.0
32.3	4.4	30.3	4.9	1.9	0.1	1.5	0.2	0.0
30.3	4.0	25.5	3.6	1.8	0.0	1.4	0.1	0.0
31.2	4.3	29.8	4.8	1.7	0.0	1.1	0.1	0.0
29.7	4.1	28.6	4.7	1.9	0.0	1.1	0.1	0.0
33.4	4.5	30.3	4.8	1.6	0.0	1.0	0.1	0.0
30.2	4.2	28.7	4.6	1.7	0.0	0.9	0.1	0.0
33.8	4.6	30.9	4.8	1.9	0.0	0.9	0.1	0.0
33.0	4.5	30.1	4.9	1.8	0.0	1.0	0.1	0.0
31.9	4.4	29.9	4.8	1.5	0.0	1.1	0.1	0.0
33.0	4.4	30.3	4.8	1.6	0.1	1.9	0.4	0.0
32.2	4.5	30.6	5.2	2.5	0.0	1.1	0.1	0.0
34.5	4.7	31.8	5.0	1.9	0.0	1.2	0.1	0.0
45.1	6.0	39.7	5.9	1.9	0.0	0.7	0.1	0.0
31.2	4.2	29.0	4.6	2.5	0.0	1.0	0.1	0.0
33.1	4.5	30.9	4.9	1.9	0.0	1.0	0.1	0.0
30.0	4.1	29.2	4.8	2.1	0.0	1.0	0.1	0.0
29.2	3.9	24.7	3.7	1.7	0.0	0.8	0.1	0.0
28.8	4.0	28.8	4.7	2.4	0.0	1.1	0.1	0.0
29.2	3.9	27.1	4.3	1.5	0.0	0.9	0.1	0.0
30.3	4.1	27.9	4.3	1.9	0.0	0.8	0.1	0.0
31.3	4.3	27.3	4.5	2.0	0.0	0.9	0.1	0.0
30.6	4.1	26.9	4.3	2.0	0.0	0.8	0.1	0.0
30.5	4.1	26.9	4.3	2.0	0.0	0.8	0.1	0.0
29.1	4.0	26.4	4.1	1.8	b.d.l.	1.1	0.1	0.0
28.6	3.8	25.6	4.0	1.8	b.d.l.	0.8	0.1	0.0

Table A1.11: continued

Info	Position	Li ⁶	Li ⁷	Na	Mg	Al	Si	P	K	Ca	Sc	Ti	Mn	Fe	Rb	Sr	Y	Zr	Nb	Cs	Ba	La	Ce	Pr	Nd	Sm	Eu	Tb	Dy	Ho		
MFT-maf-2-8	larger grain - Core	10.9	11.1	1794	34438	3078	233733	16.9	b.d.l.	116181	162.1	1054.1	20.1	5940	163400	0.1	3.9	253.1	31.9	0.2	b.d.l.	0.5	36.2	148.6	28.2	148.4	49.3	1.3	53.4	88.8	56.4	11.1
MFT-maf-2-9	larger grain - Core	10.2	11.2	1821	35683	3086	233733	9.8	b.d.l.	117631	159.7	1031.4	21.2	5798	160915	b.d.l.	3.7	251.8	31.4	0.2	b.d.l.	b.d.l.	35.8	146.9	27.5	147.2	47.3	1.3	52.5	8.8	55.8	10.7
MFT-maf-2-10	larger grain - Core	11.8	11.6	1903	35484	3136	233733	b.d.l.	92.6	120127	161.5	1031.3	20.7	5719	159271	0.4	3.6	256.0	31.7	0.3	b.d.l.	b.d.l.	36.2	150.1	28.0	149.0	49.0	1.3	52.8	8.8	55.7	11.0
MFT-maf-2-11	larger grain - Core	12.3	10.9	1895	35464	3062	233733	b.d.l.	53.6	118723	154.8	986.8	20.9	5532	152459	0.3	3.5	256.0	30.1	0.2	b.d.l.	b.d.l.	36.2	148.3	27.8	147.2	47.7	1.3	52.0	8.5	54.0	10.4
MFT-maf-2-12	larger grain - Core	12.4	11.0	1821	35181	3073	233733	10.9	b.d.l.	121671	162.5	1012.9	21.7	5625	157073	b.d.l.	3.8	256.2	31.0	0.2	b.d.l.	b.d.l.	37.8	154.7	28.8	154.1	49.4	1.4	53.9	8.9	56.8	10.8
MFT-maf-2-13	larger grain - Core	12.5	11.3	1847	33005	3012	233733	13.5	207.1	111660	150.3	951.8	20.8	5892	162625	0.9	3.6	235.3	27.8	0.4	0.1	1.0	35.3	140.0	26.0	139.4	43.5	1.4	49.6	8.1	52.1	10.0
MFT-maf-2-15	larger grain - Core	11.5	11.3	1886	34991	3076	233733	241.7	b.d.l.	124339	165.6	1000.8	21.8	5730	158992	0.1	4.0	261.0	30.4	0.2	b.d.l.	1.2	41.4	160.6	29.4	158.0	49.2	1.4	54.7	9.1	56.7	11.1
MFT-maf-2-16	larger grain - Core	11.1	11.3	1844	36212	3116	233733	16.9	b.d.l.	130573	160.3	995.1	21.7	5623	158863	0.1	3.6	256.6	29.6	0.2	b.d.l.	1.8	38.2	158.0	29.7	156.6	49.4	1.5	53.9	9.1	57.4	11.2
MFT-maf-2-17	larger grain - Core	12.0	11.3	1845	38040	3080	233733	16.5	b.d.l.	125615	150.8	936.1	22.8	5457	151646	0.1	3.6	245.6	28.1	0.2	b.d.l.	1.3	37.0	150.8	28.0	147.7	47.5	1.3	52.6	8.8	55.2	10.6
MFT-maf-2-18	larger grain - Core	11.5	11.3	1857	37869	3099	233733	216.0	6.8	124028	149.4	936.3	21.8	5399	152437	0.1	3.9	249.4	27.3	0.3	b.d.l.	1.6	41.6	160.8	29.0	151.6	49.1	1.3	52.6	8.7	55.0	10.5
MFT-maf-2-19	larger grain - Core	12.0	11.3	1936	36286	3029	233733	18.2	127.3	123970	159.8	996.3	21.8	5599	152713	0.6	3.7	250.5	30.5	0.3	b.d.l.	1.5	38.2	154.3	28.7	153.5	48.8	1.4	52.0	8.7	55.6	10.7
MFT-maf-2-21	larger grain - Core	12.2	11.4	1827	35435	3150	233733	23.5	19.2	118549	173.7	1148.5	19.4	5854	164735	0.1	4.0	253.5	34.8	0.2	b.d.l.	0.6	37.9	157.9	29.2	156.2	49.1	1.4	53.7	8.9	55.2	11.0
MFT-maf-2-22	larger grain - Core	11.6	11.4	1881	35797	3169	233733	b.d.l.	31.8	120946	168.9	1115.0	20.9	5713	162975	0.1	4.0	255.5	35.2	0.3	b.d.l.	b.d.l.	39.1	158.2	29.6	158.6	49.7	1.5	54.6	9.0	54.8	11.1
MFT-maf-2-23	larger grain - Core	10.9	11.4	1840	35308	3078	233733	16.6	b.d.l.	120170	160.1	1028.2	21.7	5621	160818	b.d.l.	3.9	245.4	31.7	0.2	b.d.l.	b.d.l.	38.0	153.3	28.1	148.9	48.6	1.2	52.3	8.8	55.3	10.7
MFT-maf-2-24	larger grain - Core	9.9	11.1	1845	34951	3123	233733	b.d.l.	66.0	121437	164.5	1065.3	20.9	5817	162102	0.4	3.9	247.2	31.8	0.2	b.d.l.	b.d.l.	38.6	156.2	29.0	151.2	48.4	1.5	51.8	8.5	55.5	10.7
MFT-maf-2-26	larger grain - Core	12.8	11.5	1885	34602	3119	233733	9.5	79.5	120069	163.5	1027.1	19.8	5709	162753	0.4	3.5	250.8	30.7	0.3	b.d.l.	b.d.l.	37.5	151.1	28.1	148.9	48.6	1.2	52.3	8.8	55.4	10.9
MFT-maf-2-27	larger grain - Core	10.5	11.3	1852	35003	3002	233733	16.4	b.d.l.	122203	156.6	968.3	20.0	5538	159193	b.d.l.	3.2	250.0	29.1	0.2	b.d.l.	0.4	41.1	163.3	30.4	159.1	49.9	1.4	53.4	9.0	56.4	10.6
MFT-maf-2-28	larger grain - Core	12.3	11.5	1876	35172	3213	233733	9.9	53.2	122866	166.3	1056.6	20.0	5751	163272	0.7	4.1	260.5	32.2	0.5	0.4	1.8	38.4	157.1	29.5	153.5	49.4	1.3	53.9	9.0	57.7	11.1
MFT-maf-2-29	larger grain - Core	11.8	11.5	1851	34443	3063	233733	b.d.l.	b.d.l.	119254	165.5	1123.8	19.6	5773	165094	0.1	4.3	250.1	34.4	0.2	b.d.l.	0.4	39.3	161.1	30.1	155.1	50.0	1.3	54.6	8.8	55.6	10.9
MFT-maf-2-30	larger grain - Core	12.6	11.5	1819	33027	3027	233733	b.d.l.	b.d.l.	120972	174.1	1114.8	19.7	5898	168829	0.1	4.3	250.1	34.4	0.2	b.d.l.	0.4	41.1	163.3	30.4	159.1	49.9	1.4	53.4	9.0	56.4	10.6
MFT-maf-2-31	larger grain - Core	13.1	11.2	1825	31860	2971	233733	13.1	b.d.l.	117763	169.2	1113.4	18.6	5995	172193	0.1	4.1	249.2	34.2	0.2	b.d.l.	0.2	41.0	164.3	30.4	160.9	49.3	1.3	54.0	8.7	55.1	10.8
MFT-maf-2-40	larger grain - Core	10.8	11.4	1851	30295	2744	233733	26.0	b.d.l.	120303	146.3	1042.7	12.4	5859	172939	0.1	2.9	249.8	28.0	0.4	b.d.l.	b.d.l.	39.7	156.4	28.6	147.3	49.1	1.2	53.4	8.7	55.7	10.7
MFT-maf-2-41	larger grain - Core	12.3	11.3	1846	30329	2787	233733	19.9	b.d.l.	124264	145.0	1040.8	11.5	6017	176808	0.2	2.9	257.7	27.4	0.9	0.1	0.7	40.4	160.2	29.1	151.7	48.4	1.2	54.1	8.9	58.6	11.1
MFT-maf-2-53	larger grain - Rim	10.8	10.3	1887	25865	2700	233733	66.0	25.5	117962	150.9	973.9	14.9	5608	178105	0.3	4.6	228.1	28.5	0.3	0.1	b.d.l.	38.4	152.8	27.8	144.2	46.4	1.4	49.3	8.1	51.4	9.9
MFT-maf-3-1	larger grain - Rim	9.5	10.5	1913	24509	3096	233733	b.d.l.	b.d.l.	130060	174.7	1250.2	14.2	5925	179793	b.d.l.	5.9	253.9	39.5	0.3	b.d.l.	b.d.l.	46.9	181.1	32.5	171.3	52.9	1.8	54.9	9.3	57.6	11.1
MFT-maf-3-2	larger grain - Core	10.2	10.9	1874	26996	2832	233733	b.d.l.	b.d.l.	128667	158.5	1012.2	12.9	5937	183083	b.d.l.	3.8	246.5	30.1	0.1	b.d.l.	b.d.l.	41.5	162.0	29.2	157.2	49.6	1.3	53.8	8.8	56.4	10.6
MFT-maf-3-3	larger grain - Core	10.9	11.0	1868	29639	2882	233733	b.d.l.	b.d.l.	126294	143.2	1051.5	14.2	5757	180883	0.1	3.9	244.9	31.8	0.2	b.d.l.	b.d.l.	39.7	156.4	28.7	157.7	49.3	1.5	53.0	8.7	54.8	10.5
MFT-maf-3-4	larger grain - Core	11.4	11.0	1868	29639	2882	233733	b.d.l.	b.d.l.	126294	143.2	1051.5	14.2	5757	180883	0.1	3.9	244.9	31.8	0.2	b.d.l.	b.d.l.	39.7	156.4	28.7	157.7	49.3	1.5	53.0	8.7	54.8	10.5
MFT-maf-3-5	larger grain - Core	10.5	11.1	1829	31897	2686	233733	16.7	b.d.l.	126425	149.7	905.4	9.4	5693	169417	b.d.l.	2.3	251.6	24.6	0.2	b.d.l.	b.d.l.	35.5	142.9	26.4	139.8	47.5	0.9	52.7	8.8	57.2	11.1
MFT-maf-3-6	larger grain - Core	10.9	11.1	1810	33686	2736	233733	b.d.l.	b.d.l.	127473	149.9	947.5	10.2	5743	169684	b.d.l.	2.6	252.2	26.5	0.2	b.d.l.	b.d.l.	37.0	148.1	27.6	145.6	48.9	1.0	54.1	9.1	58.3	11.0
MFT-maf-3-7	larger grain - Core	11.3	11.5	1883	32295	2984	233733	9.2	b.d.l.	124141	161.3	1122.0	16.2	5805	172643	b.d.l.	4.2	252.3	32.8	0.2	b.d.l.	b.d.l.	40.1	140.1	29.7	157.8	50.7	1.2	54.1	8.9	56.7	11.0
MFT-maf-3-8	larger grain - Core	12.0	11.5	1848	32215	2936	233733	73.4	9.6	133523	174.2	1097.9	15.0	6445	184742	0.1	4.4	242.5	34.2	0.2	b.d.l.	b.d.l.	39.4	160.8	29.7	157.1	49.4	1.2	52.9	8.6	54.5	10.4
MFT-maf-3-37	larger grain - Core	14.7	12.2	1831	31363	3075	233733	73.4	9.6	133523	174.2	1097.9	15.0	6445	184742	0.1	4.4	242.5	34.2	0.2	b.d.l.	b.d.l.	39.4	160.8	29.7	157.1	49.4	1.2	52.9	8.6	54.5	10.4
MFT-maf-3-39	larger grain - Core	12.3	11.2	1872	28629	2784	233733	77.8	b.d.l.	117746	153.4	989.6	14.6	5666	164825	0.1	3.6	238.0	30.0	0.3	b.d.l.	0.6	39.0	154.5	28.1	150.3	45.0	1.2	50.6	8.5	55.1	10.3
MFT-maf-3-40	larger grain - Core	11.6	11.8	1977	28605	4027	233733	88.4	293.7	119826	155.5	1067.8	13.8	5849	171818	1.9	5.9	247.0	41.7	0.1	0.8	1.7	46.6	190.2	30.5	157.5	48.2	1.3	53.2	8.8	55.5	1

Table A1.11: continued

Er	Tm	Yb	Lu	Hf	Ta	Pb	Th	U
297	40	261	40	1.7	bd.l.	0.9	0.1	0.0
294	40	255	40	1.9	0.0	0.8	0.1	0.0
294	39	258	40	1.8	0.0	0.9	0.1	0.0
288	38	251	37	1.7	0.0	0.8	0.1	0.0
288	39	261	39	1.7	0.0	0.9	0.1	0.0
273	36	247	38	1.5	0.0	1.2	0.1	0.1
297	40	261	40	1.6	0.0	0.9	0.1	0.0
292	40	259	40	1.5	bd.l.	0.9	0.1	0.0
286	38	238	36	1.6	0.0	0.8	0.1	0.0
285	37	241	36	1.4	0.0	0.7	0.2	0.0
290	40	254	39	1.7	0.0	0.9	0.2	0.0
293	40	264	40	2.0	0.0	0.8	0.1	0.0
290	41	258	41	1.9	0.0	0.8	0.1	0.0
283	37	246	39	1.7	bd.l.	0.8	0.1	0.0
285	38	250	40	1.8	0.0	0.9	0.1	0.0
292	40	258	40	1.7	0.0	0.9	0.1	0.0
287	39	243	39	1.6	0.0	0.9	0.1	0.0
298	40	269	42	1.7	0.0	2.0	0.1	0.0
293	39	263	41	1.9	0.0	1.6	0.1	0.0
294	39	263	41	1.8	0.0	1.0	0.1	0.0
289	39	263	41	1.7	0.0	1.3	0.1	0.0
290	39	259	41	1.6	0.0	1.0	0.1	0.0
296	40	267	42	1.6	0.0	1.4	0.1	0.0
265	36	249	41	1.6	bd.l.	1.2	0.1	0.0
301	40	287	45	1.7	0.0	1.2	0.1	0.0
278	39	270	46	2.1	0.0	1.1	0.1	0.0
292	38	266	42	1.6	0.0	1.0	0.1	0.0
284	38	261	43	1.6	0.0	1.0	0.1	0.0
290	39	266	42	1.7	0.0	0.9	0.1	0.0
300	39	267	43	1.5	bd.l.	0.9	0.0	0.0
296	40	268	43	1.6	0.0	0.9	0.1	0.0
297	40	264	43	1.9	0.0	0.9	0.1	0.0
282	39	256	41	1.6	0.0	0.8	0.1	0.0
321	42	278	48	1.8	0.0	1.3	0.1	0.0
273	39	257	42	1.5	0.0	1.0	0.1	0.0
290	39	265	42	2.0	0.3	6.7	1.5	0.1
316	43	279	45	1.8	0.0	1.5	0.3	0.1
322	44	279	46	1.8	0.0	1.4	0.4	0.0
304	40	277	44	1.8	0.0	1.6	0.5	0.1
300	42	277	45	1.8	0.0	1.5	0.3	0.0
293	42	273	44	1.9	0.1	1.9	0.7	0.1
292	40	271	44	2.1	0.2	4.8	0.8	0.1
285	40	273	46	1.9	0.0	1.1	0.1	0.0
289	40	275	45	1.7	0.0	1.0	0.1	0.0
293	39	265	43	1.7	0.1	1.9	0.3	0.0
290	39	265	43	1.9	0.0	1.7	0.2	0.0
299	40	273	44	2.0	0.0	1.9	0.2	0.0
296	39	264	44	1.6	0.0	4.6	0.1	0.0
301	42	288	45	1.7	0.0	2.0	0.1	0.0
313	42	276	47	1.9	0.0	1.3	0.1	0.0
294	41	283	47	2.1	0.0	1.5	0.1	0.0
300	41	274	46	1.9	0.0	1.0	0.1	0.0
302	41	279	46	1.7	0.0	1.0	0.1	0.0
299	42	281	46	1.8	0.0	1.1	0.2	0.1

Table A1.11: continued

Info	Position	Li ⁶	Li ⁷	Na	Mg	Al	Si	P	K	Ca	Sc	Ti	V	Mn	Fe	Rb	Sr	Y	Zr	Nb	Cs	Ba	La	Ce	Pr	Nd	Sm	Eu	Gd	Tb	Dy	Ho	
MFT-maf-3 - 69	larger grain -Core	10.8	11.9	1854	27653	2992	233733	b.d.l.	11.3	125592	150.1	1071.7	12.6	6246	179359	0.1	4.0	285.6	333.0	2.2	b.d.l.	0.3	42.6	166.1	30.8	161.6	52.2	1.4	56.2	9.6	60.8	11.5	
MFT-maf-3 - 71	larger grain -Core	12.9	11.5	1877	26426	2974	233733	b.d.l.	12.3	129772	152.0	1039.4	11.6	6180	178237	0.1	4.5	251.6	333.1	0.2	b.d.l.	0.2	42.9	168.4	30.8	160.8	51.1	1.5	54.2	9.0	57.4	10.9	
MFT-maf-3 - 72	larger grain -Core	11.0	11.6	1906	24958	3196	233733	b.d.l.	b.d.l.	135508	173.2	1247.6	15.3	6254	186014	b.d.l.	5.6	258.9	40.7	0.3	b.d.l.	0.4	48.2	187.4	34.1	177.9	56.3	1.9	57.7	9.4	60.6	11.5	
MFT-maf-3 - 73	larger grain -Core	11.7	11.4	1945	24528	3139	233733	b.d.l.	8.6	129303	164.1	1266.3	16.8	6094	180344	0.2	7.7	245.6	44.6	1.5	b.d.l.	15.0	48.1	237.2	33.2	170.3	52.9	1.7	57.4	9.0	56.6	10.6	
MFT-maf-3 - 74	larger grain -Core	12.4	11.0	1922	24234	3053	233733	b.d.l.	b.d.l.	129332	164.7	1208.3	17.1	6179	180365	0.1	6.5	241.0	39.2	0.8	b.d.l.	2.5	46.7	185.2	32.8	170.3	51.5	1.8	54.2	8.9	55.3	10.5	
MFT-maf-3 - 75	larger grain -Rim	12.5	11.7	2018	24888	3396	233733	1.9	61.8	131509	162.0	1177.9	16.9	5948	180873	1.2	21.1	245.4	42.4	5.0	0.9	16.0	48.8	201.2	32.9	170.7	52.2	1.7	55.5	8.9	55.9	10.7	
MFT-maf-12 - 1	larger grain -Rim	12.5	11.0	1891	24629	3166	233733	b.d.l.	b.d.l.	130842	167.3	1247.8	19.2	6000	183954	0.1	7.5	229.0	40.6	0.5	0.0	0.7	48.2	185.1	33.6	173.6	51.9	1.9	55.4	9.0	57.3	10.5	
MFT-maf-12 - 2	larger grain -Core	10.7	11.1	1930	21285	3188	233733	b.d.l.	b.d.l.	130980	167.5	1303.5	17.8	6000	186351	0.1	7.7	229.0	43.6	0.3	b.d.l.	50.2	188.3	34.3	177.7	53.0	2.2	54.2	8.4	52.9	9.9		
MFT-maf-12 - 3	larger grain -Core	10.1	11.4	1919	21340	3610	233733	b.d.l.	9.1	128756	160.6	1352.8	21.3	5995	187770	0.3	8.8	220.6	48.2	1.4	0.1	3.0	50.8	195.2	34.1	174.9	51.4	2.4	51.9	8.3	50.8	9.5	
MFT-maf-12 - 4	larger grain -Core	11.5	11.8	2234	20558	3787	233733	b.d.l.	544.0	122708	162.3	1420.8	22.2	6278	187981	3.4	8.9	210.7	49.3	1.7	0.3	3.9	51.9	198.1	34.1	174.4	50.2	2.4	49.9	8.1	49.9	9.2	
MFT-maf-12 - 5	larger grain -Core	11.1	11.3	1813	30844	2822	233733	b.d.l.	7.3	136623	195.0	1013.9	21.2	5988	181070	b.d.l.	3.0	273.7	28.7	0.2	b.d.l.	15.1	37.8	151.3	28.8	153.6	50.4	1.1	54.0	9.7	63.1	11.4	
MFT-maf-12 - 6	larger grain -Core	10.8	11.1	1934	29014	2809	233733	14.5	12.0	125155	180.2	991.3	22.3	6043	174143	0.2	3.3	255.1	26.5	0.6	0.1	1.1	35.3	145.2	26.6	139.8	48.6	1.1	52.7	9.0	57.0	11.0	
MFT-maf-12 - 7	larger grain -Core	12.5	11.0	1893	28815	2699	233733	b.d.l.	15.6	127252	180.6	998.5	22.7	5962	179299	0.3	3.7	252.7	27.0	0.2	0.0	0.8	36.1	147.5	27.2	143.2	47.6	1.2	53.4	8.9	57.1	11.0	
MFT-maf-12 - 10	larger grain -Core	12.1	12.0	1984	24378	3661	233733	21.0	b.d.l.	126781	170.7	1630.6	32.3	6158	185680	0.1	9.1	224.8	57.7	0.5	0.0	0.5	50.6	191.5	34.9	175.6	50.2	2.4	53.4	8.4	51.3	9.8	
MFT-maf-12 - 16	larger grain -Core	12.2	12.4	2332	29477	4388	233733	17.4	518.4	119092	159.0	1503.3	31.2	5822	168730	2.1	9.9	205.9	58.1	0.9	0.1	12.0	45.5	171.1	31.3	158.0	46.0	2.5	47.9	7.3	45.9	8.8	
MFT-maf-12 - 17	larger grain -Core	12.3	12.3	1949	29931	3771	233733	59.9	49.0	124559	170.8	1544.6	31.3	6060	175772	0.3	10.2	220.6	56.1	1.0	0.4	0.1	1.9	46.6	181.2	32.5	167.6	48.2	2.7	48.8	8.0	49.5	9.5
MFT-maf-12 - 18	larger grain -Core	13.3	12.5	1903	29803	3848	233733	b.d.l.	18.0	122526	169.6	1531.6	31.0	6037	176377	0.3	9.9	227.6	56.3	1.0	0.3	2.6	45.4	181.5	32.6	168.7	49.6	2.6	51.6	8.0	51.7	9.9	
MFT-maf-12 - 19	larger grain -Core	13.7	12.1	1970	28911	3794	233733	17.5	9.6	124642	178.6	1525.2	33.0	6267	180298	0.3	9.7	241.9	52.1	1.2	0.2	6.9	46.9	188.5	33.1	173.8	53.3	2.4	54.6	8.7	54.5	10.4	
MFT-maf-12 - 21	larger grain -Core	12.0	11.5	1975	27410	3528	233733	7.0	b.d.l.	128631	185.6	1497.3	28.6	6120	184187	b.d.l.	7.9	254.0	46.3	0.0	0.0	0.2	47.5	186.5	33.6	178.4	54.8	2.1	57.1	9.1	58.1	11.0	
MFT-maf-12 - 22	larger grain -Core	12.6	11.4	1938	27210	5270	233733	224.9	101.2	118149	159.6	1211.7	22.7	5730	170348	1.4	9.5	258.9	54.6	6.9	0.1	18.1	49.8	211.3	31.8	165.9	51.5	1.7	55.6	9.1	58.7	11.0	
MFT-maf-12 - 23	larger grain -Core	11.6	11.8	1929	28896	3339	233733	21.2	19.9	128110	167.9	1280.7	26.0	6249	182649	0.3	6.7	270.3	41.4	1.5	0.2	2.7	41.2	172.2	30.9	163.0	50.9	1.7	56.1	9.6	60.8	11.6	
MFT-maf-12 - 24	larger grain -Core	11.7	11.1	1894	28819	3629	233733	30.4	b.d.l.	160.5	116177	147.3	1181.4	21.1	6483	187356	1.4	7.2	252.7	46.3	1.6	0.7	12.4	37.1	178.0	27.3	142.7	45.9	1.3	51.5	8.6	56.4	10.8
MFT-maf-12 - 25	larger grain -Core	12.1	11.0	1975	27836	3436	233733	19.5	116.4	124893	154.9	1232.2	23.5	6125	181821	1.3	7.1	266.0	45.5	4.9	0.6	9.1	40.1	188.1	29.9	154.9	50.8	1.5	54.8	9.3	58.9	11.6	
MFT-maf-12 - 26	larger grain -Core	10.8	11.1	1999	28490	3848	233733	9.8	204.4	125981	166.5	1226.8	21.5	5989	176272	2.1	8.0	265.2	50.9	7.3	1.3	14.5	39.8	189.1	29.0	153.3	49.3	1.4	54.9	9.2	59.8	11.3	
MFT-maf-12 - 27	larger grain -Core	13.4	11.6	1940	30369	3125	233733	16.0	19.2	133736	168.5	1238.4	25.1	6441	188655	0.1	5.3	279.0	36.9	1.0	0.0	0.7	42.0	169.6	31.3	162.4	53.9	1.6	58.9	9.9	62.9	12.3	
MFT-maf-12 - 29	larger grain -Core	12.6	12.4	1935	28489	3922	233733	37.9	157.5	120417	146.1	1188.4	24.7	6431	186101	1.8	7.6	260.0	50.3	6.8	0.9	15.6	38.2	191.9	28.5	151.2	49.5	1.5	54.4	9.0	58.0	11.1	
MFT-maf-12 - 30	larger grain -Core	11.2	11.8	1919	28569	3471	233733	11.3	37.5	126484	154.3	1239.1	24.7	6184	180698	0.7	6.2	266.8	42.7	3.1	0.5	5.7	40.1	175.8	29.7	159.2	50.6	1.6	56.5	9.3	60.6	11.7	
MFT-maf-12 - 31	larger grain -Core	13.3	11.6	1828	30353	3674	233733	45.9	37.9	120541	146.0	1302.5	24.2	7017	196451	3.4	7.3	248.9	42.4	2.6	0.3	7.2	38.9	165.5	28.7	152.7	49.9	1.5	54.6	9.1	58.6	11.1	
MFT-maf-12 - 32	larger grain -Core	12.2	12.1	1802	28648	3652	233733	32.8	139.4	105933	130.1	1282.2	24.2	7017	196451	1.8	6.6	275.1	50.3	2.4	0.4	6.5	44.7	189.8	33.0	176.4	55.2	2.0	59.9	9.7	62.9	11.8	
MFT-maf-12 - 33	larger grain -Core	13.9	12.0	1988	28362	3740	233733	20.8	33.7	126926	159.2	1498.9	30.0	6499	188457	0.6	8.6	275.1	50.3	2.4	0.4	6.5	44.7	189.8	33.0	176.4	55.2	2.0	59.9	9.7	62.9	11.8	
MFT-maf-12 - 34	larger grain -Core	12.0	11.7	1958	29037	3711	233733	10.8	17.3	126395	158.1	1305.2	24.7	6205	190598	1.6	7.8	285.3	49.2	3.6	0.7	18.1	43.0	186.2	31.5	170.3	53.7	1.8	58.9	9.7	60.9	11.4	
MFT-maf-12 - 37	larger grain -Core	13.4	12.6	1958	29772	3676	233733	27.5	91.8	125745	177.9	1476.5	30.3	6447	182939	2.6	8.9	252.2	49.8	1.4	0.2	6.8	44.2	183.4	32.9	173.4	52.6	2.4	56.4	8.9	57.5	10.9	
MFT-maf-12 - 38	larger grain -Core	14.1	13.6	2399	28559	5724	233733	44.4	663.4	122383	176.9	1554.3	31.9	6228	183882	3.5	10.4	246.6	57.2	3.5	0.4	20.4	46.8	196.2	33.0	177.2	52.3	2.3	55.0	8.8	57.2	10.5	
MFT-maf-12 - 39	larger grain -Core	10.7	11.9	2001	27434	3873	233733	323.2	47.0	130631	187.3	1529.4	29.0	6210	187315	0.8	8.3	257.4	56.5	4.1	0.5	9.7	50.2	219.3	34.9	181.4	54.2	2.0	58.0	9.2	58.8	11.0	
MFT-maf-12 - 40	larger grain -Rim	13.1	11.9	2037	24270	3453	233733	481.5	21.0	133170	180.0	1529.4</																					

Table A1.11: continued

Er	Tm	Yb	Lu	Hf	Ta	Pb	Th	U
31.3	4.2	28.4	4.7	1.8	0.0	1.0	0.1	0.0
30.5	4.0	26.7	4.5	1.8	0.0	1.1	0.1	0.0
29.9	4.1	28.3	5.0	2.2	0.0	1.3	0.1	0.0
28.9	4.0	28.0	4.6	2.3	0.2	5.7	0.9	0.1
28.0	3.9	27.1	4.5	2.2	0.0	1.6	0.2	0.0
29.0	3.9	26.5	4.5	2.2	0.3	6.2	1.1	0.1
29.1	4.0	27.3	4.6	2.2	0.0	1.3	0.1	0.0
27.2	3.7	25.4	4.5	2.3	0.0	1.1	0.1	0.0
25.9	3.6	24.5	4.3	2.3	0.1	1.9	0.3	0.0
25.3	3.3	24.0	4.1	2.4	0.1	2.2	0.4	0.1
32.6	4.4	29.2	4.8	1.6	b.d.l.	1.0	0.1	0.0
30.1	4.1	27.9	4.5	1.5	0.0	1.5	0.1	0.0
29.8	4.1	27.8	4.5	1.5	0.0	1.4	0.1	0.0
26.5	3.5	24.3	4.1	2.7	0.0	1.1	0.1	0.0
24.3	3.2	22.0	3.5	2.5	0.1	1.4	0.4	0.1
25.3	3.5	23.0	3.7	2.6	0.0	0.9	0.1	0.1
26.4	3.7	23.6	3.7	2.6	0.0	1.4	0.1	0.0
27.9	3.9	25.7	4.1	2.4	0.0	2.9	0.2	0.0
30.1	4.1	28.0	4.5	2.5	0.0	1.1	0.1	0.0
29.4	4.2	27.1	4.3	2.6	0.5	4.5	1.6	0.1
31.9	4.2	28.2	4.7	2.2	0.1	2.0	0.3	0.0
29.9	4.1	27.4	4.3	2.2	0.3	4.6	1.2	0.1
31.9	4.2	28.7	4.6	2.2	0.3	4.0	1.1	0.0
31.4	4.2	28.8	4.6	2.5	0.6	4.8	1.4	0.1
32.9	4.4	29.7	4.8	1.9	0.0	1.4	0.3	0.0
30.7	4.1	27.2	4.4	2.5	0.4	5.0	1.3	0.1
31.6	4.2	29.3	4.6	2.2	0.1	2.8	0.5	0.0
31.4	4.3	28.8	4.4	2.2	0.1	2.7	0.9	0.1
29.2	4.0	27.0	4.2	1.9	0.1	3.4	1.0	0.1
32.0	4.3	28.8	4.6	2.5	0.1	2.5	0.5	0.1
31.2	4.4	29.5	4.6	2.4	0.2	3.8	0.8	0.1
30.7	4.0	26.8	3.9	2.4	0.1	1.9	0.5	0.1
28.3	3.9	25.7	3.9	2.8	0.2	5.9	1.2	0.1
29.9	4.0	27.4	4.5	2.7	0.3	3.4	0.9	0.1
29.8	4.0	27.9	4.5	2.4	0.0	1.2	1.0	0.2
33.1	4.5	29.1	4.7	1.4	0.1	4.0	0.6	0.0
32.5	4.4	29.1	4.6	1.4	0.0	1.4	0.1	0.0
32.9	4.4	28.9	4.7	1.4	0.0	1.4	0.1	0.0
34.3	4.6	30.9	4.9	1.5	0.0	1.9	0.1	0.0
35.1	4.8	31.3	4.8	1.4	0.0	1.2	0.1	0.0
35.4	4.7	31.2	5.0	1.3	0.0	1.0	0.1	0.0
32.9	4.4	29.3	4.6	1.4	0.0	1.2	0.1	0.0
33.6	4.4	29.4	4.6	1.4	0.0	1.1	0.1	0.1
31.3	4.3	28.9	4.6	1.4	0.0	1.0	0.1	0.0
32.2	4.3	28.6	4.5	1.6	0.0	1.2	0.1	0.0
34.0	4.5	30.2	4.8	1.6	0.1	9.4	0.4	0.1
32.1	4.3	28.9	4.5	1.5	0.0	1.6	0.1	0.0
33.0	4.5	29.4	4.7	1.5	0.0	1.1	0.1	0.0
31.7	4.4	29.1	4.6	1.7	0.0	0.9	0.1	0.0
32.2	4.3	28.9	4.6	1.4	b.d.l.	1.1	0.1	0.0
32.7	4.3	28.9	4.6	1.4	0.0	1.1	0.1	0.0
32.2	4.3	29.8	4.7	1.5	b.d.l.	1.1	0.1	0.0
32.5	4.4	29.0	4.7	1.6	b.d.l.	1.0	0.1	0.0
33.0	4.4	30.1	4.7	1.7	0.0	1.0	0.1	0.0

Table A1.11: continued

Info	Position	I _h ^f	L ₁ ^f	Na	Mg	Al	Si	P	K	Ca	Sc	Ti	V	Mn	Fe	Rb	Sr	Y	Zr	Nb	Cs	Ba	La	Ce	Pr	Nd	Sm	Eu	Gd	Tb	Dy	Ho
MFT-mat-13 - 28	larger grain - Core	9.5	10.8	1866	33797	2618	233733	b.d.l.	b.d.l.	128828	163.1	806.3	7.9	6000	164236	b.d.l.	1.8	273.0	22.7	0.3	b.d.l.	b.d.l.	31.4	130.9	24.8	132.7	47.0	0.8	54.0	9.2	60.6	12.0
MFT-mat-13 - 30	larger grain - Core	11.7	10.8	1860	32561	2809	233733	b.d.l.	4.2	129841	160.6	873.3	7.0	5931	165758	0.2	2.3	281.2	27.0	0.8	0.1	1.4	35.6	147.9	27.0	143.4	49.3	0.8	57.5	9.8	63.5	11.9
MFT-mat-13 - 31	larger grain - Core	10.8	10.7	1893	32705	2746	233733	b.d.l.	b.d.l.	127794	163.8	871.1	7.7	5879	164849	b.d.l.	2.0	284.9	26.3	0.2	b.d.l.	b.d.l.	35.4	144.8	27.3	145.0	50.7	0.8	58.0	10.0	62.5	12.2
MFT-mat-13 - 32	larger grain - Core	10.8	11.0	1844	32590	2769	233733	b.d.l.	b.d.l.	128446	160.9	874.6	7.9	5902	165211	0.1	2.1	282.9	26.4	0.2	b.d.l.	b.d.l.	35.5	145.2	27.4	142.6	50.1	0.8	58.2	9.9	64.1	12.1
MFT-mat-13 - 33	larger grain - Core	11.6	10.8	1887	32593	2769	233733	b.d.l.	b.d.l.	131176	163.7	871.5	8.1	5971	166388	b.d.l.	2.3	287.5	25.6	0.2	b.d.l.	b.d.l.	35.8	144.1	27.4	142.6	50.9	0.8	58.2	9.9	63.8	12.4
MFT-mat-13 - 34	larger grain - Core	10.9	10.9	1861	32672	2726	233733	14.4	b.d.l.	128888	159.9	861.0	7.7	5926	165383	0.1	2.1	279.4	25.4	0.2	b.d.l.	b.d.l.	34.4	142.2	26.7	141.7	49.4	0.8	57.1	9.6	61.7	12.2
MFT-mat-13 - 35	larger grain - Core	10.8	11.2	1878	32889	2712	233733	b.d.l.	b.d.l.	130842	158.4	860.8	7.5	6000	166399	0.1	2.2	279.9	24.5	0.2	b.d.l.	b.d.l.	33.5	140.0	26.1	138.7	48.9	0.7	56.8	9.7	62.6	12.1
MFT-mat-13 - 39	larger grain - Core	10.3	10.7	1871	33466	2819	233733	13.3	b.d.l.	133543	161.1	862.4	7.2	5993	165663	0.1	2.2	292.0	26.3	0.4	0.0	1.4	36.5	149.0	28.2	145.7	52.2	0.9	59.8	10.2	66.1	12.7
MFT-mat-13 - 40	larger grain - Core	11.3	10.7	1841	33243	2775	233733	b.d.l.	b.d.l.	131654	157.6	867.5	7.1	5996	165108	b.d.l.	2.0	286.6	25.3	0.3	b.d.l.	0.8	34.9	142.4	26.8	144.5	49.4	0.8	57.9	10.0	64.9	12.4
MFT-mat-13 - 41	larger grain - Core	11.7	10.7	1873	33961	2941	233733	b.d.l.	10.6	133790	165.3	887.1	7.8	6114	167163	0.2	2.5	294.4	29.8	1.9	0.1	4.1	36.0	160.2	28.0	146.8	52.6	0.8	60.2	10.1	66.5	12.5
MFT-mat-13 - 42	larger grain - Core	11.6	10.9	1862	33762	2953	233733	b.d.l.	13.0	130041	162.4	889.4	7.4	5998	166968	0.2	2.3	294.6	29.1	2.5	0.2	1.1	36.2	164.9	27.6	147.1	52.8	0.8	59.9	10.3	66.4	12.7
MFT-mat-13 - 45	larger grain - Core	10.2	11.0	1881	33952	2956	233733	11.1	4.8	134370	166.0	875.3	7.4	6069	168075	0.1	2.2	299.6	27.5	0.5	0.1	1.0	37.3	152.6	28.4	151.8	51.6	0.9	60.7	10.3	66.4	12.9
MFT-mat-13 - 46	larger grain - Core	10.6	11.0	1883	33717	2956	233733	b.d.l.	b.d.l.	135633	165.8	867.8	7.6	6036	166215	0.1	2.3	294.0	26.6	0.4	b.d.l.	0.8	36.6	152.8	28.0	146.2	52.0	0.9	60.2	10.4	65.4	12.6
MFT-mat-13 - 47	larger grain - Core	10.0	11.2	1850	34427	2753	233733	10.7	b.d.l.	134907	163.5	861.9	7.8	6131	166459	0.1	2.2	294.5	24.7	0.2	b.d.l.	b.d.l.	35.1	141.9	27.1	142.3	50.9	0.8	58.5	10.1	64.1	12.5
MFT-mat-13 - 48	larger grain - Core	11.6	11.0	1844	34218	2745	233733	b.d.l.	b.d.l.	133660	166.5	846.4	7.5	6000	166592	b.d.l.	2.1	290.4	24.3	0.3	b.d.l.	0.7	34.4	142.7	26.7	141.4	49.9	0.8	57.5	10.0	63.7	12.2
MFT-mat-13 - 49	larger grain - Rim	10.6	10.9	1864	33567	2890	233733	b.d.l.	7.5	131668	163.7	828.0	7.1	6075	164757	0.2	2.3	287.4	25.1	0.5	0.1	1.3	34.0	142.0	26.4	139.8	49.6	0.9	55.3	9.9	63.7	12.2
MFT-mat-11 - 1	larger grain - Rim	10.6	11.0	1914	24001	3112	233733	b.d.l.	b.d.l.	128726	173.2	1279.1	32.8	5915	182423	b.d.l.	7.5	221.4	40.8	0.7	0.0	0.7	48.2	190.5	32.7	171.3	51.3	2.0	54.0	8.4	51.9	9.7
MFT-mat-11 - 1	larger grain - Core	11.2	11.1	1923	24956	3084	233733	b.d.l.	b.d.l.	126838	167.5	1293.6	42.1	5736	175726	b.d.l.	7.1	220.9	39.8	0.2	b.d.l.	b.d.l.	45.4	177.6	32.3	164.3	48.9	1.9	51.9	8.2	50.5	9.4
MFT-mat-11 - 1	larger grain - Core	11.9	11.4	1994	26112	3213	233733	b.d.l.	b.d.l.	127145	163.9	1277.6	49.2	5606	171871	b.d.l.	7.2	223.1	40.9	0.2	b.d.l.	b.d.l.	45.6	179.0	32.2	165.0	49.7	2.0	52.0	8.2	51.4	9.5
MFT-mat-11 - 1	larger grain - Core	12.9	12.2	1929	43584	4095	233733	130.0	b.d.l.	124479	141.6	1311.5	77.7	4958	142086	0.1	8.4	239.3	53.0	0.3	b.d.l.	0.3	44.2	173.9	30.5	158.9	45.8	2.1	49.2	8.2	51.8	10.0
MFT-mat-11 - 1	larger grain - Core	11.8	11.4	1887	44949	4115	233733	316.6	15.4	122025	134.4	1317.7	68.4	4913	138915	0.1	8.0	237.8	38.9	0.2	b.d.l.	0.2	46.0	173.3	31.3	156.4	46.3	2.1	50.2	8.4	51.2	10.2
MFT-mat-11 - 1	larger grain - Core	12.4	11.9	2059	46314	4809	233733	13.3	445.0	119365	130.7	1307.1	63.3	4665	133675	1.8	8.2	228.4	40.3	0.7	0.0	4.4	39.1	158.2	28.1	147.4	42.9	2.1	47.2	7.7	49.2	9.5
MFT-mat-11 - 1	larger grain - Core	12.3	11.7	1978	47639	4600	233733	17.3	136.6	123062	140.1	1357.0	68.2	4738	136910	0.5	8.0	239.8	40.8	0.5	b.d.l.	1.2	41.1	165.5	30.2	156.1	45.9	2.0	50.6	8.0	51.4	10.2
MFT-mat-11 - 1	larger grain - Core	10.6	11.0	1867	48297	3956	233733	9.8	45.4	121380	155.7	1296.6	54.0	4620	135751	0.4	7.4	225.5	38.7	2.6	0.2	4.0	38.8	162.8	27.5	143.8	42.6	1.9	45.2	7.6	48.4	9.3
MFT-mat-11 - 1	larger grain - Core	11.4	11.0	1606	47821	3479	233733	15.3	24.3	106976	140.8	1115.3	47.9	4764	142497	0.5	6.2	200.1	33.6	2.2	0.3	4.1	34.0	142.8	24.2	125.5	37.5	1.4	40.5	6.8	42.2	8.3
MFT-mat-11 - 24	larger grain - Core	11.3	11.4	1958	26798	3614	233733	117.1	24.5	129506	169.7	1296.2	44.9	6149	183590	0.2	7.1	246.6	65.1	1.5	0.1	3.1	47.3	188.3	33.4	173.0	52.4	1.8	55.7	9.0	56.0	10.7
MFT-mat-11 - 26	larger grain - Core	11.6	11.5	1953	24362	3563	233733	27.3	22.5	129105	171.2	1253.7	26.1	6095	187263	0.3	7.5	228.3	42.9	1.6	0.2	3.4	48.2	191.9	32.6	171.8	51.3	1.8	54.1	8.6	52.8	10.0
MFT-mat-11 - 27	larger grain - Core	12.8	11.2	1918	25512	2946	233733	11.1	b.d.l.	130965	166.8	1128.7	20.3	6081	184075	0.1	5.6	233.2	36.5	0.6	0.1	0.7	44.2	177.6	31.7	164.8	50.3	1.8	53.4	8.7	55.6	10.2
MFT-mat-11 - 28	larger grain - Rim	11.1	11.0	1881	27806	2914	233733	37.6	12.5	128873	163.4	1030.8	17.5	6010	182380	0.1	4.7	248.4	33.2	0.9	0.1	1.7	44.2	167.3	30.5	159.9	49.6	1.3	55.9	9.2	56.8	10.9
MFT-mat-15 - 1	larger grain - Rim	10.7	11.3	1855	30291	2844	233733	b.d.l.	13.7	128284	150.5	988.7	14.1	6168	171876	0.2	4.7	238.3	31.9	4.0	0.1	10.3	36.8	180.4	27.2	143.7	48.4	1.2	53.9	9.2	58.3	11.1
MFT-mat-15 - 5	larger grain - Core	11.4	10.9	1854	33691	2513	233733	10.7	b.d.l.	125460	153.7	780.0	5.2	6283	166138	b.d.l.	1.2	299.3	22.2	0.2	b.d.l.	b.d.l.	29.5	125.6	23.6	126.7	48.3	0.6	56.5	10.1	65.9	13.0
MFT-mat-15 - 6	larger grain - Core	10.7	11.5	1894	33720	2579	233733	b.d.l.	b.d.l.	127450	148.7	814.4	4.7	6375	167522	b.d.l.	1.1	309.3	23.3	0.2	b.d.l.	b.d.l.	30.5	126.9	24.6	129.4	48.4	0.6	58.3	10.6	68.4	13.3
MFT-mat-15 - 12	larger grain - Core	12.4	11.1	1803	35365	2622	233733	20.4	b.d.l.	137203	161.0	840.9	6.0	6215	172548	0.1	1.8	289.1	23.0	0.5	b.d.l.	0.4	33.1	138.2	26.0	139.6	48.7	0.8	58.3	10.2	64.8	12.4
MFT-mat-15 - 13	larger grain - Core	10.9	11.0	1837	34579	2528	233733	10.3	b.d.l.	131274	153.4	823.4	6.6	6135	169355	b.d.l.	1.9	277.4	22.3	0.7	b.d.l.	1.5	32.1	138.6	25.2	134.1	47.1	0.7	54.6	9.6	60.3	12.0
MFT-mat-15 - 14	larger grain - Core	11.4	11.0	1876	32725	2634	233733	12.0	b.d.l.	128674	153.0	866.9	8.5	6204	173669	b.d.l.	2.5	264.6	32.7	0.3	b.d.l.	0.6	46.2	174.0								

Table A1.11: continued

Er	Tm	Yb	Lu	Hf	Ta	Pb	Th	U
31.6	4.3	27.8	4.5	1.4	0.0	1.2	0.1	0.0
32.5	4.5	30.1	4.8	1.7	0.0	1.7	0.2	0.0
33.3	4.3	29.5	4.7	1.7	0.0	1.1	0.1	0.0
32.8	4.5	29.4	4.7	1.7	0.0	1.1	0.1	0.0
33.0	4.4	30.4	4.7	1.8	0.0	1.1	0.1	0.0
32.6	4.4	29.1	4.6	1.7	b.d.l.	1.1	0.1	0.0
32.3	4.4	29.5	4.7	1.6	0.0	1.1	0.0	0.0
33.9	4.5	30.5	5.0	1.8	0.0	3.6	0.1	0.0
33.8	4.5	29.8	4.6	1.7	b.d.l.	1.6	0.1	0.0
34.5	4.6	30.4	4.8	1.8	0.1	3.9	0.4	0.0
34.4	4.6	29.7	4.8	1.9	0.2	3.2	0.5	0.0
34.8	4.5	31.2	4.9	1.8	0.0	1.7	0.3	0.0
34.2	4.6	30.0	4.9	1.6	0.0	1.7	0.3	0.0
34.5	4.5	30.6	4.8	1.6	0.0	1.4	0.1	0.0
33.9	4.5	30.5	4.8	1.5	0.0	1.5	0.1	0.0
33.6	4.5	30.4	4.9	1.6	0.0	2.0	0.3	0.0
26.0	3.6	25.8	4.4	2.0	0.0	1.3	0.2	0.0
25.7	3.5	24.7	4.3	2.0	0.0	1.2	0.1	0.0
26.0	3.5	24.9	4.1	2.0	0.0	1.0	0.1	0.0
27.4	3.7	23.7	3.5	2.2	0.0	1.2	0.2	0.0
27.6	3.6	23.5	3.5	2.0	0.0	0.9	0.2	0.0
26.6	3.5	22.9	3.2	2.0	0.0	1.1	0.4	0.1
27.3	3.7	23.3	3.5	1.9	0.0	1.0	0.2	0.0
26.2	3.4	22.6	3.3	1.8	0.1	2.2	0.3	0.0
23.2	3.1	19.6	3.1	1.7	0.1	1.9	0.4	0.0
29.9	4.1	27.6	4.6	2.3	0.1	1.9	0.4	0.1
27.0	3.7	25.7	4.4	2.2	0.1	2.0	0.4	0.3
27.4	3.7	26.5	4.4	2.0	0.0	1.3	0.1	0.0
29.5	4.0	27.2	4.6	1.7	0.1	1.7	0.5	0.0
30.7	4.2	27.9	4.5	1.8	0.2	8.2	0.6	0.0
35.3	4.8	31.9	4.9	1.5	b.d.l.	1.0	0.1	0.0
36.3	4.9	32.8	5.1	1.5	0.0	1.0	0.1	0.0
34.2	4.6	31.1	4.8	1.5	0.0	1.7	0.1	0.0
31.8	4.3	28.3	4.6	1.3	0.0	2.6	0.2	0.0
31.4	4.2	28.6	4.6	1.5	0.0	2.9	0.1	0.0
30.2	4.1	28.4	4.6	1.8	0.0	1.3	0.5	0.1
30.3	4.1	28.4	4.6	1.7	0.1	3.1	0.3	0.0
29.5	4.1	26.9	4.2	1.5	0.1	7.0	0.6	0.1
30.1	4.2	27.7	4.7	1.8	0.0	1.3	0.4	0.2
33.6	4.5	30.4	4.9	1.7	0.0	1.3	0.3	0.1
31.9	4.3	28.5	4.5	1.6	0.1	3.5	0.4	0.1
30.1	4.3	27.8	4.7	1.8	0.0	1.1	0.2	0.1
29.7	4.1	27.8	4.8	2.0	0.1	3.1	0.3	0.0

Table A1.11: continued

Info	Position	Li ⁶	Li ⁷	Na	Mg	Al	Si	P	K	Ca	Sc	Ti	V	Mn	Fe	Rb	Sr	Y	Zr	Nb	Cs	Ba	La	Ce	Pr	Nd	Sm	Eu	Gd	Tb	Dy	Ho
MFT-maf-15 - 23	larger grain	8.1	8.0	148.6	42015	1419	233733	15.9	43.3	11437	37.3	683.6	2.5	10101	289211	0.7	1.0	58.9	4.0	1.3	0.4	3.9	4.2	15.3	1.4	7.3	2.8	0.1	5.0	1.1	9.3	2.3
MFT-maf-15 - 24	larger grain	8.4	8.0	119.6	42408	1140	233733	b.d.l.	b.d.l.	10521	36.7	676.4	2.2	10064	289096	b.d.l.	b.d.l.	54.5	2.2	0.1	b.d.l.	1.2	0.7	3.0	0.6	4.3	2.3	0.1	3.9	1.0	8.6	2.2
MFT-maf-15 - 25	larger grain	7.7	8.1	124.0	41968	1157	233733	b.d.l.	b.d.l.	10866	36.8	678.8	2.4	10131	287144	0.1	b.d.l.	56.2	2.0	0.2	b.d.l.	0.2	1.2	3.0	1.4	4.1	2.3	0.0	3.9	1.2	8.2	2.3
MFT-maf-15 - 26	larger grain	7.9	8.1	119.3	41989	1165	233733	b.d.l.	b.d.l.	10511	36.5	671.3	2.1	10232	289222	b.d.l.	b.d.l.	54.9	2.0	0.1	b.d.l.	0.2	0.4	1.9	0.5	3.4	2.1	0.1	4.0	0.9	8.2	2.1
MFT-maf-15 - 27	larger grain	8.1	8.1	113.4	40995	1143	233733	b.d.l.	b.d.l.	10571	36.0	677.7	2.3	10026	285589	b.d.l.	b.d.l.	56.2	1.8	0.1	b.d.l.	b.d.l.	0.3	2.3	0.5	3.3	2.0	0.1	4.0	1.0	8.6	2.2
MFT-maf-15 - 28	larger grain	8.5	8.0	120.4	41473	1243	233733	b.d.l.	5.6	10141	36.5	702.5	2.4	10223	293739	0.1	b.d.l.	56.4	2.1	0.2	0.1	0.8	0.4	3.1	0.5	3.4	2.0	0.0	3.7	0.9	8.8	2.2
MFT-maf-15 - 30	larger grain	9.6	8.0	116.0	41722	1231	233733	b.d.l.	b.d.l.	10056	36.3	726.5	2.5	10138	293466	b.d.l.	b.d.l.	57.9	1.8	0.1	b.d.l.	b.d.l.	0.4	1.9	0.5	3.3	2.1	0.0	4.1	1.0	8.5	2.3
MFT-maf-15 - 31	larger grain	8.9	8.2	118.6	41199	1283	233733	b.d.l.	b.d.l.	10172	37.0	712.2	2.6	10280	294721	b.d.l.	0.1	59.8	2.3	0.2	0.0	0.3	0.3	2.1	0.5	3.3	2.1	b.d.l.	4.3	1.0	9.5	2.4
MFT-maf-15 - 34	larger grain	9.6	8.4	119.5	38796	1371	233733	b.d.l.	6.7	9321	35.7	680.2	2.3	9427	275351	0.1	0.2	54.1	3.5	0.7	0.1	1.8	0.4	5.2	0.4	3.3	2.1	0.1	4.1	1.0	8.5	2.2
MFT-maf-15 - 35	larger grain	8.3	8.0	109.8	41313	1274	233733	b.d.l.	b.d.l.	9929	40.5	744.9	2.8	10078	294515	b.d.l.	b.d.l.	58.7	1.9	0.1	b.d.l.	b.d.l.	0.3	1.8	0.4	3.2	2.0	0.1	4.1	1.1	9.4	2.3
MFT-maf-15 - 38	larger grain	8.8	8.4	112.1	41771	1266	233733	b.d.l.	b.d.l.	9901	39.3	724.9	2.5	10087	290285	b.d.l.	b.d.l.	59.6	2.1	0.1	b.d.l.	b.d.l.	0.3	1.8	0.5	3.4	1.9	0.1	4.2	1.0	9.1	2.4
MFT-maf-15 - 39	larger grain	7.4	8.1	118.2	42926	1458	233733	b.d.l.	b.d.l.	10918	41.1	777.8	2.9	10298	297876	0.1	0.1	61.8	2.7	0.2	0.1	0.4	0.5	2.4	0.5	3.6	2.3	0.1	4.2	1.1	9.7	2.5
MFT-maf-15 - 41	larger grain	8.1	8.1	114.4	41958	1287	233733	23.1	b.d.l.	10084	37.1	637.9	2.5	10090	288786	0.2	0.1	57.7	2.4	0.4	0.1	0.7	1.5	5.2	0.6	4.4	2.3	0.1	4.0	0.9	8.9	2.2
MFT-maf-15 - 42	larger grain	7.9	8.2	113.7	41995	1265	233733	b.d.l.	b.d.l.	9982	39.5	705.6	2.8	10135	290190	b.d.l.	b.d.l.	59.6	2.3	0.1	b.d.l.	0.2	0.5	2.5	0.5	3.8	2.2	0.1	4.4	1.1	9.3	2.3
MFT-maf-15 - 43	larger grain	8.0	7.8	111.6	41032	1248	233733	b.d.l.	b.d.l.	10166	37.7	640.4	2.5	10011	285798	b.d.l.	b.d.l.	57.3	2.2	0.3	b.d.l.	b.d.l.	0.8	2.7	0.7	3.8	2.0	0.0	4.0	1.0	8.7	2.2
MFT-maf-15 - 44	larger grain	8.1	8.2	111.4	41235	1238	233733	b.d.l.	b.d.l.	10274	37.3	670.6	2.5	10137	288485	b.d.l.	b.d.l.	57.8	2.2	0.1	b.d.l.	b.d.l.	1.9	4.0	0.7	4.4	1.9	0.1	4.0	1.0	8.9	2.4
MFT-maf-15 - 47	larger grain	8.8	8.3	130.8	39937	1203	233733	b.d.l.	b.d.l.	9883	35.1	647.0	2.6	10183	288146	0.1	0.1	54.5	2.2	0.4	b.d.l.	2.1	0.6	14.4	0.6	4.3	1.9	0.0	3.6	0.9	8.6	2.2
MFT-maf-15 - 49	larger grain	7.7	8.4	134.0	40115	1275	233733	b.d.l.	8.4	10884	39.9	756.9	2.9	10178	288839	0.3	0.3	59.8	3.8	1.2	0.1	1.5	0.8	10.9	0.5	3.9	2.2	0.0	4.3	1.1	9.2	2.3
MFT-maf-15 - 50	larger grain	8.5	7.9	120.9	39805	1216	233733	b.d.l.	6.1	10611	40.5	751.9	2.9	10177	286360	b.d.l.	0.1	60.5	2.3	0.2	b.d.l.	0.7	0.6	5.7	0.5	3.4	2.2	0.0	4.4	1.1	9.6	2.4
MFT-maf-15 - 51	larger grain	9.2	8.0	118.7	40846	1205	233733	b.d.l.	b.d.l.	10513	40.3	740.7	2.7	10320	290462	b.d.l.	b.d.l.	60.8	2.3	0.1	b.d.l.	b.d.l.	0.4	2.4	0.5	3.6	2.2	0.0	4.3	1.0	9.5	2.4
MFT-maf-15 - 52	larger grain	8.6	8.0	116.1	39214	1164	233733	b.d.l.	4.7	10665	37.5	694.2	2.2	10293	287110	0.1	b.d.l.	57.9	2.0	0.1	b.d.l.	b.d.l.	0.3	2.4	0.5	3.2	2.1	0.1	4.2	1.0	9.1	2.3
MFT-maf-15 - 53	larger grain	8.7	8.2	121.1	38025	1153	233733	b.d.l.	b.d.l.	10561	35.7	695.7	2.3	10499	293998	b.d.l.	b.d.l.	58.1	2.2	0.1	b.d.l.	0.3	0.3	2.8	0.5	3.0	2.2	0.0	4.1	1.1	9.1	2.3
MFT-maf-15 - 54	larger grain	9.9	8.0	176.7	35082	2798	233733	b.d.l.	67.4	9720	31.4	681.2	2.1	9901	274815	0.7	1.4	61.5	7.7	2.0	0.4	6.2	6.1	7.9	1.6	8.3	3.1	0.1	5.1	1.2	9.9	2.5

Table A1.11: continued

Er	Tm	Yb	Lu	Hf
8.4	1.5	11.0	1.9	0.2
8.0	1.4	11.4	1.9	0.1
8.2	1.4	11.4	1.8	0.1
7.9	1.4	11.1	1.9	0.1
8.0	1.4	11.2	1.8	0.1
8.3	1.4	11.2	1.9	0.1
8.1	1.5	11.4	1.9	0.1
8.9	1.5	11.8	2.0	0.1
7.8	1.3	10.8	1.7	0.1
8.6	1.5	11.7	1.9	0.2
8.6	1.5	11.9	2.0	0.1
9.0	1.6	11.9	2.0	0.2
8.3	1.5	11.3	1.9	0.1
8.6	1.5	12.3	2.0	0.1
8.1	1.5	11.3	1.9	0.1
8.2	1.5	11.7	1.8	0.1
8.0	1.4	11.4	1.9	0.1
8.7	1.5	11.7	2.0	0.2
8.6	1.5	12.7	2.0	0.1
8.5	1.5	12.6	2.0	0.1
8.4	1.4	11.9	1.9	0.1
8.2	1.5	11.4	2.0	0.1
8.5	1.5	11.6	1.9	0.3

Table A1.12: Major elements - olivine

Info	Position	SiO ₂	TiO ₂	Al ₂ O ₃	FeO	MgO	CaO	Na ₂ O	K ₂ O	Cr ₂ O ₃	MnO	Total	Fo	Fa	Ca-OI
mft-ol-2 - 1	smaller grain - Rim	30.1	0.9	0.0	62.5	5.1	0.2	0.0	0.0	0.0	1.8	100.6	13	87	0.3
mft-ol-2 - 2	smaller grain - Core	30.6	0.6	0.0	62.6	5.1	0.2	0.0	0.0	0.0	1.9	100.9	13	87	0.3
mft-ol-4 - 1	smaller grain - Rim	31.0	0.6	0.0	62.3	5.1	0.2	0.0	0.0	0.0	1.8	101.1	13	87	0.3
mft-ol-4 - 2	smaller grain - Core	30.6	0.6	0.0	62.3	5.1	0.2	0.0	0.0	0.0	1.8	100.5	13	87	0.3
mft-ol-4 - 3	smaller grain - Rim	30.3	0.7	0.0	62.3	5.3	0.2	0.0	0.0	0.0	1.8	100.6	13	87	0.3
mft-ol-8 - 1	smaller grain - Rim	30.7	1.0	0.0	62.5	4.9	0.2	0.0	0.0	0.0	1.7	101.0	12	87	0.3
mft-ol-8 - 2	smaller grain - Core	31.0	0.6	0.0	62.8	5.1	0.2	0.0	0.0	0.0	1.8	101.5	13	87	0.3
mft-ol-8 - 3	smaller grain - Core	30.6	0.6	0.0	62.6	5.3	0.2	0.0	0.0	0.0	1.8	101.2	13	87	0.4
mft-ol-8 - 5	smaller grain - Rim	30.5	1.0	0.0	62.8	5.1	0.2	0.0	0.0	0.0	1.8	101.5	13	87	0.3
mft-ol-24 - 1	smaller grain - Rim	30.5	0.5	0.0	62.5	5.0	0.2	0.0	0.0	0.0	1.8	100.4	12	87	0.3
mft-ol-24 - 2	smaller grain - Core	30.5	0.7	0.1	62.5	5.1	0.2	0.0	0.0	0.0	1.8	100.9	13	87	0.4
mft-ol-24 - 3	smaller grain - Rim	30.0	0.8	0.0	62.6	5.0	0.2	0.0	0.0	0.0	1.8	100.3	12	87	0.3
mft-ol-40 - 1	smaller grain - Rim	30.6	1.2	0.0	62.6	4.8	0.2	0.0	0.0	0.0	1.9	101.2	12	88	0.4
mft-ol-40 - 2	smaller grain - Core	30.3	0.5	0.0	62.7	5.0	0.2	0.0	0.0	0.0	1.8	100.6	12	87	0.4
mft-ol-40 - 3	smaller grain - Core	30.6	0.9	0.0	62.0	5.2	0.2	0.0	0.0	0.0	1.9	100.7	13	87	0.4
mft-ol-40 - 4	smaller grain - Core	30.5	0.9	0.0	62.6	5.1	0.2	0.0	0.0	0.0	1.8	101.0	13	87	0.4
mft-ol-40 - 5	smaller grain - Rim	30.6	0.8	0.0	62.7	5.0	0.2	0.0	0.0	0.0	1.9	101.3	12	87	0.3
mft-ol-41 - 1	smaller grain - Rim	30.2	0.6	0.0	62.7	4.8	0.2	0.0	0.0	0.0	1.8	100.2	12	88	0.3
mft-ol-41 - 2	smaller grain - Core	30.3	0.9	0.0	63.1	4.5	0.1	0.0	0.0	0.0	1.8	100.7	11	89	0.2
mft-ol-41 - 3	smaller grain - Core	30.4	0.9	0.0	63.4	4.2	0.2	0.0	0.0	0.0	1.9	101.0	11	89	0.3
mft-ol-41 - 4	smaller grain - Core	30.6	1.0	0.0	63.3	4.3	0.2	0.0	0.0	0.0	1.9	101.3	11	89	0.3
mft-ol-41 - 5	smaller grain - Rim	30.6	0.4	0.0	62.7	4.8	0.2	0.0	0.0	0.0	1.9	100.6	12	88	0.3
MFT-1-2	bigger grain - Rim	31.2	0.1	0.0	63.3	4.8	0.2	0.0	0.0	0.0	1.8	101.5	12	88	0.3
MFT-7-1	bigger grain - Core	31.3	0.1	0.0	63.4	5.1	0.2	0.0	0.0	0.0	1.9	101.9	12	87	0.4
MFT-7-2	bigger grain - Rim	31.1	0.1	0.0	63.4	5.0	0.2	0.0	0.0	0.0	1.9	101.7	12	87	0.3
MFT-17 - 1	bigger grain - Core	30.7	0.1	0.0	63.7	5.0	0.2	0.0	0.0	0.0	1.9	101.6	12	87	0.4
MFT-22-1	bigger grain - Core	31.1	0.1	0.0	63.7	4.9	0.2	0.0	0.0	0.0	1.9	102.0	12	88	0.4
MFT-23-1	bigger grain - Core	30.9	0.1	0.0	63.2	5.3	0.2	0.0	0.0	0.0	1.9	101.5	13	87	0.3
MFT-23-2	bigger grain - Rim	30.9	0.1	0.0	63.3	5.1	0.2	0.0	0.0	0.0	1.9	101.4	12	87	0.3
MFT-31 - 2	bigger grain - Rim	30.7	0.1	0.0	64.1	4.9	0.2	0.0	0.0	0.0	1.8	101.8	12	88	0.3
MFT-32 - 2	bigger grain - Rim	30.7	0.1	0.0	63.6	4.9	0.2	0.0	0.0	0.0	1.9	101.4	12	88	0.3
MFT-33 - 1	bigger grain - Core	30.8	0.1	0.0	63.7	5.0	0.2	0.0	0.0	0.0	1.8	101.5	12	87	0.3
MFT-33 - 2	bigger grain - Rim	30.9	0.1	0.0	63.7	5.0	0.2	0.0	0.0	0.0	1.9	101.7	12	87	0.3
MFT-35 - 1	bigger grain - Core	30.6	0.1	0.0	63.1	5.2	0.2	0.0	0.0	0.0	1.9	101.0	13	87	0.3
MFT-35 - 2	bigger grain - Rim	30.8	0.1	0.0	63.6	5.1	0.2	0.0	0.0	0.0	1.9	101.6	13	87	0.3
MFT-37 - 3	bigger grain - Rim	30.7	0.1	0.0	63.5	5.1	0.2	0.0	0.0	0.0	1.9	101.3	12	87	0.4
MFT-38 - 1	bigger grain - Core	30.9	0.1	0.0	63.9	4.8	0.2	0.0	0.0	0.0	1.9	101.7	12	88	0.3
MFT-38 - 2	bigger grain - Rim	30.9	0.1	0.0	64.0	4.8	0.2	0.0	0.0	0.0	1.9	101.9	12	88	0.3
MFT-40 - 1	bigger grain - Core	30.9	0.1	0.0	63.7	4.8	0.2	0.0	0.0	0.0	1.9	101.5	12	88	0.3
MFT-40 - 2	bigger grain - Rim	30.8	0.1	0.0	64.0	4.8	0.2	0.0	0.0	0.0	1.9	101.8	12	88	0.3
MFT-42 - 1	bigger grain - Core	30.6	0.1	0.0	63.9	5.0	0.2	0.0	0.0	0.0	1.8	101.6	12	88	0.3
MFT-42 - 2	bigger grain - Rim	31.0	0.1	0.0	64.0	4.9	0.2	0.0	0.0	0.0	1.9	102.0	12	88	0.3
MFT-44 - 1	bigger grain - Core	30.7	0.1	0.0	63.4	5.1	0.2	0.0	0.0	0.0	1.8	101.2	13	87	0.3
MFT-44 - 2	bigger grain - Rim	31.0	0.1	0.0	63.6	5.0	0.2	0.0	0.0	0.0	1.9	101.8	12	87	0.4
MFT-45 - 3	bigger grain - Rim	30.5	0.1	0.0	63.8	5.1	0.2	0.0	0.0	0.0	1.9	101.4	12	87	0.3
MFT-51 - 1	bigger grain - Core	30.4	0.0	0.0	63.9	4.9	0.2	0.0	0.0	0.0	1.9	101.3	12	88	0.4
MFT-51 - 2	bigger grain - Rim	30.4	0.1	0.0	64.0	4.9	0.2	0.0	0.0	0.0	1.9	101.3	12	88	0.4
MFT-56 - 1	bigger grain - Core	30.4	0.1	0.0	63.7	5.2	0.2	0.0	0.0	0.0	1.8	101.4	13	87	0.3
MFT-56 - 2	bigger grain - Rim	30.8	0.1	0.0	63.9	5.2	0.2	0.0	0.0	0.0	1.9	102.0	13	87	0.3
MFT-60 - 1	bigger grain - Core	30.6	0.1	0.0	63.5	5.2	0.2	0.0	0.0	0.0	1.8	101.4	13	87	0.3
MFT-60 - 2	bigger grain - Rim	30.9	0.1	0.0	63.7	4.9	0.2	0.0	0.0	0.0	1.9	101.7	12	88	0.4
MFT-62 - 1	bigger grain - Core	30.3	0.1	0.0	63.8	5.1	0.2	0.0	0.0	0.0	1.9	101.4	12	87	0.3
MFT-62 - 2	bigger grain - Rim	30.1	0.1	0.0	63.2	5.0	0.2	0.0	0.0	0.0	1.9	100.5	12	87	0.3
MFT-67 - 1	bigger grain - Core	30.8	0.1	0.0	63.4	5.3	0.2	0.0	0.0	0.0	1.9	101.7	13	87	0.4

Table A1.13: Trace elements - olivine

Info	Position	Li ⁺	Li ⁺	Na	Mg	Al	Si	P	K	Ca	Sc	Ti	V	Mn	Fe	Rb	Sr	Y	Zr	Nb	Cs	Ba	La	Ce	Pr	Nd	Sm	Eu	Gd	Tb	Dy	Ho
mit-o-2-1	smaller grain - Rim	6.0	16.1	2.9	26198	16.9	40040	41.9	4.8	259	1.3	52.1	0.3	2.12	573895	b.d.l.	0.0	16.4	0.2	0.0	b.d.l.	b.d.l.	0.0	0.3	0.0	0.2	b.d.l.	0.4	0.2	0.7	0.6	
mit-o-2-2	smaller grain - Core	9.4	19.4	25.8	26171	18.4	40040	72.0	13.1	393	0.8	55.5	0.2	2.16	558848	b.d.l.	0.0	5.9	0.3	0.0	b.d.l.	b.d.l.	0.0	0.0	0.1	b.d.l.	0.3	0.1	0.7	0.6		
mit-o-3-2	smaller grain - Core	6.1	7.8	7.6	26441	20.2	40040	71.9	4.0	373	1.2	79.3	0.3	2.02	558872	b.d.l.	0.0	6.2	0.2	0.0	b.d.l.	b.d.l.	0.0	0.0	0.1	b.d.l.	0.3	0.1	0.6	0.6		
mit-o-4-1	smaller grain - Rim	6.3	6.9	7.6	27369	4.1	40040	54.3	5.8	453	0.9	26.7	0.2	1.96	551994	b.d.l.	0.0	6.0	0.2	0.0	b.d.l.	b.d.l.	0.0	0.0	0.1	b.d.l.	0.3	0.1	0.5	0.6		
mit-o-4-2	smaller grain - Core	6.3	6.9	7.6	27516	4.8	40040	55.1	3.7	370	0.9	26.7	0.2	1.98	547635	b.d.l.	0.0	5.9	0.2	0.0	b.d.l.	b.d.l.	0.0	0.0	0.1	b.d.l.	0.3	0.1	0.5	0.6		
mit-o-8-2	smaller grain - Core	7.2	8.2	11.9	27991	16.9	40040	85.8	1.9	295	1.1	41.8	0.2	1.91	521659	b.d.l.	0.0	5.8	0.2	0.0	b.d.l.	b.d.l.	0.0	0.0	0.1	b.d.l.	0.3	0.1	0.5	0.6		
mit-o-10-1	smaller grain - Rim	6.6	6.2	6.1	27113	34.1	40040	69.6	8.8	148	0.4	92.7	0.3	1.91	509657	0.2	0.1	5.6	0.1	0.0	0.2	0.3	1.0	0.0	0.1	0.0	0.3	0.1	0.7	0.6		
mit-o-10-2	smaller grain - Core	6.7	6.7	5.9	27619	2.8	40040	78.7	7.8	497	1.1	74.3	0.3	2.15	508373	b.d.l.	0.0	8.3	0.2	0.0	0.0	b.d.l.	1.6	4.1	0.5	0.6	0.0	0.9	0.2	0.7	0.6	
mit-o-11-2	smaller grain - Rim	6.5	6.2	13.1	27561	3.0	40040	37.7	4.3	266	0.9	22.2	0.2	2.10	510953	b.d.l.	0.0	5.9	0.2	0.0	b.d.l.	b.d.l.	0.0	0.0	0.1	0.0	0.3	0.1	0.7	0.6		
mit-o-11-3	smaller grain - Rim	6.7	6.3	7.5	27415	5.4	40040	39.2	3.2	351	1.1	42.1	0.3	2.03	505581	b.d.l.	0.0	5.8	0.2	0.0	b.d.l.	b.d.l.	0.0	0.0	0.1	0.0	0.3	0.1	0.5	0.6		
mit-o-12-2	smaller grain - Rim	7.6	7.1	7.3	28051	7.6	40040	39.8	1.7	300	0.6	69.1	0.2	2.32	519567	b.d.l.	0.0	5.5	0.1	0.0	b.d.l.	b.d.l.	0.0	0.0	0.1	0.0	0.3	0.1	0.5	0.6		
mit-o-12-3	smaller grain - Core	6.4	6.2	8.2	27441	9.6	40040	31.3	7.2	200	0.6	71.9	0.3	2.14	508368	0.2	0.0	5.7	0.2	0.1	0.3	0.2	0.0	0.2	0.0	0.1	0.0	0.3	0.1	0.7	0.6	
mit-o-13-1	smaller grain - Rim	7.0	6.9	18.9	27691	3.3	40040	46.8	2.6	306	1.1	108.0	0.3	2.40	522079	b.d.l.	0.0	5.9	0.2	0.0	0.0	b.d.l.	0.0	0.0	0.1	0.0	0.3	0.1	0.7	0.6		
mit-o-13-2	smaller grain - Rim	5.7	5.5	6.1	27079	43.7	40040	45.4	4.1	333	0.6	100.9	0.4	2.17	514440	0.1	0.1	6.7	0.3	0.3	0.1	0.7	0.4	2.4	0.1	0.5	0.2	b.d.l.	0.5	0.2	0.6	
mit-o-18-1	smaller grain - Rim	6.4	5.5	8.3	26361	3.1	40040	31.5	2.6	393	1.1	15.9	0.3	2.05	511567	b.d.l.	0.0	5.6	0.2	0.0	b.d.l.	b.d.l.	0.0	0.0	0.1	0.0	0.3	0.1	0.7	0.6		
mit-o-18-2	smaller grain - Core	8.7	8.9	12.7	26364	3.1	40040	85.1	8.8	381	1.6	204.6	0.3	2.19	521008	b.d.l.	0.0	6.1	0.2	0.0	b.d.l.	0.6	0.2	0.5	0.1	0.3	0.1	0.0	0.4	0.2	0.7	
mit-o-19-1	smaller grain - Rim	4.2	3.9	4.7	26814	4.8	40040	35.8	4.3	384	0.8	28.8	0.3	1.68	529433	b.d.l.	0.0	6.1	0.2	0.0	b.d.l.	0.0	0.0	0.0	0.1	0.0	0.3	0.1	0.7	0.6		
mit-o-20-2	smaller grain - Core	7.5	8.1	11.7	27196	2.1	40040	70.5	3.2	291	0.7	69.6	0.3	2.16	529433	b.d.l.	0.0	6.3	0.2	0.0	b.d.l.	0.0	0.0	0.0	0.1	0.0	0.3	0.1	0.7	0.6		
mit-o-20-4	smaller grain - Rim	9.3	8.4	21.0	27267	20.0	40040	66.9	3.5	305	0.7	44.2	0.4	2.19	527908	b.d.l.	0.2	6.3	0.2	0.0	b.d.l.	0.6	0.2	0.6	0.1	0.3	0.2	0.2	0.7	0.6		
mit-o-23-3	smaller grain - Rim	7.7	6.8	23.0	26981	4.8	40040	52.5	2.5	273	0.9	21.5	0.3	2.05	535998	b.d.l.	0.0	5.8	0.2	0.0	b.d.l.	0.1	0.1	0.1	0.0	0.2	0.1	0.0	0.4	0.1	0.6	
mit-o-24-3	smaller grain - Rim	5.9	5.6	9.2	26788	1.1	40040	29.5	3.6	246	1.0	109.7	0.2	2.14	545262	b.d.l.	0.0	5.9	0.1	0.0	b.d.l.	b.d.l.	0.0	0.0	0.1	0.0	0.3	0.1	0.7	0.6		
mit-o-27-1	smaller grain - Rim	6.2	6.0	3.6	26753	8.5	40040	41.7	7.7	309	0.6	91.5	0.3	2.01	519893	b.d.l.	0.0	5.3	0.2	0.0	b.d.l.	b.d.l.	0.0	0.0	0.1	0.0	0.3	0.1	0.7	0.6		
mit-o-27-2	smaller grain - Rim	6.6	5.8	5.2	26912	44.6	40040	49.1	10.7	120	0.6	93.7	0.5	2.38	522818	0.1	0.2	6.7	0.3	0.1	0.0	2.6	4.6	0.2	0.6	0.2	b.d.l.	0.5	0.2	0.9	0.6	
mit-o-30-1	smaller grain - Rim	8.1	6.7	11.6	26174	27.1	40040	48.1	3.8	242	0.7	93.5	0.3	2.44	518327	0.2	0.1	5.7	0.2	0.1	0.2	0.4	1.2	0.0	0.2	0.1	0.0	0.4	0.1	0.7	0.6	
mit-o-31-1	smaller grain - Rim	7.6	7.0	9.0	27192	48.7	40040	47.8	5.6	360	0.5	94.6	0.3	2.09	503423	b.d.l.	0.0	5.7	0.1	0.0	b.d.l.	0.0	0.0	0.0	0.1	0.0	0.3	0.1	0.7	0.6		
mit-o-31-3	smaller grain - Rim	8.4	6.3	2.2	27062	3.0	40040	36.8	3.0	226	1.4	10.5	0.3	2.19	497783	b.d.l.	0.0	6.6	0.2	0.0	b.d.l.	0.2	0.2	0.6	0.1	0.3	0.1	0.0	0.4	0.1	0.6	
mit-o-36-2	smaller grain - Core	7.0	6.8	11.0	27696	25.9	40040	52.0	3.4	185	0.4	28.1	0.4	2.17	462547	b.d.l.	0.0	6.8	0.2	0.0	b.d.l.	0.8	0.4	2.7	0.1	0.5	0.2	0.4	0.2	0.8		
mit-o-36-3	smaller grain - Rim	9.9	9.0	11.9	27686	15.9	40040	43.9	2.4	200	0.9	27.3	0.2	2.25	462403	b.d.l.	0.0	6.0	0.2	0.0	b.d.l.	0.0	0.0	0.0	0.1	0.1	0.1	0.1	0.1	0.1	0.1	
mit-o-38-1	smaller grain - Rim	6.7	6.7	9.9	28526	4.2	40040	49.8	b.d.l.	374	1.1	22.6	0.3	2.19	458114	b.d.l.	0.1	23.0	0.2	0.0	b.d.l.	b.d.l.	0.0	0.0	0.1	0.1	0.1	0.1	0.1	0.1	0.1	
mit-o-38-2	smaller grain - Core	6.3	6.4	11.1	28331	3.7	40040	97.2	b.d.l.	521	1.1	106.3	0.2	2.16	457695	b.d.l.	0.1	23.0	0.2	0.0	b.d.l.	b.d.l.	6.6	15.9	2.2	9.6	2.3	0.0	2.7	0.4	3.4	
mit-o-40-1	smaller grain - Rim	6.0	5.9	3.5	28370	16.9	40040	35.7	b.d.l.	282	0.9	30.2	0.3	2.23	453223	b.d.l.	0.0	5.9	0.2	0.0	b.d.l.	b.d.l.	0.0	0.0	0.1	0.1	0.1	0.1	0.1	0.1	0.1	
mit-o-40-2	smaller grain - Core	6.0	5.9	3.5	28421	39.8	40040	73.4	7.4	247	0.8	27.2	0.4	2.10	448820	0.1	0.2	5.9	0.2	0.0	0.1	0.9	1.4	0.0	0.2	0.1	0.1	0.1	0.1	0.1	0.1	
MP-17-1	bigger grain - Core	5.9	5.8	12.3	28950	9.8	40040	26.2	b.d.l.	1296	1.1	97.0	0.1	2.18	480648	b.d.l.	0.1	7.3	0.2	0.0	b.d.l.	b.d.l.	0.0	0.0	0.1	0.1	0.1	0.1	0.1	0.1	0.1	

Table A1.13: continued

Pr	Tm	Yb	Lu	Hf	Ta	Pb	Th	U
3.1	0.7	6.9	4.0	0.0	b.d.l.	1.7	0.0	0.0
3.0	0.7	6.7	4.0	0.0	b.d.l.	b.d.l.	0.0	b.d.l.
3.0	0.7	6.9	4.0	0.0	b.d.l.	b.d.l.	0.0	b.d.l.
2.9	0.7	6.9	4.0	0.0	b.d.l.	0.4	b.d.l.	0.0
2.9	0.7	6.9	4.0	0.0	b.d.l.	b.d.l.	0.0	0.0
3.0	0.7	6.4	4.0	0.0	b.d.l.	b.d.l.	0.0	0.0
3.3	0.7	6.8	3.0	0.0	b.d.l.	2.7	0.0	0.0
3.3	0.7	7.4	4.0	0.0	b.d.l.	0.5	0.1	0.0
2.9	0.7	6.7	4.0	0.0	b.d.l.	b.d.l.	0.0	0.0
3.0	0.7	6.8	4.0	0.0	b.d.l.	b.d.l.	0.0	0.0
2.8	0.7	6.6	3.0	0.0	b.d.l.	0.1	b.d.l.	0.0
2.8	0.7	6.8	4.0	0.0	b.d.l.	4.7	0.0	b.d.l.
3.1	0.7	6.8	4.0	0.0	0.0	12.0	0.0	0.0
3.0	0.7	6.7	4.0	0.0	b.d.l.	0.9	b.d.l.	0.0
2.9	0.7	6.7	4.0	0.0	b.d.l.	0.9	b.d.l.	0.0
3.0	0.7	6.9	4.0	0.0	b.d.l.	b.d.l.	0.0	0.0
3.1	0.7	6.9	4.0	0.0	b.d.l.	2.5	0.0	0.0
2.9	0.7	6.6	3.0	0.0	b.d.l.	0.8	0.0	b.d.l.
2.9	0.7	6.7	4.0	0.0	b.d.l.	b.d.l.	0.0	b.d.l.
2.9	0.7	6.5	3.0	0.0	b.d.l.	0.1	b.d.l.	b.d.l.
3.1	0.7	6.7	3.0	0.0	b.d.l.	8		

Table A1.13: continued

Info	Position	Li ⁺	Na	Mg	Al	Si	P	K	Ca	Sc	Ti	V	Mn	Fe	Rb	Sr	Y	Zr	Nb	Cs	Ba	La	Ce	Pr	Nd	Sm	Eu	Gd	Tb	Dy	Ho
MF-33-1	bigger grain - Core	8.6	7.6	1.3	27524	0.9	40240	4.7	33.0	1.7	108.2	0.3	2499	46903.7	b.d.	b.d.	7.3	0.2	0.0	b.d.	b.d.	0.0	0.0	0.0	0.0	0.1	b.d.	0.3	0.2	9	0.6
MF-33-2	bigger grain - Rim	7.5	6.9	3.4	27085	6.3	40240	25.0	33.4	1.5	70.7	0.2	2419	46870.9	b.d.	b.d.	7.2	0.2	0.0	b.d.	b.d.	0.0	0.0	0.0	0.1	0.1	b.d.	0.3	0.1	8	0.9
MF-33-3	bigger grain - Core	5.9	6.4	1.7	28907	3.9	40240	3.9	37.4	2.9	140.9	0.2	2481	46785.7	b.d.	b.d.	7.8	0.2	0.0	b.d.	b.d.	0.0	0.0	0.0	0.1	0.1	b.d.	0.4	0.2	9	0.6
MF-33-4	bigger grain - Core	6.8	6.8	10.9	27772	3.1	40240	33.9	31.6	2.7	205.3	0.2	2481	46458.1	b.d.	b.d.	7.8	0.2	0.0	b.d.	b.d.	0.0	0.0	0.0	0.1	0.1	b.d.	0.4	0.2	8	0.9
MF-33-5	bigger grain - Core	8.1	6.8	0.1	28449	10.7	40240	3.9	36.1	20.8	7	94.3	0.3	2519	46406.5	b.d.	b.d.	7.2	0.1	0.0	b.d.	b.d.	0.0	0.0	0.1	0.1	b.d.	0.4	0.2	8	0.7
MF-33-6	bigger grain - Core	7.0	6.3	1.1	29333	1.7	40240	3.9	38.7	1.7	87.8	0.2	2519	46333.2	b.d.	b.d.	7.1	0.1	0.0	b.d.	b.d.	0.0	0.0	0.0	0.1	0.1	b.d.	0.4	0.2	7	0.7
MF-33-7	bigger grain - Core	7.2	6.6	2.0	30774	9.4	40240	25.9	42.3	2.8	91.0	0.1	2904	47403.8	b.d.	b.d.	7.3	0.2	0.1	b.d.	b.d.	0.0	0.0	0.0	0.1	0.1	b.d.	0.3	0.2	8	0.6
MF-33-8	bigger grain - Rim	6.4	6.0	10.9	28754	14.4	40240	26.6	40.2	1.8	92.0	0.3	2432	47387.1	b.d.	b.d.	7.2	0.2	0.1	0.0	0.8	0.0	0.7	0.0	0.1	0.0	0.4	0.1	11	0.9	
MF-33-9	bigger grain - Rim	6.3	6.9	1.3	27550	9.6	40240	29.6	34.3	1.5	83.8	0.2	2463	47378.2	b.d.	b.d.	7.5	0.2	0.0	b.d.	b.d.	0.0	0.0	0.0	0.1	0.0	0.4	0.1	11	0.7	
MF-33-10	bigger grain - Core	6.3	6.5	3.7	26985	26.6	40240	26.6	31.8	1.6	90.9	0.2	2463	47378.2	b.d.	b.d.	9.0	0.0	0.0	0.0	0.0	0.6	3.1	0.2	0.7	0.3	0.0	0.6	0.2	11	0.7
MF-33-11	bigger grain - Core	6.3	6.4	7.8	27069	8.4	40240	31.5	42.1	1.1	83.1	0.2	2476	47346.4	b.d.	b.d.	7.3	0.1	0.0	b.d.	b.d.	0.0	0.0	0.0	0.0	0.1	0.0	0.4	0.1	11	0.6
MF-33-12	bigger grain - Core	5.9	6.4	7.4	27848	3.3	40240	3.5	38.1	1.4	34.9	0.3	2476	47346.4	b.d.	b.d.	7.3	0.2	0.0	b.d.	b.d.	0.0	0.0	0.0	0.0	0.1	0.0	0.4	0.1	11	0.6
MF-33-13	bigger grain - Core	7.0	7.4	11.4	27524	7.8	40240	25.8	33.7	1.8	145.0	0.3	2502	47338.5	b.d.	b.d.	7.8	0.2	0.0	b.d.	b.d.	0.0	0.0	0.0	0.1	0.1	b.d.	0.3	0.2	7	0.9
MF-33-14	bigger grain - Core	6.0	5.9	8.9	28774	1.8	40240	3.3	39.1	6	106.3	0.2	2502	47338.5	b.d.	b.d.	7.3	0.2	0.0	b.d.	b.d.	0.0	0.0	0.0	0.1	0.1	b.d.	0.3	0.2	7	0.9
MF-33-15	bigger grain - Core	6.3	6.4	10.3	28146	7.3	40240	34.9	35.9	9	105.9	0.2	2443	47319.2	b.d.	b.d.	7.7	0.2	0.0	b.d.	b.d.	0.0	0.0	0.0	0.1	0.1	b.d.	0.3	0.2	8	0.6
MF-33-16	bigger grain - Core	6.9	6.4	1.1	28283	3.2	40240	24.1	35.9	5	118.7	0.2	2491	47319.2	b.d.	b.d.	7.7	0.2	0.0	b.d.	b.d.	0.0	0.0	0.0	0.1	0.1	b.d.	0.3	0.2	8	0.6
MF-33-17	bigger grain - Core	8.3	7.8	2.8	28901	3.3	40240	61.0	38.3	9	85.9	0.2	2432	47255.2	b.d.	b.d.	7.6	0.2	0.0	b.d.	b.d.	0.0	0.0	0.0	0.1	0.1	b.d.	0.3	0.2	8	0.9
MF-33-18	bigger grain - Rim	7.9	7.5	9.2	26882	19.8	40240	49.2	34.0	3.6	78.3	0.2	2463	47255.2	b.d.	b.d.	8.0	0.2	0.0	b.d.	b.d.	0.0	0.0	0.0	0.1	0.1	b.d.	0.3	0.2	8	0.9
MF-33-19	bigger grain - Rim	6.2	6.4	6.7	27029	3.2	40240	31.5	38.9	1.3	93.7	0.2	2476	47103.3	b.d.	b.d.	7.3	0.2	0.0	b.d.	b.d.	0.0	0.0	0.0	0.1	0.1	b.d.	0.3	0.1	7	0.6
MF-33-20	bigger grain - Rim	6.9	6.8	8.8	27501	16.0	40240	29.2	39.8	1.3	93.7	0.2	2476	47103.3	b.d.	b.d.	7.3	0.2	0.0	b.d.	b.d.	0.0	0.0	0.0	0.1	0.1	b.d.	0.3	0.1	7	0.6
MF-33-21	bigger grain - Rim	6.2	6.8	9.2	28191	6.6	40240	29.2	39.8	1.3	93.7	0.2	2476	47103.3	b.d.	b.d.	7.3	0.2	0.0	b.d.	b.d.	0.0	0.0	0.0	0.1	0.1	b.d.	0.3	0.1	7	0.6
MF-33-22	bigger grain - Core	6.2	6.8	9.2	28191	6.6	40240	29.2	39.8	1.3	93.7	0.2	2476	47103.3	b.d.	b.d.	7.3	0.2	0.0	b.d.	b.d.	0.0	0.0	0.0	0.1	0.1	b.d.	0.3	0.1	7	0.6
MF-33-23	bigger grain - Core	6.2	6.8	9.2	28191	6.6	40240	29.2	39.8	1.3	93.7	0.2	2476	47103.3	b.d.	b.d.	7.3	0.2	0.0	b.d.	b.d.	0.0	0.0	0.0	0.1	0.1	b.d.	0.3	0.1	7	0.6
MF-33-24	bigger grain - Core	6.2	6.8	9.2	28191	6.6	40240	29.2	39.8	1.3	93.7	0.2	2476	47103.3	b.d.	b.d.	7.3	0.2	0.0	b.d.	b.d.	0.0	0.0	0.0	0.1	0.1	b.d.	0.3	0.1	7	0.6
MF-33-25	bigger grain - Core	6.2	6.8	9.2	28191	6.6	40240	29.2	39.8	1.3	93.7	0.2	2476	47103.3	b.d.	b.d.	7.3	0.2	0.0	b.d.	b.d.	0.0	0.0	0.0	0.1	0.1	b.d.	0.3	0.1	7	0.6
MF-33-26	bigger grain - Core	6.2	6.8	9.2	28191	6.6	40240	29.2	39.8	1.3	93.7	0.2	2476	47103.3	b.d.	b.d.	7.3	0.2	0.0	b.d.	b.d.	0.0	0.0	0.0	0.1	0.1	b.d.	0.3	0.1	7	0.6
MF-33-27	bigger grain - Core	6.2	6.8	9.2	28191	6.6	40240	29.2	39.8	1.3	93.7	0.2	2476	47103.3	b.d.	b.d.	7.3	0.2	0.0	b.d.	b.d.	0.0	0.0	0.0	0.1	0.1	b.d.	0.3	0.1	7	0.6
MF-33-28	bigger grain - Core	6.2	6.8	9.2	28191	6.6	40240	29.2	39.8	1.3	93.7	0.2	2476	47103.3	b.d.	b.d.	7.3	0.2	0.0	b.d.	b.d.	0.0	0.0	0.0	0.1	0.1	b.d.	0.3	0.1	7	0.6
MF-33-29	bigger grain - Core	6.2	6.8	9.2	28191	6.6	40240	29.2	39.8	1.3	93.7	0.2	2476	47103.3	b.d.	b.d.	7.3	0.2	0.0	b.d.	b.d.	0.0	0.0	0.0	0.1	0.1	b.d.	0.3	0.1	7	0.6
MF-33-30	bigger grain - Rim	8.3	7.8	2.8	28901	3.3	40240	61.0	38.3	9	85.9	0.2	2432	47255.2	b.d.	b.d.	7.6	0.2	0.0	b.d.	b.d.	0.0	0.0	0.0	0.1	0.1	b.d.	0.3	0.2	8	0.9

Table A1.13: continued

	Fr	Tm	Yb	Lu	Hf
33	0.8	7.3	5	b.d.l.	
33	0.7	7.3	5	b.d.l.	
33	0.8	7.9	6	0.0	
33	0.8	7.9	6	b.d.l.	
33	0.7	7.3	6	0.0	
33	0.7	7.3	5	b.d.l.	
33	0.8	7.3	5	0.0	
33	0.7	7.4	5	b.d.l.	
33	0.8	7.8	6	0.0	
33	0.9	7.3	5	b.d.l.	
33	0.8	7.3	5	0.0	
33	0.8	7.3	5	b.d.l.	
33	0.9	7.3	5	b.d.l.	
33	0.7	7.3	5	0.0	
33	0.7	7.1	4	b.d.l.	
33	0.7	7.1	3	b.d.l.	
36	0.8	7.6	6	0.0	
36	0.8	7.0	5	b.d.l.	
37	0.9	7.4	5	b.d.l.	
37	0.7	7.3	5	0.0	
37	0.7	7.3	5	0.0	
37	0.6	6.7	3	b.d.l.	
37	0.6	6.0	3	0.0	
37	0.6	5.0	3	0.0	
37	0.6	5.6	3	b.d.l.	
38	0.6	5.0	3	0.0	
37	0.6	5.0	3	b.d.l.	
37	0.6	3.6	1	b.d.l.	
37	0.6	3.9	3	b.d.l.	
38	0.9	6.3	3	b.d.l.	
38	0.7	6.3	3	b.d.l.	
39	0.7	6.3	3	b.d.l.	
37	0.6	5.4	3	0.0	
37	0.6	2.7	3	b.d.l.	
37	0.9	6.0	3	b.d.l.	
37	0.7	2.9	3	0.0	
38	0.6	6.0	3	0.0	
37	0.6	6.0	3	0.0	
39	0.9	3.6	3	b.d.l.	
39	0.7	3.9	3	0.0	
39	0.6	3.8	2	b.d.l.	
37	0.6	3.8	3	0.0	
36	0.6	3.8	3	0.0	
36	0.6	3.8	2	0.0	
2.6	0.6	6.0	1	b.d.l.	

Table A1.13: continued

Info	Position	L _j	L _j	Na	Mg	Al	Si	P	K	Ca	Sc	Ti	V	Mn	Fe	Rb	Sr	Y	Zr	Nb	Cs	Ba	La	Ce	Pr	Nd	Sm	Eu	Gd	Tb	Dy	Ho
MFT-mat-33-31	bigger grain - Rim	17.0	15.9	15.0	21.649	9.0	140240	32.8	b.d.l.	1162	9.5	64.3	0.2	11806	395566	b.d.l.	b.d.l.	14.3	0.2	0.0	b.d.l.	0.8	0.0	0.1	b.d.l.	b.d.l.	b.d.l.	0.4	0.1	1.6	0.5	
MFT-mat-33-32	bigger grain - Rim	15.9	15.9	15.2	21.770	14.0	140240	30.1	b.d.l.	1234	9.6	77.7	0.1	11944	409038	b.d.l.	b.d.l.	14.5	0.1	0.0	b.d.l.	0.4	b.d.l.	0.1	b.d.l.	b.d.l.	0.1	0.0	0.3	0.1	1.3	0.5
MFT-mat-32-2	bigger grain - Rim	17.1	15.7	15.2	21.624	52.9	140240	43.0	9.1	1198	9.8	105.1	0.2	11764	404541	b.d.l.	0.2	14.6	0.2	0.0	0.1	1.3	0.0	0.5	b.d.l.	0.1	b.d.l.	0.3	0.1	1.6	0.5	
MFT-mat-32-3	bigger grain - Rim	14.7	14.5	12.8	21.482	18.0	140240	43.5	b.d.l.	1378	9.6	109.6	0.2	11482	394525	b.d.l.	b.d.l.	14.1	0.2	b.d.l.	b.d.l.	b.d.l.	b.d.l.	0.0	0.0	b.d.l.	0.1	b.d.l.	0.4	0.1	1.5	0.5
MFT-mat-32-4	bigger grain - Rim	15.5	15.5	25.6	22.183	17.3	140240	46.8	14.8	1414	9.8	106.7	0.2	11773	412819	0.2	1.9	14.7	0.2	0.0	0.1	11.4	0.4	0.8	0.1	0.7	0.2	b.d.l.	0.4	0.1	1.5	0.6
MFT-mat-32-5	bigger grain - Core	15.8	15.7	16.0	22.705	13.6	140240	38.4	b.d.l.	968	10.3	104.0	0.2	11816	411845	b.d.l.	b.d.l.	14.7	0.2	b.d.l.	b.d.l.	0.3	0.1	0.0	0.2	0.2	0.0	0.4	0.1	1.4	0.5	
MFT-mat-32-6	bigger grain - Core	15.8	15.4	12.1	21.812	17.0	140240	45.0	b.d.l.	1344	9.8	91.4	0.3	11694	403748	b.d.l.	b.d.l.	14.5	0.2	0.0	b.d.l.	b.d.l.	b.d.l.	0.0	0.0	0.1	0.1	b.d.l.	0.4	0.1	1.3	0.5
MFT-mat-32-8	bigger grain - Core	15.9	15.0	13.0	22.281	17.0	140240	43.1	b.d.l.	1237	9.6	103.9	0.2	11633	398968	b.d.l.	b.d.l.	13.9	0.2	0.0	b.d.l.	b.d.l.	0.0	0.0	0.0	0.1	0.1	b.d.l.	0.3	0.1	1.3	0.5
MFT-mat-32-9	bigger grain - Core	15.2	15.1	14.6	22.315	15.8	140240	48.4	b.d.l.	839	9.3	106.9	0.2	11661	396886	b.d.l.	b.d.l.	14.0	0.2	0.0	b.d.l.	b.d.l.	0.4	1.2	0.1	0.4	0.2	b.d.l.	0.3	0.1	1.5	0.5
MFT-mat-32-10	bigger grain - Core	15.4	15.1	12.7	22.548	14.4	140240	41.8	b.d.l.	1201	9.6	101.1	0.2	11821	404487	b.d.l.	b.d.l.	14.4	0.2	b.d.l.	b.d.l.	b.d.l.	0.0	0.4	0.0	0.2	0.1	b.d.l.	0.2	0.1	1.4	0.5
MFT-mat-32-11	bigger grain - Core	15.9	14.7	14.2	22.071	15.6	140240	41.6	b.d.l.	1361	9.9	90.2	0.2	11466	394627	b.d.l.	b.d.l.	13.9	0.1	0.1	b.d.l.	b.d.l.	0.8	2.7	0.3	1.0	0.3	b.d.l.	0.6	0.2	1.6	0.6
MFT-mat-32-12	bigger grain - Core	17.8	16.0	14.5	22.748	15.0	140240	55.6	b.d.l.	1274	9.8	103.5	0.2	11786	411842	b.d.l.	b.d.l.	14.1	0.2	0.0	b.d.l.	b.d.l.	0.4	1.9	0.2	0.6	0.2	b.d.l.	0.5	0.1	1.5	0.5
MFT-mat-32-13	bigger grain - Core	17.9	16.3	13.3	22.956	16.6	140240	70.6	7.7	1233	9.8	117.9	0.3	12271	418096	b.d.l.	b.d.l.	14.6	0.2	b.d.l.	b.d.l.	b.d.l.	0.2	0.9	0.1	0.4	0.2	b.d.l.	0.3	0.1	1.5	0.5
MFT-mat-32-14	bigger grain - Core	16.7	17.2	16.0	22.374	19.8	140240	84.6	b.d.l.	1066	9.7	114.8	0.2	11696	403080	b.d.l.	b.d.l.	14.6	0.2	0.0	b.d.l.	b.d.l.	0.1	0.3	0.0	0.2	0.1	b.d.l.	0.4	0.1	1.6	0.5
MFT-mat-32-15	bigger grain - Core	16.7	16.0	13.1	22.377	15.2	140240	78.2	b.d.l.	1295	9.4	110.8	0.3	11460	395720	b.d.l.	b.d.l.	14.1	0.1	0.0	b.d.l.	b.d.l.	0.1	0.2	b.d.l.	0.2	0.1	b.d.l.	0.3	0.1	1.7	0.5
MFT-mat-32-19	bigger grain - Core	16.3	17.1	30.7	23.353	30.8	140240	61.0	16.7	1205	9.5	95.9	0.6	11828	408477	0.1	0.5	16.3	0.1	0.0	0.1	1.7	0.9	3.5	0.3	1.2	0.5	b.d.l.	0.7	0.2	1.9	0.7
MFT-mat-32-20	bigger grain - Core	15.8	16.3	16.6	22.718	20.9	140240	65.4	13.2	1266	9.6	103.5	0.3	11531	401818	b.d.l.	b.d.l.	13.5	0.2	0.0	b.d.l.	0.4	0.0	0.4	0.0	0.4	0.1	b.d.l.	0.2	0.1	1.4	0.5
MFT-mat-32-21	bigger grain - Core	17.8	17.7	18.3	22.393	20.6	140240	85.1	6.5	1001	9.6	123.0	0.3	11893	405730	b.d.l.	b.d.l.	14.2	0.2	b.d.l.	b.d.l.	b.d.l.	0.0	0.3	b.d.l.	0.1	0.1	0.0	0.3	0.1	1.5	0.6
MFT-mat-32-22	bigger grain - Core	18.2	17.4	18.6	22.553	21.8	140240	77.1	b.d.l.	1384	9.8	126.8	0.2	11562	405700	0.1	0.1	14.2	0.2	0.0	b.d.l.	0.5	0.1	0.3	0.0	0.2	0.1	b.d.l.	0.2	0.1	1.6	0.5
MFT-mat-32-23	bigger grain - Core	16.8	16.4	15.1	22.433	22.6	140240	54.9	b.d.l.	1045	9.6	122.7	0.3	11622	405825	b.d.l.	0.1	14.0	0.2	0.0	b.d.l.	0.3	0.0	0.1	0.0	b.d.l.	0.2	0.0	0.4	0.1	1.4	0.5
MFT-mat-32-32	bigger grain - Core	15.3	15.5	41.8	22.974	59.5	140240	93.7	04.2	1298	10.0	149.0	0.3	11795	410518	0.3	b.d.l.	14.9	0.4	0.3	b.d.l.	1.0	0.6	2.0	0.2	0.9	0.3	0.0	0.5	0.1	1.7	0.6
MFT-mat-32-42	bigger grain - Core	16.9	15.4	14.4	22.625	22.3	140240	91.6	b.d.l.	1134	9.6	122.6	0.4	11924	412289	b.d.l.	0.1	15.0	0.1	0.1	b.d.l.	0.4	1.0	4.7	0.2	1.2	0.3	b.d.l.	0.6	0.2	1.8	0.6
MFT-mat-32-43	bigger grain - Rim	15.8	14.9	13.6	22.263	19.4	140240	71.9	b.d.l.	1256	9.6	117.9	0.3	11821	409239	b.d.l.	b.d.l.	14.9	0.2	0.1	b.d.l.	0.4	0.2	1.7	0.1	0.4	0.2	b.d.l.	0.3	0.1	1.4	0.5
MFT-mat-32-45	bigger grain - Rim	16.0	15.7	14.3	22.537	42.5	140240	42.5	5.4	1313	10.0	116.8	0.4	12098	415118	0.2	0.2	14.7	0.2	0.0	0.1	0.7	0.2	1.7	0.1	0.2	0.1	b.d.l.	0.5	0.1	1.5	0.6
MFT-mat-32-46	bigger grain - Rim	14.9	15.8	19.3	21.799	24.9	140240	50.7	b.d.l.	1238	10.1	112.9	0.4	11870	409991	b.d.l.	0.2	16.4	0.2	0.0	b.d.l.	1.7	0.6	1.0	0.2	0.8	0.4	b.d.l.	0.7	0.2	1.7	0.6
MFT-mat-1-3	bigger grain - Rim	14.9	14.7	34.3	20.916	28.1	140240	20.4	11.7	1217	9.6	52.2	0.2	11243	387918	b.d.l.	b.d.l.	14.0	0.2	0.1	b.d.l.	0.3	0.1	0.7	0.0	0.1	0.1	b.d.l.	0.4	0.1	1.4	0.5
MFT-mat-1-5	bigger grain - Rim	15.1	14.8	15.3	20.901	13.8	140240	19.7	5.6	1139	9.6	53.1	0.2	11329	391509	b.d.l.	b.d.l.	14.1	0.2	0.1	b.d.l.	b.d.l.	0.0	1.0	0.0	0.1	0.1	b.d.l.	0.2	0.1	1.5	0.5
MFT-mat-1-7	bigger grain - Rim	15.9	14.5	36.9	20.585	20.3	140240	20.0	15.2	1263	10.0	53.5	0.2	11048	385724	0.1	0.2	14.3	0.1	0.1	b.d.l.	0.8	0.1	1.5	0.1	0.3	0.2	b.d.l.	0.4	0.1	1.4	0.5
MFT-mat-1-8	bigger grain - Core	15.4	14.7	12.7	21.378	13.9	140240	15.7	b.d.l.	1147	9.6	51.7	0.2	11512	395494	b.d.l.	b.d.l.	14.2	0.2	0.1	b.d.l.	0.4	0.0	0.5	0.0	0.1	0.1	b.d.l.	0.3	0.1	1.5	0.5
MFT-mat-1-9	bigger grain - Core	14.5	14.0	13.8	20.192	6.5	140240	26.5	b.d.l.	1047	9.0	43.2	0.1	10933	377993	b.d.l.	b.d.l.	13.7	0.1	0.0	b.d.l.	b.d.l.	0.0	0.2	0.0	0.1	0.1	b.d.l.	0.3	0.1	1.3	0.5
MFT-mat-1-10	bigger grain - Core	15.0	14.4	10.4	20.862	8.9	140240	23.6	4.9	1115	9.5	44.9	0.1	11353	394885	b.d.l.	0.1	14.1	0.1	0.0	b.d.l.	b.d.l.	0.0	0.1	0.0	0.1	0.1	0.0	0.3	0.1	1.4	0.5
MFT-mat-1-11	bigger grain - Core	15.3	14.5	16.2	20.877	8.7	140240	21.8	b.d.l.	1223	9.7	49.6	0.2	11242	388841	b.d.l.	b.d.l.	14.3	0.1	b.d.l.	b.d.l.	b.d.l.	0.1	0.0	0.1	0.1	b.d.l.	0.3	0.1	1.4	0.5	
MFT-mat-1-12	bigger grain - Core	15.9	14.8	10.2	20.967	7.7	140240	18.6	b.d.l.	1068	9.7	53.4	0.2	11427	393398	b.d.l.	b.d.l.	14.5	0.1	0.0	b.d.l.	b.d.l.	b.d.l.	0.0	0.0	0.0	0.1	b.d.l.	0.4	0.1	1.5	0.5
MFT-mat-1-13	bigger grain - Core	15.6	14.5	10.9	21.165	8.0	140240	17.2	b.d.l.	1283	9.7	58.1	0.2	11435	395599	b.d.l.	b.d.l.	14.5	0.1	0.0	b.d.l.	b.d.l.	0.0	0.0	0.1	0.1	b.d.l.	0.4	0.1	1.5	0.5	
MFT-mat-1-14	bigger grain - Core	15.3	15.6	12.4	21.075	4.1	140240	28.2	b.d.l.	1149	9.4	55.9	0.2	11574	393494	b.d.l.	b.d.l.	14.5	0.1	0.0	b.d.l.	b.d.l.	b.d.l.	0.0	0.0	0.1	0.0	b.d.l.	0.3	0.1	1.5	0.5
MFT-mat-1-15	bigger grain - Core	15.2	14.6	13.4	20.435	5.6	140240	26.8	b.d.l.	1042	9.2	55.5	0.3	11164	382946	b.d.l.	b.d.l.	13.7	0.2	0.0	b.d.l.	b.d.l.	b.d.l.	0.0	0.0	0.1	0.0	b.d.l.	0.3	0.1	1.4	0.5
MFT-mat-1-16	bigger grain - Core	14.6	15.2	11.5	20.647	8.4	140240	40.2	b.d.l.	1394	9.5	53.7	0.2	11258	386821	b.d.l.	b.d.l.	13.9	0.1	b.d.l.	b.d.l.	b.d.l.	0.0	0.0	0.1	0.1	b.d.l.	0.2	0.1	1.4	0.5	
MFT-mat-1-19	bigger grain - Core	14.7	15.1	13.6	21.071	11.6	14024																									

Table A1.13: continued

Er	Tm	Yb	Lu	Hf	Ta	Pb	Th	U
2.8	0.6	5.8	1.2	b.d.l.	0.0	0.1	b.d.l.	0.0
2.7	0.6	5.8	1.2	0.0	b.d.l.	0.0	b.d.l.	b.d.l.
2.7	0.7	6.0	1.2	0.0	b.d.l.	0.2	0.0	b.d.l.
2.5	0.6	6.0	1.2	0.0	b.d.l.	b.d.l.	b.d.l.	b.d.l.
2.7	0.7	5.9	1.2	b.d.l.	0.0	b.d.l.	0.0	0.0
2.7	0.7	6.2	1.2	b.d.l.	b.d.l.	b.d.l.	b.d.l.	b.d.l.
2.6	0.6	5.9	1.2	0.0	b.d.l.	b.d.l.	0.0	b.d.l.
2.6	0.5	6.0	1.2	b.d.l.	b.d.l.	b.d.l.	b.d.l.	0.0
2.8	0.6	5.7	1.2	b.d.l.	b.d.l.	b.d.l.	0.0	b.d.l.
2.7	0.6	6.0	1.2	0.0	b.d.l.	b.d.l.	0.0	b.d.l.
2.7	0.6	5.5	1.2	b.d.l.	b.d.l.	b.d.l.	0.0	0.0
2.7	0.6	6.2	1.2	b.d.l.	b.d.l.	0.0	0.0	0.0
2.9	0.6	6.3	1.2	b.d.l.	b.d.l.	b.d.l.	0.0	0.0
2.6	0.6	6.2	1.2	b.d.l.	b.d.l.	0.0	0.0	b.d.l.
2.7	0.6	6.0	1.2	0.0	0.0	b.d.l.	0.0	b.d.l.
2.9	0.7	6.2	1.3	0.0	b.d.l.	9.6	0.0	0.0
2.7	0.5	5.7	1.2	0.0	b.d.l.	0.4	b.d.l.	b.d.l.
2.6	0.6	5.9	1.1	b.d.l.	b.d.l.	0.2	b.d.l.	b.d.l.
2.7	0.6	5.7	1.2	b.d.l.	b.d.l.	0.2	b.d.l.	b.d.l.
2.7	0.6	5.8	1.2	b.d.l.	b.d.l.	0.1	0.0	0.0
2.9	0.6	5.8	1.2	0.0	0.0	0.1	0.1	0.0
2.8	0.6	6.2	1.2	0.0	b.d.l.	1.1	0.0	0.0
2.8	0.6	6.0	1.2	b.d.l.	b.d.l.	0.4	0.0	0.0
2.9	0.6	6.5	1.3	0.0	b.d.l.	2.5	0.0	b.d.l.
2.9	0.6	6.1	1.2	0.0	b.d.l.	1.4	0.0	0.0
2.4	0.6	6.1	1.2	0.0	b.d.l.	0.7	0.0	b.d.l.
2.5	0.6	6.0	1.2	0.0	b.d.l.	0.4	0.0	0.0
2.8	0.6	5.8	1.2	b.d.l.	b.d.l.	1.9	0.0	b.d.l.
2.6	0.6	5.9	1.2	b.d.l.	b.d.l.	0.5	0.0	0.0
2.5	0.6	5.4	1.1	b.d.l.	b.d.l.	0.1	0.0	b.d.l.
2.8	0.6	5.6	1.2	0.0	b.d.l.	0.1	b.d.l.	b.d.l.
2.7	0.6	5.8	1.2	b.d.l.	b.d.l.	0.0	b.d.l.	b.d.l.
2.6	0.6	6.1	1.2	b.d.l.	b.d.l.	0.0	b.d.l.	0.0
2.7	0.6	5.7	1.2	0.0	b.d.l.	0.0	b.d.l.	b.d.l.
2.6	0.6	5.8	1.2	b.d.l.	b.d.l.	b.d.l.	b.d.l.	0.0
2.3	0.6	5.9	1.2	b.d.l.	b.d.l.	b.d.l.	b.d.l.	b.d.l.
2.7	0.6	5.9	1.2	b.d.l.	b.d.l.	b.d.l.	b.d.l.	b.d.l.
2.6	0.6	5.7	1.2	0.0	b.d.l.	1.2	0.0	b.d.l.
2.5	0.6	5.7	1.1	0.0	b.d.l.	0.5	b.d.l.	b.d.l.
2.6	0.6	5.8	1.2	b.d.l.	b.d.l.	1.3	0.0	b.d.l.
2.7	0.6	6.0	1.2	0.0	b.d.l.	0.6	0.0	b.d.l.
2.7	0.6	6.1	1.3	b.d.l.	b.d.l.	3.5	b.d.l.	0.0
2.8	0.6	6.0	1.2	b.d.l.	b.d.l.	0.5	0.0	0.0
2.6	0.6	5.6	1.2	b.d.l.	b.d.l.	2.3	0.0	0.0
2.6	0.7	5.7	1.2	0.0	b.d.l.	2.5	0.0	0.0
2.6	0.6	6.0	1.2	0.0	b.d.l.	1.1	0.0	b.d.l.

Table A1.14: Trace elements - melt inclusions

Info	Li ⁺	Li ⁺	Na	Mg	Al	Si	P	K	Ca	Sc	Ti	V	Mn	Fe	Rb	Sr	Y	Zr	Nb	Cs	Ba	La	Ce	Pr	Nd	Sm	Eu	Gd	Tb	Dy	Ho	Er	Tm	Yb
180207-a05.x	325	363	30262	255	82100	327194	78.4	57889	4680	4.3	1291	1.4	273	11465	282	11.2	33.2	196	43.1	3.4	154	88	185	17.2	60.4	11.0	0.3	8.4	3.3	9.3	2.0	5.4	0.7	4.7
180207-a06.x	401	349	23879	307	84121	327196	81.7	59244	6619	3.9	928	b.d.l.	286	12191	302	4.7	64.7	178	53.1	5.3	52	80	159	16.6	53.9	1.1	0.4	10.5	1.7	12.3	2.3	7.6	0.9	6.9
180207-a07.x	191	182	35225	248	79642	327227	52.2	57707	4405	3.2	1118	0.7	257	10587	296	6.4	55.2	187	47.6	5.2	83	85	180	16.9	56.2	1.1	0.3	10.2	1.6	9.8	2.0	6.1	0.9	5.6
180207-a08.x	230	129	35245	294	79241	327225	54.9	58480	3996	2.6	979	0.5	254	11000	307	5.7	53.7	178	47.4	5.7	63	79	172	16.1	52.9	0.3	0.3	9.8	1.5	9.9	2.0	6.3	0.9	5.7
180207-a09.x	130	129	33045	240	83270	327240	53.1	54329	4226	b.d.l.	743	0.4	257	1374	286	2.1	33.9	150	53.7	5.4	13	62	128	2.4	41.9	8.5	0.2	8.6	4	9.7	1.9	6.8	0.9	6.1
180207-a10.x	124	109	32987	230	81091	327252	34.6	57082	4196	2.8	877	0.1	281	1918	306	2.4	66.8	166	53.1	6.6	17	75	154	5.0	50.1	10.8	0.2	10.4	8	11.7	2.4	7.6	1.1	7.2
180207-a104.x	366	340	30348	274	81975	327206	74.3	60238	4902	4.2	762	0.3	335	13593	319	4.7	70.3	188	57.7	5.7	39	89	190	18.0	61.9	12.4	0.3	11.3	1.9	12.4	2.5	7.8	1.2	8.3
180207-a016.x	264	251	34147	246	84817	327222	57.7	53263	4902	3.8	947	0.2	294	11991	283	7.5	79.7	225	61.7	5.4	108	103	205	20.1	69.7	3.7	0.4	3.5	2.1	14.3	2.9	8.7	1.3	8.7
180207-a017.x	277	276	31542	291	84687	327220	44.2	53557	4903	3.1	947	0.2	306	12538	272	12.0	80.7	272	63.7	4.2	206	121	232	22.4	84.0	5.9	0.5	4.4	2.3	15.2	2.9	8.9	1.2	8.7
180207-a018.x	353	320	30492	265	86290	327213	b.d.l.	55611	4800	3.3	1064	0.2	292	1336	275	14.1	80.9	282	61.5	4.6	263	131	248	24.6	86.8	16.2	0.6	4.9	2.3	15.4	3.1	9.3	1.2	8.8
180207-a019.x	64	70	33660	250	84137	327232	b.d.l.	55325	5801	3.3	188	0.2	287	10923	340	2.3	83.4	157	59.9	6.5	19	84	159	16.4	56.7	1.0	0.1	2.2	2.0	14.0	3.1	9.5	1.2	8.8
180207-a020.x	304	297	34040	295	84802	327200	45.4	50947	5246	3.4	984	0.4	347	14680	226	22.4	79.5	266	64.7	3.6	435	157	268	26.5	95.2	7.3	1.1	4.5	2.3	15.2	3.0	8.8	1.3	8.3
180207-a021.x	139	137	32845	278	83826	327227	45.7	55304	4432	0.5	939	0.1	305	3201	322	4.0	70.8	163	54.9	6.4	38	79	163	15.9	53.2	1.2	0.2	10.5	1.7	12.4	2.5	8.2	1.2	7.8
180207-a022.x	83	70	34260	276	88437	327206	150.3	58540	5107	1.5	744	b.d.l.	378	8899	349	2.1	16.9	164	61.2	7.2	11	74	168	16.7	55.7	1.8	0.2	1.5	2.0	13.3	2.7	7.3	1.1	7.4
180207-a023.x	325	295	34664	214	83666	327222	43.8	57985	5082	2.9	1273	0.6	294	12666	308	6.2	56.0	179	47.4	6.3	57	93	177	17.5	57.4	1.0	0.3	9.2	3.5	10.0	1.9	6.1	0.8	5.5
180207-a024.x	269	255	33033	236	82036	327195	35.6	58824	4910	3.5	853	0.2	292	14067	332	5.0	62.4	189	59.0	5.9	36	87	193	17.8	58.8	1.1	0.3	10.4	1.6	10.8	2.2	6.7	1.0	6.0
180207-a025.x	437	397	34330	236	80802	327242	18.9	57507	5788	3.3	1273	0.6	283	12215	322	6.3	84.7	180	52.5	6.1	47	76	179	16.5	55.9	10.1	0.3	9.6	1.4	9.5	2.0	5.8	0.7	4.8
180207-a027.x	252	246	30972	231	80217	327220	49.2	62048	4435	3.3	1224	1.0	302	13845	336	9.6	36.3	193	49.0	5.1	169	97	204	19.4	65.1	1.9	0.4	10.0	1.5	10.2	2.0	6.0	0.8	5.5
180207-a028.x	235	231	35615	176	78142	327223	50.9	59664	4510	4.5	1436	1.5	304	13964	308	13.3	52.4	204	48.3	5.1	236	94	201	19.2	63.5	1.6	0.5	9.0	1.4	9.1	1.8	5.1	0.8	4.6
180207-a029.x	298	287	32672	295	84518	327221	32.2	57163	4587	2.7	1011	b.d.l.	253	10428	330	2.9	67.8	169	57.6	6.3	18	162	161	16.1	53.5	0.5	0.3	10.4	1.7	11.1	2.5	7.6	1.0	7.1
180207-a031.x	105	101	36581	246	80192	327240	47.9	57485	4381	2.7	778	b.d.l.	306	12860	363	1.7	70.1	152	61.6	7.0	10	64	140	13.5	45.5	0.0	0.2	9.8	1.7	10.7	2.4	7.2	1.1	7.3
180207-a032.x	140	131	35809	288	80320	327211	34.0	54346	5004	2.4	734	0.2	362	15761	333	1.2	80.2	145	64.7	8.0	4	65	137	3.4	42.8	0.1	0.1	10.5	1.9	12.6	2.8	8.4	1.4	8.5
180207-a033.x	73	73	31866	238	80954	327244	36.9	59438	5141	3.0	897	0.2	337	13862	335	9.8	69.5	234	70.1	5.4	167	95	195	19.0	64.9	2.8	0.5	1.4	1.8	11.8	2.4	7.3	1.0	7.0
180207-a038.x	307	325	25001	214	90053	327214	41.2	55001	4911	4.2	1349	0.3	279	11789	309	0.3	61.5	201	50.2	5.9	60	86	181	17.0	58.0	2.0	0.4	10.0	1.6	10.0	2.2	5.8	0.9	6.6
180207-a039.x	307	325	25001	214	90053	327214	41.2	55472	4625	b.d.l.	1019	0.6	284	11935	286	6.8	65.4	209	46.4	5.0	65	91	170	17.9	62.7	2.4	0.2	10.1	1.8	11.6	2.4	7.2	0.9	5.6
180207-a041.x	301	277	35939	202	83338	327216	37.5	50730	5530	2.7	1069	0.1	350	13682	232	20.4	86.0	311	68.8	4.1	339	132	261	26.8	94.2	19.1	1.1	16.1	2.6	15.6	3.2	9.5	1.4	9.3
180207-a042.x	318	317	32740	218	83486	327223	42.6	53528	5800	3.1	1150	0.3	344	13761	239	21.0	82.0	297	63.9	3.7	422	130	253	25.9	89.1	17.3	1.1	16.4	2.3	15.0	3.1	8.5	1.2	8.2
180207-a043.x	305	311	34100	237	82390	327229	26.1	55470	5566	3.4	1234	0.4	309	12303	254	18.1	83.3	302	64.0	3.9	370	136	271	26.6	92.4	20.9	1.1	15.6	2.4	15.1	3.0	9.7	1.3	8.6

Table A1.14: continued

Lu	Hf	Ta	Pb	Th	U
0.8	7.0	3.8	43.6	39.9	8.3
0.8	8.1	4.3	52.8	40.6	10.1
0.8	7.4	3.7	44.5	37.8	9.0
0.8	7.3	3.4	46.7	39.0	9.2
0.9	7.5	4.6	50.5	41.7	10.0
1.0	7.3	4.3	48.8	42.8	11.0
1.0	8.9	4.6	47.0	40.7	10.6
1.2	10.1	5.1	44.4	42.2	9.8
1.3	10.2	4.4	41.1	39.8	8.3
1.2	11.1	4.4	40.9	39.9	8.3
1.2	10.5	4.7	36.5	42.4	8.6
1.0	6.9	4.5	47.3	46.0	10.1
1.0	7.7	4.8	53.2	44.7	11.0
0.8	6.6	3.7	41.6	39.3	10.1
0.9	7.4	4.2	46.5	36.6	10.2
0.8	6.3	3.7	41.1	37.4	10.7
0.8	6.6	3.4	43.4	37.7	9.1
0.7	6.4	3.2	43.2	36.3	8.8
1.1	7.1	4.5	44.4	44.0	10.6
1.0	6.8	4.3	49.2	40.8	11.5
1.1	6.5	5.4	50.4	47.5	13.0
0.9	8.8	3.9	45.8	45.3	9.0
1.0	8.6	4.6	49.0	53.8	9.0
0.9	5.7	4.2	44.8	41.0	9.2
0.9	7.3	3.8	40.1	43.5	8.7
1.2	11.8	4.6	39.3	38.9	8.5
1.1	10.5	4.3	42.1	37.4	7.5
1.2	10.6	4.4	42.8	37.6	7.8

Table A1.15: Lithium isotopes

Sample			Li (ppm)	Li (ppm)	d ⁷ Li	2SD
			ICPMS	MC-ICP-MS		
MFT Bulk 1			36.6	39.0	4.28	0.15
MFT Bulk 2			39.3	37.3	3.94	0.29
MFT Olivine 1			32.2	30.6	3.05	0.41
MFT Olivine 2			25.4	24.1	3.10	0.19
MFT Groundmass Glass1			29.3	32.8	6.92	0.57
MFT Groundmass Glass2			26.2	27.2	6.48	0.42
MFT Groundmass Glass3			26.8	26.5	7.31	0.27
MFT Groundmass Glass4			27.9	27.3	7.46	0.47
MFT Quartz 1			24.2	17.1	7.24	0.19
MFT Quartz 2			25.9	18.8	6.69	0.34
MFT Plagioclase 1			13.4	12.9	-1.39	0.36
MFT Plagioclase 2			15.5	13.4	-2.31	0.54
MFT Orthopyroxene 1			12.2	11.9	-2.10	0.41
MFT Orthopyroxene 2			13.1	13.7	-1.95	0.33
MFT Clinopyroxene 1			12.6	13.7	-0.11	0.16
MFT Clinopyroxene 2			11.0	11.1	1.02	0.22
MFT Sanidine 1			5.42	4.16	-0.11	0.18
MFT Sanidine 2			5.47	4.74	-0.58	0.37
Reference rocks						
BHVO-2	basalt	USGS		4.4	4.59	0.28
BCR-2	basalt	USGS		9.4	2.94	0.07
JG-2	granite	GSJ		40.7	0.46	0.26
JR-2	rhyolite	GSJ		69.5	3.88	0.45
JB-2	basalt	GSJ		8.11	4.83	0.07
UB-N	serpentine	CNRS-CRPG		24.5	-2.72	0.27

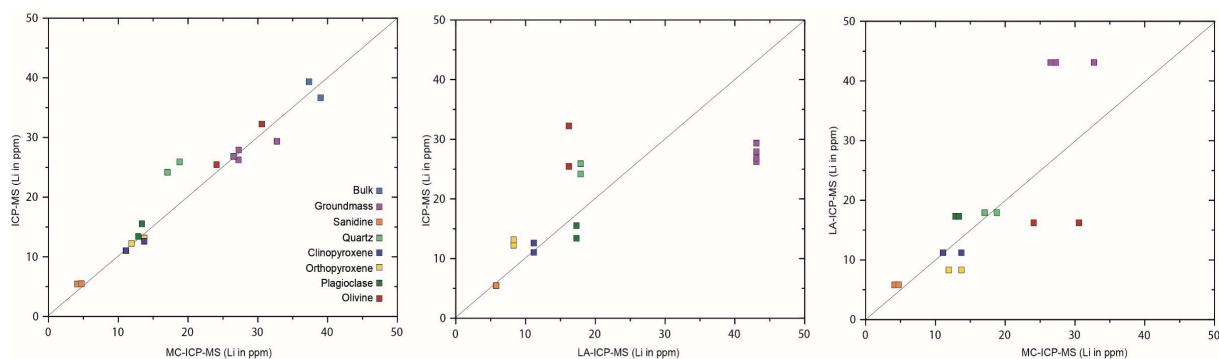


Fig. A1. Trace elements and lithium isotopes

Table A1.16: continued

	MFT Groundmass Glass1	MFT Groundmass Glass2	MFT Groundmass Glass3	MFT Groundmass Glass4	Mean value Groundmass Glass
Li	29.3	26.2	26.8	27.9	43.1
Sc	3.1	2.1	2.2	2.8	2.8
V	23.1	24.4	34.0	33.5	0.5
Cr	5.1	4.7	6.5	7.0	
Co	4.0	3.2	2.5	2.2	
Ni	6.2	3.4	2.9	3.1	
Cu	8.0	6.5	5.7	5.5	
Zn	98.5	69.4	103	105	
Ga	29.2	28.7	29.9	25.4	
Rb	164	143	145	151	253.3
Sr	43.8	64.5	62.6	34.5	14.6
Y	88.2	68.6	78.6	93.1	75.7
Nb	61.3	43.6	41.9	46.4	58.3
Zr	165	134	145	150	176.5
Cd	0.7	0.6	0.7	0.7	
Cs	6.0	5.0	6.0	7.0	6.9
Ba	298	404	311	284	133.5
La	152	87.7	73.3	99.4	81.4
Ce	305	174	140	186	151.1
Pr	29.4	16.5	12.4	17.3	16.7
Nd	101	56.9	54.9	61.1	58.8
Sm	19.5	12.0	10.9	14.5	12.3
Eu	1.1	1.6	1.5	0.9	0.4
Gd	19.6	12.5	11.7	14.9	11.3
Tb	2.7	1.9	1.9	2.4	2.0
Dy	15.4	11.1	11.7	14.4	12.6
Ho	3.2	2.4	2.5	3.0	2.6
Er	9.0	6.9	7.3	8.7	7.6
Tm	1.2	0.9	1.0	1.2	1.1
Yb	7.7	5.9	6.8	8.2	7.4
Lu	1.3	1.0	1.0	1.2	1.0
Hf	6.8	5.4	5.9	6.0	6.9
Ta	4.2	3.1	2.9	3.1	4.0
W	2.4	1.9			
Tl	2.8	2.4	2.9	3.1	
Pb	36.3	33.8	33.3	35.7	40.7
Th	43.7	27.7	21.4	29.3	31.9
U	6.5	5.2	5.4	5.9	7.4

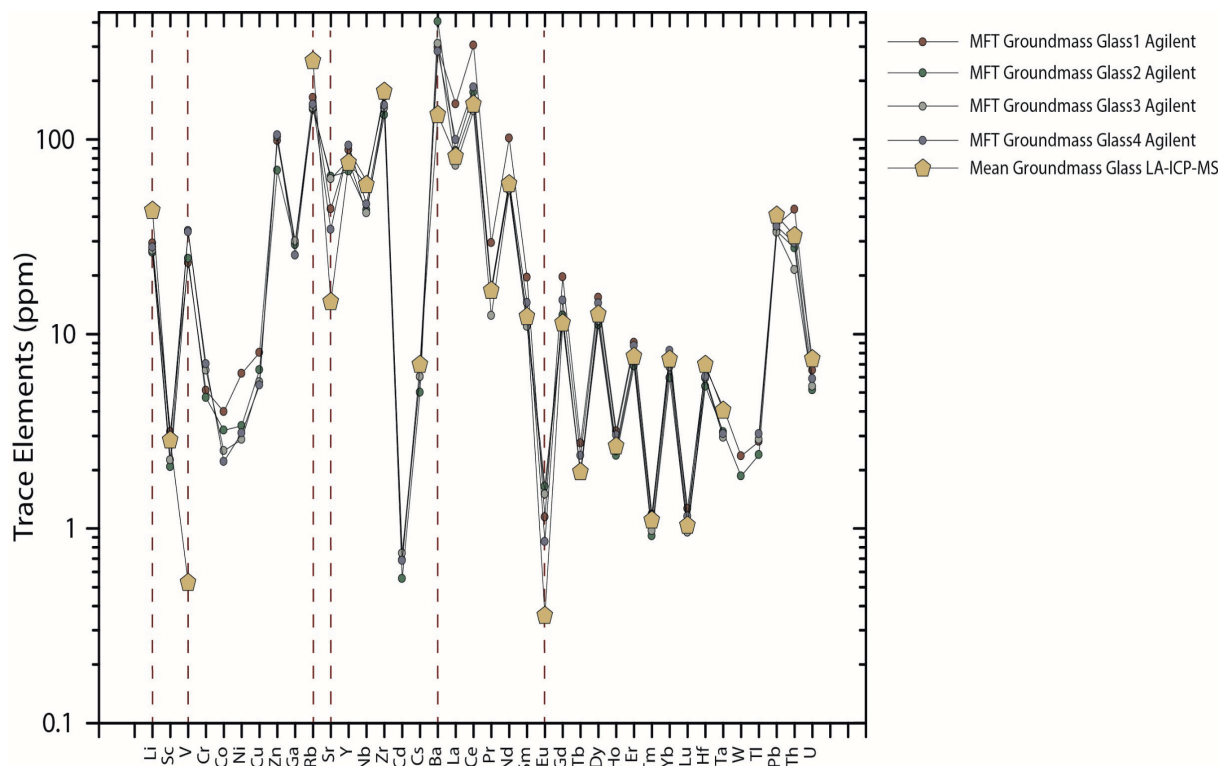


Fig. A2. Trace elements

Table A1.17: LA-ICP-MS standards

Standards for Glass																														
Li ⁶	Li ⁷	Na	Mg	Al	Si	P	K	Ca	Sc	Ti	V	Mn	Fe	Rb	Sr	Y	Zr	Nb	Cs	Ba	La	Ce	Pr	Nd	Sm	Eu	Gd	Tb	Dy	
GSD-G	43.9	42.7	27376	20826	67212	245419	764	29125	47517	46.9	75761	40.5	207.3	98991	38.8	64.6	36.5	37.1	40.4	32.5	63.2	34.8	41.7	39.4	42.9	36.4	43.4	42.2	44.8	
GSD-G	41.8	42.7	27255	21286	68207	245419	783	29265	48614	47.5	71913	40.7	203.6	101263	38.7	63.9	37.0	37.1	39.6	31.9	64.2	35.1	40.8	39.4	42.2	36.1	42.6	42.6	45.4	
GSD-G	43.3	41.2	26549	20320	66986	245419	720	34671	46882	46.6	7442.5	40.5	201.1	101493	37.7	63.4	37.0	37.0	39.2	31.5	63.0	34.5	36.6	40.3	39.0	41.9	36.2	42.6	42.7	45.8
GSD-G	43.1	42.0	26696	21408	67437	245419	695	31082	48643	46.4	7537.5	40.7	202.9	94172	37.2	63.5	36.8	36.8	39.0	31.6	62.6	34.5	36.5	40.4	38.9	42.8	36.4	42.7	42.5	46.4
GSD-G	38.8	42.0	26630	20139	66670	245419	844	28639	47464	47.4	7701.1	39.7	201.3	100286	38.1	62.6	36.8	37.1	38.9	31.7	63.7	36.3	37.6	39.8	38.3	41.8	36.0	42.8	42.0	45.5
GSD-G	45.1	42.1	27144	20972	68970	245419	791	28798	48601	48.9	7757.3	41.4	206.3	112208	38.6	65.6	37.5	38.1	39.9	32.0	63.7	36.3	37.6	41.4	39.3	42.9	37.9	45.3	44.2	47.3
GSD-G	41.9	41.8	26587	20961	68276	245419	788	28685	47705	48.1	7814.7	40.2	202.1	96791	38.1	64.4	37.3	37.8	39.3	31.7	64.2	35.3	37.4	41.2	38.9	43.4	37.1	44.5	43.8	47.0
GSD-G	43.8	41.3	26356	20096	66970	245419	785	29454	46769	47.1	7376.7	40.1	200.8	94963	38.3	62.4	36.8	37.3	39.2	31.6	62.1	34.9	36.9	40.3	39.3	42.2	36.2	43.0	42.6	46.1
GSD-G	43.4	42.6	26699	21301	68631	245419	773	31234	48577	48.5	7681.3	40.4	204.0	97668	37.7	65.3	38.3	38.7	40.3	31.8	65.5	35.9	38.0	41.6	40.5	43.7	37.7	44.9	44.2	46.6
GSD-G	41.5	42.5	26813	20849	68623	245419	749	28692	47518	48.0	7604.7	40.9	200.0	91437	38.3	64.5	37.7	37.5	39.4	31.9	63.9	35.6	37.6	41.2	40.4	44.2	37.4	43.8	43.7	46.7
GSD-G	45.4	42.1	26717	20273	67673	245419	826	29719	47557	47.9	7381.2	40.0	202.1	104377	37.9	65.2	37.8	37.1	39.5	32.5	65.1	35.5	37.0	40.7	39.4	43.2	36.8	43.2	43.3	47.3
Standards for Cpx, Opx, Ol																														
Li ⁶	Li ⁷	Na	Mg	Al	Si	P	K	Ca	Sc	Ti	V	Mn	Fe	Rb	Sr	Y	Zr	Nb	Cs	Ba	La	Ce	Pr	Nd	Sm	Eu	Gd	Tb	Dy	
GSD-G	42.0	42.3	25915	22666	66947	245419	742	27785	47729	46.9	7817.0	40.2	203.1	106909	36.4	64.5	35.9	36.1	41.0	30.9	63.3	35.3	37.6	41.5	38.9	42.6	36.9	42.3	42.1	45.0
GSD-G	41.6	41.4	26112	20803	67575	245419	713	28296	47228	47.0	7506.2	40.1	200.4	105500	37.3	63.4	36.3	36.5	39.1	31.0	63.3	34.4	36.7	40.2	38.5	42.8	36.2	42.3	41.5	44.9
GSD-G	41.8	41.1	26116	20830	67665	245419	770	29078	47337	46.7	7779.4	39.8	199.7	112374	37.2	62.7	36.2	35.7	38.9	30.8	63.2	34.3	36.6	40.0	38.7	41.7	36.1	42.2	42.0	45.0
GSD-G	42.8	41.1	26077	20706	66284	245419	751	28278	46591	45.8	7570.9	39.9	198.4	100205	36.8	62.8	36.1	36.5	39.0	30.7	61.1	34.3	36.7	39.9	38.4	41.8	35.5	42.1	41.4	44.4
GSD-G	43.0	41.6	26561	22391	67813	245419	757	29140	47881	47.0	7815.7	41.1	202.5	92509	37.8	64.1	37.2	37.3	39.5	31.7	62.7	35.2	37.6	41.0	39.2	42.9	36.6	43.1	42.7	45.8
GSD-G	39.5	41.7	26466	21919	68131	245419	777	29832	48620	48.0	7728.2	40.2	200.0	131374	37.5	65.1	38.0	37.4	40.4	31.1	62.9	35.7	37.8	41.3	40.4	43.0	36.8	44.1	44.0	46.2
GSD-G	39.6	41.4	26732	20919	68018	245419	841	30729	48767	48.5	7354.9	41.1	199.1	139174	37.4	64.6	37.6	38.3	39.6	31.3	63.8	35.8	38.1	41.4	39.7	43.4	36.7	43.2	43.3	47.3
GSD-G	46.8	40.7	26475	22345	66808	245419	857	29531	46324	46.4	7449.5	40.4	195.2	296808	37.0	62.4	37.5	38.1	40.0	31.0	61.6	34.8	37.1	40.3	40.4	43.2	36.9	43.5	42.7	45.2
GSD-G	41.7	42.0	26816	20303	68656	245419	774	28808	48461	47.2	7831.0	41.0	201.2	126321	37.5	64.2	37.6	39.0	39.5	31.1	65.0	35.8	37.3	41.3	40.1	43.4	37.3	43.0	44.2	46.6
GSD-G	44.2	42.1	26463	21066	69041	245419	944	29772	48511	48.0	7324.2	40.6	199.7	105191	37.4	64.9	37.8	38.3	40.0	31.7	63.9	35.8	37.3	41.3	39.2	43.3	37.5	44.3	44.3	47.0
GSD-G	38.84	40.63	25323	16855	65608	245419	867	25339	45710	43.69	6605	37.87	192.79	85850	37.45	61.21	35.94	35.04	37.89	30.12	60.26	33.80	36.05	39.53	37.35	42.07	34.72	43.11	40.23	43.74
GSD-G	41.08	41.77	25822	17384	66314	245419	902	25618	45612	46.20	6700	39.55	195.83	86348	37.76	63.67	35.84	36.98	38.52	30.27	63.27	35.84	37.21	40.32	39.93	42.75	35.34	43.19	41.67	45.31
GSD-G	41.67	41.28	26104	17110	65347	245419	942	25308	46356	45.57	6630	38.52	194.71	87798	37.01	62.83	36.54	36.57	38.29	30.45	60.26	34.22	36.53	40.74	38.53	41.57	35.39	42.42	40.82	44.47
GSD-G	39.25	40.82	26146	17200	65406	245419	875	25078	44965	45.27	6633	38.42	193.69	90778	36.44	62.06	36.13	35.47	37.99	30.06	61.69	34.46	36.37	40.24	37.85	41.90	35.93	42.25	40.84	44.04
GSD-G	42.32	42.19	26212	17472	66243	245419	918	25566	44887	45.56	6865	39.00	199.67	89505	36.96	62.75	36.38	36.01	38.50	30.24	61.73	34.57	36.48	40.51	39.10	41.85	35.82	43.21	41.95	45.03
GSD-G	42.99	41.48	26216	17335	65547	245419	937	25659	44905	44.57	6569	39.40	194.16	85833	38.11	62.28	35.90	36.28	38.64	30.01	62.88	34.43	36.25	40.42	39.74	41.43	35.68	42.73	41.95	45.05
GSD-G	41.34	40.64	25947	17259	65340	245419	915	25224	47332	45.39	6773	39.70	194.23	90021	37.64	62.37	36.21	36.84	38.77	29.94	62.11	34.35	36.76	40.58	38.98	42.24	36.21	42.24	41.05	45.05
GSD-G	42.68	42.51	26253	17733	67033	245419	954	25720	47178	46.20	6862	40.41	198.10	89009	38.22	63.95	37.05	36.98	39.38	31.20	63.52	35.15	36.78	40.36	39.22	43.23	36.28	42.97	42.01	45.56
GSD-G	41.73	41.75	26253	17764	67159	245419	923	25668	46300	46.03	6763	39.66	197.46	86597	37.93	62.63	36.57	35.97	38.11	30.40	64.41	34.62	36.41	40.70	38.55	41.46	36.17	42.45	41.89	45.44
GSD-G	41.82	41.01	25876	17908	66681	245419	950	25267	47318	44.76	6810	40.14	198.73	92145	37.81	62.98	37.30	37.56	39.75	30.43	63.03	35.15	37.05	41.44	38.55	42.40	36.41	42.59	41.76	45.25
GSD-G	40.06	41.31	26128	17688	66213	245419	919	26342	46841	46.04	6666	39.72	196.14	87204	38.36	62.03	36.15	36.49	38.34	30.01	64.39	34.75	36.75	40.52	39.19	41.93	36.11	43.97	41.91	45.28
GSD-G	41.99	41.40	26037	17634	66040	245419	920	25654	45877	44.88	6761	39.00	197.54	88155	36.65	61.76	35.30	36.18	38.23	30.76	61.96	35.05	36.73	40.23	39.10	41.17	36.25	43.75	41.45	44.46
GSD-G	43.15	42.40	26019	17761	67709	245419	962	26179	47725	46.63	6885	39.63	198.96	89207	37.32	63.80	37.00	38.11	39.34	30.77	63.45	35.90	38.01	41.49	39.58	43.88	37.34	45.21	42.58	45.46
Standards for Feldspar																														
Li ⁶	Li ⁷	Na	Mg	Al	Si	P	K	Ca	Sc	Ti	V	Mn	Fe	Rb	Sr	Y	Zr	Nb	Cs	Ba	La	Ce	Pr	Nd	Sm	Eu	Gd	Tb	Dy	
GSD-G	40.8	41.5	26319	17332	67041	245419	639	28867	47639	46.7	7490	40.3	200.5	89615	37.3	63.3	36.4	36.9	39.1	31.5	62.6	35.3	37.3	40.9	39.4	42.8	36.5	42.4	43.3	45.4
GSD-G	44.4	41.6	26050	19838	67563	245419	681	27990	47732	47.6	7571	39.9	196.0	90130	37.1	64.2	37.4	36.9	39.3	31.4	63.2	35.2	37.3	40.8	38.6	43.4	37.0	43.5	43.4	45.9
GSD-G	43.6	41.2	26091	20001	68230	245419	710	28711	48037	48.0	7759	40.6	201.9	89062	37.4	65.3	37.4	37.7	39.7	30.9	65.1	35.5	37.7	40.9	40.8	43.0	37.6	43.7	43.6	46.8
GSD-G	43.6	41.9	26629	20174	68239	245419	692	28470	48416	48.8	7870	40.9	204.5	92778	37.8	65.5	37.8	38.5	40.0	31.5	65.1	36.0	38.0	41.6	41.1	43.7	37.9	45.2	43.9	47.4
GSD-G	41.7	41.4	26172	20437	68338	245419	725	28526	48748	48.3	7621	40.9	203.4	95061	37.5	64.8														

Table A.1.17: continued

Ho	Er	Tm	Yb	Lu	Hf	Ta	Pb	Th	U
43.5	33.5	42.8	44.9	45.3	34.5	37.1	47.4	35.1	37.7
44.0	34.5	43.5	45.6	45.9	35.0	37.6	47.1	36.2	38.2
44.2	34.1	44.3	45.6	46.5	35.6	37.0	45.5	36.5	37.4
44.4	34.2	44.2	46.1	47.0	35.6	36.9	45.9	36.1	37.4
44.7	33.9	44.1	45.3	46.2	35.1	36.8	46.0	36.3	37.3
45.4	35.8	45.9	46.8	47.8	36.4	38.1	47.5	37.5	37.9
45.6	35.2	45.8	47.6	47.5	36.3	37.8	46.4	37.6	38.0
45.0	35.4	44.3	45.5	46.6	35.9	37.3	46.4	38.2	37.5
46.3	36.5	46.3	48.4	48.1	37.1	38.0	47.4	42.8	38.1
45.9	36.0	45.5	47.1	47.2	36.7	37.5	46.7	38.7	38.0
45.2	35.2	45.3	46.6	47.3	36.8	37.1	47.1	37.6	38.2
Ho	Er	Tm	Yb	Lu	Hf	Ta	Pb	Th	U
43.8	33.5	43.1	44.9	45.4	34.7	37.0	46.6	35.1	37.7
43.7	33.5	43.3	45.0	45.1	35.5	36.4	44.3	34.3	37.0
43.5	33.7	43.5	45.3	45.7	34.9	36.3	44.8	34.5	37.1
43.1	33.6	43.0	45.2	44.8	34.5	36.3	44.6	34.9	36.9
44.5	34.6	44.3	46.2	46.6	35.7	37.0	46.0	35.6	37.1
45.8	36.0	46.0	47.9	48.5	37.2	37.6	45.9	36.3	38.0
46.0	36.3	45.3	47.2	47.8	36.0	37.5	45.6	36.4	37.9
45.4	35.4	44.4	45.9	47.5	36.2	37.0	45.1	35.4	37.8
46.1	35.9	45.7	48.6	48.4	37.0	38.6	46.1	37.2	38.2
41.66	33.43	42.29	42.73	43.87	34.31	35.47	44.92	41.37	37.10
43.59	34.29	44.10	44.27	45.56	36.12	36.67	45.45	35.84	38.12
43.39	34.09	43.60	43.60	44.54	35.52	36.57	45.00	35.07	37.20
43.03	34.39	43.19	44.32	45.07	35.58	36.10	44.49	34.66	36.92
43.53	34.18	43.63	44.69	45.53	35.31	36.41	46.11	36.14	37.99
43.16	34.04	43.66	44.43	45.03	35.75	36.37	45.26	35.02	37.47
43.32	33.55	43.30	43.32	44.75	34.79	36.38	45.08	36.09	36.75
44.38	34.00	43.85	44.45	45.67	35.76	37.14	45.07	41.10	38.30
43.79	34.31	43.86	44.81	45.53	36.32	36.51	45.27	35.77	37.41
43.88	34.30	43.73	45.19	45.56	36.06	36.40	45.27	35.99	37.90
42.88	33.62	44.39	43.51	45.09	35.64	36.32	45.82	35.22	37.46
43.07	34.64	43.29	43.95	44.90	35.66	36.13	45.60	36.05	37.73
44.39	35.43	44.51	44.63	45.80	35.75	36.89	46.87	40.39	38.22
Ho	Er	Tm	Yb	Lu	Hf	Ta	Pb	Th	U
44.2	34.1	43.7	46.4	45.9	35.5	36.7	45.5	46.7	37.0
44.9	34.9	44.5	46.8	46.8	35.8	37.7	46.0	47.8	37.7
45.5	35.4	45.0	47.5	47.3	36.0	37.8	46.3	45.6	37.9
45.5	35.5	45.5	47.2	47.8	36.5	37.9	48.0	40.5	38.3
45.7	36.0	45.7	48.1	47.4	36.6	37.8	46.7	39.9	38.3
47.2	36.2	46.8	49.3	49.1	38.0	38.9	46.6	43.5	38.9
46.1	36.3	45.6	48.3	47.8	36.5	38.0	46.1	45.6	38.8
43.3	34.5	43.5	43.1	45.5	35.0	35.8	45.1	35.8	36.9
43.3	34.7	43.6	45.1	45.4	35.4	36.1	45.1	34.9	37.3
43.3	34.0	43.6	43.9	45.5	35.3	36.6	46.2	35.4	37.8
41.3	32.5	41.5	42.0	43.2	33.3	35.6	44.1	34.2	36.7
43.7	34.6	44.3	44.2	45.6	36.3	36.6	44.9	37.4	37.6
42.9	33.8	42.6	44.3	44.4	35.2	36.2	45.0	36.7	37.4

Table A1.17: continued

Standard for Feldspar		Li ⁷	Na	Mg	Al	Si	P	K	Ca	Sc	Ti	V	Mn	Fe	Rb	Sr	Y	Zr	Nb	Cs	Ba	La	Ce	Pr	Nd	Sm	Eu	Gd	Tb	Dy	Ho
GSD-1G	40.9	41.8	26075	17611	65503	245419	926	23511	47215	44.8	6608	38.7	193.7	88180	37.7	62.9	37.3	36.4	38.4	30.4	63.3	34.9	37.2	40.8	38.9	40.6	35.5	44.4	41.9	44.8	43.4
GSD-1G	41.8	42.2	26562	17416	65441	245419	899	26160	45897	44.7	6780	40.0	198.2	93209	37.7	62.2	36.4	38.3	38.2	31.0	62.2	34.7	36.5	40.5	37.5	42.6	36.9	41.8	42.0	46.0	43.7
GSD-1G	41.5	42.1	26124	17757	66483	245419	888	25684	46584	46.0	6815	40.0	200.3	90535	37.7	63.1	36.9	36.5	36.3	30.5	61.0	34.7	37.5	40.5	39.8	43.2	35.7	44.1	41.9	46.0	44.0
GSD-1G	42.2	42.1	26588	17678	67555	245419	915	26389	46311	45.6	6815	39.7	203.0	91657	38.2	62.9	36.5	37.7	38.9	31.6	65.0	35.3	37.7	40.4	39.3	42.0	36.3	43.5	41.5	45.0	43.6
GSD-1G	41.2	42.1	26657	17419	66412	245419	938	26196	46627	44.2	6727	39.6	196.9	90348	38.0	62.4	36.3	36.6	38.2	31.2	64.3	35.1	37.4	40.7	39.6	41.6	36.2	43.6	42.0	45.8	43.8
GSD-1G	41.9	42.4	26438	17872	66238	245419	928	25649	46908	45.1	6689	40.3	202.2	89856	38.2	61.9	36.4	36.0	38.7	30.9	62.4	35.4	37.1	40.9	39.4	41.4	35.8	42.5	41.8	44.0	43.3
GSD-1G	45.3	42.7	26759	17896	66768	245419	939	26123	47747	46.1	6804	40.4	200.4	90677	39.1	63.2	36.6	37.8	38.9	30.5	63.4	35.1	37.2	40.3	40.0	41.8	36.4	43.8	42.4	45.3	44.0
GSD-1G	40.3	42.2	26100	18023	67266	245419	940	25942	47697	45.9	6688	39.7	197.9	91105	36.8	63.2	37.3	36.0	38.9	30.7	64.3	35.9	37.7	41.4	39.4	43.1	37.0	44.4	42.7	46.2	44.0
GSD-1G	45.0	44.1	26106	19154	74393	245419	806	25942	52031	50.3	7339	41.7	207.2	94845	37.6	69.1	40.1	39.9	40.4	29.4	67.6	37.8	39.6	43.8	42.6	48.1	39.8	48.8	46.9	51.6	49.5
GSD-1G	40.7	38.3	24959	17393	69480	245419	892	24552	42804	43.3	6547	37.8	191.2	85385	34.9	59.4	34.7	36.4	36.7	27.1	63.9	33.0	34.7	37.9	38.0	41.6	34.1	42.5	40.7	44.2	42.5
GSD-1G	37.6	40.5	25793	17625	72913	245419	951	25368	44122	42.8	6890	38.8	195.0	95668	38.0	62.5	36.5	36.4	36.7	30.2	60.2	34.9	36.1	39.5	39.0	42.2	35.0	44.6	41.0	44.7	44.0
GSD-1G	40.5	41.5	26320	17996	75463	245419	870	25706	45590	47.6	6946	39.8	201.2	92388	36.1	63.4	37.1	37.9	39.0	30.0	66.8	35.7	37.2	41.1	39.1	44.4	37.3	45.8	42.9	46.9	45.5
GSD-1G	39.0	40.6	25450	18154	72882	245419	933	24801	44204	43.8	6607	39.3	194.9	91165	36.0	60.1	36.1	37.0	37.3	29.2	60.5	34.4	36.1	39.6	38.1	41.9	35.4	43.0	41.2	46.6	43.4
GSD-1G	41.8	39.4	25006	17342	71217	245419	957	24729	43916	42.2	6436	38.2	201.0	87915	34.1	60.8	35.1	35.1	36.4	28.9	62.0	33.9	35.7	39.4	38.1	41.5	35.3	43.7	41.0	44.2	43.6
GSD-1G	41.3	38.9	25058	17807	72411	245419	1005	24222	44647	43.4	6548	36.9	188.0	89923	35.7	60.7	36.4	36.4	37.1	29.1	60.7	34.3	35.4	39.2	38.3	40.9	35.4	43.4	41.1	46.1	43.1
GSD-1G	40.1	39.0	24927	17028	69755	245419	899	24991	42364	41.7	6262	37.5	184.8	87422	34.8	61.6	34.4	34.8	37.0	28.6	61.1	33.2	34.3	38.2	36.5	40.5	34.1	40.7	40.0	42.6	42.1
GSD-1G	38.9	38.9	24904	17728	71622	245419	900	23940	43493	42.7	6582	37.3	190.2	89052	34.8	60.4	36.4	35.3	36.9	29.0	57.5	34.2	36.1	39.8	38.4	40.9	35.1	43.8	41.3	45.6	43.2
GSD-1G	43.4	41.4	25811	18178	74924	245419	959	25241	45672	46.9	6630	39.0	196.6	93101	39.0	65.1	38.2	37.9	38.5	30.5	64.8	36.3	37.6	41.6	39.5	42.9	36.3	45.4	43.5	47.0	46.1
GSD-1G	39.6	40.0	25280	17507	72627	245419	923	24301	43667	45.3	6562	38.3	187.0	86208	36.0	62.3	37.0	36.8	38.4	29.7	60.7	34.5	35.1	39.1	37.5	41.8	35.8	43.0	41.1	45.2	43.7
GSD-1G	39.4	40.1	25729	17013	73228	245419	919	25409	44662	44.4	6632	38.1	201.5	89908	35.5	61.2	37.1	37.3	38.3	28.6	63.2	34.3	35.7	39.6	38.2	40.3	35.6	42.6	41.8	46.0	44.2
GSD-1G	39.6	40.1	25748	17407	72864	245419	871	24985	43787	44.6	6608	39.0	197.7	87332	36.0	63.0	35.8	37.0	36.8	27.9	60.4	33.9	35.8	39.1	38.6	42.9	35.5	44.4	41.3	44.8	42.7
GSD-1G	40.9	39.6	25517	17112	71824	245419	878	25225	43559	44.0	6420	38.1	195.5	85065	36.5	59.9	35.8	35.0	35.8	29.5	59.0	33.8	35.7	39.0	37.8	40.6	35.9	42.0	40.4	45.5	43.2
GSD-1G	40.2	38.2	25013	17082	71035	245419	896	24576	42964	43.3	6487	36.7	189.5	83023	35.5	61.5	34.7	37.9	35.6	29.0	63.1	32.8	34.9	38.7	37.5	39.7	35.2	41.8	40.3	43.2	42.3
GSD-1G	41.8	39.4	25363	17176	70434	245419	915	24974	42633	42.8	6372	38.8	190.0	87076	35.9	58.8	34.5	34.8	36.8	29.7	57.5	32.9	34.2	38.7	37.7	42.1	34.7	42.8	40.9	43.7	41.8
GSD-1G	41.8	41.0	26026	16868	63114	245419	936	24595	44222	44.6	6525	38.5	194.4	84201	37.0	60.1	35.0	35.7	36.7	30.7	62.1	33.8	35.3	38.4	37.8	40.6	34.3	42.2	40.4	44.0	42.2
GSD-1G	41.0	42.3	25766	18183	63769	245419	920	23788	46761	45.3	6813	38.9	193.5	89147	36.7	61.6	34.6	35.1	37.5	31.9	63.0	33.5	36.2	38.6	37.9	42.3	34.1	42.0	40.4	43.4	42.2
GSD-1G	42.6	41.2	25554	17024	64072	245419	904	24877	46954	45.5	6770	39.9	197.3	85006	37.2	63.3	36.4	36.0	37.6	29.6	62.1	34.3	36.9	40.0	37.8	41.8	35.3	43.3	42.1	44.6	43.6
GSD-1G	40.7	41.2	26459	17550	65842	245419	872	25244	46439	45.7	6658	38.8	194.6	87606	37.7	62.5	36.7	37.4	38.0	30.0	61.9	34.3	36.0	39.8	38.0	42.2	35.6	43.3	40.6	44.8	43.1
GSD-1G	39.9	40.3	25511	16997	64613	245419	894	25328	44728	43.9	6845	39.1	190.1	86231	36.1	62.0	35.7	35.8	36.8	29.9	60.9	33.5	35.8	39.1	37.5	39.9	35.1	44.1	40.5	44.8	42.0
GSD-1G	40.3	39.8	25270	16539	63442	245419	918	23892	44332	43.7	6643	37.6	185.2	90637	36.8	59.1	34.6	34.7	37.3	29.7	57.7	33.6	35.2	37.9	35.1	40.7	35.6	40.8	39.0	43.3	41.6
GSD-1G	42.5	41.6	26196	17339	65502	245419	907	25594	47236	45.0	6891	39.7	198.2	87458	37.7	62.3	36.4	37.7	37.4	29.7	62.5	34.8	38.2	41.2	37.8	41.7	35.5	43.1	41.9	45.3	43.3
GSD-1G	45.8	43.3	26355	19511	67272	245419	974	25379	45203	45.3	6779	39.9	202.8	96807	37.0	64.0	36.8	36.3	41.1	30.3	66.4	38.9	36.4	39.8	38.7	44.6	37.4	43.7	40.9	47.0	42.2
GSD-1G	44.5	41.5	25686	17078	65003	245419	974	26020	45798	44.8	6597	40.6	194.3	87587	36.9	61.6	36.6	36.5	37.6	30.5	60.2	34.5	35.7	39.7	38.4	43.6	36.8	43.1	41.1	47.0	43.7
GSD-1G	39.0	40.2	25846	17136	65824	245419	936	25571	47392	45.3	6669	39.2	192.9	87055	37.0	61.5	36.6	37.3	37.9	29.8	59.6	33.8	36.2	39.7	38.7	41.8	34.9	44.0	40.9	45.1	43.2
GSD-1G	42.6	43.4	25454	18307	65298	245419	1017	25113	46882	44.6	6783	39.4	201.5	89236	36.4	63.5	36.4	36.5	41.4	29.3	61.8	35.1	35.8	39.8	38.4	43.5	37.3	43.7	41.0	47.7	44.3
GSD-1G	41.2	41.9	26722	17756	66317	245419	943	25411	48021	45.1	6618	40.4	194.4	90122	37.4	63.7	36.7	37.2	38.0	30.4	63.3	34.3	36.5	43.4	39.7	42.1	36.1	43.4	41.1	45.4	44.7
GSD-1G	41.9	41.6	25482	17523	65876	245419	900	25258	45565	45.7	6769	44.4	195.7	88434	36.8	62.6	36.6	36.5	38.7	29.5	64.1	35.5	36.0	39.2	40.4	42.5	35.8	43.3	41.4	44.5	43.2

Table A1.17: continued

Fr	Tm	Yb	Lu	Hf	Ta	Pb	Th	U
34.8	44.1	44.0	45.2	35.9	36.9	44.6	36.8	37.6
33.7	43.6	45.6	44.7	34.9	36.2	46.7	34.6	37.9
34.7	44.3	44.4	45.9	36.0	36.9	45.3	35.7	37.9
34.4	44.1	43.6	44.9	35.6	36.3	44.8	35.6	37.9
34.2	43.3	44.4	44.8	34.7	36.5	44.7	35.1	37.4
34.1	43.4	44.5	45.2	36.1	37.2	46.0	35.7	37.1
34.5	44.2	44.1	46.0	36.3	36.8	46.4	36.1	38.0
34.9	44.4	45.7	46.2	36.2	37.1	45.5	36.1	38.5
38.6	49.7	50.1	50.2	39.8	39.7	42.9	39.6	40.6
34.0	44.3	45.3	44.9	35.3	36.6	43.6	34.2	37.6
36.0	45.5	44.9	46.8	35.8	36.2	46.4	37.7	38.9
33.6	44.3	44.6	45.0	35.9	36.1	43.9	36.2	38.3
33.8	43.8	46.3	44.6	35.4	35.9	46.6	34.3	36.5
35.4	44.0	43.0	45.2	34.6	36.1	42.6	36.6	36.0
32.9	42.8	43.2	42.8	32.3	35.2	43.7	34.5	36.3
34.2	44.2	43.9	45.1	35.1	36.3	42.7	34.2	36.2
37.3	46.4	48.0	47.3	37.7	37.1	42.8	35.6	38.5
33.1	44.2	45.0	45.4	33.7	35.2	44.0	33.6	37.1
33.9	44.3	44.6	44.9	35.5	36.5	43.7	38.9	36.5
33.4	44.0	42.4	44.9	36.1	34.6	42.3	34.9	35.2
33.4	42.7	43.4	43.5	34.7	35.4	42.6	34.5	35.2
32.1	42.6	42.5	43.8	35.6	35.5	44.0	33.5	35.6
33.2	42.0	41.9	44.2	34.7	34.9	45.6	35.2	36.2
33.8	41.5	42.6	43.1	33.6	35.2	42.8	32.9	37.5
33.9	43.3	43.8	45.1	36.0	36.0	44.7	34.9	36.9
33.6	43.2	42.8	45.1	35.8	35.9	44.5	35.6	36.5
33.2	43.4	43.4	44.7	34.9	35.5	44.3	33.7	36.4
32.5	42.2	42.0	43.0	34.0	34.7	43.4	35.8	35.8
34.8	43.2	44.5	45.1	35.2	36.3	44.5	34.5	36.7
34.0	43.3	44.4	44.6	34.7	35.8	52.8	35.9	37.2
34.4	44.8	45.1	45.6	36.1	36.1	44.6	35.3	38.3
34.2	42.8	43.8	44.9	34.5	35.6	44.9	35.0	36.5
33.8	43.5	45.2	45.1	35.5	36.0	44.7	35.1	36.3
34.7	44.4	44.8	45.1	35.8	36.2	46.6	35.3	36.5

Table A1.17: continued

Standards - trace elements - Quartz																			
Li ⁶	Li ⁷	Na	Mg	Al	Si	P	K	Ca	Ti	Mn	Fe	Ce	Rb	Sr	Sn	Cs	Pb	Ba	
NQS_AA	29.1	29.3	<0.24318	<0.27551	46698	62.5	<5.0072	<323.9743	51.9	0.4	<5.4395	1.5	<0.02598	<0.016114	1.2	<0.016578	0.1	<0.015321	
NQS_AA	28.7	29.4	<0.11158	0.3	166.5	46698	63.2	<3.602	<251.5587	0.4	<4.014	1.3	<0.01773	0.0	1.5	<0.0069166	0.1	<0.0017757	
NQS_AA	33.6	32.5	<0.37224	0.2	163.9	46698	64.6	<3.2197	<205.9389	54.9	0.4	<3.3461	1.5	<0.024372	<0.01918	1.4	<0.014072	0.0	<0.019509
NQS_AA	32.7	29.3	0.4	0.3	158.3	46698	71.6	<4.54	<285.8515	51.7	0.3	<5.0865	1.5	<0.017357	<0.0065001	0.7	<0.010296	0.1	<0.0079444
NQS_AA	28.5	28.0	0.2	<0.15679	168.2	46698	73.9	<2.9681	<195.5482	54.0	0.3	<2.8455	1.4	<0.015185	0.0	0.6	<0.0057634	0.0	<0.006109
NQS_AA	29.6	30.2	0.5	<0.23496	157.4	46698	74.9	<3.9843	<249.9998	54.5	0.3	<3.6559	1.7	0.0	0.9	<0.0046562	<0.024759	0.0	0.0
NQS_AA	32.7	31.8	0.6	0.2	156.3	46698	71.1	<3.4565	<216.6434	54.3	0.3	<3.0909	1.6	<0.013592	<0.0078139	1.0	<0.0073267	0.0	0.0
NQS_AA	34.3	30.9	0.5	0.2	159.0	46698	61.9	<10.3418	<471.922	53.3	<0.36193	<6.8043	1.4	<0.035103	<0.016645	0.6	<0.017198	<0.062458	<0.0044752
NQS_AA	28.6	30.4	3.1	0.4	158.0	46698	70.7	<5.4446	<287.3904	53.0	0.3	<3.8657	1.6	<0.023274	0.0	1.0	<0.012708	0.0	<0.0074539
NQS_AA	30.1	30.0	2.2	0.3	156.3	46698	72.8	<6.0797	<319.0457	54.0	0.5	<4.2273	1.8	<0.024291	<0.0095896	0.8	<0.0072687	<0.026532	0.0
NQS_AA	31.9	31.7	0.6	<0.37954	168.4	46698	75.1	<8.9171	<474.2802	55.7	0.5	<5.8802	1.4	<0.041508	<0.016588	0.7	<0.018248	<0.036445	<0.014012
NQS_AA	30.2	29.5	0.2	0.5	154.3	46698	75.5	<5.5444	<310.626	52.8	0.4	<3.8909	1.2	<0.024078	<0.015292	0.6	<0.0098954	<0.026261	<0.010743
NQS_AA	30.0	31.5	11.5	0.4	165.4	46698	76.0	12.7	<351.2727	55.9	0.4	5.0	1.2	<0.030401	0.0	0.9	<0.016755	0.0	0.0
NQS_AA	29.9	28.2	<0.19038	0.3	149.8	46698	81.1	7.5	<318.485	52.4	0.4	<4.1295	1.9	<0.029693	<0.01057	1.0	<0.010337	<0.032643	<0.0089244
NQS_AA	34.7	32.2	9.3	0.3	166.3	46698	56.4	11.4	<545.7952	55.6	0.4	<7.2634	1.9	0.0	<0.38933	<0.012322	<0.038074	<0.0046703	
NQS_AA	30.6	29.7	2.3	0.3	157.5	46698	63.9	<11.1478	<515.8422	23.5	0.4	<7.8145	<1.0895	<0.0472	0.0	<0.50513	<0.022725	<0.061457	<0.018357
NQS_AA	34.5	31.3	3.8	0.3	166.5	46698	60.2	25.2	<684.9082	54.0	0.7	<8.4276	1.6	<0.055095	<0.039217	<0.52329	<0.016228	<0.054164	<0.022774
NQS_AA	30.6	29.6	3.1	<0.48277	155.0	46698	61.3	<11.6093	<627.1415	53.7	<0.4492	<8.1605	2.5	<0.043455	0.0	0.6	<0.033904	<0.055759	<0.016744
Standards for Quartz																			
Li ⁶	Li ⁷	Na	Mg	Al	Si	P	Sc	Ti	Ge										
NQS_AA	31.0	31.1	17.9	222.9	46698	33.1	1.2	64.5	1.3										
NQS_AA	31.7	31.6	1.9	164.2	46698	20.3	1.0	61.5	1.5										
NQS_AA	31.5	30.6	2.5	158.2	46698	16.5	0.9	62.0	<1.4077										
NQS_AA	31.9	31.5	35.3	240.0	46698	43.9	0.9	63.4	1.9										
NQS_AA	33.3	32.8	55.0	344.6	46698	30.7	0.9	68.1	1.3										
NQS_AA	32.0	31.3	64.5	161.9	46698	16.0	1.0	61.6	1.1										
NQS_AA	30.1	29.8	<0.34734	153.0	46698	14.0	0.9	60.2	1.4										
NQS_AA	29.8	30.2	0.4	156.6	46698	16.9	0.7	62.7	1.8										
NQS_AA	30.7	30.6	0.8	155.8	46698	<11.8684	0.8	63.2	1.5										
NQS_AA	29.7	29.5	1.8	156.8	46698	21.1	0.7	61.6	<1.2362										
NQS_AA	31.2	30.7	5.3	152.8	46698	11.0	0.8	63.3	1.7										
NQS_AA	28.3	28.5	8.1	144.8	46698	14.0	0.9	59.0	1.6										
NQS_AA	31.6	31.1	10.8	257.2	46698	19.7	0.7	62.3	1.3										
NQS_AA	31.6	30.7	<0.3965	181.7	46698	<12.084	0.9	61.5	1.9										
NQS_AA	33.1	32.2	6.9	192.7	46698	16.2	0.8	59.7	1.8										

Appendix A

Table A1.18: Standards - major elements - feldspars

Info	SiO ₂	TiO ₂	Al ₂ O ₃	FeO	MgO	CaO	Na ₂ O	K ₂ O	BaO	SrO	Total
ANO	43.86	0.02	36.11	0.50	0.03	19.29	0.49	0.00	0.07	0.02	100.39
ANO	43.92	0.05	36.11	0.47	0.01	19.15	0.47	0.00	0.00	0.06	100.24
ANO	43.94	0.04	36.26	0.50	0.06	19.32	0.49	0.01	0.00	0.00	100.63
ANO	44.02	0.06	36.00	0.48	0.05	19.30	0.48	0.00	0.03	0.00	100.43
ANO	43.43	0.05	36.25	0.48	0.04	19.15	0.49	0.00	0.08	0.04	100.01
ANO	43.64	0.04	36.08	0.45	0.04	19.25	0.53	0.00	0.00	0.03	100.05
ANO	43.78	0.06	36.30	0.44	0.02	19.41	0.49	0.01	0.10	0.06	100.68
ANO	43.56	0.04	35.97	0.43	0.04	19.26	0.51	0.00	0.00	0.00	99.80
ANO	43.70	0.05	36.12	0.44	0.08	19.27	0.51	0.01	0.00	0.03	100.21
ANO	43.48	0.02	36.03	0.48	0.01	19.24	0.52	0.01	0.00	0.02	99.80
ANO	43.59	0.04	36.19	0.48	0.03	19.29	0.47	0.01	0.00	0.07	100.18
ANO	43.46	0.06	36.07	0.52	0.05	19.28	0.51	0.00	0.00	0.05	100.00
ANO	43.15	0.02	35.78	0.44	0.05	19.06	0.48	0.00	0.00	0.00	98.98
ANO	43.16	0.01	35.82	0.45	0.02	19.12	0.47	0.00	0.00	0.04	99.09
ANO	43.49	0.04	36.15	0.51	0.05	19.22	0.47	0.01	0.06	0.03	100.03
ANO	43.23	0.06	35.81	0.45	0.02	19.01	0.48	0.01	0.00	0.04	99.11
ANO	43.54	0.01	35.64	0.44	0.03	19.23	0.47	0.01	0.00	0.08	99.45
ANO	43.55	0.02	35.59	0.46	0.01	19.17	0.49	0.00	0.00	0.02	99.31
ANO	44.19	0.03	36.40	0.44	0.02	19.41	0.55	0.01	0.01	0.03	101.09
ANO	43.64	0.06	36.24	0.44	0.03	19.32	0.54	0.01	0.00	0.03	100.31
ANO	44.24	0.05	36.27	0.43	0.04	19.32	0.48	0.01	0.01	0.07	100.92
ANO	43.89	0.04	36.22	0.48	0.03	19.20	0.48	0.02	0.00	0.00	100.37
ANO	44.06	0.05	36.37	0.45	0.06	19.13	0.48	0.01	0.08	0.07	100.77
ANO	44.03	0.07	36.18	0.44	0.05	19.27	0.50	0.00	0.00	0.01	100.55
ANO	44.29	0.07	36.58	0.47	0.05	19.22	0.49	0.02	0.02	0.00	101.22
ANO	44.24	0.07	36.79	0.44	0.03	19.25	0.50	0.01	0.00	0.02	101.36
ANO	44.15	0.01	36.09	0.49	0.06	18.84	0.48	0.00	0.00	0.04	100.17
ANO	43.99	0.07	35.97	0.51	0.03	19.04	0.45	0.00	0.01	0.07	100.14
ANO	44.00	0.03	36.44	0.44	0.01	19.23	0.49	0.01	0.00	0.05	100.72
ANO	43.93	0.04	36.31	0.48	0.04	19.17	0.47	0.01	0.00	0.06	100.51
ANO	43.80	0.06	36.40	0.47	0.03	19.34	0.52	0.01	0.00	0.04	100.67
ANO	43.85	0.04	36.14	0.47	0.01	19.28	0.54	0.01	0.00	0.03	100.37
ANO	42.74	0.06	35.87	0.49	0.03	19.10	0.51	0.00	0.00	0.00	98.80
ANO	42.95	0.04	35.87	0.48	0.04	19.12	0.52	0.01	0.00	0.04	99.08
ANO	43.00	0.07	35.98	0.46	0.03	19.17	0.49	0.02	0.00	0.06	99.28
ANO	42.75	0.05	35.66	0.43	0.06	19.10	0.52	0.00	0.00	0.01	98.58
ANO	43.29	0.05	35.92	0.50	0.03	19.08	0.50	0.01	0.08	0.01	99.47
ANO	43.15	0.05	36.08	0.48	0.06	19.24	0.47	0.01	0.00	0.03	99.57
Info	SiO ₂	TiO ₂	Al ₂ O ₃	FeO	MgO	CaO	Na ₂ O	K ₂ O	BaO	SrO	Total
LAB	51.30	0.08	30.77	0.43	0.11	13.31	3.64	0.14	0.03	0.02	99.83
LAB	51.09	0.08	30.86	0.43	0.12	13.27	3.64	0.12	0.02	0.05	99.67
LAB	51.13	0.07	30.66	0.45	0.13	13.13	3.68	0.13	0.00	0.00	99.38
LAB	51.31	0.08	30.93	0.42	0.11	13.29	3.73	0.13	0.01	0.04	100.06
LAB	50.42	0.05	30.73	0.42	0.13	13.22	3.69	0.13	0.00	0.00	98.79
LAB	50.82	0.09	30.85	0.45	0.10	13.11	3.74	0.13	0.00	0.03	99.32
LAB	51.27	0.06	30.75	0.43	0.14	13.27	3.73	0.12	0.00	0.00	99.77
LAB	51.21	0.05	30.58	0.45	0.11	13.24	3.77	0.12	0.00	0.04	99.57
LAB	50.69	0.07	30.48	0.44	0.14	13.26	3.65	0.14	0.05	0.03	98.95
LAB	50.91	0.04	30.57	0.47	0.13	13.06	3.66	0.13	0.00	0.06	99.03
LAB	51.22	0.07	30.99	0.44	0.11	13.12	3.81	0.13	0.06	0.00	99.96
LAB	51.12	0.09	30.65	0.46	0.11	13.22	3.70	0.12	0.05	0.00	99.52
LAB	50.70	0.08	30.42	0.44	0.13	13.17	3.71	0.15	0.00	0.02	98.82
LAB	51.06	0.06	30.48	0.41	0.12	13.20	3.72	0.13	0.02	0.00	99.20
LAB	50.94	0.06	30.63	0.46	0.13	13.18	3.69	0.13	0.07	0.01	99.29
LAB	51.07	0.05	30.36	0.44	0.10	13.12	3.65	0.13	0.04	0.00	98.97
LAB	50.95	0.07	30.28	0.47	0.13	13.11	3.70	0.13	0.00	0.06	98.90
LAB	51.01	0.07	30.63	0.44	0.11	13.13	3.62	0.13	0.05	0.01	99.21
LAB	51.50	0.07	31.08	0.41	0.13	13.24	3.85	0.14	0.00	0.00	100.43
LAB	51.54	0.08	30.93	0.51	0.16	13.31	3.83	0.14	0.03	0.06	100.57
LAB	51.36	0.06	30.93	0.43	0.12	13.12	3.77	0.12	0.06	0.01	99.98
LAB	51.78	0.07	30.61	0.43	0.15	13.03	3.68	0.14	0.08	0.05	100.02
LAB	51.79	0.08	30.84	0.42	0.12	13.13	3.70	0.13	0.00	0.00	100.23
LAB	51.72	0.10	30.91	0.43	0.12	13.18	3.68	0.15	0.04	0.00	100.33
LAB	51.56	0.08	31.03	0.49	0.12	13.11	3.70	0.12	0.01	0.00	100.23
LAB	51.72	0.06	30.47	0.47	0.13	13.04	3.46	0.14	0.00	0.04	99.52
LAB	51.62	0.07	31.06	0.42	0.15	13.09	3.55	0.13	0.02	0.03	100.14
LAB	51.51	0.09	30.99	0.44	0.11	13.15	3.91	0.12	0.00	0.01	100.34
LAB	51.62	0.09	30.75	0.45	0.12	13.16	3.88	0.14	0.07	0.04	100.33
LAB	51.33	0.10	30.62	0.47	0.09	12.99	3.84	0.14	0.00	0.04	99.61
LAB	51.32	0.08	30.89	0.43	0.15	13.09	3.83	0.14	0.03	0.00	99.96
LAB	51.67	0.09	30.81	0.47	0.10	13.29	3.86	0.13	0.00	0.04	100.46
LAB	51.49	0.10	30.87	0.47	0.12	13.13	3.84	0.13	0.03	0.04	100.22
Info	SiO ₂	TiO ₂	Al ₂ O ₃	FeO	MgO	CaO	Na ₂ O	K ₂ O	BaO	SrO	Total
MCL	64.70	0.03	18.72	0.02	0.00	0.03	1.25	15.36	0.23	0.00	100.34
MCL	64.67	0.04	18.87	0.00	0.00	0.01	1.17	15.32	0.18	0.00	100.25
MCL	64.52	0.04	18.96	0.00	0.00	0.00	1.25	15.37	0.20	0.00	100.34
MCL	64.51	0.05	19.09	0.00	0.00	0.00	1.31	15.30	0.28	0.02	100.56
MCL	64.44	0.04	19.02	0.04	0.01	0.00	1.24	15.47	0.21	0.04	100.50
MCL	64.64	0.05	19.23	0.01	0.00	0.03	1.22	15.48	0.33	0.00	100.99
MCL	64.57	0.05	18.91	0.01	0.00	0.00	1.28	15.44	0.21	0.02	100.48
MCL	64.82	0.04	18.86	0.02	0.00	0.00	1.27	15.42	0.23	0.00	100.65
MCL	64.31	0.04	19.04	0.02	0.00	0.00	1.24	15.43	0.22	0.03	100.34
MCL	64.47	0.03	18.95	0.01	0.01	0.00	1.27	15.31	0.29	0.03	100.37
MCL	64.30	0.03	19.14	0.00	0.00	0.00	1.26	15.28	0.32	0.01	100.34
MCL	63.81	0.03	18.73	0.00	0.00	0.00	1.10	15.50	0.30	0.01	99.49

Table A1.18: continued

MCL	64.28	0.02	18.96	0.00	0.01	0.02	1.21	15.28	0.27	0.00	100.04
MCL	64.12	0.05	18.74	0.02	0.00	0.00	1.25	15.04	0.26	0.02	99.50
MCL	64.73	0.03	18.94	0.01	0.00	0.00	1.28	15.60	0.25	0.00	100.85
MCL	64.52	0.06	18.86	0.01	0.00	0.00	1.25	15.48	0.17	0.02	100.37
MCL	64.68	0.08	18.97	0.01	0.00	0.01	1.29	15.53	0.20	0.00	100.78
MCL	64.83	0.05	18.95	0.00	0.03	0.00	1.30	15.63	0.25	0.03	101.07
MCL	63.86	0.00	18.74	0.00	0.00	0.00	1.24	15.51	0.25	0.00	99.60
MCL	63.91	0.06	18.83	0.00	0.00	0.00	1.26	15.55	0.26	0.04	99.92
MCL	64.50	0.06	19.13	0.00	0.01	0.01	1.07	15.76	0.25	0.00	100.78
MCL	64.59	0.04	19.03	0.03	0.00	0.00	1.20	15.45	0.26	0.02	100.62
MCL	64.14	0.05	18.59	0.01	0.00	0.00	1.17	15.43	0.25	0.00	99.64
MCL	64.37	0.03	18.88	0.00	0.00	0.02	1.14	15.64	0.28	0.00	100.36
MCL	64.09	0.03	18.76	0.03	0.00	0.00	1.20	15.54	0.27	0.01	99.94
MCL	64.82	0.04	18.95	0.03	0.00	0.02	1.19	15.56	0.27	0.00	100.86
MCL	64.35	0.04	18.80	0.00	0.00	0.00	1.25	15.53	0.25	0.01	100.24
MCL	64.57	0.05	18.96	0.02	0.00	0.00	1.26	15.66	0.26	0.00	100.80
MCL	64.26	0.03	18.96	0.02	0.00	0.03	1.29	15.50	0.28	0.05	100.43
MCL	64.24	0.02	18.89	0.00	0.00	0.00	1.27	15.56	0.25	0.00	100.23
MCL	64.20	0.03	19.01	0.00	0.00	0.00	1.37	15.48	0.24	0.00	100.33
MCL	63.92	0.04	19.11	0.01	0.01	0.00	1.28	15.57	0.27	0.00	100.21
MCL	63.91	0.04	18.95	0.00	0.00	0.00	1.06	15.73	0.29	0.00	99.98
MCL	64.06	0.06	18.95	0.00	0.00	0.01	1.30	15.50	0.22	0.00	100.09

Table A1.19: Standards - major elements - glass

Info	SiO ₂	TiO ₂	Al ₂ O ₃	FeO	Cr ₂ O ₃	MnO	MgO	CaO	Na ₂ O	K ₂ O	P ₂ O ₅	Cl	Total
ATHO-G	75.34	0.29	12.50	3.23	0.19	0.09	0.11	1.65	3.74	2.71	0.00	0.03	99.88
ATHO-G	75.75	0.35	12.55	3.06	0.06	0.08	0.08	1.75	3.68	2.84	0.00	0.04	100.25
ATHO-G	75.59	0.37	12.54	3.06	0.03	0.13	0.10	1.62	3.70	2.76	0.00	0.04	99.94
ATHO-G	75.47	0.28	12.59	3.00	0.15	0.11	0.05	1.69	3.88	2.83	0.00	0.05	100.09
ATHO-G	75.75	0.23	12.69	3.09	0.00	0.16	0.11	1.66	3.51	2.82	0.01	0.03	100.07
ATHO-G	75.93	0.25	12.60	2.99	0.06	0.12	0.12	1.69	3.76	2.71	0.06	0.04	100.33
ATHO-G	75.66	0.27	12.48	3.11	0.00	0.05	0.07	1.73	3.66	2.80	0.06	0.04	99.93
ATHO-G	75.79	0.26	12.35	3.02	0.00	0.10	0.08	1.61	3.66	2.82	0.04	0.04	99.77
ATHO-G	75.72	0.28	12.49	3.03	0.35	0.08	0.09	1.70	3.59	2.79	0.07	0.02	100.21
ATHO-G	75.21	0.24	12.76	3.08	0.00	0.11	0.09	1.64	3.63	2.80	0.00	0.05	99.60
ATHO-G	75.55	0.30	12.47	2.97	0.00	0.13	0.10	1.68	3.55	2.85	0.00	0.03	99.63
ATHO-G	75.39	0.31	12.51	3.20	0.10	0.08	0.07	1.65	3.61	2.85	0.00	0.02	99.80
ATHO-G	75.84	0.28	12.41	3.29	0.00	0.12	0.11	1.63	3.68	2.84	0.00	0.02	100.22
ATHO-G	75.45	0.34	12.43	3.19	0.00	0.12	0.04	1.74	3.75	2.76	0.02	0.02	99.86
ATHO-G	75.65	0.34	12.41	3.19	0.00	0.12	0.12	1.67	3.75	2.82	0.07	0.03	100.16
ATHO-G	75.58	0.33	12.55	3.08	0.00	0.13	0.06	1.69	3.64	2.81	0.04	0.05	99.95

Info	SiO ₂	TiO ₂	Al ₂ O ₃	FeO	Cr ₂ O ₃	MnO	MgO	CaO	Na ₂ O	K ₂ O	P ₂ O ₅	Cl	Total
NIST-610	70.00	0.16	2.13	0.06	0.15	0.07	0.04	11.30	13.21	0.06	0.12	0.04	97.34
NIST-610	70.18	0.14	2.15	0.05	0.05	0.12	0.07	11.55	13.25	0.08	0.10	0.03	97.77
NIST-610	70.15	0.12	2.04	0.06	0.18	0.07	0.04	11.36	13.34	0.04	0.14	0.04	97.57
NIST-610	70.08	0.13	2.09	0.03	0.03	0.02	0.06	11.31	13.18	0.08	0.05	0.02	97.09
NIST-610	69.41	0.13	2.06	0.06	0.00	0.09	0.07	11.21	13.24	0.04	0.06	0.05	96.42
NIST-610	69.48	0.16	2.14	0.07	0.22	0.05	0.09	11.23	13.62	0.06	0.09	0.05	97.26
NIST-610	69.48	0.13	2.13	0.06	0.00	0.03	0.05	11.42	13.32	0.08	0.08	0.04	96.82
NIST-610	69.75	0.12	2.02	0.03	0.04	0.03	0.00	11.36	13.29	0.07	0.08	0.02	96.81
NIST-610	68.85	0.18	2.01	0.03	0.18	0.05	0.03	11.06	13.27	0.09	0.10	0.02	95.87
NIST-610	69.09	0.13	2.11	0.02	0.04	0.06	0.05	11.36	13.18	0.08	0.16	0.01	96.29
NIST-610	70.12	0.11	2.13	0.09	0.08	0.05	0.06	11.33	13.25	0.09	0.13	0.02	97.44
NIST-610	69.81	0.20	2.13	0.05	0.00	0.05	0.03	11.37	13.04	0.05	0.04	0.04	96.81
NIST-610	70.01	0.15	2.14	0.06	0.11	0.07	0.09	11.38	13.34	0.06	0.05	0.03	97.48
NIST-610	70.28	0.14	2.12	0.04	0.18	0.04	0.08	11.44	13.26	0.05	0.03	0.02	97.68
NIST-610	69.35	0.21	2.13	0.07	0.00	0.08	0.04	11.19	12.92	0.09	0.11	0.02	96.20
NIST-610	69.81	0.12	1.98	0.06	0.08	0.06	0.10	11.24	12.94	0.04	0.12	0.03	96.58
NIST-610	69.44	0.14	2.01	0.05	0.00	0.07	0.00	11.42	12.82	0.09	0.10	0.06	96.20
NIST-610	69.69	0.18	2.08	0.05	0.24	0.03	0.10	11.38	13.11	0.06	0.07	0.03	97.02

A2: KDs and literature data

Table A2.1: Overview of literature data used

Sample number	Unit name	UAT (N)	LONG (W)	Comment	published by
BE SRP 14 038	Huckleberry Ridge Tuff	43.91273	111.5358	Teton dam Embree location basal vitrophyre	Ellis et al., 2018
BP5-23-12-8	Kilgore Tuff	43.48842	111.90332	Basal vitrophyre Kilgore Tuff	Ellis et al., 2018
BP5-23-12-6	Kilgore Tuff	43.65009	111.68466	Upper vitrophyre Kilgore Tuff	Ellis et al., 2018
BP4-19-12-2	Kilgore Tuff	43.53290	111.69989	Basal vitrophyre, Kilgore tuff, reference section (Morgan and McIntosh, 2005)	Ellis et al., 2018
BP5-25-12-2	Kilgore Tuff	44.1277	112.5379	upper vitrophyre, Kilgore Tuff	Ellis et al., 2018
BP140625-1	Conant Creek Tuff	44.06265	110.92682	glassy sample of Conant Creek Tuff at type section, S Boome Creek	Ellis et al., 2018
DS13003	Wolverine Creek Tuff	43.52775	111.69442	Massive, dark grey deposit, full of on-size pumice and dense clasts up to 1.5 cm	Szymanowski et al., 2015
DS14038	Wolverine Creek Tuff	43.64805	111.68558	Massive unweilded, pumice-rich, black deposit	Szymanowski et al., 2015
DS13018	Walcott Tuff	43.80732	112.84908	Basal part of Walcott Tuff at reference section (Morgan and McIntosh, 2005), black layer with spherulites	Szymanowski et al., 2015; Ellis et al., 2018
BP5-23-12-9	Walcott Tuff	43.42539	111.90997	Basal vitrophyre	Szymanowski et al., 2015
BP4-19-12-1	Blacktail Creek	43.5049	111.76157	Upper vitrophyre, Blacktail Creek Tuff, type section (Morgan and McIntosh, 2005)	Szymanowski et al., 2015; Ellis et al., 2018
DS13019	Winnetou Ignimbrite	43.80732	112.84908	Upper vitrophyre from enigmatic red ignimbrite at base of Walcott ref section	Ellis et al., 2017b
BE SRP 11 032	Greys Landing	42.21137	114.73346	Upper perlitic vitrophyre GL, Salmon Falls dam	Ellis et al., 2015
BE SRP 09 039	Greys Landing	42.06757	114.76372	Basal vit GL Backwaters	Ellis et al., 2015
BE SRP 09 031	Gwin Springs	43.18005	114.65634	Upper vitrophyre of the Tuff of Gwin Springs	This study
BE SRP 13 002	Wooden Shoe Butte	42.34459	114.29541	Wooden Shoe Butte next to the road in Rock Creek	Ellis et al., 2018
BE SRP 09 023	Tuff of Knob	43.23937	114.9171	Upper vitrophyre of Knob	Ellis et al., 2018
BE SRP 09 020	Tuff of Knob	43.20672	115.0054	Basal vitrophyre Tuff of Knob	Ellis et al., 2018
CPT XIII					This study
BE SRP 09 015	Rhyolite of Deer Springs	43.2137	114.98688	Vitrophyre of the Deer Springs Unit	This study
Samples from the drillcore	Unit name	Depth (m)			
14002	Upper Rhyolite	154.5			Ellis et al., 2017b
14006	Upper Rhyolite	181.7			Ellis et al., 2017b
14008	Upper Rhyolite	189.9			Ellis et al., 2017b
14018	Upper Rhyolite	498.3			Ellis et al., 2017b
14020	Upper Rhyolite	516.0			Ellis et al., 2017b
14021	Upper Rhyolite	518.8			Ellis et al., 2017b
14027	Middle Rhyolite	591.9			Ellis et al., 2017b

Table A2.2: Li concentration overview

Sample	Filtered Glass data				n	taken out
	Mean	Min	Max	2SD		
Mesa Falls Tuff	42.5	36.1	148.7	6.5	70	3
Huckleberry Ridge Tuff	46.9	42.0	51.8	5.2	50	0
Upper Rhyolite	23.4	4.1	31.5	8.2	283	33
Middle Rhyolite	11.7	4.5	126.4	11.7	25	0
Kilgore Tuff	27.0	23.0	31.2	4.3	134	20
Conant Creek Tuff	36.5	35.5	37.7	1.3	26	0
Wolverine Creek Tuff	30.0	27.4	32.7	2.7	85	12
Walcott Tuff	35.8	26.6	53.7	16.7	53	2
Blacktail Creek Tuff	33.3	14.3	47.3	19.1	32	1
Winnetou Ignimbrite	14.8	11.9	17.0	3.2	21	0
Greys Landing	23.5	16.8	26.2	5.5	34	6
Tuff of Gwin Spring	24.9	23.2	26.1	2.0	10	0
Wooden Shoe Butte	25.5	18.0	32.2	8.5	54	0
Tuff of Knob	30.3	24.1	36.5	6.2	34	2
Cougar Point Tuff XIII	38.8	22.2	50.6	16.7	22	1
Rhyolite of Deer Springs	25.7	19.9	29.2	4.6	35	14

Table A2.3: Kds

	MFT	Mean	Min	Max	n	HRT	Mean	Min	Max	n	Walcott Tuff	Mean	Min	Max	n	Tuff of Knob	Mean	Min	Max	n	
rim	Sanidine	0.11	0.03	0.18	69	Sanidine	0.04	0.02	0.10	119	Sanidine	-	-	-	-	Sanidine	-	-	-	-	
rim	Plagioclase	0.52	0.41	0.67	68	Plagioclase	0.13	0.08	0.19	10	Plagioclase	0.16	0.09	0.23	36	Plagioclase	0.22	0.12	0.33	189	
rim2	Plagioclase	0.28	0.11	0.42	97	Orthopyroxene	-	-	-	-	Orthopyroxene	0.24	0.22	0.38	19	Orthopyroxene	0.37	0.28	0.53	27	
rim	Orthopyroxene	0.20	0.18	0.22	58	Clinopyroxene	-	-	-	-	Clinopyroxene	0.30	0.26	0.33	31	Clinopyroxene	0.25	0.21	0.38	14	
rim	Clinopyroxene	0.26	0.23	0.29	74	Favallite	-	-	-	-	Favallite	-	-	-	-	Favallite	-	-	-	-	
rim	Favallite	0.39	0.31	0.58	168	Quartz	0.50	0.39	0.56	51	Quartz	-	-	-	-	Quartz	-	-	-	-	
rim	Quartz	0.45	0.35	0.53	148																
core	Sanidine	0.15	0.09	0.28	338	Middle Rhvolutite	Mean	Min	Max	n	Blacktail Creek	Mean	Min	Max	n	CPT XIII	Mean	Min	Max	n	
core	Plagioclase	0.43	0.27	0.63	276	Sanidine	0.14	0.11	0.17	20	Sanidine	0.12	0.07	0.45	82	Sanidine	-	-	-	-	
core	Clinopyroxene	0.27	0.23	0.32	185	Plagioclase	-	-	-	-	Plagioclase	0.38	0.26	0.55	68	Plagioclase	0.16	0.09	0.22	14	
core	Favallite	0.38	0.33	0.46	84	Orthopyroxene	-	-	-	-	Orthopyroxene	0.32	0.22	0.56	10	Orthopyroxene	-	-	-	-	
core	Quartz	0.41	0.31	0.58	570	Clinopyroxene	-	-	-	-	Clinopyroxene	0.31	0.25	0.83	131	Clinopyroxene	-	-	-	-	
						Favallite	-	-	-	-	Favallite	-	-	-	-	Favallite	-	-	-	-	
						Quartz	-	-	-	-	Quartz	-	-	-	-	Quartz	-	-	-	-	
						Upper Rhvolutite	Mean	Min	Max	n	Winnetou Ignimbrite	Mean	Min	Max	n	Rhyolite of Deer Springs	Mean	Min	Max	n	
						Sanidine	0.09	0.06	0.13	42	Sanidine	-	-	-	-	Sanidine	0.07	0.05	0.10	31	
						Plagioclase	0.29	0.13	0.48	74	Plagioclase	0.44	0.14	0.74	35	Plagioclase	0.25	0.15	0.44	26	
						Orthopyroxene	-	-	-	-	Orthopyroxene	-	-	-	-	Pigeonite	0.59	0.42	0.86	15	
						Clinopyroxene	-	-	-	-	Clinopyroxene	-	-	-	-	Clinopyroxene	0.30	0.19	0.47	4	
						Favallite	-	-	-	-	Favallite	-	-	-	-	Favallite	-	-	-	-	
						Quartz	-	-	-	-	Quartz	-	-	-	-	Quartz	-	-	-	-	
						Kilgore Tuff	Mean	Min	Max	n	Greys Landing	Mean	Min	Max	n						
						Sanidine	0.08	0.04	0.18	118	Sanidine	-	-	-	-						
						Plagioclase	0.23	0.04	0.49	245	Plagioclase	0.24	0.14	0.42	59						
						Orthopyroxene	0.27	0.23	0.48	98	Orthopyroxene	-	-	-	-						
						Clinopyroxene	0.33	0.21	0.42	71	Clinopyroxene	-	-	-	-						
						Favallite	-	-	-	-	Favallite	-	-	-	-						
						Quartz	-	-	-	-	Quartz	-	-	-	-						
						Conant Creek Tuff	Mean	Min	Max	n	Tuff of Gwin Springs	Mean	Min	Max	n						
						Sanidine	-	-	-	-	Sanidine	-	-	-	-						
						Plagioclase	0.13	0.08	0.18	30	Plagioclase	0.19	0.10	0.27	44						
						Orthopyroxene	-	-	-	-	Orthopyroxene	-	-	-	-						
						Clinopyroxene	-	-	-	-	Clinopyroxene	-	-	-	-						
						Favallite	-	-	-	-	Favallite	-	-	-	-						
						Quartz	-	-	-	-	Quartz	-	-	-	-						
						Wolverine Creek Tuff	Mean	Min	Max	n	Tuff of Wooden Shoe Butte	Mean	Min	Max	n						
						Sanidine	0.17	0.06	0.38	23	Sanidine	-	-	-	-						
						Plagioclase	0.07	0.04	0.16	18	Plagioclase	0.17	0.07	0.27	95						
						Orthopyroxene	-	-	-	-	Orthopyroxene	-	-	-	-						
						Clinopyroxene	-	-	-	-	Clinopyroxene	0.44	0.28	0.81	20						
						Favallite	-	-	-	-	Favallite	0.58	0.43	0.76	46						
						Quartz	-	-	-	-	Quartz	-	-	-	-						

Appendix A

Table A2.4: Whole rock data

MESA FALLS TUFF - Whole rock data						
Unnormalized Major Elements (Weight %):						
SiO ₂	76.1	73.5	72.6	73.8	75.4	76.2
TiO ₂	0.2	0.2	0.2	0.2	0.2	0.1
Al ₂ O ₃	11.1	11.6	12.2	11.8	12.3	11.6
FeO*	1.9	1.6	1.6	1.9	1.8	1.2
MnO	0.0	0.0	0.0	0.0	0.0	0.0
MgO	0.1	0.1	0.1	0.1	0.1	0.0
CaO	0.9	0.7	0.7	0.8	0.5	0.5
Na ₂ O	2.6	2.6	2.3	2.6	3.2	3.5
K ₂ O	4.9	5.1	5.5	5.2	5.2	4.8
P ₂ O ₅	0.0	0.0	0.0	0.0	0.0	0.0
Sum	97.8	95.3	95.6	96.2	98.8	98.0
Normalized Major Elements (Weight %):						
SiO ₂	77.8	77.1	75.9	76.6	76.3	77.8
TiO ₂	0.2	0.2	0.2	0.2	0.2	0.1
Al ₂ O ₃	11.4	12.2	12.7	12.2	12.4	11.9
FeO*	1.9	1.7	1.7	1.9	1.8	1.3
MnO	0.0	0.0	0.0	0.0	0.0	0.0
MgO	0.1	0.1	0.1	0.1	0.1	0.0
CaO	0.9	0.8	0.8	0.8	0.5	0.5
Na ₂ O	2.7	2.7	2.9	2.7	3.3	3.6
K ₂ O	5.0	5.3	5.7	5.4	5.3	4.9
P ₂ O ₅	0.0	0.0	0.0	0.0	0.0	0.0
Total	100.0	100.0	100.0	100.0	100.0	100.0
Unnormalized Trace Elements (ppm):						
Ni	4	4	4	12	3	3
Cr	6	3	3	4	3	3
Sc	4	2	3	3	3	1
V	5	4	5	4	6	2
Ba	1006	444	595	423	527	42
Rb	97	180	174	173	175	230
Sr	56	29	38	32	33	3
Zr	250	242	266	296	283	173
Y	40	73	69	71	64	76
Nb	21.7	43.6	41.6	43.4	41.5	60.7
Ga	17	20	21	20	22	24
Cu	3	2	2	1	3	2
Zn	54	65	66	69	55	75
Pb	24	30	30	28	25	47
La	57	82	86	91	85	72
Ce	105	157	161	166	172	119
Th	14	30	28	30	31	30
Nd	44	61	62	65	61	48
U	2	7	5	5	5	8
sum tr.	1808	1477	1657	1535	1599	1018
in %	0	0	0	0	0	0
sum m+tr	98	95	96	96	99	98
M+1oxides	98	96	96	96	99	98
Major elements are normalized on a volatile-free basis, with total Fe expressed as FeO. "R" denotes a duplicate bead made from the same rock powder.						
NiO	5.6	4.5	5.0	15.1	6.1	3.8
Cr ₂ O ₃	8.6	4.8	4.7	6.4	5.0	4.2
Sc ₂ O ₃	5.7	3.1	4.1	3.8	4.4	2.8
V ₂ O ₅	7.4	6.0	7.8	5.9	8.5	2.4
BaO	1123.4	495.8	663.8	472.4	587.9	46.6
Rb ₂ O	105.9	197.3	189.7	188.8	191.6	251.9
SrO	66.6	34.3	45.2	37.5	39.1	3.3
ZrO ₂	337.0	326.6	359.3	399.3	382.1	234.0
Y ₂ O ₃	51.1	93.1	87.0	90.4	80.8	96.1
Nb ₂ O ₅	31.0	62.4	59.5	62.1	59.4	86.8
Ga ₂ O ₃	22.6	27.0	27.8	27.2	30.1	32.4
CuO	3.5	2.0	2.0	1.1	3.8	1.9
ZnO	67.9	81.3	82.4	86.7	68.6	93.6
PbO	25.9	31.9	32.4	30.3	26.7	50.1
La ₂ O ₃	66.5	96.6	100.7	106.3	100.0	84.7
CeO ₂	128.5	192.7	197.9	203.8	210.9	145.8
ThO ₂	15.7	32.8	30.6	32.9	33.9	33.5
Nd ₂ O ₃	51.0	70.7	72.5	75.9	71.4	56.5
U ₃ O ₈	1.7	7.2	5.5	5.8	5.4	9.1
Cs ₂ O	103.9	101.2	101.6	102.2	104.9	104.0
As ₂ O ₅	0.0	0.0	0.0	0.0	0.0	0.0
W ₂ O ₆	0.0	0.0	0.0	0.0	0.0	0.0
sum tr.	2229	1871	2080	1954	2021	1343
in %	0.22	0.19	0.21	0.20	0.20	0.13

Table A2.5: Melts modell

MELTS - Results		MELT FRACTION at temperature (°C)		TEMPERATURE at melt fraction (%)	
MINERALS IN	MINERALS OUT				
feldspar	960	feldspar	790	675	-
quartz	1030	quartz	850	700	-
spinel	940	spinel	800	725	-
Rhm-oxide		Rhm-oxide		750	35.0
olivine	920	olivine	780	775	70.0
orthopyroxene	940	orthopyroxene	810	800	84.1
clinopyroxene	910	clinopyroxene	780	825	92.9
amphibole		amphibole		850	96.6
biotite		biotite		875	99.6
muscovite		muscovite		900	100.0
cummingtonite		cummingtonite		925	100.0
apatite		apatite		950	100.0
whitlockite		whitlockite		975	100.0
garnet		garnet		1000	100.0
sillimanite		sillimanite		1025	100.0
leucite		leucite		1050	100.0
crystalite		crystalite		1075	100.0
tridymite		tridymite		1100	100.0
corundum		corundum			
water	1300	water	930		

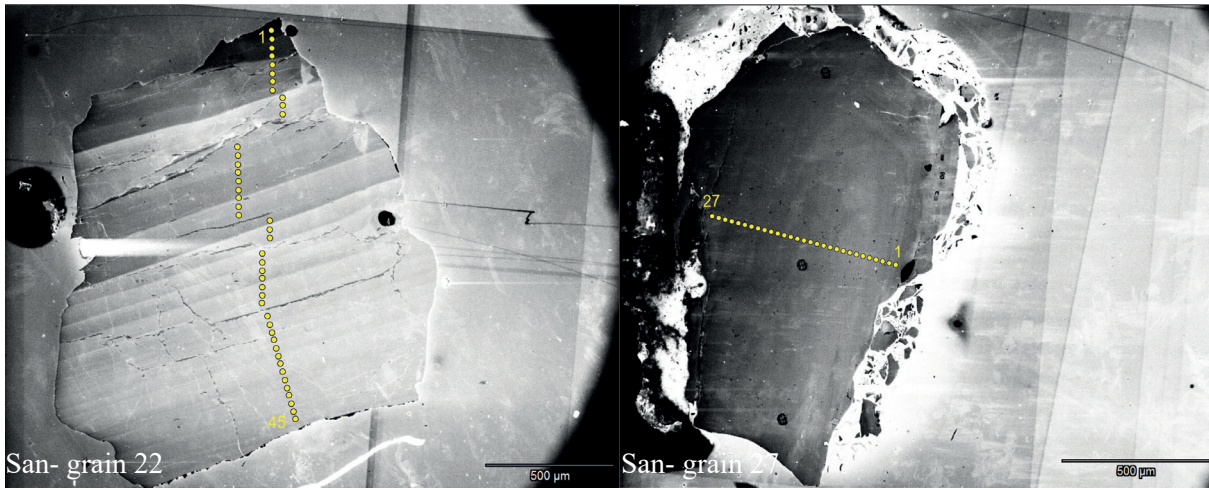


Fig. A3. CL images of sanidine

Appendix

Appendix B: Supplementary material for Chapter 3

B: Plagioclase major and trace element data and Fs-LA-MC-ICP-MS data

Table B1: Plagioclase grain 7 - Line 1

Distance	L ¹⁶ ppm	2SD	L ¹⁷ ppm	2SD	Na ppm	2SD	Mg ppm	2SD	Al ppm	2SD	K ppm	2SD	Ca ppm	2SD	Ti ppm	2SD	Fe ppm	2SD	Rb ppm	2SD	Sr ppm	2SD	Ba ppm	2SD	La ppm	2SD
core	2	20	2	19	54577	3367	18	5	118448	7045	12758	770	27200	917	51	8	1432	106	4	1	171	12	308	20	23	2
core	7	21	2	21	61027	4331	18	5	124693	8128	13884	776	28436	980	57	8	1413	140	4	1	82	12	339	26	24	2
core	17	20	2	19	55914	5630	21	5	14384	6250	12708	742	25366	1532	51	9	1246	114	3	0	170	10	327	26	23	2
core	12	20	2	19	54428	2543	18	4	16504	5283	12951	616	26240	2041	45	7	1368	114	3	0	175	7	335	21	24	2
core	27	19	2	19	53110	2787	18	4	14870	5037	12748	770	25460	1631	41	8	1302	98	4	1	69	9	314	21	23	2
core	27	20	2	19	54283	3780	19	3	13621	6971	12504	797	26144	2314	41	5	1305	108	3	1	73	12	319	22	23	2
core	32	18	2	18	52408	3399	17	5	112691	8130	12249	794	26033	2310	47	10	1337	108	4	1	174	12	302	29	21	2
core	37	19	2	18	52666	3022	22	7	114311	7289	12118	675	25033	1612	46	8	1248	86	3	1	165	12	311	21	20	1
core	42	23	3	19	55696	4596	19	4	119285	9920	12820	1071	28000	3154	48	6	1304	150	3	1	177	14	332	29	23	2
core	47	20	2	20	54477	2729	21	6	124552	8191	13277	910	28977	2072	49	10	1344	126	4	0	175	11	314	25	22	1
core	52	21	2	20	57853	4109	20	6	124552	8191	13277	910	28977	2072	49	10	1344	126	4	0	175	11	314	25	22	1
core	57	19	2	19	53235	2257	21	5	118271	4131	12205	571	26128	1589	43	7	1271	74	3	1	170	7	300	16	23	2
core	62	21	1	20	55230	3906	17	4	18221	8778	12975	567	28079	2260	53	10	1384	136	4	1	172	15	320	37	23	2
core	67	21	2	20	58060	3771	19	5	123788	6519	13312	678	27999	1641	51	10	1443	122	4	0	182	11	322	22	24	2
core	72	20	2	19	54935	2405	19	5	18088	5592	12782	606	27006	1448	40	8	1345	75	4	1	170	8	292	17	22	2
core	77	20	2	19	54151	2910	21	4	16214	5792	12819	613	27519	2037	45	6	1386	105	4	1	174	9	304	21	21	2
core	82	20	3	18	52194	2624	18	4	113437	5734	12367	641	26695	1446	40	8	1249	91	3	0	162	8	275	22	21	2
core	87	23	3	20	56275	2942	20	5	118575	6190	12922	689	27332	1751	44	8	1412	119	3	0	178	10	290	17	22	2
core	92	22	3	20	56648	4424	19	5	120921	8394	13067	925	27587	1949	47	10	1318	115	4	1	171	15	304	23	23	2
core	97	19	2	18	52721	3624	19	4	112321	7797	12352	876	25904	1961	40	8	1299	155	4	1	158	12	268	25	21	2
core	102	22	3	19	53060	2394	19	5	115132	5136	12983	629	26134	1818	41	6	1249	61	4	1	166	8	269	15	20	1
core	107	19	2	19	53098	2693	19	6	113124	5823	12594	649	25499	1887	42	9	1218	92	4	1	159	9	262	18	20	1
core	112	20	2	20	56091	2967	19	5	19517	5607	13445	671	27546	1655	37	6	1358	95	4	0	167	9	284	20	22	2
core	117	23	3	21	56853	4269	21	4	120373	9073	13413	866	26493	2687	46	9	1311	132	4	1	172	12	289	26	22	2
core	122	20	3	20	56211	4621	21	5	19415	9138	13533	1129	26892	2144	41	7	1390	156	4	1	161	11	270	24	21	2
core	127	20	2	20	54587	2940	18	6	16440	5954	12762	642	26674	1811	50	7	1237	115	4	1	162	9	281	18	20	1
core	132	19	2	20	56432	3412	18	3	118539	6689	13053	721	27595	2013	37	6	1323	109	4	1	164	11	273	19	21	1
core	137	23	2	20	56786	3423	17	5	118514	6832	13315	789	26891	2205	38	9	1299	116	4	1	162	10	268	22	21	2
core	142	19	1	18	51219	2671	14	4	109087	6131	12004	589	24252	1203	40	6	1192	90	3	0	143	7	257	16	20	1
core	147	20	1	20	54913	3219	20	5	117179	4838	13364	572	25669	1728	41	7	1303	92	4	1	159	7	272	12	21	1
core	152	22	2	20	56026	3127	19	5	118331	7290	13436	959	27982	1843	45	8	1308	94	4	1	162	11	274	19	22	2
core	157	20	2	20	55419	3985	22	5	116530	5757	13268	874	23859	2080	42	7	1256	94	4	1	156	10	255	20	22	2
core	162	20	2	20	54621	3126	20	3	117749	5521	13137	642	23872	1858	44	9	1271	128	5	1	153	9	261	18	23	2
core	167	18	2	19	54498	2717	14	4	118184	5145	12805	542	24325	1434	33	8	1248	72	4	1	151	9	262	20	22	2
core	172	20	1	19	53465	2751	18	4	118184	5145	12805	542	24325	1434	33	8	1248	72	4	1	151	9	262	20	22	2
core	177	20	1	19	52607	2212	18	5	112202	5347	12785	500	25655	1629	39	5	1202	96	4	1	142	7	256	16	20	1
core	182	20	2	19	53596	3041	23	5	112822	5474	12923	687	25639	2377	39	7	1231	92	4	1	141	9	248	14	21	1
core	187	18	2	19	54131	3037	13	4	113096	6279	12939	659	25030	1692	39	5	1199	98	4	1	141	9	248	14	21	1
core	192	20	2	20	55295	2532	15	5	116003	4969	13193	603	25789	1941	42	5	1184	78	4	1	148	8	256	17	21	1
core	197	19	2	19	53672	2760	17	4	111815	6260	12886	610	25041	1391	40	6	1132	64	4	1	138	7	256	15	21	2
core	202	22	2	21	57727	3988	19	5	119921	6353	13754	781	27409	1969	46	7	1348	138	4	1	145	9	276	16	21	1
core	207	21	2	20	55408	2824	20	6	117282	6944	13089	644	23881	1462	44	7	1194	94	4	1	140	8	246	16	21	1
core	212	20	2	19	55069	3025	21	6	117468	7319	13175	723	26241	1967	48	8	1275	86	4	0	137	8	236	20	21	2
core	217	18	2	18	54188	3085	20	6	113753	6492	12619	760	25159	1592	41	8	1233	102	4	0	130	8	222	17	22	2
core	222	20	4	18	54686	4349	17	4	14202	8018	12971	984	25185	2315	46	9	1212	147	4	1	132	10	230	19	20	2
core	227	19	2	17	53995	2991	18	5	11914	6437	12982	677	24969	1609	37	5	1202	63	4	1	130	9	210	16	22	2
core	232	17	2	17	52902	2938	20	4	109372	5528	12948	819	24813	1837	41	8	1163	94	4	1	121	7	196	12	19	2
core	237	17	2	17	54235	2372	16	3	112147	4954	13202	610	23762	1515	41	6	1150	67	4	0	123	7	194	13	20	2
core	242	18	2	18	57913	3037	22	4	114018	5162	14128	717	25874	3650	44	15	1217	90	4	1	126	6	188	14	21	1
core	247	18	2	18	57904	1954	28	6	118579	4167	14092	605	25341	1428	40	7	1198	78	5	1	127	8	188	14	21	1
core	252	17	2	17	57357	3499	26	6	118216	6650	13912	907	26917	1850	40	6	1272	108	4	1	128	8	159	17	20	1
rim	257	14	2	15	56822	3215	22	5	116678	4210	13919	853	24556	1830	36	5	1176	63	4	1	117	7	136	8	20	2
rim	262	15	2	14	58110	3319	18	4	117657	6703	13981	729	24148	248	39	9	1227	119	5	1	126	9	135	13	20	2
rim	267	16	2	14	58110	3319	18	4	117657	6703	13981	729	24148	248	39	9	1227	119	5	1	126	9	135	13	20	2
rim	272	15	2	13	53166	3245	14	3	109870	6043	13295	676	24594	1653	41	5	1108	88	5	1	118	7	138	12	21	2
rim	276	13	1	12	53782	2108	15	3	109368	4672	13071	935	23396	1289	40	6	1092	73	3	1	119	6	127	8	18	1
rim	281	13	1	12	55504	3146	16	4	112753	6390	13235	747	24556</													

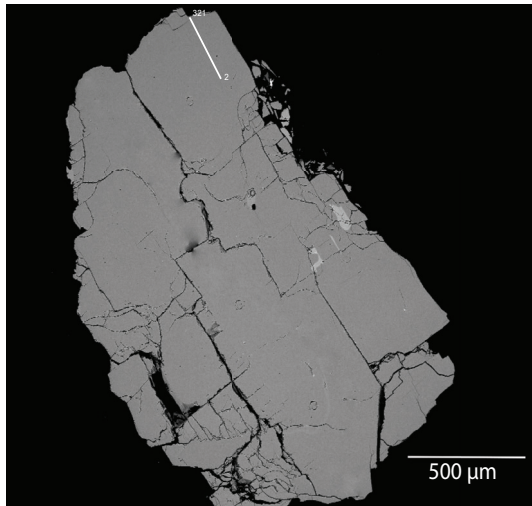
Table B1: continued

	Ce ppm	2SD	Pr ppm	2SD	Nd ppm	2SD	Sm ppm	2SD	Eu ppm	2SD	Gd ppm	2SD	Pb ppm	2SD	SiO ₂	TiO ₂	Al ₂ O ₃	FeO	MgO	CaO	Na ₂ O	K ₂ O	BaO	SrO	Total	An mol%	Ab mol%	Or mol%		
24	2	0	2	0	5	1	1	0	5	1	0	0	0	13	2															
26	2	0	2	0	5	1	0	0	5	1	0	0	0	13	2															
22	2	0	2	0	4	1	0	0	4	1	0	0	0	12	2															
24	2	0	2	0	5	1	0	0	5	1	0	0	0	12	1															
23	2	0	2	0	4	1	0	0	4	1	0	0	0	12	1															
22	2	0	2	0	4	1	0	0	4	1	0	0	0	12	2	63.1	0.1	22.9	0.2	0.0	4.3	8.1	1.5	0.0	0.0	100.2	21		71	9
22	2	0	2	0	4	1	0	0	4	1	0	0	0	13	1	63.1	0.1	22.8	0.2	0.0	4.2	8.0	1.6	0.0	0.0	99.9	20		71	9
22	2	0	2	0	4	1	0	0	4	1	0	0	0	12	2	63.0	0.1	23.0	0.2	0.0	4.1	8.1	1.6	0.0	0.0	100.1	20		71	9
24	2	0	2	0	5	1	0	0	5	1	0	0	0	12	2	63.1	0.1	23.1	0.2	0.0	4.3	8.1	1.5	0.1	0.0	100.4	21		71	9
22	2	0	2	0	4	1	1	0	4	1	0	0	0	12	1	63.1	0.1	22.8	0.2	0.0	4.1	8.2	1.3	0.1	0.0	100.2	20		71	9
24	2	0	2	0	4	1	0	0	4	1	0	0	0	13	1	63.4	0.0	22.7	0.2	0.0	3.9	8.1	1.6	0.0	0.0	99.8	19		72	9
23	2	0	2	0	5	1	1	0	5	1	0	0	0	12	1	63.5	0.1	22.9	0.2	0.0	3.8	8.1	1.6	0.0	0.0	100.3	19		72	9
22	2	0	2	0	4	1	1	0	4	1	0	0	0	14	1	63.4	0.1	22.8	0.2	0.0	4.0	8.1	1.6	0.0	0.0	100.2	19		71	9
24	2	0	2	0	4	1	0	0	4	1	0	0	0	13	1	63.3	0.1	22.8	0.2	0.0	4.0	8.0	1.6	0.0	0.1	100.0	20		71	9
23	2	0	2	0	4	1	1	0	4	1	0	0	0	13	1	63.0	0.1	22.8	0.2	0.0	4.0	8.1	1.5	0.0	0.0	99.8	20		72	9
22	2	0	2	0	5	1	0	0	5	1	0	0	0	12	1	63.2	0.1	22.7	0.2	0.0	4.0	8.0	1.6	0.0	0.0	99.8	20		71	9
23	2	0	2	0	5	1	1	0	4	1	0	0	0	12	1	63.0	0.1	22.9	0.2	0.0	4.2	8.1	1.5	0.0	0.1	100.1	20		71	9
22	2	0	2	0	5	1	0	0	4	1	0	0	0	14	2	63.2	0.1	22.7	0.2	0.0	4.0	8.2	1.2	0.0	0.0	99.9	19		72	9
22	2	0	2	0	4	1	0	0	4	1	0	0	0	12	1	63.3	0.1	22.8	0.2	0.0	4.1	8.1	1.5	0.0	0.0	100.2	20		71	9
21	2	0	2	0	4	1	0	0	4	1	0	0	0	13	1	63.1	0.1	22.9	0.2	0.0	4.2	8.1	1.5	0.0	0.0	100.1	20		71	9
20	2	0	2	0	5	1	0	0	4	1	0	0	0	13	1	63.1	0.1	22.8	0.2	0.0	4.2	8.1	1.5	0.0	0.0	100.0	20		71	9
22	2	0	2	0	3	1	0	0	5	1	0	0	0	13	1	63.1	0.1	23.0	0.2	0.0	4.2	8.1	1.5	0.1	0.0	100.2	20		71	9
23	2	0	2	0	4	1	0	0	5	1	0	0	0	14	1	63.2	0.1	22.8	0.2	0.0	4.0	8.1	1.6	0.0	0.0	100.0	20		71	9
22	2	0	2	0	3	1	0	0	5	1	0	0	0	13	2	63.4	0.1	22.6	0.2	0.0	3.9	8.2	1.6	0.0	0.0	100.0	19		72	9
21	2	0	2	0	3	1	1	0	5	1	0	0	0	13	1	63.3	0.1	22.9	0.2	0.0	4.1	8.1	1.6	0.1	0.0	100.3	20		71	9
20	2	0	2	0	4	1	0	0	4	1	0	0	0	12	1	63.3	0.1	22.8	0.2	0.0	4.1	8.1	1.6	0.0	0.0	100.2	20		71	9
22	2	0	2	0	4	1	0	0	4	1	0	0	0	12	1	63.1	0.1	22.8	0.2	0.0	4.0	8.0	1.6	0.0	0.0	99.8	20		71	9
20	2	0	2	0	4	1	1	0	5	1	0	0	0	12	1	63.1	0.1	22.7	0.2	0.0	4.1	8.0	1.6	0.1	0.0	99.8	20		71	9
21	2	0	2	0	4	1	0	0	4	1	0	0	0	12	1	63.1	0.0	22.5	0.2	0.0	4.0	8.0	1.6	0.0	0.0	99.4	20		71	9
22	2	0	2	0	4	1	0	0	4	1	0	0	0	14	1	63.1	0.1	22.9	0.2	0.0	4.0	8.2	1.6	0.0	0.0	100.1	19		72	9
22	2	0	2	0	4	1	0	0	4	1	0	0	0	13	1	63.2	0.1	22.6	0.2	0.0	4.0	8.0	1.6	0.0	0.0	99.7	20		71	9
21	2	0	2	0	4	1	0	0	4	1	0	0	0	13	1	63.0	0.1	23.0	0.2	0.0	4.2	8.0	1.5	0.0	0.1	100.1	19		71	9
21	2	0	2	0	4	1	0	0	5	1	0	0	0	13	2	63.1	0.1	23.0	0.2	0.0	4.0	8.2	1.6	0.1	0.0	100.1	19		72	9
22	2	0	2	0	3	1	0	0	4	1	0	0	0	12	1	63.2	0.1	22.9	0.2	0.0	4.0	8.0	1.6	0.1	0.0	100.0	20		71	9
20	2	0	2	0	4	1	1	0	4	1	0	0	0	13	1	63.1	0.1	22.9	0.2	0.0	4.1	8.0	1.6	0.0	0.0	99.9	20		71	9
21	2	0	2	0	3	1	0	0	4	1	0	0	0	12	1	63.2	0.1	22.8	0.2	0.0	4.0	8.1	1.6	0.0	0.0	99.9	19		71	9
20	2	0	2	0	3	1	0	0	4	1	0	0	0	13	2	63.2	0.1	22.7	0.2	0.0	4.1	8.1	1.6	0.0	0.0	99.9	20		71	9
22	2	0	2	0	4	1	0	0	4	1	0	0	0	12	1	63.3	0.1	23.0	0.2	0.0	4.0	8.0	1.6	0.0	0.0	100.2	20		71	9
23	2	0	2	0	5	1	0	0	4	1	0	0	0	13	2	63.0	0.1	22.8	0.2	0.0	4.0	8.0	1.6	0.0	0.1	99.6	20		71	9
21	2	0	2	0	4	1	0	0	4	1	0	0	0	13	2	63.1	0.1	22.9	0.2	0.0	4.2	7.9	1.6	0.1	0.0	100.1	21		70	9
24	3	0	2	0	4	1	1	0	4	1	0	0	0	14	2	63.5	0.1	22.6	0.2	0.0	3.9	8.1	1.6	0.0	0.0	99.9	19		72	9
22	2	0	2	0	4	1	0	0	4	1	0	0	0	13	1	63.4	0.1	22.6	0.2	0.0	3.9	8.1	1.6	0.0	0.0	99.9	19		72	9
22	2	0	2	0	4	1	0	0	4	1	0	0	0	13	1	63.3	0.1	22.7	0.2	0.0	4.0	8.0	1.6	0.0	0.0	99.9	19		71	9
21	2	0	2	0	5	1	0	0	3	1	0	0	0	12	1	63.3	0.1	22.9	0.2	0.0	4.1	8.0	1.5	0.0	0.0	100.1	20		71	9
21	2	0	2	0	4	1	0	0	4	1	0	0	0	12	1	63.2	0.1	22.7	0.2	0.0	4.1	8.1	1.6	0.0	0.0	99.9	20		71	9
20	2	0	2	0	3	1	1	0	3	1	0	0	0	13	2	63.2	0.1	22.8	0.2	0.0	4.0	8.1	1.6	0.0	0.0	99.9	19		71	9
20	2	0	2	0	3	1	0	0	3	1	0	0	0	13	1	63.1	0.1	22.7	0.2	0.0	4.1	8.1	1.6	0.0	0.1	99.9	20		71	9
21	2	0	2	0	4	1	0	0	3	1	0	0	0	14	1	63.1	0.1	22.9	0.2	0.0	4.0	8.0	1.6	0.0	0.0	99.8	19		71	9
21	2	0	2	0	4	1	0	0	4	1	0	0	0	17	2	63.2	0.1	22.7	0.2	0.0	4.1	7.9	1.6	0.0	0.0	99.8	20		71	9
19	1	0	2	0	3	1	0	0	3	1	0	0	0	25	5	63.5	0.0	22.5	0.2	0.0	3.9	8.0	1.7	0.0	0.0	100.0	19		71	10
21	2	0	2	0	3	1	0	0	3	1	0	0	0	14	2	63.5	0.1	22.6	0.2	0.0	3.9	8.0	1.7	0.0	0.0	100.0	19		71	10
21	2	0	2	0	3	1	1	0	3	1	0	0	0	13	1	63.6	0.1	22.5	0.1	0.0	3.9	8.1	1.6	0.0	0.0	100.0	19		71	9
21	2	0	2	0	4	1	0	0	4	1	0	0	0	14	2	63.4	0.1	22.6	0.2	0.0	3.9	8.0	1.6	0.0	0.0	99.8	19		71	10
20	2	0	2	0	3	1	0	0	3	1	0	0	0	13	2	63.6	0.1	22.8	0.2	0.0	3.9	8.1	1.6	0.0	0.0	100.2	19		71	9
18	2	0	2	0	4	1	0	0	3	1	0	0	0	13	1	63.2	0.0	22.7	0.2	0.0	3.9	8.2	1.6	0.0	0.0	99.8	19		72	9
19	2	0	2	0	4	1	0	0	3	1	0	0	0	14	1	63.2	0.1	22.5	0.2	0.0	3.8	8.2	1.7	0.0	0.0	99.7	19		72	10
20	2	0</																												

Table B2: continued

Nd ppm	2SD	Sm ppm	2SD	Eu ppm	2SD	Cd ppm	2SD	Pb ppm	2SD
4.0	0.0	0.0	0.0	4.8	0.1	0.1	0.0	1.3	2
4.2	0.2	0.2	0.2	5.3	0.5	0.5	0.0	2.4	2
4.6	0.1	0.1	0.1	4.8	0.2	0.2	0.0	1.9	1
4.0	0.3	0.3	0.3	4.9	0.2	0.2	0.0	1.4	1
4.3	0.4	0.4	0.4	5.1	0.3	0.3	0.0	0.9	2
5.1	0.2	0.2	0.2	4.4	0.0	0.0	0.0	1.1	1
3.9	0.3	0.3	0.3	4.9	0.0	0.0	0.0	3.3	2
4.1	0.2	0.2	0.2	4.8	0.0	0.0	0.0	1.9	1
4.5	0.2	0.2	0.2	4.9	0.0	0.0	0.0	2.5	1
4.8	0.1	0.1	0.1	4.5	0.5	0.5	0.0	1.0	1
4.9	0.1	0.1	0.1	5.0	0.2	0.2	0.0	1.8	2
4.9	0.8	0.8	0.8	3.9	0.9	0.9	0.0	1.9	2
4.8	0.6	0.6	0.6	5.0	0.1	0.1	0.0	2.0	1
3.7	2	2	2	4.8	0.1	0.1	0.0	2.0	1
3.8	0.6	0.6	0.6	4.3	0.1	0.1	0.0	1.9	1
3.8	0.6	0.6	0.6	4.7	0.1	0.1	0.0	1.9	1
4.7	0.3	0.3	0.3	4.6	0.2	0.2	0.0	1.8	2
4.5	0.3	0.3	0.3	5.0	0.1	0.1	0.0	2.2	2
5.6	0.5	0.5	0.5	3.2	0.0	0.0	0.0	2.1	1
4.4	0.6	0.6	0.6	4.6	0.4	0.4	0.0	2.9	1
3.5	0.4	0.4	0.4	5.0	0.2	0.2	0.0	1.9	1
4.3	0.4	0.4	0.4	4.1	0.1	0.1	0.0	2.3	2
4.8	0.4	0.4	0.4	4.6	0.3	0.3	0.0	2.6	2
3.9	0.2	0.2	0.2	4.6	0.1	0.1	0.0	3.1	1
4.1	0.6	0.6	0.6	4.6	0.1	0.1	0.0	3.4	1
4.0	0.2	0.2	0.2	4.0	0.1	0.1	0.0	2.3	1
4.7	0.3	0.3	0.3	4.6	0.2	0.2	0.0	2.4	2
3.8	0.4	0.4	0.4	4.5	0.2	0.2	0.0	1.7	1
4.0	0.2	0.2	0.2	4.0	0.2	0.2	0.0	3.1	1
4.8	0.2	0.2	0.2	4.0	0.3	0.3	0.0	2.0	1
4.8	0.4	0.4	0.4	4.3	0.2	0.2	0.0	2.8	2
4.8	0.4	0.4	0.4	4.1	0.2	0.2	0.0	2.4	2
4.8	0.6	0.6	0.6	4.0	0.2	0.2	0.0	2.7	1
3.7	0.8	0.8	0.8	4.1	0.2	0.2	0.0	3.1	1
3.7	0.5	0.5	0.5	4.3	0.3	0.3	0.0	3.5	1
4.6	0.2	0.2	0.2	4.2	0.2	0.2	0.0	3.0	1
4.0	0.5	0.5	0.5	4.0	0.1	0.1	0.0	3.0	1
4.0	0.7	0.7	0.7	4.3	0.2	0.2	0.0	2.9	1
3.8	0.7	0.7	0.7	4.3	0.2	0.2	0.0	2.6	1
4.9	0.4	0.4	0.4	3.8	0.1	0.1	0.0	3.3	2
4.9	0.4	0.4	0.4	3.8	0.3	0.3	0.0	3.3	2
3.4	0.6	0.6	0.6	3.2	0.0	0.0	0.0	3.0	2
3.5	0.6	0.6	0.6	3.1	0.2	0.2	0.0	3.5	2
4.1	0.2	0.2	0.2	3.2	0.2	0.2	0.0	2.1	2
4.3	0.2	0.2	0.2	3.1	0.1	0.1	0.0	2.8	2
3.9	0.4	0.4	0.4	3.3	0.2	0.2	0.0	3.3	2
3.9	0.4	0.4	0.4	3.1	0.1	0.1	0.0	2.7	2
3.6	0.3	0.3	0.3	2.6	0.3	0.3	0.0	3.9	2
3.9	0.4	0.4	0.4	3.7	0.2	0.2	0.0	1.9	1
3.4	0.2	0.2	0.2	2.4	0.4	0.4	0.0	3.4	2
3.3	0.2	0.2	0.2	3.8	0.0	0.0	0.0	4.0	2
3.6	0.6	0.6	0.6	3.7	0.2	0.2	0.0	4.1	2
3.9	0.4	0.4	0.4	3.1	0.2	0.2	0.0	3.9	2
3.6	0.4	0.4	0.4	3.1	0.1	0.1	0.0	3.2	2
3.6	0.4	0.4	0.4	3.1	0.1	0.1	0.0	3.1	2
4.4	0.2	0.2	0.2	3.9	0.2	0.2	0.0	0.8	3
1.7	2	2	2	2.9	0.1	0.1	0.0	2.6	3

grain7 - line 1



grain 7 - line 2

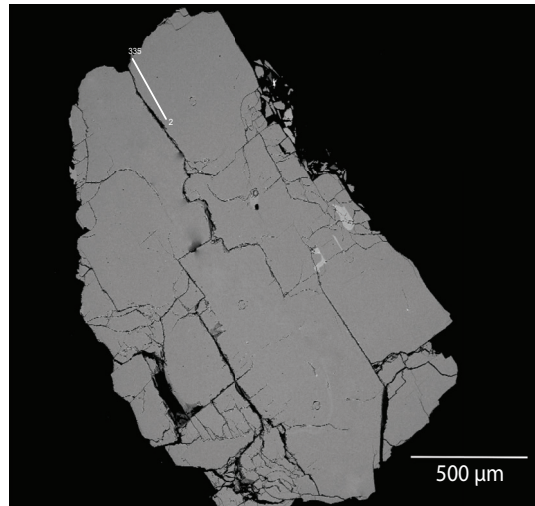


Fig. B1. BSE images of plagioclase grain 7 with trace element lines (by LA-ICP-MS) indicated.

Table B3: Plagioclase grain 7 - Lithium isotopes

	MEASURED		background		Results (BLK + tau corr.)						
	⁷ Li (V)	⁶ Li (cps)	⁷ Li (V)	⁶ Li (cps)	⁷ Li/ ⁶ Li	SE	SD	1 SD	n	D time (min)	
1	0.00547	21260	0.00034	0.0000496	240	16.1250	0.0129	0.1416	802	119	5.6
2	0.00819	31865	0.00051	0.0000428	228	16.1009	0.0097	0.1094	601	129	4.5
3	0.00947	36709	0.00059	0.0000474	224	16.1004	0.0096	0.1073	599	124	5.2
4	0.01063	41418	0.00066	0.0000420	217	16.0680	0.0087	0.0983	541	129	5.2
5	0.01053	41075	0.00066	0.0000403	221	16.0320	0.0093	0.1061	583	129	5.0
6	0.01140	44599	0.00071	0.0000402	223	15.9816	0.0082	0.0922	512	129	4.2
7	0.01059	41420	0.00066	0.0000432	226	15.9450	0.0086	0.0933	538	121	4.4
8	0.01076	42230	0.00068	0.0000398	216	15.9213	0.0094	0.1038	592	120	4.1
9	0.00991	38857	0.00062	0.0000541	266	15.9239	0.0083	0.0930	524	124	4.8

std drift	^δ Li (‰) rel	2 s	^δ Li (‰) rel	RepRate	integr.	distance	Li	2 σ	d ⁷ Li	2 σ	
⁷ Li/ ⁶ Li	GOR132-G		IRMM-016	Hz	time (s)						
0.7	-9.0	2.3	-0.1	28	1.049	rim	35	12.4	1.0	-0.1	2.3
-0.8	-10.5	2.0	-1.6	28	1.049	core	70	16.6	1.0	-1.6	2.0
1.7	-10.2	1.8	-1.3	23	1.049	core	103	18.1	1.4	-1.3	1.8
-0.5	-11.6	1.7	-2.7	23	1.049	core	143	19.3	1.1	-2.7	1.7
-0.1	-14.1	1.8	-5.2	23	1.049	core	185	19.9	1.4	-5.2	1.8
1.4	-16.5	1.7	-7.6	25	1.049	core	216	18.6	0.9	-7.6	1.7
1.8	-19.1	1.8	-10.2	25	1.049	core	252	18.8	1.0	-10.2	1.8
1.9	-18.7	1.9	-9.8	25	1.049	core	290	18.3	1.3	-9.8	1.9
-0.7	-18.0	1.8	-9.1	25	1.049	core	329	16.1	1	-9.1	1.8

grain 7 - isotopes

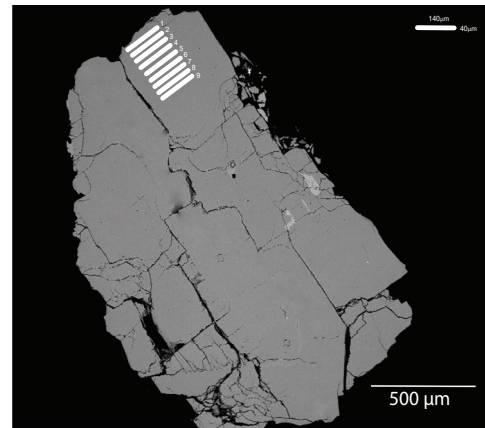


Fig. B2. BSE image of plagioclase grain 7 with Fs-LA-MC-ICP-MS lines indicated.

Table B4: continued

Sm	Dm	Zr	Hf	Eu	Gd	Pb	2SD	Pb	ppm	2SD	SiO ₂	TiO ₂	Al ₂ O ₃	FeO	MgO	CaO	Na ₂ O	K ₂ O	Br	Cl	SO ₄	Total	An	mol%	Ab	mol%	Or	mol%
0.4	0	4.2	0	4.2	0	0.3	0	12.7	1	1	61.7	0.1	23.0	0.2	0.0	4.6	7.7	1.4	0.1	0.0	0.0	98.8	23					8
0.3	0	4.8	1	4.8	1	0.4	0	13.9	1	1	61.8	0.1	22.9	0.2	0.0	4.5	7.8	1.4	0.1	0.0	0.0	98.9	22					8
0.3	0	4.9	1	4.9	1	0.4	0	13.6	1	1	61.8	0.1	23.2	0.2	0.0	4.4	7.9	1.5	0.0	0.0	0.0	99.0	22					8
0.3	0	5.3	1	5.3	1	0.1	0	13.0	1	1	61.6	0.0	22.8	0.2	0.0	4.3	7.8	1.5	0.1	0.0	0.0	98.3	21					8
0.2	0	4.2	0	4.2	0	0.2	0	12.7	1	1	61.7	0.1	22.9	0.2	0.0	4.3	8.0	1.5	0.1	0.0	0.0	98.9	21					8
0.6	0	5.0	1	5.0	1	0.3	0	11.6	1	1	61.9	0.1	22.5	0.2	0.0	4.3	7.9	1.5	0.1	0.0	0.0	98.4	21					8
0.3	0	4.7	1	4.7	1	0.2	0	12.6	1	1	61.7	0.0	22.8	0.2	0.0	4.3	8.0	1.5	0.0	0.0	0.0	98.5	21					8
0.5	0	5.3	1	5.3	1	0.3	0	13.0	1	1	61.9	0.0	22.9	0.2	0.0	4.3	7.9	1.5	0.1	0.0	0.0	98.7	21					8
0.3	0	5.1	1	5.1	1	0.2	0	12.6	1	1	62.0	0.1	22.9	0.2	0.0	4.3	8.0	1.5	0.1	0.0	0.0	99.0	21					8
0.3	0	5.5	1	5.5	1	0.2	0	12.7	1	1	61.9	0.1	22.5	0.2	0.0	4.3	7.9	1.5	0.1	0.0	0.0	98.4	21					8
0.4	0	4.7	1	4.7	1	0.3	0	11.7	1	1	62.0	0.1	22.7	0.2	0.0	4.2	7.9	1.5	0.0	0.0	0.0	98.6	21					8
0.4	0	5.4	1	5.4	1	0.5	0	12.0	1	1	62.0	0.1	22.7	0.2	0.0	4.2	7.9	1.5	0.0	0.0	0.0	98.6	21					8
0.4	0	4.7	1	4.7	1	0.1	0	12.1	1	1	62.0	0.1	22.5	0.2	0.0	4.1	7.9	1.6	0.0	0.0	0.0	98.4	20					8
0.6	0	5.7	1	5.7	1	0.3	0	13.4	1	1	62.3	0.0	22.7	0.2	0.0	4.1	7.9	1.6	0.0	0.0	0.0	98.8	20					8
0.3	0	4.7	1	4.7	1	0.1	0	11.6	1	1	62.3	0.1	22.6	0.2	0.0	4.0	7.9	1.5	0.0	0.0	0.0	98.8	20					8
0.5	0	5.1	1	5.1	1	0.1	0	13.2	1	1	62.1	0.1	22.8	0.2	0.0	4.1	7.9	1.6	0.1	0.0	0.0	98.8	20					8
0.2	0	4.6	1	4.6	1	0.0	0	11.7	1	1	62.1	0.0	22.9	0.1	0.0	4.1	8.0	1.6	0.1	0.0	0.0	98.9	20					8
0.3	0	5.4	1	5.4	1	0.0	0	11.8	1	1	62.2	0.1	22.7	0.2	0.0	4.1	7.9	1.5	0.0	0.0	0.0	98.7	20					8
0.5	0	4.7	1	4.7	1	0.2	0	11.8	2	1	62.0	0.1	22.9	0.2	0.0	4.4	7.9	1.5	0.0	0.0	0.0	99.0	21					8
0.3	0	4.8	1	4.8	1	0.4	0	11.9	1	1	62.1	0.1	22.9	0.2	0.0	4.2	8.0	1.5	0.1	0.0	0.0	99.1	20					8
0.1	0	5.3	1	5.3	1	0.4	0	11.8	1	1	62.2	0.1	22.8	0.2	0.0	4.1	7.8	1.5	0.0	0.0	0.0	98.8	20					8
0.4	0	4.6	1	4.6	1	0.3	0	12.5	1	1	61.9	0.1	22.7	0.2	0.0	4.1	8.0	1.5	0.1	0.0	0.0	98.6	20					8
0.4	0	4.5	1	4.5	1	0.7	0	11.8	1	1	62.1	0.1	23.0	0.2	0.0	4.2	8.0	1.6	0.1	0.1	0.0	99.3	20					8
0.6	0	5.1	1	5.1	1	0.2	0	13.5	2	1	62.0	0.0	22.6	0.2	0.0	4.1	7.9	1.6	0.1	0.1	0.0	98.5	20					8
0.5	0	5.1	1	5.1	1	0.2	0	11.5	1	1	62.1	0.0	23.2	0.2	0.0	4.1	8.0	1.6	0.1	0.0	0.0	99.3	20					8
0.5	0	5.2	1	5.2	1	0.3	0	11.4	1	1	62.1	0.1	22.8	0.2	0.0	4.1	7.9	1.5	0.1	0.0	0.0	98.8	20					8
0.4	0	5.2	1	5.2	1	0.1	0	12.1	1	1	62.2	0.1	22.8	0.2	0.0	4.1	7.9	1.6	0.1	0.0	0.0	99.0	20					8
0.2	0	4.6	1	4.6	1	0.1	0	10.5	1	1	62.0	0.1	22.7	0.2	0.0	4.1	8.0	1.6	0.1	0.0	0.0	98.7	20					8
0.3	0	5.4	1	5.4	1	0.5	0	12.4	1	1	62.3	0.1	22.8	0.2	0.0	4.1	7.9	1.6	0.1	0.0	0.0	99.1	20					8
0.3	0	5.6	1	5.6	1	0.3	0	11.7	1	1	62.0	0.1	22.8	0.2	0.0	4.1	8.1	1.6	0.1	0.0	0.0	98.9	20					8
0.4	0	5.0	0	5.0	0	0.4	0	11.2	1	1	62.1	0.1	22.6	0.2	0.0	4.0	7.9	1.6	0.1	0.0	0.0	98.6	20					8
0.2	0	5.1	0	5.1	0	0.4	0	12.1	1	1	62.1	0.1	22.7	0.2	0.0	4.0	7.9	1.6	0.1	0.0	0.0	98.7	20					8
0.7	1	5.6	1	5.6	1	0.3	0	11.7	1	1	61.9	0.0	22.7	0.2	0.0	4.1	8.0	1.6	0.0	0.0	0.0	98.5	20					8
0.5	0	4.7	0	4.7	0	0.3	0	10.7	1	1	62.0	0.0	22.8	0.2	0.0	4.0	7.9	1.6	0.1	0.0	0.0	98.9	20					8
0.5	0	4.8	1	4.8	1	0.2	0	11.5	1	1	61.8	0.1	22.7	0.2	0.0	4.1	7.8	1.6	0.1	0.0	0.0	98.3	20					8
0.3	0	4.8	1	4.8	1	0.5	0	11.2	1	1	61.6	0.1	22.7	0.2	0.0	4.0	8.0	1.6	0.0	0.0	0.0	98.3	20					8
0.2	0	4.9	1	4.9	1	0.5	0	11.2	1	1	62.1	0.1	22.8	0.2	0.0	4.1	7.9	1.6	0.1	0.1	0.0	98.9	20					8
0.2	0	4.9	1	4.9	1	0.2	0	11.2	1	1	62.1	0.1	22.8	0.2	0.0	4.1	7.9	1.6	0.1	0.1	0.0	98.9	20					8
0.3	0	5.4	1	5.4	1	0.7	1	12.3	1	1	61.7	0.1	22.6	0.2	0.0	4.1	8.0	1.6	0.0	0.0	0.0	98.6	20					8
0.2	0	5.4	1	5.4	1	0.4	0	12.1	1	1	62.0	0.1	22.9	0.2	0.0	4.1	7.9	1.6	0.0	0.0	0.0	98.9	20					8
0.2	0	5.2	1	5.2	1	0.4	0	11.3	1	1	61.7	0.1	22.7	0.2	0.0	4.2	7.8	1.6	0.1	0.0	0.0	98.3	21					8
0.1	0	4.8	1	4.8	1	0.1	0	11.7	1	1	62.0	0.1	22.8	0.2	0.0	4.1	8.0	1.6	0.0	0.0	0.0	98.7	20					8
0.4	0	5.1	1	5.1	1	0.3	0	12.1	1	1	61.6	0.1	22.6	0.2	0.0	4.1	8.1	1.6	0.1	0.0	0.0	98.3	20					8
0.3	0	4.9	1	4.9	1	0.7	1	12.7	2	1	61.9	0.1	22.7	0.2	0.0	4.1	7.9	1.6	0.1	0.0	0.0	98.5	20					8
0.4	0	5.6	1	5.6	1	0.3	0	12.4	1	1	61.5	0.1	22.8	0.2	0.0	4.1	7.9	1.6	0.0	0.0	0.0	98.1	20					8
0.7	0	4.7	1	4.7	1	0.2	0	11.7	1	1	62.1	0.1	22.8	0.2	0.0	4.2	8.0	1.6	0.0	0.0	0.0	99.0	20					8
0.4	0	4.4	1	4.4	1	0.3	0	11.2	1	1	62.1	0.1	22.7	0.2	0.0	4.0	8.0	1.6	0.1	0.0	0.0	98.7	20					8
0.2	0	4.8	1	4.8	1	0.2	0	11.9	1	1	61.6	0.1	22.6	0.2	0.0	4.1	7.9	1.6	0.0	0.0	0.0	98.0	20					8
0.4	0	4.9	1	4.9	1	0.4	0	12.1	1	1	62.0	0.1	22.9	0.2	0.0	4.1	8.0	1.6	0.0	0.0	0.0	98.9	20					8
0.4	0	4.6	1	4.6	1	0.2	0	11.4	1	1	61.5	0.1	22.6	0.2	0.0	4.1	7.8	1.6	0.1	0.0	0.0	98.0	20					8
0.2	0	4.4	1	4.4	1	0.5	0	10.5	1	1	61.9	0.1	22.8	0.2	0.0	4.1	8.0	1.6	0.0	0.0	0.0	98.7	20					8
0.2	0	5.1	1	5.1	1	0.1	0	11.9	1	1	61.9	0.1	22.7	0.2	0.0	4.1	7.9	1.6	0.0	0.0	0.0	98.5	20					8
0.5	0	4.9	1	4.9	1	0.3	0	12.2	1	1	61.9	0.1	22.8	0.2	0.0	4.1	8.0	1.6	0.0	0.0	0.0	98.5	20					8
0.7	0	4.7	1	4.7	1	0.2	0	11.4	1	1	61.7	0.0	22.8	0.2	0.0	4.2	7.9	1.5	0.1	0.0	0.0	98.7	20					8
0.3	0	4.9	1	4.9	1	0.3	0	11.3	1	1	61.8	0.1	22.6	0.2	0.0	4.2	7.9	1.5	0.1	0.0	0.0	98.4	21					8
0.3	0	4.3	1	4.3	1	0.2	0	11.4	1	1	61.6	0.0	22.6	0.2	0.0	4.2	7.9	1.5	0.1	0.0	0.0	98.1	21					8
0.2	0	5.3	1	5.3	1	0.2	0	11.1	1	1	61.8	0.0	22.7	0.2	0.0	4.2	7.9	1.5	0.1	0.0	0.0	98.6	21					8
0.3	0																											

Table B5: continued

Sim	ppm	2SD	Eu	ppm	2SD	Cd	ppm	2SD	Pb	ppm	2SD
0.2	0	3.0	0	0.3	0	1.8	1	1.8	1	1.8	1
0.4	0	3.7	1	0.2	0	1.0	1	1.0	1	1.0	1
0.3	0	4.9	1	0.3	0	0.9	1	0.9	1	0.9	1
0.1	0	5.9	1	0.3	0	2.7	1	2.7	1	2.7	1
0.4	0	5.2	1	0.4	0	1.8	1	1.8	1	1.8	1
0.3	0	5.4	1	0.0	0	2.1	1	2.1	1	2.1	1
0.6	0	5.2	1	0.1	0	2.9	1	2.9	1	2.9	1
0.6	0	4.8	1	0.8	0	1.5	1	1.5	1	1.5	1
0.4	0	5.8	1	0.4	0	1.9	1	1.9	1	1.9	1
0.2	0	4.9	1	0.3	0	2.8	1	2.8	1	2.8	1
0.6	0	3.1	1	0.5	1	1.1	1	1.1	1	1.1	1
0.2	0	4.9	1	0.2	0	0.8	1	0.8	1	0.8	1
0.1	0	5.9	1	0.0	0	2.4	1	2.4	1	2.4	1
0.6	0	5.5	1	0.1	0	2.3	1	2.3	1	2.3	1
0.5	0	5.1	1	0.2	0	1.5	1	1.5	1	1.5	1
0.2	0	5.7	1	0.1	0	1.9	1	1.9	1	1.9	1
0.5	0	4.6	0	0.5	0	2.7	1	2.7	1	2.7	1
0.4	0	5.0	0	0.4	0	1.9	1	1.9	1	1.9	1
0.3	0	4.8	0	0.2	0	1.3	2	1.3	2	1.3	2
0.6	0	3.9	0	0.5	0	1.8	1	1.8	1	1.8	1
0.2	0	3.3	0	0.2	0	1.6	1	1.6	1	1.6	1
0.2	0	3.1	0	0.0	0	1.2	1	1.2	1	1.2	1
0.3	0	3.0	0	0.2	0	1.9	1	1.9	1	1.9	1
0.4	0	5.3	1	0.4	0	1.6	1	1.6	1	1.6	1
0.3	0	6.1	0	0.2	0	2.5	1	2.5	1	2.5	1
0.7	0	5.4	0	0.5	0	1.2	1	1.2	1	1.2	1
0.4	0	5.7	0	0.3	0	1.7	1	1.7	1	1.7	1
0.5	0	4.4	0	0.4	0	1.1	1	1.1	1	1.1	1
0.4	0	5.0	0	0.3	0	2.0	1	2.0	1	2.0	1
0.5	0	4.8	0	0.0	0	2.0	1	2.0	1	2.0	1
0.0	0	4.8	0	0.3	1	3.0	2	3.0	2	3.0	2
0.5	0	5.0	0	0.1	0	2.1	1	2.1	1	2.1	1
0.1	0	5.3	1	0.1	0	2.1	1	2.1	1	2.1	1
0.3	0	5.2	0	0.4	0	1.3	1	1.3	1	1.3	1
0.2	0	5.6	0	0.3	0	1.5	1	1.5	1	1.5	1
0.6	0	6.2	0	0.5	0	2.8	1	2.8	1	2.8	1
0.4	0	5.5	0	0.2	0	2.4	2	2.4	2	2.4	2
0.2	0	3.3	0	0.2	0	2.4	1	2.4	1	2.4	1
0.5	0	3.1	0	0.1	0	2.8	1	2.8	1	2.8	1
0.2	0	3.0	0	0.2	0	2.5	1	2.5	1	2.5	1
0.6	0	4.8	0	0.4	0	2.4	1	2.4	1	2.4	1
0.9	1	5.6	0	0.2	0	2.8	1	2.8	1	2.8	1
0.8	0	5.4	0	0.3	0	0.8	1	0.8	1	0.8	1
0.5	0	5.2	0	0.3	0	0.8	1	0.8	1	0.8	1
0.6	0	4.5	0	0.1	0	2.0	2	2.0	2	2.0	2
0.2	0	5.9	0	0.2	0	2.9	1	2.9	1	2.9	1
0.6	0	5.8	0	0.6	0	1.6	2	1.6	2	1.6	2
0.0	0	3.1	0	0.2	0	2.5	1	2.5	1	2.5	1
0.4	0	3.0	0	0.5	0	0.8	1	0.8	1	0.8	1
0.4	0	3.4	0	0.3	0	2.1	1	2.1	1	2.1	1
0.5	0	3.8	0	0.4	0	2.2	1	2.2	1	2.2	1
0.3	0	5.8	0	0.4	0	2.1	20	2.1	20	2.1	20
0.5	0	5.4	0	0.0	0	1.0	1	1.0	1	1.0	1
0.5	1	5.6	0	0.4	0	2.1	1	2.1	1	2.1	1
1.0	0	4.7	0	0.2	0	2.8	1	2.8	1	2.8	1

Table B5: continued

rim	323	20.3	3	18.7	1	56621	3243	19.6	5	124083	7652	12173	541	25936	2642	47.4	9	1454	104	3.1	1	178	10	584	39	20.3	2	23.3	2	1.4	0	4.3	1	10.5	0
rim	328	17.6	2	17.6	1	57304	4281	18.4	4	118692	7157	12199	736	27243	2356	47.0	14	1480	161	3.7	1	179	11	582	41	20.8	2	23.3	2	1.9	0	4.8	1	10.3	0
rim	333	17.8	3	17.3	1	65323	8000	30.4	7	122341	4126	12804	623	27031	1719	55.2	8	1490	125	3.8	1	178	8	630	45	20.1	2	23.5	2	1.7	0	4.0	1	10.3	0
rim	338	15.1	3	17.2	3	54885	2740	19.9	6	115845	5273	12377	737	25708	1762	39.1	10	1366	141	3.7	1	174	11	572	20	19.5	2	22.7	2	1.5	0	3.0	1	10.5	0
rim	343	14.3	2	14.3	2	56245	3256	21.4	5	118174	7115	12175	629	27285	2572	56.7	10	1393	118	3.3	1	172	10	575	45	20.2	2	22.6	2	1.2	0	5.5	1	10.4	1
rim	348	13.1	3	13.4	2	55477	2618	21.7	6	119848	5112	12133	481	25996	1789	44.0	14	1433	127	3.7	1	177	7	607	41	19.3	2	23.2	2	1.7	0	4.1	1	10.3	0
rim	353	11.1	2	12.4	2	58116	3487	27.0	6	123880	7225	12424	674	24817	1727	54.7	9	1459	155	3.3	1	182	15	648	51	22.7	2	23.1	2	1.6	0	4.0	1	10.3	0
rim	358	11.6	4	10.2	2	56111	3269	18.9	6	118752	6493	12361	743	27747	2304	47.8	14	1397	114	3.6	1	171	14	605	47	20.6	2	21.3	2	1.3	0	4.6	1	10.2	0
rim	363	8.0	2	8.8	1	54709	2296	19.5	4	118646	4925	12297	467	25249	1642	52.5	13	1336	133	4.1	1	168	10	601	42	20.0	1	23.4	2	1.6	0	3.5	1	10.3	0
rim	368	6.6	2	7.3	2	55570	3497	29.3	8	116211	7007	11660	562	26554	2040	46.8	11	1387	136	3.9	1	172	12	613	45	20.4	2	22.0	2	1.6	0	4.4	1	10.7	0
rim	373	4.5	2	5.9	1	56470	2800	28.4	5	120017	5127	12847	811	26317	1920	51.2	10	1418	131	3.9	1	169	11	632	38	20.8	2	22.7	2	1.6	0	3.4	1	10.5	0

Table B5: continued

4.8	1	0.3	0	11.5	1
4.7	1	0.0	0	11.4	2
5.6	0	0.8	1	11.7	1
4.9	1	0.2	0	12.0	1
5.6	1	0.2	0	11.2	1
4.9	1	0.5	0	11.4	1
4.5	1	0.8	1	12.5	1
4.7	1	0.2	0	12.2	1
5.1	1	0.5	1	12.2	1
5.0	1	0.3	0	11.7	1
4.6	1	0.1	0	12.4	2

grain 11 - Line 1.2

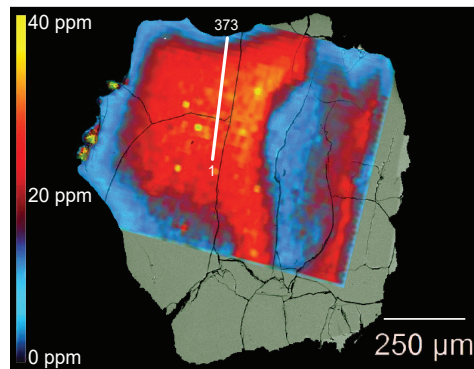


Fig. B4. BSE image of plagioclase grain 11 with trace element line 1.2 (by LA-ICP-MS) indicated.

grain 11 - Line 2

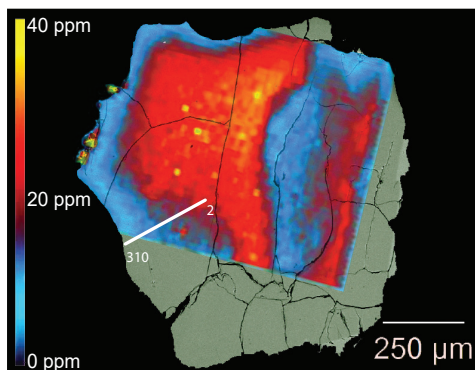


Fig. B5. BSE image of plagioclase grain 11 with trace element line 2 (by LA-ICP-MS) indicated.

grain 11 - Isotopes

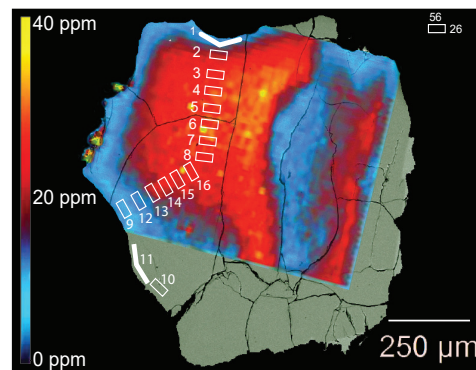


Fig. B6. BSE image of plagioclase grain 11 with Fs-LA-MC-ICP-MS lines indicated.

Table B6: Plagioclase grain 11 - Line 2

	Distance	L ¹⁶	J ¹⁶	J ¹⁶	Na	Mg	Al	Si	Ca	Ti	Fe	Rb	Sr	Ba	La	Ce	Pr	Nd	ppm															
cracked	2	23.0	3	22.8	3	57125	2439	23.3	5	16216	3868	12167	764	23078	991	51.1	6	1473	116	3.8	183	9	469	27	21.2	1	22.1	2	23.4	1	5	0	4.3	1
cracked	6	23.5	2	21.1	1	64741	13319	25.2	7	18850	5345	2470	681	26659	1975	55.1	14	464	118	3.8	187	11	487	30	21.5	2	23.4	1	22.3	2	16	0	4.8	1
cracked	11	24.2	4	22.5	2	72727	3001	21.6	6	17902	5210	1833	584	20959	1935	50.4	11	459	124	4.8	189	11	479	30	21.5	2	23.3	2	16	0	4.3	1		
cracked	16	20.1	4	22.4	3	57059	5223	18.6	5	11749	7609	11890	987	24501	2499	50.0	6	432	117	3.6	184	14	456	32	20.2	2	23.0	2	16	0	3.9	1		
cracked	21	24.4	3	21.0	2	55899	2455	21.1	6	18093	4133	12121	595	27411	1455	55.0	11	427	117	3.9	187	12	504	32	21.0	1	22.9	2	15	0	4.2	1		
cracked	26	22.6	3	21.1	2	54782	2823	23.0	5	118292	6203	12214	676	28035	2487	42.3	10	388	148	3.7	194	12	493	25	21.0	2	22.9	2	14	0	4.2	1		
cracked	31	19.0	3	20.5	2	57790	5469	22.7	7	21614	7182	12914	615	28288	2400	47.2	9	379	145	3.4	201	13	492	37	23.3	2	24.3	2	20	0	3.7	1		
cracked	36	19.5	3	20.0	2	56623	3655	20.5	8	21584	6654	12148	594	26684	1956	48.8	10	436	130	3.3	195	13	483	27	23.1	2	23.3	2	15	0	4.8	1		
cracked	41	17.4	2	19.1	1	56988	4330	24.9	3	21880	6144	12775	941	27944	2178	50.9	12	581	154	4.4	201	13	512	35	22.4	2	23.9	2	14	0	3.8	1		
cracked	46	18.6	3	19.8	1	55888	3366	24.5	6	18200	5158	12043	776	27184	1738	48.6	10	412	123	3.4	187	12	495	31	21.0	1	23.1	1	15	0	3.8	1		
cracked	51	18.6	3	19.4	1	54266	2356	19.1	6	20165	4848	12035	588	26884	2011	47.9	12	542	124	4.0	193	8	512	37	22.4	2	23.7	2	15	0	4.0	1		
cracked	56	19.8	2	19.4	2	56407	4940	22.1	7	21294	7737	12210	770	27369	2481	51.2	16	411	112	4.5	195	14	519	37	22.1	2	24.4	2	14	0	3.4	1		
cracked	61	19.3	3	18.8	2	53883	3613	17.5	6	16328	5795	11773	694	26743	1790	46.0	9	271	111	3.4	191	15	503	30	20.9	2	24.6	3	15	0	4.5	1		
cracked	66	19.3	3	18.9	1	53683	1530	20.6	6	23365	4440	12672	782	27618	1828	50.4	7	496	165	3.8	196	7	500	29	22.4	2	23.6	1	17	0	4.5	1		
cracked	71	17.6	3	19.6	2	56392	2654	22.2	7	18202	5540	12203	600	25869	1228	46.3	14	430	146	3.5	186	10	508	26	22.2	2	23.6	2	17	0	4.7	1		
cracked	76	19.4	3	19.3	2	55506	3391	20.8	3	17611	6585	12310	734	25673	1939	49.9	10	536	138	3.8	180	11	494	32	22.3	2	24.1	2	16	0	4.7	1		
cracked	81	21.5	3	19.0	2	55137	3304	18.2	6	17511	7408	12287	898	26726	2320	46.3	10	491	185	4.8	191	13	504	34	22.7	2	23.3	2	19	0	3.7	1		
cracked	86	18.3	2	17.5	2	53857	2917	20.5	5	18855	6656	12301	653	28112	2514	54.3	7	450	196	3.2	193	13	504	37	22.7	2	24.5	2	18	0	3.2	1		
cracked	91	20.0	4	18.2	2	56131	4132	20.6	7	20834	8239	12332	1101	27342	1813	42.1	11	380	98	3.7	191	13	503	34	21.6	2	25.1	2	16	0	4.6	2		
cracked	96	17.2	3	17.5	2	57694	4893	20.0	6	17239	7085	13005	978	27464	2009	52.1	13	444	175	3.6	188	11	502	29	22.5	2	24.1	2	17	0	5.0	1		
cracked	101	17.9	3	17.1	2	55959	5815	21.3	7	17286	5252	12102	645	26824	2391	59.1	12	345	141	4.3	192	9	509	25	22.2	2	24.1	2	16	0	4.0	1		
cracked	106	8.7	3	17.3	2	53983	3060	18.3	6	19133	8404	12105	831	27527	2467	47.7	12	359	117	3.8	188	17	512	39	23.8	2	25.3	2	18	0	3.9	1		
cracked	111	6.2	3	15.2	1	54359	2785	22.9	4	21414	7683	12608	1130	27283	2395	56.4	3	385	93	3.7	184	11	506	34	22.3	2	22.7	2	15	0	5.2	1		
cracked	116	5.6	3	15.5	1	52661	3023	27.6	11	17611	4474	12092	696	25622	1483	61.6	3	415	154	3.5	184	11	503	32	22.0	2	22.2	2	18	0	4.4	1		
cracked	120	5.5	2	18.2	2	53868	3247	24.3	5	23894	6197	12899	827	28410	2211	57.5	15	439	140	3.6	198	15	531	37	23.5	2	25.5	2	17	0	4.4	1		
cracked	125	6.7	2	17.9	2	57479	3256	22.8	5	19676	4463	12565	848	27101	1518	57.0	10	481	134	3.1	193	11	545	30	21.5	2	24.1	2	14	0	4.9	1		
cracked	130	5.4	4	14.9	1	53512	4301	27.3	6	14516	8665	11555	959	26277	2674	55.9	12	269	149	3.7	187	15	471	36	20.5	2	23.0	2	17	0	5.1	1		
cracked	135	6.4	4	15.6	2	54547	4361	19.2	5	12633	8227	11655	868	26105	2559	54.9	12	420	230	4.3	179	14	487	44	19.8	2	22.7	3	16	0	4.9	1		
cracked	140	7.8	3	15.8	2	56432	3666	23.0	9	20932	7125	12102	888	27213	1791	63.4	14	487	106	3.9	188	10	502	38	22.4	2	23.8	2	16	0	4.4	1		
cracked	145	14.7	2	15.2	2	62502	10127	17.7	6	19401	4618	11904	616	28271	2097	49.8	11	308	123	4.0	190	10	492	24	23.3	2	24.1	2	17	0	4.4	1		
cracked	150	15.7	4	14.7	2	56479	3431	21.6	6	22256	5378	12196	620	28459	2470	43.3	9	401	114	4.4	195	8	515	36	22.9	1	24.2	2	16	0	4.5	1		
cracked	155	6.2	4	17.4	2	56742	4688	20.5	7	24109	6281	12431	1228	27734	1885	58.2	12	418	140	3.2	192	9	497	39	22.6	2	24.3	2	17	0	4.7	1		
cracked	160	3.8	2	16.7	2	54550	2374	20.9	6	22143	5959	12157	851	27617	1756	67.2	12	488	131	3.4	192	13	516	28	23.8	2	25.6	2	16	0	4.8	1		
cracked	165	5.2	3	15.9	2	55581	2886	21.7	5	20762	6656	12035	784	26902	2164	62.9	13	442	115	3.9	193	14	505	27	21.9	2	24.6	2	19	0	5.2	1		
cracked	170	8.8	3	16.5	3	53965	2970	21.0	7	18271	7446	12451	1109	27836	2291	64.1	13	336	182	3.2	187	13	478	36	21.7	2	23.9	3	20	0	4.2	1		
cracked	175	6.9	2	15.8	2	54676	3349	23.6	7	17152	3980	11511	547	25052	2082	52.8	12	321	95	3.2	177	11	478	36	22.6	2	22.4	2	17	0	5.0	1		
cracked	180	7.1	3	16.8	2	58050	3330	17.6	7	21668	5849	11969	554	27611	1826	62.6	12	400	137	4.0	191	11	503	29	22.7	2	26.5	2	15	0	4.5	1		
cracked	185	5.3	3	15.0	2	55624	2338	24.0	6	19436	4409	12638	558	26573	1876	59.3	12	438	107	3.4	182	12	492	34	22.6	2	26.5	2	14	0	5.0	2		
cracked	190	14.5	2	14.2	1	59722	6372	18.8	4	16421	7104	11575	839	26415	1783	51.9	10	397	131	3.4	180	13	463	37	21.6	2	23.6	2	19	0	4.2	1		
cracked	195	17.1	3	14.6	2	56852	3900	20.0	6	20111	5704	12301	979	27955	1559	51.4	8	413	174	3.7	195	13	517	31	22.4	2	25.2	2	17	0	4.4	1		
cracked	200	16.5	4	14.9	2	60335	4890	16.5	4	22567	7502	12400	911	29441	1779	53.0	9	436	171	4.0	189	13	469	37	21.9	1	24.6	2	14	0	3.8	1		
cracked	205	3.0	1	15.5	1	55452	3554	26.2	6	19117	5085	11758	535	27079	2050	47.9	11	434	158	4.1	181	11	474	33	21.0	2	24.6	2	15	0	5.1	1		
cracked	210	8.8	5	15.6	2	56192	3965	18.7	4	20762	6923	12303	925	29821	2448	61.0	13	482	122	3.7	193	11	483	28	21.6	2	25.3	2	14	0	4.2	1		
cracked	215	6.7	2	15.7	2	56308	4769	18.2	5	19621	8748	11980	954	26978	1972	41.7	11	535	160	3.9	182	14	473	31	22.5	3	25.6	2	16	0	5.1	1		
cracked	220	4.9	2	15.6	3	58403	4884	21.1	6	19980	8979	11674	931	27264	2689	42.7	11	475	217	3.4	182	14	470	38	22.5	2	25.0	2	16	0	3.5	1		
cracked	225	1.2	2	14.3	2	55906	3890	24.1	6	11057	7																							

Table B6: continued

Sm ppm	Eu ppm	Gd ppm	Zr ppm	Pb ppm	2SD Pb ppm	Ti ppm	Al ppm	Fe ppm	Mg ppm	Ca ppm	Na ppm	K ppm	Ba ppm	Sr ppm	Total ppm	An mol%	Ab mol%	Or mol%	
0.2	0	4.5	1	0	10.9	63.2	0.1	22.7	0.2	0.0	4.2	8.1	5	0.1	0.0	100.1	20	71	9
0.3	0	4.7	1	0.4	13.0	63.4	0.0	22.8	0.2	0.0	4.2	8.0	5	0.0	0.0	100.2	21	71	9
0.2	0	4.8	1	0.4	12.6	63.1	0.0	23.0	0.2	0.0	4.2	7.9	5	0.0	0.0	99.9	21	70	9
0.1	0	4.8	1	0.3	3	63.4	0.1	22.7	0.2	0.0	4.1	7.9	5	0.1	0.0	100.0	20	71	9
0.3	0	4.8	1	0.0	2.7	63.4	0.1	22.7	0.2	0.0	4.2	7.8	5	0.0	0.0	100.0	21	70	9
0.3	0	4.9	1	0.1	13.1	63.3	0.1	22.7	0.2	0.0	4.2	7.9	5	0.0	0.0	100.4	21	70	9
0.3	0	5.5	1	0.5	12.8	63.4	0.1	22.5	0.2	0.0	4.1	7.9	5	0.1	0.0	99.8	20	71	9
0.2	0	5.5	1	0.2	13.4	63.6	0.1	22.8	0.2	0.0	4.2	7.9	5	0.1	0.0	100.5	21	70	9
1.0	1	5.3	1	0.4	12.8	63.4	0.1	22.8	0.2	0.0	4.3	7.8	5	0.1	0.0	100.3	21	70	9
0.3	0	4.7	1	0.1	12.8	63.5	0.1	22.8	0.2	0.0	4.2	8.0	5	0.1	0.0	100.2	21	71	9
0.4	0	4.3	1	0.2	12.0	63.5	0.1	22.8	0.2	0.0	4.2	7.9	5	0.1	0.0	100.3	20	71	9
0.4	0	5.2	1	0.2	11.8	63.5	0.1	22.8	0.2	0.0	4.1	8.0	6	0.1	0.0	100.2	20	71	9
0.5	0	4.9	1	0.2	12.3	63.4	0.0	22.6	0.2	0.0	4.1	8.0	5	0.1	0.0	100.0	20	71	9
0.5	0	5.2	1	0.6	12.3	63.4	0.1	22.6	0.2	0.0	4.2	7.9	5	0.1	0.0	100.0	21	71	9
0.4	0	4.6	1	0.6	4.6	63.4	0.1	22.9	0.2	0.0	4.2	7.9	5	0.1	0.0	100.2	21	70	9
0.6	0	4.8	1	0.2	12.2	63.4	0.1	22.7	0.2	0.0	4.3	7.9	5	0.2	0.0	99.8	21	70	9
0.5	0	4.7	1	0.2	12.2	63.4	0.1	22.9	0.2	0.0	4.4	7.9	5	0.0	0.0	100.5	21	70	9
0.3	0	5.5	1	0.2	12.0	63.1	0.1	22.9	0.2	0.0	4.4	7.8	5	0.0	0.0	99.8	22	70	9
0.3	0	5.5	1	0.2	11.8	63.1	0.1	22.8	0.2	0.0	4.4	7.8	5	0.0	0.0	99.9	22	70	9
0.5	0	5.4	1	0.3	12.9	63.2	0.1	22.9	0.2	0.0	4.3	7.9	4	0.0	0.0	100.0	21	71	8
0.3	0	4.8	1	0.1	12.0	63.2	0.0	22.9	0.2	0.0	4.3	7.9	5	0.1	0.0	100.1	21	70	9
0.4	0	4.7	1	0.5	12.4	63.6	0.1	23.0	0.2	0.0	4.2	7.9	5	0.1	0.0	100.5	21	71	9
0.4	0	5.1	1	0.5	11.6	63.4	0.1	23.0	0.2	0.0	4.2	7.9	5	0.1	0.0	100.2	20	71	9
0.2	0	5.0	1	0.3	11.7	63.5	0.1	22.6	0.2	0.0	4.1	7.9	5	0.0	0.0	100.0	20	71	9
0.4	0	5.3	1	0.4	12.6	63.3	0.1	22.6	0.2	0.0	4.4	8.0	5	0.1	0.0	100.0	21	70	9
0.5	0	5.4	1	0.5	11.7	63.4	0.1	23.0	0.2	0.0	4.3	7.9	5	0.0	0.0	100.4	21	70	9
0.5	0	5.2	1	0.2	10.9	63.4	0.1	22.7	0.2	0.0	4.3	7.9	5	0.0	0.0	100.1	21	70	9
0.8	1	5.2	1	0.3	11.2	63.3	0.1	22.8	0.2	0.0	4.4	7.8	5	0.0	0.0	100.2	22	70	9
0.4	0	5.0	1	0.2	12.2	63.0	0.0	22.8	0.2	0.0	4.3	7.7	5	0.1	0.0	99.7	22	70	9
0.6	0	5.1	1	0.6	12.4	63.2	0.1	22.9	0.2	0.0	4.4	7.8	5	0.1	0.0	100.2	22	70	9
0.5	0	5.5	1	0.4	11.2	63.5	0.1	23.1	0.2	0.0	4.4	7.8	4	0.1	0.0	100.3	22	70	8
0.2	0	4.7	1	0.6	11.8	63.5	0.1	22.8	0.2	0.0	4.3	7.9	5	0.1	0.0	100.4	21	70	9
0.5	0	4.4	1	0.1	11.9	63.2	0.1	22.7	0.2	0.0	4.3	7.9	5	0.0	0.0	99.9	21	70	9
0.4	0	4.8	1	0.8	11.4	63.1	0.1	22.8	0.2	0.0	4.3	7.9	5	0.0	0.0	99.9	21	70	9
0.3	0	4.8	1	0.4	13.2	63.5	0.1	22.7	0.2	0.0	4.4	7.9	5	0.1	0.0	100.4	21	70	9
0.4	0	4.8	1	0.3	11.4	63.2	0.0	23.0	0.2	0.0	4.4	7.8	4	0.0	0.0	100.2	22	70	8
0.4	0	5.1	1	0.2	12.0	63.3	0.1	22.8	0.2	0.0	4.4	7.8	4	0.1	0.0	100.1	22	70	8
0.6	0	5.1	1	0.4	11.4	63.0	0.0	23.1	0.2	0.0	4.4	7.8	4	0.0	0.0	100.1	22	70	8
0.5	0	4.9	1	0.4	12.0	63.1	0.1	22.9	0.2	0.0	4.4	7.8	4	0.1	0.0	100.1	22	70	8
0.4	0	5.0	1	0.7	12.2	62.9	0.1	22.9	0.2	0.0	4.4	7.7	5	0.1	0.0	99.8	22	70	8
0.5	0	4.9	1	0.1	12.3	63.3	0.1	23.0	0.2	0.0	4.4	7.8	4	0.0	0.0	100.3	22	70	8
0.5	0	5.5	1	0.2	12.7	63.3	0.1	22.8	0.2	0.0	4.3	7.8	5	0.1	0.0	100.1	21	70	9
0.7	1	5.0	1	0.2	12.5	63.4	0.1	22.8	0.2	0.0	4.3	7.9	5	0.0	0.0	100.2	21	70	9
0.6	1	5.3	1	0.4	13.1	63.4	0.1	22.8	0.2	0.0	4.3	7.9	5	0.1	0.0	100.2	21	70	9
0.4	0	4.6	1	0.3	12.2	63.2	0.1	22.6	0.2	0.0	4.4	7.8	4	0.2	0.0	99.8	22	70	8
0.4	0	4.7	1	0.5	12.9	63.2	0.1	22.9	0.2	0.0	4.3	7.6	4	0.1	0.0	99.9	22	69	8
0.5	0	4.4	1	0.4	10.6	62.9	0.1	23.0	0.2	0.0	4.3	7.9	4	0.1	0.0	100.0	22	70	8
0.5	0	4.4	1	0.4	11.4	63.3	0.1	22.8	0.2	0.0	4.3	7.8	4	0.0	0.0	100.2	22	69	8
0.5	0	4.3	1	0.3	12.3	63.4	0.1	23.0	0.2	0.0	4.4	7.9	5	0.0	0.0	100.4	22	70	8
0.3	0	5.5	1	0.1	11.7	63.3	0.1	22.6	0.2	0.0	4.2	7.8	5	0.0	0.0	99.8	21	70	8
0.2	0	4.4	1	0.1	12.5	62.8	0.1	22.8	0.2	0.0	4.3	8.0	5	0.1	0.0	99.7	21	70	8
0.3	0	4.5	1	0.1	11.7	63.0	0.1	23.0	0.2	0.0	4.3	7.9	5	0.0	0.0	99.9	21	70	9
0.4	0	4.5	1	0.2	12.2	63.0	0.0	23.1	0.2	0.0	4.4	7.8	4	0.1	0.0	100.0	22	70	8
0.3	0	4.9	1	0.2	12.1	63.0	0.0	23.1	0.2	0.0	4.5	7.9	4	0.1	0.0	100.0	22	70	8
0.2	0	4.6	1	0.6	12.4	62.7	0.1	23.5	0.2	0.0	4.6	7.9	4	0.1	0.0	100.2	22	70	8
0.5	0	4.6	1	0.7	11.2	62.5	0.1	23.6	0.2	0.0	4.7	7.7	4	0.0	0.0	100.1	23	69	8
0.1	0	4.9	1	0.2	11.7	62.1	0.1	23.6	0.2	0.0	4.9	7.8	3	0.1	0.0	100.2	24	69	8
0.3	0	4.7	1	0.2	11.4	62.3	0.1	23.5	0.2	0.0	4.9	7.7	3	0.1	0.0	100.0	24	68	7
0.2	0	5.2	1	0.6	11.7	62.4	0.0	23.4	0.2	0.0	4.7	7.8	3	0.1	0.0	99.9	23	69	8
0.3	0	4.7	1	0.2	11.8	62.8	0.1	23.4	0.2	0.0	4.8	7.8	3	0.1	0.0	100.5	23	69	8
0.5	0	5.1	1	0.1	12.0	63.0	0.1	23.2	0.2	0.0	4.5	7.9	4	0.0	0.0	100.3	22	70	8
0.3	0	5.1	1	0.3	12.8	63.2	0.0	22.9	0.2	0.0	4.2	8.0	5	0.0	0.0	100.0	21	71	8
0.4	0	4.1	1	0.2	12.3	63.1	0.0	22.9	0.2	0.0	4.2	8.0	5	0.0	0.0	100.0	20	71	9

Table B7: Plagioclase grain 11 - Lithium isotopes

Run	0.5 pt		background		Results (BLK + tau corr.)		D time (min)	std drift	δ ⁷ Li (‰)	rel GOR132-G	2 σ			
	⁷ Li (V)	⁶ Li (cps)	⁶ Li (V)	⁷ Li (V)	6Li (cps)	⁷ Li/ ⁶ Li						SE	SD	1 RSD
1	0.0070	32362.7836	0.0005	0.0001	697.5950	13.3574	0.0134	0.1038	1003	60	15.1	1.6	-5.7	2.5
2	0.0158	73725.3802	0.0012	0.0001	674.1693	13.3222	0.0086	0.0910	649	110	6.1	-0.8	-7.9	1.9
3	0.0177	83128.5559	0.0013	0.0001	613.0078	13.3035	0.0073	0.0763	552	107	4.9	0.5	-9.5	1.8
4	0.0142	66626.4843	0.0011	0.0001	574.7694	13.2871	0.0077	0.0836	577	119	4.8	-1.1	-11.0	1.9
5	0.0117	55363.6839	0.0009	0.0001	565.1176	13.2800	0.0098	0.1013	734	109	5.0	1.1	-11.5	2.0
6	0.0123	57731.7148	0.0009	0.0001	446.0795	13.2792	0.0089	0.0948	672	113	4.9	1.3	-10.5	2.3
7	0.0118	55213.5691	0.0009	0.0001	443.4655	13.2875	0.0075	0.0805	567	117	4.1	-1.3	-9.9	2.0
8	0.0097	45077.8599	0.0007	0.0001	736.3028	13.4737	0.0111	0.1184	827	114	4.6	0.7	-7.8	2.1
9	0.0059	27474.2157	0.0004	0.0001	590.4535	13.3128	0.0158	0.1222	1185	60	8.0	-0.3	-8.6	2.7
10	0.0031	14732.1037	0.0002	0.0001	552.0140	13.3275	0.0214	0.1598	1602	55	6.9	0.7	-7.3	3.5
11	0.0032	15210.1102	0.0002	0.0001	530.7668	13.3162	0.0156	0.1708	1171	119				

Table B7: Plagioclase grain 13 - Line 1.1

ID	Distance [μm]	L _a [ppm]	L _b [ppm]	L _c [ppm]	Na [ppm]	Mg [ppm]	Si [ppm]	Al [ppm]	Ca [ppm]	Ti [ppm]	Fe [ppm]	Rb [ppm]	Sr [ppm]	Ba [ppm]	La [ppm]	Ce [ppm]	Pr [ppm]	Nd [ppm]																		
core	0	27.1	2.2	0	49731	1221	35.3	3	107456	34	8055	92	28888	30	28888	1	1.9	0	4.6																	
core	3	26.5	3	26.6	1	55627	2049	23.9	6	25217	3029	9406	341	32036	1060	76.5	3	356.2	3	8.0																
core	8	30.1	3	26.5	1	20459	5508	91.48	389	33074	2651	85.8	3	1605	147	2.6	1	26.3	0	5.7																
core	13	30.1	3	27.5	2	54529	2351	27.9	7	20859	4567	9275	385	32926	1722	75.3	4	179	168	3	6.9															
core	18	30.0	3	26.8	2	54149	2332	25.6	8	33738	4708	9099	355	32575	2342	84.4	8	630	39	34.8	2	7.2														
core	23	30.0	3	27.5	1	56666	2277	30.3	6	32632	4670	9440	437	33991	2584	77.3	3	717	148	2.5	0	7.5														
core	28	27.6	3	25.3	1	54673	1987	32.4	8	26055	4418	9077	334	33756	1952	78.5	6	555	44	35.6	2	6.1														
core	33	26.4	4	25.6	2	55307	3430	25.4	11	29757	8280	9427	595	35654	2498	84.4	4	1846	133	32.1	2	6.9														
core	38	26.2	4	25.0	2	53005	2171	29.4	11	25393	8280	9427	595	35654	2498	84.4	4	1846	133	32.1	2	6.9														
core	43	26.3	3	24.5	2	54034	1786	30.2	7	38331	3077	9077	331	33250	1998	81.7	4	1647	117	2.6	1	7.0														
core	48	23.3	3	22.3	1	54815	2911	30.9	8	30865	5417	9143	357	36065	1863	80.2	5	1618	149	2.8	1	6.7														
core	53	20.2	2	19.6	1	52488	2188	27.4	7	22429	6325	8653	286	33180	1548	76.9	4	1607	115	2.8	1	7.4														
core	58	17.1	2	17.1	1	50640	2828	24.7	6	21630	4195	8510	306	33180	1548	76.9	4	1607	115	2.8	1	7.4														
crack	63	18.0	3	16.5	1	51176	2630	28.7	5	31083	6659	9233	510	34990	2966	83.1	4	1636	162	2.4	0	5.5														
crack	68	16.1	2	14.2	1	53929	2763	32.7	7	28709	5271	9198	398	34561	2297	81.1	3	1687	49	35.5	2	6.2														
crack	73	13.9	3	12.6	1	55981	3815	32.3	8	32780	9521	9531	615	35591	2821	77.3	11	623	180	2.9	1	6.3														
crack	78	11.3	2	10.0	1	58962	3926	31.6	9	37391	7068	9833	542	37300	2466	87.9	12	1817	190	3.2	1	8.3														
crack	83	9.6	2	8.0	1	56423	3677	37.2	8	33733	7619	9473	471	36655	2570	91.3	14	1602	150	2.3	1	8.4														
crack	88	6.6	2	6.6	1	56708	1913	28.5	5	33464	4243	9294	437	35847	2950	77.3	16	1737	129	2.7	1	8.8														
crack	93	7.0	2	6.3	1	53495	2383	34.9	7	33495	6194	9432	441	34827	2081	95.3	18	1619	175	2.0	1	9.2														
crack	98	5.3	1	7.0	1	57218	2386	27.8	7	37597	4336	9723	347	36595	2098	80.9	2	1667	186	2.0	1	8.0														
crack	103	6.8	2	7.8	1	55523	2942	31.4	8	30740	7064	9166	498	33421	2728	86.3	20	1617	192	2.2	1	8.0														
crack	108	8.4	2	9.5	2	53864	2454	22.9	5	25225	5462	8964	359	34098	2204	70.6	2	1665	153	2.5	1	7.0														
crack	113	10.8	2	11.7	2	54361	3248	26.0	6	26994	6872	8781	452	35245	2650	81.5	2	1556	135	2.8	1	7.8														
crack	118	16.9	3	14.1	1	56873	4446	32.5	8	34278	9118	9239	611	34987	3336	92.7	4	580	131	2.4	1	8.8														
crack	123	16.0	3	15.0	1	53642	2009	24.2	9	25480	5096	8682	335	34330	2299	84.5	16	666	140	2.6	1	7.9														
crack	127	17.6	3	17.0	2	53657	2798	24.5	7	28337	6491	8891	501	33782	2405	81.3	3	531	152	2.6	1	7.7														
core	132	20.8	3	20.6	2	54716	2425	29.2	8	30260	4709	9022	379	34044	1720	81.0	15	1723	161	2.3	1	8.2														
core	137	23.3	3	21.5	1	54986	2628	35.8	6	32103	7217	9266	475	36307	2515	80.1	12	1649	131	2.0	1	7.9														
core	142	23.7	4	22.7	1	52505	2228	33.5	9	28184	5683	8853	412	33600	2578	74.6	2	1611	165	2.5	1	7.5														
core	147	28.2	3	25.0	1	53508	3266	30.9	8	29754	7621	8847	527	33982	2985	76.7	4	1696	227	2.4	1	7.3														
core	152	28.0	3	26.1	2	55275	2016	40.9	11	33390	5182	9191	394	36485	2514	92.8	4	1658	154	2.6	1	8.2														
core	157	28.7	3	27.0	2	56738	3160	44.4	12	33588	2613	78.3	5	1735	175	2.3	1	276	17	739	40	37.0	4	41.5	2	3.0	1	8.2								
core	162	26.6	3	25.7	1	54091	2762	28.0	6	29914	6591	9099	391	33947	2284	78.8	16	739	40	37.0	4	41.5	2	3.0	1	8.2										
core	167	29.1	4	26.3	1	51726	2855	19.3	3	28360	7077	8638	451	33308	2335	95.4	8	1666	140	2.6	1	7.9	2	2.9	1	7.9	2	2.9	1	7.9						
core	172	27.6	3	26.3	1	54650	2364	25.1	6	29469	5222	8737	457	33275	2941	84.5	3	698	97	1.9	1	268	15	750	42	36.7	2	38.8	3	39.0	2	4.0	2	7.7	2	7.7
core	177	27.6	3	26.3	1	53638	3088	32.0	8	22713	7230	8909	436	34477	3049	87.7	5	1635	147	2.8	1	257	18	684	36	33.6	2	40.6	3	3.0	1	7.7	1	7.7		
core	182	25.6	3	26.8	1	53172	2544	28.4	7	25240	4230	8437	352	34911	1339	71.8	12	1550	148	2.9	1	280	13	689	33	35.7	3	40.7	3	2.0	1	7.4	1	7.4		
core	187	26.7	4	26.4	2	54003	3071	26.9	7	29412	6723	8814	508	36378	3007	76.8	11	1502	91	2.8	1	254	16	693	40	36.3	3	40.4	3	2.7	0	8.5	2	8.5		
core	192	28.7	3	27.2	2	54054	3071	26.9	7	29412	6723	8814	508	36378	3007	76.8	11	1502	91	2.8	1	254	16	693	40	36.3	3	40.4	3	2.7	0	8.5	2	8.5		
core	197	29.9	4	28.2	2	54168	2519	28.2	6	30515	6120	9020	423	36214	2125	73.8	5	1716	145	1.7	1	254	9	700	42	37.8	2	38.8	2	2.8	0	8.5	2	8.5		
core	202	27.6	3	27.2	2	54441	3727	22.0	9	29198	7780	8969	523	36611	2828	84.2	7	1678	223	2.5	1	249	14	710	57	34.9	3	40.3	3	2.6	0	9.3	2	9.3		
core	207	29.4	4	26.5	3	51990	5118	23.1	5	27192	12962	8325	758	35847	3868	80.6	9	523	193	2.2	1	240	25	678	71	36.7	4	38.6	4	3.3	1	8.9	2	8.9		
core	212	28.2	3	29.1	2	53159	3843	29.6	7	32190	9605	8580	500	36349	2738	100.1	4	1611	192	2.0	1	253	17	666	60	36.6	3	40.2	4	2.5	0	9.5	2	9.5		
core	217	30.6	4	28.6	2	54719	1925	26.8	8	30015	4926	8858	353	36116	2666	101.4	4	1611	192	2.0	1	253	17	666	60	36.6	3	40.2	4	2.5	0	9.5	2	9.5		
core	222	30.8	3	27.2	2	53039	3353	22.9	6	29430	6604	8846	350	36038	2845	86.9	10	536	153	2.3	1	255	14	685	44	37.1	3	40.0	3	2.4	0	7.8	2	7.8		
core	227	27.1	3	28.0	2	54474	2625	27.5	6	34310	7209	8795	399	36568	2292	82.1	14	1468	125	2.3	1	256	15	658	43	35.8	3	39.4	4	2.8	0	7.0	2	7.0		
core	232	26.7	3	28.7	3	54891	2110	22.4	7	32414	4026	8824	280	36577	2022	84.2	20	1559	186	2.4	1	242	11	658	39	38.6	2	39.0	3	2.9	0	7.9	1	7.9		
core	237	29.4	3	26.4	2	55784	3699	26.9	7	30345	6472	8674	455	35866	2975	88.4	13	1413	142	2.1	1	245	18	658	35	37.1	3	38.1	2	3.0	1	6.9	1	6.9		
core	242	32.2	4	29.0	2	55234	2736	28.3	7	32340	5612	9056	450	37341	2260	69.8	19	1386	154	2.9	1	250	19	687	41	36.1	3	39.9	3	2.4	0	8.6	2	8.6		
core	247	30.3	4	28.3	1	55694	2522	28.5	6	33208	6256	8970	526	38476	2193	87.3	16	1574	160	2.4	1	247	13	688	49	36.1	3	39.5	3	3.1	1	6.4	1	6.4		
core	252	28.5	4	26.5	2	52564	2669	26.8	6	29412	6723	8814	508	36378	3007	76.8	11	1502	91	2.8	1	254	16	693	40	36.3	3	40.4	3	2.7	0	8.5	2	8.5		
core	257	25.3	3	26.7	1	51908	2095	25.5	7	25250	4079	8323	285	34898	2064	77.9	4	1483	125	1.8	1	233	12	603	29	32.5	3	35.8	2	2.4	0	6.8	2	6.8		
core	262	27.5	4	27.2	2	52518	3337	19.6	8	31148	5300	8651	407	36112	2039	85.9	16	520	111	2.4	1	228	11	585	46	33.										

Table B7: continued

Sm ppm	Zr ppm	Hf ppm	Th ppm	U ppm	2SD Pb ppm	2SD Cd ppm	2SD Sr ppm	2SD Ba ppm	2SD SrO	2SD SiO ₂	2SD TiO ₂	2SD Al ₂ O ₃	2SD FeO	2SD MgO	2SD CaO	2SD Na ₂ O	2SD K ₂ O	2SD BaO	2SD SrO	Total	An mol%	Ab mol%	Or mol%	
1.3	2.8	1	0.9	9.6	2																			
0.4	0	0	0.4	0	2.8	1	0.9	9.6	2															
0.5	0	3.9	1	0.3	0	4.2	1																	
0.4	0	4.4	1	0.4	0	3.9	1																	
0.7	0	4.8	1	0.3	0	3.0	1																	
0.6	0	4.8	1	0.7	0	4.6	2																	
0.5	0	5.9	1	0.7	0	3.9	1																	
1.1	1	4.6	1	0.3	0	3.4	1																	
0.8	1	4.7	1	0.9	1	2.7	1																	
0.7	1	5.4	1	0.3	0	2.7	1																	
0.6	0	5.2	1	0.4	0	3.0	1																	
0.4	0	5.1	1	0.3	0	3.0	1																	
0.6	0	4.6	1	0.4	0	1.7	1																	
0.9	1	4.2	1	0.8	1	2.5	1																	
0.3	0	5.0	1	0.4	0	2.6	1																	
0.6	0	4.7	1	0.8	0	3.2	1																	
0.3	0	5.2	1	0.4	1	3.0	1																	
0.8	1	5.1	1	1.0	1	3.4	1																	
1.1	1	4.8	1	0.4	0	2.5	1																	
0.5	0	5.5	1	0.8	1	2.8	1																	
0.5	0	5.1	1	0.3	0	3.8	1																	
0.7	0	4.3	1	0.4	1	2.3	1																	
1.0	1	4.9	1	0.7	1	2.0	1																	
0.5	0	4.7	1	0.2	0	1.1	1																	
0.9	1	5.5	1	0.2	0	2.4	1																	
0.4	0	4.9	1	0.3	0	2.1	1																	
0.5	0	4.9	1	0.1	0	1.9	1																	
1.2	1	4.9	1	1.1	1	2.4	1																	
1.0	1	4.6	1	0.8	1	3.1	1																	
0.7	0	4.7	1	0.1	0	3.1	1																	
0.5	0	4.4	1	1.2	1	2.4	1																	
0.5	0	4.9	1	0.3	1	3.0	1																	
0.9	1	5.3	1	0.2	0	3.2	1																	
0.5	0	5.4	1	0.9	1	2.6	1																	
1.0	1	5.2	1	0.5	1	1.5	1																	
0.5	1	4.6	1	0.1	0	2.3	1																	
0.7	0	5.1	1	1.5	1	2.3	1																	
0.5	0	5.2	1	0.5	1	1.8	1																	
1.2	1	5.2	1	1.0	1	2.6	1																	
1.2	1	6.1	1	0.8	0	2.5	1																	
1.1	1	5.8	1	0.7	0	0.9	1																	
1.0	1	5.3	1	0.7	1	1.2	1																	
0.5	0	5.1	1	0.9	1	1.6	2																	
1.1	1	5.6	1	0.8	1	2.0	1																	
0.9	0	5.4	1	0.9	1	3.0	1																	
0.8	1	4.9	1	0.3	0	3.1	1																	
0.4	0	4.9	1	0.3	0	3.1	1																	
0.8	1	5.4	1	0.6	0	3.2	1																	
0.7	1	5.5	1	0.4	0	2.2	1																	
0.7	1	6.1	1	0.4	1	2.6	1																	
0.5	0	5.8	1	0.3	0	1.3	1																	
0.6	0	4.8	1	0.2	0	1.3	1																	
0.4	0	5.1	1	0.4	0	1.4	1																	
0.8	1	5.3	1	0.5	0	2.5	1																	
0.7	0	5.1	1	0.5	1	0.9	1																	
1.1	1	5.6	1	0.4	0	2.1	1																	
1.1	1	4.9	1	1.1	1	3.1	1																	
0.4	0	4.9	1	1.1	1	1.4	1																	
1.0	1	5.8	1	0.6	1	1.4	1																	
0.6	0	5.3	1	0.3	0	2.6	2																	
0.5	0	5.9	1	0.8	1	1.3	1																	
0.5	0	4.6	1	0.4	0	2.4	1																	
0.4	0	4.9	1	0.3	0	2.7	1																	
0.7	0	4.6	1	0.5	1	2.5	2																	
1.0	1	5.3	1	0.5	1	2.1	1																	

grain 13 - Line 1.1

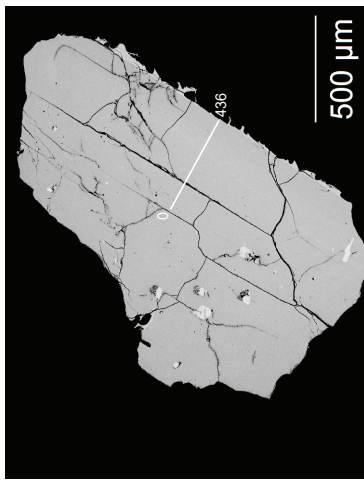


Fig. B7. BSE image of plagioclase grain 13 with trace element line 1.1 (by LA-ICP-MS) indicated.

grain 13 - Line 1.2

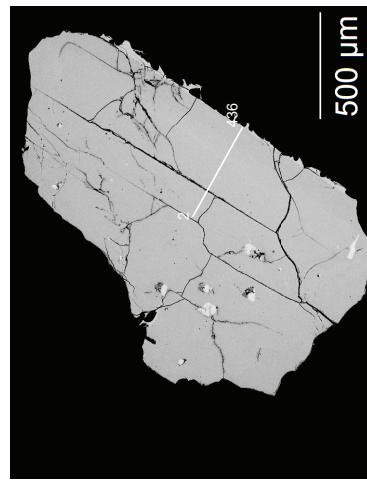


Fig. B8. BSE image of plagioclase grain 13 with trace element line 1.2 (by LA-ICP-MS) indicated.

Table B8: continued

core	182	27.6	3	27.3	3	52433	3478	36.6	9	121020	8592	8944	552	32443	2801	77.1	19	579	87	3.1	1	247	17	707	52	33.3	2	39.4	4	2.7	0	7.8
core	187	25.6	3	27.0	3	53886	2083	33.5	6	26323	5405	9278	420	34511	2493	89.9	13	632	20	2.5	2	246	10	750	48	33.2	2	38.3	2	2.6	1	7.4
core	192	28.4	4	27.0	2	54211	2938	37.7	6	29498	6940	9587	577	34281	2600	96.6	17	632	65	2.3	1	233	16	778	65	34.9	3	39.6	3	2.4	0	7.7
core	197	30.1	7	24.7	2	52461	3570	29.8	8	32382	7016	8885	622	34360	3532	79.5	20	632	230	1.8	1	249	20	722	61	33.5	4	39.2	4	2.7	0	6.9
core	202	26.0	4	29.6	7	54783	4002	27.4	9	124011	7895	9182	624	32893	2511	89.0	12	1493	185	2.9	1	254	16	729	51	36.2	2	38.8	2	2.7	1	7.5
core	207	26.1	4	25.9	2	52542	2922	27.9	9	12192	7547	9188	575	33510	2041	88.3	21	1494	147	2.3	0	241	15	664	51	34.3	3	38.6	3	3.3	0	8.4
core	212	29.9	4	27.8	3	54086	3805	26.4	7	125705	7613	8891	582	35448	3784	71.1	16	1631	169	2.1	1	236	17	692	45	33.0	3	38.7	3	2.9	1	7.0
core	217	35.9	12	30.0	3	54454	3362	24.7	7	133696	8038	9277	555	36673	2949	88.5	15	1674	199	2.6	1	265	15	730	65	36.0	3	39.5	3	2.5	1	7.0
core	222	29.5	5	32.5	5	58631	4681	33.0	10	130290	7722	9397	664	34790	2242	92.6	19	1656	53	2.4	4	252	19	717	69	37.6	3	39.3	4	2.3	0	4.9
core	227	25.7	3	24.7	2	54780	3319	19.6	6	127942	7312	9048	465	34554	2436	85.2	8	694	178	2.9	1	241	14	694	65	32.9	3	38.4	3	2.8	0	7.1
core	232	27.1	4	26.3	2	50133	4129	24.8	7	115938	9315	8599	813	31505	2982	70.9	17	408	69	2.3	1	231	22	627	60	32.9	3	35.5	4	2.5	0	7.2
core	237	34.3	4	28.6	2	54994	3199	26.8	6	126943	6837	9145	591	33434	1874	85.3	7	548	59	2.3	1	233	16	651	40	33.9	3	41.0	3	2.7	0	7.3
core	242	29.2	4	27.2	1	54465	2642	25.1	7	123216	5508	8704	410	37188	2356	83.2	7	633	70	1.6	1	227	13	662	45	33.9	3	37.8	2	2.3	0	6.7
core	247	32.2	4	29.3	2	54212	1165	28.9	7	128636	4082	9237	405	34793	2203	96.4	18	584	20	2.0	1	240	13	669	32	34.4	2	37.8	2	2.3	0	8.0
core	252	30.0	3	30.7	2	57498	3744	30.9	8	130203	4584	9500	557	35900	2066	84.5	14	1537	147	2.5	1	246	16	647	32	33.4	2	38.1	3	2.7	1	6.3
core	257	32.3	3	28.8	2	52542	2153	22.9	7	120982	5771	8948	895	33970	2665	92.5	16	1486	185	1.9	1	224	14	589	52	29.9	3	35.2	2	2.8	1	7.2
core	262	32.1	3	31.7	3	53921	16186	26.5	6	122173	7256	8251	489	32936	2321	103.6	15	1438	146	1.6	0	222	15	614	43	32.2	2	36.9	3	2.3	0	8.1
core	267	32.9	4	31.7	2	52826	3949	26.0	8	131290	7599	8238	435	39860	3734	108.3	17	1492	156	2.3	1	241	18	620	48	34.7	3	39.1	3	2.9	1	7.7
core	272	31.5	4	31.2	3	53762	2515	29.0	8	131839	5976	7771	541	39559	2334	108.4	8	637	21	2.3	1	220	9	563	36	35.1	2	40.6	3	2.8	1	8.4
core	276	32.5	5	31.2	2	54438	4559	21.8	6	132055	4581	7632	373	39664	3044	13.2	9	503	48	1.7	1	229	9	562	30	36.2	3	42.0	2	3.4	0	9.3
core	281	34.9	4	33.2	4	56601	3919	27.5	7	135896	6662	7850	496	42141	2914	201.6	19	577	26	2.1	1	233	16	548	39	35.4	2	41.7	2	3.6	1	9.1
core	286	35.0	5	29.9	3	54005	3181	29.3	6	136293	8507	8187	533	37705	2850	28.2	22	585	39	1.9	1	230	14	583	29	34.8	2	40.8	4	2.8	1	7.3
core	291	31.7	6	32.1	3	55850	4059	29.2	6	135900	7758	8944	1101	37532	1968	116.1	17	569	83	1.7	1	233	18	581	57	36.4	3	44.2	4	3.5	1	10.3
core	296	29.9	4	30.4	3	54860	4288	22.2	5	133071	9017	8415	593	36745	2934	129.2	20	1499	54	2.1	1	225	17	567	39	33.2	2	37.3	4	2.6	1	7.6
core	301	34.2	7	26.4	2	53237	7681	24.7	6	124109	6890	7839	538	34630	1817	104.9	17	1485	148	2.3	1	207	13	558	48	28.0	2	34.3	3	2.6	1	8.1
core	306	29.2	2	30.0	3	60027	8278	30.7	9	133828	7280	8613	374	36638	2505	102.9	14	1391	158	2.8	1	211	13	554	26	33.6	2	39.6	4	2.5	0	7.1
core	311	30.9	3	30.1	3	56960	4788	26.5	7	128310	6547	9012	596	35150	2545	86.6	20	1642	158	2.0	1	215	11	586	39	32.9	3	40.4	3	2.8	1	7.0
core	316	31.9	3	29.9	3	56173	4660	27.4	8	129915	7034	8787	540	34824	2738	88.1	13	537	118	3.2	1	210	16	576	42	34.5	3	39.6	3	2.3	0	8.1
core	321	32.4	7	31.0	5	55591	2687	28.9	8	134931	7353	9103	491	35038	2401	114.2	14	581	145	2.4	1	216	13	572	34	34.6	3	37.7	3	2.4	0	8.3
core	326	30.6	7	29.1	4	52942	2775	30.7	7	131123	6945	9440	494	34347	2407	87.3	23	453	59	2.3	0	210	13	574	36	35.0	3	37.4	3	2.4	0	8.3
core	331	26.0	2	26.4	3	53730	2494	27.1	9	131265	5842	9299	968	34363	1534	92.0	18	533	54	2.2	0	205	13	576	33	35.6	3	37.9	3	2.8	0	7.3
core	336	26.7	5	27.0	4	56468	3600	26.5	8	132974	6733	9326	655	34894	2482	108.7	25	564	146	2.0	0	211	12	558	44	33.6	3	39.5	3	2.7	1	6.4
core	341	32.1	6	25.4	3	55962	3811	26.4	5	131555	7748	9464	558	33601	2575	80.0	14	528	106	3.0	1	205	17	545	50	34.9	3	39.8	4	2.6	1	6.5
core	346	19.8	3	24.2	4	54634	5877	19.9	7	124565	11975	9016	858	31557	2883	84.8	16	1448	54	1.8	1	183	18	535	55	33.4	4	35.7	4	2.4	0	7.0
core	351	22.7	4	24.9	4	54036	2766	30.8	7	126713	5311	9342	575	33196	2643	88.0	15	1573	88	2.1	0	192	10	577	31	31.8	2	34.5	2	3.0	1	6.0
core	356	22.9	4	20.6	2	52511	2533	24.8	7	124900	5828	10258	1697	33422	2460	87.0	12	1451	143	2.5	1	182	10	577	31	31.8	3	34.2	2	2.4	0	6.9
core	361	21.5	2	22.3	3	56255	2986	21.6	8	127909	6155	10176	651	31735	2699	85.9	15	1385	111	2.7	1	186	11	513	34	30.8	2	34.6	3	2.5	1	7.1
core	366	23.7	4	19.5	2	57282	3007	24.5	5	128557	6941	10785	548	32437	2521	67.8	12	1445	29	3.6	1	183	12	508	29	27.8	3	30.0	2	2.2	0	6.0
core	371	17.7	3	17.1	1	55409	2730	22.9	6	124714	6198	10594	569	29754	2435	59.8	12	1424	116	2.4	0	180	12	492	35	24.2	2	27.3	2	1.6	0	5.0
rim	376	18.6	3	16.5	2	54496	2761	18.1	4	119011	5800	10574	661	28607	2565	42.8	10	1366	163	3.3	1	167	11	468	32	23.3	2	25.8	2	1.9	1	4.9
rim	381	17.6	2	16.6	2	54287	3194	18.2	5	122139	6295	10947	503	28120	2858	49.7	10	1328	97	3.0	1	164	9	475	27	21.4	2	23.2	2	1.7	0	4.8
rim	386	15.6	2	14.9	1	55521	3059	22.3	5	124227	5923	11504	901	26636	2061	57.2	18	1328	97	3.0	1	164	9	468	28	22.2	2	24.5	2	1.8	0	5.6
rim	391	22.3	2	14.2	2	55426	4056	21.8	9	119454	6116	1042	692	27081	1827	43.7	12	1413	22	2.7	1	165	11	460	37	19.6	2	22.5	2	1.7	0	3.9
rim	396	13.1	2	12.5	2	56031	6209	22.6	7	115008	6357	11648	1273	25604	2411	54.4	13	1260	20	3.5	1	155	11	449	32	19.4	2	22.7	2	1.2	0	3.7
rim	401	11.9	3	12.5	2	59159	5845	18.2	5	121975	5854	11450	590	25504	2127	52.8	12	1369	184	3.6	1	154	13	440	35	22.2	3	21.5	2	1.5	0	4.9
rim	406	15.4	4	12.7	2	56424	2632	21.6	6	123014	5015	12235	668	27349	2462	69.3	15	1457	161	3.9	1	162	8	436	26	21.7						

Table B8: continued

2SD	Si	ppm	2SD	Eu	ppm	2SD	Gd	ppm	2SD	Pb	ppm	2SD	SO ₄	TiO ₂	Al ₂ O ₃	FeO	MgO	CaO	Na ₂ O	K ₂ O	BaO	SrO	Total	An mol%	Ab mol%	Or mol%
1	0.5	0	4.6	0	0.3	0	14.1	2	61.6	0.1	22.5	0.2	0.0	4.1	8.0	1.5	0.0	0.0	0.0	0.0	0.0	98.1	20	71		9
1	0.6	0	4.3	0	0.3	0	4.1	1	61.7	0.1	22.7	0.2	0.0	4.2	7.8	1.5	0.0	0.0	0.0	0.0	0.0	98.1	21	70		9
2	0.3	0	4.0	0	0.3	0	3.6	1	61.8	0.1	22.4	0.2	0.0	4.2	7.9	1.5	0.1	0.0	0.0	0.0	0.0	98.1	21	71		9
1	0.4	0	4.4	0	0.6	0	17.1	6	61.8	0.1	22.4	0.2	0.0	4.2	7.9	1.5	0.1	0.0	0.0	0.0	0.0	98.1	21	71		9
1	0.3	0	4.6	0	0.3	0	3.8	1	61.4	0.1	22.8	0.2	0.0	4.4	7.8	1.4	0.1	0.0	0.0	0.0	0.0	98.0	22	70		8
2	0.5	0	4.5	0	0.2	0	2.6	1	60.7	0.1	23.4	0.3	0.0	5.0	7.6	1.2	0.1	0.0	0.0	0.0	0.0	98.3	25	68		7
2	1.0	1	4.8	1	0.3	0	2.9	1	60.3	0.1	23.4	0.2	0.0	5.3	7.5	1.1	0.0	0.0	0.0	0.0	0.0	98.0	26	67		7
2	0.7	1	4.3	0	0.4	0	12.0	1	60.6	0.1	23.6	0.2	0.0	5.3	7.6	1.1	0.1	0.0	0.0	0.0	0.0	98.5	26	68		6
2	0.8	0	4.8	0	0.5	0	3.7	1	60.3	0.1	23.4	0.2	0.0	5.3	7.4	1.1	0.1	0.0	0.0	0.0	0.0	98.0	26	67		6
2	0.6	1	5.0	0	0.5	0	3.5	2	60.0	0.1	23.7	0.2	0.0	5.5	7.5	1.0	0.1	0.0	0.0	0.0	0.0	98.0	27	67		6
2	0.7	1	4.3	0	0.3	0	3.5	1	59.9	0.1	24.0	0.2	0.0	5.8	7.3	1.0	0.1	0.0	0.0	0.0	0.0	98.4	29	65		6
2	0.5	0	4.8	0	0.9	0	1.9	1	59.2	0.1	24.4	0.2	0.0	6.2	7.2	0.9	0.1	0.0	0.0	0.0	0.0	98.3	31	64		5
2	0.7	0	5.4	0	0.6	0	1.7	1	60.1	0.1	23.8	0.2	0.0	5.5	7.4	1.0	0.1	0.0	0.0	0.0	0.0	98.2	27	67		6
2	0.6	0	4.6	0	0.3	0	2.5	1	60.3	0.1	23.8	0.2	0.0	5.5	7.4	1.0	0.1	0.0	0.0	0.0	0.0	98.4	27	67		6
2	0.5	0	5.4	0	0.4	0	2.2	1	60.5	0.1	23.6	0.2	0.0	5.4	7.5	1.1	0.1	0.0	0.0	0.0	0.0	98.4	27	67		6
2	0.6	0	4.8	0	0.6	0	1.7	1	60.5	0.1	23.6	0.2	0.0	5.4	7.5	1.1	0.1	0.0	0.0	0.0	0.0	98.4	27	67		6
2	1.1	1	4.3	0	0.5	0	2.0	0	60.5	0.1	23.6	0.2	0.0	5.4	7.5	1.1	0.1	0.0	0.0	0.0	0.0	98.4	27	67		6
2	0.7	0	4.6	0	0.1	0	1.7	1	60.5	0.1	23.6	0.2	0.0	5.3	7.4	1.1	0.1	0.0	0.0	0.0	0.0	98.3	26	67		7
2	0.7	0	5.0	0	0.6	0	2.0	0	60.4	0.1	23.5	0.2	0.0	5.2	7.5	1.1	0.1	0.0	0.0	0.0	0.0	98.1	26	67		6
1	0.8	0	5.1	0	0.7	0	1.9	1	60.3	0.1	23.6	0.2	0.0	5.3	7.5	1.1	0.2	0.0	0.0	0.0	0.0	98.2	26	67		6
1	0.8	0	4.8	0	0.6	0	1.9	1	60.3	0.1	23.6	0.2	0.0	5.3	7.5	1.1	0.2	0.0	0.0	0.0	0.0	98.2	26	67		6
2	0.5	0	4.2	0	0.8	0	3.2	1	60.7	0.1	23.4	0.3	0.0	5.4	7.4	1.1	0.1	0.0	0.0	0.0	0.0	98.3	27	67		6
2	0.9	0	5.5	0	0.7	0	1.3	1	60.1	0.1	23.6	0.2	0.0	5.4	7.5	1.1	0.1	0.0	0.0	0.0	0.0	98.1	27	67		6
2	0.6	1	4.4	0	0.5	0	1.9	1	60.1	0.1	23.6	0.2	0.0	5.4	7.5	1.1	0.1	0.0	0.0	0.0	0.0	98.1	27	67		6
2	0.6	0	4.8	0	0.2	0	1.8	1	60.1	0.1	23.6	0.2	0.0	5.4	7.5	1.1	0.1	0.0	0.0	0.0	0.0	98.1	27	67		6
2	0.5	0	4.7	0	0.1	0	1.7	1	60.1	0.1	23.7	0.2	0.0	5.4	7.6	1.1	0.1	0.0	0.0	0.0	0.0	98.7	26	67		6
2	0.4	0	4.6	0	0.3	0	3.3	2	60.6	0.1	23.5	0.2	0.0	5.3	7.5	1.1	0.0	0.0	0.0	0.0	0.0	98.4	26	67		7
2	0.5	1	5.0	0	0.0	0	4.7	2	60.7	0.1	23.6	0.2	0.0	5.2	7.6	1.1	0.1	0.0	0.0	0.0	0.0	98.7	26	67		7
2	0.2	0	5.3	0	0.1	0	2.5	1	60.7	0.1	23.6	0.2	0.0	5.2	7.6	1.1	0.1	0.0	0.0	0.0	0.0	98.7	26	67		7
1	0.6	0	5.6	0	0.6	0	1.0	1	60.6	0.1	23.5	0.2	0.0	5.2	7.5	1.1	0.0	0.0	0.0	0.0	0.0	98.3	26	67		7
1	0.9	0	5.6	0	0.4	0	1.0	1	60.6	0.1	23.6	0.2	0.0	5.2	7.6	1.1	0.1	0.0	0.0	0.0	0.0	98.3	26	67		7
2	0.4	0	4.6	0	0.4	0	1.2	1	60.6	0.1	23.6	0.2	0.0	5.2	7.5	1.1	0.0	0.0	0.0	0.0	0.0	98.3	26	67		7
1	1.1	1	5.5	0	0.6	0	2.4	1	60.6	0.1	23.6	0.2	0.0	5.2	7.6	1.1	0.1	0.0	0.0	0.0	0.0	98.5	26	68		7
2	0.5	1	5.5	0	0.5	0	3.6	1	60.6	0.1	23.6	0.2	0.0	5.2	7.6	1.1	0.1	0.0	0.0	0.0	0.0	98.5	26	68		7
2	0.7	1	4.9	0	0.8	0	1.4	1	60.6	0.1	23.6	0.2	0.0	5.1	7.5	1.2	0.1	0.0	0.0	0.0	0.0	98.3	26	67		7
2	1.0	1	5.3	0	0.8	0	1.9	1	60.5	0.1	23.2	0.2	0.0	5.1	7.5	1.2	0.2	0.0	0.0	0.0	0.0	98.0	25	68		7
2	0.6	0	4.8	0	0.8	0	2.6	0	60.7	0.1	23.5	0.2	0.0	5.1	7.5	1.2	0.2	0.0	0.0	0.0	0.0	98.0	25	68		7
2	1.0	1	5.7	0	0.2	0	2.6	0	60.7	0.1	23.5	0.2	0.0	5.2	7.5	1.1	0.1	0.0	0.0	0.0	0.0	98.4	26	67		7
2	0.8	1	5.3	0	0.3	0	1.8	0	60.9	0.0	23.6	0.3	0.0	5.1	7.6	1.1	0.1	0.0	0.0	0.0	0.0	98.8	25	68		7
2	0.4	0	5.3	0	0.3	0	1.3	2	60.7	0.1	23.3	0.2	0.0	5.2	7.6	1.1	0.1	0.0	0.0	0.0	0.0	98.3	26	68		7
2	1.2	1	5.6	0	0.1	0	3.1	1	60.5	0.1	23.8	0.2	0.0	5.2	7.6	1.1	0.1	0.0	0.0	0.0	0.0	99.0	26	68		6
2	0.6	0	4.9	0	0.2	0	1.0	1	60.5	0.1	23.8	0.2	0.0	5.3	7.7	1.1	0.1	0.0	0.0	0.0	0.0	99.0	26	68		6
2	0.5	0	4.9	0	0.2	0	2.4	0	60.5	0.1	23.8	0.2	0.0	5.3	7.7	1.1	0.1	0.0	0.0	0.0	0.0	99.0	26	68		6
2	0.5	0	5.7	0	1.0	0	1.0	1	60.5	0.1	23.8	0.2	0.0	5.3	7.7	1.1	0.1	0.0	0.0	0.0	0.0	99.0	26	68		6

Table B8: continued

2	1.0	0	5.3	0	0.6	0	1	12.9	1	60.2	0.1	23.6	0.2	0.0	5.2	7.6	1.1	0.0	0.0	0.0	98.0	26	68		7
2	0.6	0	5.3	0	0.8	0	1	13.0	1	60.1	0.1	23.5	0.2	0.0	5.3	7.5	1.1	0.1	0.0	0.0	98.0	26	67		7
2	0.4	0	4.5	0	0.5	0	1	11.9	1	60.1	0.1	23.5	0.2	0.0	5.3	7.5	1.1	0.1	0.0	0.0	98.0	26	67		7
1	0.7	1	5.6	0	0.6	0	1	12.5	1	60.1	0.1	23.5	0.2	0.0	5.3	7.5	1.1	0.1	0.0	0.0	98.0	26	67		7
2	0.5	0	5.2	0	0.7	0	2	12.7	2	60.5	0.1	23.5	0.2	0.0	5.3	7.5	1.1	0.1	0.0	0.0	98.4	26	67		7
2	0.9	1	4.4	0	0.3	0	2	12.6	2	60.5	0.1	23.5	0.2	0.0	5.3	7.5	1.1	0.1	0.0	0.0	98.4	26	67		7
1	0.4	0	5.0	0	0.2	0	1	11.7	1	60.6	0.0	23.8	0.2	0.0	5.2	7.7	1.1	0.1	0.0	0.0	98.9	26	68		7
2	0.7	1	4.9	0	0.7	0	1	13.2	1	60.6	0.1	23.7	0.2	0.0	5.3	7.5	1.1	0.1	0.0	0.0	98.7	26	67		7
2	0.7	0	4.2	0	0.2	0	2	12.6	2	60.6	0.1	23.7	0.2	0.0	5.3	7.5	1.1	0.1	0.0	0.0	98.7	26	67		7
1	0.5	0	4.8	0	0.3	0	1	12.5	1	60.6	0.1	23.7	0.2	0.0	5.3	7.5	1.1	0.1	0.0	0.0	98.7	26	67		7
2	0.5	0	3.8	0	0.4	0	1	12.9	1	60.5	0.1	23.7	0.2	0.0	5.2	7.6	1.1	0.1	0.0	0.0	98.5	26	68		7
1	0.6	0	4.4	0	0.7	0	1	12.4	1	60.5	0.1	23.7	0.2	0.0	5.2	7.6	1.1	0.1	0.0	0.0	98.5	26	68		7
1	0.3	0	4.6	0	0.7	0	1	11.5	1	60.6	0.1	23.7	0.2	0.0	5.2	7.5	1.1	0.1	0.0	0.0	98.5	26	67		7
2	0.4	0	4.5	0	0.3	0	1	12.1	1	60.7	0.1	23.6	0.2	0.0	5.2	7.6	1.1	0.1	0.0	0.0	98.7	26	67		7
1	0.3	0	3.8	0	0.5	0	1	12.0	1	60.7	0.1	23.6</													

Table B9: continued

Nd ppm	Zr ppm	Sm ppm	Eu ppm	Gd ppm	Pb ppm	2SD Pb	TiO ₂	Al ₂ O ₃	FeO	MgO	CaO	Na ₂ O	K ₂ O	BaO	SrO	Total	An mol%	Ab mol%	Or mol%
8.4	2	0.5	0	4.2	0.1	0	3.7												
7.8	1	0.6	0	4.3	0.1	0	3.4												
7.2	2	0.3	0	4.8	0.3	0	3.7												
6.2	1	0.3	0	4.3	0.2	0	3.2												
9.1	1	0.8	0	4.3	0.5	0	3.1												
7.9	2	0.7	1	4.4	0.6	0	2.7												
7.6	2	0.7	0	4.2	0.8	0	2.7												
7.4	1	0.5	0	4.7	0.7	0	2.3												
8.4	1	0.6	0	5.2	0.6	0	3.6												
8.5	2	0.8	1	4.3	0.2	0	3.0												
9.0	2	1.0	1	4.7	0.5	0	3.0												
7.6	1	0.8	1	4.4	0.5	0	1.9												
6.6	2	0.6	1	5.4	0.4	0	1.4												
7.1	1	0.3	0	4.4	0.3	0	1.7												
6.4	2	0.6	0	4.7	0.5	0	1.7												
7.3	2	0.7	0	4.9	0.2	0	1.5												
6.7	1	0.6	1	4.5	1.0	0	1.4												
8.0	1	0.8	0	4.7	0.3	0	1.8												
6.4	1	0.6	0	4.2	0.8	0	1.4												
5.8	2	0.5	0	4.6	0.9	0	1.8												
8.9	2	0.4	1	4.3	0.9	0	2.5												
9.6	2	0.7	1	4.6	1.3	0	2.1												
7.8	2	0.8	0	5.4	1.4	0	2.5												
7.7	2	0.4	0	5.1	0.8	0	2.2												
8.9	2	0.8	0	3.4	0.1	0	3.0												
8.2	2	0.6	0	5.3	0.5	0	3.2												
8.4	2	0.8	0	4.8	0.4	0	2.0												
7.5	2	1.0	0	4.9	0.8	0	2.0												
7.9	2	1.4	1	5.5	0.8	0	1.6												
8.5	2	0.7	1	5.7	0.1	0	2.0												
10.1	2	1.2	1	5.2	0.5	0	2.5												
9.7	2	1.3	1	5.4	0.6	0	2.0												
9.4	2	0.3	0	5.1	0.5	0	2.3												
10.0	2	1.0	1	5.1	0.9	0	2.0												
8.2	1	0.5	0	3.0	1.3	0	2.4												
7.1	1	0.4	0	3.0	1.3	0	1.4												
9.5	2	0.6	1	5.3	0.6	0	1.7												
7.4	2	0.3	0	5.4	0.6	0	1.8												
7.0	1	0.4	0	4.9	0.4	0	1.3												
5.4	2	0.6	0	4.9	0.3	0	2.0												
6.5	1	0.5	0	5.2	0.1	0	1.8												
8.5	2	0.5	1	4.7	0.1	0	1.8												
6.3	2	0.7	1	5.4	0.6	0	1.4												
7.0	2	0.4	0	3.2	0.1	0	1.7												
6.6	1	0.3	0	3.2	0.4	0	1.9												
8.1	2	0.6	0	5.3	0.4	0	1.0												
7.6	1	1.0	1	5.3	0.1	0	1.5												
7.0	2	0.3	0	5.4	0.4	0	2.1												
7.1	1	0.2	0	5.2	0.3	0	1.2												
6.8	1	0.6	1	5.7	0.5	0	1.0												
7.1	2	0.6	1	5.2	0.2	0	2.0												
6.3	1	0.3	0	5.7	0.5	0	2.0												
6.9	1	1.1	1	6.1	0.1	0	1.7												
6.2	1	0.5	0	5.0	0.0	0	1.7												
7.6	1	1.3	1	5.8	0.4	0	1.2												
6.4	1	0.3	0	5.9	0.4	0	1.2												
5.2	2	0.6	0	5.9	0.3	0	1.5												
5.5	1	0.5	0	5.1	0.1	0	2.2												
7.5	2	0.6	0	5.1	0.2	0	2.8												
7.3	1	0.7	1	4.7	0.1	0	2.3												
5.2	1	0.2	0	5.3	0.3	0	1.3												

Table B10: Plagioclase grain 13 - Lithium isotopes

MEASURED		background		Results (BLK + tau corr.)										
⁷ Li (V)	⁶ Li (cps)	⁷ Li (V)	⁶ Li (cps)	⁷ Li/ ⁶ Li	SE	SD	1 RSD	n	ID time (min)	std drift	⁷ Li/ ⁶ Li (‰)	rel GOR132-G	2 σ	
1	0.00642	31117	0.000050	0.0001205	667	12.8516	0.0125	0.1059	971	75	10.4	-0.6	-10.1	2.4
2	0.01637	79349	0.00127	0.0001166	645	12.7974	0.0102	0.0928	796	85	5.8	0.2	-14.4	2.1
3	0.01647	80354	0.00129	0.0001127	610	12.7721	0.0086	0.0942	673	119	4.2	-0.9	-16.7	2.1
4	0.01781	87223	0.00140	0.0001081	597	12.7495	0.0071	0.0775	555	119	4.4	1.6	-18.1	2.0
5	0.01630	80029	0.00128	0.0001054	583	12.7514	0.0083	0.0911	652	119	7.0	-0.3	-17.3	1.8
6	0.01428	69995	0.00112	0.0001038	565	12.7544	0.0077	0.0827	602	119	4.5	-0.1	-17.2	1.7
7	0.00978	47666	0.00076	0.0001025	557	12.8101	0.0113	0.1176	884	107	5.3	-1.5	-13.7	2.2
8	0.01443	70559	0.00113	0.0001019	557	12.7849	0.0074	0.0804	579	119	4.2	0.1	-16.4	1.8
9	0.00767	36573	0.00059	0.0000958	531	12.8782	0.0162	0.1362	1255	70	4.5	-1.6	-8.4	2.9
10	0.01594	77444	0.00124	0.0000895	485	12.8455	0.0155	0.1630	1204	110	5.3	0.3	-11.2	2.8
11	0.00916	44999	0.00072	0.0000908	465	12.8102	0.0228	0.1780	1779	60	4.4	-0.1	-13.8	3.8
12	0.01779	87268	0.00140	0.0000851	456	12.7306	0.0126	0.1203	990	90	4.6	1.7	-19.1	2.4
13	0.01696	83486	0.00134	0.0000820	433	12.7119	0.0078	0.0857	615	119	4.4	-0.5	-20.0	1.8

⁶ Li (‰) rel IRMM-016	RepRate Hz	Integr.time (s)	distance	Li	2 σ d	Li	2 σ
-1.2	50	1.049	rim	35	11.0	1	-1.2 2.4
-5.5	28	1.049	core	81	19.5	2	-5.5 2.1
-7.8	20	1.049	core	137	26.9	1	-7.8 2.1
-9.2	17	1.049	core	193	28.3	1	-9.2 2.0
-8.4	16	1.049	core	275	25.7	1	-8.4 1.8
-8.3	16	1.049	core	305	20.6	2	-8.3 1.7
-4.8	14	1.049	core	399	25.0	2	-4.8 2.2
-7.5	14	1.049	core	437	26.6	1	-7.5 1.8
0.5	50	1.049	rim	37	20.0	2	0.5 2.9
-2.3	33	1.049	core	100	20.0	2	-2.3 2.8
-4.9	25	1.049	crack	157	9.7	2	-4.9 3.8
-10.2	25	1.049	core	225	29.4	2	-10.2 2.4
-11.1	17	1.049	core	297	29.6	2	-11.1 1.8

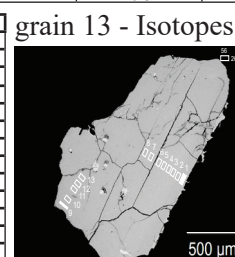


Fig. B9. BSE image of plagioclase grain 13 with Fs-LA-MC-ICP-MS lines indicated.

Table B11: continued

Sm ppm	Zr ppm	La ppm	Ce ppm	Pr ppm	2SD	Pb ppm	2SD	SiO ₂	TiO ₂	Al ₂ O ₃	FeO	MgO	CaO	Na ₂ O	K ₂ O	BaO	StrO	Total	An mol%	Ab mol%	Or mol%
0.4	0	6.4	1	0.0	0	3.7	1	61.4	0.1	23.4	0.2	0.0	4.3	7.9	1.5	0.1	0.0	98.8	21	70	9
0.5	0	7.8	1	0.5	0	3.7	1	61.4	0.1	23.3	0.2	0.0	4.2	8.1	1.5	0.0	0.0	98.7	20	71	9
0.5	0	6.8	1	0.2	0	3.7	1	61.3	0.0	23.2	0.2	0.0	4.1	8.1	1.5	0.0	0.0	98.6	20	71	9
0.3	0	7.0	1	0.1	0	3.3	1	61.6	0.1	23.3	0.2	0.0	4.2	8.0	1.5	0.1	0.0	99.0	20	71	9
0.1	0	6.8	1	0.2	0	2.8	2	61.1	0.1	23.4	0.2	0.0	4.4	8.0	1.5	0.1	0.0	98.7	21	70	8
0.0	0	6.7	1	0.5	0	3.4	1	61.3	0.0	23.4	0.2	0.0	4.3	8.0	1.5	0.1	0.0	98.8	21	71	9
0.6	0	5.5	1	0.4	0	3.6	1	61.3	0.0	23.3	0.2	0.0	4.2	8.0	1.5	0.0	0.0	98.6	20	71	9
0.5	0	6.2	1	0.2	0	2.1	1	61.6	0.1	23.3	0.2	0.0	4.1	8.0	1.5	0.0	0.0	98.9	21	71	9
0.2	0	6.9	1	0.0	0	3.0	1	61.1	0.1	23.4	0.2	0.0	4.4	8.0	1.5	0.1	0.0	98.7	21	70	8
0.5	0	5.9	1	0.5	0	3.0	2	61.3	0.0	23.4	0.2	0.0	4.3	8.0	1.5	0.1	0.0	98.8	21	71	9
0.8	1	7.4	1	0.3	0	2.5	1	61.5	0.0	23.2	0.2	0.0	4.2	8.0	1.5	0.1	0.0	98.7	21	71	9
0.2	0	6.3	1	0.1	0	2.9	1	61.3	0.0	23.2	0.2	0.0	4.2	8.0	1.5	0.1	0.0	98.7	21	71	9
0.5	0	6.7	1	0.3	0	2.8	1	61.3	0.0	23.1	0.2	0.0	4.2	8.0	1.5	0.0	0.0	98.6	20	71	9
0.1	0	5.7	1	0.6	1	2.6	1	61.6	0.1	23.2	0.2	0.0	4.2	8.1	1.5	0.0	0.0	98.9	21	71	9
0.9	1	6.3	1	0.2	0	3.6	1	61.8	0.1	23.5	0.2	0.0	4.1	8.0	1.5	0.1	0.0	98.6	20	71	9
0.6	0	6.1	1	0.8	1	1.7	1	61.6	0.1	23.0	0.3	0.0	4.0	8.1	1.6	0.0	0.0	98.8	20	71	9
0.9	0	6.2	1	0.0	0	2.1	1	61.7	0.1	23.0	0.2	0.0	4.0	8.1	1.6	0.0	0.0	98.8	20	71	9
0.8	1	5.6	1	0.5	0	2.2	1	62.0	0.1	23.1	0.2	0.0	4.0	8.1	1.6	0.0	0.0	99.0	19	71	9
0.6	1	6.1	1	0.5	0	1.8	1	62.3	0.1	22.7	0.2	0.0	3.7	8.1	1.7	0.0	0.0	98.8	18	72	10
0.1	0	6.0	1	0.1	0	2.3	1	62.2	0.0	22.5	0.2	0.0	3.5	8.1	1.9	0.1	0.0	98.5	17	72	11
0.3	0	5.6	1	0.1	0	1.3	1	62.3	0.1	22.5	0.2	0.0	3.7	8.2	1.8	0.0	0.0	98.7	18	72	10
0.0	0	5.5	1	0.4	1	2.1	1	62.2	0.1	22.5	0.2	0.0	3.6	8.1	1.8	0.0	0.0	98.4	18	72	10
0.3	0	5.0	1	0.2	0	2.0	1	62.2	0.1	22.7	0.2	0.0	3.8	8.1	1.7	0.0	0.0	98.8	19	72	10
0.2	0	5.5	1	0.1	0	3.1	1	61.5	0.1	23.1	0.2	0.0	4.2	8.0	1.6	0.1	0.0	98.8	20	70	9
0.5	0	5.8	1	0.3	0	2.4	1	61.6	0.1	23.1	0.2	0.0	4.1	8.1	1.6	0.1	0.0	98.8	20	71	9
0.5	0	5.8	1	0.5	0	2.6	1	62.0	0.1	23.1	0.2	0.0	4.0	8.1	1.6	0.1	0.0	99.0	20	71	9
0.6	0	5.0	1	0.5	1	2.1	1	61.9	0.1	22.9	0.2	0.0	4.1	8.1	1.6	0.1	0.0	99.0	20	71	9
0.6	0	5.4	1	0.2	0	3.3	1	62.2	0.1	23.1	0.2	0.0	4.0	8.0	1.6	0.1	0.0	99.3	19	71	9
0.7	1	5.2	1	0.2	0	2.4	1	61.9	0.1	22.9	0.2	0.0	4.1	8.0	1.6	0.1	0.0	98.9	20	71	9
0.6	0	5.7	1	0.3	0	1.6	1	62.0	0.1	23.1	0.2	0.0	4.1	8.0	1.6	0.1	0.0	99.1	20	71	9
0.9	1	5.4	1	0.5	1	2.9	1	62.3	0.1	22.8	0.2	0.0	3.8	8.2	1.9	0.1	0.0	99.0	19	72	10
0.2	0	5.1	0	0.2	0	8.2	3	62.3	0.1	22.6	0.2	0.0	3.8	8.1	1.7	0.1	0.0	98.7	19	72	10
0.2	0	5.1	1	0.1	0	3.6	1	62.0	0.1	22.8	0.2	0.0	4.1	7.9	1.6	0.0	0.0	98.7	20	70	9
0.4	0	5.2	1	0.2	0	1.8	1	61.8	0.1	22.8	0.2	0.0	4.0	7.9	1.6	0.1	0.0	98.5	20	71	9
0.6	1	5.2	1	0.4	0	2.9	2	62.1	0.0	23.0	0.2	0.0	4.1	7.9	1.5	0.1	0.0	99.0	20	71	9

grain 15 - Line 1.1



Fig. B10. BSE image of plagioclase grain 15 with trace element line 1.1 (by LA-ICP-MS) indicated.

grain 15 - Line 3.1



Fig. B11. BSE image of plagioclase grain 15 with trace element line 3.1 (by LA-ICP-MS) indicated.

Table B12: continued

Sm ppm	Zr ppm	La ppm	Ce ppm	Pr ppm	2SD	Pb ppm	2SD	SiO ₂	TiO ₂	Al ₂ O ₃	FeO	MgO	CaO	Na ₂ O	K ₂ O	BaO	StrO	Total	An mol%	Ab mol%	Or mol%
0.4	0	4.2	1	0.3	0	2.5	2	63.2	0.1	23.9	0.2	0.0	4.0	8.0	1.6	0.1	0.1	100.2	20	71	9
0.6	0	4.4	1	0.4	0	3.5	2	63.3	0.1	23.2	0.2	0.0	4.2	8.0	1.5	0.0	0.0	100.5	21	71	9
0.4	0	4.3	1	0.2	0	3.6	2	63.3	0.1	23.2	0.2	0.0	4.2	8.0	1.5	0.0	0.0	100.5	21	71	9
0.3	0	4.1	1	0.3	0	2.9	2	63.1	0.1	23.2	0.2	0.0	4.2	8.1	1.5	0.1	0.0	100.5	20	71	9
0.3	0	5.0	1	0.1	0	1.9	1	63.4	0.1	23.1	0.1	0.0	4.1	8.0	1.6	0.1	0.0	100.5	20	71	9
0.4	0	4.6	1	0.5	0	2.7	1	63.2	0.1	23.3	0.2	0.0	4.3	8.0	1.5	0.1	0.0	100.6	21	70	9
0.6	0	4.7	1	0.7	1	2.5	1	63.2	0.1	22.9	0.2	0.0	4.1	8.0	1.6	0.0	0.0	100.1	20	71	9
0.7	1	4.5	1	0.3	0	3.2	2	63.2	0.1	23.0	0.2	0.0	4.2	8.0	1.6	0.0	0.0	100.3	20	70	9
0.3	0	4.0	1	0.4	0	3.2	1	63.3	0.1	23.2	0.2	0.0	4.1	8.0	1.6	0.1	0.0	100.5	20	71	9
0.2	0	4.9	1	0.1	0	3.3	1	63.2	0.0	23.1	0.2	0.0	4.1	8.1	1.5	0.0	0.0	100.3	20	71	9
0.5	0	4.3	1	0.4	0	2.7	2	63.4	0.1	23.1	0.2	0.0	4.2	8.0	1.5	0.0	0.0	100.5	20	71	9
0.5	0	3.9	1	0.1	0	1.5	1	63.7	0.0	22.7	0.2	0.0	3.8	8.2	1.8	0.1	0.0	100.4	18	71	10
0.1	0	3.9	0	0.2	0	1.3	1	63.5	0.1	23.1	0.2	0.0	4.0	8.0	1.6	0.0	0.0	100.6	19	71	9
0.4	0	4.8	1	0.6	1	1.4	1	63.2	0.0	23.0	0.2	0.0	4.2	8.1	1.5	0.0	0.0	100.3	20	71	9
0.4	0	3.9	1	0.1	0	3.4	2	63.3	0.1	23.0	0.2	0.0	4.3	8.1	1.5	0.0	0.0	100.5	21	71	9
0.3	0	5.0	1	0.0	0	1.8	1	63.2	0.1	23.1	0.2	0.0	4.3	8.1	1.5	0.1	0.0	100.6	21	71	9
0.3	0	4.1	1	0.2	0	1.2	1	63.0	0.1	23.1	0.2	0.0	4.0	8.0	1.5	0.0	0.0	100.2	21	70	9
0.8	1	3.8	1	0.4	0	2.9	1	63.4	0.1	23.1	0.2	0.0	4.1	8.2	1.5	0.1	0.0	100.7	20	71	9
0.1	0	4.0	1	0.3	0	1.4	1	63.1	0.1	23.1	0.2	0.0	4.3	8.0	1.5	0.1	0.0	100.4	21	70	9
0.6	0	3.0	1	0.2	0	1.9	1	63.5	0.0	22.8	0.2	0.0	4.2	8.1	1.5	0.1	0.0	100.4	21	70	9
0.6	1	3.1	1	0.0	0	3.9	1	63.4	0.1	22.9	0.2	0.0	4.2	8.1	1.6	0.0	0.0	100.3	20	71	9
0.3	0	3.5	1	0.2	0	1.4	2	63.4	0.1	23.0	0.2	0.0	4.1	8.1	1.6	0.0	0.0	100.4	20	71	9

Table B13: Plagioclase grain 15 - Line 1.2

	Distance	L ¹	ppm	2SDI	L ¹	ppm	2SDI	Na	ppm	2SDI	Na	ppm	2SDI	Mg	ppm	2SDI	Mg	ppm	2SDI	Ca	ppm	2SDI	Ca	ppm	2SDI	Ti	ppm	2SDI	Ti	ppm	2SDI	Fe	ppm	2SDI	Fe	ppm	2SDI	Rb	ppm	2SDI	Rb	ppm	2SDI	Sr	ppm	2SDI	Sr	ppm	2SDI	Ba	ppm	2SDI	Ba	ppm	2SDI	Pr	ppm	2SDI	Pr	ppm	2SDI	Ce	ppm	2SDI	Ce	ppm	2SDI	La	ppm	2SDI	La	ppm	2SDI	Nd	ppm	2SDI	Nd	ppm	2SDI
core	2	32.0	5	3.11	2	59230	6758	19.9	6	120974	7737	1086	830	30375	23588	108.0	15	1440	185	25	1	268	5	453	110	4.4	2	14.0	1	10	0	2.4	1																																														
core	7	28.6	4	3.10	2	56210	2054	26.7	7	124288	13988	10420	394	32210	21441	90.0	15	1513	12	3.3	1	274	9	414	62	3.4	1	15.9	2	1.3	0	3.9	1																																														
core	12	26.5	4	28.0	2	56503	3246	25.6	7	124769	6051	10836	856	32173	21653	85.5	20	1468	154	3.9	1	282	18	126	89	4.0	2	16.4	1	1.2	0	4.7	2																																														
core	17	30.5	3	27.7	2	57925	3813	28.8	6	122410	6676	1075	50	32173	21788	103.5	18	1603	155	3.6	1	288	17	1450	92	4.7	2	16.9	2	1.2	0	3.7	1																																														
core	22	27.7	4	26.4	2	56922	3813	20.3	6	122448	6536	10897	760	29947	19871	95.0	3	424	142	3.5	1	278	15	345	85	3.9	1	17.8	2	1.0	0	3.0	1																																														
core	27	28.1	5	28.5	3	57003	2320	19.5	6	127645	6114	1093	642	31259	23130	112.8	8	516	131	2.9	1	265	5	367	55	4.5	1	17.7	2	0.9	0	2.8	2																																														
core	32	23.5	4	27.8	3	54614	2489	20.7	7	120488	5171	11103	551	29851	2138	102.0	7	463	176	3.2	1	265	5	369	56	4.4	1	16.7	1	2.9	0	3.5	1																																														
core	37	27.2	4	25.6	3	54931	2618	25.0	7	124419	6340	1183	606	29816	2083	83.6	7	472	132	3.7	1	275	7	388	75	3.8	1	17.7	2	1.4	0	3.7	1																																														
core	41	25.7	4	25.2	2	56390	3413	26.0	7	124945	5950	11810	632	30186	2659	82.7	9	364	151	3.4	1	276	8	339	71	4.5	1	17.7	2	1.6	0	3.4	1																																														
core	46	25.6	3	25.4	2	59297	4990	26.7	7	124945	5950	11810	632	30186	2659	82.7	9	364	151	3.4	1	276	8	339	71	4.5	1	17.7	2	1.6	0	3.4	1																																														
core	51	23.9	3	25.3	3	54961	3601	19.6	6	121235	5591	12033	837	27884	1904	90.4	20	544	145	3.1	1	264	4	297	76	5.0	1	6.0	1	1.2	0	3.2	1																																														
core	56	25.9	3	22.8	3	68032	25030	22.4	7	123887	13705	12633	393	27483	1787	77.9	8	440	111	4.0	1	267	12	355	77	6.2	1	18.2	1	1.5	0	3.5	1																																														
core	61	24.2	3	23.6	3	57522	4865	26.3	8	122928	17151	12824	734	27136	22584	104.6	20	1338	182	5.1	1	260	19	339	78	17.4	2	17.4	1	1.1	0	3.4	1																																														
core	66	22.4	4	21.6	2	56151	2828	24.3	7	121734	5685	12581	609	27808	1725	81.2	14	308	129	3.8	1	261	14	276	85	17.6	2	18.5	1	1.5	0	3.4	1																																														
core	71	21.4	3	20.7	1	54571	2211	21.4	6	116948	4348	12358	457	25800	2202	60.9	16	399	123	3.9	1	242	15	267	71	17.7	2	20.6	2	1.5	0	3.2	1																																														
core	76	22.3	3	20.7	1	54977	2340	20.0	6	119708	4543	12379	563	27505	1760	67.2	11	383	131	3.9	1	246	15	232	65	20.1	2	20.5	2	1.6	0	4.0	1																																														
core	81	24.3	5	21.5	2	54452	3432	17.6	6	121254	6798	12636	511	28108	2158	58.9	5	366	128	4.3	1	247	7	265	84	20.1	1	21.8	2	1.7	0	4.2	1																																														
core	86	18.6	3	20.2	2	54452	3432	17.6	6	121254	6798	12636	511	28108	2158	58.9	5	366	128	4.3	1	247	7	265	84	20.1	1	21.8	2	1.7	0	4.2	1																																														
core	91	20.4	4	19.6	2	52599	1990	23.2	8	118159	4662	12124	503	24781	1870	54.6	9	377	108	3.4	1	248	8	1065	47	21.9	2	22.0	2	1.7	0	4.8	1																																														
core	96	19.8	4	18.8	1	53912	2398	16.3	6	120435	3186	12209	430	24793	1706	49.3	13	317	142	3.4	1	239	10	1053	50	22.2	2	24.4	2	1.3	0	4.4	1																																														
core	101	5.3	2	20.7	2	56760	3415	21.2	7	123633	5559	12639	584	28114	1913	57.8	4	378	139	3.4	1	242	5	1035	77	23.3	2	24.9	2	1.9	0	4.4	1																																														
core	106	4.9	2	19.2	2	53345	2560	19.8	6	119991	6384	12632	935	28343	2198	56.0	12	464	157	4.0	1	238	14	978	58	23.5	2	26.0	2	1.5	0	3.6	1																																														
core	111	18.7	3	18.4	1	58729	4079	20.6	6	124485	15208	12638	538	27908	2292	59.8	11	386	118	4.5	1	240	14	995	51	25.3	2	26.6	2	1.6	0	4.7	1																																														
core	116	16.2	3	17.7	2	57101	3442	26.3	9	122520	15356	13319	906	28520	2352	62.0	17	506	167	3.9	1	240	8	951	44	23.2	2	26.4	2	1.6	0	4.7	1																																														
core	121	4.9	3	15.8	1	53868	2755	24.8	7	118957	6578	12497	561	28446	2590	52.6	3	385	151	4.3	1	231	12	860	46	23.4	2	23.2	1	1.6	0	4.3	1																																														
core	126	3.3	2	15.5	2	54142	2143	17.8	5	123261	5803	12804	898	28279	2030	59.9	3	384	136	4.2	1	229	14	855	52	21.7	2	23.8	2	1.5	0	5.8	2																																														
core	131	3.5	2	15.2	3	54381	2315	24.0	7	120285	4799	12908	481	27577	1631	58.0	3	305	154	3.8	1	222	2	834	44	21.8	2	25.4	1	1.6	0	4.4	2																																														
crack	136	4.6	3	14.1	2	54102	2636	16.1	4	120501	5073	12845	686	28657	1824	53.2	9	438	108	4.1	1	218	14	810	36	23.3	2	24.5	2	1.5	0	4.9	1																																														
crack	141	1.5	2	12.6	1	55932	3148	15.2	5	119738	4834	12414	584	27743	1622	53.2	9	438	108	4.1	1	218	14	810	36	23.3	2	24.5	2	1.5	0	5.5	1																																														
crack	146	1.7	3	13.2	3	55998	4700	23.3	6	122335	6243	12414	633	28029	3359	48.3	3	368	176	3.5	1	214	15	690	49	22.2	2	24.2	2	1.4	0	4.9	2																																														
crack	151	0.1	2	13.6	4	56007	3520	21.7	7	124025	6243	12407	593	28710	2387	50.3	3	351	122	3.8	1	212	11	662	47	22.3	2	24.3	2	1.4	0	4.6	2																																														
crack	156	0.2	2	11.2	1	53078	3757	18.0	8	120266	6848	11773	791	28040	1971	53.2	11	294	128	3.3	1	200	14	598	38	21.6	2	23.3	2	1.5	0	4.6	1																																														
crack	161	11.4	3	10.5	1	53491	3469	19.7	6	121157	5284	12978	659	22815	1723	46.8	10	186	130	2.7	1	201	13	621	44	22.7	2	23.6	2	1.7	0	5.9	1																																														
crack	166	10.9	4	8.6	1	53323	2745	18.8	6	116869	6470	15151	789	28303	1994	44.2	10	186	130	2.7	1	187	13	580	48	21.8	2	21.8	2	1.7	0	4.3	2																																														
crack	171	6.4	2	7.5	1	57923	3420	25.8	6	126537	7285	12846	978	29844	2514	52.1	11	307	126	3.8	1	205	13	613	46	23.2	2	26.5	2	1.6	0	5.1	1																																														

Table B14: Plagioclase grain 15 - Line 3.2

	Distance	L ¹	ppm	2SDI	L ¹	ppm	2SDI	Na	ppm	2SDI	Na	ppm	2SDI	Mg	ppm	2SDI	Mg	ppm	2SDI	Ca	ppm	2SDI	Ca	ppm	2SDI	Ti	ppm	2SDI	Ti	ppm	2SDI	Fe	ppm	2SDI	Fe	ppm	2SDI	Rb	ppm	2SDI	Rb	ppm	2SDI	Sr	ppm	2SDI	Sr	ppm	2SDI	Ba	ppm	2SDI	Ba	ppm	2SDI	Pr	ppm	2SDI	Pr	ppm	2SDI	Ce	ppm	2SDI	Ce	ppm	2SDI	La	ppm	2SDI	La	ppm	2SDI	Nd	ppm	2SDI	Nd	ppm	2SDI
core	2	20.8	5	21.1	2	62772	2	17.1	6	114834	7091	12797	673	25373	2077	53.3	10	364	82	4.1	1	197	40	452	26	18.9	3	21.6	2	1.3	0	3.5	1																																														
core	6	22.2	3	24.6	4	58842	4	23.4	7	115311	5159	13995	843	26066	2821	61.8	13	330	107	5.2	1	184	9	442	21	20.2	1	21.9	2	1.5	0	2.6	1																																														
core	11	21.2	2	20.1	2	58634	2	15.1	4	109740	4909	13087	188	24285	1857	42.5	12	267	104	4.2	1	177	11	402	26	19.9	2	19.6	2	1.2	0	3.8	1																																														
core	16	22.5	4	17.5	2	53592	2	20.7	7	119191	6353	12344	795	23899	2256	48.8	11	280	167	4.4	1	167	13	387	33	17.5	2	19.6	2	1.4	0	2.8	1																																														
core	21	21.1	3	18.6	2	59888	2	18.8	8	118576	7864	13654	860	24803	2472	54.7	15	439	129	3.9	1	172	12																																																								

Table B13: continued

Sm ppm	ZSD	Eu ppm	ZSD	Gd ppm	ZSD	Pb ppm	ZSD	Pb ppm	ZSD	TiO ₂	Al ₂ O ₃	FeO	MgO	CaO	Na ₂ O	K ₂ O	Or	mol%	Ab	mol%	Or	mol%	Total	An	mol%	Ab	mol%	Or	mol%
0.2	0	7.8	0.5	1	2.7	1	63.3	0.1	22.9	0.2	0.0	4.3	8.0	5	0.3	0.0	100.6	21	70	9	9	9	100.6	21	70	9	9	9	9
0.3	0	9.0	0.1	0	3.5	1	63.6	0.1	23.1	0.2	0.0	4.3	7.8	5	0.3	0.0	100.9	21	70	9	9	9	100.9	21	70	9	9	9	9
0.5	0	8.1	0.1	0	3.4	1	63.6	0.1	23.1	0.2	0.0	4.3	7.8	5	0.3	0.0	100.5	21	70	9	9	9	100.5	21	70	9	9	9	9
0.0	0	7.9	0.2	0	4.0	2	62.6	0.1	23.6	0.2	0.0	4.9	7.7	3	0.3	0.0	100.7	24	68	8	8	8	100.7	24	68	8	8	8	8
0.3	0	8.5	0.1	0	2.6	2	62.8	0.1	23.4	0.2	0.0	4.7	7.8	3	0.2	0.0	100.4	23	69	8	8	8	100.4	23	69	8	8	8	8
0.1	0	8.0	0.3	0	3.2	1	63.0	0.1	23.2	0.2	0.0	4.5	7.9	4	0.2	0.1	100.6	22	70	8	8	8	100.6	22	70	8	8	8	8
0.2	0	7.6	0.3	0	2.1	1	63.1	0.1	23.4	0.2	0.0	4.5	7.8	4	0.2	0.0	100.8	22	69	8	8	8	100.8	22	69	8	8	8	8
0.2	0	7.9	0.4	0	3.9	1	63.1	0.1	23.1	0.2	0.0	4.5	7.7	4	0.2	0.0	100.3	22	69	8	8	8	100.3	22	69	8	8	8	8
0.5	0	7.6	0.5	0	3.2	1	62.9	0.1	23.3	0.2	0.0	4.7	7.8	3	0.2	0.1	100.6	23	69	8	8	8	100.6	23	69	8	8	8	8
0.2	0	7.8	0.1	0	2.4	1	62.9	0.1	23.4	0.2	0.0	4.8	7.7	3	0.2	0.0	100.6	24	69	8	8	8	100.6	24	69	8	8	8	8
0.4	0	7.3	0.4	0	1.8	1	63.0	0.1	23.3	0.2	0.0	4.6	7.7	3	0.2	0.0	100.6	23	69	8	8	8	100.6	23	69	8	8	8	8
0.7	1	7.1	0.7	0	1.4	1	63.0	0.1	23.4	0.2	0.0	4.7	7.7	3	0.2	0.0	100.6	23	69	8	8	8	100.6	23	69	8	8	8	8
0.3	0	6.5	0.1	0	2.1	1	62.8	0.1	23.0	0.2	0.0	4.5	7.7	4	0.2	0.0	98.8	23	69	8	8	8	98.8	23	69	8	8	8	8
0.3	0	6.9	0.1	0	2.8	1	62.7	0.1	23.1	0.2	0.0	4.3	7.8	4	0.2	0.0	100.0	22	70	8	8	8	100.0	22	70	8	8	8	8
0.4	0	6.9	0.5	1	2.2	1	63.1	0.1	23.1	0.2	0.0	4.3	7.8	4	0.2	0.0	100.7	22	69	8	8	8	100.7	22	69	8	8	8	8
0.0	0	7.2	0.4	1	1.3	1	63.3	0.1	23.4	0.2	0.0	4.5	7.9	4	0.2	0.0	100.9	22	70	8	8	8	100.9	22	70	8	8	8	8
0.7	0	6.6	0.1	0	2.6	1	63.3	0.1	22.9	0.2	0.0	4.3	7.9	5	0.2	0.0	100.4	21	70	9	9	9	100.4	21	70	9	9	9	9
0.7	1	7.0	0.4	0	1.8	1	63.5	0.1	22.9	0.2	0.0	4.2	8.0	6	0.2	0.0	100.7	20	71	9	9	9	100.7	20	71	9	9	9	9
0.5	0	7.4	0.4	0	1.8	1	63.6	0.1	22.9	0.2	0.0	4.3	7.9	5	0.2	0.0	100.7	21	70	9	9	9	100.7	21	70	9	9	9	9
0.4	0	7.3	0.2	0	2.2	1	63.3	0.1	22.9	0.2	0.0	4.2	8.0	5	0.2	0.0	100.5	21	70	9	9	9	100.5	21	70	9	9	9	9
0.7	1	6.7	0.3	0	2.2	1	63.5	0.1	22.5	0.2	0.0	4.2	7.8	6	0.2	0.0	100.0	21	70	9	9	9	100.0	21	70	9	9	9	9
0.6	1	6.7	0.5	1	1.9	1	63.5	0.1	22.7	0.2	0.0	4.1	7.9	6	0.1	0.0	100.2	20	71	9	9	9	100.2	20	71	9	9	9	9
0.2	0	7.0	0.6	0	2.7	1	63.4	0.1	22.7	0.2	0.0	4.2	7.8	6	0.2	0.1	100.2	20	71	9	9	9	100.2	20	71	9	9	9	9
0.6	0	6.1	0.1	0	2.6	1	63.3	0.1	22.8	0.2	0.0	4.3	7.9	6	0.2	0.0	100.3	21	70	9	9	9	100.3	21	70	9	9	9	9
0.5	0	6.2	0.3	0	4.0	1	63.3	0.1	22.8	0.2	0.0	4.2	7.9	6	0.1	0.1	100.6	21	70	9	9	9	100.6	21	70	9	9	9	9
0.4	0	7.2	0.1	0	2.8	1	63.6	0.1	22.7	0.2	0.0	4.2	7.8	5	0.2	0.0	100.4	21	70	9	9	9	100.4	21	70	9	9	9	9
0.1	0	6.6	0.3	0	2.9	1	63.6	0.1	23.0	0.2	0.0	4.2	7.9	5	0.1	0.0	100.7	21	70	9	9	9	100.7	21	70	9	9	9	9
0.5	0	5.9	0.6	0	3.0	1	63.3	0.1	22.8	0.2	0.0	4.2	7.9	5	0.1	0.0	100.2	21	70	9	9	9	100.2	21	70	9	9	9	9
0.4	0	6.3	0.3	0	2.1	1	63.5	0.1	23.0	0.2	0.0	4.4	8.0	5	0.2	0.0	100.8	21	70	9	9	9	100.8	21	70	9	9	9	9
0.1	0	6.0	0.0	0	2.8	1	63.2	0.1	22.8	0.2	0.0	4.4	7.7	5	0.1	0.0	100.0	22	69	9	9	9	100.0	22	69	9	9	9	9
0.8	1	5.6	0.4	0	1.8	1	63.6	0.1	22.9	0.2	0.0	4.3	7.8	5	0.1	0.0	100.5	21	70	9	9	9	100.5	21	70	9	9	9	9
0.4	0	5.9	0.1	0	1.2	1	63.6	0.1	22.6	0.2	0.0	4.3	7.9	5	0.1	0.0	100.4	21	70	9	9	9	100.4	21	70	9	9	9	9
0.7	0	5.7	0.2	0	2.0	1	63.8	0.1	22.8	0.2	0.0	4.3	7.9	5	0.1	0.0	100.6	21	70	9	9	9	100.6	21	70	9	9	9	9
0.3	0	5.7	0.4	0	2.2	1	63.7	0.1	22.9	0.2	0.0	4.3	7.9	5	0.2	0.0	100.7	21	70	9	9	9	100.7	21	70	9	9	9	9
0.4	0	5.5	0.3	0	2.9	1	63.7	0.1	22.9	0.2	0.0	4.2	8.0	1.5	0.2	1.0	100.6	20	71	9	9	9	100.6	20	71	9	9	9	9

grain 15 - Line 1.2

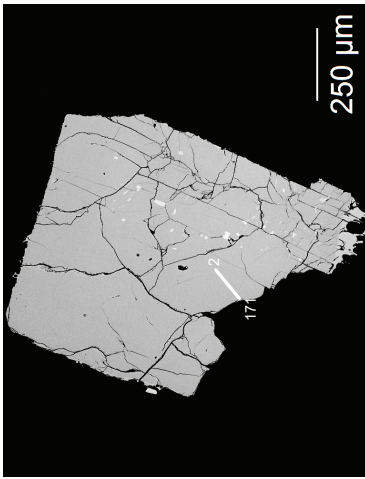


Fig. B12. BSE image of plagioclase grain 15 with trace element line 1.2 (by LA-ICP-MS) indicated.

grain 15 - Line 3.2

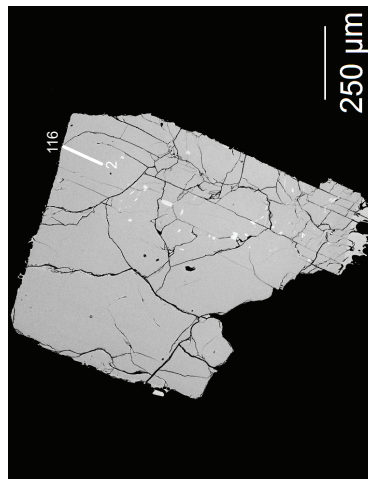


Fig. B13. BSE image of plagioclase grain 15 with trace element line 3.2 (by LA-ICP-MS) indicated.

Table B14: continued

Sm ppm	ZSD	Eu ppm	ZSD	Gd ppm	ZSD	Pb ppm	ZSD	Pb ppm	ZSD	TiO ₂	Al ₂ O ₃	FeO	MgO	CaO	Na ₂ O	K ₂ O	Or	mol%	Ab	mol%	Or	mol%	Total	An	mol%	Ab	mol%	Or	mol%
0.6	0	4.6	1	0.0	0	4.1	2	63.3	0.1	23.0	0.2	0.0	4.2	8.1	1.5	0.0	0.0	100.4	20	71	9	9	100.4	20	71	9	9	9	9
0.5	0	5.1	1	0.2	0	4.5	1	63.4	0.1	22.9	0.2	0.0	4.2	8.0	1.5	0.1	0.0	100.5	20	71	9	9	100.5	20	71	9	9	9	9
0.3	0	4.7	1	0.3	0	2.5	1	63.3	0.1	22.7	0.2	0.0	4.1	8.1	1.6	0.0	0.0	100.1	20	71	9	9	100.1	20	71	9	9	9	9
0.4	0	4.6	1	0.3	0	2.9	2	63.4	0.1	22.7	0.2	0.0	4.0	8.0	1.6	0.1	0.0	100.1	20	71	9	9	100.1	20	71	9	9	9	9
0.5	0	5.4	1	0.2	0	3.7	2	63.8	0.1	22.7	0.2	0.0	4.0	8.0	1.7	0.1	0.0	100.5	20	71	9	9	100.5	20	71	9	9	9	9
0.5	0	4.8	1	0.0	0	2.9	2	63.4	0.1	22.7	0.2	0.0	4.0	8.0	1.6	0.0	0.0	100.0	20	71	9	9	100.0	20	71	9	9	9	9
0.6	1	5.2	1	0.2	0	3.6	2	63.4	0.1	22.9	0.2	0.0	4.1	8.0	1.6	0.0	0.0	100.2	20	71	9	9	100.2	20	71	9	9	9	9
0.5	1	4.7	1	0.4	0	2.8	1	63.4	0.1	23.0	0.2	0.0	4.1	8.2	1.6	0.0	0.0	100.7	20	71	9	9	100.7	20	71	9	9	9	9
0.5	0	4.1	1	0.5	1	2.1	1	63.9	0.1	22.7	0.2	0.0	3.7	8.1	1.7	0.0	0.0	100.4	18	72	10	10	100.4	18	72	10	10	10	10
0.6	0	4.3	1	0.8	1	3.8	2	63.9	0.1	22.5	0.2	0.0	3.8	8.0	1.8	0.0	0.0	100.3	19	71	10	10	100.3	19	71	10	10	10	10
0.1	0	4.1	1	0.4	1	2.3	1	63.7	0.1	22.9	0.2	0.0	4.1	8.0	1.6	0.0	0.0	100.6	20	71	9	9	100.6	20	71	9	9	9	9
0.1	0	4.7	1	0.1	0	2.5	1	64.3	0.1	22.2	0.2	0.0	3.7	7.8	1.8	0.0	0.0	100.1	18	71	11	11	100.1	18	71	11	11	11	11
0.5	0	4.6	1	0.4	0	3.4	1	64.2	0.1	22.6	0.2	0.0	3.7	8.1	1.8	0.0	0.0	100.6	18	72	10	10	100.6	18	72	10	10	10	10
0.4	0	3.8	1	0.6	1	2.0	1	64.4	0.1	22.9	0.2	0.0	4.2	8.1	1.5	0.1	0.0	100.4	20	71	9	9	100.4	20	71	9	9	9	9
0.9	1	4.6	1	0.2	0	3.2	2	63.2	0.1	23.0	0.2	0.0																	

Table B14: continued

Sm ppm	2SD	Eu ppm	2SD	Gd ppm	2SD	Ph ppm	2SD	SiO ₂	TiO ₂	Al ₂ O ₃	FeO	MgO	CaO	Na ₂ O	K ₂ O	SiO ₂	Total	An mol%	Ab mol%	Or mol%	
0.2	0	6.2	0	0.3	0	2.4	0	61.9	0.1	23.0	0.2	0.0	4.1	7.9	1.5	0.1	0.0	98.9	20	71	9
0.5	0	5.9	0	0.2	0	2.2	0	61.6	0.1	22.8	0.2	0.0	4.1	8.0	1.5	0.1	0.0	98.3	20	71	9
0.3	0	6.4	0	0.5	0	3.9	0	61.6	0.1	22.8	0.2	0.0	4.1	8.0	1.5	0.1	0.0	98.3	20	71	9
0.4	0	6.4	0	0.2	0	4.6	0	61.5	0.0	23.0	0.2	0.0	4.1	8.1	1.5	0.1	0.0	98.4	20	71	9
0.5	0	6.4	0	0.2	0	3.9	0	61.5	0.0	23.0	0.2	0.0	4.1	8.1	1.5	0.1	0.0	98.4	20	71	9
0.3	0	6.7	0	0.2	0	3.7	0	61.5	0.1	23.3	0.2	0.0	4.3	8.0	1.5	0.0	0.0	98.8	21	70	9
0.2	0	5.8	0	0.5	0	3.4	0	61.5	0.1	23.3	0.2	0.0	4.3	8.0	1.5	0.0	0.0	98.8	21	70	9
0.4	0	6.2	0	0.5	0	2.5	0	61.6	0.1	23.0	0.2	0.0	4.1	8.0	1.6	0.0	0.0	98.6	20	71	9
0.3	0	5.5	0	0.1	0	1.3	0	61.6	0.1	23.0	0.2	0.0	4.1	8.0	1.6	0.0	0.0	98.6	20	71	9
0.2	0	5.8	0	0.3	0	1.7	0	61.6	0.1	23.0	0.2	0.0	4.1	8.0	1.6	0.0	0.0	98.6	20	71	9
0.3	0	5.3	0	0.3	0	2.6	0	61.6	0.1	23.3	0.2	0.0	4.3	8.0	1.5	0.0	0.0	99.0	21	70	9
0.1	0	6.3	0	0.2	0	2.3	0	61.8	0.1	22.9	0.2	0.0	4.1	7.9	1.6	0.1	0.0	98.7	20	71	9
0.1	0	6.2	0	0.3	0	2.2	0	61.8	0.1	22.9	0.2	0.0	4.1	7.9	1.6	0.1	0.0	98.7	20	71	9
0.4	0	6.6	0	0.4	0	3.5	0	61.9	0.1	22.6	0.2	0.0	3.8	8.1	1.7	0.0	0.0	98.5	19	72	10
0.1	0	6.6	0	0.4	0	1.2	0	61.9	0.1	22.6	0.2	0.0	3.8	8.1	1.7	0.0	0.0	98.5	19	72	10
0.3	0	5.8	0	0.4	0	2.7	0	62.3	0.1	22.2	0.2	0.0	3.6	8.1	1.8	0.0	0.0	98.3	18	72	10
0.5	0	6.1	0	0.7	0	1.9	0	62.1	0.1	22.3	0.2	0.0	3.7	8.2	1.8	0.1	0.0	98.4	18	72	10
0.6	0	5.3	0	0.5	0	2.8	0	62.1	0.1	22.3	0.2	0.0	3.7	8.2	1.8	0.1	0.0	98.4	18	72	10
0.7	0	5.6	0	0.4	0	2.7	0	61.5	0.1	23.0	0.2	0.0	4.2	8.0	1.6	0.0	0.0	98.5	20	71	9
0.4	0	5.0	0	0.5	0	1.3	0	61.5	0.1	23.0	0.2	0.0	4.2	8.0	1.6	0.0	0.0	98.5	20	71	9
0.3	0	4.6	0	0.5	0	1.4	0	61.9	0.0	23.1	0.2	0.0	4.1	8.0	1.6	0.1	0.0	99.2	20	71	9
0.3	0	5.3	0	0.8	0	2.9	0	61.9	0.0	23.1	0.2	0.0	4.1	8.0	1.6	0.1	0.0	99.2	20	71	9
0.5	0	5.1	0	0.2	0	2.9	0	61.9	0.1	22.9	0.2	0.0	4.1	8.0	1.6	0.1	0.0	98.7	20	71	9
0.4	0	4.9	0	0.1	0	3.5	0	61.9	0.1	22.9	0.2	0.0	4.1	8.0	1.6	0.1	0.0	98.7	20	71	9
0.4	0	3.5	0	0.7	0	2.4	0	61.7	0.1	22.9	0.2	0.0	4.0	8.1	1.6	0.1	0.1	98.7	20	71	9
0.5	0	5.2	0	0.0	0	2.4	0	61.7	0.1	22.9	0.2	0.0	4.0	8.1	1.6	0.1	0.1	98.7	20	71	9
0.4	0	4.8	0	0.2	0	2.5	0	61.7	0.1	22.9	0.2	0.0	4.0	8.1	1.6	0.1	0.1	98.7	20	71	9
0.3	0	4.3	0	0.6	0	2.2	0	61.5	0.1	23.0	0.2	0.0	4.0	8.0	1.6	0.1	0.0	98.4	20	71	9
0.5	0	5.0	0	0.3	0	2.3	0	61.5	0.1	23.0	0.2	0.0	4.0	8.0	1.6	0.1	0.0	98.4	20	71	9
0.2	0	4.9	0	0.2	0	2.0	0	61.6	0.1	22.9	0.2	0.0	4.0	8.1	1.6	0.0	0.0	98.5	19	71	9
0.2	0	5.5	0	0.1	0	2.5	0	61.6	0.1	22.9	0.2	0.0	4.0	8.1	1.6	0.0	0.0	98.5	19	71	9
0.5	0	4.8	0	0.1	0	2.8	0	61.3	0.0	22.9	0.2	0.0	4.1	8.1	1.6	0.0	0.0	98.1	20	71	9
0.1	0	5.4	0	0.6	0	1.8	0	61.3	0.0	22.9	0.2	0.0	4.1	8.1	1.6	0.0	0.0	98.1	20	71	9
0.8	0	4.0	0	0.2	0	2.0	0	61.5	0.1	23.0	0.2	0.0	4.1	8.0	1.6	0.0	0.0	98.5	20	71	9
0.4	0	4.8	0	0.1	0	1.6	0	61.5	0.1	23.0	0.2	0.0	4.1	8.0	1.6	0.0	0.0	98.5	20	71	9
0.1	0	4.4	0	0.2	0	3.1	0	61.5	0.0	23.1	0.2	0.0	4.1	8.0	1.6	0.0	0.0	98.5	20	71	9
0.2	0	4.8	0	0.2	0	2.3	0	61.5	0.0	23.1	0.2	0.0	4.1	8.0	1.6	0.0	0.0	98.5	20	71	9
0.8	0	4.2	0	0.1	0	1.9	0	61.5	0.1	22.9	0.2	0.0	4.0	8.2	1.6	0.0	0.1	98.5	19	72	9
0.2	0	4.7	0	0.1	0	2.5	0	61.4	0.1	23.1	0.2	0.0	4.1	8.1	1.6	0.0	0.0	98.6	20	71	9
0.2	0	5.1	0	0.2	0	3.0	0	62.0	0.1	22.7	0.2	0.0	3.8	8.1	1.6	0.0	0.0	98.6	19	72	10
0.6	0	5.3	0	0.3	0	1.8	0	61.6	0.1	22.9	0.2	0.0	4.1	8.0	1.6	0.0	0.0	98.5	20	71	9
0.6	0	4.4	0	0.1	0	2.1	0	61.5	0.1	22.9	0.2	0.0	4.0	8.2	1.6	0.0	0.1	98.5	19	72	9
0.6	0	4.8	0	0.1	0	0.9	0	61.5	0.1	22.9	0.2	0.0	4.0	8.2	1.6	0.0	0.1	98.5	19	72	9
0.5	0	5.1	0	0.2	0	2.5	0	62.0	0.1	22.7	0.2	0.0	3.8	8.1	1.6	0.0	0.0	98.6	19	72	10
0.2	0	4.7	0	0.5	0	1.5	0	62.0	0.1	22.7	0.2	0.0	3.8	8.1	1.6	0.0	0.0	98.6	19	72	10
0.4	0	4.9	0	0.2	0	2.0	0	62.1	0.1	22.9	0.2	0.0	3.8	8.1	1.7	0.0	0.0	98.8	19	72	10
0.2	0	4.6	0	0.7	0	1.5	0	62.1	0.1	22.9	0.2	0.0	3.8	8.1	1.7	0.0	0.0	98.8	19	72	10
0.5	0	4.0	0	0.0	0	1.8	0	61.8	0.1	22.6	0.2	0.0	3.8	8.1	1.6	0.0	0.0	98.2	19	72	10
0.3	0	4.4	0	0.2	0	1.7	0	61.8	0.1	22.6	0.2	0.0	3.8	8.1	1.6	0.0	0.0	98.2	19	72	10
0.0	0	5.0	0	0.4	0	2.1	0	61.7	0.1	23.0	0.2	0.0	3.9	8.1	1.6	0.0	0.0	98.5	19	72	9
0.4	0	4.3	0	0.0	0	2.6	0	61.7	0.1	23.0	0.2	0.0	3.9	8.1	1.6	0.0	0.0	98.5	19	72	9
0.2	0	4.3	0	0.5	0	3.0	0	61.7	0.0	23.2	0.2	0.0	4.1	8.0	1.5	0.0	0.0	98.7	20	71	9
0.6	0	4.3	0	0.6	0	2.0	0	61.7	0.0	23.2	0.2	0.0	4.1	8.0	1.5	0.0	0.0	98.7	20	71	9
0.8	0	4.4	0	0.6	0	2.4	0	61.7	0.1	22.9	0.2	0.0	4.1	8.0	1.6	0.1	0.0	98.6	20	71	9
0.6	0	4.6	0	0.9	0	2.7	0	61.7	0.1	22.9	0.2	0.0	4.1	8.0	1.6	0.1	0.0	98.6	20	71	9
0.2	0	3.6	0	0.4	0	3.2	0	61.7	0.1	23.1	0.2	0.0	4.0	8.0	1.6	0.1	0.0	98.7	20	71	9
0.3	0	3.8	0	0.3	0	1.9	0	61.7	0.1	23.1	0.2	0.0	4.0	8.0	1.6	0.1	0.0	98.7	20	71	9
0.7	0	3.4	0	0.5	0	2.2	0	61.7	0.0	22.9	0.2	0.0	4.0	8.0	1.5	0.0	0.0	98.4	20	71	9
0.7	0	3.7	0	0.2	0	2.8	0	61.7	0.0	22.9	0.2	0.0	4.0	8.0	1.5	0.0	0.0	98.4	20	71	9
0.5	0	3.5	0	0.6	0	3.6	0	61.5	0.1	22.9	0.2	0.0	4.1	8.1	1.6	0.0	0.0	98.5	20	71	9
0.4	0	3.5	0	0.5	0	1.9	0	61.5	0.1	22.9	0.2	0.0	4.1	8.1	1.6	0.0	0.0	98.5	20	71	9
0.4	0	3.2	0	0.3	0	3.5	0	61.6	0.1	23.1	0.2	0.0	4.1	8.1	1.5	0.0	0.0	98.8	20	71	9
0.0	0	3.3	0	0.2	0	3.3	0	61.6	0.1	23.1	0.2	0.0	4.1	8.1	1.5	0.0	0.0	98.8	20	71	9
0.4	0	3.6	0	0.4	0	1.6	0	61.7	0.0	22.9	0.2	0.0	4.1	8.0	1.5	0.0	0.0	98.4	20	71	9
0.7	0	3.1	0	0.1	0	4.1	0	61.7	0.0	22.9	0.2	0.0	4.1	8.0	1.5	0.0	0.0	98.4	20	71	9
0.3	0	3.2	0	0.3	0	3.3	0	61.7	0.0	22.9	0.2	0.0	4.1	8.0	1.5	0.0	0.0	98.4	20	71	9
0.2	0	2.7	0	0.4	0	3.3	0	61.7	0.0	22.9	0.2	0.0	4.1	8.0	1.5	0.0	0.0	98.4	20	71	9
0.6	0	2.7	0	0.4	0	3.6	0	61.7	0.0	22.9	0.2	0.0	4.1	8.0	1.5	0.0	0.0	98.4	20	71	9

grain 15 - Line 2.1

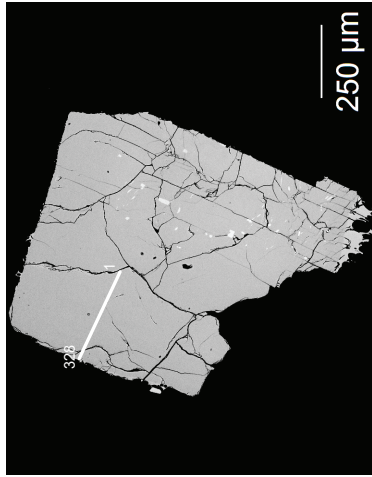


Fig. B12. BSE image of plagioclase grain 15 with trace element line 2.1 (by LA-ICP-MS) indicated.

grain 15 - Line 2.2

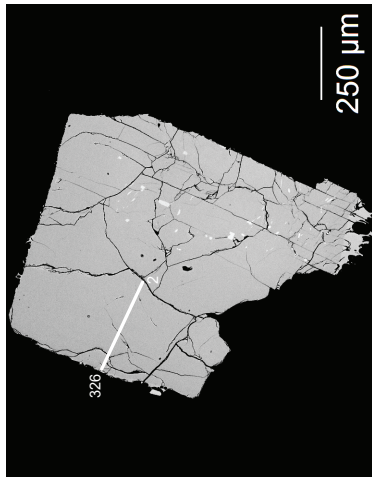


Table B15: Plagioclase grain 15 - Line 2.2

Distance	Lr	ppm	ZSDI	Na	ppm	ZSD	Mg	ppm	ZSDA	ppm	ZSDIA	ppm	ZSDIK	ppm	ZSD	Ca	ppm	ZSD	Ti	ppm	ZSDI	Fe	ppm	ZSDIRb	ppm	ZSDI	Sr	ppm	ZSDI	Rb	ppm	ZSDI	Ba	ppm	ZSDI	Pb	ppm	ZSDI	Ce	ppm	ZSDI	Pr	ppm	ZSDI	Nd	ppm	ZSDI	Sm	ppm	ZSDI	Eu	ppm	ZSDI	Gd	ppm	ZSDI	Tb	ppm	ZSDI	Dy	ppm	ZSDI	Ho	ppm	ZSDI	Er	ppm	ZSDI	Tm	ppm	ZSDI	Yb	ppm	ZSDI	Lu	ppm	ZSDI
core	2	16.0	3	16.2	2	57724.8	2301	22.4	7	75033.4663	3701	582	25559	1944	48.3	0	403	123	4.0	202	9	735	43	20.0	2	22.6	2	1.9	0	3.5																																															
core	7	16.0	3	5.3	2	56146.2	4339	15.5	5	12974.8474	3099	857	24609	2217	53.7	0	352	115	4.2	194	4	714	63	18.7	2	21.2	2	1.9	0	4.5																																															
core	12	16.1	3	6.3	2	58252.9	2777	24.1	8	18923.4322	3185	682	25284	2023	45.5	0	398	51	4.5	204	1	708	46	20.9	3	23.0	2	1.6	0	3.7																																															
core	17	17.1	3	7.2	2	57364.4	2679	29.0	7	20011.5484	2936	651	27337	1526	61.4	0	380	46	4.5	205	2	710	36	22.2	2	23.4	2	1.9	0	3.5																																															
core	22	19.3	3	7.8	2	55582.1	3424	20.2	7	19062.6428	2945	950	26283	1622	67.8	0	371	69	4.5	201	15	663	47	21.7	2	23.1	2	1.6	0	4.4																																															
core	27	22.3	4	18.9	1	58056.8	3230	24.3	7	22024.6155	2644	771	26891	2135	57.8	0	406	68	4.1	208	1	666	38	21.7	2	23.3	2	1.6	0	5.4																																															
core	32	22.4	4	21.4	1	54384.5	2715	20.6	4	18209.6100	2083	848	27149	2409	57.7	0	392	48	3.2	203	12	619	39	22.8	2	22.8	2	1.4	0	3.9																																															
core	37	22.4	4	23.4	3	55526.3	3677	24.9	6	18206.6186	2077	812	25949	2082	51.7	0	433	58	3.2	199	13	633	43	20.9	2	22.8	2	1.4	0	4.4																																															
core	42	24.2	4	27.3	2	55707.3	2501	19.7	6	18905.5034	2524	585	25448	1643	56.5	0	373	42	3.8	199	13	634	41	21.2	2	21.7	2	1.5	0	3.9																																															
core	47	24.5	3	27.7	2	56960.2	3109	26.0	6	18942.7142	3149	862	27765	1824	61.0	0	346	66	4.3	205	3	642	37	21.6	2	21.7	2	1.3	0	3.2																																															
core	52	25.3	4	27.2	3	57040.8	3054	22.0	5	22755.9441	3273	147	26951	2470	70.6	0	316	52	4.3	212	20	626	38	19.2	2	22.4	2	1.3	0	4.2																																															
core	57	25.9	2	24.3	2	54002.4	2748	20.3	6	16948.8085	2758	846	25322	2015	57.1	0	369	52	4.3	201	16	610	37	20.3	2	21.9	2	1.3	0	4.4																																															
core	62	23.0	3	23.8	6	53869.8	2924	18.1	6	14749.5585	2693	750	24504	2288	49.4	0	324	78	3.4	192	9	609	37	20.3	2	21.9	2	1.3	0	4.6																																															
core	67	28.3	3	27.2	2	57704.4	4610	19.8	6	19680.6699	3111	701	27498	2397	52.5	0	427	46	4.5	197	18	597	37	22.2	2	23.5	2	1.1	0	3.7																																															
core	72	27.5	3	25.0	2	54796.8	4550	20.3	8	19341.8557	2479	972	27334	2190	58.7	0	361	51	4.1	201	17	577	50	24.3	3	23.7	2	1.6	0	5.5																																															
core	77	28.6	3	25.8	2	56571.4	2934	22.5	9	21066.5216	2784	781	28888	2136	58.8	0	499	86	4.0	200	4	605	43	24.6	2	24.0	2	1.4	0	4.6																																															
core	82	27.2	4	25.5	2	54620.2	5197	18.2	6	16847.5946	1858	663	28572	2740	50.5	0	329	94	3.9	186	10	529	43	22.9	2	22.9	2	1.4	0	4.6																																															
core	87	27.4	3	27.3	2	54628.9	1980	19.6	7	23856.4783	2752	679	27105	1614	53.7	0	413	111	3.7	208	8	562	28	22.8	2	24.3	2	1.5	0	3.8																																															
core	92	26.7	4	26.3	2	52264.9	2689	22.1	6	15435.5565	1678	655	25984	1154	46.3	0	342	165	4.0	183	14	495	34	22.4	2	23.5	3	1.6	0	4.7																																															
core	97	29.2	4	29.4	2	57148.5	2726	25.8	6	21702.6163	2709	368	29276	1456	51.9	0	459	23	4.6	196	10	525	26	23.4	2	22.8	2	1.7	0	3.6																																															
core	102	27.7	5	28.0	2	54907.8	3199	20.4	5	21107.6318	2182	529	28669	2505	54.0	0	458	76	3.4	186	4	497	34	22.9	2	22.8	2	1.8	0	4.7																																															
core	107	27.5	4	27.2	2	56046.0	3192	22.6	6	20463.6810	2114	723	26689	2018	48.6	0	399	31	3.6	188	6	461	39	20.5	2	22.4	2	1.4	0	4.0																																															
core	112	29.0	3	25.2	1	55227.9	2855	18.6	6	19253.5440	2435	539	26402	1883	57.9	0	326	116	3.9	178	9	464	31	20.6	1	22.3	2	1.6	0	3.4																																															
core	117	31.6	5	28.6	2	53358.6	3120	22.2	6	20732.5961	2557	823	25971	1972	60.8	0	321	146	3.4	183	12	485	33	21.7	2	23.6	2	1.6	0	4.7																																															
core	122	27.5	4	27.1	2	56254.9	4076	20.0	4	19232.6507	2552	810	26431	2029	50.1	0	315	32	3.1	188	12	467	38	22.3	2	23.0	2	1.9	0	5.1																																															
core	127	28.1	3	26.3	2	53789.1	2306	21.4	8	18202.5194	2705	705	26928	1502	46.4	0	310	110	3.6	177	2	441	36	19.6	2	23.3	2	1.8	0	3.9																																															
core	132	27.9	4	27.0	2	53326.0	2933	22.6	7	16971.5763	2849	814	24544	1872	56.8	0	350	164	3.6	175	2	410	31	19.9	2	21.3	2	1.3	0	4.2																																															
core	137	28.5	3	28.8	2	57356.0	3394	23.5	8	22533.5520	3503	822	25624	1712	43.4	0	382	33	4.7	188	17	453	22	20.6	2	25.2	2	1.5	0	3.4																																															
core	142	28.2	3	28.2	2	54082.3	2616	23.9	6	14381.4777	3309	659	24170	1754	31.5	0	334	36	4.7	174	12	423	37	19.5	2	21.3	2	1.3	0	4.4																																															
core	147	28.2	3	28.2	2	57596.7	2389	23.4	8	19309.4088	4023	833	24971	1784	46.0	0	308	109	4.3	179	1	438	33	19.2	2	21.8	2	1.3	0	3.7																																															
core	152	27.9	3	26.3	2	54117.9	2448	24.5	8	20329.4194	3485	754	23361	2013	49.4	0	427	143	4.2	165	10	381	23	18.8	2	21.2	1	1.3	0	3.5																																															
core	157	28.3	4	27.8	3	56524.6	4409	15.4	6	16173.8623	3652	754	23361	2290	62.9	0	296	168	4.5	164	10	418	28	21.7	2	24.3	3	1.7	0	4.1																																															
core	162	28.6	4	33.4	4	54421.7	3521	21.2	7	13447.5658	3871	708	23749	2033	56.1	0	421	278	4.0	171	10	395	36	21.7	2	21.9	2	1.4	0	3.9																																															
core	167	28.6	4	29.1	5	52261.3	2178	21.0	7	18452.4398	3571	708	23845	1947	48.0	0	200	138	5.6	164	8	363	23	19.8	2	21.9	2	1.4	0	3.9																																															
core	172	29.0	3	28.3	3	72377.0	29566	19.2	6	20664.8061	3901	1173	26346	1883	58.5	0	282	32	4.4	173	14	393	35	21.5	2	23.5	2	1.3	0	5.9																																															
core	177	29.6	4	26.7	2	54510.4	2956	22.8	8	18314.6773	3805	1049	26759	1955	67.4	0	314	40	4.2	172	2	354	30	19.6	2	23.1	3	1.6	0	4.8																																															
core	182	29.6	4	25.6	2	53259.2	2180	16.8	6	17900.4233	2765	682	25662	1775	40.6	0	294	48	4.4	163	1	346	30	20.5	2	22.7	2	1.4	0	5.1																																															
core	187	23.4	3	25.3	2	53257.5	3286	17.9	6	16719.7377	3067	907	25951	2009	50.6	0	367	30	4.6	161	2	329	30	18.3	2	22.1	2	1.4	0	4.1																																															
core	192	26.4	3	25.3	2	56968.0	4101	19.5	5	20328.8847	2914	851	26072	1982	48.8	0	191	41	3.8	166	1	346	39	8.6	2	22.8	2	1.4	0	3.6																																															
core	196	26.2	3	24.8	2	57284.5	2740	21.0	6	22722.4312	4138	849	26292	1917	50.2	0	547	22	5.3	176	8	349	24	9.9	2	22.8	2	1.6	0	4.6																																															
core	201	27.5	3	27.8	2	57530.7	3433	14.9	6	24612.7113	3272	523	27796	2684	51.4	0	283	34	4.0	165	9	316	22	9.8	2	20.4	1	1.4	0	4.1																																															
core	206	25.5	4	25.0	3	54530.2	4260	24.5	6	15507.8064	3606	1203	25345	2460	39.8	0	291	55	4.1	158	13	285	21	9.4	1	21.4	2	1.4	0	2.7																																															
core	211	23.8	4	22.9	1	54135.4	2288	20.3	7	17468.4283	2697	516	25972	1841	41.0	0	1	277	73	151	164	8	296	18	8.5	2	20.3	1	1.5	0	3.6																																														
core	216	23.2	4	22.9	2	58856.4	2626	23.5	5	22833.7700	3517	642	25285	2655	41.5	0	236	126	3.8	156	8	297	18	8.5	2	20.3	1	1.5	0	2.7																																															
core	221	23.1	3	21.5	2	54148.1	4012	17.7	4	15479.8606	2825	891	23033	2188	37.3	0	219	26	4.1	151	1	380	27	9.0	2	20.6	3	1.3	0	3.4																																															
core	226	22.1	3	20.0	2	55459.7	6297	21.4	8	19513.5638	3445	810	25744	2036	50.4																																																														

Table B18: continued

Sm	ppm	2SD	Eu	ppm	2SD	Gd	ppm	2SD	Pb	ppm	2SD
0.9	338	20.5	13.8	18.0	21.5	54274	2329	27.5	9	22579	6053
0.9	338	17.8	7.51	55574	2561	25.8	8	19847	6071	1691	483
0.9	343	17.0	7.8	52477	3005	24.5	7	12830	852	26430	2035
0.2	0	3.8	0	0	0	0	0	394	21	37	35.8
0.5	0	3.2	0	0	0	0	0	348	3	38	28.9
0.4	0	3.5	0	0	0	0	0	353	3	39	30.2
0.4	0	3.9	0	0	0	0	0	383	63	3	34.8
0.7	1	3.1	2	0	0	0	0	353	14	3	35.3
0.4	0	3.5	0	0	0	0	0	352	14	3	35.3
0.5	0	4.1	0	0	0	0	0	362	20	7	33.2
0.1	0	2.8	0	0	0	0	0	352	20	7	33.2
0.5	0	1.9	0	0	0	0	0	362	20	7	33.2
0.2	0	3.7	0	0	0	0	0	372	18	0	37
0.2	0	4.1	0	0	0	0	0	372	18	0	37
0.3	0	3.5	0	0	0	0	0	382	17	3	35.9
0.7	1	3.6	0	0	0	0	0	382	17	3	35.9
0.5	0	2.5	0	0	0	0	0	392	19	3	34.6
0.5	0	2.9	0	0	0	0	0	392	19	3	34.6
0.3	0	3.7	0	0	0	0	0	402	17	2	34.6
0.4	0	3.7	0	0	0	0	0	402	17	2	34.6
0.3	0	2.7	0	0	0	0	0	412	17	2	34.6
0.4	0	2.9	0	0	0	0	0	412	17	2	34.6
0.2	0	3.3	0	0	0	0	0	422	17	2	34.6
0.2	0	3.6	0	0	0	0	0	422	17	2	34.6
0.6	0	2.8	0	0	0	0	0	432	17	2	34.6
0.5	0	3.0	0	0	0	0	0	432	17	2	34.6
0.5	0	3.4	0	0	0	0	0	442	17	2	34.6
0.4	0	3.4	0	0	0	0	0	442	17	2	34.6
0.2	0	1.6	0	0	0	0	0	452	17	2	34.6
0.6	0	1.5	0	0	0	0	0	452	17	2	34.6
0.6	0	1.5	0	0	0	0	0	462	16	3	34.6
0.4	0	3.0	0	0	0	0	0	462	16	3	34.6
0.5	0	3.3	0	0	0	0	0	472	15	3	34.6
0.5	0	3.6	0	0	0	0	0	472	15	3	34.6
0.5	0	4.0	0	0	0	0	0	482	15	3	34.6
0.4	0	0.9	0	0	0	0	0	482	15	3	34.6
0.4	0	0.9	0	0	0	0	0	492	16	2	34.6
0.4	0	0.9	0	0	0	0	0	492	16	2	34.6
0.3	0	0.3	0	0	0	0	0	502	16	2	34.6
0.2	0	0.2	0	0	0	0	0	502	16	2	34.6
0.4	0	0.6	0	0	0	0	0	512	16	2	34.6
0.8	0	0.6	0	0	0	0	0	512	16	2	34.6
0.3	0	0.4	0	0	0	0	0	522	15	3	34.6
0.4	0	0.4	0	0	0	0	0	522	15	3	34.6
0.5	0	0.5	0	0	0	0	0	532	15	3	34.6
0.4	0	0.5	0	0	0	0	0	532	15	3	34.6
0.1	0	0.9	0	0	0	0	0	542	15	3	34.6
0.3	0	0.3	0	0	0	0	0	542	15	3	34.6
0.3	0	0.3	0	0	0	0	0	552	15	3	34.6
0.6	0	1.0	0	0	0	0	0	562	14	3	34.6
0.5	0	1.0	0	0	0	0	0	562	14	3	34.6
0.5	0	1.0	0	0	0	0	0	572	13	3	34.6
0.4	0	0.4	0	0	0	0	0	572	13	3	34.6
0.4	0	0.4	0	0	0	0	0	582	13	3	34.6
0.3	0	0.3	0	0	0	0	0	582	13	3	34.6
0.3	0	0.3	0	0	0	0	0	592	12	3	34.6
0.2	0	0.2	0	0	0	0	0	592	12	3	34.6
0.2	0	0.2	0	0	0	0	0	602	12	3	34.6
0.5	0	0.6	0	0	0	0	0	602	12	3	34.6
0.5	0	0.6	0	0	0	0	0	612	11	3	34.6
0.2	0	0.2	0	0	0	0	0	612	11	3	34.6
0.5	0	0.8	0	0	0	0	0	622	11	3	34.6
0.2	0	0.2	0	0	0	0	0	622	11	3	34.6
0.2	0	0.2	0	0	0	0	0	632	11	3	34.6
0.4	0	0.8	0	0	0	0	0	632	11	3	34.6
0.4	0	0.8	0	0	0	0	0	642	10	3	34.6
0.3	0	0.3	0	0	0	0	0	642	10	3	34.6
0.4	0	0.4	0	0	0	0	0	652	10	3	34.6
0.4	0	0.4	0	0	0	0	0	652	10	3	34.6
0.3	0	0.3	0	0	0	0	0	662	9	3	34.6
0.2	0	0.2	0	0	0	0	0	662	9	3	34.6
0.2	0	0.2	0	0	0	0	0	672	9	3	34.6
0.3	0	0.3	0	0	0	0	0	672	9	3	34.6
0.3	0	0.3	0	0	0	0	0	682	8	3	34.6
0.4	0	0.4	0	0	0	0	0	682	8	3	34.6
0.4	0	0.4	0	0	0	0	0	692	8	3	34.6
0.3	0	0.3	0	0	0	0	0	692	8	3	34.6
0.3	0	0.3	0	0	0	0	0	702	7	3	34.6
0.4	0	0.4	0	0	0	0	0	702	7	3	34.6
0.4	0	0.4	0	0	0	0	0	712	7	3	34.6
0.3	0	0.3	0	0	0	0	0	712	7	3	34.6
0.3	0	0.3	0	0	0	0	0	722	6	3	34.6
0.4	0	0.4	0	0	0	0	0	722	6	3	34.6
0.4	0	0.4	0	0	0	0	0	732	6	3	34.6
0.3	0	0.3	0	0	0	0	0	732	6	3	34.6
0.3	0	0.3	0	0	0	0	0	742	5	3	34.6
0.4	0	0.4	0	0	0	0	0	742	5	3	34.6
0.4	0	0.4	0	0	0	0	0	752	5	3	34.6
0.3	0	0.3	0	0	0	0	0	752	5	3	34.6
0.3	0	0.3	0	0	0	0	0	762	4	3	34.6
0.4	0	0.4	0	0	0	0	0	762	4	3	34.6
0.4	0	0.4	0	0	0	0	0	772	4	3	34.6
0.3	0	0.3	0	0	0	0	0	772	4	3	34.6
0.3	0	0.3	0	0	0	0	0	782	3	3	34.6
0.4	0	0.4	0	0	0	0	0	782	3	3	34.6
0.4	0	0.4	0	0	0	0	0	792	3	3	34.6
0.3	0	0.3	0	0	0	0	0	792	3	3	34.6
0.3	0	0.3	0	0	0	0	0	802	2	3	34.6
0.4	0	0.4	0	0	0	0	0	802	2	3	34.6
0.4	0	0.4	0	0	0	0	0	812	2	3	34.6
0.3	0	0.3	0	0	0	0	0	812	2	3	34.6
0.3	0	0.3	0	0	0	0	0	822	1	3	34.6
0.4	0	0.4	0	0	0	0	0	822	1	3	34.6
0.4	0	0.4	0	0	0	0	0	832	1	3	34.6
0.3	0	0.3	0	0	0	0	0	832	1	3	34.6
0.3	0	0.3	0	0	0	0	0	842	0	3	34.6
0.4	0	0.4	0	0	0	0	0	842	0	3	34.6
0.4	0	0.4	0	0	0	0	0	852	0	3	34.6
0.3	0	0.3	0	0	0	0	0	852	0	3	34.6
0.3	0	0.3	0	0	0	0	0	862	0	3	34.6
0.4	0	0.4	0	0	0	0	0	862	0	3	34.6
0.4	0	0.4	0	0	0	0	0	872	0	3	34.6
0.3	0	0.3	0	0	0	0	0	872	0	3	34.6
0.3	0	0.3	0	0	0	0	0	882	0	3	34.6
0.4	0	0.4	0	0	0	0	0	882	0	3	34.6
0.4	0	0.4	0	0	0	0	0	892	0	3	34.6
0.3	0	0.3	0	0	0	0	0	892	0	3	34.6
0.3	0	0.3	0	0	0	0	0	902	0	3	34.6
0.4	0	0.4	0	0	0	0	0	902	0	3	34.6
0.4	0	0.4	0	0	0	0	0	912	0	3	34.6
0.3	0	0.3	0	0	0	0	0	912	0	3	34.6
0.3	0	0.3	0	0	0	0	0	922	0	3	34.6
0.4	0	0.4	0	0	0	0	0	922	0	3	34.6
0.4	0	0.4	0	0	0	0	0	932	0	3	34.6
0.3	0	0.3	0	0	0	0	0	932	0	3	34.6
0.3	0	0.3	0	0	0	0	0	942	0	3	34.6
0.4	0	0.4	0	0	0	0	0	942	0	3	34.6
0.4	0	0.4	0	0	0	0	0	952	0	3	34.6
0.3	0	0.3	0	0	0	0	0	952	0	3	34.6
0.3	0	0.3	0	0	0	0	0	962	0	3	34.6
0.4	0	0.4	0	0	0	0	0	962	0	3	34.6
0.4	0	0.4	0	0	0	0	0	972	0	3	34.6
0.3	0	0.3	0	0	0	0	0	972	0	3	34.6
0.3	0	0.3	0	0	0	0	0	982	0	3	34.6
0.4	0	0.4	0	0	0	0	0	982	0	3	34.6
0.4	0	0.4	0	0	0	0	0	992	0	3	34.6
0.3	0	0.3	0	0	0	0	0	992	0	3	34.6
0.3	0	0.3	0	0	0	0	0	1002	0	3	34.6

Table B18: continued

core	676	21.4	3.3	22.2	3.3	57.2	6.5	88.0	24.9	7	20.590	75.42	10.967	6.72	27.93	5.23	44.9	8	48.4	76	3.7	146.6	5.50	7.8	20.5	2.2	24.0	11	8.0	5.1	10.6	0.1	5.0	0.2	0.10	4.9		
core	68	120.9	3.3	22.6	3.3	54.7	5.3	87.6	27.6	8	25.821	60.21	13.36	5.58	28.84	1.2	38.8	40.3	12	42.7	0.7	3.1	43.2	4.5	9	21.3	2.2	25.0	2	6.0	4.6	10.4	0.2	0.20	4.3			
core	686	19.0	2.2	8.3	1.6	23.5	3.9	66.6	11.2	25.329	66.65	11.37	6.43	19.43	15.5	9	2.5	5.3	12	5.3	5.4	2.9	46.9	4.2	6	22.4	2.2	25.6	2	9.0	4.7	10.2	0.1	0.20	5.1			
core	69	19.3	3.3	20.1	3.3	52.7	5.0	95.4	30.5	9	21.404	58.22	10.895	5.17	29.06	4.1	53.7	15	5.10	30	2.9	44.3	5.1	9	21.2	2.2	24.7	2	8.0	4.4	10.3	0.1	0.40	4.5				
core	696	20.5	2.2	8.8	1.6	25.6	3.9	68.2	11.2	26.000	67.22	10.05	6.66	29.28	20.7	5.8	12	5.43	40	3.3	4.5	4.2	46.4	4.3	6	20.9	2.2	25.2	2	6.0	5.1	10.6	1.1	0.40	4.5			
core	70	22.3	4.3	18.7	3.3	52.0	3.9	69.2	35.0	8	186.24	58.22	10.833	5.72	29.06	4.1	53.7	15	5.10	30	2.9	44.3	5.1	9	21.2	2.2	24.7	2	8.0	4.4	10.3	0.1	0.40	4.4				
core	706	21.3	3.3	22.1	3.3	54.2	7.2	81.3	34.3	11	28.094	56.17	11.421	3.5	3.7	46.9	4.3	68.8	8	22.3	3.7	46.9	4.3	68.8	8	22.3	3.7	46.9	4.3	68.8	8	22.3	3.7	46.9	4.3	68.8	8	
core	71	21.3	3.3	20.3	3.3	52.5	2.9	62.6	31.1	6	21.292	62.61	10.49	6.33	4.5	6.2	3	4.3	4.3	4.3	4.3	4.3	4.3	4.3	4.3	4.3	4.3	4.3	4.3	4.3	4.3	4.3	4.3	4.3	4.3	4.3		
core	716	21.1	3.3	19.9	3.3	52.9	2.8	32.1	9	22.600	67.22	10.05	6.66	29.28	20.7	5.8	12	5.43	40	3.3	4.5	4.2	46.4	4.3	6	20.9	2.2	25.2	2	6.0	5.1	10.6	1.1	0.40	4.5			
core	72	22.2	4.3	20.9	2.2	54.8	3.3	43.7	12	129.107	103.83	12.235	1.77	28.79	2.52	61.2	4	46.8	75	3.5	48.6	4.0	3.2	46.2	6.0	3	24.2	2.2	26.3	3	8.0	5.1	10.4	0.1	0.20	5.8		
core	726	23.0	4.3	21.2	3.3	54.2	1.9	34.9	33.8	10	21.585	66.40	13.38	7.77	28.79	2.52	61.2	4	46.8	75	3.5	48.6	4.0	3.2	46.2	6.0	3	24.2	2.2	26.3	3	8.0	5.1	10.4	0.1	0.20	5.8	
core	73	24.6	4.3	21.2	3.3	54.2	1.9	34.9	33.8	10	26.740	65.77	14.05	5.53	29.49	2.0	49.2	12	62.3	75	3.2	47.5	5.3	6.6	5.2	2.0	2.0	2.0	2.0	2.0	2.0	2.0	2.0	2.0	2.0	2.0		
core	736	26.3	5.3	20.5	1.2	54.8	6.4	19.7	28.0	8	25.482	30.28	14.78	6.35	29.40	19.8	6.1	12	45.8	66	2.8	47.5	6.9	6.6	2.8	4.7	3.3	2.6	2.9	3.5	10.3	0.1	0.40	5.3				
core	74	20.0	3.3	19.6	2.2	53.96	4.8	29.5	6	20.845	76.11	12.75	5.55	27.53	23.40	46.6	11	42.0	24	3.2	48.4	6.6	5.9	2.2	2.2	7.0	5.4	10.6	0.1	0.20	4.9							
core	746	24.8	3.3	21.4	3.3	54.9	0.7	32.8	8	28.819	59.75	12.87	5.33	29.94	21.5	50.4	11	41.9	89	3.5	49.8	4.0	2.9	2.5	7.2	7.0	4.5	10.5	0.1	0.20	5.6							
core	75	19.4	3.3	22.8	3.3	57.8	3.9	89.9	30.6	8	26.603	66.92	11.5	6.46	3.0	16.2	20.4	14	62.7	41	2.9	51.3	4.7	9	24.6	2.2	25.7	2	10.4	0.1	0.20	5.6						
core	756	22.3	4.3	21.5	3.3	55.2	3.9	67.7	34.3	9	29.683	72.12	13.22	6.23	28.96	25.0	50.9	14	52.8	73	3.7	50.8	4.9	3	23.5	3.5	2.2	2.0	4.2	10.4	0.1	0.20	5.6					
core	76	124.9	4.3	22.3	3.3	54.0	6.0	32.4	8	23.187	70.41	12.66	8.80	28.87	23.00	52.5	4	41.4	68	3.7	50.3	7.0	0.2	2.3	2.6	1.1	7.0	5.0	10.3	0.1	0.20	5.1						
core	766	22.2	4.3	22.5	3.3	54.0	6.0	32.4	8	20.029	58.16	14.93	4.81	29.96	24.26	36.6	10	35.0	25	3.1	48.2	6.7	8	0.2	2.3	2.6	1.1	7.0	5.0	10.3	0.1	0.20	4.7					
core	77	22.0	4.3	22.5	3.3	54.0	6.0	32.4	8	16.904	82.31	18.73	10.10	29.90	24.26	36.6	10	35.0	25	3.1	48.2	6.7	8	0.2	2.3	2.6	1.1	7.0	5.0	10.3	0.1	0.20	4.7					
core	776	24.6	4.3	22.5	3.3	54.0	6.0	32.4	8	24.288	78.28	19.03	7.44	29.92	27.1	53.0	13	37.5	6	4.0	46.0	3.3	4.9	4.5	1.6	2.4	2.4	2.4	2.4	2.4	2.4	2.4	2.4	2.4	2.4			
core	78	125.1	4.3	23.0	3.3	54.4	3.9	44.3	31.1	7	29.339	76.78	14.79	8.38	23.89	24.65	63.4	18	35.6	3	3.7	46.6	4.3	5	2.0	2.2	2.5	3.3	5.0	4.2	10.7	0.1	0.20	4.8				
core	786	22.3	3.3	23.4	3.3	58.2	1.2	56.3	28.3	8	20.409	81.68	19.79	8.72	26.63	25.55	46.2	12	29.8	55	3.2	50.1	5.7	1	0.2	2.2	2.4	2.2	2.4	2.2	2.4	2.2	2.4	2.2	2.4	2.2		
core	79	21.4	3.3	21.8	1.1	55.5	3.3	24.6	26.3	7	22.032	49.63	13.08	9.5	26.90	8.43	62.0	16	60.1	64	3.8	49.7	3.7	9	2.1	2.3	1.1	5.0	4.2	10.3	0.1	0.20	4.5					
core	796	21.5	4.3	22.0	2.2	55.7	4.0	28.0	10	12.774	8.13	22.30	8.20	26.57	8.54	45.6	12	45.6	92	3.6	49.3	5.7	4	2.1	2.1	2.1	2.1	2.1	2.1	2.1	2.1	2.1	2.1	2.1	2.1	2.1		
core	80	124.4	3.3	21.9	2.2	55.8	4.0	28.0	10	19.909	63.59	16.89	5.20	26.48	15.51	56.8	13	51.2	63	3.6	46.2	4.3	6	2.2	2.2	2.2	2.2	2.2	2.2	2.2	2.2	2.2	2.2	2.2	2.2	2.2	2.2	
core	806	25.6	3.3	22.8	2.2	59.0	3.3	53.1	28.0	7	12.740	78.05	12.43	8.62	28.19	30.99	51.8	12	38.6	16	3.3	50.3	4.6	6	2.5	3.2	8.0	4.1	10.5	0.1	0.20	6.7						
core	81	23.2	4.3	24.2	2.2	59.70	6.5	24.4	11	124.79	63.19	17.76	7.26	28.57	28.87	59.4	10	41.5	13	3.2	47.6	4.7	8	2.2	2.2	2.2	2.2	2.2	2.2	2.2	2.2	2.2	2.2	2.2	2.2	2.2	2.2	
core	816	22.0	2.2	24.2	2.2	56.0	3.6	35.9	7	24.071	62.95	18.70	6.42	28.24	20.32	54.7	10	53.1	94	3.2	50.3	3.3	6.8	5	2.3	2.2	2.2	2.2	2.2	2.2	2.2	2.2	2.2	2.2	2.2	2.2	2.2	
core	82	24.4	3.3	22.2	2.2	55.7	3.7	31.9	30.0	9	12.758	6.92	17.56	6.08	28.17	1.86	52.1	16	48.7	69	3.4	48.2	4.6	8.2	3	2.2	2.2	2.2	2.2	2.2	2.2	2.2	2.2	2.2	2.2	2.2	2.2	
core	826	24.4	3.3	21.9	2.2	57.0	1.2	25.9	22.4	8	12.038	4.96	17.89	5.16	29.87	2.26	62.4	12	45.9	47	3.5	49.2	3.3	4	2.3	2.2	2.2	2.2	2.2	2.2	2.2	2.2	2.2	2.2	2.2	2.2	2.2	
core	83	26.4	6.3	21.6	3.3	53.7	2.8	3.3	8	18.568	54.60	10.68	5.99	28.17	22.59	49.0	11	49.9	50	3.7	47.5	4.6	6.5	6	2.1	2.2	2.2	2.2	2.2	2.2	2.2	2.2	2.2	2.2	2.2	2.2	2.2	
core	836	21.4	3.3	21.1	2.2	53.7	3.5	28.5	24.3	8	18.991	47.10	10.920	4.53	27.43	19.81	49.6	12	32.5	22	2.7	48.1	3.0	7	2.2	2.2	2.2	2.2	2.2	2.2	2.2	2.2	2.2	2.2	2.2	2.2	2.2	2.2
core	84	124.5	3.3	20.7	2.2	54.0	1.1	19.0	25.2	6	22.066	4.56	10.95	4.24	28.01	19.8	58.6	13	44.8	42	3.1	49.4	3.8	2	2.2	2.2	2.2	2.2	2.2	2.2	2.2	2.2	2.2	2.2	2.2	2.2	2.2	2.2
core	846	22.6	3.3	21.7	2.2	57.3	0.1	34.3	31.1	8	29.519	63.29	18.32	7.54	29.47	22.20	58.3	11	52.4	36	3.6	48.6	4.6	3	2.5	3.2	2.8	3.2	2.5	3.2	2.5	3.2	2.5	3.2	2.5	3.2	2.5	3.2
core	85	124.9	4.3	22.4	3.3	52.4	1.2	52.4	31.7	8	26.972	76.77	13.91	6.11	32.18	24.72	60.2	15	50.2	36	3.6	45.3	4.4	6.9	4	2.5	3.2	2.8	3.2	2.5	3.2	2.5	3.2	2.5	3.2	2.5	3.2	
core	856	19.9	2.2	21.9	1.2	56.1	6.0	29.0	28.3	8	27.456	4.68	15.20	5.18	30.08	23.69	49.5	9	38.6	33	4.3	51.9	4.3	2	2.4	2.2	2.2	2.2	2.2	2.2	2.2	2.2	2.2	2.2	2.2	2.2	2.2	2.2
core	86	117.8	3.3	18.2	1.2	56.7	3.6	27.8	3	22.387	72.93	10.984	8.45	29.59	32.29	41.6	14	44.4	16	3.3	50.1	4.7	6.8	2	2.4	2.2	2.2	2.2	2.2	2.2	2.2	2.2	2.2	2.2	2.2	2.2	2.2	2.2
core	866	20.2	2.2	18.7	1.2	56.0	3.3	21.0	7	24.099	76.49	11.53	6.77	29.59	22.07	51.7	8	51.2	55	3.6	50.0	4.7	1	0.2	2.4	2.2	2.2	2.2	2.2	2.2	2.2	2.2	2.2	2.2	2.2	2.2	2.2	2.2
core	87	15.9	2.2	16.3	1.2	54.1	5.9	4.3	6	19.023	6.347	10.972	5.63	28.35	20.31	54.7	14	44.9	47	3.8	50.0	5.7	1	0.2	2.4	2.2	2.2	2.2	2.2									

Table B19: Plagioclase grain 21 - Line 2

Crackled	2	1.4	3	2.2	59918	4482	25.1	7	20650	7971	2477	1020	2845	2487	50.4	8	468	145	4	74.2	8	24.7	2	27.0	3	1.4	0	3.6
Crackled	6	1.5	2	1.7	57993	3203	29.3	6	19651	6160	1955	679	26330	2245	54.8	12	421	171	3	77.4	6	22.1	2	26.9	3	1.9	0	4.8
Crackled	11	2.5	2	58488	4668	30.0	6	17200	7392	6338	712	25510	2449	58.0	4	691	450	3	5	71.1	13	23.0	2	27.5	3	1.9	0	5.7
Crackled	16	14.7	4	55082	3214	33.1	9	41103	6696	931	1041	27425	2336	46.7	10	433	36	3	59.8	8	21.9	2	26.8	2	2.0	0	6.2	
Crackled	21	13.5	3	54739	3588	24.2	8	17786	7089	1179	645	26515	2277	45.7	11	559	97	3	70.9	9	22.3	2	26.4	2	2.0	0	5.4	
Crackled	26	13.2	2	57824	2597	28.3	7	20591	5653	1063	672	27754	1965	66.5	16	473	123	3	71.3	11	23.3	2	27.4	3	1.9	0	3.9	
Crackled	31	1.9	3	54203	2243	26.2	6	14808	3514	1033	517	25345	1688	46.5	12	425	117	3	71.3	10	23.3	2	27.4	2	2.0	0	4.9	
Crackled	36	12.1	1	53964	2502	27.0	8	17780	5268	1235	657	26973	1604	50.1	12	423	188	3	71.3	10	23.3	2	27.4	2	2.0	0	4.9	
Crackled	41	1.1	3	59336	3639	31.4	7	24872	7759	1664	853	29171	2719	70.0	13	606	122	2	71.2	12	26.4	2	27.7	2	2.3	0	5.3	
Crackled	46	10.5	2	58914	7109	30.1	8	20005	6380	1127	676	28615	2471	44.3	8	519	166	2	71.0	11	23.8	2	27.0	3	1.7	0	3.2	
Crackled	51	3.4	3	53187	2627	24.7	6	20709	6109	1010	532	29288	2168	42.8	17	449	176	4	71.0	10	24.8	2	29.2	2	2.4	0	5.1	
Crackled	56	2.2	4	56536	3082	36.8	9	21746	6199	1448	576	29379	2007	55.3	13	677	133	4	70.8	9	25.0	2	29.6	2	2.0	0	3.4	
Crackled	61	14.8	3	56026	3360	28.5	8	16233	6650	1508	735	28652	2134	49.6	11	632	210	3	71.0	9	26.1	2	29.9	3	2.0	0	4.6	
Crackled	66	11.7	3	56193	4399	26.1	7	20601	6981	1592	1024	28233	2550	58.4	10	497	173	4	71.0	9	26.1	2	28.5	2	1.7	0	4.9	
Crackled	71	1.5	2	57157	3944	38.7	10	18874	8152	1310	689	27710	2600	45.6	12	452	150	3	80.8	13	24.4	2	28.2	2	1.8	0	5.4	
Crackled	76	14.0	3	59096	6493	33.6	10	22058	8806	1468	1018	28734	3258	57.2	15	441	173	3	71.3	10	29.1	4	28.7	3	2.6	1	7.4	
Crackled	81	15.2	4	56652	4103	40.4	9	25109	8247	1868	876	28539	2491	51.6	15	542	167	4	68.2	9	26.3	3	32.3	3	2.1	1	6.5	
Crackled	86	14.7	4	58336	6117	39.2	15	13343	8290	1742	869	25101	2279	57.9	12	343	164	3	71.1	13	23.0	2	27.7	2	1.3	0	6.0	
Crackled	91	12.3	3	59495	4249	34.7	7	11681	5976	2873	1181	23773	2143	44.7	10	356	120	3	75.7	11	22.0	2	25.2	2	1.9	0	4.0	
Crackled	96	11.1	3	55255	3209	33.4	7	11811	6406	2197	747	24877	2280	48.9	12	434	148	3	75.7	11	22.0	2	25.2	2	1.6	0	3.9	
Crackled	101	1.2	2	57062	3859	30.5	8	18975	7001	2133	637	26527	2387	50.9	12	418	150	4	73.5	10	24.5	2	26.5	2	1.8	0	4.2	
Crackled	106	1.6	3	53082	2990	22.8	6	2687	5080	2140	653	23845	1391	47.6	10	392	106	3	71.4	10	23.1	2	33.8	2	1.7	0	4.8	
Crackled	111	10.3	4	54757	3105	23.4	7	4205	5530	1409	542	24797	2026	58.2	14	403	168	4	76.3	7	23.2	2	35.4	3	1.7	0	4.6	
Crackled	116	9.4	3	55017	3250	29.5	8	18809	8188	1201	756	26212	2223	57.3	10	413	168	4	79.6	11	24.3	2	37.1	2	2.0	0	5.0	
Crackled	21	9.6	2	55365	4165	31.8	10	14654	6878	2006	950	27217	2233	49.8	10	315	135	4	81.3	10	24.2	3	25.4	2	2.0	1	4.9	
Crackled	26	7.3	2	57243	3530	23.2	9	21253	6581	2443	640	26922	2325	48.1	12	417	174	3	66.5	7	23.3	2	28.1	2	1.8	0	3.9	
Crackled	31	6.2	3	58165	3294	32.0	8	21591	6574	2681	877	25840	1890	47.2	14	400	220	3	84.7	9	24.7	2	27.3	2	1.4	0	4.2	
Crackled	36	10.4	3	55190	3180	26.5	8	11529	4884	2435	734	24845	1924	45.3	9	378	169	4	87.0	13	23.3	2	25.8	2	2.2	0	5.2	
Crackled	41	7.4	2	56045	2706	32.7	8	20008	4689	2459	554	26071	1331	52.0	10	410	148	3	86.2	11	23.8	2	27.3	3	1.6	0	4.4	
Crackled	46	10.0	3	54451	2664	26.4	6	15398	5232	2210	656	26103	2359	49.1	11	343	144	3	89.0	12	23.8	2	25.8	2	1.7	0	3.9	
Crackled	51	7.6	2	56256	2955	24.5	6	18125	5252	2450	529	24553	1452	51.3	13	364	23	4	84.9	10	21.9	2	25.2	2	1.6	0	4.2	
Crackled	56	12.8	3	55416	2272	29.6	7	4538	5788	2901	648	25160	1930	55.7	13	434	142	4	73.0	10	23.2	2	35.0	2	1.6	0	4.4	
Crackled	61	2.6	3	51875	2170	30.0	8	10605	4185	2165	600	23578	1695	49.1	13	246	99	3	73.1	11	21.4	2	34.8	2	1.6	0	4.0	
Crackled	66	14.5	3	57263	2729	19.4	8	18050	5785	2489	641	28236	2757	54.9	13	481	149	3	76.7	10	23.8	2	26.1	1	1.8	0	5.5	
Crackled	71	14.5	3	56948	3701	24.5	8	15718	5934	2108	633	26125	2750	46.9	12	313	151	3	81.3	10	24.2	2	26.9	2	1.9	0	3.6	
Crackled	76	9.3	4	58619	4290	27.2	9	19001	6858	2547	800	26733	2216	47.5	12	408	153	3	78.4	9	23.6	2	26.6	2	1.6	0	3.1	
Crackled	81	2.9	3	58214	2718	23.2	6	25546	6506	2724	616	29146	1951	54.9	15	589	200	4	90.4	10	24.3	2	26.1	2	1.8	0	4.4	
Crackled	86	14.4	4	54937	2413	20.8	7	15871	3119	2419	522	27076	1911	47.1	14	408	150	4	92.1	11	24.4	2	26.2	2	1.7	0	4.0	
Crackled	91	13.2	3	59517	3828	31.9	8	26046	7777	2912	858	27194	2208	62.2	15	433	233	4	92.1	14	24.2	2	27.2	3	2.0	0	5.0	
Crackled	96	15.0	3	56036	3567	26.7	8	17099	6327	2059	697	26992	2027	50.5	13	404	121	3	79.8	11	24.9	3	25.7	2	1.3	0	3.9	
Crackled	201	4.1	3	55105	3590	27.0	7	14754	6232	1817	619	25418	1933	47.7	10	379	166	3	86.2	11	25.0	3	29.5	2	1.8	0	3.8	
Crackled	206	5.3	2	58031	2706	23.0	7	21106	4738	2186	519	27748	2058	57.4	15	591	160	3	86.2	11	25.0	3	29.5	2	1.9	0	3.2	
Crackled	211	19.7	3	54468	2830	36.3	9	17826	9561	1665	725	26087	1875	45.9	9	291	233	3	73.0	7	22.4	2	27.3	2	1.9	0	4.8	
Crackled	216	18.4	4	54977	2774	24.8	5	11719	5498	1936	689	25797	1461	62.8	16	429	204	3	73.8	7	22.4	2	25.9	2	1.8	0	4.6	
Crackled	221	16.2	3	56843	3762	32.7	8	20553	8263	2327	753	29672	3243	61.7	12	483	186	4	88.3	10	23.5	2	28.0	3	2.0	1	6.3	
Crackled	226	21.0	3	58704	6294	27.8	10	16435	8346	2619	853	26504	2506	48.2	12	465	188	4	84.8	13	24.6	3	26.2	2	1.6	0	5.7	
Crackled	231	15.3	3	57180	2976	35.7	11	20955	6731	2741	689	27602	1865	50.3	12	519	138	3	87.8	9	23.5	2	28.8	3	2.2	0	4.4	
Crackled	236	22.0	4																									

Table B21: continued

Sm ppm	Zr	Df	Eu	ppm	Zr	Df	Cd	ppm	Zr	Df	Pb	ppm	Zr	Df	SiO ₂	THO	Al ₂ O ₃	FeO	MgO	CaO	Na ₂ O	K ₂ O	BaO	SrO	Total	An mol%	Ab mol%	Or mol%				
0.5	0	1.2	0.1	8.6	2																											
0.4	0	1.6	0.4	6.6	2																											
0.3	0	4	0.2	6.8	1																											
0.8	0	4	0.3	8.0	2																											
0.7	1	4	0.1	6.6	1	63.5	0.1	23.0	0.2	0.0	4.4	7.9	5	0.0	0.0	100.5	22															
0.4	0	3	0.3	9.6	3	63.1	0.1	23.1	0.2	0.0	4.4	8.0	4	0.0	0.0	100.3	21															
1.0	1	4	0.2	6.5	2	63.6	0.0	23.0	0.2	0.0	4.4	7.8	5	0.0	0.0	100.4	21															
0.6	1	1	0.7	7.9	1	63.2	0.0	22.8	0.2	0.0	4.3	7.9	5	0.0	0.0	100.0	21															
0.6	0	1	0.6	7.4	2	63.2	0.1	23.1	0.2	0.0	4.3	7.9	4	0.0	0.0	100.3	21															
1	1	3	0.2	6.3	2	63.2	0.1	23.0	0.2	0.0	4.4	7.9	5	0.1	0.0	100.3	21															
0.5	0	0.8	0.7	7.7	2	63.5	0.1	22.7	0.2	0.0	4.2	7.9	5	0.0	0.0	100.2	21															
0.3	0	1.4	0.2	7.8	3	63.8	0.1	22.6	0.2	0.0	4.1	8.0	5	0.1	0.1	100.4	20															
1	1	1	0.5	6.5	2	63.5	0.1	22.6	0.2	0.0	4.1	8.0	5	0.1	0.1	100.2	30															
0.4	0	7	0.6	6.8	2	63.1	0.1	22.8	0.2	0.0	4.3	8.1	5	0.0	0.0	100.0	31															
0.9	0	4	0.9	6.7	2	63.3	0.1	22.9	0.2	0.0	4.4	7.9	4	0.0	0.0	100.3	31															
0.3	0	4	0.2	6.8	2	63.2	0.1	22.9	0.2	0.0	4.3	8.0	5	0.0	0.0	100.3	31															
0.5	0	4	0.6	6.9	3	63.4	0.1	22.9	0.2	0.0	4.3	8.0	5	0.0	0.0	100.3	31															
0.1	0	2	0.5	6.7	2	63.1	0.1	22.9	0.2	0.0	4.4	7.9	5	0.0	0.0	100.0	22															
0.5	0	4	0.6	6.9	2	63.2	0.1	22.9	0.2	0.0	4.3	7.8	4	0.0	0.0	100.1	22															
0.8	0	1	0.4	5.3	2	62.8	0.1	22.9	0.2	0.0	4.3	7.9	4	0.0	0.0	99.7	22															
0.7	0	3	0.1	5.2	2	62.5	0.1	23.0	0.2	0.0	4.4	7.7	4	0.0	0.0	99.4	22															
0.6	0	4	0.5	4.9	2	63.1	0.1	23.0	0.2	0.0	4.5	7.8	4	0.0	0.0	100.1	22															
0.6	0	4	0.4	7.8	2	63.2	0.1	22.9	0.2	0.0	4.4	7.8	4	0.0	0.0	100.0	22															
0.4	0	3	0.3	5.9	2	63.3	0.0	23.1	0.2	0.0	4.5	7.4	4	0.0	0.0	99.9	23															
0.7	1	0	0.3	7.0	2	63.2	0.1	23.2	0.2	0.0	4.5	7.3	4	0.1	0.0	99.9	23															
0.2	0	5	0.7	4.1	2	63.0	0.1	23.2	0.2	0.0	4.6	7.3	4	0.0	0.0	99.9	24															
0.6	0	0	0.2	4.8	2	63.1	0.1	23.2	0.2	0.0	4.5	7.4	4	0.0	0.0	99.9	23															
0.8	1	0	0.3	5.4	1	63.1	0.1	23.0	0.2	0.0	4.6	7.7	3	0.0	0.0	100.0	23															
0.6	0	5	0.4	6.1	2	62.8	0.0	23.0	0.2	0.0	4.6	7.8	3	0.0	0.0	99.8	23															
0.6	0	2	0.4	4.4	4.7	2	63.0	0.1	22.9	0.2	0.0	4.5	7.8	4	0.0	0.0	99.9	22														
0.5	0	10	0.2	6.1	2	63.2	0.1	23.0	0.2	0.0	4.5	7.9	4	0.0	0.0	100.3	22															
0.6	0	4	0.4	5.9	1	63.0	0.0	23.0	0.2	0.0	4.6	8.0	4	0.0	0.0	100.2	22															
0.9	0	4	0.4	5.5	1	63.0	0.1	22.8	0.2	0.0	4.5	7.9	4	0.1	0.0	100.0	22															
0.3	0	2	0.3	2.2	1	63.3	0.1	22.8	0.2	0.0	4.5	7.9	4	0.1	0.0	100.6	22															
0.3	0	2	0.3	4.8	2	62.9	0.1	23.2	0.2	0.0	4.4	7.9	4	0.0	0.0	99.6	22															
0.3	0	2	0.5	4.8	2	62.9	0.1	23.1	0.2	0.0	4.4	7.9	4	0.0	0.0	99.8	22															
0.2	0	4	0.6	6.8	2	62.9	0.1	23.0	0.2	0.0	4.6	8.0	3	0.0	0.0	100.2	22															
0.2	0	1	0.1	4.5	1	62.9	0.0	23.2	0.2	0.0	4.6	8.0	3	0.0	0.0	100.2	22															
0.7	0	3	0.6	5.9	1	62.8	0.1	22.9	0.2	0.0	4.6	7.9	4	0.0	0.0	100.4	22															
0.3	0	3	0.0	5.6	2	63.3	0.1	23.1	0.2	0.0	4.5	8.0	3	0.0	0.0	99.7	22															
0.7	0	3	0.2	5.4	2	63.2	0.1	23.0	0.2	0.0	4.6	7.9	4	0.0	0.0	100.3	22															
0.6	0	0	0.1	6.7	1	63.0	0.1	22.9	0.2	0.0	4.5	7.9	4	0.0	0.0	100.0	22															
0.5	0	2	0.5	5.2	2	62.9	0.1	22.8	0.2	0.0	4.5	7.9	3	0.0	0.0	99.8	22															
0.6	0	4	0.2	6.3	2	63.1	0.1	23.3	0.2	0.0	4.6	7.9	4	0.0	0.0	100.5	22															
0.3	0	6	0.1	5.0	2	62.9	0.0	23.2	0.2	0.0	4.6	8.0	4	0.0	0.0	100.3	22															
0.2	0	2	0.3	6.0	2	63.1	0.1	23.1	0.2	0.0	4.5	8.0	3	0.0	0.0	100.3	22															
0.6	0	1	0.6	5.8	1	62.9	0.1	23.1	0.2	0.0	4.5	8.0	4	0.0	0.0	100.2	22															
0.5	0	1	0.4	6.8	2	62.7	0.1	23.0	0.2	0.0	4.5	7.9	3	0.0	0.0	99.7	22															
1	1	3	0.6	5.9	2	63.1	0.1	23.1	0.2	0.0	4.3	7.9	3	0.0	0.0	100.0	21															
0.6	1	2	0.4	5.1	1	63.2	0.1	22.9	0.2	0.0	4.2	7.9	4	0.0	0.0	99.8	21															
0.6	1	6	0.4	4.8	1	63.2	0.1	22.8	0.2	0.0	4.2	8.0	4	0.0	0.0	99.9	21															
0.3	0	3	0.3	5.7	2	63.2	0.0	23.0	0.2	0.0	4.4	8.0	4	0.1	0.0	100.3	21															
0.3	0	3	0.3	6.0	2	63.3	0.1	23.1	0.2	0.0	4.4	7.9	5	0.1	0.0	100.6	22															
0.9	0	4	0.3	5.1	1	63.3	0.1	22.7	0.2	0.0	4.4	8.0	3	0.0	0.0	100.0	21															
0.9	0	4	0.1	5.1	2	63.3	0.1	22.7	0.2	0.0	4.4	8.0	3	0.0	0.0	100.2	21															
0.5	0	3	0.1	4.5	2	63.2	0.1	23.0	0.2	0.0	4.3	8.0	3	0.0	0.0	100.2	21															
0.2	0	4	0.1	4.1	1	63.2	0.1	22.9	0.2	0.0	4.3	8.0	4	0.0	0.0	100.1	21															
0.4	1	5	0.2	5.8	1	63.2	0.1	22.9	0.2	0.0	4.4	8.0	4	0.0	0.0	100.5	21															
0.3	0	1	0.6	6.4	2	63.3	0.1	22.9	0.2	0.0	4.3	7.9	4	0.0	0.0	100.1	21															
0.7	1	1	0.6	6.6	4.3	1	63.5	0.1	22.8	0.2	0.0	4.2	8.0	5	0.0	0.0	100.2	21														
0.4	0	4	0.3																													

Table B22: Plagioclase grain 21 - Lithium isotopes

MEASURED	Background		Results (BLK + tau corr.)		D time (min)	n	std drift ⁷ Li/ ⁶ Li	δ ⁷ Li (‰) rel GOR132-G	2 σ	δ ⁷ Li (‰) rel IRMM-016	RepRate Hz	integr-time (s)	dis-tance	Li (ppm)	2 σ	d/Li	2 σ		
	⁷ Li (V)	⁶ Li (cps)	⁷ Li (V)	⁶ Li (cps)														SE	SD
1	0.00673	31267	0.00050	0.00014	18	79	13.4088	0.0109	0.0866	81.4	65	12.0	-1.1	-12.7	2.1	15.9	-3.8	2.1	
2	0.01632	75767	0.0012	0.000386	758	13.4986	0.0112	0.1025	83.5	85	5.1	0.49	rim	30	21.2	2.1	15.9	-4.6	2.1
3	0.01535	71637	0.00115	0.000340	720	13.4006	0.0101	0.0829	72.2	85	4.5	0.49	core	36	21.5	3	3.4	2.1	
4	0.01622	75939	0.00122	0.000306	712	13.3562	0.0096	0.0824	72.2	84	4.2	0.49	core	31	19.4	3	-3.4	2.1	
5	0.01575	73739	0.00118	0.000305	695	13.3487	0.0089	0.0826	66.3	87	4.4	0.49	core	168	18.6	1	-6.2	1.9	
6	0.01442	67499	0.00108	0.0002758	675	13.3334	0.0102	0.0912	76.5	80	4.2	0.49	core	210	18.6	1	-6.2	1.9	
7	0.01360	63713	0.00102	0.000194	660	13.3585	0.0128	0.1154	96.0	80	4.9	0.49	core	256	18.6	3	-7.0	2.0	
8	0.01457	68289	0.00109	0.000212	631	13.3584	0.0143	0.1178	107.1	60	4.1	0.49	core	310	16.9	1	-5.1	2.4	
9	0.01324	61805	0.00099	0.000186	625	13.3782	0.0093	0.0831	69.5	80	4.3	0.49	core	358	17.2	1	-5.7	2.6	
10	0.0134	52787	0.00084	0.000146	611	13.4120	0.0103	0.0915	76.8	80	4.2	0.49	cracked	416	17.5	1	-4.4	2.0	
11	0.00951	44330	0.00071	0.000121	610	13.4192	0.0133	0.1196	99.0	80	4.2	0.49	core	481	6.2	3	-0.9	2.4	
12	0.01331	62132	0.00099	0.000163	593	13.3799	0.0099	0.0889	73.8	80	5.5	0.49	core	537	19.2	3	-0.9	2.4	
13	0.01237	57988	0.00093	0.000127	596	13.3571	0.0104	0.0963	78.2	85	4.3	0.49	core	592	20.0	2	-3.4	2.1	
14	0.01212	56866	0.00091	0.0001092	583	13.3266	0.0094	0.0895	70.8	90	4.3	0.49	core	643	19.3	2	-5.1	2.1	
15	0.01141	53631	0.00086	0.0001078	578	13.3131	0.0093	0.0880	69.6	90	4.0	0.49	core	698	18.9	2	-7.3	1.9	
16	0.01235	58135	0.00093	0.0001088	570	13.2888	0.0121	0.1079	90.8	80	4.2	0.49	core	750	19.0	1	-7.9	1.9	
17	0.01303	61307	0.00098	0.0001077	565	13.2912	0.0118	0.1041	88.7	80	4.2	0.49	core	803	19.4	1	-9.7	2.2	
18	0.00971	45501	0.00073	0.0001046	552	13.3521	0.0179	0.1615	134.4	80	4.3	0.49	core	849	18.7	1	-10.2	2.2	
19	0.00663	30839	0.00049	0.0001028	532	13.4149	0.0142	0.1299	105.7	85	4.0	0.49	cracked	892	14.4	1	-5.3	3.1	
20	0.01228	58511	0.00094	0.0000738	380	13.1398	0.0131	0.1164	99.7	80	7.5	0.49	cracked	940	12.2	1	-0.4	2.5	
21	0.00507	23950	0.00038	0.0000818	389	13.2219	0.0148	0.1328	111.6	80	5.1	0.49	cracked	929	5.0	1	-0.1	2.7	
22	0.00592	27800	0.00044	0.0000744	389	13.2949	0.0167	0.1260	126.6	110	4.3	0.49	cracked	964	12.1	1	5.1	2.9	
23	0.00578	27065	0.00043	0.0000807	407	13.2504	0.0135	0.1162	102.1	90	4.1	0.49	cracked	1015	13.5	3	1.6	2.6	
24	0.00653	30773	0.00049	0.0000733	365	13.2713	0.0119	0.1123	89.7	88	4.2	0.49	cracked	1061	9.0	1	3.8	2.4	
25	0.00816	38417	0.00051	0.0000797	366	13.2791	0.0155	0.1392	116.5	80	5.3	0.49	cracked	1110	14.9	3	3.8	2.7	
26	0.00677	31757	0.00051	0.0000732	370	13.2737	0.0131	0.1278	98.8	95	4.2	0.49	cracked	1152	13.5	1	3.5	2.3	
27	0.00562	26432	0.00042	0.0000766	365	13.2631	0.0144	0.1369	108.8	90	4.5	0.49	cracked	1215	12.7	2	2.3	2.6	
28	0.00457	21436	0.00034	0.0000720	368	13.2905	0.0143	0.1352	107.8	88	4.2	0.49	cracked	1296	9.3	1	4.2	2.6	
30	0.01065	50252	0.00050	0.0000701	360	13.2134	0.0162	0.1437	122.3	80	6.9	0.49	cracked	1343	7.6	1	0.6	2.4	
31	0.00726	34136	0.00035	0.0000667	351	13.2133	0.0170	0.1271	128.5	55	5.8	0.49	rim	35	16.8	2	-1.9	2.9	
32	0.00526	26191	0.00042	0.0000678	338	13.2214	0.0131	0.1247	98.8	90	5.1	0.49	rim	32	16.8	2	-2.2	2.9	
33	0.01763	83371	0.00133	0.0000667	336	13.1937	0.0106	0.0949	80.4	82	4.0	0.49	rim	30	26.4	5	-4.3	2.1	
34	0.01606	76167	0.00121	0.0000671	331	13.1880	0.0097	0.0875	73.8	80	4.4	0.49	core	91	26.4	5	-4.3	2.1	
35	0.01195	56884	0.00091	0.0000669	331	13.1763	0.0089	0.0821	67.2	109	4.2	0.49	core	134	25.8	3	-4.9	2.1	
36	0.01099	52255	0.00084	0.0000657	331	13.1567	0.0088	0.0957	67.2	109	4.7	0.49	core	183	27.5	2	-5.6	2.1	
37	0.01075	51181	0.00082	0.0000691	333	13.1481	0.0103	0.1129	78.4	119	4.4	0.49	core	229	30.8	3	-7.1	2.1	
38	0.01051	50049	0.00080	0.0000682	329	13.1401	0.0095	0.1010	72.0	113	4.1	0.49	core	277	28.1	3	-8.2	2.2	

grain 21 - Isotopes

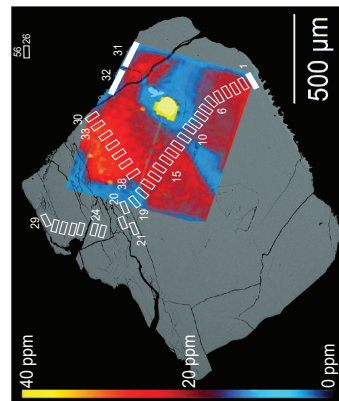


Fig. B20. BSE image of plagioclase grain 21 with Fs-LA-MC-ICP-MS lines indicated.

Table B24: Plagioclase grain 25 - Lithium isotopes

MEASURED		background		Results (BLK + tau corr.)											
⁷ Li (V)	⁶ Li (cps)	⁷ Li (V)	⁶ Li (V)	⁶ Li (cps)	⁷ Li/ ⁶ Li	SE	SD	1 RSD	n	D time (min)	std drift ⁷ Li/ ⁶ Li	δ ⁷ Li (‰) rel GOR132-G	2 σ	2 σ	
1	0.00571	22400	0.00036	0.0000401	218	16.0141	0.0146	0.1700	910	135	8.2	-0.5	-3.0	2.4	2.4
2	0.00342	13429	0.00021	0.0000381	212	15.9538	0.0130	0.1495	816	135	5.0	2.0	-6.0	2.2	2.2
3	0.00462	18155	0.00029	0.0000382	211	15.9161	0.0124	0.1384	781	123	4.2	-1.3	-8.0	2.1	2.1
4	0.00826	32315	0.00052	0.0000365	195	15.9409	0.0100	0.1159	628	135	4.8	0.4	-6.9	2.0	2.0
5	0.01009	39446	0.00063	0.0000368	187	15.9308	0.0104	0.1205	656	135	4.4	-0.5	-7.6	2.1	2.1
6	0.00896	35095	0.00056	0.0000329	178	15.9313	0.0122	0.1396	768	131	4.4	0.9	-7.4	2.1	2.1
7	0.01164	45677	0.00073	0.0000362	181	15.8936	0.0096	0.1110	603	135	4.2	-0.6	-9.6	1.8	1.8
8	0.01133	44694	0.00072	0.0000344	185	15.7986	0.0092	0.1056	582	133	4.0	0.4	-15.6	1.9	1.9
9	0.01096	43197	0.00069	0.0000328	174	15.7918	0.0095	0.1080	605	130	5.2	-0.1	-15.9	2.0	2.0
10	0.00977	38605	0.00062	0.0000292	175	15.8134	0.0103	0.1167	652	131	4.8	0.9	-14.2	1.9	1.9
11	0.00913	36086	0.00058	0.0000354	176	15.7881	0.0093	0.1069	587	135	4.2	-0.2	-15.5	1.8	1.8
12	0.01118	44160	0.00071	0.0000310	165	15.8262	0.0085	0.0984	539	133	4.7	1.2	-12.6	1.8	1.8
13	0.01165	46065	0.00074	0.0000310	173	15.8130	0.0090	0.0980	568	119	4.0	-0.4	-13.0	2.0	2.0
14	0.01124	44324	0.00071	0.0000344	163	15.8386	0.0085	0.0993	538	135	4.6	-1.0	-12.1	2.0	2.0
15	0.01093	43082	0.00069	0.0000305	162	15.8492	0.0085	0.0987	534	135	4.7	0.7	-11.6	1.9	1.9

Table B24: continued

δ ⁷ Li (‰) rel IRMM-016	RepRate Hz	integr.time (s)		distance	Li	2 σ	d ⁷ Li	2 σ
5.9	26	1.049	rim	20	9.4	1	5.9	2.4
2.9	29	1.049	rim	20	14.7	1	2.9	2.2
0.9	42	1.049	rim	20	14.7	1	0.9	2.1
2.0	42	1.049	core	65	20.4	1	2.0	2.0
1.3	38	1.049	core	100	22.5	1	1.3	2.1
1.5	38	1.049	core	85	16.7	1	1.5	2.1
-0.7	38	1.049	core	167	23.4	1	-0.7	1.8
-6.7	38	1.049	core	235	23.4	1	-6.7	1.9
-7.0	38	1.049	core	290	21.8	1	-7.0	2.0
-5.3	33	1.049	core	340	20.3	1	-5.3	1.9
-6.6	33	1.049	core	405	19.3	1	-6.6	1.8
-3.7	33	1.049	core	460	19.1	1	-3.7	1.8
-4.1	33	1.049	core	535	18.6	1	-4.1	2.0
-3.2	33	1.049	core	610	18.7	1	-3.2	2.0
-2.7	33	1.049	core	670	19.9	1	-2.7	1.9

grain 25 - Isotopes

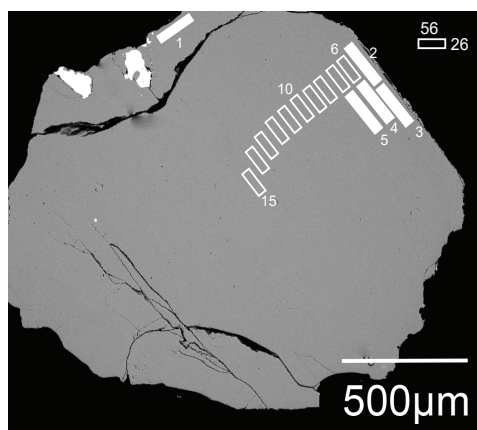


Fig. B23. BSE image of plagioclase grain 25 with Fs-LA-MC-ICP-MS lines indicated.

Table B28: EPMA Standards

	SiO	TiO ₂	AlO ₃	FeO	MgO	CaO	Na O	K O	BaO	SrO	Total
Ref value	64.67	0.01 ²	18.90 ³	0.04	0.03	0.02	1.30	15.14			100.11
MCL-1	63.9	0.1	18.7	0.0	0.0	0.0	1.2	15.3	0.2	0.1	99.5
MCL-2	64.0	0.1	18.8	0.0	0.0	0.0	1.3	15.2	0.3	0.0	99.6
MCL-3	64.0	0.0	18.6	0.0	0.0	0.0	1.3	15.2	0.3	0.0	99.3
MCL-4	63.4	0.1	18.4	0.0	0.0	0.0	1.2	15.0	0.3	0.0	98.3
MCL-5	64.5	0.1	18.8	0.0	0.0	0.0	1.2	15.1	0.2	0.1	99.8
MCL-6	64.1	0.1	19.0	0.0	0.0	0.0	1.3	15.3	0.2	0.0	100.0
MCL-7	64.0	0.1	18.7	0.0	0.0	0.0	1.2	15.4	0.2	0.0	99.6
MCL-8	64.4	0.1	18.7	0.0	0.0	0.0	1.2	15.3	0.2	0.0	99.8
MCL-9	63.6	0.0	18.3	0.0	0.0	0.0	1.2	14.9	0.2	0.0	98.3
MCL-10	64.5	0.1	18.8	0.0	0.0	0.0	1.3	15.0	0.2	0.0	99.8
Ref value	44.00 ¹	0.03 ²	36.03 ³	0.62	0.02	19.09	0.53	0.03			100.35
ANO-1	43.9	0.1	36.7	0.5	0.0	19.3	0.5	0.0	0.0	0.1	101.0
ANO-2	44.1	0.1	36.6	0.4	0.0	19.2	0.5	0.0	0.0	0.0	101.0
ANO-3	44.1	0.1	35.9	0.5	0.1	19.6	0.5	0.0	0.0	0.0	100.7
ANO-4	44.2	0.1	36.0	0.5	0.0	19.5	0.5	0.0	0.0	0.0	100.8
ANO-5	43.8	0.1	35.8	0.5	0.0	19.3	0.5	0.0	0.0	0.1	100.1
ANO-6	44.1	0.1	36.0	0.5	0.0	19.5	0.5	0.0	0.0	0.0	100.6
ANO-7	43.8	0.1	36.6	0.5	0.0	19.1	0.5	0.0	0.0	0.0	100.6
ANO-8	44.1	0.1	36.7	0.4	0.0	19.3	0.6	0.0	0.0	0.0	101.3
ANO-9	44.0	0.1	35.9	0.5	0.1	19.3	0.5	0.0	0.0	0.0	100.3
ANO-10	44.2	0.1	36.0	0.5	0.0	19.5	0.5	0.0	0.0	0.0	100.8
ANO-11	43.8	0.1	36.0	0.5	0.0	19.5	0.5	0.0	0.0	0.1	100.5
ANO-12	44.0	0.1	36.0	0.5	0.0	19.4	0.5	0.0	0.0	0.0	100.5
Ref value	51.60 ¹	0.05 ²	30.91 ³	0.46	0.14	13.64	3.45	0.18			100.43
LAB-1	51.8	0.1	31.1	0.5	0.2	13.3	3.8	0.1	0.0	0.0	100.9
LAB-2	51.6	0.1	30.5	0.4	0.1	13.1	3.6	0.1	0.0	0.0	99.6
LAB-3	51.7	0.1	31.0	0.4	0.1	13.2	3.8	0.1	0.0	0.0	100.5
LAB-4	51.6	0.1	31.2	0.5	0.1	13.3	3.8	0.1	0.0	0.0	100.8
LAB-5	51.6	0.1	30.6	0.4	0.1	13.3	3.8	0.1	0.0	0.0	100.2
LAB-6	51.2	0.1	30.2	0.4	0.1	13.2	3.7	0.1	0.0	0.0	99.1
LAB-7	51.5	0.1	30.4	0.5	0.1	13.2	3.7	0.1	0.0	0.0	99.8
LAB-8	51.9	0.1	30.7	0.5	0.1	13.1	3.7	0.1	0.1	0.1	100.4
Ref value	64.67	0.01 ²	18.90 ³	0.04	0.03	0.02	1.30	15.14			100.11
MCL-1	63.9	0.1	18.6	0.0	0.0	0.0	1.2	15.3	0.2	0.0	99.3
MCL-2	63.7	0.1	18.5	0.0	0.0	0.0	1.3	15.2	0.2	0.0	98.9
MCL-3	63.7	0.0	18.6	0.0	0.0	0.0	1.2	15.1	0.3	0.0	99.0
MCL-4	63.8	0.0	18.6	0.0	0.0	0.0	1.2	15.1	0.2	0.1	99.1
MCL-5	63.8	0.1	18.6	0.0	0.0	0.0	1.3	15.4	0.2	0.0	99.5
MCL-6	63.8	0.0	18.4	0.0	0.0	0.0	1.3	15.2	0.2	0.0	99.0
MCL-7	64.0	0.1	18.6	0.0	0.0	0.0	1.2	15.3	0.3	0.0	99.6
MCL-8	64.0	0.1	18.5	0.0	0.0	0.0	1.3	15.1	0.3	0.0	99.3
Ref value	44.00 ¹	0.03 ²	36.03 ³	0.62	0.02	19.09	0.53	0.03			100.35
ANO-1	43.7	0.1	36.0	0.5	0.0	19.4	0.5	0.0	0.0	0.0	100.2
ANO-2	43.7	0.1	35.8	0.5	0.1	19.4	0.5	0.0	0.0	0.0	100.2
ANO-3	43.7	0.0	35.7	0.5	0.0	19.3	0.5	0.0	0.0	0.0	99.9
ANO-4	43.8	0.0	35.8	0.5	0.0	19.4	0.5	0.0	0.0	0.1	100.1
ANO-5	43.7	0.1	36.3	0.5	0.0	19.4	0.5	0.0	0.0	0.0	100.5
ANO-6	43.6	0.1	35.6	0.4	0.0	19.3	0.5	0.0	0.0	0.0	99.5
ANO-7	43.4	0.1	35.3	0.5	0.0	19.4	0.5	0.0	0.0	0.1	99.3
ANO-8	43.7	0.0	35.9	0.5	0.0	19.3	0.6	0.0	0.0	0.0	99.9
Ref value	51.60 ¹	0.05 ²	30.91 ³	0.46	0.14	13.64	3.45	0.18			100.43
LAB-1	51.5	0.1	30.8	0.5	0.1	13.2	3.9	0.1	0.0	0.0	100.2
LAB-2	51.2	0.1	30.2	0.4	0.1	13.2	3.7	0.1	0.0	0.0	99.1
LAB-3	51.3	0.1	30.9	0.5	0.1	13.4	3.9	0.1	0.0	0.0	100.3
LAB-4	51.4	0.1	30.4	0.4	0.1	13.2	3.9	0.1	0.0	0.0	99.7
LAB-5	51.3	0.1	30.3	0.5	0.2	13.1	3.8	0.1	0.0	0.0	99.4
LAB-6	51.3	0.1	30.4	0.4	0.1	13.2	3.8	0.1	0.0	0.0	99.5
LAB-7	51.3	0.1	30.1	0.5	0.1	13.2	3.8	0.1	0.0	0.0	99.2
Ref value	64.67	0.01 ²	18.90 ³	0.04	0.03	0.02	1.30	15.14			100.11
MCL-1	64.4	0.1	18.7	0.0	0.0	0.0	1.2	15.2	0.3	0.0	100.0
MCL-2	64.9	0.1	18.8	0.0	0.0	0.0	1.3	15.1	0.2	0.0	100.4
MCL-3	64.9	0.1	18.9	0.0	0.0	0.0	1.2	14.6	0.3	0.0	100.1
MCL-4	64.8	0.1	18.8	0.0	0.0	0.0	1.3	14.9	0.2	0.0	100.1
MCL-5	65.0	0.1	19.1	0.0	0.0	0.0	1.2	14.8	0.2	0.0	100.5
MCL-6	64.7	0.1	19.0	0.0	0.0	0.0	1.3	15.2	0.3	0.0	100.6
MCL-7	64.9	0.0	19.0	0.0	0.0	0.0	1.3	15.1	0.2	0.0	100.6
MCL-8	64.8	0.1	18.9	0.0	0.0	0.0	1.3	15.1	0.3	0.0	100.4
MCL-9	64.6	0.1	18.9	0.0	0.0	0.0	1.3	15.2	0.3	0.0	100.3
MCL-10	65.1	0.1	19.1	0.0	0.0	0.0	1.2	15.3	0.3	0.0	101.0
MCL-11	64.9	0.1	18.8	0.0	0.0	0.0	1.3	15.1	0.2	0.0	100.4
MCL-12	64.7	0.1	19.0	0.0	0.0	0.0	1.2	15.2	0.2	0.0	100.4
MCL-13	64.9	0.1	18.7	0.0	0.0	0.0	1.2	15.3	0.2	0.0	100.5
MCL-14	65.0	0.0	18.9	0.0	0.0	0.0	1.3	15.1	0.3	0.0	100.6
MCL-15	65.0	0.1	19.0	0.0	0.0	0.0	1.3	15.1	0.3	0.0	100.7
MCL-16	64.9	0.1	18.9	0.0	0.0	0.0	1.3	14.9	0.3	0.0	100.4
MCL-17	64.7	0.1	18.7	0.0	0.0	0.0	1.3	15.2	0.2	0.0	100.2
MCL-18	64.5	0.1	18.8	0.0	0.0	0.0	1.2	15.1	0.2	0.0	99.9
MCL-19	64.3	0.1	18.8	0.0	0.0	0.0	1.3	15.1	0.3	0.0	99.9
MCL-20	64.6	0.1	18.7	0.0	0.0	0.0	1.2	15.0	0.2	0.1	99.9
MCL-21	64.4	0.1	18.6	0.0	0.0	0.0	1.2	15.1	0.4	0.0	99.8
MCL-22	64.4	0.1	18.7	0.0	0.0	0.0	1.2	15.3	0.2	0.0	100.0
MCL-23	64.4	0.0	18.8	0.0	0.0	0.0	1.2	15.1	0.3	0.0	99.7
MCL-24	64.4	0.1	18.8	0.0	0.0	0.0	1.3	15.1	0.3	0.0	99.9
MCL-25	64.6	0.1	18.9	0.0	0.0	0.0	1.2	15.0	0.3	0.0	100.1
MCL-26	64.3	0.1	18.9	0.0	0.0	0.0	1.2	15.1	0.3	0.1	99.9
MCL-27	64.4	0.1	18.8	0.0	0.0	0.0	1.2	15.1	0.3	0.0	100.0
MCL-28	64.4	0.1	18.6	0.0	0.0	0.0	1.2	14.9	0.2	0.0	99.4
MCL-29	64.7	0.1	18.8	0.0	0.0	0.0	1.3	15.0	0.4	0.1	100.3
MCL-30	64.8	0.1	18.8	0.0	0.0	0.0	1.3	15.1	0.3	0.0	100.4
MCL-31	64.8	0.1	18.8	0.0	0.0	0.0	1.3	15.0	0.2	0.1	100.2
MCL-32	64.5	0.1	18.8	0.0	0.0	0.0	1.3	15.1	0.2	0.0	100.0
MCL-33	64.4	0.0	18.9	0.0	0.0	0.0	1.3	15.1	0.2	0.0	99.9
MCL-34	64.7	0.1	18.7	0.0	0.0	0.0	1.3	15.0	0.2	0.0	100.0
MCL-35	64.8	0.1	18.7	0.0	0.0	0.0	1.3	15.1	0.2	0.0	100.3
MCL-36	64.6	0.1	18.8	0.0	0.0	0.0	1.3	15.1	0.3	0.0	100.2
MCL-37	64.6	0.0	18.7	0.0	0.0	0.0	1.2	15.1	0.2	0.0	99.9
MCL-38	64.2	0.0	18.7	0.0	0.0	0.0	1.2	14.9	0.2	0.1	99.4
MCL-39	64.4	0.1	18.9	0.0	0.0	0.0	1.3	14.8	0.3	0.0	99.6

Table B28: continued

	SiO	TiO	AlO	FeO	MgO	CaO	Na O	K O	BaO	SrO	Total
Ref value	44.00 ²	0.03 ²	36.03 ²	0.62	0.02	19.09	0.53	0.03			100.35
ANO-1	43.8	0.1	35.9	0.5	0.0	19.4	0.5	0.0	0.0	0.0	100.3
ANO-2	44.0	0.1	35.7	0.5	0.0	19.0	0.5	0.0	0.0	0.1	99.9
ANO-3	44.0	0.1	35.7	0.5	0.0	19.4	0.5	0.0	0.0	0.0	100.3
ANO-4	44.0	0.1	36.1	0.5	0.0	19.4	0.5	0.0	0.0	0.0	100.3
ANO-5	44.3	0.1	35.9	0.5	0.1	19.5	0.5	0.0	0.1	0.0	100.7
ANO-6	44.0	0.1	36.2	0.5	0.0	19.4	0.5	0.0	0.0	0.1	100.8
ANO-7	44.0	0.0	36.0	0.5	0.0	19.5	0.5	0.0	0.0	0.0	100.6
ANO-8	44.1	0.1	36.3	0.4	0.1	19.3	0.5	0.0	0.0	0.0	100.8
ANO-9	44.1	0.1	36.0	0.5	0.0	19.5	0.5	0.0	0.1	0.0	100.7
ANO-10	44.1	0.1	36.0	0.5	0.1	19.3	0.5	0.0	0.1	0.1	100.7
ANO-11	44.1	0.1	35.9	0.4	0.0	19.4	0.5	0.0	0.0	0.1	100.5
ANO-12	44.2	0.1	35.9	0.5	0.0	19.4	0.5	0.0	0.0	0.1	100.7
ANO-13	44.2	0.1	36.0	0.5	0.0	19.4	0.5	0.0	0.0	0.0	100.7
ANO-14	44.1	0.1	36.0	0.4	0.0	19.4	0.5	0.0	0.0	0.1	100.7
ANO-15	43.7	0.1	36.0	0.5	0.0	19.2	0.5	0.0	0.1	0.0	100.1
ANO-16	43.7	0.1	35.9	0.5	0.0	19.2	0.5	0.0	0.1	0.0	99.9
ANO-17	43.9	0.1	35.9	0.5	0.0	19.2	0.5	0.0	0.0	0.0	100.2
ANO-18	43.8	0.1	35.7	0.5	0.0	19.2	0.5	0.0	0.0	0.1	99.8
ANO-19	43.7	0.1	35.5	0.5	0.0	19.2	0.5	0.0	0.0	0.0	99.6
ANO-20	43.8	0.1	36.0	0.5	0.0	19.2	0.5	0.0	0.0	0.0	100.0
ANO-21	43.9	0.0	36.0	0.5	0.0	19.2	0.5	0.0	0.0	0.1	100.2
ANO-22	43.9	0.1	36.0	0.4	0.1	19.2	0.5	0.0	0.0	0.1	100.3
ANO-23	43.8	0.1	36.0	0.5	0.1	19.1	0.5	0.0	0.0	0.0	100.1
ANO-24	43.8	0.1	35.9	0.4	0.0	19.2	0.5	0.0	0.0	0.0	99.9
ANO-25	43.8	0.1	36.1	0.5	0.0	19.2	0.5	0.0	0.0	0.0	100.3
ANO-26	43.6	0.1	35.9	0.4	0.0	19.2	0.5	0.0	0.0	0.1	99.8
ANO-27	43.9	0.1	35.8	0.5	0.1	19.3	0.5	0.0	0.1	0.0	100.3
ANO-28	43.9	0.1	35.8	0.5	0.1	19.3	0.5	0.0	0.1	0.0	100.3
ANO-29	43.9	0.1	36.2	0.4	0.0	19.1	0.5	0.0	0.0	0.0	100.3
ANO-30	43.9	0.1	36.2	0.4	0.0	19.1	0.5	0.0	0.0	0.0	100.3
ANO-31	43.6	0.1	35.9	0.4	0.0	19.2	0.5	0.0	0.0	0.1	100.0
ANO-32	43.9	0.1	36.0	0.5	0.0	19.1	0.5	0.0	0.0	0.1	100.1
ANO-33	43.8	0.1	36.0	0.5	0.1	19.0	0.6	0.0	0.1	0.0	100.2
ANO-34	43.6	0.1	35.8	0.5	0.0	19.4	0.5	0.0	0.0	0.0	99.9
ANO-35	43.9	0.1	36.0	0.5	0.0	19.0	0.5	0.0	0.0	0.1	100.2
ANO-36	43.5	0.1	36.0	0.4	0.0	19.2	0.5	0.0	0.0	0.0	99.8
ANO-37	43.7	0.1	35.8	0.5	0.1	19.2	0.5	0.0	0.0	0.1	99.7
ANO-38	44.1	0.1	35.9	0.5	0.1	19.2	0.5	0.0	0.0	0.0	100.4

	SiO	TiO	AlO	FeO	MgO	CaO	Na O	K O	BaO	SrO	Total
Ref value	51.60 ²	0.05 ²	30.91 ²	0.46	0.14	13.64	3.45	0.18			100.43
LAB-1	50.7	0.1	31.1	0.4	0.1	13.9	3.6	0.1	0.0	0.0	100.0
LAB-2	50.9	0.1	31.1	0.4	0.1	14.0	3.4	0.1	0.0	0.0	100.2
LAB-3	50.7	0.1	31.1	0.4	0.1	14.0	3.4	0.1	0.0	0.0	100.1
LAB-4	50.6	0.1	31.3	0.4	0.1	13.9	3.5	0.1	0.0	0.1	100.0
LAB-5	50.9	0.1	31.4	0.4	0.1	14.0	3.4	0.1	0.0	0.1	100.4
LAB-6	50.8	0.1	31.3	0.4	0.1	14.1	3.5	0.1	0.0	0.1	100.5
LAB-7	50.9	0.1	31.2	0.4	0.1	13.9	3.4	0.1	0.0	0.0	100.2
LAB-8	50.8	0.1	31.4	0.4	0.1	14.1	3.4	0.1	0.0	0.1	100.5
LAB-9	50.8	0.1	31.2	0.4	0.1	14.2	3.5	0.1	0.0	0.1	100.4
LAB-10	50.9	0.1	31.1	0.4	0.1	13.9	3.4	0.1	0.0	0.0	100.2
LAB-11	51.0	0.1	31.1	0.4	0.2	13.9	3.4	0.1	0.0	0.1	100.3
LAB-12	50.8	0.1	30.9	0.4	0.2	14.2	3.4	0.1	0.0	0.0	100.1
LAB-13	50.8	0.1	31.1	0.4	0.1	14.1	3.4	0.1	0.0	0.0	100.3
LAB-14	51.0	0.1	31.1	0.4	0.1	14.1	3.4	0.1	0.0	0.1	100.4
LAB-15	50.9	0.1	31.3	0.5	0.1	14.0	3.4	0.1	0.0	0.0	100.4
LAB-16	50.9	0.1	31.1	0.4	0.1	13.8	3.4	0.1	0.0	0.1	100.1
LAB-17	50.5	0.1	31.0	0.4	0.1	13.9	3.5	0.1	0.0	0.0	99.7
LAB-18	50.5	0.1	31.3	0.4	0.2	14.0	3.5	0.1	0.0	0.1	100.0
LAB-19	50.3	0.1	31.1	0.4	0.1	13.9	3.4	0.1	0.0	0.1	99.5
LAB-20	50.5	0.1	30.8	0.4	0.2	13.8	3.4	0.1	0.0	0.0	99.2
LAB-21	50.6	0.1	31.1	0.4	0.2	13.8	3.4	0.1	0.0	0.0	99.6
LAB-22	50.7	0.1	31.2	0.4	0.1	14.0	3.5	0.1	0.0	0.1	100.2
LAB-23	50.6	0.1	31.0	0.4	0.1	13.8	3.4	0.1	0.0	0.0	99.5
LAB-24	50.6	0.1	31.3	0.4	0.1	14.0	3.5	0.1	0.0	0.0	100.1
LAB-25	50.4	0.1	31.3	0.4	0.1	14.0	3.4	0.1	0.1	0.0	100.1
LAB-26	50.5	0.1	31.1	0.4	0.1	13.9	3.5	0.1	0.0	0.0	99.8
LAB-27	50.5	0.1	31.3	0.4	0.1	13.9	3.5	0.1	0.0	0.0	99.9
LAB-28	50.5	0.1	31.2	0.4	0.1	13.8	3.5	0.1	0.0	0.0	99.7
LAB-29	50.5	0.1	31.2	0.4	0.1	13.8	3.5	0.1	0.0	0.0	99.7
LAB-30	50.5	0.1	31.2	0.4	0.2	14.0	3.4	0.1	0.0	0.0	100.1
LAB-31	50.5	0.1	31.2	0.4	0.2	14.0	3.4	0.1	0.0	0.0	100.1
LAB-32	50.7	0.1	31.1	0.4	0.1	13.8	3.4	0.1	0.1	0.1	99.8
LAB-33	50.5	0.1	31.2	0.4	0.1	14.0	3.6	0.1	0.0	0.0	100.0
LAB-34	50.6	0.1	31.0	0.5	0.1	13.8	3.4	0.1	0.0	0.0	99.8
LAB-35	50.6	0.1	31.0	0.4	0.1	14.0	3.5	0.1	0.1	0.0	99.8
LAB-36	50.3	0.1	31.2	0.4	0.1	14.1	3.5	0.1	0.1	0.0	99.9
LAB-37	50.5	0.1	31.1	0.4	0.1	13.9	3.4	0.1	0.0	0.1	99.8
LAB-38	50.4	0.1	31.2	0.4	0.1	13.9	3.5	0.1	0.0	0.1	99.8

	SiO ₂	TiO ₂	AlO ₂	FeO	MgO	CaO	Na O	K O	SrO	BaO	Total
Ref value	44.00	0.03	36.03 ²	0.62	0.02	19.09	0.53	0.03			100.35
ANO-1	44.0	0.0	36.4	0.5	0.1	19.2	0.5	0.0	0.0	0.0	100.7
ANO-2	43.8	0.0	36.4	0.5	0.1	19.1	0.5	0.0	0.0	0.1	100.4
ANO-3	43.9	0.0	36.1	0.5	0.0	19.1	0.6	0.0	0.0	0.0	100.3
ANO-4	44.1	0.0	36.2	0.5	0.1	19.4	0.5	0.0	0.1	0.0	100.8
ANO-5	44.3	0.0	36.4	0.5	0.0	19.2	0.5	0.0	0.0	0.0	100.9
ANO-6	44.0	0.0	36.2	0.5	0.0	19.3	0.5	0.0	0.0	0.0	100.7
ANO-7	44.0	0.1	36.2	0.5	0.0	19.1	0.5	0.0	0.0	0.0	100.5
ANO-8	44.1	0.0	36.1	0.5	0.0	19.1	0.5	0.0	0.0	0.0	100.4
ANO-9	44.1	0.0	36.0	0.5	0.0	19.4	0.5	0.0	0.0	0.0	100.6
ANO-10	44.0	0.0	36.2	0.5	0.1	19.3	0.6	0.0	0.0	0.0	100.7

	SiO ₂	TiO ₂	AlO ₂	FeO	MgO	CaO	Na O	K O	SrO	BaO	Total
Ref value	51.6 ²	0.1	30.9	0.5	0.1	13.6	3.5	0.2			100.4
LAB-1	50.6	0.0	31.2	0.4	0.2	13.9	3.5	0.1	0.1	0.0	100.0
LAB-2	50.6	0.0	31.6	0.4	0.1	13.9	3.5	0.1	0.1	0.0	100.3
LAB-3	51.2	0.0	30.9	0.4	0.1	13.2	3.8	0.1	0.1	0.0	99.9
LAB-4	51.4	0.1	30.9	0.4	0.1	13.3	3.8	0.1	0.1	0.0	100.1
LAB-5	51.3	0.0	30.7	0.4	0.1	13.3	3.7	0.1	0.0	0.0	99.8
LAB-6	51.2	0.1	30.8	0.4	0.1	13.4	3.8	0.1	0.1	0.1	100.0
LAB-7	51.6	0.0	31.0	0.4	0.1	13.5	3.8	0.1	0.1	0.0	100.5
LAB-8	51.4	0.0	31.0	0.4	0.1	13.4	3.9	0.1	0.0	0.0	100.3
LAB-9	51.4	0.0	30.6	0.4	0.1	13.3	3.9	0.1	0.1	0.0	99.9

	SiO ₂	TiO ₂	AlO ₂	FeO	MgO	CaO	Na O	K O	SrO	BaO	Total
MCL-1	64.7	0.0	18.9	0.0	0.0	0.0	1.3	15.1			100.1
MCL-2	64.6	0.0	18.7	0.0	0.0	0.0	1.2	15.1	0.0	0.2	100.1
MCL-3	64.9	0.0	18.9	0.0	0.0	0.0	1.3	15.0	0.0	0.2	99.9
MCL-4	64.8	0.0	18.9	0.0	0.0	0.0	1.3	15.1	0.0	0.2	100.2
MCL-5	64.8	0.0	18.0	0.0	0.0	0.0	1.4	15.1	0.0	0.1	100.6
MCL-6	65.3	0.0	18.7	0.0	0.0	0.0	1.3	15.0	0.1	0.2	100.3
MCL-7	65.1	0.0	18.7	0.0	0.0	0.0	1.3	15.0	0.1	0.2	100.5
MCL-8	65.2	0.0	18.8	0.0	0.0	0.0	1.3	15.1	0.0	0.2	100.6
MCL-9	65.0	0.0	19.1	0.0	0.0	0.0	1.4	15.1	0.1	0.2	100.7

Appendix

Appendix C: Supplementary material for Chapter 4

C: Melt inclusion data

Table C1: Glassy and crystallised melt inclusion - Lithium concentration and isotopic composition (by SIMS), H₂O and CO₂ data (by FTIR), major element data (by EPMA) and trace elements (by La-ICP-MS)

Sample	MI Type	Li ppm	d ⁷ L/2 SE	MI thickness (µm)	% of total thickness	Band absorbance (cm ⁻¹)	H ₂ O (wt%)	1 SD CO ₂ (ppm)	1 SD SiO ₂	Na ₂ O	Al ₂ O ₃	MgO	K ₂ O	CaO	TiO ₂	Cl	FeO	MnO	P ₂ O ₅	Cr ₂ O ₃	Total	
11022-g1-MI3-1	glassy	27.0	-5.1	1.5					77.8	2.6	11.7	0.0	5.2	0.5	0.1	0.1	1.2	0.1	0.0	0.0	99.3	
11022-g1-MI3-2	glassy								77.5	2.6	11.6	0.1	5.1	0.6	0.1	0.1	1.2	0.0	0.0	0.0	98.9	
11022-g1-MI3-3	glassy																					
11022-g1-MI3-4	glassy																					
11022-g1-MI3-5	glassy																					
11022-g1-MI2-1	glassy	46.6	-2.9	1.4					76.2	2.2	11.5	0.0	5.6	0.5	0.1	0.1	1.2	0.1	0.0	0.0	97.5	
11022-g1-MI2-2	glassy	62.8	3.3	1.9					77.0	2.1	11.3	0.0	5.4	0.5	0.1	0.1	1.2	0.1	0.0	0.0	97.8	
11022-g1-MI2-3	glassy	46.0	-2.7	1.3					76.4	2.2	11.4	0.0	5.5	0.5	0.1	0.1	1.1	0.0	0.0	0.0	97.4	
11022-g1-MI2-4	glassy								76.6	2.2	11.5	0.0	5.5	0.6	0.1	0.1	1.3	0.0	0.0	0.0	97.9	
11022-g1-MI1-1	glassy	29.8	-4.8	1.4	12.5	19.6	0.055	2.8	77.2	2.5	11.7	0.0	5.2	0.5	0.1	0.1	1.2	0.0	0.0	0.0	98.7	
11022-g1-MI1-2	glassy	30.0	2.8	1.3	12.5	19.6	0.055	2.8	77.9	2.6	11.7	0.0	5.2	0.5	0.1	0.1	1.3	0.0	0.0	0.0	99.5	
11022-g1-MI1-3	glassy	29.7	-4.1	1.5	12.5	19.6	0.055	2.8	77.8	2.6	11.9	0.0	5.2	0.6	0.1	0.1	1.2	0.0	0.0	0.0	99.6	
11022-g1-MI1-4	glassy				12.5	19.6	0.055	2.8	77.7	2.5	11.6	0.0	5.1	0.5	0.1	0.1	1.2	0.0	0.1	0.0	99.1	
11022-g1-MI1-5	glassy				12.5	19.6	0.055	2.8	77.7	2.7	11.7	0.0	5.3	0.5	0.1	0.1	1.2	0.0	0.0	0.0	99.4	
11022-g8-MI2-1	glassy	79.4	2.9	1.3	71	13.2	0.032	2.9	76.4	2.0	11.4	0.1	5.5	0.5	0.1	0.2	1.0	0.0	0.1	0.0	97.2	
11022-g8-MI2-2	glassy				71	13.2	0.032	2.9	76.2	2.1	11.7	0.0	5.3	0.5	0.1	0.2	1.0	0.0	0.1	0.1	97.4	
11022-g8-MI2-3	glassy				71	13.2	0.032	2.9	76.7	2.2	11.5	0.0	5.3	0.5	0.1	0.2	1.2	0.1	0.0	0.0	97.8	
11022-g8-MI2-4	glassy				71	13.2	0.032	2.9	77.3	2.1	11.4	0.0	5.5	0.5	0.1	0.1	1.1	0.1	0.1	0.1	98.3	
11022-g14-MI1-1	glassy	18.8	-6.7	1.8	150	35.5	0.065	2.8	76.8	1.8	11.6	0.1	5.4	0.4	0.1	0.1	1.0	0.1	0.1	0.0	97.6	
11022-g14-MI1-2	glassy	18.7	-8.0	1.6	150	35.5	0.065	2.8	77.5	1.9	11.7	0.1	5.5	0.5	0.1	0.2	0.9	0.0	0.1	0.0	98.5	
11022-g14-MI1-3	glassy				150	35.5	0.065	2.8	77.6	1.9	12.1	0.1	5.3	0.5	0.1	0.2	1.1	0.0	0.1	0.0	98.9	
11022-g14-MI1-4	glassy				150	35.5	0.065	2.8	76.2	1.9	11.7	0.0	5.6	0.4	0.1	0.1	1.0	0.0	0.1	0.0	97.3	
11022-g14-MI1-5	glassy				150	35.5	0.065	2.8	76.7	2.0	11.6	0.0	5.3	0.4	0.1	0.2	1.0	0.0	0.1	0.0	97.4	
11022-g10-MI2-1	glassy	61.0	-7.1	1.2	77	13.3	0.038	3.1	77.2	2.0	11.4	0.0	5.3	0.4	0.1	0.1	0.9	0.1	0.1	0.0	97.6	
11022-g10-MI2-2	glassy	61.9	-7.4	1.3	77	13.3	0.038	3.1	76.9	2.0	11.4	0.0	5.4	0.5	0.1	0.2	1.0	0.1	0.1	0.0	97.7	
11022-g10-MI2-3	glassy								77.2	2.0	11.6	0.1	5.3	0.5	0.1	0.1	1.0	0.1	0.1	0.1	98.1	
11022-g10-MI2-4	glassy								76.4	1.9	11.5	0.0	5.2	0.4	0.1	0.1	1.2	0.0	0.2	0.0	97.1	
11022-g10-MI3-1	glassy	59.5	-6.7	1.1	96	13	0.041	3.2	77.5	1.9	11.3	0.1	5.3	0.5	0.1	0.1	1.2	0.1	0.0	0.0	98.0	
11022-g10-MI3-2	glassy								76.9	2.0	11.3	0.1	5.5	0.5	0.1	0.1	1.2	0.0	0.1	0.0	97.8	
11022-g10-MI3-3	glassy								76.8	2.0	11.6	0.0	5.3	0.5	0.2	0.1	1.2	0.0	0.1	0.0	97.7	
11022-g1-MI1-1	glassy	62.8	-7.1	1.5	90	13.8	0.061	3.7	76.3	1.6	12.0	0.0	5.5	0.5	0.1	0.1	1.3	0.1	0.0	0.0	97.6	

Table C1: continued

L ^a	L ^b	B	Na	Mg	Al	Si	P	K	Ca	Sc	Ti	V	Cr	Mn	Fe	Co	Ni	Cu	Zn	Ga	Ge	Rb	Sr	Y	Zr	Nb	Mo	Sb	Te	Cs	Ba	La	Ce	Pr	Nd	Sm	Eu	Gd	Tb	Dy	Ho	Er	Tm	Yb	Lu	Hf	Ta	W	Tl	Pb	Bi	Th	U	
12	13	25289	187	62635	355274	44	39293	3334	2	594	bd	bd	223	9215	bd	bd	3	64	21	bd	221	8	61	153	51	5	7	0	0	4	105	71	141	151	51	10	0	11	2	11	2	7	1	6	1	6	3	3	1	32	1	29	7	
13	13	23291	164	56932	355274	24	36697	3069	2	522	bd	bd	197	8675	bd	bd	3	53	18	3	198	7	55	136	44	4	7	bd	bd	4	95	65	128	13	47	9	0	9	1	9	2	6	1	6	1	5	3	3	1	29	0	26	6	
13	13	25575	182	61398	355274	31	39519	3394	2	580	0	5	220	9180	0	4	3	67	21	bd	218	8	62	150	49	5	7	0	bd	4	107	71	139	151	50	11	0	9	2	11	2	7	1	6	1	6	3	3	1	32	0	29	7	
16	14	13	26077	185	62195	355274	41	40463	3378	2	595	bd	bd	221	9226	0	bd	6	68	21	5	223	7	61	150	50	5	6	bd	bd	4	104	70	140	151	50	11	0	10	2	11	2	6	1	6	1	6	3	3	1	33	1	29	7
14	13	125155	164	60702	355274	38	40786	3353	2	563	bd	bd	222	9371	0	bd	6	72	22	bd	225	7	59	147	51	5	7	0	bd	4	104	69	137	14	49	11	0	9	2	11	2	6	1	5	3	3	1	33	0	28	7			
20	20	23697	186	62325	355274	32	42685	3380	2	610	bd	bd	218	9533	bd	1	bd	71	21	bd	219	7	61	151	50	5	7	bd	bd	4	106	73	143	151	51	10	0	9	2	11	2	7	1	6	1	6	3	4	2	33	0	29	7	
18	21	123805	181	61896	355274	34	43537	3754	2	601	bd	bd	224	9602	0	bd	1	65	21	bd	230	7	62	152	51	5	7	0	bd	4	109	73	143	151	52	11	0	11	2	11	2	7	1	6	1	6	4	3	2	31	0	29	7	
22	22	123590	165	62555	355274	27	43373	3682	2	586	0	bd	226	9540	bd	bd	bd	69	22	bd	227	7	62	152	50	4	7	0	bd	4	108	74	144	151	54	11	0	10	2	11	2	6	1	6	1	6	4	2	32	0	29	7		
24	23	14	23918	179	61684	355274	37	44114	3492	3	1603	0	4	219	9602	bd	bd	bd	72	22	bd	233	7	61	147	50	4	7	bd	bd	4	102	72	142	141	50	10	0	9	2	10	2	7	1	6	1	7	3	3	2	34	0	28	7
14	16	12	27440	204	66702	355274	40	41620	3825	2	621	bd	bd	231	9836	0	bd	3	82	22	4	236	8	62	155	52	3	8	bd	bd	4	106	74	150	151	52	11	0	10	2	12	2	7	1	6	1	8	4	2	33	0	28	8	
14	15	12	25418	176	61162	355274	40	39082	3346	2	568	bd	bd	213	9263	0	bd	5	61	22	3	221	7	61	153	50	5	7	bd	bd	4	105	72	141	151	52	11	0	10	2	11	2	7	1	6	1	6	3	3	1	33	0	29	7
15	15	13	25516	164	61876	355274	36	39901	3249	2	582	0	bd	213	9218	bd	bd	3	65	21	3	222	8	61	149	51	4	6	bd	bd	4	100	73	142	151	53	11	0	10	2	11	2	6	1	7	1	6	4	3	2	32	0	28	7
16	15	13	25050	155	59032	355274	44	39876	3289	2	568	bd	bd	216	9433	0	2	70	22	bd	220	7	59	149	46	4	7	0	bd	4	107	68	133	141	48	9	0	9	2	9	2	7	1	6	1	7	4	3	2	32	0	27	7	
34	34	16	23115	195	59008	355274	38	38711	3083	1	551	0	bd	183	7237	1	bd	bd	49	18	bd	240	2	54	114	41	5	6	0	1	5	14	57	107	111	38	8	0	8	1	9	2	6	1	5	1	6	3	3	2	31	0	30	7
38	37	15	25148	211	66900	355274	23	43353	3431	2	605	bd	bd	209	8086	bd	bd	bd	57	19	3	273	2	61	130	46	9	7	bd	bd	5	15	62	123	13	41	9	0	8	2	11	2	6	1	7	1	6	4	5	2	36	1	34	8
10	11	19	25079	262	65887	355274	38	41613	3413	2	bd	bd	bd	183	7389	0	1	bd	46	20	bd	251	3	59	150	45	6	6	0	bd	5	40	64	123	13	45	8	0	8	2	10	2	6	1	5	1	6	4	4	2	33	0	37	8
12	10	16	25248	278	65793	355274	40	42712	3401	2	729	bd	8	181	7381	bd	bd	bd	46	19	3	247	3	59	153	46	6	7	bd	bd	5	39	64	124	13	45	9	0	9	1	10	2	6	1	6	1	7	4	3	2	32	0	38	8
13	11	17	26609	290	68064	355274	38	44608	3253	1	715	0	bd	186	7231	0	bd	bd	51	21	bd	264	4	58	150	43	8	6	bd	bd	5	44	64	125	12	43	10	0	8	2	10	2	6	1	6	1	8	4	4	2	33	0	36	9
33	31	16	25207	248	64540	355274	25	41219	3343	3	713	bd	bd	180	7524	bd	bd	bd	45	20	bd	245	2	52	129	43	7	7	bd	bd	5	17	58	112	12	42	9	0	8	1	10	2	6	1	5	1	5	3	3	2	32	0	31	8
32	31	16	25259	269	65269	355274	41	42833	3242	1	715	bd	bd	188	7518	bd	1	47	19	bd	247	2	53	132	42	6	7	bd	bd	5	16	58	114	12	42	8	0	8	1	9	2	6	1	6	1	5	3	3	2	35	0	34	8	
35	33	16	26381	243	66273	355274	34	42281	3257	2	732	bd	8	184	7779	bd	bd	1	50	20	bd	261	2	54	130	42	6	6	bd	bd	5	17	58	117	12	42	9	0	8	1	10	2	6	1	5	1	6	3	3	2	37	0	34	8
35	32	15	25355	252	64084	355274	39	43071	3005	2	704	bd	bd	182	7891	bd	1	bd	48	17	4	255	3	54	129	41	7	7	0	bd	5	16	59	114	12	41	9	0	8	1	9	2	6	1	5	1	5	3	4	2	32	0	33	8
32	27	10	23756	177	62274	355274	16	41574	3240	2	747	bd	bd	216	8350	1	bd	bd	54	19	bd	199	9	54	151	42	5	5	bd	bd	4	137	80	153	151	51	11	0	8	2	9	2	7	1	5	1	6	3	2	27	0	25	6	
28	32	12	28280	226	71664	355274	41	44016	4357	1	729	bd	bd	214	8298	1	bd	bd	57	19	bd	192	7	55	177	49	6	8	bd	bd	4	125	84	159	16	54	14	0	10	2	9	2	6	1	6	1	8	3	1	2	34	0	30	7
31	29	12	24092	342	67641	355274	26	38289	3223	2	621	bd	9	183	7614	bd	bd	bd	58	19	4	194	6	52	158	46	3	5	bd	4	4	115	74	171	151	53	12	0	10	2	9	2	6	1	4	1	5	3	2	32	1	27	6	
26	27	21	24297	181	66855	355274	32	44793	3476	2	580	bd	bd	216	9687	bd	bd	1	58	20	bd	273	1	60	127	48	7	7	bd	bd	6	8	57	111	12	39	8	0	9	2	10	2	6	1	6	1	6	4	4	2	34	0	33	9

Table C1: continued

Sample	MI Type	Li (ppm)	d(Li)	2 SE	Lj ^a	Lj ^b	B	Na	Mg	Al	Si	P	K	Ca	Sc	Ti	V	Cr	Mn	Fe	Co	Ni	Cu	Zn	Ga	Ge	Rb	Sr	Y	Zr	Nb	Mo	Sb	Te	Cs	Ba	La	Ce	Pr	Nd	Sm	Eu		
13005-g1-M11-1	cryst	144.4	-1.6	1.0	75	70	15	27841	177	64479	355274	29	39178	2771	3	541	bdl	bdl	219	8788	bdl	1	bdl	61	23	bdl	235	3	68	148	56	3	7	0	bdl	5	8	66	130	14	47	10	0	
13005-g1-M11-2	cryst				79	81	15	28505	176	63721	355274	30	37537	3048	2	529	0	bdl	222	8693	0	bdl	61	22	bdl	247	3	64	139	52	4	7	0	bdl	6	11	64	127	13	47	10	0		
13005-g1-M11-3	cryst				57	55	15	28600	187	64270	355274	27	37150	2908	2	523	bdl	bdl	226	8735	0	bdl	59	23	3	200	6	62	140	53	5	8	0	1	5	8	64	127	13	45	10	0		
13005-g4-M11-1	cryst	165.8	-4.2	1.4	85	84	17	26036	160	62882	355274	20	40007	3168	2	546	bdl	bdl	201	8795	0	bdl	3	63	21	3	239	4	57	143	47	4	6	0	bdl	5	36	66	121	14	49	0		
13005-g4-M11-2	cryst	190.9	-3.5	1.2	79	76	13	21848	159	57451	355274	34	39477	3351	1	571	bdl	bdl	199	8060	0	bdl	4	57	19	bdl	225	4	54	133	48	3	6	0	bdl	4	42	60	123	13	44	10		
13005-g4-M11-3	cryst	205.4	-5.0	1.4	87	83	14	26455	200	65435	355274	35	42977	3635	2	575	bdl	bdl	217	8811	0	bdl	2	62	23	4	250	5	61	150	52	5	7	0	1	5	33	69	139	14	51	10		
13005-g4-M11-4	cryst	207.9	-6.2	1.2	75	69	16	26937	179	65651	355274	42	41609	2938	2	579	bdl	bdl	222	9311	0	bdl	4	63	22	bdl	216	5	62	155	53	6	0	bdl	5	30	70	138	14	51	11	0		
13005-g4-M11-5	cryst				85	90	17	27899	174	67244	355274	31	40138	3869	2	603	bdl	bdl	236	9362	0	bdl	3	66	25	6	252	5	68	156	55	5	8	0	bdl	6	23	75	145	15	54	11	0	
13005-g4-M11-6	cryst				87	86	15	28895	192	64463	355274	37	39051	4063	2	577	bdl	bdl	216	9082	0	bdl	2	4	59	23	bdl	237	4	63	154	51	6	7	0	bdl	5	24	70	138	14	51	11	0
13005-g4-M11-7	cryst				83	85	15	27981	188	63520	355274	41	38589	3657	1	583	0	bdl	220	8985	bdl	bdl	3	63	21	bdl	232	5	60	149	50	5	7	0	bdl	5	20	69	137	15	50	10	0	
13005-g4-M11-8	cryst				93	86	15	28349	174	64813	355274	41	39125	3592	4	579	bdl	bdl	222	9137	0	bdl	1	2	68	20	5	240	5	63	150	52	5	7	0	bdl	5	20	70	139	15	52	10	
13005-g4-M11-9	cryst				90	87	15	27590	176	63491	355274	32	38988	3550	2	601	5	227	9147	0	bdl	1	2	64	21	7	237	4	64	146	52	4	8	0	bdl	5	15	67	136	14	48	11	0	
13005-g6-M11-1	cryst	325.7	-0.1	1.5	176	169	13	27564	201	67792	355274	32	39745	2135	2	1051	2	bdl	155	7852	bdl	bdl	7	41	18	bdl	206	10	37	161	31	6	6	bdl	2	4	66	69	135	12	42	7	0	
13005-g6-M11-2	cryst	408.8	-0.9	2.0	206	190	13	24338	211	77421	355274	44	48606	4752	2	937	1	bdl	159	7323	bdl	bdl	8	48	13	bdl	205	12	37	167	34	4	3	bdl	bdl	3	96	69	137	14	46	7	0	
13005-g6-M11-3	cryst				114	112	12	28753	267	65860	355274	49	37805	2853	2	970	1	bdl	163	7492	0	bdl	1	10	32	19	bdl	188	9	40	165	33	4	4	bdl	bdl	4	49	74	140	14	48	8	0
13005-g6-M11-4	cryst				120	113	12	27607	301	64779	355274	60	39696	2735	3	993	1	bdl	162	8475	0	2	7	45	19	bdl	188	8	41	165	32	4	4	bdl	bdl	4	62	73	138	14	45	8	0	
13005-g6-M11-5	cryst				130	119	13	30540	269	67047	355274	52	37660	3249	2	984	1	bdl	152	7676	bdl	1	10	39	19	bdl	182	8	41	169	34	5	4	0	bdl	4	50	75	143	14	48	9	0	
13005-g6-M12-1	cryst				118	114	13	29215	267	65125	355274	53	36009	2982	3	962	1	bdl	158	7739	bdl	bdl	8	44	19	3	180	8	41	171	32	5	5	0	bdl	4	54	72	137	14	47	9	0	
13005-g6-M12-2	cryst	25.2	3.2	1.5	17	18	22	33583	261	66069	355274	36	32671	3784	2	564	bdl	bdl	121	7288	bdl	4	1	57	20	3	115	8	54	122	45	6	8	1	2	20	58	112	12	41	7	0		
13005-g7-M12-1	cryst	9.38	0.63	18.21	20	20	16	29926	283	67909	355274	26	40990	2988	2	532	bdl	bdl	152	7200	bdl	bdl	1	39	21	bdl	233	4	47	122	41	4	6	bdl	1	5	18	51	102	10	35	8	0	
13005-g7-M12-2	cryst				19	18	18	34262	278	66921	355274	35	37467	2255	1	521	0	8	162	7129	0	bdl	10	34	23	3	170	3	50	118	47	3	6	1	bdl	3	15	56	108	11	36	7	0	
13005-g10-M11-1	cryst	6.06	1.26	6.10	6	6	49	27498	130	78246	355274	57	62834	1001	1	423	bdl	48	84	3976	0	167	2	33	22	4	306	2	42	138	45	1	6	0	bdl	6	8	46	80	7	23	4	0	
13005-g10-M11-2	cryst				9	12	54	29833	119	74842	355274	48	55987	1321	1	330	bdl	45	74	3339	0	189	4	26	22	bdl	270	3	40	131	38	2	4	bdl	bdl	6	11	39	68	6	21	4	bdl	
13005-g10-M11-3	cryst				79	75	24	14897	105	39680	355274	36	30425	1978	1	407	bdl	23	84	4987	bdl	89	2	24	11	bdl	229	1	36	73	35	3	7	0	bdl	4	13	38	82	9	29	6	0	
13005-g10-M11-4	cryst				63	61	31	15787	81	43108	355274	46	33389	1608	2	876	bdl	24	73	8099	bdl	99	3	21	13	bdl	240	1	32	87	53	3	11	0	bdl	3	12	36	72	7	24	5	0	
13005-g12-M11-1	cryst	11.80	0.49	149.15	13	11	11	27105	272	75957	355274	41	58855	3827	2	672	bdl	6	166	7466	0	bdl	bdl	32	22	bdl	353	1	49	144	39	4	6	0	2	7	52	99	10	33	7	0		
13005-g12-M11-2	cryst				23	22	13	23810	286	72764	355274	35	58379	3097	3	610	bdl	bdl	203	7772	0	bdl	bdl	36	17	bdl	370	1	48	134	36	3	6	bdl	bdl	7	52	100	10	37	8	0		
13005-g13-M11-1	cryst	12.85	0.90	11.63	9	9	15	44909	291	81482	355274	34	33245	4315	2	733	bdl	1474	196	8920	0	bdl	bdl	49	24	5	180	2	62	153	56	42	8	0	bdl	6	2	53	93	9	30	6	bdl	
13005-g13-M11-2	cryst				22	22	9	24929	215	73212	355274	31	59431	3550	2	601	bdl	151	173	7558	bdl	bdl	31	39	23	bdl	352	1	58	133	45	4	6	1	bdl	7	5	49	93	10	33	8	0	
13005-g15-M11-1	cryst	5.44	1.02	9.80	46	47	15	29592	233	72191	355274	32	49173	2986	2	629	bdl	18	157	7246	bdl	bdl	34	22	bdl	276	1	55	139	45	5	7	0	bdl	6	5	48	123	13	42	10	0		
13005-g15-M11-2	cryst				77	78	14	20526	201	59500	355274	38	45975	3036	2	560	bdl	59	148	7090	1	bdl	1	44	17	3	270	1	39	109	40	4	6	1	bdl	5	4	46	86	8	26	6	0	
13005-g16-M11-1	cryst	10.12	0.30	107.81	74	72	12	22745	210	60676	355274	44	44332	2429	2	795	0	170	160	7850	bdl	bdl	43	1																				

Table C1: continued

Gd	Tb	Dy	Ho	Er	Tm	Yb	Lu	Hf	Ta	W	Ti	Pb	Bi	Th	U	
9	2	11	2	7	1	7	1	6	4	4	2	29	0	32	9	
10	2	11	2	7	1	7	1	6	3	3	1	30	0	30	8	
10	2	11	2	7	1	7	1	6	4	4	1	41	0	32	9	
9	2	10	2	6	1	6	1	6	3	3	2	33	0	27	8	
9	1	9	2	6	1	5	1	5	3	3	1	31	0	26	7	
10	2	11	2	7	1	6	1	7	4	3	2	31	0	29	8	
10	2	10	2	7	1	6	1	7	3	3	2	30	0	30	8	
10	2	12	2	7	1	7	1	6	4	4	2	27	0	32	8	
9	2	11	2	7	1	6	1	6	3	5	2	28	0	29	8	
11	2	11	2	6	1	7	1	6	4	3	2	28	0	29	8	
11	2	11	2	7	1	6	1	7	3	3	2	29	0	30	8	
9	2	11	2	6	1	6	1	6	4	3	2	31	0	28	7	
6	1	7	1	4	1	4	1	4	2	3	1	27	0	26	6	
9	1	7	1	4	1	3	1	5	2	4	2	38	1	31	7	
8	1	8	1	4	1	4	1	6	2	2	1	25	0	28	6	
7	1	7	1	4	1	4	1	6	2	3	2	25	0	27	6	
7	1	7	1	4	1	4	1	5	2	2	1	25	0	28	6	
8	1	7	1	5	1	4	1	6	2	2	2	25	0	29	6	
7	1	7	1	4	1	4	1	6	3	3	1	25	0	28	6	
8	1	9	2	6	1	6	1	6	4	4	1	52	0	32	8	
7	1	8	2	5	1	5	1	5	3	3	2	34	bdl	31	8	
7	1	8	2	5	1	5	1	6	4	5	2	34	5	30	9	
5	1	7	2	5	1	5	1	6	4	4	3	30	0	30	11	
5	1	6	1	5	1	4	1	7	4	3	3	34	0	28	9	
6	1	6	1	4	0	4	0	3	3	6	1	22	0	22	5	
5	1	5	1	4	1	4	0	4	4	5	2	25	0	25	6	
7	1	8	2	5	1	5	1	6	4	3	3	45	0	32	7	
7	1	9	2	5	1	5	1	6	3	3	3	39	0	31	7	
6	1	10	2	7	1	7	1	7	5	4	2	42	1	38	12	
9	1	9	2	6	1	5	1	6	3	4	3	47	0	36	9	
9	1	10	2	6	1	6	1	5	4	4	4	44	0	35	10	
5	1	6	1	4	1	4	1	4	3	3	4	3	47	0	29	7
9	1	9	2	5	1	5	1	4	3	2	2	39	1	32	8	
10	2	11	2	5	1	5	1	8	4	3	2	38	0	32	8	
10	1	8	2	7	1	6	1	6	4	5	2	39	0	33	9	
7	1	9	2	6	1	5	1	6	3	3	3	31	0	31	8	
8	1	9	2	6	1	5	1	6	3	4	2	30	0	32	9	
7	1	7	2	6	1	5	1	4	2	2	2	32	1	28	7	
8	2	10	2	7	1	6	1	5	3	4	1	28	0	28	7	
11	2	11	2	6	1	6	1	6	4	3	2	32	0	30	7	
12	2	13	2	5	1	6	1	6	3	1	3	52	0	29	8	
6	1	6	2	4	0	4	1	4	2	7	2	22	1	26	5	
11	2	11	2	7	1	6	1	7	3	3	2	32	1	27	6	
11	2	11	2	6	1	6	1	7	4	3	2	32	0	28	6	
11	2	11	2	7	1	7	1	7	4	3	2	34	0	29	7	
9	1	10	2	6	1	6	1	6	4	5	2	44	1	28	9	

Appendix C

Table C2: Groundmass glass 13005 and 11022 - Lithium concentration and isotopic composition (by SIMS), major element data (by EPMA) and trace elements (by La-ICP-MS).

Sample	d ⁷ Li	2SE	Li ppm	SiO ₂	Na ₂ O	Al ₂ O ₃	MgO	K ₂ O	CaO	TiO ₂	Cl	FeO	MnO	P ₂ O ₅	Cr ₂ O ₃	Total
13005 glass1-1	9.07	0.73	40.95	76.1	2.3	11.8	0.0	5.4	0.6	0.1	0.1	1.3	0.0	0.0	0.0	97.8
13005 glass1-2				76.2	2.3	11.7	0.0	5.4	0.6	0.1	0.1	1.2	0.0	0.0	0.0	97.6
13005 glass1-3				76.6	2.1	11.7	0.0	5.5	0.5	0.1	0.1	1.3	0.0	0.0	0.0	98.0
13005 glass2-1	18.00	0.50	35.44	76.6	2.4	11.7	0.0	5.3	0.4	0.1	0.1	1.3	0.0	0.0	0.0	98.1
13005 glass2-2	17.83	0.46	33.38	76.4	2.2	11.6	0.0	6.0	0.4	0.1	0.1	1.3	0.0	0.1	0.0	98.2
13005 glass2-3	13.57	0.40	40.85	76.3	2.2	11.7	0.0	6.2	0.5	0.1	0.1	1.2	0.0	0.1	0.0	98.4
13005 glass2-4				76.5	2.2	11.5	0.0	5.8	0.4	0.1	0.1	1.4	0.0	0.0	0.0	98.1
13005 glass4-1	15.23	0.42	36.83	77.0	2.2	11.7	0.0	6.0	0.4	0.1	0.1	1.1	0.0	0.0	0.0	98.6
13005 glass4-2	17.86	0.39	41.62	77.3	2.3	12.0	0.0	5.4	0.5	0.1	0.1	1.3	0.0	0.0	0.0	99.2
13005 glass4-3	17.45	0.63	40.34	76.1	2.2	11.6	0.0	5.8	0.4	0.1	0.2	1.3	0.0	0.0	0.0	97.8
13005 glass4-4				76.7	2.2	12.1	0.0	6.0	0.4	0.1	0.1	1.1	0.0	0.0	0.0	98.7
13005 glass4-5				76.7	2.3	12.0	0.0	5.5	0.4	0.1	0.1	1.3	0.0	0.1	0.0	98.5
13005 glass5-1	14.48	0.40	42.00	77.8	2.2	11.7	0.0	5.8	0.4	0.1	0.1	1.3	0.0	0.0	0.0	99.5
13005 glass5-2	14.78	0.42	37.07	76.3	2.3	11.7	0.1	5.5	0.6	0.1	0.1	1.3	0.1	0.0	0.1	98.1
13005 glass5-3	14.87	0.39	41.69	77.5	2.1	11.5	0.0	5.6	0.4	0.1	0.1	1.2	0.1	0.1	0.0	98.8
13005 glass5-4				77.1	2.3	11.7	0.0	5.6	0.4	0.1	0.1	1.2	0.0	0.0	0.0	98.6
13005 glass5-5				76.3	2.4	11.7	0.0	5.4	0.5	0.1	0.1	1.2	0.1	0.0	0.0	97.9
13005 glass5-6				77.6	2.3	11.8	0.0	5.7	0.5	0.1	0.2	1.3	0.0	0.0	0.0	99.6
13055 glass6-1	13.11	0.49	42.28	76.9	2.3	11.7	0.0	5.6	0.4	0.1	0.1	1.3	0.1	0.0	0.0	98.6
13005 glass6-2	14.67	0.42	42.71	77.7	2.3	11.7	0.0	5.8	0.5	0.1	0.1	1.3	0.0	0.1	0.0	99.6
13005 glass6-3				76.6	2.1	11.7	0.0	5.8	0.4	0.1	0.1	1.2	0.0	0.0	0.0	98.2
13005 glass7-1	17.77	0.56	43.34	76.1	2.3	11.8	0.0	5.4	0.5	0.1	0.2	1.3	0.0	0.0	0.0	97.7
13005 glass7-2	17.42	0.59	39.74	76.8	2.2	11.8	0.0	5.6	0.4	0.1	0.1	1.3	0.0	0.1	0.0	98.4
13005 glass7-3				76.7	2.3	11.9	0.0	5.6	0.5	0.1	0.1	1.3	0.1	0.1	0.0	98.7
13005 glass8-1	15.12	0.62	36.17	76.3	2.4	11.9	0.0	5.6	0.5	0.1	0.1	1.2	0.0	0.1	0.0	98.3
13005 glass8-2	7.61	1.60	32.16	76.1	2.2	11.4	0.0	5.4	0.6	0.1	0.1	1.2	0.0	0.1	0.0	97.2
13005 glass8-3				75.9	2.2	11.6	0.0	5.5	0.5	0.1	0.1	1.3	0.0	0.0	0.0	97.5
13005 glass8-4				76.5	2.3	11.8	0.1	5.5	0.5	0.1	0.1	1.3	0.0	0.0	0.0	98.1
13005 glass9-1	13.47	0.70	43.55	76.6	2.3	11.7	0.0	5.8	0.4	0.1	0.1	1.2	0.0	0.0	0.0	98.4
13005 glass9-2	20.49	0.66	36.44	77.0	2.2	12.0	0.0	6.2	0.4	0.1	0.1	1.2	0.1	0.1	0.0	99.2
13005 glass9-3	20.47	0.99	36.71	77.1	2.3	11.7	0.0	5.5	0.4	0.1	0.1	1.3	0.0	0.0	0.0	98.6
13005 glass9-4				77.1	2.3	11.9	0.0	5.5	0.5	0.1	0.1	1.2	0.0	0.0	0.0	98.8
13005 glass10-1	16.46	0.60	38.44	75.9	2.2	11.8	0.0	5.3	0.5	0.1	0.1	1.3	0.0	0.0	0.0	97.4
13005 glass10-2				76.7	2.2	11.8	0.0	5.5	0.6	0.1	0.1	1.3	0.0	0.0	0.0	98.3
13005 glass10-3	15.00	0.62	40.04	76.6	2.2	11.8	0.0	5.3	0.6	0.1	0.1	1.3	0.0	0.0	0.0	98.0
13005 glass10-4				77.1	2.2	11.6	0.0	5.5	0.5	0.1	0.1	1.3	0.1	0.1	0.0	98.6
13005 glass10-5				77.0	2.3	11.7	0.0	5.4	0.4	0.1	0.1	1.2	0.0	0.0	0.0	98.2
13005 glass10-6				76.5	2.1	11.6	0.1	5.5	0.4	0.1	0.1	1.3	0.0	0.1	0.0	97.9
13005 glass11-1	14.64	0.62	41.11	77.7	2.3	11.8	0.0	5.7	0.5	0.1	0.1	1.4	0.0	0.1	0.0	99.8
13005 glass11-2	10.16	0.76	41.57	76.0	2.3	11.8	0.0	5.3	0.5	0.1	0.1	1.3	0.0	0.0	0.0	97.5
13005 glass11-3	14.49	0.73	27.35	76.2	2.2	11.7	0.0	5.7	0.4	0.1	0.1	1.3	0.0	0.0	0.0	97.9
13005 glass11-4				76.5	2.4	11.8	0.0	5.5	0.5	0.1	0.1	1.3	0.0	0.1	0.0	98.2
13005 glass12-1	14.78	0.61	40.73	76.0	2.3	11.7	0.0	5.4	0.5	0.1	0.1	1.2	0.0	0.0	0.0	97.4
13005 glass12-2	15.18	0.55	43.98	76.0	2.2	11.7	0.0	5.6	0.5	0.1	0.1	1.2	0.0	0.1	0.0	97.5
13005 glass12-3	19.75	0.61	37.07	76.0	2.3	11.5	0.0	5.5	0.6	0.1	0.1	1.3	0.0	0.0	0.0	97.5
13005 glass12-4				76.7	2.2	11.8	0.0	5.3	0.5	0.1	0.1	1.3	0.1	0.0	0.0	98.1
13005 glass12-5				76.9	2.1	11.9	0.0	5.8	0.4	0.1	0.1	1.3	0.0	0.0	0.0	98.7
13005 glass13-1				75.9	2.2	11.7	0.0	5.4	0.5	0.1	0.1	1.2	0.0	0.0	0.0	97.2
13005 glass13-2	10.54	0.57	47.52	76.0	2.3	11.8	0.0	5.3	0.5	0.1	0.1	1.4	0.0	0.0	0.0	97.4
13005 glass13-3				77.7	2.2	11.8	0.0	5.8	0.4	0.1	0.1	1.3	0.0	0.0	0.0	99.4
13005 glass14-1	16.61	0.56	44.23	77.7	2.2	11.6	0.1	5.5	0.5	0.1	0.1	1.2	0.0	0.0	0.0	98.9
13005 glass14-2	19.46	0.63	38.28	76.6	2.2	12.0	0.0	6.0	0.5	0.1	0.1	1.3	0.1	0.1	0.0	99.0
13005 glass14-3	15.13	0.99	22.70	76.5	2.2	11.5	0.0	5.4	0.5	0.1	0.1	1.1	0.0	0.1	0.0	97.5
13005 glass14-4				76.0	2.3	11.6	0.0	5.3	0.5	0.1	0.1	1.2	0.0	0.1	0.0	97.3
13005 glass15-1	13.60	0.56	42.48	75.5	2.3	11.5	0.0	5.5	0.5	0.1	0.1	1.3	0.1	0.0	0.0	97.0
13005 glass15-2	15.60	0.74	39.18	76.1	2.3	12.1	0.0	5.5	0.5	0.1	0.1	1.4	0.0	0.0	0.0	98.2
13005 glass15-3	14.67	0.58	42.59	76.3	2.4	12.1	0.0	5.8	0.4	0.1	0.1	1.2	0.0	0.0	0.0	98.5
13005 glass15-4				75.7	2.3	11.9	0.0	5.4	0.4	0.1	0.1	1.3	0.0	0.0	0.0	97.3
13005 glass16-1	13.77	0.55	43.38	76.1	2.2	11.6	0.0	5.6	0.5	0.1	0.1	1.1	0.0	0.0	0.0	97.4
13005 glass16-2	13.69	1.57	34.83	76.6	2.4	11.5	0.0	5.4	0.6	0.1	0.1	1.3	0.0	0.0	0.0	98.0
13005 glass16-3	19.34	0.74	36.19	77.1	2.3	11.6	0.0	5.4	0.4	0.1	0.1	1.2	0.0	0.0	0.0	98.4
13005 glass16-4				77.6	2.3	11.8	0.0	5.8	0.4	0.1	0.1	1.2	0.0	0.0	-0.1	99.4
13005 glass18-1	14.48	0.56	42.49	76.5	2.3	11.7	0.0	5.2	0.5	0.1	0.2	1.3	0.0	0.1	0.0	97.8
13005 glass18-2				77.3	2.2	11.6	0.0	5.6	0.4	0.1	0.1	1.3	0.0	0.1	0.0	98.9
13005 glass19-1	12.81	0.56	42.38	75.8	2.3	11.7	0.0	5.3	0.5	0.1	0.1	1.2	0.1	0.0	0.0	97.1
13005 glass19-2	9.42	0.67	44.44	76.6	2.3	11.5	0.0	5.4	0.6	0.1	0.1	1.3	0.0	0.0	0.0	98.0
13005 glass19-3	15.02	0.56	41.99	76.3	2.3	11.7	0.0	5.3	0.5	0.1	0.1	1.2	0.1	0.0	0.0	97.7
13005 glass19-4				75.3	2.4	12.0	0.0	5.3	0.5	0.1	0.1	1.3	0.1	0.1	0.0	97.1
13005 glass20-1	18.15	0.55	43.75	75.8	2.2	11.8	0.0	5.2	0.5	0.1	0.1	1.3	0.0	0.1	0.0	97.2
13005 glass20-2	16.85	0.58	38.79	76.3	2.3	11.7	0.0	5.3	0.5	0.1	0.1	1.4	0.0	0.0	0.0	97.7
13005 glass20-3	15.09	0.56	42.01	76.2	2.1	11.5	0.0	5.6	0.5	0.1	0.1	1.3	0.0	0.0	0.0	97.5
13005 glass21-1	17.72	0.60	36.84	77.1	2.2	11.5	0.0	5.8	0.4	0.1	0.2	1.2	0.0	0.1	0.0	98.6
13005 glass21-2	10.06	2.30	31.82	77.7	2.2	11.7	0.0	5.7	0.5	0.1	0.1	1.3	0.1	0.0	0.0	99.2
13005 glass21-3				76.1	2.2	11.6	0.0	5.7	0.5	0.1	0.1	1.3	0.0	0.0	0.0	97.6
13005 glass21-4				77.2	2.3	12.0	0.0	5.6	0.4	0.1	0.1	1.3	0.0	0.0	0.0	99.0

Table C2:continued

Li	Be	B	Na	Mg	Al	Si	P	K	Ca	Sc	Ti	V	Cr	Mn	Fe	Co	Ni	Cu	Zn	Ga	Rb	Sr	Y	Zr	Nb	Cs	Ba	La	Ce	Pr	Nd	Sm	Eu	Gd	Th	Dy	Ho	Er	Tm	Yb	Lu	Hf	Ta	Pb	Th	U
38	38	13	22168	192	66553	355274	39	48280	3548	2	590	0	bd	214	8756	0	3	2	74	25	227	8	63	155	51	5	95	75	143	15	53	11	0	9	2	11	2	7	1	6	1	6	4	37	29	7
46	42	11	22927	375	74774	355274	53	49577	3512	2	656	1	bd	195	9933	0	5	5	62	33	218	24	72	156	52	6	355	78	131	17	59	12	1	11	2	12	2	7	1	7	1	6	4	37	29	7
42	41	12	20262	379	67416	355274	52	50336	3159	2	642	1	bd	239	11833	1	bd	3	46	26	230	14	73	166	52	6	128	80	146	17	57	12	0	12	2	12	3	7	1	7	1	6	4	40	32	7
30	37	12	19380	318	68927	355274	bd	56827	3214	2	624	0	bd	189	9146	2	3	3	30	25	232	17	74	165	31	6	123	78	145	16	50	11	0	12	2	12	2	7	1	7	1	6	4	43	30	7
42	43	14	20595	271	63717	355274	bd	51352	3131	2	609	0	bd	208	9745	2	bd	4	45	25	224	12	67	155	51	7	116	73	137	15	54	11	0	10	2	11	2	7	1	6	1	6	4	35	28	7
45	48	12	20414	513	63337	355274	30	48239	3556	2	614	1	bd	206	13550	0	2	3	96	29	225	14	64	157	52	5	126	72	136	15	50	10	0	10	2	11	2	6	1	6	1	6	4	43	28	7
46	41	12	23783	209	63737	355274	27	46509	3898	2	607	0	bd	232	9865	0	bd	2	74	22	233	7	69	166	53	4	89	80	157	17	57	12	0	11	2	12	3	8	1	7	1	7	4	36	32	8
41	37	11	22369	286	68312	355274	42	51113	3151	2	624	1	bd	207	8573	1	2	3	58	25	229	13	72	164	53	6	112	78	146	16	58	12	0	11	2	12	2	7	1	7	1	6	4	44	30	7
41	42	11	20879	395	65310	355274	45	48347	3405	2	648	2	bd	218	11850	1	bd	2	63	27	232	12	73	171	57	7	110	77	145	16	55	11	0	10	2	12	2	7	1	7	1	7	4	42	31	7
37	39	12	21380	264	64748	355274	39	51403	2757	2	620	0	bd	212	8713	6	bd	9	51	23	237	10	71	161	52	6	105	78	148	16	55	11	0	11	2	12	2	7	1	7	1	7	4	37	31	7
48	43	12	23337	237	69688	355274	bd	47731	3554	2	616	bd	bd	224	9645	5	3	3	51	25	223	9	69	163	53	5	92	79	149	16	56	12	0	11	2	12	2	7	1	7	1	6	4	36	31	7
49	44	12	21872	283	67014	355274	37	48985	3530	2	632	0	bd	222	10427	0	2	3	68	25	229	11	70	166	53	5	108	78	151	16	56	11	0	11	2	12	2	7	1	7	1	7	4	39	32	7
48	42	11	22419	207	61836	355274	bd	49234	3261	2	627	bd	bd	214	9293	0	bd	0	60	24	228	9	65	157	51	5	96	77	146	16	54	11	0	10	2	12	2	7	1	7	1	6	4	37	30	7
39	42	12	22649	205	62726	355274	bd	49448	3339	2	597	bd	bd	218	9517	1	bd	1	67	26	232	9	63	155	52	6	94	74	142	15	51	10	0	10	2	11	2	7	1	6	1	6	4	41	29	8
43	40	16	14682	653	71467	355274	bd	47838	2470	2	555	1	bd	170	8365	1	8	4	62	41	216	20	52	128	50	10	132	53	89	11	38	8	0	7	1	8	1	5	1	5	1	5	3	56	20	5
44	43	10	21375	301	70798	355274	35	50221	3347	2	633	0	bd	217	9849	1	3	2	56	25	232	12	67	164	55	6	117	73	143	15	54	11	0	10	2	11	2	7	1	7	1	7	4	38	30	7
42	43	10	24108	428	71583	355274	49	48143	7453	2	652	1	bd	198	9120	1	4	2	51	28	222	37	78	164	54	6	157	83	145	16	56	12	0	11	2	13	3	8	1	7	1	6	4	43	30	6
40	39	11	21700	227	63431	355274	48	49105	2874	2	592	0	bd	199	8880	0	2	1	57	25	224	10	66	155	51	5	101	74	140	15	52	11	0	10	2	12	2	7	1	7	1	6	4	40	29	7
52	45	12	21072	392	66894	355274	62	49856	2873	2	622	1	bd	213	14023	1	2	2	52	25	232	12	75	158	54	6	128	79	147	17	57	11	0	12	2	12	3	7	1	7	1	6	4	39	31	7
50	42	13	19821	356	66146	355274	75	51064	3336	2	601	bd	bd	192	8916	bd	3	1	54	31	234	13	65	151	53	6	125	73	139	15	51	11	0	10	2	11	2	7	1	6	1	6	4	45	30	7
47	44	11	22657	231	63857	355274	bd	48692	3485	2	615	0	bd	218	9984	0	1	1	75	24	231	9	67	160	55	5	95	76	147	16	53	11	0	11	2	11	2	7	1	7	1	7	4	36	31	8
38	42	12	21254	278	67208	355274	29	50756	3411	2	622	bd	bd	218	11339	1	2	9	64	25	235	12	70	168	55	6	121	77	146	16	54	11	0	11	2	12	2	7	1	7	1	7	4	36	31	8
46	38	15	20641	238	65935	355274	bd	51456	2625	2	577	0	bd	209	9064	bd	4	4	20	26	242	10	63	149	51	6	90	71	134	14	49	10	0	9	2	11	2	7	1	6	1	6	4	41	28	7
42	39	11	20124	268	67051	355274	51	54480	2304	2	609	0	bd	204	9064	bd	2	1	49	26	232	12	72	163	54	6	110	78	145	16	55	11	0	11	2	12	3	8	1	7	1	6	4	41	31	7
29	35	13	18199	407	70874	355274	bd	52860	2630	2	561	1	bd	169	9734	bd	6	2	29	26	235	16	68	140	52	9	105	64	112	14	45	10	0	9	1	10	2	6	1	6	1	5	4	41	23	6
47	45	11	22122	339	67021	355274	bd	49562	3287	2	610	0	bd	217	10978	0	bd	1	55	24	236	10	73	173	56	6	85	80	147	17	57	12	0	12	2	13	3	8	1	7	1	7	4	37	33	8
48	45	13	18950	513	75792	355274	38	48899	3376	2	707	1	bd	189	10980	0	5	2	64	33	225	6	71	174	61	8	113	76	129	16	53	12	0	11	2	12	2	7	1	7	1	7	4	40	30	7
44	51	10	21228	361	72225	355274	bd	50605	3356	2	743	1	bd	218	10144	1	3	2	53	27	228	15	70	162	57	6	163	77	144	16	58	13	0	10	2	13	2	7	1	7	1	6	4	36	28	7
36	41	13	20012	407	69104	355274	bd	50472	3252	2	648	1	bd	211	9989	bd	5	1	54	27	224	15	73	160	54	6	138	79	133	16	54	11	0	11	2	11	2	7	1	6	1	6	4	37	30	7
41	42	10	23643	194	63106	355274	37	48614	3599	2	634	bd	bd	222	9265	bd	0	56	23	233	8	66	158	52	4	97	75	147	15	53	11	0	10	2	11	2	7	1	7	1	6	4	35	30	7	
41	38	11	21524	218	65993	355274	bd	50521	3413	2	591	0	bd	210	9039	bd	2	2	62	24	229	9	67	160	51	5	107	78	144	16	54	11	0	11	2	12	2	7	1	7	1	6	4	35	30	7
45	41	12	23365	209	63402	355274	bd	47880	3411	2	602	bd	bd	218	9099	bd	1	55	24	225	8	64	155	51	4	97	74	141	15	52	11	0	10	2	11	2	7	1	7	1	6	4	34	29	7	
36	41	12	19705	368	69319	355274	49	52797	2518	2	630	1	bd	190	9550	1	3	2	36	26	230	14	71	158	55	7	137	74	135	15	52	11	0	10	2	11	2	7	1	6	1	6	4	39	28	6
37	41	12	18351	587	70223	355274	bd	55364	2718	2	626	1	bd	188	10509	2	4	7	49	28	243	21	65	152	51	8	165	70	122	14	49	11	0	10	2	11	2	6	1	6	1	5	4	43	26	6
46	40	14	20593	319	65664	355274	bd	53355	3215	2	594	0	bd	207	9371	1	bd	2	43	28	239	12	65	157	50	6	133	75	143	15	52	11	0	10	2	11	2	6	1	6	1	6	4	40	29	7

Table C2: continued

	Li ⁺	B	Na	Mg	Al	Si	P	K	Ca	Sc	Ti	V	Cr	Mn	Fe	Co	Ni	Cu	Zn	Ga	Rb	Sr	Y	Zr	Nb	Cs	Ba	La	Ce	Pr	Nd	Sm	Eu	Gd	Tb	Dy	Ho	Er	Tm	Yb	Lu	Hf	Ta	Pb	Th	U	
11022GLASS-1	36	37	12	21367	232	63054	355274	bd	48534	3778	2	622	0	bd	225	9707	bd	bd	1	64	25	240	10	66	58	51	5	140	76	44	16	54	11	0	10	2	11	2	7	1	6	1	6	4	35	30	7
11022GLASS-2	34	36	13	19429	433	68537	355274	39	49089	3956	2	670	1	bd	235	1076	0	4	2	73	28	244	16	80	66	54	7	200	79	44	16	57	12	0	12	2	13	3	8	1	7	1	7	4	40	31	7
11022GLASS-3	33	35	12	20832	208	62790	355274	bd	49881	3378	2	602	0	bd	223	9857	0	bd	1	65	26	239	11	66	59	53	5	138	77	47	15	53	11	0	10	2	11	2	7	1	6	1	6	4	36	30	7
11022GLASS-4	39	38	11	22446	224	63156	355274	34	48511	3589	2	617	0	bd	224	9806	0	2	69	24	239	11	66	59	53	5	145	77	45	15	56	11	0	10	2	11	2	7	1	6	1	6	4	36	32	8	
11022GLASS-5	38	39	13	19572	240	59502	355274	bd	48099	3439	2	580	0	bd	212	9655	bd	1	75	29	234	11	66	51	5	141	74	36	15	51	11	0	10	2	11	2	7	1	6	1	6	4	43	28	7		
11022GLASS-6	33	37	14	17939	490	68320	355274	93	53955	3520	2	622	bd	3	225	9440	0	bd	0	71	23	233	8	66	60	52	4	108	79	50	16	54	11	0	10	2	12	2	7	1	6	1	6	4	49	32	7
11022GLASS-7	45	43	12	23019	182	61798	355274	35	47645	3539	2	622	bd	3	225	9440	0	bd	0	71	23	233	8	66	60	52	4	108	79	50	16	54	11	0	10	2	12	2	7	1	6	1	6	4	34	31	8
11022GLASS-8	47	43	13	20349	290	69404	355274	59	49727	3709	2	667	0	bd	223	10683	0	4	2	83	28	237	13	82	175	57	5	174	82	150	17	60	13	0	12	2	14	3	8	1	8	1	7	4	40	32	7
11022GLASS-9	42	39	14	20154	233	60355	355274	38	49074	3407	2	592	0	bd	216	9823	bd	2	4	76	29	232	11	63	52	51	5	149	71	37	15	50	11	0	10	2	11	2	7	1	6	1	6	4	39	28	7
11022GLASS-10	31	32	13	17347	224	62578	355274	64	51668	3648	2	598	0	bd	216	9745	0	3	63	28	247	17	80	61	54	6	203	83	42	17	57	12	0	12	2	13	3	7	1	6	1	6	4	35	28	7	
11022GLASS-11	35	39	11	18903	371	67987	355274	35	52846	3159	2	636	1	bd	246	10518	0	3	2	63	28	247	17	80	61	54	6	203	83	42	17	57	12	0	12	2	13	3	7	1	6	1	6	4	42	30	7
11022GLASS-12	27	28	15	17069	226	55082	355274	bd	52007	3119	2	511	bd	bd	207	9316	bd	bd	2	53	32	240	11	56	33	47	5	150	64	21	13	44	9	0	9	1	10	2	6	1	5	3	49	25	6		
11022GLASS-13	33	34	11	18835	235	62173	355274	49	52841	3783	2	588	0	bd	219	9854	0	bd	1	48	26	249	14	66	160	51	5	175	77	44	16	53	11	0	10	2	12	2	7	1	6	1	6	4	35	31	7
11022GLASS-14	43	37	10	20185	194	60209	355274	38	49774	3859	2	588	0	bd	219	9854	0	bd	1	48	26	249	14	66	160	51	5	175	77	44	16	53	11	0	10	2	12	2	7	1	6	1	6	4	34	29	7
11022GLASS-15	42	39	13	21917	194	61652	355274	63	53197	3578	2	603	bd	bd	223	9788	0	2	1	79	27	237	9	66	59	51	5	119	76	49	15	54	11	0	10	2	12	2	7	1	6	1	6	4	40	30	7
11022GLASS-16	31	35	13	18166	368	68272	355274	4	47733	3729	2	636	1	bd	215	10415	1	5	2	68	29	245	16	84	65	53	6	254	80	43	17	59	12	0	12	2	14	3	9	1	8	1	7	4	38	30	7
11022GLASS-17	36	33	13	18366	339	65328	355274	47	53119	3642	2	651	1	bd	213	10237	0	4	3	51	28	252	17	78	57	51	6	224	73	33	15	51	11	0	10	2	12	2	7	1	6	1	6	4	38	28	7
11022GLASS-18	41	44	11	23402	229	65288	355274	30	46795	3988	2	632	1	bd	228	9800	0	bd	1	69	23	252	9	69	162	53	5	109	80	150	16	57	12	0	11	2	12	2	7	1	7	1	7	4	36	32	8
11022GLASS-19	41	44	12	23582	196	63130	355274	41	47440	3308	2	635	0	bd	227	9733	bd	1	71	23	248	8	71	163	53	4	101	80	151	16	56	12	0	11	2	12	3	7	1	7	1	7	4	35	32	8	
11022GLASS-20	48	44	11	22795	354	64843	355274	43	49663	4007	2	634	1	bd	238	10106	1	2	3	69	24	245	10	71	165	53	5	120	80	49	16	56	12	0	11	2	12	3	8	1	7	1	7	4	35	31	7
11022GLASS-21	43	44	11	23560	230	62675	355274	31	46677	3767	2	626	0	bd	229	9743	0	2	77	23	247	8	69	166	53	5	100	79	150	17	56	11	0	11	2	12	2	7	1	7	1	7	4	35	31	7	
11022GLASS-22	45	43	11	24094	180	61175	355274	bd	47266	3996	2	606	bd	bd	227	9364	0	bd	1	70	22	244	7	65	160	52	4	90	78	49	16	53	11	0	10	2	11	2	7	1	6	1	7	4	34	30	7
11022GLASS-23	45	43	12	24245	180	61599	355274	27	47235	3537	2	604	bd	bd	225	9315	0	bd	1	72	23	241	7	65	160	52	4	92	78	150	16	54	11	0	10	2	12	2	7	1	6	1	7	4	34	31	8
11022GLASS-24	41	44	12	24046	183	61763	355274	bd	47431	3564	2	660	1	bd	192	10429	0	bd	0	71	22	235	7	65	160	53	4	91	78	150	16	54	11	0	11	2	11	2	7	1	7	1	7	4	34	31	8
11022GLASS-25	46	44	12	24038	204	65312	355274	34	47516	3604	2	640	0	bd	220	9788	0	2	1	76	24	237	9	74	167	54	4	119	81	154	17	56	12	0	11	2	12	3	8	1	7	1	7	4	35	32	8
11022GLASS-26	46	43	12	22033	181	61440	355274	30	46913	3405	2	610	0	bd	220	9561	0	3	2	67	21	243	8	68	55	51	6	110	77	47	16	54	12	0	11	2	12	2	7	1	6	1	6	4	37	31	8
11022GLASS-27	45	45	13	23904	198	63370	355274	38	47347	3673	2	629	0	bd	226	9595	bd	bd	1	74	23	236	8	66	61	53	4	104	77	49	16	54	12	0	10	2	12	2	7	1	6	1	6	4	35	31	8
11022GLASS-28	44	38	12	19582	288	62174	355274	40	51540	3620	2	611	0	bd	199	9812	0	3	2	66	26	240	18	77	149	50	5	181	82	34	16	60	12	0	12	2	12	3	7	1	6	1	6	4	39	27	7
11022GLASS-29	42	40	13	17998	362	66443	355274	69	51912	3384	2	660	1	bd	192	10429	0	bd	3	49	28	252	14	78	153	50	5	142	73	32	15	58	10	11	2	12	3	7	1	6	1	6	4	43	26	6	
11022GLASS-30	35	40	13	22013	193	66693	355274	bd	54548	3165	2	651	1	bd	115	10290	0	3	2	67	21	243	8	68	55	51	6	110	77	47	16	54	12	0	11	2	12	2	7	1	6	1	6	4	40	29	7
11022GLASS-31	37	42	10	22979	181	60771	355274	38	46844	3405	2	610	0	bd	220	9561	0	bd	1	66	27	234	22	57	41	47	4	302	69	33	14	48	10	1	9	2	10	2	6	1	6	3	34	27	7		
11022GLASS-32	42	37	10	25311	161	66312	355274	bd	51227	4533	2	563	bd	bd	198	8850	bd	bd	1	66	27	234	22	57	41	47	4	302	69	33	14	48	10	1	9	2	10	2	6	1	6	3	34	27	7		
11022GLASS-33	40	39	11	22817	232	68308	355274	56	53084	3270	2	611	0	bd	199	9812	0	3	2	66	26	240	18	77	149	50	5	181	82	34	16	60	12	0	12	2	12	3	7	1	6	1	6	4	39	27	7
11022GLASS-34	52	33	13	18557	258	59562	355274	bd	44758	4470	2	591	1	bd	100	9441	0	4	6	71	26	246	11	72	146	50	5	142	73	32	15	58	10	11	2	11	2	7	1	6	1	6	4				

Table C3: Quartz - Trace elements (by La-ICP-MS).

Info		Position	Li ⁶	Li ⁷	B	Na	Mg	Al	Si	P	Sc	Ti	Ga	Ge
13005-g1-P1-2	with crust -MI	next to MI	18.0	17.6	0.5	bdl	0.6	102.7	466998.0	14.1	0.7	86.8	bdl	bdl
13005-g1-P1-3	with crust -MI	core	17.6	17.5	0.6	0.2	0.7	95.2	466998.0	11.2	0.8	89.0	bdl	bdl
13005-g1-P1-4	with crust -MI	core	16.3	16.5	0.5	bdl	0.5	92.8	466998.0	9.8	0.8	74.9	bdl	0.7
13005-g1-P1-5	with crust -MI	core	17.4	16.1	bdl	0.3	0.5	93.5	466998.0	11.6	0.8	72.0	bdl	0.6
13005-g1-P1-6	with crust -MI	core	17.4	17.0	0.8	0.2	0.6	98.5	466998.0	11.2	0.8	86.1	bdl	0.8
13005-g1-P1-7	with crust -MI	core	17.4	17.1	0.6	0.2	0.8	105.5	466998.0	11.3	0.8	98.1	bdl	bdl
13005-g1-P1-8	with crust -MI	core	17.7	17.7	0.6	bdl	0.9	108.5	466998.0	11.5	0.9	110.0	bdl	0.7
13005-g1-P1-9	with crust -MI	core	19.0	18.7	0.7	bdl	0.7	114.1	466998.0	11.5	0.9	129.7	bdl	0.7
13005-g1-P1-10	with crust -MI	core	19.6	19.0	0.5	bdl	1.0	115.6	466998.0	10.7	1.0	146.0	bdl	bdl
13005-g1-P1-11	with crust -MI	core	19.0	19.3	0.7	bdl	1.1	118.9	466998.0	11.7	0.9	151.1	bdl	0.6
13005-g1-P1-12	with crust -MI	core	18.8	18.7	0.5	bdl	0.8	117.0	466998.0	11.3	0.9	141.8	bdl	0.7
13005-g1-P1-13	with crust -MI	core	19.0	18.7	0.7	0.2	0.8	116.4	466998.0	10.5	0.9	137.4	bdl	bdl
13005-g1-P1-14	with crust -MI	core	18.9	18.3	0.5	bdl	0.7	115.9	466998.0	9.9	0.9	136.0	bdl	bdl
13005-g1-P1-15	with crust -MI	core	19.8	18.6	0.4	bdl	0.7	116.4	466998.0	11.3	0.9	136.5	bdl	0.8
13005-g1-P1-16	with crust -MI	core	18.5	18.1	0.5	0.2	0.6	115.1	466998.0	11.0	0.9	139.1	0.0	0.7
13005-g1-P1-17	with crust -MI	core	18.4	18.3	0.6	bdl	0.9	115.4	466998.0	10.2	0.9	140.7	bdl	0.6
13005-g1-P1-18	with crust -MI	core	18.4	18.1	0.5	bdl	1.0	114.0	466998.0	11.2	0.9	136.2	bdl	bdl
13005-g1-P1-19	with crust -MI	core	18.1	18.2	0.8	bdl	0.8	114.3	466998.0	12.5	0.9	136.5	0.0	bdl
13005-g1-P1-20	with crust -MI	core	18.6	18.5	0.6	bdl	0.8	114.0	466998.0	11.7	0.9	131.9	bdl	0.7
13005-g1-P1-21	with crust -MI	core	18.5	18.6	0.6	0.3	0.9	116.0	466998.0	10.9	0.9	132.9	bdl	0.8
13005-g1-P1-22	with crust -MI	core	19.5	19.1	0.7	0.3	0.8	116.4	466998.0	10.8	0.9	133.6	bdl	0.8
13005-g1-P1-23	with crust -MI	core	18.9	18.5	0.6	bdl	0.8	118.3	466998.0	12.4	0.9	136.0	bdl	bdl
13005-g1-P1-24	with crust -MI	core	16.0	16.8	bdl	bdl	0.6	118.1	466998.0	14.2	0.7	132.0	bdl	bdl
13005-g1-P1-25	with crust -MI	core	17.3	17.0	bdl	0.2	1.0	119.4	466998.0	12.7	0.8	138.6	bdl	bdl
13005-g1-P1-26	with crust -MI	core	18.4	17.8	bdl	bdl	0.7	119.6	466998.0	13.6	0.8	140.6	bdl	0.8
13005-g1-P1-27	with crust -MI	core	22.6	20.8	0.7	0.2	1.0	114.6	466998.0	12.1	1.0	147.9	bdl	bdl
13005-g1-P1-28	with crust -MI	core	21.7	21.1	bdl	0.2	1.0	114.9	466998.0	10.5	0.9	139.5	0.0	bdl
13005-g1-P1-29	with crust -MI	core	21.4	21.2	0.6	0.2	0.8	116.8	466998.0	11.2	0.8	135.9	bdl	bdl
13005-g1-P1-30	with crust -MI	core	21.7	21.8	0.6	0.2	0.6	111.3	466998.0	10.7	0.9	110.3	bdl	0.5
13005-g1-P1-31	with crust -MI	core	20.9	21.1	bdl	0.2	0.8	108.1	466998.0	11.9	0.9	104.6	0.0	bdl
13005-g1-P1-32	with crust -MI	core	21.6	21.2	0.7	0.2	0.8	109.3	466998.0	11.6	0.9	98.8	bdl	bdl
13005-g1-P1-33	with crust -MI	core	22.7	21.8	0.9	0.3	0.8	109.5	466998.0	11.9	0.8	93.8	bdl	0.8
13005-g1-P1-34	with crust -MI	core	22.4	22.8	0.5	0.3	0.8	106.4	466998.0	11.4	0.9	93.5	bdl	bdl
13005-g1-P1-35	with crust -MI	rim	22.5	23.2	0.6		0.8	107.9	466998.0	10.5	0.9	89.7	bdl	0.7
13005-g1-P2-1	with crust -MI	core	17.6	17.7	1.0	0.3	0.8	116.5	466998.0	12.3	0.8	135.1	0.0	0.7
13005-g1-P2-2	with crust -MI	core	20.3	18.8	0.9	0.2	0.9	115.5	466998.0	11.3	0.8	137.1	bdl	bdl
13005-g1-P2-3	with crust -MI	core	20.0	19.5	0.9	0.3	0.8	115.5	466998.0	12.1	0.9	136.7	bdl	bdl
13005-g1-P2-4	with crust -MI	core	20.6	20.1	0.6	0.2	0.7	115.1	466998.0	11.4	0.9	136.9	0.0	bdl
13005-g1-P2-5	with crust -MI	core	20.3	19.8	0.6	0.4	0.8	116.8	466998.0	11.8	0.8	136.0	bdl	0.9
13005-g1-P2-6	with crust -MI	core	19.8	19.7	0.8	bdl	0.8	108.4	466998.0	11.6	0.8	118.8	bdl	0.6
13005-g1-P2-7	with crust -MI	core	20.1	19.7	0.9	0.2	0.6	102.2	466998.0	11.8	0.8	103.1	0.0	0.6
13005-g1-P2-8	with crust -MI	core	20.5	20.1	0.8	bdl	0.8	104.1	466998.0	11.7	0.8	101.1	bdl	0.7
13005-g1-P2-9	with crust -MI	core	21.3	21.0	0.9	bdl	0.6	105.2	466998.0	10.9	0.8	98.9	bdl	bdl
13005-g1-P2-10	with crust -MI	core	20.8	20.4	1.0	bdl	0.4	100.4	466998.0	11.2	0.8	91.8	bdl	bdl
13005-g1-P2-11	with crust -MI	core	21.1	20.5	1.1	0.2	0.8	96.6	466998.0	12.2	0.9	85.3	bdl	0.5
13005-g1-P2-12	with crust -MI	core	22.0	22.3	0.7	0.1	0.8	102.0	466998.0	11.0	0.9	87.5	bdl	0.7
13005-g1-P2-13	with crust -MI	core	22.0	21.6	1.0	0.2	0.6	97.1	466998.0	10.8	0.8	84.4	bdl	0.6
13005-g1-P2-14	with crust -MI	core	23.5	22.6	0.8	0.2	0.6	100.7	466998.0	12.0	0.9	81.2	bdl	0.5
13005-g1-P2-15	with crust -MI	rim	23.2	22.3	0.8	0.3	0.5	96.0	466998.0	10.5	0.9	81.4	0.0	0.6
13005-g10-P1-1	with crust -MI	next to MI	19.3	18.7	1.5	0.3	0.8	104.7	466998.0	13.8	0.8	94.4	bdl	bdl
13005-g10-P1-2	with crust -MI	Core	19.5	19.2	1.6	bdl	0.7	105.2	466998.0	13.6	0.8	96.1	bdl	bdl
13005-g10-P1-3	with crust -MI	Core	20.0	19.1	1.5	0.3	0.6	102.8	466998.0	13.6	0.9	99.9	bdl	0.7
13005-g10-P1-4	with crust -MI	Core	19.5	18.6	1.5	bdl	0.8	101.3	466998.0	12.4	0.9	99.1	bdl	bdl
13005-g10-P1-5	with crust -MI	Core	19.0	17.9	1.9	0.8	0.6	99.5	466998.0	11.7	0.9	98.1	bdl	0.6
13005-g10-P1-6	with crust -MI	Core	18.7	18.0	1.6	0.4	0.6	100.7	466998.0	14.0	0.9	98.5	bdl	0.8
13005-g10-P1-7	with crust -MI	Core	18.8	18.5	1.4	0.3	0.6	102.3	466998.0	13.2	1.0	99.6	0.0	bdl
13005-g10-P1-8	with crust -MI	Core	19.4	18.9	1.5	0.2	0.8	103.3	466998.0	12.7	1.0	101.0	bdl	0.5
13005-g10-P1-9	with crust -MI	Core	18.7	18.5	1.8	bdl	0.7	105.1	466998.0	13.3	0.9	100.4	bdl	0.5
13005-g10-P1-10	with crust -MI	Core	18.4	17.8	1.5	bdl	0.8	103.6	466998.0	13.2	0.9	96.5	bdl	bdl
13005-g10-P1-11	with crust -MI	Core	18.2	18.0	1.8	bdl	0.8	101.6	466998.0	11.9	0.9	98.4	bdl	0.5
13005-g10-P1-12	with crust -MI	Core	18.2	17.7	1.6	0.8	0.8	101.6	466998.0	13.9	0.9	98.5	bdl	bdl
13005-g10-P1-13	with crust -MI	Core	19.4	18.3	1.4	0.2	0.7	100.1	466998.0	12.3	1.0	97.6	bdl	0.6
13005-g10-P1-14	with crust -MI	Core	19.2	18.5	2.1	bdl	0.7	103.1	466998.0	12.2	1.0	97.5	0.0	bdl
13005-g10-P1-15	with crust -MI	Core	19.5	19.0	1.3	0.2	0.8	98.5	466998.0	11.9	1.1	98.8	bdl	0.7
13005-g10-P1-16	with crust -MI	Core	19.1	18.3	1.4	bdl	0.6	96.4	466998.0	13.3	1.0	92.1	0.0	0.6
13005-g10-P1-17	with crust -MI	Core	20.1	18.8	1.8	0.2	0.7	97.0	466998.0	13.3	1.0	88.1	0.0	0.5
13005-g10-P1-18	with crust -MI	Core	20.5	19.4	1.5	0.2	0.6	96.5	466998.0	13.3	1.0	88.5	bdl	0.5
13005-g10-P1-19	with crust -MI	Core	20.5	19.2	1.5	bdl	0.7	97.2	466998.0	13.6	0.9	86.6	bdl	bdl
13005-g10-P1-20	with crust -MI	Core	22.5	20.7	1.3	0.2	0.7	94.6	466998.0	12.1	1.0	86.8	bdl	bdl
13005-g10-P1-21	with crust -MI	Core	20.7	20.7	1.7	0.2	0.7	94.9	466998.0	12.7	1.0	78.5	0.0	bdl
13005-g10-P1-22	with crust -MI	Core	21.5	21.2	1.6	0.2	0.6	95.4	466998.0	12.1	0.9	78.5	0.0	0.7
13005-g10-P1-23	with crust -MI	rim	23.0	22.0	1.6	bdl	0.5	96.2	466998.0	12.1	1.0	78.9	bdl	0.6
13005-g10-P1-24	with crust -MI	rim	25.7	23.5	1.0	bdl	1.2	147.2	466998.0	9.0	1.2	82.5	0.1	bdl
13005-g10-P2-1	with crust -MI	next to MI	24.1	22.6		bdl		97.5	466998.0	8.8	1.4	92.6	bdl	bdl
13005-g10-P2-2	with crust -MI	Core	22.1	21.2	1.5	bdl	0.7	97.6	466998.0	13.5	1.0	93.1	0.0	bdl
13005-g10-P2-3	with crust -MI	Core	21.7	20.9	1.2	8.9	0.7	95.2	466998.0	12.3	1.0	84.5	bdl	0.6
13005-g7-P1-1	with crust -MI	next to MI	13.3	12.8		bdl		95.7	466998.0	19.2	0.8	85.9	bdl	bdl
13005-g7-P1-2	with crust -MI	Core	16.3	15.5	1.4	1.6	0.7	97.8	466998.0	15.5	0.7	59.6	bdl	bdl
13005-g7-P1-3	with crust -MI	Core	14.9	14.9	1.3	0.8	0.5	97.4	466998.0	14.9	0.8	61.4	bdl	0.8
13005-g7-P1-4	with crust -MI	Core	16.0	15.2	1.5	0.7	0.6	103.1	466998.0	16.1	0.7	60.2	bdl	0.8
13005-g7-P1-5	with crust -MI	Core	15.9	15.2	1.6	5.2	0.7	104.2	466998.0	14.2	0.8	82.0	0.0	bdl
13005-g7-P1-6	with crust -MI	Core	15.9	15.9	1.7	3.4	0.7	107.7	466998.0	12.8	0.9	93.2	bdl	0.6
13005-g7-P1-7	with crust -MI	Core	17.2	17.1	1.4	bdl	0.9	113.7	466998.0	14.1	0.9	126.5	0.0	0.6
13005-g7-P1-8	with crust -MI	Core	18.4	17.6	1.1	bdl	1.0	116.3	466998.0	12.7	1.0	118.1	0.0	bdl
13005-g7-P1-9	with crust -MI	Core	18.8	17.5	1.8	bdl	0.9	117.9	466998.0	13.7	1.0	118.2	0.0	bdl

Appendix C

Table C3: continued

Info		Position	Li ⁶	Li ⁷	B	Na	Mg	Al	Si	P	Sc	Ti	Ga	Ge
13005-g7-P1-10	with cryst -MI	Core	18.3	18.5	1.5	5.3	0.8	114.8	466998.0	13.2	1.0	128.6	0.0	bdl
13005-g7-P1-11	with cryst -MI	Core	18.2	17.1	1.6	3.5	0.8	113.3	466998.0	13.1	0.9	128.3	bdl	bdl
13005-g7-P1-12	with cryst -MI	Core	18.1	17.7	1.7	2.5	0.8	111.8	466998.0	12.5	0.9	122.0	0.0	0.5
13005-g7-P1-13	with cryst -MI	Core	18.7	17.4	1.5	2.4	0.6	108.5	466998.0	12.6	1.0	112.9	0.0	0.5
13005-g7-P1-14	with cryst -MI	Core	18.2	18.0	1.2	1.2	0.7	107.2	466998.0	13.8	1.0	121.4	bdl	bdl
13005-g16-P1-1	with cryst -MI	next to MI	17.7	17.7	1.9	0.5	0.9	109.0	466998.0	18.3	0.8	105.8	0.0	bdl
13005-g16-P1-2	with cryst -MI	Core	21.7	19.5	1.3	bdl	0.9	106.2	466998.0	16.7	0.7	106.3	0.0	0.7
13005-g16-P1-3	with cryst -MI	Core	20.5	20.7	1.3	bdl	0.7	105.1	466998.0	16.5	0.9	106.0	bdl	0.6
13005-g16-P1-4	with cryst -MI	Core	22.1	20.9	1.2	1.1	0.7	101.6	466998.0	16.2	1.0	106.2	0.0	bdl
13005-g16-P1-5	with cryst -MI	Core	22.7	21.8	1.2	0.3	0.8	106.3	466998.0	15.3	1.0	113.2	0.0	0.7
13005-g16-P1-6	with cryst -MI	Core	23.3	22.6	1.2	0.5	0.7	105.7	466998.0	16.2	1.0	110.1	bdl	bdl
13005-g16-P1-7	with cryst -MI	Core	21.9	22.1	1.0	bdl	0.9	106.6	466998.0	16.0	0.9	112.8	bdl	0.8
13005-g16-P1-8	with cryst -MI	Core	22.2	21.8	1.1	0.2	0.7	108.1	466998.0	17.8	0.9	115.3	bdl	0.6
13005-g16-P1-9	with cryst -MI	Core	22.1	22.3	1.1	0.2	0.8	107.5	466998.0	16.6	0.9	110.3	bdl	0.5
13005-g16-P1-10	with cryst -MI	Core	23.0	22.1	1.3	bdl	0.8	106.2	466998.0	15.7	1.0	105.7	0.0	bdl
13005-g16-P1-11	with cryst -MI	Core	23.5	23.0	1.0	0.4	0.8	108.6	466998.0	16.3	1.0	106.4	bdl	0.8
13005-g16-P1-12	with cryst -MI	Core	23.9	23.9	1.0	0.2	0.6	106.7	466998.0	16.5	1.0	107.7	bdl	bdl
13005-g16-P1-13	with cryst -MI	Core	22.4	22.2	0.8	0.3	0.7	105.6	466998.0	16.4	0.9	101.3	bdl	bdl
13005-g16-P1-14	with cryst -MI	Core	23.0	22.0	0.9	bdl	0.8	106.0	466998.0	15.7	0.8	100.1	0.0	0.5
13005-g16-P1-15	with cryst -MI	rim	23.0	23.1	0.8	bdl	0.7	104.4	466998.0	16.4	0.9	97.2	bdl	bdl
13005-g16-P1-16	with cryst -MI	rim	24.7	23.7	0.9	0.1	0.7	111.7	466998.0	15.5	0.9	94.9	bdl	0.7
13005-g16-P2-1	with cryst -MI	next to MI	18.1	17.9	0.9	bdl	0.9	105.0	466998.0	14.6	0.8	109.5	0.0	0.7
13005-g16-P2-2	with cryst -MI	Core	20.4	19.8	1.0	bdl	0.8	108.5	466998.0	14.5	0.9	107.1	bdl	1.0
13005-g16-P2-3	with cryst -MI	Core	21.1	21.3	0.8	0.4	0.9	102.9	466998.0	13.1	1.0	103.1	0.0	0.6
13005-g16-P2-4	with cryst -MI	Core	21.2	21.1	0.9	0.2	0.7	101.0	466998.0	14.5	1.0	100.0	bdl	0.7
13005-g16-P2-5	with cryst -MI	Core	22.1	20.9	0.8	bdl	0.6	104.2	466998.0	14.1	0.9	92.6	0.0	bdl
13005-g16-P2-6	with cryst -MI	Core	22.5	22.0	1.1	0.4	0.6	105.2	466998.0	13.8	1.0	101.6	bdl	bdl
13005-g16-P2-7	with cryst -MI	Core	22.6	21.0	1.0	0.2	0.7	104.5	466998.0	13.7	1.0	96.6	0.0	0.6
13005-g16-P2-8	with cryst -MI	Core	23.1	21.9	1.1	0.3	0.6	99.8	466998.0	13.4	1.0	92.1	bdl	0.6
13005-g16-P2-9	with cryst -MI	Core	21.8	20.7	1.0	bdl	0.6	97.7	466998.0	13.9	0.9	86.5	0.0	0.5
13005-g16-P2-10	with cryst -MI	Core	24.1	22.1	1.0	bdl	0.7	96.8	466998.0	13.9	1.0	88.6	bdl	0.8
13005-g16-P2-11	with cryst -MI	Core	21.6	21.7	0.9	0.2	0.8	96.8	466998.0	12.9	0.9	86.7	0.0	0.8
13005-g16-P2-12	with cryst -MI	Core	22.6	21.3	1.0	0.3	0.5	93.3	466998.0	13.9	0.9	83.2	bdl	0.7
13005-g16-P2-13	with cryst -MI	rim	22.6	23.0	0.7	0.2	0.8	100.6	466998.0	14.0	0.9	92.3	0.0	0.6
11022-g1-P1-1	with glassy -MI	next to MI	13.1	12.7	1.2	0.7	0.9	106.1	466998.0	16.5	0.7	94.5	bdl	bdl
11022-g1-P1-2	with glassy -MI	core	10.6	9.4	1.1	bdl	0.6	104.6	466998.0	15.1	0.7	93.4	bdl	0.7
11022-g1-P1-3	with glassy -MI	core	10.2	9.5	0.9	bdl	0.8	104.3	466998.0	15.3	0.8	92.2	bdl	0.9
11022-g1-P1-4	with glassy -MI	core	10.3	9.9	1.1	bdl	0.8	107.1	466998.0	13.1	0.8	110.8	bdl	0.6
11022-g1-P1-5	with glassy -MI	core	10.7	9.9	1.0	bdl	0.8	109.7	466998.0	14.4	0.8	111.3	bdl	0.7
11022-g1-P1-6	with glassy -MI	core												
11022-g1-P1-7	with glassy -MI	core												
11022-g1-P1-8	with glassy -MI	core												
11022-g1-P1-9	with glassy -MI	core												
11022-g1-P1-10	with glassy -MI	core												
11022-g1-P1-11	with glassy -MI	core	11.0	9.6	1.0	bdl	0.9	114.0	466998.0	14.8	0.8	84.6	bdl	0.7
11022-g1-P1-12	with glassy -MI	core	10.0	9.8	0.9	bdl	0.8	106.4	466998.0	14.2	0.8	83.2	bdl	0.6
11022-g1-P1-13	with glassy -MI	core	10.5	10.0	0.9	bdl	0.9	105.4	466998.0	14.0	0.9	84.0	0.0	1.0
11022-g1-P1-14	with glassy -MI	core	11.1	9.9	0.6	bdl	0.7	104.0	466998.0	13.6	0.9	83.4	0.0	0.6
11022-g1-P1-15	with glassy -MI	core	10.1	10.0	0.8	1.5	0.7	103.1	466998.0	13.1	0.8	77.6	0.0	0.8
11022-g1-P1-16	with glassy -MI	core	10.5	9.7	0.9	0.7	0.6	101.1	466998.0	13.0	0.9	80.3	bdl	0.6
11022-g1-P1-17	with glassy -MI	core	10.3	9.5	0.8	0.2	0.6	103.8	466998.0	13.8	0.8	78.1	bdl	0.7
11022-g1-P1-18	with glassy -MI	core	9.7	9.5	0.8	bdl	0.6	103.0	466998.0	13.3	0.8	76.0	bdl	0.5
11022-g1-P1-19	with glassy -MI	core	10.1	10.1	0.8	0.3	0.7	103.9	466998.0	13.6	0.9	78.7	bdl	bdl
11022-g1-P1-20	with glassy -MI	core	10.5	10.0	0.7	0.2	0.6	105.7	466998.0	13.7	0.9	91.0	0.0	0.6
11022-g1-P1-21	with glassy -MI	core	9.7	9.9	0.7	0.2	0.7	101.0	466998.0	12.6	0.9	93.8	bdl	0.6
11022-g1-P1-22	with glassy -MI	core												
11022-g1-P1-23	with glassy -MI	core	10.7	9.8	0.7	0.2	0.7	103.6	466998.0	13.4	0.9	93.8	bdl	bdl
11022-g1-P1-24	with glassy -MI	core	10.6	9.6	0.7	0.3	0.7	99.2	466998.0	13.4	0.8	92.4	bdl	0.7
11022-g1-P1-25	with glassy -MI	core	10.5	10.7	0.6	0.2	0.5	98.9	466998.0	12.5	1.0	91.3	bdl	0.5
11022-g1-P1-26	with glassy -MI	core	10.3	9.5	0.8	bdl	0.5	96.9	466998.0	12.2	0.9	86.4	bdl	0.5
11022-g1-P1-27	with glassy -MI	rim	10.2	10.0	0.8	0.2	0.6	90.7	466998.0	12.7	0.9	82.2	0.0	0.7
11022-g1-P2-1	with glassy -MI	core	10.4	9.9	1.3	0.4	0.7	103.0	466998.0	10.8	1.0	83.3	bdl	0.7
11022-g1-P2-2	with glassy -MI	core	9.8	9.6	1.3	0.4	0.6	102.7	466998.0	11.7	1.0	83.2	bdl	bdl
11022-g1-P2-3	with glassy -MI	core	9.8	9.5	0.9	0.6	0.7	102.5	466998.0	10.8	0.9	84.6	bdl	0.6
11022-g1-P2-4	with glassy -MI	core	9.2	9.6	1.2	0.3	0.7	101.0	466998.0	9.7	1.0	85.5	bdl	0.6
11022-g1-P2-5	with glassy -MI	core	9.7	9.8	0.9	0.7	0.7	102.8	466998.0	10.1	1.0	89.1	0.0	0.7
11022-g1-P2-6	with glassy -MI	core	10.1	9.6	0.9	0.5	0.7	106.8	466998.0	10.5	1.0	92.9	bdl	bdl
11022-g1-P2-7	with glassy -MI	core	10.6	9.7	0.6	0.6	0.9	105.6	466998.0	11.9	1.0	97.4	0.0	0.8
11022-g1-P2-8	with glassy -MI	core	10.2	9.1	0.6	0.7	0.5	104.7	466998.0	11.1	0.9	93.8	bdl	0.8
11022-g1-P2-9	with glassy -MI	core	9.9	9.7	0.7	1.1	0.7	101.1	466998.0	10.8	1.0	98.3	0.0	bdl
11022-g1-P2-10	with glassy -MI	core	9.4	9.3	0.9	0.7	0.7	99.5	466998.0	10.4	0.9	94.7	bdl	0.7
11022-g1-P2-11	with glassy -MI	core	9.8	9.5	0.6	0.6	0.5	98.8	466998.0	10.6	1.0	91.6	bdl	0.6
11022-g1-P2-12	with glassy -MI	core	10.0	9.2	0.4	0.4	0.5	95.3	466998.0	10.2	1.0	90.3	0.0	bdl
11022-g1-P2-13	with glassy -MI	core	9.9	9.7	bdl	0.2	0.6	101.0	466998.0	10.6	0.9	95.1	0.0	0.7
11022-g1-P2-14	with glassy -MI	core	11.0	10.0	0.5	0.2	0.6	100.1	466998.0	9.4	1.0	96.8	bdl	0.5
11022-g1-P2-15	with glassy -MI	core	11.1	11.8	0.6	0.3	0.6	99.5	466998.0	10.8	0.9	96.4	bdl	0.6
11022-g1-P2-16	with glassy -MI	core	11.6	11.3	0.5	bdl	0.6	96.2	466998.0	11.8	0.9	89.6	bdl	0.7
11022-g1-P2-17	with glassy -MI	core	12.6	11.9	bdl	bdl	0.7	92.8	466998.0	11.6	0.9	87.1	0.0	0.8
11022-g1-P2-18	with glassy -MI	rim	15.4	14.5	0.5	0.2	0.7	97.6	466998.0	10.8	0.9	81.8	bdl	1.0
11022-g1-P3-1	with glassy -MI	core	8.9	9.0	0.8	bdl	0.6	105.4	466998.0	11.6	0.8	84.8	bdl	0.8
11022-g1-P3-2	with glassy -MI	core	10.0	9.4	1.1	0.8	0.6	103.5	466998.0	10.8	0.9	85.3	bdl	bdl
11022-g1-P3-3	with glassy -MI	core	10.7	10.0	1.1	bdl	0.8	106.8	466998.0	10.6	1.0	94.5	bdl	bdl
11022-g1-P3-4	with glassy -MI	core	10.6	10.7	1.3	bdl	0.7	110.5	466998.0	11.0	1.0	102.9	0.0	0.8
11022-g1-P3-5	with glassy -MI	core	10.1	9.6	1.0	0.9	0.7	109.3	466998.0	11.6	0.8	101.7	0.0	bdl

Table C3: continued

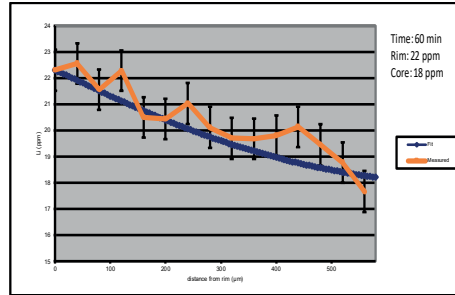
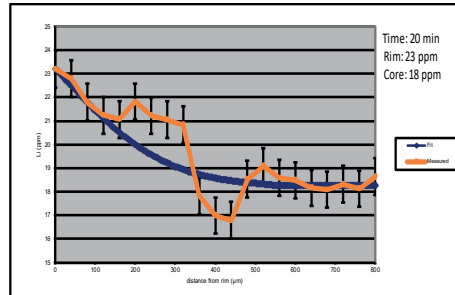
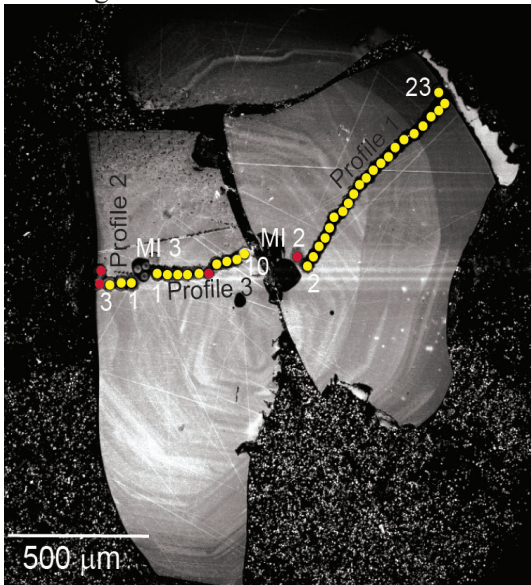
Info		Position	Li ⁶	Li ⁷	B	Na	Mg	Al	Si	P	Sc	Ti	Ga	Ge
11022-g1-P3-6	with glassy -MI	core	9.9	9.1	0.6	0.4	0.9	109.2	466998.0	11.5	0.8	112.0	0.0	0.9
11022-g1-P3-7	with glassy -MI	core	8.7	8.6	1.1	0.9	0.6	100.6	466998.0	11.9	0.9	91.5	bdl	0.9
11022-g1-P3-8	with glassy -MI	core	8.7	8.4	0.8	0.2	0.5	99.4	466998.0	10.9	0.8	90.5	bdl	0.6
11022-g1-P3-9	with glassy -MI	core	9.0	8.6	bdl	0.4	0.6	98.8	466998.0	11.5	0.8	84.8	bdl	bdl
11022-g1-P3-10	with glassy -MI	core	9.0	8.5	0.6	0.2	0.4	93.4	466998.0	11.4	0.8	86.3	bdl	bdl
11022-g1-P3-11	with glassy -MI	core	9.1	8.5	0.7	0.4	0.5	93.5	466998.0	11.8	0.9	81.7	bdl	1.0
11022-g1-P3-12	with glassy -MI	core	8.7	8.7	0.9	bdl	0.6	96.4	466998.0	12.4	0.9	87.2	bdl	bdl
11022-g1-P3-13	with glassy -MI	rim	9.3	9.1	0.6	bdl	0.4	92.0	466998.0	11.3	0.8	75.7	bdl	1.0
11022-g8-P1-1	with glassy -MI	next to MI	9.3	9.2	0.7	1.4	0.5	98.4	466998.0	12.9	0.8	75.6	bdl	0.6
11022-g8-P1-2	with glassy -MI	core	10.0	9.8	0.4	0.2	0.7	100.0	466998.0	13.7	0.9	75.8	bdl	0.7
11022-g8-P1-3	with glassy -MI	core	10.6	10.2	0.6	0.2	0.7	96.8	466998.0	13.0	0.9	71.6	bdl	bdl
11022-g8-P1-4	with glassy -MI	rim	12.3	11.7	0.6	bdl	0.7	99.6	466998.0	12.6	1.0	73.7	bdl	0.7
11022-g8-P1-5	with glassy -MI	rim	13.7	13.7	0.6	bdl	0.7	102.7	466998.0	12.6	1.1	78.8	bdl	0.6
11022-g8-P2-1	with glassy -MI	rim	12.4	12.4	0.6	1.7	0.5	99.8	466998.0	14.0	0.8	72.3	bdl	0.9
11022-g8-P2-2	with glassy -MI	core	10.1	10.1	0.5	0.8	0.5	93.5	466998.0	13.1	0.9	71.3	bdl	bdl
11022-g8-P2-3	with glassy -MI	core	9.2	9.0	0.5	0.5	0.7	93.6	466998.0	12.8	0.9	70.0	0.0	0.6
11022-g8-P2-4	with glassy -MI	core	8.5	8.5	0.7	0.3	0.6	93.5	466998.0	13.1	0.9	75.1	0.0	bdl
11022-g8-P2-5	with glassy -MI	core	9.4	9.4	0.5	0.3	0.7	95.3	466998.0	11.7	1.0	76.2	bdl	bdl
11022-g8-P2-6	with glassy -MI	core	9.0	9.0	0.4	0.3	1.0	94.5	466998.0	12.2	0.9	79.4	bdl	bdl
11022-g8-P2-7	with glassy -MI	core	8.7	8.6	0.7	bdl	0.7	99.1	466998.0	12.0	0.9	79.5	bdl	1.0
11022-g8-P2-8	with glassy -MI	core	9.8	9.1	0.6	0.2	0.8	98.5	466998.0	12.3	1.0	83.7	bdl	0.9
11022-g8-P2-9	with glassy -MI	core	9.1	8.8	0.7	bdl	0.8	95.7	466998.0	12.5	0.9	83.8	bdl	0.6
11022-g8-P2-10	with glassy -MI	core	10.1	9.9	0.5	0.2	0.7	101.9	466998.0	12.9	1.0	100.8	0.0	0.6
11022-g8-P2-11	with glassy -MI	core	10.8	10.3	0.4	0.2	0.7	110.2	466998.0	11.5	1.0	119.8	bdl	bdl
11022-g8-P2-12	with glassy -MI	core	11.1	11.0	0.5	0.3	0.7	113.0	466998.0	12.5	1.0	122.6	bdl	0.6
11022-g8-P2-13	with glassy -MI	core	11.3	11.1	0.5	0.3	1.0	113.2	466998.0	11.8	1.0	126.0	0.0	0.6
11022-g8-P2-14	with glassy -MI	core	11.2	11.4	0.5	0.6	0.8	109.6	466998.0	10.7	1.1	123.4	bdl	bdl
11022-g8-P2-15	with glassy -MI	core	11.2	11.3	0.3	0.3	0.8	109.6	466998.0	11.9	1.1	125.4	bdl	bdl
11022-g8-P2-16	with glassy -MI	core	11.4	11.0	0.5	0.2	1.0	111.3	466998.0	11.9	1.1	124.6	0.0	0.6
11022-g8-P2-17	with glassy -MI	core	10.5	10.1	0.5	bdl	0.8	108.7	466998.0	11.0	1.0	111.7	0.0	bdl
11022-g8-P2-18	with glassy -MI	core	10.9	10.3	0.6	bdl	0.9	107.0	466998.0	11.6	1.0	102.5	bdl	0.6
11022-g10-P1-2	with glassy -MI	next to MI	9.7	9.2	0.9	0.3	0.8	104.4	466998.0	13.1	0.8	104.4	bdl	0.5
11022-g10-P1-3	with glassy -MI	core	10.1	9.4	1.2	0.3	0.6	104.0	466998.0	14.1	0.7	98.7	bdl	0.7
11022-g10-P1-4	with glassy -MI	core	9.9	9.5	0.9	0.3	0.7	102.9	466998.0	12.8	0.8	99.4	bdl	0.8
11022-g10-P1-5	with glassy -MI	core	10.1	10.0	0.7	bdl	0.7	104.9	466998.0	12.5	0.8	99.3	bdl	bdl
11022-g10-P1-6	with glassy -MI	core	10.8	9.8	0.6	0.4	0.9	104.0	466998.0	11.8	0.9	104.1	0.0	bdl
11022-g10-P1-7	with glassy -MI	core	10.3	9.8	1.1	0.2	0.8	104.1	466998.0	12.4	0.9	100.4	0.0	0.8
11022-g10-P1-8	with glassy -MI	core	10.0	9.4	0.7	bdl	0.7	101.6	466998.0	12.4	0.8	95.1	bdl	bdl
11022-g10-P1-9	with glassy -MI	core	9.6	9.7	0.9	bdl	0.7	106.1	466998.0	13.3	0.8	102.4	0.0	0.8
11022-g10-P1-10	with glassy -MI	core	10.6	9.7	0.7	0.2	0.8	105.6	466998.0	14.5	0.9	106.3	0.0	bdl
11022-g10-P1-11	with glassy -MI	core	10.6	9.9	1.6	bdl	0.6	105.0	466998.0	13.0	1.0	96.6	bdl	bdl
11022-g10-P1-12	with glassy -MI	core	9.7	9.7	0.9	bdl	0.6	106.1	466998.0	12.7	0.8	90.9	bdl	0.8
11022-g10-P1-13	with glassy -MI	core	9.9	9.5	bdl	bdl	0.4	109.7	466998.0	14.6	0.8	86.8	0.0	0.7
11022-g10-P1-14	with glassy -MI	core	10.3	9.8	1.3	0.2	0.9	104.6	466998.0	13.1	0.9	84.2	bdl	0.7
11022-g10-P1-15	with glassy -MI	core	10.6	9.7	1.2	0.2	0.7	100.1	466998.0	12.5	0.9	82.8	bdl	bdl
11022-g10-P1-16	with glassy -MI	core	10.8	10.2	1.2	0.5	0.7	101.8	466998.0	12.4	1.0	82.8	bdl	bdl
11022-g10-P1-17	with glassy -MI	core	11.0	9.8	0.9	0.2	0.5	97.0	466998.0	12.4	0.9	79.7	bdl	0.7
11022-g10-P1-18	with glassy -MI	core	10.6	10.1	0.9	bdl	0.5	98.7	466998.0	14.8	0.8	76.9	bdl	0.7
11022-g10-P1-19	with glassy -MI	core	10.1	9.5	0.8	bdl	0.7	97.8	466998.0	12.3	0.7	64.4	bdl	bdl
11022-g10-P1-20	with glassy -MI	core	13.2	11.6	1.9	bdl	0.7	94.8	466998.0	12.4	1.0	67.8	bdl	0.5
11022-g10-P1-21	with glassy -MI	core	12.0	11.3	0.9	bdl	0.5	97.5	466998.0	12.4	0.9	64.6	bdl	0.7
11022-g10-P1-22	with glassy -MI	rim	14.5	13.6	1.2	0.3	0.6	98.5	466998.0	13.8	0.8	67.2	bdl	bdl
11022-g10-P1-23	with glassy -MI	rim	14.0	13.4	1.6	0.4	0.8	102.7	466998.0	13.3	0.8	67.5	bdl	bdl
11022-g10-P2-1	with glassy -MI	next to MI	12.3	12.2	1.0	0.2	0.8	107.3	466998.0	14.3	0.8	99.3	bdl	bdl
11022-g10-P2-2	with glassy -MI	core	11.5	11.0	1.1	bdl	0.7	104.7	466998.0	14.1	0.8	89.7	0.0	0.7
11022-g10-P2-3	with glassy -MI	next to MI	13.0	12.9	1.0	0.3	0.7	102.6	466998.0	13.4	0.9	91.4	0.0	bdl
11022-g10-P3-1	with glassy -MI	next to MI	10.6	10.0	0.7	bdl	0.9	105.3	466998.0	14.4	0.9	93.3	0.0	bdl
11022-g10-P3-2	with glassy -MI	core	10.6	10.2	0.8	bdl	0.7	98.3	466998.0	11.8	1.0	93.3	0.0	0.7
11022-g10-P3-3	with glassy -MI	core	10.6	10.2	0.7	bdl	0.6	104.1	466998.0	12.4	1.0	97.1	bdl	bdl
11022-g10-P3-4	with glassy -MI	core	10.4	9.9	0.7	bdl	0.7	101.6	466998.0	11.9	1.0	100.6	0.0	bdl
11022-g10-P3-5	with glassy -MI	core	11.8	10.9	0.7	bdl	0.9	106.0	466998.0	10.7	1.2	104.5	0.0	0.5
11022-g10-P3-6	with glassy -MI													
11022-g10-P3-7	with glassy -MI	core	10.2	9.8	0.9	bdl	0.7	104.5	466998.0	12.0	1.0	95.9	0.0	0.5
11022-g10-P3-8	with glassy -MI	core	10.4	10.3	0.8	bdl	0.9	106.4	466998.0	12.1	1.0	105.0	bdl	0.5
11022-g10-P3-9	with glassy -MI	core	15.3	13.1	0.8	bdl	0.8	102.8	466998.0	12.6	1.0	104.4	bdl	bdl
11022-g10-P3-10	with glassy -MI	next to MI	15.1	13.6	0.7	bdl	1.2	116.7	466998.0	12.8	1.0	100.9	0.0	0.6
11022-g11-P1-1	with glassy -MI	next to MI	14.9	14.2	0.9	bdl	0.4	98.1	466998.0	15.3	0.7	62.5	bdl	0.6
11022-g11-P1-2	with glassy -MI	core	14.8	14.5	1.2	0.9	0.7	99.3	466998.0	15.0	0.8	97.4	bdl	0.7
11022-g11-P1-3	with glassy -MI	core	14.8	14.3	0.9	bdl	0.8	99.1	466998.0	13.7	0.8	91.3	bdl	0.5
11022-g11-P1-4	with glassy -MI	core	14.8	14.8	1.3	0.2	0.7	96.2	466998.0	14.2	0.8	86.2	bdl	0.7
11022-g11-P1-5	with glassy -MI	core	15.1	13.7	1.2	bdl	0.6	96.2	466998.0	13.3	0.9	94.2	0.0	bdl
11022-g11-P1-6	with glassy -MI	core	14.5	14.0	1.1	0.3	0.6	98.8	466998.0	15.2	0.8	88.9	bdl	0.7
11022-g11-P1-7	with glassy -MI	core	13.5	13.3	0.8	bdl	0.4	95.6	466998.0	13.4	0.8	86.8	bdl	0.5
11022-g11-P1-8	with glassy -MI	core	12.7	11.4	1.2	0.4	0.6	92.6	466998.0	12.5	0.8	82.0	bdl	0.6
11022-g11-P1-9	with glassy -MI	core	11.0	10.7	1.2	bdl	0.8	96.1	466998.0	13.5	0.8	78.1	bdl	0.8
11022-g11-P1-10	with glassy -MI	core	11.1	11.1	1.0	0.7	0.7	98.6	466998.0	13.0	0.9	82.8	0.0	0.8
11022-g11-P1-11	with glassy -MI	core	11.6	10.6	1.1	bdl	0.7	98.3	466998.0	12.5	0.8	82.7	bdl	bdl
11022-g11-P1-12	with glassy -MI	core	11.9	10.4	1.4	0.2	0.7	94.2	466998.0	14.1	0.8	79.6	bdl	0.7
11022-g11-P1-13	with glassy -MI	core	11.5	10.8	0.8	bdl	0.6	93.4	466998.0	12.5	0.8	72.7	0.0	0.8
11022-g11-P1-14	with glassy -MI	core	11.2	11.2	1.0	bdl	0.6	93.7	466998.0	13.9	0.8	73.7	bdl	bdl
11022-g11-P1-15	with glassy -MI	core	11.4	11.4	1.0	0.8	0.8	95.2	466998.0	13.9	0.8	76.2	bdl	0.7
11022-g11-P1-16	with glassy -MI	core	12.3	11.3	0.8	0.8	0.4	93.3	466998.0	12.8	0.8	70.1	bdl	bdl
11022-g11-P1-17	with glassy -MI	core	12.6	12.6	0.8	0.3	0.6	91.8	466998.0	11.9	0.8	67.2	0.0	bdl

Appendix C

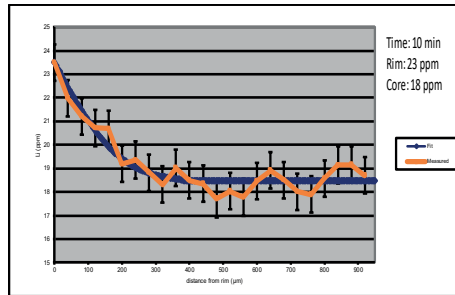
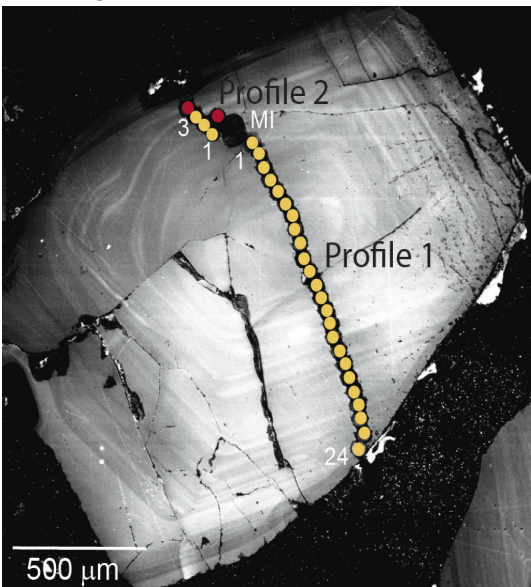
Table C3: continued

Info		Position	Li ⁶	Li ⁷	B	Na	Mg	Al	Si	P	Sc	Ti	Ga	Ge
11022-g11-P1-18	with glassy -MI	rim	13.7	12.7	1.0	bdl	0.6	90.6	466998.0	12.3	0.8	68.3	bdl	0.8
11022-g11-P2-1	with glassy -MI	next to MI	13.2	12.7	1.2	bdl	0.7	89.6	466998.0	12.6	0.8	74.2	0.0	0.6
11022-g11-P2-2	with glassy -MI	core	9.5	9.6	0.8	0.9	0.5	92.5	466998.0	12.7	0.8	67.7	bdl	0.6
11022-g11-P2-3	with glassy -MI	core	10.1	9.8	0.9	0.5	0.6	92.7	466998.0	12.9	0.9	68.5	bdl	0.8
11022-g11-P2-4	with glassy -MI	core	10.7	10.1	0.9	bdl	0.6	97.3	466998.0	15.3	0.8	67.1	bdl	0.7
11022-g11-P2-5	with glassy -MI	core	9.8	9.8	1.6	0.3	0.5	92.9	466998.0	13.2	0.8	63.6	bdl	0.8
11022-g11-P2-6	with glassy -MI	core	10.5	10.3	0.9	0.2	0.4	99.8	466998.0	13.0	0.8	68.8	bdl	0.5
11022-g11-P3-1	with glassy -MI	next to MI	14.8	14.3	0.9	1.6	0.6	95.8	466998.0	13.0	0.9	70.8	0.0	0.6
11022-g11-P3-2	with glassy -MI	core	13.1	11.5	0.9	0.6	1.1	99.6	466998.0	13.9	0.9	69.3	bdl	bdl
11022-g11-P3-3	with glassy -MI	core	11.4	11.3	0.8	0.5	0.8	99.6	466998.0	12.4	0.9	66.0	0.0	bdl
11022-g11-P3-4	with glassy -MI	core	12.1	11.9	1.0	bdl	1.3	107.9	466998.0	12.4	0.8	68.2	0.0	bdl
11022-g11-P3-5	with glassy -MI	core	10.8	10.4	0.9	0.4	0.5	95.0	466998.0	11.3	0.9	66.1	0.0	0.5
11022-g11-P3-6	with glassy -MI	next to MI	12.8	12.0	1.0	0.6	0.5	96.7	466998.0	13.6	0.8	69.4	bdl	0.5
11022-g14-P1-1	with glassy -MI	next to MI	9.2	9.2	0.8	bdl	0.8	110.8	466998.0	15.1	0.8	103.6	bdl	0.7
11022-g14-P1-2	with glassy -MI	core	9.9	9.7	0.5	bdl	0.9	110.8	466998.0	13.6	0.8	101.6	bdl	bdl
11022-g14-P1-3	with glassy -MI	core	10.2	9.9	0.6	bdl	0.7	106.9	466998.0	13.8	0.9	100.8	bdl	0.7
11022-g14-P1-4	with glassy -MI	core	10.2	9.6	0.6	bdl	0.7	107.3	466998.0	13.0	0.9	102.6	bdl	bdl
11022-g14-P1-5	with glassy -MI	core	10.8	9.7	0.5	bdl	0.9	107.7	466998.0	14.3	1.0	104.2	bdl	bdl
11022-g14-P1-6	with glassy -MI	core	9.8	9.3	0.7	bdl	1.0	106.2	466998.0	12.2	0.9	101.6	bdl	bdl
11022-g14-P1-7	with glassy -MI	core	9.6	8.8	0.6	0.2	0.7	103.7	466998.0	12.8	0.9	102.3	bdl	bdl
11022-g14-P1-8	with glassy -MI	core	10.0	9.4	0.7	0.2	0.5	100.8	466998.0	13.8	0.9	95.5	bdl	0.7
11022-g14-P1-9	with glassy -MI	core	10.4	9.9	0.5	0.3	0.6	100.6	466998.0	11.9	1.0	91.5	0.0	0.8
11022-g14-P1-10	with glassy -MI	core	9.3	8.6	0.6	bdl	0.6	99.4	466998.0	14.2	0.8	87.3	bdl	bdl
11022-g14-P1-11	with glassy -MI	core	9.2	9.0	0.5	bdl	0.7	102.3	466998.0	13.5	0.8	92.8	bdl	0.8
11022-g14-P1-12	with glassy -MI	core	10.0	9.5	0.6	bdl	0.8	105.9	466998.0	12.3	0.9	93.7	0.0	0.6
11022-g14-P1-13	with glassy -MI	core	10.1	9.5	bdl	bdl	0.5	97.3	466998.0	13.5	1.0	87.3	0.0	bdl
11022-g14-P1-14	with glassy -MI	core	9.7	9.4	0.7	bdl	0.6	100.1	466998.0	12.7	1.0	86.7	bdl	0.6
11022-g14-P1-15	with glassy -MI	core	9.6	10.2	0.5	bdl	0.6	99.2	466998.0	12.5	1.0	84.7	bdl	0.6
11022-g14-P1-16	with glassy -MI	core	10.4	10.2	0.5	bdl	0.8	100.9	466998.0	12.7	0.9	83.7	0.0	bdl
11022-g14-P1-17	with glassy -MI	core	12.4	10.3	0.4	bdl	0.8	100.4	466998.0	12.9	1.0	81.7	bdl	0.6
11022-g14-P1-18	with glassy -MI	core	10.2	9.6	0.9	0.5	0.7	96.9	466998.0	13.1	1.0	79.3	bdl	bdl
11022-g14-P1-19	with glassy -MI	core	9.9	9.2	0.8	0.2	0.6	95.3	466998.0	14.0	1.0	74.3	0.0	0.6
11022-g14-P1-20	with glassy -MI	core	9.6	9.1	0.6	0.4	0.6	95.3	466998.0	11.8	1.0	76.3	0.0	bdl
11022-g14-P1-21	with glassy -MI	core	10.4	9.3	0.6	0.8	0.7	96.2	466998.0	13.8	0.9	77.1	bdl	bdl
11022-g14-P1-22	with glassy -MI	core	9.7	9.3	0.4	0.2	0.5	95.4	466998.0	13.3	1.0	74.1	bdl	0.9
11022-g14-P1-23	with glassy -MI	core	9.8	9.0	0.5	0.3	0.9	95.3	466998.0	13.6	0.9	70.3	bdl	bdl
11022-g14-P1-24	with glassy -MI	core	9.9	9.6	0.6	0.3	0.8	99.5	466998.0	12.7	1.0	75.6	0.0	bdl
11022-g14-P1-25	with glassy -MI	core	10.1	9.5	0.4	bdl	0.7	95.9	466998.0	12.8	1.0	74.7	bdl	0.7
11022-g14-P1-26	with glassy -MI	core	9.9	9.5	0.5	0.2	0.7	92.5	466998.0	12.6	1.0	73.2	bdl	bdl
11022-g14-P1-27	with glassy -MI	rim	9.6	9.1	0.5	1.9	0.6	94.8	466998.0	14.3	0.8	68.6	bdl	bdl
11022-g14-P2-1	with glassy -MI	next to MI	9.8	9.4	0.4	1.6	0.8	109.1	466998.0	15.3	0.8	100.0	bdl	bdl
11022-g14-P2-2	with glassy -MI	core	10.5	9.8	0.5	0.7	0.9	108.3	466998.0	13.0	0.9	98.8	0.0	0.7
11022-g14-P2-3	with glassy -MI	core	10.4	10.4	0.3	0.8	0.7	108.0	466998.0	12.4	1.0	101.6	bdl	0.9
11022-g14-P2-4	with glassy -MI	core	10.3	10.5	0.4	0.6	0.8	102.9	466998.0	12.9	1.0	100.3	0.0	0.5
11022-g14-P2-5	with glassy -MI	core	10.0	9.6	0.5	0.5	0.8	104.6	466998.0	12.7	0.9	101.1	0.0	bdl
11022-g14-P2-6	with glassy -MI	core	10.1	9.9	0.4	0.7	0.6	102.3	466998.0	14.0	1.0	94.2	bdl	0.6
11022-g14-P2-7	with glassy -MI	core	10.4	9.7	0.5	0.5	0.7	102.0	466998.0	13.3	1.0	94.7	bdl	0.8
11022-g14-P2-8	with glassy -MI	core	10.4	9.7	0.6	0.5	0.8	100.9	466998.0	11.4	1.0	91.3	bdl	0.9
11022-g14-P2-9	with glassy -MI	core	10.4	10.1	0.5	1.0	0.5	100.8	466998.0	11.8	1.1	94.1	bdl	bdl
11022-g14-P2-10	with glassy -MI	core	10.0	9.6	0.5	0.3	0.6	94.5	466998.0	12.2	1.0	92.2	bdl	0.6
11022-g14-P2-11	with glassy -MI	core	9.9	9.5	0.6	0.2	0.5	96.6	466998.0	12.8	1.0	92.7	bdl	0.8
11022-g14-P2-12	with glassy -MI	core	11.1	9.5	0.5	bdl	0.5	95.2	466998.0	12.9	1.1	85.5	bdl	0.5
11022-g14-P2-13	with glassy -MI	core	9.6	9.1	0.6	bdl	0.6	92.7	466998.0	13.0	1.0	82.1	0.0	bdl
11022-g14-P2-14	with glassy -MI	core	10.5	9.8	0.3	0.3	0.6	92.3	466998.0	12.2	1.0	80.0	bdl	0.7
11022-g14-P2-15	with glassy -MI	core	10.4	9.1	0.5	0.3	0.6	87.5	466998.0	11.2	1.0	77.9	bdl	1.0
11022-g14-P2-16	with glassy -MI	core	10.2	9.0	0.6	0.2	0.6	89.8	466998.0	11.2	1.1	73.9	bdl	bdl
11022-g14-P2-17	with glassy -MI	core	10.5	9.8	0.6	0.2	0.6	91.0	466998.0	11.9	1.0	84.9	bdl	0.8
11022-g14-P2-18	with glassy -MI	rim	11.8	11.4	0.5	0.2	0.6	91.3	466998.0	11.7	1.1	88.7	bdl	0.5

13005- grain 1



13005- grain 10



13005- grain 7

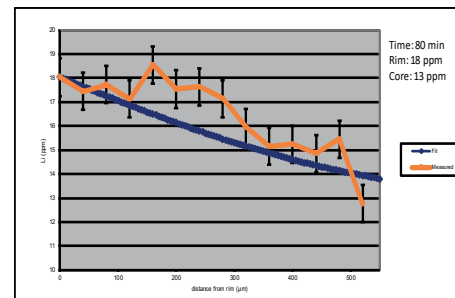
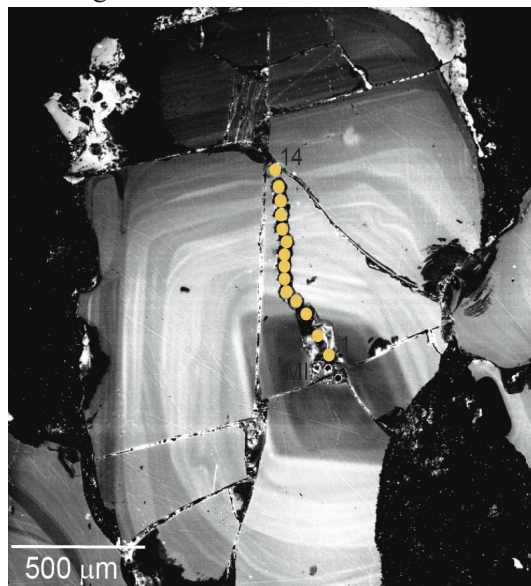


Fig. C1. CL images of quartz grains with trace element profiles and diffusion models.

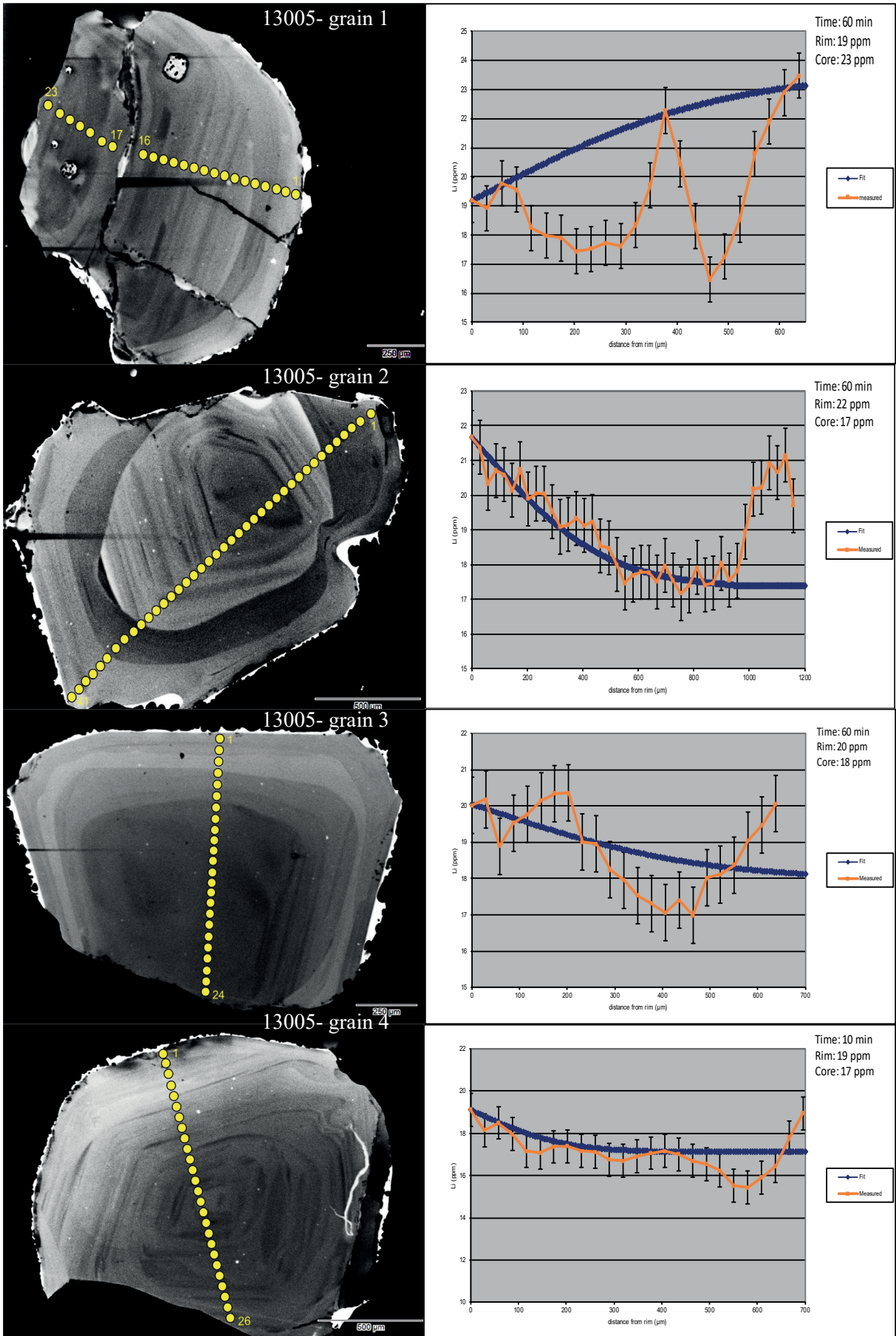


Fig. C1. continued

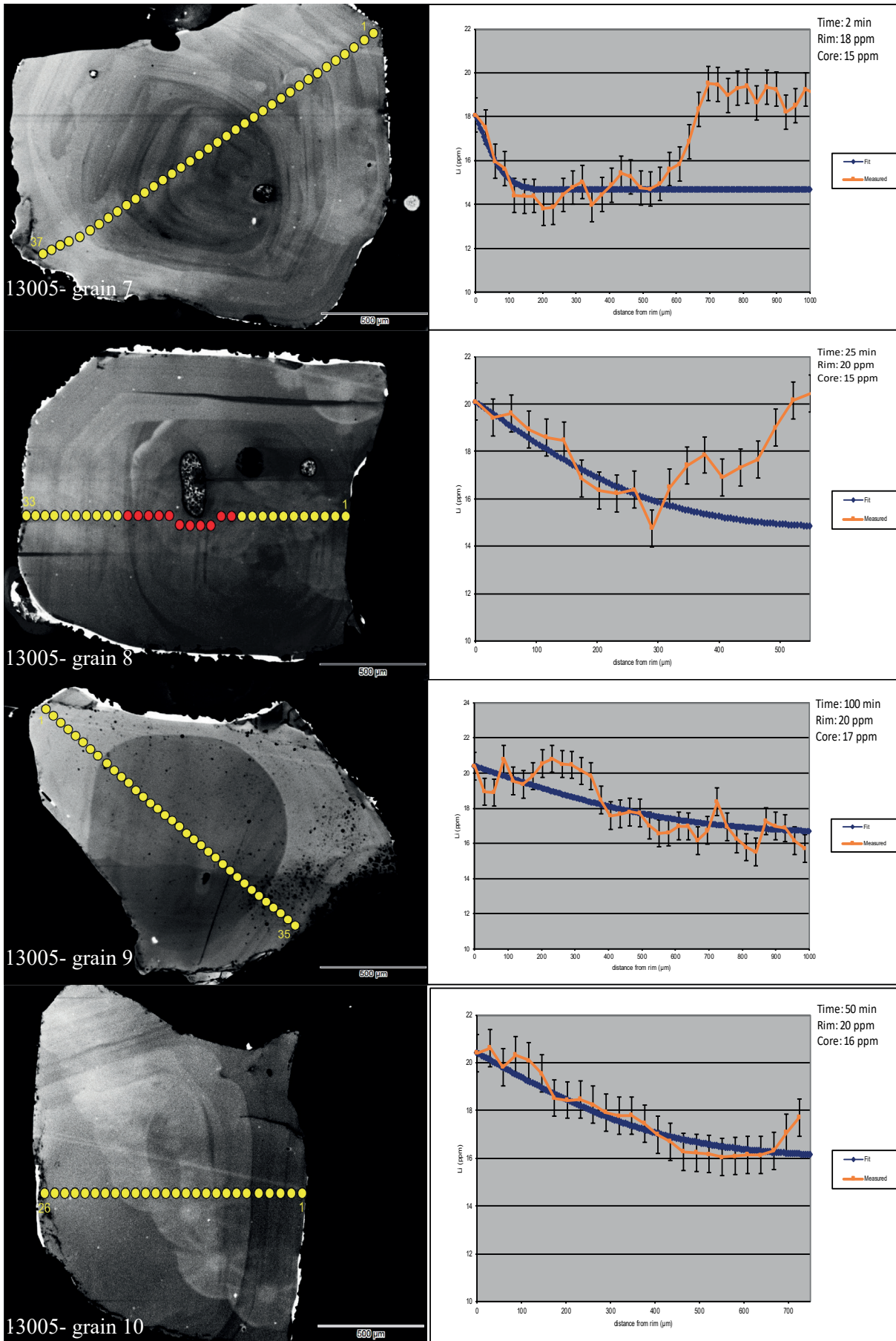


Fig. C1. continued

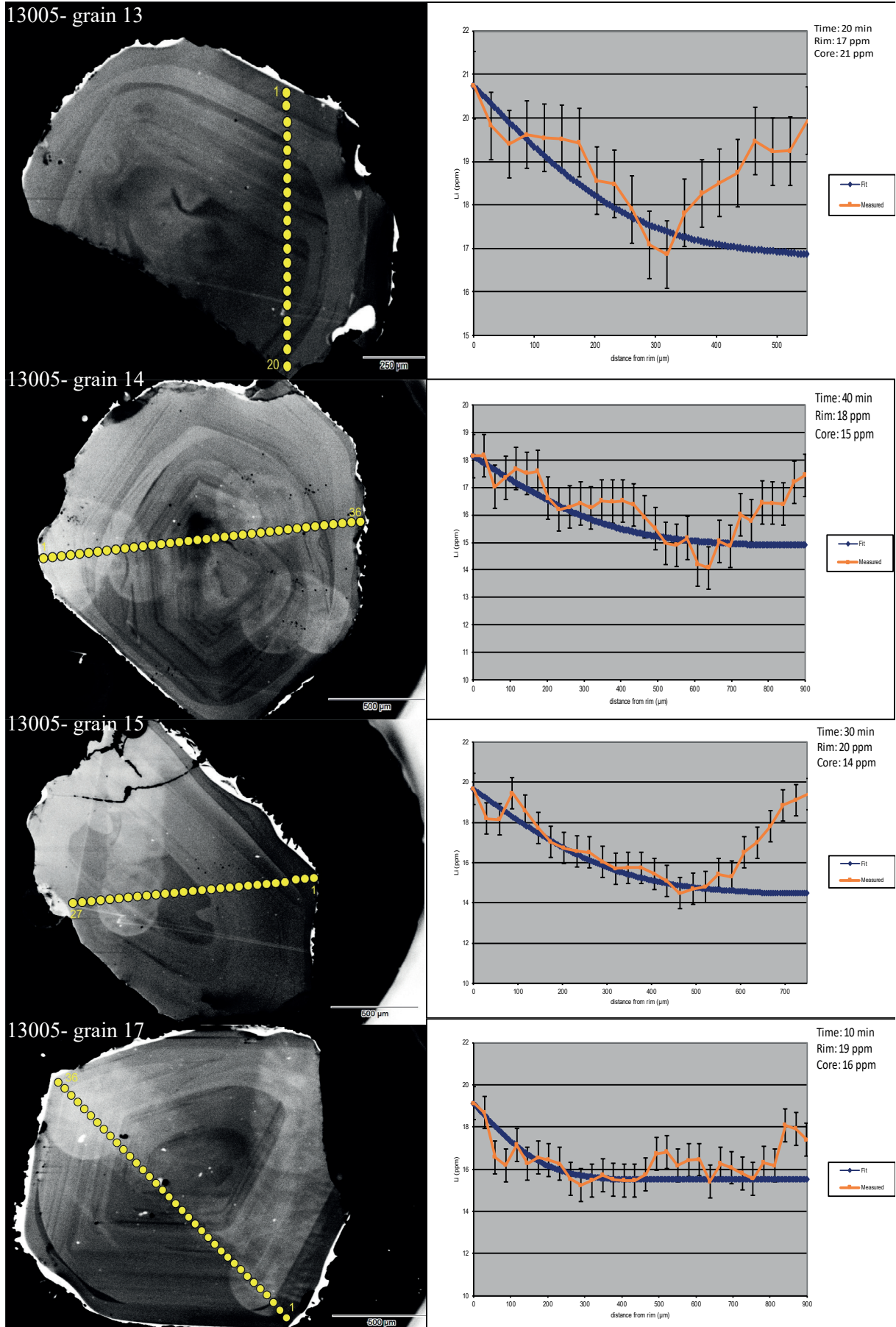


Fig. C1. continued

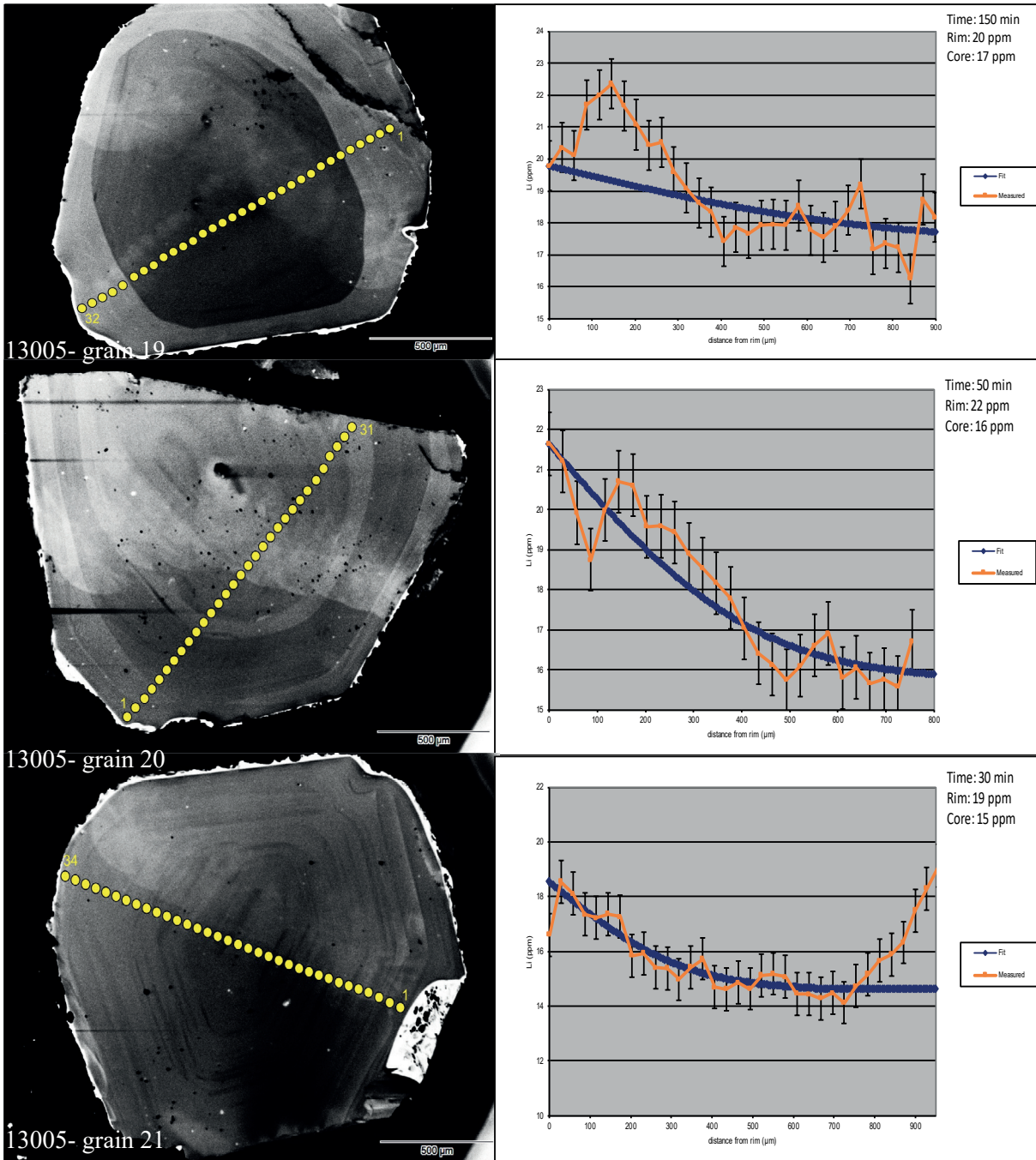


Fig. C1. continued

Curriculum vitae

Julia Neukampf

Clausiusstrasse 25, 8092 Zürich, Switzerland

☎ (+49) 172 8425 680 - ✉ julia.neukampf@erdw.ethz.ch

Research Interests

- silicic magma generation, especially large scale silicic volcanism
- non-traditional stable isotope systems
- volatiles and timescales of degassing and eruption timescales
- intraplate and subduction volcanism
- physical volcanology with emphasis on explosive volcanism

Education

Doctor of Sciences, ETH Switzerland	Thesis: <i>Lithium behaviour in shallow, silicic magmatic Systems</i> Advs.: Dr. B. Ellis; Prof. Dr. O. Bachmann	01.09.2016- 30.09.2020
M.Sc., FU Berlin, Germany	Geodynamics and Geomaterials Thesis: <i>Magma chambers beneath the Cape Verde Islands: Petrology and Thermobarometry of alkaline differentiated magmas</i> Advs.: Prof. Dr. T. John; Dr. A. Freundt	23.03.2014- 18.07.2016
B.Sc., Fu Berlin	Geological Sciences Thesis: <i>Petrographie der Lapilli und Bomben aus dem Meerfelder Maar, Westeifel</i> Advs.: Dr. K. Hammerschmidt; Dr. R. Milke	01.10.2009- 23.03.2014

Awards and Funding

Grant	DAAD group scholarship for field trip to Iceland	July 2013
-------	--	-----------

Research Experience

Graduate Research Assistant	ETH Zürich responsibilities: Electron Probe Micro-Analyser assistant Karl-Fischer (KF) titration assistant	2018-present
Laboratory work	clean laboratory (chemical separation for isotopic measurements), thin section preparation, mineral separation (crushing, milling, heavy liquids), sample preparation for XRD/XRF analysis, SIMS mount preparation, FTIR mount preparation	

Teaching/Advising

M.Sc. Co-advisor	Alejandro Cortes; Geochronology and Geochemistry of an Explosive Oceanic Volcano, The Fataga Group, Gran Canaria	2018-2019
Teaching assistant at ETH	<ul style="list-style-type: none">– Crystals and minerals (BSc Level)– Electron Microprobe Course (MSc and PhD Level)– Mark Exams (Dyn. Earth) (BSc Level)– Integrated Earth systems (BSc Level)– Volcanology Field Trip (MSc Level)– Geological Field Trip (BSc Level)	2016-2020
Teaching	<ul style="list-style-type: none">– Introductory Microscopy (BSc Level)	2016

Teaching assistant at FU	– Lab practical - Mineral and rock identification (BSc Level)	2013-2016
	– Introductory Microscopy (B.Sc. Level)	
	– Igneous Rock Microscopy (B.Sc. Level)	
	– Metamorphic Microscopy (B.Sc. Level)	
	– Introduction to Mineralogy/Crystallography (BSc Level)	

Instrument Proficiencies

- **EPMA:** JEOL JXA-8230 and JEOL JXA-8200
- **LA-ICP-MS:** Physik excimer ArF and Resonetics ArF excimer laser systems, Nexion2000 and Thermo Element XR ICP-MS systems
- **MC-ICP-MS:** Thermo Fisher Scientific Neptune
- **SEM:** JEOL JSM-6390LA SEM/Thermo Fisher
- **SIMS:** CAMECA IMS 1280HR
- **FTIR:** Bruker Tensor 27 spectrometer with globar infrared source attached to a Bruker Hyperion 3000 microscope
- **KFT:** EUROTHERM type 818 controller coupled to a titration cell

Short Courses

Prof. D. Dingwell	Melts, Glasses, Magmas	June 2019
Prof. S. Chakraborty	Diffusion modelling workshop	Oct. 2018
Prof. H. Marschall	Radiogenic and non-traditional isotopes – analytical methods and application	Mar. 2018
Dr. M. Wiedenbeck	SIMS	Nov. 2017
Prof. C. Breitkreuz	Introduction to physical volcanology and volcanic textures	Sept. 2014
Prof. H.U. Schmincke	Volcano-magma systems with emphasis on explosive processes and deposits	Oct. 2012
Dr. Hennie Theart	The Role of the Geologist in the Mineral Business	Dez. 2011

Professional Memberships

- Deutsche Vulkanologische Gesellschaft
- Deutsche Mineralogische Gesellschaft (DMG)
- Deutsche Geologische Gesellschaft - Geologische Vereinigung (DGGV)
- Geochemical Society

Publications

Neukampf, J., Ellis, B.S., Magna, T., Laurent, O., Bachmann, O. (2019). Partitioning and isotopic fractionation of lithium in mineral phases of hot, dry rhyolites: The case of the Mesa Falls Tuff, Yellowstone. *Chemical Geology* **506**, 175-186.

Kueppers, U., Pimentel, A., Ellis, B.S., Forni, F., **Neukampf, J.**, Pacheco, J.M.R., Perugini, D., Queiroz, G. (2019). Biased volcanic hazard assessment due to incomplete eruption records on ocean islands: an example of Sete Cidades Volcano, Azores. *Frontiers in Earth Science* **7**, 122.

Tollan, P., Ellis, B.S., Troch, J., **Neukampf, J.** (2019). Assessing magmatic volatile equilibria through FTIR spectroscopy of unexposed melt inclusions and their host quartz: a new technique and application to the Mesa Falls Tuff, Yellowstone. *Contrib. Mineral. Petrol.* 174:24.

Ellis, B.S., Szymanowski, D., Magna, T., **Neukampf, J.**, Dohmen, R., Bachmann, O., Ulmer, P., Guillong, M. (2018). Post-eruptive mobility of lithium in volcanic rocks. *Nat. Commun.*, **9**, 3228.

Neukampf, J., Ellis, B.S., Laurent, O., Steinmann, L.K., Ubide, T., Oeser, M., Magna, T., Weyer, S., Bachmann, O. (2020). Time scales of syn-eruptive volatile loss in silicic magmas quantified by Li-isotopes. *Geology* **49**.

Conference presentations

Neukampf, J., Ellis, B.S., Bouvier, A.S., Tollan, P., Ulmer, P., Magna, T., Bachmann, O. (2020): Tracking degassing in rhyolite using lithium isotopes. (Oral) Goldschmidt 2020. Hawaii, USA

Ellis, B.S., **Neukampf, J.**, Laurent, O., Steinmann, L., Weyer, S., Magna, T., Ubide, T., Bachmann, O. (2020): Plagioclase as a witness of syn-eruptive degassing in rhyolitic magmas. EGU General Assembly Conference, 2020. Vienna, Austria

Cortes-Calderon, E.A., Ellis, B.S., **Neukampf, J.**, Harris, C., Wolff, J.A., Mark, D.F., Bachmann, O. (2020): The role of contamination in the tightrope of Gran Canaria peralkaline magma differentiation. EGU General Assembly Conference, 2020. Vienna, Austria

Neukampf, J., Ellis, B.S., Bouvier, A.S., Tollan, P., Ulmer, P., Magna, T., Bachmann, O. (2020): Tracking degassing in rhyolite using lithium isotopes. (Poster) 56th Annual Meeting of the Volcanic and Magmatic Studies Group. Plymouth, UK

Ellis B.S., Cortes-Calderon, E.A., **Neukampf, J.**, Mark, D.F., Wolff, J.A., Harris, C., Bachmann, O. (2020): Fataga Volcanism on Gran Canaria. 56th Annual Meeting of the Volcanic and Magmatic Studies Group. Plymouth, UK

Neukampf, J., Ellis, B.S., Laurent, O., Steinmann, L.K., Dohmen, R., Ubide, T., Oeser, M., Magna, T., Weyer, S., Bachmann, O. (2019): Timescales of degassing in rhyolitic magmas tracked by Li in plagioclase. (Oral) Goldschmidt 2019. Barcelona, Spain

Cortes-Calderon E.A., Ellis B.S., **Neukampf J.**, Wolff J.A., Bachmann O. (2019): Chemical Fingerprinting of Volcanic deposits from the Fataga Group, Gran Canaria (Spain). Goldschmidt 2019. Barcelona, Spain

Neukampf, J., Steinmann, L.K., Ellis, B.S., Oeser, M., Dohmen, R., Laurent, O., Ubide, T., Magna, T., Weyer, S., Bachmann, O. (2019): Tracking degassing of explosive eruption with lithium isotopes. (Oral) 55th Annual Meeting of the Volcanic and Magmatic Studies Group. St. Andrews, UK

Ellis B.S., **Neukampf J.**, Magna T., Harris, C., Bachmann, O. (2019): Biotites as recorders of the magmatic-hydrothermal transition. 55th Annual Meeting of the Volcanic and Magmatic Studies Group. St. Andrews, UK

Tollan, P., Ellis, B.S., Troch, J., **Neukampf, J.** (2019): An assessment of magmatic volatile equilibria by FTIR spectroscopy of unexposed melt inclusions and their host quartz: a new technique and application to the Mesa Falls Tuff, Yellowstone. 55th Annual Meeting of the Volcanic and Magmatic Studies Group. St. Andrews, UK

Neukampf J., Steinmann L.K., Ellis B.S., Oeser-Rabe M., Dohmen R., Ubide T., Magna T., Weyer S., Bachmann O. (2018): Lithium isotopic and concentration gradients in plagioclase – implications for pre- and syn-eruptive magmatic processes. (Poster) AGU Fall Meeting. Washington, D.C., USA

Neukampf J., Ellis B.S., Magna T., Laurent O., Bachmann O. (2018): Li isotopic variations between magmatic minerals and indications of degassing of a rhyolitic magma (Mesa Falls Tuff, Yellowstone). (Poster) Goldschmidt 2018. Boston, USA

Kueppers U., Pimentel A., Ellis B.S., Forni F., **Neukampf J.**, Pacheco J.M.R., Perugini D., Queiroz G. (2018): Gone with the Wind: how to quantify the risk based on incomplete eruptive records on volcanic islands. An example of Sete Cidades volcano, Azores. EGU General Assembly Conference, 2018. Vienna, Austria

Ellis B.S., Bachmann O., **Neukampf J.**, Magna T. (2017): Lithium in silicic magmatic systems. Royal Society meeting on magma reservoir architecture and dynamics. Chicheley, Newport Pagnell, UK

Neukampf J., Ellis B.S., Magna T., Bachmann O. (2017): Lithium abundance and isotopic variations between phases in a rhyolite (the Mesa Falls Tuff, Yellowstone). (Poster) IAVCEI 2017. Portland, Oregon, USA. Abstract volume, p.760

Ellis B.S., Szymanowski D., Magna T., **Neukampf J.**, Bachmann O., Ulmer P., Guillong M. (2017): Post-eruptive behaviour of Li in volcanic rocks: implications for element cycling. IAVCEI 2017. Portland, Oregon, USA. Abstract volume, p. 299

Neukampf J., Ellis, B.S.; Magna T., Bachmann O (2017): Li isotopic variations between phases in Mesa Falls Tuff. (Oral) Journée Magmatique annual meeting. Geneva, Switzerland

Ellis B.S., Szymanowski D., Magna T., **Neukampf J.**, Bachmann O., Guillong M. (2017): The effect of cooling rates on lithium in rhyolites. Volcanic and Magmatic Studies Group annual meeting. Liverpool, UK. Abstract volume, p. 89

Neukampf, J., Freundt, A., John, T. (2015): Study of the evolution of the intra-plate magma plumbing system beneath Fogo (Cape Verde Archipelago). (Poster) DMG Annual Meeting. Berlin, Germany

Outreach

Meet a Scientist at ETH Zürich	2017-present
Assistance for the course “Children at University” at FU Berlin	2015
Girls day - course instructor for “Minerals in everyday life” at FU Berlin	2015
Participation and supervision of experiments at the “Night of Science” at FU Berlin	2011-2013
Mentor for freshmen at FU Berlin	2011-2012
Active member of the Student Council of Geological Science at FU Berlin	
Co-organisation of the Meeting of German Student Council 2012 in Berlin	
Helped with the organisation and supervision of field trips for freshmen	2011-2014

Languages

- German: native
- English: fluent
- Spanish: A1 level
- Latin: A2